DESIGNING WITH
GEOSYNTHETICS

FIFTH EDITION

ROBERT M. KOERNER

Designing with Geosynthetics

Fifth Edition

Robert M. Koerner

Director, Geosynthetic Institute
Emeritus Professor of Drexel University

PEARSON
Prentice
Hall

Upper Saddle River, New Jersey 07458

Vice President and Editorial Director, ECS: *Marcia J. Horton*	Director of Creative Services: *Paul Belfanti*
Executive Editor: *Eric Svendsen*	Creative Director: *Jayne Conte*
Editorial Assistant: *Andrea Messineo*	Cover Designer: *Bruce Kenselaar*
Vice President and Director of Production and Manufacturing, ESM: *David W. Riccardi*	Art Editor: *Greg Dulles*
	Manufacturing Buyer: *Lisa McDowell*
Executive Managing Editor: *Vince O'Brien*	Marketing Manager: *Holly Stark*
Managing Editor: *David A. George*	About the Cover: *Cover images courtesy of the author.*
Production Editor: *Kevin Bradley*	

Pearson Prentice Hall™ is a trademark of Pearson Education, Inc.

The author and publisher of this book have used their best efforts in preparing this book. These efforts include the development, research, and testing of the theories and programs to determine their effectiveness. The author and publisher make no warranty of any kind, expressed or implied, with regard to these programs or the documentation contained in this book. The author and publisher shall not be liable in any event for incidental or consequential damages in connection with, or arising out of, the furnishing, performance, or use of these programs.

Printed in the United States of America

10 9 8 7 6 5 4 3 2 1

Dedication

To the member organizations of the Geosynthetic Institute for their confidence, interaction, friendship, and financial support over the past 20 years and to Drexel University for the opportunities provided over the past 40 years.

Contents

Preface

While the first monograph on the subject we now call "geosynthetics" appeared in 1980, it was not until 1986 that the subject was unified into a formalized structure. This occurred thanks to the publication of the first edition of *Designing with Geosynthetics*. Subsequent editions have appeared in 1990, 1994, 1998, and (now) 2005.

At this point it is clear that geosynthetic materials (aided by the dissemination and use of *Designing with Geosynthetics*) have entered the mainstream of the targeted professional groups—that is, with transportation, geotechnical, environmental, hydraulics, and private site development designers and related personnel. Many conferences, short courses, seminars, workshops, and internet tutorials have emerged that are very helpful in advancing the geosynthetics knowledge base. No longer considered a new construction material, geosynthetics have matured and entered into academia as well. At least 15 stand-alone courses are given on geosynthetics (mostly in North America), and they are included in partial form in various courses at hundreds of colleges and universities. It should be mentioned that the geosynthetic industry continues to be shaped by manufacturers and entrepreneurs in private business, which leaves academics and researchers to play "catch-up" insofar as investigating the nuances of how geosynthetics work. Hopefully, this book will continue to help in this regard.

The structure of the book remains as in the past few editions, with the first chapter presenting an overview of all types of geosynthetics as well as a description of the elements of polymer chemistry and the related manufacturing and fabrication techniques. Each of the chapters that follow focus on a particular type of geosynthetic material. Any one of these chapters can be taught/learned in isolation, although it is helpful to couple a particular chapter with the relevant section in Chapter 1. Descriptive examples, references, and problems accompany each chapter.

Significant new material has been added to this edition. For example, in the chapter on geotextiles, the discussion of containers and tubes has been greatly expanded; in the chapter on geogrids, walls and slope design including seismic analysis are now discussed; in the chapter on geomembranes, we now look at wet landfills, agricultural waste, waste stability, and dam waterproofing; in the chapter on geosynthetic clay liners new products and related performance are addressed; in the chapter on geocomposites new products and related behavior including fiber reinforcement and wall drainage are presented. In addition, a completely new chapter on geofoam has been added. Whenever possible, suggested areas for further research and development are mentioned. A printed instructor's solutions manual is available from your Prentice Hall sales rep, or by emailing engineering @prenhall.com.

ROBERT M. KOERNER

Acknowledgments

1

Overview of Geosynthetics

1.0   INTRODUCTION

According to ASTM D4439, a geosynthetic is defined as follows:

> **geosynthetic,** *n*—a planar product manufactured from polymeric material used with soil, rock, earth, or other geotechnical engineering related material as an integral part of a human-made project, structure, or system.

Geosynthetics have emerged as exciting engineering materials in a wide array of applications—transportation, geotechnical, environmental, hydraulics, and private development applications—and the rapidity at which the related products are being developed and used is nothing short of amazing. At no time in the author's experience has a new engineering material come on so strong. The reasons for this explosion of

geosynthetic materials into new products are numerous and include the following:

- They are quality-control manufactured in a factory environment.
- They can be installed rapidly.
- They generally replace raw material resources.
- They generally replace difficult designs using soil or other construction materials.
- Their timing is very appropriate.
- Their use is required by regulations in some cases.
- They are generally cost competitive against the soils or other construction materials that they replace or augment.
- They have made heretofore impossible designs and applications possible.
- They are being actively marketed and are widely available.
- Their technical database (both design and testing) is reasonably established.
- They are being integrated into the profession via generic specifications.

The professional groups most strongly influenced are transportation, geotechnical, environmental, hydraulics, and private development engineering communities, although all soil-, rock-, and groundwater-related activities fall within the general scope of the various applications. This being the case, the term geosynthetics seems appropriate. *Geo*, of course, refers to the earth. The realization that the materials are almost exclusively from human-made products gives the second part to the name—*synthetics*. The materials used in the manufacture of geosynthetics are almost entirely from the plastics industry—that is, they are polymers made from hydrocarbons, although fiberglass, rubber, and natural materials are occasionally used. Interestingly, the case could easily be made that the entire technology might better be called *geopolymers*, but the term geosynthetics took hold before this realization. The sections that follow in this opening chapter present an overview of the various types of geosynthetic materials and serve as an introduction to the remainder of the text—namely Chapters 2 through 9—where each particular type of geosynthetic will be discussed.

1.1 BASIC DESCRIPTION OF GEOSYNTHETICS

Lost to history are the initial attempts to reinforce soils; the adding of materials that would enhance the behavior of the soil itself was no doubt done long before our first historical records of this process. It seems reasonable to assume that first attempts were made to stabilize swamps and marshy soils using tree trunks, small bushes, and the like. These soft soils would accept the fibrous material until a mass was formed that had adequate properties for the intended purpose. It also seems reasonable to accept that either the continued use of such a facility was possible because of the properly stabilized nature of the now-reinforced soil (probably by trial-and-error), or was impossible due to a number of factors, among which were

- insufficient reinforcement material for the loads to be carried;
- the pumping of the soft soil up through the reinforcement material; and

- the degradation of the fibrous material with time, leading back to the original unsuitable conditions.

Such stabilization attempts were undoubtedly continued with the development of a more systematic approach in which timbers of nearly uniform size and length were lashed together to make a mattressed surface. Such split-log "corduroy" roads over peat bogs date back to 3000 B.C. [1]. This art progressed to the point where the ridged surface was filled in smooth. Some of these systems were surfaced with a stabilized soil mixture or even paved with stone blocks. Here again, however, deterioration of the timber and its lashings over time was an obvious problem.

The concept of reinforcing soft soils has continued until the present day. The first use of fabrics in reinforcing roads was attempted by the South Carolina Highway Department in 1926 [2]. A heavy cotton fabric was placed on a primed soil subgrade, hot asphalt was applied to the fabric, and a thin layer of sand was placed on the asphalt. In 1935 results were published of this work, describing eight separate field experiments. Until the fabric deteriorated, the results showed that the roads were in good condition and that the fabric reduced cracking, raveling, and localized road failures. This project was certainly the forerunner of the separation and reinforcement functions of geosynthetic materials as we know them today. The separation and reinforcement of unsuitable soils is a major topic area of this book.

Another major topic area is that of providing an intermediate barrier between two dissimilar materials for the purpose of liquid drainage (usually water) and soil filtration. When requiring liquid flow across such a barrier, it must obviously be porous, yet the voids must not be open so much as to lose the retained soil—thus the necessity of using some sort of intermediate filter. Again the historical development of filtration provides an important background for understanding the work that followed. Naturally occurring sands and gravels that were found to be well graded had been used as filter material since ancient times. The idea of systematizing filtration criteria seems to have been originated by Karl Terzaghi and Arthur Casagrande in the 1930s and brought to use by Bertram [3] shortly thereafter. This idea of soil filters, even multiple-grade soil filters, is a target area for the geosynthetic materials described in this book—now for reasons of construction quality control and cost effectiveness.

The last major topic area is that of providing a waterproof barrier for preventing liquid movement from a given containment area. Such liners have historically been made using low-permeability clay soils. The Roman aqueducts were lined in such a manner, and the technology undoubtedly preceded them by many years [4]. Liners made from bitumen and various cements have been used since the 1900s, but it was the synthetic rubber material "butyl" in the 1930s that ushered in polymeric liners [5]. Today, such liners (there are many different types) are regulatory-mandated for use in certain environmentally related applications. Interestingly, the newest barrier materials are combinations of both geosynthetics and bentonite soil used as a composite material.

Thus geosynthetic materials perform five major functions: (1) separation, (2) reinforcement, (3) filtration, (4) drainage, and (5) containment (of liquid and/or gas). The use of geosynthetics has basically two aims: (1) to perform better (e.g., with no deterioration of material or excessive leakage) and (2) to be more economical than using

traditional materials and solutions (either through lower initial cost or through greater durability and longer life, thus reducing maintenance and replacement costs).

1.1.1 Types of Geosynthetics

There are eight types of geosynthetics: (1) geotextiles, (2) geogrids, (3) geonets, (4) geomembranes, (5) geosynthetic clay liners, (6) geopipe, (7) geofoam, and (8) geocomposites. They are shown in Figure 1.1 and are discussed next.

Geotextiles.   Geotextiles (see Section 1.3 and Chapter 2) form one of the two largest groups of geosynthetics described in this book. Their rise in growth during the past 25 years has been nothing short of extraordinary. They are indeed textiles in the traditional sense, but they consist of synthetic fibers rather than natural ones such as cotton, wool, or silk. Thus biodegradation and subsequent short lifetime is not a problem. These synthetic fibers are made into flexible, porous fabrics by standard weaving machinery or are matted together in a random nonwoven manner. Some are also knitted. The major point is that geotextiles are porous to liquid flow across their manufactured plane and also within their thickness, but to a widely varying degree. There are at least 100 specific application areas for geotextiles that have been developed; however, the fabric always performs at least one of four discrete functions: separation, reinforcement, filtration, and/or drainage.

Geogrids.   Geogrids (see Section 1.4 and Chapter 3) represent a rapidly growing segment within the geosynthetics. Rather than being a woven, nonwoven, or knitted textile fabric, geogrids are plastics formed into a very open, gridlike configuration—i.e., with large apertures between individual ribs in the machine and cross machine directions. Geogrids are formed in various ways: (1) stretched in one or two directions for improved physical properties, (2) made on weaving or knitting machinery by standard and well-established methods, or (3) made by bonding rods or straps together. There are many application areas, however, and they function almost exclusively as reinforcement materials.

Geonets.   Geonets, called *geospacers* by some (see Section 1.5 and Chapter 4), constitute another specialized segment within the geosynthetics area. They are formed by a continuous extrusion of parallel sets of polymeric ribs at acute angles to one another. When the ribs are opened, relatively large apertures are formed into a netlike configuration. Their design function is completely within the drainage area where they are used to convey liquids of all types.

Geomembranes.   Geomembranes (see Section 1.6 and Chapter 5) represent the other largest group of geosynthetics described in this book, and in dollar volume their sales are greater than that of geotextiles. Their growth in the United States and Germany was stimulated by governmental regulations originally enacted in the early 1980s. The materials themselves are relatively thin, impervious sheets of polymeric material used primarily for linings and covers of liquid- or solid-storage facilities. This includes all types of landfills, reservoirs, canals, and other containment facilities. Thus the
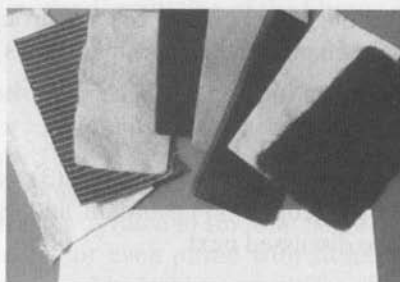
(a) Geotextiles
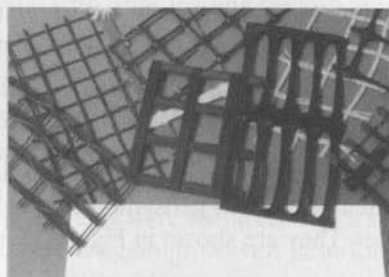
(b) Geogrids
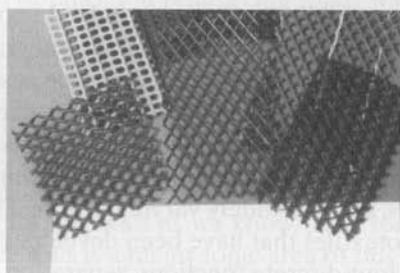
(c) Geonets
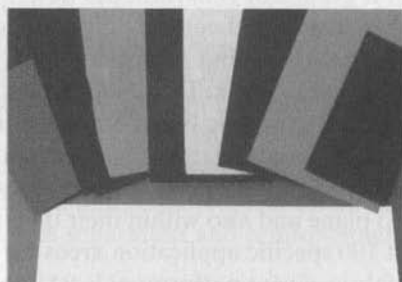
(d) Geomembranes
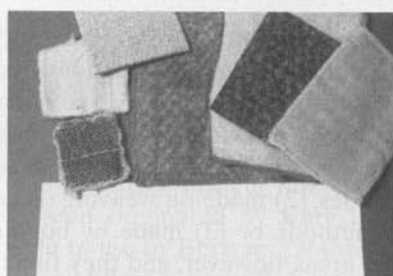
(e) Geosynthetic clay liners

(f) Geopipe

(g) Geofoam
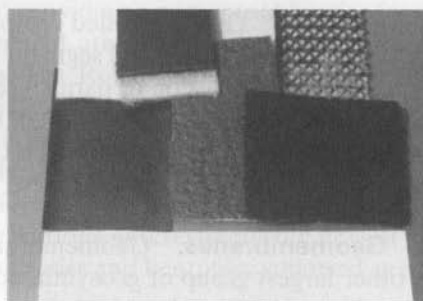
(h) Geocomposites

Figure 1.1   The eight types of geosynthetics.

primary function is always containment as a liquid or vapor barrier or both. The range of applications, however, is great, and in addition to the environmental area, applications are rapidly growing in geotechnical, transportation, hydraulic, and private development engineering.

Geosynthetic Clay Liners.   Geosynthetic clay liners (GCLs) (see Section 1.7 and Chapter 6) are an interesting juxtaposition of polymer and natural soil materials. They are rolls of factory-fabricated thin layers of bentonite clay sandwiched between two geotextiles or bonded to a geomembrane. Structural integrity of the composite is obtained by needle-punching, stitching, or physical bonding. GCLs are used as a composite component beneath a geomembrane or by themselves in environmental and containment applications as well as in transportation, geotechnical, hydraulic, and various private development applications.

Geopipe (aka Buried Plastic Pipe).   Geopipe, or buried plastic pipe (see Section 1.8 and Chapter 7), is perhaps the original geosynthetic material still available today. This orphan of typical engineering curricula is included here because of an obvious awareness that geopipe is being used in all aspects of geotechnical, transportation, environmental, hydraulic, and private development engineering most often with little design and testing, attributable to a general lack of formalized training. The critical nature of leachate collection pipes coupled with high compressive loads makes geopipe a bona fide member of the geosynthetics family and one that is focused completely on the drainage function.

Geofoam.   Geofoam (see Section 1.9 and Chapter 8) is a product created by polymeric expansion process resulting in a "foam" that consists of many closed but gas-filled cells. The skeletal nature of the cell walls is the unexpanded polymeric material. The resulting product is generally in the form of large, but extremely light, blocks that are stacked side-by-side, providing lightweight fill in numerous applications. Although the primary function is dictated by the application, separation is always a consideration and geofoam will be included in this category rather than creating a separate one.

Geocomposites.   Geocomposites (see Section 1.10 and Chapter 9) consist of a combination of geotextiles, geogrids, geonets, and/or geomembranes in a factory-fabricated unit. Also, any one of these four materials can be combined with another synthetic material (e.g., deformed plastic sheets or steel cables) or with soil. For example, a geonet with geotextiles on both surfaces and a GCL consisting of a geotextile/bentonite/geotextile sandwich are both geocomposites. This exciting area brings out the best creative efforts of the engineer, manufacturer, and contractor. The application areas are numerous and growing steadily. They encompass the entire range of functions previously listed for geosynthetics: separation, reinforcement, filtration, drainage, and containment.

Geo-Others.   The general area of geosynthetics has exhibited such innovation that many systems defy categorization. For want of a better phrase, *geo-others* describes items such as threaded soil masses, polymeric anchors, and encapsulated soil

cells. As with geocomposites, the primary function of geo-others is product-dependent and can be any of the five major functions of geosynthetics. These materials will be discussed in those chapters that they are most closely related to, or in Chapter 9 on the basis of their primary function.

1.1.2 Organization by Function

The juxtaposition of the various types of geosynthetics just described with the primary function that the material is called upon to serve allows for the creation of a matrix that will be used throughout this book. In essence, this matrix is the "scorecard" for understanding the entire geosynthetic field and its design-related methodology. Table 1.1 illustrates the primary function that each of the geosynthetics can be called upon to serve. Note that these are primary functions, and in many (if not most) cases there are secondary functions, and perhaps tertiary ones as well. For example, a geotextile placed on soft soil will usually be designed on the basis of its reinforcement capability, but separation and filtration might certainly be secondary and tertiary considerations. A geomembrane is obviously used for its containment capability, but separation will always be a secondary function.

The greatest variability from a manufacturing and materials viewpoint is the category of geocomposites. The primary function will depend upon what is actually created, manufactured, and installed.

Note that Table 1.1 will be constantly referred to throughout this book. It will clearly identify each geosynthetic material vis-à-vis the primary function (usually by application) that is being served.

1.1.3 Market Activity

To say that the geosynthetic market activity, as indicated by sales volume, is strong is decidedly an understatement. All existing application areas are seeing constant growth, albeit at different rates. Current geosynthetics growth is approximately 5% in

TABLE 1.1   IDENTIFICATION OF THE USUAL PRIMARY FUNCTION FOR EACH TYPE OF GEOSYNTHETIC

Type of Geosynthetic (GS)	Primary Function					Chapter in Book
	Separation	Reinforcement	Filtration	Drainage	Containment	
Geotextile (GT)	✓	✓	✓	✓		2
Geogrid (GG)		✓				3
Geonet (GN)				✓		4
Geomembrane (GM)					✓	5
Geosynthetic Clay Liner (GCL)					✓	6
Geopipe (GP)				✓		7
Geofoam (GF)	✓					8
Geocomposite (GC)	✓	✓	✓	✓	✓	9

Note: This table will be referred to in every chapter of this book.

the transportation and environmental sector, and approximately 10% in the geotechnical sector, while the hydraulics and private development sectors are seeing growth rates in excess of 15%. The motivators for such growth are decreased cost/benefit ratio over conventional materials and solutions, and (in certain applications) requirements by federal or state regulations. This is evidenced by steady growth rates over a long period of approximately 30 years for geotextiles and geogrids influenced by low cost/benefit ratios in the private construction sector), and a rapid increase after 1982 for geomembranes and geonets when the first government regulations were promulgated.

Current geosynthetic sales are difficult to assess, but the author's estimate for 2003 on a worldwide basis is as follows (note that the values are in millions of square meters and millions of US dollars):

Geotextiles	1000 M m^2 @ $0.90/m^2	=	$900M
Geogrids	100 M m^2 @ $2.50/m^2	=	250
Geonets	50 M m^2 @ $2.00/m^2	=	100
Geomembranes	200 M m^2 @ $8.00/m^2	=	1,600
Geosynthetic clay liners	75 M m^2 @ $4.00/m^2	=	300
Geopipe	not applicable	=	300
Geofoam	not applicable	=	100
Geocomposites	50 M m^2 @ $4.00/m^2	=	200
			$3,750M

While the total expenditure is impressive and indicates that geosynthetics are well-entrenched construction materials, the situation could, perhaps even should, be larger than indicated. This can be explained by the fact that relatively few colleges teach geosynthetics as a specialized course. It appears as though the subject is being introduced to students (often only graduate students) as part of existing courses, which is a logical way to contrast geosynthetics with traditional materials. Geosynthetics can also, of course, be studied in professional courses taken after graduation. These are offered on intermittent schedules by numerous associations, institutes, and continuing education organizations. Perhaps the Internet will eventually be the educational outreach vehicle of the future for geosynthetics, but that remains to be seen. Whatever vehicle form it takes, education in geosynthetics is still a major objective of this field and the one to which this book dedicates itself.

1.2   POLYMERIC MATERIALS

The vast majority (well over 95%) of the geosynthetics discussed in this book are made from synthetic polymers. Thus a brief discussion on the topics of polymer composition, structure, and identification is in order. This section is not meant to make a polymer engineer or a polymer scientist out of the reader, but only to afford an appreciation of (1) the wealth of information that is available, (2) the sophistication of the topic area,

and (3) the need for at least a rudimentary understanding of geosynthetics at the molecular level, which will prove beneficial for the topics discussed throughout the book.

The polymer industry is enormous. Worldwide sales are over $50 billion per year and the distribution reflects both the strength and diversity of consumption. For example, the consumption in tons of thermoplastic polymers (of the type used in geosynthetics) in 2000 was as follows:

United States	26,797,000
Western Europe	27,071,000
Eastern Europe	4,111,000
Canada	2,525,000
Mexico	2,224,000
Central/South America	6,201,000
Japan	8,069,000
Other Asia	34,242,000
Africa/Middle East	6,091,000
Total	117,331,000 tons

Fortunately, the area of geosynthetics utilizes very few of the thousands of commercialized polymers in existence. The following are the most commonly used in the manufacturing of geosynthetics:

- High-density polyethylene (HDPE)—developed in 1941
- Linear low-density polyethylene (LLDPE)—developed in 1956
- Polypropylene (PP)—developed in 1957
- Polyvinyl chloride (PVC)—developed in 1927
- Polyester (PET)—developed in 1950
- Expanded polystyrene (EPS)—developed in 1950
- Chlorosulphonated polyethylene (CSPE)—developed around 1965
- Thermoset polymers such as ethylene propylene diene terpolymer (EPDM)—developed in 1960

1.2.1 Brief Overview

The basic "feedstock" for almost all of the polymers used to make geosynthetics is ethylene gas. As can be seen in Figure 1.2, almost all of the polymers mentioned previously are included in the various branches. Ethylene is reacted by a catalyst to form discrete particles, called "flake," in a huge refinery, as shown in Figure 1.3. To say that the chemistry involved in the reaction is complex is a vast understatement, as evidenced by Ziegler and Natta who shared the Noble Prize for their respective discoveries of the catalysts for polyethylene and for polypropylene in 1963. Subsequently, Flory received the Noble Prize in 1974 for understanding the physical chemistry of polymers. Polymer manufacturing and properties are a significant component of chemistry and materials engineering departments at every college.

```
                              ┌─────────────────────┐
                         ┌───▶│ Polyethylene and    │
                         │    │ copolymers          │
                         │    └─────────────────────┘
          + chloride     │    ┌──────────────┐      ┌─────────────────────┐
              ┌──────────┴───▶│ Vinyl chloride│────▶│ Polyvinyl chloride  │
   ┌────────┐ │                └──────────────┘      └─────────────────────┘
   │Ethylene│─┤ + benzene      ┌──────────────┐      ┌─────────────────────┐
   └────────┘ ├──────────────▶│ Styrene       │────▶│ Polystyrene         │
              │                └──────────────┘      └─────────────────────┘
          + oxygen             ┌──────────────────┐  ┌─────────────────────┐
              └──────────────▶│ Ethylene oxide,   │─▶│ Polyethylene and    │
                               │ ethylene glycol   │  │ polyesters          │
                               └──────────────────┘  └─────────────────────┘
```

```
                              ┌─────────────────────┐
                         ┌───▶│ Polypropylene       │
                         │    └─────────────────────┘
          + ammonia      │    ┌──────────────┐      ┌─────────────────────┐
              ┌──────────┴───▶│ Acrylonitrile │────▶│ Acrylic fiber, plastic│
   ┌─────────┐│                └──────────────┘      │ and rubber          │
   │By-product││ + oxygen                             └─────────────────────┘
   │propylene │┤                ┌──────────────┐      ┌─────────────────────┐
   └─────────┘│ + benzene      │ Propylene oxide│────▶│ Urethane foams      │
              ├──────────────▶ └──────────────┘      └─────────────────────┘
              │                ┌──────────────────┐  ┌─────────────────────┐
              └──────────────▶│ Cumene, then      │─▶│ Phenolic resins     │
                               │ phenol and acetone│  └─────────────────────┘
                               └──────────────────┘
                          + HCN │ methanol
                               ┌──────────────┐      ┌─────────────────────┐
                               │ Methacrylates │────▶│ Poly (methyl        │
                               └──────────────┘      │ methacrylate)       │
                                                      └─────────────────────┘
```

```
                              ┌─────────────────────┐
                         ┌───▶│ Polybutadiene       │
                         │    └─────────────────────┘
          + styrene      │    ┌──────────────┐      ┌─────────────────────┐
              ┌──────────┴───▶│ SBR rubber    │      
   ┌─────────┐│                └──────────────┘      
   │By-product││ + chloride                           
   │butadiene │┤                ┌──────────────┐      ┌─────────────────────┐
   └─────────┘│                │ Chloroprene   │────▶│ Neoprene rubber     │
              │ + ammonia      └──────────────┘      └─────────────────────┘
              └──────────────▶┌──────────────────┐  ┌─────────────────────┐
                               │ Hexamethylene     │─▶│ Nylon 66            │
                               │ diamine           │  └─────────────────────┘
                               └──────────────────┘
```

Figure 1.2 Major polymeric products derived from ethylene and its by-products, after Rodriguez [6]. The major polymers used in geosynthetics manufacturing are shaded.

The word *polymer* comes from the Greek *poly* meaning "many" and *meros* meaning "parts." Thus a polymeric material consists of many parts joined together to make the whole. Each part, or unit, is called a *monomer*, the molecular compound used to produce the polymer. It should be recognized that the monomers and the repeating molecular units are different. This is due to the polymerization process. The functionality

Figure 1.3 Polyethylene production facility.

(i.e., the number of sites at which a monomeric molecule can link with other monomer molecules) determines the type and length of the chain.

The molecular weight of a polymer is the degree of polymerization (i.e., the number of times a repeating unit occurs) multiplied by the molecular weight of the repeating unit. The average molecular weight and its statistical distribution are very important in the resulting behavior of the polymer, since increasing *average molecular weight* has several results: increased textile strength, increased elongation, increased impact strength, increased stress crack resistance, increased heat resistance, decreased flow behavior, and decreased processability. Narrowing the *molecular weight distribution* also has several results: increased impact strength, decreased stress crack resistance, decreased flow behavior, and decreased processability.

While most of the polymers used in the manufacture of geosynthetics are from one type of monomer, thus called *homopolymers*, there are other possibilities. A polymer made from two repeating units in its chain is called a *copolymer*. It is important to note here the manner of linking or joining the repeating units, which can be random, alternating, block, or branch (graft).

Such copolymerization greatly expands the structural properties of the resulting polymer. Furthermore, it is possible to have three repeating units in the chain in what is called a *terpolymer*. It is easy to see that the options are essentially limitless, which explains why there are approximately 50,000 commercialized polymers in existence.

As previously mentioned, there are only a few polymers that make up the majority of geosynthetic materials. Table 1.2 presents the repeating molecular units of polymers used in manufacture of geosynthetics. Among the groups shown, polyethylene and polypropylene are the most common and are collectively called *polyolefins*.

Bonding between polymer molecules and their chains is critically important in understanding their behavior and performance. A number of excellent references are available for in-depth study [6–9]; however, Moore and Kline [10] is particularly well suited for an introduction to the subject. The bonds between polymer molecules are van der Waals forces, permanent dipoles, or hydrogen bonds. Between molecular chains, however, the bonds are usually much weaker and often must be supplemented by some form of cross-linking by means of covalent bonds or covalent bonding systems. Cross-links can be formed

- by the use of monomers having a functionality greater than two,
- by the use of chemical agents (sometimes called *curing*), and
- by the use of nuclear radiation methods.

Cross-linking is an important conceptual consideration because it separates the two major types of polymeric materials—i.e., thermoplastic and thermoset. A *thermoplastic polymer* can be repeatedly heated to its softening point, shaped or worked as desired, and then cooled to preserve that remolded shape; the polymer structure remains essentially unaltered. In a *thermoset polymer* the process cannot be repeated. Any additional heat after first forming will lead only to charring and degradation of the material. The key to this behavior in thermoset materials is, of course, cross-linking, which does not exist to such a degree in thermoplastic materials. Examples of thermoplastic materials are polyethylene (PE), polypropylene (PP), polyvinyl chloride (PVC), and polyester (PET); examples of thermoset materials are nytrile, butyl, and ethylene propylene diene terpolymer (EPDM). As mentioned previously, however, geosynthetics consist almost entirely of thermoplastic materials. With the exception of EPDM geomembranes, there are essentially no thermoset materials currently used in geosynthetic applications.

Crystallinity can indeed exist in polymeric materials but does so to widely varying degrees. In a rather difficult to visualize manner, the aligned portions of the polymer chain(s) in small regions are called "crystallites." The nonaligned regions are called *amorphous*. The crystallinity patterns are very complex and are still being researched. For example, the aligned molecular chain can loop back on itself in a series of folds called *spherulites* and can form exotic configurations such as "snowflakes" and "shish kebabs." The amount of crystallinity gives rise to a further polymer classification of semicrystalline or noncrystalline, hence amorphous. (No polymer is completely crystalline.) Thus the three major classifications of polymers that can be used for geosynthetic materials are (1) semicrystalline thermoplastic, (2) amorphous thermoplastic,

TABLE 1.2 REPEATING MOLECULAR UNITS OF POLYMERS USED IN THE MANUFACTURE OF GEOSYNTHETICS

Polymer	Repeating Unit	Types of Geosynthetics
Polyethylene (PE)		Geotextiles, geomembranes, geogrids, geopipe, geonets, geocomposites
Polypropylene (PP)		Geotextiles, geomembranes, geogrids, geocomposites
Polyvinyl chloride (PVC)		Geomembranes, geocomposites, geopipe
Polyester (polyethylene terephthalate) (PET)		Geotextiles, geogrids
Polyamide (PA) (nylon 6/6)		Geotextiles, geocomposites, geogrids
Polystyrene (PS)		Geocomposites, geofoam

and (3) thermoset; the latter is rarely used for geosynthetics, and essentially all of the polymers used in the manufacture of geosynthetics are of the first two varieties.

The amount of crystallinity varies from nil to 30% in some polyvinyl chlorides (PVCs), to as high as 65% in high-density polyethylene (HDPE). Crystallinity is significant, and in some instances critical, in the behavior of polymeric geosynthetics. It can be shown that increasing crystallinity results in the following: increased stiffness or hardness, increased heat resistance, increased tensile strength, increased modulus, increased chemical resistance, decreased diffusive permeability (or vapor transmission), decreased elongation or strain at failure, decreased flexibility, decreased impact strength, and decreased stress crack resistance.

Finally, in this brief section on polymer chemistry, there are two fundamental temperatures that are important to keep in mind: (1) the glass transition temperature, T_g, and (2) the melting temperature, T_m. These values are given in Table 1.3 for the common polymers that are made into geosynthetics. Although the melting temperature is intuitive, the glass transition temperature is not. In a physical sense, T_g is the temperature below which the polymer is glassy, hence rigid and essentially brittle. Above the T_g temperature, the polymer is rubbery, hence flexible and essentially fluid-like. The implications with respect to mechanical properties such as creep and stress relaxation are important in this regard.

1.2.2 Polymer Identification

There are a number of possible ways to identify the specific polymer from which a material (in our case, a geosynthetic) has been made. Table 1.4 gives an indication of polymer type on the basis of its burning characteristics.

It must be recognized, however, that the burning tests described in Table 1.4 are very subjective. For a significantly more accurate identification of the particular type of synthetic polymer, there are a number of *chemical analysis tests*. Such tests are finding a place in geosynthetic materials analysis for the following reasons:

- They are used in quality assurance and product certification.
- They are used to evaluate the estimated lifetime of field-retrieval samples.
- They are used in laboratory investigations into material degradation and subsequent lifetime prediction.

TABLE 1.3 TRANSITION TEMPERATURES FOR SELECTED POLYMERS

Monomer unit	Glass Transition Temperature (T_g, °C)	Melting Temperature (T_m, °C)
Ethylene (linear)	−125	141
Propylene (isotactic)	−7	187
Styrene (isotactic)	100	240
Vinyl chloride (syndiotactic)	81–98	273
Vinyl alcohol	85	265
Ethylene terephthalate	60–85	280
Nylon 66	50	280

TABLE 1.4   BURNING CHARACTERISTICS OF POLYMERIC MATERIALS USED IN GEOSYNTHETICS

Polymer Type*	Behavior Beginning, During, and After Burning
Polyethylene (HDPE and LLDPE)	Before touching the flame, the material melts, shrinks, and curls. Burns readily and is not self-extinguishing. Burns rapidly when moved away from the flame. Becomes clear when molten and tends to drip. When the flame is extinguished, smells of molten wax. Ash is soft and same color as material.
Polypropylene (PP)	Before touching the flame, the material shrinks, melts, and curls. Burns in a manner similar to polyethylene and is not self-extinguishing. Burns slowly when moved away from the flame. Burns with no clear blue color at the base of the flame, except with carbon black. Faint odor of burning asphalt is given off. Ash is hard and light tan.
Polyvinyl chloride (PVC), unplasticized	Burns with difficulty and is self-extinguishing. Flame is yellow, green at the bottom edges, with spurts of green and yellow. White smoke is given off. The material softens on ignition and has an unpleasant acidic smell.
Polyvinyl chloride (PVC), plasticized	Flammability behavior depends on amount of plasticizer present; most plasticizers burn readily with a yellow, smoky flame. Black smoke is given off. Odors are mostly floral (esterlike) but with an unpleasant acidic smell.
Polyester (PET)	Burns slowly with a yellow smoky flame. Floral (ester) odor. Flame jitters and dances. Molten material drips.
Polyamide (PA)	Difficult to ignite and is self-extinguishing. Slight green flame occurs due to chlorine. Flame is blue with a yellow top. Material froths on ignition. Odor is of burning wool or hair.
Polystyrene (PS)	Burns readily and is not self-extinguishing. Flame is orange-yellow, and black dense smoke containing soot is given off. Flame jitters and dances somewhat. On ignition, material softens and odor is characteristic of benzene.
Chlorosulphonated polyethylene (CSPE) (Hypalon)	Difficult to ignite. White smoke while in flame. Black smoke while burning. Slight green flame. Self-extinguishing. No drops. Wax odor.
Most thermosets, such as ethylene propylene diene terpolymer (EPDM)	Rapid burning, very intense. No drops. Chars at edges. Orange flame with black smoke. Char is tacky.

*To conduct final check on a chlorine-containing polymer: Heat copper wire in a flame and press the heated wire into the sample; then slowly put the wire back into the flame. A green flame indicates a chlorine-containing polymer.

- They are valuable in the forensic analysis of field failures.
- They are used for research and development into new additive packages (stabilizers, antioxidants, plasticizers, and additives).
- They are used for new geosynthetic product development and application investigations.

A brief description of the most frequently used chemical analysis tests as applied to the polymers used in the manufacture of geosynthetics follows; see Halse et al. [11] for additional insight into these methods.

Thermogravimetric Analysis (TGA).   Thermogravimetric analysis (TGA) is one of a series of thermal methods in which a property of the polymer is tracked as a function of a controlled temperature program (see Thomas and Verschoor [12] for a review). TGA follows mass change as a function of temperature. Continuous weighing of the decreasing mass of a specimen that is being subjected to a constantly increasing temperature produces curves such as those shown in Figure 1.4. The pronounced decreases in weight at specific temperatures signify vaporization of specific components. For example, the plasticizer in the PVC is removed at about 300°C, while the resin is removed between 450°C and 500°C. What remains beyond 500°C is carbon black and ash, since the tests were performed in a nitrogen atmosphere. The weight percentage of each component is computer obtained, since the device automatically normalizes the vertical axis.
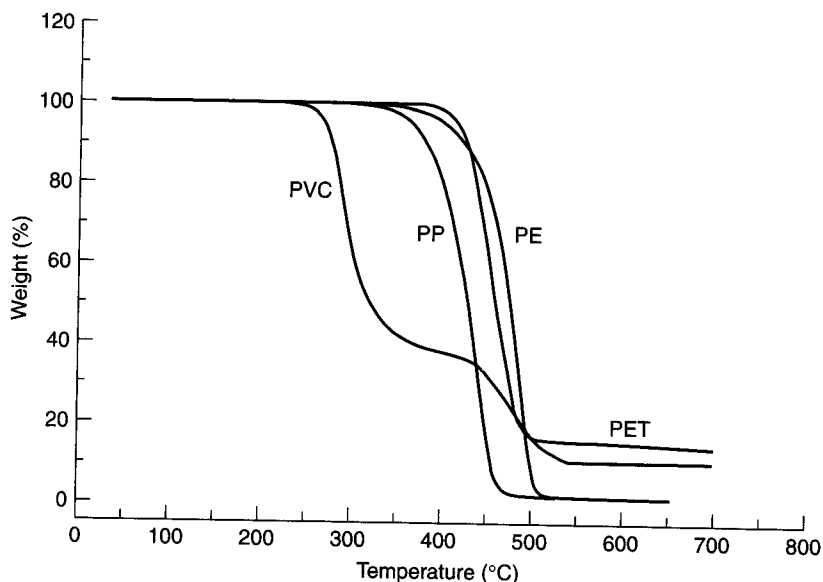
Figure 1.4   Thermogravimetric analysis curves of some common geosynthetic polymers. (After Thomas and Veschoor [12])

The technique can also be used to determine kinetic information concerning the stability of the polymer and the energy of activation for thermal decomposition. This latter piece of information can be used in an Arrhenius plot to predict in-service lifetime at a specific temperature.

Differential Scanning Calorimetry (DSC). Using a differential scanning calorimeter (DSC) a temperature balance between a reference cell and a test specimen cell can be maintained and the heat flow into and out of a specimen can be monitored and plotted as a function of temperature. Figure 1.5 shows such a response for polyester [12]. The glass transition temperature is at 80.36°C, the exothermic crystallization of the polymer backbone is at 164.20°C, and the endothermic melting of the crystallites is at 251.43°C. The area under the curve of the crystallization melt—that is, the value of 31.56 J/g—is proportional to the percent crystallinity of the polymer. Reference standards are used as a calibration for obtaining the actual percent crystallinity value. Lastly, the beginning of melting of the crystalline portion of the polymer at 236.43°C is important, as it relates to proper field seaming. This can be seen in the DSC curves of Figure 1.6 for different types of polyethylene [13]. Here the crystalline melting zone is clearly defined, and the higher the density of the PE, the higher the melting temperature and the narrower the temperature window over which melting takes place. In this regard it is inferred that HDPE can be a challenging material to properly seam.
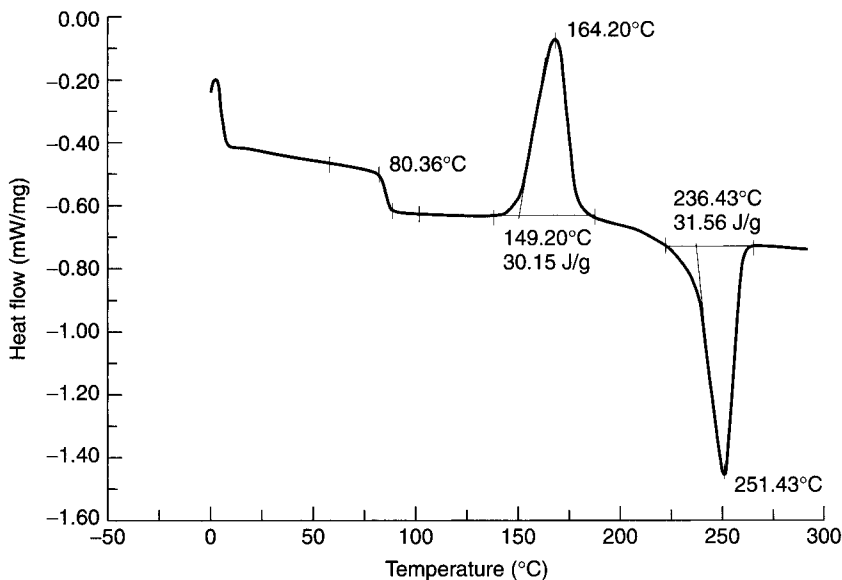
Figure 1.5 Differential scanning calorimeter curves for quenched polyester. (After Thomas and Verschoor [12])
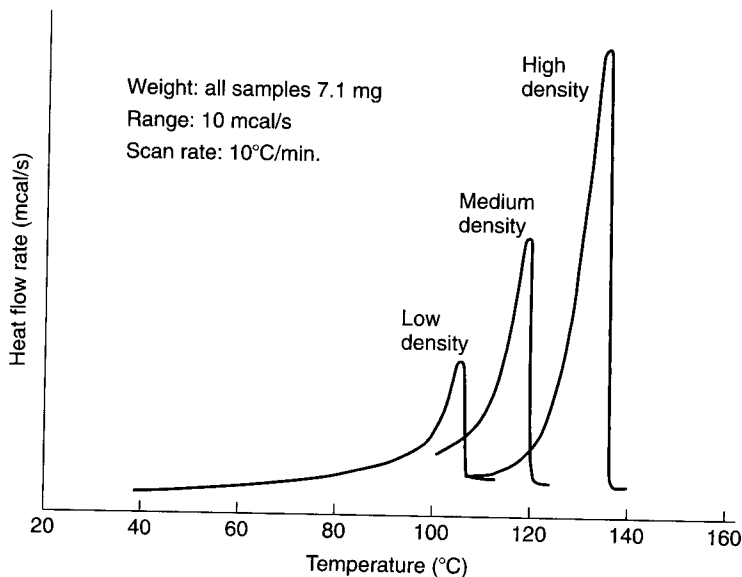
Figure 1.6   Differential scanning calorimeter curves for various densities of polyethylenes. (Compliments of Perkin-Elmer Instrument Co.)

The curves of Figure 1.6 are also instructive with respect to field welding of different polyethylenes. For example, LLDPE geomembranes are essentially impossible to weld to HDPE geopipe since the melting "windows" for the two materials do not overlap. The net result of such an attempt would be to either completely melt the LLDPE, or not sufficiently melt the HDPE.

Oxidative Induction Time (OIT).   The oxidative induction time (OIT) test uses a differential scanning calorimeter with a special testing cell capable of sustaining pressure. In the standard OIT (Std-OIT) test, per ASTM D3895, a 5 mg specimen is heated from room temperature to 200°C at a rate of 20°C/mm under a nitrogen atmosphere. Oxygen is then introduced and the test is terminated when an exothermal peak is reached (see Figure 1.7a) and the OIT time is readily obtained. This time is related to the quantity and type of antioxidants used in the polymer formulation. As seen in Figure 1.7(b), the OIT time is also related to laboratory incubation time of HDPE geomembrane samples in forced-air ovens at elevated temperatures [14]. Data such as this can be used to predict antioxidant depletion lifetime at in situ (and lower) temperatures.

The high pressure OIT (HP-OIT) test uses higher pressure and lower temperature than the standard test just described. It is designated ASTM D5885. Unless otherwise stated by the parties involved, the test is conducted at a pressure of 3.4 MPa and a temperature of 150°C. A response similar to Figure 1.7(a) is obtained. This test is felt to be more representative of the in situ behavior of low-temperature-functioning antioxidants insofar as prediction methods are concerned.
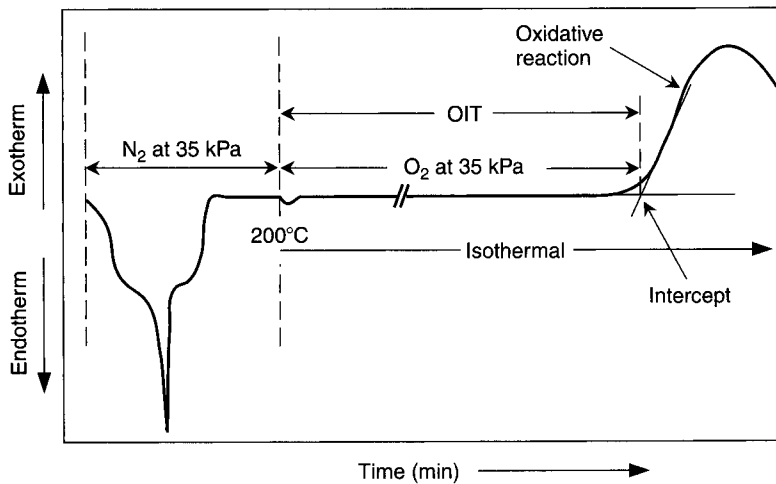
(a) Typical OIT response curve
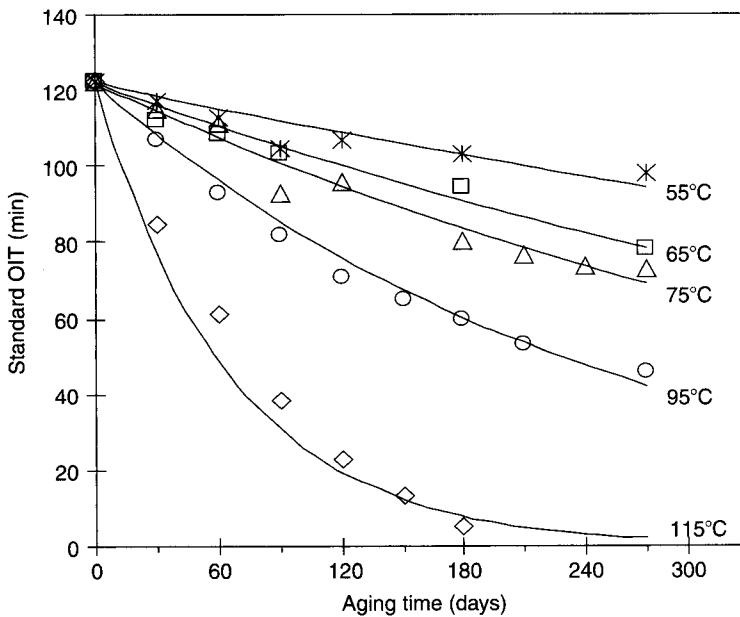
(b) OIT behavior of HDPE geomembrane

Figure 1.7   Oxidative induction time response and test behavior. (After Hsuan and Guan [14])

Still further, Li and Hsuan [15] have followed the oxidation of polyolefin geosynthetics by OIT procedures after incubation at extremely high pressures. The pressures, up to 6.3 MPa, provide for greatly reduced laboratory incubation times.

Thermomechanical Analysis (TMA). Thermomechanical analysis (TMA) measures a particular dimension of the polymer specimen under a controlled increase in temperature. A quartz probe rests on the test specimen, and its displacement is precisely measured as the temperature increases (or decreases). The modes of operation are expansion, penetration, or shear flow of the polymer. The most straightforward property to obtain using TMA is the coefficient of thermal expansion. It is simply the slope of the temperature-deformation curve. Figure 1.8 shows the results of such a test for PET, where the linear coefficient of thermal expansion is 76.4 μm/m°C for the initial (called the "glassy" state) stage and 132 μm/m°C for the final (or "rubbery" state) stage. The transition value between the two stages clearly defines the glass transition temperature, which is 80.55°C.

Dynamic Mechanical Analysis (DMA). Dynamic mechanical analysis (DMA) is a thermal technique that measures the mechanical response of a polymer as it is deformed under a periodic stress in a controlled temperature environment. Thus the viscoelastic properties can be evaluated. The test measures the dynamic storage modulus, E' (a measure of stiffness), the dynamic loss modulus, E'' (to measure glass transition and softening points), and the ratio of storage-to-loss moduli, which is called the damping, or "tan δ" value. Figure 1.9 gives the response of a HDPE geomembrane sample under the following conditions: fixed frequency of 1.0 Hz, heated at 4°C per minute, under 5.7 J of energy. The amplitude of the frequency is 0.20 mm (peak-to-peak).
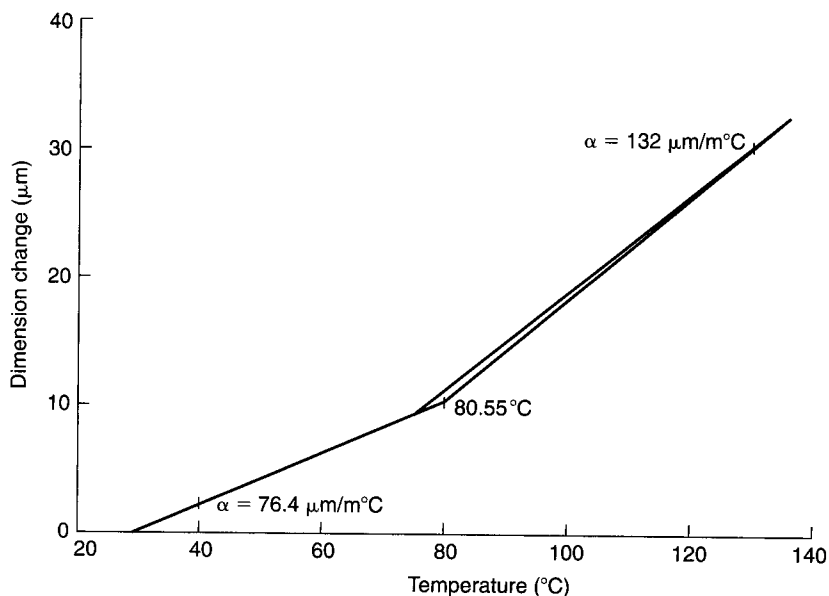
Figure 1.8   Thermomechanical analysis curves for PET under a temperature increase of 10°C/min. (After Thomas and Verschoor [12])
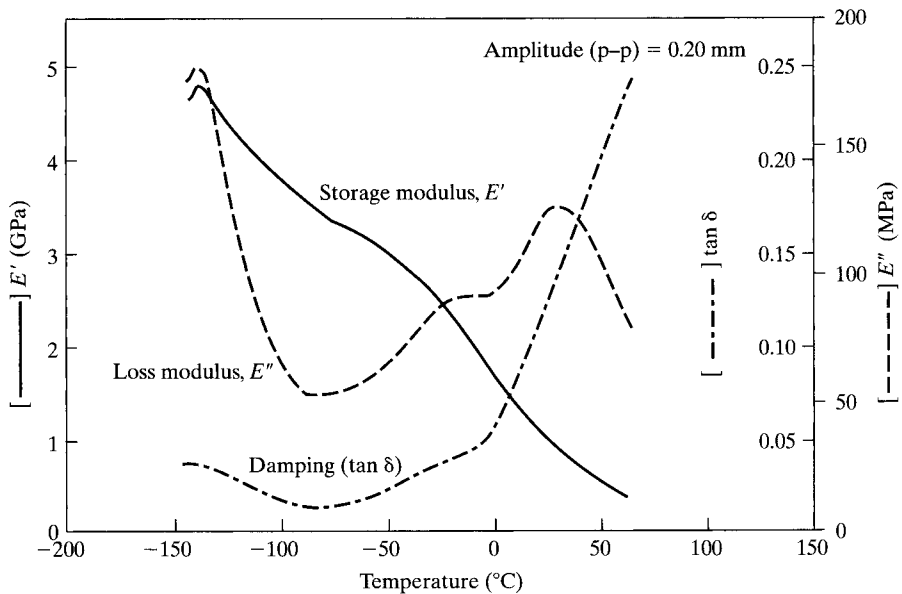
Figure 1.9   Dynamic mechanical analysis curves at fixed frequency for a HDPE geomembrane test specimen.

DMA devices are of additional interest in evaluating the viscoelastic engineering properties via either creep or stress relaxation test modes. Since DMA units are computer controlled, one can either preset the load and measure changing deformation (i.e., the creep mode) or preset the deformation and measure the sustaining force (i.e., the stress relaxation mode). By repeating the particular test at a series of increasing (or decreasing) temperature increments, a family of curves results. Additionally, a master curve can be generated using the time-temperature superposition principle for use in long-term studies and lifetime prediction.

Infrared Spectroscopy (IR).   The concept of infrared spectroscopy (IR), generally used as Fourier transform infrared spectroscopy (FTIR), is based upon the realization that the functional groups in molecules (such as the –CH– group in polyethylene) are always in motion. During an FTIR analysis, the polymer test specimen is subjected to radiation. The frequency of the incident radiation is in the infrared region. If the frequency matches a natural motion of the functional group, the polymer will absorb this energy and an absorption band will appear on the FTIR frequency sweep.

      Figure 1.10 shows the spectrum of a polyethylene specimen without compounding agents. Each peak in the spectrum represents the motion of a functional group either in bending or in stretching. For example, the strong peak at a frequency of 2850 cm^{-1} is the absorption peak due to C–H stretching motion. The area under the curve in this region is represented as I_{2850}.
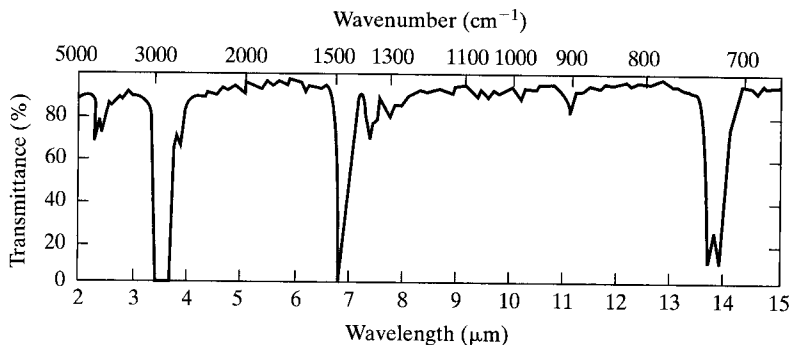
Figure 1.10   Infrared spectrum of a HDPE geomembrane test specimen. (After Halse et al. [11])

For a majority of polymers, carbonyl groups ($-C=O-$) would be produced after a certain amount of oxidation reaction (degradation) has occurred. The frequency corresponding to the motion of this molecular group is approximately 1715 cm^{-1}. (This frequency range does not appear in Figure 1.10 since it was a virgin nondegraded material). The area of the peak (I_{1715}) is proportional to the amount of carbonyl groups formed in the polymer. Hence it can be used to monitor the progress of oxidation. Often the results are normalized with another peak area taken from the polymer spectrum. For example, using polyethylene, the I_{1715} value would be normalized with the peak area at 2850 cm^{-1}—i.e., a ratio of I_{1715}/I_{2850} would be obtained. It is then defined as the *carbonyl index*.

Chromatography (GC, LC, and HPLC).   Chromatography is an analysis method that allows for the separation, isolation, and identification of complex mixtures. After a polymer specimen is liquefied in a solvent carrier, the components of the mixture are carried through a stationary column and the migration rates indicate fundamental differences. The soluble mobile phase either dissolves, absorbs or reacts with the stationary phase within the column.

In gas chromatography (GC) the mobile phase is a gas, which is passed through the column, and a detector produces a plot of concentration versus time. The position of the peaks serve to identify the components, and the area under the peaks the concentration. Plasticizers in PVC geomembranes have been identified by this method.

In liquid chromatography (LC) the mobile phase is liquid and the stationary phase is either liquid or solid. The separation process is very time-consuming, which has led to a technique known as high-pressure liquid chromatography (HPLC), which results in much-improved flow rates. Additives in various polymers have been identified and quantified by HPLC.

Molecular Weight Determination (GPC and MI).   There are four molecular weight averages in common use [9]: (1) the number-average molecular weight, M_n; (2)

the weight-average molecular weight, M_w; (3) the z-average molecular weight, M_z; and (4) the viscosity-average molecular weight, M_v. These are defined below in terms of the number of molecules, N_i, having molecular weights M_i; or the weight of species, w_i, with molecular weights M_i.

$$M_n = \frac{\Sigma_i N_i M_i}{\Sigma_i N_i} = \frac{\Sigma_i w_i}{\Sigma_i (w_i/M_i)} \tag{1.1}$$

$$M_w = \frac{\Sigma_i N_i M_i^2}{\Sigma_i N_i M_i} = \frac{\Sigma_i w_i M_i}{\Sigma_i w_i} \tag{1.2}$$

$$M_z = \frac{\Sigma_i N_i M_i^3}{\Sigma_i N_i M_i^2} = \frac{\Sigma_i w_i M_i^2}{\Sigma_i w_i M_i} \tag{1.3}$$

$$M_v = \left[\frac{\Sigma_i N_i M_i^{1+a}}{\Sigma_i N_i M_i} \right]^{1/a} \tag{1.4}$$

These values are seen on the molecular weight distribution curves of Figure 1.11, which is for a HDPE geomembrane. M_n is seen to be close to the mean value (approximately 50,000 for this material) while M_w is near the upper inflection point (approximately 170,000). M_z is an indicator of the upper end of the curve (above M_w) and M_v is a zone
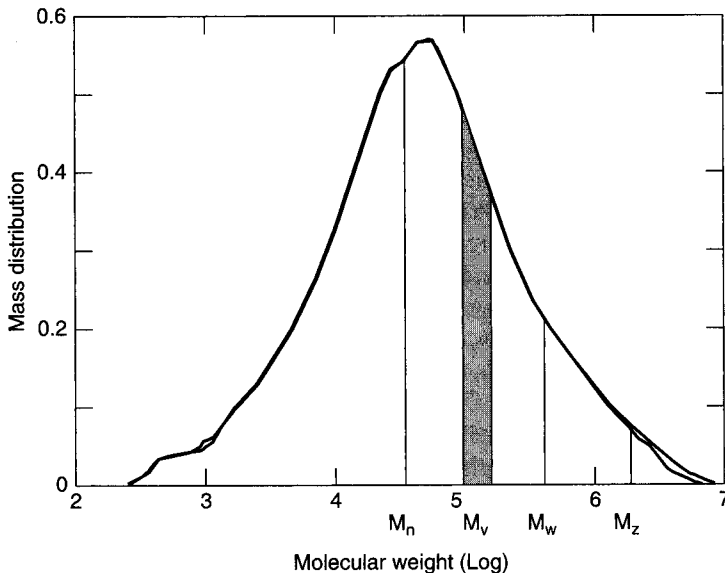
Figure 1.11 Gel permeation chromotography results of normalized molecular weight on HDPE geomembrane test specimens. There are two curves shown: one with one melt cycle, the other with two melt cycles. (After Struve [16])

varying between M_n and M_w. The curve (along with its various descriptors) is probably the most powerful indicator of any available method regarding the molecular structure of polymers and its subsequent degradation behavior. There are actually two curves lying almost on top of one another illustrating the noneffect of an additional heat cycle in degrading the molecular weight of the geomembrane [16].

To determine the entire distribution of molecular weight, gel permeation chromatography (GPC) is sometimes performed. This is essentially a process for the fractionation of polymers according to their molecular size and, therefore, according to their molecular weight. The molecular weight is determined indirectly by calibration of the system in terms of the elution time expected for a particular polymer molecular-weight fraction with a particular piece of equipment. The column packages are made with microporous glass beads and powdered, swelled, cross-linked polystyrene. It is a tedious test, requiring care and precision, but it is one that has had a dramatic effect on the procedures for polymer characterization and molecular weight determination [17].

It should be noted that a qualitative test to indirectly measure the molecular weight of a polymer is the *melt-flow index*. ASTM D1238 or ISO 01133 are commonly used for geosynthetics. In this test, the polymer is heated in a small oven attached to the device until it melts. A constant load is applied to the polymer melt and pushes the molten polymer from within the oven through an orifice. The weight extruded in 10 min. is defined as the melt index (MI) value. The lower the MI, other things being equal, the higher the molecular weight. By repeating the test at two different constant loads, the respective MI values can be made into a flow-rate ratio (FRR). High values of FRR, other things being equal, indicate broader molecular weight distributions.

These melt flow tests, particularly the melt index test, are routinely used by the industry for quality control, conformance, and quality assurance testing of the incoming resin and the final geosynthetic product. Melt index testing, along with density testing (which is simply the specimen's weight in air divided by its weight in water [ASTM D792 or ISO 1183], are considered by many to be the "workhorses" of all types of polymer manufacturing, including geosynthetics).

Intrinsic Viscosity Determination (IV).   The molecular weight of the polymer from which geosynthetics are made can also be indirectly determined using solution viscosity methods. The results are empirically related to the molecular weight in that higher viscosity values come about from higher molecular-weight resins, all other things being equal. The intrinsic viscosity value is particularly applicable to polyester (PET) resins, fibers, yarns, straps, and rods used in the manufacture of reinforcement geotextiles and geogrids.

According to ASTM D4603, the inherent viscosity is obtained using a 0.50% concentration of PET resin in a 60/40 phenol/1-2-3-3-tetrachloroethane solution. The flow time of the solution is measured in a capillary viscometer at 30°C. The pure solvent is also measured under the identical test conditions and the ratio of the two values is the relative viscosity, i.e.,

$$\eta_r = t/t_o \tag{1.5}$$

where

    η_r = relative viscosity
    t = average solution flow time (sec)
    t_o = average solvent flow time (sec)

This value can then be used to calculate a inherent viscosity, if desired.

$$\eta_{\text{inh}} = \frac{\ln \eta_r}{C} \tag{1.6}$$

where

    η_{inh} = inherent viscosity at 0.5% and 30°C
    C = polymer solution concentration, g/dL

Finally, the intrinsic viscosity is determined to be

$$[\eta] = \frac{0.25(\eta_r - 1 + 3 \ln \eta_r)}{C} \tag{1.7}$$

where
    $[\eta]$ = intrinsic viscosity

In its specification for PET geosynthetic reinforcement of walls and slopes, the Association of State Highway and Transportation Officials (AASHTO) requires that the minimum number average molecular weight (M_n) is 25,000 or higher. To obtain this value from intrinsic viscosity, the Mark-Honwock-Sakmada equation is used.

$$[\eta] = K M_n^a, or \tag{1.8}$$

$$M_n = \exp\left[\frac{[\eta]}{K}\right]^{1/a} \tag{1.9}$$

where K and a are constants for a particular solvent and temperature. For example, for a test performed at 35°C, K = 125 ml/g and a = 0.65.

    Carboxyl End Group Analysis (CEG).   An analysis of carboxyl end group for polyester (PET) resins, fibers, yarns, straps, and rods is an important indicator of the polymer's long-term durability. According to Pohl [18], a semimicroprocedure for the rapid determination of the number of carboxyl end groups of a polyester specimen entails dissolving the polymer in benzyl alcohol rapidly at a high temperature (e.g, at 200°C) then quickly mixing the solution with chloroform and titrating with sodium hydroxide and the aid of a phenol red indicator. The result of the procedure is expressed in equivalents per million grams. A maximum value of 30 is sometimes referenced for PET used in reinforcement geosynthetics (e.g., the AASHTO specifications).

Commentary on Chemical Fingerprinting.   The previously described series of chemical analyses are sometimes referred to as "chemical fingerprinting." However, fingerprinting is perhaps too descriptive a word, since no two products will give identical response curves to one another. Nevertheless, such response curves should be close enough to one another to substantiate their equivalency, or fundamental differences. In this sense perhaps "signature" would be a better descriptive term, but the term generally used is fingerprinting.

Taken collectively, the tests are very strong in their identification capability. Table 1.5 gives a summary of the advantages and disadvantages of each method. While this collection of tests may initially be felt by the engineering designer to be excessive and unwarranted, there are numerous instances where the typical physical and mechanical engineering tests (weight, strength, elongation, puncture, etc.) are simply not sensitive enough to evaluate the situation under study. The fallback position, which is invariably the use of these chemical analysis tests, will be used frequently. They have an ongoing importance in many facets of geosynthetic engineering; see Halse et al. [11] for specifics on most of the tests.

1.2.3 Polymer Formulations

No geosynthetic product is 100% of the polymer resin associated with its name. In all cases, the primary resin is mixed, or formulated, with antioxidants, screening agents, fillers, and/or other materials for a variety of purposes. The total amount of each additive in a given formulation varies widely—from a minimum of 1% to as much as 50%. The additives, either in particulate or liquid form, are used as ultraviolet (UV) light absorbers, antioxidants, thermal stabilizers, plasticizers, biocides, flame retardants, lubricants, colorants, foaming agents, or antistatic agents. The resulting mixture can be homogeneous or heterogeneous, depending upon the solubility parameters of the additives versus the primary resin polymer. Heterogeneous mixtures can also be particulate or fibrous [10].

Common particulate additives include carbon blacks; various antioxidants; calcium carbonate; metallic powders and flakes; silicate minerals such as clay, talc, and mica; silica minerals such as quartz, diatomaceous earth, and novaculite; metallic oxides such as alumina, biocides, and other synthetic polymers. Carbon blacks of different particle sizes are very common additives. This is due to polymers being relatively sensitive to ultraviolet degradation and the low cost of carbon black. Carbon black content is determined according to ASTM D1603 or ISO 6964. In addition to the amount of carbon black, its uniform dispersion in the final product is important. The test method for dispersion is ASTM D5596 or ISO 11420.

Common liquid additives include plasticizers, fillers, and colorants. Common fibrous additives (although rarely used in geosynthetic materials) include glass; carbon and graphite; cellulosics such as alpha cellulose; synthetic polymers such as nylon; metals such as steel fibers and strands; and boron.

The resulting formulation varies from product to product but can be generalized for the most common polymers used to manufacture geosynthetics, as shown in Table 1.6. Manufacturing of the particular product is addressed in many polymer and

TABLE 1.5 CHEMICAL FINGERPRINTING METHODS AND RELATED COMMENTS

Method	Information Obtained	Advantages*	Disadvantages
TGA	• Polymer, additives, and ash content • Carbon black amount • Decomposition temperatures	• Straightforward measurement • High accuracy • All polymers	• Qualitative results • High cost
DSC, Std-OIT and HP-OIT	• Melting point • Crystallinity • Oxidative induction time • Glass transition	• Straightforward measurement • High accuracy • All polymers	• Qualitative results • Limited to chlorinated polymers • High cost
TMA	• Coefficient of linear thermal expansion • Softening point • Glass transition	• Straightforward measurement • High accuracy • All polymers	• High cost
DMA	• Elastic constants • Loss modulus • Creep behavior • Stress relaxation behavior	• High accuracy • Versatile • All polymers • Temp. controlled	• High cost • High maintenance • Complex unit
IR	• Identifies additives • Identifies fillers • Identifies plasticizers • Rate of oxidation reaction	• All polymers	• Difficult specimen preparation • No resin information • High cost
GC, LC, and HPLC	• Identifies additives • Identifies plasticizers	• Straightforward measurement	• Difficult specimen preparation • No resin information • High cost
GPC	• Molecular weight distribution • Average molecular weight	• Accurate values • Only valid technique for molecular weight • All polymers	• Tedious test • Difficult specimen preparation • Uses strong solvents • Very high cost
MF and FRR	• Indication of molecular weight • Indication of molecular weight distribution	• Straightforward • Low cost • Used throughout industry	• None
Density	• Density	• Straightforward • Low cost • Used throughout the industry	• None
IV	• Intrinsic viscosity • Average molecular weight	• Straightforward measurement • Common test • Assesses susceptibility to hydrolysis	• Indirect measurements • Need correlations • Uses strong solvents
CEG	• Titration method • Carboxyl end group	• Assesses susceptibility to hydrolysis	• Tedious test • Uses strong solvents

*An advantage common to all methods is the extremely small specimen size required for testing in comparison to traditional physical and mechanical test specimen sizes.

TABLE 1.6   COMMONLY USED GEOSYNTHETIC POLYMERS AND THEIR APPROXIMATE WEIGHT
FORMULATIONS

Polymer Type	Resin	Filler	Carbon Black or Pigment	Additives	Plasticizer
Polyethylene (PE)	95–98	0	2–3	0.5–2.0	0
Polypropylene (PP)	85–96	0–13	2–3	1–2	0
Polyvinyl chloride (PVC) (unplasticized)	70–85	5–15	5–10	2–3	0
Polyvinyl chloride (PVC) (plasticized)	30–40	20–30	5–10	2–3	25–30
Polyester (PET)	96–98	0	2–3	0.5–1.0	0
Polyamide (PA) (nylon)	96–98	0	2–3	0.5–1.0	0
Polystyrene (PS)	96–98	0	2–3	0.5–1.0	0
Chlorosulphonated polyethylene (CSPE)	40–60	40–50	5–10	5–15	0
Ethylene propylene diene terpolymer (EPDM)	25–30	20–40	20–40	1–5	0

(Note: All values are percent on the basis of weight measurement)

materials engineering books, however, EPA/600/R-93/182 is focused specifically on
geosynthetic materials.

Thus, an understanding of a polymeric material insofar as its formulation is con-
cerned is a complex and formidable task, but it is a "doable" one. Unfortunately, it is
rarely given a high priority in engineering curricula, the obvious exception being in a
polymer (or materials) engineering program. Rarely (if at all) does a civil, mechanical,
or industrial engineer have any formal training in polymers, and even many chemical
engineering programs are quite lean in this area. Future college curricula must be more
attuned to the necessities of modern material systems, in which polymers play a key
and ever-expanding role.

1.3 OVERVIEW OF GEOTEXTILES

1.3.1 History

Geotextiles, as they are known and used today, were intended to be an alternative to
granular soil filters. Thus the original, and still sometimes used, term for geotextiles is
filter fabrics. Barrett [19], in his now classic 1966 paper, tells of work originating in the
late 1950s using geotextiles behind precast concrete seawalls, under precast concrete
erosion control blocks, beneath large stone riprap, and in other erosion control situa-
tions. He used different styles of woven monofilament fabrics, all characterized by a
relatively high percentage open area (varying from 6 to 30%). He discussed the need
for both adequate permeability and soil retention, along with adequate fabric strength
and proper elongation and set the tone for geotextile use in filtration situations. Note
should be made that an earlier paper by Agerschou [20] discussed applications along
the same general lines.

In the late 1960s Rhone-Poulenc Textiles in France began working with nonwoven needle punched fabrics for quite different applications. Here emphasis was on unpaved roads, beneath railroad ballast, within embankments and earth dams, and the like. The primary function in many of these applications was that of separation and/or reinforcement. Additionally, a distinctly different use of this particular style of fabric was also recognized—that is, that thick feltlike fabrics can also transmit water within the plane of their structure, acting as drains. Such uses as dissipation of pore-water pressures, and horizontal and vertical flow interceptors, grew out of this particular drainage function. Today's use of the word *geotextiles* recognizes these many possible functions of fabrics when used within a soil mass.

Credit for early work in the use of geotextiles should also be given to the Dutch and the English. ICI Fibres was a major influence in the use of nonwoven, heat bonded fabrics in a wide variety of uses. The first nonwovens used in the United States were imported in the late 1970s from ICI Fibres by Mirafi, Inc. Rankilor [21] describes this worldwide movement of geotextiles in the formative years. ICI Fibres provided early design-related literature that was very significant in proper use of geotextiles in a variety of applications. Chemie Linz (now Polyfelt) in Austria, Naue Fasertechnik in Germany, and du Pont and Mirafi in Europe and the United States (now BBA Nonwovens and TC Nicolon, respectively) were also early leaders in the technology. These firms and many others have continued to introduce geotextiles on a worldwide basis. Today many manufacturers are involved in the production, sales, and distribution of geotextiles.

A number of early conferences were held exclusively on the subject of geotextiles. More recently, the conferences have branched into the entire breadth of geosynthetics. They began in Paris in 1977 and have continued to be held every four years under the auspices of the International Geosynthetics Society (IGS) in locations around the world. The original two books on the subject— those of Koerner and Welsh [22] in 1980 and Rankilor [21] in 1981—appeared almost simultaneously. Today, additional books dealing with geotextiles along with thousands of separate papers and reports are available. In addition dedicated journals have been launched dealing with all types of geosynthetics [24, 25]. This massive generation and dissemination of information was led initially by geotextile manufacturers. Their influence in this market continues to be active, and indeed is very positive and welcome. It has been followed by the entire community of governmental, industrial, consulting, research, testing, and academic institutions.

Perhaps the culmination of this activity was the formation of the International Geosynthetics Society (IGS), which currently has 27 national and regional chapters. All are active with separate venues on a variety of geosynthetic-related topics and activities.

1.3.2 Manufacture

As noted, the role of the fabric manufacturer in the stimulation and growth of the geotextile market has been both large and positive. Many fiber types and fabric styles have been developed both for general use and for specific applications. In fact, it seems that

these two approaches to the marketing of geotextiles typify all geotextile manufacturers: manufacturers tend to target products either for the larger, customary (or commodity) market or for the smaller, specialized (or engineered) market. Whatever the case, three points are relevant insofar as manufacturing is concerned: (1) type of polymer, (2) type of fiber, and (3) fabric style. Each will be discussed separately in the sections that follow.

Type of Polymer.   The polymers used in the manufacture of geotextile fibers are made from the following polymeric materials, listed in order of decreasing use:

- Polypropylene ($\simeq$92%)
- Polyester ($\simeq$5%)
- Polyethylene ($\simeq$2%)
- Polyamide (nylon) ($\simeq$1%)

Their respective repeating units were given in Table 1.2; Table 1.7 presents some of their relevant properties. Note that moisture plays a relatively minor role in strength, that only polyolefins (polypropylene and polyethylene) are lighter than water, that polyester absorbs the least amount of water, and all polymeric materials have quite high melting points. While an extremely large database [27, 28] is available on these and other polymers, it is the final manufactured product that is of primary interest to the engineering designer and end user.

Type of Fiber.   There are five principal types of fibers used in the construction of geotextiles: (1) monofilament, (2) multifilament, (3) staple fiber yarn, (4) slit film monofilament, and (5) slit-film multifilament; see Figure 1.12. The properly formulated polymers are made into fibers (or yarns, where a yarn can consist of one or more fibers) by melting them and forcing them through a spinneret, similar in principle to a bathroom showerhead. The resulting fiber filaments are then hardened or solidified by one of three methods: (1) wet, (2) dry, or (3) melt. Most geotextile fibers are made by the melt process; these include polyolefins, polyester, and nylon. Here hardening is by cooling, and simultaneously or subsequently the fibers are stretched. Stretching reduces the fiber diameter and causes the molecules in the fibers to arrange themselves in an orderly fashion. When this happens, the fiber's strength increases, its elongation at failure decreases, and its modulus increases. A wide range of stress versus strain responses can be achieved. These monofilaments can also be twisted together to form a multifilament yarn. Note that the diameter of the fiber is characterized by its *denier*—the weight in grams of 9000 m of fiber or yarn. The related textile term, *tex*, is the weight in grams of 1000 m of yarn.

Staple fibers are different than those described above. They are produced by continuous filaments of specific denier gathered in a large ropelike bundle called a *tow*. A tow can contain thousands of continuous filaments, and it can be converted directly into yarn. More often, however, these filament bundles are then crimped and cut into short lengths of 25 to 100 mm. The short fibers, or *staple*, are then opened and subsequently twisted or spun into long yarns for eventual fabric manufacturing.

TABLE 1.7 SOME PHYSICAL PROPERTIES OF SYNTHETIC FIBERS (STANDARD LABORATORY CONDITIONS FOR FIBER TESTS: 20°C AND 65% RELATIVE HUMIDITY)

Fiber	Breaking Tenacity (g/denier)*		Specific Gravity	Standard Moisture Regain (%)	Coefficient of Thermal Expansion ($\times 10^{-5}$ per 1°C)	Effect of Heat
	Standard	Wet				
Polyethylene (high-density)	—	—	0.96	2.0	13	Melts at 110–140°C
Polypropylene (filament and staple)	4.8–7.0	4.8–7.0	0.91	3.0	6	Melts at 160–170°C
Polyester Regular-tenacity filament	4.0–5.0	4.0–5.0	1.22 or 1.38	0.4 or 0.8	4–5	Melts at 250–290°C
High-tenacity filament	6.3–9.5	6.2–9.4	1.22 or 1.38	0.4 or 0.8	4–5	Melts at 250–290°C
Regular-tenacity staple	2.5–5.0	2.5–5.0	1.22 or 1.38	0.4 or 0.8	4–5	Melts at 250–290°C
High-tenacity staple	5.0–6.5	5.0–6.4	1.22 or 1.38	0.4 or 0.8	4–5	Melts at 250–290°C
Nylon						
Nylon 66 (regular-tenacity filament)	3.0–6.0	2.6–5.4	1.14	4.0–4.5	5.5	Sticks at 230°C Melts at about 260°C
Nylon 66 (high-tenacity filament)	6.0–9.5	5.0–8.0	1.14	4.0–4.5	5.5	Same as above
Nylon 66 (staple)	3.5–7.2	3.2–6.5	1.14	4.0–4.5	5.5	Same as above
Nylon 6 (filament)	6.0–9.5	5.0–8.0	1.14	4.5	5.0	Melts at 210°C and 220°C
Nylon 6 (staple)	2.5	2.0	1.14	4.5	5.0	Melts at 160–220°C

Source: Modified from Shreve and Brink [26].

* Denier is equivalent to the grams per 9000 meters of the thread used to make synthetic fabrics. The higher the denier, the heavier the fabric.
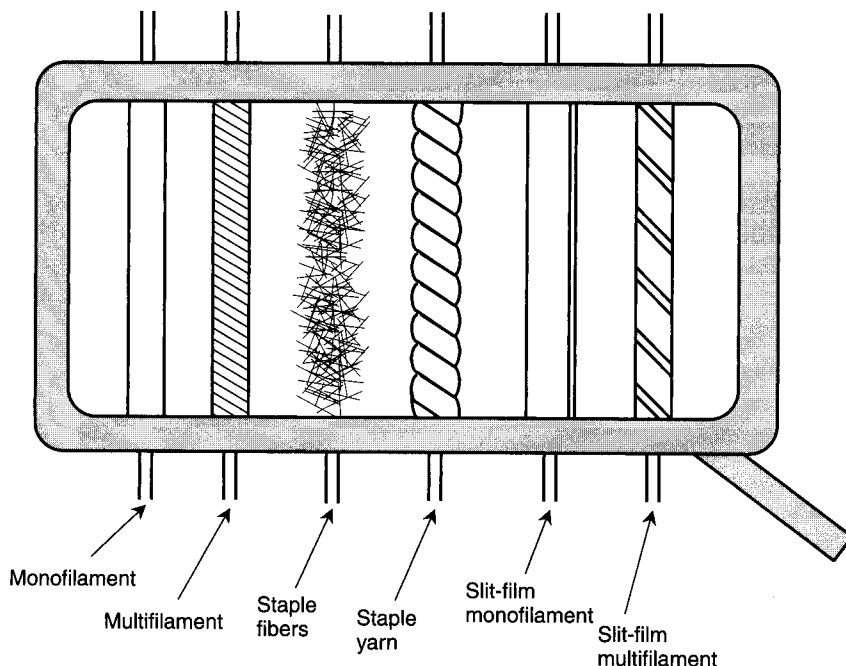
Figure 1.12   Types of polymeric fibers (or yarns) used in the manufacture of geotextiles.

The last type of fiber to be discussed here is made completely differently from those described above. These fibers, called slit (or split) film or tapes, are made from a continuous sheet of polymer that is cut into fibers by knives or lanced by air jets. The resulting ribbonlike fibers are referred to as *slit film monofilament fibers*. Obviously, these fibers can be twisted together to make a slit film multifilament.

Fabric Style.   Once the *yarns*, as they would be referred to in the textile industry, are made, they must be manufactured into fabrics. The basic manufacturing choices are woven, nonwoven, or knit, although knit fabrics are seldom used as geotextiles. Various woven and nonwoven types are shown in Figure 1.13. The woven fabrics are made on conventional textile weaving machinery into a wide variety of fabric weaves. Kaswell [27] gives an excellent review of weaving technology in which each of the various fabric weaves is clearly illustrated. Variations are many and most have direct influence on the physical, mechanical, and hydraulic properties of the fabric.

For conventional industrial fabrics (of which geotextiles form a subset), the weaves are usually kept relatively simple. The particular pattern of the weave is determined by the sequence in which the warp yarns are threaded into the weaving loom and the position of the warp harness for each filling pick (see Figure 1.14a). As shown in Figure 1.14b, reeds shed the warp yarns up, allowing a shuttle to insert the weft
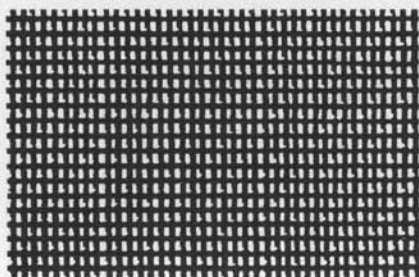
(a) Woven monofilament
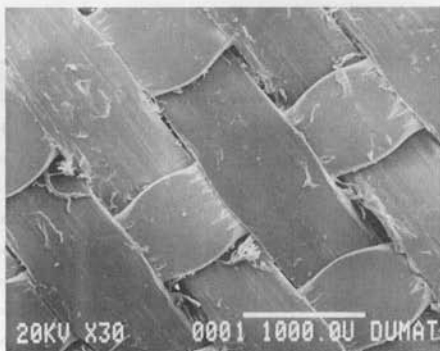
(b) Woven monofilament, calendered
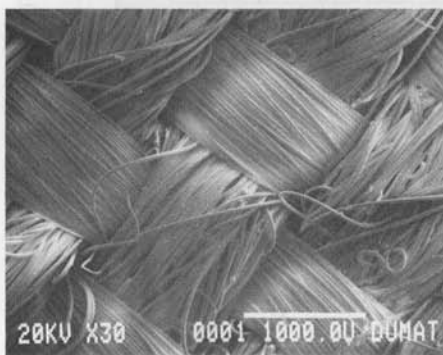
(c) Woven multifilament
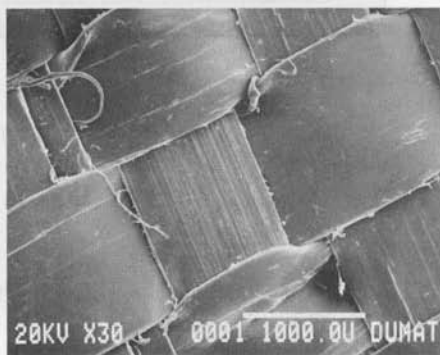
(d) Woven slit (split) film
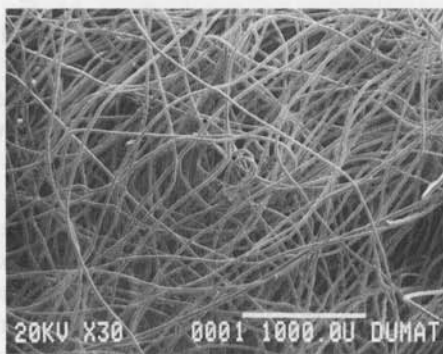
(e) Nonwoven needle punched
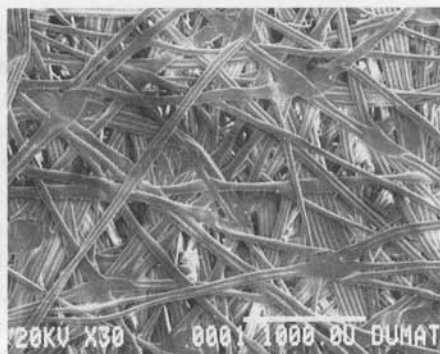
(f) Nonwoven heat bonded

Figure 1.13 Photomicrographs of various fabrics used as geotextiles. Magnification of (a) is ×5; all others are ×30.

(a) Main components and identification of terms

(b) Reed action for insertion of weft (or fill) yarn
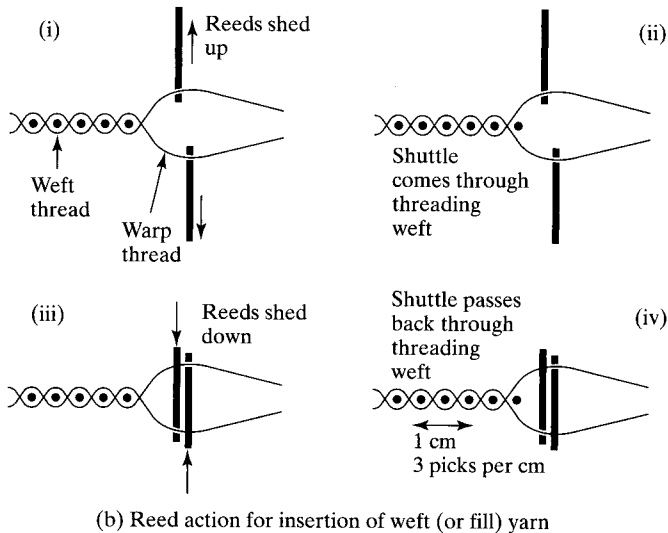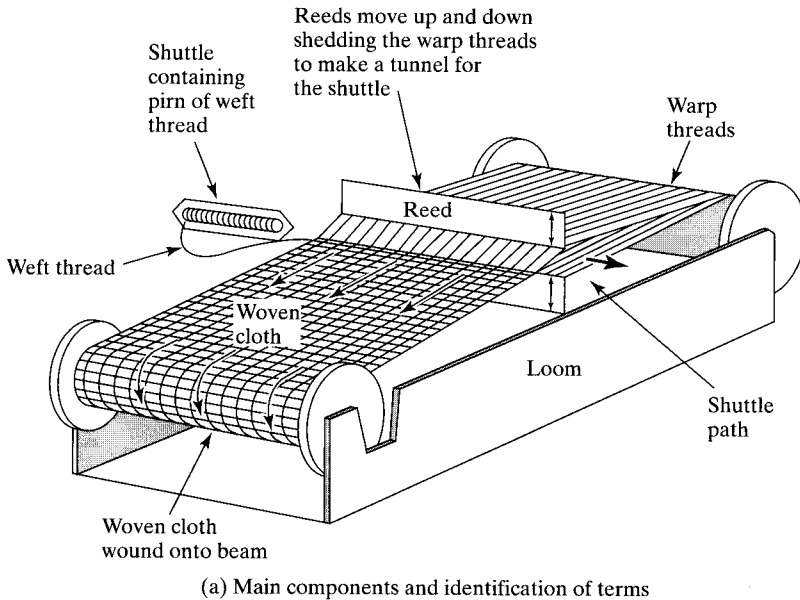
Figure 1.14   Basic functioning of a weaving loom. (After Rankilor [21])

yarn. The reeds then shed downward, encapsulating the weft yarn and allowing the return of the shuttle in the opposite direction with another weft yarn. The reeds then shed back upward and the process continues as a cycle. This action gives rise to nomenclature in woven fabrics of warp direction (the direction the fabric is being made, or

machine direction), weft or fill direction (the cross direction, or cross machine direction), and selvedge (edges of the fabric where the weft yarns reverse direction and gather the outer warp yarns on each side of the fabric). This action gives rise to the various types of weaves common to the formation of fabrics for use as geotextiles.

- *Plain weave*: The simplest and most common weave; also known as "one up and one down."
- *Basket weave*: A weave using two or more warp and/or filling yarns as one. For example, a "two-by-two basket weave" takes two warp and two weft yarns acting as individual units.
- *Twill weave*: A weave in which a diagonal or "twill" line moves across the fabric by moving yarn intersections one pick higher on successive warp yarns. Related patterns—e.g., steep twills, broken twills—can also be formed.
- *Satin weave*: A weave in which the warp (or weft) yarn is carried over many weft (or warp) yarns, resulting in a smooth and shiny fabric surface. It is generally not used for geotextile fabrics.

Additional details on the weaving process using both natural and synthetic fibers are found in Kaswell [27].

The manufacture of nonwoven fabrics is very different from that of woven fabrics. Each nonwoven manufacturing system generally includes four basic steps: (1) fiber preparation, (2) web formation, (3) web bonding, and (4) post-treatment. Within each category are many possibilities, so only those most common to current geotextiles will be described.

Of these four steps, fiber preparation has already been discussed. The process of *spun bonding* encompasses the remaining three steps in one operation. Spun bonding is a continuous process used to produce a finished fabric from a polymer. The polymer formulation is fed into an extruder. As the polymer melt flows from the extruder, it is forced through a spinneret or a series of spinnerets. The fibers are then stretched, usually by air, and after cooling are laid on a moving conveyor belt to form a continuous web. In the lay-down process, the desired orientation of the fibers is achieved by various means, such as rotation of the spinneret, electrical charges, introduction of controlled air-streams, or by varying the speed of the conveyor belt. Of course, a random orientation is possible and is very common. The mat of fabric is then bonded (i.e., the filaments are made to adhere to one another) by thermal, chemical, or mechanical treatment before being wound up into finished roll form (see Figure 1.15).

Alternatively, the web can be formed by starting the process with short, crimped fibers—i.e., with staple fibers—of 25 to 100 mm in length. The fibers are directly made or purchased by the geotextile manufacturer in the form of bales, which are opened by forced air in what is referred to as a "carding" process. The discrete fibers are then moved by conveyer in a lay-down process to form a web of desired width, orientation, and mass per unit area. The process has enormous flexibility, particularly in the choice of initial fiber selection. Once the loose web is formed, one of three processes are used to bond the filaments of the web together: (1) needle punching, (2) resin bonding, and (3) melt bonding.
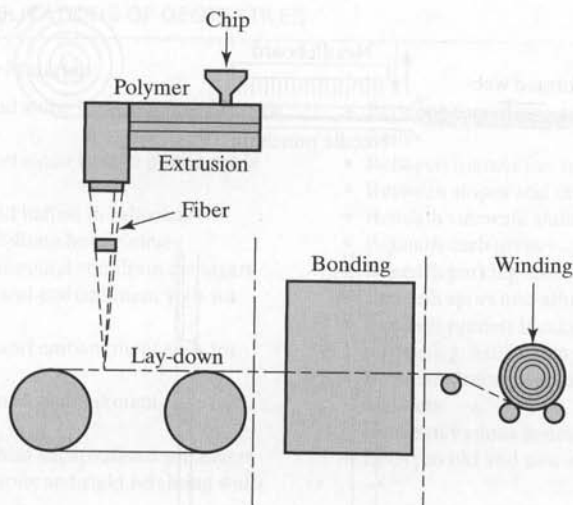
Figure 1.15 Diagram of the spun bonding process to manufacture geotextiles. Note that bonding can be by needle punching, heat bonding, or resin bonding. (Compliments of INDA)

In needle punching, the most common nonwoven geotextile bonding method, a fibrous web is introduced into a machine equipped with hundreds of specially designed needles. The needles are about 75 mm long and each have three or four downward-oriented barbs (see Figure 1.16). While the web is trapped between a bed plate and a stripper plate, the barbed needles punch through it and reorient the fibers so that mechanical bonding is achieved throughout the length and width of the fabric. It is generally on the downstroke where the entanglement process occurs. Often, the web or *batt* of laid-down fibers is carried into the needle punching section of the machine on a lightweight support material or substrate. This is done to improve finished fabric strength and integrity. The needle punching process is generally used to produce fabrics that have high mass per unit area yet retain considerable bulk. Fabric weights up to 750 g/m^2 can be made in a single pass and, if desired, such fabrics can be stacked and needled together, forming weights in excess of 2000 g/m^2. Of course, the thickness and related properties increase proportionately.

In the resin bonding process, a fibrous web is either sprayed or impregnated with an acrylic resin. After curing and/or calendering, bonds are formed between filaments. Often a forced air drying operation is used to reestablish the fabric's open-pore structure before the resin has hardened or cured.

In the melt bonding process (also called *heat bonding* or *heat setting*), the web, which is composed of continuous filaments or staple fibers, is melted together at filament or fiber crossover points. The resultant fabrics are rather stiff in texture and feel. Somewhat higher fabric strength can be achieved with this type of manufacture at lower fabric weights than for other fabric styles, owing to the fiber bonding utilized in
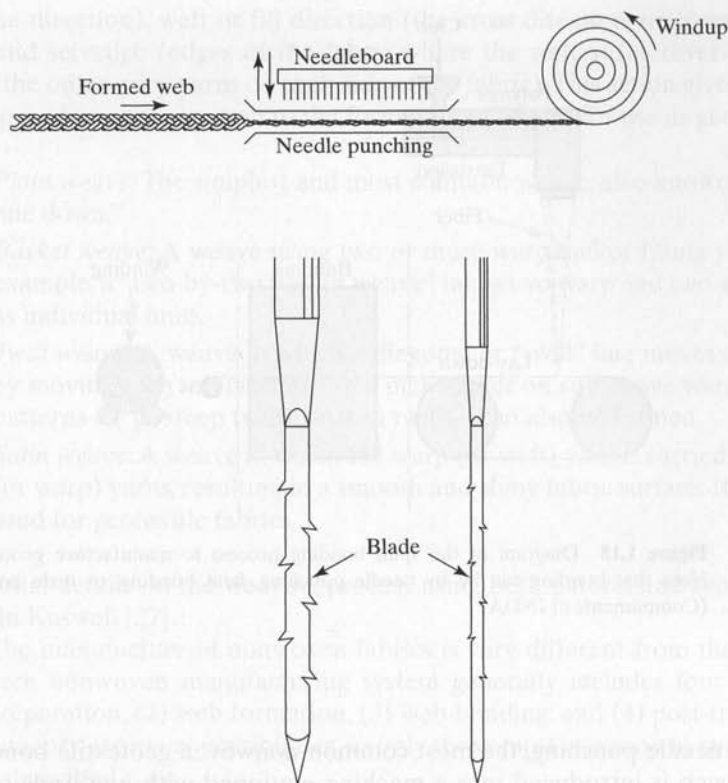
Figure 1.16 Diagram of needle punched process and details of typical needles. (Compliments of INDA)

the process. The bonding operations differ between the commercially available fabrics, depending on the basic fiber characteristics.

A major point to be emphasized is that the textile industry is a very mature and sophisticated one that can produce a tremendous variety of fabrics. Indeed, tailoring a fabric for a specific purpose or property is well within the state-of-the-practice.

1.3.3 Current Uses

Although Chapter 2 will deal with the applications of geotextiles more thoroughly, a few remarks can be made here. As already mentioned, the functions of geotextiles are separation, reinforcement, filtration, and drainage. Within these functions, however, there are a large number of use areas or applications, as shown in Table 1.8. Obviously this is not an all-inclusive list and it is constantly growing, but it does give an idea of the scope of the geotextile market.

TABLE 1.8   MAJOR APPLICATIONS OF GEOTEXTILES

Separation of Dissimilar Materials

- Between subgrade and stone base in unpaved roads and airfields
- Between subgrade and stone base in paved roads and airfields
- Between subgrade and ballast in railroads
- Between landfills and stone base courses
- Between geomembranes and soil drainage layers
- Between foundation and embankment soils for surcharge loads
- Between foundation and embankment soils for roadway fills
- Between foundation and embankment soils for earth and rock dams
- Between foundation and encapsulated soil layers
- Between foundation soils and rigid retaining walls
- Between foundation soils and flexible retaining walls
- Between foundation soils and storage piles
- Between slopes and downstream stability berms
- Beneath sidewalk slabs
- Beneath curb areas
- Beneath parking lots
- Beneath sport and athletic fields
- Beneath precast blocks and panels for aesthetic paving, e.g. hardscaping
- Between drainage layers in poorly graded filter blankets
- Between various zones in earth dams
- Between old and new asphalt layers

Reinforcement of Weak Soils and Other Materials

- Over soft soils for unpaved roads
- Over soft soils for airfields
- Over soft soils for railroads
- Over soft soils for landfills
- Over soft soils in sport and athletic fields
- Over karst and thermokarst areas
- Over unstable landfills as closure systems
- For lateral containment of railroad ballast
- To wrap soils in encapsulated fabric systems, e.g. geotextile tubes
- To construct fabric-reinforced walls
- To reinforce embankments
- To aid in construction of steep slopes
- To reinforce earth and rock dams
- To reinforce stacked gabions
- To reinforce stacked geofoam
- To stabilize slopes temporarily
- To halt or diminish creep in soil slopes
- To reinforce jointed flexible pavements
- As basal reinforcement over soft soils
- As basal reinforcement over karst areas
- As basal reinforcement over thermokarst areas
- As basal reinforcement between deep foundation caps
- To bridge over cracked or jointed rock
- To hold graded-stone filter mattresses
- As a substrate for articulated concrete blocks and block mattresses
- To stabilize unpaved storage yards and staging areas
- To anchor facing panels in reinforced earth walls
- To anchor concrete blocks in retaining walls
- To prevent puncture of geomembranes by subsoils
- To prevent puncture of geomembranes by landfill materials or stone base
- To create more stable side slopes due to high frictional resistance
- To contain soft soils in earth dam construction
- For use in membrane-encapsulated soils
- For use in in-situ compaction and consolidation of marginal soils
- To bridge over uneven landfills during closure of the site
- To aid in bearing capacity of shallow foundations

Filtration (Cross-Plane Flow)

- In place of granular soil filters
- Beneath stone base for unpaved roads and airfields
- Beneath stone base for paved roads and airfields
- Beneath ballast under railroads
- Around crushed stone surrounding underdrains
- Around crushed stone without underdrains (i.e., French drains)
- Around perforated underdrain pipe
- Around stone and perforated pipe in tile fields
- Beneath landfills that generate leachate
- To filter hydraulic fills
- As a silt fence
- As a silt curtain
- As a snow fence
- As a flexible form for containing sand, grout, or concrete in erosion control systems
- As a flexible form for reconstructing deteriorated piles

(continued)

TABLE 1.8 (*continued*)

- As a flexible form for restoring underground mine integrity
- As a flexible form for restoring scoured bridge pier bearing capacity
- To protect chimney drain material
- To protect drainage gallery material
- Between backfill soil and voids in retaining walls
- Between backfill soil and gabions
- Around molded cores in fin drains

- Around molded cores in wick, sheet and edge drains
- Against geonets to prevent soil intrusion
- Against geocomposites to prevent soil intrusion
- Around sand columns in sand drains
- Around porous tips for wells
- Around porous tips for piezometers
- As a filter beneath stone riprap
- As a filter beneath precast blocks

Drainage (In-Plane Flow)

- As a chimney drain in an earth dam
- As a drainage gallery in an earth dam
- As a drainage interceptor for horizontal flow
- As a drainage blanket beneath a surcharge fill
- As a drain behind a retaining wall
- As a drain at the base of a retaining wall
- As a drain beneath railroad ballast
- As a water drain beneath geomembranes
- As an gas drain beneath geomembranes

- As a drain beneath sport and athletic fields
- As a drain for roof gardens
- As a pore water dissipator in earth fills
- As a replacement for sand or wick drains
- As a capillary break in frost-sensitive areas
- As a capillary break for salt migration in arid areas
- To dissipate seepage water from exposed soil or rock surfaces

1.3.4 Sales

Between 1977 (the date of the first conference on geosynthetics) and 2000, geotextiles have experienced enormous growth. Actual sales by application area are given in Table 1.9. Estimated quantities in North America are approaching 500 million square meters. Although no data are now available, European sales quantities of geotextiles are thought to be about equivalent to North America. The remainder of the world has perhaps 50% of the sales of North America or Europe.

TABLE 1.9 UTILIZATION OF GEOTEXTILES IN NORTH AMERICA BY APPLICATION AREA

Applications	1987	1990	1992	1995	2000
Separation/stabilization	65	85	87	115	130
Reinforcement	12	16	18	25	35
Filtration/drainage	31	35	37	55	62
Protection for geomembranes	14	30	58	85	90
Erosion control	12	15	16	20	35
Silt fence	12	15	17	23	30
Asphalt overlays	75	88	88	77	60
Total market	221	284	321	400	442

*In millions of square meters.

Source: After Jagielski [29] and extended by the Geosynthetic Materials Association [30].

Within the above total, the distribution on the basis of end use is approximately as follows. Distribution of geotextiles from the manufacturer to the ultimate user is handled (1) from the mill directly, (2) by means of commissioned agents, and (3) through individual distributors. Generally, but certainly not always, direct-mill sales efforts are focused on unusually large jobs, where competition is very intense. Commissioned agents, who are often very well versed in geotextile applications, functions, properties, and design, work with professional engineers and consultants, and generally service the engineered job applications. Individual distributors service the standard applications and are often "wired-into" certain segments of the industry (e.g., specific road work or erosion control projects).

Sales of geotextiles, and to a similar extent the other geosynthetics, are strongly related to government spending and private sector development. Both are tied to the general economy and reflect slow and accelerating cycles. Growth also reflects educational outreach programs; the more activity there is in professional courses, seminars, conferences, and tutorials, the more vibrant will be sales and use of geotextiles and related geosynthetics.

1.4 OVERVIEW OF GEOGRIDS

1.4.1 History

The development of methods of preparing high-modulus polymer materials by tensile drawing [31], in a sense "cold working," raised the possibility that such materials could be used in the reinforcement of a soils for walls, steep slopes, roadway bases, and foundation soils. Thus, the major function of such geogrids is in the area of reinforcement. This area, as in many others, is very active, with a number of different products, materials, and connections making up today's geogrid market. The key feature of all geogrids is that the *apertures*—the openings between the adjacent longitudinal and transverse ribs—are large enough to allow for soil communication, or strike-through, from one side of the geogrid to the other. The ribs of geogrids are often quite stiff compared to the fibers of geotextiles. As will be discussed later, not only is rib strength important, but also is junction strength. The reason for this is that in certain situations the soil strike-through within the apertures bears against the transverse ribs, which transmits the load to the longitudinal ribs via the junctions. The junctions are, of course, where the longitudinal and transverse ribs meet and are connected. They are sometimes called *nodes*.

The original geogrids (which are categorized as unitized or homogeneous) were made in the United Kingdom by Netlon Ltd., and they were brought in 1982 to North America by the Tensar Corporation. A similar type of drawn geogrid, which originated in Italy by Tenax, is also available, as are products by new manufacturers in Asia. More flexible, textilelike geogrids using bundles of polypropylene-coated polyester fibers as the reinforcing component were developed by ICI in the United Kingdom around 1980. This led to the development of polyester yarn geogrids made on textile weaving machinery. In this process hundreds of continuous fibers are gathered together to form

yarns that are woven into longitudinal and transverse ribs with large open spaces between. The crossovers are joined by knitting or intertwining before the entire unit is protected by a subsequent coating. Geogrids within this group are manufactured by many companies having various trademarked products. There are possibly as many as 25 companies manufacturing coated yarn-type polyester geogrids on a worldwide basis. The third group of geogrids are made by laser or by ultrasonically bonding together polyester rods or straps in a gridlike pattern.

1.4.2 Manufacture

Each of the three different types of geogrids will be described. The polymers used to manufacture unitized or homogenous geogrids are HDPE for the unidirectional types and PP for the bidirectional types. The former is used in walls and slopes where the principal stress direction is known; the latter is used in base and foundation reinforcement where load orientation can be in all directions. The process begins with heavy gauge sheet of the appropriate polymer. Typical thicknesses are 4 to 6 mm. Holes are then punched into the sheeting on a regular pattern, and the sheet is then drawn uniaxially or biaxially (see Figure 1.17). Drawing is done under controlled temperatures and strain rates, so as to avoid fracture while allowing ductile flow of the molecular chains into an elongated condition. The key variable in the process is the draw ratio, but other variables, such as molecular weight, molecular weight distribution, and degree of branching or cross-linking, are also important [32, 33]. Aside from significant

Punched sheet

Unidirectional
geogrid

Bidirectional
geogrid
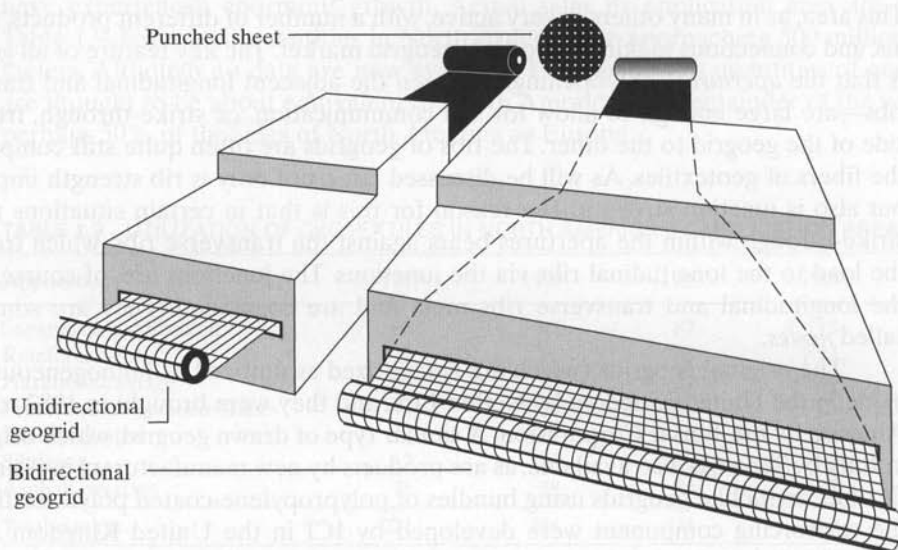
Figure 1.17 Method of manufacturing homogeneous, unitized geogrids. (After Netlon/Tensar [33])

increases in modulus and strength, the creep sensitivity of the elongated ribs is greatly reduced by the drawing process. The resulting geogrids are referred to as unitized or homogeneous geogrids and are relatively stiff with respect to the coated yarn types.

Coated yarn-type geogirds are made from high-tenacity polyester yarns, woven into an open structure with the junctions being knitted together or physically intertwined to link the transverse and longitudinal ribs. The entire geogrid is then coated with PVC, latex, or bitumen for dimensional stability and to provide protection for the ribs during soil backfilling [34]. Although PET yarns are by far the most widely used, fiberglass, nylon, and PVA yarns are also possible. The resulting geogrids are referred to as coated yarn types and are relatively flexible with respect to the others. They are available in the widest widths of the various classes of geogrids.

Polyester rod or strap geogrids are made from the same material used to package, bind, and ship various articles and materials. Parallel sets of straps approximately 10 mm wide are joined to perpendicular sets by laser or ultrasonic welding [35, 36]. Depending on the number and spacing of the rods or straps, these are the stiffest of all types and, depending on the rib spacing, can be the highest strength.

There are other types of prototype geogrids currently under development. Many are composite materials with intriguing junction assemblies, while some are continuous sheets of "super-tuff" polymeric materials with large holes punched in them. This activity in the geogrid area stems from the excellent anchorage and pullout resistance afforded when placed in a soil system. As will be seen in the design portion of Chapter 3, the reinforcement function can profit handsomely from this type of geosynthetic material.

1.4.3 Current Uses

The geogrids that result from the processes described are relatively high-strength, high-modulus, low-creep-sensitive polymers with apertures varying from 10 to 100 mm in size. These apertures are either elongated ellipses, near-squares with rounded corners, squares, or rectangles. Under some circumstances, separation may be a function, but only with very coarse gravels and large particle size materials. Invariably, geogrids are involved in the primary function of reinforcement. The following uses have been reported in the literature.

- Beneath or within aggregate in unpaved roads
- Beneath or within ballast in railroad construction
- Beneath or within surcharge fills or temporary construction sites
- As mechanically stabilized earth for a variety of wall facings
- As wraparound walls providing reinforcement and facing
- Reinforcement of embankment fills and earth dams
- Repairing slope failures and landslides
- As gabions for wall and bridge abutment construction
- As gabions for erosion control structures
- As basal reinforcement over soft soils
- As basal reinforcement over karst areas

- As basal reinforcement over thermokarst curves
- As basal reinforcement between pile and other deep foundation caps
- As lateral confinement to stone for constructing stone columns
- As a bridge over cracked or jointed rock
- To construct mattresses for fills over soft soils
- To construct mattresses over peat, tundra, and muskeg
- As sheet anchors for retaining-wall facing panels
- As sheet anchors and facing panels to form an entire retaining wall
- As asphalt reinforcement in pavements
- As cement or concrete reinforcement in a wide variety of applications
- To reinforce disjointed rock sections
- To reinforce disjointed concrete sections
- As composite forms with nonwoven geotextiles
- As inserts between geotextiles
- As inserts between geomembranes
- As inserts between a geotextile and a geomembrane
- To reinforce landfills to allow for vertical expansion
- To reinforce landfills to allow for lateral expansion
- To stabilize leachate collection stone as veneer reinforcement
- To stabilize landfill cover soil as veneer reinforcement
- As three-dimensional mattresses for landfill bearing capacity
- As three-dimensional mattresses for embankments over soft soils

1.4.4 Sales

In serving as a reinforcement material, geogrids compete directly against geotextiles in many of the above uses. Some of the manufacturers of geogrids also manufacture high-strength geotextiles. As such, sales are difficult to separate out for the different products. We estimate the global geogrid market to be approximately 100 million square meters. For example, a 1998 survey of walls reinforced by geosynthetics shows that over 90% of the geosynthetic reinforced walls built in North America have been reinforced by geogrids. The current area, called *segmental retaining walls* (SRWs), consists of dry-laid masonry blocks reinforced by geogrids, and it is the fastest growing application of geosynthetics, with the possible exception of polymer pipe.

1.5 OVERVIEW OF GEONETS

1.5.1 History

Geonets were originally developed by Bryan Mercer of Netlon Ltd. in the United Kingdom. Mercer patented the machinery and processing methods for the lightweight plastic nets commonly seen in supermarkets for carrying produce, fruits, and vegetables. Experimentation with gradually thicker ribs in various configurations led to drainage

nets of the type used in geosynthetic engineering. The first known use was in 1984 for the environmental application of leak detection in a double-lined hazardous liquid waste impoundment. Although geonets are indeed gridlike materials and were included in the geogrid chapter of the first edition of this book, current use dictates a separate identity. The reason for this separate treatment lies not in the material or its configuration but in its function. Geonets are used for their *in-plane drainage* capability, while geogrids (as just discussed) are used for *reinforcement*. It should be stated at the outset, however, that geonets are not weak, flimsy materials. They have reasonable tensile strength, but they are used exclusively in drainage applications. Note that geonets are generally used with a geotextile, geomembrane, or other material on their upper and lower surfaces to prevent soil intrusion into the apertures that would block the in-plane drainage function of the material. Hence, they are used as a composite and could equally as well as be included in the chapter on geocomposites, but they deserve mention in their own right. They can also be used by themselves—for example, when placed between two geomembranes.

1.5.2 Manufacture

Almost all geonets are made of polyethylene. The specific gravity of most geonets is in the range of 0.937 to 0.947, thus they are in the upper range of medium density or lower range of high density, depending on the classification system used. The division between medium- and high-density polyethylene established by the American Society for Testing and Materials (ASTM) is 0.940/0.941. The only additives in geonets are carbon black (1 to 2%) and a processing/antioxidant package (0.5 to 1.0%); thus the material is almost pure resin.

In the manufacture of *biplanar geonets*, the ingredients are mixed and forced through an extruder that ejects the melt into a die with slotted counter-rotating segments. This is called a "stenter" (see Figure 1.18). Here the polymer melt flows at angles forming discrete parallel ribs in two planes. As continuous pressure on the ejected material forces the semisolid mass forward, it is forced over a gradually increasing diameter core (or mandrel), which separates the ribs and opens the net. Thus diamond-shaped apertures are formed that are typically 12 mm long by 8 mm wide. The resulting angles between sets of ribs are on the order of 70 to 110 degrees, resulting in a diamond-shaped pattern. By the time the net has cooled completely, its full diameter is realized. The geonet is quenched in a water bath and cut along its manufactured axis and formed into rolls for shipment. Final widths have been increasing with the development of newer production facilities so as to produce geonets up to 4.5 m wide. Because of this formation process, the intersecting ribs generally are not perpendicular to one another but are at slight angles. This is an important consideration when it comes to normal load-carrying capability.

The geonets described above are typically 5.0 to 9.0 mm in thickness. Since thickness is a key factor in generating in-plane drainage capability, it seems logical to try to increase the above values. One way to do this is to add a foaming agent to the ingredients. The foaming agent reacts upon cooling to form microspheres in the solidified polymer. Although this has been done by a few manufacturers and results in nets up to 10 to 13 mm in thickness, foamed-rib geonets are seldom used currently.
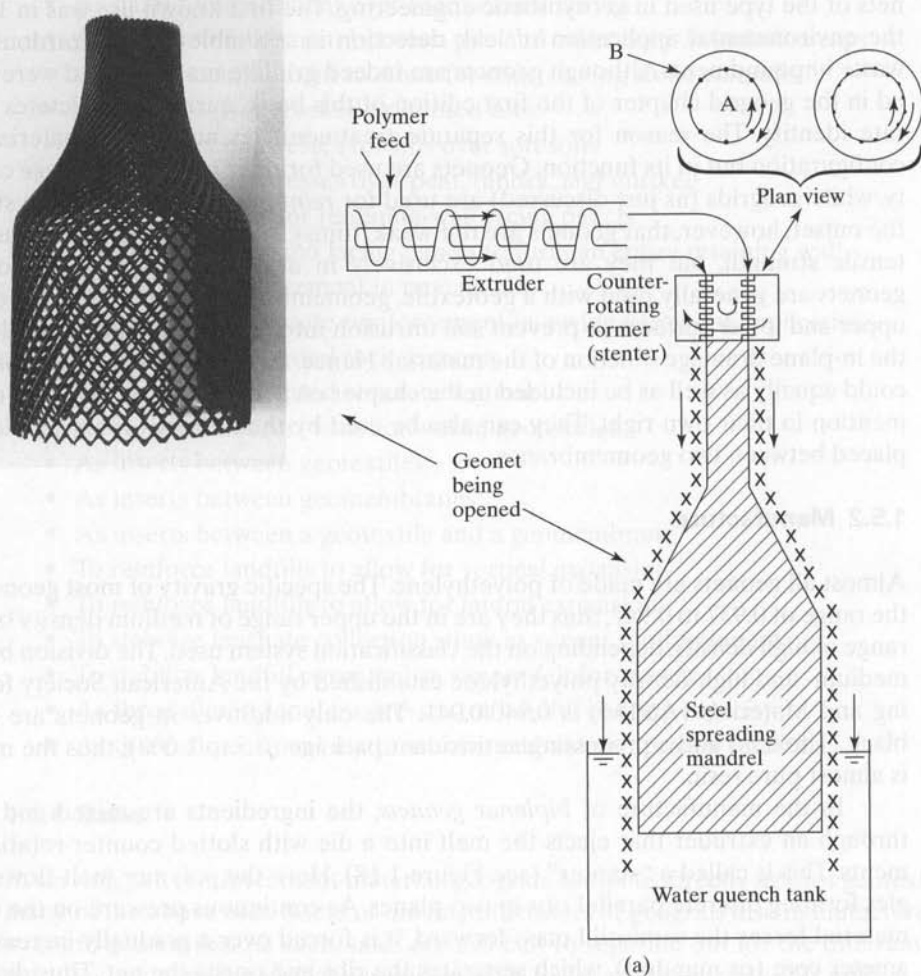
Figure 1.18 Diagram of geonet manufacturing process along with prototype shape as expanded over a steel spreading mandrel.

An alternative geonet is known as a *triplanar geonet* [37]. The die used to manufacture triplanar nets has three segments. The largest and central set of ribs are oriented in the principal flow or machine direction. Thus, field placement must be oriented hydraulic gradientwise in this direction. The upper and lower sets of ribs are smaller and closer together to maintain the structure of the central ribs and to minimize geotextile intrusion into the flow channels. The resulting triplanar geonets have flow rates considerably higher in their manufactured direction than the conventional diamond-shaped biplanar geonets. The cross-machine direction, however, has lower flow rates; hence these geonets are used on slopes where flow is unidirectional and known in its orientation.

A variety of prototype nets have also been formed by casting, injection molding, and other methods and can serve equally well, provided their mechanical and hydraulic properties are adequate. We can anticipate future geonets being quite different than the biplanar and triplanar types just described. Their cost/benefit ratio, however, will have to be comparable or better than those currently available [38].

1.5.3 Current Uses

As just described, geonets are used almost exclusively for their drainage capability. As such, they are single-function geosynthetics. The following uses have been documented in the literature:

- For water drainage behind retaining walls
- For water drainage of seeping rock slopes
- For water drainage of seeping soil slopes
- For water drainage behind geomembranes in dams and canals
- For water drainage beneath sport fields, golf courses, and other athletic facilities
- For water drainage of frost-susceptible soils
- For water drainage beneath building foundations
- For water drainage of plaza decks
- For water drainage beneath highways and airfields
- For leachate collection in landfills and waste piles
- For leachate collection in heap leach pads
- To detect leaks between double liners in landfills and surface impoundments
- As underdrain systems beneath landfills
- As surface water drains in landfills caps and closures
- To detect leaks between two geomembranes in vertical containment walls
- As drainage blankets beneath a surcharge fill

1.5.4 Sales

Geonets as drainage materials fall at an intermediate point in their flow capability between needle punched nonwoven geotextiles and thick-molded types of drainage geocomposites. These other types of drainage geocomposites will be described later. As such, geonets compete with each of these materials at each end of their use spectrum. Yet their use has increased dramatically, from virtually nil in 1984 to an estimated 50 million square meters in 2002, of which approximately 80% of the usage was in North America. Other types of drainage materials are more common elsewhere and

these materials will be covered in Section 1.10 and in Chapter 9. They are indeed viable geosynthetic materials in their own right.

1.6 OVERVIEW OF GEOMEMBRANES

1.6.1 History

In 1839, Charles Goodyear used vulcanization to cure natural rubber with sulfur, resulting in a synthetic rubber that is the current classification of *thermoset polymers*. The impetus was the inherent instability of natural (gum) rubber—i.e., it was brittle in cold weather and sticky in hot weather. Today, the production of various synthetic rubber materials is a major industry. The original geomembrane was a rubber product and was used as a water reservoir pond liner. It was butyl rubber, which is a copolymer of isobutylene with approximately 2% isoprene. Butyl rubber is quite impermeable and has its major use as inner tubes and as the liners of tubeless tires. Many other combinations and variants of rubber materials are possible—for example, nitrile and EPDM. Since the 1980s, however, the geosynthetics industry has shifted from thermoset polymers to *thermoplastic polymers*, the exception being EPDM geomembranes. Thus, almost all of the geomembrane materials we will discuss fall into the category of polymers classified as thermoplastic materials. By definition, these are materials that become soft and pliable when heated without any substantial change in inherent properties and when cooled revert back to their original properties. Thus they are readily seamed by heat, extrusion, or chemical methods.

Polyethylene is formed by the polymerization of compounds containing an unsaturated bond between two carbon atoms. Production in quantity began in 1943. Its main original uses were (and continue to be) in the packaging and molding industries. In its various densities, polyethylene is the most widely used polymer in the manufacturing of geomembranes. The development of crystallizing polypropylene is an outgrowth of low-pressure polymerization of ethylene and is the basic material from which many geosynthetics are made (recall Figure 1.2). Polyvinyl chloride is another member of this group commonly used to manufacture geopipe and, when plasticized, geomembranes. This resin was developed in 1939 and has extensive uses. It ranks second in use to the various density polyethylenes. It is interesting to note that polyethylene geomembranes were first used in Europe and South Africa and moved to North America, while polyvinyl chloride used for geomembranes had its roots in the United States and moved to Europe and elsewhere. Other types of geomembranes were being developed in the 1960s and were used by the U.S. Bureau of Reclamation. These geomembranes served primarily as canal liners, and their use spread to Canada, Russia, Taiwan, and Europe. Another early geomembrane, chlorosulfonated polyethylene (CSPE), resulting from the reaction of chlorine and sulfur chloride on polyethylene, was introduced for reservoir and landfill liners in the late 1960s. This geomembrane type was used in Europe shortly thereafter. Today's polymeric geomembranes are made from various thermoplastic resins and are manufactured and distributed throughout the world, making all types of products readily available. However, what

matters most to the owner/designer/specifier, and what is the focus of this book, is to use the proper material for the particular project. *That* is the essence of the design-by-function concept.

1.6.2 Manufacture

The manufacturing of geomembranes begins with the production of the raw materials, which include the polymer resin itself; various additives such as antioxidants, plasticizers, fillers, carbon black; and lubricants (as a processing aid). Recall Table 1.6, which gave the approximate amounts of different materials used to make geosynthetic materials. These raw materials are then processed into geomembrane sheets of various widths and thicknesses by one of the three ways shown in Figure 1.19: (1) extrusion, (2) calendering, and (3) spread coating.

High-density polyethylene (HDPE), linear low-density polyethylene (LLDPE), and flexible polypropylene (fPP) geomembranes are manufactured by an *extrusion* method. The polymer resin in pelletized form is mixed with a pelletized master batch that contains carbon black, stabilizers, and antioxidants in a carrier resin. The two pelletized material systems are carefully metered to result in the proper formulation and pneumatically loaded into the feed hopper of an extruder (see Figure 1.20). The extruder contains a heated rotating continuous flight screw. The formulation passes successively through a feed section, compression section, and metering section where it
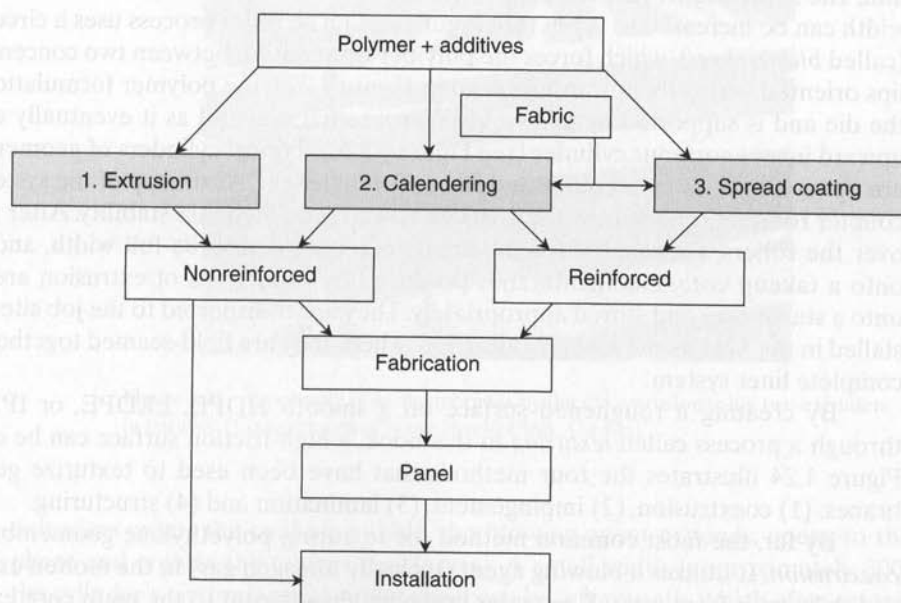
Figure 1.19 Three methods used to manufacture geomembranes. (After Haxo [39])
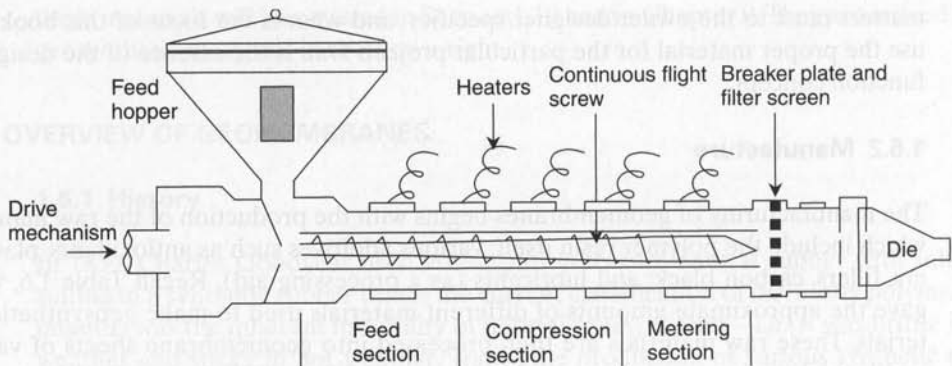
Figure 1.20   Cross-section diagram of a horizontal single-screw extruder for polymer processing.

finally emerges as a mixed and molten material that is passed through a breaker plate and filter screen and then fed directly into a die. Two variations of extrusion processing are then used to make geomembranes. One process uses a flat die (called *cast sheet*), which forces the polymer formulation between two horizontal die lips, in a coathanger-like manner, resulting in polymer sheet of closely controlled thickness from 0.75 to 3.0 mm. The sheet widths vary from 1.8 to 4.6 m. When two parallel extruders are used, the width can be increased to 9.5 m (see Figure 1.21). The other process uses a circular die (called *blown sheet*), which forces the polymer formulation between two concentric die lips oriented vertically upward. As seen in Figure 1.22a, the polymer formulation exits the die and is supported by a large circular internal mandrel as it eventually extends upward in an enormous cylinder (see Figure 1.22b). Typical cylinders of geomembrane are up to 10 m in circumference and 30 to 40 m in height. At the top of the system, two counter rotating rollers draw the cylinder upward and maintain stability. After passing over the rollers, the sheet is longitudinally cut, unfolded to its full width, and rolled onto a takeup core. Geomembranes produced by both types of extrusion are rolled onto a stable core and stored appropriately. They are transported to the job site and installed in the field as shown in Figure 1.23a, where they are field-seamed together into a complete liner system.

By creating a roughened surface on a smooth HDPE, LLDPE, or fPP sheet through a process called *texturing* in this book, a high-friction surface can be created. Figure 1.24 illustrates the four methods that have been used to texturize geomembranes: (1) coextrusion, (2) impingement, (3) lamination and (4) structuring.

By far, the most common method for texturing polyethylene geomembranes is *coextrusion*. It utilizes a blowing agent (typically nitrogen gas) in the molten extrudate and delivers it from a small extruder immediately adjacent to the main core extruder. When both sides of the sheet are to be textured, two small extruders are used. (For blown film, one internal and one external to the main extruder are needed; for cast sheet, one above and below the main extruder.) As the extrudate from these smaller
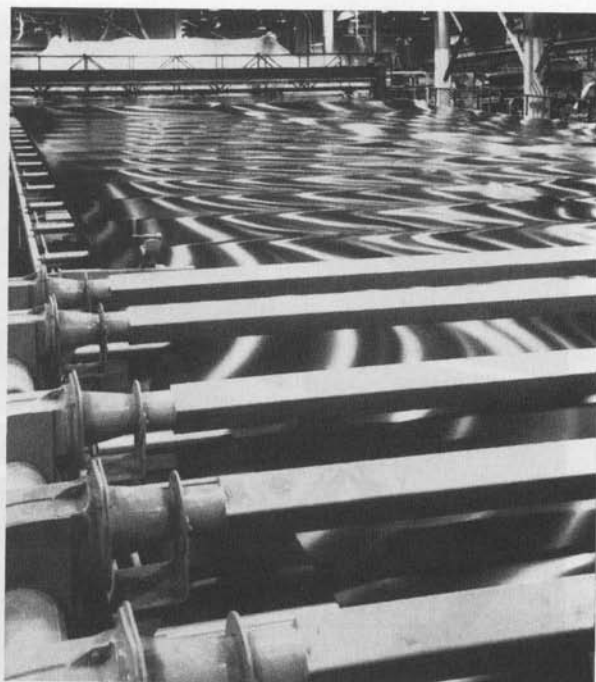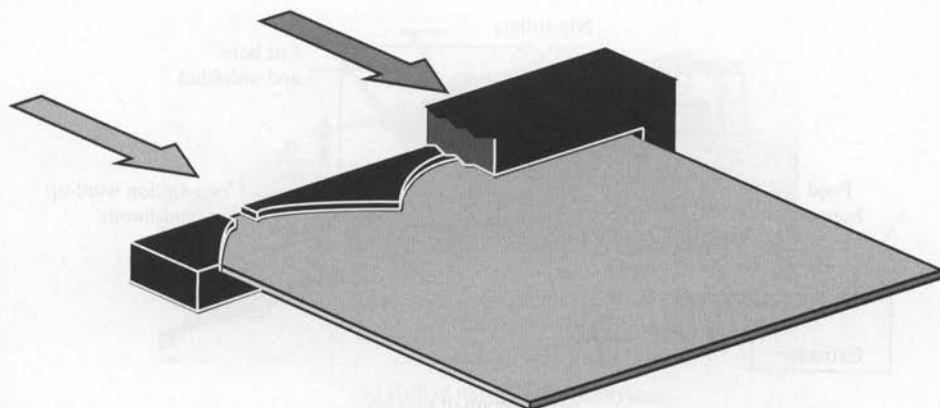
Figure 1.21   Processing of geomembranes by flat die extrusion using two extruders in parallel. (Compliments of Naue Fasertechnik, GmbH)

extruders meets the cool air bubble, the blowing agent expands, opens to the atmosphere and creates the textured surface(s). A small width (approximately 300 mm) of the cylinder's circumference or flat sheet can be left smooth, which after central cutting or trimming, becomes the two lengthwise edges of the roll for ease of seaming.

The second method of texturing is *impingement*, a process in which hot polyethylene particles are actually projected onto the previously manufactured smooth sheet
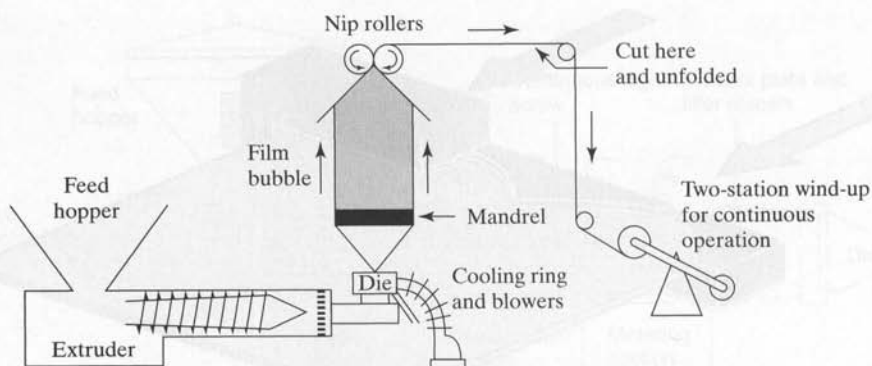
(a) Diagram of process

(b) Film bubble

Figure 1.22   Processing of geomembranes by blown sheet extrusion. (Compliments of GSE Lining Technology, Inc.)

(a) Roll of extruded polyethylene

(b) Accordion-folded pallet of
calendered polyvinyl chloride

Figure 1.23   Geomembranes being deployed in the field.

on one or both of its surfaces in a secondary operation. The adhesion of the hot parti-
cles to the cold surface(s) should be as great, or greater, than the shear strength of the
adjacent soil or other abutting material. The lengthwise edges of the sheets are left
nontextured for approximately 150 mm for ease of seaming. The method is common in
Europe but not often used in the United States due to its relatively high cost during
manufacturing.

The third method of texturing is *lamination*, a process that involves a foam on the
previously manufactured smooth sheet in a secondary operation. In this method a
foaming agent contained within molten polyethylene provides a froth that is adhered
to the previously manufactured smooth sheet providing a rough textured surface. The
degree of adhesion is important with respect to the shear strength of the adjacent soil
or other abutting material. If texturing on both sides of the geomembrane is necessary,
the roll must go through another cycle but now on its opposite side. The lengthwise
edges of the sheets are left nontextured for approximately 150 mm so that field-seaming
can be readily accomplished. This method is expensive and is rarely used.

(a) Coextrusion with nitrogen gas

(b) Impingement of hot polyethylene particles

(c) Lamination with polyethylene foam

(d) Structuring, or patterning, a surface
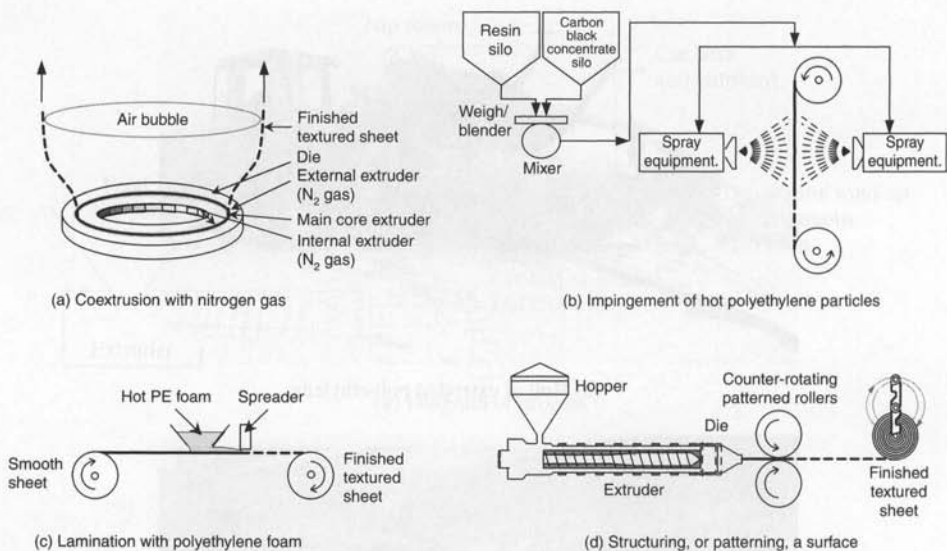
Figure 1.24 The four methods used to produce textured surfaces on HDPE, LLDPE, and fPP geomembranes.

The fourth method of texturing is *structuring*, or *patterning*. In this method a smooth sheet is made by the flat die method and immediately upon leaving the die lips passes between two counter-rotating patterned rollers. These rollers have patterned surface(s) allowing the still hot sheet (approximately at 120°C) to pass between and deform into the inverse pattern of the rollers. This gives a single or multiple raised surface patterns on the sheet as it exits the rollers; the most typical is a box and point pattern, but the variations are endless. For example, the patterned rollers can have a very knurled and rough pattern and the subsequent sheet will reflect the inverse of this pattern. The lengthwise edges of the sheets are left nontextured for approximately 150 mm so that field-seaming can be readily accomplished. This texturing method is a common one, particularly for geomembranes manufactured in Europe.

PVC, CSPE, and scrim-reinforced geomembranes including CSPE-R and fPP-R are not produced as described above and are manufactured by *calendering*, a method in which the polymer resin, carbon black, filler, plasticizer (if any), and additive package are weighed (recall Table 1.6) and mixed in a batch (Banbury-type) or continuous mixer (Farrel-type). During mixing, heat is added, which initiates a reaction between the components. The material exits the mixer and moves by conveyor to a roll mill where it is further blended and homogenized, or "masticated." Now in the form of a continuous mass, it is conveyed through a set of counter-rotating rollers (called a "calender") to form the final sheet. The versatility of calenders is seen in Figure 1.25. This type of manufacturing gives rise to the concept of multiple plies of laminated geomembranes, sometimes with an open-weave fabric (called *scrim*) inserted between the individual plies. The openings in the scrim must be large enough to allow the plies to
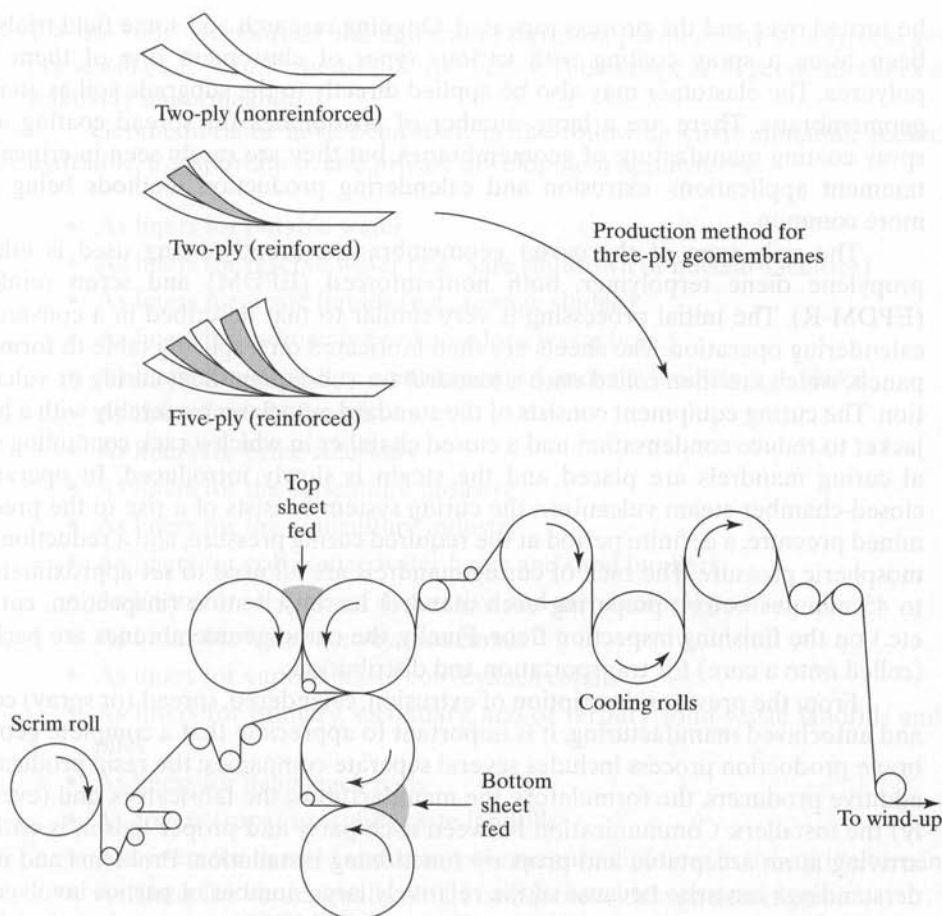
Figure 1.25   Processing of geomembranes by calendering, utilizing multiple plies of material. (Compliments of JPS Elastomerics, Inc.)

adhere to one another (called "*strike through*") with adequate ply adhesion to prevent delamination. When the fabric scrim is included, geomembranes are called "reinforced" and carry the designation accordingly—for example, CSPE-R or fPP-R. Geomembranes produced by calendering are available in widths of up to 2 to 3 m. To produce much wider widths (called *panels*), the rolls are sent to a fabricator who factory-seams the roll edges together and packages them in a double accordion-folded manner for shipment to the field (see Figure 1.23b).

Reinforced geomembranes can also be made by a manufacturing method called *spread coating*. In this method the molten polymer (whatever its formulation) is spread in a relatively thin coating over a tightly woven fabric or even a nonwoven fabric. Generally, the open pore spaces of the fabric are insufficient to allow for penetration to the opposite side; hence, if coating on both sides of the fabric is required, the material must

be turned over and the process repeated. Ongoing research and some field trials have been using a spray coating with various types of elastomers, one of them being polyurea. The elastomer may also be applied directly to the subgrade soil as an in situ geomembrane. There are a large number of possibilities for spread coating and/or spray coating manufacture of geomembranes, but they are rarely seen in critical containment applications, extrusion and calendering production methods being much more common.

The only type of thermoset geomembrane currently being used is ethylene propylene diene terpolymer, both nonreinforced (EPDM) and scrim reinforced (EPDM-R). The initial processing is very similar to that described in a conventional calendering operation. The sheets are then fabricated on a splicing table to form large panels, which are then rolled onto a mandrel for subsequent heat curing or vulcanization. The curing equipment consists of the standard autoclave, preferably with a heated jacket to reduce condensation and a closed chamber in which a rack containing several curing mandrels are placed and the steam is slowly introduced. In operating a closed-chamber steam vulcanizer, the curing system consists of a rise to the predetermined pressure, a definite period at the required curing pressure, and a reduction to atmospheric pressure. The rack of curing mandrels are allowed to set approximately 30 to 45 minutes before preparing each mandrel for observation (inspection, cut plan, etc.) on the finishing/inspection floor. Finally, the cured geomembranes are packaged (rolled onto a core) for transportation and distribution.

From the previous description of extrusion, calendered, spread (or spray) coated, and autoclaved manufacturing, it is important to appreciate that a complete geomembrane production process includes several separate companies: the resin producer, the additive producers, the formulators, the manufacturers, the fabricators, and (eventually) the installers. Communication between each party and proper liaison is critical in arriving at an acceptable and properly functioning installation. Problems and misunderstandings can arise because of the relatively large number of parties involved. It is critical that proper manufacturing quality control (MQC) measures be taken by the manufacturer and fabricator in bringing to the job site the geomembrane that was designed, specified, and purchased. The quality procedures embodied in ISO 9000 and ISO 14,000 indicate to the designer, specifier, and purchaser that a manufacturing quality control (MQC) system has been developed and is being practiced by the manufacturer. In this same light, manufacturing quality assurance (MQA)—seeing that the proper geomembrane has been manufactured per the project plans and specifications—is important and routinely practiced in the geomembrane industry.

1.6.3 Current Uses

A wide range of uses of geomembranes have been developed, all of which relate to the primary function of a material being "impermeable." Note at the outset that nothing is *strictly* impermeable in an absolute sense. Here we are speaking of relative impermeability compared to that of competing materials. In the case of solid- or liquid-waste containment geomembranes, the competing material is often natural or amended clay, which usually has a targeted hydraulic conductivity (permeability) of approximately

1×10^{-9} m/s. By contrast, the equivalent diffusion permeability of a typical geomembrane will be 1×10^{-11} m/s to 1×10^{-14} cm/s. Thus we speak of geomembranes as being relatively impermeable.

Geomembranes have been used in the following environmental, geotechnical, hydraulic, transportation, and private development applications:

- As liners for potable water
- As liners for reserve water (e.g., safe shutdown of nuclear facilities)
- As liners for waste liquids (e.g., sewage sludge)
- As liners for radioactive or hazardous waste liquid
- As liners for secondary containment of underground storage tanks
- As liners for solar ponds
- As liners for brine solutions
- As liners for the agriculture industry
- As liners for the aquiculture industry
- As liners for golf course water holes and sand bunkers
- As liners for all types of decorative and architectural ponds
- As liners for water conveyance canals
- As liners for various waste conveyance canals
- As liners for primary, secondary, and/or tertiary solid-waste landfills and waste piles
- As liners for heap leach pads
- As covers (caps) for solid-waste landfills
- As covers for aerobic and anaerobic manure digesters in the agriculture industry
- As liners for vertical walls: single or double with leak detection
- As cutoffs within zoned earth dams for seepage control
- As linings for emergency spillways
- As waterproofing liners within tunnels and pipelines
- As waterproof facing of earth and rockfill dams
- As waterproof facing for roller compacted concrete dams
- As waterproof facing for masonry and concrete dams
- Within cofferdams for seepage control
- As floating reservoirs for seepage control
- As floating reservoir covers for preventing pollution
- To contain and transport liquids in trucks
- To contain and transport potable water and other liquids in the ocean
- As a barrier to odors from landfills
- As a barrier to vapors (radon, hydrocarbons, etc.) beneath buildings
- To control expansive soils
- To control frost-susceptible soils

- To shield sinkhole-susceptible areas from flowing water
- To prevent infiltration of water in sensitive areas
- To form barrier tubes as dams
- To face structural supports as temporary cofferdams
- To conduct water flow into preferred paths
- Beneath highways to prevent pollution from deicing salts
- Beneath and adjacent to highways to capture hazardous liquid spills
- As containment structures for temporary surcharges
- To aid in establishing uniformity of subsurface compressibility and subsidence
- Beneath asphalt overlays as a waterproofing layer
- To contain seepage losses in existing above-ground tanks
- As flexible forms where loss of material cannot be allowed

1.6.4 Sales

Although there are always a few new resins being developed in the geomembrane field, the U. S. market currently is divided between HDPE, LLDPE, fPP, PVC, CSPE-R and EPDM-R and others, such as ethylene interpolymer alloy (EIA-R) and can we summarized as follows:

(Note that Mm^2 refers to millions of square meters).

High-density polyethylene (HDPE)	$\simeq40\%$ or 30 Mm^2
Linear low-density polyethylene (LLDPE)	$\simeq25\%$ or 19 Mm^2
Polyvinyl chloride (PVC)	$\simeq20\%$ or 15 Mm^2
Chlorosulphonated polyethylene (CSPE)	$\simeq5\%$ or 4 Mm^2
Flexible polypropylene (fPP)	$\simeq5\%$ or 4 Mm^2
Ethylene propylene diene terpolymer (EPDM)	$\simeq5\%$ or 3 Mm^2

Data are available for sales of HDPE and LLDPE insofar as various applications and geographic use is concerned. The data for 2002 in millions of kilograms of polymer (Mkg) are shown below.

Application	HDPE	LLDPE
Landfill liners	82.7 Mkg	4.9 Mkg
Landfill covers	16.5	15.2
Liquid impoundments	16.6	2.4
Floating covers	2.9	0.1
Canal liners	4.6	0.1
Secondary containment	3.9	0.2
Heap leach pads	8.1	4.3
Geotechnical uses	7.9	0.2
Total	143.2 Mkg	27.4 Mkg

Location	HDPE	LLDPE
Eastern United States	31.2 Mkg	12.4 Mkg
Western United States	27.0	5.8
Canada	3.9	0.6
Latin America	9.8	3.9
Europe	41.1	3.4
Asia	17.9	0.8
Africa	9.7	0.4
Australia	2.6	0.1
Total	143.2 Mkg	27.4 Mkg

Projections for geomembrane sales are strongly dependent on application and geographic location, as just suggested. Landfill liners and covers in North America and Europe will probably see modest growth ($\approx 5\%$), while in other parts of the world growth could be dramatic (10–15%). Other applications depend on the degree of education and marketing, but in the aggregate should be 10% or more.

1.7 OVERVIEW OF GEOSYNTHETIC CLAY LINERS

1.7.1 History

Geosynthetic clay liners (GCLs) are factory-manufactured hydraulic barriers consisting of a thin layer of bentonite (or other very low permeability material) supported by geotextiles and/or geomembranes, being mechanically held together by needling, stitching, or chemical adhesives.

The use of GCLs as a separate category of geosynthetics appears to have first occurred in the United States in 1988 in the field of solid waste containment as a backup to a geomembrane. The product was Claymax, which is bentonite mixed with an adhesive so as to bond the clay between two geotextiles—one below (the *carrier*) and the other above (the *cover*). About the same time a different product in Germany, named Bentofix, was manufactured by placing bentonite powder between two geotextiles and then needle-punching the three-component system together.

Other names for GCLs are "clay blankets," "bentonite blankets," "bentonite mats," "prefabricated bentonite clay blankets," and "clay geosynthetic barriers," the latter currently favored by the International Standards Organization (ISO). The engineering function of a GCL is containment as a hydraulic barrier to water, leachate, or other liquids and sometimes to gases. As such, GCLs are used as replacements to either compacted clay liners or geomembranes, or they are used in a composite manner to augment the more traditional liner materials.

1.7.2 Manufacture

There are many GCLs available today. In addition to the above-mentioned products, these would include Bentomat, which consists of two geotextiles needle-punched

together containing bentonite powder; Gundseal, which uses an adhesive to bond bentonite powder onto a HDPE or LLDPE geomembrane; and Na Bento, which consists of two geotextiles containing bentonite powder and stitch-bonded together. Figure 1.26 illustrates the related products available in the United States with a small hydrated sample placed above the as-received products.

Figure 1.27 presents the production concept for GCLs, with part (a) depicting the two adhesive bonded products and part (b) depicting the needle punched and stitch bonded products. All of the GCL products manufactured in North America use a sodium bentonite in the mass per unit area range of 3.2 to 6.0 kg/m^2. The clay thickness varies in the range of 4.0 to 6.0 mm. The hydraulic conductivity (permeability) is typically in the range of $(5 \text{ to } 1) \times 10^{-11}$ m/s, thus 20 to 100 times lower than the typical compacted clay liner. The various products come to the job site at a humidity equilibrated moisture state that varies from 10 to 30%. This is due in part to the extremely high hydrophilic nature of bentonite. The types of geotextiles used with the different products vary widely in their manufacturing (e.g., needle punched nonwoven, woven silt film, spunlaced, composite) and in their mass per unit area (e.g., varying from 90 g/m^2 to 600 g/m^2). The particular product with a geomembrane backing can also vary in its type, thickness, and surface texture. Some recent GCL variations include a thin polymeric film on or beneath the cover geotextile and a polymer impregnated cover geotextile. In addition, a polymer modified bentonite GCL has been introduced.

GCLs are factory-made in widths of 4.0 to 5.2 m and lengths of 30 to 60 m. Upon manufacturing, they are wrapped around a core and covered with a plastic film to prevent additional moisture absorption or wetting (i.e., premature hydration) during storage, transportation, and placement prior to their eventual covering with an overlying layer.

Figure 1.26 Various types of geosynthetic clay liners currently available, showing the corresponding hydrated product directly on top of the as-received product.
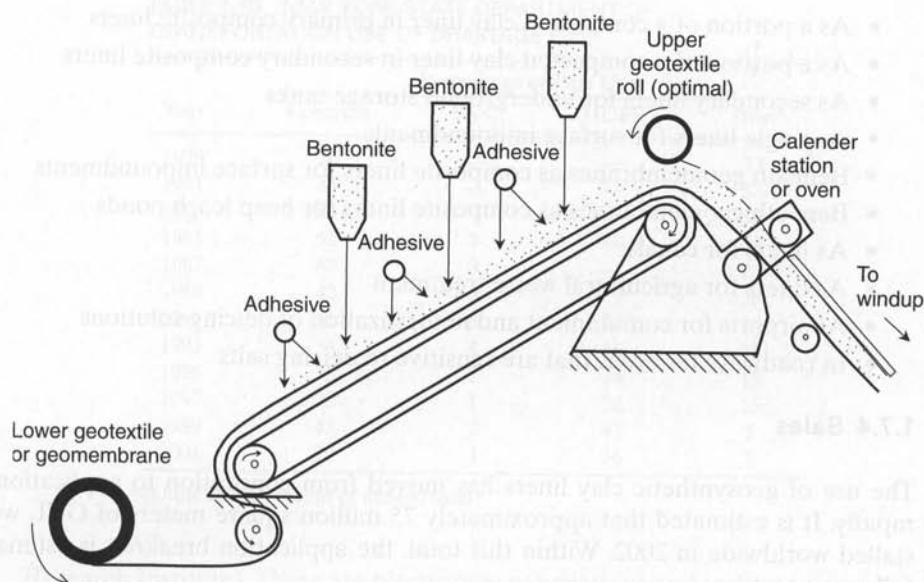
(a) Adhesive mixed with clay
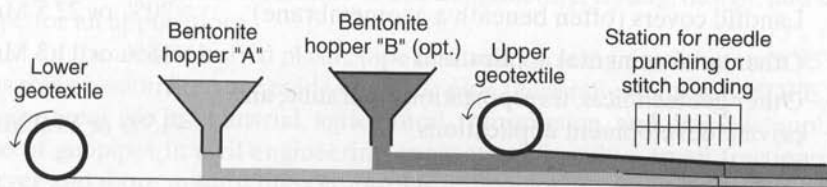
(b) Needle punched or stitch bonded through clay

Figure 1.27   Methods of manufacturing different types of geosynthetic clay liners.

1.7.3 Current Uses

GCLs are indeed hydraulic barriers to liquid movement, and as such they are competitive or complementary wherever geomembranes and compacted clay liners are used. GCL applications reported in the literature are as follows:

- Beneath geomembranes in the primary liners of landfills
- Beneath geomembranes in the secondary liners of landfills
- Beneath geomembranes and above clay liners of landfills—i.e., three-component liners
- Beneath geomembranes in the covers of landfills
- Adjacent to geomembranes in vertical cutoff walls
- Above geomembranes as puncture protection against coarse gravel

- As a portion of a compacted clay liner in primary composite liners
- As a portion of a compacted clay liner in secondary composite liners
- As secondary liners for underground storage tanks
- As single liners for surface impoundments
- Beneath geomembranes as composite liners for surface impoundments
- Beneath geomembranes as composite liners for heap leach ponds
- As liners for canals
- As liners for agricultural waste treatment
- At airports for containment and neutralization of deicing solutions
- In roadways for areas that are sensitive to deicing salts

1.7.4 Sales

The use of geosynthetic clay liners has moved from conception to application quite rapidly. It is estimated that approximately 75 million square meters of GCL were installed worldwide in 2002. Within this total, the application breakout is estimated as follows:

Landfill liners (usually beneath a geomembrane)	$\simeq$40% or 30 Mm^2
Landfill covers (often beneath a geomembrane)	$\simeq$30% or 22.5 Mm^2
Other environmental applications	$\simeq$15% or 11.3 Mm^2
Other geotechnical, transportation, hydraulic, and private development applications	$\simeq$15% or 11.2 Mm^2

1.8 OVERVIEW OF GEOPIPE (AKA PLASTIC PIPE)

1.8.1 History

The traditional materials used for underground pipeline transmission of water, gas, oil, and various other liquids have been steel, cast iron, concrete, and vitrified clay. These pipe materials are classified as "rigid" and are strength-related as far as their material behavior is concerned. Plastics, however, are making significant inroads in these markets, and they certainly deserve a separate chapter in a book devoted to polymeric-based geosynthetic materials. For example, the use of corrugated, or profiled, HDPE pipe has increased to 56% of the drainage pipe market in New York State since 1989 (see Table 1.10). Pipes made from polymeric materials are classified as "flexible" and are deflection governed as far as their mechanical behavior is concerned. To be consistent with other geo-terms in this book, the category is titled "geopipe," which obviously refers to plastic pipe placed beneath the ground surface and subsequently backfilled.

Plastic pipe predates other geosynthetics and was one of the very first polymer materials manufactured and used to a wide extent. The area is very well organized with a large institute (the Plastic Pipe Institute) and a world renown research arm (the Gas

TABLE 1.10   NEW YORK STATE DEPARTMENT OF
TRANSPORTATION USE OF DRAINAGE PIPE

Year	Percentage of Pipe Use			
	Concrete	PVC	HDPE	Steel
1979	26	—	—	73
1981	44	—	—	53
1983	48	—	—	52
1985	52	7	—	38
1987	67	3	—	21
1989	42	5	1	38
1991	31	8	24	24
1993	33	4	16	21
1995	35	2	34	15
1997	23	1	38	15
1999	43	1	47	5
2001	29	3	56	5

(Units are in percent of annual total)

Research Institute). There are plastic pipe associations and institutes in most of the industrialized countries in the world. Annual plastic pipe conferences disseminate information and lend great credibility to the manufacture, testing, design, and use of plastic pipe for all applications.

In the area of buried plastic pipe it should be recognized that over 95% of natural gas transmission lines are made of plastic pipe (generally solid-wall HDPE). Additional major areas are in industrial, agricultural, transmission, and drainage applications. The use of geopipes in civil engineering applications is only a small fraction of this much larger and more mature market. Insofar as geopipe is concerned within the context of this book, there are five areas of application focus: (1) environmental, (2) transportation, (3) geotechnical, (4) private development, and (of course) (5) hydraulic.

1.8.2 Manufacture

There are a number of polymer resins being used in the fabrication of plastic pipe. Currently they are nonplasticized polyvinyl chloride (PVC), high-density polyethylene (HDPE), polypropylene (PP), polybutylene (PB), acrylonitrile butadiene styrene (ABS), and cellulose acetate buytrate (CAB). The focus of applications discussed in this book is almost completely related to the use of PVC and HDPE. PVC and HDPE entered the market as solid wall, constant thickness pipes of relatively small diameter. For example, every hardware store handles small diameter PVC pipe and fittings for household water and drainage systems for "do-it-your-selfers." Today's plastic pipes, however, can be very large in diameter (up to 4 m) and very thick in wall dimension (up to 150 mm).

Plastic pipe consists of a specific formulation (recall Table 1.6) that is fed into a extruder of the type shown in Figure 1.20. As the polymer melt exits the filter screen, however, the die is circular in its shape, with a concentric circular insert contained within it. The polymer that flows in the annular space has controlled outer and inner diameters.

Obviously, the support system for the inner core must be appropriately designed, but plastic pipe manufacturing design is very developed in this regard; extremely close tolerances of diameter and thickness can be achieved.

In order to optimize behavior, economize on resin, and aid in installation, a number of differing types of wall sections consisting of ribs, cores, and corrugated profiles of a wide variety of cross-sectional shapes and sizes have appeared. These latter pipes are referred to as corrugated, or profiled, wall pipes. Additionally, many applications such as agriculture drains and leachate collection systems require holes, slots, or other types of perforations in the wall section to allow for inflow of liquids. This has led to the following designation system for corrugated plastic pipe:

$$CPP = \text{corrugated (outside) plastic pipe}$$
$$CPP\text{-}S = \text{CPP pipe with smooth inside}$$
$$CPP\text{-}C = \text{CPP pipe with corrugated inside}$$
$$CPP\text{-}SP = \text{CPP-S pipe with perforations}$$
$$CPP\text{-}CP = \text{CPP-C with perforations}$$

Both solid-wall and corrugated-walled plastic pipe are shown in Figure 1.28.

1.8.3 Current Uses

Solid-wall and corrugated-wall plastic pipes are used in a wide variety of civil engineering applications, including the following:

- As highway, railway, and airfield edge- and under-drains
- As seepage drains in tunnels
- As pore water drains behind retaining walls
- As interceptor drains in seeping soil and rock slopes
- As interceptor drains for groundwater seepage
- For dewatering projects
- In fluid transmission lines by gravity
- In force transmission lines under pressure
- In waste water drainage systems
- For piping in leach fields of various types
- In chemical transmission pipelines
- In primary leachate removal systems in landfills and waste piles
- In secondary leachate removal systems in landfills and waste piles
- In pipe risers in landfill sidewalls
- In pipe manifold systems for landfill gas collection and removal
- In pipe manifold systems for leachate reinjection into landfills
- In surface water removal systems in landfill covers
- For dredging pipelines

Figure 1.28   Smooth and corrugated plastic pipe (geopipe) used in below-ground construction.

1.8.4 Sales

It is difficult to estimate sales of geopipe in the application areas focused upon in this book because the data cannot be placed on a unit area basis and such pipe is regularly used for "non-geo" uses. The estimate of $300 million worldwide sales given earlier is based on approximate resin sales, recognizing that geopipe manufacturing can range from large multinational companies to extremely small operations with one extruder. Suffice it to say that the plastic pipe industry is interested in geosynthetics applications, and this interest is certainly reciprocated by offering the topic as a separate chapter in this book.

1.9 OVERVIEW OF GEOFOAM

1.9.1 History

Geofoam is a foamed polymeric geosynthetic material (generally expanded poly-styrene) manufactured in slab or block form and used primarily for its lightweight and sometimes for its insulating properties. The original applications as a lightweight fill were in Norway in 1972 and subsequently throughout Scandinavia. Early use has also been in Japan and Southeast Asia. These uses invariably take advantage of geofoam fills being only 1 to 3% as heavy as conventional soil fills. Thus carrying loads, such as highways over compressible soils, frost-sensitive soils, and other settlement-prone situations favor the use of geofoam.

The first use in the United States was to relieve lateral earth pressures behind a retaining wall [40]. An international conference in 1995 [41] and subsequent publications by Horvath [42] and Negussey [43] have greatly helped in the proper positioning of geofoam for the civil engineering designer and specifier.

1.9.2 Manufacture

The resin styrene was developed in 1937. Expanded polystyrene (EPS), the general material for the manufacture of geofoam, was developed by the BASF Corporation in 1950. Their manufacturing process is described.

The molecular structure of polystyrene (PS) is given in Table 1.2 and its genesis from ethylene is shown in Figure 1.2. The public knows the material best as packaging material and insulating container material. Geofoam production follows the three processing stages, shown in Figure 1.29.

In the first stage, styrene with various additives is introduced with pentane as a blowing agent via water into a polymerization unit. Using steam as the heat transfer medium, the resin softens and the increased vapor pressure of the blowing agent expands the resin beads to about 50 times their original size. During this increase in volume, the close-cell foam structure of the beads is formed. The apparent density is an extremely low value ranging between 10 and 30 kg/m^3.

During the second stage, which is called intermediate bead processing, steam is again used along with rotary blowers or blower injectors for the following purposes:

- Air diffuses through the cell walls, making the particles mechanically stable.
- Moisture is dissipated to the atmosphere, aiding in the flow properties of the beads.
- Any residual blowing agent diffuses out through the walls of the beads.

The now-stabilized beads are then stored in a silo for 5 to 28 hours.

The third stage is final processing in which slabs or blocks of geofoam are made. Again steam is used on the beads placed in the appropriate forms, causing the polymer beads to soften. The free space between beads is closed, causing a polyhedral structure to form and the touching surfaces to bond together. When cooled, the finished slabs or
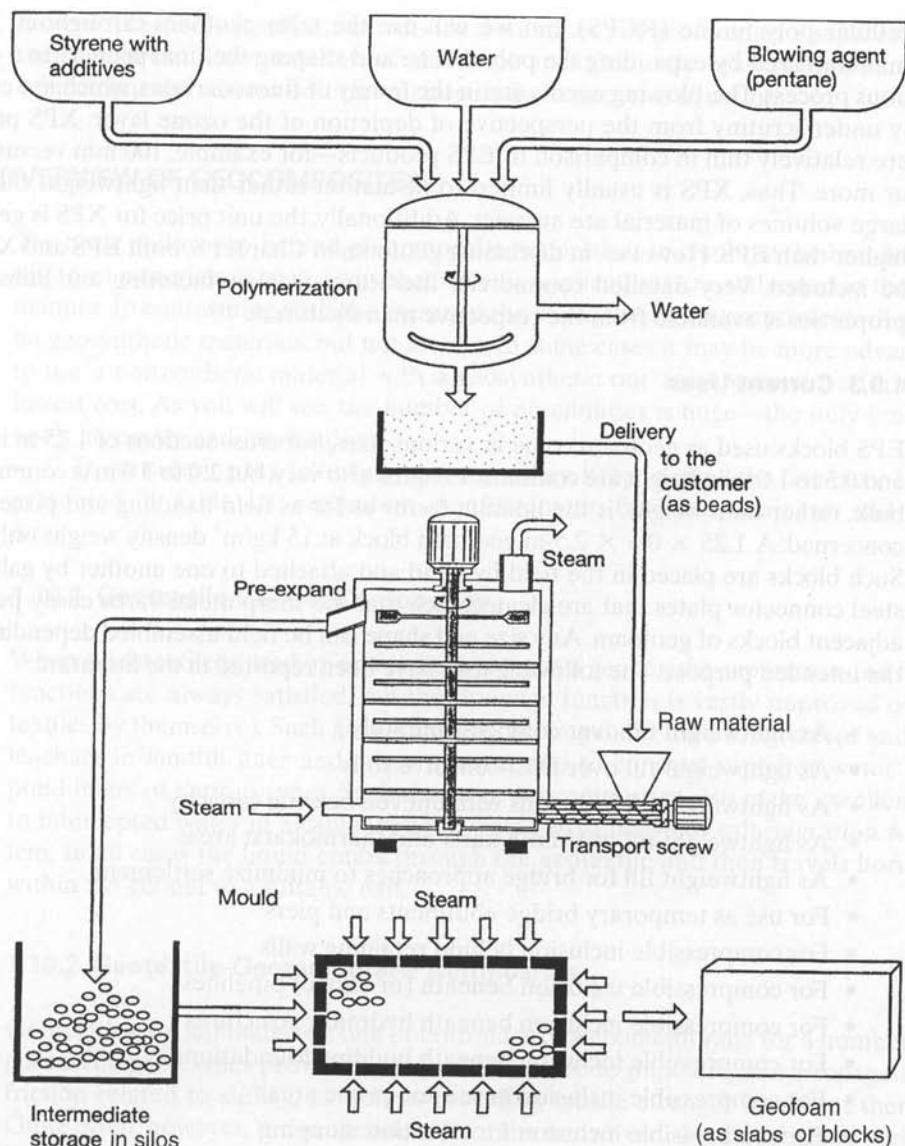
Figure 1.29   BASF Inc. production method of Styropor expanded polystyrene (EPS) slabs and blocks.

blocks are removed, sent to a sizing operation, and eventually shipped to the customer. Modern production also allows for continuous production (rather than the batch process described above).

A somewhat different geofoam manufacturing process produces extruded polystyrene (XPS). Note that EPS and XPS are referred to in ASTM standards as rigid

cellular polystyrene (RCPS), but we will use the term geofoam throughout. XPS is manufactured by expanding the polystyrene and shaping the final product in a continuous process. The blowing agents are in the family of fluorocarbons, which are currently under scrutiny from the perspective of depletion of the ozone layer. XPS products are relatively thin in comparison to EPS products—for example, 100 mm versus 1.0 m, or more. Thus, XPS is usually limited to insulation rather than lightweight fill where large volumes of material are an asset. Additionally, the unit price for XPS is generally higher than EPS. However, in discussing geofoam in Chapter 8, both EPS and XPS will be included. Very detailed commercial literature on manufacturing and subsequent properties is available from the respective manufacturers.

1.9.3 Current Uses

EPS blocks used as geofoam come in various sizes, but cross sections of 1.25 m in width and 0.5 to 1.0 m in height are common. Lengths also vary, but 2.0 to 3.0 m is common. The bulk, rather than weight, is the limiting factor as far as field handling and placement is concerned. A $1.25 \times 0.5 \times 2.5$-m geofoam block at 15 kg/m^3 density weighs only 23 kg. Such blocks are placed in the field by hand and attached to one another by galvanized steel connector plates that are cleated such that the sharp metal barbs easily penetrate adjacent blocks of geofoam. Any size and shape can be field-assembled depending upon the intended purpose. The following uses have been reported in the literature:

- As lightweight fill over compressible soils
- As lightweight fill over frost-sensitive soils
- As lightweight fill over soils with uneven bearing capacity
- As lightweight fill over both karst and thermokarst areas
- As lightweight fill for bridge approaches to minimize settlement
- For use as temporary bridge abutments and piers
- For compressible inclusion behind retaining walls
- For compressible inclusion beneath (or above) pipelines
- For compressible inclusion beneath hydraulic structures
- For compressible inclusion beneath building foundations
- For compressible inclusion in seismic-prone areas
- For compressible inclusion for vibration damping
- As thermal insulation for below-grade construction
- As thermal insulation to avoid frost pressures
- For use as a fluid transmission medium when properly machined

1.9.4 Sales

Similar to geopipe, it is difficult to estimate sales of geofoam since it is regularly used for "non-geo" uses. The estimate of $100 million worldwide sales given earlier is largely not in the United States. The major users are in Scandinavia and Japan. The growth,

however, certainly justifies the individual treatment of geofoam as a separate geosynthetic material. Prior editions of this book included only brief commentary on the subject, but the current edition will hopefully correct this situation.

1.10   OVERVIEW OF GEOCOMPOSITES

The basic philosophy behind geocomposite materials is to combine the best features of different materials in such a way that specific applications are addressed in the optimal manner. In conforming with the theme of the book, these geocomposites will generally be geosynthetic materials, but not always. In some cases it may be more advantageous to use a nonsynthetic material with a geosynthetic one for optimum performance or lowest cost. As you will see, the number of possibilities is huge—the only limits being one's ingenuity and imagination.

In considering the following geocomposites, keep in mind the five basic functions presented in Table 1.1: separation, reinforcement, filtration, drainage, and containment.

1.10.1 Geotextile-Geonet Composites

When a geotextile is used on one or both sides of a geonet, the separation and filtration functions are always satisfied, but the drainage function is vastly improved over geotextiles by themselves. Such geocomposites are regularly used to intercept and convey leachate in landfill liner and cover systems and to conduct vapor or water beneath pond liners of various types. Such drainage geocomposites also make excellent drains to intercepted water in a capillary zone where frost heave or salt migration is a problem. In all cases the liquid enters through the geotextile and then travels horizontally within the geonet to a suitable exit.

1.10.2 Geotextile-Geomembrane Composites

Geotextiles are laminated on one or both sides of a geomembrane for a number of purposes. The geotextiles provide increased resistance to puncture, tear propagation, and friction related to sliding, as well as providing tensile strength in and of themselves. Quite often, however, the geotextiles are of the nonwoven, needle punched variety and are of relatively heavy weight. In such cases the geotextile component acts as a drainage media, since its in-plane transmissivity feature can conduct water, leachate or gases away from direct contact with the geomembrane.

1.10.3 Geomembrane-Geogrid Composites

Since some types of geomembranes and geogrids can be made from the same material (e.g., high-density polyethylene), they can be bonded together to form an impervious barrier with enhanced strength and friction capabilities.

1.10.4 Geotextile-Geogrid Composites

A needle punched nonwoven geotextile bonded to a geogrid provides in-plane drainage while the geogrid provides tensile reinforcement. Such geocomposites are used for internal drainage of low-permeability backfill soils for reinforced walls and slopes. The synergistic properties of each component enhances the behavior of the final product.

1.10.5 Geotextile-Polymer Core Composites

A core in the form of a quasi-rigid plastic sheet can be extruded or deformed in such a way as to allow very large quantities of liquid to flow within its structure; it thus acts as a drainage core. The core must be protected by a geotextile, acting as a filter and separator, on one or both sides. Three main systems are available. The first type is called a wickdrain in the United States and a prefabricated vertical drain (PVD) in Europe. The 100 mm wide by 5 mm thick polymer core is often fluted for ease of conducting water. A geotextile acting as a filter and separator is socked around the core. The emergence of such geotextile polymer-core composites has all but eliminated traditional sand drains as a rapid means of consolidating fine-grained saturated soils.

   The second type of system, called a sheet drain, is in the form of panels, the rigid polymer core being nubbed, columned, or dimpled, or formed as a three-dimensional net. With a geotextile on one side, it makes an excellent drain on the backfilled side of retaining walls, basement walls, and plaza decks. The cores are often vacuum-formed dimples, as shown in Figure 1.30(a), or stiff, three-dimensional meshes, as shown in Figure 1.30(b). As with wick drains, the geotextile is the filter/separator and the thick polymer core is the drain. Many systems of this type are available, the latest addition having a thin pliable geomembrane on the side facing the wall and functioning as a vapor barrier.

   The third system within this area of drainage geocomposites is the category of prefabricated edge drains. These materials, typically 500 mm high by 20 to 30 mm wide, are placed adjacent to a highway pavement, airfield pavement, or railroad right-of-way, for lateral drainage out of and away from the pavement section. The systems are incredibly rapid in their installation and extremely cost effective.

1.10.6 Geosynthetic-Soil Composites

As typified by the geosynthetic clay liners described in Section 1.7, many other variations of geosynthetic products and soil can be developed. For example, geocells are geomembrane or geotextile strips that have been cleverly arranged vertically in a box-like fashion, placed horizontally (standing upright) and filled with soil. Thus the material forms a cellular structure and, acting with the contained sand or gravel, makes an impressively strong and stable mattress for vehicular trafficking. Sizable earth embankments have been built on such systems with the possibility of supporting structures over weak soils in the near future (i.e., an inexpensive mat foundation).
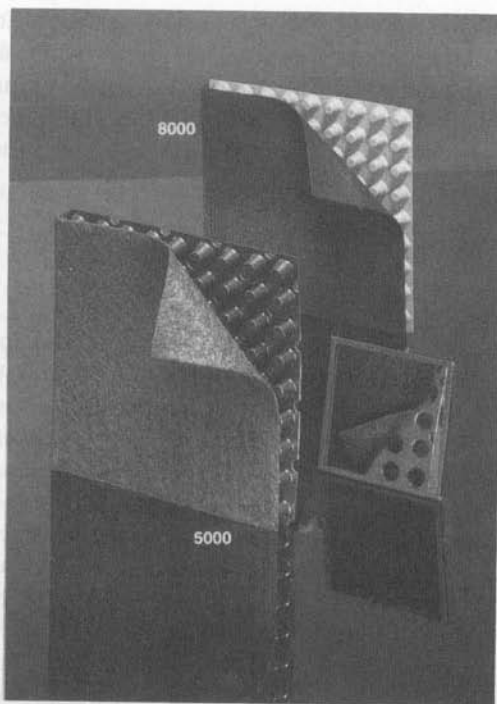
(a) Vacuum-formed dimpled drainage core
(Compliments of TC. Nicolon, Inc.)
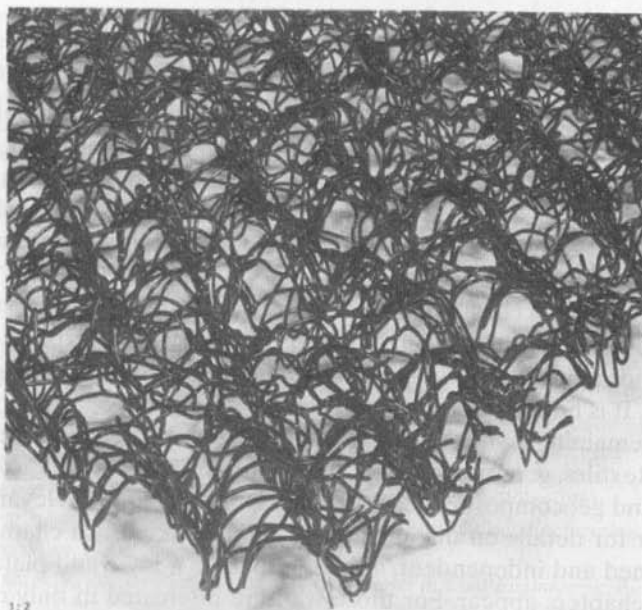
(b) Three-dimensional stiff nylon mesh type of drainage core
(Compliments of Colbond Geosynthesis, Inc.)

Figure 1.30   Various types of non-geonet geocomposite drainage materials.

Another variation is to use continuous polymer fibers and sand to form steep soil slopes with excellent strength properties. The fibers give the composite material a very pronounced apparent cohesion. The area called *geofibers* has resulted in impressive shear strength gains for deep-seated soil stability as well as near-surface soil stability in an area called *turf reinforcement*. The latter applications include horse racetracks, sport fields, golf courses, and parking and picnicking areas.

1.10.7 Other Geocomposites

Weaving steel strands within a geotextile matrix can result in incredible composite material strengths. Used as a substrate, extremely large loads can be sustained. Large composite mattresses have been constructed in this manner. A measurable increase in bearing capacity for the support of light structures is also possible.

Geotextiles with prefabricated holes for the insertion of steel rod anchors (called anchored spider netting) have been used to stabilize slopes and as in situ compaction and consolidation systems. The rods act as anchors, stressing the geotextile against the soil, which is put into compression. The geotextile thus acts dually as a tensile-stressing mechanism and as a filter allowing the pore water to escape while retaining the subsurface soil particles.

Another example of a new geocomposite trend is the *articulated concrete mattress*, interconnected steel strand concrete paving blocks that are bonded to a geotextile acting as a separator and filter. It competes against traditional hard armor alternatives like rock riprap. The possibilities are essentially endless.

1.11 OUTLINE OF BOOK

To the author, and hopefully to many others, the area of geosynthetics is a vibrant, exciting and rapidly growing field within geotechnical, transportation, environmental, hydraulics, and private development engineering. The sales information presented in Section 1.1.3 (which is based on the author's best estimates) reflects this dynamic growth in each geosynthetic area. The data are approximate, but they are indicative of the general worldwide pattern.

The field is in a constant state of flux, and the designs and test method to be presented here might be superseded in the future. This is to be expected. Nevertheless, the area demands a specific *design-by-function* methodology—an end to which this book is committed. It is hoped that time will validate the effort.

The remaining eight chapters of this book will each focus on one of the following topics: geotextiles, geogrids, geonets, geomembranes, geosynthetic clay liners, geopipe, geofoam, and geocomposites. Each chapter will refer to the relevant part of this opening chapter for details on manufacturing and the like. Each chapter is also relatively self-contained and independent, although there is a logic and plan to the sequence in which the chapters appear. For those who are interested in only one type of geosynthetic, that chapter can be studied in isolation, but the background given in this first chapter should be read thoroughly, particularly those parts related to materials manufacturing. Design-by-function is emphasized throughout the book, with illustrative

problems and homework problems in each chapter. Reference lists unique to each chapter are included.

REFERENCES

1. Dewar, S., "The Oldest Roads in Britain," *The Countryman*, vol. 59, no. 3, 1962, pp. 547–555.
2. Beckham, W. K., and Mills, W. H., "Cotton-Fabric-Reinforced Roads," *Engineering News-Record*, October 3, 1935, pp. 453–455.
3. Bertram, G. E., "An Experimental Investigation of Protective Filters," Graduate School of Engineering, Harvard University, Publ. 267, January 1940, 140 pp.
4. Kays, W. B., *Construction of Linings for Reservoirs, Tanks, and Pollution Control Facilities*, 2nd ed. New York: Wiley 1982.
5. Lauritzen, C. W., "Plastic Films for Water Storage," *Journal of American Water Works* Association, vol. 53, no. 2, February 1963 pp. 135–140.
6. Rodriguez, F., *Principles of Polymer Systems*. 4th ed. New York: McGraw Hill, 1996.
7. Mascia, L., *Thermoplastics: Engineering*. New York: Applied Science Publishers, 1982.
8. Rosen, S. L., *Fundamental Principles of Polymeric Materials*. New York: Wiley, 1982.
9. Sperling, L. H., *Introduction to Physical Polymer Science*. New York: Wiley, 1986.
10. Moore, G. R., and Kline, D. E., *Properties and Processing of Polymers for Engineers*. Englewood Cliffs, NJ: Prentice Hall 1984.
11. Halse, Y., Wiertz, J., Rigo, J.-M., and Cazzuffi, D. A., "Chemical Indentification Methods Used to Characterize Polymeric Geomembranes." In *Geomembranes: Identification and Performance Testing*, edited by A. Rollin and J-M Rigo, RILEM Report 4, London: Chapman and Hall 1991, pp. 316–336.
12. Thomas, R. W., and Verschoor, K. L., *Thermal Analysis of Geosynthetics*, Geotechnical Fabrics Report, IFAI, vol. 6, no. 3, May/June 1988, pp. 24–30.
13. Brennan, W. P., *Characterization of Polyethylene Films by Differential Scanning Calorimetry*, Norwalk, CT: Perkin-Elmer Instrument Division, March 1978, 25 pp.
14. Hsuan, Y. G., and Guan, Z., "Evauation of Oxidation Behavior of Polyethylene Geomembranes Using Pressure Different Scanning Calorimetry." In *Oxidative Behavior of Materials by Thermal Analytical Techniques*, ASTM STP1326, ed. A. T. Riga and G. H. Patterson, American Society for Testing and Materials, 1997, pp. 76–90.
15. Li, M., and Hsuan, Y. G., "Pressure Effects on the Oxidation of High Density Polyethylene Geogrids," *Proceedings from Geosynthetics '04*, Winnipeg, Canada, 2004, 8 pp.
16. Struve, F., "Extrusion Fillet Welding of Geomembranes," *Journal of Geotextiles and Geomembranes*, vol. 9, nos. 4–6, 1990, pp. 1–14.
17. Allcock, H., *Contemporary Polymer Chemistry*. Englewood Cliffs, NJ: Prentice Hall, 1981.
18. Pohl, H. A., "Determination of Carboxyl End Groups in a Polyester (Polyethylene Terephthalate)," *Journal of Analytical Chemistry*, vol. 26, no. 10, October 1954, pp. 1614–1616.
19. Barrett, R. J., "Use of Plastic Filters in Coastal Structures," *Proceedings from the 16th International Conference Coastal Engineers*, Tokyo, September 1966, pp. 1048–1067.
20. Agerschou, H. A., "Synthetic Material Filters in Coastal Protection," *Journal of Waterways Harbors Division*, ASCE, vol. 87, no. WW1, February 1961, pp. 111–124.
21. Rankilor, P. R., *Membranes in Ground Engineering*. New York: Wiley 1981.
22. Koerner, R. M., and Welsh, J. P., *Construction and Geotechnical Engineering Using Synthetic Fabrics*. New York: Wiley, 1980.
23. van Zantan, R. V., ed., *Geotextiles and Geomembranes in Civil Engineering*. Rotterdam: A. A. Balkema, 1986.
24. Rowe, R. K., ed., *Journal of Geotextiles and Geomembranes*. Elsevier Applied Science Publishers.
25. Ingold, T., ed., *Geosynthetics International*. T. Telford Publishers Ltd.

26. Shreve, R. N., and Brink, J. A. Jr., *Chemical Process Industries*, 4th ed. New York: McGraw-Hill, 1977.

27. Kaswell, E. R., *Handbook of Industrial Textiles*. New York: West Point Pepperall, 1963.

28. INDA, Association of Nonwoven Fabrics Industry, 10 East 40th Street, New York, NY 10016.

29. Jagielski, K., "Lining Systems Show Growth," *GFR Magazine* vol. 9, no. 6, September 1991, IFAI Publ, pp. 26–28.

30. Geosynthetic Materials Association, IFAI, Rosemont, MN, 2001.

31. Capaccio, G., and Ward, I. M., "Properties of Ultra-high Modulus Linear Polypropylene," *Nature Physical Sciences*, vol. 243, 1974, pp. 130–143.

32. Ward, I. M., "The Orientation of Polymers to Produce High Performance Materials," *Proceedings of the Symposium on Polymer Grid Reinforcement in Civil Engineering*, Institution of Civil Engineers, UK, 1984.

33. Netlon Ltd. Blackburn, United Kingdom (product literature) and Tensar Inc., Morrow, GA (product literature).

34. Paulson, J. N., "Flexible Geogrids," *Proceedings GRI-8, Geosynthetic Resins, Formulations, and Manufacturing*, IFAI Publishers, 1995, pp. 199–204.

35. Heerten, G., Floss, R. and Brau, G., "Safe and Economical Soil Reinforcement Using a New Style Geogrid." In *Landmarks in Earth Reinforcement*, edited by H. Ochiai, J. Otani, N. Yasufuku and K. Omine. Rotterdam: A. A. Balkema, IS Kyushu 2001, pp. 43–48.

36. Voskamp, W., "Index and Performance Testing of a New Geogrid Made of Highly Oriented Straps," *Proceedings of GeoDenver 2000, Advances in Transportation and GeoenvironmentalSystems Using Geosynthetics*, edited by J. G. Zornberg and B. R. Christopher GSP No. 103, GeoInstitute of ASCE, 2000, pp. 360–372.

37. Austin, R. A., "The Manufacture of Geonets and Composite Products," *Proceedings of Geosynthetic Resins, Formulations and Manufacturing*, edited by Y. G. Hsuan and R. M. Koerner, IFAI, 1995, pp. 127–138.

38. Rimoldi, P., "The Future of Geonets and Geocomposites," *Proceedings of the GRI-13 Conference Geosynthetics in the Future: Year 2000 and Beyond*. Folsom, PA: Geosynthetic Information Institute, 1999, pp. 49–66.

39. Haxo, H. E. Jr., "Quality Assurance of Geomembranes Used as Linings for Hazardous Waste Containment," *Journal of Geotextiles and Geomembranes*, vol. 3, no. 4, 1986, pp. 225–248.

40. Partos, A. M., and Kazaniwsky, P. M., "Geoboard Reduced Lateral Earth Pressure," *Proceedings of Geosynthetics '87*, IFAI, 1987, pp. 628–638.

41. Horvath, J. S., *Proceedings International Geotechnical Symposium on Polystyrene Foam in Below-Ground Applications*, New York, Manhattan College, May 1995.

42. Horvath, J. S., *Geofoam Geosynthetic*, Scarsdale, NY: Horvath Engineering P.C., 1995.

43. Negussey, D., *Properties and Applications of Geofoam*, Society of Plastics Industries, 1997.

PROBLEMS

1.1. This book deals exclusively with geosynthetics—synthetic materials placed in the ground. What materials would *not* be considered in this category? That is, what would be some *non*synthetic geotextiles, *non*synthetic geomembranes, and *non*synthetic composites?

1.2. Regarding the unit prices of geosynthetics given in Section 1.1.3, what factors do you think would influence these values?

1.3. Regarding the installation of geosynthetics, what labor group(s) would be involved in installing the following, considering both union and nonunion situations?
   (a) Geotextiles
   (b) Geogrids

    (c) Geonets

    (d) Geomembranes

    (e) Geosynthetic clay liners

    (f) Geopipe

    (g) Geofoam

1.4. What complications might you see arising in purchasing and providing quality-assurance geomembranes versus geotextiles? (*Hint:* Consider how many different firms are involved in the manufacture of each of the types mentioned.)

1.5. Name some major corporations that produce the following resins:

    (a) Polyethylene

    (b) Polypropylene

    (c) Polyester

    (d) Polyvinyl chloride

1.6. Identify the common polymer used to manufacture the following commonly used products:

    (a) Milk containers

    (b) Soft drink bottles

    (c) Disposable coffee containers

    (d) Household plumbing pipe

    (e) Automobile battery cases

    (f) Lightweight plastic canoes

1.7. The PVC curve in Figure 1.4 was described as consisting of plasticizer, resin, carbon black/ash. What percentages of each were in this material?

1.8. Identify the components and their percentages in Figure 1.4 of PP, PE, and PET.

1.9. The DSC traces shown in Figure 1.6 list LDPE, MDPE, and HDPE. Identify the temperature window at which each type begins to melt, when melting is complete, and the difference—i.e., the "melting window."

1.10. Using the OIT data of Figure 1.7, estimate the time for depletion of all of the antioxidant in this particular geomembrane formulation at a service temperature of 20°C. Proceed using the following steps:

    (a) Replot the data on a semilong axis omitting the 115°C data.

    (b) Extrapolate each of the curves down to "zero" minutes.

    (c) Plot these values on a logarithmic y-axis against inverse temperature on the x-axis.

    (d) Determine the average slope of the resulting four points.

    (e) Extrapolate this slope down to an estimated service life temperature of 20°C to obtain the estimated time for antioxidant depletion.

1.11. Use the coefficients of thermal expansion shown in Figure 1.8 to determine the following:

    (a) What change in length is involved in 10 m of PET yarn if there is a 20°C change in temperature below the glass transition temperature (T_g)?

    (b) Recalculate part (a) for temperature changes above T_g.

1.12. You have been asked to perform a forensic analysis of a failure involving a geosynthetic product in which the polymeric material itself was suspect. Which tests in Table 1.5 would you perform under the following circumstances:

    (a) The material is a polypropylene geotextile.

    (b) The material is a polyester geogrid.

    (c) The material is a polyethylene geonet.

    (d) The material is a polyvinyl chloride geomembrane.

1.13. Name five major functions that geosynthetics perform and illustrate them by means of sketches.

1.14. In placing a geotextile beneath railroad ballast, the materials can serve in four different functions simultaneously. Describe and illustrate these functions.

1.15. The first person to describe the general use of geotextiles was Barrett in 1966 [19]. What major function did the geotextile serve? List the various uses he describes.

1.16. Plot the trend lines for the geotextile applications listed in Table 1.9. What is the fastest growing application area in current geotextile usage?

1.17. Permeability of geotextiles refers to liquid moving through the voids created by the fibers and yarns that make up the fabric. This permeability is called *Darcian permeability*.
    (a) Give the equation for Darcy's law.
    (b) Identify the various terms.
    (c) What are the major variables involved in variations of the k-value?

1.18. Permeability of geomembranes refers to liquid vapor moving through the amorphous structure of the polymer. This permeability is called *diffusion permeability*.
    (a) Give the equation for 'Fick's law.'
    (b) Identify the terms.
    (c) What are the major variables involved in variations of the diffusion coefficient?

1.19. If a hole is created in a geomembrane, the flow through the hole is governed by Bernoulli's equation.
    (a) State Bernoulli's equation.
    (b) Identify the terms.
    (c) What kind of relationship do you think there would be between the diffusion permeability of an intact geomembrane and the Bernoulli flow through one or more holes in a geomembrane?

1.20. What is a "corduroy" road, and how does it function?

1.21. Other than geosynthetics, what are some methods for strengthening soils (i.e., adding tensile strength to them)?

1.22. How would you estimate geosynthetic performance in the following severe climatic conditions: (*Hint:* How do plastics respond to cold and hot temperatures in general?)
    (a) Arctic conditions
    (b) Desert conditions

1.23. What two commonly used polymers in the manufacture of geosynthetic materials are in the polyolefin family?

1.24. Assume that you are familiar with the molecular structure of the polymers used to make geosynthetics.
    (a) What are typical lengths of the molecular chains?
    (b) What is meant by the "backbone" of the molecular chain?
    (c) Sketch the crystalline and amorphous molecular chains of polyethylene and show how they are linked together.

1.25. The molecular structure of high-molecular-weight polymeric materials has often been described as a "bowl of spaghetti." Assuming that this is the case, answer the following questions:
    (a) What would be the length of a high-molecular-weight polymer like polyester, if the diameter was typical of spaghetti, e.g. 1.5 mm?
    (b) What happens to the "bowl of spaghetti" as the polymer structure is stressed?
    (c) What happens if it is stressed too high?

1.26. Degradation of polymeric materials involves a decrease in its molecular weight and is often called *chain scission.*
(a) Describe this process.
(b) What mechanisms can bring it about?

1.27. In general, all polymeric materials are susceptible to UV attack. Considering their chemical structure, why is this the case?

1.28. The usual processing step taken to avoid UV light degradation of polymers is the addition of carbon black. How does this material function? Are there other additives that can be used instead of carbon black such that the resulting geosynthetic is not black in color?

1.29. In the absence of ultraviolet light degradation, what would cause a polymer structure to "age"?

1.30. What are the major causes of degradation of the following polymers considering that they have been covered in a timely manner and that no high level radiation is involved?
(a) Polyethylene
(b) Polypropylene
(c) Polyester
(d) Plasticized polyvinyl chloride
(e) Polyamide

1.31. In considering the manufacturing of geomembranes as described in Section 1.6.2, do you think that residual stresses could exist in the as-manufactured sheet? If so, how would you measure the magnitude and orientation?

1.32. Regarding the production cost of geotextiles, rank the following styles on the basis of an equivalent mass per unit area (i.e., consider that they are all the same in terms of g/m^2 weight and the same polymer type).
(a) Woven monofilament
(b) Woven slit film
(c) Nonwoven heat bonded
(d) Nonwoven resin bonded
(e) Nonwoven needle punched

1.33. Regarding the material cost of geomembranes, rank the relative cost of the following styles on the basis of an equivalent thickness of material.
(a) High density polyethylene (HDPE)
(b) Linear low density polyethylene (LLDPE)
(c) Polyvinyl chloride (PVC)
(d) Flexible polypropylene (fPP)
(e) Chlorosulphonated polyethylene–scrim reinforced (CSPE-R)

1.34. Assume that you have been asked to write a report on geosynthetic clay liners (GCLs):
(a) List some advantages and disadvantages over a geomembrane (GM).
(b) List some advantages and disadvantages over a compacted clay liner (CCL).

1.35. You have been asked to explain the use of a three-component liner consisting of a geomembrane over a GCL and over a CCL. i.e., a GM/GCL/CCL, composite liner.
(a) List some advantages and disadvantages over a GM/CCL composite.
(b) List some advantages and disadvantages over a GM/GCL composite.

1.36. You have been asked to explain soil-backfilled plastic pipe (or *geopipe*).
(a) List some advantages and disadvantages of a polymer geopipe over concrete pipe.
(b) List some advantages and disadvantages of a polymer geopipe over metal pipe.

    (c) List some advantages and disadvantages of HDPE polymer geopipe over PVC polymer geopipe

1.37. Geofoam is listed in Table 1.1 as having the primary function of separation.
    (a) What other function could it serve?
    (b) If an additional primary function were added for geofoam, what would be the test descriptor?

1.38. List what you feel are the most relevant and unique properties of geofoam.

1.39. Someone has just coined the new geoword *geospacer*: What types of geosynthetic materials would it likely include?

2

Designing with Geotextiles

2.0 INTRODUCTION

According to ASTM D4439, a geotextile is defined as follows:

Geotextile: A permeable geosynthetic comprised solely of textiles. Geotextiles are used with foundation, soil, rock, earth, or any other geotechnical engineering-related material as an integral part of a human-made product, structure, or system.

The area of geotextiles is a well-established and exciting field, with new uses being developed regularly. As such, there are a number of possible applications and an even greater number of geotextiles to choose from. The vast majority of geotextiles are made from polypropylene (although some are polyester or polyethylene) polymers; formed into fibers or yarns (the choices being monofilament, multifilament, staple yarn, continuous yarn, slit-film monofilament, or slit-film multifilament); and finally manufactured as a woven or nonwoven fabric. When placed in the ground, these textile fabrics are called *geotextiles*. In general, the words "fabric" and "geotextile" are used interchangeably. The following choices of fabric styles are available:

- Woven monofilament
- Woven multifilament
- Woven slit-film monofilament
- Woven slit-film multifilament
- Nonwoven continuous filament heat bonded
- Nonwoven continuous filament needle-punched
- Nonwoven staple needle-punched
- Nonwoven heat bonded
- Nonwoven resin bonded (rare)
- Other woven or nonwoven combinations
- Knitted (very rare)

A complete description of the methods of manufacturing geotextiles is presented in Section 1.3.

Due to the very wide range of applications and the tremendous variety of available geotextiles having widely different properties, the selection of a particular design method or design philosophy is a critical decision that must be made before the actual mechanics of the design process are initiated.

2.1 DESIGN METHODS

While many possible design methods or combinations of methods are available to the geotextile designer, the ultimate decision for a particular application usually takes one of three directions: (1) design by cost and availability, (2) design by specification, and (3) design by function.

2.1.1 Design by Cost and Availability

Design by cost and availability is quite simple. The funds available are divided by the area to be covered, and a maximum available unit price that can be allocated for the geotextile is calculated. The geotextile with the best properties for the primary function intended (recall Table 1.1) is then selected within this unit price limit and according to its availability. The method is obviously weak technically but is one that is still sometimes practiced. It perhaps typified the situation in the early days of geotextiles, but it is somewhat outmoded by current standards of practice.

2.1.2 Design by Specification

Design by specification is very common and is used almost exclusively when dealing with public agencies and many private owners as well. In this method several application categories are listed in association with various physical, mechanical, hydraulic, and/or endurance properties. The application areas are usually related to the intended primary function. A specification of this type used by the Pennsylvania Department of Transportation is shown in Table 2.1. Subsurface filtration focuses on underdrain systems and related drainage applications. The combined category of separation/stabilization/reinforcement is distinguished by the condition of the soil subgrade, thickness of aggregate base course, and type of vehicular loading; note the gradual increase in properties from Type A to Type C. Erosion control refers to geotextiles beneath rock riprap and articulated concrete mattress. The categories are distinguished by the site-specific installation survivability requirements. Sediment control refers to geotextile silt fences and is distinguished by having no geogrid support (Type A) and having a geogrid support (Type B). While the Penn DOT specification is typical in its format (listing the various common applications against minimum or maximum property values), it is not typical insofar as the numeric values of the various properties. In this case it is higher than most. Different agencies have different perspectives as to what properties and numeric values are important, and sometimes as to the test method of obtaining the numeric values.

 A federal agency that has formulated a unified approach in the United States is the American Association of State Highway and Transportation Officials (AASHTO). In its M288 geotextile specifications, AASHTO provides for three different strength classifications (see Table 2.2a) The classifications are essentially a list of strength properties meant to withstand varying degrees of installation survivability stresses. It is the first step in the process:

- *Class 1*: For severe or harsh survivability conditions where there is a greater potential for geotextile damage.
- *Class 2*: For typical survivability conditions; this is the default classification to be used in the absence of site specific information.
- *Class 3*: For mild survivability conditions where there is little or no potential for geotextile damage.

TABLE 2.1 PENNSYLVANIA DEPARTMENT OF TRANSPORTATION GEOTEXTILE REQUIREMENTS BASED ON APPLICATION AREA[1]

Geotextile Properties	Test Method	Subsurface Filtration	Separation Type A	Stabilization Type B	Reinforcement Type C	Erosion Control Type A	Erosion Control Type B	Sediment Control Type A	Sediment Control Type B
Grab tensile strength, N	ASTM D 4632	700	1200	1500[5]	1500[5]	900	400	900	400
Grab tensile elongation, %	ASTM D4632	20 min	50 min	20	20	15–50	15 min	15–50	15 min
Burst strength, kPa	ASTM D 3786	1300	3000	—	—	2200	960	2200	960
Puncture, N (8.0 mm flat-end rod)	ASTM D 4833	250	450	620	900	360	180	360	180
Trapezoidal tear strength, N	ASTM D 4533	250	450	—	—	220	130	220	130
Apparent opening size (AOS) sieve no.	ASTM D 4751	(2), (3)	(2), (3)	> No. 30	> No. 30	(2), (3)	(2), (3)	No. 20 max	No. 20 max
Permeability, K, cm/sec	ASTM D 4491	K fabric ≥ 10K soil[3]	K fabric ≥ 10K soil[3]	—	—	K fabric ≥ 10K soil[3]	K fabric ≥ 10K soil[3]	K fabric ≥ 10K soil[3]	K fabric ≥ 10K soil[3]
Permittivity, sec^{-1}	ASTM D4491	0.2	—	—	—	—	—	0.01	0.01
Seam strength, N[4]	ASTM D 4632	310	1070	1600	2000	800	360	360	—
Ultraviolet resistance strength retention, %	ASTM D 4355	70 @ 150 hr	70 @ 150 hr	70 @ 150 hr	70 @ 150 hr	70 @ 150 hr	70 @ 150 hr	70 @ 150 hr	70 @ 150 hr

Notes:

(1) Numerical values indicate minimum average roll value, or minimum to maximum range.

(2) Soil with 50% or less particles by weight passing No. 200 sieve, AOS≥No. 50 sieve. Soil with more than 50% particles by weight passing No. 200 sieve, AOS >No. 50 sieve

(3) Design specified.

(4) Applies to both field and/or manufactured seams.

(5) Minimum grab tensile strength for the warp and fill direction at maximum elongation.

83

TABLE 2.2a   AASHTO M288 GEOTEXTILE STRENGTH PROPERTY REQUIREMENTS

	Test Methods	Units	Geotextile Classification[1]					
			Class 1		Class 2		Class 3	
			Elongation <50%[2]	Elongation ≥50%[2]	Elongation <50%[2]	Elongation ≥50%[2]	Elongation <50%[2]	Elongation ≥50%[2]
Grab strength	ASTM D4632	N	1400	900	1100	700	800	500
Sewn seam strength[3]	ASTM D4632	N	1200	810	990	630	720	450
Tear strength	ASTM D4533	N	500	350	400[4]	250	300	180
Puncture strength[5]	ASTM D4833	N	500	350	400	250	300	180
Permittivity	ASTM D4491	sec^{-1}	Minimum property requirements for permittivity, AOS, and UV stability are based on geotextile application. Refer to Table 2.2b for subsurface filtration, Table 2.2c for separation, Table 2.2d for stabilization, or Table 2.2e for permanent erosion control.					
Apparent opening size	ASTM D4751	mm						
Ultraviolet stability	ASTM D4355	%						

Notes:

(1) Required geotextile classification is designated in Tables 2.2b, c, d, e for the indicated application. The severity of installation conditions for the application generally dictate the required geotextile class. Class 1 is specified for more severe or harsh installation conditions where there is a greater potential for geotextile damage and Classes 2 and 3 are specified for less severe conditions.

(2) As measured in accordance with ASTM D4632. *Note:* Woven geotextiles fail at elongations (strains) <50%, while nonwovens fail at elongation (strains) >50%.

(3) When sewn seams are required. Overlap seam requirements are application specific.

(4) The required MARV tear strength for woven monofilament geotextiles is 250 N.

(5) Puncture strength will likely change from ASTM D4833 to ASTM D6241 with approximately five times higher values.

The second step is to select one of different tables according to the specific application. These applications follow the intended primary function:

- *Table 2.2(b)*: Filtration applications as in highway underdrains.
- *Table 2.2(c)*: Separation when placed on firm strength subgrades.
- *Table 2.2(d)*: Stabilization when placed on moderate strength subgrades.
- *Table 2.2(e)*: Erosion control—for example, geotextiles serving as a filter beneath rock riprap.
- *Table 2.2(f)*: Temporary silt fences for sediment control.
- *Table 2.2(g)*: Geotextiles used for the prevention of reflective cracking in flexible pavement overlays.

TABLE 2.2b AASHTO M288 SUBSURFACE FILTRATION (CALLED "DRAINAGE" IN THE ACTUAL SPECIFICATION) GEOTEXTILE REQUIREMENTS

Property	Test Methods	Units	Requirements		
			Percent In-Situ Soil Passing 0.075 mm[1]		
			<15	15 to 50	>50
Geotextile class			Class 2 from Table 2.2a[2]		
Permittivity[3][4]	ASTM D4491	sec^{-1}	0.5	0.2	0.1
Apparent opening size[3][4]	ASTM D4751	mm	0.43 max. avg. roll value	0.25 max. avg. roll value	0.22[5] max. avg. roll value
Ultraviolet stability (retained strength)	ASTM D4355	%	50% after 500 hr of exposure		

Notes:

(1) Based on grain size analysis of in situ soil in accordance with AASHTO T88.

(2) Default geotextile selection. The engineer may specify a Class 3 geotextile from Table 2.2a for trench drain applications based on one or more of the following.

   (a) The engineer has found Class 3 geotextiles to have sufficient survivability based on field experience.

   (b) The engineer has found Class 3 geotextiles to have sufficient survivability based on laboratory testing and visual inspection of a geotextile sample removed from a field test section constructed under anticipated field conditions.

   (c) Subsurface drain depth is less than 2 m, drain aggregate diameter is less than 30 mm and compaction requirement is equal to or less than 95% of AASHTO-T99.

(3) These default filtration property values are based on the predominant particle sizes of the in situ soil. In addition to the default permittivity value, the engineer may require geotextile permeability and/or performance testing based on engineering design for drainage systems in problematic soil environments.

(4) Site specific geotextile design should be performed especially if one or more of the following problematic soil environments are encountered: unstable or highly erodable soils such as noncohesive silts; gap-graded soils; alternating sand/silt laminated soils; dispersive clays; and/or rock flour.

(5) For cohesive soils with a plasticity index greater than seven, geotextile maximum average roll value for apparent opening size is 0.30 mm.

TABLE 2.2c   AASHTO M288 SEPARATION GEOTEXTILE PROPERTY REQUIREMENTS

Property	Test Methods	Units	Requirements
Geotextile class			Class 2 from Table 2.2a[1]
Permittivity	ASTM D4491	$\sec^{-1}$	0.02[2]
Apparent opening size	ASTM D4751	mm	0.60 max. avg. roll value
Ultraviolet stability (retained strength)	ASTM D4355	%	50% after 500 hr. of exposure

Notes:
(1) Default geotextile selection. The engineer may specify a Class 3 geotextile from Table 2.2a based on one or more of the following:

    (a) The engineer has found Class 3 geotextiles to have sufficient survivability based on field experience.

    (b) The engineer has found Class 3 geotextiles to have sufficient survivability based on laboratory testing and visual inspection of a geotextile sample removed from a field test section constructed under anticipated field conditions.

    (c) Aggregate cover thickness of the first lift over the geotextile exceeds 300 mm and aggregate diameter is less than 50 mm.

    (d) Aggregate cover thickness of the first lift over the geotextile exceeds 150 mm, aggregate diameter is less than 30 mm, and construction equipment contact pressure is less than 550 kPa.

(2) Default value. Permittivity of the geotextile should be greater than that of the soil ($\Psi_g > \Psi_s$). The engineer may also require the permeability of the geotextile to be greater than that of the soil ($k_g > k_s$).

TABLE 2.2d   AASHTO M288 STABILIZATION GEOTEXTILE PROPERTY REQUIREMENTS

Property	Test Methods	Units	Requirements
Geotextile class			Class 1 from Table 2.2a[1]
Permittivity	ASTM D4491	$\sec^{-1}$	0.05[2]
Apparent opening size	ASTM D4751	mm	0.43 max. avg. roll value
Ultraviolet stability (retained strength)	ASTM D4355	%	50% after 500 hr of exposure

Notes:
(1) Default geotextile selection. The engineer may specify a Class 2 or 3 geotextile from Table 2.2a based on one or more of the following:

    (a) The engineer has found the class of geotextile to have sufficient survivability based on field experience.

    (b) The engineer has found the class of geotextile to have sufficient survivability based on laboratory testing and visual inspection of a geotextile sample removed from a field test section constructed under anticipated field conditions.

(2) Default value. Permittivity of the geotextile should be greater than that of the soil ($\Psi_g > \Psi_s$). The engineer may also require the permeability of the geotextile to be greater than that of the soil ($k_g > k_s$).

The following example illustrates the use of these AASHTO tables; the individual properties will be described later.

Example 2.1

Using the AASHTO M288 Specification of Table 2.2, determine what geotextile properties (to be described in detail in Section 2.3) are needed for the following applications:

TABLE 2.2e   AASHTO M288 PERMANENT EROSION CONTROL GEOTEXTILE REQUIREMENTS

			Requirements		
			Percent In Situ Soil Passing .075 mm [1]		
Property	Test Methods	Units	<15	15 to 50	>50
Geotextile class					
Woven monofilament geotextiles			Class 2 from Table 2.2a[2]		
All other geotextiles			Class 1 from Table 2.2a[2,3]		
Permittivity[4]	ASTM D4491	sec^{-1}	0.7	0.2	0.1
Apparent opening size[4]	ASTM D4751	mm	0.43 max. avg. roll value	0.25 max. avg. roll value	0.22[5] max. avg. roll value
Ultraviolet stability (retained strength)	ASTM D4355	%	50% after 500 hr of exposure		

Notes

(1) Based on grain size analysis of in situ soil in accordance with AASHTO T88.

(2) As a general guideline, the default geotextile selection is appropriate for conditions of equal or less severity than either of the following:

  (a) Armor layer stone weights do not exceed 100 kg, stone drop height is less than 1 m, and no aggregate bedding layer is required.

  (b) Armor layer stone weighs more than 100 kg, stone drop height is less than 1 m, and the geotextile is protected by a 150-mm thick aggregate bedding layer designed to be compatible with the armor layer. More severe applications require an assessment of geotextile survivability based on a field trial section and may require a geotextile with higher strength properties.

(3) The engineer may specify a Class 2 geotextile from Table 2.2a based on one or more of the following:

  (a) The engineer has found Class 2 geotextiles to have sufficient survivability based on field experience.

  (b) The engineer has found Class 2 geotextiles to have sufficient survivability based on laboratory testing and visual inspection of a geotextile sample removed from a field test section constructed under anticipated field conditions.

  (c) Armor layer stone weighs less than 100 kg, stone drop height is less than 1 m, and the geotextile is protected by a 150 mm thick aggregate bedding layer designed to be compatible with the armor layer.

  (d) Armor layer stone weights do not exceed 100 kg, stone is placed with a zero drop height.

(4) These default filtration property values are based on the predominant particle sizes of the in situ soil. In addition to the default permittivity value, the engineer may require geotextile permeability and/or performance testing based on engineering design for erosion control systems over problematic soil environments.

(5) (a) Site-specific geotextile design should be performed especially if one or more of the following problematic soil environments are encountered: unstable or highly erodable soils such a noncohesive silts; gap-graded soils; alternating sand/silt laminated soils; dispersive clays; and/or rock flour.

  (b) For cohesive soils with a plasticity index greater than seven, geotextile maximum average roll value for apparent opening size is 0.30 mm.

  (a) A nonwoven geotextile ($\varepsilon > 50\%$) pavement underdrain filter adjacent to soil with 60% passing the 0.075 mm sieve and under typical installation survivability conditions.

  (b) A woven geotextile ($\varepsilon < 50\%$) pavement separator between firm soil subgrade and stone base course, under typical survivability conditions according to the design engineer.

TABLE 2.2f   AASHTO M288 TEMPORARY SILT FENCE PROPERTY REQUIREMENTS

Property	Test Methods	Units	Supported Silt Fence[1]	Unsupported Silt Fence Geotextile Elongation $\geq 50\%$ [2]	Unsupported Silt Fence Geotextile Elongation < 50 [2]
Maximum Post Spacing			1.2 m	1.2 m	2.0 m
Grab strength	ASTM D4632	N			
Machine direction			400	550	550
X-Machine direction			400	450	450
Permittivity	ASTM D4491	sec^{-1}	0.05	0.05	0.05
Apparent opening size[3]	ASTM D4751	mm	0.60 max. avg. roll value	0.60 max. avg. roll value	0.60 max. avg. roll value
Ultraviolet stability (retained strength)[2]	ASTM D4355	%	70% after 500 hr of exposure	70% after 500 hr of exposure	

Notes

(1) Silt fence support shall consist of 14 gage steel wire with a mesh spacing of 150 mm by 150 mm or prefabricated polymeric mesh of equivalent strength.

(2) As measured in accordance with ASTM D4632.

(3) These default filtration property values are based on empirical evidence with a variety of sediments. For environmentally sensitive areas, a review of previous experience and/or site or regionally specific geotextile tests should be performed by the agency to confirm suitability of these requirements.

TABLE 2.2g   AASHTO M288 PREVENTION OF REFLECTIVE CRACKING, I.E., PAVING FABRICS, PROPERTY REQUIREMENTS

Property	Test Method	Units	Requirements
Grab strength	ASTM D4632	N	450
Mass per unit area	ASTM D3776	g/m^2	140
Ultimate elongation	ASTM D4632	%	≥ 50
Asphalt retention	Texas DOT Item 3099	lit/m^2	Notes (1) and (2)
Melting point	ASTM D276	°C	150

Notes

(1) Asphalt required to saturate paving fabric only. Asphalt retention must be provided in manufacturer certification. Value does not indicate the asphalt application rate required for construction. Refer to appendix in AASHTO M288 titled "Construction/Installation Guidelines" for discussion of asphalt application rate.

(2) Product asphalt retention property must meet the MARV provided by the manufacturer's certification.

Solution: Tables 2.2b to 2.2g are used for the appropriate application properties and then Table 2.2a is used for the required strength properties.

(a) First from Table 2.2b and then from Table 2.2a the required properties for the non-woven geotextile filtration fabric are as follows:

- Permittivity $\geq 0.1 \text{ sec}^{-1}$
- AOS ≤ 0.22 mm
- Grab strength ≥ 700 N
- Sewn seam strength ≥ 630 N
- Tear strength ≥ 250 N
- Puncture strength ≥ 250 N
- UV stability $\geq 50\%$ of 700 N, i.e., ≥ 350 N after 500 hrs.

(b) First from Table 2.2c and then from Table 2.2a the required properties for the woven geotextile separation fabric are as follows:
- Permittivity $\geq 0.02 \text{ sec}^{-1}$
- AOS ≤ 0.60 mm
- Grab strength ≥ 1100 N
- Sewn seam strength ≥ 990 N
- Tear strength ≥ 400 N
- Puncture strength ≥ 400 N
- UV stability $\geq 50\%$ of 1100 N—i.e., ≥ 550 N after 500 hrs

It must be cautioned that when using a design-by-specification method, the specifications sometimes list *minimum* required fabric properties, whereas some manufacturers' literature may list either *average-lot* or *minimum-average-roll* property values. (In this regard, the word *lot* is defined as any unit of production taken for sampling or statistical testing, having one or more common properties and being readily separable from other similar units. Thus, a lot can be as large as an entire production run, or as small as a few rolls of fabric for a specific project. The point is that a lot is arbitrary and must be agreed upon by the parties involved.) By comparing such a specification value to the manufacturer's listed values, you may be comparing different sets of numbers. This is so because average lot value is the mean value for the particular property in question from all the tests made on that lot of fabrics. This may be the compilation of thousands of tests made over many months or even years of production of that particular geotextile style. Thus the average lot value is considerably higher than the minimum value (see Figure 2.1). An intermediate value between these two extremes is the *minimum average roll value* (MARV)—the average of a representative number of tests made on selected rolls of the lot in question, which is limited in area to the particular site in question. This value is numerically equivalent to two standard deviations lower than the mean, or average, lot value. Thus we can see that MARV is the minimum of a limited series of average roll values. These different values are shown schematically in Figure 2.1.

Note that in a true statistical sense about 16% of all values will be lower than $\overline{X} - S$; 2.5% will be lower than $\overline{X} - 2S$; and 0.15% will be lower than $\overline{X} - 3S$,

where

$\overline{X}$ = mean value, and
S = standard deviation.
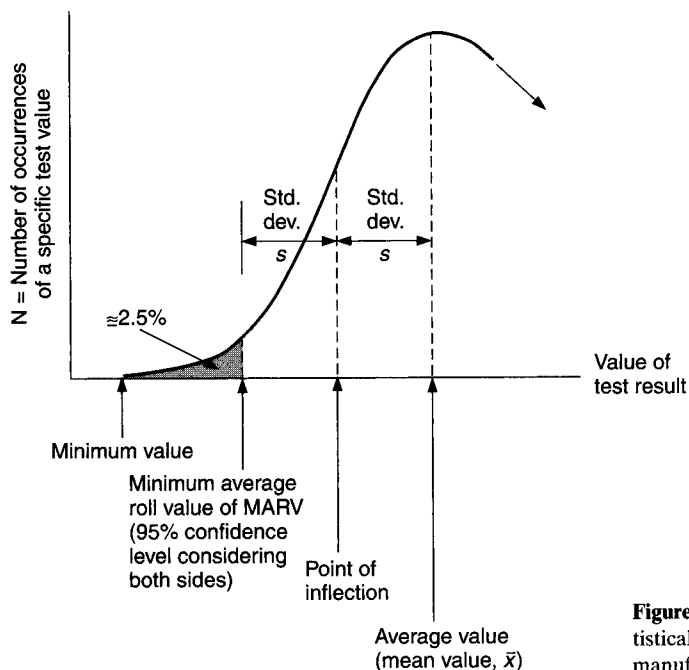
Figure 2.1   Relative relationships of different statistical values used in geotextile specifications and manufacturers' literature.

Furthermore, the minimum average roll value (MARV), with 2.5% of the values falling below $\overline{X} - 2S$ is also called the 95% confidence level. (The other 2.5% is above $\overline{X} + 2S$ and is obviously not of concern since these values are well in excess of that required). One other consideration should be mentioned: the case where one is targeting a maximum value, such as a maximum AOS opening size value. Here we are considering the right side of the curve of Figure 2.1 and the comparable value to MARV would logically become MaxARV.

The mean value $(\overline{X})$ is calculated using $\Sigma X_i / N$ and the standard deviation using

$$S = \left[\frac{(X_1 - \overline{X})^2 + (X_2 - \overline{X})^2 + \cdots + (X_N - \overline{X})^2}{N - 1} \right]^{1/2} \qquad (2.1)$$

where

$\overline{X}$ = mean value
X_i = measured value, and
N = number of measurements.

These are, of course, standard statistical definitions. Still further, the coefficient of variation "V," or simply "variance," is calculated using $(S/\overline{X})$ (100). The variance should be as low as possible, thereby indicating good quality control during manufacturing. Most

agencies, including AASHTO in its M288 specifications, presented in Tables 2.2a–g, recommend the use of MARV or MaxARV for use in both the specification and the listing of manufacturers' product data. Example 2.2 illustrates the meaning of MARV insofar as field conformance testing is concerned.

Example 2.2

Consider a field construction site where 150 rolls of geotextile are delivered. This value then defines the *lot*. The quality control or quality assurance inspector would *sample** a representative number of these rolls to determine MARV and see that it conforms with the value called for in the specification. Assume that the targeted value is grab tensile strength. A geotextile sample, full roll width and 1.0 m long, is taken from each of six randomly selected rolls in the lot. Note that according to ASTM D4354 on sampling technique, a lot consisting of from 126 to 216 rolls requires at least 6 rolls to be sampled. It is actually the cube root of the number of rolls in the lot. These samples are sent to an approved laboratory for testing. Within each sample, eight test *specimens* are taken and tested according to ASTM D4632, the grab tensile test method. Given the test data shown in the table below, determine MARV.

Solution: Assume that each of the six samples were cut into eight individual grab tensile specimens, were properly tested, and resulted in the following data set in units of newtons (N) at failure.

Specimen Test Number	Sample Number					
	1	2	3	4	5	6
1	643 N	627 N	637 N	642 N	652 N	637 N
2	627	615	643	646	641	624
3	652	621	628	658	639	631
4	629	616	662	641	657	620
5	632	619	646	635	642	618
6	641	621	633	642	651	633
7	662	622	619	658	641	641
8	<u>635</u>	<u>628</u>	<u>636</u>	<u>662</u>	<u>645</u>	<u>625</u>
Average	640	621	638	648	646	629

From this data set it is seen that MARV is 621 N, which must equal, or exceed, the MARV value of grab-tensile strength required by the specification. Note that there are six individual test values in the entire data set that are numerically less than 621. These represent the statistical 2.5% of the values less than MARV as illustrated by the shaded portion in Figure 2.1.

---

*Throughout this book, a roll of geosynthetics is *sampled* by cutting a piece or swatch from it. This sample is then taken to a laboratory from which *specimens* are cut to exact size for subsequent testing according to a particular test protocol. In some cases, the sample will be cut into sections and incubated in an oven, or in liquid, or under light exposure, etc. It is then called a *coupon*, which is subsequently cut into specimens for actual testing purposes. Thus, the order of size hierarchy for all geosynthetics is a lot, roll, sample, coupon (sometimes), and specimen.

In summary, the design-by-specification method must compare like sets of numbers. If the intent of the specification is to list MARVs (as it is with Tables 2.1 and 2.2a–g), then manufacturer's listed mean or average values must be decreased by two standard deviations (approximately 5 to 20%) if average lot values are given. Only if MARVs are given by the manufacturer can they be directly compared to a MARV-based specification value on a like-set-of-number basis.

In closing, it is hoped that both specifications and manufacturer's literature come together with a common unit that centers on MARV, or in a few cases MaxARV. It is a concept that everyone can live with, a value that can be field-verified, and a number that reflects the inherent variation in quality control of the manufacture of geotextiles.

2.1.3 Design by Function

Design by function consists of assessing the primary function that the geotextile will be asked to serve and then calculating the required numerical value of a particular property for that function. By dividing this value into the candidate geotextile's allowable property value, a factor of safety (FS) will result:

$$\text{factor of safety (FS)} = \frac{\text{allowable (test) property}}{\text{required (design) property}} \qquad (2.2a)$$

where

allowable property = a numeric value based on a laboratory test that models the actual situation or is adjusted accordingly,

required property   = a numeric value obtained from a design method that models the actual situation, and

factor of safety (FS) = FS against unknown loads and/or uncertainties in the analytic or testing process; sometimes called a *global factor of safety*.

If the factor of safety is sufficiently greater than 1.0, the candidate geotextile is acceptable. The above process can be repeated for a number of available geotextiles; if others are acceptable, then the final choice becomes one of availability and least cost. The individual steps in this process are as follows:

1. Assess the particular application, considering not only the candidate geotextile but the material system on both sides of it.
2. Depending on the criticality of the situation (i.e., "If it fails, what are the consequences?"), decide on a minimum factor of safety. This value may be suggested or imposed through regulations.
3. Decide on the geotextile's primary function.
4. Calculate numerically the required geotextile property value in question on the basis of its primary function.

5. Test for, or otherwise obtain, the candidate geotextile's allowable value of this particular property (recall the discussion in Section 2.1.2 on the recommended use of MARV values).
6. Calculate the factor of safety on the basis of the allowable property (Step 5) divided by required property (Step 4) per equation (2.2a).
7. Compare this factor of safety with the required value decided upon in Step 2.
8. If not acceptable, repeat the process with a geotextile having more appropriate properties.
9. If it is acceptable, determine whether any secondary function of the geotextile is more critical.
10. Repeat the process for other available geotextiles; if more than one satisfy the factor of safety requirement, select the geotextile on the basis of least cost and availability.

Note that the design-by-function process can also be used to solve for the required property value:

$$\text{required (design) property} = \frac{\text{allowable (test) property}}{\text{factor of safety}} \qquad (2.2b)$$

Both calculation procedures will be illustrated later.

The design-by-function approach will be used throughout this book. This method obviously necessitates identifying the primary function that the geotextile is to serve; thus this chapter (and the subsequent chapters) has been laid out accordingly. A brief treatment of the major functions that a geotextile can serve is given in the next section.

2.2 GEOTEXTILE FUNCTIONS AND MECHANISMS

Section 1.3.3, which provided an overview of geotextiles, alluded to the many applications falling into categories vis-à-vis their major function (recall Table 1.8). These categories—separation, reinforcement, filtration, drainage and containment—when properly identified, lead to the design-by-function method. The purpose of this section is to demonstrate technically what these functions mean with respect to geotextiles and to elaborate on the actual mechanisms embodied within each type of function.

2.2.1 Separation

The concept of separation can perhaps be illustrated by the engineering adage, "10 kilograms of stone placed on 10 kilograms of mud results in 20 kilograms of mud." With this in mind, a geotextile serving in a separation function can be defined as follows:

> *Geotextile separation:* The placement of a flexible porous textile between dissimilar materials so that the integrity and functioning of both materials can remain intact or be improved.

When placing stone aggregate on fine-grained soils, there are two simultaneous mechanisms that tend to occur over time. One is that the fine soils attempt to enter into the voids of the stone aggregate, thereby ruining its drainage capability; the other is that the stone aggregate attempts to intrude into the fine soil, thereby ruining the stone aggregate's strength. When this occurs we have a situation that has been called *sacrificial aggregate*, which is all too often the case without the use of a proper separating geotextile. The two mechanisms are shown schematically in Figure 2.2.

2.2.2 Reinforcement

Because geotextiles are materials possessing tensile strength, they can nicely complement those materials good in compression but weak in tension. Thus low-strength fine-grained silt and clay soils are prime targets for geotextile reinforcement. The following definition will clarify this point:

> *Geotextile reinforcement:* The synergistic improvement of a total system's strength created by the introduction of a geotextile (that is good in tension) into a soil (that is good in compression but poor in tension) or other disjointed and separated material.

Improvement in strength can be evaluated in a number of ways. The triaxial tests conducted by Broms [1] illustrate the beneficial effects of a geotextile when properly placed. Figure 2.3 shows two sets of triaxial tests on dense sand samples at confining pressures of 21 kPa and 210 kPa for different soil and geotextile configurations. In both parts, Curve 1 represents the baseline shear strength data of the sand by itself; Curve 2 has geotextiles on the extreme top and bottom of the soil and does not show improved shear strength behavior. Since these locations of the geotextiles are in the nonacting

Without geotextile   With geotextile
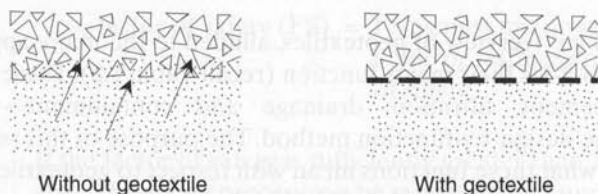
(a) Mechanism of fine soils pumping into stone aggregate voids
and prevention using geotextiles

Without geotextile   With geotextile
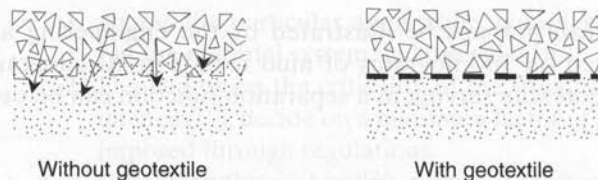
(b) Mechanism of stone aggregate intrusion into fine soil subgrade
and prevention using geotextiles

Figure 2.2   Different mechanisms involved in the use of geotextiles involved in the separation function.
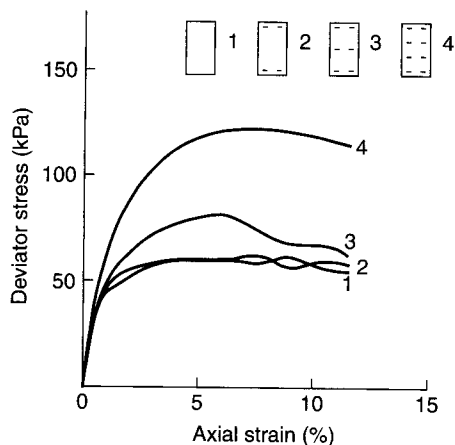
(a) Dense sand at 21 kPa confining pressure
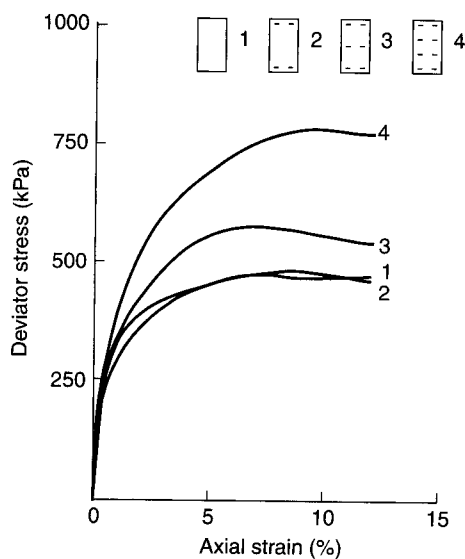
(b) Dense sand at 210 kPa confining pressure

Figure 2.3 Triaxial test results showing influence of geotextiles placed at various locations within soil specimen. (After Broms [1])

dead zones in conventional triaxial tests, this behavior is both logical and instructive. It is instructive because it is teaching us that if the geotextile is placed at the wrong location, it will have no beneficial effect. Upon placing the geotextile in the center of the sample, as with Curve 3, or at the one-third points, as with Curve 4, however, beneficial effects are easily seen. Here the geotextile interrupts potential shear planes and has the influence of increasing the overall shear strength of the now-reinforced soil. As expected, the double layers placed at the one-third points (Curves 4) are more beneficial than the single layer placed at the center of the sample (Curves 3).

Within the general function of geotextile reinforcement of soils, there are three different reinforcement mechanisms: (1) membrane type, (2) shear type, and (3) anchorage type.

Membrane Type. Membrane reinforcement occurs when a vertical force is applied to a geotextile that has been placed on a deformable subgrade. Depending on the depth at which the geotextile is placed from the force application, it is well established [2] that

$$\sigma_h = \frac{P}{2\pi z^2}\left[3\sin^2\theta\cos^3\theta - \frac{(1 - 2\mu)\cos^2\theta}{1 + \cos\theta}\right] \tag{2.3}$$

where

σ_h = horizontal stress at depth z and angle θ,

P = applied vertical force,

z = depth beneath surface where σ_h is being calculated,

μ = Poisson's ratio, and

θ = angle from the vertical beneath the surface load P.

Note that directly beneath the load, where $\theta = 0$ deg.,

$$\sigma_h = -\frac{P}{2\pi z^2}\left(\frac{1}{2} - \mu\right) \tag{2.4}$$

Since μ is less than 0.5, σ_h is negative (which is tension); that is, the applied vertical downward force produces tension on a horizontal plane beneath it. Thus tension results in the geotextile, which is precisely the objective of placing it there. As seen in equation (2.4), the larger the magnitude of P, the higher the tensile stress and the higher requirement of tensile strength of the geotextile. Also, the closer the geotextile is to the force (i.e., low values of z), the higher will be the applied stress on the geotextile. Many situations in which geotextiles are placed on soft soils or in a yielding situation use this particular reinforcement mechanism. When geotextiles are placed in closely spaced layers, as in walls and slopes, the situation is more complex but the principle is the same.

Shear Type. Shear reinforcement was illustrated by the triaxial tests of Figure 2.3 but can be better visualized by means of direct shear tests. Here a geotextile placed on a soil is loaded in a normal direction, and then the two materials are sheared at their interface. The resulting geotextile-to-soil shear strength parameters (adhesion and friction angle) can be obtained as described in a traditional geotechnical manner using an adapted form of the Mohr-Coulomb failure criterion,

$$\tau = c_a + \sigma'_n \tan\delta \tag{2.5a}$$

where

τ = shear strength (between the geotextile and soil),

σ_n' = effective normal stress on the shear plane,

c_a = adhesion (of the geotextile to the soil), and

δ = friction angle (between the geotextile and soil).

The shear strength parameters c_a and δ can be compared with the shear strength parameters of the soil by itself (i.e., soil against soil) as follows:

$$\tau = c + \sigma_n' \tan \phi \qquad (2.5b)$$

where

c = cohesion (of soil-to-soil)

ϕ = friction angle (of soil-to-soil)

Furthermore,

$$E_c = (c_a/c)\ 100 \qquad (2.6)$$

$$E_\phi = (\tan \delta/\tan\phi)\ 100 \qquad (2.7)$$

where

E_c = efficiency of cohesion mobilization, and

E_ϕ = efficiency of soil friction angle mobilization.

These ratios, generally called *efficiencies*, have limiting values of zero to unity. While a numeric value higher than unity is possible, such values cannot be mobilized since the failure plane would simply move into the soil itself and the situation reverts from equation (2.5a) to (2.5b).

Anchorage Type.   Anchorage reinforcement is similar to the shear type just described, but now the soil acts on both sides of the geotextile as a tensile force tends to pull the geotextile out of the soil. The laboratory modeling of this type of mechanism is similar to direct shear except that now the upper and lower soil is stationary in both halves of the test device and the geotextile extends out of the device at its center. It is gripped externally and pulled, while normal compressive stresses act on the soil and geotextile within the test box setup. The situation is readily described in terms of shear strength parameters by themselves and efficiencies as just discussed. Another approach could be to express the efficiency as a function of the amount of mobilized geotextile strength. Wide-width tensile values should be used in this case. Here anchorage efficiencies greater than unity can occur but are usually limited by the tensile strength of the geotextile. As with the other types of mechanisms of geotextile reinforcement,

this category of geotextile anchorage is used quite often. The applications mentioned in Section 1.3.3 illustrate the point.

For calculations, we will use the shear strength mobilized by the geotextile with the soil above and with the soil below and arithmetically sum the two values as the limiting anchorage value. In the absence of anchorage tests, we will use direct-shear-generated values for this purpose.

2.2.3 Filtration

The geotextile function of filtration involves the movement of liquid through the geotextile itself—i.e., across its manufactured plane. At the same time, the geotextile must serve the purpose of retaining the soil on its upstream side. Both adequate permeability requiring an open fabric structure and soil retention requiring a tight fabric structure are required simultaneously. A third factor is also involved: a long-term soil-to-geotextile flow compatibility that will not excessively clog the fabric during the lifetime of the system. Thus geotextile filtration can be defined as follows:

> *Geotextile filtration:* The equilibrium soil-to-geotextile system that allows for adequate liquid flow with limited soil loss across the plane of the geotextile over a service lifetime compatible with the application under consideration.

This function of filtration is a major one for the geotextile industry (recall the application areas presented in Section 1.3.3). Geotextiles, when properly designed and constructed, offer a practical remedy to many problems involving the flow of liquids.

Permeability.   This particular discussion of geotextile permeability refers to cross-plane permeability when liquid flow is perpendicular to the plane of the fabric. Some of the geotextiles used for this purpose are relatively thick and compressible. For this reason the thickness is included in the permeability coefficient and is used as *permittivity*, which is defined as follows:

$$\psi = \frac{k_n}{t} \tag{2.8}$$

where

ψ = permittivity,
k_n = cross-plane permeability coefficient (the subscript n is often
         omitted), and
t = thickness at a specified normal pressure.

The testing for geotextile permittivity follows similar lines as used for testing soil permeability. It should be noted that some designers prefer to work directly with permeability and require the geotextile's permeability to be some multiple of the adjacent soil's permeability—e.g., 0.1, 1.0, or 10.0 (see Christopher and Fisher [3]).

Soil Retention.   For the required flow of liquid to be allowed through the geotextile, the void spaces in it must be sufficiently large. There is, however, a limit—that being when the upstream soil particles start to pass through the geotextile voids along with the flowing liquid. This can lead to an unacceptable situation called *soil piping*, in which soil particles are carried through the geotextile, leaving unstable soil voids behind. The velocity of the liquid then increases, accelerating the process, until the upstream soil structure begins to collapse. This collapse often leads to small sinkhole-type patterns that grow larger with time.

This process is prevented by making the geotextile voids tight enough to retain the soil on the upstream side of the fabric. It is the coarser soil fraction that must be initially retained and that is the targeted soil size in the design process. These coarser-sized particles eventually block the finer-sized particles and build up a stable upstream soil structure. Fortunately, filtration concepts are well established in the design of soil filters, and those same ideas will be used to design an adequate geotextile filter.

There are many formulas that can be applied to soil-retention design, most of which use the soil particle size characteristics and compare them to the 95% opening size of the geotextile—i.e., defined as O_{95} of the geotextile. The test method used in the United States to determine this value is called the *apparent opening size* (AOS) and is obtained using a dry-sieving method. In Europe and Canada, the test method is called *filtration opening size* (FOS), and it is accomplished by wet or hydrodynamic sieving. Both of these latter methods are preferable to the dry-sieving method used in the United States.

The simplest of the design procedures examines the percentage of soil passing the No. 200 sieve, whose openings are 0.074 mm. According to AASHTO [4], the following is recommended:

- For soil with $\leq 50\%$ passing the No. 200 sieve: $O_{95} < 0.60$ mm—i.e., AOS of the fabric $\geq$ No. 30 sieve.
- For soil $>50\%$ passing the No. 200 sieve: $O_{95} < 0.30$ mm—i.e., AOS of the fabric $\geq$ No. 50 sieve.

Beginning in 1972, a series of direct comparisons of geotextile-opening size (O_{95}, O_{50}, or O_{15}) was made in ratio form to some soil particle size to be retained (d_{90}, d_{85}, d_{50}, or d_{15}; see Christopher and Fischer [3]). The numeric value of the ratio depends upon the geotextile type, soil type, flow regime, etc. For example, Carroll [5] recommends the following:

$$O_{95} < (2 \text{ or } 3) \, d_{85} \qquad\qquad (2.9)$$

where d_{85} is the soil particle size in mm, for which 85% of the total soil is finer.

In contrast to the simplified methods above, a more comprehensive approach toward soil retention criteria is given in Figure 2.4(a) and (b), for steady-state and dynamic flow conditions, respectively (Luettich et al. [6]). To utilize the figures, we must first characterize the upstream soil. A grain-size distribution, along with Atterberg limits and dispersivity characteristics for the fine fraction, are necessary. An example illustrates the use of each of the figures.

Figure 2.4a Soil retention criteria for geotextile filter design using *steady-state flow* conditions. (After Luettich et al. [6])

From soil property tests

More than 90% gravel
($d_{10} > 4.8$ mm)

Less than 10% fines and less than 90% gravel
($d_{10} > 0.075$ mm, and $d_{10} < 4.8$ mm)

Less than 20% clay and more than 10% fines
($d_{20} > 0.002$ mm, and $d_{10} < 0.075$ mm)

More than 20% clay
($d_{20} < 0.002$ mm)

Nonplastic soil
(PI < 5)

Plastic soil
(PI > 5)

Nondispersive soil
(DHR < 0.5)

Dispersive soil
(DHR > 0.5)

Application favors permeability

Application favors retention

Stable soil
($1 < C_c < 3$)

Unstable soil
($C_c > 3$ or $C_c < 1$)

Use straight line drawn tangent at d_{50} to obtain C_u'

Use straight line through d_{30} and d_{10} to obtain C_u'

Use straight line through d_{60} and d_{30} to obtain C_u'

Uniformly graded
$C_u' < 3$

Widely graded
$C_u' > 3$

Loose
($I_D < 35\%$)

Medium
($35\% < I_D < 65\%$)

Dense
($I_D > 65\%$)

Loose
($I_D < 35\%$)

Medium
($35\% < I_D < 65\%$)

Dense
($I_D > 65\%$)

$O_{95} < C_u' d_{50}$

$O_{95} < 1.5 C_u' d_{50}$

$O_{95} < 2 C_u' d_{50}$

$O_{95} < \dfrac{9}{C_u'} d_{50}$

$O_{95} < \dfrac{13.5}{C_u'} d_{50}$

$O_{95} < \dfrac{18}{C_u'} d_{50}$

$O_{95} < 0.21$ mm

Use 75 to 150 mm of fine sand between soil and geotextile, then design the geotextile as a filter for the sand

NOTES:

d_x is the particle size of which x percent is smaller

$$C_u' = \sqrt{\dfrac{d'_{100}}{d'_0}}$$

where d'_{100} and d'_0 are the extremities of a straight line drawn through the particle-size distribution, as directed above; and d'_{50} is the midpoint of this line.

$$C_u = \dfrac{d_{60}}{d_{10}}$$

$$C_c = \dfrac{(d_{30})^2}{d_{60} \times d_{10}}$$

I_D = relative density of the soil
PI = plasticity index of the soil
DHR = double-hydrometer ratio of the soil

$O_{95} < 10\ d_{50}$; $O_{95} < d_{90}$; and $O_{95} < 0.1$ mm

Use 75 to 150 mm of fine sand, then design the geotextile as a filter for the sand

$O_{95} < d_{50}$

$O_{95} < 2.5\ d_{50}$ and $O_{95} < d_{90}$

$d_{50} < O_{95} < d_{90}$

Nondispersive soil (DHR < 0.5)

Dispersive soil (DHR > 0.5)

Plastic soil (PI > 5)

Nonplastic soil (PI < 5)

Widely graded ($C_u > 5$)

Uniformly graded ($C_u \le 5$)

Severe wave attack

Mild water currents

More than 30% clay ($d_{30} < 0.002$ mm)

Less than 30% clay and more than 50% fines ($d_{30} > 0.002$ mm, and $d_{50} < 0.075$ mm)

Less than 50% fines and less than 90% gravel ($d_{50} > 0.075$ mm, and $d_{10} < 4.8$ mm)

More than 90% gravel ($d_{10} > 4.8$ mm)

From soil property tests

NOTES: $C_u = \dfrac{d_{60}}{d_{10}}$

d_x = particle size of which x percent is smaller
PI = plasticity index of the soil
DHR = double-hydrometer ratio of the soil
O_{95} = geotextile opening size

Figure 2.4b Soil retention criteria for geotextile filter design under *dynamic flow* conditions.
(After Luettich et al. [6])

Example 2.3

What is the appropriate formula to obtain the required O_{95} of a geotextile filter under steady-state flow conditions if the upstream soil is 25% less than 0.002 mm and the fine fraction is nondispersive?

Solution: From Figure 2.4(a), we see that $O_{95} < 0.21$ mm, which is equivalent to a #70 sieve or tighter.

Example 2.4

What is the appropriate formula to obtain the required O_{95} of a geotextile filter under dynamic flow conditions if the upstream soil is less than 50% fines and less than 90% gravel and the situation is one of severe wave attack.

Solution: From Figure 2.4(b), we see that $O_{95} < d_{50}$, where d_{50} is the median particle size of the upstream soil.

Long-Term Flow Compatibility.   Perhaps the most frequently asked question regarding the use of geotextiles in hydraulic-related systems is, "Will it eventually clog?" Obviously, some soil particles will embed themselves on, or within, the geotextile structure and an understandable reduction in permeability or permittivity will almost always occur. This type of *partial clogging* is expected. A more perceptive question asks if the geotextile will *excessively clog*, such that the flow of liquid through it will be decreased to the point where the system will not adequately perform its function. There are guidelines available for noncritical, nonsevere cases [3], but the question can be answered directly by taking a soil sample and the candidate geotextile(s) and testing them in the laboratory. We must perform one of three techniques: (1) the gradient ratio (GR) tests [7] such that the $GR \leq 3.0$, (2) long-term flow (LTF) tests [8] such that the terminal slope of the flow rate versus time curve is adequate for site specific conditions, or (3) the hydraulic conductivity ratio (HCR) tests [9], such that resulting HCR values are between 0.7 and 0.3. These tests will be described later.

A different approach to the excessive clogging question is simply to avoid situations that have been known to lead to such problems. Experience will show that the following conditions give rise to concerns about geotextile filter applications:

- Poorly graded (i.e., all uniform size) fine, cohesionless, soils such as loess, rock flour, and stone quarry fines.
- Cohesionless soils consisting of gap-graded, particle-size distributions and functioning under high hydraulic gradients.
- Dispersive clays that separate into individual fine particles over time. Note, however, that nondispersive clays possessing true cohesion are generally not troublesome due to these same cohesive forces keeping the upstream soil structure intact.
- High-alkalinity groundwater where the slowing of the liquid as it flows through the geotextile can cause a calcium, sodium, or magnesium precipitate to be deposited.
- High-suspended solids in the permeating liquid, as found in turbid river water or dredged water that can build up on, or within, the geotextile.

- High-suspended solids coupled with high-microorganisms content, as in landfill leachates [10] and agricultural wastes, can combine to build up on, or within, the geotextile.

For all of these cases we could use a relatively open geotextile and allow for fine particles, sediment, or microorganisms to pass through into the downstream drain. In such cases we would generally consider two options:

- woven geotextiles with open area ≥ 10%
- nonwoven geotextiles with porosity ≥ 50% (under site specific normal stress conditions)

Recognize, however, that whatever the downstream drain is (gravel, drainage core, perforated pipe, etc.) it must be designed to adequately accept and transport the particulate matter without itself excessively clogging.

This discussion of soil-to-geotextile compatibility assumes the establishment of a set of mechanisms that are in equilibrium with the flow regime being imposed on the system. Numerous attempts at insight into these phenomena have been attempted (see McGown [11], Heerten [12], and Giroud [13]). There exists a number of possibilities, including upstream soil filter formation, blocking, arching, partial clogging, and depth filtration. These are shown schematically in Figure 2.5. With respect to how these mechanism interact, it has been suggested that the geotextile serves as a *catalyst* to promote the upstream soil and the now soil-modified geotextile to generate its own internal filter system. Obviously, a number of phenomena are working together simultaneously, and just what mechanism dominates under what conditions of soil type, geotextile type, and flow regime is still an issue that deserves further investigation.

2.2.4 Drainage

Fabrics placed in such a way as to transmit liquid within the plane of their structure provide a drainage function. Thus drainage can be defined as follows:

> *Geotextile drainage:* The equilibrium soil-to-geotextile system that allows for adequate liquid flow with limited soil loss within the plane of the geotextile over a service lifetime compatible with the application under consideration.

All geotextiles can provide such a function but to widely varying degrees [14]. For example, thin woven geotextiles, by virtue of their fibers crossing over and under one another, can transmit liquid within the spaces created at these crossover points, but to an extremely low degree. Conversely, thick, nonwoven needle-punched geotextiles have considerable void space in their structure, and this space is available for liquid transmission. Furthermore (to preview the discussion in Chapters 4 and 9), geonets and drainage geocomposites can transmit much more liquid than can geotextiles—even thick, bulky ones. Obviously, proper design will dictate just what type of geosynthetic drainage material is necessary.

(a) Formation of an upstream soil filter

(b) Upstream particles blocking geotextile openings

(c) Upstream particles arching over geotextile openings

(d) Soil particles clogged within geotextile structure

(e) Depth filtration concept using thick geotextiles
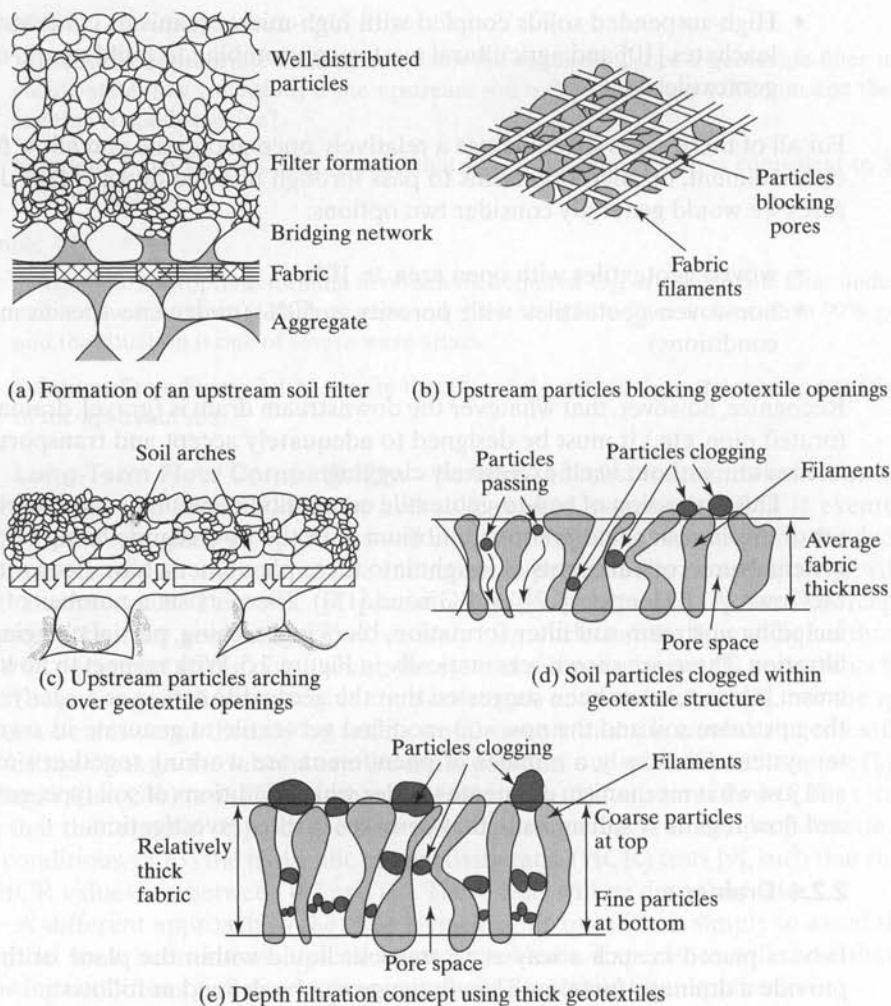
Figure 2.5 Various hypothetical mechanisms involved in long-term soil-to-fabric flow compatibility. (Parts [a–d] after McGown [11]; part [e] after Heerten [12])

Note that this discussion on drainage overlaps considerably the preceding section on filtration. For these two functions (except for the consideration of flow direction) the soil retention and long-term compatibility concepts are the same.

Permeability.   Referring now to in-plane permeability for the drainage function, we must recognize that the geotextile's thickness will decrease with increasing normal stress on it. For this reason we will define a term called *transmissivity* as follows:

$$\theta = k_p t \qquad (2.10)$$

where

> θ = transmissivity,
> k_p = in-plane permeability coefficient (the subscript p is often omitted), and
> t = thickness at a specified normal pressure.

The testing method for geotextile transmissivity will be covered later.

Soil Retention.   The criteria used to design the opening spaces of a geotextile so that it retains the adjacent soil were covered in Section 2.2.3. The concepts and design guides are precisely the same for the drainage function as they were for filtration.

Long-Term Flow Compatibility.   As with the filtration function, we must ensure the compatibility of the soil with the geotextile over the lifetime of the system being built. The criteria discussed in Section 2.2.3 hold for the drainage function the same as they do for filtration.

2.2.5 Containment

By virtue of their inherent porosity, geotextiles rarely serve in the containment function. The exception is when the geotextile is purposely impregnated with bitumen or polymer. These few applications will be noted accordingly.

2.2.6 Combined Functions

The introduction to this chapter described design-by-function. The procedure as outlined identified the geotextile's primary function and set the design accordingly. Where geotextiles are used for a single function, this can indeed be done. However, geotextiles often serve multiple or combined functions. Some examples will illustrate this:

- Beneath railroad ballast, where separation, reinforcement, filtration, and drainage can all be involved.
- In flexible-forming systems to contain concrete, grout, or soil, where separation, reinforcement, and filtration are involved.
- For prevention of crack reflection in asphalt pavement overlays, where both reinforcement and waterproofing functions are involved.

In these situations all functions—primary, secondary, tertiary, and so on—must be evaluated. They must all satisfy the required factor of safety (FS). If the situation is properly assessed, the calculated FS should increase progressively as we proceed through the primary, secondary, tertiary, etc., functions. If not (i.e., if the factors of safety jump around as we proceed through the calculations), it means that the critical functions were not properly assessed to begin with. Thus the minimum FS will always indicate the primary function, the next highest value of FS will indicate the secondary function, and so on. This approach, of course, assumes that a reasonably accurate quantitative

analysis can be developed for each of the functions described. Before we discuss this, however, we will treat a very important aspect of the subject dealing with specific geotextile properties and how they are obtained. That subject is a quantification of geotextile properties via their current test methods and procedures that follows.

2.3 GEOTEXTILE PROPERTIES AND TEST METHODS

This section presents the necessary test methods, relevant details, and selected data for the design-by-function procedure to be developed in the remainder of the chapter. (It also applies to the design-by-specification procedure.) The reader should refer back to this section continuously as the various design methods are developed, since results from these test methods become the numerator of the design-by-function equation (recall equations 2.2a and 2.2b).

2.3.1 General Comments

In a growing area such as geotextiles, it should come as no surprise that a completely unified set of worldwide standards and test methods is currently not available. Yet the activity toward such an ultimate goal is very intense. Organizations that are involved in this activity are spread across the entire spectrum of potential users: raw material suppliers, manufacturers, manufacturers representatives, contractors and installers, testing organizations, design engineering firms, owners, regulators, research institutes, and (of course) universities.

Within these groups we will often hear reference to either *index* or *performance* tests. This terminology is somewhat unfortunate, since a particular index test to one group might be (and usually is) very much a performance test to another group. For example, a geotextile puncture test using a steel probe may be of an index variety to a geotechnical engineer, but to the manufacturer it is instead a measure of the quality control performance of the particular manufacturing process. Thus, this book does not make continual reference to a test method as being either index- or performance-related, but when it does so, the test method is identified from the perspective of the design engineer.

In the review of available geotextile test methods that follows, it should be recognized that many of the test methods are not fully harmonized between countries as far as their test procedures are concerned [15]. The two main groups developing and promoting test methods are American Society for Testing and Materials (ASTM) and the International Organization for Standardization (ISO). The standards from these two groups will be constantly referenced in this book.

It should come as no surprise that many physical and mechanical test methods for geotextiles are partially, or completely, taken from existing textile standards [16–19]. The tests that differ between textiles and geotextiles are those that involve hydraulic, endurance, and environmental properties. These are generally new tests oriented completely toward geotextiles.

The section will be subdivided into the following major categories: (1) physical properties, (2) mechanical properties, (3) hydraulic properties, (4) endurance properties, and (5) degradation considerations.

2.3.2 Physical Properties

The properties discussed in this subsection all refer to the geotextile in its manufactured or as-received condition. These tests are often referred to as being index tests.

Specific Gravity.   The specific gravity of the fibers from which geotextiles are made is actually the specific gravity of the polymeric feed stock (see ASTM D792 or D1505). As customary, specific gravity is defined as the ratio of the material's unit volume weight (without any voids) to that of distilled, de-aired water at 4°C. Some typical values of the specific gravity of commonly used polymeric materials made into geotextiles are listed below (steel, soil, glass and cotton are added for comparison).

- Steel = 7.87
- Soil/rock = 2.9 to 2.4
- Glass = 2.54
- Polyvinyl chloride = 1.69
- Cotton = 1.55
- Polyester = 1.38 to 1.22
- Nylon = 1.14 to 1.05
- Polyethylene = 0.96 to 0.90
- Polypropylene = 0.91

Note that the specific gravity of some of the polymers (e.g., the polyolefins) is less than 1.0, which must be considered when working in water because they will float.

Mass per Unit Area (Weight).   *Mass per unit area* is the proper term for what most people mean when they state or ask for the "weight" of a geotextile. It is also sometimes called *basis weight*, but this is equally incorrect, since neither weight nor basis weight explicitly considers area. Geotextile mass per unit area (the proper term) is given in units of grams per square meter (g/m^2). Unfortunately, still other values are listed in the literature, such as grams per linear meter for a geotextile of given width. Sometimes the latter value is given inversely as linear meters per kilogram. The point here is that we must clearly state what value is being communicated. Methods for the test are ASTM D5261 and ISO 9864.

Testwise, the mass (or weight) should be measured to the nearest 0.01% of the total specimen mass, and length and width should be measured under zero geotextile tension. The range of typical values for most geotextiles is from 150 to 750 g/m^2 although geotextiles in excess of 2000 g/m^2 have been used. Since fabric cost (and, in general, mechanical properties) is directly related to mass per unit area, it is an important property.

Thickness.   The thickness of geotextiles is sometimes mentioned in specifications, but this is really more of a descriptive property than design-oriented property. It is measured as the distance between the upper and lower surface of the fabric, measured at a specified pressure. ASTM D5199 stipulates that the thickness of a geotextile is to

be measured to an accuracy of at least 0.02 mm under a pressure of 2.0 kPa. The comparable ISO 9863 test method allows for the specifier to select the pressure. The thicknesses of commonly used geotextiles range from 0.25 to 3.5 mm.

Stiffness.   Stiffness, or flexibility, of a geotextile should not be confused with its modulus (which is determined as the initial portion of the stress-versus-strain curve). In this test, stiffness is a measure of the interaction between the geotextile mass and its bending stiffness as shown by the manner in which the geotextile gravitationally bends under its own weight; the test method is designated as ASTM D1388. It is more appropriately called *flex stiffness*. The method takes a 25-mm-wide strip of geotextile specimen and slides it out lengthwise over the edge of a horizontal surface. The length of overhang is measured when the tip of the geotextile bends under its own weight and just touches an inclined plane making an angle of 41.5° with the horizontal. One-half of this length is the bending length of the specimen. The cube of this quantity multiplied by the mass per unit area of the geotextile is its flexural rigidity or stiffness. The value is expressed in mg-cm units.

The property is indicative of the geotextile's inherent capability of providing a suitable working surface for installation. In placing a geotextile on extremely soft soils, a high geotextile stiffness is very desirable. Haliburton et al. [20] have related this property to various soil subgrade strength values as given in Table 2.3.

2.3.3 Mechanical Properties

The mechanical properties to be discussed here indicate a geotextile's resistance to tensile stresses mobilized from applied loads and/or installation conditions. Some are

TABLE 2.3 RECOMMENDED GEOTEXTILE STIFFNESS VALUES FOR VARYING DEGREES OF REQUIRED WORKABILITY

Subgrade CBR[1] (%)	Workability Benefit of Vegetative Cover[2]	Field Workability Requirements	Minimum Fabric Stiffness[3] (mg · cm)
CBR ≤ 0.5	Poor	Very high	25,000
	Good	High	15,000
0.5 < CBR ≤ 1.0	Poor	High	15,000
	Good	Moderate	10,000
1.0 < CBR ≤ 2.0	Poor	Moderate	10,000
	Good	Low	5,000
CBR > 2.0	Poor	None	1,000
	Good	None	1,000

1. CBR refers to *soaked* California Bearing Ratio (CBR) which is a test routinely used in geotechnical engineering to evaluate soil subgrade strength. The values for *unsoaked* CBR are considerably higher. The test, both soaked and unsoaked alternatives, is standardized as ASTM D1883.

2. Medium to dense root system will probably exhibit some inherent workability benefits, whereas little to no root system will be of no benefit.

3. Test conforms to ASTM D1388, except uses 300 mm long by 50 mm wide test specimens.

Source: After Haliburton et al. [20].

performed with the geotextile by itself (i.e., often called *index*, or *in-isolation tests*) while others are associated with a standard soil or with the site-specific soil (i.e., often called *performance tests*).

Compressibility.   The compressibility of a geotextile is its thickness at varying applied normal stresses. For most geotextiles, the compressibility is relatively low and of little direct consequence as far as design is concerned (e.g., with woven fabrics and with nonwoven heat-bonded and heavily calendered geotextiles). For nonwoven needle-punched or bulky resin-bonded geotextiles, however, compressibility is important. This is because such geotextiles are often used to convey liquid within the plane of their structure. The more a fabric compresses under load, the lower its transmissivity. Figure 2.6 illustrates the compressibility of several geotextile types, where the influence of normal stress on thickness is clearly seen. The nonwoven needle-punched geotextiles are the most compressible, and this in turn is directly related to their mass per unit area.

Tensile Strength.   Perhaps the single most important property of a geotextile is its tensile strength. In this regard, "strength" is defined as the maximum tensile stress that the test specimen can sustain at the point of failure. Invariably all geotextile applications rely on this property either as the primary function (as in reinforcement applications) or as a secondary function (as in separation, filtration, or drainage). The actual performance of the test contains the geotextile test specimen within a set of clamps or grips, then places this assembly in a constant rate of extension (CRE) testing machine,
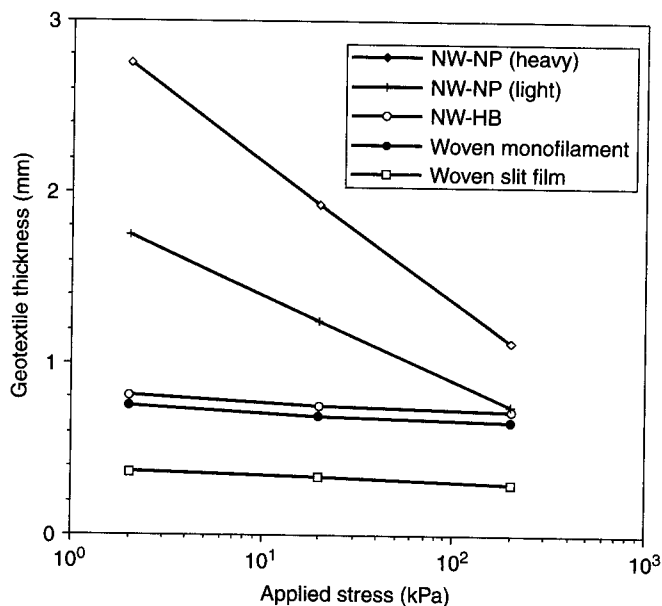
Figure 2.6   Compressibility of different types of geotextiles, including nonwoven needle-punched (NW-NP) and nonwoven heat-bonded (NW-HB).

and then stretches the geotextile in tension until failure occurs. Fabric failure is generally easy to identify and often it is even audible. During the extension process, it is customary to measure both load and deformation in such a way that a stress-versus-strain curve can be generated. Stress here is usually given as force per unit width. From the stress-versus-strain curve (strain calculated as deformation divided by original specimen length), four values are obtained:

1. Maximum tensile stress (referred to as the geotextile's *strength*)
2. Strain at failure (generally referred to as *maximum elongation*, or simply *elongation*)
3. Toughness (work done per unit volume before failure, usually taken as the area under the stress-strain curve)
4. Modulus of elasticity (which is the slope of the initial portion of the stress-versus-strain curve)

Typical responses of geotextiles made from different manufacturing processes are given in Figure 2.7. Note that the vertical axis is in units of force per unit width of fabric (i.e., kN/m) which is not a bona fide stress unit. To obtain true stress units, this value would have to be divided by the geotextile's thickness. This is not conventionally done, since the thickness varies greatly under load and during the extension process. This, of course, has implications in the toughness and modulus values as well, since they too would have to be divided by thickness to obtain conventional engineering units. The example that follows illustrates these features.

Example 2.5

For the nonwoven heat-bonded geotextile illustrated in Figure 2.7 (Curve D), determine the strength, elongation, toughness, and modulus in common geotextile units and (on the basis of a nominal thickness of 0.33 mm) in standard engineering units.

Solution: By observation, the strength is

$$T_{\max} = 23 \text{ kN/m}$$

and for 0.33 mm thickness,

$$\sigma_{\max} = 69{,}700 \text{ kN/m}^2 = 69{,}700 \text{ kPa}$$

The elongation, i.e., maximum strain, is also determined by observation:

$$\epsilon_f = 69\%$$

The toughness (U) is then calculated as 1/2 ($T_{max} \times \epsilon_f$) (actually this is an approximation since it should be the area under the curve):

$$U_g = \frac{1}{2}(23 \times 0.69)$$

$$= 7.9 \text{ kN/m}$$

and for 0.33 mm thickness,

$$U = 24{,}000 \text{ kN/m}^2 = 24{,}000 \text{ kPa}$$

To 60 kN/m at
30% strain

Curve	Manufacturing Type	Mass/Unit Area (g/m^2)	Thickness (mm)
A	Woven monofilament	200	0.38
B	Woven slit-film	170	0.25
C	Woven multifilament	270	0.71
D	Nonwoven heat-bonded	135	0.33
E	Nonwoven needle-punched	200	0.63
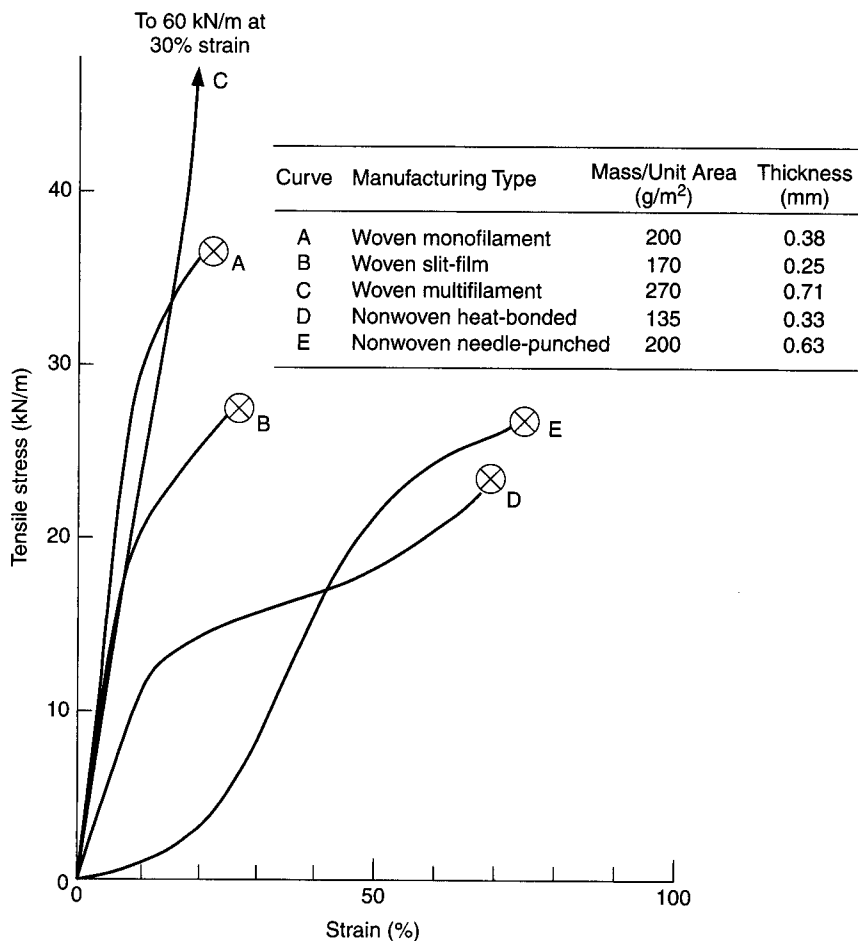
Figure 2.7   Tensile test response of various geotextiles manufactured by different processes. All are polypropylene fabrics; specimens were initially 200 mm wide by 100 mm high and tested according to ASTM D4595.

Finally, the modulus is taken from the initial slope of the curve as

$$E = \frac{12}{0.10} = 120 \text{ kN/m}$$

and for 0.33 mm thickness,

$$E = 364,000 \text{ kN/m}^2 = 364,000 \text{ kPa}$$
$$= 364 \text{ mPa}$$

There are several features of the tensile test that require further discussion, since they have implications for subsequent design procedures, the major ones being the

modulus and the specimen size. Regarding the modulus, several choices are available for measuring the initial slope of the curve:

- *Initial tangent modulus:* This is straightforward for many woven geotextiles in both their warp and weft directions and for nonwoven heat-bonded geotextiles. Here the initial slope is quite linear (as in conventional soil testing) and a reasonably accurate modulus value can be obtained.
- *Offset tangent modulus:* This concept is sometimes used when the initial slope is very low and is typical of nonwoven needle-punched geotextiles (see Figure 2.7, Curve E). To obtain the relevant modulus, we avoid the initial portion of the curve and essentially shift the *y*-axis to the right, where it meets the downward extension of the linear portion of the response curve. The slope is then taken from this adjusted axis location.
- *Secant modulus:* To avoid the some arbitrariness of the above-mentioned methods, we could stipulate the procedure of obtaining a modulus value—e.g., a secant modulus at 10% strain. Here we draw a line from the axes' origin to the designated curve at 10% strain and measure its slope from the origin irrespective of the actual curve to this point. Example 2.6 illustrates these various procedures.

Example 2.6

For the nonwoven needle-punched fabric E shown in Figure 2.7, determine the initial tangent modulus, offset tangent modulus, and secant moduli at 10% and 35% strain in units of kN/m and kN/m^2 (kPa) based on an initial thickness of 0.63 mm.

Solution: Scaling directly from the curve:

$$E_T = \frac{4.3}{0.50} = 8.6 \text{ kN/m or } 13{,}600 \text{ kN/m}^2$$

$$E_{OT} = \frac{20}{0.46 - 0.20} = 77 \text{ kN/m or } 122{,}000 \text{ kN/m}^2$$

$$E_{S10} = \frac{1.1}{0.10} = 11 \text{ kN/m or } 17{,}500 \text{ kN/m}^2$$

$$E_{S35} = \frac{11.6}{0.35} = 33 \text{ kN/m or } 52{,}600 \text{ kN/m}^2$$

Regarding the test specimen size (length, width, and aspect ratio, or length-to-width ratio), much has been written. ASTM standards D1682, D751, D4632, and D4595 along with ISO 10319 allow for a number of variations. Figure 2.8 illustrates the current most popular test specimen sizes. The grab tensile test D4632 is a very widely used and reported test. The geotextile specimen dimensions are 100 mm wide and 150 mm long, but the jaws of the clamps grip only the central 25 mm of the test specimen. Almost all geotextile manufacturers and geotextile specifications use this value (recall Tables 2.1 and 2.2). Narrow strip tests (usually 25 or 50 mm wide) are used in many research and development studies since they use a minimum amount of geotextile. The reason

(a) ASTM D4632 grab

(b) ASTM D751 "narrow strip"

(c) ASTM D4595 and ISO 10319 wide-width

(d) Very wide-width
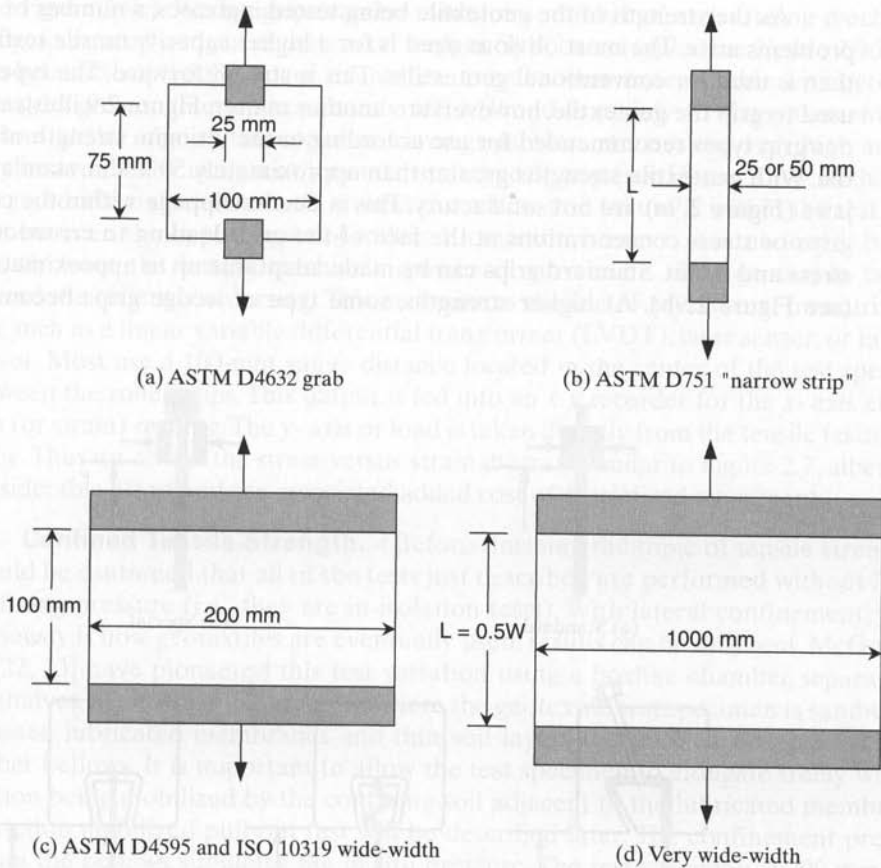
Figure 2.8   Various tensile test specimen sizes used to obtain fabric strength properties.

wide-width specimens are necessary is that geotextiles (particularly nonwovens) when tensioned tend to have a severe Poisson's ratio effect under increasing stress and they rope-up, giving artificially high values. Thus the tendency for design-related tests is to use wide-width specimens. The most common wide-width tests are ASTM D4595 and ISO 10319, both of which use a 200 mm wide specimen that is 100 mm long between the faces of the opposing grips. Such a test is not intended to be a routine or index test. The grab specimen should continue to be used in this regard (e.g., as a manufacturer's quality-control or conformance test). There are no universal relationships between the different test specimen sizes or shapes, and therefore the choice of specimen size depends on the intended use of the data. Proper identification of the specimen size on the test data is always necessary. Regarding other features of tensile testing of geotextiles (effect of conditioning, load rate, load method, etc.), the applicable standard(s) should be consulted.

As the strength of the geotextile being tested increases, a number of operational problems arise. The most obvious need is for a higher capacity tensile testing machine than is used for conventional geotextiles. This is straightforward. The types of devices used to grip the geotextile, however, are another matter. Figure 2.9 illustrates the various grip types recommended for use according to the ultimate strength of the geotextile. With geotextile strengths greater than approximately 50 kN/m, standard clamping jaws (Figure 2.9a) are not satisfactory. This is due to slippage within the conventional grips or stress concentrations at the face of the grips leading to erroneous values of stress and strain. Standard grips can be made adaptable up to approximately 90 kN/m (see Figure 2.9b). At higher strengths, some type of wedge grips become necessary

(a) Standard

(b) Special

Mechanical   Serrated   Epoxy or soft metal

(c) Various types of wedges

(d) Split barrel   (e) Roller (capstan)
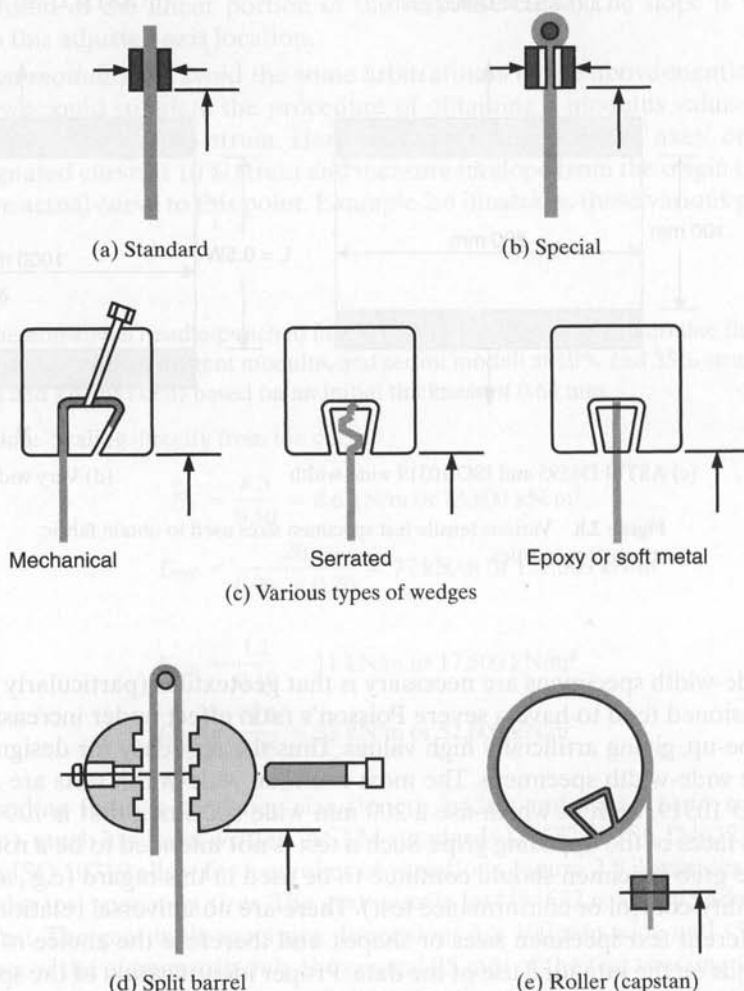
Figure 2.9 Various grip types for testing geotextiles and geogrids. (Adapted from Myles and Carswell [21])

(see Figure 2.9c). Wedge grips can be made in a number of styles, using mechanical wedges, serrated wedges, of cast metal wedges. Split barrel types (see Figure 2.9d) have also been attempted. However, even these grips become unacceptable with geotextile strengths greater than approximately 180 kN/m, due mainly to stress concentration failures at the edge of the upper or lower grips. Here stresses are very high and can only be avoided by using a roller or capstan type of grip (see Figure 2.9e). In this case, the geotextile tightens on itself around the rollers and failure is within the test specimen between the opposing set of rollers. Elongation, however, can no longer be read directly from the testing machine's crosshead movement, since geotextile take-up around the rollers is occurring. This necessitates the use of an external measuring device such as a linear variable differential transformer (LVDT), laser sensor, or infrared sensor. Most use a 100-mm gauge distance located in the center of the test specimen between the roller grips. This output is fed into an x-y recorder for the x- axis elongation (or strain) reading. The y- axis or load is taken directly from the tensile testing machine. Thus we obtain the stress-versus-strain diagram similar to Figure 2.7, albeit with considerable effort and the associated added cost of specialized equipment.

Confined Tensile Strength.   Before finishing the topic of tensile strength, it should be cautioned that all of the tests just described are performed without lateral confining pressure (i.e., they are in-isolation tests). With lateral confinement, which obviously is how geotextiles are eventually used, results can be different. McGown et al. [22, 23] have pioneered this test variation using a boxlike chamber separated in two halves, as shown in Figure 2.10, where the geotextile test specimen is sandwiched between lubricated membranes and thin soil layers that have been pressurized by rubber bellows. It is important to allow the test specimen to elongate freely without friction being mobilized by the confining soil adjacent to the lubricated membranes. A friction mobilized pull-out test will be described later. The confinement pressure within the bellows simulates the in situ pressure. The test specimen is 200 mm wide and 100 mm long in the test zone. Although this process is tedious and relatively complex, it is the best attempt at obtaining a true tensile strength/elongation response known to the author. It is particularly important for obtaining the modulus value of nonwoven needle-punched geotextiles if a finite element method for design is being used.

In order to assess a wide range of geosynthetic materials tested in this manner, Wilson-Fahmy et al. [24] have evaluated four different styles of geotextiles (see Figure 2.11). It is important to note from this study that *only* the nonwoven needle-punched geotextiles show significantly improved stress-versus-strain behavior under confinement (see Figures 2.11c and d). This apparently comes from the confining pressure that holds the randomly oriented fibers in their original positions. Thus the low initial modulus response seen in Figure 2.71 (Curve E) is eliminated. For the other geotextiles tested under confining pressure, the woven in Figure 2.11a and the nonwoven heat-bonded in Figure 2.11b, there is essentially no difference except as failure is approached. Although not shown in Figure 2.7, there was no measurable improved strength behavior noted with geonets, geomembranes, or GCLs with woven slit-film geotextiles, when they were placed under confinement; see [24] for details.
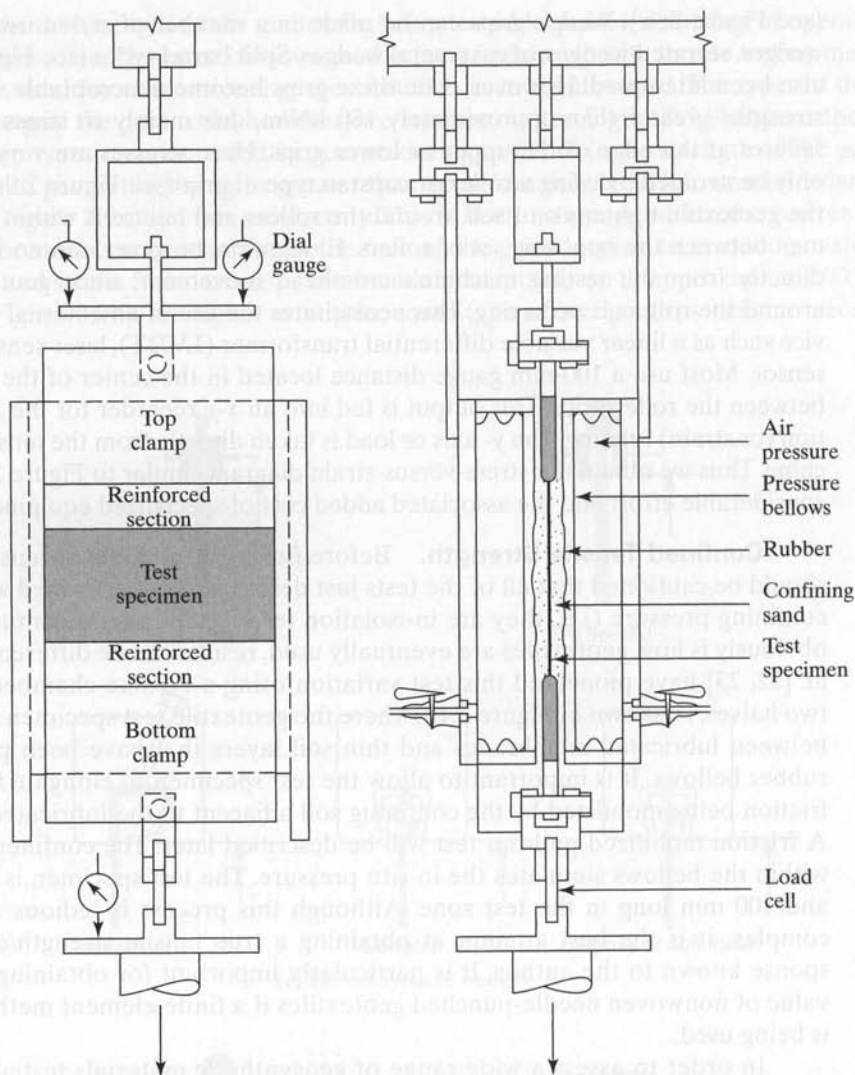
Figure 2.10 Geotextile placed under lateral confinement during tensile testing. (After McGown et al. [22, 23])

Seam Strength. Often the ends or sides of rolls of geotextiles have to be joined together for the purpose of transferring tensile stress. By far, the most common method is by sewing. Various styles of sewn seams will be described later, but whatever the type, they must be laboratory-evaluated for their load-transfer capability from one geotextile roll to another. ASTM D4884 and ISO 13426 test methods call for the following requirements:

- The shape of the seamed test specimen is 200 mm wide except at the seam itself. Here an additional 25 mm of seamed material is allowed to protrude from both
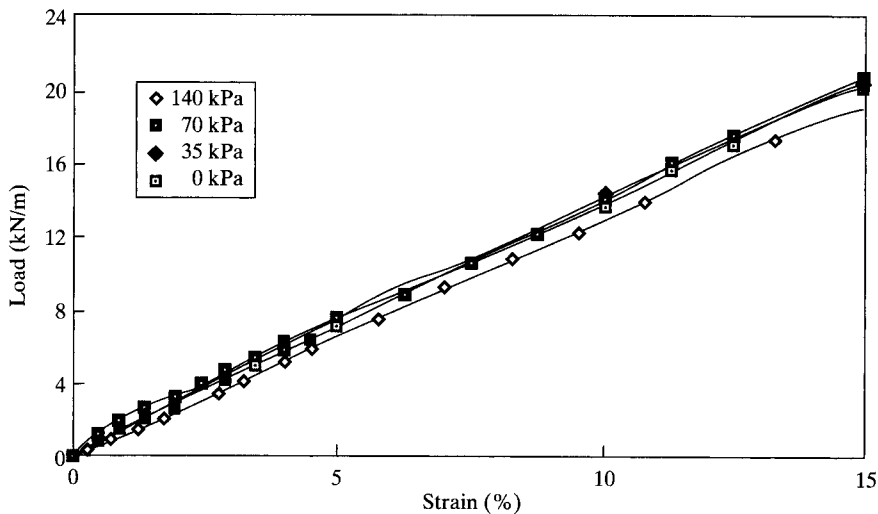
(a) 190 g/m² woven polypropylene monofilament geotextile
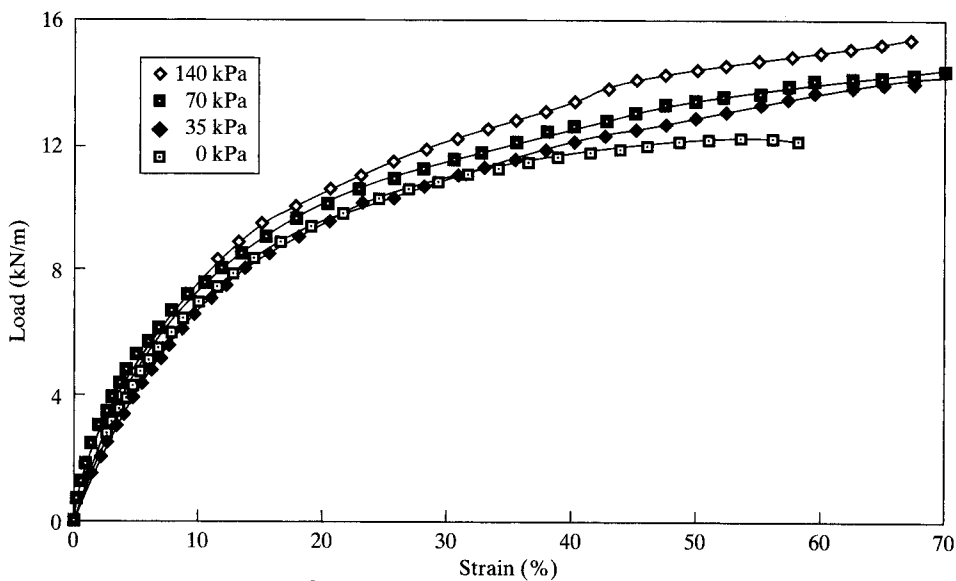
(b) 200 g/m² nonwoven heat-bonded polypropylene geotextile

Figure 2.11   Confined wide-width tensile strength response of different types of geotextiles. (After Wilson-Fahmy et al. [24])
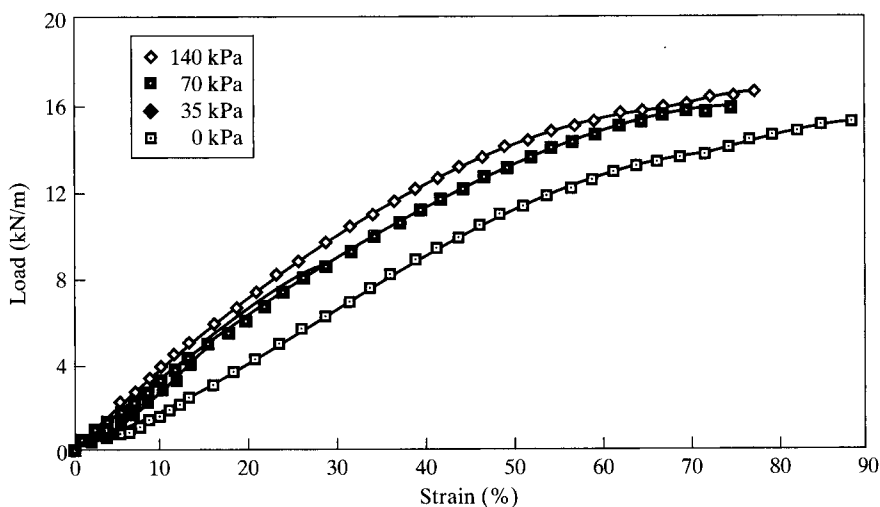
(c) 270 g/m^2 nonwoven needle-punched polypropylene geotextile
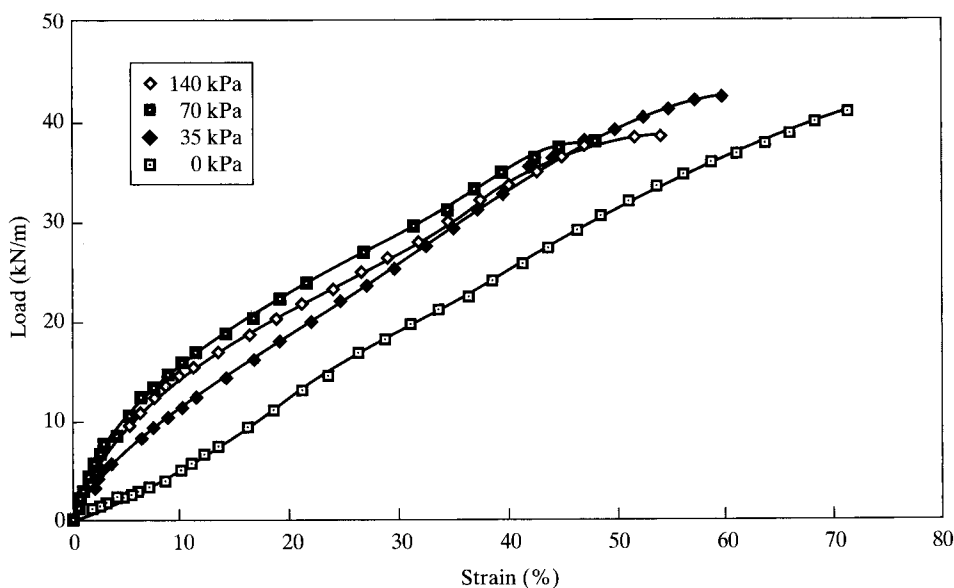
(d) 550 g/m^2 nonwoven needle-punched polyester geotextile

Figure 2.11 (*continued*)

sides; that is, at the seam the test specimen is 250 mm wide. This accounts for a certain amount of loss of seam strength when the seaming yarns are cut during specimen preparation, but to what degree is quite uncertain.

- The resulting ultimate load is divided by a 200-mm width and reported in units of kN/m. The appropriateness of this computational step is questionable.

- The rate of extension is 10%/min.
- Elongation across the seam is not required to be measured—i.e., the test measures only tensile strength.

Test results from the evaluation of well-made sewn seams of geotextiles having wide-width strengths up to approximately 20 kN/m usually result in sewn-strength efficiencies above 85%; i.e.,

$$E(\%) = \frac{T_{\text{seam}}}{T_{\text{geotextile}}} \times 100 \qquad (2.11)$$

where

E = seam efficiency (%),
T_{seam} = wide-width seam strength, and
$T_{\text{geotextile}}$ = wide-width geotextile strength (i.e., unseamed).

As the geotextile strength becomes higher, seam strengths become progressively less efficient (see Figure 2.12, where the upper bound is typical of good factory seams and the lower bound is typical of poor field seams). Above 50 kN/m, most seams fall beneath 75% efficiency, and beyond 200 to 250 kN/m, the best we can do is approximately 50% seam efficiency. Note that by this point poorly made seams become extremely low in their load-transfer capabilities. The seaming of high-strength geotextiles simply
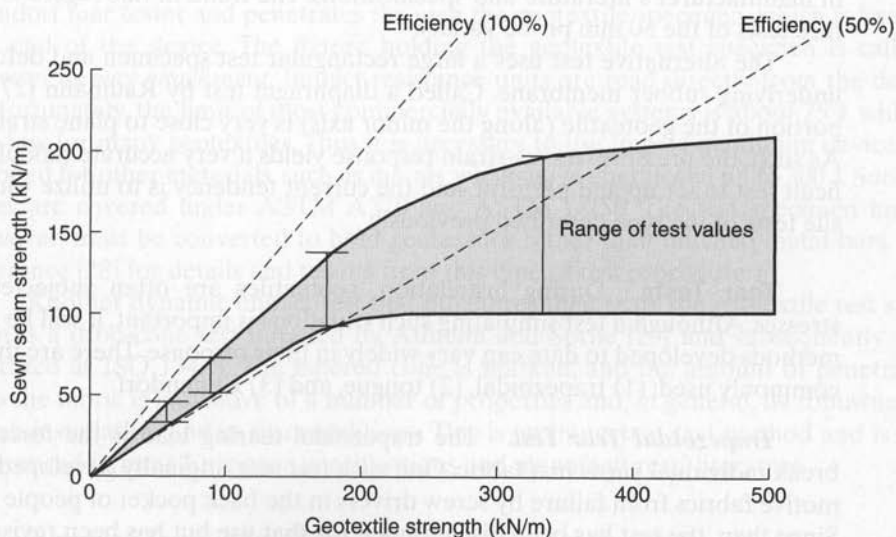
Figure 2.12   Behavior of sewn geotextile strength in comparison to the parent (unseamed) geotextile strength.

begs for better joining or bonding methods than sewing. Other possibilities that are available are the use of epoxy resins [25] or mechanical joining.

Fatigue Strength. Fatigue strength, or fatigue resistance, is the ability of a geotextile to withstand repetitive loading before undergoing failure. A tensile test specimen, usually of a wide-width variety, is stressed longitudinally at a constant rate of extension to a predetermined load (less than failure) and then back to a lower, or zero, load. This cycling is repeated until failure occurs. The resulting cyclic stress-versus-strain response (i.e., the hysteresis loops) can be used to calculate a cyclic modulus that becomes evident after a number of load cycles are applied. Also important, is the number of cycles required to bring the geotextile to failure and the respective loads that were applied. The load resulting in failure is converted to stress, and this value is usually expressed as a fraction of the quasi-statically applied failure stress (strength) described previously. As expected, the lower the stress level, the larger the number of cycles required before failure.

Although many variables remain to be defined (primarily, the decision as to what loads to apply during testing), the test reasonably simulates in situ conditions for applications such as seismic and railroad loadings, and wave or tidal action. Research in this area seems justified (see Ashmawy and Bourdeau [26]).

Burst Strength. There are two test methods that stress geotextiles out of plane, thereby mobilizing tension until failure occurs. The most common is the Mullen burst test, which was covered in ASTM D3786 but is now depreciated. In this test, an inflatable rubber membrane is used to distort the geotextile into the shape of a hemisphere of 30 mm diameter. Bursting of the geotextile occurs when no further deformation is possible. The test has been used for quality control but is seeing less and less use in manufacturer's literature and specifications. The trend in this regard is to use puncture tests of the 50 mm probe variety.

The alternative test uses a large rectangular test specimen and deforms it by an underlying rubber membrane. Called a diaphragm test by Raumann [27], the central portion of the geotextile (along the minor axis) is very close to plane strain conditions. As such, the pressure-versus-strain response yields a very accurate modulus. It is a difficult test to set up and perform, and the current tendency is to utilize wide-width tensile tests of the type described previously.

Tear Tests. During installation, geotextiles are often subjected to tearing stresses. Although a test simulating such situations is important, it will be seen that the methods developed to date can vary widely in their response. There are three tear tests commonly used: (1) trapezoidal, (2) tongue, and (3) Elmendorf.

Trapezoidal Tear Test. The trapezoidal tearing load is the force required to break individual yarns in a fabric. One such test was originally developed to test automotive fabrics from failure by screw drivers in the back pocket of people sitting down. Since then, the test has been discontinued for that use but has been revised and modified for geotextiles. The current trapezoidal tear tests are ASTM D4533 and ISO 13434. In these tests, the geotextile is inserted into a tensile testing machine on the bias, which

causes the yarns to tear progressively. An initial 15 mm cut is made to start the process. The load actually stresses the individual yarns gripped in the clamps rather than stressing the fabric structure. The value—commonly referred as *trap tear*—is reported by all manufacturers and used in most specifications.

Tongue Tear Test.   As indicated in ASTM D751, the tongue tear test, uses a 75 mm by 200 mm geotextile specimen with a 75 mm long initiation cut. The geotextile is placed in a testing machine with the cut ends in the grips of the machine. An increasing tensile force is applied to make the geotextile tear along the initiation cut. The test configuration permits the yarns to rope-up and work together to resist tear propagation. Thus the values resulting from tongue tear tests are usually much higher than those from trapezoidal tear tests.

Elmendorf Tear Test.   The Elmendorf tear test is covered in ASTM D1424, and it involves a procedure for the determination of the average force required to dynamically propagate a single-rip tongue type tear starting from a premade cut in a woven geotextile. The cut is then continued by means of a rotating pendulum apparatus. The tearing force is the force required to continue the tear previously started in the test specimen. The strength is calculated as the work done in tearing the specimen divided by twice the length of the tear. The test is often used in Europe to measure tear strength. It is generally not used for nonwoven geotextiles.

Impact Tests.   Since falling objects such as rocks, tools, and other construction items can readily create punctures and tears in geotextiles, a number of tests have been developed to assess the impact resistance of geotextiles. One such test that measures impact resistance directly in energy units (Joules) has been developed for an Elmendorf tear apparatus. The impacting cone is attached to the pendulum arm of the Elmendorf tear tester and penetrates through the geotextile specimen, which is fixed on the end of the device. The fixture holding the geotextile test specimen is called a *Spencer impact attachment*. Impact resistance units are read directly from the device. Unfortunately, the limit of most commercially available systems is about 25 J, which is too low for many geotextiles. Thus it is necessary to use impact pendulum devices developed for other materials, such as metals, which have energies of up to 300 J. Such devices are covered under ASTM A370 and ASTM D256. The test specimen holder, however, must be converted to hold geotextiles rather than notched metal bars. (See reference [28] for details and results from this type of test procedure.)

Another dynamic impact test that punctures then tears the geotextile test specimen is a drop-cone test initiated by Alfheim and Sorlie [29] and subsequently standardized as ISO 13433. The tapered cone is marked, and the amount of penetration into the fabric is indicative of a number of properties and, in general, its robustness to harsh installation and in situ conditions. This is an important test method and is seen referenced in most European specifications and manufacturers' literature.

Puncture Tests.   In addition to the dynamic tests just described for impact resistance, there is need for an assessment of geotextile resistance to objects such as stones and stumps under quasi-static conditions. Such a test is described under ASTM

D4833. This test uses a penetrating steel rod of 8.0 mm in diameter. The geotextile test specimen is firmly clamped in an empty cylinder of 45 mm inside diameter and the rod pushed through it via a compression testing machine at a prescribed rate. Resistance to puncture is measured in force units.

   This test is a popular one due to its simplicity and ability to be automated. It is reported by all manufacturers and listed in most specifications. A considerably large database exists using this test method (e.g., see [28]). It is important to note the exact shape of the end of the metal rod. Three types are in current use: (1) hemispherical, (2) flat, and (3) beveled flat. The latter type, with a 0.8 mm, 45° bevel around its circumference is preferred and covered in ASTM D4833.

   The small size of the device described above is of concern. For example, a lightweight nonwoven geotextile can selectively be chosen in a low density fiber region or in a high density fiber region. The differences in puncture resistance will be very large.

   With such a concern in mind, a larger-sized puncture test has been developed [30]. It uses a conventional soil testing CBR plunger and mold. The penetrating steel rod is 50 mm in diameter and the geotextile is firmly clamped in an empty mold of 150 mm inside diameter. The circumference of the plunger should be beveled 0.80 mm on a 45° angle so as not to cut the yarns at the edge of the penetrating rod. This test is formalized as ASTM D6241 and ISO 12236. Table 2.4 presents data from this type of test on both woven and nonwoven geotextiles.

   There is a direct relationship between the CBR puncture-resistance value and the wide-width tensile strength of geotextiles. This is because the geotextile between the inner edge of the specimen holder and the outer edge of the puncturing rod is in a state of pure axi-symmetric tension. Cazzuffi and Venesia [31] propose the following empirical equation as a correlation between the puncture breaking force of the CBR test and the wide-width tensile strength for isotropic, nonwoven geotextiles

$$T_f = F_p/\pi r \qquad (2.12)$$

where

   T_f = tensile force per unit width of fabric (kN/m),
   F_p = puncture breaking force (kN), and
   r = radius of the puncturing rod (m).

Both the German and Italian standards have correlations between the CBR test results and the wide-width tensile elongation of the geotextile. According to the German (DIN) standard, the tensile elongation at failure (ϵ_f) is calculated as follows:

$$\epsilon_f = \frac{(x - a)}{a} \times 100 \qquad (2.13)$$

where

   x = diagonal elongation of the geosynthetic at failure (m), and
   a = horizontal distance between the outer edge of the plunger and the inner
        edge of the mold (m)

TABLE 2.4 RELATIONSHIP BETWEEN CBR PUNCTURE STRENGTH AND WIDE-WIDTH TENSILE STRENGTH OF VARIOUS GEOTEXTILES*

Geotextile Designation	CBR Puncture Strength (kN)	Wide-Width Strength Using Eq.(2.12) (kN/m)	Measured Wide-Width Tensile Strength (kN/m)	Variation (%)	CBR Calculated Elongation (%) Using Eqs (2.13) and (2.14) DIN	ENEL	Measured Wide-Width Elongation (%)	Variation (%) DIN	ENEL
WGT-1									
Fill			36.0	38.1			23.5	15.3	23.4
Warp			23.6	5.5			28.8	30.9	37.5
Average	3.55	22.3	29.8	25.2	19.9	18.0	26.2	24.0	31.3
WGT-2									
Fill			33.1	03.9			24.2	37.2	43.0
Warp			50.0	36.4			13.0	16.9	6.2
Average	5.06	31.8	41.5	23.4	15.2	13.8	18.6	18.3	25.8
WGT-3									
Fill			17.5	41.7			23.0	—	—
Warp			9.2	10.9			23.9	—	—
Average	1.62	10.2	13.4	23.9	—	—	23.4	—	—
WGT-4									
Fill			15.1	13.9			11.9	—	—
Warp			10.8	20.4			11.4	—	—
Average	2.07	13.0	13.0	0.0	—	—	11.6	—	—
WGT-5									
Fill			24.2	17.4			11.6	—	—
Warp			20.1	0.5			17.3	—	—
Average	3.18	20.0	22.2	9.9	—	—	14.4	—	—
WGT-6									
Fill			32.0	16.2			18.7	—	—
Warp			30.1	11.0			13.5	—	—
Average	4.27	26.8	31.0	13.5	—	—	16.1	—	—
NWGT-1									
MD			5.9	30.5			134.0	—	—
XMD			6.9	11.6			135.2	—	—
Average	1.23	7.7	6.4	20.3	—	—	134.6	—	—

TABLE 2.4 (continued)

124

Geotextile Designation	CBR Puncture Strength (kN)	Wide-Width Strength Using Eq.(2.12) (kN/m)	Measured Wide-Width Tensile Strength (kN/m)	Variation (%)	CBR Calculated Elongation (%) Using Eqs (2.13) and (2.14)		Measured Wide-Width Elongation (%)	Variation (%)	
					DIN	ENEL		DIN	ENEL
NWGT-2									
MD			14.4	22.9			152.8	—	—
XMD			20.7	14.5			162.2	—	—
Average	2.72	17.7	17.5	1.1	—		157.5	—	—
NWGT-3									
MD			16.7	35.3			167.1	62.1	65.7
XMD			23.9	5.4			152.2	58.4	62.4
Average	3.60	22.6	20.3	11.3	63.3	57.2	159.6	60.3	64.2
NWGT-4									
MD			6.5	12.3			44.7	17.9	25.7
XMD			8.1	9.9			60.4	39.2	45.0
Average	1.16	7.3	7.3	0.0	36.7	33.2	52.5	30.1	36.8
NWGT-5									
MD			13.0	11.5			51.1	17.6	25.4
XMD			9.8	17.3			45.5	7.5	16.3
Average	1.83	11.5	11.4	0.9	42.1	38.1	48.3	12.8	21.1

*Description of the geotextiles tested in this study:

Designation	Type (mass per unit area)
WGT-1	Woven monofilament polypropylene (200/gm^2)
WGT-2	Woven slit-film polypropylene (240/gm^2)
WGT-3	Woven monofilament polyvinyl chloride (390/gm^2)
WGT-4	Woven slit-film polypropylene (100/gm^2)
WGT-5	Woven slit-film polypropylene (150/gm^2)
WGT-6	Woven slit-film polypropylene (200/gm^2)
NWGT-1	Nonwoven needle-punched polypropylene (200/gm^2)
NWGT-2	Nonwoven needle-punched polypropylene (400/gm^2)
NWGT-3	Nonwoven needle-punched polypropylene (600/gm^2)
NWGT-4	Nonwoven heat-bonded polypropylene (140/gm^2)
NWGT-5	Nonwoven heat-bonded polypropylene (200/gm^2)

Source: After Murphy and Koerner [30].

The Italian (ENEL) standard uses the following equation to calculate the tensile elongation at failure:

$$\epsilon_f = \frac{[\pi(R + r)x + \pi r^2 - \pi R^2]}{\pi R^2} \times 100 \qquad (2.14)$$

where

R = radius of the mold (m), and
r = radius of the puncturing rod (m)

Included in Table 2.4 are the wide-width tensile strengths and elongation at failure for the same geotextiles that were tested in CBR (puncture) strength. Also included according to equations (2.12)–(2.14) are the calculated wide-width strengths and elongations at failure, the latter according to both DIN and ENEL equations. From this information a percentage variation can be calculated.

It appears that the strength predictions are reasonable, with the nonwovens being more accurate than the wovens. The variation in predicted elongation at failure has more scatter but is still reasonable. Clearly, the CBR test for puncture strength or as a form of axi-symmetric tensile strength has considerable merit.

Friction Behavior.   In many design problems it is necessary to know the soil-to-geotextile friction behavior. The generally accepted test setup is an adaptation of the direct shear test used in geotechnical engineering [32]. As shown in Figure 2.13(a), the geotextile is firmly fixed to one-half of the test device with soil (or another geosynthetic) in the other half. After normal stress is applied and equilibrates, a shear force is mobilized until sliding occurs between the geotextile and the soil with no further increase in required shear force. When the test is repeated at different normal stresses, the data are plotted and trends are established, as shown in Figure 2.13(b). From these trend curves, limiting data (peak and residual stresses) can be obtained and then the curves of Figure 2.13(c) can be drawn. These curves result in the establishment of the Mohr-Coulomb failure parameters (adhesion and friction angle) of the interface being tested (recall equation 2.5a). From a comparison of the geotextile-to-soil response versus the soil-to-soil response, the shear strength efficiencies on the soil's cohesion and friction angle can be obtained (recall equations 2.5b, 2.6, and 2.7). Note that the soil's shear-strength parameters are the upper limit—that is, an efficiency of 100%. This implies that if the soil-to-geotextile interface is stronger than the shear strength of the soil itself, failure will occur entirely in the soil either above or beneath the geotextile inclusion.

Also shown in parts (b) and (c) of Figure 2.13 is a residual strength lower than the peak strength. This is not uncommon in carrying out geosynthetic-to-soil direct shear tests, including those tests that have geotextiles. Such data present to the design engineer a major decision as to what value to select. If peak values are used, traditional factor of safety values can generally be used, the assumption being that the movement of the interface in the field cannot go beyond the deformation needed to mobilize peak strength. If the interface deformations in the field go beyond peak, then a lower shear
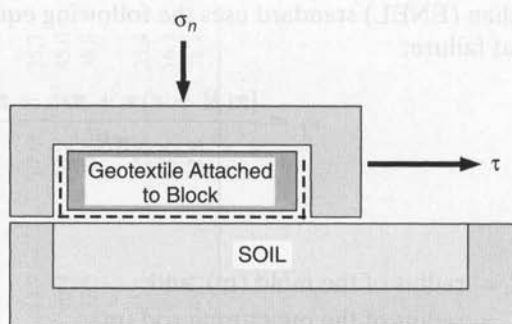
(a) Direct shear test device
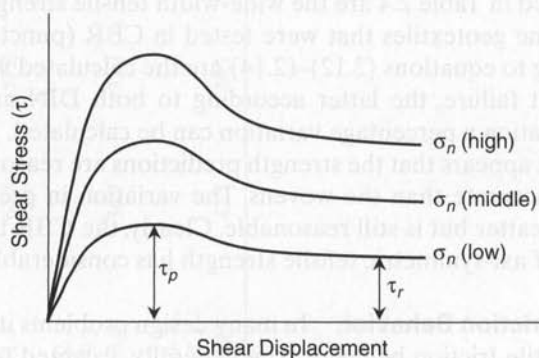
(b) Direct shear test data
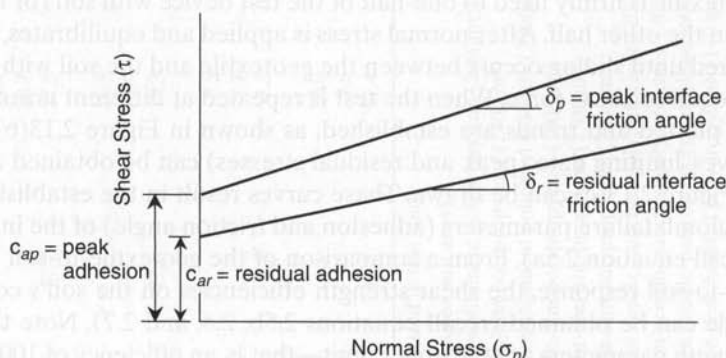
(c) Failure envelopes on Mohr-Coulomb stress space

Figure 2.13 Test setup and procedure to assess interface shear strengths involving geotextiles.

strength must be used and, in the limit, the residual shear strength. Using less than peak strength, the factor of safety value can probably be lower, but how much so is not clear. This issue of peak, residual, or somewhere in-between is very significant when considering the multigeosynthetic-lined slopes that are typical in landfill liners and covers [33, 34]. The issue will be further discussed in Chapter 5 on geomembranes.

The results from such a test by Martin et al. [35] are presented in Table 2.5 for four geotextile types against three different cohesionless soils. *Peak* soil-to-geotextile friction angles are given (in all cases the adhesion was zero), as well as the geotextile efficiency versus the peak soil friction angle by itself as per equation (2.7). Here it is seen that most geotextiles can mobilize a high percentage of the soil's friction and can be used to advantage in situations requiring this feature.

Both ASTM D5321 and ISO 12957 direct shear tests (as with many other geosynthetic standardization groups) call for a shear box of 300 mm × 300 mm in size. While such a large test box is appropriate for geonets, geogrids, many geocomposites, and large particle-sized soils, this author considers it to be excessive for geotextiles (and certainly for geomembranes) against sands, silts, and clays and against one another. Standard geotechnical engineering laboratory shear boxes (e.g., 100 mm × 100 mm), are felt to be satisfactory for geotextile testing and focus should be on more relevant shear strength testing parameters such as the following:

- Use of site-specific soil types as well as product-specific geotextile types
- Control of density and moisture content of the as-placed soil
- Geotextile fixity conditions to the end platen
- Saturation conditions during consolidation and shear testing
- Specific type of saturating fluid (e.g., leachate)
- Use of field anticipated strain rates
- Adequate shear box deformation to achieve residual shear strength

Pullout (Anchorage) Tests.   Geotextiles are often called upon to provide anchorage for many applications within the reinforcement function. Such anchorage usually has the geotextile sandwiched between soil on either side. The resistance can be modeled in the laboratory using a pullout test, which will be detailed in Section 3.1.2 on geogrids. The pullout resistance of the geotextile is obviously dependent on the normal force applied to the soil, which mobilizes shearing resistances on both surfaces of the geotextile.

TABLE 2.5 PEAK SOIL-TO-GEOTEXTILE FRICTION ANGLES AND EFFICIENCIES (IN PARENTHESES) IN SELECTED COHESIONLESS SOILS

Geotextile Type	Concrete Sand $\phi = 30°$	Rounded Sand $\phi = 28°$	Silty Sand $\phi = 26°$
Woven, monofilament	26° (84%)	—	—
Woven, slit-film	24° (77%)	24° (84%)	23° (87%)
Nonwoven, heat-bonded	26° (84%)	—	—
Nonwoven, needle-punched	30° (100%)	26° (92%)	25° (96%)

Source: After Martin et al. [35].
Note: Values such as the above should *not* be used in critical designs. Site specific geotextiles and soils must be individually tested and evaluated in accordance with the particular project conditions—e.g., saturation, type of liquid, normal stress, consolidation time, shear rate, and displacement amount.

Since the test greatly resembles a direct shear test, albeit with stationary soil on both sides of the tensioned geotextile, a possible design strategy is to take direct shear test results (for both sides of the geotextile) and use these values for pullout design purposes. However, this may not be a conservative practice.

Test results by Collios et al. [36] show a relationship of pullout test results to shear test results with some notable exceptions. For pullout testing, if the soil particles are smaller than the geotextile openings, efficiencies are high; if not, they can be low. In all cases, however, pullout test resistances are less than the sum of the direct shear test resistances. This is due to the fact that the geotextile is taut in the pullout test and exhibits large deformations. This in turn causes the soil particles to reorient themselves into a reduced shear strength mode at the soil-to-geotextile interfaces, resulting in lower pullout resistance. The stress state mobilized in this test is both interesting and complex as evidenced by a large number of technical references on this topic.

2.3.4 Hydraulic Properties

Unlike the physical and mechanical properties just discussed, traditional tests on textile materials rarely have hydraulic applications; that is, the garment and industrial fabrics industry obviously does not test for liquid flow. As a result, hydraulic testing of geotextiles has required completely new and original test concepts, methods, devices, interpretation, and databases. Both geotextile tests in-isolation and with soil will be described in this section.

Porosity.   As conventionally defined with soils in geotechnical engineering, the porosity of a geotextile is the ratio of void volume to total volume. It is related to the ability of liquid to flow through or within the geotextile but is rarely measured directly. Instead, it is calculated from other properties of the geotextile:

$$n = 1 - \frac{m}{\rho t} \tag{2.15}$$

where

n = porosity (dimensionless),
m = mass per unit area, i.e., weight, (g/m^2),
ρ = density (g/m^3), and
t = thickness (m).

It is seen in equation (2.15) that for a given geotextile's weight and density, the porosity is directly related to thickness. Thickness in turn is related to the applied normal stress (see again Figure 2.6).

Pore size can be measured by careful sieving with controlled-size glass beads (see the AOS test later in this section), by the use of image analyzers [37], or by the use of

mercury intrusion [38]. Bhatia et al. [39] have compared these different measurement techniques on a variety of geotextiles illustrating behavioral trends and comparisons. The image analyzer results presented by ICI Fibers [40] for their various weights of geotextiles are instructive in showing that the pore size shifts gradually lower as the geotextile weight increases (see Figure 2.14a). McGown [41] has provided information of the same type comparing different geotextile manufacturing styles (see Figure 2.14b). These results are for the as-manufactured geotextile. Recognize, however, that geotextiles have pore sizes that are sensitive to changes in geotextile thickness due to applied normal stresses and adjacent soil gradations as would be typical of in situ conditions.

Percent Open Area.   Percent open area (POA) is a geotextile property that has applicability only for woven geotextiles, and even then only for woven monofilament geotextiles. POA is a comparison of the total open area (the void areas between adjacent yarns) to the total specimen area. A convenient way to measure the open area is to project a light through the geotextile onto a large poster-sized piece of cardboard. The magnified open spaces (resembling a window screen) can be mapped by a planimeter. Alternatively, a cardboard background that is crosshatched like graph paper can be used. Here the squares are counted and summed up for the open area. The total area (yarns plus voids) must be measured at the same magnification as the voids measurement. A library-type microfiche reader can also be used. Woven monofilament geotextiles vary from essentially a closed structure (POA $\cong$ 0%) to one that is extremely open (POA = 36%), with many commercial woven monofilament geotextiles being in the range of 6 to 12%.

The test is not applicable to nonwovens, since the overlapping yarns block any light from passing directly through the geotextile. Thus a different test method is required to measure void sizes in nonwovens.

Apparent Opening Size (or Equivalent Opening Size).   A test for measuring the apparent opening size was developed in the 1970s by the U.S. Army Corps of Engineers to evaluate woven geotextiles. The test has since been extended to cover all geotextiles, including the nonwoven types. The apparent opening size (AOS) or equivalent opening size (EOS)—AOS and EOS are essentially equivalent terms—are defined in CW-02215 as the U.S. standard sieve number that has openings closest in size to the openings in the geotextile. The subsequent ASTM test is designated D4751. The test uses known-diameter glass beads and determines the O_{95} size by standard *dry* sieving. Sieving is done using beads of successively different diameters until the weight of beads passing through the test specimen is 5%. This defines the O_{95}-size of the geotextile's openings in millimeters. Values of O_{95} are indicated on the curves shown in Figure 2.14. Note, however, that the O_{95} value defines only one particular opening size of the geotextile, not the total pore-size distribution. A conversion of the O_{95} size in millimeters can then be made using Table 2.6 to obtain the closest U.S. sieve size, and its number defines the AOS (or EOS) value. Thus AOS, EOS, and O_{95} all refer to the same specific pore size, the difference being that AOS and EOS are sieve numbers, while O_{95} is the corresponding sieve-opening size in millimeters. It should also be noted in the conversion on Table 2.6 that as the AOS sieve number increases, the O_{95} particle size value decreases;

(a) Fabric pore size distribution for geotextiles produced by BBA Nonwovens Inc. [40]. Note that geotextile mass per unit area increases progressively from Terram 500 up to Terram 3000

(b) Pore size distributions of different types of geotextiles (After McGown [41])
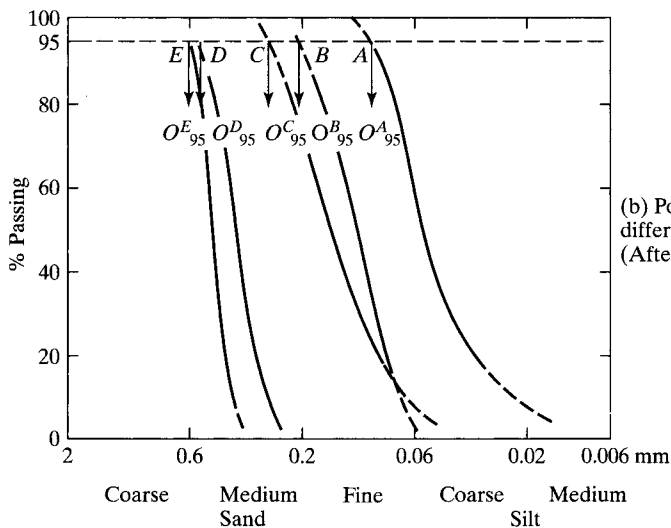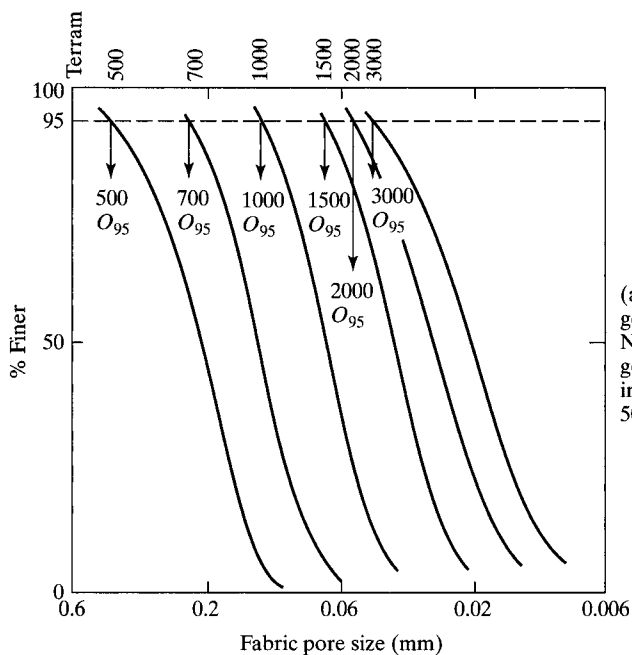
Legend
A. 250 gm/m^2 resin-bonded
B. 300 gm/m^2 needle-punched
C. 140 gm/m^2 heat-bonded
D. 380 gm/m^2 hessian woven
E. 185 gm/m^2 woven terylene

Figure 2.14   Various fabric pore size distribution curves.

TABLE 2.6 CONVERSION OF U.S. STANDARD
SIEVE SIZES TO EQUIVALENT SQUARE
OPENING SIZES

Sieve Size (No.)	Opening Size (mm)
4	4.750
6	3.350
8	2.360
10	2.000
16	1.180
20	0.850
30	0.600
40	0.425
50	0.300
60	0.250
70	0.210
80	0.180
100	0.150
140	0.106
170	0.088
200	0.075
270	0.053
400	0.037

that is, the numbers are inversely related to one another. In this book we will generally use the O_{95} value since it is the target value for design purposes.

The AOS test per ASTM D4751 as just described is a poor test, having many problems, but simplicity of the test and its inertia seems to sustain its use in the United States. Some of the problems associated with the test are as follows:

- The test is conducted dry, whereas filtration and drainage always involve liquids.
- The glass beads can easily get trapped in the geotextile itself (particularly in thick nonwovens) and not pass through at all.
- Electrostatic charges often result in the finer glass beads clinging to the inside of the sieve and not participating in the test at all.
- Yarns in some geotextiles easily move with respect to one another (as they do in woven slit-film geotextiles), thereby allowing the beads to pass through an enlarged void not representative of the total geotextile test specimen.
- Slight changes in fabric structure do not result in different O_{95} values. This is perplexing since structure, temperature, humidity, bead size variation, and test duration all potentially influence the test results.
- The test is directed only at the 5% size (equivalent to the 95% passing size), which allows for determination of the O_{95} size. The remainder of the pore size curve is not defined.

Alternatives to the dry sieving test just described include the following wet-sieving methods [42]:

- In Canada (CGSB-148.1) and France, a frame containing the geotextile specimen has well-graded glass beads placed on it and is repeatedly submerged in water. The bead fraction that passes is calculated and a O_{95} equivalent particle size is obtained.
- In Germany, the setup is similar but a water spray is used. The soil fraction that passes as well as an effective opening diameter are calculated.
- The ISO 12956 test is also a wet-sieving test and will undoubtedly be seeing greater use than dry sieving in the future.

In general, these wet-sieving tests avoid many of the problems of dry sieving and are felt to be more representative of site conditions. In addition, even more sophisticated measurement techniques are emerging, including bubble point, mercury intrusion, and image analysis. Figure 2.15 illustrates that the differences in pore size may be quite pronounced.

Permittivity (Cross-Plane Permeability).   One of the major functions that geotextiles perform is that of filtration. (Note that most transportation agency specifications and some manufacturers' literature incorrectly call this "drainage.") In filtration, the liquid flows perpendicularly through the geotextile into crushed stone, a perforated pipe, a geosynthetic drainage core, or some other drainage system. It is important that the geotextile allow for this flow to occur and not be impeded. Hence the geotextile's cross-plane permeability must be quantified. As we discussed in the
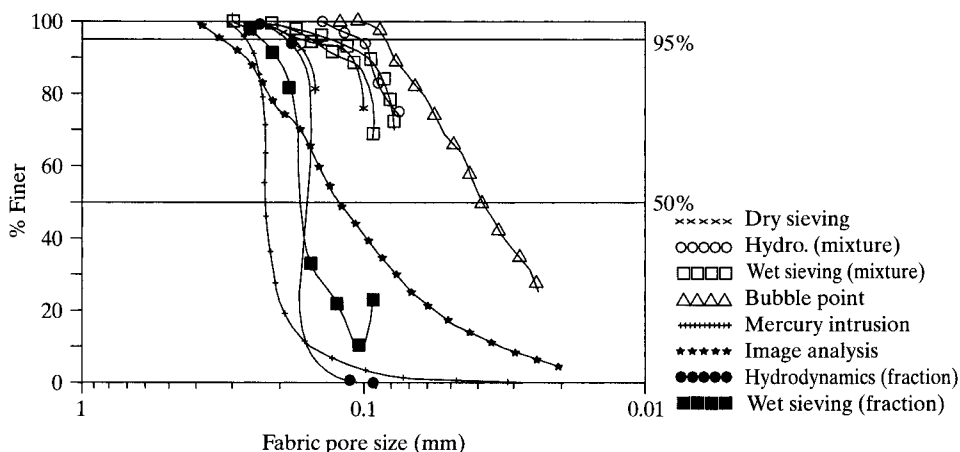
Figure 2.15   Complete pore size distribution curves for a continuous filament needle-punched nonwoven geotextile using different test methods. (After Bhatia et al. [39])

compressibility section, however, fabrics deform under load (recall Figure 2.6). Thus a new term, permittivity (Ψ) as was previously defined as equation (2.8), is repeated here:

$$\Psi = \frac{k_n}{t}$$

where

Ψ = permittivity (sec^{-1}),

k_n = permeability (properly called *hydraulic conductivity*) normal to the geotextile where the subscript n is often omitted (m/sec), and

t = thickness of the geotextile (m).

The above equation is used in Darcy's formula as follows:

$$q = k_n i A$$

$$q = k_n \frac{\Delta h}{t} A$$

$$\frac{k_n}{t} = \Psi = \frac{q}{(\Delta h)(A)} \tag{2.16}$$

where

q = flow rate (m^3/sec),

i = hydraulic gradient (dimensionless),

Δh = total head lost (m), and

A = total area of geotextile test specimen (m^2).

The formulation above is used for constant head tests in an identical manner as with soil permeability testing. Typically, the flow rate (q) is measured at one value of Δh, and then the test is repeated at different values of Δh. These different values of Δh produce correspondingly different values of q. When plotted as ($\Delta h A$) on the horizontal axis and (q) on the vertical axis, the slope of the resulting straight line yields the desired value of Ψ.

The test can also be conducted using a falling (variable) head procedure as is also performed on soils. In this case, Darcy's formula is integrated over the head drop in an interval of time and used in the following equation:

$$\frac{k_n}{t} = \Psi = 2.3 \frac{a}{A \Delta t} \log_{10} \frac{h_o}{h_f} \tag{2.17}$$

where

Ψ = permittivity (sec^{-1}),

a = area of water supply standpipe (m^2),

A = total area of geotextile test specimen (m^2),

Δt = time change between h_0 and h_f (sec),

h_o = head at beginning of test (m), and

h_f = head at end of test (m).

In either case, the resulting permittivity value can be multiplied by the geotextile thickness to obtain the traditional permeability value, if so desired.

If the permeating fluid is not water (e.g., is leachate or waste oil.) compensation for differences in density and viscosity must be made (Hausmann [43]). This is done by using the following conversion:

$$\Psi_f = \Psi_w \frac{\rho_f}{\rho_w} \frac{\mu_w}{\mu_f} \tag{2.18}$$

where

Ψ_f = permittivity of the fluid under consideration,

Ψ_w = permittivity using water,

ρ_f = density of the fluid,

ρ_w = density of water,

μ_w = viscosity of water, and

μ_f = viscosity of the fluid.

ASTM D4491 uses the device shown in Figure 2.16 to measure the permittivity of geotextile test specimens. It is similar to ISO 11058. Either constant head or falling head can be used, although the standard is written around the constant head test, at a head of 50 mm. As with the permeability of soils, geotextile values of permittivity (and permeability) range over several orders of magnitude:

- Permittivity, ψ: from 0.02 to 2.2 s^{-1}
- Permeability, k_n: from 8×10^{-6} to 2×10^{-3} m/s

Some important test considerations are preconditioning of the test specimen, temperature, and the use of de-aired water. ASTM D4491 requires a dissolved oxygen content of the permeating water to be less than 6.0 mg/l. Tap water is allowed unless disputes arise, in which case deionized water should be used. Note that conventional soil-testing permeameters cannot be used to test geotextiles, since the size of their water outlets is rarely large enough to handle the flow coming through most geotextiles. The testing of soil and geotextile systems for long-term flow compatibility will be treated later under endurance properties in Section 2.3.5.

Permittivity Under Load.   The previously described permittivity test had the geotextile test specimen under zero normal stress, a situation rarely encountered in the field. To make the test more performance-oriented, numerous attempts to construct a
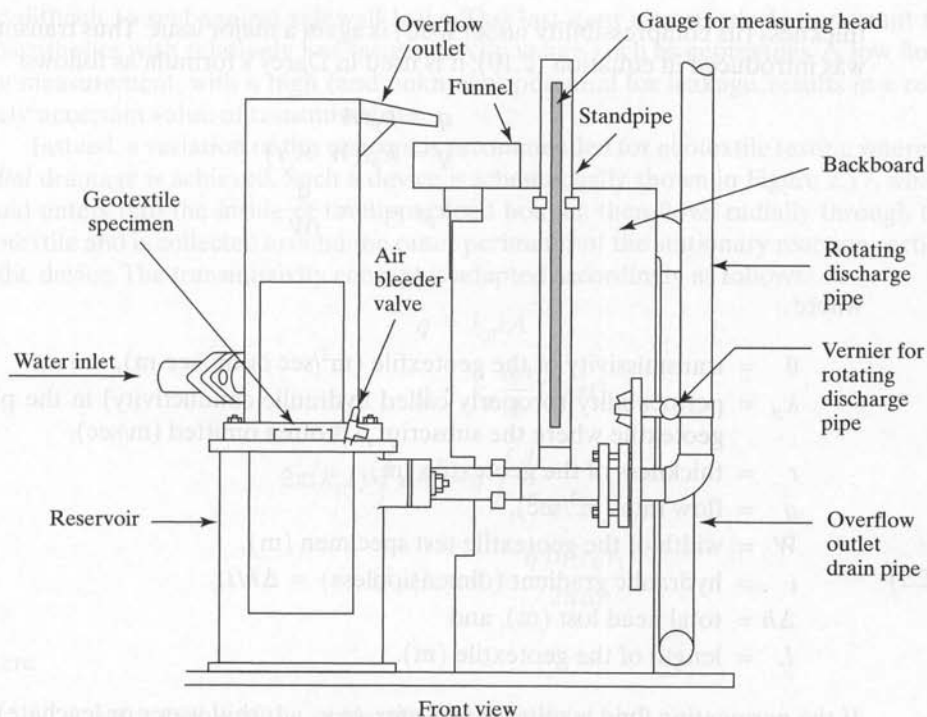
Figure 2.16   Permeability device for measuring geotextile permittivity (cross-plane flow).

permittivity-under-load device have been made. Generally, a number of layers of geotextile (2 to 5) are placed upon one another with an open-mesh stainless steel grid on the top and bottom. This assembly is placed inside a permeameter and loaded normally via ceramic balls having a diameter of approximately 12 mm. Thus normal stress is imposed on the geotextile, but flow is only nominally restricted. Loading by soil itself (which would definitely affect flow) is completely avoided. The test has been standardized as ASTM D5493, and results seem to indicate the following trends between standard permittivity and permittivity-under-load;

- Woven monofilament geotextiles: no change to a slight increase when under load.
- Woven slit-film geotextiles: data scatter too large to establish trends.
- Nonwoven heat-bonded geotextiles: no change to slight decrease when under load.
- Nonwoven needle-punched geotextiles: slight decrease to moderate decrease depending on magnitude of load and mass/unit area of geotextile.

Transmissivity (In-Plane Permeability).   For flow of water within the plane of the geotextile, (e.g., in the utilization of the drainage function), the variation of geotextile

thickness (its compressibility under load) is again a major issue. Thus transmissivity (θ) was introduced in equation (2.10); it is used in Darcy's formula as follows:

$$q = k_p i A$$
$$q = k_p i (W \times t) \tag{2.19}$$

$$k_p t = \theta = \frac{q}{iW} \tag{2.20}$$

where

θ = transmissivity of the geotextile (m^2/sec or m^3/sec-m),

k_p = permeability (properly called hydraulic conductivity) in the plane of the geotextile where the subscript p is often omitted (m/sec),

t = thickness of the geotextile (m),

q = flow rate (m^3/sec),

W = width of the geotextile test specimen (m),

i = hydraulic gradient (dimensionless) = $\Delta h / L$,

Δh = total head lost (m), and

L = length of the geotextile (m).

If the permeating fluid is other than water, (e.g., a turbid water or leachate), the density and viscosity can be accommodated for by using equation (2.18). Also, note in equation (2.20) that θ and q/W carry the same units, but they are numerically equal *only* at a hydraulic gradient i, of unity.

A number of test devices are configured to model the above formulation, where liquid (usually water) flows in the plane of the geotextile (of dimensions L × W × t) in a *parallel* flow trajectory; ASTM D4716 and ISO 12958 use such a device. Koerner and Bove [44] provide a review of such devices, and Table 2.7, after Gerry and Raymond [14], gives typical values. These test devices are necessary for high-flow geonets and drainage geocomposites (discussed in Chapters 4 and 9, respectively), but they are somewhat unwieldy for geotextiles. Such devices are large, time-consuming to set up

TABLE 2.7 TYPICAL VALUES OF TRANSMISSIVITY AND IN-PLANE PERMEABILITY OF GEOTEXTILES*

Type of Geotextile	Transmissivity m^2/s	Permeability Coefficient m/s
Nonwoven, heat-bonded	3.0×10^{-9}	6×10^{-6}
Woven, slit-film	1.2×10^{-8}	2×10^{-5}
Woven, monofilament	3.0×10^{-8}	4×10^{-5}
Nonwoven, needle-punched	2.0×10^{-6}	4×10^{-4}

*Values are measured at an applied normal stress of 40 kPa.

Source: Data after Gerry and Raymond [14].

and difficult to seal against sidewall leaks. This last item is particularly important for geosynthetics with relatively low transmissivity values such as geotextiles. A low flow-rate measurement, with a high (and unknown) potential for leakage, results in a relatively uncertain value of transmissivity.

Instead, a variation of this concept is recommended for geotextile testing whereby *radial* drainage is achieved. Such a device is schematically shown in Figure 2.17, where liquid enters into the inside of the upper load bonnet, then flows radially through the geotextile and is collected around the outer perimeter of the stationary reaction section of the device. The transmissivity concept is adapted accordingly as follows:

$$q = k_p i A$$

$$q = k_p \frac{dh}{dr}(2\pi rt)$$

$$2\pi(k_p t) \int dh = q \int \frac{dr}{r}$$

$$(k_p t) = \theta = \frac{q \, ln(r_2/r_1)}{2\pi\Delta h} \qquad (2.21)$$

where

r_2 = outer radius of the geotextile test specimen, and
r_1 = inner radius of the geotextile test specimen.
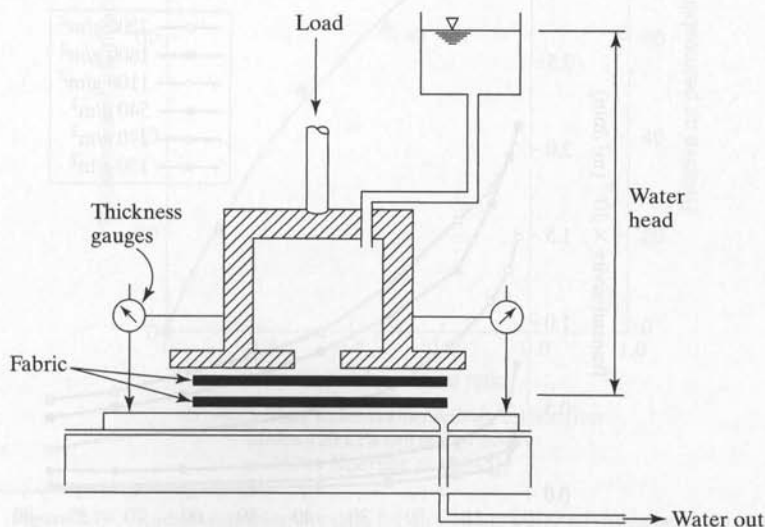
Figure 2.17 Permeability device for measuring geotextile transmissivity (radial in-plane flow).

The thicker nonwoven geotextiles are best suited to convey water in the drainage function, but these are the same geotextiles that are subject to relatively high compression under load. Thus the exponential decrease in transmissivity of the geotextiles shown in Figure 2.18 should come as no surprise. Fortunately, most geotextiles reach constant values after approximately 100 kPa, beyond which the yarn structure is sufficiently tight and dense to hold the load and still convey liquid to the extent shown. Note also the increase in transmissivity with increasing mass per unit area (or number of layers).

Lastly, it should be noted that the radial device shown in Figure 2.17 can readily be adapted to measure the in-plane flow of gases (e.g., air, methane, or radon) by placing a shroud around the outside of the load bonnet. The gas is introduced under controlled pressure and measured at the outlet for its flow rate. Typical air transmissivity data are given in Figure 2.19(a). The same device can be used under combined airflow through partially saturated geotextiles to assess *permselectivity*, as shown in Figure 2.19(b).

Soil Retention: Underwater Turbidity Curtains. One variation of a soil-retention test is directed primarily toward the use of geotextiles as *underwater turbidity (or silt) curtains*. The test device consists of two rectangular tanks that are placed end to end with slide gates facing one another. Between these two slide gates is the geotextile test specimen. The upstream tank (with the slide gate closed) is now filled with water that has a known amount of uniformly mixed silt in it. The gate valve at the exit end of the downstream tank is opened. The test begins by lifting up the slide gates on each side of the geotextile and allowing the (turbid) water to pass through the geotextile,
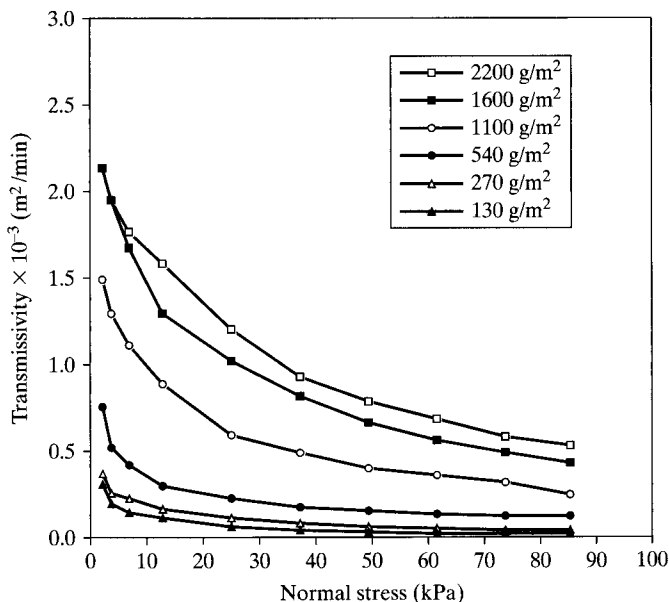
Figure 2.18 Transmissivity test results for different mass per unit area of nonwoven needle-punched geotextiles.
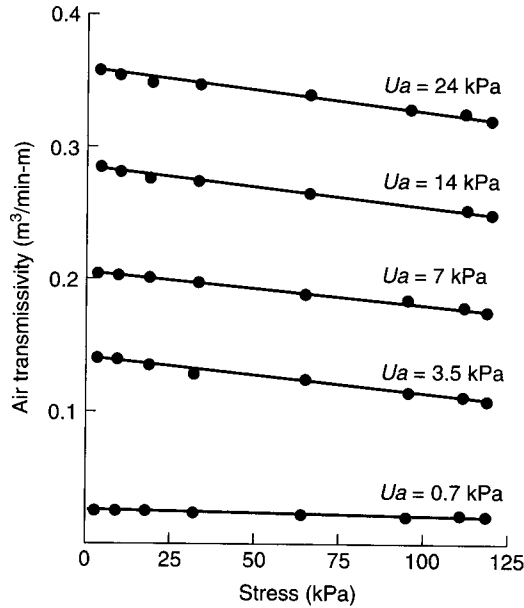
(a) Air transmissivity data
(after Koerner and Bove [44])
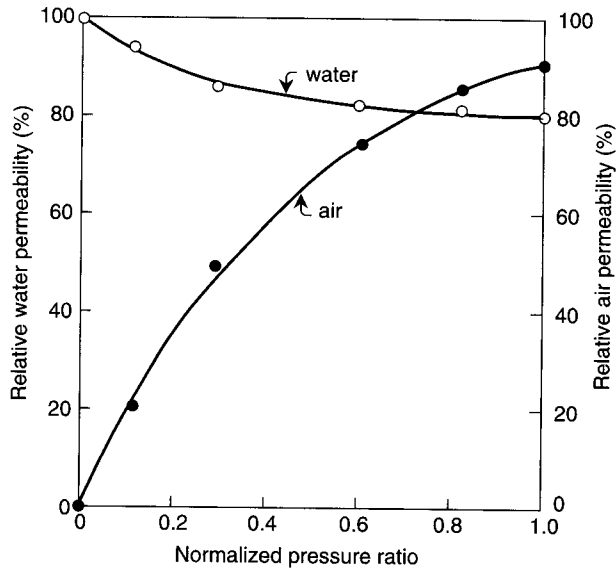
(b) Air versus water transmissivity interaction
under 120 kPa normal pressure
(after Koerner, et al. [45])

Figure 2.19   Radial transmissivity data for air and air/water mixtures on a 550 g/m^2 nonwoven needle-punched geotextile.

which is acting as a submerged soil filter. Clear water is continually added to the upstream tank to maintain a constant head. Two values are generated:

1. The flow rate and velocity through the geotextile, which is indicative of its void space and the amount of clogging that occurs.
2. The percentage of solids passing through the geotextile during the test process, which is indicative of the geotextile's retention capability.

This test, developed by the New York Department of Transportation, is aimed at an assessment of turbidity of rivers and streams during adjacent construction activities.

Soil Retention: Above-Ground Silt Fences.   The second variation of a soil retention test is directed toward the use of geotextiles as *above-ground silt fences*. The test protocol and setup is covered in ASTM D5141. Here the soil (usually a silty sand) is slurried in water and poured into a flume box measuring 1200 mm long × 800 mm wide × 300 mm high. The candidate geotextile, measuring 800 mm × 300 mm, forms the downstream end of the box, which is set at an 8% slope. The flow rate of the soil-water mixture is monitored with time, and the amount of fines passing through the geotextile is measured to determine the soil retention capability. The process is repeated at least three times to determine the degree of clogging that has occurred. Two values are generally reported:

1. The slurry flow rate (1/min-m)
2. The retention efficiency (%)

The recommended procedure, developed by the Virginia Department of Transportation under designation VTM-51, also includes a field method with the same objective of determining the filtering efficiency of the geotextile.

2.3.5 Endurance Properties

Thus far the testing of geotextiles has concentrated on the short-term material behavior of the as-manufactured fabric. Yet, the question remains regarding their behavior during service conditions over the design lifetime of the system; in other words, *endurance* is of concern. This section addresses some of the tests that focus on this question. The reader should also see ASTM D5819 and ISO 13429, which are guides for selecting various endurance test methods.

Installation Damage.   It should be obvious that harsh installation stresses can cause geotextile damage. In some cases installation stresses might be more severe than the actual design stresses for which the geotextile is intended. There are a number of references available, but most involve removal of the geotextile after considerable time, usually years. In this section, focus is on the immediate damage that can be caused by the contractors' operations during installation.

In order to assess this situation, 100 field sites were evaluated by removing approximately 1.0 m^2 of the geotextile within hours after placement. The procedure followed closely the ISO 13437 protocol. Most of the geotextiles were used for highway base separation, but some were for embankments, walls, underdrains, erosion control, staging areas, access ways, and so on. The entire exhumed sample was brought into the laboratory along with an equal size of the unused and uninstalled geotextile for comparison purposes. Test specimens were taken from the exhumed and unused geotextiles and were tested. The percentage of strength reduction was calculated. The following mechanical tests were performed:

- Grab tensile (3 to 6 tests per site)
- Puncture resistance (3 to 6 tests per site)
- Trapezoidal-tear resistance (3 to 6 tests per site)
- Burst resistance (3 to 6 tests per site)
- Wide-width strength in machine direction (1 to 2 tests per site)
- Wide-width strength in cross-machine direction (1 to 2 tests per site)

A hole count was also made of the exhumed geotextiles. In Figure 2.20a, the relationship between retained strength (the weighted average of the above tests) and number of holes per square meter is observed. The entire data set was arbitrarily divided into three groups: (1) acceptable, (2) questionable, and (3) nonacceptable (Regions A, B, and C, respectively, in Figure 2.20b). While loss of strength can be accommodated via a suitable installation-damage reduction factor (the inverse of the numeric strength retained value shown in Figure 2.20), we could well wonder how the separation and filtration functions can properly work with the occurrence of so many holes. It should be noted that the recommendations of this study by Koerner and Koerner [46], suggests that no geotextile less than 270 g/m^2 should be used unless special precautions are taken, such as a sand cushioning layer along with lightweight construction equipment, to avoid installation damage.

Creep (Constant Stress) Tests.   *Creep* is the common name applied to the elongation of a geotextile under constant load. Since polymers are generally considered creep-sensitive materials, it is an important property to evaluate. The test specimens should be of the wide-width variety (recall Figure 2.8c) and are usually stressed by means of stationary hanging weights. Since the test duration should be long, a number of tests are often conducted simultaneously by cascading the test specimens and their respective loads. The setup can also be horizontal with a number of specimens connected to one another.

Selection of the load is important, and it is usually based on a percentage of the geotextile's strength as determined from a conventional test, as described in Section 2.3.3. If such a value is considered to be 100%, creep test stresses of 20%, 40%, and 60% are sometimes evaluated. Stresses are commonly applied for 1000 to 10,000 hours (depending on the particular application) and deformation readings are taken
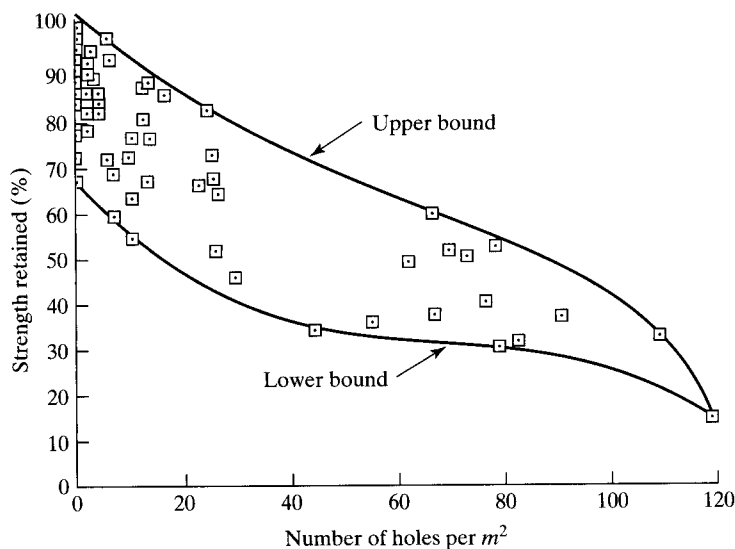
(a) Number of holes versus strength retained of all tests
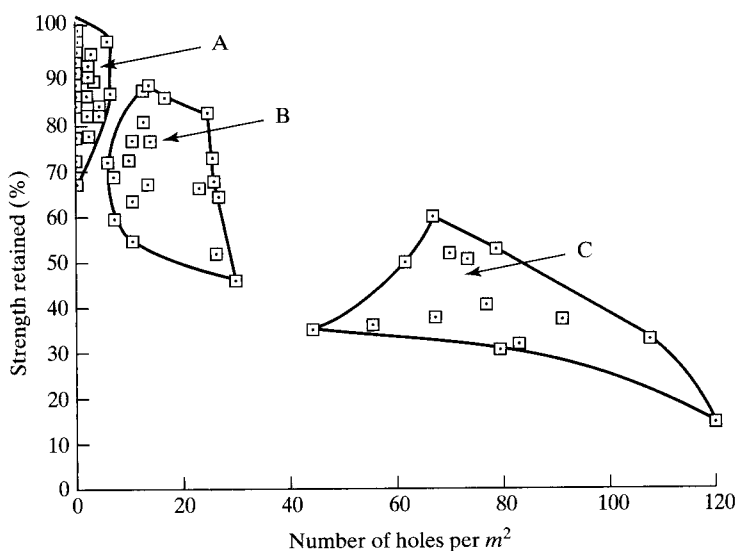
(b) Number of holes versus strength retained separated into zones

Figure 2.20   Results of field exhuming of geotextiles immediately after installation to assess installation damage. (After Koerner and Koerner [46])

at progressively longer time increments from the beginning of the test (e.g., 1, 2, 5, 10, and 30 min, then 1, 2, 5, 10, 30, 100, 250, 500, 750 and 1000 hrs). For creep tests longer than 1000 hrs, readings every 250 hrs are usually adequate. Obviously, continuous de-formation readings can be taken by LVDTs or other electronic monitoring equipment.

The elongation or percent strain (deformation divided by original length) versus time should be plotted for each stress increment. Both ASTM D5262 and ISO 13431 describe details of the testing procedure. Although completely arbitrary, the slope of the terminal portion of the curve (in units of mm/hr) is then reported. The resulting values can then be empirically compared to maximum allowable values or used directly in a predictive procedure, as described by Shrestha and Bell [47]. Creep rates can also be calculated from these response curves, plotted and compared to some agreed upon limiting value of strain,—for example, at 10%.

Numerous references are available on the creep behavior of geotextile-forming yarns and fabrics. Perhaps the greatest sensitivity is due to stress level and polymer type (see Figure 2.21). Such information is very important in design, since the inverse of the quasi-static strength at which no (or a minimum) creep occurs is used as a value
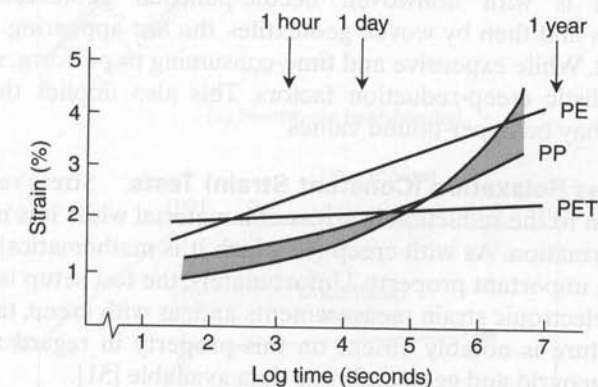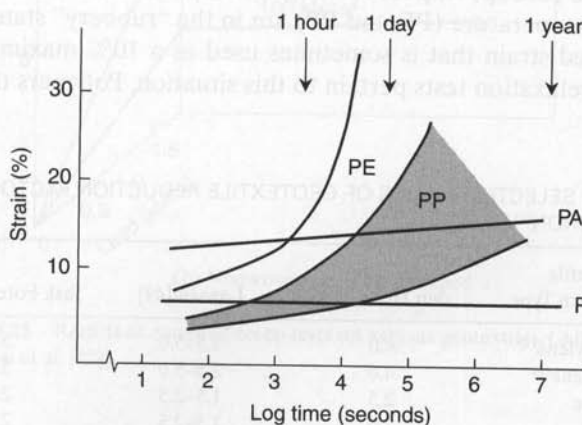
Figure 2.21 Results of creep tests on various yarns of different polymers. (After den Hoedt [48])

for the reduction factor necessary to avoid objectionable creep deformation. Trends from den Hoedt [48] are shown in Figure 2.21 and creep reduction factors from the literature are given in Table 2.8. Care in using these values is suggested, however, since the tests should be geotextile-specific (e.g., polymer type, polymer processing, geotextile type), have similar environmental conditions (e.g., temperature, moisture), model the in-situ stresses (e.g., confinement), and be adjusted for the anticipated service lifetime. Typically the lower values in Table 2.8 are for short lifetimes while the higher numbers are for long lifetimes; all, however, are felt to be relatively conservative.

Confined Creep Tests.   As with the confined wide-width tensile test device shown in Figure 2.10, McGown et al. [22, 23] have also performed confined creep tests in such a device. Some of the results obtained are shown in Figure 2.22. The general tendency of these tests is to show that the creep behavior is improved with soil confinement. As with the short-term confined tensile tests of Section 2.3.3, the major improvement is with nonwoven needle-punched geotextiles, followed by other nonwovens and then by woven geotextiles, the last appearing to show little if any improvement. While expensive and time-consuming to perform, such tests are important to set realistic creep-reduction factors. This also implies that the values given in Table 2.8 may be upper-bound values.

Stress Relaxation (Constant Strain) Tests.   Stress relaxation is the common name given to the reduction in stress of a material while it is maintained under a constant deformation. As with creep (to which it is mathematically related), stress relaxation is an important property. Unfortunately, the test setup is difficult, requiring load cells and electronic strain measurements and, as with creep, taking considerable time. The literature is notably absent on this property in regard to geotextiles, however, there are geogrid and geomembrane data available [51].

Stress (Creep) Rupture.   In general, polymers used in-service above their glass transition temperature (PE and PP) are in the "rubbery" state and are governed by a creep-limited strain that is sometimes used as a 10% maximum. The previous creep and stress relaxation tests pertain to this situation. Polymers that function below their

TABLE 2.8 SELECTED VALUES OF GEOTEXTILE REDUCTION FACTORS AGAINST CREEP DEFORMATION[1]

Geotextile Fiber or Yarn Type	den Hoedt[48]	Lawson[49]	Task Force #27[50]	Koerner[51]
Polypropylene[2]	4.0	2.5–5.0	5.0	3.0–4.0
Polyethylene[2]	4.0	2.5–5.0	5.0	3.0–4.0
Polyamide	2.5	1.5–2.5	2.9	2.0–2.5
Polyester	2.0	1.5–2.5	2.5	2.0–2.5

1. These values are for use in avoiding creep deformation completely—i.e., the zero-creep condition.

2. Refers to polyolefin geotextile yarns, *not* to oriented homogeneous geogrids that are less sensitive to creep and are discussed in Chapter 3.
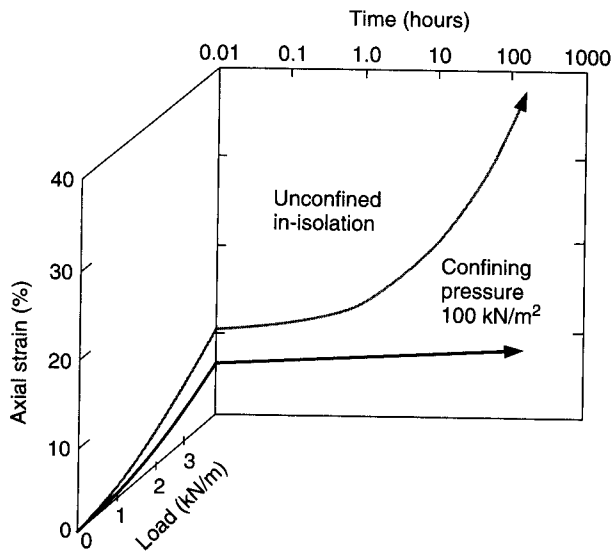
(a) Nonwoven heat-bonded
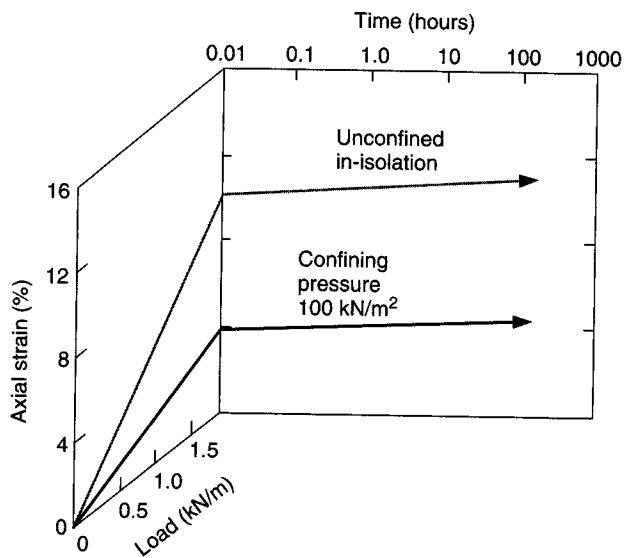
(b) Nonwoven needled-punched

Figure 2.22   Results of confined creep tests on various geotextiles. (After McGown et al. [22])

glass transition temperature (PET, PA, PVA) are in the "glassy" state. Hence, the creep strains are generally quite low and stress (creep) rupture will probably occur before a given strain value is reached. Thus the need for a variation in the creep test method.

Fortunately, the test setup and configuration for stress rupture is identical to that described in ASTM D5262 and ISO 13431. The difference is that the applied stresses are significantly higher. They must be sufficiently high so as to cause rupture, or failure, of the test specimens in a reasonable time. As many as 10 to 15 replicate specimens are brought to failure under different loads and analyzed accordingly. Ingold et al. [52] describe the process that will be addressed in detail in Chapter 3, which deals with geogrids that are always used in the reinforcement function. It should be mentioned that rupture at low loads is difficult to accomplish at typical laboratory testing temperatures and elevated temperatures are sometimes used accordingly. As a result, time-temperature superposition (TTS) per ASTM D5292 and stepped isothermal testing (SIM) per ASTM D6992 along with the necessary curve shifting is necessary. Both methods significantly decrease testing time, while the latter has the added advantage of using a single test specimen.

Abrasion Tests.   The abrasion of geotextiles when in service can be the cause of failure of soil-geotextile systems. The ASTM test methods for abrasion resistance of textile fabrics are designated D1175 and cover six procedures: (1) inflated diaphragm, (2) flexing and abrasion, (3) oscillatory cylinder, (4) rotary platform-double head, (5) uniform abrasion, and (6) impeller tumble.

In all cases, abrasion is the wearing away of any part of a material by rubbing against another surface. There are, however, a large number of variables to be considered in such a test. Results are reported as the percent weight loss or strength/elongation retained under the specified test and its particular conditions.

One of the tests for evaluating the abrasion resistance of geotextiles is the rotary platform–double head (Taber Test, Model 503) method. In this test, both heads are fitted with 1000-g weights and vitrified (CS-17) abrasion wheels. The test specimen is disk-shaped with a 90 mm outer diameter and a 60 mm inner diameter. The specimen is placed on a rubber base on a platform that is rotated and abraded by the stationary abrasion wheels for up to 1000 cycles. Two strip tensile specimens are then cut from the abraded geotextile and tested for their tensile strengths. The average value is then compared to the tensile strength of nonabraded geotextile and the results reported as a percentage of strength retained by the geotextile after abrasion. The percentage of elongation retained after abrasion can also be reported. Figure 2.23 gives results of a series of different types of geotextiles, all of which were approximately 200 g/m^2.

Although this particular test is straightforward to perform and many devices are commercially available, the ASTM and ISO preference is for a uniform (sandpaper) abrasion test. The designations are D4886 and 13427, respectively. Data presentation and analyses are similar to that just described.

All of these tests, however, are questionable simulators of field abrasion conditions. In many cases it would be better to use some sort of tumble test, such as the German Test Standard DIN 5385, which is a large test using a basalt-stone aggregate abrading a geotextile test specimen within a 1.0-m diameter rotating drum.

(a) Strength response

(b) Strain response
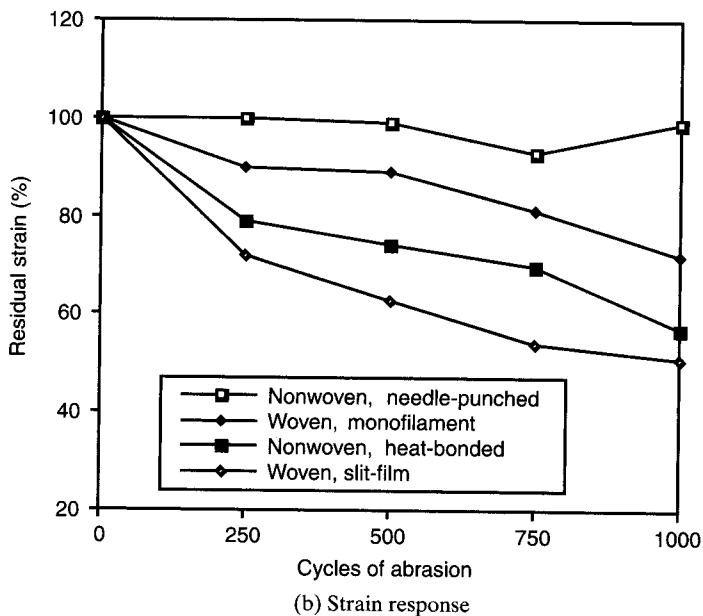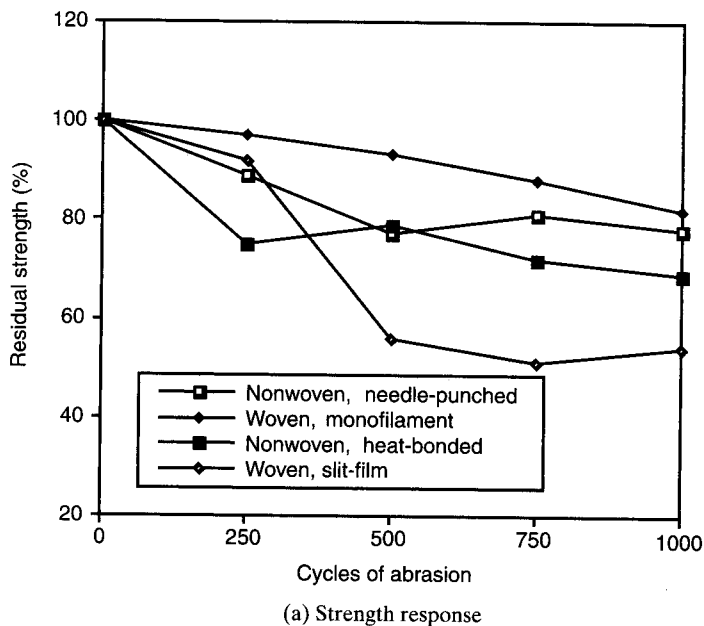
Figure 2.23   Abrasion test results for various geotextiles using the Taber Test, Model 503.

Long-Term Flow (Clogging) Test.   One of the greatest endurance concerns is that of the long-term flow capability of a geotextile with respect to the hydraulic load coming from the upstream soil. Tests are needed to assess the potential of *excessive* geotextile clogging.

The most direct testing approach is to take a sample of the soil at the site and place it above the candidate geotextile, which is fixed in position in a test cylinder. It is then evaluated under constant head flow over a long period of time. A set of such test units can be built and a series of candidate geotextiles tested simultaneously (see Figure 2.24a). The general response is piecewise linear, with the initial portion due largely to hydraulic densification of the soil and not of direct interest. At a transition time of approximately 10 hr (for granular soils) to 200 hr (for fine-grained soils), the soil-geotextile system will enter its field-simulated behavior. If the slope of the response curve becomes essentially zero after this transition time, the geotextile is compatible with the soil at least under the imposed test conditions (hydraulic gradient, temperature, water, etc; see Figure 2.24b). Assuming that the flow rate value at equilibrium is adequate for the situation, the candidate geotextile(s) should be appropriate. If the slope continues to be negative, however, increased clogging is indicated and eventually excessive clogging could occur. In such a case, the geotextile is probably not suited for this type of soil and these test conditions. The database for this particular test has been extended for both clear and turbid water using a number of soil-to-geotextile conditions [54]. If the slope reverses and goes positive, upstream soil loss (also called "piping") is indicated. This is equally unsatisfactory as is excessive clogging, but for a different reason. Piping indicates that the geotextile is too open for the upstream soil, while excessive clogging indicates that the voids are too tight. The test is a good discriminator in this regard.

Although seemingly straightforward in its approach to answering the clogging question, there are drawbacks to the test, the major one being time. The test should normally run for 1000 hr ($\cong 40$ days) to clearly establish the slope of the curve beyond the transition time. (Note that the time axis in Figure 2.24b is logarithmic.) This is unfortunately too long for many real-time situations, where an answer regarding potential clogging is usually needed within a few days. Also, the test chamber can develop bacteria growth in a warm laboratory environment over the required test time, and periodic flushing with a detergent is necessary; this could cause changes in the soil-geotextile system. Finally, the question of de-aired and/or de-ionized water must always be addressed in hydraulic tests of this type.

Gradient Ratio (Clogging) Test.   A test that may be performed in a considerably shorter time than the long-term flow test and that is aimed at determining the hydraulic compatibility of a soil-geotextile system is the U.S. Army Corps of Engineer's Gradient Ratio Test CW-02215. It has been adopted (with slight variations) by ASTM as the D5101 Test Method. In this test, the flow configuration is set up similarly to the long-term flow test just described. Now, however, instead of measuring flow rates, the hydraulic head at various locations in the soil-geotextile column is measured. Head
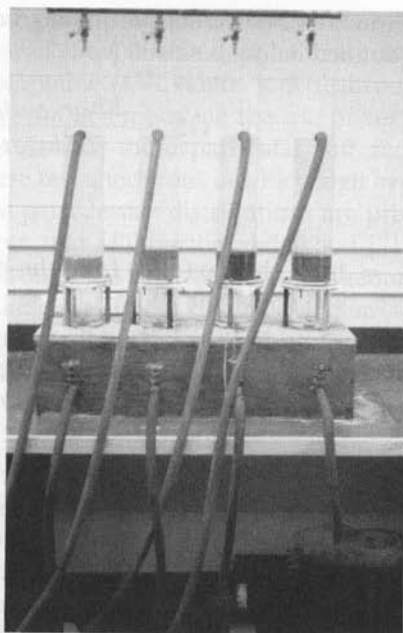
(a) Photograph of setup
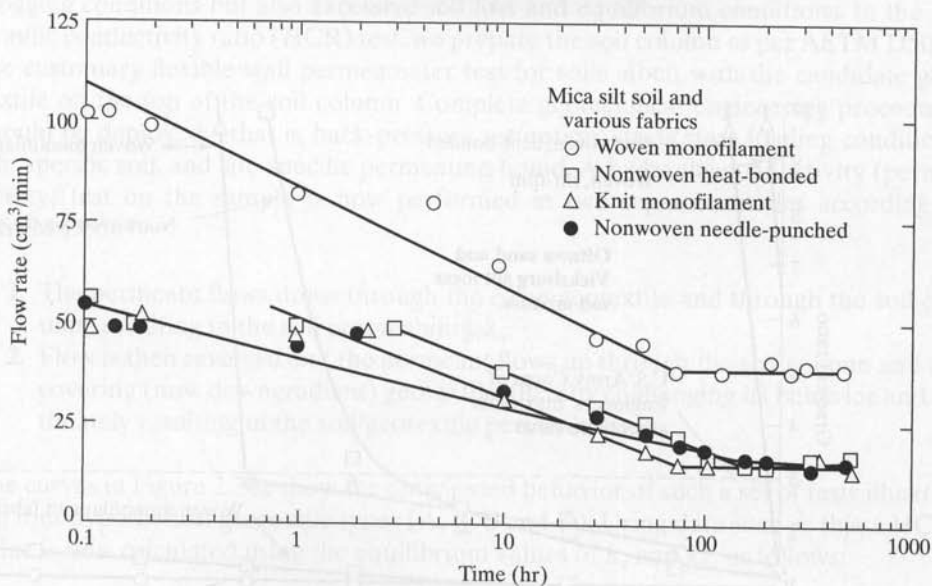
(b) Response curves

Figure 2.24   Long-term flow tests on soil-geotextile systems and typical response curves. (After Koerner and Ko [53])

differences are then converted to hydraulic gradients and finally the gradient ratio (GR) value, as defined below, is calculated:

$$GR = \frac{\Delta h_{GT+25S}/t_{GT+25}}{\Delta h_{50S}/t_{50}} \qquad (2.22)$$

where

Δh_{GT+25S} = head change (mm) from the bottom of the geotextile to 25 mm of soil above the geotextile,

t_{GT+25} = geotextile thickness (mm) plus 25 mm of soil,

Δh_{50S} = head change (mm) between 50 mm of soil above the geotextile, and

t_{50} = 50 mm of soil.

The Corps of Engineers suggests that gradient ratio values greater than 3.0 indicate nonacceptable geotextiles for the type of soil under test. Figure 2.25 gives data illustrating various combinations of soil types and geotextiles. The soil types were systematically varied from an "ideal" rounded sand (Ottawa test sand) to controlled mixtures of sand and cohesionless silt, by varying the percentage of silt added; that is, the creation of gap-graded soils of increasing silt content. When different geotextile types were evaluated with each soil type, the GR response was measured. It is seen that the
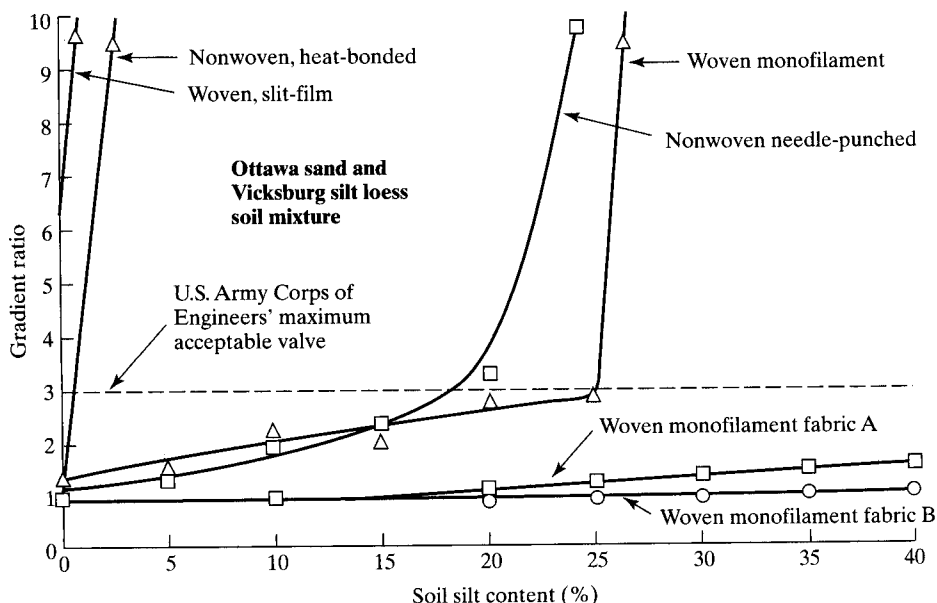
Figure 2.25   Gradient ratio test data used to illustrate geotextile clogging potential. (After Haliburton and Wood [7])

heat-bonded nonwoven and woven slit-film geotextiles were not acceptable $(GR > 3.0)$ as even a nominal percentage of silt was added. In contrast, the woven monofilament geotextiles A and B were acceptable $(GR$ values $< 3.0)$ throughout the silt addition. This type of response is powerful in supporting the use of very open $(POA > 25\%)$ woven monofilament geotextiles for these particular soil and hydraulic conditions. Note that these are very severe test conditions in which high hydraulic gradients, cohesionless soils, and gap-graded particle size distributions are present. Also in these test results, it is important to note that Haliburton and Wood [7] did not report on the amount of silt that passed through the high POA woven geotextiles that had the low gradient ratio values. How the downstream drainage system accommodates the fines that are carried through the geotextile and the possible lack of stability of the upstream soil are both important design issues. The intermediate responses of the nonwoven needle-punched and lower POA woven geotextiles are felt to be a good compromise in this rather unique situation.

The test is not without its share of problems and complications, including long-term stability of the gradient ratio value [8], piping along the test cylinder walls, use of de-aired or deionized water, and air pockets in the soil, geotextile, and head monitoring system.

Hydraulic Conductivity Ratio (Clogging) Test.

Williams and Abouzakhm [55] propose the use of a flexible wall permeameter test to assess not only excessive clogging conditions but also excessive soil loss and equilibrium conditions. In the hydraulic conductivity ratio (HCR) test, we prepare the soil column as per ASTM D5084, the customary flexible wall permeameter test for soils albeit with the candidate geotextile on the top of the soil column. Complete geotechnical engineering procedures should be deployed—that is, back-pressure saturation, stress state loading conditions, site-specific soil, and site-specific permeating liquid. A hydraulic conductivity (permeability) test on the sample is now performed in two separate modes according to ASTM D5567:

1. The permeant flows down through the *clean* geotextile and through the soil column, resulting in the soil permeability, k_s.
2. Flow is then reversed and the permeant flows up through the soil column and the covering (now downgradient) geotextile, thereby challenging its behavior and ultimately resulting in the soil/geotextile permeability, k_{sg}.

The curves in Figure 2.26a show the anticipated behavior of such a set of tests illustrating four hypothetical geotextile types (A, B, C and D). Using data such as this, a HCR-value is now calculated using the equilibrium values of k_s and k_{sg} as follows:

$$HCR = k_{sg}/k_s \qquad (2.23)$$

Values of HCR are then plotted against pore volumes passed through the system, as shown in Figure 2.26b. An interpretation of these curves is suggested by Luettich and Williams [56] whereby high values of HCR suggest soil loss, low values of HCR suggest

(a) Typical response curves

(b) Analysis method using hydraulic conductivity ratio testing
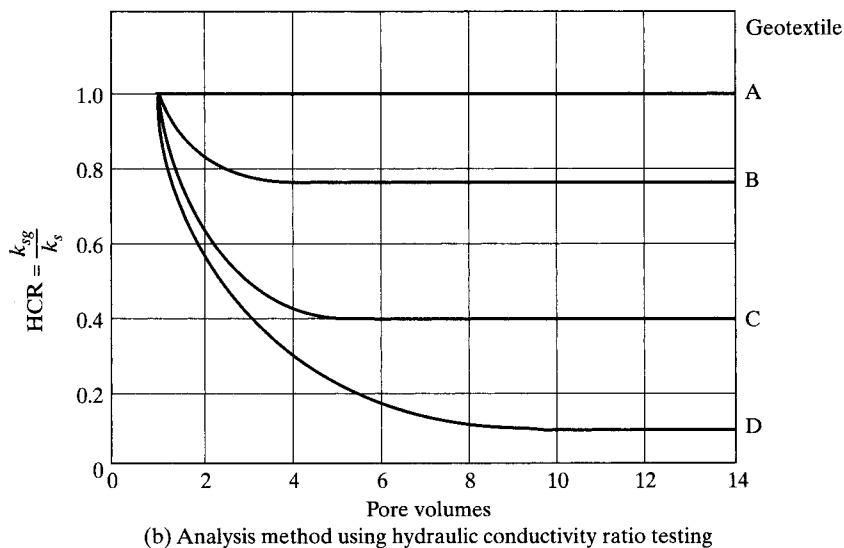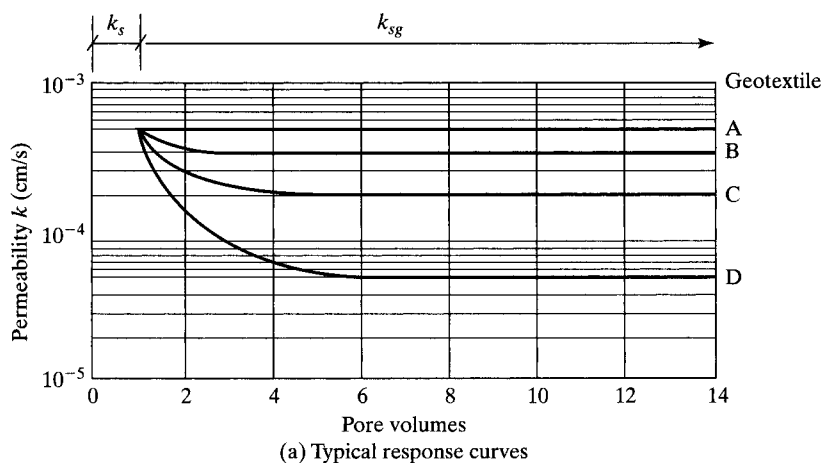
Figure 2.26   Suggested response curves utilizing hydraulic conductivity ratio after testing. (After Leuttich and Williams [56])

excessive clogging, and intermediate values of HCR (for example, between 0.4 and 0.8) suggest soil-to-geotextile equilibrium. The author feels that this test is the premier laboratory test to assess the potential of excessive geotextile clogging and/or soil retention concerns.

2.3.6 Degradation Considerations

"How long will the geotextile last?" This important question for permanent and/or critical applications is asked more frequently than any other in geosynthetics. It will

be addressed through a description of different degradation mechanisms and testing procedures in this subsection. It should be noted that all of the degradation mechanisms to be described result in some form of molecular chain scission, bond breaking, cross-linking, or the extraction of formulated components. Thus there is a fundamental change (albeit it extremely slow in a buried environment) in the polymer at the molecular level from its as-manufactured state. While many chemical fingerprinting methods can be used to detect these changes (recall Table 1.4) they are time-consuming, expensive, and tedious to perform. At the macroscopic level, the mechanical properties will eventually change from the as-manufactured state. For example, a stress-versus-strain curve will gradually transition from a plastic to brittle behavior in that; the modulus will increase, the elongation at failure will decrease, and the strength will often temporarily increase but will eventually decrease. The reader should also see ASTM D5819 and ISO 13429, which are guides for selecting various degradation test methods.

Sunlight (Ultraviolet) Degradation.   Sunlight is an important cause of degradation to all organic materials, including the polymers from which geosynthetics are made. For geosynthetic purposes, energy from the sun is divided into three parts:

- Infrared, with wavelengths longer than 760 nm
- Visible, with wavelengths between 760 and 400 nm
- Ultraviolet (UV), with wavelengths shorter 400 nm

The UV region is further subdivided into UV-A (400 to 315 nm), which causes some polymer damage; UV-B (315 to 280 nm), which causes severe polymer damage; and UV-C (280 to 100 nm), which is only found in outer space.

From summer to winter there are changes in both the intensity and the spectrum of sunlight (see Figure 2.27), most significant being the loss of shorter-wavelengths of UV radiation during the winter months. Other factors in the UV degradation process of polymers are geographic location, temperature, cloud cover, wind, moisture, and atmospheric pollution. These should be considered in any test method. Laboratory simulations are, at best, approximate but nonetheless very important.

For laboratory simulation of sunlight, artificial light sources (lamps) are generally compared with worst-case conditions, or the "solar maximum condition." The actual degradation is caused by photons of light breaking the polymer's chemical bonds. For each type of bond, there is a threshold wavelength for bond scission; above the threshold the bonds will not break, below it they will. Thus the short wavelengths are critical. The literature [57] shows that polyethylene is most sensitive to UV degradation around 300 nm, polyester around 325 nm, polypropylene around 370 nm, polyvinyl chloride around 312 nm, and polystyrene around 315 nm; that said, they are all within the UV-A or UV-B range of the wavelength spectrum.

Of the variety of laboratory exposure devices, Xenon Arc exposure is widely used and is often recommended for use on geotextiles. Two features are very important: (1) the filters (used to reduce unwanted radiation) and (2) the irradiance settings (used to compensate for lamp aging). The recommended ASTM test for geotextiles is D4355, which uses either Type BH or C as described in ASTM G26. Specimens are
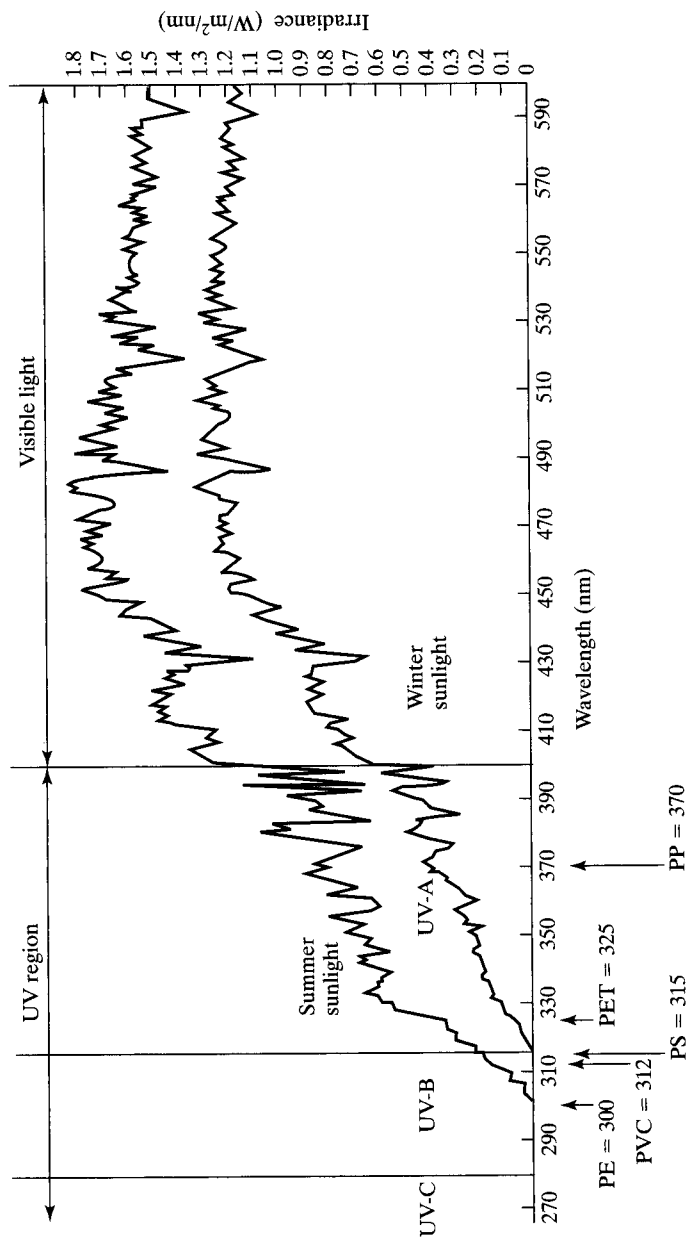
Figure 2.27 The wavelength spectrum of visible and UV solar radiation. (After Q-Panel Co., Cleveland, OH)

exposed for 0, 150, 300, and 500 hr. The exposure consists of 120-min cycles; light only (102 min), then water spray and light (18 min). The test procedure allows the user to develop a curve to assess the amount of degradation, but it should be recognized that the device requires significant operational costs, is very expensive, and can be challenged on technical grounds as to its similitude to actual conditions.

Another laboratory exposure device (the type favored by the author) is the Ultraviolet Fluorescent Light Test Method covered under ASTM test methods G53 and D5208. While this method can also be challenged as to its simulation relevancy and use in comparing different polymer types, the device is easy to maintain and quite reasonable in its initial cost and operational costs. The exposure is similar to that described above—that is, cycles of light only, followed by water spray and light.

Using either exposure device the test coupons are removed at designated times, cut into strip-tension test specimens, and evaluated for their retained strength and elongation. The results are then compared to the unexposed geotextile for percent retained values (see Figures 2.28a and b). Alternatively, we can use the information obtained in a predictive manner to determine the equivalent field behavior at a specific location.

Example 2.7

Assume that a geotextile reaches its half-life elongation in a laboratory weathering device (Energy $= 517.8$ W/m^2) in 2000 hr. What is the equivalent lifetime in Philadelphia with a known average exposure energy of 5021 MJ/m^2-yr? *Note*: Joule (J) $=$ watts (W) $\times$ seconds (sec)

Solution:

$$E_{test} = (517.8)(2000)(3600)(1 \times 10^{-6})$$
$$= 3728 \text{ MJ/m}^2$$
$$E_{Phila} = (5021 \text{ MJ/m}^2 - \text{yr})(1/4 \text{ sun time})$$
$$= 1255 \text{ MJ/m}^2 - \text{year}$$
$$T_{Phila} = \frac{3728}{1255} = 2.97 \text{ years}$$

Thus, the acceleration factor (AF) of the exposure device over real-time exposure is

$$AF = \frac{(2.97)(365)}{(2000)(1/24)} = 13$$

Ultraviolet degradation is also covered by ASTM under the title "Outdoor Weathering of Plastics," designated D1435. This procedure is intended to define site-specific conditions for the exposure of plastic materials to light and weather. It is a comparative test depending on a defined climate, time of year, atmospheric conditions, and so on. Racks are constructed with the geotextile coupons to be evaluated fixed to them. Samples can be placed at 0, 45°, or 90° to the horizontal and in different solar orientations. Exposure test samples should simulate service conditions of the end-use application as much as practical. A specific version of this test is available as ASTM D5970, which was used to generate the data in Figure 2.28c and 2.28d. Clearly, if a test of site-specific UV degradation is desired at a critical field site where the geotextile is

to be exposed for months or years, outdoor weathering tests of this type should be considered.

Whatever the test method used to produce UV-degradation results, it is clear that geotextiles must be shielded from prolonged ultraviolet light exposure. Geotextile rolls are always shipped with a protective plastic covering and only when the material is ready for use should it be unrolled and exposed. The manufacturer's recommendations for "timely cover" (backfilling) must be rigidly met. Cover placement (soil or another geosynthetic) for polypropylene geotextiles should generally be within 14 days (per AASHTO M288), with polyesters being allowed longer exposure times. For long-term exposed applications, testing of the type reported in Figure 2.28c and 2.28d is necessary—that is, actual outdoor weathering tests that can be performed on a site-specific basis.
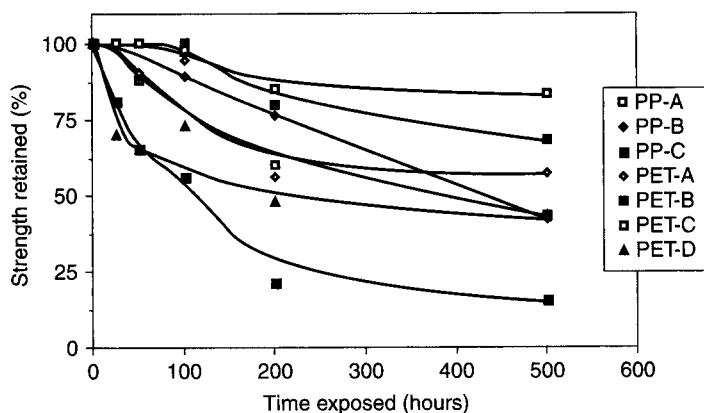
(a) Strength retained after exposure in laboratory ultraviolet
fluorescent device, per ASTM D5208.
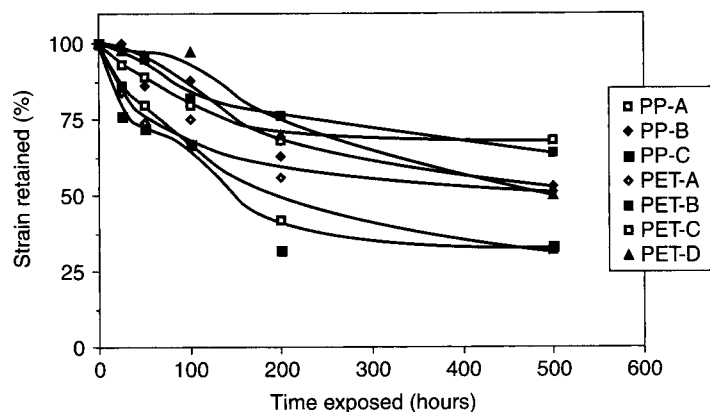
(b) Strain retained after exposure in laboratory ultraviolet
fluorescent device, per ASTM D5208.

Figure 2.28   Degradation of various geotextiles due to ultraviolet exposure.
(After Koerner et al. [58])
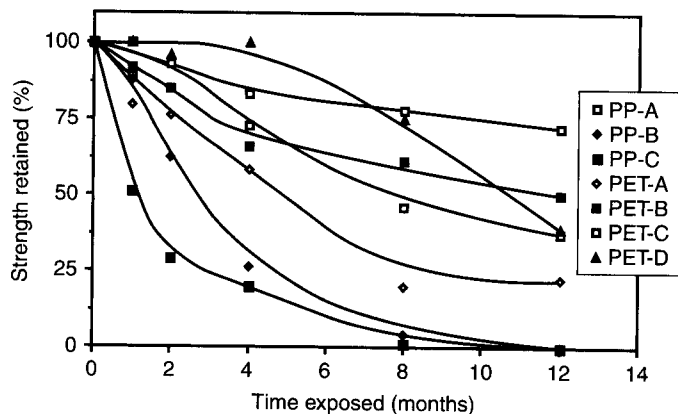
(c) Strength retained after outdoor exposure in Austin, Texas
    per ASTM D5970
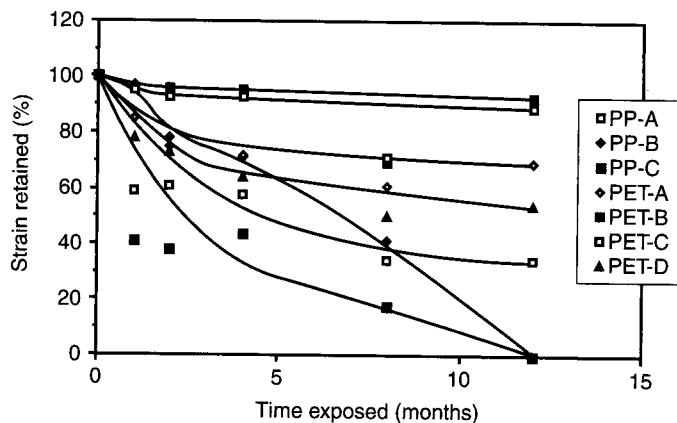
(d) Strain retained after outdoor exposure in Austin, Texas
    per ASTM D5970

Figure 2.28   (*continued*)

Temperature Degradation.   Extremely high temperature causes all polymer
degradation mechanisms to occur at an accelerated rate. In fact, at the heart of *time-
temperature-superposition* lifetime prediction techniques (used in Arrhenius model-
ing) is to test laboratory specimens at temperatures from 50°C to 100°C and extrapolate
the accelerated degradation down to field-anticipated temperatures. Thus high temper-
ature is an acceleration phenomenon acting with other degradation mechanisms like
sunlight, oxidation, hydrolysis, chemical, radiation, biological, and so on. As such, labo-
ratory temperature testing (per se) as an individual degradation mechanism will not be
discussed separately.

Regarding the mechanical behavior of plastics (insofar as engineering properties
are concerned), hot and cold temperatures cause a softening and stiffening respectively,

as would be expected. For geotextiles, high temperatures slightly increase flexibility, and ASTM D1388 can be used to quantify the behavior (recall Section 2.3.2).

ASTM Test Method D746 addresses the effect of cold temperatures on plastics and, in particular, on brittleness and impact strength. At severely cold temperatures, specimens are tested by a specified impact device (recall Section 2.3.3).

For geotextiles, however, neither hot nor cold *field* temperatures are generally important topics or issues, except in extreme environmental situations.

Oxidation Degradation.   While all types of polymers react with oxygen causing degradation, the polyolefins (polypropylene and polyethylene) are generally considered to be the most susceptible to this phenomenon. Hsuan et al. [59] describe the chemical mechanism. It will be presented in detail in Chapter 5 since geomembranes are seeing the most research activity, and data are now becoming available.

ASTM Recommended Practice D794 describes high-temperature oxidation testing for plastics. Only the incubation procedure for heat exposure is specified, the test method(s) for assessment being governed by the potential end use. Heat is applied using a forced-air oven with controlled airflow and with substantial fresh-air intake. Two types of incubation are described: (1) continuous heat and (2) cyclic heat. In the former, heat is gradually increased until failure occurs. Failure is defined as a change in appearance, weight, dimension, or other properties that alter the material to a degree that it is no longer serviceable for the purpose. The test may be very short or require months, depending on the rate of temperature increase. The cyclic heat test repeatedly applies heat up to a constant value until failure.

A number of research efforts are ongoing to assess geotextile oxidative behavior using forced-air ovens at (constant) elevated temperatures; the higher the temperature, the greater the rate of oxidative degradation. Changes in tensile strength, elongation, and modulus are tracked over time. Properly plotted, these trends are back-extrapolated to a site-specific (i.e., lower) temperature to arrive at a predicted lifetime. The procedure is the essence of time-temperature-superposition, followed by Arrhenius modeling.

Caution should be exercised in the incubation of geotextiles at extremely high temperature. Polypropylene melts at 165°C and polyethylene melts at 125°C. Such high temperatures should obviously be avoided and oxidative incubation should be at significantly lower temperatures.

Hydrolytic Degradation.   Hydrolysis can cause degradation via either internal or external fiber or yarn reactions. Geosynthetics manufactured using polyester resins are particularly affected when the immersion liquid has a very high (pH > 10) or very low (pH < 3) alkalinity.

Table 2.9 gives an indication of trends in degradation behavior insofar as loss of strength is concerned [60]. As seen, extremely high pH values can affect some polyesters, while extremely low pH values can be harsh on some polyesters and polyamides. It is important that the polyester resin used for permanent geotextile applications has a high molecular weight (e.g., $>25,000$) and a low carboxyl end group (CEG) concentration (e.g., <30). These effects are further described by Hsuan et al. [59] and Hsieh et al. [61].

TABLE 2.9 EFFECT OF HYDROLYSIS ON STRENGTH LOSS AT DIFFERENT pH LEVELS ON VARIOUS GEOTEXTILES AT 20°C AFTER 120 DAYS

Geotextile Type	Solution	Weight (g/m^2)	pH = 2	pH = 4	pH = 7	pH = 10	pH = 12
PP monofilament woven (Manufacturer 1)	$Ca(OH)_2$	220	—	—	nc	nc	nc
PP needle-punched nonwoven (Manufacturer 2)	$Ca(OH)_2$	770	—	—	nc	nc	nc
PP heat-bonded nonwoven (Manufacturer 3)	$Ca(OH)_2$	100	—	—	nc	nc	incl.
PVC monofilament woven (Manufacturer 4)	$Ca(OH)_2$	95	—	—	nc	nc	nc
PET staple needle-punched nonwoven (all white fibers, Manufacturer 5)	$Ca(OH)_2$	550	—	—	nc	nc	nc
PET heat-bonded nonwoven (Manufacturer 3)	$Ca(OH)_2$	100	—	—	nc	nc	nc
PET staple needle-punched nonwoven (Mixture of white and black fibers, Manufacturer 5)	$Na(OH)$	450	—	—	nc	−33%	−53%
PET heat-bonded nonwoven (Manufacturer 3)	$Na(OH)$	100	—	—	nc	nc	nc
PET staple needle-punched nonwoven "A" (Mixture of white and black fibers, Manufacturer 6)	$Na(OH)$	150	−18%[+]	nc	nc	−27%	−32%
PET staple needle-punched nonwoven "B" (Mixture of white and black fibers, Manufacturer 6)	$Na(OH)$	150	nc	nc	nc	−13%	−16%
PET staple needle-punched nonwoven (all white fibers, Manufacturer 6)	$Na(OH)$	150	nc	nc	nc	nc	nc
PET needle-punched nonwoven "A" (carbon black blended fibers, Manufacturer 6)	$Na(OH)$	134	−12%	−15%	nc	nc	nc
PET needle-punched nonwoven "B" (carbon black blended fibers, Manufacturer 6)	$Na(OH)$	134	nc	nc	nc	nc	nc
PET staple needle-punched nonwoven (bottle grade resin, Manufacturer 7)	$Na(OH)$	264	nc	nc	nc	nc	nc

Note: All fibers are continuous unless otherwise noted.

Abbreviations: nc—*no change* within estimated experimental accuracy of ±10%; incl.—*inconclusive* due to large scatter of the data; +—longer testing time required to draw a meaningful conclusion.

Source: After Halse et al. [60].

In cases of concern, the candidate geotextile should be incubated in water having the prevailing pH levels at 20°C and 50°C for at least 120 days and then tested for changes in strength and elongation. For a base-line comparison, it is important to have a complete parallel set of samples incubated in distilled water (pH = 7) at the same temperatures.

Chemical Degradation. ASTM Method D543 covers chemical degradation under the title "Resistance of Plastics to Chemical Reagents." The test method includes provisions for reporting changes in weight, dimensions, appearance, and strength. Provisions are also made for various exposure times and exposure to reagents at elevated temperatures. A list of 50 standard reagents is supplied in order to attempt some sort of standardization.

For example, the DuPont Company has evaluated most of its yarns (including acetate, dacron, nylon, orlon, rayon, cotton, wool, and silk) under a wide range of chemicals (sulfuric acid, hydrochloric acid, nitric acid, hydrofluoric acid, phosphoric acid, organic acids, sodium hydroxide, bleaching agents, scouring and laundering agents, salt solutions, and organic and miscellaneous chemicals), many of which were at different concentrations and at different temperatures. After the specified exposure, the coupons were rinsed, air dried, and then conditioned at 21°C and 65% relative humidity for 16 hours. Data on test specimen strength, elongation, and toughness of the exposed yarns were compared to control specimens of the yarns that were not exposed to the chemical. Similar information is available from most raw material suppliers and some geotextile manufactures for their particular products in many standard chemical environments.

Notable exceptions to the use of literature values using standard incubation liquids are geotextiles used at landfill sites, heap leach pads, and agriculture waste facilities. Here the liquid can be very aggressive and uniquely site-specific. In such cases, the actual leachate, or a synthetized version thereof, is to be used as the incubation liquid. ASTM D5322 presents the laboratory incubation methodology and ASTM D5496 gives an alternative field incubation methodology. Upon removal of the geotextile coupons (typically 120 days at 50°C) they are tested according to ASTM D6389 to assess the percent change from the nonincubated samples. Decisions as to the geotextile's compatibility or noncompatibility to the site-specific leachate are made accordingly.

Biological Degradation. In order for microorganisms such as bacteria or fungi to degrade polymers, the organisms must attach themselves to the fiber or yarn surfaces and use the polymer as a feedstock. This is highly unlikely. All the resins used for geosynthetics are very high in molecular weight with relatively few chain endings for the biodegradation process to be initiated. In fact, there is a concerted effort ongoing to develop polymers that will biodegrade, with little apparent success. Irrespective of the above comment, ISO 12961 is focused on microbiological degradation.

The additives to the polymer, however, might be somewhat more vulnerable than the resin itself. Plasticizers or processing aids could be vulnerable, although there is no authoritative research on the subject to my knowledge.

Converse to biological *degradation*, biological *clogging* is clearly a concern depending on the characteristics of the permeating liquid. For those liquids high in microorganism content, exacerbated by high suspended solids content, excessive clogging

has occurred. Clearly landfill leachates have been problematic in this regard [62, 63], and animal waste runoff from large farms promises to be likewise.

Radioactive Degradation.   While there are no references in the open literature on the radioactive degradation of geotextiles, the subject is generally discussed when dealing with radioactive waste disposal. It is assumed, though clearly not proven, that low-level radioactive exposure (by hospital garments, nuclear power plant tools and clothing, ground emanating radon, etc.) is orders of magnitude too low to cause chain scission of geosynthetic-related polymers. Conversely, high-level radioactive waste (e.g., spent nuclear fuel rods) is suspect and, if in the proximity of geotextiles, could cause radiation degradation. The situation must be experimentally evaluated if radioactive conditions are anticipated, although such testing will involve major health and safety issues and be extremely expensive.

Other Degradation (and Damage) Processes.   Other processes that may degrade geotextiles are ozone attack (only in certain climates and when exposed) and rodent or muskrat attack (which is site specific and has happened when the animal was trapped). Also, seagulls, hawks, and vultures have been known to pull apart exposed geotextiles at many landfill and reservoir sites. In spite of these degradation and/or damage mechanisms, the performance record for geotextile durability has been quite good as will be described in the next section.

Geotextile Aging.   While specific test standards are not available to measure the aging of geotextiles (due to the complexity of the many mechanisms involved), field-exhuming work is continually being reported. Perhaps the longest functioning geotextile that is periodically exhumed is at the Volcros Dam in France (Gourc and Faure [64]). Both mechanical and hydraulic properties are examined and compared to original properties. Losses were generally nominal with maximum reductions (perhaps installation-related) being 30%.

Numerous studies on the exhuming of geotextiles have been reported in the literature. Tests on these recovered samples show that geotextiles remain in good to excellent condition. This indicates to the author that the proper polymers and formulations are at hand and are being utilized in the manufacture of geotextiles used in the applications to be discussed. For extremely long service lifetimes a laboratory procedure using time-temperature-superposition and Arrhenius modeling will be presented in Chapter 5.

2.3.7 Summary

This section on geotextile properties is very important and could have been dealt with in greater detail than we have. The subject deserves this attention, for any quantifiable design method will result in numbers to be compared to the candidate geotextile's actual properties. This section dealt with the relevant properties and subsequent test values, how they are obtained, their authenticity, and their reliability. In some cases, additional inquiry and research was recommended.

The section included a mixture of in-isolation (or index) properties and soil-to-geotextile related (or performance) properties. Eventually, the tests for these different properties will sort out into their respective categories and uses, but most organizations are looking at the complete collection of tests as they were presented here.

Regarding a summary of geotextile properties, the rapidly changing market and its demands make it difficult to give precise values. However, for many commercially available geotextiles, Table 2.10 gives the range of current values. For specific values of a particular type of geotextile the respective manufacturers should be consulted; all have up-to-date Web sites that can be freely accessed.

2.4 ALLOWABLE VERSUS ULTIMATE GEOTEXTILE PROPERTIES

It is important to recognize that many of the preceding geotextile test properties represent idealized conditions and therefore result in the maximum possible numeric values when used directly in design; that is, they result in upper-bound values. In the design-by-function concept described in Section 2.1.3, the factor of safety was formulated around an allowable test value (equations 2.2a and 2.2b). Generally, most laboratory test values cannot be used directly; they must be suitably reduced for the in situ conditions. This could be done directly in the test procedure—for example, by conducting a completely simulated performance test; but in most cases, this simply is not possible. Simulating installation damage, performing long-term creep testing, using site-specific liquids, reproducing in situ pore water stresses, providing complete stress state modeling, and so on are generally not feasible. To account for such differences between the laboratory measured test value and the desired performance value, two approaches can be taken:

1. Use an extremely high factor of safety at the end of a problem.
2. Use reduction factors on the laboratory-generated test value to make it into a site-specific allowable value.

The latter alternative of *reduction factors* will be used in this book. By doing this, the usual value of the factor of safety can be assessed in the final analysis. Our approach will be to refer to the general laboratory-obtained value as an "ultimate" value and to modify it by reduction factors to an "allowable" value.

2.4.1 Strength-Related Problems

For problems dealing with geotextile strength, such as those involving separation and reinforcement applications, the formulation of the allowable values takes the form of equation (2.24a). Typical ranges of values for reduction factors for different applications are given in Table 2.11. These values must be tempered by the site-specific considerations. Also, note that if the laboratory test includes the mechanism listed, it appears in the equation as a value of 1.0.

TABLE 2.10 TYPICAL RANGE OF PROPERTIES FOR CURRENTLY AVAILABLE GEOTEXTILES

Physical Properties	
Specific gravity	0.9–1.7
Mass per unit area	135–2000 g/m²
Thickness	0.25–7.5 mm
Stiffness	nil–25,000 mg-cm

Mechanical Properties	
Compressibility	nil–high
Tensile strength (grab)	0.45—4.5 kN
Tensile strength (wide width)	9–180 kN/m
Confined tensile strength	18–180 kN/m
Seam strength	50–100% of tensile
Cyclic fatigue strength	50–100% of tensile
Burst strength	350–5200 kPa
Tear strength	90–1300 N
Impact strength	14–200 J
Puncture strength	45–450 N
Friction behavior	60–100% of soil friction
Pullout behavior	50–100% of geotextile strength

Hydraulic Properties	
Porosity (nonwovens)	50–95%
Percent open area (wovens)	nil–36%
Apparent opening size (sieve size)	2.0–0.075 mm (#10–#200)
Permittivity	0.02–2.2 s⁻¹
Permittivity under load	0.01–3.0 s⁻¹
Transmissivity	0.01–2.0 × 10⁻³ m²/min
Soil retention: turbidity curtains	m.b.e.
Soil retention: silt fences	m.b.e.

Endurance Properties	
Installation damage	0–70% of fabric strength
Creep response	g.n.p if <40% strength is being used
Confined creep response	g.n.p. if <50% strength is being used
Stress relaxation	g.n.p. if <40% strength is being used
Abrasion	50–100% of geotextile strength
Long-term clogging	m.b.e. for critical conditions
Gradient ratio clogging	m.b.e. for critical conditions
Hydraulic conductivity ratio	0.4–0.8 appear to be acceptable

Degradation Considerations	
Temperature degradation	high temperature accelerates degradation
Oxidative degradation	m.b.e. for long service lifetimes
Hydrolysis degradation	m.b.e. for long service lifetimes
Chemical degradation	g.n.p. unless aggressive chemicals
Biological degradation	g.n.p.
Radioactive degradation	g.n.p. unless high level
Sunlight (UV) degradation	major problem unless protected
Synergistic effects	m.b.e.
General aging	actual record to date is excellent

Abbreviations: m.b.e.—must be evaluated; g.n.p.—generally no problem

TABLE 2.11 RECOMMENDED STRENGTH-REDUCTION FACTOR VALUES FOR USE IN EQUATION (2.24a)

Area	Range of Reduction Factors		
	Installation Damage	Creep[1]	Chemical/Biological Degradation[2]
Separation	1.1 to 2.5	1.5 to 2.5	1.0 to 1.5
Cushioning	1.1 to 2.0	1.2 to 1.5	1.0 to 2.0
Unpaved roads	1.1 to 2.0	1.5 to 2.5	1.0 to 1.5
Walls	1.1 to 2.0	2.0 to 4.0	1.0 to 1.5
Embankments	1.1 to 2.0	2.0 to 3.5	1.0 to 1.5
Bearing and foundations	1.1 to 2.0	2.0 to 4.0	1.0 to 1.5
Slope stabilization	1.1 to 1.5	2.0 to 3.0	1.0 to 1.5
Pavement overlays	1.1 to 1.5	1.0 to 2.0	1.0 to 1.5
Railroads (filter/sep.)	1.5 to 3.0	1.0 to 1.5	1.5 to 2.0
Flexible forms	1.1 to 1.5	1.5 to 3.0	1.0 to 1.5
Silt fences	1.1 to 1.5	1.5 to 2.5	1.0 to 1.5

1. The low end of the range refers to applications that have relatively short service lifetimes and/or situations where creep deformations are not critical to the overall system performance.

2. Previous editions of this book have listed biological degradation as a separate reduction factor. As described in Section 2.3.6, however, there is no evidence of such degradation for the polymers used to manufacture geotextiles.

$$T_{\text{allow}} = T_{\text{ult}} \left(\frac{1}{\text{RF}_{ID} \times \text{RF}_{CR} \times \text{RF}_{CBD}} \right) \qquad (2.24a)$$

$$T_{\text{allow}} = T_{\text{ult}} \left(\frac{1}{\Pi \text{RF}} \right) \qquad (2.24b)$$

where

T_{allow} = allowable tensile strength,

T_{ult} = ultimate tensile strength,

RF_{ID} = reduction factor for installation damage (≥ 1.0),

RF_{CR} = reduction factor for creep (≥ 1.0),

RF_{CBD} = reduction factor for chemical and biological degradation (≥ 1.0), and

ΠRF = value of cumulative reduction factor (≥ 1.0).

Note that equation (2.24a) could have included additional site-specific terms, such as re-duction factors for seams and intentionally made holes. It also could have been formu-lated with fractional multipliers (values ≤ 1.0) and placed in the numerator of the equation or on the opposite side of the equation as with the *load and reduction factor de-sign method* (LRFD). It has been put in this form following other studies (e.g., Voskamp

and Risseeuw [65]). Although the equation indicates tensile strength, it can be applied to burst strength, tear strength, puncture strength, impact strength, and so on.

2.4.2 Flow-Related Problems

For problems dealing with flow through or within a geotextile, such as filtration and drainage applications, the formulation of the allowable values takes the form of equation (2.25a). Typical values for reduction factors are given in Table 2.12. Note that these values must be tempered by the site-specific conditions, as in Section 2.4.1. If the laboratory test includes the mechanism listed, it appears in the equation as a value of 1.0.

$$q_{\text{allow}} = q_{\text{ult}} \left(\frac{1}{RF_{SCB} \times RF_{CR} \times RF_{IN} \times RF_{CC} \times RF_{BC}} \right) \tag{2.25a}$$

$$q_{\text{allow}} = q_{\text{ult}} \left(\frac{1}{\Pi RF} \right) \tag{2.25b}$$

where

q_{allow} = allowable flow rate,

q_{ult} = ultimate flow rate,

RF_{SCB} = reduction factor for soil clogging and blinding (≥ 1.0),

RF_{CR} = reduction factor for creep reduction of void space (≥ 1.0),

RF_{IN} = reduction factor for adjacent materials intruding into geotextile's void space (≥ 1.0),

RF_{CC} = reduction factor for chemical clogging (≥ 1.0),

TABLE 2.12 RECOMMENDED FLOW-REDUCTION FACTOR VALUES FOR USE IN EQUATION (2.25a)

	Range of Reduction Factors				
Application	Soil Clogging and Blinding[1]	Creep Reduction of Voids	Intrusion into Voids	Chemical Clogging[2]	Biological Clogging
Retaining wall filters	2.0–4.0	1.5–2.0	1.0–1.2	1.0–1.2	1.0–1.3
Underdrain filters	2.0–10	1.0–1.5	1.0–1.2	1.2–1.5	2.0–4.0[3]
Erosion control filters	2.0–10	1.0–1.5	1.0–1.2	1.0–1.2	2.0–4.0
Landfill filters	2.0–10	1.5–2.0	1.0–1.2	1.2–1.5	2.0–5.0[3]
Gravity drainage	2.0–4.0	2.0–3.0	1.0–1.2	1.2–1.5	1.2–1.5
Pressure drainage	2.0–3.0	2.0–3.0	1.0–1.2	1.1–1.3	1.1–1.3

1. If stone riprap or concrete blocks cover the surface of the geotextile, use the upper values or include an addition reduction factor.

2. Values can be higher, particularly for high alkalinity groundwater.

3. Values can be higher for turbidity and/or microorganism contents greater than 5000 mg/l.

RF_{BC} = reduction factor for biological clogging (≥ 1.0), and

ΠRF = value of cumulative reduction factor (≥ 1.0).

As with the equation (2.24a) for strength reduction, this flow reduction equation could also have additional site specific terms included—e.g., blocking of a portion of the geotextile's surface by riprap or concrete blocks.

2.5 DESIGNING FOR SEPARATION

Application areas for geotextiles used for the separation function were given in Section 1.3.3. There are indeed many specific applications, and it could said, in a general sense, that geotextiles always serve a separation function. If they do not serve this function, any other function, including the primary function, will not be served properly. This should not give the impression that the geotextile function of separation always plays a secondary role. Many situations call for separation only, and in such cases the geotextiles do serve a significant and worthwhile purpose.

2.5.1 Overview of Applications

Perhaps the target application that best illustrates the use of geotextiles as separators is its placement between a reasonably firm soil subgrade (beneath) and a stone base course, aggregate, or ballast (above). We say "reasonably firm" because it is assumed that the subgrade deformation is not sufficiently large to mobilize uniformly high tensile stress in the geotextile. (The application of geotextiles in unpaved roads on soft soils with membrane-type reinforcement is treated in Section 2.6.1.) Thus for a separation function to occur the geotextile has only to be placed on the soil subgrade and then to have stone placed, spread, and compacted on top of it. The subsequent deformations are very localized and occur around each individual stone particle. A number of scenarios can be developed showing what geotextile properties are required for this type of situation.

2.5.2 Burst Resistance

Consider a geotextile on a soil subgrade with stone of average particle diameter (d_a) placed above it. If the stone is uniformly sized, there will be voids within it that will be available for the geotextile to enter. This entry is caused by the simultaneous action of the traffic loads being transmitted to the stone, through the geotextile, and into the underlying soil. The stressed soil then tries to push the geotextile up into the voids within the stone. The situation is shown schematically in Figure 2.29. Giroud [66] provides a formulation for the required geotextile strength that can be adopted for this application.

$$T_{\text{reqd}} = \frac{1}{2} p' d_v [f(\epsilon)] \qquad (2.26)$$
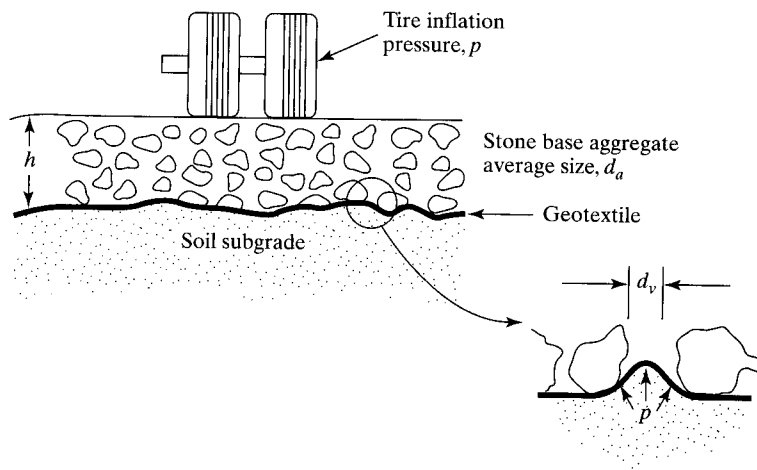
Figure 2.29   Geotextile being forced up into voids of stone base by traffic tire loads.

where

T_{reqd} = required geotextile strength,

p' = stress on the geotextile, which is slightly less than p, the tire inflation pressure at the ground surface,

d_v = maximum void diameter of the stone $\cong 0.33 d_a$,

d_a = the average stone diameter,

$f(\epsilon)$ = strain function of the deformed geotextile,

$$= \frac{1}{4}\left(\frac{2y}{b} + \frac{b}{2y}\right), \text{ in which}$$

b = width of opening (or void), and

y = deformation into the opening (or void).

The field situation is analogous to the ASTM D3786 (Mullen) burst test, which has the geotextile being stressed into a gradually increasing hemispherical shape until it fails (recall Section 2.2.2). Thus, the adapted form of equation (2.26) is

$$T_{ult} = \frac{1}{2} p_{test} d_{test}[f(\epsilon)] \tag{2.27}$$

where

T_{ult} = ultimate geotextile strength,

p_{test} = burst pressure of the geotextile at failure (its strength), and

d_{test} = diameter of the burst test device (= 30 mm).

Knowing that $T_{\text{allow}} = T_{\text{ult}}/(\Pi\text{RF})$, where ΠRF = cumulative reduction factors, we can formulate an expression for the factor of safety (FS) as follows:

$$FS = \frac{T_{\text{allow}}}{T_{\text{reqd}}}$$

$$= \frac{(p_{\text{test}}d_{\text{test}})}{(\Pi\text{RF})p'd_v}$$

For example, if $d_{\text{test}} = 30$ mm; $d_v = 0.33\, d_a$; and $\Pi\text{FS} = 1.5$ (which is reasonable since creep is not an issue with this application), then the FS-value is the following, with d_a in units of mm:

$$FS = \frac{p_{\text{test}}(30)}{(1.5)p'(0.33\, d_a)}$$

$$FS = \frac{60.6 p_{\text{test}}}{p'd_a} \tag{2.28}$$

Example 2.8

Given a truck with 700 kPa tire inflation pressure on a poorly graded aggregate layer consisting of 50 mm maximum-sized stone, what is the factor of safety using a geotextile beneath the aggregate having an ultimate burst strength of 2000 kPa and cumulative reduction factors of 1.5?

Solution: Assuming that the tire inflation pressure is not significantly reduced through the thickness of the stone base, we can solve equation (2.28) as follows:

$$FS = \frac{60.6(2000)}{700(50)}$$
$$FS = 3.5$$

Note that with the reduction factors of 1.5 already included, the resulting factor of safety value is acceptable.

For a range of stone base particle diameters (d_a), values of tire inflation pressure (p'), and cumulative reduction factors of 1.5, along with a factor of safety of 2.0, we can generate the design guide in Figure 2.30. Here it can be seen that stone size is quite significant insofar as the required burst pressure values are concerned. Note also that these are poorly graded aggregates and that the presence of fines will lessen the severity of the design; hence this approach should be considered to be a worst-case design.

2.5.3 Tensile Strength

Continuing the discussion of geotextile roadway separation, there are other processes acting on the geotextile simultaneous with its tendency to burst in an out-of-plane
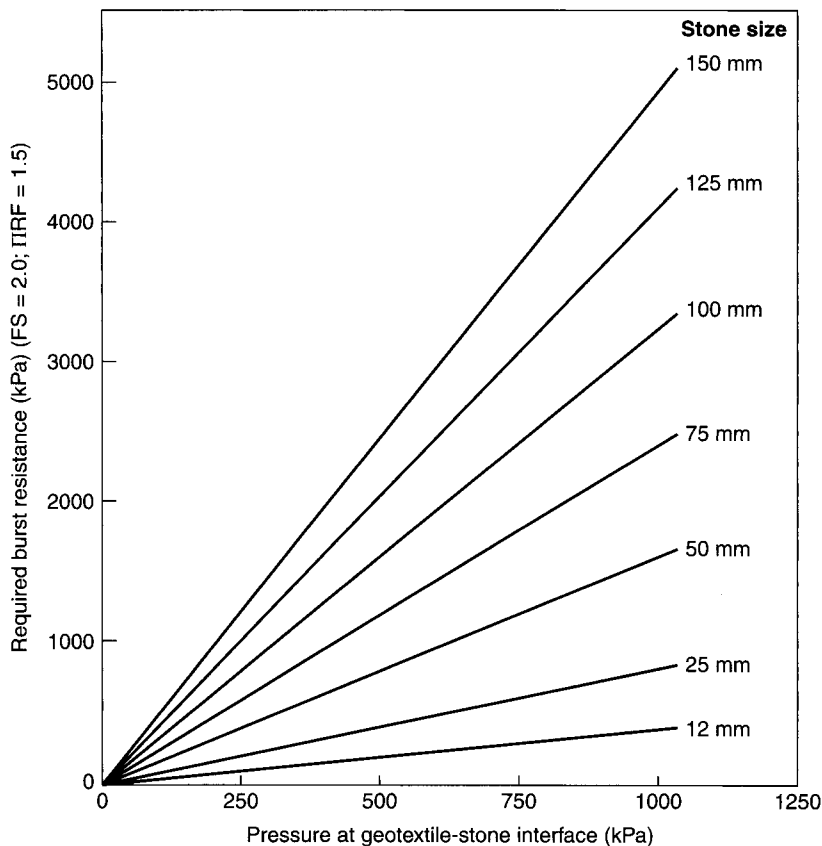
Figure 2.30   Design guide for burst analysis of geotextile used in a separation function based on cumulative reduction factors of 1.5 and a factor of safety of 2.0.

mode. One of these is tensile stress being mobilized by in-plane deformation. This occurs as the geotextile is locked into position by stone-base aggregate above it and soil subgrade below it. A lateral, or in-plane, tensile stress in the geotextile is mobilized when an upper piece of aggregate is forced between two lower pieces that are in contact with the geotextile. The analogy to the grab tensile test can be readily visualized, as illustrated in Figure 2.31. Here we must estimate the maximum strain that the geotextile will undergo as the upper stone wedges itself down to the level of the geotextile. Using the dimensions shown (where $S \simeq d/2$ and l_f = deformed geotextile length), the maximum strain with no slippage, as with nonwoven geotextiles, or stone breakage can be calculated:

$$\epsilon = \frac{l_f - l_o}{l_o}(100)$$

$$= \frac{[d + 2(d/2)] - 3(d/2)}{3(d/2)}(100)$$
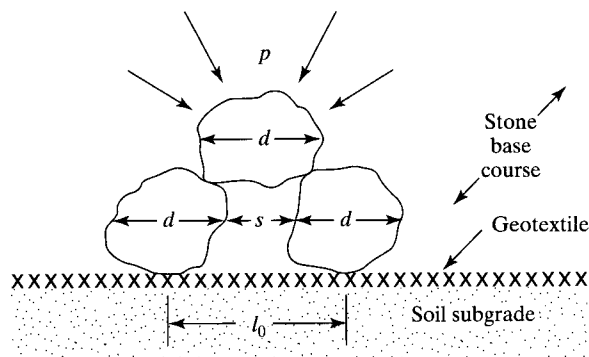
(a) Actual situation
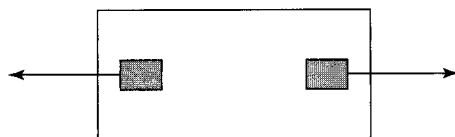
(b) Analogous grab tensile test

Figure 2.31   Geotextile being subjected to tensile stress as surface pressure is applied and stone base attempts to spread laterally.

$$= \frac{4(d/2) - 3(d/2)}{3(d/2)}(100)$$

$$\epsilon = 33\%$$

Note that the preceding assumptions result in a strain that is independent of particle size. Thus the strain in the geotextile could be 33% given the hypothetical assumptions stated above. With woven geotextiles, slippage probably occurs and the strain value would be significantly decreased. Now the tensile force being mobilized is related to the pressure exerting on the stone as follows [66]:

$$T_{\text{reqd}} = p'(d_v)^2[f(\epsilon)] \tag{2.29}$$

where

T_{reqd} = required grab tensile force,
p' = applied pressure,
d_v = maximum void diameter $\simeq 0.33\, d_a$, where
d_a = average stone diameter; and
$f(\epsilon)$ = strain function of the deformed geotextile

$$= \frac{1}{4}\left(\frac{2y}{b} + \frac{b}{2y}\right), \text{ where}$$

b = width of stone void, and

y = deformation into stone void.

Example 2.9

Given a truck with 700 kPa tire inflation pressure on a stone base course consisting of 50 mm maximum-sized stone with a geotextile beneath it, calculate (**a**) the required grab tensile stress on the geotextile, and (**b**) the factor of safety for a geotextile whose maximum grab strength is 500 N with cumulative reduction factors of 2.5. Use a value of $f(\epsilon) = 0.52$.

Solution: (a) Using an empirical relationship that $d_v = 0.33\, d_a$ and the value of $f(\epsilon) = 0.52$, the required grab tensile strength is as follows:

$$
\begin{aligned}
T_{\text{reqd}} &= p'(d_v)^2(0.52) \\
&= p'(0.33\, d_a)^2(0.52) \\
&= 0.057 p' d_a^2 \\
&= 0.057(700)(1000)(0.050)^2 \\
T_{\text{reqd}} &= 100\ N
\end{aligned}
$$

(b) The factor of safety on a 500 N maximum grab tensile geotextile with reduction factors of 2.5, is as follows:

$$
\begin{aligned}
FS &= \frac{T_{\text{allow}}}{T_{\text{reqd}}} \\
&= \frac{500/2.5}{100}
\end{aligned}
$$

$FS = 2.0$, which is acceptable.

2.5.4 Puncture Resistance

The geotextile must always survive the installation process. This is not just related to the roadway separation function; indeed, fabric survivability is critical in all types of applications; without it the best of designs are futile (recall Figure 2.20). In this regard, sharp stones, tree stumps, roots, miscellaneous debris, and other items, either on the ground surface beneath the geotextile or placed above it, could puncture through the geotextile during backfilling and when traffic loads are imposed. The design method suggested for this situation is shown schematically in Figure 2.32. For these conditions, the vertical force exerted on the geotextile (which is gradually tightening around the protruding object) is as follows:

$$
F_{\text{reqd}} = p' d_a^2 S_1 S_2 S_3 \tag{2.30}
$$

where

F_{reqd} = required vertical puncturing force to be resisted,

d_a = average diameter of the puncturing aggregate or sharp object,
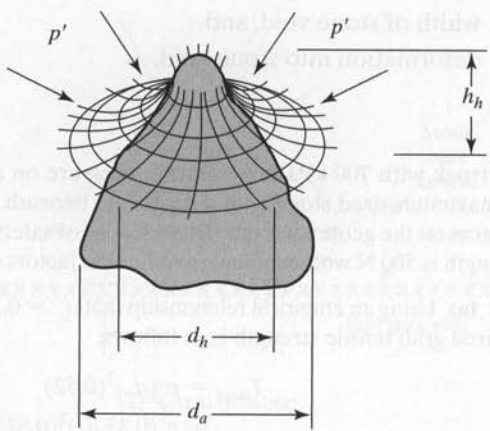
Figure 2.32 Visualization of a stone puncturing a geotextile as pressure is applied from above.

p' = pressure exerted on the geotextile (approximately 100% of tire inflation pressure at the ground surface for thin covering thicknesses),

S_1 = protrusion factor of the puncturing object (see Table 2.13),

S_2 = scale factor to adjust the ASTM D4833 puncture test value that uses a 8.0 mm diameter puncture probe to the actual puncturing object (see Table 2.13), and

S_3 = shape factor to adjust the ASTM D4833 flat puncture probe to the actual shape of the puncturing object (see Table 2.13).

Example 2.10

What is the factor of safety against puncture of a geotextile from a subrounded 25 mm diameter stone on the ground surface mobilized by a loaded truck with tire inflation pressure of 550 kPa traveling on the surface of the base course? The geotextile has an ultimate puncture strength of 300 N according to ASTM D4833.

TABLE 2.13 RECOMMENDED VALUES FOR FACTORS USED IN PUNCTURE ANALYSIS (DIMENSIONLESS)

Puncturing Object	S_1	S_2	S_3
Angular and relatively large	0.9	0.8	0.9
Angular and relatively small	0.6	0.6	0.7
Subrounded and relatively large	0.7	0.6	0.6
Subrounded and relatively small	0.4	0.4	0.5
Rounded and relatively large	0.5	0.4	0.4
Rounded and relatively small	0.2	0.2	0.3

S_1 = protrusion factor ⎫
S_2 = scale factor ⎬ see equation (2.30)
S_3 = shape factor ⎭

Solution: Using the full stress on the geotextile of 550 kPa and factors from Table 2.13 of 0.55, 0.50, and 0.55 for S_1, S_2, and S_3 respectively, we see that

$$F_{\text{reqd}} = p' d_a^2 S_1 S_2 S_3$$

$$= (550)(1000)(25 \times 0.001)^2 (0.55)(0.50)(0.55)$$

$$F_{\text{reqd}} = 52 \text{ N}$$

Assuming that the cumulative reduction factors are 2.0, the factor of safety is as follows:

$$\text{FS} = \frac{F_{\text{allow}}}{F_{\text{reqd}}}$$

$$= \frac{300/2.0}{52}$$

$$\text{FS} = 2.9, \text{ which is acceptable}$$

2.5.5 Impact (Tear) Resistance

As with the puncture requirement just described, the resistance of a geotextile to impact is as much a survivability criterion as it is a separation function. Yet in many instances of separation the geotextile must resist the impact of various objects. The most obvious one is that of a rock falling on it, but there are also situations in which construction equipment and materials can cause or contribute to impact damage on geotextiles.

The problem addresses the energy mobilized by a free-falling object of known weight and height of drop. Rarely will an object be intentionally impelled onto an exposed geotextile with additional force, so only gravitational energy will be assumed.

To develop a design procedure, we assume a free-falling rock of specific gravity of 2.60, varying in diameter from 25 to 600 mm and falling from heights of 0.5 to 5 m. Using this data, the design curves in Figure 2.33 are developed. The relationship used is as follows:

$$E = mgh$$

$$= (V \times \rho)gh$$

$$= [V \times (\rho_w G_s)]gh$$

$$= \left(\frac{\pi (d_a/1000)^3}{6} \right) \left(\frac{1000 \; kg}{m^3} \right) (2.6)(9.81)h$$

$$E = 13.35 \times 10^{-6} \, d_a^{\,3} h \qquad\qquad (2.31)$$

where

E = energy developed (Joules),

m = mass of the falling object (kg),

g = acceleration due to gravity (m/sec^2),
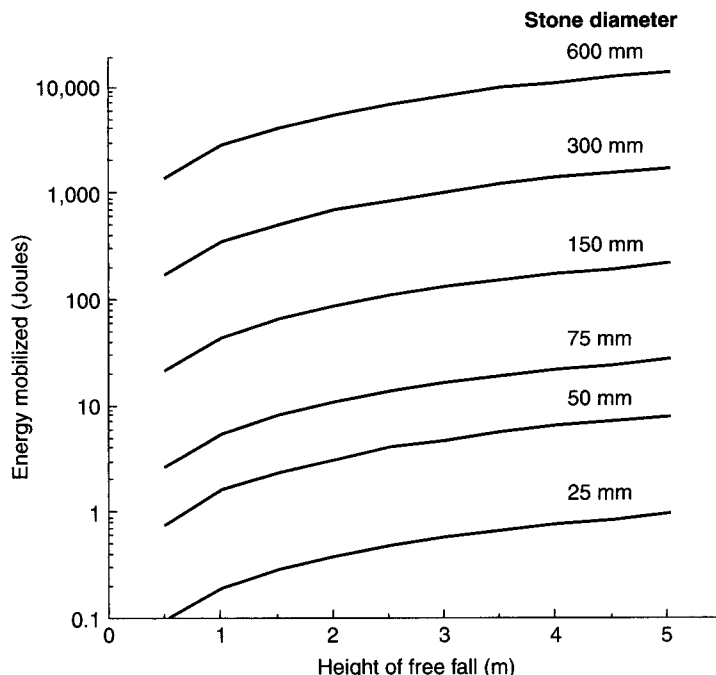
Figure 2.33 Energy mobilization by a free-falling rock on a geotextile with an unyielding support.

h = height of fall (m),

V = volume of the object (m³),

ρ = density of the object (kg/m³),

ρ_w = density of water (kg/m³),

G_s = specific gravity of the object (dimensionless), and

d_a = diameter of the object, (mm).

Note that these calculated energies are based on the geotextile resting on an unyielding surface, which is the worst possible condition. As the soil beneath the geotextile deforms, the geotextile can absorb greater amounts of impacting energy. Since this is usually the case, the modification factors in Figure 2.34 are to be used in conjunction with the curves in Figure 2.33. Once the required energy is calculated, it should be compared to the allowable impact strength of the geotextile (e.g., the Elmerdorf tear or dynamic cone drop test as discussed in Section 2.3.3).

Example 2.11

What energy is mobilized by a free-falling rock of 300 mm size falling 1.5 m onto a geotextile? The geotextile is supported by a poor subsoil having an unsoaked CBR strength of 4.0. If the geotextile has an allowable impact strength of 36 J, what is the factor of safety?
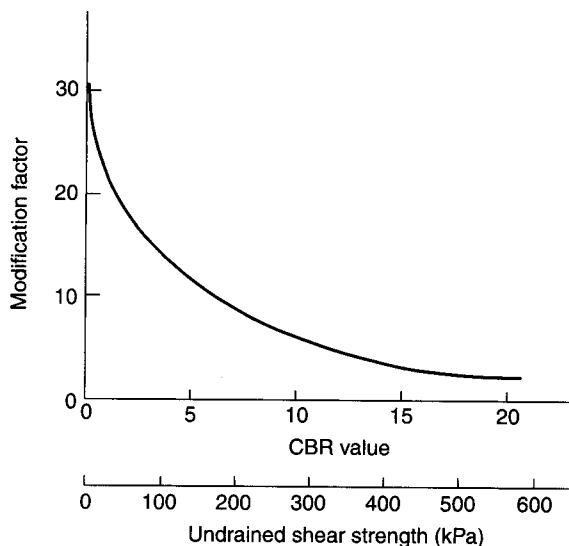
Figure 2.34   Modification factor to be used with energy mobilized by objects falling on geotextiles of varying support resistances characterized by their unsoaked CBR values or undrained shear strength.

Solution: Using equation (2.31) we calculate the required impact energy

$$E_{max} = 13.35 \times 10^{-6}(d_a^3)(h)$$

$$= 13.35 \times 10^{-6}(300)^3(1.5)$$

$$E_{max} = 540 \text{ J}$$

Note that this value is substantiated by the design chart of Figure 2.33. Of course, other design charts can be made for different assumptions. This value is now reduced according to the subgrade conditions of Figure 2.34.

$$E_{reqd} = 540/13$$

$$= 41.5 \text{ J}$$

This results in a factor of safety calculation as follows:

$$FS = \frac{E_{allow}}{E_{reqd}}$$

$$= \frac{36}{41.5}$$

$$FS = 0.87, \text{ which is not acceptable.}$$

Thus holes are likely to be formed when free-falling objects of this size fall directly on the exposed geotextile. Not included in this analysis is the effect of the contact area of the falling object on the geotextile; for a very rounded rock, the effect is much less severe than for a sharp, angular one, which could easily cut through the fabric.

It should be emphasized that the last two methods of puncture and impact design refer not only to roadway separation per se, but to construction survivability of geotextiles in general (recall Table 2.2a). In all cases the considerations of this section should be examined, for they are critical in many situations.

2.5.6 Summary

Of all the geotextile functions, separation is the most underrated—underrated because every use of geotextiles carries with it the separation function, yet rarely is separation designed on its own merit. Hopefully, the designs in this section will allow the engineer to determine quantitatively which geotextile is suitable for a specific situation.

Last, and in a sense most important, is the economic justification for the use of geotextiles in the separation function. It lies in the greater use and service lifetime of the system with geotextiles than without. When a geotextile separator is used in roadway cross sections, geotextiles could well double or triple lifetime; however, field data for such quantification is just now becoming available [67]. Figure 2.35 is the photograph of a 40 m long driveway test plot, which was subdivided into four elongated quadrants, two with geotextiles and two without. Further, the two geotextiles were different and placed diagonally across from one another. After 16 years of service, no cracks have surfaced on the paving and the test is continuing with the objective of providing lifetime data with and without geotextiles and which is the preferred type of geotextile. A database of like projects (in 300 m sections) is under development [68].
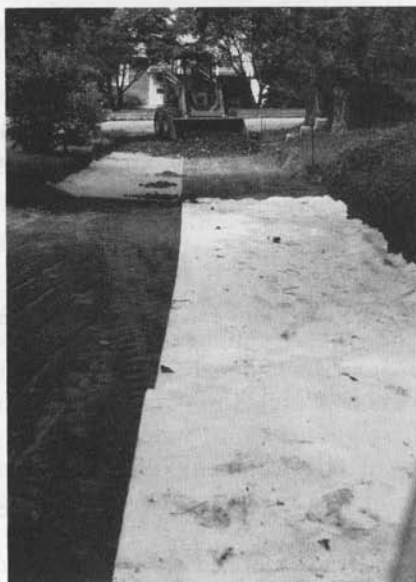
Figure 2.35 Different separation geotextiles being used to determine pavement (driveway) lifetime contrasted to sections with no geotextile.

2.6 DESIGNING FOR ROADWAY REINFORCEMENT

The combined use of soil (good in compression and poor in tension) and a geotextile (good in tension and poor in compression) suggests a number of situations in which geotextiles have made existing designs work better or provided for the development of entirely new applications. These applications were previewed in Section 1.3, together with a brief history of the original uses in this particular area. This section focuses on the design methods using geotextiles for various roadway reinforcement situations.

2.6.1 Unpaved Roads

Overview.   The application in this section is for use of geotextiles in unpaved roads, in which soft soil subgrades have sand or stone aggregate placed directly above. No permanent surfacing, such as concrete or asphalt pavement, is immediately placed on the stone. At most, the road is surfaced with quarry crusher run or chip seal for reasonable ridability. There are many thousands of kilometers of unpaved secondary roads, haul roads, access roads, and the like, with no permanent surfacing on them. At a later time, perhaps years after settlement takes place and ruts are backfilled, a permanent surfacing may be placed.

　　This particular application triggered the high volume use and acceptance of geotextiles in the 1970s, since calculations can be made for the thickness of stone required without a geotextile, then with a geotextile; the difference being the thickness of stone that is saved. By determining the cost of saved stone versus the cost of the geotextile, the value of using a geotextile is known immediately. The particular design process used in arriving at the respective thicknesses is the focus of this section.

　　Before beginning, however, it is important to realize that the geotextile must have its tensile modulus or strength mobilized via deformation of the soil subgrade. Although this can be done intentionally by prestressing the fabric, this is usually not the case, because of the construction difficulties involved. Instead, the yielding of the soil subgrade by the imposed traffic is the triggering phenomenon, allowing for geotextile deformation and the mobilization of its tensile properties. How much deformation is necessary with regard to the vehicular loading, the particular geotextile, the time it takes for adequate strength mobilization, and so on, are all pressing questions, but the deformation characteristics of the soil subgrade takes precedence. A soft, yielding soil subgrade is needed to mobilize the geotextile's strength—but how soft? In light of the tremendous variety of situations, we must use a broad generality; and in this case it will be based on the California Bearing Ratio (CBR) of the soil subgrade. The CBR test is used throughout the world and standardized accordingly (e.g, see ASTM D1883 or ISO 12236). The CBR-value is a comparison of the subgrade soil's resistance to the force of a 50 mm diameter plunger at a given deformation, with that of a standardized crushed stone base material. It is actually a percentage value, although rarely expressed as such. The test on the soil subgrade can be performed at the in situ moisture content, or the soil can be saturated for 24 hr and then tested. These two conditions give rise to unsoaked and soaked CBR values, respectively. Typical unsoaked CBR values are given in Table 2.14, where a considerable body of empirical correlations is presented. Soaked

TABLE 2.14 CORRELATION CHART FOR ESTIMATING UNSOAKED CBR VALUES FROM SOIL STRENGTH OR PROPERTY VALUES

Approximate CBR	Identification Procedure
Less than 2	Easily penetrated with thumb
2–3	Moderate effort to penetrate with thumb
3–6	Indented with thumb
6–16	Indented with thumbnail
Over 16	Difficult to indent with thumbnail

Group Symbols	Soil Group Name
ML	Silt
MH	Micaceous silt
OL	Organic silt
CL	Silty clay
CH	High plastic clay
OH	Organic clay
PT	Peat and muck

Source: After Portland Cement Association and E.I. DuPont literature.

CBR values are generally lower than unsoaked values, but the difference depends on the soil type. Table 2.15 is given as a guide in this regard; note that it correlates well to the Penn DOT specification of Table 2.1.

It should also be noted that *resilient modulus* (obtained from a cyclic triaxial soils test) is beginning to replace CBR as an indicator of soil subgrade strength in pavement design. Charts comparable to those in Table 2.14, however, are not yet available.

For the purposes of using geotextiles in roadway applications on soil subgrades of different strength characteristics, we will subdivide the functions per Table 2.15. Here we can see that with medium to firm soil subgrades [CBR (unsoaked) ≥8 and CBR (soaked) ≥3] the function is uniquely separation. The design for this condition is described in Section 2.5. For poor to very soft soil subgrades—CBR (unsoaked) ≤3 and CBR (soaked) ≤1—the function is both reinforcement and separation. This is the topic of this section. The intermediate category is only loosely defined; it is generally called *stabilization*. This term represents an interrelated group of functions (separation, reinforcement, and filtration) and is essentially a transition category between the two extremes.

Manufacturers' Methods.   All of the major geotextile manufacturers have an unpaved-road design method for use with their particular geotextiles. They usually show CBR (or other related soil strength values) on the x-axis and the required stone thickness (with and without a geotextile) on the y-axis. All result in logical behavior, with the geotextile providing greater savings in stone aggregate as the soil subgrade becomes weaker. Since most manufacturers have a range of geotextiles available for reinforcement of unpaved roads, it is also seen that the heavier and stronger geotextiles result in greater stone savings than the lighter and weaker ones. Because each manufacturer's set of curves has its own background (based on theory, laboratory work, field observation, or empirical observation), it is nearly impossible to compare one method with another. Yet the designs have served the industry well and generally with excellent success. Their use is certainly acceptable and if only one geotextiles is available, its manufacturer's method should continue to be used. If, however, a number of geotextiles are available, a method that views them on the basis of a specific, well-defined property is needed. Such a property could well be the geotextile's modulus, which

TABLE 2.15 RECOMMENDED SOIL SUBGRADE CBR VALUES TO DISTINGUISH DIFFERENT GEOTEXTILE FUNCTIONS IN ROADWAY CONSTRUCTION

Geotextile Function(s)	CBR - Value	
	Unsoaked	Soaked
Separation	≥8	≥3
Stabilization*	8–3	3–1
Reinforcement (and separation)	≤3	≤1

*A frequently used but poorly defined transition term that always includes separation, some unknown amount of reinforcement, and usually filtration as well.

is the basis of design in the procedure to follow. It should be noted, however, that a number of generic techniques are available, and that Hausmann [69] has assessed and compared them to one another.

Analytic Method.   Giroud and Noiray [70] use the geometric model shown in Figure 2.36 for a tire wheel load of pressure p_{ec} on a $B \times L$ area, which dissipates through h_o thickness of stone base without geotextile and h thickness of stone base with a geotextile. The geometry indicated results in a stress on the soil subgrade of p_o (without geotextile) and p (with geotextile) as follows:

$$p_o = \frac{P}{2(B + 2h_o \tan \alpha_o)(L + 2h_o \tan \alpha_o)} + \gamma h_o \qquad (2.32)$$

$$p = \frac{P}{2(B + 2h \tan \alpha)(L + 2h \tan \alpha)} + \gamma h \qquad (2.33)$$

where

   P = axle load, and

   γ = unit weight of the stone aggregate.

Since the pressure exerted by the axle load through the aggregate and into the soil subgrade is known, the shallow-foundation theory of geotechnical engineering can now be utilized. We have assumed throughout the analysis that the soil is functioning in its undrained condition and thus that its shear strength is represented completely by the cohesion (i.e., $\tau = c$). The tacit assumption is that the soil subgrade consists of saturated fine-grained silt and clay soils. Critical in this design method are the assumptions that without the geotextile the maximum pressure that can be maintained corresponds to the elastic limit of the soil, that is,

$$p_o = \pi c + \gamma h_o \qquad (2.34)$$

(a) Case without geotextile   (b) Case with geotextile
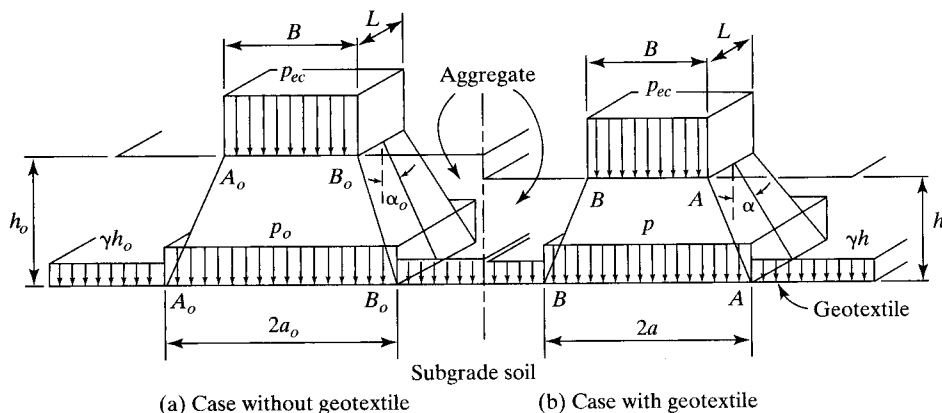
Figure 2.36   Load distribution by aggregate layer. (After Giroud and Noiray [70])

and that with the geotextile the limiting pressure can be increased to the ultimate bearing capacity of the soil, that is,

$$p^* = (\pi + 2)c + \gamma h \qquad (2.35)$$

These assumptions reasonably agree with the earlier findings of Barenberg and Bender [71] using small-scale laboratory tests, where on a deformation basis they found that large-scale ruts began at a $3.3c$ value with no fabric reinforcement, versus a $6.0c$ value with fabric (where c is the undrained soil shear strength).

Thus for the case of no geotextile reinforcement, equations (2.32) and (2.34) can be solved, resulting in equation 2.36, which yields the desired aggregate thickness response curve without the use of a geotextile:

$$c = \frac{P}{2\pi\left(\sqrt{P/p_c} + 2h_o \tan \alpha_o\right)\left(\sqrt{P/2p_c} + 2h_o \tan \alpha_o\right)} \qquad (2.36)$$

where

c = soil cohesion,
P = axle load,
p_c = tire inflation pressure,
h_o = aggregate thickness, and
α_0 = angle of load distribution ($\cong 26°$).

For the case where geotextile reinforcement is used, p^* in equation (2.35) is replaced by $(p - p_g)$, where p_g is a function of the tension in the geotextile; hence its elongation is significant. On the basis of the probable deflected shape of the geotextile-soil system,

$$p_g = \frac{E\epsilon}{a\sqrt{1 + (a/2S)^2}} \qquad (2.37)$$

where

E = modulus of geotextile,
ϵ = elongation (strain),
a = geometric property (see again Figure 2.36), and
S = settlement under the wheel (rut depth).

Combining equations (2.33), (2.35), and (2.37) and using $p^* = p - p_g$, gives equation 2.38, where h is the unknown aggregate thickness. It can be graphed for various rut-depth thicknesses and various moduli of geotextiles.

$$(\pi + 2)c = \frac{P}{2(B + 2h \tan \alpha)(L + 2h \tan \alpha)} - \frac{E\epsilon}{a\sqrt{1 + (a/2S)^2}} \qquad (2.38)$$

With these two sets of equations, the design method is essentially complete, since both h_o (thickness without a geotextile) and h (thickness with a geotextile) can be calculated. From these two values $\Delta h = h_o - h$ can be obtained, which represents the savings in aggregate due to the presence of the geotextile. For convenience, however, it can be read directly from Figure 2.37. This figure also considers the effects of traffic. In this case, the required thickness h' becomes $h' = h'_o - \Delta h$, which is obtainable from the curves by subtracting the two ordinate values of h'_o and Δh. Note that the effect of service lifetime takes the form of number of vehicle passages.

Two examples follow: one illustrating the general design procedure [70] and the other showing a specific example with an economic analysis included. The influence of rut depth has been further evaluated by Holtz and Sivakugan [72].
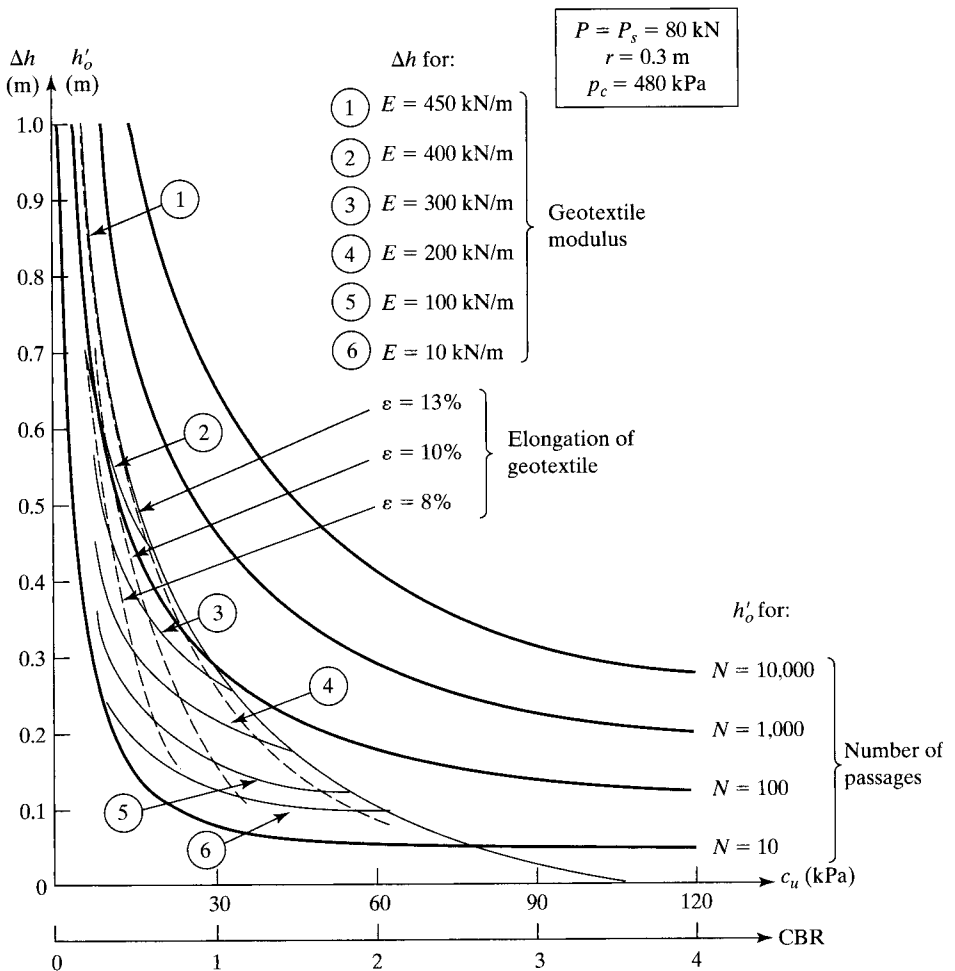
Figure 2.37 Design curves for determining aggregate thickness of unpaved roads and aggregate saved using various geotextiles. (after Giroud and Noiray [70])

Example 2.12

Given 340 passages of 80 kN single axle-load vehicles, assume the following: tire inflation pressure pressure $= 480$ kPa; soft soil CBR $= 1$; geotextile modulus $E = 90$ kN/m; and an allowable rut depth $= 0.3$ m. What is the required aggregate thickness of an unpaved road?

Solution: Figure 2.37 gives $h'_o = 0.35$ m for $N = 340$ and $CBR = 1$, (i.e., thickness when no geotextile is used). It also gives $\Delta h = 0.15$ m for $E = 90$ kN/m and $CBR = 1$ (i.e., the reduction in aggregate thickness when a geotextile-reinforcement layer is used). The difference between the two values, or 0.20 m, is the required aggregate depth when the geotextile is used.

Example 2.13

Assume the following: 1000 passages of 80 kN single-axle-load vehicles with a tire inflation pressure of 480 kPa on a soft soil CBR $= 2$, a candidate geotextile modulus $E = 170$ kN/m, and an allowable rut depth $= 0.3$ m (a) Plot the response curve from Figure 2.37; (b) Determine the aggregate savings; and (c) Do an economic analysis based on the distance the project is from the stone quarry and geotextile supplier, respectively, using the following data (the stone unit weight is 20 kN/m^3):

Distance (km)	Aggregate Cost (dollars/kN)	Geotextile Cost (dollars/m^2)
<5	0.90	0.72
5–20	1.20	0.76
20–50	1.70	0.78
50–100	2.50	0.84
100–200	3.80	0.90

Solution: (a) The required complementary curve to Figure 2.37 is shown below.
(b) At CBR $= 2.0$

$$h'_o \text{ (without geotextile)} = 300 \text{ mm}$$
$$h' \text{ (with geotextile)} = 205 \text{ mm}$$
$$\Delta h \text{ (savings in stone)} = 95 \text{ mm}$$

(c) Based on 20 kN/m^3, this is a 0.020 kN/m^2-mm stone thickness, which results in the table below. It is easily seen that the use of the geotextile is very economical and becomes more so as the distance from the stone quarry to the project site becomes greater.

Distance (km)	Aggregate Cost (dollars/kN)	Aggregate Cost (dollars/m^2-mm)	Aggregate Savings (dollars/m^2)	Geotextile Cost (dollars/m^2)	Geotextile Savings (dollars/m^2)
<5	0.90	0.018	1.71	0.72	0.99
5–20	1.20	0.024	2.31	0.76	1.55
20–50	1.70	0.035	3.31	0.78	2.53
50–100	2.50	0.050	4.79	0.84	3.95
100–200	3.80	0.075	7.13	0.90	6.23
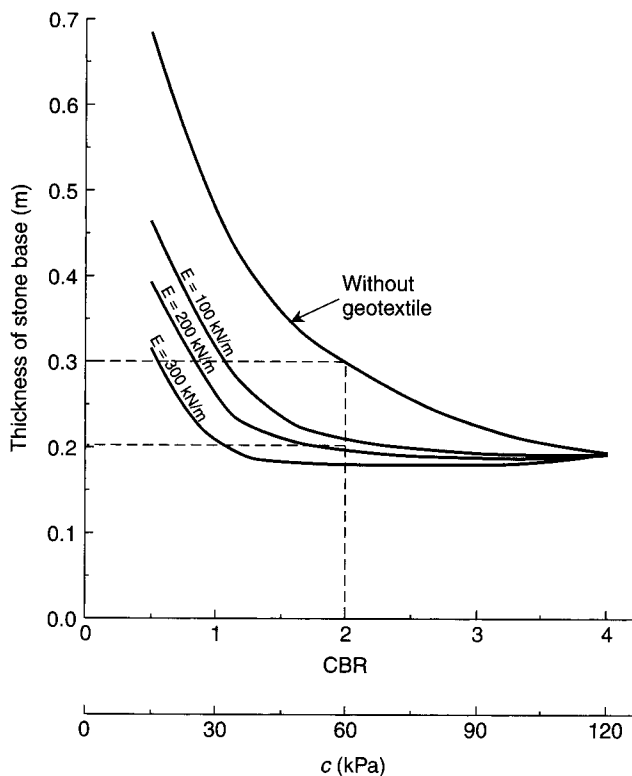
Laboratory Method. If laboratory facilities are available, it is possible to model the situation so as to arrive at a reinforcement ratio provided by the geotextile. The procedure is as follows:

1. Take the lower portion of a standard laboratory CBR mold and fill it with the soil in question at its in situ density and water content.
2. Place crushed stone in the upper portion of the mold.
3. With the load piston on top of the stone, perform a load-versus-deflection test at discrete intervals of piston deflection and record the data.
4. Using a CBR mold that has been modified to hold a geotextile at the interface between the soil subgrade and the crushed stone, repeat the test with the candidate geotextile in position and record the data. (The modification can be made by welding flanges to the upper and lower sections of the CBR mold and clamping or bolting the geotextile between the flanges.)
5. Calculate the ratio of the loads at each deflection increment. The data in Table 2.16 show this reinforcement ratio for four separate test sets of a geotextile placed on a kaolinite clay at different water contents. Here we see that the reinforcement ratio increases as both the deflection and the water content increase.

TABLE 2.16 LABORATORY OBTAINED REINFORCEMENT RATIOS[1]
(WITH AND WITHOUT A GEOTEXTILE) FROM MODIFIED CBR TESTS

	Kaolinite Clay[2] Soil at Water Content			
Deflection (mm)	32%	35%	38%	41%
3.3	1.0	1.0	1.2	1.4
6.7	1.0	1.1	1.3	1.7
10	1.0	1.2	1.5	2.0
13	1.1	1.3	1.7	2.2
25	1.3	1.5	2.0	2.4
37	1.5	1.8	2.4	3.0
50	1.8	2.2	3.0	3.4

1. Ratio = soil with geotextile/soil without geotextile.
2. Shrinkage limit, $w_s = 18\%$; plastic limit, $w_p = 32\%$; liquid limit, $w_l = 41\%$.

6. Assuming that this reinforcement ratio can be used as a multiplier to the in situ CBR of the soil, a number of accepted design procedures can be used to arrive at an aggregate thickness with and without geotextiles.

Example 2.14

Using the U.S. Army Corps of Engineers Modified CBR Design Method (WES TR 3-692), calculate the required stone base thickness for an unpaved road carrying 5000 coverages of 45 kN equivalent single-wheel loads using a tire contact area of 300 × 450 mm for (**a**) stone on a kaolinite clay soil at 41% water content with a $CBR = 1.0$ with no geotextile reinforcement, and (**b**) the same conditions but with a geotextile whose data are typical of Table 2.16 at 25 mm deflection. Then (**c**) compare the resulting thicknesses.

Solution: The essential formula is the following:

$$h = (3.24 \log C + 2.21)\left(\frac{P}{36.0 \times \text{CBR}} - \frac{A}{2030}\right)^{1/2} \tag{2.39}$$

where

- h = aggregate thickness (mm),
- C = traffic in terms of coverages,
- P = equivalent single wheel load (N), and
- A = tire contact area (mm²).

This leads to the general relationship:

$$h = (3.24 \log 5000 + 2.21)\left(\frac{45{,}000}{36.0 \times \text{CBR}} - \frac{(300)(450)}{2030}\right)^{1/2}$$

$$h = (14.19)\left(\frac{1250}{\text{CBR}} - 66.5\right)^{1/2}$$

(a) For no geotextile reinforcement and CBR $= 1.0$, the required thickness is

$$h'_o = (14.19)(34.4)$$
$$= 488 \text{ mm}$$

(b) When using a geotextile that results in an equivalent CBR $= 2.4$ (from Table 2.16; $2.4 \times 1.0 = 2.4$), the thickness is

$$h' = (14.19)(21.3)$$
$$= 302 \text{ mm}$$

(c) Thus the savings in stone base (Δh) afforded by using a geotextile is

$$\Delta h = h'_o - h'$$
$$= 488 - 302$$
$$\Delta h = 186 \text{ mm } (\cong 38\% \text{ savings})$$

Sewn Seams.   With the soft compressible subgrade soils under consideration in this section on unpaved roads, the matter of geotextile overlap for transferring stress across rolls becomes an issue. This overlap affects both the longitudinal sides and the transverse ends of the geotextile rolls. As expected, the softer the soil, the greater the necessary amount of overlap. Figure 2.38 gives a guide for different types of use on the basis of overlap required. It is easily seen that large overlap distances are required for low-strength soils. Not only is this wasted geotextile but it necessitates the calculation of geotextile-to-geotextile friction (recall the shear tests of Section 2.3.3). As a result, field-sewing of the geotextiles is generally preferred (see Figure 2.39). Example 2.15 illustrates how field-sewing of geotextiles can be very economical.

Example 2.15

Using the overlap guide of Figure 2.38, calculate when geotextile sewing becomes more economical than geotextile overlap for a single seam down the center of a 2000 m long access road. The costs are $1.75/m^2 for heavy geotextile, $1.37/m^2 for medium geotextile, and $1.00/m^2 for light geotextile. Sewing costs are $400 per day for sewing machine rental and thread and $175 per day for three laborers each, who can easily sew a 2000 m seam in one day.

Solution: The chart below is taken from data in Figure 2.38 and the costs provided.

Unsoaked Subgrade CBR	Type of Loads	Overlap Required (m)	Geotextile Required (m^2)	Overlap Geotextile Cost ($/2000 m)		
				Heavy ($1.75/m^2)	Medium ($1.37/m^2)	Light ($1.00/m^2)
1.0	Heavy	0.86	1720	3010	2360	1720
	Medium	0.71	1420	2480	1940	1420
	Light	0.58	1160	2030	1590	1160
2.5	Heavy	0.57	1140	1990	1560	1140
	Medium	0.51	1020	1780	1400	1020
	Light	0.44	880	1540	1200	880
4.0	Heavy	0.37	740	1300	1010	740
	Medium	0.35	700	1220	960	700
	Light	0.33	660	1150	900	660
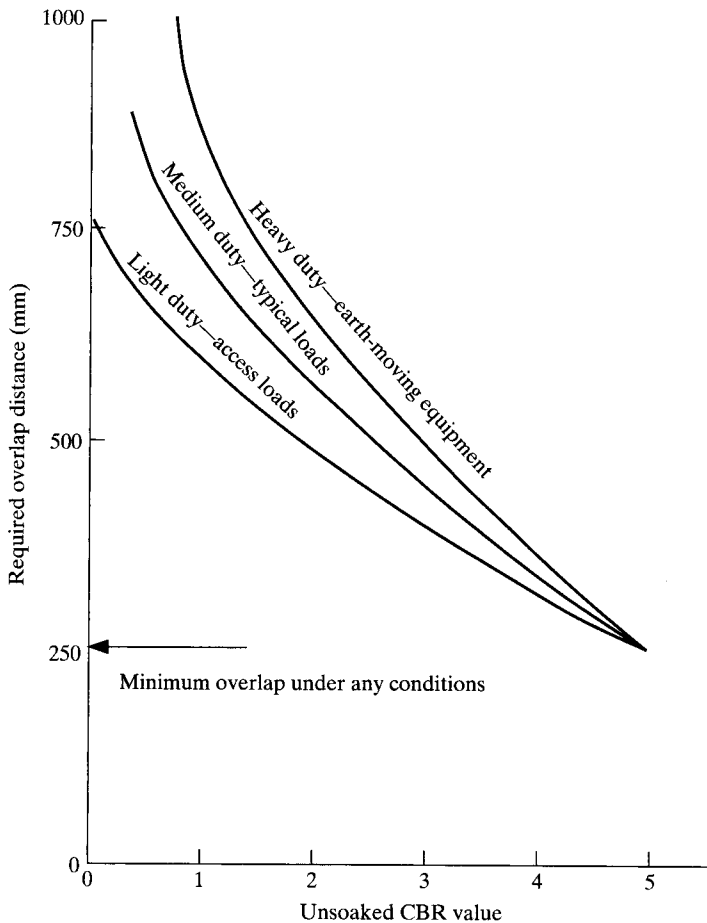
Figure 2.38   Recommended overlap for geotextiles used in unpaved roads as a function of unsoaked soil subgrade CBR value.

Since the total sewing costs are $925 per day, it is seen that only on the lower-right portion of the chart (on relatively strong subgrades with light geotextiles for light- and medium-duty vehicles) does sewing not pay for itself.

When considering the field-sewing of geotextiles, a number of details must be addressed. They are:

- *Thread type*: The choices are polypropylene, polyester, and polyamides (the same thread types as geotextile fiber type should be used, certainly not a stronger type).
- *Thread tension*: Usually adjusted in the field, this should be sufficiently tight without cutting the geotextile.
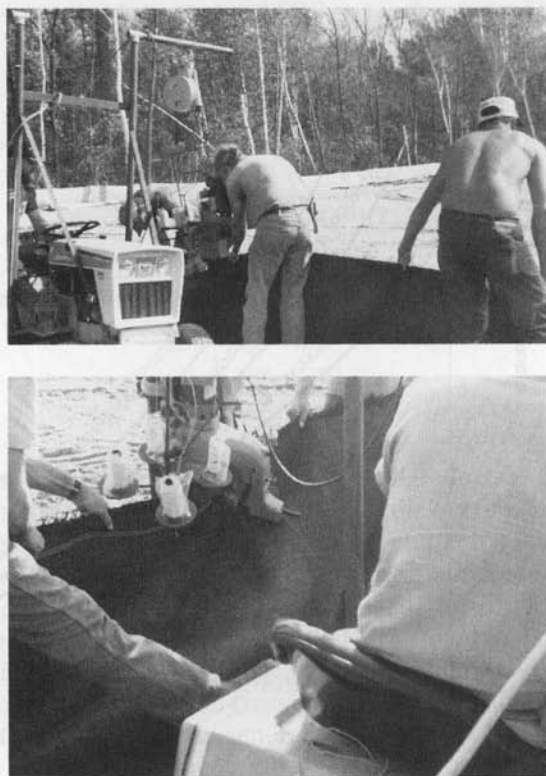
Figure 2.39 Field sewing of geotextiles. (Compliments of Union Special Corp.)

- *Stitch density*: Two, three or four stitches per 25 mm are customary.
- *Stitch type*: The choices are prayer, J-type, or butterfly (see Figure 2.40), the strongest being the butterfly type.
- *Number of rows*: One, two, or three can be used, but generally two are recommended (see Figure 2.40).
- *Type of chain stitch*: The 401 two-thread is recommended.

The sewing of geotextiles has rapidly advanced to the point where all geotextile construction on soft soil sites should consider its use. A geotextile sewing guide is provided in [74]. Tensile seam strengths of 170 kN/m have been attained (recall Figure 2.12) and productivity has reached a point where sewing is no longer an obstacle for rapid progress of the work.

2.6.2 Membrane-Encapsulated Soils

Concept and Overview. It is beyond question that well-graded angular sands and gravels make the best base course materials for both paved and unpaved roads.

(a) "Flat" or "prayer" seam

(b) "J" seam

(c) "Butterfly" seam

(d) "101" single thread chainstitch

(e) "401" two-thread chainstitch
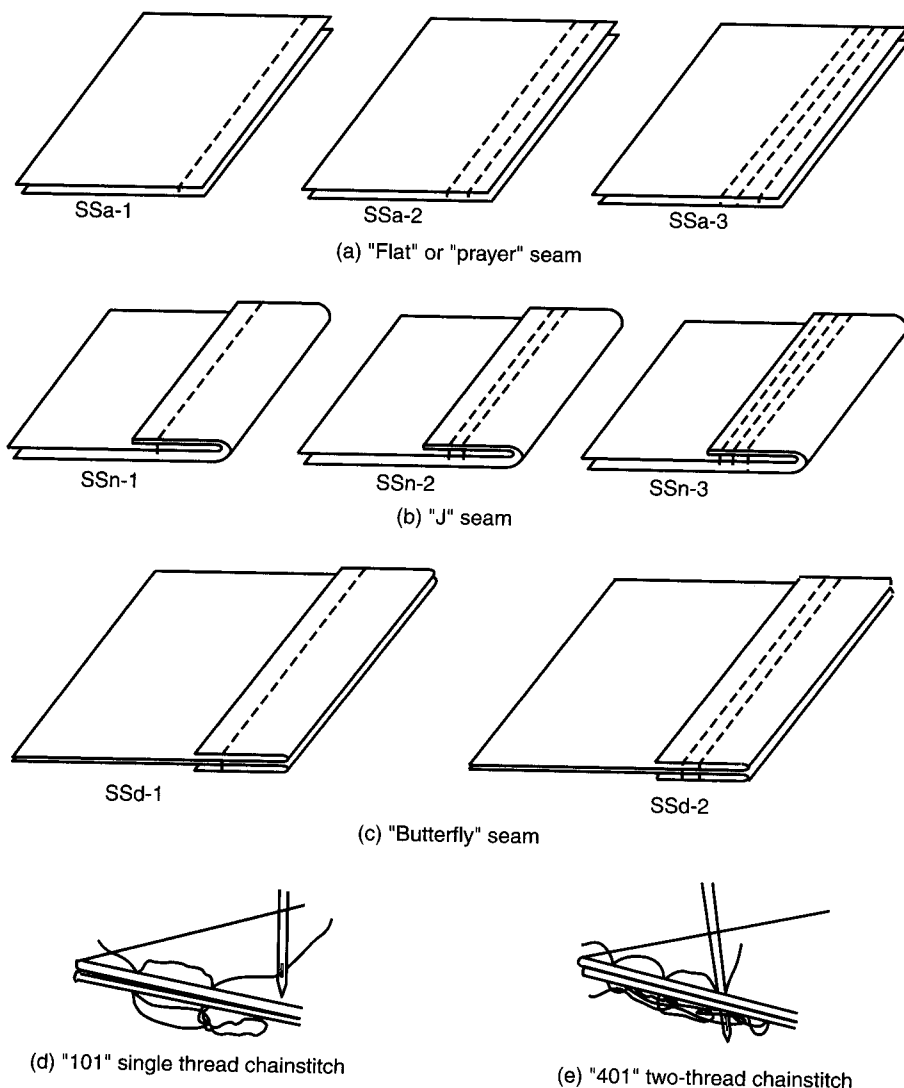
Figure 2.40   Various types of sewn seams for joining geotextiles. (After Diaz [73])

Such coarse-grained soils provide good structural stability and adequate drainage in both vertical and horizontal directions. Yet in many areas of the world, such soil types are simply not available. In abundance, however, are fine-grained silts, clays, and related mixed soils. Although such materials can be placed in a stable condition (by careful control of their moisture content), their performance over time is generally poor. During wet seasons, they take up moisture and become excessively wet and soft, while during dry seasons they lose moisture and become friable and weak. Their behavior is particularly poor in cold regions, where such fine-grained soils exhibit marked frost

susceptibility, which involves excessive heave while frozen and rapid collapse during thaw periods.

The idea of encapsulating such fine-grained soils in a state just lower than their optimum moisture content and preventing moisture migration from occurring has created a good deal of interest in places that lack good-quality stone aggregate. Beginning in 1930 when the Bavarian Highway Department used prefabricated asphalt panels [75], the concept was extended by Casagrande in 1937 using bitumen-coated jute fabric in the same area of Germany. It should also be noted that the Asphalt Institute had recommended an asphalt barrier, with or without geotextile carrier, as capillary cutoffs even before 1930 [76]. The use of geomembranes (i.e., impermeable plastic sheets) for encapsulation began about 1953 by Bell and Yoder [77] at Purdue University. They used both polyethylene and polyvinyl chloride sheets that were sealed at their overlapping seams. Later systems developed by the U.S. Army Cold Regions Research and Engineering Laboratory [78] were hybrids, in that a geomembrane was used beneath and on the sides of the soil to be encapsulated, and an asphalt emulsion-impregnated geotextile was used as a cover.

All of these early attempts at encapsulating poor-quality soils were aimed at providing a moisture-tight barrier beneath the roadway's wearing surface. Thus, in the context of this book, the primary function of the geosynthetic material so used is clearly as a *moisture barrier*, although there is a secondary function of containment reinforcement as well. Today the major applications are the following:

- To encapsulate frost-sensitive silt soils from problems associated with freeze-thaw cycles.
- To encapsulate expansive and heavy clays from volume changes associated with wet-dry cycles.
- To protect subgrade soils from being exposed to water from rainfall or snowmelt.
- To minimize the amount of granular soil used to bridge over weaker or moisture sensitive subsoils.
- To make it possible to use a substandard type of granular soil when its saturated strength is too low for the imposed traffic loads or its gradation is improper.

As currently practiced, membrane-encapsulated soil layers (MESLs) utilize geotextiles as the base material, which are then impregnated with a sprayed-on bituminous or elastomeric product (see Figure 2.41), thereby forming bottom, sides, and top around the enclosed soil. There are good reasons for using geotextiles over other materials to solve this problem:

- Geotextiles, being made from plastic materials, do not degrade with time as do jute or cotton fabrics.
- Geotextiles mobilize good friction resistance and have high survivability characteristics (puncture, tear, and impact resistance) compared with geomembranes.
- Bitumen- or polymeric-impregnated geotextiles, although not watertight under hydrostatic pressure, are adequate for eliminating water migration across them
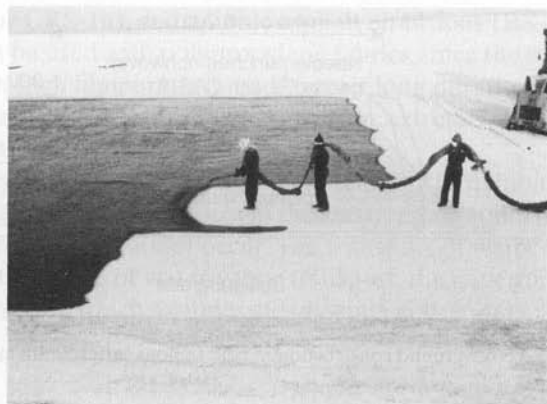
Figure 2.41   Spraying of a geotextile to form the bottom of a membrane encapsulating soil layer. (Photo compliments of Chevron/Phillips Co.)

under most circumstances (to provide a completely watertight barrier is usually not necessary).

- Overlapped or sewn seams can easily be made using geotextiles.
- Geotextiles offer the most cost-effective solution.

Design Methods.   MESL designs can be characterized as being either above grade or below grade. An example [79] of an above-grade scheme is shown in Figure 2.42(a), in which a frost-sensitive silt soil near Fairbanks, Alaska, has been encapsulated in a nonwoven needle-punched geotextile sprayed with CRS-2 emulsified asphalt. A MESL approach was made necessary by a general lack of granular soils in the arctic and subarctic areas together with the problem of permafrost. Conversely, moisture-sensitive silt is very available. Upon thawing, these silt soils weaken considerably, causing surface distortion (deep ruts) and local bearing-capacity failures. The subgrade was prepared, rolled, and covered with the geotextile. CRS-2-emulsified asphalt was used to seal the geotextile and included the overlapped centerline joint. A road grader was used to mix the silt so as to bring it to its optimum water content. The silt was then placed in three lifts of 250 mm each to a total height of 750 mm. The upper surface and sides were covered with the same type of geotextile, and sealing was done using the same type of emulsified asphalt. A 40 mm layer of gravelly sand was spread over the top surface so that traffic would not travel directly on the geotextile.

Using the same MESL concept in a semiarid region of Australia, Lawson and Ingles [80] report on two below-grade case histories (see Figure 2.42b). Both sites were subjected to water infiltration into the subgrade and had low unsoaked CBR values, typically three in the wet season and about seven in the dry season. The soil encapsulated in the nonwoven heat-bonded geotextile was more granular than the subgrade, and a reinforcing function was the goal in addition to waterproofing. A sprayed-on bituminous product was used as the sealant. Note that the longitudinal section of Site 2 had
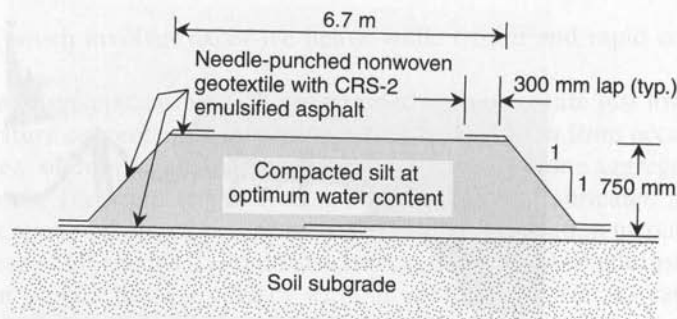
(a) Above-ground construction in cold regions (after Smith and Pazsint [79])
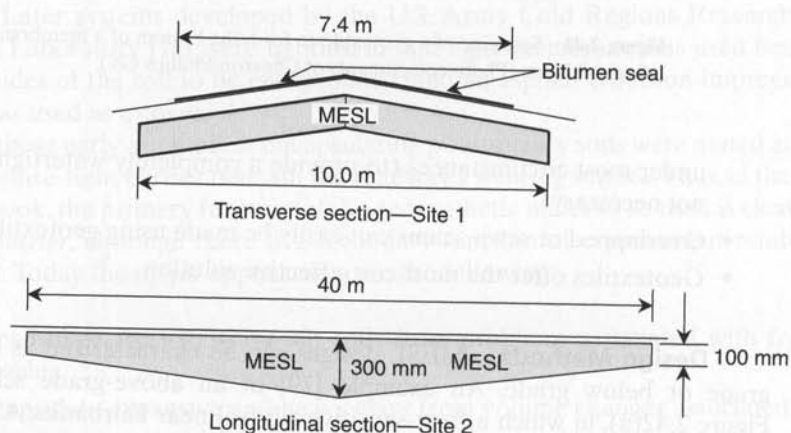
(b) Below-ground construction in semiarid regions (after Lawson and Ingles [80])

Figure 2.42   Various cross sections of membrane-encapsulated soil layers.

a varying thickness of 300 mm at the center, tapering to 100 mm at each end. The transverse section was uniform, as was the case for the entire Site 1.

In order to implement a design methodology for providing a water barrier using MESLs, it is essential that the geotextiles be impregnated with a proper sealant. This is usually bitumen, although coal tar [80] and various elastomers [81] have also been used. Sometimes polyester geotextiles are used rather than polypropylene, due to their lower tendency to swell when subjected to hydrocarbons. The impregnation process is similar to the use of geotextiles beneath bituminous overlays to prevent reflection cracking, which will be treated in Section 2.10.2. To saturate geotextiles, Murray [82] has found that 0.25 to 1.5 l/m² is necessary for geotextiles in the weight range of 100 to 200 g/m². Unlike the reflective cracking application, more sealant can be used than is required for saturation, and the figures above should be considered as minimum values. Recommended sealants [83] are asphaltic cement (AC-10 or AC-20), cationic asphalt

emulsion (CRS-2 or CRS-1h), and anionic asphalt emulsions (RS-2 or RS-1). Cutback asphalts should not be used with polypropylene fabrics, since the solvent in them reacts with the polymer at high temperatures and/or over long durations. The cure period for most of these sealants is 30 min to 4 hr; however, extremely cold temperatures will greatly extend the time required.

Properly done, this saturation of the geotextile will exhibit a wetting pressure within it greater than the water pressure in the surrounding soil. Thus water movement into and through the barrier cannot occur. The transport of water *vapor*, however, will occur. To quantify this value of water-vapor transport, the governing equation that can be used is Fick's first law, which assumes steady-state conditions:

$$\frac{\partial W}{\partial t} = -KA\frac{\partial C}{\partial x} \tag{2.40}$$

where

$\dfrac{\partial W}{\partial t}$ = rate of water diffused, by weight,

$\dfrac{\partial C}{\partial x}$ = vapor gradient across the barrier,

A = surface area of the barrier, and

K = diffusion constant of the barrier.

The critical parameter is K, which is also known as the *water-vapor transmission constant* (not to be confused with k, the *permeability coefficient*, which is related to water flow) and can be found experimentally using the water-vapor transmission test, ASTM E96. The procedure is given in Lord and Koerner [84] together with other diffusion and transmission measurement techniques, and values are given by Lawson and Ingles [85].

The preceding first-order differential equation (equation 2.40) is integrated over boundary conditions of

$$At \ \chi = 0: \text{then } C = C_1$$
$$At \ \chi = L: \text{then } C = C_2$$

which yields

$$W = \frac{KA(C_2 - C_1)\Delta t}{L}$$

and if $K' = K/L$

$$W = K'A\,\Delta C\,\Delta t \tag{2.41}$$

where

K' = permeance,

K = water-vapor transmission,

L = thickness,

A = surface area,

ΔC = change in vapor pressure,

Δt = elapsed time, and

W = amount of water, via vapor transmission, gained or lost over time Δt.

The design procedure becomes one of calculating the water weight gained or lost within the MESL to see if an acceptable condition exists. Example 2.16 illustrates this procedure.

Example 2.16

Assume that you have been given a below-grade MESL constructed from a bitumen-impregnated geotextile with a permeance $K' = 5 \times 10^{-5}$ day^{-1}, the cross section shown below, and a vapor-pressure gradient over the 4-month wet season of 6.0 kPa. What will be the increase in moisture content of the soil within the MESL if it is placed at a unit weight of 18 kN/m^3 and at 12% moisture content?

Surface-sealed
wearing course

ML soil

600 mm

10 m
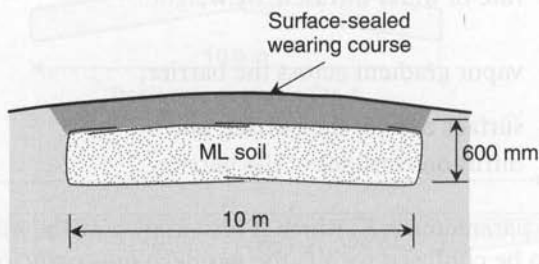
Solution: The weight of water gained, W, is

$$W = K' A \Delta C \Delta t$$
$$= (5 \times 10^{-5})(21.2)(6.0)(1000)(121)$$
$$W = 770 \ N/m$$

Now using standard soil mechanics principles, calculate the change in water content.

As constructed:

Total weight, $W_w + W_s = 10 \times 0.6 \times 18,000 = 108,000$ N/m   but

$$W_w/W_s = 0.12$$

Therefore, total weight water, $W_w = 11,600$ N/m.

After the wet season:

Total weight water, $W_w = 11,600 + 770$

$$= 12,400 \ N/m$$

Total weight dry soil, $W_s = 108,000 - 11,600 = 96,400$ N/m

Water content, $w = \dfrac{12,400}{96,400}(100)$

$$w = 12.9\%$$

Thus the water content of the soil has increased from 12.0 to 12.9% after four months of exposure under these stated conditions. Clearly, the bitumen-impregnated geotextile is performing its intended function as a barrier.

Some comments on the design procedure and its assumptions using this approach are in order. First, there is a problem concerning the units of permeance. Water vapor-transmission is given in units of g/m²-day, which when divided by the vapor-pressure gradient gives metric-perms. Its units are as follows:

$$\left(\frac{g}{m^2 - day} \frac{1}{mm\ Hg} \right)$$

This must be converted to day^{-1} to use the design procedure described above. Second, the driving force in the problem is the anticipated vapor-pressure gradient in the field, ΔC, which is very difficult to estimate in the absence of tensiometers and field measurements. In addition, the time frame for the calculations is also an assumption. A factor of safety can be effectively used in design in light of the statements above, and a value of 3.0 is recommended.

Field Behavior. Regarding the cross sections of the MESLs shown in Figure 2.42, all were test sections and were carefully monitored over long periods. The above-grade MESL encapsulating silt in Alaska (Figure 2.42a) performed satisfactorily, although two problems occurred. One was an area of significant rutting, the other was a section where a seam separated. Both occurred when the geotextile was exposed to surface water; thus both problems were related to the cover material—the 40 mm of gravelly sand—rather than the performance of the MESL itself. Clearly, a more durable surface course is warranted in this situation. An additional measure would have been to sew all seams, particularly those on the top and sides of the MESL, where overburden pressures from cover soils are low.

A large amount of information was gained from the below-grade MESLs in Australia shown in Figure 2.42b. Observations were made over a period of seven years, corresponding to 300,000 standard axle loads, which is approximately one-half of its design life. Moisture content and surface deflections were taken periodically on both MESL sections and on the adjacent control sections that did not have MESLs. General conclusions were as follows:

1. No degradation of the bitumen-sealed geotextile was observed, even though it is a relatively thin, nonwoven heat-bonded geotextile.
2. There was good bond between the adjacent soil and the impregnated geotextile. At Site 2 surface cracking was successfully arrested by the MESL.
3. The moisture content of the MESL encapsulated soil was better than in the control sections, which in turn led to lower surface deflections of the MESL sections. The overall performance of the MESL sections was unquestionably superior to the control sections. Severe crack crazing and edge failures occurred in control sections on both sides of the MESL of Site 2, but none within the MESL section itself.

4. No estimate of service life equivalence could be obtained, since even the thinnest MESL of 100 mm has continued to perform satisfactorily for seven years under traffic.

2.6.3 Paved Roads

Whenever geotextile use in unpaved roads is discussed, the question of the material's use in paved roads usually follows. To address this properly, we must focus on the general characteristics of the situation. It is most important to recognize that if the road is to be paved with concrete or asphalt immediately (i.e., during initial construction), it cannot be placed on an excessively yielding soil subgrade. If the subgrade yields, the road section will deform and the surfacing will simply crack after a few load repetitions. Many agencies put the *lower limit* of acceptable unsoaked CBR values in the range 10 to 15. As just described, however, the geotextile must deform in order to mobilize its strength, and the *upper limit* of soil subgrade strength for such mobilization as suggested in Table 2.15 is an unsoaked CBR of 3 to 8. This contradiction begs the question of how the geotextile is to reinforce if it is not significantly deformed. Advocates of a reinforcement function in paved roads on firm soil subgrades will suggest that the geotextile deformation around the coarse-aggregate base course (when heavily rolled) is sufficient to mobilize the geotextile's strength. Thus the design can proceed in a manner similar to unpaved roads.

Those who feel this is not the case still desire a geotextile under the stone base, but for reasons other than soil subgrade reinforcement. Here the primary function becomes separation (discussed in Sections 2.2.1 and 2.5) or filtration (Sections 2.2.3 and 2.8). The economic justification is the longer service lifetime with a geotextile separator than without. (Recall the discussion in Section 2.5.6 and the photograph in Figure 2.35.)

When separation is the primary function in paved road applications, it is important to recognize where the geotextile is located with respect to the pavement cross section and applied loads. In a trial test site with 40 mm of asphalt paving, 150 mm of base course, and 100 mm of large crushed stone, a lightweight geotextile (150 g/m^2) failed under 165,000 repetitions of a standard 80 kN axle load [86]. This premature geotextile failure was evidenced by abrasion of the yarns followed by fines pumping up from the subgrade into the stone base. Although no specific design is available to explain the situation, it does illustrate that a minimum set of geotextile properties is required in most situations. In other words, an adequate survivability criterion is required to ensure reasonable performance in general situations.

To specifically add reinforcement for paved roads on firm subsoils, a geotextile pretensioning system is required. By pretensioning the geotextile, the stone base will be placed in compression (i.e., thereby providing a lateral confinement) and will effectively increase its modulus over the nonreinforced case. Some of these concepts are discussed in Section 2.7.4; however, they are extremely difficult to implement.

2.7 DESIGNING FOR SOIL REINFORCEMENT

This section continues the discussion of the use of geotextiles in the primary function of reinforcement. Since this was the topic of the preceding section involving road systems, it could easily have been incorporated into that section. However, this type of soil reinforcement raises a unique set of design issues, whereby the geotextile in horizontal layers and the interspersed soil form a *mechanically stabilized earth* (MSE) system rather than acting as a discrete material element. Three applications are involved here: (1) geotextile reinforced walls (facing angle ≥70° to the horizontal), (2) geotextile reinforced slopes (facing angle <70° to the horizontal), and (3) geotextile reinforced foundations (also called basal reinforcement).

2.7.1 Geotextile Reinforced Walls

Background. Conventional gravity and cantilever wall systems made from masonry and concrete resist lateral earth pressure by virtue of their large mass. They act as rigid units and have served the industry well for centuries. However, a new era of retaining walls was introduced in the 1960s by H. Vidal with Reinforced Earth. Here metal strips extending from exposed facing panels back into the soil serve the dual role of anchoring the facing units and being restrained through frictional stresses mobilized between the strips and the backfill soil. The backfill soil both creates the lateral pressure and interacts with the strips to resist it. The walls are very flexible compared with conventional gravity structures. They offer many advantages, including significantly lower cost per square meter of exposed surface. A steady series of variations followed Vidal's steel strips, all of which can be put into the MSE wall category:

- Facing panels with metal strip reinforcement
- Facing panels with metal wire mesh reinforcement
- Solid panels with tieback anchors
- Anchored gabion walls
- Anchored crib walls
- Geotextile-reinforced walls (to be described here)
- Geogrid-reinforced walls (to be described in Chapter 3)

In all cases, the reinforced soil mass behind the wall facing is said to be mechanically stabilized earth and the wall system is generically called an MSE wall.

Construction Details. A critical factor in the successful functioning of a geotextile-reinforced MSE wall is proper construction, which is done on a planned sequential basis. Upon preparing an adequate soil foundation, which consists of removing unsuitable material and compacting in situ or replacement foundation soils, the wall itself is begun. There is no concrete footing with these walls, and the lowest

geotextile layer is placed directly on the foundation soil. An iterative construction sequence, developed by the U.S. Forest Service (see Figure 2.43) can be summarized as follows. The resulting wall is referred to as a "wrap-around" MSE wall.

1. A wooden form of a height slightly greater than the individual soil layer thickness, called the *lift height*, is placed on the ground surface or on the previously placed lift after the first layer is completed. This form is nothing more than a series of metal L brackets with a continuous wooden brace board running along the face of the wall.

2. The geotextile is unrolled and positioned so that approximately 1.0 m extends over the top of the form and hangs free. If it is sufficiently wide, the geotextile can be unrolled parallel to the wall. In this way the geotextile's cross machine direction is oriented in the maximum stress direction. This will depend on the required design length and geotextile strength, which will be discussed later. If a single roll is not wide enough, two of them can be sewn together. The sewn strength is then a governing factor. Alternatively, the geotextile can be deployed perpendicular to the wall in full-width strips and adjacent roll edges can be overlapped or sewn. In this way the geotextile's machine direction is oriented in the maximum stress direction.

3. Backfill is now placed on the geotextile for 1/2 to 3/4 of its lift height and compacted. This is typically 200 to 400 mm and is done with lightweight construction equipment. The choice of backfill soil type is important. If it is angular gravel, drainage can easily occur but high installation damage to the geotextile must be considered. If it is fine-grained silts or clays, drainage cannot occur and hydrostatic pressures must be considered. This leaves sand, which the author considers the ideal backfill soil for MSE walls that are reinforced by geotextiles or geogrids.

4. A windrow is made 300 to 600 mm from the face of the wall with a road grader or is dug by hand. Care must be exercised not to damage the underlying geotextile.

5. The free end of the geotextile—that is, its "tail"—is then folded back over the wooden form into the windrow.

6. The remaining lift thickness of soil is then completed to the planned lift height and suitably compacted.

7. The wooden form is then removed from in front of the wall, and the metal brackets from beneath the lift, and the assembly is reset on top in preparation for the next higher lift. Note that it is usually necessary to have scaffolding in front of the wall when the wall is higher than 1.5 or 2.0 m.

When completed, this sequence provides walls similar to those shown in Figure 2.44. The exposed face of the wall must now be covered to prevent the geotextile's weakening due to UV exposure (recall Section 2.3.6) and possible vandalism. Bituminous emulsions or other asphalt products have been used for covering wall faces and have the advantage of being flexible, as are the walls themselves. Unfortunately, oxidation of the bitumen causes deterioration after a few years, and it must be periodically reapplied. Alternatively, the surface of wrap-around geotextile walls can be covered with shotcrete (wet-mixed cement/sand/water paste with air supplied at the nozzle) or gunite (dry cement/sand mix

1. Set form on completed lift.

2. Unroll geotextile and position it so that a ± 1 m-wide tail drapes over the form.

3. Place backfill to about half of the total lift height.

4. Make a windrow to slightly greater than full lift height against the form.

5. Place the geotextile tail over the windrow and lock into place with backfill.

6. Complete backfilling for planned lift thickness.

7. Reset the form to the next lift and repeat the sequence.

Figure 2.43 Construction sequence for geotextile wrap-around walls followed by U.S. Forest Service.

Figure 2.44　Geotextile wrap-around walls. (Compliments of Crown Zellerbach Corp.)

with water and air supplied at the nozzle). A wire mesh anchored between the geotextile layers may be necessary to keep the coating adhered to the vertical face of the wall. Still further, a precast concrete or cast-in-place concrete facing can be used, but only after deformation equilibrium of the wrap-around wall has occurred.

Design Methods.　There are two somewhat different approaches to the design of geotextile walls: the method used by Broms [87] and the one used by the U.S. Forest Service, as discussed in Steward et al. [88] and Whitcomb and Bell [89]. The latter method will be followed in this book. This method follows the work that Lee et al. [90] did on reinforced earth walls with metallic strip reinforcement and was originally adapted to geotextile walls by Bell et al. [91]. The design progresses in parts, as follows:

- Internal stability is first addressed to determine geotextile spacing, geotextile length, and overlap distance.
- External stability against overturning, sliding, and foundation failure is investigated and the internal design verified or modified accordingly.
- Miscellaneous considerations, including wall facing details and external drainage, are completed.

To determine the geotextile layer separation distances, earth pressures are assumed to be linearly distributed using Rankine active "earth pressure" conditions for

the soil backfill and "at rest" conditions for the surcharge. A prediction conference at the Canadian Royal Military College, however, showed that the entire design to be presented here is quite conservative (see Jarrett and McGown [92]). Therefore, active earth pressure (K_a) conditions will be used throughout. An even less conservative approach would be to use a Coulomb analysis for the earth pressure values. This is the approach used in several computer programs and will be discussed later. Boussinesq elastic theory for live loads on the soil backfill is used. As shown in Figure 2.45, the following earth pressures result:

$$\sigma_{hs} = K_a \gamma z \tag{2.42}$$

$$\sigma_{hq} = K_a q \tag{2.43}$$

$$\sigma_{hl} = P \frac{x^2 z}{R^5} \tag{2.44}$$

$$\sigma_h = \sigma_{hs} + \sigma_{hq} + \sigma_{hl} \tag{2.45}$$

where

σ_{hs} = lateral pressure due to soil,

K_a = $\tan^2(45 - \phi/2)$ = coefficient of active earth pressure, where

ϕ = angle of shearing resistance of backfill soil,

γ = unit weight of backfill soil,

z = depth from ground surface to layer in question,
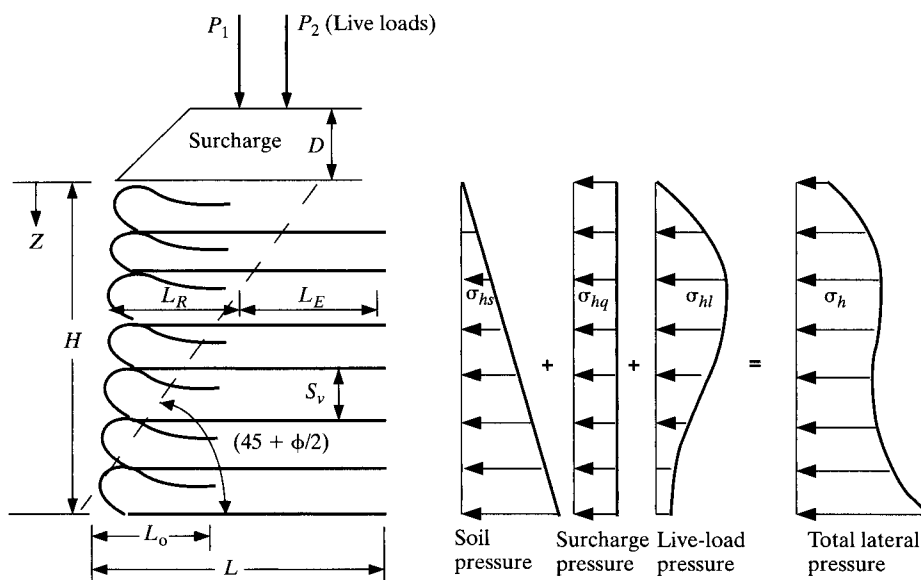
Figure 2.45 Earth pressure concepts and theory for geotextile wall design.

σ_{hq} = lateral pressure due to surcharge load,

q = $\gamma_q D$ = surcharge load on ground surface, where,

γ_q = unit weight of surcharge soil, and

D = depth of surcharge soil,

σ_{hl} = lateral pressure due to live load,

P = concentrated live load on backfill surface,

x = horizontal distance load is away from wall,

R = radial distance from load point on wall where pressure is being calculated, and

σ_h = total, or cumulative, lateral earth pressure on wall.

The calculations of σ_{hs} and σ_{hq} are quite straightforward, but σ_{hl} presents problems, particularly for multiwheeled truck loads where superposition of each wheel must be performed. Figure 2.46 greatly aids in such calculations.

By taking a free body at any depth in the total lateral pressure diagram and then summing the forces in the horizontal direction, we obtain the equation for the lift thickness:

$$\sigma_h S_v = \frac{T_{\text{allow}}}{\text{FS}}$$

$$S_v = \frac{T_{\text{allow}}}{\sigma_h \text{ FS}} \tag{2.46}$$

where

S_v = vertical spacing (lift thickness),

T_{allow} = allowable stress in the geotextile (recall equation 2.24 and Table 2.11),

σ_h = total lateral earth pressure at depth considered, and

FS = factor of safety (use 1.3 to 1.5 when using T_{allow} as determined above).

The same free-body approach can be taken for obtaining the length of embedment of the geotextile layers in the anchorage zone, L_e. Note that when these values are obtained they must be added to the nonacting lengths (L_R) of geotextile within the active zone for the total geotextile lengths (L); that is,

$$L = L_e + L_R \tag{2.47}$$

where

$$L_R = (H - z) \tan\left(45 - \frac{\phi}{2}\right) \tag{2.48}$$

Left graph: axes — Value of $n = Z/H$ (vertical, 0 to 1.0), Value of $\sigma_H \left(\dfrac{H}{Q_L}\right)$ (horizontal, 0 to 1.0). Curves labeled $m = 0.1$, $m = 0.5$, $m = 0.7$, $m = 0.3$.

m	R
0.1	.60H
0.3	.60H
0.5	.56H
0.7	.48H

Right graph: axes — Value of $n = Z/H$ (vertical, 0 to 1.0), Value of $\sigma_H \left(\dfrac{H^2}{Q_P}\right)$ (horizontal, 0 to 1.5). Curves labeled $m = 0.6$, $m = 0.2$, $m = 0.4$.

m	$\dfrac{P}{H}\left(\dfrac{H}{Q_P}\right)$	R
0.2	.78	.59H
0.4	.78	.59H
0.6	.45	.48H

Point load Q_P

Line load Q_L

For $m \le 0.4$:

$$\sigma_H \left(\frac{H}{Q_L}\right) = \frac{0.20n}{(0.16 + n^2)^2}$$

$$P_H = 0.55\, Q_L$$

For $m > 0.4$:

$$\sigma_H \left(\frac{H}{Q_L}\right) = \frac{1.28m^2n}{(m^2 + n^2)^2}$$

Resultant $P_H = \dfrac{0.64Q_L}{(m^2 + 1)}$

Pressure from line load Q_L
(Boussinesq equation modified
by experiment)

For $m \le 0.4$:

$$\sigma_H \left(\frac{H^2}{Q_P}\right) = \frac{0.28n^2}{(0.16 + n^2)^3}$$

For $m > 0.4$:

$$\sigma_H \left(\frac{H^2}{Q_P}\right) = \frac{1.77m^2n^2}{(m^2 + n^2)^3}$$

$$\sigma'_H = \sigma_H \cos^2 (1.1\theta)$$

Section A-A
Pressures from point load Q_P
(Boussinesq equation modified by experiment)

Figure 2.46 Lateral earth pressure due to a surface load. Left side is for line load; right side is for point load. (After NAVFAC [93])

and

$$S_v \sigma_h \text{ FS} = 2\tau L_e$$
$$= 2(c_a + \sigma_v \tan \delta)L_e$$
$$= 2(c_a + \gamma Z \tan \delta)L_e$$
$$L_e = \frac{S_v \sigma_h \text{ FS}}{2(c_a + \gamma Z \tan \delta)} \tag{2.49}$$

where

τ = shear strength of the soil to the geotextile,

L_e = required embedment length (minimum is one meter),

S_v = vertical spacing (lift thickness),

σ_h = total lateral pressure at depth considered,

FS = factor of safety,

c_a = soil adhesion between soil and geotextile (zero if granular soil is used),

γ = unit weight of backfill soil,

Z = depth from ground surface, and

δ = angle of shearing resistance (friction) between soil and geotextile.

Finally, the overlap distance L_o is obtained in a manner similar to that above with a few exceptions—namely, that the distance Z should be measured to the middle of the layer and σ_h is not as large as that illustrated in Figure 2.45. It is reasonably well-established that the stress in reinforcement elements is maximum near the failure plane and falls off sharply to either side [94]. As an approximation, $0.5\sigma_h$ will be used, which results in the following equation:

$$L_o = \frac{S_v \sigma_h \text{ FS}}{4(c_a + \gamma Z \tan \delta)} \tag{2.50}$$

where L_o is the required overlap length (minimum is one meter).

Next, we must consider external stability of the geotextile reinforced MSE mass, which includes overturning, sliding, and foundation failures. These are illustrated in Figure 2.47. These features are common to all wall systems and can be treated exactly the same way as with gravity or crib walls. They are generally site-specific insofar as calculations are concerned. In general, it is recommended that for overturning and foundation-bearing capacity the FS value ≥ 2.0 and for sliding the FS-value ≥ 1.5.

The miscellaneous considerations that generally must be addressed are facing details; facing connections (if applicable); seaming methods (if necessary); drainage behind,

(a) Overturning considerations

(b) Sliding considerations

(c) Foundation considerations
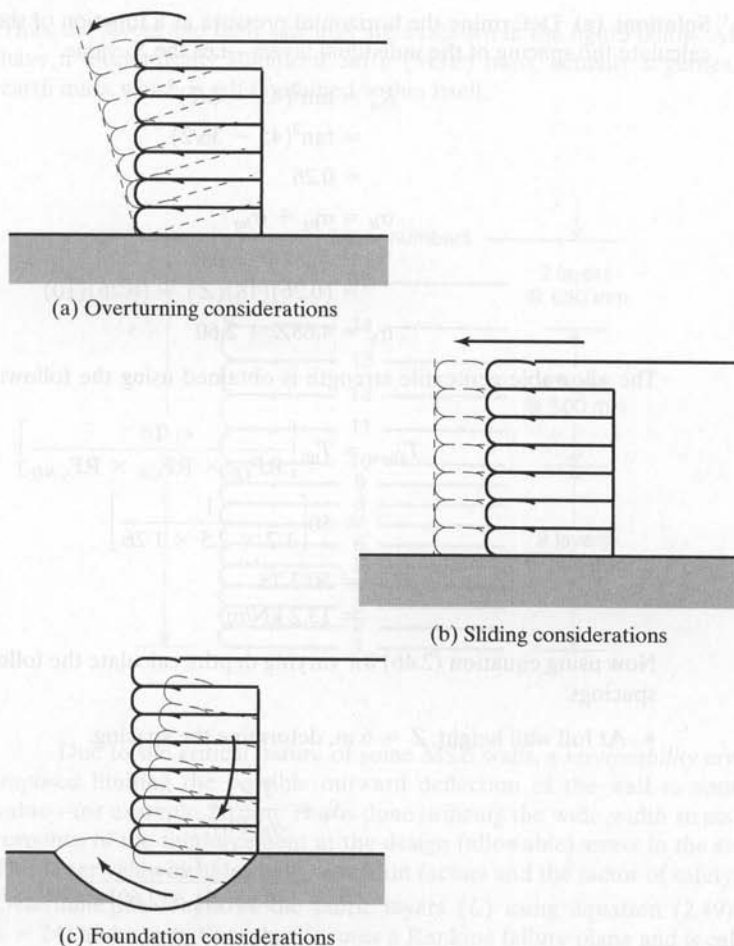
Figure 2.47   External stability considerations for geotextile walls.

beneath and in front of wall; erosion above and in front of wall, guard post, light posts, fencing and other appurtenances with or without deep foundations.

Example 2.17

Design a 6-m-high wrap-around type of geotextile wall that is to carry a storage area of equivalent dead load of 10 kPa. The wall is to be backfilled with a granular soil (SP) having properties of $\gamma = 18$ kN/m^3, $\phi = 36°$, and $c = 0$. A woven slit-film geotextile with warp (machine) direction ultimate wide-width tensile strength of 50 kN/m and friction angle with granular soil of $\delta = 24°$ (see again Table 2.5) is intended to be used in its construction. The orientation of the geotextile is perpendicular to the wall face and the edges are to be overlapped or sewn to handle the weft (cross machine) direction. A factor of safety of 1.4 is to be used along with site-specific reduction factors.

Solution: (a) Determine the horizontal pressure as a function of the depth Z in order to calculate the spacing of the individual layers—i.e., the S_v value.

$$K_a = \tan^2(45 - \phi/2)$$
$$= \tan^2(45 - 36/2)$$
$$= 0.26$$

$$\sigma_h = \sigma_{hs} + \sigma_{hq}$$
$$= K_a \gamma z + K_a q$$
$$= (0.26)(18)(Z) + (0.26)(10)$$
$$\sigma_h = 4.68Z + 2.60$$

The allowable geotextile strength is obtained using the following reduction factors:

$$T_{allow} = T_{ult}\left[\frac{1}{RF_{ID} \times RF_{CR} \times RF_{CBD}}\right]$$
$$= 50\left[\frac{1}{1.2 \times 2.5 \times 1.26}\right]$$
$$= 50/3.78$$
$$= 13.2 \text{ kN/m}$$

Now using equation (2.46) for varying depths, calculate the following geotextile layer spacings:

- At full wall height, $Z = 6$ m, determine the spacing.

$$S_v = \frac{T_{allow}}{\sigma_h(FS)}$$
$$= \frac{T_{allow}}{[4.68(Z) + 2.60]\, 1.4}$$
$$= \frac{13.2}{[4.68(6.0) + 2.60]\, 1.4}$$
$$S_v = 0.307 \text{ m; use } 0.30 \text{ m}$$

- By trial and error, see if the spacing can be opened up to 0.50 m at $Z = 3.3$ m.

$$S_v = \frac{13.2}{[(4.68)(3.3) + 2.60]\, 1.4}$$
$$S_v = 0.52 \text{ m; use } 0.50 \text{ m}$$

- By trial and error, see if the spacing can be further opened up to 0.65 m at $Z = 1.3$ m.

$$S_v = \frac{13.2}{[(4.68)(1.3) + 2.60]\, 1.4}$$
$$S_v = 1.08 \text{ m; use } 0.65 \text{ m}$$

Thus, the layers and their spacings are as shown in the figure below. At this point we have a mechanically stabilized earth (MSE) mass, actually a geotextile stabilized earth mass, which is self-contained within itself.
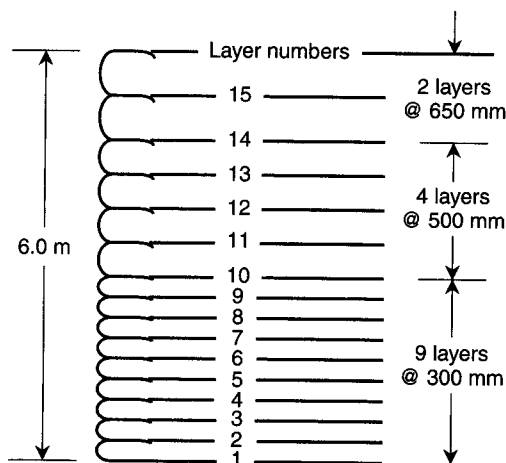
Due to the critical nature of some MSE walls, a *serviceability* criterion can be imposed limiting the possible outward deflection of the wall to some acceptable value—for example, 20 mm. This is done utilizing the wide-width stress versus strain response of the reinforcement at the design (allowable) stress in the reinforcement. This latter value includes both reduction factors and the factor of safety.

(b) Determine the length of the fabric layers (L) using equation (2.49) for L_e with $\delta = 24°$ and $c = 0$. Note that L_R uses a Rankine failure plane and is calculated from equation (2.48).

$$L_e = \frac{S_v \sigma_h (\text{FS})}{2(c + \gamma Z \tan \delta)}$$

$$= \frac{S_v (4.68Z + 2.60)\, 1.4}{2(0 + 18Z \tan 24°)}$$

$$L_e = \frac{S_v (6.55Z + 3.64)}{16.0Z}, \text{ and}$$

$$L_R = (H - Z) \tan\left(45 - \frac{36}{2}\right)$$

$$L_R = (6.0 - Z)(0.509)$$

Layer No.	Depth, z (m)	Spacing, S_v (m)	L_e (m)	L_e min (m)	L_R (m)	L_{calc} (m)	L_{spec} (m)
15	0.65	0.65	0.49	1.0	2.72	3.72	Use 4.0
14	1.30	0.65	0.38	1.0	2.39	3.39	
13	1.80	0.50	0.27	1.0	2.14	3.14	
12	2.30	0.50	0.26	1.0	1.88	2.88	Use 3.0
11	2.80	0.50	0.25	1.0	1.63	2.63	
10	3.30	0.50	0.24	1.0	1.37	2.37	
9	3.60	0.30	0.14	1.0	1.22	2.22	
8	3.90	0.30	0.14	1.0	1.07	2.07	
7	4.20	0.30	0.14	1.0	0.92	1.92	Use 2.0
6	4.50	0.30	0.14	1.0	0.76	1.76	
5	4.80	0.30	0.14	1.0	0.61	1.61	
4	5.10	0.30	0.14	1.0	0.46	1.46	
3	5.40	0.30	0.14	1.0	0.31	1.31	
2	5.70	0.30	0.14	1.0	0.15	1.15	
1	6.00	0.30	0.13	1.0	0.00	1.00	

Note that the calculated L_e values are very small (this is typically the case with geotextile walls) and the minimum value of 1.0 m should be used. When this is added to L_R for the total length, you should round up to a even number of meters. Also, the important consideration of total geotextile width must be addressed. Three cases can be envisioned.

- *Case 1*: If the geotextile rolls are wide enough, they can be deployed parallel to the wall, and the weft or cross machine direction is the important property insofar as its wide width strength is concerned. Although this is possible for the lower fabric layers, it is not for the uppermost, since, 4.0 + 0.65 + 1.0 = 5.65 m, which is wider than many commercially available geotextiles.
- *Case 2*: Alternatively, two adjacent rolls of fabric can be used parallel to the wall, but a sewn seam, or large overlap, must be used for the uppermost layers. If sewn seams are used, an appropriate reduction factor must be used.
- *Case 3*: The fabric layers can be deployed perpendicular to the wall, thereby utilizing their warp or machine direction wide-width strength in the major principal stress direction. This was the case posed in this example. This requires sewn seams, or overlaps, in the opposite direction. However, in this (the minor principal stress) direction the required forces are significantly lower—for example, 33 to 50% of the major principal stress direction.

(c) Check the overlap length L_o, to see if it is less than the 1.0 m recommended value using equation (2.50):

$$L_o = \frac{S_v \sigma_h (\text{FS})}{4(c_a + \gamma Z \tan \delta)}$$

$$= \frac{S_v [4.68(Z) + 2.60] \, 1.4}{4[0 + (18)Z \tan 24°]}$$

This is maximum at the upper layer at $z = 0.65$ m:

$$L_o = \frac{0.65[4.68(0.65) + 2.60]\ 1.4}{4[0 + (18)(0.65) \tan 24°]}$$

$$= 0.25 \text{ m; use 1.0 m throughout}$$

The solution at this point in the design, appears as in the figure below.
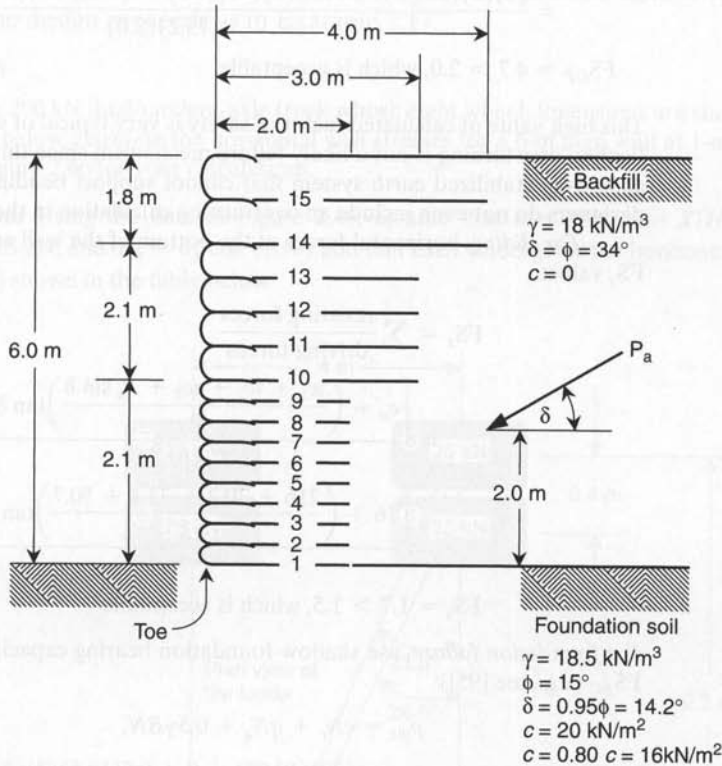
(d) Since the internal stability of the wall has been provided for, focus now shifts to external stability. Standard geotechnical engineering concepts are used to analyze overturning, sliding, and bearing capacity. See the above figure where

$$K_a = \tan^2(45 - \phi/2) = \tan^2(45 - 34/2)$$

$$= 0.28$$

$$P_a = 0.5\gamma\, H^2\, K_a$$

$$= 0.5(18)(6)^2(0.28)$$

$$= 90.7 \text{ kN/m}$$

$$P_a \cos 34 = 75.2 \text{ kN/m}$$

$$P_a \sin 34 = 50.7 \text{ kN/m}$$

For overturning, moments are taken about the toe of the wall to generate a FS_{OT} value.

$$FS_{OT} = \sum \frac{\text{resisting moments}}{\text{driving moments}}$$

$$= \frac{w_1 x_1 + w_2 x_2 + w_3 x_3 + P_a \sin \delta(4)}{P_a \cos \delta(2)}$$

$$= \frac{(6)(2)(18)(1) + (3.9)(1)(18)(2.5) + (1.8)(1.0)(18)(3.5) + (50.7)(4)}{(75.2)(2.0)}$$

$FS_{OT} = 4.7 > 2.0$, which is acceptable

This high value of calculated factor of safety is very typical of walls of this type. Even further, overturning is not a likely failure mechanism since this is a very flexible mechanically stabilized earth system that cannot support bending stresses. Thus many designers do not even include an overturning calculation in the design process.

For sliding, horizontal forces at the bottom of the wall are summed to obtain a FS_s value:

$$FS_s = \sum \frac{\text{resisting forces}}{\text{driving forces}}$$

$$= \frac{\left[c_a + \left(\dfrac{w_1 + w_2 + w_3 + P_a \sin \delta}{2} \right) \tan \delta \right] 2}{P_a \cos \delta}$$

$$= \frac{\left[16 + \left(\dfrac{216 + 70.2 + 32.4 + 50.7}{2} \right) \tan 14.2 \right] 2}{75.2}$$

$FS_s = 1.7 > 1.5$, which is acceptable

For foundation failure, use shallow-foundation bearing capacity theory to determine FS_{BC} (e.g., see [95]):

$$p_{ult} = cN_c + qN_q + 0.5\gamma B N_\gamma$$

$$= (20)(10.98) + 0 + 0.5(18.5)(2)(2.65)$$

$$= 219.6 + 49.0$$

$$= 269 \text{ kN/m}^2$$

$$p_{act} = (18)(6) + (10)$$

$$= 118 \text{ kN/m}^2$$

$$FS_{BC} = \frac{p_{ult}}{p_{act}}$$

$$= \frac{269}{118}$$

$$FS_{BC} = 2.3 > 2.0, \text{ which is acceptable}$$

Both internal and external designs are now complete. The wall uses 15 layers of fabric (the lowest nine at 0.30 m spacing; the middle four at 0.50 m spacing; the upper two at 0.65 m spacing). The fabric lengths are 3.3 m $(2 + 0.3 + 1)$ at the lowest level, 4.5 m $(3 + 0.5 + 1)$ at the intermediate level, and 5.65 m $(4 + 0.65 + 1)$ at the upper level.

Although this example illustrates the design of a wrap-around geotextile retaining wall design for static loads, it does *not* take into account the incorporation of live loads as produced by traffic. Example 2.18 will illustrate how this is done, but just to the point of calculating the additional horizontal stress distribution against the wall. Beyond this, the design proceeds as in Example 2.17.

Example 2.18

For the 200 kN dual-tandem-axle truck whose eight wheel dimensions are shown in the diagram below, calculate the horizontal wall stresses for a 6-m high wall at 1-m increments. Use Figure 2.46 for your calculations.

Solution: Using the data in Figure 2.46, assume that $n = Z/H$, $m = X/H$, $H = 6.0$ m, $Q_p = 25$ kN, and $\sigma'_h = \sigma_h \cos^2(1.1\theta)$ and that each wheel gives the horizontal stresses (in kN/m²) shown in the table below.
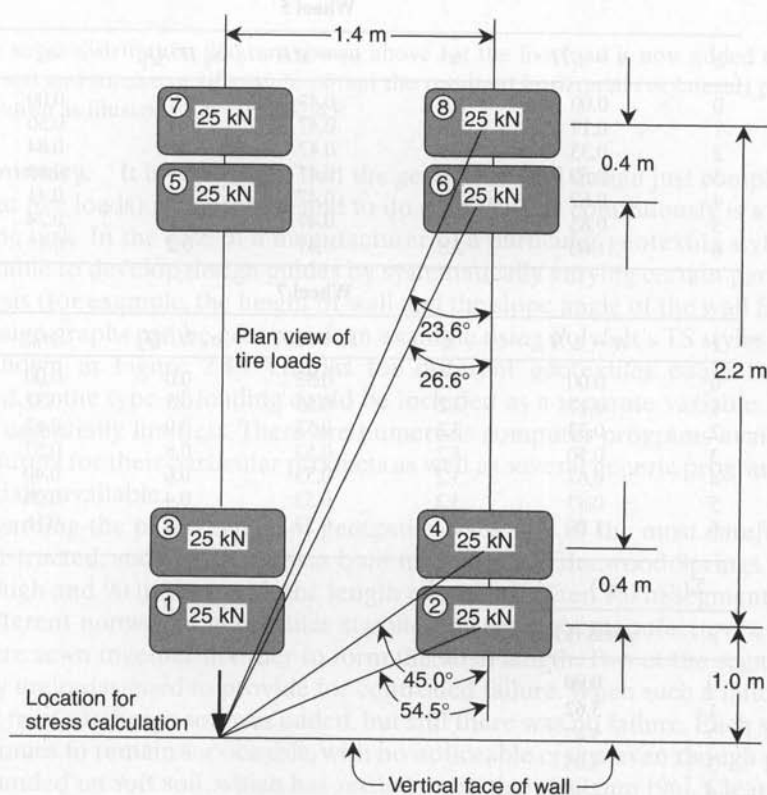
			Wheel 1			**Wheel 2**
z	$n = z/H$	x	$m = x/H$	$\sigma_h H^2/Q_p$	σ_h	$\sigma_h' = 0.25\sigma_h$
0	0.00	1.0	0.17	0.0	0.00	0.00
1	0.17	1.0	0.17	1.2	0.82	0.18
2	0.33	1.0	0.17	1.6	1.08	0.24
3	0.50	1.0	0.17	1.0	0.71	0.16
4	0.67	1.0	0.17	0.6	0.39	0.09
5	0.83	1.0	0.17	0.3	0.22	0.05
6	1.00	1.0	0.17	0.2	0.12	0.03

			Wheel 3			**Wheel 4**
z	$n = z/H$	x	$m = x/H$	$\sigma_h H^2/Q_p$	σ_h	$\sigma_h' = 0.42\sigma_h$
0	0.00	1.4	0.23	0.0	0.00	0.00
1	0.17	1.4	0.23	1.2	0.82	0.34
2	0.33	1.4	0.23	1.6	1.08	0.46
3	0.50	1.4	0.23	1.0	0.71	0.30
4	0.67	1.4	0.23	0.6	0.39	0.16
5	0.83	1.4	0.23	0.3	0.22	0.09
6	1.00	1.4	0.23	0.2	0.12	0.05

			Wheel 5			**Wheel 6**
z	$n = z/H$	x	$m = x/H$	$\sigma_h H^2/Q_p$	σ_h	$\sigma_h' = 0.76\sigma_h$
0	0.00	2.8	0.47	0.0	0.00	0.00
1	0.17	2.8	0.47	0.7	0.50	0.38
2	0.33	2.8	0.47	1.2	0.84	0.64
3	0.50	2.8	0.47	0.9	0.65	0.50
4	0.67	2.8	0.47	0.6	0.41	0.31
5	0.83	2.8	0.47	0.4	0.24	0.19
6	1.00	2.8	0.47	0.2	0.15	0.11

			Wheel 7			**Wheel 8**
z	$n = z/H$	x	$m = x/H$	$\sigma_h H^2/Q_p$	σ_h	$\sigma_h' = 0.81\sigma_h$
0	0.00	3.2	0.53	0.0	0.00	0.00
1	0.17	3.2	0.53	0.5	0.32	0.26
2	0.33	3.2	0.53	0.9	0.63	0.51
3	0.50	3.2	0.53	0.8	0.57	0.46
4	0.67	3.2	0.53	0.6	0.40	0.33
5	0.83	3.2	0.53	0.4	0.26	0.21
6	1.00	3.2	0.53	0.2	0.16	0.13

$\Sigma(\sigma_h + \sigma_h')$	
z	stress (kPa)
0	0.00
1	3.62
2	5.47
3	4.05
4	2.48
5	1.47
6	0.89

Horizontal stress (kPa)
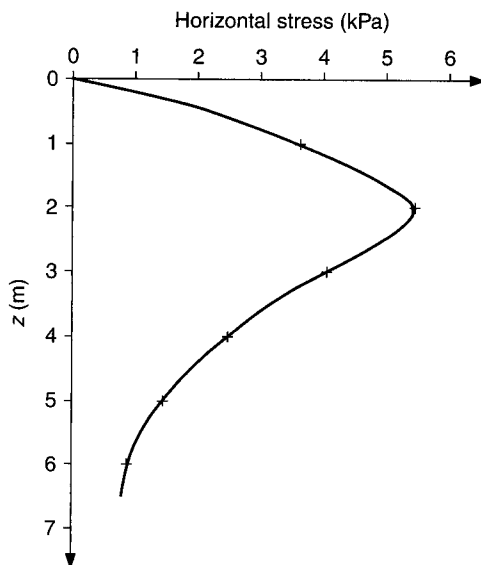
The stress distribution diagram shown above for the live load is now added to that from the soil and surcharge (if any) to obtain the resultant horizontal (or lateral) pressure distribution as illustrated in Figure 2.45.

Summary.   It is easily seen that the geotextile wall design just completed (with or without live loads) is not trivial, and to do such designs continuously is a very time-consuming task. In the case of a manufacturer of a particular geotextile style, it would be preferable to develop design guides by systematically varying certain parameters in the analysis (for example, the height of wall and the slope angle of the wall face). Innovative design graphs can be generated; an example using Polyfelt's TS styles of geotextiles is shown in Figure 2.48. Graphs for different geotextiles could be similarly developed, or the type of loading could be included as a separate variable. The variations are essentially limitless. There are numerous computer programs available from manufacturers for their particular products as well as several generic programs that are commercially available.

Regarding the performance of geotextile walls, one of the most carefully developed, constructed, and monitored was built in 1982 near Glenwood Springs, Colorado. It is 5 m high and 90 m long, with the length consisting of ten 9.0 m segments. Consisting of different nonwoven geotextiles supplied by separate manufacturers, these segments were sewn together in order to form the 90 m length. Two of the segments were purposely underdesigned to provide for controlled failure. When such a failure did not occur, 5.2 m of surcharge soil was added, but still there was no failure. Each segment of wall continues to remain serviceable, with no noticeable creep, even though part of the wall is founded on soft soil, which has settled more than 600 mm [96]. Clearly, geotextile reinforced walls are intrinsically sound in concept, but this case history suggests that the design method may be quite conservative. Several other noteworthy geotextile

① Type of load

② Fill material

③ Height of wall

④ Slope inclination

⑤ Type of geotextile

⑥ Lift thickness

Height (m)

$\beta = 60°$ $\beta = 80°$ $\beta = 89°$

Traffic load 1

(Silty) sand
($c' = 0$, $\phi' = 30°$)

TS 600
TS 500

TS 900
TS 750
TS 700

Spacing of
geotextile
layers

(cm)

⑦ Length curve

② Anchorage length
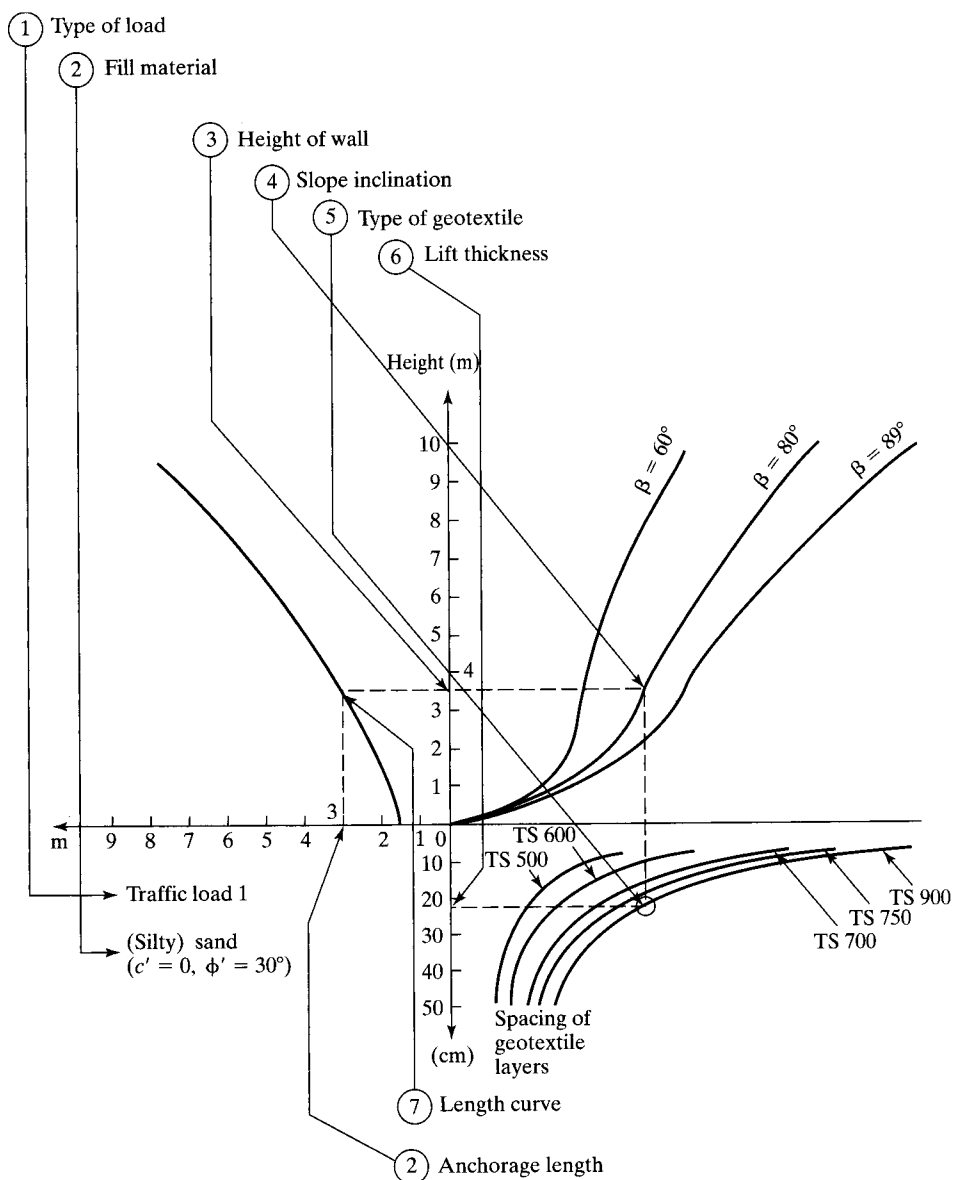
Figure 2.48   Design guide for geotextile walls using Polyfelt geotextiles. (Available from Polyfelt, GmbH)

reinforced walls have appeared in the literature. For example, a 12.6 m high wall was constructed to form support for an additional 5 m of surcharge soil fill in Seattle, Washington (Allen et al. [97]), and a 12.2 m high vertical wall was used to support a high bridge approach while its adjacent section was being constructed (Stevens and Souiedan [98]).

When we compare geotextile walls to gravity walls (and, to a lesser extent, other types of flexible walls), there are the following advantages and disadvantages to using geotextiles:

- *Advantages*: A flexible wall system is created; minimum excavation is needed behind the face of wall; there are no corrosion problems; the backfill need not be gravel; drainage can occur using certain geotextiles; unskilled labor can be used; no heavy equipment is required; and the cost per square meter of exposed wall is very low.
- *Disadvantages*: The design method appears to be quite conservative, the geotextile interaction in the analysis (perhaps via arching theory) is not currently considered; creep is potentially a problem, thereby requiring a relatively high reduction factor; the wall face must be coated to prevent UV degradation and vandalism; and the coatings (shotcrete, gunite, or asphalt) are not particularly attractive.

The above disadvantage regarding the appearance of wrap-around walls is being dealt with ever more effectively. For instance, it is becoming popular to use wall facing panels made from large-sized timbers, gabions, or decorative concrete panels. The geotextiles are fixed to or placed between the facing and extend into the backfill soil exactly as described and designed in this section. For walls less than 5 m in height, timber can be used for the facing. The attachment detail is important, as described by Richardson and Behr [99].

However, the type of wall (both reinforced and nonreinforced) growing fastest in popularity consists of concrete-block facing elements. These precast masonry blocks, weighing up to 400 N each, are laid in a stacked configuration as is a masonry wall; however, they are laid dry—that is, no mortar is used. Small walls of this type (less than one meter in height) can be nonreinforced. Larger walls have the reinforcement placed between the blocks. When geotextiles (or flexible geogrids) are used for the reinforcement, the mated surfaces of the upper and lower blocks provide an interlocking mechanism. This adds to the frictional resistance of the reinforcement between the surfaces of the blocks. Stiff geogrids (and other block types described in Chapter 3) can rely on mechanical anchorage using pins or connections in the lower and/or upper blocks. The various block/reinforcement systems are sometimes called *modular block walls* (MBW) or *segmental retaining walls* (SRWs) and are proliferating due to the aesthetics of very attractive surface finishes on the blocks, their adaptability to curving around trees, ponds, poles, and other obstructions, the ease of construction by nonskilled labor, the lack for need of heavy construction equipment (e.g., cranes), the availability of generic computer programs [100, 101], and all the advantages of flexible walls mentioned earlier.

Perhaps the greatest economy can be realized by the nature of the backfill soil. Large stone, (e.g., AASHTO 8 or 57) need not be used, since the installation damage is likely to be excessive; rather a sand backfill, with sufficient permeability for drainage, is recommended. Table 2.17 gives a suggested gradation. In many cases, sand is locally available and is generally significantly less expensive than quarried stone or river gravel.

TABLE 2.17 RECOMMENDED SOIL BACKFILL GRADATION
FOR GEOTEXTILE AND GEOGRID REINFORCEMENT
APPLICATIONS (WALLS AND SLOPES) TO PROVIDE
ADEQUATE DRAINAGE AND TO AVOID EXCESSIVE
INSTALLATION DAMAGE

Sieve Size (No.)	Particle Size (mm)	Percent Passing
4	4.76	100
10	2.0	90–100
40	0.42	0–60
100	0.15	0–5
200	0.074	0

Source: After Koerner et al. [102].

Even backfill soils that are finer-grained than sand are possible, but then a geosynthetic drainage system behind or within the backfill must be considered. Use of external or internal drainage systems to accompanying silt or clay backfills will be addressed in Chapters 3 and 9.

2.7.2 Geotextile Reinforced Embankments

Background.   It should come as no surprise that if vertical walls can be built using geotextiles, steep soil embankments can be stabilized by them also. In fact, as the slope angle with the horizontal (β) decreases, a wall transitions into an embankment, albeit one in which the exposed face is not covered with anything except vegetation aided by some type of erosion-control material. In this section, geotextiles will be deployed in horizontal layers with no upturned facing treatment or hard-faced wall surface. When this is the case, the design methodology transitions from lateral earth pressure theory to slope stability analyses. At what β-value the transition occurs is an academic issue, although 70° has often been used. Various geotextile deployment schemes for embankments are shown in Figure 2.49. Pattern (a) is typical. The uneven spacing pattern of (b) reflects those cases where stresses are higher in the lower regions of the slope than in the top. The short edge strips shown in (c) and (d), sometimes called *secondary reinforcement*, represent compaction aids, necessary since high compaction at the edge of the slope is difficult to achieve. These short geotextile layers also eliminate shallow sloughing failures between widely spaced reinforcement layers. Note that all of these schemes require the embankment to be built at the same time as placement of the geotextile proceeds; that is, they are not in situ stabilization schemes (these are discussed later in this section).

Construction Details.   Geotextile placement in embankment stabilization situations is relatively simple in that the sheets are usually horizontally placed as directed by the design. When using woven geotextiles (more so than when using nonwovens) it is important to recognize the direction of maximum stress. For two-dimensional plane strain cases this is typically in the direction of the embankment face. If the geotextile is

(a) Even spaced-even length   (b) Uneven spaced-even length   (c) Even spaced-even length with
                                                                           short facing layers

(d) Even spaced–uneven length
with short facing layers
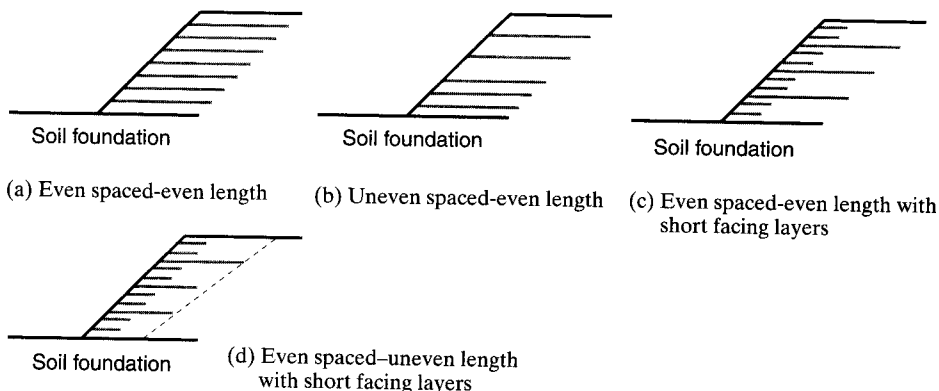
Figure 2.49   Various geotextile deployment schemes for stabilizing steep soil embankments on firm foundations.

sufficiently wide, it can be used parallel to the face of the slope, and the weft, or cross machine direction, must carry the major principal stresses; the fabric must be manufactured and specified accordingly. If the geotextile is not sufficiently wide and is still to be used parallel to the face of the slope, sewn seams will be required, which will have to be included with an appropriate reduction factor in arriving at a T_{allow}-value.

If the geotextile is oriented perpendicular to the face of the slope, the warp or machine direction will carry the major principal stress. Now the weft or cross-machine direction of these rolls will have to carry the minor principal stress, which is typically 33 to 50% of the major principal stress and can be handled by sewing or by an overlap sufficient to mobilize the required strength by frictional resistance. Although either method can effectively transmit the mobilized tensile stresses in the minor principal direction from one geotextile sheet to the next, the labor cost of sewn seams usually becomes small when many seams are required. Thus the cost comparison discussed in Section 2.6.1 swings even further than illustrated in favor of sewn seams.

Limit Equilibrium Design.   The usual geotechnical engineering approach to slope-stability problems is to use limit equilibrium concepts on an assumed circular arc failure plane, thereby arriving at an equation for the factor of safety. Alternatively, a two-part wedge analysis can be used and will be illustrated in Chapter 3 on geogrids. The resulting equations for a circular arc failure for total stresses and effective stresses, respectively, are given below and are also illustrated in Figure 2.50, which diagrams the case of several layers of geotextile reinforcement.

$$FS = \frac{\sum_{i=1}^{n} (N_i \tan \phi + c\Delta l_i)R + \sum_{i=1}^{m} T_i y_i}{\sum_{i=1}^{n} (W_i \sin \theta_i)\, R}$$

(2.51)

Figure 2.50 Details of circular are slope stability analysis for (c, ϕ) shear strength soils.

$$\text{FS} = \frac{\sum\limits_{i=1}^{n} \left(\overline{N_i} \tan \overline{\phi} + \overline{c}\Delta l_i\right)R + \sum\limits_{i=1}^{m} T_i y_i}{\sum\limits_{i=1}^{n} \left(\overline{W_i} \sin \theta_i\right) R}$$ (2.52)

where

$\quad$ FS $\quad$ = factor of safety (against instability);

$\quad N_i \quad$ = $W_i \cos \theta_i$;

$\quad W_i, \overline{W_i}$ = total and effective weight of each slice;

θ_i = angle of intersection of horizontal to tangent at center of each slice;

Δl_i = arc length of each slice;

R = radius of failure circle;

$\phi, \overline{\phi}$ = total and effective angles of shearing resistance, respectively;

$c, \overline{c}$ = total and effective cohesions, respectively;

T_i = allowable geotextile tensile strength;

y_i = moment arm for geotextiles (note that in large-deformation situations these moment arms could become equal to R, which is generally a larger value):

n = number of slices;

m = number of geotextile layers;

$\overline{N}_i$ = $N_i - u_i \, \Delta x_i$, in which

u_i = $h_i \gamma_\omega$ = pore-water pressure,

h_i = height of water above base of circle for each slice,

γ_ω = unit of weight of water, and

Δx_i = width of slices.

The use of equation (2.51)—the total stress analysis equation—is recommended for embankments where water is not involved or when the soil is at less than saturation conditions. The effective stress analysis equation (equation 2.52), is for conditions where water and saturated soil are involved—conditions typical of earth dams and delta areas involving fine-grained cohesive soils.

These equations are tedious to solve, and when additional consideration is given to finding the minimum value of factor of safety by varying the radius and coordinates of the origin of the circle, the process becomes unbearable to do by hand. Fortunately, many computer programs exist that either include, or can readily be modified to include, the contribution of the geotextile reinforcement—i.e., the $\Sigma T_i y_i$ term.

The moment arm y has been the topic of discussion in that its placement as shown is likely to be distorted as rotational deformation occurs. In the limit, this distortion could orient the geotextile along the potential failure arc, changing (and increasing) the moment arm from y to R. Kaniraj [103] has found that this transition can add as much as 45% to the resisting moment of the geotextile. While this is certainly possible, it is quite site-specific and the more conservative value of y is preferred.

For fine-grained cohesive soils whose shear strength can be estimated by undrained conditions, the entire analysis becomes quite simple. (Recall that this is the same assumption as was used in Section 2.6.1 on unpaved roads.) Here slices need not be taken, since the soil strength does not depend on the normal force on the shear plane. Figure 2.51 gives the details of this situation, which results in equation (2.53). Examples 2.19 and 2.20 illustrate its use.

$$\text{FS} = \frac{cL_{\text{arc}}R + \sum_{i=1}^{m} T_i y_i}{W X} \tag{2.53}$$
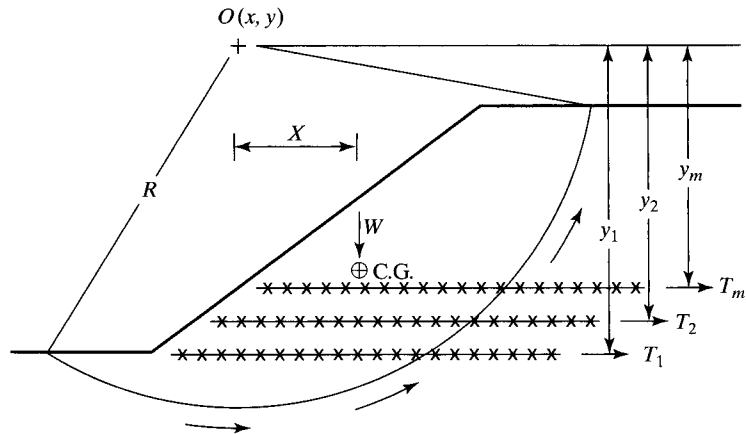
Figure 2.51 Details of circular arc slope stability analysis for soil strength represented by undrained conditions.

where

FS = factor of safety (against instability)

c = cohesion = $0.5q_u$,

q_u = unconfined compression strength of soil,

L_{arc} = length of the failure arc,

R = radius of the failure circle,

T_i = allowable tensile strength of various geotextile layers,

y_i = moment arm of geotextile layers,

W = weight of failure zone, and

X = moment arm to center of gravity of failure zone.

Example 2.19

Assume you are dealing with a 10-m-high, 50° angle slope shown in the diagram below, which consists of a silty clay embankment ($\gamma = 19$ kN/m³, $\phi = 0°, c = 15$ kPa, area $= 60$ m², center of gravity as indicated) on a silty clay foundation ($\gamma = 20$ kN/m³, $\phi = 0°$, $c = 18$ kPa, area $= 55$ m², center of gravity as indicated).

(a) Determine the factor of safety with no geotextile reinforcement.

(b) Determine the factor of safety with a geotextile of *allowable* tensile strength 40 kN/m (note that with a cumulative reduction factor of 3.0, this is an ultimate strength geotextile of 120 kN/m) placed along the surface between the foundation soil and the embankment soil.

(c) Determine the factor of safety with 10 layers of the same geotextile placed at one meter intervals from the foundation interface to the top of the embankment. Assume
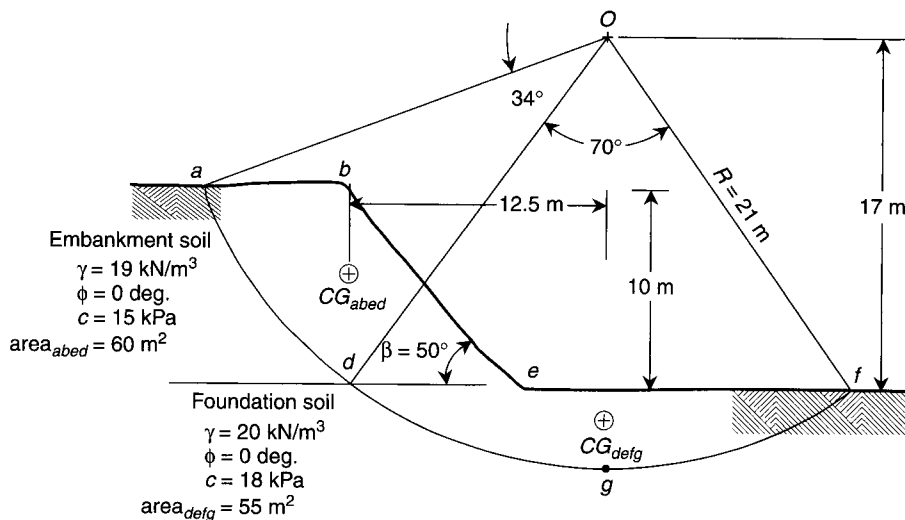
that sufficient anchorage behind the slip circle shown is available to mobilize full geotextile strength.

(d) How would the problem solutions differ if granular soil were involved?

Solution: The following computational data are needed in all parts of the problem:

$$W_{abed} = (60)(19) = 1140 \text{ kN/m}$$

$$W_{defg} = (55)(20) = 1100 \text{ kN/m}$$

$$L_{ad} = 2(21)\pi\left(\frac{34}{360}\right) = 12.5 \text{ m}$$

$$L_{df} = 2(21)\pi\left(\frac{70}{360}\right) = 25.7 \text{ m}$$

(a) Slope as shown (with no geotextile reinforcement):

$$FS = \sum \frac{\text{resisting moments}}{\text{driving moments}}$$

$$FS = \frac{(c_e L_{ad} + c_f L_{df})R}{W_{abed}(12.5) + W_{defg}(0)}$$

$$= \frac{[(15)(12.5) + (18)(25.7)]21}{1140(12.5) + 0}$$

$$FS = \frac{13650}{14250} = 0.96; \text{ not acceptable and failure is indicated}$$

(b) Slope with a geotextile along surface *ed* with sufficient anchorage beyond point *d*:

$$FS = \frac{13650 + 40(17)}{14250}$$

$$FS = 1.01; \text{ still not acceptable and failure is incipient}$$

(c) Slope with 10 layers at one meter intervals from surface *ed* upward, all of which have sufficient anchorage behind the slip surface:

$$FS = \frac{13650 + 40(17 + 16 + 15 + \cdots \cdots + 9 + 8)}{14250}$$

$$FS = 1.31; \text{ which is marginally acceptable}$$

(d) Regarding geotextile reinforcement of *granular* embankment soils—that is, those with a frictional component—the design method involves taking slices and making the modifications described in Figure 2.50 and equation 2.51 or 2.52. This is certainly possible but it requires a computer program with search capabilities to find the critical arc radius and coordinates. Note that even in the undrained example presented here, this same type of search is required, but the calculations are much simpler because slices are not necessary.

Example 2.20

Assume you are dealing with the slope shown in Example 2.19,

(a) Determine how much embedment (or anchorage length) is required *behind* the potential slip circle in order to mobilize the allowable tensile strength of the geotextile. Assume that the transfer efficiency of the geotextile to the shear strength of the soil is 0.80 and base the calculation on FS = 1.5.

(b) Determine the total length of the geotextile, using the maximum distance from the slope face to the failure plane to be 8.0 m.

(c) Comment on the effect of the possible placement orientations of the geotextile rolls.
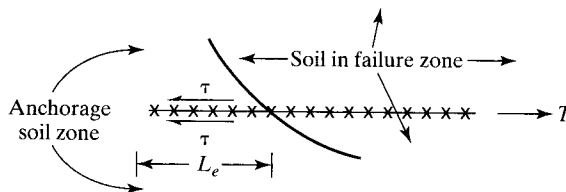
Solution:

(a) When the anchorage test was explained in Section 2.3.3, it was assumed that the resistance was uniformly distributed over the geotextile's embedment and that the strength was entirely mobilized. This is almost certainly not the case. It appears that the concentration decreases rapidly as the embedment length increases and that separate mobilized and fixed portions of the geotextile exist. For this problem, however, a linear distribution will be assumed over a continuous displaced length, since it results

in a conservative length. Taking force summation in the X-direction results in the following equation:

$$2\tau E L_e = T_{allow}(FS)$$
$$2(15)(0.8)(L_e) = 40(1.5)$$
$$L_e = 2.5 \text{ m}$$

This is the required embedment length beyond the potential slip circle for sufficient anchorage of each geotextile layer

(b) The total length of each geotextile layer will be 2.5 + 8.0 = 10.5 m.
(c) Since the typical widths of commercially available geotextiles range from 3 to 4.5 m, seams will be necessary in at least one direction. If the geotextile rolls are oriented parallel to the slope face at least two seams will be required and they will be oriented perpendicular to the major stress direction. If this is the case, a reduction factor for seam strength will have to be included to arrive at the value of T_{allow}. Figure 2.12 provides guidance in this regard. However, if the geotextile is oriented perpendicular to the slope face, sewn seams will be required along the edges of each roll of geotextile and will therefore be in the minor principal stress direction. Overlaps could also be considered, but they would probably not be an economic solution for the higher-strength geotextiles used in this problem; for these, sewn seams are the logical choice.

Finite Element Methods.   Finite element methods (FEM) have been used to study the performance of geotextile-reinforced embankments in both analysis and design situations [104, 105]. Although these computer-based methods might not be routinely used for noncritical situations, they do give great insight into the behavior of geosynthetically reinforced systems.

To illustrate the results of the technique, Rowe and Soderman [106] evaluated two instrumented test embankments on very soft soils in Holland. The embankments, one with geotextile and one without, were purposely brought to failure. The one without geotextile reinforcement failed as the height was brought to 1.75 m (see Figure 2.52a). The other, reinforced with a geotextile, reached a height of 2.75 m before failure (see Figure 2.53a). Using a plane strain nonlinear elastoplastic FEM program with over 1000 triangular elements, the velocity field and the plastic region are shown in Figure 2.52(b) and (c) for a fill height of 1.8 m for the case without reinforcement. Both figures clearly show that continuous failure is mobilized at approximately the height when it did indeed fail (i.e., 1.75 m versus the predicted 1.8 m). To adapt the FEM to the soil-geotextile interface for the reinforced section, the displacement of the soil and geotextile are assumed to be compatible until the shear stress reaches the limiting shear stress defined by the Mohr-Coulomb failure criterion. Once this shear stress is attained, slip occurs. Note from Figure 2.53(b), the FEM-generated plastic zone at a height of 1.8 m, that a continuous plastic region does not yet exist (i.e., the embankment has not yet failed). The plastic zone does begin to be continuous at a height of 2.05 m (Figure 2.53c), and is fully mobilized at a height of 2.66 m. This FEM predicted height of 2.66 m corresponds nicely with the actual failure height of 2.75 m.

Techniques such as this certainly are important for understanding the behavior of geotextile-related designs of permanent and/or critical situations (see Rowe and Soderman [107]).
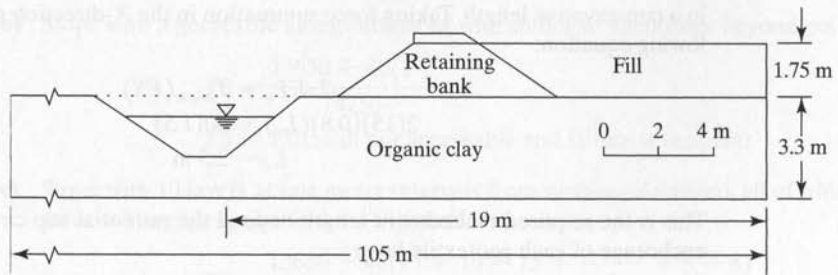
(a) Cross section at failure of 1.75 m
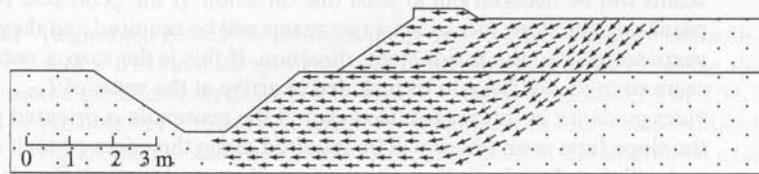
(b) Velocity field at 1.8 m from FEM
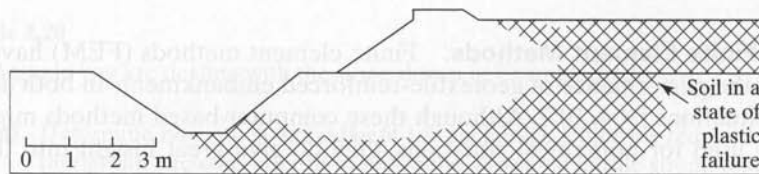
(c) Plastic region at 1.8 m from FEM

Figure 2.52 Test embankment on a soft clay soil with corresponding FEM velocity field and plastic region. (After Rowe and Soderman [107])

Summary.   Geotextile reinforced embankments have been shown to be a practical expedient in many situations. When reinforced, slope heights and/or angles can be significantly increased over the nonreinforced situation. Designwise, the process involves modifications to limit equilibrium procedures that are within the realm of geotechnical engineering practice and seem to be a rational approach. There are several questions that must be asked, however, and additional research is warranted:

- What reduction factors should be used to adapt an ultimate strength value to an allowable value?
- Should load factors be used on the other side of the equation as in load and reduction factor design (LRFD) methods?
- Should the factor of safety be on the soil and the geotextile? If so, should they be the same values?
- What moment arm should be used?
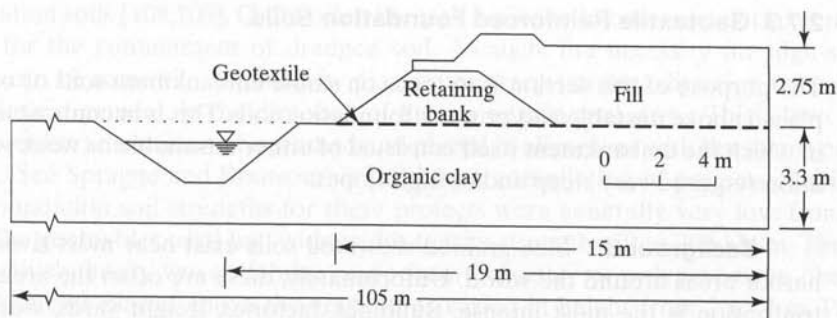
(a) Cross section at failure of 2.75 m
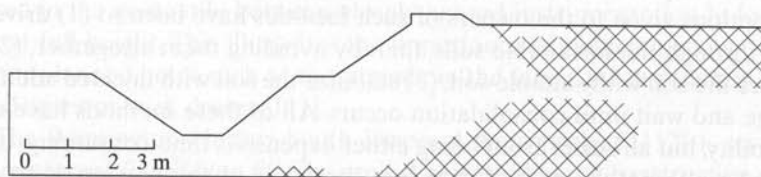
(b) Plastic region at 1.8 m from FEM
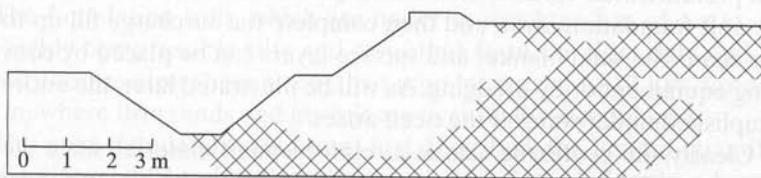
(c) Plastic region at 2.05 m from FEM

Figure 2.53 Geotextile reinforced test embankment shown in Figure 2.52 with corresponding FEM plastic regions. (After Rowe and Soderman [107])

- How are shear stresses transmitted from the soil to the geotextile?
- Is there interaction between closely spaced geotextile layers? If so, how do we address this interaction?
- What anchorage is needed, and how is it mobilized?
- How is strain compatibility of the soil and geotextile(s) considered?
- What type of surface slope treatment is necessary to provide erosion protection?

In this section the focus was on the stabilization of the embankment soil, not of its underlying foundation soil. While it is very similar in its concept to the reinforcement of embankments, geotextile reinforcement of foundations consisting of very weak soils is a rapidly growing area in its own right and will be treated separately in the next section.

2.7.3 Geotextile Reinforced Foundation Soils

The purpose of this section is to focus on stable embankment soils or other structures placed above unstable and/or weak foundation soils. This is in contrast to Section 2.7.2, in which the embankment itself consisted of either unsuitable or weak soils or the situation required very steep and/or high slopes.

Background. Fine-grained saturated soils exist near most river estuaries and harbor areas around the world. Unfortunately, these are often the areas where industrialization is the most intense. Buildings, factories, freight yards, stockpiles, storage tanks, access roads, roadways, highways, railroads, and other appurtenances of industry are all incompatible with such weak foundation soil conditions. The traditional foundation options given to the owners of such facilities have been to (1) drive deep foundations through the unsuitable soils, thereby avoiding them altogether, (2) excavate and replace the soil with suitable soil, (3) stabilize the soil with injected additives, or (4) surcharge and wait until consolidation occurs. All of these methods have a degree of applicability, but all suffer from being either expensive, time-consuming, or both.

An alternative method, which is the focus of this section, is to deploy a high-strength geotextile over the site, place a sand drainage layer/working blanket above it, install prefabricated vertical wick drains (to be described in Chapter 9) to the bottom of the soft foundation layer, and then complete the surcharge fill up to the equivalent design load. The sand blanket and surface layers can be placed by conventional earthmoving equipment or by dredging. As will be illustrated later, the entire process can be accomplished under water if the need arises.

Clearly, the geotextile acts as a reinforcement material, since the shear strength of the foundation soils are often less than 10 kPa, which would hardly support the weight of an individual. The vertical wick drains (also called *prefabricated vertical drains* or *strip drains*) are geosynthetic composites and are used to drain the excess pore water from the foundation soil as it is mobilized by the surcharge fill, which usually consists of locally available soils.

There are two somewhat different variations for the configurations of these projects. One is a large *areal fill* in which the length and width of the site are approximately equal. In such cases there is no clearly defined principal stress direction, and the strength of the geotextile must be equally balanced in all directions. This, of course, is required of the seams in both directions as well as for the material itself. Actual situations in this category are often industrial- or building-site development projects. The second variation is one in which the length of the fill is much larger than the width, called a *linear fill*. In these cases, the major principal stress direction can be identified and the geotextile reinforcement can be aligned accordingly. Seams can often be avoided or placed in the minor principal stress directions. Situations in this category are roadway embankments and containment dikes. Both areal and linear fill situations will be illustrated by case histories.

Construction Details. The U.S. Army Corps of Engineers has been the leading agency behind the use of high-strength woven geotextiles to reinforce very soft

foundation soils [108,109]. Quite often the task has been to construct permanent linear dikes for the containment of dredged soil. As such, the necessity for high-strength seams can be somewhat avoided by placing the warp (strong) direction transverse to the dike's alignment, in the direction of the major principal stress. This allows for the weft (weaker) direction to be seamed and placed in alignment with the minor principal stress. (See Sprague and Koutsourais [110] for a compilation of projects of this type.) The foundation soil strengths for these projects were generally very low, from 1 to 8 kPa. The geotextiles used had wide-width tensile strengths 80 to 700 kN/m. They were all relatively heavy woven fabrics made from polyester or polypropylene fibers. The embankments placed above the geotextiles varied in height from 2 to 7 m. Postcon-struction consolidation settlements varied from 1 to 5 m. To my knowledge all have been successful with only one known problem: at one site a propagating tensile failure occurred in the geotextile between closely-spaced instrumentation holes as surcharge was near full height. This illustrates the importance of reducing geotextile strength to allow for planned holes such as those made in the fabric for installation of instrumen-tation devices or wick drains [111].

The Wilmington Harbor South Disposal Area project [112] is an example of a *linear reinforced foundation fill.* The project consisted of the construction of a U-shaped dike from land out into a major river to provide storage capacity for dredged material from maintenance dredging.

The foundation soils, which are under as much as 5 m of water, consist of the weak, highly compressible silts and clays that form the tidal flats and shallows. Un-confined compression shear strengths range from zero to 10 kPa for depths averag-ing 27 m, where firm sands and gravels are eventually encountered.

The poor foundation conditions just described, the limited quantity of granular borrow soil available, and environmental considerations led to the adoption of a wide-bermed embankment to enclose this disposal area. The concept behind the design in-volves "floating" the dike on the soft foundation soil with the use of a high-strength geotextile for tensile reinforcement. The chosen geotextile deployed on this project was a woven polyester fabric and was specifically designed for this application. The geotextile specifications are given in Table 2.18. After placement of the high-strength geotextile, the dike was constructed of dredged granular soil placed in two stages. The first stage averaged approximately 3 m deep by 180 m in width and formed the wide berm of the dike section. This first stage construction consisted of five separate hy-draulic fills [112]. When constructing the embankment, the outer two fills were placed concurrently, so as to contain the foundation soil and prevent its lateral extrusion. This is a critical aspect of the construction since the lateral containment that is provided forces the central soil to subsequently consolidate (and not laterally extrude), thereby providing long-term stability. This also placed the central section of the geotextile in tension and provided added support for the subsequent three fills. These fills applied load whenever the geotextile rose above the level of the water due to high pressures from the underlying foundation soils. This first stage reached an average top-of-fill ele-vation of 2.1 m, which was approximately 1.0 m above mean high water.

Prefabricated vertical wick drains were installed through the granular fill and geotextile to a depth of 12 m. The drains were in a triangular pattern of 3 m. Upon the

TABLE 2.18 COMPARISON OF SPECIFICATIONS FOR TWO HIGH-STRENGTH GEOTEXTILE FOUNDATION STABILIZATION PROJECTS

Geotextile Specification Properties	Linear Fill (Containment Dike; Wilmington Harbor; U.S. Army Corps of Engineers)	Areal Fill (Industrial Development; Seagrit, MD; Maryland Port Admin.)
Polymer type	PET	PP & PET
Tensile strength (kN/m)	260	180
Modulus (kN/m)	3300	500
Elongation (%)	10–35	15–35
Stiffness (mg-cm)	—	30,000
Friction angle (°)	30	30
Seam strength		
Warp (kN/m)	none	105
Weft (kN/m)	140	105
Seam type	J	J
Seam thread type	PET	PA, PET

completion of primary consolidation settlement (measured via piezometers, settlement anchors, and inclinometers), the second stage embankment was placed on top of the first stage up to an elevation of +4.6 m. The outboard slope has a riprap erosion control system protecting it, and the inboard slope has a low permeability soil liner.

The contractor chose to fabricate the high-strength geotextile reinforcement mat from rolls measuring 3.7 and 5.2 m in width. These rolls were continuous for their full length in the warp direction, since the contract specifications allowed no seams in the warp direction (recall Table 2.18). The geotextile supplier seamed four rolls together to form a 17.4 m wide panel from two 5.2 m wide and two 3.7 m wide rolls at an off-site location. The seamed panels were then rolled onto axles for shipment to the actual construction site. Upon arrival at the site, the axles were attached to wheels, loaded onto barges, unrolled, and then field-seamed to one another. This resulted in an accordion-folded mat of the proper (and unseamed) length in the warp direction and continuous (albeit seamed) length in the weft direction.

When the field-seaming of the panels on the barges was completed, the now continuous geotextile mat was deployed on the soft foundation subsoil beneath the river's surface. The normal means of accomplishing this was to move the interconnected laying barges forward along the centerline of the embankment, letting the geotextile feed off the barge over rollers and down into place on the river bottom. When starting off a new leg of the embankment, this process was reversed with the geotextile being pulled from the barge, which was temporarily anchored. The hydraulic placement of dredged granular fill was begun once the high-strength geotextile was properly positioned. The contractor chose to branch five lines off of a primary supply line to allow the selective placement of the granular material on the five fill segments, as was described.

Prefabricated vertical wick drains were installed following completion of the stage one fill, as explained earlier. The subcontractor's wide-tracked installation crane

was rigged to install the drains to depths of 18 m. The mandrel point and flat anchor system employed by the drain installer was very satisfactory. (Details of the wick drain aspect of the project will be described in Chapter 9).

An example of an *areal fill* on dredged soil using a high-strength geotextile was at Seagirt, Maryland, for the Maryland Port Administration [113]. This 45 ha site contains 6 to 11 m of dredged soil at water contents of 50 to 150%. The goal was to prepare the site for ground surface loads of approximately 30 kPa within the extraordinarily short time of six months. This goal was achieved by deploying a 1000 g/m^2 woven geotextile having wide-width strength of approximately 210 kN/m. The required seam strength was 105 kN/m, which was the limiting design constraint. (See again Table 2.18 for a comparison of the geotextile specification of this project with the previously described linear fill project.) In this areal fill project, sewn seams were particularly critical since the direction of the maximum principal stress was not known. Thus seam strength dominated the design (recall Figure 2.12 for seam efficiencies of high-strength geotextiles that must be included in equation 2.24 as an additional reduction factor). A single 0.75 m thick lift of granular soil, serving as the drainage blanket/working platform, was placed and wick drains at 1.5 m centers were installed to the bottom of the in situ soil. Note that the allowable geotextile strength must make accommodation for these holes and must be included as still another reduction factor in equation (2.24). The final operation was to place a 2.5 m surcharge fill over the entire site. Settlement plates and piezometers were the main control instruments from which the surcharge fill placement rate and dwell time were controlled. The project was very successful in that consolidation occurred to the anticipated degree within the desired six-month time frame. The entire area is currently paved and used for heavy truck storage, loading, and unloading.

Design Methods.   In considering an embankment placed upon very soft foundation soil and supported by a geotextile, a number of design elements, all of which are potential failure scenarios, are present. Figure 2.54 illustrates these various possibilities. In sequentially going from one design scenario to the next, the overall geotextile/embankment design gradually becomes more defined.

Bearing capacity	$\rightarrow$	for overall embankment geometry
Global stability	$\rightarrow$	for strength design in major principal stress direction
	$\rightarrow$	for strength design in minor principal stress direction
Elastic deformation	$\rightarrow$	for modulus and maximum strain in major principal stress direction
	$\rightarrow$	for modulus and maximum strain in minor principal stress direction
Pullout or anchorage	$\rightarrow$	for anchorage length behind slip plane(s)
Lateral spreading	$\rightarrow$	for frictional resistance against embankment sliding

Bearing Capacity.   Regarding bearing capacity as shown in Figure 2.54(a), the limiting embankment height that can be placed on a given foundation soil is essentially independent of the geotextile. If a mass failure occurs beyond the limits of the reinforced

(a) Bearing capacity

(b) Global stability

(c) Elastic deformation

(d) Pullout or anchorage

(e) Lateral spreading
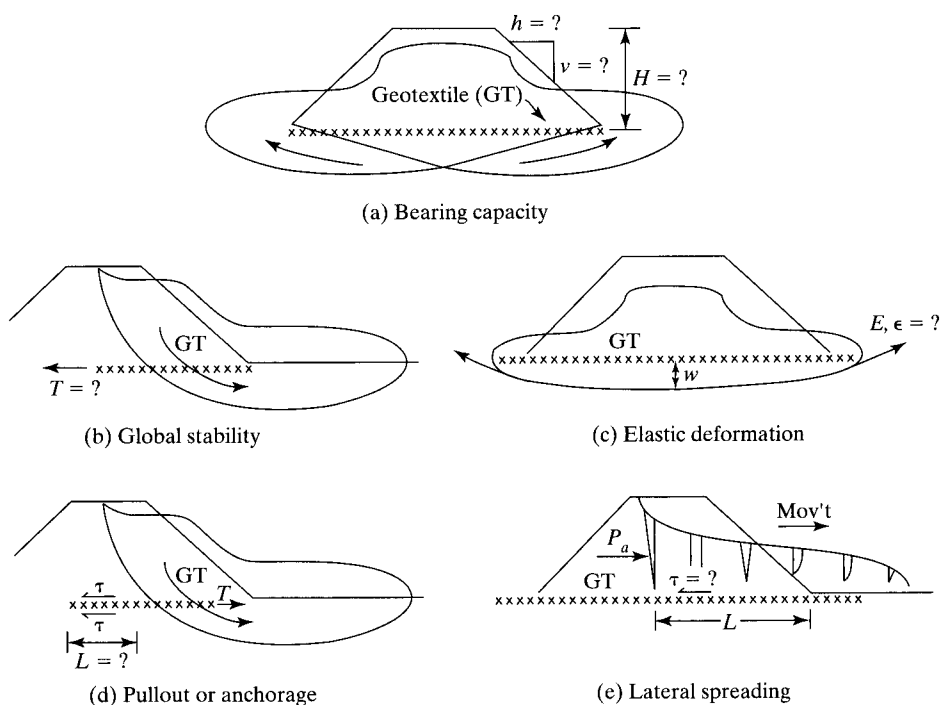
Figure 2.54   Geotextile design models for use in soft stabilization. (After Koerner et al. [111])

zone, the geotextile will be carried along en masse. Thus conventional geotechnical engineering theory can be used directly:

$$q_{\text{allow}} = cN_c/\text{FS} \tag{2.54}$$

where

q_{allow} = γH_{allow} = allowable bearing capacity, in which

γ = unit weight of embankment soil, and

H_{allow} = allowable height of embankment,

c = cohesion of the foundation soil,

N_c = bearing capacity factor (= 3.5 to 5.7), and

FS = factor of safety.

Calculations based on equation (2.54) are surely worst-case situations, for soil strength invariably increases with depth (see Humphrey [114]).

Global Stability.   Figure 2.54(b) shows the type of global stability model that results in the required strength of the geotextile. It is precisely the same as formulated in equation (2.53), since the soil foundation strength can generally be estimated by its undrained shear strength, and a single reinforcement layer is usually being placed. The strength of the embankment soil above the geotextile is another matter. Depending upon the soil's thickness, this shear strength is often taken as being zero—the assumption being that if tension cracks occur in the embankment soil due to lateral deformation, the shear strength can easily be lost. The three parts of Figure 2.55 show the required geotextile strength values for cases of surcharge weight only, surcharge weight plus placement bulldozer, and surcharge weight plus wick drain installation crane, respectively. For weak foundation soils and typical slope angles in the 20 to 40° range, the required tensile strength of the geotextile is seen to be quite high.

Example 2.21

What are the required, allowable and ultimate wide-width geotextile strengths for a 4.0 m high reinforced embankment whose face is on a slope of 3(*H*) to 1(*V*) using a factor of safety of 1.3 and reduction factors from Table 2.11. The undrained shear strength of the foundation soil is 2 kPa.

Solution: Using a slope angle of 18.4° and Figure 2.55(a) results in

$$T_{\text{reqd}} = 66 \text{ kN/m}$$

from which

$$FS = \frac{T_{\text{allow}}}{T_{\text{reqd}}}$$

$$1.3 = \frac{T_{\text{allow}}}{66}$$

$$T_{\text{allow}} = 86 \ kN/m$$

Using equation (2.24) and Table 2.11 gives the necessary ultimate wide-width laboratory test strength.

$$T_{\text{allow}} = T_{\text{ult}}\left[\frac{1}{RF_{ID} \times RF_{CR} \times RF_{CBD}}\right]$$

$$86 = T_{\text{ult}}\left[\frac{1}{1.2 \times 2.0 \times 1.2}\right]$$

$$T_{\text{ult}} = 86(2.88)$$

$$T_{\text{ult}} = 250 \text{ kN/m}$$

Note that the above is for the geotextile itself. If seams are involved in the direction of the principal stress, see Figure 2.12 for typical efficiencies. Here it is seen that maximum efficiency for a 250 kN/m geotextile seam is approximately 0.75. This is comparable to a
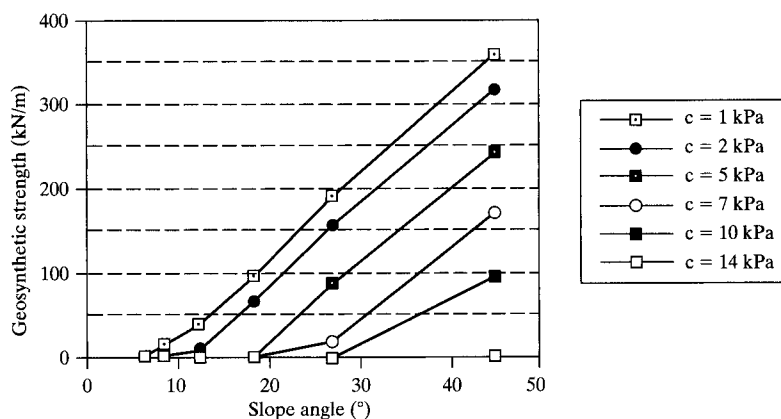
(a) Required geosynthetic strength based on FS = 1.3. Chart reflects soil surcharge height of 4 m.
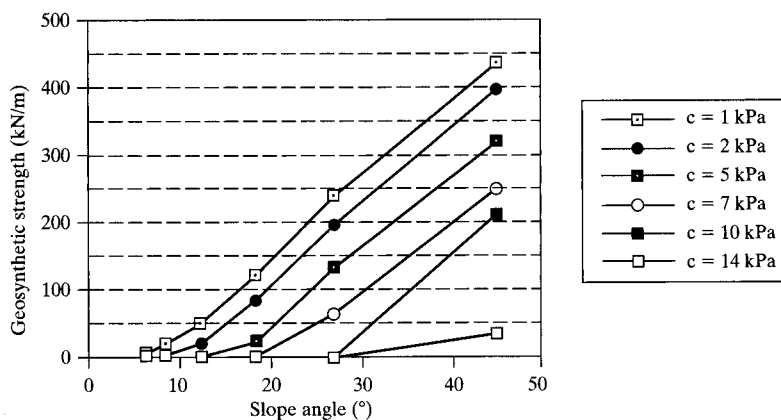
(b) Required geosynthetic strength based on FS = 1.3. Chart reflects soil surcharge height of 4 m plus 13 kPa dozer on embankment.
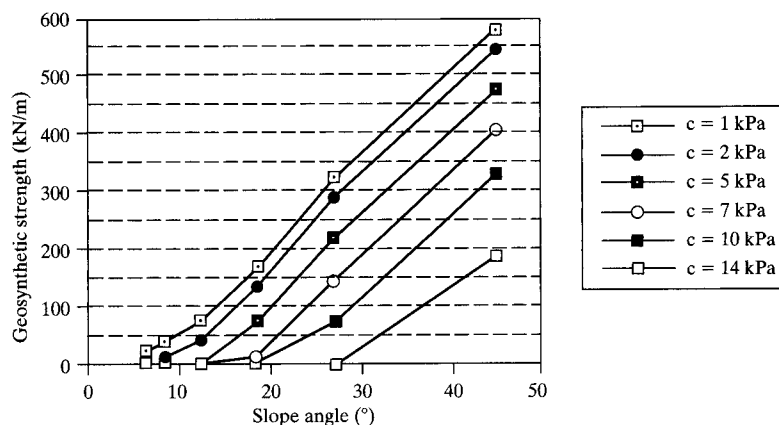
(c) Required geosynthetic strength based on FS = 1.3. Chart reflects soil surcharge height of 4 m plus 42 kPa wick drain installation equipment on embankment.

Figure 2.55 Studies for global stability, using geotextile reinforcement.

reduction factor of 1.33. If holes are involved via the insertion of wick drains, the loss of strength is approximately linear with hole dimension [111]. Thus wick drains at 3 m centers making geotextile holes of 300 mm size will require another reduction factor of $10/9 = 1.11$. Using these two additional factors makes the formulation as follows:

$$T_{\text{allow}} = T_{\text{ult}} \left[\frac{1}{RF_{ID} \times RF_{CR} \times RF_{CBD} \times RF_{\text{Seams}} \times RF_{\text{Holes}}} \right]$$

$$86 = T_{\text{ult}} \left[\frac{1}{1.2 \times 2.0 \times 1.2 \times 1.33 \times 1.11} \right]$$

$$T_{\text{ult}} = 86(4.25)$$

$$= 365 \text{ kN/m}$$

Elastic Deformation.   The amount of elastic deformation allowed by the geotextile will govern the deformation of the embankment, as shown in Figure 2.54(c). Obviously, too great an amount will cause unwanted embankment deformation and loss of underlying foundation soil. Thus relatively high modulus values of the geotextile are desirable. Unfortunately, "relatively high" is a poorly defined term. The U.S. Army Corps of Engineers desired value of maximum strain at the required stress is approximately 10%, thus

$$E = T_{\text{reqd}}/\epsilon_f$$

$$E = T_{\text{reqd}}/0.10$$

$$E_{\text{reqd}} = 10\, T_{\text{reqd}} \tag{2.55}$$

However, to obtain this E_{reqd} value requires a significantly stronger geotextile than T_{reqd} without this condition. The modulus requirement will dominate over the strength requirement if this condition is imposed. Note that these comments are based on the geotextile itself and do not consider seamed areas. The latter situation is difficult to consider and only recently has the deformation monitoring of seams been attempted (Guglielmetti et al. [115]).

Pullout or Anchorage.   With the mobilization of all, or part, of the geotextile reinforcement's strength comes an equal and opposite requirement that the soil behind the slip zone resist pullout. As shown in Figure 2.54(d), the situation is one in which an anchorage problem can be envisioned. Extending the work of Section 2.7.2, an equation can be formulated as follows:

$$T_{\text{act}} = 2\tau L$$

$$= 2(c_a + \sigma_v \tan \delta)L$$

and

$$L_{\text{reqd}} = \frac{T_{\text{act}}}{2(c_a + \sigma_v \tan \delta)} \tag{2.57}$$

or

$$L_{\text{reqd}} = \frac{T_{\text{act}}}{2E(c_a + \sigma_v \tan \phi)} \tag{2.58}$$

where

L_{reqd} = required anchorage length behind the slip plane,
T_{act} = actual stress in the geosynthetic,
c = cohesion of the soil,
c_a = adhesion of the soil to the geosynthetic,
ϕ = friction angle of the soil,
δ = friction angle of the soil to the geosynthetic,
σ_v = average vertical stress = γH, in which
γ = unit weight of embankment soil, and
H = average height of embankment above geosynthetic, and
E = anchorage, or pullout, efficiency of geosynthetic to soil.

For geotextiles, $E = 0.8–1.2$; for geogrids, $E = 1.3–1.5$. If insufficient anchorage distance is available to mobilize the required strength, physical methods of attachment—rolling of the material around stone or attachment to timber cribbing—is necessary.

Lateral Spreading. On occasion, tension cracks have been observed on the surface of embankments as shown schematically in Figure 2.54e. The situation of lateral spreading can be analyzed using the following equation for active earth pressure and considering granular soil fills to be above the geotextile.

$$P_a = \tau L$$
$$P_a = (\sigma_{v_{ave}} \tan \delta) L$$
$$0.5\gamma H^2 K_a = (0.5\gamma H \tan \delta) L$$
$$\tan \delta_{reqd} = (H K_a)/L \tag{2.59}$$

where

δ_{reqd} = required friction angle of geosynthetic-to-soil,
H = embankment height,
K_a = coefficient of active earth pressure = $\tan^2(45 - \phi/2)$, in which
ϕ = friction angle of embankment soil,
L = length of zone involved in spreading, and
$\tan \delta_{\text{reqd}}$ = $E(\tan \phi)$, in which
E = shear, or frictional, efficiency of geosynthetic-to-soil, for geotextiles, $E = 0.6–0.8$; for geogrids, $E = 1.0–1.5$.

Geotextile Implications.   The previous designs focus entirely on quantitative analyses and procedures that lead to the ultimate selection of the reinforcement geotextile. However, there are other considerations, many of which are qualitative, that must be brought into focus. These include the specific gravity and rigidity (or stiffness) of the geotextile, and the size and weight of rolls.

If the site under consideration is at, or under, the surface of water, buoyancy is usually not a desirable feature. Thus the geotextile should not float and its specific gravity must be greater than one. Rigidity, or stiffness, of the geotextile is desirable for providing some type of working platform for deployment. The ASTM stiffness test described in Section 2.3.2 can be used for specifications. The minimum value is related to the CBR of the foundation soil (recall Table 2.3). This is an important feature and an area where additional investigation is warranted. The size and weight of geotextile rolls must be considered by everyone involved in the process. It is obviously a site-specific situation, but one that is paramount in the success of the project. Designs that can not be reasonably constructed *should not* be designed to begin with.

Summary.   It is the author's perception that soft soil stabilization using geotextiles has been implemented from two different perspectives. The first is by the geotechnical engineer, who has modified traditional design methods to accommodate the inclusion of reinforcement; the second is by the manufacturer, who has provided a means of accomplishing an end. In this case, the means is a high-strength geotextile.

For designs and installations that are both economical and safe, the perspectives of engineer and manufacturer must be brought together. Beginning with the design elements illustrated in Figure 2.54, the stress-strain characteristics are progressively defined. The initial technical design is then modified by other site-specific considerations, the applicable yarns, and fabrication of the geotextile. The next, and very significant, question is whether the result is a balanced design. For example, where is the critical aspect of the design? If it is the field-sewn seams, then everything (warp, weft, modulus, elongation, etc.) should be formulated from this point. Last, there is the question of whether the resulting geotextile is constructible in light of the actual site situation. Here considerations of workability and survivability are very important.

In the final analysis, we should be able to arrive at a geotextile design that is both optimally safe and economical. It is indeed a very worthwhile pursuit, for finally the profession has a technique whereby we can almost walk on water.

2.7.4 Geotextiles for Improved Bearing Capacity and Basal Reinforcement

With the recognition that multiple layers and/or high-strength geotextiles can reinforce flexible walls, slopes, and foundations, it follows that soils beneath rigid walls, footings, piers, etc., having poor bearing capacity should also be a target for improved performance using geotextiles. The situation follows that of Binquet and Lee [116, 117] on the improved bearing capacity of compressible sands using metal strips (thereby creating mechanically stabilized earth). They found definite improvement, which was further evidenced by an economic analysis showing cost savings. However, when corrosion was

considered, the economic benefits were essentially lost. With noncorroding geotextiles as the reinforcement, the problem of corrosion is obviated. What remains is the research needed to quantify the possible improvements.

Laboratory studies by Guido et al. [118] using layers of geotextiles on a loose sand produce the results shown in Figure 2.56(a). Here it is seen that multiple (up to three) layers produced beneficial results, but only after a measurable settlement had occurred. This is to be expected, since the geotextile must deform before its reinforcing benefit is realized. Their tests used a nonwoven heat-bonded geotextile and varied a number of parameters, including distance to the upper geotextile, the spacing between layers, and the distance the geotextile extends beyond the edge of the footing.

Laboratory studies at the Geosynthetic Research Institute on soft compressible fine-grained soils at saturations above their plastic limit have produced the curves shown in Figure 2.56(b). Here, using a woven slit-film geotextile, similar behavioral trends are noticed; some improvement in bearing pressure is noted throughout, but only at large deformations is the improvement noteworthy. It can be seen that for both of the studies portrayed in Figure 2.56, a method of prestressing the geotextile would be an advantage so as to eliminate the required deformation before significant improvement is noted. How to do this in a cost-effective manner, however, is not known. In lieu of prestressing the geotextile, design must consider improved bearing capacity only after relatively large settlement. Also, the laboratory-generated curves shown must be utilized with considerable caution, since scale effects are essentially unknown.

(a) Nonwoven heat-bonded geotextile at 140 mm spacings on loose sand ($D = 50\%$) using 560 mm square footing. (After Guido et al. [118])

(b) Woven slit-film geotextile at 40 mm spacings on soft saturate clay silt using 150 mm round footing, (Geosynthetic Research Institute)
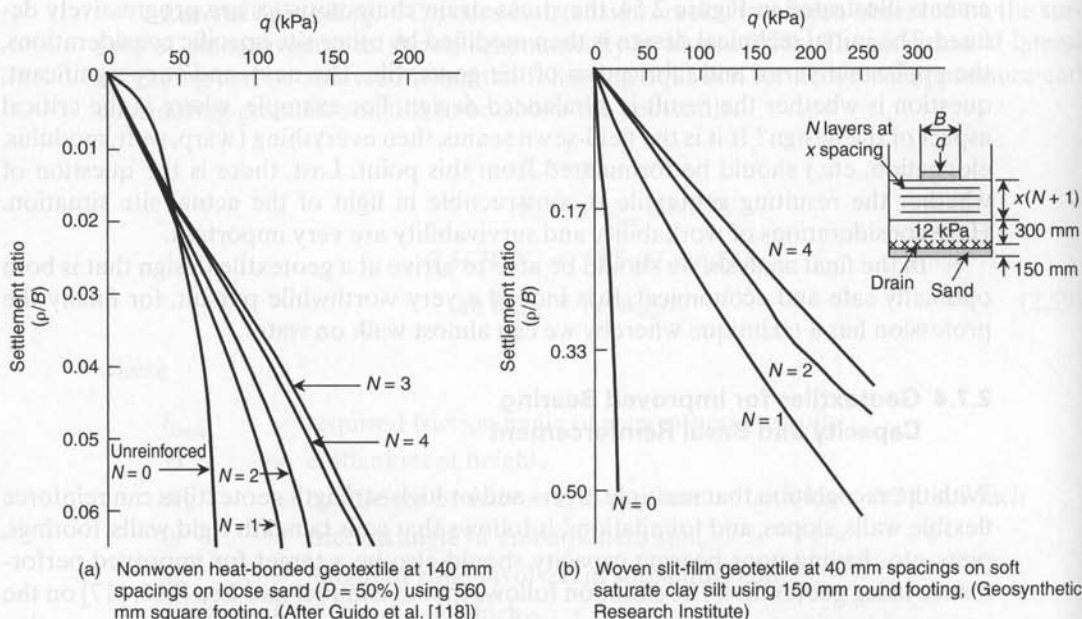
Figure 2.56 Laboratory-developed curves showing improvement in bearing capacity of soils using geotextiles; ρ is the footing settlement and B is the footing width.

In proceeding with a design, four modes of failure must be considered. They are shown schematically in Figure 2.57 and are explained below.

- *Bearing capacity failure above the upper geotextile*. This is probably avoidable if the upper geotextile is within 300 mm of the ground surface.
- *Anchorage pullout of geotextiles due to insufficient embedment length*. Anchorage pullout is avoidable if the geotextile extends far enough beyond the potential failure zone to mobilize the required resisting anchorage force. This is described in Sections 2.7.2 and 2.7.3.
- *Tensile failure breaking of geotextiles*. This is the main design element and uses information such as that presented in Figure 2.55.
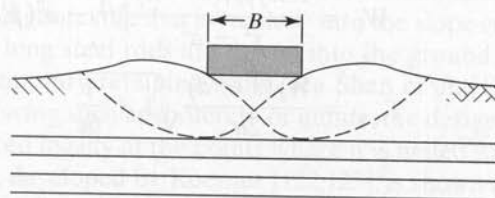
(a) Bearing capacity failure above upper geotextile layer
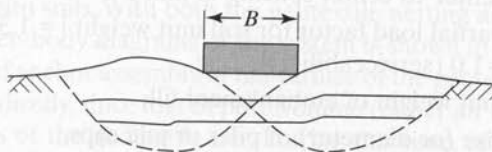
(b) Anchorage pullout of geotextiles due to insufficient embedment length
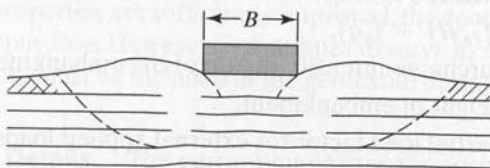
(c) Tensile failure (breaking) of geotextiles
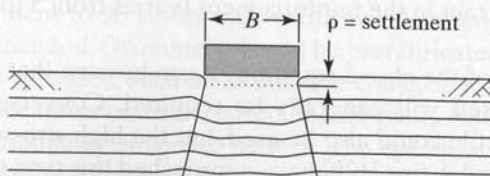
(d) Excessive long-term deformations (creep)

Figure 2.57   Possible modes of failure of geotextile-reinforced shallow foundations.

- *Excessive long-term deformations (creep)*. This is due to the sustained surface loads and subsequent geotextile stress relaxation, which can be avoided if low-enough allowable stresses in the geotextile are used. Allowable tensile strength values should be very conservatively chosen (see equation 2.24 and Table 2.11).

A variation on this theme is to use a high-strength geotextile (or geogrid) to span between pile caps, stone columns, or related deep foundation systems thus providing *basal reinforcement* between discrete supports. The reinforcement is considered as a tensioned membrane under an imposed soil loading which may, or may not, have arching considered. The application of support between deep foundations is nicely covered in the British Standard Code of Practice [119], which presents the following equations for load (W_T) and the required geosynthetic strength (T_{reqd}).

$$W_T = \frac{1.4 s f_{fs} \gamma (s - a)}{s^2 - a^2} [s^2 - a^2 (p_c'/\sigma_v')] \tag{2.60a}$$

$$T_{reqd} = \frac{W_T(s - a)}{2a} \sqrt{1 + \frac{1}{6\epsilon}} \tag{2.60b}$$

where

W_T	=	distributed load carried by the reinforcement,
s	=	center-to-center spacing of piles,
f_{fs}	=	partial load factor for soil unit weight [= 1.3 (ultimate), =1.0 (serviceability)],
γ	=	unit weight of embankment fill,
a	=	size (or diameter) of piles or pile caps,
p_c'	=	vertical stress on piles or pile caps,
σ_v'	=	factored average stress at base of embankment,
	=	$(f_{fs}\gamma H + f_q q)$,
q	=	surcharge intensity on top of the embankment,
H	=	height of embankment,
f_q	=	partial load factor for external applied loads, [= 1.3 (ultimate), =1.0 (serviceability)],
T_{reqd}	=	required tensile strength of the geosynthetic reinforcement
ϵ	=	strain in the reinforcement (varies from 5 to 10%)

In calculations of the above equations it can be seen that a very high-strength geotextile used by itself will generally be required. Conversely, several layers of lower-strength geotextile could also be used, but the high stresses on the lowest layer are of concern. Han and Akins [120] have approached this type of situation using a finite element model with interesting results. It is a fruitful topic of research covering a number of possible geotextile (and geogrid) application areas.

2.7.5 Geotextiles for In Situ Slope Stabilization

Background.   Thus far the methods described in this section are all oriented toward new construction, where the geotextiles are placed simultaneously with the earthwork involved. However, there are many situations in which existing soil slopes and embankments are at or near their failure state. Oftentimes homes or other structures are precariously close to the edge of the slope. Landslides cause losses of billions of dollars and, sometimes, lives as well. The usual indicators of slope instability are bulges of soil at the toe of the slope, springs near the toe of the slope, tension cracks along the soil slope or at the crest, and vegetative growth that is leaning toward the downstream toe. The basic problem in such cases is insufficient shear strength of the soil with respect to the slope angle and/or height of the embankment. This often suggests low relative density in granular soils and high water content in cohesive soils. Both of these situations could be positively influenced by some type of in situ stabilization system. The addition of a surface deployed geotextile that is "nailed" into the slope could provide such a system. In *soil nailing*, long steel rods are driven into the ground and then shotcreted or gunited to form temporary retaining walls (see Shen et al. [121]). Instead of using a rigid impermeable facing such as shotcrete or gunite, the designer could consider using a geotextile reinforced locally at the points where it is nailed to the soil slope.

Such a system, developed by Koerner [122,123], is shown in Figure 2.58. Here the anchored geotextiles (also called *anchored spider netting* since the surface appears quilted and tucked into the soil on regular patterns) are used in the compaction and/or consolidation of the in situ soils. With both the geotextile netting and the steel-rod nails in tension, the set of free-body diagrams of the system is shown in Figure 2.59. Figure 2.60 illustrates one type of anchor assembly at the surface of the geotextile. The system should be reanchored periodically, since loss of pore volume (either air or water) will result in a relaxed tensile stress of the geotextile net. During this time, of course, the soil itself is gaining in shear strength either by increased densification and/or by consolidation. This improvement in shear strength is precisely what is necessary to reinstate the slope's stability. Once the soil properties are sufficiently improved, the geotextile no longer serves a useful strengthening purpose. However, it continues to serve as an erosion control material; thus UV inhibitors must be included in the geotextile during its manufacture.

Construction Details.   The current guidelines for anchored geotextiles are as follows. Geotextiles of 35 kN/m wide-width tensile strength and opening size tight enough to prevent soil loss are being used. Local reinforcement of the geotextiles at anchor points equivalent to 90 kN/m wide-width tensile strength for 150 mm around the anchor is recommended. Grommets should be prefabricated into the geotextile unless an alternative is provided; such an alternative could be localized fabric reinforcement at the anchor locations or an oversized anchor plate. Anchor points should be at 1.5 m centers on a triangular or square pattern. The option of a prefabricated grid or net with localized reinforced zones has been used. Steel-rod anchors should be 13 mm in diameter or larger. Anchor lengths should exceed the potential failure plane by at least 1.5 m, which for base failures can mean rods of considerable length.

(a)

(b)

(c)
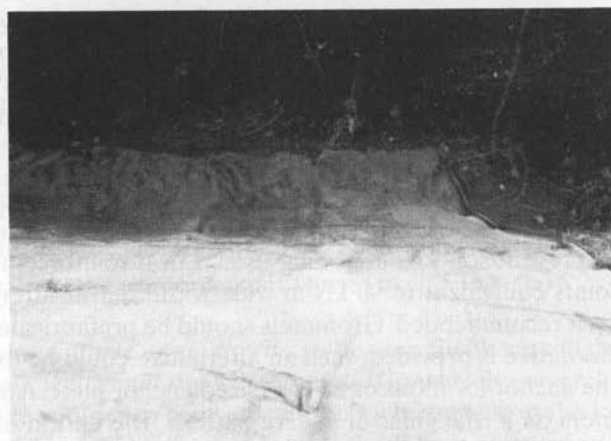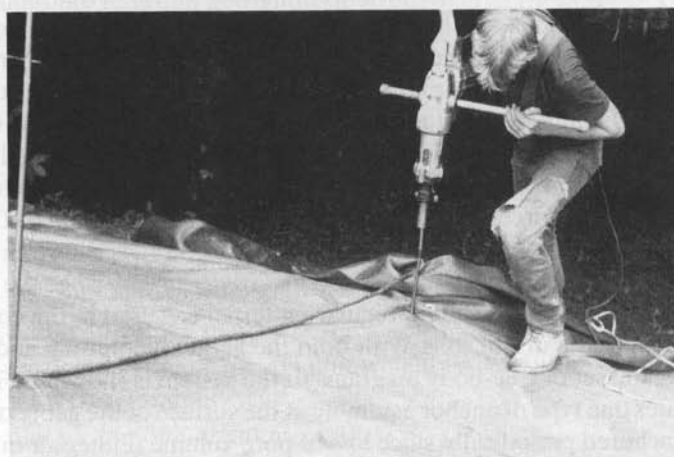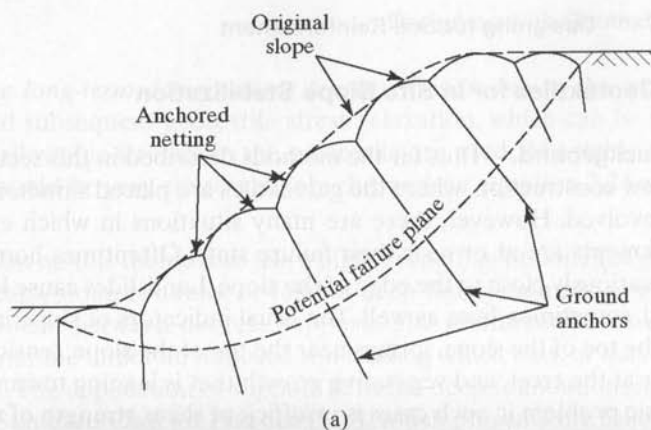
Figure 2.58 Cross section and photographs of in situ slope stabilization using anchored geotextiles. (After Koerner [122, 123])

Netting in tension

Free-body diagram of netting

Soil in compression

Free-body diagram of anchor

Free-body diagram of contained soil
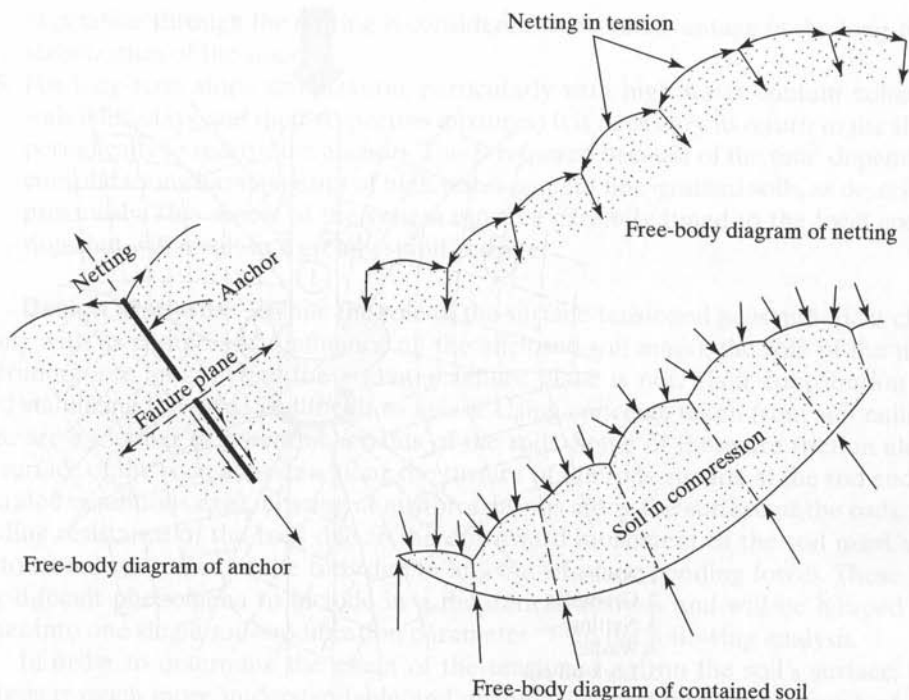
Figure 2.59 Free-body diagrams of various components of anchored geotextiles. (After Koerner [122, 123])

The following steps illustrate the usual manner of deploying anchored geotextile netting on a soil slope in need of stabilization. It should be mentioned that it is done without the aid of heavy construction machinery or equipment, which for working on quasi-stable slopes is a great advantage.

1. Rough-grade the slope so as to eliminate abrupt high spots and fill in holes and sharp depressions. This can usually be done by hand, depending on existing site conditions.

2. Unroll and spread the netting, with its prefabricated grommets or localized reinforced zones in place, on the slope from the upper levels downward and horizontally across it.

3. Under windy conditions, or if part of the slope is beneath water, it may be necessary to staple the netting to the soil. L-shaped nails or U-shaped pins are recommended. They should be approximately 300 mm long.

4. Beginning at the upper part of the slope, place steel anchor rods through the anchor holes and hand-drive them as far as possible. If threaded rod or pipe is being used, it will be necessary to have an adapter put over the threads so as not to damage them during driving. These rods should be driven to within 75 to 90% of their intended depth. In most cases it will be necessary to use an impact hammer, or other type of mechanized driving tool.
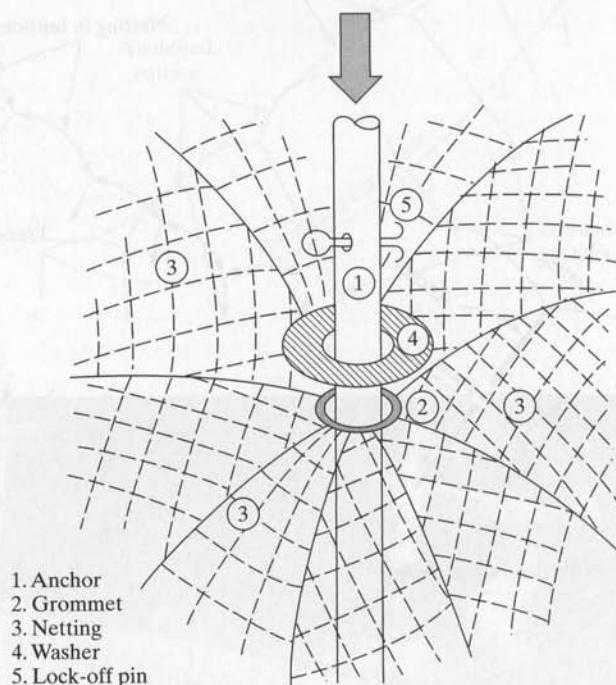
Figure 2.60 Sketch of anchor lock-off assembly at points where anchor passes through grommet in netting. (After Koerner [123])

1. Anchor
2. Grommet
3. Netting
4. Washer
5. Lock-off pin

5. When this depth is reached, fix the washer and lock-off assembly to the anchor.
6. Continue driving the anchor into the soil. At this time the netting is being pulled along with the anchor and it is being stressed (tensioned) in a radial manner.
7. Temporarily stop driving a short distance (approximately 5%) from the final design depth or refusal.
8. Repeat Steps 4 through 7 on each of the immediately adjacent anchors.
9. Return to the original anchor and drive it to design depth or refusal.
10. Continue in this manner down the slope and across it, progressing in a uniform manner.
11. As an alternative to Steps 4 through 10, it should be possible to explosively drive the anchors into the soil, carrying the net along with it. Myles and Bridle [124] have developed such a method for installing nails and anchors into soil.
12. At the end of each roll of netting, positive fixity by means of sewing or clamping of the geotextile netting—is required. At least 75% of the basic strength of the netting should be available at all roll edges.
13. The top, bottom, and extreme ends of the total stabilized slopes should end with anchors of the same type as the interior of the system.
14. Depending on site conditions, seed the slope either before or after placement of geotextile netting, although seeding before is generally preferred. Growth of

vegetation through the netting is considered to be an advantage in the long-term stabilization of the slope.

15. For long-term slope stabilization, particularly with high water content cohesive soils (silts, clays, and their respective mixtures) it is necessary to return to the slope periodically to redrive the anchors. This is required because of the time-dependent consolidation characteristics of high water content fine-grained soils, as described previously. This aspect of the system must be carefully tuned to the local conditions but will result in a greatly stabilized site.

Design Methods.   While the role of the surface-tensioned geosynthetic is clear (along with its compressive influence on the enclosed soil mass), the role of the nails protruding into and beyond the potential failure plane is not. Their contribution toward stabilizing the slope is difficult to assess. Using concepts taken from soil nailing, there are a number of potential benefits of the rods. Some of these are friction along the surface of the rods, adhesion along the surface of the rods, suction at the rod ends if saturated conditions exist, bearing at any protrusions along the surface of the rods, the bending resistance of the rods due to the downward movement of the soil mass, and the torsional resistance of the rods due to any out-of-plane bending forces. These are very difficult phenomena to include in a theoretical analysis and will be lumped together into one single soil-modification parameter "f" in the following analysis.

In order to determine the effect of the tensioned net on the soil's surface, the analysis is much more understandable and analytically tractable. The purpose of the tensioned net is clearly to place the encapsulated soil mass in compression. This will add normal forces to the slope, which will increase its stability by causing the soil to densify. For granular soils, this densification is rapid and takes the form of compaction where pore air or pore water is expelled. For saturated cohesive soils, this densification is slower and takes the form of consolidation where the pore water is expelled, but over a considerably longer time than when dealing with granular soil masses. In both cases, the need for a porous netting at the soil's surface is obvious. Use of an impervious geomembrane is not applicable for this method.

The time-dependent densification process just described will ultimately cause an increase in soil shear strength by means of an increase in friction and/or cohesion, thereby increasing the slope's stability. This densification (hence volume reduction) process will require redriving of the anchors to greater depths on a periodic basis. Eventually the increased shear strength parameters will allow for the slope to support itself without the need for the anchored spider netting at all.

To begin the analysis that follows, the modified Bishop method based on effective stresses is used [125]. Effective stress analyses are necessary since the slope soils are often wet and they invariably have a frictional component requiring use of the method of slices. Both moment and vertical force equilibrium are satisfied in the analysis, resulting in the following equations.

$$\overline{S}_i = (\overline{c}l_i + \overline{\sigma}l_i \tan\overline{\phi})/FS \qquad (2.61)$$

$$\overline{\sigma}l_i = (W_i - \mu_i l_i \cos\theta_i - \overline{S}_i \sin\theta_i) \sec\theta_i \qquad (2.62)$$

Solved simultaneously, equations (2.61) and (2.62) result in the following equation for the factor of safety:

$$\text{FS} = \sum_{i=1}^{n} \frac{\bar{c}l_i + (W_i - \mu_i l_i \cos\theta) \tan\bar{\phi} \sec\theta_i}{(W_i \sin\theta_i)\left(1 + \dfrac{\tan\bar{\phi} \tan\theta_i}{\text{FS}}\right)} \qquad (2.63)$$

Note in equation (2.63) that the factor of safety is not an explicit function and that an iterative solution is necessary. Added to the complexity of the equation is the necessity of summing each of the individual slices and finding the minimum factor of safety. Thus a computer solution is required.

With the addition of anchored spider netting on the surface of the slope, as shown in Figure 2.58, a number of features are added. Moment and force equilibrium after Koerner and Robbins [126] now yield the following equations:

$$\bar{S}_i = [(1 + f)(\bar{c}_m l_i + \bar{\sigma}l_i \tan\bar{\phi}_m)]/\text{FS} \qquad (2.64)$$

$$\bar{\sigma}l_i = (W_i + F_i \cos\beta_i - \mu l_i \cos\theta_i - \bar{S}_i \sin\theta_i) \sec\theta_i \qquad (2.65)$$

which when solved simultaneously result in equation (2.66) for the desired factor of safety:

$$\text{FS} = (1 + f) \sum_{i=1}^{n} \frac{\bar{c}_m l_i + (W_i + F_i \cos\beta_i - \mu_i l_i \cos\theta_i) \tan\bar{\phi}_m \sec\theta_i}{[W_i \sin\theta_i - (F_i d_i/R)]\left[1 + \dfrac{(1 + f) \tan\bar{\phi}_m \tan\theta_i}{\text{FS}}\right]} \qquad (2.66)$$

where

f = factor to account for soil anchors (nails)
$\bar{c}$ = effective cohesion,
$\bar{\phi}$ = effective angle of shearing resistance,
W_i = slice weight,
l_i = arc length of slice,
μ_i = pore water pressure in the slice,
θ_i = angle that the midpoint of the slice makes with the horizontal, and
n = number of slices, which is arbitrary.

If we now compare equation (2.63) to equation (2.66), the influence of the anchored spider netting can be seen. These features (all of which positively influence the factor of safety) are as follows:

where

$\bar{c}_m$ = modified effective cohesion (where $\bar{c}_m \geq \bar{c}$),
$\bar{\phi}_m$ = modified angle of shear resistance (where $\bar{\phi}_m \geq \bar{\phi}$),

$(1 + f)$ = contribution of the anchors (nails) penetrating the failure plane to stability,

$(F_i d_i / R)$ = moment due to the pressure of the stressed net at the ground surface, and

$(F_i \cos \beta_i)$ = contribution of the stressed net at the bottom of the slice (where the equilibrium equations are taken) to stability.

In order to investigate the numeric influence of these added terms to the slope's factor of safety, a computer-based sensitivity analysis has been performed [126]. The analysis uses a uniform slope of height 7.6 m, a slope angle of 55°, a soil unit weight 16.8 kN/m³, a cohesion of 9.5 kPa, and a friction angle of 20°. The factor of safety of the slope using equation (2.63) without anchored spider netting is 0.97.

Now using anchored spider netting on the slope and only the influence of the rods in equation (2.66), with $(1 + f)$ varying from 0 to 25%, the factor of safety increases, as shown in Figure 2.61a. Using only the influence of the surface loading term, $\Sigma(F_i/d_i)/R$, in equation (2.66), with the netting pressure σ varying from 0 to 2700 Pa, the factor of safety increases as shown in Figure 2.61b. Using only the influence of an
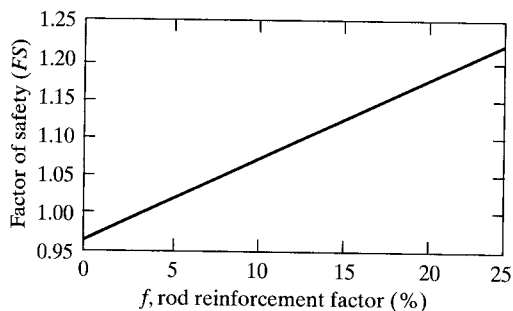
(a) Effect of rods on factor of safety
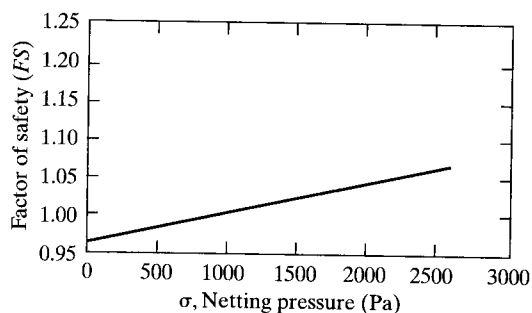
(b) Effect of $\Sigma(Fd)/R$ term on factor of safety
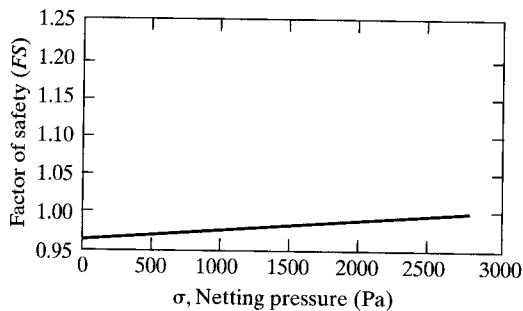
(c) Effect of $F(\cos \beta)$ term on factor of safety
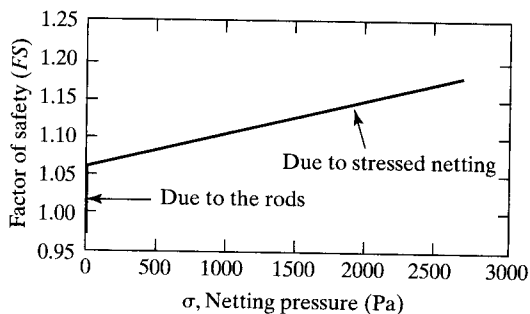
(d) Total effect of spider netting system on factor of safety with $f = 10\%$

Figure 2.61   Parametric study of factors influencing soil slope stability when using anchored spider netting. (After Koerner and Robins [126])

increased normal force at the base of the slice, $F_i \cos \beta_i$, in equation (2.66), with σ varying from 0 to 2700 Pa, the factor of safety increases as shown in Figure 2.61c. Finally, taking all of the short-term gains collectively in equation (2.66) gives Figure 2.61d. Here the increase in the global factor of safety of a slope due to a properly designed and constructed anchored spider net is quite obvious and, indeed, very beneficial. Note that the analysis could also be extended to account for long-term gains in the shear strength parameters $(\overline{c}_m)$ and $(\overline{\phi}_m)$. However, their influence is typical of strength gains in any slope-stability analysis. They are indeed significant and well understood by geotechnical engineers. The theoretical aspects of the anchored netting concept has been extended and modeled in large-scale laboratory tests (see Ghiassian et al. [127]). In a companion paper, Ghiassian et al. [128] have investigated the seepage considerations in the soil slope beneath the geosynthetic using a number of surface deformation patterns.

2.8 DESIGNING FOR FILTRATION

When liquid flows *across the plane* of the geotextile, the geotextile acts and is designed as a filter. Unfortunately, some literature including many highway specifications and numerous manufacturers brochures, identifies this topic incorrectly as drainage. Drainage, a distinct and separate topic, will be discussed in Section 2.9.

2.8.1 Overview of Applications

In Section 1.3.3 a number of applications were presented in which geotextiles are used adjacent to soil for the purpose of allowing liquid to pass through them while retaining the soil on the upstream side. Generally, the situations represent liquid moving in one direction only, but in some cases reversing flow was mentioned—for example, in tidal areas. Furthermore, the situations that will be discussed here all involve flow conditions designed on a worst-case scenario basis. This should come as no surprise, since it is the same type of conservatism that is used in all engineering design. Time-dependent random or dynamic flow situations will only be considered peripherally, because too little information is currently available for handling such situations. The factor of safety can always be increased to account for such considerations. Hopefully, the designs to follow cover most of the commonly encountered situations. The following specific designs will be discussed: geotextile filters behind retaining walls, geotextile filters wrapped around underdrains, geotextile filters used beneath erosion control systems, and geotextiles used as silt fences.

2.8.2 General Behavior

The general behavior of a filter simultaneously demands adequate permeability and proper soil retention. Permeability is required to allow the liquid to pass the filter so as not to build up excess hydrostatic pore pressure. At the same time, it is necessary to retain the majority of the upstream soil to avoid soil piping—the gradual loss of upstream soil fines, which results in higher flow rates, which in turn causes more soil loss, and so on. Thus we are asking for the design of an open geotextile structure that allows liquid to pass and, at the same time, a closed geotextile structure that retains the soil on the

upstream side of the geotextile. While these are indeed contradictory demands, such a geotextile filter design is possible because the amount of liquid flow through the soil is related primarily to particle size. For example, a commonly used empirical relationship between permeability coefficient and soil particle size is the following:

$$k = Cd_{10}^2 \qquad (2.67)$$

where

k = permeability coefficient (hydraulic conductivity) of the soil,

C = site specific constant, and

d_{10} = effective soil particle size (i.e., size at which 10% of the soil is finer).

Thus large particle-size soils can generate high-flow conditions (requiring geotextiles with relatively large voids), while small particle-size soils are associated with low-flow conditions (requiring geotextiles with relatively small voids). This results in a completely possible design situation, which is addressed in this section.

Before beginning with actual designs it must be repeated that long-term soil-to-geotextile compatibility is also a necessary requirement. This third aspect of the design was treated in Section 2.2.3, and the particular details will not be repeated here.

2.8.3 Geotextiles Behind Retaining Walls

Behind conventional reinforced concrete retaining walls there must be a vertical drainage layer, typically consisting of granular soil that serves as a flow path allowing water from the backfill soil to escape into an underdrain system (Figure 2.62a), or through weep holes (Figure 2.62b). Without this drainage layer, hydrostatic pressures will build up and together with the horizontal soil pressure, could easily cause failure. Such hydrostatic pressures, if not dissipated by adequate drainage, can double the pressure against the wall. Also, the drainage sand must stay free-draining for the lifetime of the wall. If it excessively clogs from the retained backfill soil within this time span, the sand becomes as useless as if it were not there at all. Thus it must be protected by a soil filter (which is expensive and difficult to place) or by a geotextile filter.

An identical situation, as far as the geotextile is concerned, is in the construction of flexible wall systems that are free-draining in themselves but would, without a soil filter or geotextile filter, allow the backfill soil to move into and through the open spaces. Such walls are illustrated in Figure 2.62c and d in which the gabion style consists of wire baskets filled with 100 mm and larger stones. To backfill against such walls with no filter media (soil or geotextile) would be completely unacceptable. Since the soil filter option is difficult to place in a vertical or near-vertical manner and may even require a series of graded filter soils, the geotextile filter becomes very attractive. Geotextile filter design is illustrated in the example that follows.

Example 2.22

Given a 3.5 m high gabion wall consisting of three $1 \times 1 \times 3$ m long baskets sitting on $0.5 \times 2 \times 3$ m long mattresses, as shown in the diagram below, the backfill soil is a medium-dense silty sand of $d_{10} = 0.03$ mm, $CU = 2.5$, $k = 0.0075$ m/s, and $D_R = 70\%$. Check the

(a) Rigid retaining wall with underdrains

(b) Rigid retaining wall with weep holes

(c) Temporary retaining wall with open sheeting

(d) Flexible retaining wall made from gabions
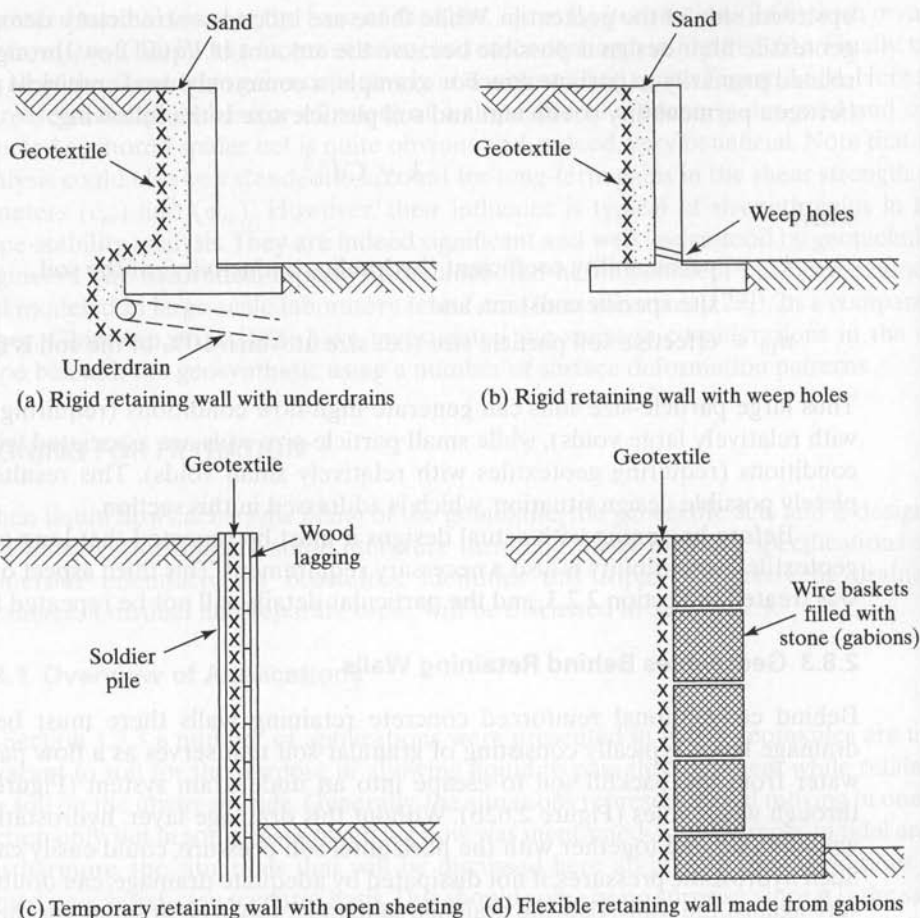
Figure 2.62 Various types of retaining walls in which geotextiles have been used as filters.

adequacy of three candidate geotextiles whose laboratory test properties are given in the table below. Use a cumulative reduction factor in equation (2.25b) of 15.0, in order to adjust the ultimate laboratory-obtained permittivity value to an allowable field-oriented value.

No.	Geotextile Type	Permittivity (sec^{-1})	AOS* (mm)
1	Nonwoven needle punched	2.0	0.30
2	Woven monofilament	1.2	0.42
3	Nonwoven heat bonded	0.4	0.21

*Note that if the AOS is given in sieve size number, it must be converted to O_{95} in mm using Table 2.6.

Solution:
The design is in two stages: (1) a determination of the flow factor of safety of the geotextile and (2) a consideration of opening size.

1. The first part of the design is done by calculating the required permittivity, ψ.
   - Calculate the actual flow rate using a flow net as shown.
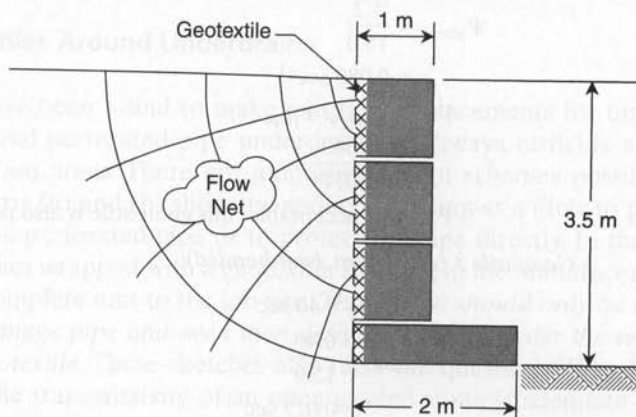
$$q = kh\left(\frac{F}{N}\right)$$

$$= (0.0075)(3.5)\left(\frac{4}{5}\right)$$

$$q = 0.021 \text{ m}^2/\text{sec}$$

   - Calculate the required permittivity.

$$q = kiA$$

$$q = k\frac{\Delta h}{t}A$$

$$\frac{k}{t} = \frac{q}{(\Delta h)(A)}$$

$$\Psi_{\text{reqd}} = \frac{0.021}{(3.5)(3.5 \times 1)}$$

$$= 1.71 \times 10^{-3} \text{ sec}^{-1}$$

   - Check against the allowable permittivity of the candidate geotextiles.
     Geotextile 1 (nonwoven, needle-punched):

$$\Psi_{\text{ult}} = 2.0 \text{ sec}^{-1}$$

$$\Psi_{\text{allow}} = \Psi_{\text{ult}}\left(\frac{1}{RF_{SCB} \times RF_{CR} \times RF_{IN} \times RF_{CC} \times RF_{BC}}\right)$$

$$= \frac{2.0}{15.0}$$

$$= 0.13 \text{ sec}^{-1}$$

$$FS = \Psi_{\text{allow}}/\Psi_{\text{reqd}}$$

$$= \frac{0.13}{0.00171}$$

FS = 76 acceptable; the geotextile has a high factor of safety

Geotextile 2 (woven, monofilament):

$$\Psi_{ult} = 1.2 \text{ sec}^{-1}$$

$$\Psi_{allow} = \frac{1.2}{15.0}$$

$$= 0.080 \text{ sec}^{-1}$$

$$FS = \Psi_{allow}/\Psi_{reqd}$$

$$= \frac{0.080}{0.00171}$$

FS = 47 acceptable; this geotextile is also permeable enough

Geotextile 3 (nonwoven, heat-bonded):

$$\Psi_{ult} = 0.40 \text{ sec}^{-1}$$

$$\Psi_{allow} = \frac{0.40}{15.0}$$

$$= 0.027 \text{ sec}^{-1}$$

$$FS = \Psi_{allow}/\Psi_{reqd}$$

$$= \frac{0.027}{0.00171}$$

FS = 16 acceptable; this geotextile is also adequate

The above shows that many commercially available geotextiles can easily handle the required flow.

2. The second part of the design relates to the geotextile's opening size, which prevents excessive soil loss. The three candidate geotextiles have AOS values of 0.30, 0.42, and 0.21 mm, respectively.

   • The appropriate criterion for opening size must first be selected. Since this is a noncritical situation, Carroll's criterion (recall Section 2.2.3) will be used. This is as follows:

$$O_{95} < 2.5 \, d_{85}$$

   Since $d_{10} = 0.03$ mm and $CU = 2.5$, an approximate value of $d_{85} = 0.15$ mm, which results in:

$$O_{95} < 2.5(0.15)$$

$$< 0.375 \text{ mm}$$

   • Check against the candidate geotextiles' AOS values:

   Geotextile 1: AOS = 0.30 mm < 0.375 mm, acceptable with FS = 1.25
   Geotextile 2: AOS = 0.42 mm > 0.375 mm, not acceptable with FS = 0.89
   Geotextile 3: AOS = 0.21 mm < 0.375 mm, acceptable with FS = 1.79

Thus geotextile 2 is too open and will experience excessive soil loss based upon this soil-retention criterion. (If such a woven monofilament style were used, it would have

to have a tighter AOS value, which is possible since the permittivity factor of safety was 47, a very high FS.) Candidate geotextiles 1 and 3 are both acceptable. The technical decision as to which of these geotextiles to use will be based on the site-specific concern as to which mechanism (permittivity or soil retention) is more important. The nontechnical, but important, final decision is based on cost and availability.

2.8.4 Geotextiles Around Underdrains

Geotextiles have been found to make excellent replacements for uniform or graded soil filters around perforated pipe underdrains. Highways, airfields, and railroads are major application areas. There are numerous design schemes possible, as shown in Figure 2.63. Parts (a) and (b) show the geotextile acting as a filter to protect the stone surrounding the perforated pipe or to protect the pipe directly. In the latter case, the pipe is sometimes wrapped with a geotextile stocking in the manufacturing plant and is shipped as a complete unit to the job site. *This design should only be used with slotted corrugated drainage pipe and even then design should consider the reduced flow area through the geotextile.* These sketches also raise the question: "Why have the pipe at all?" Indeed, the transmissivity of an open-graded stone is adequate to handle many flow situations, as long as its long-term protection against fine soil contamination is ensured. The point is precisely why the geotextile is involved. By wrapping the stone as shown in Figure 2.63c and 2.63d, no pipe at all is required. This is the design for a

(a) Conventional pipe underdrain with geotextile around stone

(b) Geotextile wrapped pipe underdrain with sand backfill (generally not recommended)

(c) Geotextile wrapped stone (no pipe) retangular section

(d) Geotextile wrapped stone (no pipe) trapezoidal section
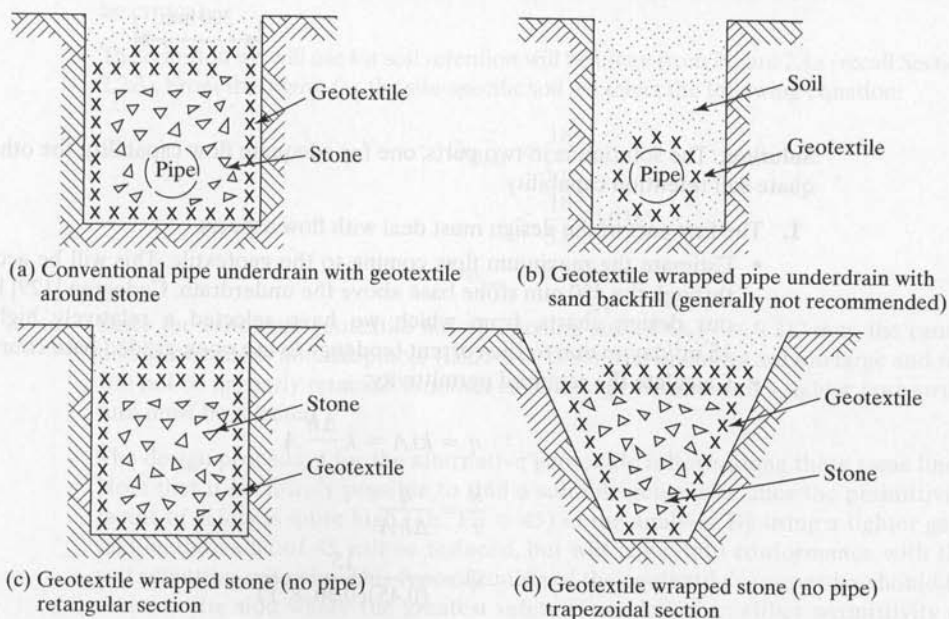
Figure 2.63   Typical cross sections of underdrain systems with and without perforated pipes.

French drain system, but unlike those in the past, one that will remain free from fine soil contamination if the geotextile is properly designed.

Example 2.23

Design the geotextile filter surrounding an open-graded stone aggregate that in turn surrounds a perforated pipe underdrain, as shown in the diagram below. Flow will enter through the stone base from the upper part of the underdrain, while soil infiltration will come from the surrounding native soil. This soil is a dense sandy silt (ML) with the relevant properties of 15% nonplastic fines with $C_c = 2.0$, $C_U = 5.0$, $I_D = 80\%$, $d_{50} = 0.035$ mm and $k = 1 \times 10^{-5}$ m/sec. The geotextile being considered is nonwoven needle-punched with laboratory tested values of $\psi = 1.5$ sec^{-1} and AOS = 0.212 mm.
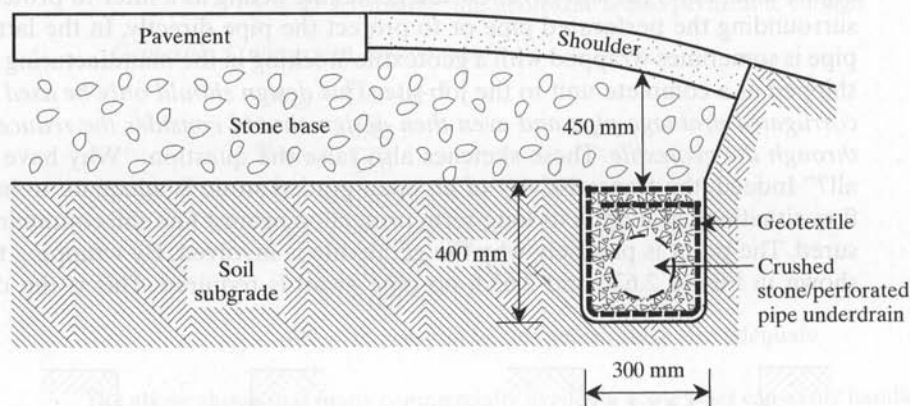
Solution: The solution is in two parts, one for adequate flow capability, the other for adequate soil retention capability.

1. The first part of the design must deal with flow aspects.
   - Estimate the maximum flow coming to the geotextile. This will be accomplished through the 450 mm stone base above the underdrain. Cedegren [129] has numerous design charts, from which we have selected a relatively high value of 15 m^3/day-m due to the current tendency to use open-graded base courses.
   - Calculate the required permittivity:

$$q = kiA = k\frac{\Delta h}{t}A$$

$$\frac{k}{t} = \frac{q}{\Delta hA}$$

$$\psi = \frac{15}{(0.45)(0.30 \times 1)}$$

$$\psi = 111 \text{ day}^{-1} = 1.3 \times 10^{-3} \text{ sec}^{-1}$$

• Check this required permittivity against the allowable permittivity of the geotextile. Using data from Table 2.12 substituted into equation (2.25a) gives the allowable permittivity (the values of reduction factors were estimated):

$$\psi_{allow} = \psi_{ult} \left[\frac{1}{RF_{SCB} \times RF_{CR} \times RF_{IN} \times RF_{CC} \times RF_{BC}} \right]$$

$$= 1.5 \left[\frac{1}{7.0 \times 1.2 \times 1.1 \times 1.4 \times 2.0} \right]$$

$$= 1.5 \left[\frac{1}{25.9} \right]$$

$$= 0.058 \ \text{sec}^{-1}$$

$$FS_{flow} = \psi_{allow}/\psi_{reqd}$$

$$= \frac{0.058}{0.0013}$$

$$FS_{flow} = 45 \ \text{acceptable}$$

2. The second part of the design has to do with soil retention of all of the soils surrounding the geotextile-enclosed drainage stone. Since the stone base course above the geotextile is of no real concern, the finer soil subgrade adjacent to the geotextile and beneath it becomes the focus of attention. Another consideration is that siltation of the perforated pipe within the enclosure is a possibility and therefore that the drainage stone must not become contaminated. This situation is considered to be critical.

The criterion we will use for soil retention will be taken from Figure 2.4a (recall Section 2.2.3). From this figure for the site-specific soil we select the following equation:

$$O_{95_{reqd}} < \frac{18}{C_U} d_{50}$$

$$< \frac{18}{5.0} (0.035)$$

$$O_{95_{reqd}} < 0.126 \ \text{mm}$$

Since the candidate geotextile has an opening size of $O_{95_{act}} = 0.212$ mm, the candidate geotextile is not acceptable (i.e., FS = 0.59). The openings are too large and soil will not be properly retained. Another candidate geotextile with a tighter pore structure must be selected.

The design procedure for the alternative geotextile follows along these same lines. Note that it is entirely possible to find a suitable geotextile since the permittivity factor of safety is quite high (i.e., FS = 45) in the analysis. By using a tighter geotextile, the value of 45 will be reduced, but will come into conformance with the soil retention criterion. This type of tuning of the geotextile's properties should be done on the side where the greatest safety is needed—i.e., either permittivity or soil retention.

2.8.5 Geotextiles Beneath Erosion-Control Structures

Geotextiles have been used beneath erosion-control structures since the late 1950s. Section 1.3.1 mentions some of the original applications. In these applications, both rock riprap and precast concrete blocks or mattresses were placed on the geotextile, and the geotextile was referred to as a *filter fabric*. In today's designs, depending primarily on the care exercised by the contractor in placing riprap, a sand cushion may be needed to protect the geotextile from impact damage during installation or abrasion damage during its lifetime (e.g., due to wave action agitating the rock riprap). If precast concrete blocks or mattresses are being used, a sand layer can still be used, not so much as a cushion, but as a pore water dissipater, since a major part of the geotextile will be directly covered by the blocks. This feature will be illustrated in Example 2.24. In Figure 2.64, part (a) shows a geotextile filter in place with riprap armor above it; part (b) shows the newer concept of a prefabricated concrete block mattress; part (c) shows precast concrete paving blocks that cover essentially all of the underlying geotextile; part (d) shows the failure that results by not allowing for dissipation of pore water from the underlying soil subgrade.

Example 2.24

Evaluate the filtration adequacy of a candidate geotextile for placement beneath a rock riprap erosion control system in a coastal inlet area with 1 m tides (i.e., reversing flow conditions with mild water currents) as shown in the diagram below. The candidate geotextile laboratory properties are $\psi = 0.5 \ \text{sec}^{-1}$ and AOS = 0.21 mm. The in situ soil is a beach sand (SP) with $C_u = 3.5$, $d_{50} = 0.10$ mm, $d_{90} = 0.40$ mm and porosity = 0.40.
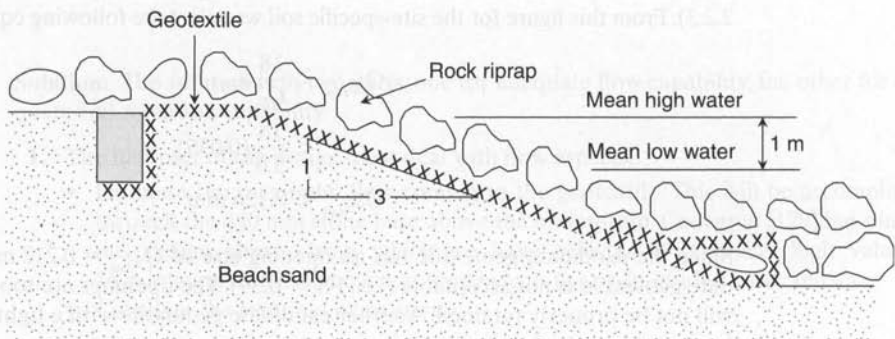
Solution: As with all filtration designs, this requires a two-part solution, one for adequate flow and the other for soil retention.

   1. For adequate flow, the procedure is as follows.

     • Estimate the maximum flow rate due to the 1 m tidal lag, assuming the water profile shown in the diagram that follows on page 256.

(a) Partial coverage by riprap
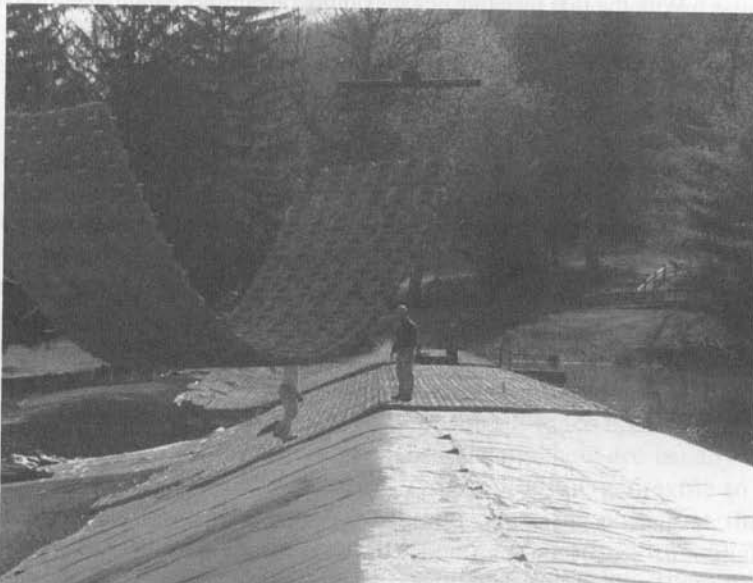
(b) Partial coverage by concrete block mattress
(Compliments of InterGeo Company)

(c) Complete coverage by paving blocks

(d) Problem with complete coverage

Figure 2.64 Geotextiles being used as filters beneath erosion-control structures.
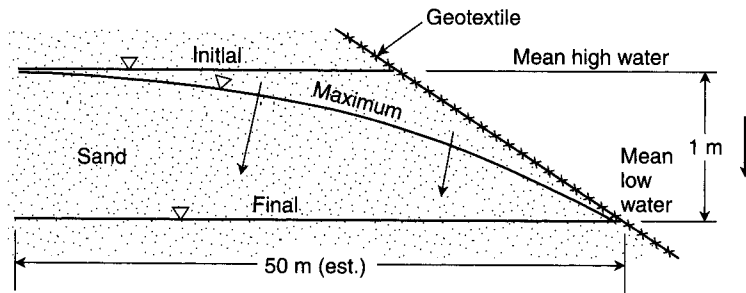
With the tide receding at a maximum rate during an initial period of 2 hr as shown, then

$$q_{max} = \frac{50 \times 1 \times 1}{2} \times \frac{0.4}{2}$$

$$= 5.0 \text{ m}^2/\text{hr}$$

$$q_{max} = 1.39 \times 10^{-3} \text{ m}^2/\text{sec}$$

- Calculate the required permittivity.

$$q = kiA = k\frac{\Delta h}{t} A$$

$$\frac{k}{t} = \frac{q}{\Delta h A}$$

$$= \frac{0.00139}{(1.0)(3.16)}$$

$$\Psi_{reqd} = 0.00044 \text{ sec}^{-1}$$

- Since the candidate geotextile has a laboratory obtained ultimate permittivity of 0.5 sec^{-1}, it must be modified with reduction factors for site-specific conditions.
- The allowable permittivity is found in equation (2.25a) and the values in Table 2.12, where the reduction factor for blinding is used as its maximum value of 10.0 since the rock riprap will cover a large portion of the geotextile's surface area.

$$\Psi_{allow} = \Psi_{ult}\left(\frac{1}{RF_{SCB} \times RF_{CR} \times RF_{IN} \times RF_{CC} \times RF_{BC}}\right)$$

$$= 0.50\left[\frac{1}{10.0 \times 1.2 \times 1.2 \times 2.5 \times 3.0}\right]$$

$$= 0.50\left[\frac{1}{108}\right]$$

$$= 0.0046 \text{ sec}^{-1}$$

- The factor of safety is then

$$FS = \frac{\Psi_{allow}}{\Psi_{reqd}} = \frac{0.0046}{0.00044}$$

$$FS = 10 \text{ acceptable}$$

2. The geotextile is now evaluated with respect to its adequacy to retain the soil beneath it.
   - Since these ocean-control structures are destroyed when the contained soil passes through the geotextile voids (resulting in subsidence and loss of stability of the riprap) and the flow regime is pulsating and cyclic, we will use Figure 2.4(b), which results in the following criterion:

$$d_{50} < O_{95} < d_{90} \qquad \text{or} \qquad d_{50} < AOS < d_{90}$$

   - Check this against the AOS of the candidate geotextile, which is 0.21 mm.

$$0.10 \text{ mm} < 0.21 \text{ mm} < 0.40 \text{ mm, which is acceptable.}$$

   Since 0.21 mm is within the proper bounds, excessive soil loss will not occur and the geotextile is proper as far as soil retention is concerned. The filtration design is essentially complete with the candidate geotextile's flow and retention properties both being adequate.
   - Another part of the design, however, is to see that the geotextile has adequate strength properties to withstand the impact of falling riprap and/or puncture from equipment moving on the surface of the riprap. These strength-related design issues were described in Section 2.5.

2.8.6 Geotextile Silt Fences

Silt fences consist of above-ground textiles attached vertically onto posts to prevent sediment-carrying sheet runoff from entering into downstream creeks, rivers, or sewer systems. Since all construction activities must have an associated sedimentation and erosion control plan, this concept is used regularly and has replaced bales of straw, hay, and other makeshift methods. The bottom of the silt fence is embedded in a small anchor trench; the posts, to which the geotextile is attached, are usually at 1.5 to 3.0 m spacings. Sometimes a geogrid backup is required on the geotextile to provide additional support; in this case, the geogrid is attached to the posts first, then to the geotextile, both facing upslope. Since the geotextile is exposed to sunlight, it must be UV-stabilized. Figure 2.65 illustrates three typical installations, showing a silt fence (a) as placed, (b) working as designed and intended, and (c) improperly constructed without an adequate anchor trench and being undermined.

The physical model utilized in the original development was developed by Bell and Hicks [130] and has sediment-carrying runoff water depositing soil particles within and on the surface of the geotextile as it first acts as a true filter, then eventually clogs with soil particles in its lower part so that water can no longer pass freely through it. The impoundment created by this action causes coarse sediment to settle behind the clogged portion of the silt fence and the water carrying finer particles to try to reach higher levels on the silt fence above the clogged region. With time, an equilibrium situation such as the one shown in Figure 2.66 is established.

Richardson and Middlebrooks [131] provide a design method based upon the required site-specific storage volume to be contained by the silt fence. The method assumes that the ground surface is smooth and bare, with sheet erosion (versus rill or gully erosion) being the predominant erosion mechanism. The recommended procedure, albeit somewhat modified here, follows a sequential series of calculations.

(a) Cascading silt fences after installation

(b) Properly functioning silt fence

(c) Silt fence that has been undercut by erosion

Figure 2.65   Geotextile silt fences and examples of field performance.
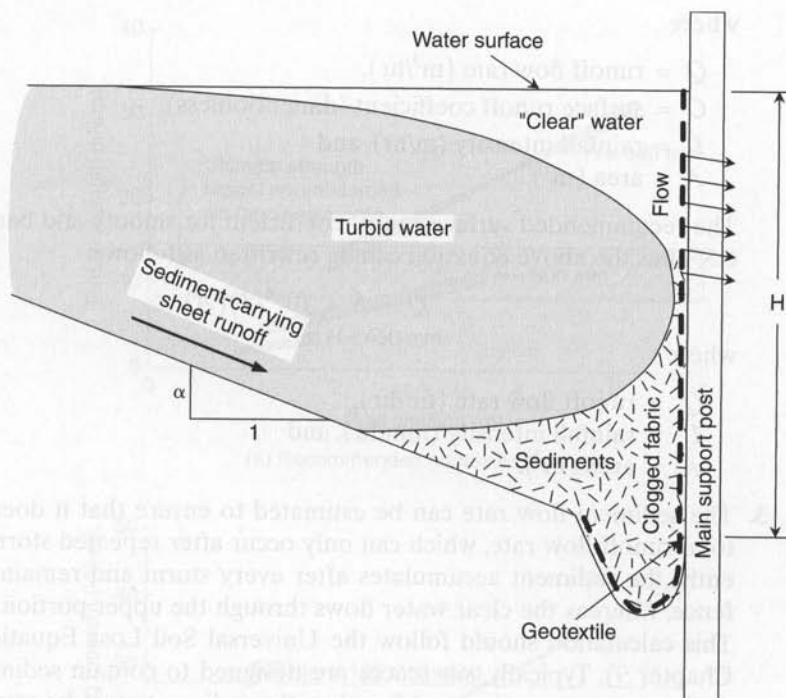
Figure 2.66   Cross section of geotextile silt fence and suggested manner in which system functions.

1. The maximum slope length that can be contained by a single silt fence is obtained from the following equation for a given slope angle under the above assumed conditions:

$$L_{max} = 36.2e^{-11.1\alpha} \qquad (2.68)$$

where

L_{max} = slope length (m), and

α = slope inclination as measured by its steepness, i.e., vertical rise to horizontal length (dimensionless)

For greater slope lengths than indicated from equation (2.68), a set of cascading silt fences must be used, each of which is individually designed.

2. The runoff flow rate (water plus sediment) is calculated using the site-specific value of rainfall intensity. This is somewhat subjective and may be controlled by local regulations. Using the hourly rainfall based on a 10-year recurrence interval the runoff is recommended:

$$Q = CIA \qquad (2.69a)$$

where

Q = runoff flow rate (m^3/hr),
C = surface runoff coefficient (dimensionless),
I = rainfall intensity (m/hr), and
A = area (m^2).

The recommended surface runoff coefficient for smooth and bare soil surfaces is 0.5. Thus the above equation can be rewritten as follows:

$$Q = 5 \times 10^{-4}(I)(A) \tag{2.69b}$$

where

Q = runoff flow rate (m^3/hr),
I = rainfall intensity (mm/hr), and
A = area (m^2).

3. The sediment flow rate can be estimated to ensure that it does not exceed the total runoff flow rate, which can only occur after repeated storms. Stated differently, the sediment accumulates after every storm and remains behind the silt fence, whereas the clear water flows through the upper portion of the silt fence. This calculation should follow the Universal Soil Loss Equation (described in Chapter 9). Typically, silt fences are designed to contain sediments for at least three major storm events. After that, the sediment must be removed and/or the silt fence replaced.

4. The height of the silt fence is then determined using the value of Q obtained previously on the basis of single-event storm intensity. A factor is then applied that represents the number of recurring storm events (i.e., a FS = 3 represents three similar storms). Thus

$$V = Qt = H\left(\frac{H}{\alpha}\right)$$

$$H = [(Q)(t)(\alpha)]^{1/2} \tag{2.70}$$

where

V = total runoff volume (m^3),
Q = runoff flow rate (m^3/hour),
t = storm duration (hr), assumed to be 1.0 hr based on the value of I selected in the calculation of Q,
H = silt fence height to contain a single storm (m), and
α = slope inclination (vertical-to-horizontal ratio).

5. The spacing of the silt fence posts is then arbitrarily selected and is integrated into the design per the next two steps.

6. The geotextile is selected on the basis of its ultimate wide-width tensile strength in the weakest direction. Figure 2.67(a) can be used for this determination. A reduction factor can be included. Note that the opening size of the geotextile is not a governing criterion since excessive clogging via turbidity is the issue and with
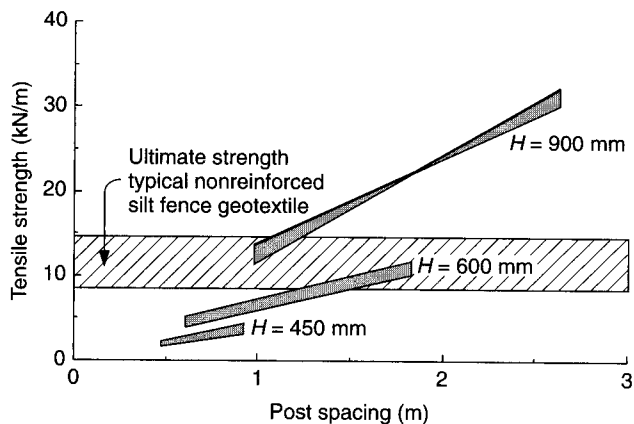
(a) Recommended geotextile strength
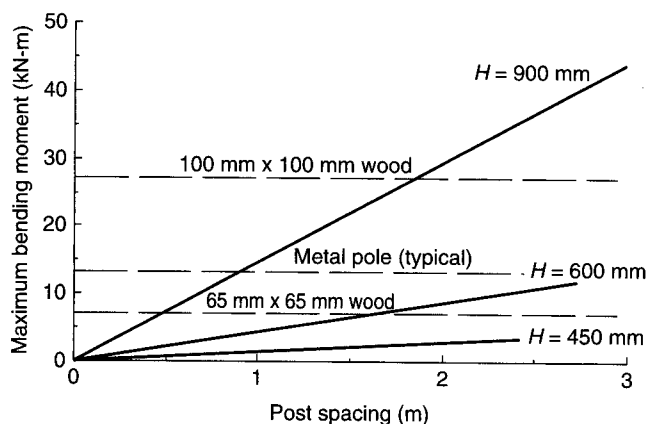
(b) Recommended post strength

Figure 2.67   Design recommendations for silt fence geotextile and post strengths. (After Richardson and Middlebrooks [131])

individual soil particle sediment, this will occur. Thus woven slit-film geotextiles predominate in this particular application; they are rapidly clogged, yet possess high tensile strength.

7. The type of fence post is selected. This can be done using the guide given in Figure 2.67(b).

Example 2.25

Design a silt fence for a 60 m long relatively smooth surface construction site where top-soil has been stripped and the average slope inclination is 5%. The 10-year recurring single-storm intensity is 100 mm/hr.

Solution: Using the procedure just described, the problem is solved in successive steps.

1. Calculate the maximum slope length per silt fence:

$$L_{max} = 36.2e^{-11.1\alpha}$$
$$= 36.2e^{-11.1(0.05)}$$
$$L_{max} = 21 \text{ m; use 20 m as the maximum slope length}$$

Therefore, three cascading silt fences will be needed for this construction site.

2. Calculate the runoff flow rate:

$$Q = 5 \times 10^{-4}(I)(A)$$
$$= 5 \times 10^{-4}(100)(20 \times 1)$$
$$Q = 1.0 \text{ m}^3/\text{hour}$$

3. Either calculate the sediment flow rate, or make an assumption about the number of storm events that the silt fence must contain. Here, we select

$$\text{number} = 3 \text{ events}$$

This establishes the factor that will be used on the calculated height of the silt fence.

4. Calculate the height of the silt fence:

$$H = [(Q)(t)(\alpha)]^{1/2}$$
$$= [(1.0)(1.0)(0.05)]^{1/2}$$
$$= 0.22 \text{ m}$$

For three storms, the total height is

$$3 \times H = 3 \times 0.22$$
$$= 0.66 \text{ m}$$
$$H = 660 \text{ mm}$$

5. The spacing of the silt fence posts is selected to be

$$S = 1.5 \text{ m}$$

6. The required strength of the geotextile is now taken from Figure 2.67(a)

$$T_{reqd} = 10 \text{ kN/m},$$

which is adequate without geogrid backup support. This can be increased for damage due to stapling/attachment to the fence post if so desired.

$$T_{ult} = FS(T_{reqd})$$
$$= 1.2(10)$$
$$T_{ult} = 12 \text{ kN/m}$$

7. Select, the type of post from Figure 2.67(b) to end the design procedure.

Use 65 mm $\times$ 65 mm wooden posts.

2.8.7 Summary

This section presented a series of designs in which geotextiles are serving in the filtration function. In such cases the liquid (often water) is moving across the plane of the geotextile. Thus, the designs allow for a required flow capacity that is expressed in terms of permittivity (ψ), a term that includes both the permeability coefficient and the geotextile's thickness. However, more than just required flow capability is necessary; soil retention is also necessary. Since these two demands are contradictory (flow requiring large geotextile voids and adequate soil retention requiring small geotextile voids), problems illustrating the criticality of each demand were presented.

The fine soils used behind flexible walls (Section 2.8.3) and adjacent to underdrains (Section 2.8.4) showed that adequate permittivity is easily achieved, yet small opening-size values are required. This means that the fibers or yarns had to be close to one another, resulting in a relatively tight or dense geotextile structure.

Conversely, the illustration of geotextiles beneath erosion-control structures (Section 2.8.5) usually occurs with free-draining sands. Thus the permittivity of the geotextile is challenged by a lower factor of safety, whereas the opening-size requirement is easily met. Note that if the erosion-control system lies directly on the geotextile and covers a high percentage of it (as with precast-concrete blocks directly on the geotextile), the permittivity design always becomes critical. In this case, the percentage of covered geotextile (sometimes as high as 70%) is included via a high reduction factor—i.e., $RF_{SCB} = 10$. A simple proportional factor is appropriate, since flow rate should be a linear function of area remaining open to flow.

In all of these problems the long-term compatibility of the soil to the geotextile should be considered. In most cases the designs illustrated should suffice; however, when the situation is critical, laboratory flow tests described in Section 2.3.5 should be considered.

Finally, the geotextile silt fence of Section 2.8.6 was considered. This design simply begs for excessive clogging of the geotextile, which must happen so that the sedimentation reservoir can form behind it. The design then becomes a structural design of the strength of the geotextile, and its supporting post spacings and type. It was discussed in this section because the geotextile above the clogged area is indeed still serving as a true filter.

2.9 DESIGNING FOR DRAINAGE

In this book, drainage refers to planar flow within the structure of the geosynthetic. Geotextiles acting as drains will be considered in this section; geonets and drainage geocomposites will be discussed in Chapters 4 and 9, respectively.

2.9.1 Overview of Applications

Although closely related to the filtration function just described, geotextile drainage occurs in the in-plane rather than cross-plane direction. The transitive verb *to drain*,

according to *Webster's New Collegiate Dictionary*, means "to draw off (liquid) gradually ... ," and it is to precisely this action, as it is performed by geotextiles, that this section is devoted. Note that all geotextiles are capable of draining liquid in their in-plane directions, but to widely varying degrees. In order of *increasing* in-plane drainage capability, the various manufactured styles are ranked as follows:

- Woven slit-film
- Woven monofilament
- Nonwoven heat-bonded
- Nonwoven resin-bonded—increasing with increasing weight and decreasing resin
- Nonwoven needle-punched—increasing with increasing weight (recall Figure 2.18)
- Hybrid drainage systems—particularly geonets and drainage geocomposites (see Chapters 4 and 9 respectively)

Although all geotextiles possess some in-plane drainage capability, the first three types of geotextiles listed above have too little to take advantage of. The nonwoven resin-bonded and needle-punched groups, however, can be made sufficiently thick to have meaningful quantities of liquid flow within them. These geotextiles, particularly the needle-punched variety, are often 5 mm thick and can be made much thicker in a cost-effective manner. Relatively thick nonwoven needle-punched geotextiles will be the focus of the designs included in this section.

For the flow capability of the geotextiles, we will be considering two general categories: gravity flow (Section 2.9.3) and pressure flow (Section 2.9.4). This distinction will become obvious in the sections that follow. Some selected applications can be noted in each category:

- Gravity drainage: as chimney drains and drainage galleries in earth and earth/rock dams, as pore water dissipaters behind retaining walls, as flow interceptors (as in fin drains), and as drains placed beneath geomembrane lined reservoirs (for water drainage or gas conveyance).
- Pressure drainage: as vertical drains for rapid soil consolidation, within the soil backfill of reinforced earth walls, within earth embankments and dams, and beneath surcharge fills.

2.9.2 General Behavior

Except for the direction of flow (in-plane rather than cross-plane), the design similarities of this drainage section with the preceding filtration section will be obvious. There are again three aspects of design: (1) adequate flow capacity, (2) proper soil retention, and (3) long-term soil-to-geotextile flow equilibrium. Since soil retention and long-term soil-to-geotextile flow equilibrium are discussed in other sections, these aspects will not be fully treated in this section; only some brief comments will be included. The reader is referred to Sections 2.3 and 2.8 for full details.

Regarding the hydraulic design parameter of major concern, we will focus on the transmissivity of the geotextile θ in equation (2.10) (repeated here),

$$\theta = k_p t$$

where

θ = transmissivity,

k_p = in-plane geotextile permeability, and

t = geotextile thickness.

The relationship will appear as $\theta = kt$, the k being understood to be in-plane permeability (rather than the filtration-related cross-plane permeability). Transmissivity will be used in conjunction with Darcy's formula under the assumption that laminar flow exists within the geotextile. This is generally valid, but when very thick geotextiles are used together with high hydraulic gradients, the assumption of a laminar flow regime becomes questionable. (Indeed, with the geonets and drainage geocomposites discussed in Chapters 4 and 9, flow is generally turbulent and Darcy's formula should not be used. For geonets and drainage geocomposites a related design based on flow rates will be used.)

2.9.3 Gravity Drainage Design

For gravity drainage problems involving liquid flow in geotextiles, the driving force is merely the slope at which the geotextile is placed. Using the geometry of the particular situation under consideration, a required transmissivity can be calculated using Darcy's formula. This value is then compared to the allowable transmissivity of the candidate geotextile for calculation of a factor of safety. Considering the severity of the situation, these values of factor of safety should be quite high, depending on how the allowable transmissivity is obtained (recall equation 2.25 and Table 2.12).

Note that the allowable geotextile transmissivity is the value at the particular normal stress that is acting upon it. This is usually calculated on the basis of the effective stress of the soil placed above, if the geotextile is horizontal. If the geotextile is vertical, the normal stress is the vertical effective stress multiplied by the appropriate coefficient of earth pressure. This can usually be taken as the at-rest value, and the relationship $K_o = 1 - \sin \phi$ is often used. If the friction angle of the soil (ϕ) is not known, K_o can be taken approximately equal to 0.5. It should be recalled from the testing section involving hydraulic properties (Section 2.3.4) that the transmissivity decreases substantially with applied normal stress on the geotextile. Figure 2.18 illustrated this behavior for various mass per unit area nonwoven, needle-punched geotextiles. However, a near-constant value of transmissivity is reached above approximately 100 kPa. Examples 2.26 and 2.27 illustrate these concepts.

Example 2.26

A 10 m high zoned earth dam will be used as an irrigation reservoir with the dam cross section as shown in the diagram that follows. A geotextile is being considered as a chimney drain and drainage gallery. The geotextile under consideration is a 2000 g/m² nonwoven,

needle-punched geotextile with $\theta_{ult} = 15 \times 10^{-4}$ m²/min. Use cumulative reduction factors of 3.0 to convert this to θ_{allow}. What factor of safety does this geotextile have for the amount of flow seeping through the core wall, which is a clayey silt of permeability 1×10^{-7} m/s?
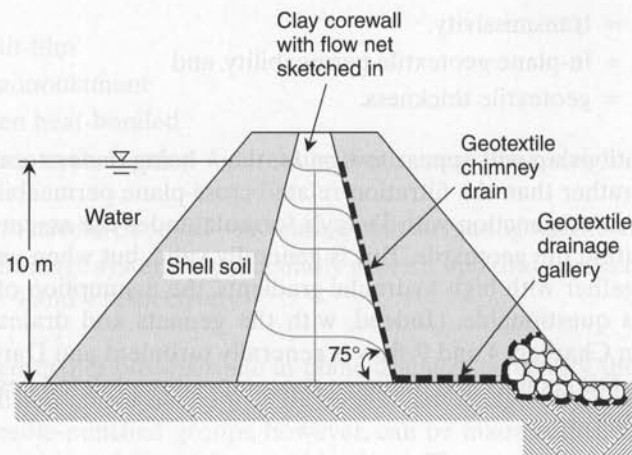
Solution: In stages, the solution is as follows:

(a) Calculate the maximum seepage coming through the clay core wall that the geotextile must carry. The use of a flow net (as shown in the diagram) gives

$$q = kh\left(\frac{F}{N}\right)$$

$$= (1 \times 10^{-7})(10)\left(\frac{5}{2}\right)$$

$$= 2.50 \times 10^{-6} \text{ m}^2/\text{sec}$$

$$q = 1.50 \times 10^{-4} \text{ m}^2/\text{min}$$

(b) Calculate the gradient of flow in the geotextile:

$$i = \sin 75°$$

$$i = 0.97$$

(c) Using Darcy's formula, calculate the required transmissivity, θ_{reqd}:

$$q = kiA$$

$$= ki(t \times w)$$

$$q = (kt)(i \times w)$$

$$kt = \frac{q}{(i)(w)}$$

$$\theta_{reqd} = \frac{1.50 \times 10^{-4}}{(0.97)(1.00)}$$

$$\theta_{reqd} = 1.55 \times 10^{-4} \text{ m}^2/\text{min}$$

(d) Determine the factor of safety:

$$FS = \frac{\theta_{allow}}{\theta_{reqd}} = \frac{\theta_{ult}/\Pi RF_p}{\theta_{reqd}}$$

$$= \frac{(15 \times 10^{-4})/3.0}{1.55 \times 10^{-4}}$$

$$FS = 3.2$$

Due to the critical nature of this application, this FS value is somewhat low, and a minimum value of 5.0 is recommended. Two options present themselves: one is to use multiple layers of geotextile (to increase θ_{allow}) in the lower part of the chimney drain and in the drainage gallery (the upper part of the chimney drain could still use one layer); the other is to use the FS = 5.0 and back-calculate the necessary geotextile's transmissivity. This latter suggestion is illustrated as follows:

$$\theta_{allow} = \theta_{reqd} \times FS$$

$$= (1.55 \times 10^{-4}) \times 5.0$$

$$\theta_{allow} = 7.75 \times 10^{-4} \text{ m}^2/\text{min}$$

This in turn requires a geotextile to have an ultimate (or as-manufactured) transmissivity considerably in excess of θ_{allow}. If the cumulative reduction factor is 3.0

$$\theta_{ult} = (7.75 \times 10^{-4}) \times 3.0$$

$$\theta_{ult} = 23.2 \times 10^{-4} \text{ m}^2/\text{min}$$

As seen in Figure 2.18, this is possible only by selecting an extremely thick, nonwoven, needle-punched geotextile, which would not be economical. Alternatively, geonets or geocomposites can be considered (see Chapters 4 and 9, respectively).

(e) Perform a soil retention analysis to see that soil particles do not embed in the geotextile and decrease its transmissivity. The analysis is the same as in Section 2.8.

(f) Determine long-term soil-to-geotextile compatibility. Here within an earth dam is where long-term flow tests, gradient ratio tests, or hydraulic conductivity ratio tests have applicability. (See Section 2.3.5 for details.)

Example 2.27

Calculate the factor of safety of a 500 g/m^2 needle-punched, nonwoven geotextile required to drain water from behind an 8 m high concrete cantilever retaining wall if it has an allowable transmissivity of $\theta_{allow} = 0.15 \times 10^{-3}$ m^2/min measured at is maximum design pressure. The soil backfill is a silty sand (ML-SW) with $k = 5 \times 10^{-5}$ m/s.

Solution: As before, we proceed in parts:

(a) Calculate the maximum flow rate coming to the geotextile. From the flow net shown in the following diagram, we have

$$q = kh\left(\frac{F}{N}\right)$$

$$= (5.0 \times 10^{-5})(60)(8)\left(\frac{5}{5}\right)$$

$$q = 0.024 \text{ m}^2/\text{min}$$
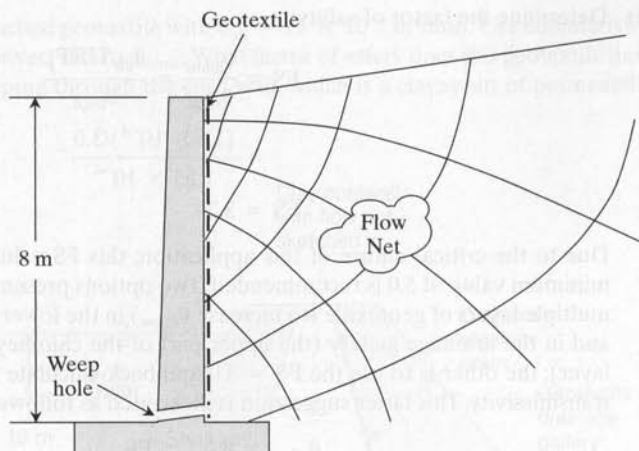
(b) Determine the flow gradient within the geotextile:

$$i = \sin 90°$$
$$= 1.0$$

(c) Calculate the required transmissivity:

$$q = kiA$$
$$= ki(t \times w)$$
$$q = (kt)(i \times w)$$
$$kt = \frac{q}{(i)(w)}$$
$$= \frac{0.024}{(1.0)(1.0)}$$
$$\theta_{reqd} = 0.024 \text{ m}^2/\text{min}$$

(d) Compare this value with the geotextile's allowable transmissivity to obtain a factor of safety:

$$FS = \frac{\theta_{allow}}{\theta_{reqd}}$$
$$= \frac{0.00015}{0.024}$$

$$FS = 0.0062 \text{ not nearly acceptable!}$$

It is easily seen is that this application is not suited for geotextiles. It is, however, a perfect situation for geonets or drainage geocomposites that have much greater in-plane flow capacity. Geonets are the subject of Chapter 4 and geocomposites are the subject of Chapter 9 where we will repeat this exact problem and note the substantial increases in the factor of safety.

2.9.4 Pressure Drainage Design

Geotextile transmissivity is the key parameter in both gravity and pressure drainage; in this sense the two topics are quite similar. The difference is that for pressure drainage water will flow from locations of higher pressure to locations of lower pressure regardless of the geotextile's orientation. Thus, flow direction depends on each specific situation; some of these situations have been identified. The following equation is formulated for a geotextile placed beneath a surcharge fill on a fine-grained compressible foundation soil (after Giroud [66]).

$$\theta_{reqd} = k_p t = \frac{B^2 k_s}{(c_v T)^{1/2}} \tag{2.71}$$

where

θ_{reqd} = geotextile transmissivity,

k_p = in-plane permeability coefficient of the geotextile,

t = thickness of the geotextile,

B = width of the surcharge layer,

k_s = permeability coefficient of the foundation soil,

c_v = coefficient of vertical consolidation of the foundation soil, and

T = time for the surcharge fill to be placed.

Example 2.28 illustrates use of the formula.

Example 2.28

You have been given a variable-width surcharge fill placed in 10 days (14,400 min) on a foundation soil of 1×10^{-9} m/s permeability and 4.6×10^{-6} m²/min coefficient of consolidation, as shown in the diagram below. (a) Determine the required geotextile transmissivity as a function of base width of the surcharge fill and graph the result; (b) Using a ultimate geotextile transmissivity of 0.75×10^{-3} m²/min and cumulative reduction factors of 5.0, find the maximum width of surcharge that can be used under these conditions.
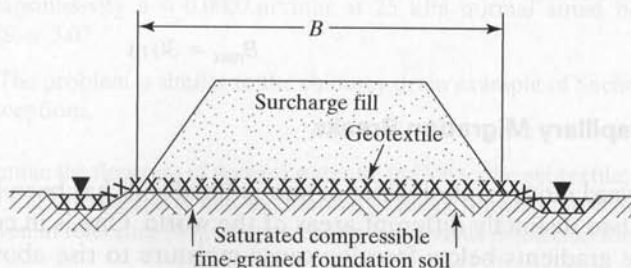
Solution:

(a) Determine the graph of B versus θ:

$$\theta_{reqd} = \frac{B^2 k_s}{(c_v T)^{1/2}}$$

$$= \frac{(1 \times 10^{-9})(60) B^2}{[(4.6 \times 10^{-6})(0.0144 \times 10^6)]^{1/2}}$$

$$= 2.33 \times 10^{-7} B^2, \text{ where } B \text{ is in units of m.}$$

When different values of B are plotted, the curve shown below results.
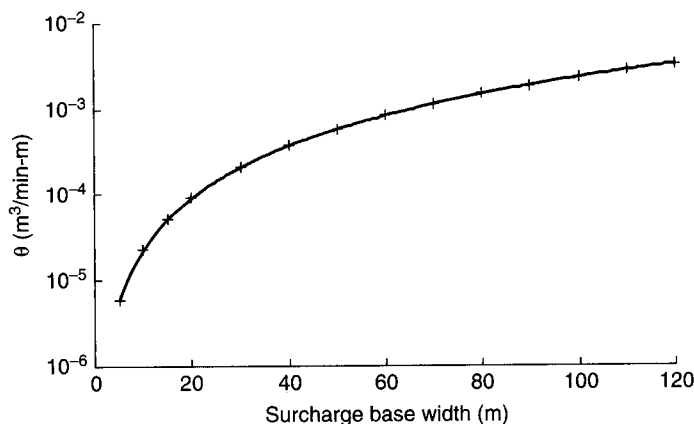
(b) Using the above graph,

$$\theta_{ult} = 0.00075 \text{ m}^2/\text{min}$$
$$\theta_{allow} = \theta_{ult}/\Pi RF$$
$$= 0.00075/5.0$$
$$= 0.00015 \text{ m}^2/\text{min}$$

and from the curve the value is as follows:

$$B_{max} = 30 \text{ m}$$

2.9.5 Capillary Migration Breaks

The upward movement of water in fine-grained soils has been known to present problems in two distinctly different areas of the world. One is in cold regions, where temperature gradients below freezing cause moisture to rise above the stationary water table. This rise occurs in the capillary zone and can eventually result in frozen layers

(ice lenses), which will expand, lifting any structure placed above it. The phenomenon is called *frost heave* and is well-documented in the geotechnical literature.

Remedies for frost heave usually involve a capillary break or cut-off placed horizontally at a depth beneath the lowest elevation of the freezing isotherm. Sands and gravels have been used, but geotextiles offer an attractive and cost-effective alternative. Use of a thick, nonwoven, needle-punched geotextile is easily placed and can be readily graded to drain the rising water away from the area of immediate concern. Several laboratory studies and case histories of geotextiles used in this manner are available [132,133].

It should be mentioned that geotextiles are generally hydrophobic—that is, they repel water—so there is no wicking action across the plane of the geotextile. This is important to note because there is a popular misconception that geotextiles can wick water, as does the wick of a candle with wax. This is not so, since both polypropylene and polyester repel water. Until the geotextile voids are saturated, there is only minor intimate contact of the water with the fibers. This is just the opposite of water in soil, where soil particles are hydrophilic, and the water nests itself around points of contact of adjacent soil particles. Once geotextiles are completely saturated, however, they can be used to siphon water in a continuous manner, thereby maintaining flow within them [134].

In a completely different part of the world—namely, deserts and arid regions— there is a similar problem involving capillary rise. Here, as groundwater rises it brings dissolved salts with it [135]. As this salt-ladened water comes near the ground surface, it kills all vegetation, which takes up the salt water through the root system. Equally severe is the salt attacking building foundations of both stone and reinforced concrete, making these usually-adequate structural materials very friable.

As with the frost cutoff, this application area of salt-migration cutoff can effectively use a geotextile exhibiting proper in-plane drainage characteristics. The design procedure uses the transmissivity parameter, as in the case of gravity drainage. Once again laminar flow is assumed, so that Darcy's formula is employed in the problem solution. Example 2.29 actually suggests gravity and pressure situations but is solved completely by a gravity approach.

Example 2.29

A storage building for frozen foods is to be founded on the site illustrated in the diagram below, with a capillary break beneath the building's foundation; a geotextile is being considered as a solution. Will a 700 g/m^2 nonwoven needle-punched geotextile having an allowable transmissivity $\theta = 0.0007$ m^2/min at 25 kPa normal stress be adequate if the required FS = 3.0?

Solution: The problem is similar to the chimney drain example of Section 2.9.3 with some obvious exceptions.

(a) Determine the flow rate of upward water migration to the geotextile, which is a function of the soil's permeability and the thermal gradient drawing the water upward. Guides are given in reference [95], where a conservative value is selected for this example.

$$q = 2.7 \times 10^{-5} \text{ m}^2/\text{min}$$
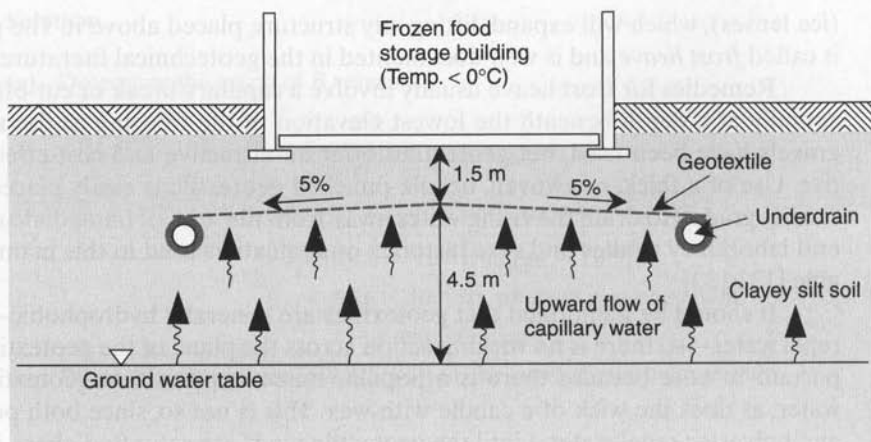
(b) Calculate the gradient of flow in the geotextile.

$$5\% \text{ slope} = 0.05 \text{ gradient}$$

(c) Calculate the required transmissivity, θ_{reqd}:

$$q = kiA$$
$$= ki(t \times w)$$
$$q = (kt)(i \times w)$$
$$kt = \frac{q}{i \times w}$$
$$\theta_{reqd} = \frac{0.000027}{(0.05)(1.0)}$$
$$= 0.00054 \text{ m}^2/\text{min}$$

(d) Determine the factor of safety:

$$FS = \frac{\theta_{allow}}{\theta_{reqd}}$$
$$= \frac{0.00070}{0.00054}$$
$$FS = 1.3 < 3.0 \text{ not acceptable}$$

Therefore, at least a triple layer of geotextile is needed or a geonet or drainage geocomposite, as will be discussed in Chapters 4 and 9.

2.9.6 Summary

Geotextiles used in the drainage function are quite attractive for use as long as the required planar flow rates are relatively low. Certainly the drainage of fine-grained soil masses (like silts and clays) is possible, along with some examples shown in this section. Nonwoven, needle-punched geotextiles are best suited for this function. High mass per

unit areas or multiple layers can be used to obtain sequentially higher flow rates. Although not shown herein, their flow rates can be further augmented by being constructed with high-denier fibers. Significantly higher flow capacity, however, requires a different approach. That will be seen to be nicely fulfilled by geonets and drainage geocomposites.

Some of the examples of this section used an allowable transmissivity for their calculations. Thus no reduction on an ultimate transmissivity value by means of equation (2.25) and Table 2.12 was illustrated. Other problems used relatively low reduction factors to obtain an allowable transmissivity from the laboratory test value. This is because the current transmissivity test procedures (ASTM D4716 and ISO 12958) are often configured as performance tests. Site-specific conditions and loads can be readily replicated, and the resulting value will then be an allowable value (or near allowable) rather than an ultimate one. If not, the procedures set forth in reducing an ultimate to an allowable value by using reduction factors must be used.

2.10 DESIGNING FOR MULTIPLE FUNCTIONS

2.10.1 Logic for Chapter

In Sections 2.5 to 2.9, the primary function of the geotextile was readily apparent. This was to orient the reader's attention toward the design-by-function concept, and also to see that most applications lend themselves to a readily definable primary function design. Nevertheless, there are other applications in which the geotextile must be designed for multiple functions. In these cases a single dominant (primary) function cannot always be identified. Thus there are primary, secondary, tertiary, and perhaps even quaternary functions that may vary in a particular application. Furthermore, these functions might vary from site to site. Such multiple-function applications are the focus in this section. They should not be taken lightly or be considered of lesser importance than those discussed previously. Some of the major uses of geotextiles are included in this section on multiple-function applications.

2.10.2 Reflection Crack Prevention in Pavement Overlays

Overview.   The resurfacing of existing pavements that have excessive cracks in them represents an ongoing and expensive task for all federal, state, local, and private organizations that own and maintain roads. Such resurfacing is usually done with bituminous overlays ranging in thickness from 25 to 100 mm. Particularly exasperating to the road owners (and to the users and their automobiles as well) is when the cracks in the original pavement reflect up through the new overlay earlier than anticipated. To combat this, thicker overlays than desirable are used but at the cost of added expense, lower curb heights, and excessive weight and thickness on the subgrade system. Due in part to the magnitude of this problem and the potential market that it represents, the use of geotextiles to remedy the situation has been attempted in a number of ways. In some instances strips of geotextile have been placed over the cracks, spanning them by

150 to 600 mm on each side, and the overlay placed above. Polyester, polypropylene, and fiberglass geotextiles as well as geogrids (see Chapter 3) have all been used in this regard. By far the major use, however, has been with full-width geotextile sheets which have been waterproofed with asphalt cement or asphalt emulsion, over the entire pavement surface, and then overlaid with the final bituminous surfacing. The goal of such a process is to either (1) decrease the thickness of the overlay while keeping a lifetime equivalent to not using a geotextile, or (2) increase the lifetime of the overlay while using the same thickness as without the use of the geotextile.

A tremendous market has developed for this use, amounting to approximately 50 million square meters in the United States in 2002. It is interesting to note that users in other countries are not nearly as involved in this application as those in the United States. This is probably due to better ongoing road maintenance using conventional techniques (i.e., cleaning and filling of cracks when they are small) than that generally practiced in the United States, but that is not known to be a fact. Finally, it should be noted that this technique is used only for existing bituminous pavements, not for Portland-Cement concrete pavements. The significantly sharper edges of concrete would generally puncture and tear the lightweight geotextiles customarily used for this application.

As with other topics in this particular section, a clear-cut primary function is difficult to identify. It probably involves either the reinforcement from one side of the existing crack to the other (via the geotextile's tensile strength), or moisture-proofing against water moving through the pavement and into the subgrade via the impregnation of the geotextile with asphalt cement or asphalt emulsion. Since either function is possible, both design concepts will be explored after the construction and related details are addressed.

Construction. The use of full-pavement-width geotextiles in reflective crack prevention for bituminous pavement overlays is seemingly quite simple and straightforward. The general process follows; however, each step has its own peculiarities and subtleties.

1. Any existing failures in foundation soils must be repaired before resurfacing is done. A geotextile of 140 to 200 g/m² weight cannot be expected to hold up highway vehicles traveling only a few centimeters above it when the foundation soil beneath the stone base is unacceptable. In some instances these primary repairs must be very extensive.

2. Cracks in the existing bituminous pavement should be filled (see Figure 2.68a). Cracks up to approximately 6 mm thick are filled with hot-liquid crack filler, while larger cracks are filled with asphalt, hot mix, or cold patch.

3. An asphalt-based sealant is then uniformly sprayed over the existing pavement (see Figure 2.68b). The amount ranges from 0.2 to 2.3 l/m², depending on the porosity of the existing pavement and the absorbency of the geotextile. Recommended sealants are asphaltic cement (AC-5 or AC-20), cationic asphalt emulsions (CRS-2 or CRS-1h), and anionic asphalt emulsions (RS-2 or RS-1). When using the asphalt emulsions, care is required to ensure that they cure adequately

(a) Filling cracks in existing bituminous pavement

(b) Spraying asphalt-based sealant over existing pavement

(c) Geotextile being placed by mechanical equipment

(d) Hot mix bituminous overlay being placed

(e) Asphalt pavement core showing the crack-arresting feature offered by the geotextile with the new overlay placed above

Figure 2.68 Construction procedures and equipment for using geotextiles in reflective crack prevention in bituminous overlays. (Compliments of Amoco Fabrics and Fibers Co.)

before the geotextile is placed. Curing takes from 30 min to 4 hr, depending on the temperature and humidity. Cutback asphalts cannot be used with polypropylene geotextiles, since the solvent in them reacts with the polymer at high temperatures.

4. The geotextile is then placed on the sealant by hand or with mechanical equipment (see Figure 2.68c). Excessive wrinkles or folds in the geotextile must be cut open and laid flat. Stiff brooms are used to obtain a good bond with the sealant and to smooth out the surface as well. Joint overlaps of 25 to 75 mm are generally used. Additional sealant should be applied at these joints. If sealant comes through the geotextile, sand can be spread over it to absorb the excess.

5. The hot mix overlay is placed directly on the geotextile as soon as possible (see Figure 2.68d). The temperature of the mix should be about 150°C with a maximum of 165°C. Care must be taken to avoid movement or damage to the geotextile from turning of the paver or truck movement, since these vehicles are riding directly on the waterproofed geotextile.

6. The resulting system should appear as the core shown in Figure 2.68e.

A few points in the procedure need additional comment. The amount of asphalt-based sealant used is very important. Too little sealant leaves the geotextile unsaturated (thus permeable to infiltrating water), and too much sealant leaves an excess above or below the geotextile (thus forming a potential slip layer when the overlay is placed). Phenomenologically, the hot overlay draws the sealant up into the geotextile, just saturating it. (Note that for this reason, cold patch cannot be used as the overlay material.) Just how much sealant should be used depends on both the quality of the existing pavement and the type of geotextile being used. Button et al. [136] present the following equation for the quantity of sealant (also called a *tack coat*) to be used:

$$Q_d = 0.36 + Q_s \pm Q_c \qquad\qquad (2.72)$$

where

Q_d = design sealant quantity (l/m²),
Q_s = saturation content of the geotextile being used (l/m²), and
Q_c = correction based on sealant demand of the existing pavement
       surface (l/m²).

Concerning the value of Q_S, most manufacturers have specific geotextiles for this application (recall Table 2.2g) and are familiar with the required amount. In the absence of this information, we can take a flat pan with the candidate geotextile placed in it and experimentally determine the required amount. The geotextile is first saturated in asphaltic cement at 120°C for 1 min. It is allowed to cool and then is pressed with a hot iron between two absorbent papers to remove the excess asphalt. The value of Q_s is measured accordingly. A related procedure can be done in the field with a completely flat piece of sheet metal beneath the geotextile. The quantity Q_s depends mainly on the geotextile's thickness and to a lesser extent on other manufacturing details. Table 2.19

TABLE 2.19 SEALANT DEMAND OF EXISTING BITUMINOUS PAVEMENT SURFACES

Surface Condition	Q_c (1/m²)
Flushed	−0.09–0.09
Smooth, nonporous	0.09–0.23
Slightly porous, slightly oxidized	0.23–0.36
Slightly porous, oxidized	0.36–0.50
Badly pocked, porous, oxidized	0.50–0.59

Source: After Button et al. [136].

provides additional information concerning the value of Q_c, where it is seen that the older more oxidized pavement surfaces require greater amounts of sealant.

Regarding geotextile selection, recall Table 2.2g. On the basis of the majority of field projects completed to date, lightweight, nonwoven, needle-punched geotextiles prevail. Such low initial modulus geotextiles make us wonder about the reinforcement possibilities made for this application. They do indeed saturate well with sealant, so that waterproofing may be the dominant function. Laboratory modeling, however, suggests something very different. Using small cross-section test specimens consisting of a cracked asphalt base layer, a waterproofed geotextile above it, and finally the overlay, Murray [82] has found a strong relationship between geotextile effectiveness with 5% secant modulus. The data in Table 2.20 show the results based on the number of dynamic cycles until the lower crack reflected through the overlay. The data plot is close to linear, indicating that higher-modulus geotextiles, via a primary reinforcement function, outperform the lower-modulus geotextiles.

TABLE 2.20 LABORATORY TEST RESULTS OF DYNAMIC CYCLE LIFE SHOWING EFFECT OF GEOTEXTILES AND MODULUS VALUES

Geotextile	Type	Mass / Unit Area (g/m²)	Secant Modulus[1] (N)	Cycles to Failure	Standard Deviation	Fabric Effectiveness Factor, FEF[2]
—	Control, no geotextile	—	—	480	50	1.0
B	Nonwoven needle-punched polypropylene	150	590	1000	55	2.1
C	Nonwoven needle-punched polyester	200	540	2300	880	4.8
D	Nonwoven needle-punched polypropylene	200	930	3260	610	6.8
E	Woven slit-film polypropylene/polyester	170	1600	2760	570	5.8
A	Nonwoven melt-bonded polyester	108	2000	7650	575	15.9

1. Values are for force at 5% strain using a grab tensile test.

2. *FEF* is the ratio of the cycles to failure of the geotextile (fabric) reinforced specimens to that of the control specimen without fabric.

Source: After Murray [82].

Since the decision as to primary function is by no means clear-cut, two separate design methods will be presented. The first is based on reinforcement as the primary function, and the second on waterproofing as the primary function.

Reinforcement-Based Design.   The key to the reinforcement-based design of geotextiles in reflective crack prevention in bituminous pavement overlays is the fabric's effectiveness as determined by laboratory testing or by experience. Quantitatively, it is defined as follows:

$$\text{FEF} = \frac{N_r}{N_n} \tag{2.73}$$

where

FEF = fabric effectiveness factor,
N_r = number of load cycles to cause failure in the geotextile reinforced case, and
N_n = number of load cycles to cause failure in the nonreinforced case.

Values of FEF vary widely when based on laboratory tests (as they usually are), the range being from 2.1 to 15.9, as shown in Table 2.20. Upon having this value, however, design can be approached by a number of procedures. Majidzadeh et al. [137] use a mechanistic design procedure influenced by both rutting (distortion) and fatigue (cracking). Another approach, however, is merely to modify existing asphalt overlay design methods. In this regard the design traffic number (DTN), upon which overlay designs are based, will be modified as follows:

$$\text{DTN}_r = \frac{\text{DTN}_n}{\text{FEF}} \tag{2.74}$$

where

DTN$_r$ = design traffic number in the fabric-reinforced case,
DTN$_n$ = design traffic number in the nonreinforced case, and
FEF   = fabric effectiveness factor.

Using the Asphalt Institute's overlay design procedure [138], Example 2.30 illustrates the procedure. It is based on an arbitrarily selected FEF value of 3.0 and uses Figure 2.69 as the basic design guide. The procedure is as follows:

1. Determine the soil subgrade strength value as represented by its CBR value.
2. Determine the initial traffic number (ITN) as discussed in reference [138]. This is a combination of each vehicle's weight and respective number of load repetitions based on traffic counting.

Figure 2.69   Thickness requirements for asphalt pavement structures using un-soaked subgrade soil CBR. (After Asphalt Institute [138])

3. Determine the adjustment factor for the desired design period and estimate traffic annual growth rate, as described in reference [138].
4. Multiply the ITN by the adjustment factor to obtain the design traffic number DTN for use in the thickness design chart.

5. Use Figure 2.69 (or equivalent) to determine the full-depth asphalt-to-pavement thickness, t_{An}, needed for the design subgrade strength value, the DTN, and the selected design period.
6. Determine the effective thickness, t_e, of the existing pavement as discussed in [138].
7. The thickness of asphalt concrete overlay required, then, is equal to $t_{An} - t_e$.
8. This process is repeated for the geotextile-reinforced case using equation (2.74), which results in a thickness t_{Ar}.
9. The resulting two thicknesses (nonreinforced and geotextile-reinforced) are then compared $(t_{An} - t_{Ar})$ to note the savings in asphalt overlay thickness Δt since the base thickness is the same in both cases.

Example 2.30

An interurban two-lane highway carries an average of 4000 vehicles per day, 400 (10%) of which are heavy trucks of 135 kN average gross mass. The single-axle load limit is 80 kN. Traffic growth rate is 4% annually. The existing pavement consists of 75 mm of asphalt concrete surface and 200 mm of crushed stone base on a soil whose CBR = 5.0. The pavement is in generally good condition, but visual evaluation indicates the need for an overlay. Find the overlay thickness for a 20-year design period **(a)** if you do not use a geotextile, and **(b)** if you use a geotextile with FEF = 3.0. **(c)** Compare the two overlay thicknesses. This problem (without geotextile reinforcement) is from [138].

Solution:

(a) Determine that the initial traffic number is 90, and the adjustment factor is 1.49, resulting in a DTN for the nonreinforced fabric case of

$$\text{DTN}_n = 90 \times 1.49$$
$$= 134$$

Using this and a CBR of 5. Figure 2.69 results in a full-depth nonreinforced asphalt pavement thickness (t_{An}) of

$$t_{An} = 245 \text{ mm}$$

The existing pavement effective thickness (t_e) calculation uses a weighing factor of 0.8 on the existing asphalt and 0.4 on the existing stone base.

$$t_e = 75 \, (0.8) + 200 \, (0.4)$$
$$= 140 \text{ mm}$$

Therefore, the required overlay thickness (t_{on}) without using a geotextile (i.e., nonreinforced) is

$$t_{on} = t_{An} + t_e$$
$$= 245 - 140$$
$$= 105 \text{ mm}$$

(b) The solution varies for the case of using a geotextile-reinforcement layer as follows:

$$DTN_r = \frac{DTN_n}{FEF}$$
$$= \frac{134}{3.0}$$
$$= 45$$

which, from Figure 2.69, results in

$$t_{Ar} = 215 \text{ mm}$$

and

$$t_{or} = 215 - 140$$
$$= 75 \text{ mm}$$

(c) Thus the savings in asphalt overlay thickness using a geotextile layer (and based on a reinforcement hypothesis) is

$$\Delta t_o = t_{on} - t_{or}$$
$$= 105 - 75$$
$$\Delta t = 30 \text{ mm}$$

Note that this same result comes about from using the values of t_{An} and t_{Ar} directly, i.e.,

$$\Delta t = t_{An} - t_{Ar}$$
$$= 245 - 215$$
$$\Delta t = 30 \text{ mm}$$

Waterproofing-Based Design.   Again using the Asphalt Institute's techniques [138], we can develop an alternate design procedure for geotextiles used in asphalt overlay situations—this time one that is based on a waterproofing hypothesis. This concept should not come as a surprise since adequate subgrade drainage of pavements has long been suspected as being the key factor for extending conventional pavement lifetimes. Cedergren [139] clearly illustrates this type of improved pavement lifetime. The particular procedure we will use, adopted from Bell [140], utilizes field-measured rebound deflections of the existing pavement system along with the design guide of Figure 2.70. The individual steps in the design are as follows:

1. Determine the representative rebound deflection as discussed in [138], which is based on Benkelman beam field deflection tests.
2. Determine the ITN as discussed in [138]. It is a combination of each vehicle's weight and respective number of load rejections based on traffic counting.
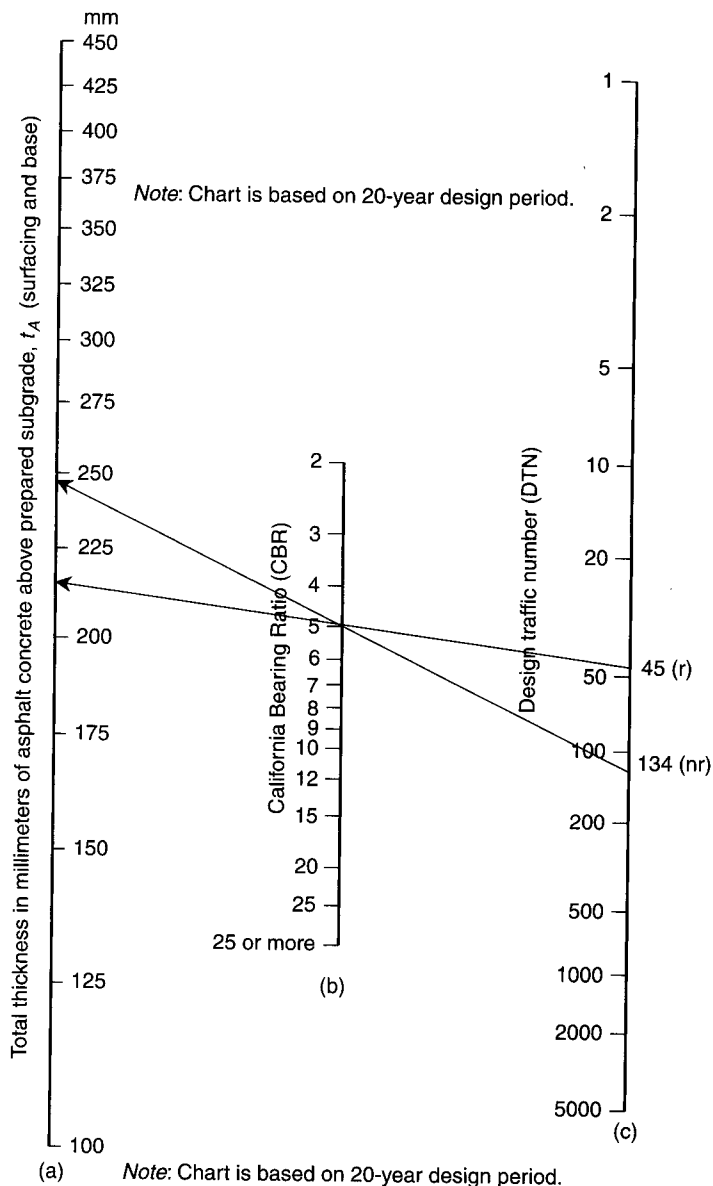3. Determine the initial traffic number adjustment factor for the desired design period as described in [138].
4. Multiply the ITN by the ITN adjustment factor to obtain the DTN for use in the overlay thickness chart.

Representative rebound deflection ($\overline{X} + 2s)fc$ (mm)
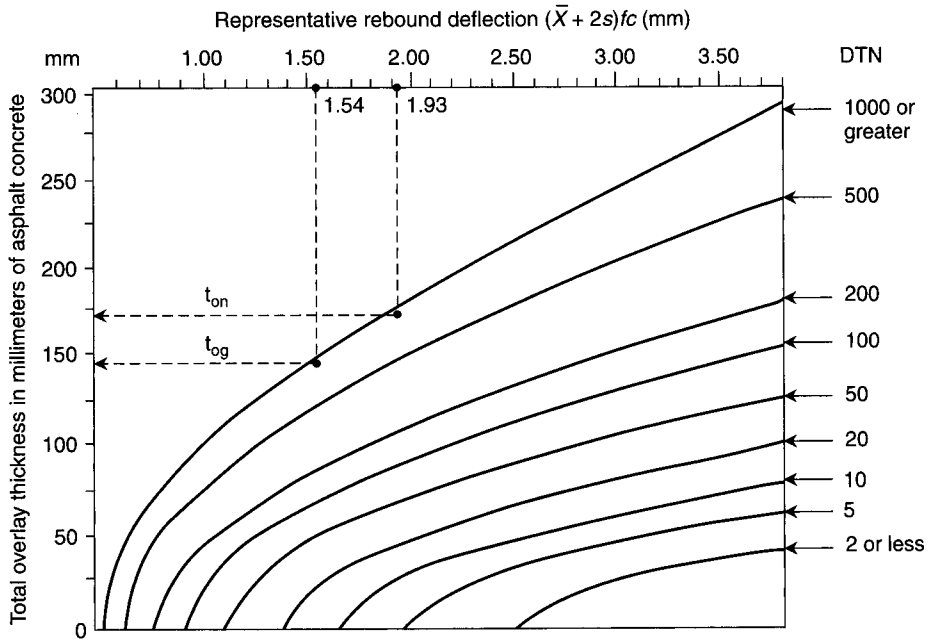
Figure 2.70 Asphalt overlay thickness required to reduce pavement deflection from a measured to a design deflection value (a rebound test). (After Asphalt Institute, [138])

5. Enter the overlay thickness chart (Figure 2.70) at the representative rebound deflection and move down vertically to the curve representing the DTN (interpolate if necessary). Move horizontally to the overlay thickness scale and read the thickness of overlay required.

6. For the case of a geotextile included in the pavement cross-section and of it being suitably waterproofed, modify the representative rebound deflection (RRD) equation as appropriate:

$$\text{RRD} = (\overline{X} + 2s)fc \qquad (2.75)$$

where

$\overline{X}$ = arithmetic mean of measured Benkelman beam deflection values,
s = standard deviation,
f = temperature adjustment (see [138]), and
c = critical period adjustment factor, which is largely influenced by moisture in the subgrade system (this is the term that will be empirically adjusted in design Example 2.31).

7. Repeat the design process as with the nongeotextile case, and compare the resulting two thicknesses to note the savings in asphalt overlay using the geotextile.

Example 2.31

A four-lane interurban highway carries an average of 16,000 vehicles per day, 2400 (15%) of which are heavy trucks with an average gross mass of 145 kN; the design lane is estimated to carry 45% of the heavy trucks; the traffic growth rate is 5% annually, and the legal single-axle load limit is 80 kN. Some cracking of the pavement surface is evident. High deflections indicate the need for an overlay. Find the overlay thickness required for a 20-year design period (**a**) if you do not use a geotextile, and (**b**) if you use a geotextile that changes the value of c in equation (2.75) from 1.25 to 1.00. (**c**) Compare the two overlay thicknesses. In the analysis use ITN = 590 and an adjustment factor of 1.67. This problem (without geotextile waterproofing) is also taken from [138].

Solution:

(**a**) Calculate the representative rebound reflection from equation (2.75) using field-gathered data of

$$\overline{X} = 1.55 \text{ mm,}$$
$$s = 0.10 \text{ mm,}$$
$$f = 0.88,$$
$$c = 1.25, \text{ and}$$
$$\text{RRD} = (1.55 + 0.20)0.88 \times 1.25$$
$$= 1.93 \text{ mm}$$

The design traffic number is also needed:

$$\text{DTN} = \text{ITN} \times \text{adjustment factor}$$
$$= 590 \times 1.67$$
$$= 985$$

Using Figure 2.70, the required overlay thickness without a geotextile is

$$t_{on} = 170 \text{ mm}$$

(**b**) For the case with a geotextile as a waterproofing layer, the constant c is changed from 1.25 to 1.00 and the process is repeated:

$$\text{RRD} = (1.55 + 0.20)\, 0.88 \times 1.00$$
$$= 1.54 \text{ mm}$$

Using this value and a DTN of 985, the required overlay waterproofed geotextile thickness from Figure 2.70 is

$$t_{og} = 140 \text{ mm}$$

(**c**) Based on these asphalt overlay thickness values, the saving using a geotextile is as follows:

$$\Delta t = t_{on} - t_{og}$$
$$= 170 - 140$$
$$\Delta t = 30 \text{ mm}$$

Note that the equivalent thickness of the existing pavement system is the same in both cases, and the resulting saving if a constant value were added to both t_{on} and t_{og} is still 30 mm.

Commentary.   As mentioned in Section 2.10.1, multiple-function geotextile applications are difficult to analyze since a clear-cut primary function cannot be easily identified. This topic of crack reflection prevention in bituminous pavement overlays illustrates the dilemma perfectly. Using two completely different hypotheses (one based on reinforcement and the other on waterproofing), two completely different designs can be developed. It simply begs the question of where the truth actually lies. Considering these two extremes, it might be that a combination of the two phenomena are working together! Further, a separation interlayer may be another function that is yet to be quantifiably developed.

It is clear that well-instrumented, well-monitored, well-analyzed, and well-reported case histories are needed in this application area. Perhaps, then, a decision as to which is the primary function will evidence itself, pointing the way to the correct design methodology. The case histories that are currently available on the topic not only do not give this identification but cast doubt on where the technique can be used.

Beginning in 1968, thirty-seven projects aimed at evaluating geotextiles used for the control of reflective cracking in bituminous overlays have been initiated by the U.S. Department of Transportation, Federal Highway Administration, under its National Experimental and Evaluation Program (NEEP). The most comprehensive test sites were conducted by Arizona, California, Florida, and North Dakota. One finding was that there is no strong evidence that the geotextile used provides a specific mechanism for extending the crack-free life of an overlay. Most reports have identified the problem as being very complex and being influenced by the type and degree of pavement distress, working versus nonworking cracks, type of pavement, loads, climate, geotextile-asphalt bonding (tack coat), geotextile type and properties, and asphalt type and mixing properties. The general conclusion of the Federal Highway Administration is that geotextiles may be used in the control of reflection cracking, but that the best results can be achieved where the existing pavement has experienced fatigue-associated alligator cracking with cracks 3 mm wide or less and located in relatively mild climates.

To be sure, the summary statements above challenge the universal use of geotextiles in the control of reflection cracking in bituminous overlays. In general, however, it is felt that reports are definitely on the positive side. Based on experiences to date, the following recommendations are offered:

- For those states that are using proprietary or competition-limiting specifications for geotextiles, the adaptation of Texas specifications for state use is encouraged.
- Prior to placement of a geotextile overlay system, the condition of the existing roadway should be documented. When an unstable roadway is suspected, deflection tests are recommended. While limiting deflection values have yet to be established for geotextile systems, it is important that data be obtained that could assist in their eventual evaluation.
- Since all geotextiles presently being marketed are not equivalent in physical properties, agencies should conduct the tests identified in the Texas specification, including the asphalt retention test, so as to develop documentation that may be useful later in assessing relative geotextile performance.

- Rather than placing the geotextile on the cracked existing pavement, an asphalt leveling course should be constructed first so as to provide a relatively unblemished surface for applying the tack coat and the geotextile. This will ensure more complete and uniform impregnation of the geotextile by the tack coat and will also assist in determining the type of tack coat to be used and the proper application rate.
- For pavement rehabilitation projects that include pavement widening with new asphaltic concrete overlays, geotextiles placed longitudinally over the shoulder pavement and/or widening joint should be considered. The state of Maine has had success in this regard [141]. Both longitudinal and transverse joints were greatly retarded by 380% and 320%, respectively, when using a high-strength geotextile directly spanning the cracks in question.
- Over jointed portland-cement concrete pavements, no evidence has been provided to support placing a geotextile system across the full roadway width in a continuous mat. Instead, the use of heavy-duty geotextile materials in strips over transverse and pavement edge joints and cracks is presently recommended.

A summary report by the U.S. Army Corps of Engineers on this particular application of geotextiles has arrived at similar conclusions [142]. Of importance insofar as current research and development is concerned is a series of RILEM conferences focused specifically on reflective cracking in pavements [143].

2.10.3 Railroad Applications

Geotextiles are often used in railroads beneath the stone ballast upon which the wooden or concrete tie system is placed. As will be discussed, a critical aspect of the design is the depth at which the geotextile is placed beneath the bottom of the tie (i.e., the thickness of overlying ballast). First, however, it is necessary to gain a perspective of the possible functions of the geotextile under various conditions.

Overview.   It is virtually impossible to identify a unique, primary function for geotextile use in railroad applications. Site-specific conditions will vary the primary function among a number of possibilities. In listing these possibilities it is important to keep in mind whether the railroad is being newly constructed or rehabilitated. If new construction, the material beneath the geotextile will probably be the in situ soil; if rehabilitation, the material beneath the geotextile will be previously placed ballast (now contaminated with soil), which has migrated into the soil over the past working history of the railroad. If both situations are being considered, the following geotextile functions are likely:

- Separation in new railroads, between in situ soil and new ballast.
- Separation in rehabilitated railroads, between old, contaminated ballast and new, clean ballast.
- Confinement-type reinforcement in order to contain the overlying ballast stone from lateral movement.

- Filtration of soil pore water rising up from the soil beneath the geotextile due to rising water conditions, or the dynamic pumping action of the individual wheel loads across the plane of the geotextile.
- Lateral drainage from water entering from above or below the geotextile moving within the geotextile.

Irrespective of the difficulty of identifying a single function of the geotextile (it is obviously a multifunction application), the acceptance of geotextiles by railroad companies is reasonable and increasing. Newby [144] reports that as far back as 1982 the Southern Pacific Railroad had used geotextiles in more than 1600 km of trackage.

Specific Design. A review of the geotextile literature on railroad applications shows some inconsistency. Railroad specifications seem to favor relatively heavy, non-woven, needle-punched geotextiles because of their high flexibility and in-plane drainage (transmissivity) characteristics. The logic for high flexibility is apparent, since the geotextiles must deform around the relatively large ballast and not fail or form a potential slip plane. In-plane drainage, however, is not itself a dominant function, because any geotextile acting as a proper separator and filter will preserve the integrity of the drainage of the ballast stone itself, where ample void volume is always present. Nevertheless, geotextile drainage has been emphasized in railroad specifications [144].

Laboratory work, even large-scale model testing, seems to be directed at a reinforcing and stiffening function provided for by the geotextile. Work by Einsenmann and Leykauf [145] (which also included the filtration function), Saxena and Wang [146], and Bosserman [147] clearly illustrates the reinforcement benefits of using a geotextile beneath the ballast stone. In the author's opinion, however, such membrane-type reinforcement can be gained only after quite high deformation of the subgrade soils. For the majority of existing railroads, as in rehabilitation work, such deformations do not seem possible or desirable, since densification of the subsoil has usually occurred many years before rehabilitation is necessary. Similarly, new railroads would never be placed on deformable soil subgrades.

For these reasons, the design of geotextiles beneath ballast in railroad applications can be addressed in the following steps:

1. Design the geotextile as a *separator*, since this function is always required. The procedures of Section 2.5 have direct applicability here. High burst strength, grab tensile strength, puncture resistance, and impact resistance all have significance in this particular application and lead to Class 1 types of geotextiles (recall Table 2.2a) or stronger.
2. Design the geotextile as a *filter*, since this function is also usually required. The general procedures discussed in Section 2.8, in particular those illustrated for walls and underdrains, are relevant in this application. The general requirements of adequate permeability, soil retention, and long-term soil-to-geotextile flow equilibrium are needed, as they are in all filtration designs. A note of caution, however: Railroad loads are dynamic; thus pore pressures must be rapidly dissipated.

For this reason high factors of safety are required in the permittivity design part of the process and the opening size would be designed using Figure 2.4(b) for dynamic flow conditions.

3. Consider geotextile *flexibility* if the cross-section is raised above the adjacent subgrade. Here a very flexible geotextile is an advantage in laterally containing the ballast stone in its proper location. Quantification of this type of lateral confinement reinforcement is, however, very subjective (recall Section 2.3.2).

4. Consider the *depth* of the geotextile beneath the bottom of the railroad tie. The very high dynamic loads of a railroad acting on ballast imparts accelerations to the stone that are gradually diminished with depth. If the geotextile is not deep enough, it will suffer from abrasion at the points of contact with the ballast. Raymond [148] has evaluated a number of geotextiles beneath Canadian and U.S. railroads and found many that are pockmarked with abrasion holes, as shown in Figure 2.71. In fact, there were so many cases that he has quantified the situation (see Figure 2.72). Here it is seen that major damage occurs within 250 mm of the tie, and that the situation becomes acceptable only at depths greater than 350 mm. From this curve it can be concluded that the minimum depth for geotextile placement is 350 mm plus 50 mm for track settlement, for a total 400 mm. If this depth is considered excessive in view of the large amount of ballast stone required, a highly abrasion-resistant geotextile must be used. Raymond [148] recommends a resin-dipped, nonwoven, needle-punched geotextile that has been forced-air dried to reestablish its porosity.

5. The last step in the design is to consider the geotextile's *survivability* during installation. To compact ballast under ties, the railroad industry customarily uses a series of vibrating steel prongs forced into the ballast. Considering both the forces exerted and the vibratory action, high geotextile-puncture resistance is required. Hence, and in keeping with the Step 4, it is necessary to keep the geotextile deep or to use a special high-puncture resistant geotextile (recall Section 2.3.5).

Commentary.   Geotextile use in railroads beneath the ballast offers a number of possible benefits. These are separation, lateral confinement-type reinforcement, filtration, and drainage. It cannot be categorically stated that one function dominates over the others in all cases. This application is indeed a multifunctioned one that must be handled on a site-specific basis. Yet some functions (e.g., separation and filtration) are always present. A recommended design procedure has been outlined.

It must be emphasized that a geotextile beneath a railroad is a very demanding application. Avoiding both puncture during installation and abrasion during service lifetime requires deep placement beneath the bottom of the tie or specially treated geotextiles designed for high-puncture resistance and abrasion resistance.

In closing, more well-planned, well-documented, and well-reported case histories of the type reported by Chrismer and Richardson [149] are recommended. Only with quantified results under specific conditions can a definitive function be associated with the geotextile. At that point the design process can advance in a position of strength.

(a) Exhumed geotextile showing large puncture holes due to installation composition stresses

(b) Exhumed geotextile showing smaller abrasion holes due to dynamic action of railroad loads

Figure 2.71 Puncture and Abrasion failures of geotextiles placed too close to the track structure. (Compliments of G. Raymond)

2.10.4 Flexible Forming Systems

The traditional method of formwork for concrete or grout is to use wood or metal. These rigid forms are properly positioned and fixed in location until the material placed in them adequately cures and has sufficient strength of its own. While the constraint of a rigid form is an obvious advantage in building a concrete wall or footing to exact line and grade, it is a decided disadvantage in a number of other applications. These situations, which can capitalize on the use of flexible forms made from geotextiles, are explored in this section.

   Overview.   It is easy to visualize that a geotextile, in the form of a bag, container, or tube, could be used as a flexible form into which concrete, grout, or soil could be
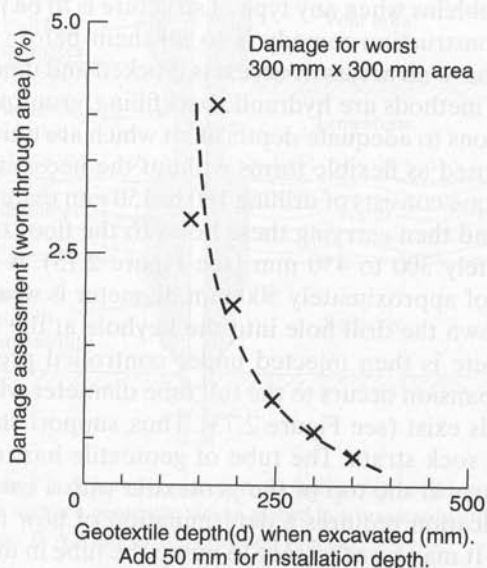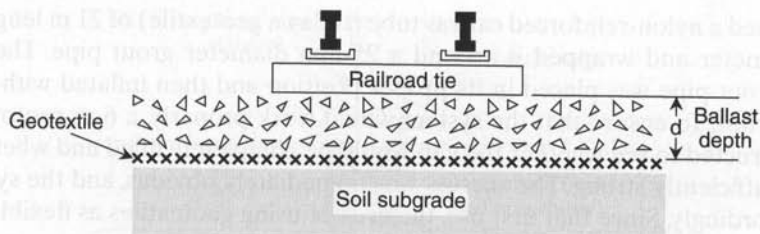
Figure 2.72   Observed geotextile abrasion damage as a function of depth beneath bottom of railroad tie. (After Raymond [148])

placed or pumped. Such a system would work as well under water (where water is displaced from within the fabric) as it would above ground (where air is displaced from within the fabric). Upon curing or stabilizing, the shape of the solidified mass takes the shape of the expanded geotextile; the number of possibilities is enormous. Additionally, the geotextiles, being flexible, can be inserted in difficult-to-reach locations and filled after proper positioning. This concept of flexible-forming systems with geotextiles can be used in many practical situations.

As a historical note, Terzaghi was the first to use geotextiles as flexible forms at Mission Dam (now Terzaghi Dam) in British Columbia, Canada, in 1955 [150]. A seepage cutoff wall was being placed within an existing dam. Since the surfaces on each side of the cutoff wall were not parallel (one side was a multicurved concrete surface and the other was steel piling), a pipe or beam closure was not possible. Instead, Terzaghi

used a nylon-reinforced canvas tube (today a geotextile) of 21 m length and 450 mm diameter and wrapped it around a 25-mm diameter grout pipe. The tube-surrounded grout pipe was placed in its proper position and then inflated with cement-bentonite grout. To ensure that the system would work properly, a 6-m prototype was first constructed to see whether the gap would be completely filled and whether the fabric was sufficiently strong. The success was immediately obvious, and the system was used accordingly. Since that first use, the area of using geotextiles as flexible forms has grown rapidly and in many different applications.

Columns for Mine and Cavern Stability. Abandoned mines and caverns are obvious problems when any type of structure is to be founded on or near them. The obvious preconstruction remedy is to fill them before subsidence can occur; however, they often have no access or access is blocked and unavailable. Under these conditions, alternative methods are hydraulic backfilling, grouting, or the construction of conventional caissons to adequate depth, all of which are quite expensive. Geotextiles, however, can be used as flexible forms without the necessity of entering the mine or cavity. The technique consists of drilling 100 to 150 mm diameter holes to intercept the roof of the mine and then carrying these holes to the floor of the mine, penetrating the floor approximately 300 to 450 mm (see Figure 2.73). A prefabricated and sewn tube of geotextile of approximately 500 mm diameter is wrapped around a grout pipe and is inserted down the drill hole into the keyhole at the floor of the opening. Fine-aggregate concrete is then injected under controlled pressure as the grout pipe is withdrawn. Expansion occurs to the full tube diameter where no resistance is met—that is, where voids exist (see Figure 2.73). Thus, support shoulders are created beneath the competent rock strata. The tube of geotextile has to be supported at the surface or through rings at the top of the geotextile with a cable system to the ground surface. Each application requires a determination of how much pressure the geotextile can withstand. It may be necessary to pump the tube in multiple lifts. Reinforcing steel can be placed either in the void area only or for the full length of the column. The critical point in this application is to get maximum support of the column of concrete under the roof of the individual rock strata. Where the cavity or mine is dry, it is feasible to observe the expanded column with a television camera from an adjacent hole. In areas where the opening is fully or partially filled with soil or other compressible or objectionable materials, it is possible to jet out an opening in this material by having the grout pipe extend through the bottom of the tube and, while jetting through this pipe, maintain an adequate head of bentonite or grout in the geotextile form. This technique has the advantage over other methods of forming grout columns in that a positive form can be installed with a relative economy, as large quantities of concrete are not lost in a wasteful base that would be needed to build up the angle of repose of the concrete.

Using this concept, it is also possible to create a bulkhead in an underground mine. By drilling holes on a predetermined line we pump alternate columns initially and allow for curing. The secondary or intermediate locations are then pumped and expanded with concrete to interlock between the originally placed columns. Two parallel walls can be created to form a bulkhead or cutoff. This technique has been used in relatively shallow mine and limestone applications; see Koerner and Welsh [83] for several case
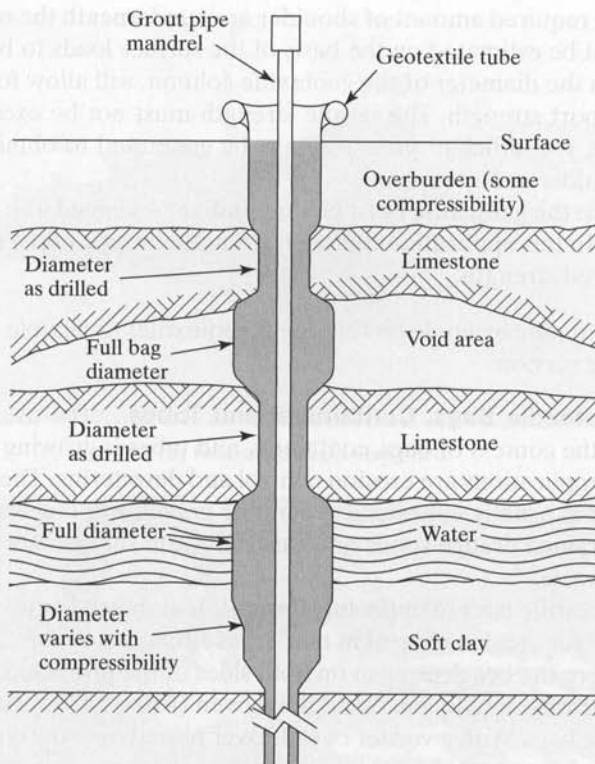
Figure 2.73 Idealized diagram of complete cross section of Fabriform mortar piles showing grout pipe within a geotextile sleeve placed in a previously drilled 150 mm diameter hole. (After B. A. Lamberton, Intrusion Prepakt)

histories. The method is very similar to the construction of secant-pile or tangent-pile cutoff walls in conventional foundation engineering.

As with other topics in this section, the geotextile to be used serves multiple functions (filtration, separation, and reinforcement through containment). The design centers on the following steps.

1. The opening size of the geotextile must be designed as a filter with emphasis on grout retention. A recommended criterion in this regard is the following:

$$O_{95} \leq 2d_{50} \tag{2.76}$$

where

O_{95} = 95% opening size of the geotextile (mm), and

d_{50} = average (50%) particle size of the cement used in the grout (mm).

Note that some "bleeding" of the grout will occur, but this should not significantly decrease its strength. It is necessary to have an open geotextile when construction is underwater so as to expel water within the fabric.

2. The required amount of shoulder area underneath the roof of the mine or cavern must be estimated on the basis of the surface loads to be imposed. This, together with the diameter of the geotextile column, will allow for a rough estimate of the support strength. The tensile strength must not be exceeded by the grout pressure, yet sufficient pressure must be generated to obtain the maximum possible shoulder area.

3. Since the geotextile must be longitudinally seamed, the sewing procedure is critical. In this application the seam strength must be equal to, or greater than, the required strength.

A numeric example on the use of geotextiles as flexible forms will be given at the end of the section.

Geotextile Bags, Containers, and Tubes.   The use of geotextiles as flexible forms in the context of bags, containers, and tubes is growing at an incredible rate. The primary applications are erosion control and dewatering. The fill in erosion control applications is usually cohesionless sand or gravel, while dewatering applications focus on fine-grained dredge spoils or industrial waste sludges, not the least of which is agricultural waste.

Geotextile bags manufactured with UV-stabilized antioxidants are being successfully used for erosion control in numerous situations. Figure 2.74 illustrates such a situation where the beach erosion on both sides of the protected section is very obvious. A composite woven (340 g/m^2) and nonwoven (610 g/m^2) fabric was used for the fabrication of the bags. With a veneer of soil cover placed over the completed bag system, both UV degradation and accidental or intentional damage are essentially avoided.

Geotextile containers represent an extension of the previous geobags, but the application differs, often involving the removal of river and harbor bottom sediments from shipping channels and navigable waterways. The technique generally utilizes high-strength woven geotextiles (greater than 50 kN/m tensile strength) and bottom dump barges (see Figure 2.75). The geotextile is placed in the empty barge and then filled with the bottom sediments. When full, the geotextile ends are folded over the top and sewn together, thereby completing the enclosure. The barge is towed to the disposal area and, when properly positioned, the split hull of the barge is opened and the sediment-filled container drops to the bottom. Subsurface embankments are being formed by this technique, which has the significant advantage that the sediments (particularly when contaminated) never leave the estuary or harbor. Furthermore, additional storage is possible behind the embankments, now reinforced by the filled containers themselves. Particularly intriguing is the design of the geotextile vis-a-vis its deformed shape, which includes the dynamic placement of the dredged sediment, its squeezing through the barge opening, and the impact stresses of its final positioning (see Leschinsky and Leshchinsky [151]).

Geotextile tubes form the logical extension to bags and containers and have been increasing in size and length since their inception. Efforts to form flexible sand-filled tubes were made as early as 1957, but they were not very successful. Eventually, a patent was granted in 1967 to a Danish firm, Aldek A. S., in conjunction with the Danish Institute of Applied Hydraulics [152]. Since that time the technology has rapidly grown, resulting in the use of tubes as large as 20 m in circumference and of

(a) Fabricated bags being filled

(b) Seamed bags being transported by barge

Cliff area successfully defended

(c) Geotextile bags protecting a shoreline

Figure 2.74 Geotextile bag protection of Historic Farm Building along North Sea, Germany. (Compliments Naue Fasertechnik, GmbH).
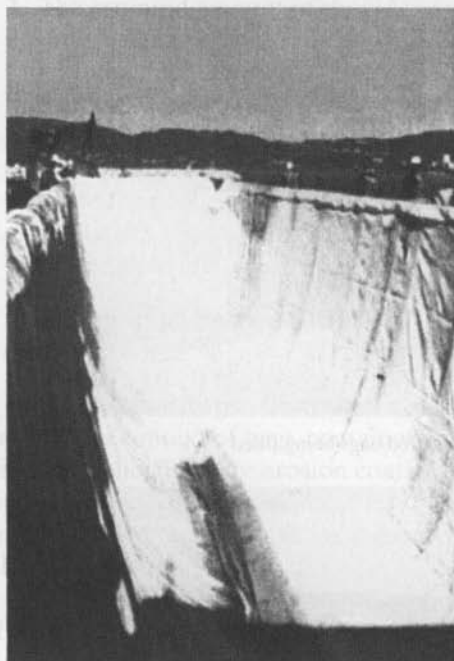
(a) Geotextile within closed barge

(b) Geotextile being filled

(c) Geotextile sewn over sediment fill forming closed container
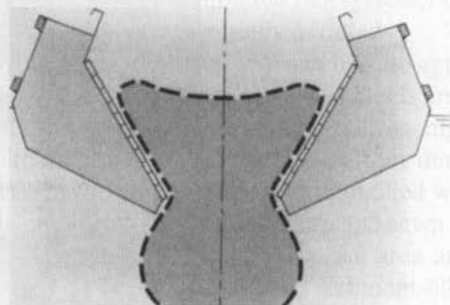
(d) Filled container being dropped out of bottom of barge at disposal site

Figure 2.75 Geotextile containers for removal of river and harbor sediment (sometimes contaminated) to construct underwater containment areas using bottom-dump barges. (Compliments TC Nicolon–TC Mirafi Corp.)

an unlimited length [153]. Figure 2.76 shows large geotextile tubes filled with dredged sand acting as a beach erosion-control system. There are a number of important design issues, among which are the following:

- Beachside anchor tube dimensions, location, and connection to main tube
- Waterside scour tube dimensions, location, and apron connection to main tube

(a) Method for sand slurry filling of prefabricated tube

(b) Filled tube showing longitudinal seam

(c) Tube after backfilling with recently planted dune grass

Figure 2.76   Sand-filled geotextile tubes for beach erosion protection.

(a)

Pressure head/circumference (dimensionless)

(b)
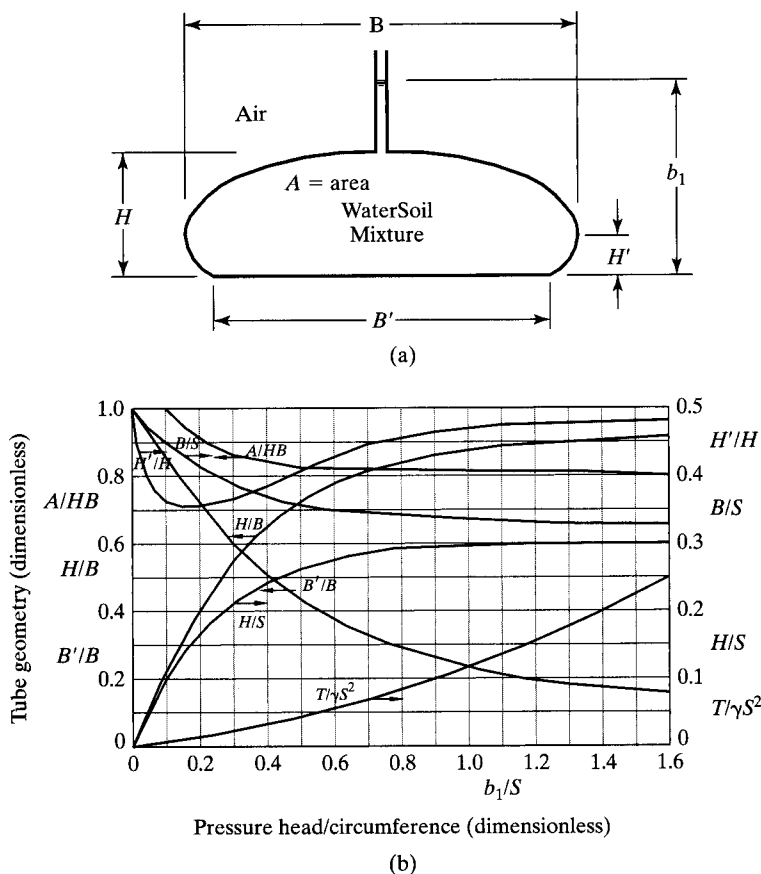
Figure 2.77 Geotextile tube definition diagram (a) and design curves for fabric strength and final dimensions. (b) (After Pilarczyk [154])

- Subsidence and/or rolling of main tube during intense storms
- Opening size of fabric vis-à-vis particle size of soil being used as infill
- Required tensile strength of the fabric and the seams, of which the seams are critical since they are invariably the weaker element
- Geometric dimensions of the main tube after final pumping and filling

Progress on these last two issues has been made and is provided by means of a design nomograph (see Figure 2.77). Example 2.32 illustrates its use.

Example 2.32

A geotextile tube is filled with sand for the purpose of beach erosion control. **(a)** Determine the factor of safety of a 200 kN/m allowable strength geotextile used under the following conditions: pressure head, $b_1 = 10.5$ m (at 100 kPa) and circumference, $S = 14$ m. **(b)** What are the dimensional properties of the filled tube?

Solution: Using Figure 2.77 the procedure uses values taken directly from the curves:

(a) For

$$b_1/S = 10.5/14 = 0.75$$
$$T/\gamma S^2 = 0.085$$
$$T_{\text{reqd}} = (0.085)(9.81)(14)^2$$
$$= 163 \text{ kN/m}$$
$$FS = T_{\text{allow}}/T_{\text{reqd}}$$
$$= 200/163$$
$$FS = 1.2; \text{ which is marginally acceptable}$$

(b) Figure 2.77 is again used for the final dimensional properties of the geotextile tube for a (b_1/S)-value of 0.75:

$$B/S = 0.34; \text{ therefore, } B = (0.34)(14) = 4.76 \text{ m}$$
$$H/S = 0.28; \text{ therefore, } H = (0.28)(14) = 3.92 \text{ m}$$
$$H'/H = 0.45; \text{ therefore, } H' = (0.45)(3.92) = 1.76 \text{ m}$$
$$B'/B = 0.27; \text{ therefore, } B' = (0.30)(4.76) = 1.43 \text{ m}$$
$$A/HB = 0.81; \text{ therefore, } A = (0.81)(3.92)(4.76) = 15.1 \text{ m}^2$$

We can now check on the curves and respective values from the following:

$$H/B = 3.92/4.76 = 0.82 \text{ vs. } 0.82, \text{ which is appropriate}$$

The extension of geotextile tubes into the dewatering of fine-grained soils, industrial sludges, sewage treatment sludges (biosolids), and agricultural farm waste is logical, but only to a certain degree. Clearly, the pumping of such sludges into a geotextile tube is possible, but the time for dewatering depends on the composition of the filter cake that is formed on the inside of the fabric. Figure 2.78 shows a field of such tubes with contaminated harbor bottom sediment being dewatered and an example of the low permeability filter cake formed on the inside of the fabric. The pumping must be carefully adjusted so that fabric or seam failure does not occur, yet the tube's capacity is optimized and stabilization time is minimized. This is a cutting edge research topic with many unknowns including the fate of the pollutants in the case of hazardous materials and of the microorganisms in the case of biosolids (see references [153–158]). It is possible that decontamination within the tube can occur if proper additives are included during filling (Hwang and Koerner [159]).

Restoration of Piles (Pile Jacketing).   All piles in a marine environment suffer deterioration at varying rates. The deterioration is caused by normal marine exposure, wet-dry cycles, freeze-thaw cycles, and chemical, industrial, and sanitary wastes. Moreover, each type of pile has its own particular problems.

1. Wood piles in a marine environment can be subject to attack by bores. There are three basic types: teredo and bankia (both mollusks), and the arthropod limnoria.
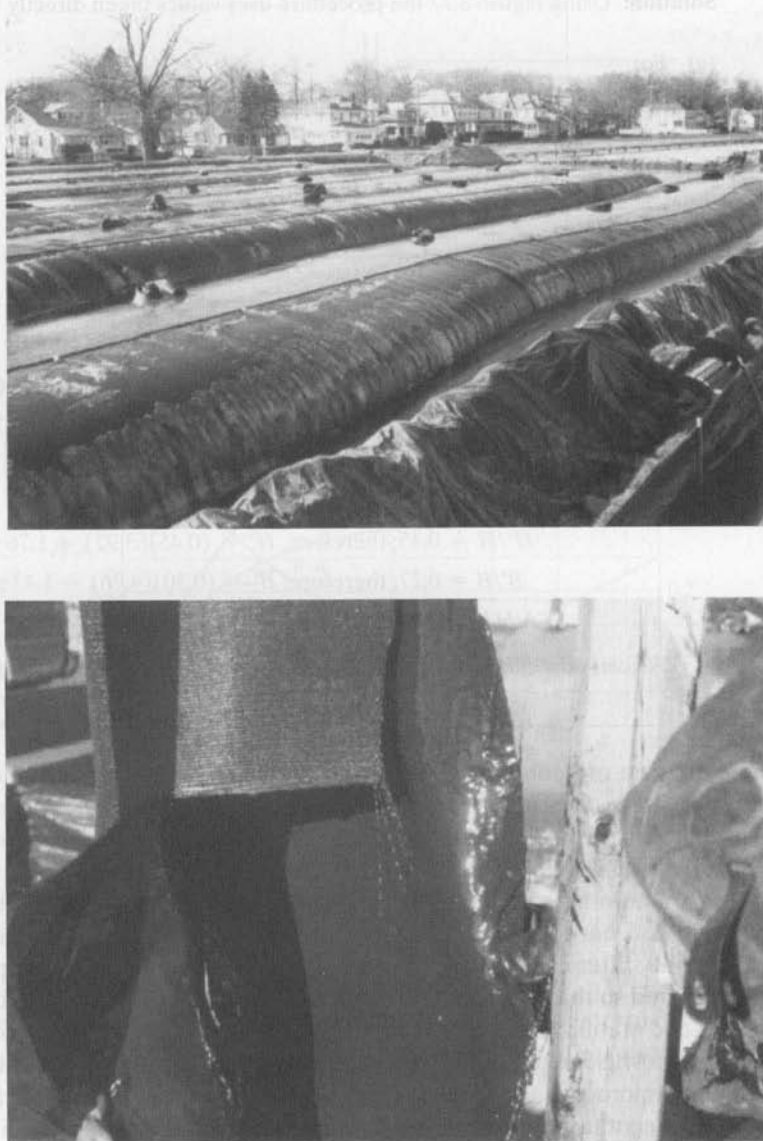
Figure 2.78   Dewatering of contaminated harbor bottom sediment using geotextile tubes (upper photograph) and the subsequent filter cake on the inside of the fabric (lower photograph).

Although the limnoria is a surface eroder and the mollusks are internal borers, it is extremely difficult to detect damage to wood piles by any of them through visual inspection until serious deterioration has occurred.

2. Concrete piles are subject to deterioration in the water and splash fluctuation zone, caused by the wet-dry, freeze-thaw cycles. Some concrete piles (both precast and cast-in-place) deteriorate below the mudline because of poor original placement techniques. This comes about from permeable or cracked concrete, which allows corrosion of the reinforcing steel and subsequent expansion and spalling of the concrete. It is also sometimes caused by a sulfite reaction of the concrete.

3. All types of steel pipes are subjected to corrosion, with average corrosion rates being 0.13 mm per year under normal conditions. However, this value can increase drastically under certain conditions. Values considerably higher have been measured, particularly under certain stress corrosion conditions.

The methods used for rehabilitation of piles are varied and constantly increasing in number. The oldest technique is to use metal forms, such as corrugated steel in half sections joined together by angles, attached to each of the half sections. Dockworkers and divers place, join, and seal the sections, which are used to contain cement grout, which bonds to the deteriorated pile section. This highly labor-intensive operation has led to the development of other, more economical techniques. Rigid plastic has been proposed as not only an economical form but as high-strength envelope to prevent further deterioration to the piling system. The annular space between the form and pile can be filled with either concrete grout or specially formulated epoxy. Another pile jacketing technique utilizes bituminized fiber forms. However, all of these systems have a problem with bottom closure and sealing when they are acting as a form and the pile is not to be jacketed down to the firm subsoils. Also, complex configurations are all but impossible to form when using rigid enclosures. It should be noted that built-up layers of epoxy or bituminous coatings have also been utilized to protect pilings from deterioration; however, most of these techniques involve hand-placement by divers, and a thorough coating of the piles is difficult and expensive to obtain.

In the 1960s, a technique was developed that utilizes geotextiles as a concrete-forming system [83]. Basically, this concept uses a geotextile jacket as a concrete form, with its lengthwise seam joined by a heavy industrial zipper prefabricated into the geotextile. The ends of the geotextile above and below the deteriorated pile zone are banded to the pile. These flexible geotextile forms possess economic advantages over other concrete-forming systems because of their light weight, ease of installation, adaptability to any configuration, relatively low cost, and ease of connection onto the piles at any location above the mudline. The geotextile is so designed that when concrete is injected into it, the excess water bleeds through the voids of the geotextile without allowing the cementatious portion to escape. This lowering of the water/cement ratio produces a dense surface of concrete to resist further deterioration of the pile. Typical installation procedures are illustrated in Figure 2.79.

The design procedure for this application is similar to other cases of using geotextiles as flexible-forming systems and will be described later. One departure worth
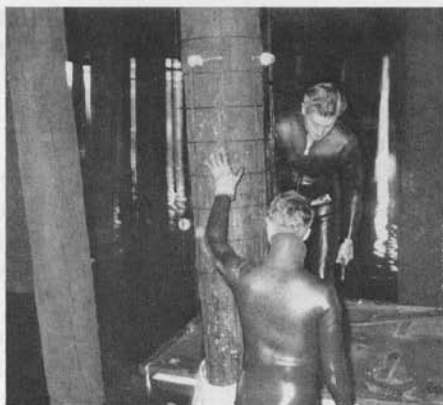
(a) Cleaning pile and placing reinforcement   (b) Banding geotextile to lower, sound pile

(c) Preparing geotextile for filling   (d) Completed pile restoration

Figure 2.79   Procedure for using geotextiles as flexible forms in pile jacketing reha-
bilitation work.

noting, however, is that elongation of the geotextile under load should be kept to a
minimum. Thus high-strength woven geotextiles are often used. As with other situa-
tions where grout is being pumped, high-strength seams meeting the required design
strength are necessary.

Bridge Pier Underpinning.   An estimate of foundation soil scour depth be-
neath shallow foundation bridge piers in rivers and streams is extremely difficult [160].
Even for bridge piers founded on rock, the rock often deteriorates and is scoured away
during floods that are accompanied by high-velocity water situations. The problem is so
severe that divers sometimes find that they can swim beneath the bridge pier itself [83].
(One has to wonder about the structural factor of safety under such circumstances!)

In a related problem, the Ambursen Hydraulic Company constructed a number of hollow-core, reinforced-concrete slab-and-buttress dams throughout the eastern and midwestern United States from 1910 until 1940. The dams consisted of flat concrete slabs positioned at 45° that were supported by vertical buttresses at 3.0 to 4.5 m spacing. Both the slabs and buttresses were relatively thin (e.g., 300 to 600 mm of reinforced concrete). Today, many of these dams are in need of repair, particularly at their buttress footing regions where compressive stresses are the highest.

Using fabrics as flexible forms, some very clever solutions to these difficult problems have been developed. Figure 2.80 illustrates a solution used by Welsh [161] for a number of scoured bridge piers. A geotextile tube is prefabricated to fit around the perimeter of the pier between the top of the stable foundation material and the bottom of the pier foundation. As grout inflation of the geotextile proceeds, pipes are placed to communicate from the outside of the pier to within the enclosure. After curing of the perimeter tube, injection of high-strength grout into the inside of the perimeter tube reestablishes the bearing capacity of the pier foundation. The previously installed pipes serve the dual function of allowing grout to enter the enclosure and allowing entrapped water to be displaced. The concrete cures as does typical tremie concrete placed under water.
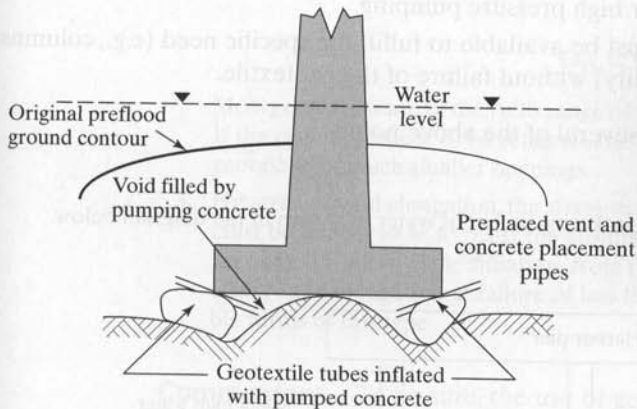
(a) Elevation view
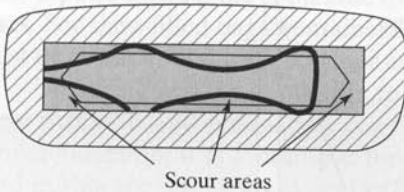
(b) Plan view

(c) Lower tube installed

(d) Completed system

Figure 2.80 Underpinning of scoured bridge pier using grout-filled geotextile forms. (After Welsh [161])

Erosion Control Mattresses. By taking two sheets of geotextile and joining them at discrete points, a form will result that can be pumped with grout to field fabricate a mattress that will conform to essentially any subsoil shape or grade. The thickness and geometry are controlled by internal spacer threads woven between the upper and lower sheets of geotextile. Thicknesses of up to 500 mm have been made with various configurations. Such mattresses must have firm soil subgrades (after curing they have no flexibility) and essentially no water to dissipate (most of the surface is covered). The articulating block mattresses shown in Figure 2.64(b) have significant advantages in this regard.

Design Procedures for Flexible Forming Systems. As shown in the preceding subsections, there are many applications for soil, grout, or concrete-filled geotextile forms. There are subtle differences between the designs, yet the basic design philosophy is quite similar. Regarding the geotextile design, the following points must be considered:

- Sufficient permeability or permittivity must be available to allow removal of water either within the forms or from within concrete or grout during its curing.
- Proper opening size of the geotextile must be present to prevent excessive loss of the soil, cement, or grout.
- Adequate strength must be available to prevent rupture of the geotextile and its seams, particularly under high pressure pumping.
- Adequate elongation must be available to fulfill the specific need (e.g., columns for mine or cavern stability) without failure of the geotextile.

Example 2.33 illustrates several of the above points.

Example 2.33

Design a geotextile for pile jacketing in 3 m of water as shown in the diagram below.
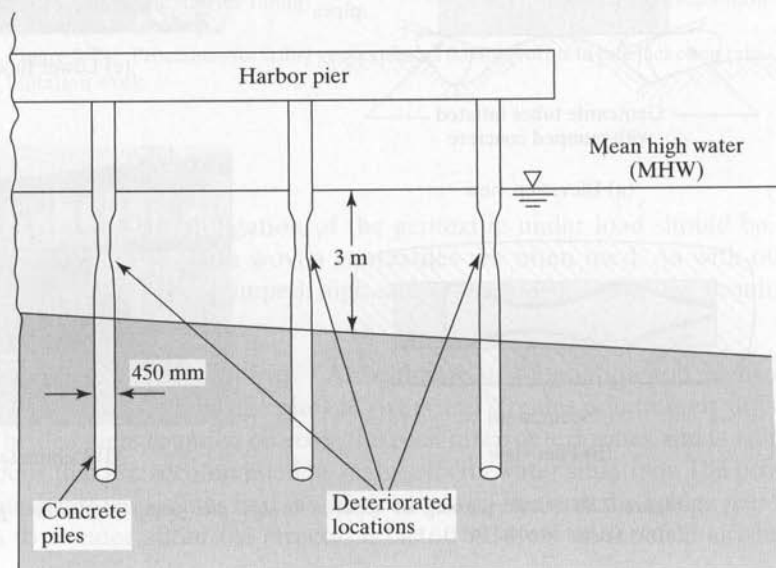
Solution: The three most important issues to be considered in the design follow:

1. For adequate permeability/permittivity, an estimate of the flow of water out of the geotextile during grouting is necessary. Using an estimated value of 0.2 m³/min, you can obtain the following:

$$q = kiA = \frac{k\,\Delta h A}{t}$$

$$\psi = \frac{k}{t} = \frac{q}{\Delta h A}$$

$$= \frac{0.2}{(3.0)\pi(0.45)(3.0)(60)}$$

$$\psi = 2.6 \times 10^{-4}\,\text{sec}^{-1}$$

Since most geotextiles are in the range of 10^{-1} to 10^{-3} sec^{-1} for their actual permittivity, there are many commercial geotextiles available.

2. For retention of grout mix, assume that d_{50} of sand is 0.4 mm and that it has a CU = 4.0; use

$$O_{95} < 9(d_{50})/\text{CU}$$

$$< \frac{(9)(0.40)}{4.0}$$

$$O_{95} < 0.9\,\text{mm}$$

Most geotextiles are in the AOS range of 0.1 to 0.5 mm, thus a wide range is available. If the cement paste is to be retained, the design is straightforward but will result in a geotextile of much smaller openings.

3. For strength and elongation, the stress-versus-strain curve of the candidate geotextile must be known so as to resist the grouting pressure and required elongation. This is very much a site-specific situation. Note that woven geotextiles with grab strength of 1000 N and elongation at failure of less than 15% are often used for geotextile flexible forms of this type.

Commentary.   To be sure, the use of geotextiles as flexible forming systems is an exciting concept simply waiting for new and innovative applications. Contrasted to other geotextile uses, the geotextile is sacrificial in most cases (e.g., when grout or concrete is placed within the geotextile form). Thus UV degradation is no problem in these cases. For sand-filled bags, containers, and tubes, however, it is a definite problem that must be considered during polymer and antioxidant selection.

The design of the geotextile follows nicely along lines of other geotextile systems. Strength and elongation considerations are invariably necessary along with proper filtration; it is a multiple-function situation. Thus the topic is being considered in this section. A good deal of future activity will undoubtedly be seen in this application of geotextiles, particularly in the areas of geotextile bags, containers, and tubes.

2.11 CONSTRUCTION METHODS AND TECHNIQUES USING GEOTEXTILES

2.11.1 Introduction

Although this book is devoted primarily to design issues, it is critically important to consider the constructability of the final design. All too often adequate designs have been negated by the inability to construct them or by use of improper construction methods. Of course, either situation can be disastrous as far as the final system is concerned.

Construction with geotextiles is not particularly difficult as long as it is remembered that the textile product being dealt with typically has a mass per unit area from 150 to 600 g/m^2—that is, it is not a steel-wire blasting mat! Most building contractors, heavy-construction contractors, land developers, and federal, state, and local construction forces that deal with other types of construction materials are well-equipped for handling geotextiles. In fact, it is most interesting to note the adaptability of these groups in devising new and clever geotextile deployment and installation procedures. Freely available literature by manufacturers is also extremely helpful in this regard. There are, however, certain areas where new and unique techniques are required, and these have been discussed in their specific sections. Most important are the reinforcement area (walls, embankments, and foundations), the reflective crack prevention area, and flexible forming systems.

One area that does require constant vigilance is that of ultraviolet (UV) light susceptibility. Contractors often fail to recognize that geotextiles can be literally destroyed by exposing them to prolonged sunlight, especially in southern climates. The work of Koerner et al. [58], originally commented on in Section 2.3.6, is reemphasized here to bring attention to this susceptibility. As was shown in Figure 2.28c and 2.28d, the strength and elongation of both polypropylene and polyester fabrics were drastically reduced when exposed to sunlight. In some cases more than 50% of the strength was lost within a few months. Clearly, there is the utmost need for the contractor to keep the geotextile in its protective plastic cover as long as possible and even perhaps to keep it in an enclosure. Once the roll is opened and the geotextile is placed in its final position, it must be backfilled *in a timely manner*. Unused portions of rolls or sampled rolls must be rerolled and suitably protected. The specification must be clear and the inspection rigid in this regard. There are numerous references available (for example, see Hsuan et al. [162]) as well as agency guidelines. The latter guidelines often estimate that 2 to 4 weeks is the maximum length of exposure unless the geotextile is of a unique type and/or especially stabilized. When the geotextile is UV-stabilized (generally using carbon black and/or high quality antioxidants in the polymer mixture), UV durability is increased, but certainly not indefinitely.

2.11.2 Geotextile Installation Survivability

Geotextile survivability refers to the ability of the geotextile to withstand handling, installation, and backfilling stresses. It is related to construction equipment, construction technique, substrate material, substrate condition, backfill material, backfill size and shape, and so on. Recall the levels of installation damage shown in Figure 2.20

and discussed in Section 2.3.5. Table 2.21 considers these features and rates general geotextile requirements of survivability in categories of low, moderate, high, very high, or not recommended. Depending on, and keyed into, these categories are a set of survivability requirements that are considered to be the minimum geotextile properties for necessary placement in the intended and final position. The numeric values of these survivability properties are given in Table 2.2(a). The classes corresponding to the requirements in Table 2.21 are as follows:

- Class 1 (highest values) ≃ "very high" to "high" survivability
- Class 2 (intermediate values) ≃ "high" to "moderate" survivability
- Class 3 (lowest) values ≃ "moderate" to "low" survivability

TABLE 2.21 REQUIRED DEGREE OF SURVIVABILITY AS A FUNCTION OF SUBGRADE CONDITIONS AND CONSTRUCTION EQUIPMENT*

Subgrade Conditions	Low ground-pressure equipment (≤25 kPa)	Medium ground-pressure equipment (> 25 kPa, ≤ 50 kPa)	High ground-pressure equipment (>50 kPa)
Subgrade has been cleared of all obstacles except grass, weeds, leaves, and fine wood debris. Surface is smooth and level so that any shallow depressions and humps do not exceed 450 mm in depth or height. All larger depressions are filled. Alternatively, a smooth working table may be placed.	Low	Moderate	High
Subgrade has been cleared of obstacles larger than small to moderate-sized tree limbs and rocks. Tree trunks and stumps should be removed or covered with a partial working table. Depressions and humps should not exceed 450 mm in depth or height. Larger depressions should be filled.	Moderate	High	Very high
Minimal site preparation is required. Trees may be felled, delimbed, and left in place. Stumps should be cut to project not more than ±150 mm above subgrade. Fabric may be draped directly over the tree trunks, stumps, large depressions and humps, holes, stream channels, and large boulders. Items should be removed only if placing the fabric and cover material over them will distort the finished road surface.	High	Very high	Not recommended

Diagonal bands: CLASS-3, CLASS-2, CLASS-1, CLASS-0

*Recommendations are for 150 to 300 mm initial lift thickness. For other initial lift thicknesses:

    300 to 450 mm: reduce survivability requirement one level;
    450 to 600 mm: reduce survivability requirement two levels;
    >600 mm: reduce survivability requirement three levels

For special construction techniques such as prerutting, increase the fabric survivability requirement one level.
Placement of excessive initial cover material thickness may cause bearing failure of the soft subgrade.
Source: After Christopher, Holtz, and DiMaggio [163].

While a Class 0 is not provided in Table 2.2(a), its values would be proportionately higher than Class 1. It should be emphasized that if the values in Table 2.21 exceed those calculated on the basis of functional design (as they sometimes will), the values in the table must be used. Thus calculated design properties do not always prevail.

2.11.3 Cost and Availability Considerations

Of prime importance to all involved with the candidate geotextile is its installed cost. Although this has been noticeably absent in the book because of changing price indices, site and climate variations, type and quantity of geotextile, and so on, a few comments are in order.

The cost of the geotextile itself is reasonably related to its mass per unit area. Heavier geotextiles cost proportionately more than lighter ones. Note, however, that the installation cost may not be significantly higher for the heavier geotextiles. The type of manufacture is also a factor, with woven slit-film types generally being the least expensive, then nonwoven heat-bonded and nonwoven needle-punched, and then woven monofilament types, which are the most expensive on the basis of an equivalent mass per unit area. These comments, however, should in no way sway a design toward preference of one geotextile over another. They are offered only to give a feeling for the costs involved. As of this writing, these costs ranged from $0.60 to $2.00 per square meter for geotextiles in the range 150 to 500 g/m^2, with installation costs being an additional $0.15 to $0.50 per square meter depending on the site conditions, quantity involved, and particular application.

It should also be recognized that geotextile availability is sometimes very important. In aggressively marketed areas, many geotextiles are available and the free-market system will sort things out. In more remote areas, however, where only one or two geotextiles are available, design must necessarily reflect this situation. It is totally unrealistic to think that manufacturers will tailor-make a geotextile to a design specification if it involves only a small quantity in a remote area. In a similar vein, labor unions have been known to affect costs, as have patent costs in a few select applications.

2.11.4 Summary

As with all construction materials, failures sometimes occur. In my personal investigations of geotextile-related failures, they primarily fall into the following groups:

1. *Construction related*: This is the largest group of failures with excessive ultraviolet degradation, installation damage, poorly constructed seams, and the lack of intimate contact being the major problems. This last issue is particularly important for filtration and erosion-control applications.
2. *Design/specification related*: Design failures per se have been relatively few. Some embankments on soft soils have had excessive deformations but they have generally been repaired on-site without insurance or litigation problems. Retaining walls backfilled with low permeability soils have been problematic (excessive deformations and collapse) particularly when adequate drainage has not been

provided. Specifications have often been lax and in many instances contributed to some of the construction-related failures mentioned before.

3. *Testing related*: There have been a number of testing-related problems, but no serious failures to my knowledge. The major concern in this regard is the use of literature values for interface shear strengths, instead of properly simulated direct shear tests. Such practices can lead to major problems. In spite of the concern over the lack of true performance tests, conservative reduction factors probably compensate for the shortcoming. In this regard, a designer should never apologize for using high reduction factors or high factors of safety.

4. *Product related*: Other than supplying the wrong product, and then accepting and installing same, product failures are sparse. The use of the MARV concept is certainly warranted and provides the needed safeguard against product variability. It also challenges the manufacturer to decrease product variability to the maximum extent possible.

While geotextile failures have indeed occurred, their number has been small in light of the number of installations. We certainly have an engineering material capable of being considered in a comparable manner with other materials conventionally used by civil engineers and related professions. Field performance to date, after more than 25 years of service life in a multitude of applications, has been excellent.

REFERENCES

1. Broms, B. B., "Triaxial Tests with Fabric-Reinforced Soil," *Proceedings of the International Conference on Soils and Textiles*, Paris, 1977, pp. 129–133.

2. Taylor, D. W., *Fundamentals of Soil Mechanics*, New York: Wiley, 1948.

3. Christopher, B. R., and Fischer, G. R., "Geotextile Filtration Principles, Practices and Problems," *Journal of Geotextiles and Geomembranes*, Elsevier, vol. 11, nos. 4–6, 1992, pp. 337–354.

4. *Report on Task Force 25*, Joint Committee Report of AASHTO-AGC-ARTBA, American Association of State, Highway and Transportation Officials, Washington, DC, January 1991.

5. Carroll, R. G., Jr., "Geotextile Filter Criteria," *Engineering Fabrics in Transportation Construction*, Transportation Research Record, Washington, DC, 1983, pp. 46–53.

6. Luettich, S. M., Giroud, J. P., and Bachus, R. C., "Geotextile Filter Design Guide," *Journal of Geotextiles and Geomembranes*, vol. 11, no. 4–6, 1992, pp. 19–34.

7. Haliburton, T. A., and Wood, P. D., "Evaluation of U.S. Army Corps of Engineers Gradient Ratio Test for Geotextile Performance," *Proceedings of Second International Conference Geotextiles*, August 1–6, 1982, IFAI, pp. 97–101.

8. Halse, Y., Koerner, R. M., and Lord, A. E. Jr., "Filtration Properties of Geotextiles Under Long-Term Testing," *Proceedings of* ASCE/PennDOT *Conference on Advances in Geotechnical Engineering*, Hershey, PA, April 1987, pp. 1–13.

9. Williams, N. D., and Abouzakhm, M. A., "Evaluation of Geotextile/Soil Filtration Characteristics Using the Hydraulic Conductivity Ratio Analysis," *Journal Geotextiles and Geomembranes*, Elsevier, vol. 8, no. 1, 1989, pp. 1–26.

10. Koerner, G. R., Koerner, R. M., and Martin, J. P., "Design of Landfill Leachate Collection Systems," *Journal of Geotechnical Engineering*, ASCE, vol. 120, no. 10, October 1994, pp. 1792–1803.

11. McGown, A., "The Properties of Nonwoven Fabrics Presently Identified as Being Important in Public Works Applications," *Index 78 Programme*, University of Strathclyde, Glasgow, Scotland, 1978.

12. Heerten, G., "A Contribution to the Improvement of Dimensioning Analogies for Grain Filters and Geotextile Filters," *Proceedings of the International Conference on Filters, Filtration and Related Phenomena*, Karlsruhe, Germany, 1992, pp. 110–122.

13. Giroud, J. P., "Granular Filters and Geotextile Filters," *Proceedings Geofilters '96*, edited by J. LaFleur and A. Rollin, 1996, pp. 565–680.

14. Gerry, G. S., and Raymond, G. P., "The In-Plane Permeability of Geotextiles," *Geotechnical Test Journal*, ASTM, vol. 6, no. 4, December 1963, pp. 181–189.

15. International Geosynthetic Society, Test Method Harmonization Committee, Brussels Belgium (see Web site at www.geosyntheticssociety.org).

16. "Textiles: Yarns, Fabrics and General Test Methods," *Annual Book of Standards*, Parts 31 and 32, West Conshohocken, PA: ASTM.

17. Kaswell, E. R., *Handbook of Industrial Textiles*. New York: West Point Peperell, 1963.

18. Booth, J. E., *Principles of Textile Testing*. London: Newnes-Butterworths, 1968.

19. Morton, W. E., and Heart, J. W., *Physical Properties of Textile Fibers*. New York: Wiley, 1975.

20. Haliburton, T. A., Fowler, J., and Langan, J. P., "Design and Construction of a Fabric Reinforced Test Section at Pinto Pass, Mobile, Alabama," *Transportation Research Record #79*, Washington, DC, 1980.

21. Myles, B., and Carswell, I., "Tensile Testing of Geotextiles," *Proceedings of the 3rd International Conference Geotextiles*, IFAI, 1986, pp. 713–718.

22. McGown, A., Andrawes, K. Z., and Kabir, M. H., "Load-Extension Testing of Geotextiles Confined in Soil," *Proceedings of the 2nd International Conference Geotextiles*, Aug. 1–6, 1982, IFAI, pp. 793–796.

23. McGown, A., Andrawes, K. Z., and Murray, R. T., "The Load-Strain-Time-Temperature Behavior of Geotextiles and Geogrids," *Proceedings of the 3rd International Conference on Geotextiles*, IFAI, 1986, pp. 707–712.

24. Wilson-Fahmy, R. F., Koerner, R. M., and Fleck, J. A., "Unconfined and Confined Wide Width Testing of Geosynthetics Used in Reinforcement Applications," edited by S. C. J. Cheng, STP 1190, ASTM 1993, pp. 49–63.

25. Wayne, M. H., Carey, J. E., and Koerner, R. M., "Epoxy Bonding of Geotextiles," *Journal of Geotextiles and Geomembranes*, vol. 9, no. 4–6, 1990, pp. 559–564.

26. Ashmawy, A. K., and Bourdeau, P. L., "Geosynthetic Reinforced Soils Under Repeated Loadings: A Review and Comparative Study," *Geosynthetics International*, vol. 2, no. 4, 1995, pp. 643–678.

27. Raumann, G., "A Hydraulic Tensile Test with Zero Transverse Strain for Geotechnical Fabrics," *Geotechnical Testing Journal*, ASTM, vol. 2, no. 2, June 1979, pp. 69–76.

28. Koerner, R. M., Monteleone, M. J., Schmidt, R. K., and Roethe, A. T., "Puncture and Impact Resistances of Geosynthetics," *Proceedings of the 3rd International Conference on Geotextiles*, IFAI, 1986, pp. 677–682.

29. Alfheim, S. L., and Sorlie, A., "Testing and Classification of Fabrics for Application in Road Construction," *Proceedings of the International Conference on Soils and Textiles*, vol. 2, 1977, pp. 333–338.

30. Murphy, V. P., and Koerner, R. M., "CBR Strength (Puncture) of Geosynthetics," *Journal of Geotechnical Engineering Testing*, ASTM, vol. 11, no. 3, September 1988, pp. 167–172.

31. Cazzuffi, D., and Venesia, S., "The Mechanical Properties of Geotextiles: Italian Standard and Interlaboratory Test Comparison," *Proceedings of the 3rd International Conference on Geosynthetics*, IFAI, 1986.

32. Ingold, T. S., "Some Observations on the Laboratory Measurement of Soil-Geotextile Bond," *Geotechnical Testing Journal*, ASTM, vol. 5, no. 3/4, 1982, pp. 57–67.

33. Koerner, R. M., "A Recommendation to Use Peak Shear Strengths for Geosynthetic Interface *Design*," *GFR*, vol. 21, no. 3, April 2003, pp. 28–30; Letters to the editor, *GFR*, vol. 21, no. 6, August 2003, pp. 14–15].

34. Marr, W. A., and Christopher, B., "Recommended Design Strength for Needle-punched GCL Products," *GFR*, vol. 21, no. 8, October/November 2003, pp. 18–23.

35. Martin, J. P., Koerner, R. M., and Whitty, J. E., "Experimental Friction Evaluation of Slippage between Geomembranes, Geotextiles and Soils," *Proceedings of the International Conference on Geomembranes*, June 20–24, 1984, IFAI, pp. 191–196.

36. Collios, A., Delmas, P., Gourc, J. P., and Giroud, J. P., "Experiments of Soil Reinforcement with Geotextiles," *Proceedings on the Use of Geotextiles for Soil Improvement*, ASCE, April 14–18, 1980, pp. 53–73.

37. Gourc, J. P., Faure, Y., Rollin, A., and LeFleur, J., "Standard Tests of Permittivity and Application of Darcy's Formula," *Proceedings of the 2nd International Conference on Geotextiles*, vol. 1, August 1, 1982, IFAI, pp. 149–154.

38. Holtz, R. D., *Mercury Intrusion Characterization of Geotextile Pore Size Distribution*, Report to Hoechst-Celanese Corp., Spartanburg, SC, 1988.

39. Bhatia, S. K., Smith, J. L., and Christopher, B. R., "Geotextile Characterization and Pore Size Distribution: Comparison of Methods and Applications to Design," *Geosynthetics International*, vol. 3, no. 3, 1996, pp. 301–328.

40. "Designing with Terram," Design Brochure from ICI Fibres, Ltd., Gwent, Wales.

41. McGown, A. W., "The Properties and Uses of Permeable Fabric Membranes," *Residential Workshop on Materials and Methods for Low Cost Roads and Reclamation Works*," 1976, pp. 663–710.

42. Dierickx, W., and Myles, B., "Wet Sieving as a European EN-Standard for Determining the Characteristic Opening Size of Geotextiles," *Recent Developments in Geotextile Filters and Prefabricated Drainage Geocomposites*, STP 1281, edited by Shobha K. Bhatia and L. David Suits, ASTM, 1996, pp. 54–64.

43. Hausmann, M., *Engineering Principles of Ground Engineering*. New York: McGraw-Hill, 1991.

44. Koerner, R. M., and Bove, J. A., "In-Plane Hydraulic Properties of Geotextiles," *Geotechnical Testing Journal*, ASTM, vol. 6, no. 4, 1983, pp. 190–195.

45. Koerner, R. M., Bove, J. A., and Martin, J. P., "Water and Air Transmissivity of Geotextiles," *Journal of Geotextiles and Geomembranes*, vol. 1, 1984, pp. 57–73.

46. Koerner, G. R., and Koerner, R. M., "The Installation Survivability of Geotextiles and Geogrids," *Proceedings of the 4th Conference on Geosynthetics*, Balkema, 1990, pp. 597–602.

47. Shrestha, S. C., and Bell, J. R., "Creep Behavior of Geotextiles Under Sustained Loads," *Proceedings of the 2nd International Conference on Geotextiles;* August 1–6, 1982, IFAI, pp. 769–774.

48. den Hoedt, G., "Creep and Relaxation of Geotextile Fabrics," *Journal of Geotextiles and Geomembranes*, vol. 4, no. 2, 1986, pp. 83–92.

49. Lawson, C. R., "Geosynthetics in Soil Reinforcement," *Proceedings of the Symposium on Geotextiles in Civil Engineering*, Institution of Engineers of Australia, July 1986, pp. 1–35.

50. Task Force #27, *Guidelines for the Design of Mechanically Stabilized Earth Walls*, AASHTO-AGC-ARTBA Joint Committee, Washington, DC, 1991.

51. Koerner, R.M., Hsuan, Y., and Lord, A. E., Jr., "Remaining Technical Barriers to Obtain General Acceptance of Geosynthetics," Inaugural Mercer Lecture, *Journal of Geotextiles and Geomembranes*, vol. 12, no. 1, 1993, pp. 1–52.

52. Ingold, T. S., Montanelli, F., and Rimoldi, P., "Extrapolation Techniques for Long-Term Strengths of Polymeric Geogrids," Proceedings of the 5th International Conference on Geosynthetics, Singapore, 1994, pp. 1117–1120.

53. Koerner, R. M., and Ko, F. K., "Laboratory Studies on Long-Term Drainage Capability of Geotextiles," *Proceedings of the 2nd International Conference on Geotextiles*, 1982, IFAI, pp. 91–95.

54. Wayne, M. H., and Koerner, R. M., "Correlation Between Long-Term Flow Testing and Current Geotextile Filtration Design Practice," *Proceedings of Geosynthetics '93*, IFAI, 1993, pp. 501–517.

55. Williams, N. D., and Abouzakhm, M. A., "Evaluation of Geotextile/Soil Filtration Characteristics Using the Hydraulic Conductivity Ratio Analysis," *Journal of Geotextiles and Geomembranes*, vol. 8, no. 1, 1989, pp. 1–26.

56. Luettich, S. M., and Williams, N. D., "Design of Vertical Drains Using the Hydraulic Conductivity Ratio Analysis," *Proceedings of the Conference on Geosynthetics*, IFAI, 1989, pp. 95–103.

57. Van Zanten, R. V. ed., *Geotextiles and Geomembranes in Civil Engineering*. Rotterdam: Balkema, 1986.

58. Koerner, G. R., Hsuan, Y., and Koerner, R. M., "Photo-Initiated Degradation of Geotextiles," *Journal of Geotechnical and Geoenvironmental Engineering*, ASCE, vol. 124, no. 12, December 1998, pp. 1159–1166.

59. Hsuan, Y. G., Koerner, R. M., and Lord, A. E., Jr., "A Review of the Degradation of Geosynthetic Reinforcement of Materials and Various Polymer Stabilization Methods," STP 1190, edited by S.C.J. Cheng, ASTM, 1993, pp. 228–244.

60. Halse, Y., Koerner, R. M., and Lord, A. E., Jr., "Effect of High Alkalinity Levels on Geotextiles—Part 1—$Ca(OH)_2$ Solutions," *Journal of Geotextiles and Geomembranes*, vol. 5 no. 4, 1987, pp. 261–282; Part 2—NaOH Solutions," *Journal of Geotextiles and Geomembranes*, vol. 6, no. 4, 1987, pp. 295–305.

61. Hsieh, C. W., Lin, C. K., and Chiu, Y. F., "The Strength Properties of Geotextiles in Ocean Environments," *Proceedings of EuroGeo3*, Munich, 2004, pp. 377–382.

62. Koerner, G. R., and Koerner, R. M., "Leachate Flow Rate Behavior Through Geotextile and Soil Filters and Possible Remediation Methods," *Journal of Geotextiles and Geomembranes*, vol. 11, no. 4–6, 1992, pp. 401–430.

63. Koerner, G. R., Koerner, R. M., and Martin, J. P., "Geotextile Filters Used for Leachate Collection Systems: Testing, Design of Field Behavior," *Journal of Geotechnical Engineering*, ASCE, vol. 120, no. 10, October 1994, pp. 1792–1803.

64. Gourc, J.-P., and Faure, Y.-H., "Soil Particles, Water and Fibers—A Fruitful Interaction Now Controlled," *Proceedings of the 4th International Conference on Geosynthehics*, 1990, pp. 949–972.

65. Voskamp, W., and Risseeuw, P., "Method to Establish the Maximum Allowable Load Under Working Conditions of Polyester Reinforcing Fabrics," *Journal of Geotextiles and Geomembranes*, vol. 6, 1988, pp. 173–184.

66. Giroud, J. P., "Designing with Geotextiles," *Mater. Const.* (Paris), vol. 14, no. 82, 1981, pp. 257–272; reprinted in *Geotextiles and Geomembranes, Definitions, Properties, and Designs*. vol. 1, IFAI, 1984, pp. 5–40.

67. Koerner, G. R., "Long-Term Benefit Cost Performance and Analysis of Geotextile Separators in Pavement Systems," *Proceeding of the Geosynthetics '97 Conference*, IFAI, 1997, pp. 701–713.

68. Suits, L. D., and Koerner, G. R., "Site Evaluation/Performance of Separation Geotextiles," *Proceedings of the Geosynthetics '01 Conference*, IFAI, 2001, pp. 451–468.

69. Hausmann, M. R., "Fabric Reinforced Unpaved Road Design Methods—Parametric Studies," *Proceedings of the 3rd International Conference on Geosynthetic*, 1986, IFAI, pp. 19–24.

70. Giroud, J. P., and Noiray, L., "Design of Geotextile Reinforced Unpaved Roads," *Journal of Geotechnical Engineering* ASCE, vol. 107, no. GT9, September 1981, pp. 1233–1254.

71. Barenberg, E. J., and Bender, D. A., "Design and Behavior of Soil-Fabric-Aggregate Systems," paper presented at 57th Transp. Research Board Meeting, June 1978.

72. Holtz, R. D., and Sivakugan, K., "Design Charts for Roads with Geotextiles," *Journal of Geotextiles and Geomembranes*, vol. 5, no. 3, 1987, pp. 191–200.

73. Diaz, V., "Thread Selector for Geotextiles," *Geotechnical Fabrics Report*, vol. 3, no. 1, January-February, 1985, IFAI, pp. 15–19.

74. Diaz, V., *Field Seaming of Geotextiles*, IFAI, 1989.

75. Proksch, H., "German Experiences with the Replacement of Granular Frost Blankets by Other Types of Construction," *Proceedings of the 3rd International Conference on the Structural Design of Asphalt Pavements*, London, 1972, pp. 115–125.

76. Sayward, J. M., *Evaluation of MESL Membrane—Puncture, Stiffness, Temperature, Solvents*, Rep. 76–22, June 1976, Cold Regions Research at Engineering Laboratory, U.S. Army, Hanover, NH.

77. Bell, J. R., and Yoder, E. J., "Plastic Moisture Barrier for Highway Subgrade Protection," *Proceedings of the Highway Research Board*, vol. 36, 1957, pp. 713–735.

78. Smith, N., "Techniques for Using MESL in Roads and Airfields in Cold Regions," ASCE *Conference on Cold Regions Technology*, Anchorage, May 17–19, 1978.

79. Smith, N., and Pazsint, D. A., *Field Test of a MESL Road Section in Central Alaska*, Technical Report 260, Cold Regions Research at Engineering Laboratory, U.S. Army, Hanover, NH, July 1975.

80. Lawson, C. R., and Ingles, O. G., "Long-Term Performance of MESL Road Sections in Australia," *Proceedings of the 2nd International Conference on Geotextiles*, August 1–6, 1982, IFAI, vol. 2, pp. 535–539.

81. Meader, A. L., Jr., "Construction of Geomembranes in Place by Spraying an Elastomer over a Geotextile," *First International Conference on Geomembranes*, June 20–24, 1984, IFAI, vol. 2, pp. 389–393.

82. Murray, C. D., "Simulation Testing of Geotextile Membranes for Reflection Cracking," *Proceedings of the 2nd International Conference on Geotextiles*, August 1–6, 1982, IFAI, vol. 2, pp. 511–516.

83. Koerner, R. M., and Welsh, J. P., *Construction and Geotechnical Engineering Using Synthetic Fabrics*. New York: Wiley, 1980.

84. Lord, A. E., Jr. and Koerner, R. M., "Fundamental Aspects of Chemical Degradation of Geomembranes," *International Conference on Geomembranes*, June 20–24, 1984, IFAI, vol. 2, pp. 293–298.

85. Lawson, C. R., and Ingles, O. G., "Water Repellency Requirements for Geomembranes," *International Conference on Geomembranes*, June 20–21, 1984, IFAI, vol. 2, pp. 169–173.

86. Hoffman, G. L., and Shamon, M. E., *Premature Failure of Permeable Subbase Pavement Sections Incorporating Geotextiles*, Pennsylvania Department of Transportation, Harrisburg, PA, April 5–6, 1984.

87. Broms, B. B., "Design of Fabric Reinforced Retaining Structures," *Proceedings of the Symposium on Earth Reinforcement*, ASCE, 1978, Pittsburgh, PA, pp. 282–303.

88. Steward, J. E., Williamson, R., and Mohney, J., "Earth Reinforcement," In *Guidelines for Use of Fabrics in Construction and Maintenance of Low Volume Roads*. Portland, OR: U.S. Forest Service, June 1977, ch. 5.

89. Whitcomb, W., and Bell, J. R., "Analysis Techniques for Low Reinforced Soil Retaining Walls," *Proceedings of the 17th Engineering Geology Symposium*, Moscow, ID, April 1979, pp. 35–62.

90. Lee, K. L., Adams, B. D., and Vagneron, J. M. J., "Reinforced Earth Retaining Walls," *Journal of Soil Mech. Fdtn. Eng. Div.*, ASCE, No. SM10, October 1973, pp. 745–764.

91. Bell, J. R., Stilley, A. N., and Vandre, B., "Fabric Retained Earth Walls," *Proceedings of the 13th Engineering Geology Symposium*, Moscow, ID, April 1975, pp. 115–126.

92. Jarrett, P. W., and McGown, A., eds., *Proceedings on the Application of Polymeric Reinforcement in Soil Retaining Structures*, Royal Military College, 1988.

93. Naval Facilities Manual *DM-7.2*, Bureau of Yards and Docks, U. S. Navy, April 1982.

94. Broms, B. B., "Polyester Fabric as Reinforcement in Soil," *Proceedings of the International Conference on Soils and Textiles*, Paris, 1977, vol. 1, pp. 129–135.

95. Koerner, R. M., *Construction and Geotechnical Methods in Foundation Engineering*. New York: McGraw-Hill, 1984.

96. Barrett, R. K., "Geotextiles in Earth Reinforcement," *Geotechnical Fabrics Report*, vol. 3, no. 2, March/April 1985, pp. 15–19.

97. Allen, T. M., Christopher, B. R., and Holtz, R. D., "Performance of a 12.6 m High Geotextile Wall in Seattle, Washington," *Proceedings Geosynthetic Reinforced Retaining Walls*, edited by J. T.H. Wu, Rotterdam: A. A. Balkema, 1992, pp. 81–100.

98. Stevens, J. B., and Souiedan, B., "Geotextile Wall Aids Bridge Construction," *Geotechnical Fabrics Report*, vol. 8, no. 3, 1990, pp. 10–15.

99. Richardson, G. N., and Behr, L. H. Jr., "Geotextile-Reinforced Wall: Failure and Remedy," *Geotechnical Fabrics, Report*, vol. 6, no. 4, 1988, IFAI, pp. 14–18.

100. Collin, J. G., ed., *Design Manual for Segmental Retaining Walls (Modular Concrete Block Retaining Wall Systems)*, 2nd ed. Herndon, VA: National Concrete Masonry Association, 1996.

101. Elias, V., Christopher, B. R., and Berg, R. R., *Mechanically Stabilized Earth Walls and Reinforced Soil Slopes: Design and Construction Guidelines*, NHI-00-043, Federal Highway Administration, U.S. Department of Transportation, Washington, DC 2001.

102. Koerner, G. R., Koerner, R. M., and Elias, V., "Geosynthetic Installation Damage Under Two Different Backfill Conditions," STP 1190, edited by S. C. J. Cheng. ASTM, 1993, pp. 163–184.

103. Kaniraj, S. R., "Direction and Magnitude of Reinforcement Force in Embankments on Soft Soil." In *Earth Reinforcement*, edited by Ochiai, Yasufuku and Omine, Rotterdam: A. A. Balkema, 1996, pp. 221–225.

104. Andrawes, K. Z., McGown, A., Wilson-Fahmy, R. F., and Mashhour, M. M., "The Finite Element Method of Analysis Applied to Soil-Geotextile Systems," *Proceedings of the 2nd International Conference on Geotextiles*, IFAI, vol. 2, 1982, pp. 690–700.

105. Rowe, R. K., "Reinforced Embankments: Analysis and Design," *Journal Geotechnical Engineering Division, ASCE*, vol. 110, no. 2, February 1984, pp. 231–246.

106. Rowe, R. K., and Soderman, K. L., "Comparison of Predicted and Observed Behavior of Two Test Embankments," *Journal of Geotextiles and Geomembranes*, vol. 1, 1984, pp. 143–160.

107. Rowe, R. K., and Soderman, K. L., "The Role of Finite Element Analyses," *Journal of Geotextiles and Geomembranes*, vol. 6, no. 1–3, 1987, pp. 53–80.

108. Haliburton, T. A., Fowler, J., and Langan, J. P., *Design and Construction of a Fabric Reinforced Test Section at Pinto Pass, Mobile, Alabama*, no. 79, Washington, DC, Transportation Research Record 1980.

109. Fowler, J., "Theoretical Design Considerations for Fabric Reinforced Embankments," *Proceedings of the 2nd International Conference on Geotextiles*, 1982, IFAI, pp. 665–676.

110. Sprague, C. J., and Koutsourais, M., "The Evolution of Geotextile Reinforced Embankments," no. 30, edited R. H., Borden, R. D. Holtz, and I. Juran, ASCE, 1992, pp. 1129–1141.

111. Koerner, R. M., Hwu, B-L., and Wayne, M. H., "Soft Soil Stabilization Designs Using Geosynthetics," *Journal of Geotextiles and Geomembranes*, vol. 6, no. 1–3, 1987, pp. 33–52.

112. Koerner, R. M., and Uibel, B. L., "Hydraulic Fill Embankments Utilizing Geosynthetics," *Proceedings of the ASCE Conference on Hydraulic Fill Structures '88*, Colorado State University, ASCE, 1988.

113. Koerner, R. M., Fowler, J., and Lawrence, C. A., *Soft Soil Stabilization Study for Wilmington Harbor South Dredge Material Disposal Area*, U.S. Army Engineer Waterways Experiment Station, GL-86-38, December 1986.

114. Humphrey, D. N., "Current Design Methods," discussion, *Journal of Geotextiles and Geomembranes*, vol.6, no. 1–3, 1987, pp. 89–92.

115. Guglielmetti, J. L., Koerner, G. R., and Battino, F. S., "Geotextile Reinforcement of Soft Landfill Process Sludge to Facilitate Final Closure," *Journal of Geotextiles and Geomembranes*, vol. 14, nos. 7/8, July/August 1996, pp. 377–392.

116. Binquet, J., and Lee, K. L., "Bearing Capacity Tests in Reinforced Earth Slabs," *Journal of Geotechnical Engineering*, ASCE, Vol. 101, No. GT12, Dec. 1975, pp. 1241–1255.

117. Binquet, J., and Lee, K. L., "Bearing Capacity Analysis of Reinforced Earth Slabs," *Journal Geotechnical Engineering*, ASCE, vol. 101, no. GT12, December 1975, pp. 1257–1276.

118. Guido, V. A., Biesiadecki, G. L., and Sullivan, M. J., "Bearing Capacity of a Geotextile Reinforced Foundation," *Proceedings of the 11th International Society Soil*, San Francisco, 1985, vol. 3, pp. 1777–1780.

119. British Standard Code of Practice, "Strengthened/Reinforced Soils and Other Fills," BS 8006, 1995, London, pp. 97–121.

120. Han, J., and Akins, K., "Use of Geogrid Reinforced and Pile Supported Earth Structures," *Proceedings of the International Deep Foundations Congress*, ASCE, 2002, pp. 668–679.

121. Shen, C. K., Bang, S., and Herrman, L. R., "Ground Movement Analysis of Earth Support System," *Journal of Geotechnical Engineering*, ASCE, Vol. 107, No. GT12, Dec. 1981, pp. 1609–1624.

122. Koerner, R. M., "Slope Stabilization Using Anchored Geotextiles: Anchored Spider Netting," *Proceedings of Specialty Geotechnical Engineering for Roads and Bridges*, PennDOT, Harrisburg, PA, 1984, pp. 1–11.

123. Koerner, R. M., "In-Situ Soil Slope Stabilization Using Anchored Nets," *Proceedings of the Conference on Low-Cost and Energy-Saving Construction Materials*, July 1984. Envo Publishing, pp. 465–478.

124. Myles, B., and Bridle, R. J., "Fired Soil Nails." In *Proceedings of the Earth Reinforcement Practice*, edited by H. Ochiai, S. Hayashi and J. Otani, A. A. Balkema, 1992, pp. 509–514.

125. Lambe, T. W., and Whitman, R. V., *Soil Mechanics*. New York: Wiley, 1969.

126. Koerner, R. M. and Robins, J. C., "In-Situ Stabilization of Soil Slopes Using Nailed Geosynthetics," *Proceedings of the 3rd Conference on Geosynthetics*, IFAI, 1986, pp. 395–399.

127. Ghiassian, H., Hryciw, R. D., and Gray, D. H., "Laboratory Testing Apparatus for Slopes Stabilized by Anchored Geosynthetics," *Geotechnical Testing Journal*, ASTM, vol. 19, no. 1, March 1996, pp. 65–73.

128. Ghiassian, H., Gray, D. H., and Hryciw, R. D., "Seepage Considerations and Stability of Sandy Slopes Reinforced by Anchored Geosynthetics," *Proceedings of Geosynthetics '97*, IFAI, 1997, pp. 581–593.

129. Cedegren, H. R. *Seepage, Drainage and Flow Nets*. New York: Wiley, 1967.

130. Bell, J. R., and Hicks, R. G., *Evaluation of Test Methods and Use Criteria for Geotechnical Fabrics in Highway Applications*, Final Report, FHwA, Contract No. DOT-FH-119353, Oregon State University, Corvallis, OR, 1984.

131. Richardson, G. R., and Middlebrooks, P., "A Simplified Design Method for Silt Fences," *Proceedings Geosynthetics '91 Conference*, IFAI, 1991, pp. 879–885.

132. Roth, H., "Filter Fabric for Improving Frost Susceptible Soils," *Proceedings of the International Conference on Soils and Textiles*, April 20–22, 1977, vol. 1, pp. 23–28.

133. Anderson, O., "The Use of Plastic Fabric for Pavement Protection During Frost Break," *Proceedings of the International Conference on Soils and Textiles*, April 20–22, 1977, vol. 1, pp. 143–149.

134. Gamski, K., and Rigo, J.M., "Geotextile Soil Drainage in Siphon or Siphon-Capillarity Conditions," *Proceedings of the 2nd International Conference on Geotextiles*, August 1–6, 1982, IFAI, Vol. 1, pp. 145–452.

135. Clough, I. R., and French, W. J., "Laboratory and Field Work Relating to the Use of Geotextiles in Arid Regions," *Proceedings of the 2nd International Conference on Geotextiles*, August 1–6, 1982, IFAI, pp. 447–452.

136. Button, J. W., Epps, J. A., Lytton, R. L., and Harmon, W. S., "Fabric Interlayer for Pavement Overlays," *Proceedings of the 2nd International Conference on Geotextiles*, August 1–6, 1982, IFAI, pp. 523–528.

137. Majidzadeh, K., Luther, M. S., and Skylut, H., "A Mechanistic Design Procedure for Fabric-Reinforced Pavement Systems," *Proceedings of the 2nd International Conference on Geotextiles*, August 1–6, 1982, IFAI, pp. 529–534.

138. The Asphalt Institute, *Asphalt Overlays and Pavement Rehabilitation*, Manual Series No. 17 (MS-17), College Park, MD, November 1977.

139. Cedergren, H. R., *Seepage, Drainage, and Flow Nets*. New York: Wiley, 1989.

140. Bell, J. R., Jr., "Designing with Geosynthetics," unpublished course notes of R. M. Koerner and J. R. Bell, 1983 to 1985.

141. Personal communication from Maine Department of Transportation, 1994.

142. Ahlrich, R. C., "Evaluation of Asphalt Rubber and Engineering Fabrics as Pavement Interlayers," GL-86-34, Vicksburg, MS: U.S. Army Corps of Engineers, 1986.

143. Conference Proceedings, on "Reflective Cracking in Pavements" *RILEM International Union of Testing and Research Laboratories for Materials and Structures*, 1989, 1993, and 1996.

144. Newby, J. E., "Southern Pacific Transportation Corporation Utilization of Geotextiles in Railroad Subgrade," *Proceedings of the 2nd International Conference on Geotextiles*, August 106, 1982, IFAI, pp. 467–472.

145. Einsenmann, J., and Leykauf, G., "Investigation of a Nonwoven Fabric Membrane in Railway Track Construction," *Proceedings of the International Conference on Soils and Textiles*, April 20–22, 1977, pp. 41–45.

146. Saxena, S. K., and Wang, S., "Model Test of a Rail-Ballast-Fabric-Soil System," *Proceedings of the 2nd International Conference on Geotextiles*, August 1–6, 1982, IFAI, pp. 495–500.

147. Bosserman, B., "Reviewing Geotextiles at FAST," *Railroad Track and Structures*, June 1981, pp. 42–58.

148. Raymond, G., "Geotextiles for Railroad Bed Rehabilitation," *Proceedings of the 2nd International Conference on Geotextiles*, August 1–6, 1982, IFAI, pp. 479–484.

149. Chrismer, S. M., and Richardson, G. R., "In-Track Performance of Geotextiles at Caldwell, Texas," No. 1071, Transportation Research Board, Washington, DC, 1986, pp. 72–80.

150. Terzaghi, K., and Lacroix, Y., "Mission Dam: An Earth and Rockfill Dam on a Highly Compressible Foundation," *Geotechnique*, vol. 1964, pp. 13–50.

151. Leshchinsky, D., and Leshchinsky, O., "Geosynthetic Confined Pressurized Slurry (GeoCoPS)," Technical Report, CPAR-GL-96-1, U.S. Army Corps of Engineers, Washington, DC, September 1996.

152. Zirbel, R., "Sand-Filled Tubes Used in Beach Protection Plan," *World Dredging Marine Construction*, 1975, pp. 28–39.

153. Lawson, C., "Geotextile Containment—International Perspectives," *Proceedings GRI-17 Conference on Hot Topics in Geosynthetics IV*, GII Publ., 2003, pp. 178–201.

154. Pilarczyk, K. W., "Application and Design Aspects of Geocontainers," *Proceedings Geosynthetics '97*, IFAI, pp. 147–160.

155. Fowler, J., American Society of Civil Engineers "Geotubes and Geocontainers for Hydraulic Applications," *Proceedings of Cleveland Section ASCE*, Cleveland, OH, 1995.

156. den Adel, H., Henrickse, C.S.H., and Pilarczyk, K. W., "Design and Application of Geotubes and Geocontainers." In *Proceedings Geosynthetics: Application, Design and Construction*, edited by M. B. deGroot, G. den Hoedt, and R. J. Termaat. Rotterdam: A. A. Balkema, 1996, pp. 925–932.

157. Gaffney, D. A., and Austin, D. N., "Engineering with Geotextile Tubes," *Proceedings of GRI-17 Conference on Hot Topics in Geosynthetics IV*, GII Publ., Folsom, PA, 2003, pp. 202–210.

158. Heibaum, M., ed., "Special Issue on Geotextile Containers," *Journal of Geotextiles and Geomembranes*, vol. 20, no. 5, October 2002, pp. 279–342.

159. Hwang W., and Koerner R.M., "An Amendment Strategy for Enhancing the Performance of Geotextile Tubes used in Decontamination of Polluted Sediments and Sludges," *Proceedings of the GRI-18 Conference, GeoInstitute of ASCE*, 2005, pp. 282–289.

160. National Academy of Engineering, *Scour at Bridge Waterways*, NCHRP Publication 5, Highway Research Board, Washington, DC, 1970.

161. Welsh, J. P., "PennDOT Uses a New Method for Solving Scour Problems Beneath Bridge Piers," *Highway Focus*, vol. 9, no. 1, May 1977, pp. 72–81.

162. Hsuan, Y. G., Koerner, R. M., and Soong, Y.-T., "Behavior of Partially Ultraviolet Degraded Geotextiles," *Proceedings of the 5th International Conference on Geosynthehics*, Sept. 5–9, 1994, pp. 1209–1212.

163. Christopher, B. R., Holtz, R. D., and DiMaggio, J. A., *Geotextile Engineering Manual*, No. DTFH 61-80-C-00094, Washington, DC Federal Highway Administration 1984.

PROBLEMS

2.1. A shopping center site developer has $15,000 available to purchase a geotextile to be used as a separator between subgrade soil and stone base, and the total area to be covered is 2.5 ha. Which of the following would the developer probably use?
   (a) 165 g/m^2 fabric at $0.75/m^2
   (b) 200 g/m^2 fabric at $0.85/m^2
   (c) 250 g/m^2 fabric at $0.95/m^2

2.2. Given available funds of $7500, how many linear meters of pipe underdrain trench could be covered with geotextile if it is 2.5 m wide and costs $0.95/m^2 in place?

2.3. Review the Pennsylvania Department of Transportation specification given in Table 2.1.
   (a) For erosion-control geotextiles, when would you use Type A versus Type B?
   (b) For sediment-control geotextiles, when would you use Type A versus Type B?

2.4. Assuming that the values listed in the specifications of Table 2.1 are MARV and that one standard deviation of a particular geotextile is 8%, convert them (with exception of AOS and UV strength retention) to the following:
 (a) Average (mean) roll values
 (b) Minimum values at $\bar{x} - 3\sigma$

2.5. Review the statistics involved in the discussion of Figure 2.1:
 (a) Define mean and standard deviation.
 (b) For a normally distributed behavior, what percentage of total occurrences falls between $\bar{x} \pm s$; $\bar{x} \pm 2s$; and $\bar{x} \pm 3s$?

2.6. Each class of geotextile in Table 2.2(a) was subdivided according to the elongation at break of 50%. Where do the following types of fabrics fall in this regard?
 (a) Woven slit-film
 (b) Woven monofilament
 (c) Nonwoven heat-bonded
 (d) Nonwoven needle-punched

2.7. Compare the Pennsylvania Department of Transportation Specification values given in Table 2.1 against the AASHTO M288 Class 2 values listed in Table 2.2(a) for the following:
 (a) Subsurface filtration versus Table 2.2(b)
 (b) Separation versus Table 2.2(c)
 (c) Erosion control—Type A versus Table 2.2(e)
 (d) Sediment control—Type A versus Table 2.2(f)

2.8. Using the M288 specification of Table 2.2, determine what geotextile properties are needed for the following applications under severe installation conditions.
 (a) Woven monofilament erosion control geotextile under stone riprap for soil subgrade of 65% passing the 0.075 mm sieve size
 (b) Unsupported woven geotextile silt fence
 (c) Nonwoven needle-punched geotextile for prevention of reflective cracking as a paving fabric

2.9. In the description of "designing-by-function" (Section 2.1.3), what would be the estimated range of required factors of safety for the following situations:
 (a) A highway underdrain in the shoulder area of a secondary road
 (b) A filter fabric behind a retaining wall, above which is a paved parking lot
 (c) A reinforcing fabric for an access road on which cranes will be setting structural steel
 (d) A filter to protect a chimney drain within an earth dam where a small town is located downstream

2.10. In designing-by-function (recall Section 2.1.3) the focus is on the primary function. How do we know what is primary? (*Hint*: Would the resulting factors of safety from various aspects of the problem be indicative in any way?)

2.11. In Section 2.2, separation was distinguished from reinforcement. In the case of geotextiles placed on soil subgrades beneath stone base courses for highways, when does the geotextile act as a separator vis-a-vis reinforcement?

2.12. Regarding liquid flow situations:
 (a) In Section 2.2, filtration was distinguished from drainage. Describe these two functions and how they are different.
 (b) In handling flow for these two different functions, ψ and θ were defined. Why is this necessary and why is the thickness of the geotextile included in each term?

2.13. Using Figure 2.4(a), determine what is the appropriate opening size formula for the following steady-state flow conditions.
 (a) Gravel with $C'_U = 5$ in a dense condition.
 (b) Stable sand favoring retention with $C'_U = 2.5$ in a loose condition.
 (c) Sandy silt that is nonplastic favoring permeability, widely graded $C'_U > 15$ and in a medium-density state.

2.14. Using Figure 2.4(b), determine what is the appropriate opening size formula for the following dynamic flow conditions.
 (a) Clayey (plastic) soil that is nondispersive.
 (b) Silty sand that is widely graded ($C_U = 13$) under mild water current.
 (c) Gravel under severe wave attack.

2.15. In geotextile testing:
 (a) What is an index test?
 (b) What is a performance test?
 (c) How can typical laboratory-test values be made into allowable values for design-by-function procedure?

2.16. Calculate the compressibility modulus and the compressibility coefficient of the four geotextiles shown in Figure 2.6. (*Note*: The thickness change must be converted to strain using original fabric thickness measured at 2.0 kPa.)

2.17. Determine the strength, maximum elongation, toughness, and initial tangent modulus of fabrics A, B, C, and E shown in Figure 2.7 in both geotextile units and standard engineering units.

2.18. Concerning the different geotextile tensile test specimen shapes shown in Figure 2.8:
 (a) Estimate the tensile strength in units of kN/m for a woven geotextile for the various shapes shown if the grab strength is 30 kN.
 (b) Estimate the tensile strength in units of kN/m for a nonwoven, needle-punched geotextile for the various shapes shown if the grab strength is 20 kN.

2.19. Comparing results of wide-width tests in-isolation versus under confinement, calculate the modulus of elasticity, the maximum stress (strength), and the elongation at failure for each of the geotextiles shown in Figure 2.11a–d. Prepare your answers in table form, calculate percentages of improvement from the in-isolation case, and describe why the major improvement is with the needle-punched nonwovens.

2.20. Concerning the type of puncture probe used in evaluating puncture resistance of geotextiles as described in Section 2.3.3, why should (a) a large-diameter probe be used for nonwovens and (b) a beveled probe used for wovens?

2.21. You have been given the following set of data from a soil-geotextile friction test:

| Normal Stress (kPa)	Shear Strength (kPa)
17	8.6
35	20
70	36
140	75

 (a) Plot the Mohr failure envelope.
 (b) Obtain the friction angle.
 (c) Calculate the fabric efficiency based on a soil friction angle of 38°.

2.22. Calculate the porosity of the following geotextiles:

Geotextile	Mass/unit area (g/m^2)	Unit Weight (kN/m^3)	Density (kN/m^3)	Thickness (mm)
A	135	4.7	480	0.33
B	200	6.0	610	0.38
C	350	5.5	560	0.63
D	600	6.0	610	1.32

2.23. What is an "image analyzer," and how could it be used to determine fabric porosity?

2.24. Given the projection of a woven monofilament geotextile shown below, determine its percent open area (POA). (*Hint*: You will have to enlarge the figure considerably. A photocopier used a number of times will get you to a convenient size to use cross section paper or a planimeter.)
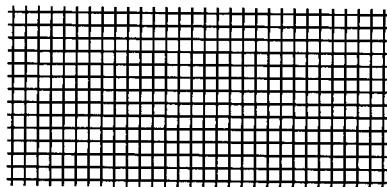
2.25. The apparent opening size test described in Section 2.3.4 is very controversial. There are three versions described in the literature; dry sieving (ASTM D4751), wet sieving (ISO 12956) and hydrodynamic sieving (used in Germany). Make a table describing the advantages and disadvantages.

2.26. If a series of glass bead sieve tests (either dry or wet) gave the following O_{95} values in mm, what would be the AOS sieve size value?

Geotextile	O_{95} (mm)
A	0.87
B	0.415
C	0.079

2.27. You have been given the following data for constant-head cross-plane flow of water through a 50 mm diameter, 0.30 mm thick geotextile. Calculate the permittivity (s^{-1}) and coefficient of permeability (cm/s).

Δh(mm)	q (cm^3/min.)
31	300
62	680
125	1010
250	1400

2.28. You have been given the following constant-head data for planar flow of water in a 1.50 mm thick geotextile that is 300 mm wide by 600 mm long. Calculate the transmissivity in m^3/min-m of fabric and then the planar coefficient of permeability in cm/sec.

Δh(mm)	q (cm^3/min.)
75	21
150	41
225	60
300	79

2.29. You have been given the following constant-head data set for radial flow of water in a 1.02 mm thick geotextile that has a 57 mm outer radius and a 28.7 mm inner radius. Calculate the transmissivity in m^3/min-m of fabric and the planar coefficient of permeability in cm/sec.

Δh(mm)	q (cm^3/min.)
150	1400
300	2900
450	4500
600	6000

2.30. Assume the data from Problem 2.29 were taken at normal pressure on the fabric of 7 kPa and the test was repeated at 14, 28, and 56 kPa, giving the additional data shown below. Plot the transmissivity (m^3/min-m) versus applied normal pressure (kN/m^2) response curve.

Pressure (kPa)	Δh(mm)	q (cm^3/min.)
14	150	820
	300	1730
	450	2500
	600	3500
28	150	570
	300	1220
	450	1730
	600	2250
56	150	540
	300	1080
	450	1650
	600	2200

2.31. What is the range of factors of safety for installation damage for the data shown in Figure 2.20b in Regions A, B and C?

2.32. Calculate the strain of the polyester fabric shown in Figure 2.21 at the end of 30 years, assuming a linear extension of the data for both 20% and 60% of failure loads.

2.33. Review the long-term flow tests in Section 2.3.5:
  (a) Describe the physical phenomena that accompany the various portions of the long-term flow behavior shown in Figure 2.24b.
  (b) Which of these phenomena is most important as to the possibility of the response shutting off flow completely?

2.34. Review the gradient ratio tests in Section 2.3.5:
  (a) In the gradient ratio test, head is measured via plastic tubing attached to a manometer board. Since it is this value that is most important in calculating the gradient ratio, what experimental problems could you envision?
  (b) In Figure 2.25, why is the value 3.0 used to separate acceptable and nonacceptable fabrics?

2.35. Concerning clogging of geotextiles in the field:
  (a) What are the main soils and conditions where excessive clogging of geotextiles is likely to occur?
  (b) In such instances, what is the logical recommendation?

2.36. The type of clogging described in Sections 2.3.5 had to do with various soils upstream of the fabric and water as the permeant. If the permeant was a liquid with a large amount of suspended solids and microorganisms in it (e.g., farm runoff or landfill leachate), what possible mechanisms of clogging could occur?

2.37. How would you evaluate the chemical resistance of a geotextile to a hazardous waste leachate of which there is no standard test data? (Recall Section 2.3.6.)

2.38. What specific portions of the ultraviolet light spectrum are damaging to polymeric materials? (Recall Section 2.3.6.) What wavelength is most sensitive to the various polymers used to manufacture geosynthetics?

2.39. How do manufacturers avoid, or minimize the harmful effects of ultraviolet degradation to exposed geotextiles?

2.40. How would you predict the *exposed* lifetime of a geotextile on the basis of accelerated weathering (ultraviolet, temperature, and moisture) laboratory-test data?

2.41. Regarding lifetime prediction of geosynthetics that are covered in a timely manner:
  (a) Devise an experiment for evaluating the long-term lifetime of a PP geotextile to be used for a reinforced wall application.
  (b) Devise the same experiment, but now for a PET geotextile.

2.42. If the ultimate strength of a geotextile from an index-type test is 45 kN/m, determine the allowable strength for the design purposes according to Table 2.11 for the following:
  (a) Separation
  (b) Reinforced embankment
  (c) Increased bearing capacity
  (d) Flexible forming system

2.43. If the ultimate flow rate of a geotextile from an index-type test is 18 l/min-m, determine the allowable flow rate for design purposes according to Table 2.12 for the following:
  (a) Gravity drainage problems
  (b) Pressure drainage problems

2.44. If the ultimate permittivity of a geotextile from an index-type test is 1.2 sec^{-1}, determine the allowable value for design purposes according to Table 2.12 for the following:
   (a) Retaining-wall filter
   (b) Highway-underdrain filter
   (c) Filter beneath rock riprap
   (d) Filter above leachate collection system

2.45. What are the mechanical properties of a geotextile that are of most importance when using it as a separator in an unpaved road situation with only stone base above it and relatively firm soil below it?

2.46. Regarding geotextiles used in separation:
   (a) What is the required burst pressure of a geotextile supporting 75 mm maximum-size stone and heavy trucks with a tire inflation pressure of 1000 kPa? Use $p \simeq 0.75 p_a$, a cumulative reduction factor of 2.0, and a factor of safety of 2.0.
   (b) What is the required burst pressure of a geotextile under the same conditions in part (a) except that now the road will haul only light vehicles of tire inflation pressure of 500 kPa.

2.47. What would be the influence on a burst analysis if well-graded stone base were used instead of poorly graded aggregate materials?

2.48. Redo Example 2.9 (in Section 2.5.3) on the basis that slippage does occur between the stone and geotextile. In your analysis assume that the $f(\epsilon)$-values mobilized are 75%, 30%, and 10%. Plot these values together with the 52% strain versus required grab tensile strength.

2.49. What is the factor of safety for a geotextile with allowable puncture strength of 250 N according to ASTM D 4833, considering a 600 kPa tire inflation pressure and relatively large stone of 30 mm size. The following types of stone come from different quarries, as described in Table 2.13.
   (a) Angular
   (b) Subrounded
   (c) Rounded

2.50. What is the factor of safety for a geotextile with ultimate puncture strength of 350 N according to ASTM D 4833, (use $\Pi RF = 2.5$) considering a 700 kPa tire inflation pressure and relatively small stone of 15 mm size. The following types of stone come from different sources, as described in Table 2.13:
   (a) Angular
   (b) Subrounded
   (c) Rounded

2.51. The data in Table 2.13 for protrusion factors, scale factors, and shape factors are limited in scope and quite subjective.
   (a) What other variables besides shape and size of the puncturing object might be important?
   (b) What type of laboratory experiment could be developed to authenticate the values?

2.52. Regarding impact resistance, determine what energy is mobilized by rock of 150 mm size falling out of a dump truck 1.5 m to the geotextile, if the geotextile rests on the following:
   (a) A "soft" soil of unsoaked $CBR = 3$
   (b) A "firm" soil of unsoaked $CBR = 9$
   (c) A "hard" soil of unsoaked $CBR = 16$

2.53. What energy is mobilized by a 250 N jackhammer falling 2.0 m out of a dump truck onto a geotextile on a "hard" soil of unsoaked $CBR = 20$? Would this situation cause a problem?

2.54. Regarding geotextiles for use in unpaved roads:
  (a) When using geotextiles as reinforcement for unpaved roads on soft subsoils, do they also act as separators?
  (b) If the answer to part (a) is yes, of what benefit is it?
  (c) From product literature, or simply gut feeling, what does this separation function amount to as far as thickness of stone base saved (if any) is concerned?

2.55. Regarding soil subgrade characteristics for roadway construction:
  (a) Describe the details of the CBR test (both unsoaked and soaked versions).
  (b) Using Table 2.14 for a soil whose CBR = 1.0, determine what the equivalent is in the following:
    • Shear strength
    • *R* value (California)
    • *S*, soil support value
    • Group index
    • *R* value (Washington)
    • Cone index (320 mm^2 probe)
    • Bearing value (300 mm plate, 5 mm deflection)
    • Bearing value (760 mm plate, 2.5 mm deflection)
    • Modulus of subgrade reaction
  (c) In Table 2.14 why do the ASTM, AASHTO, and FAA classifications not go down as far as CBR = 1.0?

2.56. You have been given a 80-kN axle-load vehicle with tire inflation pressure of 480 kPa undergoing a rut depth of 0.3 m for an unpaved road. The base course thickness is to be designed without a geotextile, then with a geotextile using Figure 2.37, and ultimately resulting in trends of thickness of stone aggregate to be saved:
  (a) What is the response for 340 passages without and with a 90-kN/m modulus geotextile? Draw the response curve to varying soil CBR values from 0.5 to 4.0.
  (b) What is the response for 340 passages and a $CBR = 1.0$? Draw the response curve for varying geotextile moduli from 450 kN/m to 10 kN/m.
  (c) What is the response for a soil of CBR = 1.0 and a geotextile modulus of 90 kN/m? Draw the response curve to a varying number of vehicle passages from 10,000 to 10.

2.57. Evaluate the sensitivity of varying rut depths (the value S in equation 2.38) on the required thickness of stone base using typical values for unpaved road problems. Plot your results. (*Hint*: It would help to go to the original reference by Giroud and Noiray [70] to gain insight into this aspect of the development.)

2.58. Using equation (2.39) in Example 2.14 of Section 2.6.1, plot the required thickness of stone base of an unpaved road as a function of CBR varying from 0.50 to 10. Use 25 kN equivalent single wheel loads for 10,000 coverages on a 300 × 450-mm tire contact area in your solution.

2.59. Regarding the sewing of geotextile seams:
  (a) What type of test would you use to evaluate the strength of a sewn seam?
  (b) In writing a specification for sewing of seams, what items would you include?
  (c) If you recommended a minimum tensile strength for the seam, what percentage of the minimum tensile strength of the geotextile would you recommend?
  (d) How would you conduct field tests for strength of sewn seams?

2.60. MESLs are usually constructed by in situ impregnation of geotextiles.
   (a) Why is in situ spraying preferred over prefabricated systems?
   (b) Why are geomembranes (Chapter 5) generally not used?
   (c) Why are needle-punched nonwovens generally used over other manufactured styles of fabrics?

2.61. Regarding the waterproofing of geotextiles for MESL construction:
   (a) What is an asphalt emulsion, and how does it waterproof after being sprayed onto a geotextile?
   (b) What is an asphaltic cement, and how does it work vis-a-vis an emulsion?
   (c) What are cutbacks, and why are they not recommended for impregnating MESLs?
   (d) How can you determine the proper quantity needed to saturate the geotextile?

2.62. In Example 2.16 (Section 2.6.2) concerning MESLs, the water content of the encapsulated soil varied only 0.8% over the conditions stated. If this soil were known to become unstable at 18% moisture content, what variations of input parameters could bring it about?

2.63. Obtain information on and briefly describe the water vapor transmission test (ASTM E96). Include comments on how the test would be different when evaluating a relatively thick impregnated geotextile to be used in construction of a MESL as opposed to when evaluating thin geomembranes films.

2.64. For geotextiles to be used to reinforce paved roads on firm soil subgrades, the geotextile must somehow be prestressed (recall Section 2.6.3).
   (a) Why is this the case?
   (b) Sketch some methods for prestressing geotextiles for such an application.
   (c) In light of your answer above, consider creep and possible stress relaxation, and postulate the road system's long-term performance.

2.65. The concept of flexible wall systems, as opposed to rigid concrete and masonry walls, is very much in style. List advantages and disadvantages of each type.

2.66. Regarding geotextile reinforced walls (this is an extremely long problem):
   (a) Design an 5.5 m high wraparound geotextile wall carrying a road consisting of 300 mm stone base ($\gamma = 22$ kN/m^3) and 150 mm asphalt ($\gamma = 24$ kN/m^3) for 180 kN dual-tandem-axle loads whose wheel pattern is shown in Example 2.18 (Section 2.7.1). The wall is to be backfilled with SW-ML soil of $\gamma = 18$ kN/m^3, $\phi = 35°$, and $c = 0$. The geotextile to be used is a nonwoven heat-bonded fabric of 200 g/m^2 with an ultimate tensile strength of 50 kN/m. Use reduction factors 1.2, 2.5, and 1.26 for installation damage, creep, and chemical/biological degradation, respectively.
   (b) Check and/or modify your answer to part (a) for external stability considering that the foundation soil is ML-CL with $\gamma = 19$ kN/m^3, $\phi = 15°$, $\delta = 0.95\phi$, $c = 24$ kPa, and $c_a = 0.90$ c.

2.67. Develop a design chart similar to Figure 2.48 for the wheel load and backfill of Problem 2.66, for vertical faced walls ($\beta = 90°$) and for wall heights varying from 1.5 to 8.0 m and geotextile allowable tensile strengths of 20, 40, 60, and 80 kN/m. (*Note:* This is another extremely long problem and even requires a computer program to be generated.)

2.68. In Examples 2.19 and 2.20 (Section 2.7.2) where geotextiles are used to stabilize embankments, the fabric's allowable tensile strength is 40 kN/m. Repeat this problem using a single fabric whose allowable strength varies from 20, 40 (the example), 80, 150, and 300 kN/m and plot the resulting FS-value against allowable strength:

2.69. Concerning the allowable geotextile strength to be used in stabilization problems (both for walls and embankments):
  (a) What tensile test method should be used?
  (b) What considerations enter into your choice of reduction factors?
  (c) How does creep enter into the situation?

2.70. A 15 m high embankment has a slope angle of $\beta = 40°$. The soil strength parameters are $\phi = 22°$ and $c = 15$ kPa in both the embankment and foundation sections. The unit weight is 16 kN/m^3. For a failure circle located at coordinates of $(+3, +18)$ with respect to the toe at $(0, 0)$ (see Figure 2.50) and a radius of 21 m, what is the factor of safety? How many layers of geotextiles spaced 300 mm apart and having an allowable tensile strength of 55 kN/m placed at the interface of the foundation and the embankment are required to raise this factor of safety to 1.40?

2.71. For Problem 2.70, find the minimum factor of safety for both the nonreinforced and reinforced conditions. (*Note:* This is a very long problem requiring a search of both variation in radius and center of circle. A computer program is necessary.)

2.72. In using high-strength geotextiles for areal stabilization projects as described in Section 2.7.3, how do you sew the transverse seams after the larger panels are already deployed? Furthermore, how do you sew the intersection where the four panels come together?

2.73. In placing fill on a high-strength geotextile used to stabilize very soft soils by the linear fill method, Section 2.7.3 mentioned the outer edges being placed first in the Wilmington Harbor South Disposal Area project. Why is this necessary? What would happen if the entire fill were advanced together? What would happen if the center were advanced first?

2.74. Describe by means of a sketch how you would instrument a high-strength geotextile of the type mentioned in Section 2.7.3 for the linear fill to verify the various design models shown in Figure 2.54.

2.75. There is considerable appeal to the use of geotextiles to improve the bearing capacity of shallow foundations (Section 2.7.4). Most efforts are aimed at showing improvement in bearing capacity as indicated in Figure 2.56.
  (a) Why are the improvements low at low deformations and considerably better at high deformations?
  (b) How could the low-deformation behavior be improved?
  (c) By observing these data, would you consider using only one high-strength geotextile instead of a number of lower-strength layers?
  (d) If the answer to (c) is yes, how would you join the geotextile ends and sides?

2.76. Regarding improved bearing capacity:
  (a) Would a geotextile placed under a large mat foundation measuring 30 × 30 m on a compressible soil prevent (total) settlement?
  (b) If the answer to (a) is no, would it be of any help insofar as reinforcement is concerned?

2.77. What is the required wide-width tensile strength of a geotextile used for basal reinforcement (recall equations 2.60 a and b) spanning between stone column deep foundations under the following conditions. Use ultimate conditions for partial load factors.
  • Column center-to-center distance = 4.0 m
  • Column diameter = 1.5 m
  • Embankment height over columns = 2.0 m

- Embankment soil unit weight $= 18$ kN/m^3
- Surcharge load above embankment $= 20$ kN/m^2
- Allowable strain in geotextile $= 10\%$

2.78. Regarding the "spider netting" of Section 2.7.5:
  (a) Illustrate the various mechanisms that soil nails can provide in soil slope stabilization.
  (b) What are the high-stress regions of the net as currently configured?
  (c) Why must the nails be continually driven into the ground even after initial installation?

2.79. The geotextile is exposed on the surface of the slope in spider netting. What advantages and disadvantages occur?

2.80. What are the three essential features that must be addressed in filtration design?

2.81. What is the difference in total active earth pressure between the two retaining wall cases shown in the diagram below? One has good drainage; the other has no drainage and full hydrostatic head.
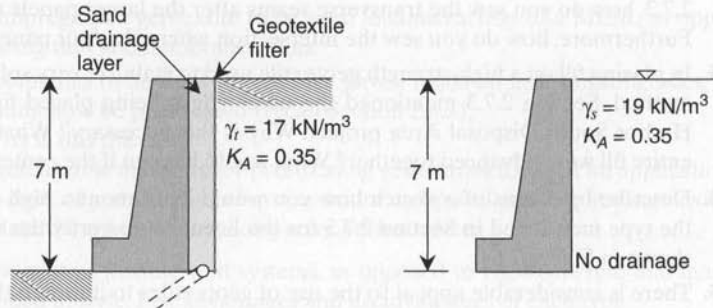
2.82. **(a)** In considering hydraulic designs involving geotextiles, why is permittivity used in filtration, and transmissivity used in drainage, rather than just the respective permeability (hydraulic conductivity) coefficients?
  (b) In the laboratory determination of a specific geotextile's permittivity or transmissivity, at what pressure should the geotextile's thickness be measured?

2.83. A stone aggregate has been placed around a highway underdrain with a geotextile.
  (a) What is the major function of the geotextile?
  (b) If properly designed, what should be the long-term condition of the stone base?
  (c) If the stone base has sufficient open space to transmit the entering water, of what necessity is the perforated pipe?
  (d) What is a French drain?

2.84. A geotextile filter is being considered to protect the stone aggregate drain behind a cantilever retaining wall, as shown in Figure 2.62a and 2.62b. The wall stem is 7.5 m high, retaining an ML soil with $k = 2.5 \times 10^{-4}$ m/s, $d_{50} = 0.05$ mm, CU $= 4.8$, and $D_R = 85\%$. The candidate geotextile is a heat-bonded nonwoven with a permittivity $(\psi) = 0.01$ sec^{-1} and an AOS $=$ No. 70 sieve. What is the factor of safety against flow and the adequacy as far as soil retention is concerned?

2.85. If the required permittivity of a sandy soil beneath a rock riprap-protected slope is 0.052 sec^{-1} slope and riprap covers 75% of the geotextile's surface, would a geotextile of $k = 3.5 \times 10^{-4}$ m/s and 0.65 mm thick be adequate? What is the factor of safety in this case?

2.86. Concerning geotextile silt fences:
   (a) While geotextile silt fences function as filters, Section 2.8.6 focused mainly on strength considerations. Why is strength so important?
   (b) How do geotextile silt fences filter the turbid water and retain the suspended soil particulates?
   (c) Discuss UV degradation of silt fences in light of their use as erosion and sedimentation control systems.

2.87. Recalculate Example 2.25 of Section 2.8.6 using the same values, except vary the storm intensity from 10, 50, 100 (the example problem), and 200 mm/hour to determine the following:
   (a) Height of the silt fence
   (b) Strength of the geotextile
   (c) Type of posts to be used for support

2.88. Regarding the drainage capability of geotextiles:
   (a) Which manufactured style is best suited to convey water in its plane?
   (b) What conditions are required to satisfy Darcy's formula?
   (c) What is the driving mechanism for water flow in gravity drainage situations?
   (d) What are some driving mechanisms for water flow in pressure drainage situations?

2.89. Geotechnical engineers are generally reluctant to use drainage geotextiles as chimney drains and drainage galleries, as shown in the earth dam Example 2.26 of Section 2.9.3. What are some reasons for this reluctance?

2.90. For the 8 m high concrete cantilever retaining wall of Example 2.27 (Section 2.9.3), recalculate the soil's permeability to determine what value is required to have the $\theta_{allow} = 0.00015$ m^2/min be adequate with FS = 4.0 (i.e., work the problem backward).

2.91. Repeat Example 2.28 illustrating pressure drainage of the consolidating soil beneath a surcharge fill (Section 2.9.4), where $B = 30$ m. Vary the time for the surcharge fill to be placed from 1 day to 1 year. Plot the results and show on the graph the acceptable zone based on FS = 5.0.

2.92. A geotextile is being used as a capillary migration break, as in Section 2.9.5:
   (a) What is to prevent the water from continuing across the barrier as though it were not there?
   (b) Does the fact that geotextiles are hydrophobic play a role in this situation?
   (c) If soil particles become clogged in the fabric structure and accumulate, does the situation change?
   (d) How might you prevent the situation in (c) from occurring?

2.93. There are some areas where full-pavement-width geotextiles should not be used in reflective crack prevention, as per Section 2.10.2. Describe why this is so for each of the following cases.
   (a) Where subsoil foundation problems exist beneath the stone base
   (b) For reinforced or nonreinforced concrete pavements
   (c) In areas of rapid and harsh cyclic freeze-thaw temperature conditions

2.94. Regarding the proper quantity of sealant for geotextile in reflective cracking applications:
  (a) Why is sealant in excess of saturation a problem?
  (b) Why is sealant less than saturation a problem?

2.95. In the reflective crack prevention discussed in Section 2.10.2, where reinforcement is assumed to be the primary function, the FEF is of paramount interest.
  (a) What is FEF?
  (b) How is it determined?
  (c) What geotextile property is it mainly dependent on?
  (d) What are the dangers in taking laboratory-generated data and using it to project field performance?

2.96. Regarding geotextiles in reflective cracking where reinforcement is assumed to be the primary function, as described in Section 2.10.2:
  (a) Using $DTN_N = 200$ and CBR values varying from 2 to 20, what is the nonreinforced value of t_A using Figure 2.69?
  (b) Using $DTN_N = 200$ and a geotextile resulting in FEF = 4.0, what is t_A if the CBR varies from 2 to 20?
  (c) Plot the two resulting curves on a graph of t_A versus CBR and comment on the results and the differences between the curves.

2.97. Postulate on the mechanism(s) that might occur in assuming waterproofing to be the major function in using geotextiles to prevent reflective cracks in asphalt pavements.

2.98. Regarding geotextiles in reflective cracking assuming moisture barrier as the primary function as described in Section 2.10.2:
  (a) Using $DTN_N = 500$ and $x = 1.57$ mm, $s = 0.15$ mm, $f = 0.80$, and $c = 1.25$, determine the asphalt overlay thickness according to Figure 2.70.
  (b) Using a fabric assumed to function as a waterproofing barrier, redo (a) for c varying from 2.5 to 0.5 in equation (2.75).
  (c) Plot the results on a graph of T_o versus c and comment on the curves and the differences.

2.99. Design and sketch a field experiment for determining whether reinforcement or waterproofing is the major function in using fabrics as preventing reflective cracks in asphalt overlays.

2.100. Regarding reflective-crack prevention using narrow strips of high-strength fabric reinforcement:
  (a) Fiberglass geotextiles have some distinct advantages and potential disadvantages over polymeric materials. What are they?
  (b) How does one anchor the sides of the geotextile strip on each side of the crack?
  (c) Are transverse or longitudinal cracks the most troublesome in old pavements? Why?

2.101. List the functions (in order of priority) that you feel are acting when geotextiles are placed beneath railroad ballast in the following situations:
  (a) New railroad track construction
  (b) Remediation of existing railroad trackage

2.102. Comment on why most railroad specifications call for thick needle-punched nonwovens and most laboratory-generated research papers use relatively thin wovens or heat-bonded nonwovens.

2.103. Regarding geotextiles used as railroad ballast separators:

(a) In the geotextile photographs shown in Figure 2.71, a few of the larger holes were probably not caused by abrasion. What was their most likely cause, and which ones were they?

(b) What is the minimum depth at which a geotextile should be placed beneath the bottom of a railroad tie to prevent abrasion problems?

2.104. In the use of geotextiles as flexible forms for columns in mine stabilization or pile jacketing (Section 2.10.4), will the resulting shape be circular? If not, why?

2.105. For the fabric used as a flexible form in mine stabilization such as that shown in Figure 2.73, what type, dimensions, and properties of geotextile should be considered?

2.106. As in Section 2.10.4, a geotextile tube has dimensionless parameters $b_1 = 10.5$ m and $S = 26.2$ m (thus, $b_1/S = 0.40$) (see Figure 2.77).

(a) What would be the necessary allowable strength of the geotextile if a FS $= 1.25$?

(b) Using $\Pi RF = 1.50$, what would be the necessary ultimate strength?

(c) Determine the geotube's dimensions B, H, H', B' and A.

2.107. In the geotextile tube shown in Figure 2.76b, is the fabric tensile strength critical? If not, estimate the longitudinal seam's efficiency as a percentage of nonseamed fabric tensile strength. (*Hint*: Recall Figure 2.12.)

2.108. In the dewatering of fine materials using geotextile tubes as shown in Figure 2.78, what could be done to reduce the negative impact of the low permeability filter cake?

2.109. If the fine sediment pumped into a geotextile tube for dewatering (as shown in the photograph of Figure 2.78) was contaminated, what two characteristics of the pollutant(s) are critical in assessing whether or not the pollutants escape with the effluent water?

2.110. Regarding the use of geotextiles as flexible forms:

(a) Is there any limit to the depth at which tremie concrete or grout can be placed under water?

(b) When placed in geotextile forms, how is the water displaced and the concrete or grout kept in?

(c) After the concrete or grout has set (hardened), what is the function of the geotextile?

2.111. Concerning the geotextile survivability concepts discussed in Section 2.11.2 and Table 2.21, what minimum mechanical properties would be required in the following cases using the specification of Table 2.2a?

(a) 35 kPa construction equipment using average site preparation

(b) Same as in (a), except no site preparation has been provided

(c) 20 kPa construction equipment on a dredged site with no vegetation or growth

2.112. What general and specific methods does the design engineer have with respect to the contractor regarding the proper care and handling of geotextiles during the installation process?

3

Designing with Geogrids

3.0   INTRODUCTION

The geotextiles discussed in Chapter 2 and the geogrids discussed in this chapter compete for use in numerous reinforcement applications. They are also designed by similar

methods but they differ in their manufacture, appearance, properties, and placement. A geogrid can be defined as follows:

> *Geogrid*: A geosynthetic material consisting of connected parallel sets of intersecting ribs with apertures of sufficient size to allow strike-through of surrounding soil, stone, or other geotechnical material.

Thus, geogrids are matrixlike materials with large open spaces called *apertures*, which are typically 10 to 100 mm between *ribs* that are called *longitudinal* and *transverse*, respectively. The ribs themselves can be manufactured from a number of different materials, and the rib cross-over joining or junction-bonding methods can vary. The primary function of geogrids is clearly reinforcement; thus sections within this chapter are organized not by function but by type of reinforcement application. In those applications where the direction of the major stresses are known, as in walls and slopes, *unidirectional,* or *uniaxial, geogrids* are used. In those where the applied stresses come from random directions, as in pavements and foundations, *bidirectional,* or *biaxial, geogrids* are used.

Figure 3.1 illustrates the three categories of geogrids that are currently available: (1) unitized polyolefin, (2) coated yarn, and (3) polyester rod (or strap). These categories will be explained in some detail, as will the testing related to their method of manufacture.

Figure 3.1(a) shows the original type of geogrids, which are characterized as being unitized insofar as the continuity of the intersecting longitudinal and transverse ribs are concerned. Both unidirectional and bidirectional products are available (recall Figure 1.7). Each style begins as a polyolefin polymer sheet (that is, a thick geomembrane) that subsequently has a uniform and controlled pattern of holes punched in it. The punched sheet is then sent over and under a number of rollers, each going faster than the one before it, thus inducing longitudinal stretching of the sheet. The elongated material between holes becomes the geogrid's ribs. In the unidirectional deformed products, circular holes punched in high density polyethylene (HDPE) sheet become elongated ellipses with stretched longitudinal ribs in the machine direction and unstretched transverse ribs in the cross machine direction. The eventual draw ratio is as high as 15 to 1. The molecular structure in the longitudinal ribs is highly elongated and the strength, modulus, and resistance to creep are increased significantly over the original nondeformed material. A number of different styles with different strength properties are available. In the bidirectional products, squares are punched in a polypropylene (PP) sheet, which is then drawn longitudinally (using rollers) as before, then transversely (using a stretcher), forming near-square or rectangular apertures. This process increases strength in both longitudinal and transverse directions in bidirectional products. Unidirectional products are for applications in which the major principal stress direction is known (such as walls and slopes), and bidirectional products are for applications in which mobilized stresses are essentially random (such as pavements and foundations).
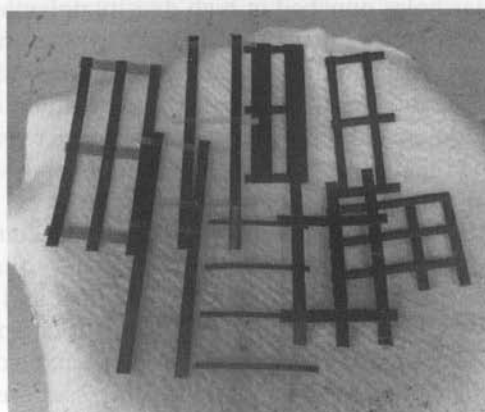
Figure 3.1(b) shows a variety of coated yarn geogrids. There are more products in this category of geogrids than any other. Most often, the yarns are bundles of high tenacity polyester (PET) filaments. (The side walls of automobile and truck tires are
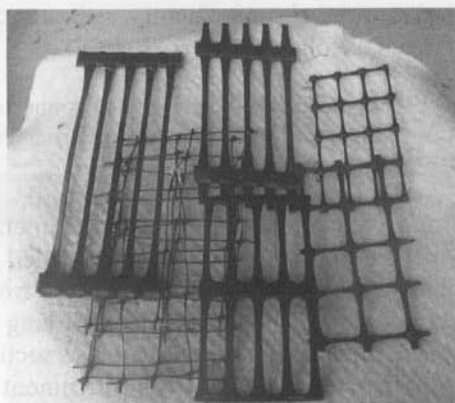
(a) Unitized polyolefin geogrids
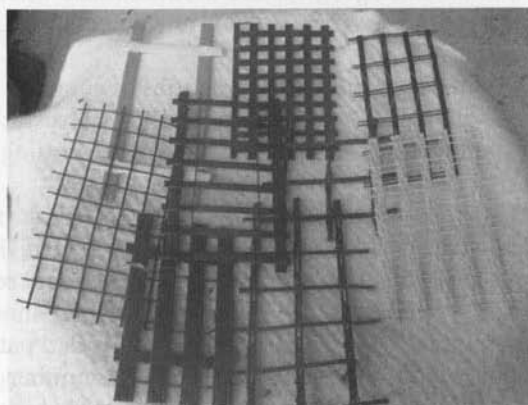
(b) Coated yarn geogrids

(c) Polymer rod (or strap) geogrids

Figure 3.1　Various categories of geogrids.

reinforced with similar filaments—that is, the so-called *tire chords*). Fiberglass and polyvinyl alcohol filaments have also been used, but PET filaments predominate. The yarn bundles are then woven or knit on conventional textile machinery into the desired grid pattern. Strength can easily be varied using more or fewer filaments per yarn in both directions, giving rise to unidirectional and bidirectional products. Yarn spacing can also be varied. The entanglement of the yarns at their intersections is an important issue and varies from product to product. There is obviously a selvedge on both edges of the manufactured material. As a secondary step, the geogrids are coated, usually by spraying and then dipping in bitumen, latex, or polyvinyl chloride (PVC). The purpose of the coating is to maintain geometric stability of the product and to protect the filaments from damage during installation and service.

Figure 3.1(c) shows geogrids made from high tenacity PET or polypropylene (PP) rods or straps. These are similar to packaging and bonding materials used for shipping purposes. Approximately 10 mm wide and 1.0 mm thick, they are manufactured by overlapping the longitudinal ribs over and/or under the transverse ribs. The crossover locations, called *junctions* or *nodes*, are either ultrasonically or laser bonded to provide junction strength. Different rib layout patterns give rise to different styles of unidirectional and bidirectional products.

3.1 GEOGRID PROPERTIES AND TEST METHODS

In contrast to the entire range of test methods described in Chapter 2, only those involved in reinforcement applications will be addressed here. Geogrid tests are unique in a number of aspects when compared with geotextiles. Properties relating to separation, filtration, drainage, and barrier applications are not included since geogrids always serve the primary function of reinforcement.

3.1.1 Physical Properties

Many of the physical properties of geogrids—including the type of structure, rib dimensions, junction type, aperture size, and thickness—can be measured directly and are relatively straightforward. Other properties that are of interest are mass per unit area, which varies over a tremendous range from 200 to 1000 g/m^2, and percent open area, which varies from 40 to 95%. The latter suggests that almost all soils will communicate, or *strike-through*, the plane of the geogrids.

Density.   The density or specific gravity of a geogrid depends upon the polymer from which it is made. Homogeneous geogrids are made from HDPE or PP and density can be measured using ASTM D792 or D1505. Values will be less than unity. Rod or strap geogrids made from PET can use the same test methods, and the resulting value will be greater than unity. Coated yarn geogrids are difficult to evaluate since the coating cannot be readily removed. In addition, the very fine filaments are troublesome to measure in their own right.

Out-of-Plane Bending Stiffness.   Bending stiffness is another physical property of geogrids that is of direct interest insofar as constructability is concerned. This

can be measured using ASTM D1388, a test for flexural rigidity. This test method slides a geogrid test specimen hanging over an inclined plane measuring an angle of 41.5° with the horizontal. When the geogrid bends and eventually touches the surface of the inclined plane, its distance is measured and then related to the mass per unit area. The test is described in Section 2.3.2. The unitized and strap geogrids are quite *stiff* and are characterized by having flexural rigidity values more than 1000 g-cm in this test. The woven or knit yarn geogrids are quite *flexible* and are characterized by having flexural rigidity values less than 1000 g-cm in this test.

In-Plane Torsional Stiffness. While not a formalized geogrid test method, Kinney [1] has proposed clamping a square bidirectional geogrid test specimen in a rigid frame and firmly gripping the central node. A torque is applied and the angular rotation versus the geogrid's resistance is measured. The resulting plot shows a near linear performance for the stiff geogrids. For the flexible geogrids, the response is initially low, but after a 5 to 10° rotation, the resisting force increases markedly. The test may have applicability for bidirectional geogrid reinforcement in pavement base courses and soft soil foundation stabilization.

3.1.2 Mechanical Properties

The mechanical properties of geogrids covered in this section all relate directly to their use in reinforcement applications. Some are index tests, while others are clearly performance-oriented.

Single Rib and Junction (Node) Strength. The initial tendency when assessing a geogrid's tensile strength is to pull a single rib in tension until failure and then to note its behavior. A secondary tendency is to evaluate the in-isolation junction strength by pulling a longitudinal rib away from its transverse rib's junction. It is important to state *in-isolation* since there is no normal stress on the junction; thus the test will not represent performance conditions. A performance junction strength test must be done with the entire geogrid structure contained within soil embedment. This is a much more complicated test and will be covered in this section under anchorage strength from soil pullout.

A *single rib tension strength test* merely uses a constant rate-of-extension testing machine to pull a single rib to failure, as described in ASTM D6637. For unidirectional geogrids, this would most likely be a longitudinal rib. For bidirectional geogrids, both longitudinal and transverse ribs require evaluation. By knowing the repeat pattern of the ribs, an equivalent wide-width strength can be calculated. Alternatively, a number of ribs can be tested simultaneously to obtain a more statistically accurate value for the wide-width strength (see below).

An *in-isolation junction* or *node strength* test can also be performed. The test method uses a clamping fixture that grips the transverse ribs of the geogrid immediately adjacent to and on each side of the longitudinal rib (see Figure 3.2). The lower portion of the longitudinal rib is gripped in a standard clamp, and each clamp is mounted in a tensile testing machine, where the test specimen is pulled apart. The strength of the junction, in force units, is obtained. Table 3.1 gives the junction strength for a number
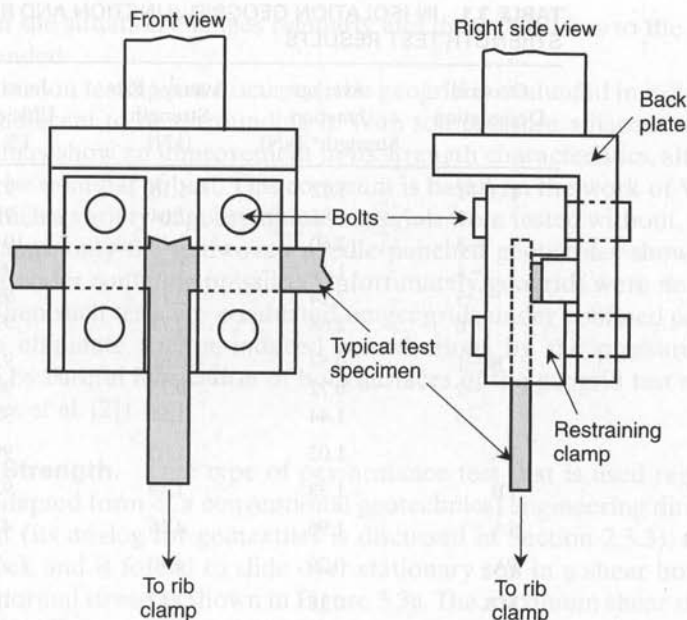
Front view   Right side view

Back plate

Bolts

Typical test specimen

Restraining clamp

To rib clamp   To rib clamp

Figure 3.2   Test fixture for measuring in-isolation geogrid junction strength.

of commercially available geogrids. Note that the rib strength can also be evaluated as described previously. Having both sets of data, a junction strength efficiency can be calculated. As the table shows, geogrid junction strength efficiencies vary from essentially 100 to 7%. It is important to note that these tests have the junction in an unconfined status. Thus, it is an index type of text. The effect of a simulated normal stress on the individual junction cannot be determined in this test, however, new approaches to this test are available that prevent the junction from rotation.

Wide-Width Tensile Strength.   Clearly the wide-width tensile strength of a geogrid, in its machine direction for unidirectional geogrids and in both machine and cross-machine directions for bidirectional geogrids, is of prime importance. When testing the products, the test clamps grip a larger test specimen than described above, including a number of repeating rib units in the width direction and perhaps repeating length sections as well. The resulting data give strength values in units of force per unit width, which is calculated by using the repeat distance of the actual geogrid structure. Obviously there is an extremely wide range in product behavior depending on type of polymer, its structure, spacing of ribs, and so on. The strength of geogrids with respect to geotextiles is also of interest. Geogrid strengths fall at an intermediate point between conventional geotextiles and those geotextiles specifically made for high-strength applications.

There are two procedural test methods used to evaluate the wide-width tensile strength of geogrids. One choice is to use ASTM D6637, which has a provision for measuring single rib strength (described previously), or multiple rib strength. The width of

TABLE 3.1   IN-ISOLATION GEOGRID JUNCTION AND RIB
STRENGTH TEST RESULTS

Geogrid Designation	Average Junction Strength* (kN)	Average Rib Strength (kN)	Junction Efficiency (%)
TU −1	1.12	1.16	97
−2	1.86	2.04	91
−3	2.60	2.49	104
−4	1.31	1.33	99
−5	2.14	2.17	99
−6	2.68	2.77	97
TB −1	0.57	0.61	93
−2	0.72	0.75	96
−3	1.44	1.51	95
TA	1.02	1.03	99
TB	1.38	1.49	93
SA	1.96	4.16	47
PA	0.29	4.40	7
MA	0.18	1.42	13
CA −1	0.50	1.18	42
−2	0.71	1.73	41
−3	0.64	1.98	32
−4	1.20	3.56	34
−5	1.25	4.00	31
NA	0.71	5.12	14
NB	0.80	8.90	9

*The junction strength tests were not laterally confined and were
evaluated in a device of the type shown in Figure 3.2.

the test specimen, its length, its clamping mechanism, its strain rate, and the method for measuring deformation are all important considerations. If this test is selected, these items must be agreed upon by the parties involved. The second choice is to use ISO 10319 for wide-width strength testing of geogrids. In this procedure the width and length of the test specimen is prescribed. The type of clamps used should conform to the guide shown in Figure 2.9. Deformation monitoring in almost all situations must be based on an external measurement system—such as, optical, laser, or transducer.

The information gained from a wide-width tension test on a geogrid comprises several factors: the tensile strength at which the test specimen fails (kN/m); the tensile elongation at which the test specimen fails—i.e., its failure strain (%); the tensile stress at different elongations prior to specimen failure—for example, stress (kN/m) at 1%, 2%, 5%, strain; and the tensile modulus (kN/m) taken from the initial portion of the strength-versus-elongation curve, or possibly other defined modulus values. Manufacturers' literature is available on the data for the particular products and styles that are in current production. Some compilations of comparative data are available in the

literature, but the situation changes regularly and direct inquiries to the manufacturer are recommended.

   In the tension testing just discussed, the geogrid is evaluated in isolation—that is, with no soil adjacent to or surrounding it. With soil pressure adjacent to the geogrid, the material may show an improvement in its strength characteristics, although the effect is felt to be nominal at best. This comment is based on the work of Wilson-Fahmy et al. [2] in which a variety of geosynthetic materials were tested without, then with, lateral confinement; only the nonwoven needle-punched geotextiles showed significant improvement under confining pressure. Unfortunately, geogrids were not evaluated in that study. When such tests are conducted on geogrids under confined conditions, it is important to eliminate friction-induced contributions by the pressurizing medium (usually soil) by careful lubrication of both surfaces of the geogrid test specimen (see Wilson-Fahmy, et al. [2]).

   Shear Strength.   One type of performance test that is used regularly on geogrids is an adapted form of a conventional geotechnical engineering direct shear test. In such a test (its analog for geotextiles is discussed in Section 2.3.3), the geogrid is fixed to a block and is forced to slide over stationary soil in a shear box while being subjected to normal stress, as shown in Figure 3.3a. The maximum shear stress, its shear strength, is obtained (see Figure 3.3b). Then a new test with a replicate geogrid specimen and soil (but now at a different normal stress) is conducted. This process is repeated sufficiently often to develop a set of shear strength-versus-normal stress points, which are plotted in Figure 3.3c. The resulting line defines what is known as the failure envelope, properly called the Mohr-Coulomb failure envelope. From this graph the shear strength parameters of the geogrid to the particular soil are obtained—that is, the values of adhesion (c_a) and friction angle (δ). Note that if a strain-softening response of the stress-versus-displacement curves occurs, two sets of values result, peak and residual. If the shear strength parameters of the soil by itself, cohesion (c) and friction angle (ϕ), are also determined in their own separate tests with soil in both halves of the shear box, a comparison or *efficiency* can be calculated as follows:

$$E_c = (c_a/c) \times 100 \tag{3.1}$$
$$E_\phi = (\tan \delta/\tan \phi) \times 100 \tag{3.2}$$

where

   E_c = efficiency on cohesion,
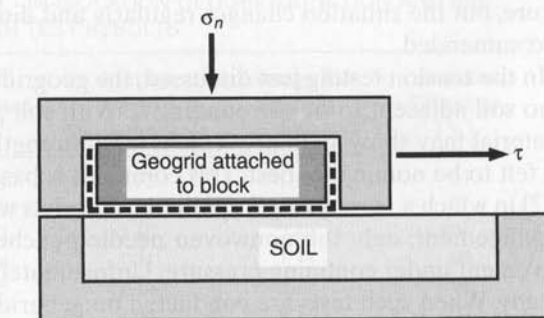 E_ϕ = efficiency on friction,
   c_a = adhesion of soil to geogrid,
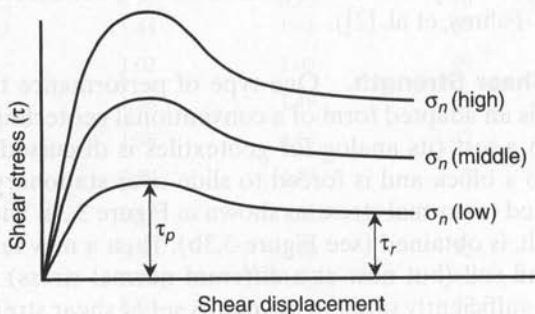 c = cohesion of soil to soil,
   δ = friction angle of soil to geogrid, and
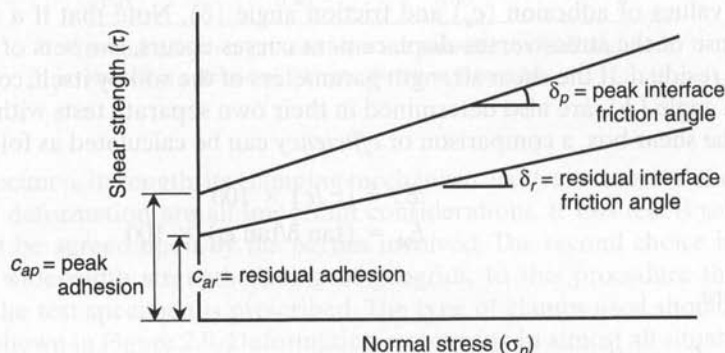 ϕ = friction angle of soil to soil.

   A large shear box must be used for geogrid testing in order to minimize scale effects. A rule of thumb used in soil testing is that the shear testing device must be

σ_n

Geogrid attached
to block

τ

SOIL

(a) Direct shear test device

σ_n (high)

σ_n (middle)

σ_n (low)

Shear stress (τ)

τ_p τ_r

Shear displacement

(b) Direct shear test data

Shear strength (τ)

δ_p = peak interface
friction angle

δ_r = residual interface
friction angle

c_{ap} = peak
adhesion

c_{ar} = residual adhesion

Normal stress (σ_n)

(c) Mohr-Coulomb failure envelope

Figure 3.3 Test setup and procedure to assess interface shear strengths involving geogrids.

more than 10 times the size of the largest soil particle. If an analogy is made with the geogrid's apertures, this would generally require a 300 × 300 mm box or larger for geogrid shear testing. Both ASTM D5321 and ISO 12957 for direct shear testing of geosynthetics require at least this size of test device.

Test results using a 450 × 450 mm shear box are shown in Table 3.2. The soil in all cases consisted of a well-graded angular sand (SW) in the dry condition and in a dense compaction state ($\cong$ 90% relative density). The cohesion of the soil was zero, hence the adhesion was also zero. The resulting peak friction angle of the soil by itself was 44°. The efficiencies were calculated on the basis of equation (3.2). Note that the efficiencies are all quite high, with many as high as the soil itself. This is understandable since the general configuration of geogrids (with their rather large apertures and relatively thick ribs) forces the failure plane into the soil itself. If any reduction in the soil's strength occurs, it is only along the surface of the geogrid's ribs. Conversely, improvement in the soil's shear strength might be gained by having an element of bearing occur against the edges of the transverse ribs of the geogrid. While it is generally prudent to do product-specific and soil-specific shear testing, the shear strength of most soils, small enough to fit into the geogrid's aperatures, will be fully mobilized by most geogrids.

An investigation of the influence of aperture size versus soil particle size on the frictional efficiency of a number of geogrids is available from Sarsby [3]. He finds that the optimum transfer of shear stress—that is, the highest efficiency—occurs when

$$B_{GG} > 3.5\, d_{50} \tag{3.3}$$

where

B_{GG} = the minimum width of geogrid aperture, and
d_{50} = the average particle size of the backfilling soil.

This is an important consideration when selecting the type of backfill to be used around geogrids. Fortunately, the criterion can readily be accommodated by a wide selection of soil types for backfilling purposes.

Anchorage Strength from Soil Pullout. The intrinsic merit of geogrids comes about by their anchorage strength or pullout resistance, which can far exceed

TABLE 3.2   RESULTS OF DIRECT SHEAR TESTS (PEAK STRENGTHS) USING VARIOUS GEOGRIDS*

| Test Condition	Test 1		Test 2	
	Friction Angle (°)	Efficiency (%)	Friction Angle (°)	Efficiency (%)
Soil to soil	44	100	44	100
Soil to bidirectional geogrid 1	43	96	44	100
Soil to bidirectional geogrid 2	45	103	45	103
Soil to bidirectional geogrid 3	46	107	46	107
Soil to unidirectional geogrid 1	35	72	37	78
Soil to unidirectional geogrid 2	37	78	39	84
Soil to unidirectional geogrid 3	42	93	43	96

*The geogrids were firmly attached to a wooden platen in the movable portion of the shear box and slid over the stationary soil in the bottom of the shear box.

the direct shear strength that was just discussed. Interesting comparison tests between steel grids, steel plate, polymer geogrids and polymer geonets are reported by Ingold [4]. This behavior comes about by virtue of the large apertures in the geogrid allowing for soil strike-through from one side of the geogrid to the other. Obviously, the soil particles must be sufficiently small to allow for full penetration; thus the d_{50} value in equation (3.3) represents the recommended maximum particle size for a particular geogrid's minimum aperture width.

The anchorage strength or pullout resistance is a result of three separate mechanisms, as illustrated in Figure 3.4. The first is the shear strength along the top and bottom of the longitudinal ribs of the geogrid. The second is the shear strength contribution along the top and bottom of the transverse ribs. The third mechanism is the passive resistance against the front of the transverse ribs. In the last mechanism the soil goes into a passive state and resists pullout by means of bearing capacity. It has been analytically shown that this bearing capacity can be a major contributor to the overall anchorage strength of geogrids [5]. It indeed is a geogrid's forte and can be used admirably in this behavioral mode. Experimental evidence follows the same trends. Example 3.1 describes this effect.

Example 3.1

For an idealized relatively stiff geogrid, such as the one shown in Figure 3.4, calculate the anchorage capacity of each of its three strength components and the percent contribution due to bearing capacity (BC). Assume that it is subjected to a normal stress of 25 kPa and that its arbitrary dimensions are L = 900 mm by W = 300 mm. The longitudinal ribs are at 50 mm spacings and the transverse ribs are at 100 mm spacings. All ribs are 15 mm wide by 3.5 mm thick. In the analysis use a shear strength of 14.4 kPa (= 25 tan 30°) and a bearing capacity of 800 kPa based on a soil friction angle of 35°.
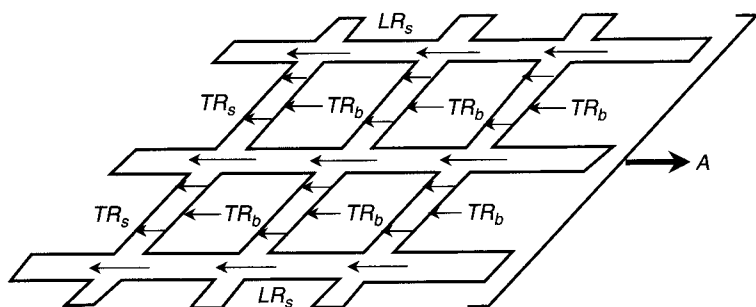
Legend

A = Total anchorage (pullout) strength
LR_s = Longitudinal rib shear strength
TR_s = Transverse rib shear strength
TR_b = Transverse rib bearing strength

Figure 3.4   Mechanisms involved in geogrid anchorage strength. (After Koerner et al. [5] and Wilson-Fahmy and Koerner [6])

Solution: The formulation based on Figure 3.4 is as follows. Note that no numeric deduction was taken at rib cross-over points. The anchorage force at failure is

$$A = 2(\Sigma LR_s + \Sigma TR_s)\tau + (\Sigma TR_b)q_o$$
$$= 2[(0.015 \times 0.900)6 + (0.015 \times 0.300)9]14.4 + [(0.0035 \times 0.300)9]800$$
$$= 2.33 + 1.17 + 7.56$$
$$A = 11.06 \text{ kN}$$
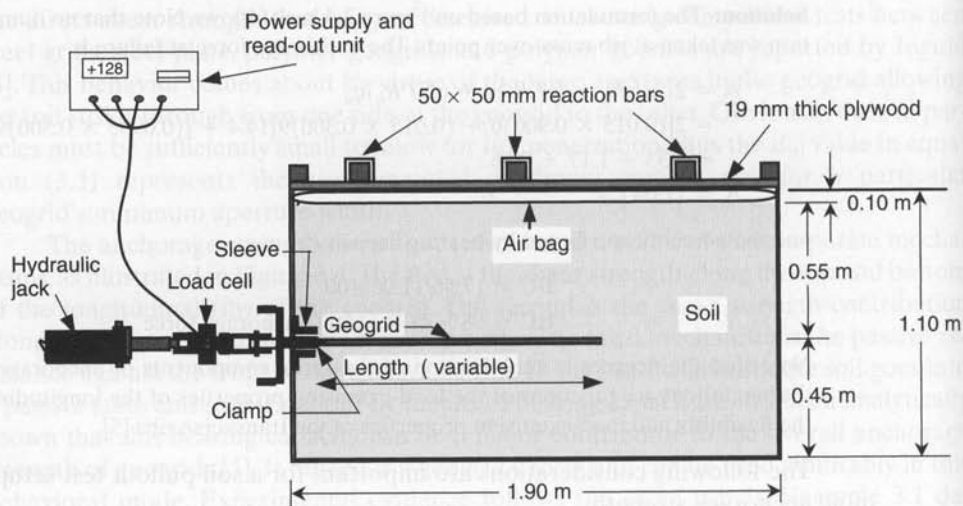
and the percent contributed by bearing capacity is

$$BC = (7.56/11.06)100$$
$$BC = 68\% \text{ of the total anchorage force}$$

Note that the degrees of mobilization of the three components of anchorage resistance during pullout are functions of the load-extension properties of the longitudinal ribs and the flexibility and load-extension properties of the transverse ribs [5].

The following considerations are important for a soil pullout test setup to determine anchorage strength:

- The test box must be deep enough to permit soil deformation above and below the geogrid as it pulls out of the soil mass. For gravel-size soils, this probably requires 300 mm of soil above and below the geogrid.
- The test box must be long enough to allow for the applied stress on the geogrid to dissipate fully. The number of transverse ribs that are required is dependent on both the geogrid structure and soil type. A box *at least* 1.0 m long is necessary.
- With such a large size test box, functioning at a high normal stress, the total forces involved can be enormous. This requires a very strongly braced and supported system.
- Using a sleeve insert, the geogrid must be gripped from within the encapsulated soil mass. If gripped from outside of the test box, passive pressure will be set up against the face of the box, which will impose additional (and quite unknown) resisting stresses on the front portion of the test specimen.
- Geogrids, being quite strong, will require a high-strength withdrawal system for the actual geogrid pullout (or tensile failure) to occur.
- To monitor the geogrid's deformation behavior, a number of deformation telltales on different parts of the embedded geogrid are necessary—that is, the incremental movement should be monitored. These telltales are often steel wires attached to the geogrid's nodes and extend out through the back of the box to which dial indicators are attached. Alternatively, strain gages attached to the longitudinal ribs can be used.

Figure 3.5 shows plan and elevation views of a soil pullout box for testing the anchorage behavior of geogrids. While the above described test is clearly not simple (the test is probably the most sophisticated and expensive of all geosynthetic performance tests at this time), many such tests have been conducted. Results from the above type of soil pullout testing are shown in Figure 3.6.

Power supply and
read-out unit

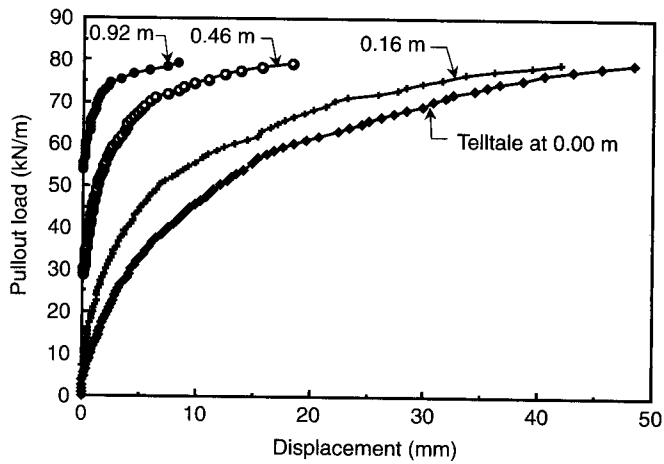+128

50 × 50 mm reaction bars

19 mm thick plywood

0.10 m

Air bag

0.55 m

Soil   1.10 m

Sleeve

Hydraulic
jack

Load cell

Geogrid

Length (variable)

Clamp

0.45 m

1.90 m

(a) Elevation view

Sleeve

Loading frame

Bearing bolts

Dial gauge

Load cell

Hydraulic jack   Geogrid   Steel wire

Geogrid clamp   Copper tubing

Pullout box
1.90 m × 0.91 m
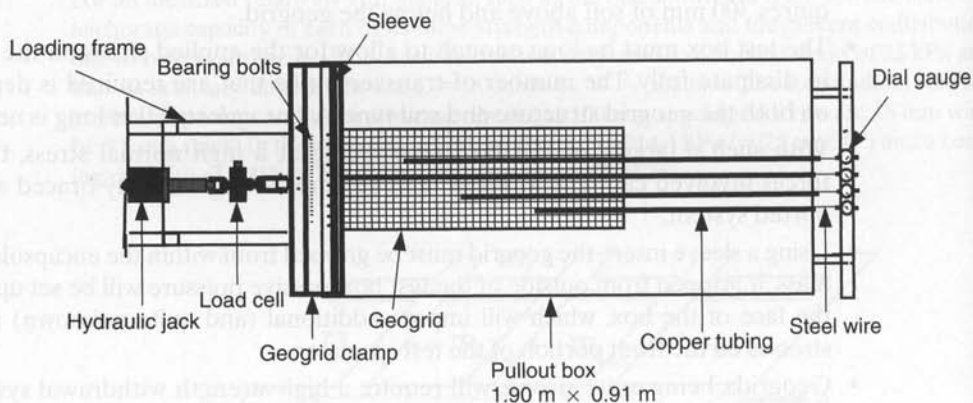
(b) Plan view

Figure 3.5   Diagrams of a soil pullout box for evaluating the anchorage behavior of
geogrids.

Analysis of the type of data shown in Figure 3.6 leads to the determination of an
interaction coefficient C_i, which can be used for the design of a specific type of geogrid
embedded in the anchorage zone behind a potential failure plane. The value of C_i is
soil type and test parameter specific. For example, if a geogrid anchorage test is con-
ducted to failure by sheet pullout, the following equation can be formulated:

$$A = 2C_i L_e \sigma'_n \tan \phi' \qquad (3.4)$$

where

A = anchorage capacity per unit width (kN/m),

C_i = interaction coefficient (dimensionless),

L_e = length of geogrid embedment (m),

σ'_n = effective normal stress in the geogrid (kPa), and

ϕ' = effective soil friction angle (°)
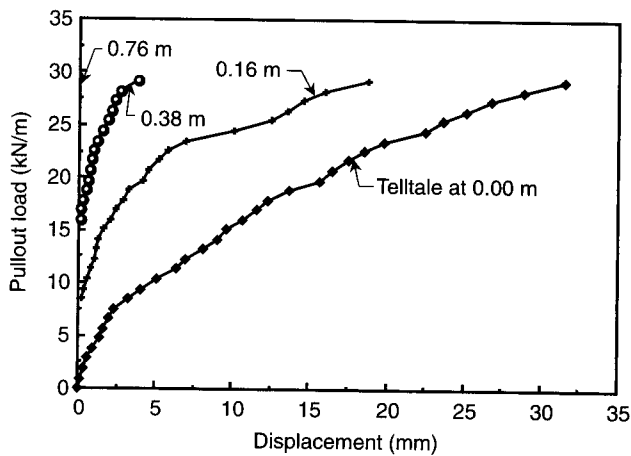
Figure 3.6   Results from selected geogrid pullout tests in a well-graded concrete sand at 69 kPa normal stress at a pullout rate of 1.5 mm/min and geogrid length of 0.92 m. (After Wilson-Fahmy and Koerner [6])

Note that the value of ϕ' is for the soil alone and not the soil-to-geogrid value. Also equation (3.4) could be modified to handle cohesive soils, but usually granular soils are selected for backfill materials; if not, the omission of a cohesion term leads to a conservative design.

Example 3.2

Given the data of Figure 3.6a (pullout), where the length was 0.92 m, the normal stress was 300 mm of 19 kN/m^3 soil plus a 70 kPa surcharge, and the effective friction angle was 35°, what is the interaction coefficient for this geogrid in this particular type of well-graded sandy soil?

Solution: First effective normal stress is calculated:

$$\sigma'_n = (0.3)(19) + (70)$$
$$= 75.7 \text{ kPa}$$

Then the interaction coefficient is calculated using equation (3.4) along with $A_{\text{ult}} = 80$ kN/m taken from Figure 3.6a:

$$80 = 2C_i(0.92)(75.7) \tan 35°$$
$$80 = 97.5C_i$$
$$C_i = 0.82$$

Note that the consideration of a soil pullout test, such as described here, completely avoids the issue of in-isolation junction strength (recall the preceding discussion of single rib and junction strength). The geogrid junctions in this test are challenged the same way they are in situ, by having a specific normal stress applied to them through soil embedment. If the junctions are inadequate, the system will fail at a low tensile stress and this will be reflected by a relatively low value of interaction coefficient.

Anchorage Strength from Wall Connections. When geogrids are used to construct reinforced retaining walls, the front edge generally terminates with a facing panel (mechanical connection) or modular block/welded wire facing (friction and/or mechanical connection). The capability of the geogrid's connection to the wall facing should generally be evaluated. Based in part on research in the literature (e.g., Bathurst and Simac [7]) ASTM has developed the D6638 Test Method. It is primarily focused on modular concrete blocks with a geogrid in its proper location and orientation, at a predetermined normal stress on the blocks. The geogrid is tensioned until failure. Failure can come about in numerous ways—from geogrid tension and connection failure to geogrid slippage or block wall failure. The test nicely exposes the mode of failure and also the ultimate strength of the entire anchorage system. However, recognize that there are a large number of modular-block wall systems, many with a matching geogrid type and facing type. Thus this test must use the specific materials that will be used in the actual wall construction. Furthermore, substitutions cannot be allowed at the time of bidding or during construction via value engineering or the like unless acceptable data are available.

3.1.3 Endurance Properties

As geogrids are used in critical reinforcement applications, some of which require long service lifetimes, it is generally necessary to evaluate selected endurance properties. Installation damage, creep, and accelerated test methods will be addressed.

Installation Damage.   As with all geosynthetics, the placement of geogrids in the field requires a considerable degree of planning and care. As happens all too often with careless field construction crews and heavy machinery, installation damage of the geogrid can occur. Other uncertainties in this same area are coarse soil impingement, falling objects, and other accidents that may occur before the geogrid is covered. A few studies have been conducted whereby geogrids have been exhumed after installation and subsequently tested with comparisons being made to the as-received material. Loss in strength has often occurred. In-house investigations (recall Figure 2.20, which had nine geogrids in the total study) show that strength reductions of 0 to 30% are possible (see Koerner et al. [8]). There is a formalized procedure available to assess installation damage, namely ISO 10722, Hsieh and Wu [9] and Sprague and Allen [10] give details and results for many geogrid samples. Generally, the higher strength-loss values come about where large, poorly graded, quarried aggregate is used and heavy construction equipment performs the placement and compaction. If it is necessary to use such materials and methods, it is prudent to first place a cushioning layer of sand above and sometimes below the geogrid.

Tension Creep Behavior.   A major endurance property involving geogrids is their sustained-load deformation or tension "creep." Since all polymers used in the manufacturing of geogrids consist of long-chain molecules arranged in crystalline regions with interspersed amorphous regions, the creep response reflects upon the percent crystallinity and the glass transition temperature (T_g). In general, this structure is reflected in the following manner:

- For nonoriented polyolefins (polypropylene and polyethylene) that function below T_g, the molecular chains slip along one another within the crystalline regions. Note that polyolefins are, in general, highly crystalline.
- For oriented polyolefins (also below T_g), the orientation creates a molecularly fibrous (or *affine*) structure, and when creep occurs it does so between fibers in the oriented, and stressed, direction.
- For polymers like polyester, polyamide, and polyvinyl alcohol, which function above T_g, creep slippage hardly occurs in the crystalline region. Here the chains break at the interface of the crystalline and amorphous regions. In this regard creep rupture (described in the next subsection) is more likely to occur before a limiting deformation is reached.

Apart from the molecular structure and T_g-values, creep is predominantly a function of stress level, time, temperature, and a number of environmental factors to be discussed

later. Creep has been extensively evaluated on many geogrids, with results for a particular HDPE product given in Figure 3.7a. Note that up to approximately 29.8 kN/m, which is 41% of the breaking load of this particular geogrid, the creep deformation is within a creep-limited strain value of 10%, which has been extrapolated as being equivalent to a 120 year design life. The allowable, or working, stress will reflect this type of information in that the reduction factor against creep will be the inverse of 41%, which is 2.4. Note in Table 2.8 that PE and PP geotextile yarns require creep reduction factors that are generally higher (i.e., 3.0 to 4.0), due to the lack of geogrid orientation effects as occurs in the manufacture of homogeneous PE and PP geogrid materials. The tension creep test has been adopted as ASTM D5262 and ISO 13431. Creep test data on polyolefin geogrids can be portrayed as isochronous creep data, shown in Figure 3.7b. The creep behavior is readily observed in such a graph.

Creep Rupture Behavior.   A variation of the tension creep test just described is the creep rupture procedure presented by Ingold et al. [12]. In this procedure higher stresses are imposed on the test specimens, causing failure to occur in a relatively short time. Upon performing a number of such tests, a graph of load-versus-log time can be generated. When extrapolated out to the desired service lifetime, an acceptable load can be obtained. When normalized to the short-term value, the inverse of this ratio becomes the reduction factor to be applied on ultimate strength (see Miyata [13]).

Accelerated Testing Methods.   Both tension creep and creep rupture can be evaluated more rapidly than conventionally done by recognizing that elevated testing temperature accelerates the relevant mechanisms. The concept utilizes time-temperature-superposition (TTS) to produce a series of curves at various elevated temperature steps. The resulting curves are then shifted along the horizontal axis (the log-time axis) to represent service lifetimes at the site-specific temperature. Based on field measurements, this can be taken as 10°C (see Hsuan et al. [14]). Using TTS, the testing time is drastically reduced and projections far into the future can be obtained.

There are two variations of TTS testing. The first (called standard TTS per ASTM D5292 Appendix) uses individual test specimens for each temperature step and load increment (see Farrag and Shirazi [15] and Farrag [16]). The second (called the Stepped Isothermal Method, or SIM, per ASTM D6992) uses the same test specimen and cascades strain measurements at each temperature increment (see Thornton et al. [17] and Greenwood and Voskamp [18]). This has the desirable effect of eliminating test specimen variation in these quite sensitive tests. For different load increments, however, individual test specimens are still required. Both of these accelerated methods are fruitful areas of research—for designers to obtain reduction factors in a timely manner and for manufacturers to investigate the behavior of modified and/or new products.

3.1.4 Degradation Issues

For all types of geogrids being used in permanent reinforcement applications, it is generally necessary to evaluate selected degradation considerations. This section briefly discusses some of these issues.
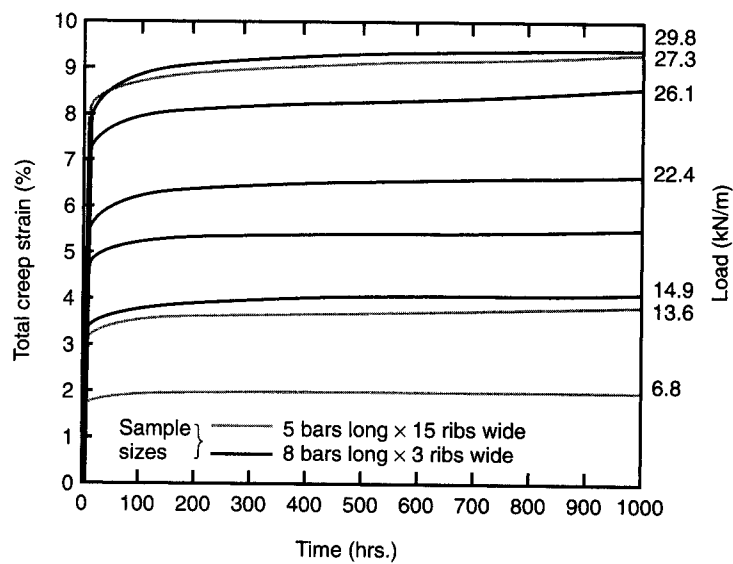
(a) Data generated directly from test
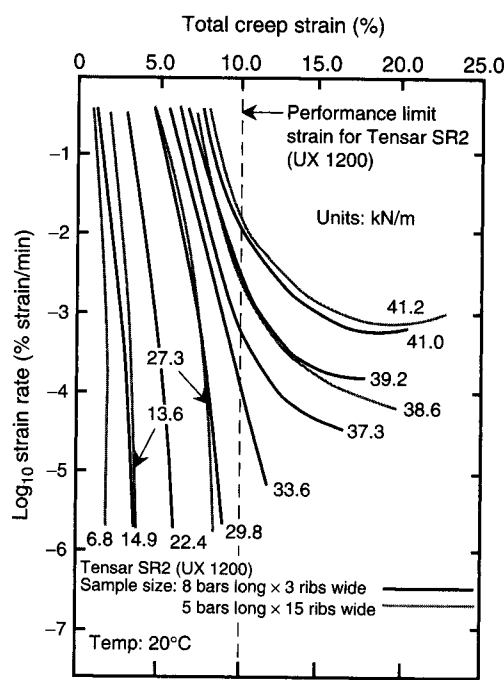
(b) Isochronous creep curves

Figure 3.7   Constant stress deformation (creep) test results on an HDPE geogrid of 72 kN/m ultimate strength. (After McGown, et al. [11])

Temperature Effects.   Given the temperature ranges of typical environments, temperature extremes (hot or cold) should have no serious adverse effects on geogrids. The one caution is that high temperature can exacerbate strains arising from tension creep, creep rupture, and/or stress relaxation. This requires actual testing at the anticipated field temperatures or the use of the TTS techniques just described.

Oxidation Effects.   This long-term mechanism, which is applicable to polyolefin (HDPE and PP) degradation, was discussed in Section 2.3.6.

Hydrolysis Effects.   This long-term mechanism, which is applicable to polyester (PET) degradation, was discussed in Section 2.3.6.

Chemical Effects.   Polyolefins and polyesters have shown excellent resistance to a wide range of chemicals. If unusual conditions exist, however, the situation may dictate specific testing in the actual chemical environment—for example, regarding such conditions as landfill leachates. The laboratory incubation procedure can utilize ASTM D5322 followed by ASTM D6213 for the actual geogrid tests to be performed. Interpretation of the test results, however, is left to the designer.

Radioactive Effects.   Unless high-level radioactive materials are in the immediate vicinity, low-level and mixed radioactive materials should pose no problem to geogrids.

Biological Effects.   The discussion on the general lack of biological degradation of geotextiles in Section 2.3.6 is applicable for geogrids, with the possible exception of the coatings on flexible geogrids. Latex, bitumen, or plasticizers in PVC may be sensitive to microorganisms, but no studies in this regard are available to my knowledge. Even if such attack on the coatings were possible, the high crystallinity polyester fibers (to which these geogrids owe their strength) would probably remain unaffected.

Sunlight (UV) Effects.   As with all polymeric materials, ultraviolet degradation can occur over time, and degradation of the polymer will follow. The discussion in Section 2.3.6 applies to geogrids as well as geotextiles. Regarding the issue of timely cover, the exposure time of geogrids can be considerably longer than geotextiles. This is due to the thickness of the ribs of the polyolefin geogrids and the good UV resistance of PET geogrids. A specification should not be left open-ended, however, and a suggested 30-day maximum exposure before covering is recommended.

Stress Crack Resistance.   Highly crystalline polymers are sometimes sensitive to brittle cracking while under stress. The test used to evaluate this tendency is ASTM D5397, which describes the notched constant tensile load (NCTL) test and the single-point version (SP-NCTL) of the appendix to D5397. Both are explained in Chapter 5, which discusses geomembranes. Only highly crystalline polyethylene geogrids are of concern and a review with respect to them is given by Wrigley [19]. It is not known to be a problem insofar as field failures are concerned.

3.1.5 Allowable Strength Considerations

The basis of the design-by-function concept is the establishment of a factor of safety. For geogrids, where reinforcement is the primary function, this factor of safety takes the following form:

$$FS = \frac{T_{allow}}{T_{reqd}} \qquad (3.5)$$

where

   FS   = factor of safety (to accommodate unanticipated loading conditions and uncertainties in design or testing),

   T_{allow} = allowable tensile strength from laboratory testing, and

   T_{reqd} = required tensile strength from design of the particular field situation.

The allowable value comes from a tensile test of the type described in Section 3.1.2, where we must compare the test setup with the intended field situation. If the test method is not completely field-simulated, the laboratory value must be suitably adjusted. This will generally be the case. Thus the laboratory-generated tensile strength is usually an ultimate value, which must be reduced before being used in design:

$$T_{allow} < T_{ult}$$

One way of accomplishing this is to place reduction factors on each of the items not modeled in the laboratory test. For example, the following equation should be considered [20]:

$$T_{allow} = T_{ult}\left[\frac{1}{RF_{ID} \times RF_{CR} \times RF_{CBD}}\right] \qquad (3.6)$$

where

   T_{ult} = ultimate tensile strength from a standardized in-isolation tensile test,

   T_{allow} = allowable tensile strength to be used in equation (3.5) for final design purposes,

   RF_{ID} = reduction factor for installation damage,

   RF_{CR} = reduction factor for avoiding creep over the duration of the structure's lifetime, and,

   RF_{CBD} = reduction factor against chemical and biological degradation.

Note that some of these values may be 1.0 or slightly above 1.0, and may therefore be inconsequential. Still others, not specifically mentioned in equation (3.6), may be included as the situation warrants. For example, reduction factors against ultraviolet degradation, RF_{UV}, field seams, RF_{seam} or penetrations, RF_{pen}, may be included on a site-specific basis. Guidelines for the usual reduction factor values are given in Table 3.3.

TABLE 3.3   RECOMMENDED REDUCTION FACTOR VALUES FOR
USE IN EQUATION (3.6) FOR DETERMINING ALLOWABLE TENSILE
STRENGTH OF GEOGRIDS

Application Area	Reduction Factor Values		
	RF_{ID}	RF_{CR}	RF_{CBD}
Unpaved roads	1.1–1.6	1.5–2.5	1.0–1.6
Paved roads	1.2–1.5	1.5–2.5	1.1–1.7
Embankments	1.1–1.4	2.0–3.0	1.1–1.5
Slopes	1.1–1.4	2.0–3.0	1.1–1.5
Walls	1.1–1.4	2.0–3.0	1.1–1.5
Foundations	1.2–1.5	2.0–3.0	1.1–1.6

Note that ranges are given rather than specific values. It is necessary to consider each item individually and make a conscious decision as to how important it is for the site-specific situation. For example, the largest is the creep reduction factor—hence its importance for proper evaluation. In Example 3.3 and 3.4 the values used are assumed on the basis of a hypothetical project and construction method.

Example 3.3

What is the allowable geogrid tensile strength to be used in the construction of an unpaved road separating stone base from subgrade soil if the ultimate strength of the geogrid is 80 kN/m?

Solution: Using estimated values from Table 3.3 in equation (3.6), the following results:

$$T_{allow} = T_{ult}\left[\frac{1}{RF_{ID} \times RF_{CR} \times RF_{CBD}}\right]$$

$$= 80\left[\frac{1}{1.3 \times 2.0 \times 1.5}\right]$$

$$= 80\left[\frac{1}{3.9}\right]$$

$$T_{allow} = 20.5 \text{ kN/m}$$

Example 3.4

What is the allowable geogrid tensile strength to be used in the construction of a permanent wall adjacent to a major highway if the ultimate strength of the geogrid is 70 kN/m?

Solution: Using estimated values from Table 3.3 in equation (3.6) gives

$$T_{allow} = T_{ult}\left[\frac{1}{RF_{ID} \times RF_{CR} \times RF_{CBD}}\right]$$

$$= 70\left[\frac{1}{1.3 \times 2.5 \times 1.3}\right]$$

$$= 70\left[\frac{1}{4.22}\right]$$

$$T_{allow} = 16.6 \text{ kN/m}$$

Note that these examples could just as well have been framed so as generate an ultimate strength from a given allowable value. This would be the case if we were working from an analytical method that generated a design value. This design value (as with the allowable) would have to be *increased* by reduction factors to arrive at a required (or ultimate) tensile strength.

3.2 DESIGNING FOR GEOGRID REINFORCEMENT

The primary function of geogrids is invariably reinforcement; this section will proceed from one reinforcement application area to another. The order will parallel that of Sections 2.6 and 2.7 on geotextile reinforcement, with the addition of several areas that are unique to geogrids.

3.2.1 Paved Roads—Base Courses

The use of geogrids in paved road aggregate base courses is an area where the large aperture size of geogrids provide an excellent advantage. Here the geogrids are placed within the granular base course, typically crushed stone, with the intention of providing an increased modulus, hence a lateral confinement to the system. This lateral confinement is intended to resist the tendency for the base course aggregate to *walk out* from beneath the repetitive traffic loads imposed on the concrete- or bitumen-pavement surface. The situation is applicable for the ballast beneath railroad tracks as well, and perhaps even more so due to the nature and intensity of the dynamic loads.

A number of laboratory tests have been conducted to assess the potential benefits and mechanisms involved, most significantly the work of Haas [21] and Abd El Halim [22, 23]. In a large test setup measuring 4.0 m long by 2.4 m wide by 2 m deep and using 10 kN loads applied sinusoidally at a frequency of 10 Hz on a 300 mm diameter circular plate, five test series (called *loops*) were performed. Loop 1 compared the response of nonreinforced and reinforced sections using both dry (strong) and saturated (weak) subgrade conditions. Failure appeared in the nonreinforced sections earlier than the reinforced sections under both conditions. Loop 2 provided data that show little difference in elastic deflection between the four trials. More significant was the angle of curvature and the elastic strain at the bottom of the asphalt pavement. Both indicate a 50% reduction for the reinforced sections, thereby indicating a significant load-spreading phenomenon. The permanent surface deformation of the reinforced section is substantially improved over the nonreinforced section. At a 20 mm failure assumption, the nonreinforced section carried 110,000 load repetitions, compared with 320,000 for the reinforced case. In the context of the discussion on geotextiles used in the control of reflective cracking of paved roadways, this would be called a geogrid effectiveness factor (GEF) equal to 2.9.

Loop 3 investigated the equivalent thickness that can be attributed to the reinforcement. The results indicate that the 150 mm reinforced section carried about 80,000 load cycles compared with only 34,000 load cycles for the 200 mm nonreinforced and 92,000 loads cycles for the 250 mm nonreinforced. In other words, 150 mm of reinforced asphalt nearly compared with 250 mm of nonreinforced asphalt. Loop 4

confirmed these results, in that reinforced sections result in a savings of 50 to 100 mm of nonreinforced asphalt. Loop 5 involved pressure cells in the soil subgrade and confirmed the load-spreading capability of the reinforcement.

Studies such as this typically indicate that a reinforcement function is provided to the pavement system by the geogrid, albeit by a rather complex set of mechanisms. Some possible contributors include the following: increasing initial stiffness, decreasing long-term vertical deformation, decreasing long-term horizontal deformation, increasing tensile strength, reducing cracking, improving cyclic fatigue behavior, and simply holding the system together. This leads to difficulties as far as a specific design methodology is concerned. We could use a geogrid effectiveness factor and divide it into the design traffic number to determine a modified value and design accordingly, that is,

$$DTN_R = \frac{DTN_N}{GEF} \tag{3.7}$$

where

DTN_R = design traffic number for the geogrid-reinforced case,

DTN_N = design traffic number under standard (nonreinforced) conditions (e.g., using the Asphalt Institute's procedures), and

GEF = geogrid effectiveness factor ($\cong 3.0$ for the unitized, homogeneous geogrid evaluated)

Carroll et al. [24] have further refined the technique using the same experimental data to calculate a structural number as per AASHTO [25]. Using the concept of a structural number, the nonreinforced (control) section is

$$SN = 25\, a_1 d_1 + 25\, a_2 d_2 \tag{3.8}$$

where

SN = structural number,

a_i = layer coefficients (0.40 for asphalt and 0.14 for granular stone base), and

d_i = thickness (mm) of each layer.

Using a soil subgrade support value S, obtained from a CBR test, the number of 80 kN single-axle equivalents for any cross section can be calculated. A load-correction factor is then calculated for geogrid-reinforced sections. An estimate of the reinforced-pavement SN is derived, and a ratio for reinforced-to-nonreinforced section is generated. When plotted against the actual reinforced base course thickness, this ratio is seen to be linear. Different values, but the same trend, are seen for geogrids placed in the middle and at the bottom of the base course. A design chart that enables a conventional nonreinforced base course thickness to be converted to a geogrid-reinforced section is given in Figure 3.8. Note that a transition occurs at 250 mm, where the geogrid can be
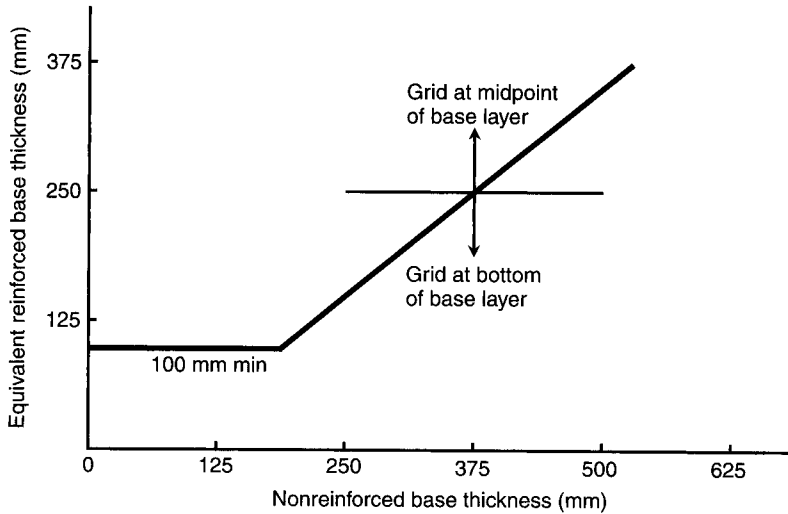
Figure 3.8   Geogrid-reinforced base course for paved highway section using HDPE geogrids. (After Carroll et al. [24])

placed either in the middle or at the bottom of the base course. It is important to recognize that this curve is based on experimental data for the specific geogrid used. An equivalency between geogrids is difficult to suggest. Longitudinal and transverse rib strength, modulus in both directions, and junction strength are all included in the reinforcement mechanisms, but to what degree needs product-specific investigation.

3.2.2 Paved Roads—Pavements

There is ongoing research on the placement of geogrids directly within the pavement itself (bitumen or concrete). This section pertains to both new construction and rehabilitation of existing pavements (i.e., the retardation of reflective cracks). Brown et al. [26] have reported that at high deformations of the pavement surface, geogrids clearly minimize rutting. However, at low deformations, the improvement is nominal. Keeping the geogrid tight during its placement (and possibly even prestressing it) appears to be logical, but it is clearly difficult to achieve. Equipment and techniques are described by Kennepohl and Kamel [27]. The material and type of geogrid is very important, since asphalt will not easily bond to the surfaces of polyethylene, polypropylene, or polyester rod (strap), but it can easily do so for yarn-type geogrids, particularly if bitumen coated. The influence of geogrid shrinkage during placement of hot asphalt may be a problem for molecular stress relaxation and loss of strength or modulus for highly oriented geogrids. In spite of the above comments, success has been reported in the prevention of reflective cracking using geogrids as crack arresters [26].

The use of geogrids to retard and minimize reflective cracking within old pavements from propagating through newly placed asphalt overlays is a topic of great interest. Results of laboratory testing by Molenaar and Nods [28] suggest the

use of a power law to calculate the rate of crack propagation through the new overlay thickness:

$$\frac{dc}{dN} = AK^n \tag{3.9}$$

where

$\frac{dc}{dN}$ = crack propagation rate per number of load cycles,

K = stress intensity factor, and

A, n = experimentally obtained constants.

Example 3.5 illustrates how equation (3.9) can be used in the prediction of overlay lifetime without, and then with, different types of geogrids and a geotextile.

Example 3.5

A 100 mm asphalt overlay is to be placed on top of a severely cracked pavement having a cement treated base. The DTN for the pavement is 100,000 load repetitions (cycles) per year. The combined overlay, existing asphalt layer and base profile, yields a design stress intensity factor (K) of 10 N/mm$^{1.5}$ and constants A of 1.0×10^{-8} and n of 4.3. **(a)** Calculate the average rate of crack growth of the new asphalt overlay. At a full-propagation failure assumption, what is the lifetime (in terms of number of cycles and years) of the new asphalt overlay without reinforcement? **(b)** Redo the problem using the inclusion of various geosynthetic reinforcement materials with A values as follows:

Nonwoven geotextile: $A_{GT} = 0.50 \ (A_{nonreinf.})$—author estimate

Polypropylene geogrid: $A_{PP} = 0.35 \ (A_{nonreinf.})$—author estimate

Polyester geogrid: $A_{PET} = 0.33 \ (A_{nonreinf.})$—Ref. [28]

Fiber glass geogrid: $A_{FG} = 0.25 \ (A_{nonreinf.})$—author estimate

Solution:

(a) Using the power law of equation (3.9), the crack propagation rate is calculated, from which the number of cycles and lifetime are obtained. The crack-propagation rate is

$$\frac{dc}{dN} = AK^n$$
$$= 1 \times 10^{-8} \times (10)^{4.3}$$
$$= 0.0002 \text{ mm/cycle}$$

from which the number of load cycles (nonreinforced) is

$$N = \frac{T}{(dc/dN)}$$
$$= \frac{100}{0.0002}$$
$$= 500,000 \text{ cycles or 5 years}$$

(b) Using the various modified A values for different types of geosynthetic reinforcement gives rise to the table below.

Reinforcement	Crack Growth Rate (mm/cycle)	Lifetime (cycles/years)
None	2.0×10^{-4}	500,000/5
Geotextile	1.0×10^{-4}	1,000,000/10
PP geogrid	0.7×10^{-4}	1,400,000/14
PET geogrid	6.6×10^{-5}	1,500,000/15
FG geogrid	5.0×10^{-5}	2,000,000/20

The technique is very intriguing and warrants additional research in this important transportation engineering application.

While many field trials are also ongoing, it is important to note that geogrids are being used directly in new pavements and in asphalt overlays to resist thermally induced stresses. This is an important consideration when designing an asphalt pavement or its overlay. The change in temperature between night and day and from season to season can be as much as 55°C. The contraction during this temperature shift is considerable, as shown in Example 3.6.

Example 3.6

Calculate the contraction of a 25 m long section of asphalt pavement undergoing a decrease in temperature of 55°C, assuming that the coefficient of expansion/contraction of the asphalt pavement is 12×10^{-6} per 1°C.

Solution: The calculation is as follows:

$$\Delta L = (25)(55)(12 \times 10^{-6})$$
$$\Delta L = 0.0165 \text{ m}$$

The resulting 16.5 mm could be in the form of a single crack or many smaller cracks. This depends upon the condition of the pavement, primarily its oxidation since its original placement.

Bidirectional geogrids are being placed on existing pavements, generally with an adhesive attached or placed separately, and then covered with a bituminous overlay. Clearly, the tensile strength of the geogrid is mobilized by such thermally induced contraction stresses and probably in a very localized region(s) where the cracks initiate. Thus the necessity for high-tensile strength is apparent. All types of polymeric geogrids are being used in this application, as are geogrids made from fiberglass. Fiberglass has some excellent tensile strength characteristics in this regard (e.g., high strength, low elongation, high modulus, and low creep). In addition, there are some ongoing attempts at using geogrids to reinforce portland-cement concrete pavements in a manner similar to that described here with asphaltic pavements.

3.2.3 Unpaved Roads

The use of geogrids to reinforce soft and/or compressible foundation soils for unpaved aggregate roads is a major application area. Many successes have been reported, together with several attempts at a design method. The most advanced analytical method, and the one that will be used here, is that of Giroud et al. [29]. The method follows along lines similar to those described in the Section 2.6.1. The nonreinforced situation is handled first, and then new concepts are developed for the reinforced case. Here the mechanisms of reinforcement are increased soil strength, enhanced load spreading, and membrane support via controlled rutting. The difference in required thickness of stone base is then compared with the cost of the installed geogrid. If the latter is less expensive (as it usually is for soft soil subgrades), it is recommended for use.

For the nonreinforced case, a U.S. Army Corps of Engineers unpaved road formula has been adapted [29] that includes the number of vehicle passages. For the geogrid-reinforced case, new concepts are developed that include the above-mentioned beneficial mechanisms attributed to inclusion of the geogrid. The effects are as follows:

1. *An increase in soil subgrade strength* from the nonreinforced case to the reinforced case as indicated by a comparison of the following equations:

$$p_e = \pi c_{uN} + \gamma h_o$$
$$p_{\lim} = (\pi + 2)c_{uN} + \gamma h$$

where

p_e = bearing capacity pressure based on the elastic limit (nonreinforced case),

$p_{\lim}$ = bearing capacity pressure based on the plastic limit (reinforced case),

c_{uN} = undrained soil strength at the Nth vehicle passage,

γ = unit weight of aggregate,

h_o = aggregate thickness without reinforcement, and

h = aggregate thickness with reinforcement.

2. *An improved load distribution* to the soil subgrade due to load spreading, which is quantified on the basis of pyramidal geometric shape. Figure 3.9 shows the angle α_0 for the nonreinforced case versus a similar construction for the reinforced case where the new and larger angle is defined as α. The ratio of reinforced to nonreinforced situations is expressed as a ratio of $\tan \alpha / \tan \alpha_0$ which is greater than 1.0.
3. *A tensioned membrane effect*, which is a function of the tensile modulus and elongation of the geogrid and the deformed surface of the subgrade soil (i.e., the rut depth).

By taking the combined effect of the first two above-mentioned geogrid reinforcement mechanisms and comparing it to the nonreinforced case, Giroud et al. [29] have developed the design chart shown in Figure 3.10. The membrane effect has been
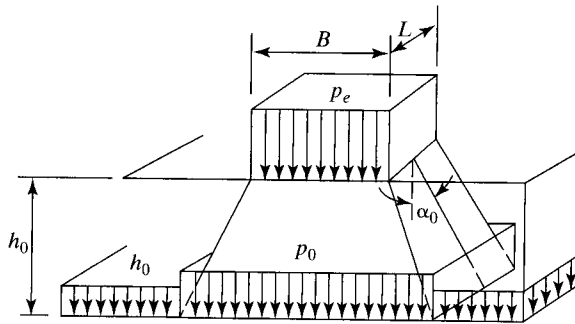
Figure 3.9   Concept of pyramidal load distribution.
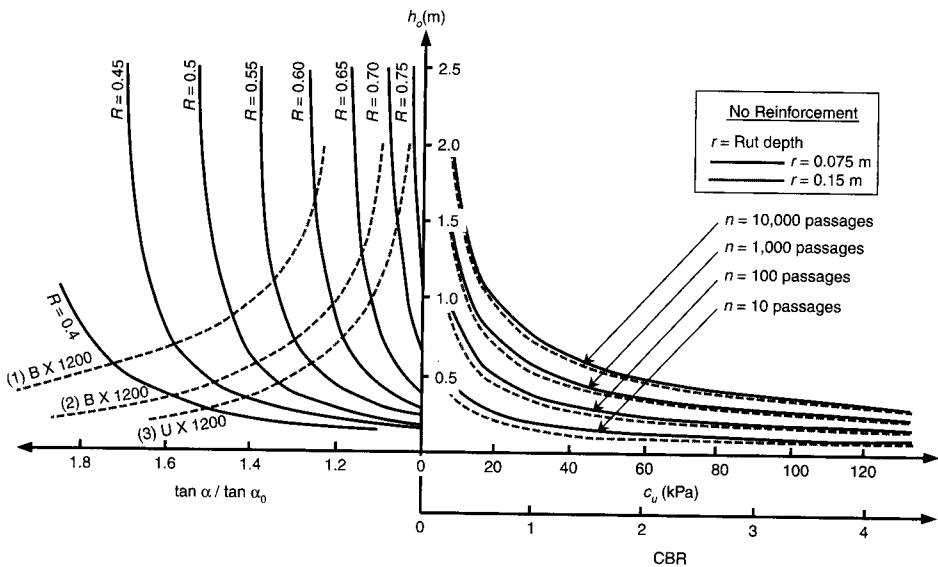
Figure 3.10   Design chart for geogrid-reinforced (left side) and nonreinforced (right side) unpaved roads. (After Giroud et al. [29])

conservatively neglected. On the right side of the graph, for a standard axle load of 80 kN and any number of vehicle passes from 10 to 10,000, a thickness of nonreinforced stone base (h_0) can be obtained upon estimation of the soil subgrade strength. The rut depth turns out to be relatively insignificant. This value is then horizontally extended to the left side of the figure, where it is intersects with one of the following:

- Curve 1, for BX 1200 geogrids, which assumes a large number of vehicle passes $(N > 1000)$ where there is a significant likelihood of aggregate contamination without the geogrid.
- Curve 2, also for BX 1200 geogrids, which assumes a low number of vehicle passes and low likelihood of aggregate contamination.

- Curve 3, for UX 1200 geogrids, which assumes a low number of vehicles passes and low likelihood of aggregate contamination.

This results in an R value that is used in the following equations to determine the aggregate thickness using geogrid reinforcement, h. The difference between h_0 (nonreinforced) and h (reinforced) is the amount of aggregate saved, Δh.

$$h = Rh_0 \qquad \text{for } r < 150 \text{ mm and no channelized traffic pattern}$$
$$h = 0.9\,Rh_0 \qquad \text{for } r \geq 150 \text{ mm with a channelized traffic pattern}$$

Example 3.7

A soil subgrade has a CBR strength of 1.0, and it is to carry 1000 standard-axle vehicle passes with a maximum rut depth of 75 mm. What is the required aggregate depth without a geogrid, the aggregate depth with BX 1200 geogrids with a low likelihood of aggregate contamination, and the difference in aggregate thickness between the two cases?

Solution: Using Figure 3.10, the nonreinforced case gives

$$h_0 = 0.60 \text{ m}$$

For the geogrid-reinforced case, Curve 2 gives $R = 0.50$:

$$h = Rh_0$$
$$= (0.50)(0.60)$$
$$= 0.30 \text{ m}$$

The aggregate saved is

$$\Delta h = 0.60 - 0.30$$
$$= 0.30 \text{ m}$$

3.2.4 Embankments and Slopes

The use of geogrids to reinforce embankments or steep soil slopes (defined as making an angle with the horizontal of less than 70°) directly parallels the techniques and designs that were developed using geotextiles (recall Section 2.7.2). The use of limit equilibrium methods via a circular arc failure plane, thereby intercepting the various layers of reinforcement, was illustrated in Figures 2.50 and 2.51. This allowed for the formulation of a factor of safety expression as follows:

$$\text{FS} = \frac{M_R + \sum_{i=1}^{n} T_i y_i}{M_D} \tag{3.10}$$

where

M_R = moments resisting failure due to the soil's shear strength,

M_D = moments causing failure due to gravity, seepage, seismic, dead, and live loads,

T_i = allowable reinforcement strength, providing force(s) resisting failure,

y_i = appropriate moment arm(s), and

n = number of separate reinforcement layers.

Forsyth and Bieber [30] used this approach to design the reconstruction of a failed slope in California. They selected a required factor of safety along with a given type of geogrid and calculated the number of layers of reinforcement to realize this value. As Example 3.8 illustrates, they used a very low allowable strength for the geogrids used (i.e., 6.67 kN/m which is only 8.4% of the ultimate value). In the context of reduction factors as per Section 3.1.5, this is equivalent to $\Pi RF = 11.8$, which is extremely high.

Example 3.8

For a failed soil slope of known centroid and radius resulting in a resisting moment of 2010 kN/m and a driving moment of 2570 kN/m, determine **(a)** the factor of safety without reinforcement, and **(b)** the number of layers of a specific geogrid with an ultimate strength of 78.7 kN/m and combined reduction factors of 11.8 using the average centroid of the reinforcement as 14.3 m and the required factor of safety to be 1.4.

Solution:

(a)   The factor of safety for the nonreinforced case is

$$FS = \frac{M_R}{M_D}$$

$$= \frac{2010}{2570}$$

$$FS = 0.78 \qquad \text{which indicates failure, as indeed did happen}$$

(b)   The geogrid-reinforced case is as follows:

$$T_{\text{allow}} = T_{ult}/(\Pi RF)$$

$$= 78.7/11.8$$

$$= 6.67 \text{ kN/m}$$

$$FS = \frac{M_R + (n)(T_{\text{allow}})(y_{\text{ave}})}{M_D}$$

$$1.4 = \frac{2010 + (n)(6.67)(14.3)}{2570}$$

$$n = 16.6 \qquad \text{use 17 layers}$$

When reconstructing such failed slopes, or when building steep soil slopes, the main reinforcement layers are usually interspersed with secondary reinforcement layers. These layers aid in compaction at the face of the slope and also tend to reduce surface erosion. Figure 3.11 shows a case of reconstructing a major highway and gaining additional space at both the toe and the top of the slope.

Example 3.8 did not go into the details of determining the location of the reinforcement layers or their lengths. For these details slope stability methods are nicely adapted to computer modeling and have resulted in a number of excellent design
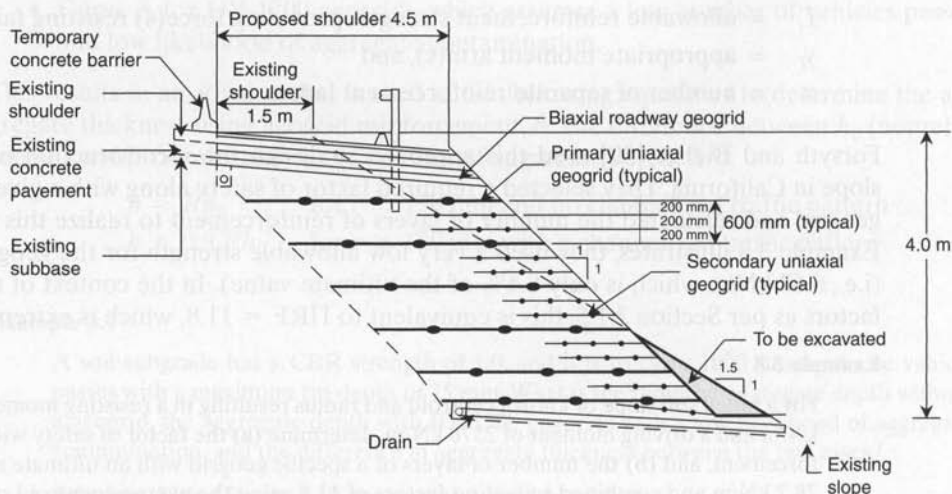
Figure 3.11   Shoulder widening of Pennsylvania Turnpike using geogrid reinforced steep soil slopes. (After Berg et al. [31])

charts. Schmertmann et al. [32] have developed a summary of the various investigators and some of the assumptions that were made in their studies (see Table 3.4). All used limit equilibrium methods to determine the reinforcement (geogrid or geotextile) spacing. However, only Jewell [35], Ruegger [38], and Schmertmann et al. [32] have given charts for the required reinforced lengths. The former two methods use constant-length reinforcement placed parallel to the slope face, whereas Schmertmann et al. use gradually decreasing lengths as the layers proceed higher in the slope. For high embankments, where the potential failure surface is curved (e.g., a logarithmic spiral), this is both accurate and more practical. However, for low and medium walls, the more conservative approach of Jewell [35] is favored by the author and will be used here.

For reinforced slopes placed on adequately strong, level foundations, limit equilibrium can be used in the form of a two-part wedge surface as shown in Figure 3.12. The design chart includes varying soil properties, slope angles, and geometric considerations; see Figure 3.13. Charts are are also available for pore water in the backfill soil. Example 3.9 illustrates the use of the chart under the assumption of zero pore water pressure.

Example 3.9

We plan to construct a soil embankment at a 70° slope angle with the horizontal and 10 m height, to be reinforced with unidirectional geogrids having an ultimate strength of 180 kN/m and combined reduction factors of 4.12. The factor of safety is to be 1.4. The soil is granular, with $\gamma = 18$ kN/m^3 and $\phi = 30°$, and it has no pore water pressure (i.e., $r_u = 0$). Determine the number, spacing, and length of the individual geogrid layers.

Solution: By observation, this slope at 70° to the vertical without reinforcement is in a failure state (that is, FS < 1.0) and is in need of some type of reinforcement. The design procedure is given in steps.

TABLE 3.4 SUMMARY OF SLOPE REINFORCEMENT DESIGN CHARTS

Investigator	Limit Equilibrium Model	Soil Strength	Pore Pressure	Slope Angle (degrees)	Length of Reinforcement	Comments
Ingold [33]	Infinite slope	$\phi' = 30°$	N.A.	30–80	N.A.	Surficial stability only
Murray [34]	Two-part wedge	ϕ'	r_u (0,0.25,0.5)	10–40	N.A.	Reinforcement load-elongation relationship included in model
Jewell [35]	Two-part wedge	ϕ'	r_u (0,0.25,0.5)	30–80	Parallel truncation	Basis for Schmertmann et al. [32], study
Leshchinsky and Reinschmidt [36]	Log spiral	c', ϕ'	N.A.	15–90	N.A.	Rigorous equilibrium model
Schneider and Holtz [37]	Two-part wedge	c', ϕ'	r_u	0–40	N.A.	Extended the work of Murray [34]; charts do not give critical surfaces
Ruegger [38]	Circular	ϕ'	N.A.	30–90	Parallel truncation	For FS = 1.3 only
Schmertmann et al. [32]	Two-part wedge	ϕ'	N.A.	30–80	General truncation	This study extended work of Jewell [35]

N.A.—Not addressed

Source: After Schmertmann et al. [32].
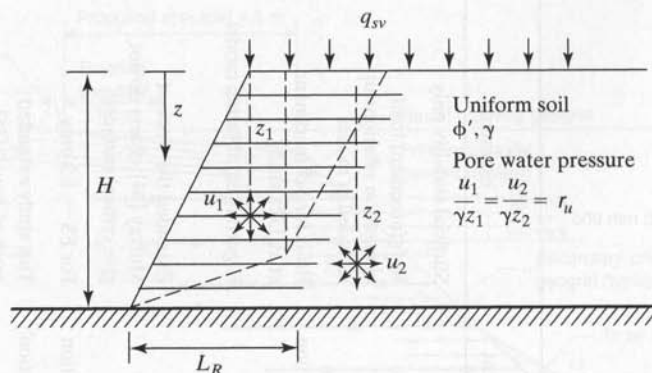
Figure 3.12 Definitions for analysis of steep reinforced soil slopes. (After Jewell [35])

(a) Calculate the allowable strength on the basis of the given reduction factors and then calculate the required strength, which includes the factor of safety

$$T_{ult} = 180 \text{ kN/m}$$

$$T_{allow} = \frac{180}{4.12}$$

$$= 43.7 \text{ kN/m}$$

$$T_{reqd} = \frac{43.7}{1.4}$$

$$= 31.2 \text{ kN/m}$$

(b) Determine the necessary values from Figure 3.13 for $r_u = 0$, $\beta = 70°$ and $\phi = 30°$. This results in the following

$$K_{reqd} = 0.19$$

$$(L_R/H)_{ovrl} = 0.51$$

$$(L_R/H)_{ds} = 0.38$$

(c) Calculate the spacing, S_v, at the base of the slope where the stresses are greatest:

$$S_v = \frac{T_{reqd}}{K_{reqd} \gamma z_{max}}$$

$$= \frac{31.2}{(0.19)(18)(10)}$$

$$S_v = 0.91 \text{ m}$$

If evenly spaced, the required number of geogrid layers will be

$$n = \frac{H}{S_v}$$

$$= \frac{10}{0.91}$$

$$n = 11 \text{ layers}$$

Steep Reinforced Slope Design Charts	Chart 1 $r_u = \dfrac{u}{\gamma_z} = 0.00$

(a) Minimum required force K_{reqd}

Minimum reinforcement length:

(1) The minimum length at the crest of the slope is that required for *overall stability*.

(2) The minimum length at the base of the slope is the greater of that required for *overall stability* and to prevent *direct sliding*.

(3) Where reinforcement of constant length is to be used, select the greater length required to satisfy equilibrium at the base of the slope, (2) above.

(4) Where *direct sliding* governs the required reinforcement length at the base of the slope, it is permissible to reduce the length uniformly from L_{ds} at the base of the slope to L_{ovrl} at the crest of the slope.

(b) Minimum required length overall stability $(L_R/H)_{ovrl}$

(c) Minimum required length direct sliding $(L_R/H)_{ds}$

Figure 3.13   Steep reinforced soil slope design charts for zero pore water pressure. (After Jewell [35])

(d) Select the reinforcement length:

- If $(L_R/H)_{\text{ovrl}} > (L_R/H)_{ds}$, use constant length $= (L_R/H_{\text{ovrl}})$.
- If not, use constant length $= (L_R/H)_{ds}$ or taper the lengths from $(L_R/H)_{ds}$ at the base to $(L_R/H)_{\text{ovrl}}$ at the crest.

Since $0.51 > 0.38$ use $L_R/H = 0.51$.

$$\therefore\ L_R = 5.1 \text{ m throughout}$$

(e) The length at the base can be checked by conventional methods using the entire mechanically stabilized earth mass, or according to the equations set forth in [35].

(f) Check among the different geogrid behaviors in the anchorage zone behind the hypothetical shear plane. Such differences must be considered from experimental results, as described in Section 3.1.2. If there is concern about the use of one geogrid product versus another, the designer always has the option of lengthening the geogrids over that required by Figure 3.13.

(g) Sketch the final reinforced slope and provide for miscellaneous details, as shown below; that is, use short (secondary) geogrids between the primary reinforcement and adjacent to the slope for compaction aid and against surface erosion (recall Figure 3.11).
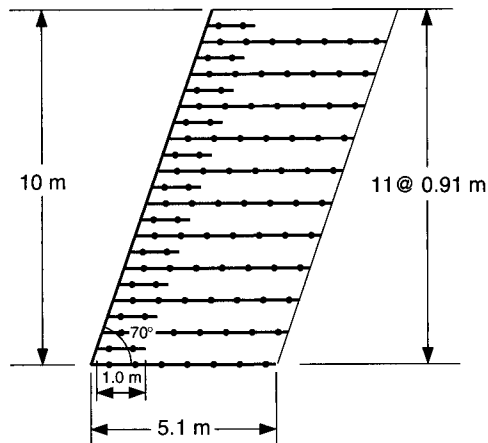
3.2.5 Reinforced Walls

A constantly increasing number of geogrid reinforced walls (defined as making an angle with the horizontal of the 70°, or more) have been constructed in the past 15 years. The current estimate is 15,000 per year in the United States and more than double that worldwide. Most have been designed directly for private owners and developers, but some have involved the public sector through the process of *value engineering*, whereby the low-bid general contractor offers the public agency an option for some particular segment of the project—for example, a geogrid-reinforced wall in place of a conventional reinforced-concrete wall or steel-reinforced wall. If the option is acceptable to the agency, the financial savings between the cost of the two different kinds of walls is shared equally between the agency and the contractor. It is a very effective

method for the introduction of new products and concepts like geogrid (and geotextile) reinforced walls. More recently, however, some state highway departments have been designing permanent geogrid-reinforced wing-walls and bridge abutments (Abu-Hejleh et al. [39]). This section addresses geogrid-reinforced wall facing types, costs, design, soil backfill considerations, and field performance.

The various types of permanent geogrid-reinforced wall facings are as follows. The geogrid reinforced soil mass—also called the mechanically stabilized earth (MSE) mass—is the same in all cases.

- *Wraparound facings*: The same as those illustrated in Section 2.7.1 with geotextile walls. Note that in order to provide protection against ultraviolet light and vandalism, a bitumen or concrete coating is usually applied.

- *Timber facings*: Railroad ties or other large treated timbers on which the geogrid is attached by batten strips and/or held by friction when placed between the timbers.

- *Articulated precast concrete panels*: Discrete precast concrete panels with inserts for attaching the geogrid. Many aesthetically pleasing facing designs are possible.

- *Full height precast panels*: Concrete panels temporarily supported until backfilling is complete. These types of walls, however, are challenging due to the vertical stresses developed on the geogrid connections to the wall after removal of the panel support [40].

- *Cast-in-place concrete panels*: Panels that are often attached to wraparound walls that are allowed to settle and after a few months are covered with a cast-in-place facing panel. These walls are currently favored in Japan [41] where the ends of the geogrid reinforcement are embedded in gabions, which then have a concrete facing panel poured against them.

- *Gabion facings*: Polymer or steel-wire baskets filled with stone, in which the geogrid is held between the baskets and fixed with rings and/or friction.

- *Welded wire-mesh facings*: Similar to gabion facings, but without stone fills. The mesh is L-shaped with the geogrids held by friction to the base of the L, or attached by metal rings or by a tapered bar called a *bodkin* (see Figure 3.14).

- *Masonry block faced walls* (also called *segmental retaining walls* [SRWs]): A variety of different block types in which a geogrid is embedded between the blocks and held by pins, keyways, and/or friction. Figure 3.15 presents two examples of such walls, and Figure 3.16 illustrates some of the many variations of modular concrete blocks. Forming an impressive segment of the industry, this type of wall is seeing the greatest growth due to its pleasing aesthetics, adaptability to design, and performance.

In addition to the walls being extremely adaptable to a wide range of conditions, they are the least expensive of all types of retaining walls, including gravity, crib/bin and MSE walls with metallic reinforcement. Figure 3.17 presents survey results of retaining wall costs (Koerner et al. [43]).

The design of the above-described walls must not be considered trivial, for many of them are critical structures that are meant to be permanent, possessing service lifetimes
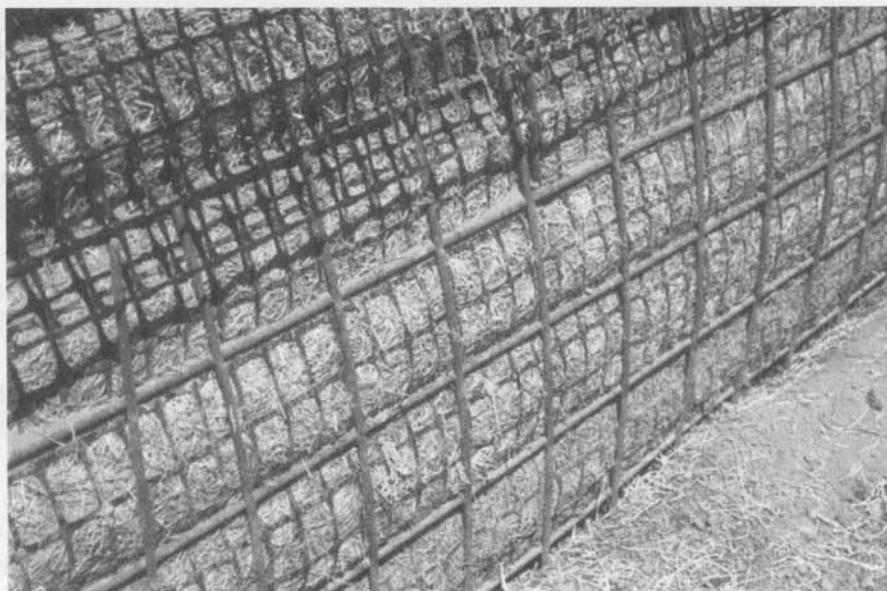
(a) Steel wire mesh with bidirectional geogrid and vegetated erosion control material behind

(b) Wall nearing completion with growing vegetation

Figure 3.14   Steel wire mesh facing of geogrid-reinforced earth wall. Note backup using bidirectional polypropylene geogrids. (Compliments of Tensar Corp.)
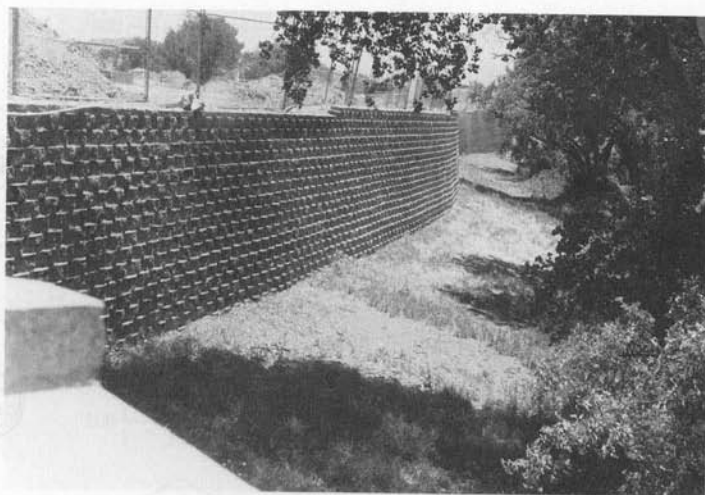
(a) Intermediate height modular concrete block wall
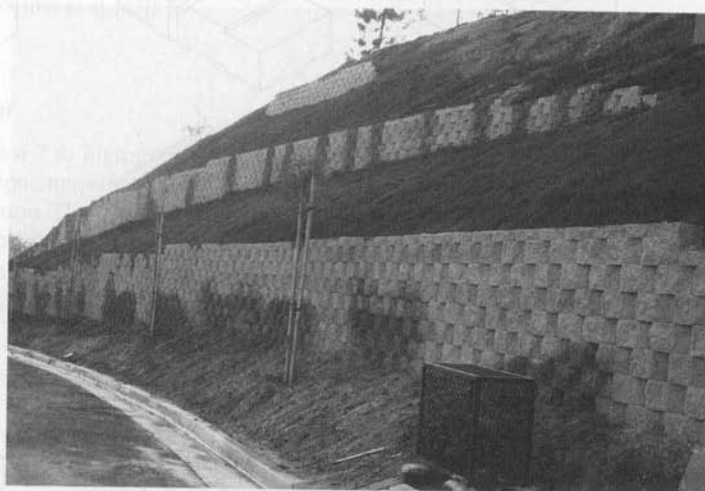
(b) Tiered walls with intermediate slopes

Figure 3.15   Geogrid reinforced modular concrete block walls (also called segmental retaining walls). (Compliments of TC Nicolon Co.)

in excess of 100 years. Design centers around the external stability of the entire mechanically stabilized mass (sliding, overturning, and bearing capacity), and the internal stability within the reinforced mass (geogrid spacing, anchorage length, and connection strength). Figure 3.18 illustrates these concepts. Each of these stability issues must be treated individually and before coming together for the final design. Example 3.10 illustrates this process using a geogrid-reinforced wall with articulated precast concrete facing panels.
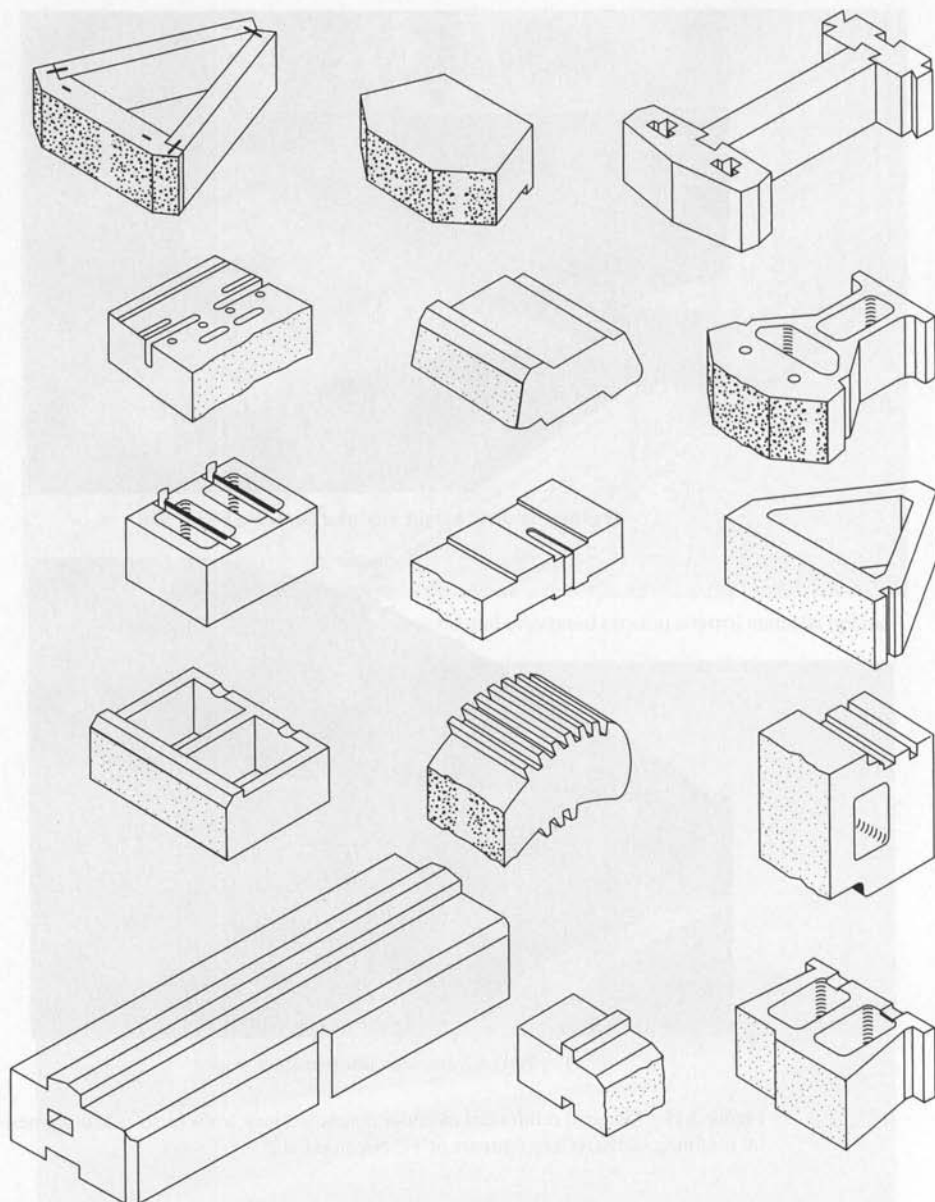
Figure 3.16 Examples of commercially available modular concrete blocks for segmental retaining walls. (After Bathurst and Simac [42])
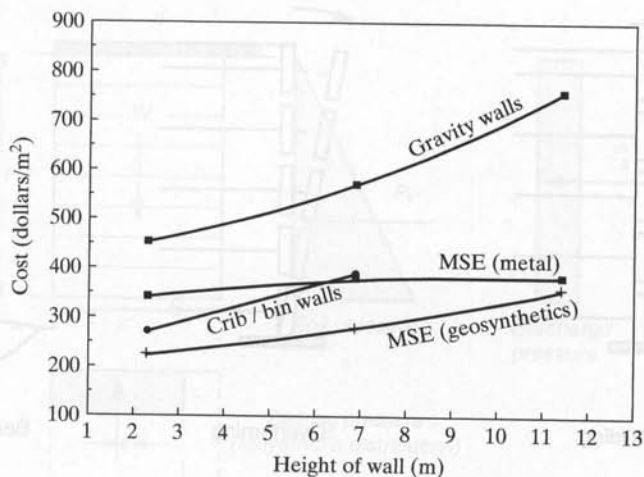
Figure 3.17   Results of retaining wall cost survey in the United States. (After Koerner et al. [43])

Example 3.10

Design a 7 m high geogrid-reinforced wall where the reinforcement spacing must be at 1.0 m spacings, since the wall facing is of the articulated precast concrete type of this same dimension. The coverage ratio is 0.8 (i.e., geogrids do not cover the entire ground surface at each lift; they are slightly separated). The length-to-height ratio of the reinforced soil wall should not be less than 0.7 (i.e., $L \geq 4.9$ m). Additional details of the problem, including soil and geogrid data are shown in the diagram below.

Sliding   Overturning   Bearing capacity

(a) External stability

Spacing   Anchorage length   Connection strength

(b) Internal stability
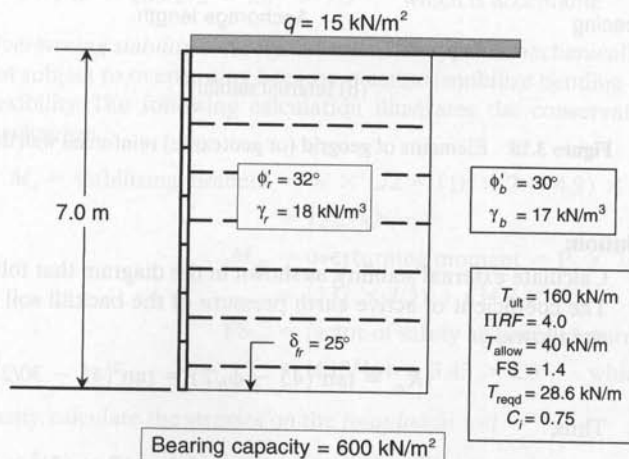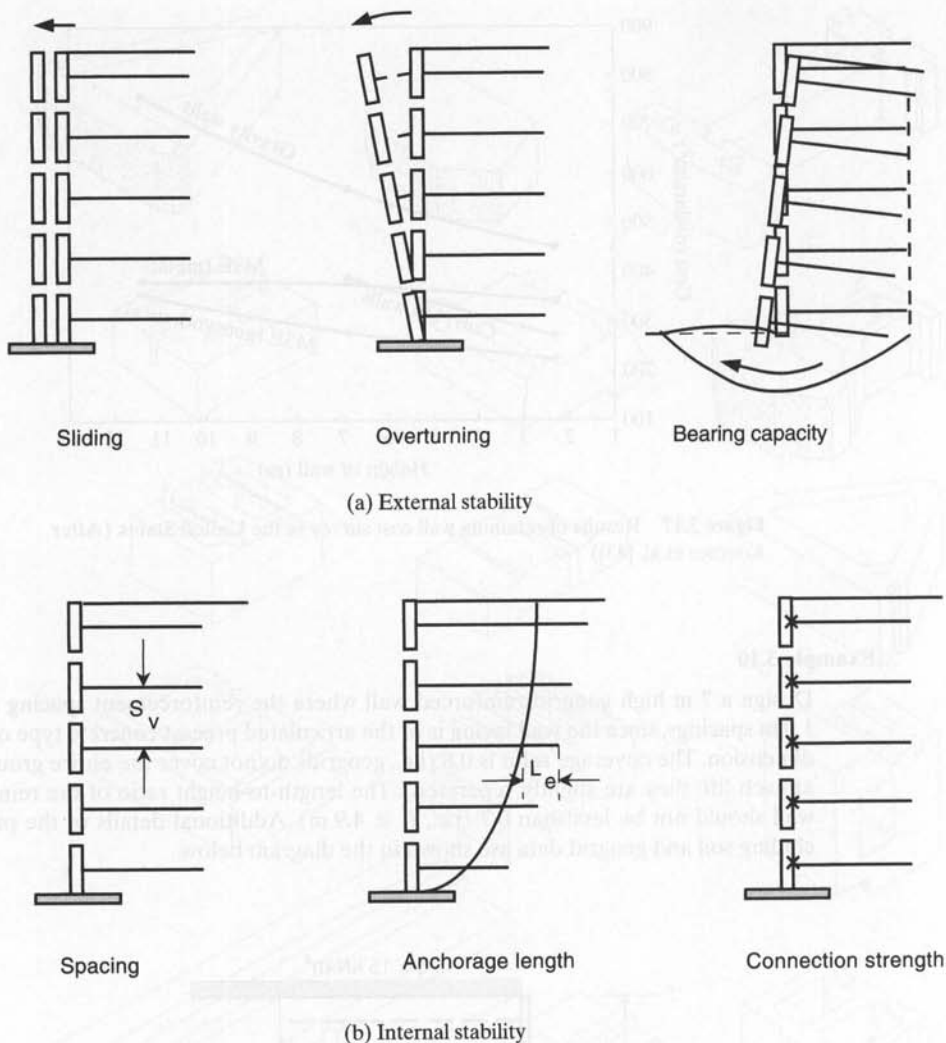
Figure 3.18 Elements of geogrid (or geotextile) reinforced wall design.

Solution:

(a) Calculate external stability, as shown in the diagram that follows, assuming L = 4.9 m. The coefficient of active earth pressure of the backfill soil behind reinforced zone is as follows:

$$K_{a_b} = \tan^2(45 - \phi_b/2) = \tan^2(45 - 30/2) = 0.33$$

Thus,

$$P_1 = 0.5 \times \gamma_b \times H^2 \times K_{a_b} = 0.5 \times 17 \times (7)^2 \times 0.33 = 137 \text{ kN/m}$$
$$P_2 = qK_{a_b} \times H = 15 \times 0.33 \times 7 = 34.7 \text{ kN/m}$$
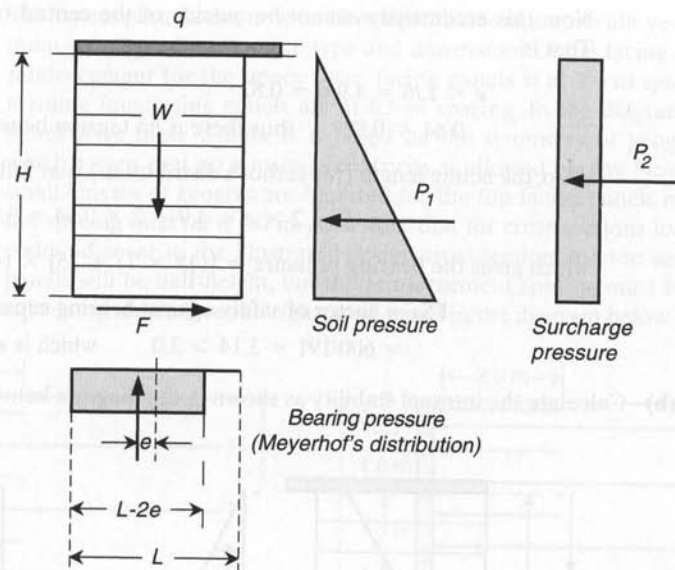
The total force is $P = 137 + 34.7 = 172$ kN/m.

1. We now calculate the *sliding stability*

$$F = \text{Resisting force} = W \times \mu$$
$$= \gamma_r \times H \times L \times \tan \delta \quad \text{(conservatively neglecting surcharge)}$$
$$= 18 \times 7 \times 4.9 \times \tan 25° = 288 \text{ kN/m}$$

FS_s = factor of safety against sliding

$$= F/P = 288/172 = 1.67 > 1.5 \quad \text{which is acceptable}$$

2. *Overturning stability* is rarely an issue. This type of mechanically stabilized wall is not subject to overturning because it cannot mobilize bending due to its inherent flexibility. The following calculation illustrates the conservative aspect of this mechanism.

$$M_s = \text{stabilizing moment} = W \times L/2 = (18 \times 7 \times 4.9) \times (4.9/2)$$
$$= 1513 \text{ kN/m}$$
$$M_{ov} = \text{overturning moment} = P_1 \times 7/3 + P_2 \times 7/2$$
$$= (137 \times 7/3) + (34.7 \times 7/2) = 441 \text{ kN/m}$$
$$FS_{ov} = \text{factor of safety against overturning}$$
$$= 1513/441 = 3.43 > 2.0 \quad \text{which is acceptable}$$

3. Lastly, calculate the stresses on the *foundation soil*

$$e = \text{eccentricity} = M_{ov}/(W + q \times L)$$
$$= 441/(18 \times 7 \times 4.9 + 15 \times 4.9) = 0.64 \text{ m}$$

Now, this eccentricity cannot be outside of the central one-third of the footing. That is

$$e < L/6 = 4.9/6 = 0.82$$
$$0.64 < 0.82 \qquad \text{thus there is no tension beneath the footing}$$

Also, the acting length (Meyerhof's distribution) is as follows:

$$= L - 2 \times e = 4.9 - 2 \times 0.64 = 3.62 \text{ m}$$

which gives the bearing pressure $= [(18 \times 7) + 15] \times (4.9/3.62) = 191 \text{ kPa}$

$$FS_b = \text{factor of safety against bearing capacity failure}$$
$$= 600/191 = 3.14 > 2.0 \qquad \text{which is acceptable}$$

(b) Calculate the internal stability as shown in the diagram below.
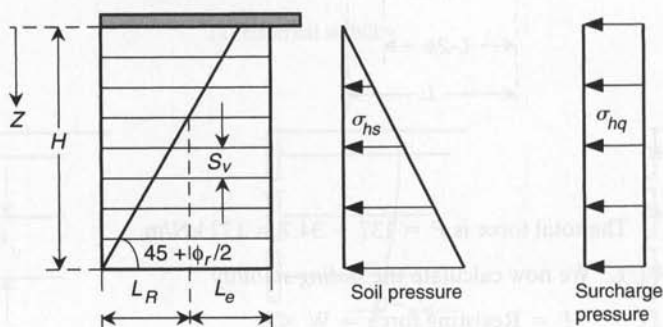
$$\sigma_h = \sigma_{hs} + \sigma_{hq}$$
$$= \gamma z K_{ar} + q K_{ar}$$
$$K_{ar} = \tan^2(45 - \phi_r/2) = 0.31$$
$$\sigma_h = (18 \times z \times 0.31) + (15 \times 0.31)$$
$$= 5.58 z + 4.65$$

1. For geogrid vertical spacing

$$T_{reqd} = s_v \sigma_h / C_r \text{ (where } C_r = \text{coverage ratio)}$$
$$28.6 = s_v (5.58 z + 4.65)/0.8$$
$$s_v = \frac{22.9}{5.58 z + 4.65}$$

Maximum depth for $s_v = 1$ m

$$1.0 = \frac{22.9}{5.58 z + 4.65} \Rightarrow z = 3.27 \text{ m}$$

Maximum depth for $s_v = 0.5$ m

$$0.5 = \frac{22.9}{5.58 z + 4.65} \Rightarrow z = 7.37 \text{ m}$$

The layout pattern can now be developed based upon the above-calculated maximum spacing values and the type and dimensions of the facing panels. Thus, the reinforcement for the upper three facing panels is at 1.0 m spacing and the remaining four facing panels are at 0.5 m spacing. In the diagram below, the left panel gives these details. It is based on the symmetry of geogrid connections, which means that no tension eccentricity is allowed on any facing panel. Hence, small lengths of geogrid are required for the top facing panels of the wall where the spacing interval is 1.0 m. Also note that for cross-sections located one facing panel adjacent to the illustrated design cross section, the top and bottom facing panels will be half-height, but the reinforcement spacing must be maintained as calculated above (see the right-hand panel in the diagram below.)
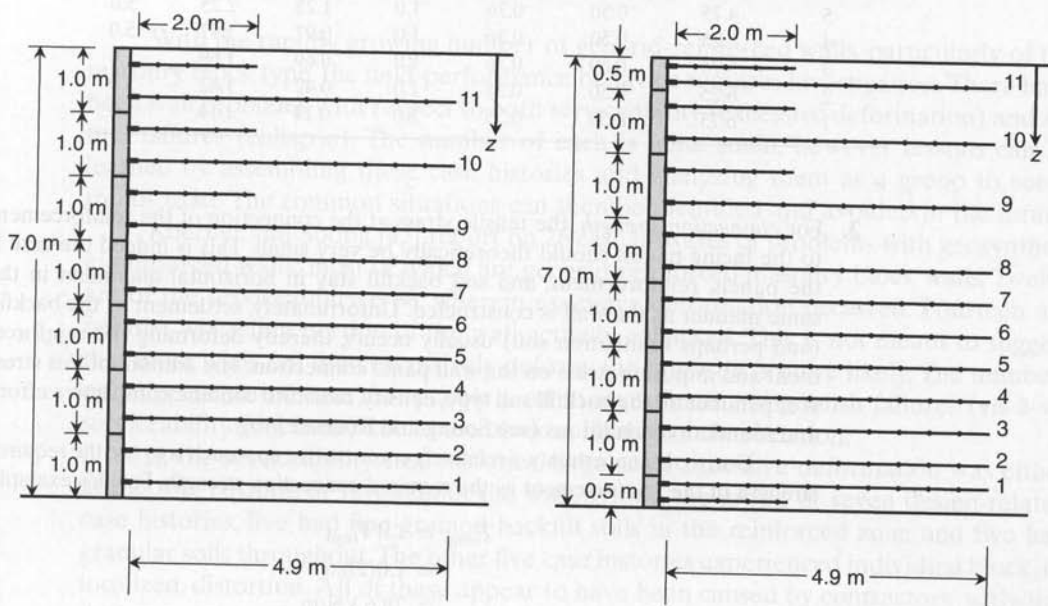
2. For the *total length* we consider the embedment plus the nonacting Rankine length. For the embedment length we have

$$s_v \times \sigma_h \times FS_{pullout} = 2 \times L_e \times C_i \times \sigma_v \tan \phi' \times C_r$$

$$s_v(5.58\,z + 4.65)1.5 = 2L_e(0.75)(18\,z)(\tan 32)(0.8)$$

$$L_e = \frac{s_v(5.58\,z + 4.65)1.5}{(2)(0.75)(18\,z)(\tan 32)(0.8)}$$

$$L_e = \frac{(0.62\,z + 0.516)s_v}{z}$$

For the nonacting Rankine length

$$L_R = (H - z) \tan\left(45 - \frac{\phi}{2}\right)$$

$$= (7 - z) \tan\left(45 - \frac{32}{2}\right)$$

$$L_R = 3.88 - 0.554\,z$$

The above relationships lead to the table below.

Layer Number	Depth z (m)	Spacing s_v (m)	L_e (m)	$L_{e_{min}}$ (m)	L_R (m)	L_{calc} (m)	L_{reqd} (m)
11	0.75	0.75	0.98	1.0	3.46	4.46	5.0
10	1.75	1.00	0.92	1.0	2.91	3.91	5.0
9	2.75	1.00	0.81	1.0	2.36	3.36	5.0
8	3.25	0.50	0.39	1.0	2.08	3.08	5.0
7	3.75	0.50	0.38	1.0	1.80	2.80	5.0
6	4.25	0.50	0.37	1.0	1.52	2.52	5.0
5	4.75	0.50	0.36	1.0	1.25	2.25	5.0
4	5.25	0.50	0.36	1.0	0.97	1.97	5.0
3	5.75	0.50	0.36	1.0	0.69	1.69	5.0
2	6.25	0.50	0.35	1.0	0.42	1.42	5.0
1	6.75	0.50	0.35	1.0	0.14	1.14	5.0

3. For *connection strength*, the tensile stress at the connection of the reinforcement to the facing panels should theoretically be very small. This is indeed the case if the panels, reinforcement, and soil backfill stay in horizontal alignment in the same manner as the wall is constructed. Unfortunately, settlement of the backfill (and perhaps foundation soil) usually occurs, thereby deforming the reinforcement and imposing stress on the wall panel connection. The amount of this stress is dependent on the backfill soil type, density, moisture content, compactive effort, and foundation conditions (see Soong and Koerner [40]).

   Due to this uncertainty, a relatively conservative approach is to use the required strength of the reinforcement as the required connection strength. For this example;

$$T_{conn} \geq 1.0\, T_{regd}$$
$$\geq 1.0(28.6)$$
$$\geq 28.6 \text{ kN/m}$$

   See Section 3.1.2 for the experiment necessary to obtain the allowable connection strength to the wall facing.

4. For drainage behind the wall, it is assumed that hydrostatic pressures are not developed. This assumes in turn that cohesionless sands (or gravels) are used as soil backfill in the reinforced zone. A recommended gradation is given in Table 3.5. While coarser particle sizes could have been given (i.e., a gravel soil), the reduction factor for installation damage might be high and gravel is generally more expensive than sand. Comments later in this section will discuss the concern over using finer-grained soils along with the necessity of then using back and base drains to conduct water away from the reinforced soil mass.

It should be noted that most wall designers do not work from the basic principles just illustrated. There are several widely distributed computer programs used for such wall designs. The program developed by Leshchinsky [44] is the most popular because of its technical accuracy, flexibility in input configurations, data generation, and graphical output.

TABLE 3.5 RECOMMENDED BACKFILL SOIL GRADATION FOR
GEOGRID- OR GEOTEXTILE-REINFORCEMENT APPLICATIONS
(WALLS AND SLOPES) TO AVOID HYDROSTATIC PRESSURE
BUILDUP AND EXCESSIVE INSTALLATION DAMAGE

Sieve Size (no.)	Particle Size (mm)	Percent Passing
4	4.76	100
10	2.0	90–100
40	0.42	0–60
100	0.15	0–5
200	0.075	0

With the rapidly growing number of geogrid-reinforced walls, particularly of the masonry block type, the field-performance behavior requires investigation. There have been wall problems with respect to both serviceability (excessive deformation) and actual failures (collapse). The number of each is quite small, however lessons can be learned by assembling these case histories and analyzing them as a group to see if trends exist. The common situations can then be identified and avoided in the future.

Koerner and Soong [45] report on 26 case histories of problems with geosynthetic-reinforced walls; most of which are geogrid-reinforced masonry block walls. Twelve are of the serviceability type, wherein excessive deformation occurred. Fourteen are failures, wherein a portion of the wall actually collapsed. This is not meant to suggest that more walls fail than excessively deform; the opposite is more likely. The numbers only appear to indicate that people tend to investigate and publish failures (vis-à-vis serviceability problems) due to the obvious finality of the situation.

In the serviceability case histories, large-scale excessive deformation was either at the top, bottom, or throughout the wall. Within the group of seven design-related case histories, five had fine-grained backfill soils in the reinforced zone and two had granular soils throughout. The other five case histories experienced individual block, or localized, distortion. All of these appear to have been caused by contractors' activities during construction. The message in both situations appears to be clear: (1) fine-grained silts and clays should be questioned insofar as backfill soils are concerned, and (2) contractors' operations must be monitored and inspected to ensure adequate construction quality control.

In the failure (or collapse) case histories, hydrostatic pressure arising from lack of drainage from fine-grained soil backfills in the reinforced zone was the overriding reason for the failures. This occurred in 10 of the 14 case histories and all are considered as design-related causes. It substantiates the concern over silt and clay backfills seen in the serviceability case histories. In three other failure case histories, contractor deficiencies were observed, again supporting the findings of the serviceability case histories insofar as lack of inspection and installation quality control are concerned.

Interestingly, in only one of the 26 case histories investigated is the problem *not* fine-grained soil backfill or inadequate construction/inspection procedures. In this case, the wall experienced a compound failure behind and beneath the entire wall structure carrying it and a much larger body of soil downslope in a large-scale failure. Once again, it was a fine-grained soil problem albeit not in the reinforced soil zone per se.

If fines (silts and/or clays) are allowed for the reinforced zone backfill soil, any possible water in front, behind, and beneath the reinforced zone must be carefully collected, transmitted, and discharged. Proper drainage control is absolutely critical in this regard. Furthermore, the top of the zone should be waterproofed—for example, by a geomembrane or a geosynthetic clay liner—to prevent water from entering the backfill zone from the surface. Surface water drainage as well as drainage from the retained earth zone is obviously of concern with respect to potential buildup of pore water pressures behind or within the reinforced soil zone. (See Koerner and Soong [46] for wall drainage system designs in this regard.)

In closing this section on geogrid reinforced walls, the current tendency to create live (or evergreen) walls with open facing should be mentioned. As we saw earlier in Figure 3.14, the sequence is a steel wire mesh (alternatively a gabion), backed by a bidirectional geogrid and then by a geosynthetic erosion control material. The reinforcing geogrids (always unidirectional types) are either attached to the steel wire mesh facing, or they are frictionally connected by sufficient overlap length. Such walls avoid masonry block durability concerns and offer a considerably less expensive wall system. Of course, the durability of the steel wire and bidirectional geogrid backup must be considered and this is a viable research topic when considering 100-year permanent wall lifetimes.

3.2.6 Foundation and Basal Reinforcement

Geogrids have been used to increase bearing capacity of poor foundation soils in different ways: as a continuous layer, as multiple closely spaced continuous layers with granular soil between layers, and as mattresses consisting of three-dimensional interconnected cells. The technical database for the single-layer continuous sheets has been reported by Jarrett [47] and by Milligan and Love [48]; in both cases large-scale laboratory tests are used. Figure 3.19 presents some of Milligan and Love's work graphed in the conventional nondimensionalized q/c_u versus ρ/B manner and also as $q/\sqrt{c_u}$ versus ρ/B where q is the bearing capacity and ρ is the settlement. The latter graph is not conventional but does sort out the data nicely. Clearly shown in both instances is the marked improvement in load-carrying capacity using geogrids at high deformation and only a nominal beneficial effect at low deformation. Beyond these observations, a precise design formulation is not currently available.

Instead of focusing on a global increase in bearing capacity, it is quite likely that single or multiple layers of geogrid (or geotextile) will aid in minimizing or eliminating differential settlement. Here localized settlements due to abruptly settling or subsiding weak zones can be spanned by the layer of reinforcement. This is known as *foundation improvement* (rather than bearing capacity via base reinforcement). Notable in this regard is a technique called *piggybacking*—the construction of new landfills above existing landfills. The approach is to use arching theory in the calculation of the vertical stress arising from localized subsidence (i.e., differential settlement) and to provide suitably strong reinforcement.

It should be recognized that arching in natural soils overlying a locally yielding foundation is well established. In the 1930s, both Karl Terzaghi in Austria (calculating
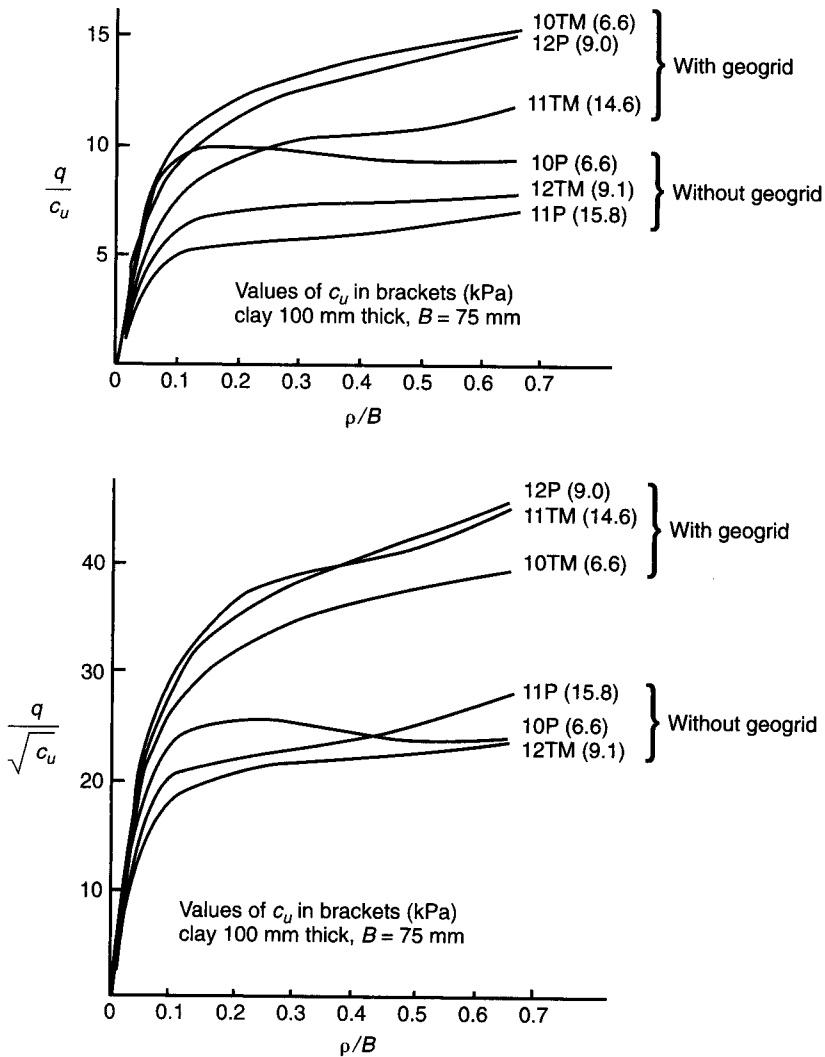
Figure 3.19   Load versus deflection curves of large laboratory tests with and without geogrid reinforcement. (After Milligan and Love [48])

stresses on deep tunnels) and Aston Marston in the United States (calculating stresses on buried pipelines) developed the analytic theory. Their work resulted in the following simplified formula for vertical stress on the surface of the particular underground structure (tunnel or pipe, respectively):

$$\sigma_z = 2\gamma_{ave}R[1 - e^{-0.5\,H/R}] + qe^{-0.5\,H/R} \tag{3.11}$$

where

σ_z = vertical stress on the structure or reinforcement layer,

γ_{ave} = average unit weight of material above the settlement area,

R = radius of differential settlement zone,

H = total height above the settlement area, and

q = surcharge pressure placed at the ground surface.

Note that for large values of H (typically $H \geq 6R$) the formula reduces to the following value of constant vertical stress:

$$\sigma_z = 2\gamma_{ave}R \tag{3.12}$$

Having a method to calculate the vertical stress, we can now use the value to calculate the stress in the reinforcement layer for a new landfill placed over an existing one. Note that the reinforcement can be either a geogrid or a geotextile. For support over a differential settlement area, the value of T_{reqd} is calculated as follows:

$$T_{reqd} = \sigma_z R \Omega \tag{3.13}$$

where

$\Omega = 0.25[(2y)/B + B/(2y)]$, where $\qquad$ (3.14)

B = width of settlement void, $\qquad$ and

y = depth of settlement void.

Giroud et al. [49] have combined the above equations to develop a design chart that can be used to avoid direct calculation (see Figure 3.20). Note that the chart can be used for either circular voids or long extended voids.

Once the value of T_{reqd} is determined, it must be compared to T_{allow} using equation (3.6), which includes the site-specific reduction factors. Example 3.11 illustrates the technique.

Example 3.11

Using the Terzaghi/Marston formulation for calculating vertical stress above localized subsidence, in this case differential settlement in an old landfill of radius 1 m, **(a)** calculate the required wide-width strength of a reinforcement layer if a new 30 m high landfill is to be placed upon the existing one—that is, if the new landfill is to be *piggybacked* on the existing landfill. The compacted unit weight of the waste is 12 kN/m³. **(b)** Check your calculated value against Figure 3.20. **(c)** Calculate the factor of safety for a geogrid with ultimate wide-width tensile strength of 125 kN/m. In the calculations use cumulative reduction factors of 5.0.

Solution:

(a) The formula for vertical stresses in arching situations under a deep fill (such as the one in this example) reduces to equation (3.12). Therefore the vertical stress is calculated as

$$\sigma_z = 2\gamma_{ave}R$$
$$= 2(12)(1.0)$$
$$= 24 \text{ kPa}$$

To transfer this vertical stress into a horizontal force, we use equation (3.13)

$$T_{reqd} = \sigma_z R \Omega$$

where Ω = strain function, f(ϵ) [recall Section 2.5.2]
  Ω = 0.97 at 5% strain
    = 0.73 at 10% strain

Assuming that Ω = 0.73,

$$T_{reqd} = 24 \times 1.0 \times 0.73$$
$$= 17.5 \text{ kN/m}$$

(b) Check this against Figure 3.20:

$$\frac{H}{R} = \frac{30}{1} = 30$$

$$\therefore \frac{T}{\gamma R^2 \Omega} = 2.0$$
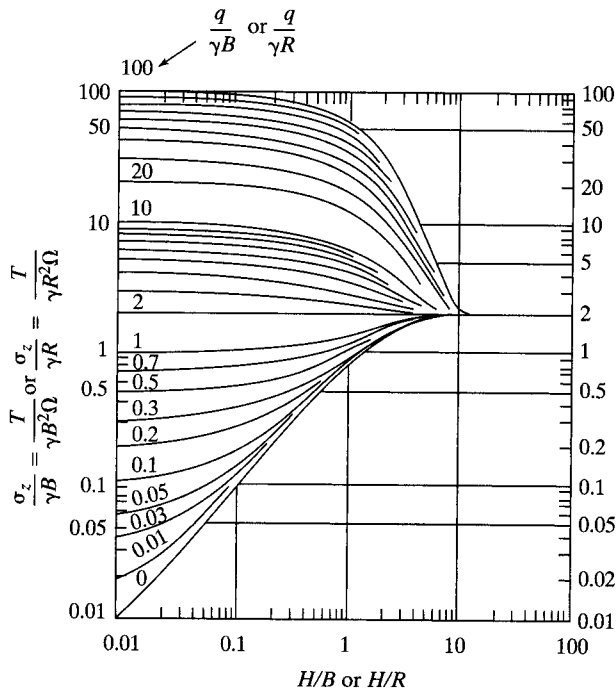
Figure 3.20 Curves of geosynthetic stress and tension that can be used for R (radius of circular void) or B (width of long voids). (After Giroud et al. [49])

$$T_{\text{reqd}} = 2.0(12)(1)^2(0.73)$$
$$= 17.5 \text{ kN/m} \quad \text{which checks}$$

(c) The factor of safety on a geogrid with 125 kN/m ultimate strength (at 10% strain) is as follows:

$$T_{\text{allow}} = T_{\text{ult}}/\Pi\text{RF}$$
$$= \frac{125}{5}$$
$$= 25 \text{ kN/m}$$

and

$$\text{FS} = T_{\text{allow}}/T_{\text{reqd}}$$
$$= 25/17.5$$
$$\text{FS} = 1.43 \quad \text{which is acceptable}$$

In a somewhat different context, but still focused on foundation and basal soil improvement, Edgar [50] reports on a three-dimensional *geogrid mattress* where 1.0 m wide unitized HDPE geogrids are placed vertically and interconnected to one another. Gravel is placed within the geogrid mattress as it is constructed over soft fine-grained foundation soils. Edgar reports on a 15 m high embankment that was successfully constructed above the mattress. It was felt that the nonreinforced slip plane was forced to pass vertically through the mattress and therefore deeper into the stiffer layers of the underlying subsoils. This improved the foundation stability to the point where the mode of failure was probably changed from a circular arc to a less critical plastic failure of the soft clay. The design was considered to be a successful and economic one. Another example of a 1 m high unitized geogrid mattress was constructed to support a 30 m high landfill over extremely soft mine tailings in Hausham, Germany [51]. The mattress was filled with gravel and the liner system constructed above it. The foundation soil was so soft that a nonwoven geotextile and a bidirectional geogrid had to be initially placed to provide a stable working area for the construction of the three-dimensional mattress. Such relatively thick mattresses can also be constructed by using closely spaced layers of bidirectional geogrids separated by granular soil.

In the design of such three-dimensional geogrid mattresses, it is felt that the following phenomena are occurring, all of which improve foundation soil stability (see Figure 3.21):

- *Global slope stability:* This is improved by forcing the potential failure plane through the mattress and deeper into the foundation soil. It is also possible that the foundation soil may improve in strength characteristics at greater depths.
- *Bearing capacity:* This is improved in a similar manner to the point where it becomes a nonissue for mattresses greater than approximately 30 m in width.
- *Lateral extrusion (or squeeze-out):* This is undoubtedly decreased because stress concentrations have been largely eliminated via a uniform pressure distribution applied through the relatively stiff geogrid mattress.

(a) Global slope stability

(b) Bearing capacity

(c) Lateral extrusion
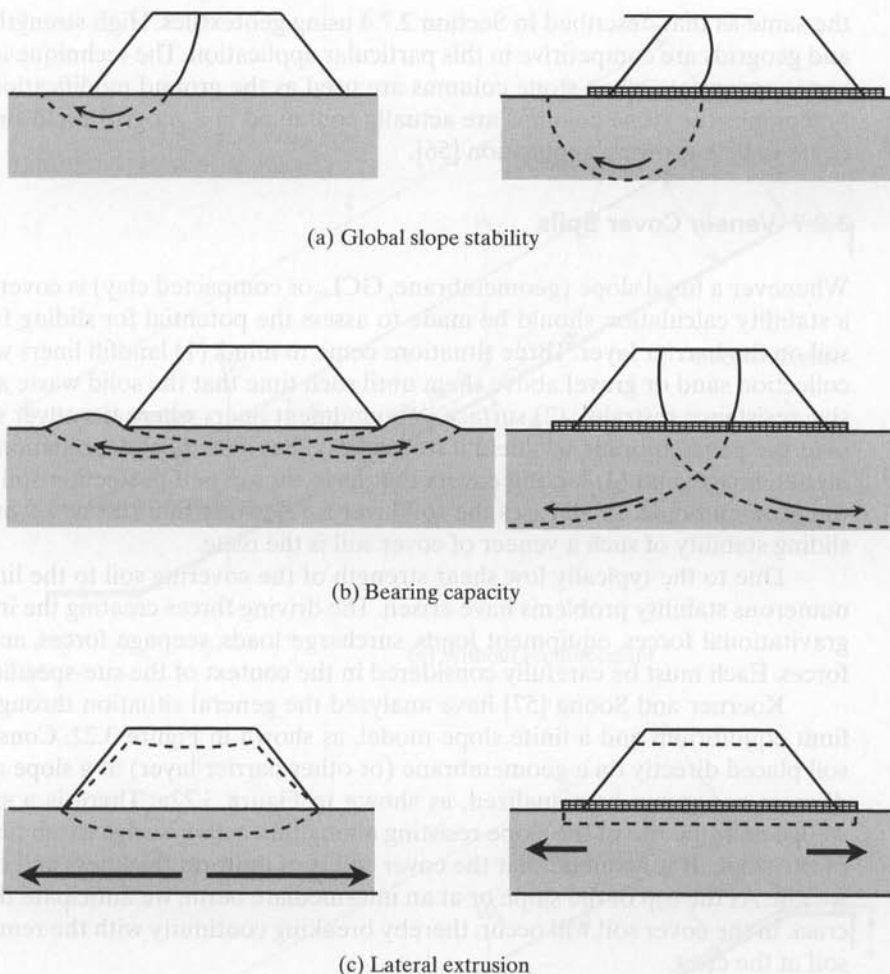
Figure 3.21 Potential improvement of embankments on soft foundation soils via three-dimensional geogrid mattresses.

In the absence of global instability, this last item is particularly important. Squeeze-out of the foundation soil is the likely service-limiting mechanism giving rise to excessive deformations. Robertson and Gilchrist [52] and Jenner et al. [53] have used slip line fields to predict the principle stresses in the soft foundation soils. Both studies give actual case histories and the monitoring feedback as to the validity of the design assumptions.

The latest application area in the context of foundation and basal soil reinforcement is the use of geogrids to span deep foundations placed through compressible soils [54, 55]. The geogrids span from pile cap to pile cap, reducing localized settlement in the supported embankment system. From a design stand point, the situation is exactly

the same as that described in Section 2.7.4 using geotextiles. High strength geotextiles and geogrids are competitive in this particular application. The technique is considered very appropriate when stone columns are used as the ground modification technique. Sometimes the stone columns are actually contained in a geogrid enclosure, which appears to be a growing application [56].

3.2.7 Veneer Cover Soils

Whenever a lined slope (geomembrane, GCL, or compacted clay) is covered with soil, a stability calculation should be made to assess the potential for sliding failure of the soil on the barrier layer. Three situations come to mind: (1) landfill liners with leachate collection sand or gravel above them until such time that the solid waste acts as a passive resistance restraint; (2) surface impoundment liners where the cover soil is placed over the geomembrane to shield it from ultraviolet light, heat degradation, and equipment damage; and (3) landfill covers that have topsoil and protection soil placed over the geomembrane. In all cases the soil layer is relatively thin (0.3 to 1.0 m), hence the sliding stability of such a veneer of cover soil is the issue.

Due to the typically low shear strength of the covering soil to the liner material, numerous stability problems have arisen. The driving forces creating the instability are gravitational forces, equipment loads, surcharge loads, seepage forces, and/or seismic forces. Each must be carefully considered in the context of the site-specific conditions.

Koerner and Soong [57] have analyzed the general situation through the use of limit equilibrium and a finite slope model, as shown in Figure 3.22. Consider a cover soil placed directly on a geomembrane (or other barrier layer) at a slope angle β. Two discrete zones can be visualized, as shown in Figure 3.22a. There is a small passive wedge near the toe of the slope resisting a long thin active wedge extending the length of the slope. It is assumed that the cover soil is of uniform thickness and constant unit weight. At the top of the slope or at an intermediate berm, we anticipate that a tension crack in the cover soil will occur, thereby breaking continuity with the remaining cover soil at the crest.

Resisting the tendency for the cover soil to slide is the interface friction and/or adhesion of the cover soil to the specific type of underlying geomembrane. The shear strength values of δ and c_a must be obtained from a laboratory direct-shear test, as described earlier. Note that the passive wedge is assumed to move on the underlying cover soil so that the shear strength parameters ϕ and c, which come from soil-to-soil friction tests, will also be required.

By taking free bodies of the passive and active wedges with the appropriate forces being applied, the formulation for the factor of safety results. The resulting equation is not an explicit solution for the FS, and it must be solved using the quadratic equation. The complete development of the equation is given in [57]. Other approaches are found in Giroud and Beech [58], Koerner and Hwu [59], and Thiel and Stewart [60].
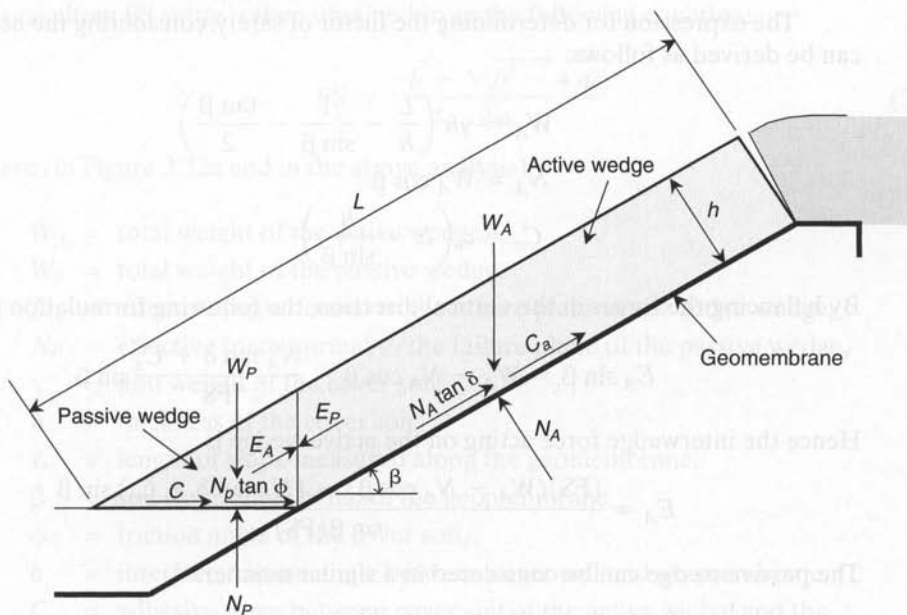
(a) Without reinforcement
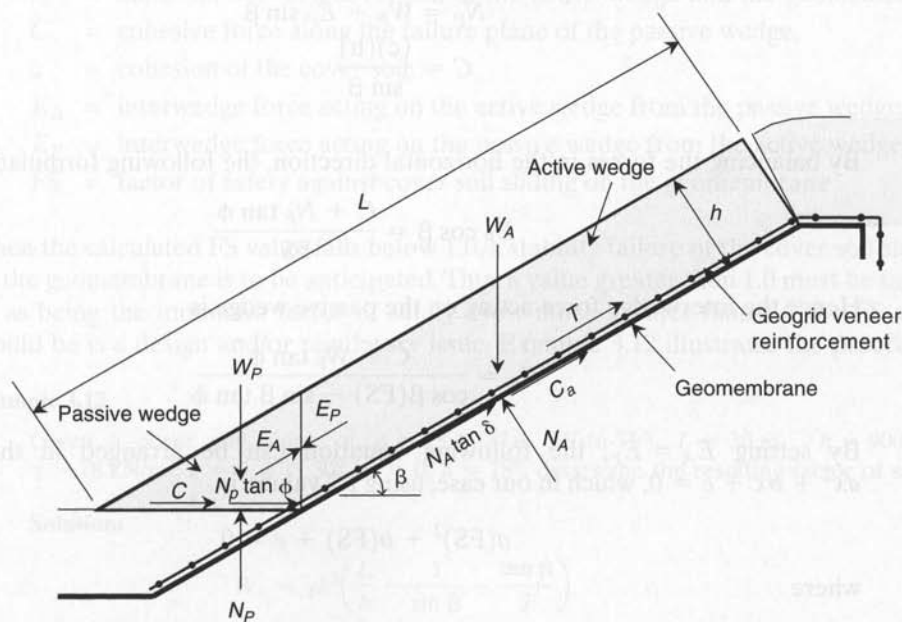
(b) With the use of geogrid veneer reinforcement

Figure 3.22   Limit equilibrium forces involved in a finite length slope analysis for a uniformly thick cover soil. (After Koerner and Soong [57])

The expression for determining the factor of safety, considering the active wedge, can be derived as follows:

$$W_A = \gamma h^2 \left(\frac{L}{h} - \frac{1}{\sin \beta} - \frac{\tan \beta}{2} \right) \tag{3.15}$$

$$N_A = W_A \cos \beta \tag{3.16}$$

$$C_a = c_a \left(L - \frac{h}{\sin \beta} \right) \tag{3.17}$$

By balancing the forces in the vertical direction, the following formulation results:

$$E_A \sin \beta = W_A - N_A \cos \beta - \frac{N_A \tan \delta + C_a}{FS} \sin \beta$$

Hence the interwedge force acting on the active wedge is

$$E_A = \frac{(FS)(W_A - N_A \cos \beta) - (N_A \tan \delta + C_a) \sin \beta}{\sin \beta (FS)}$$

The passive wedge can be considered in a similar manner:

$$W_p = \frac{\gamma h^2}{\sin 2\beta} \tag{3.18}$$

$$N_P = W_P + E_P \sin \beta \tag{3.19}$$

$$C = \frac{(c)(h)}{\sin \beta} \tag{3.20}$$

By balancing the forces in the horizontal direction, the following formulation results:

$$E_P \cos \beta = \frac{C + N_P \tan \phi}{FS}$$

Hence the interwedge force acting on the passive wedge is

$$E_P = \frac{C + W_P \tan \phi}{\cos \beta (FS) - \sin \beta \tan \phi}$$

By setting $E_A = E_P$, the following equation can be arranged in the form of $ax^2 + bx + c = 0$, which in our case, using FS values, is

$$a(FS)^2 + b(FS) + c = 0 \tag{3.21}$$

where

$$a = (W_A - N_A \cos \beta) \cos \beta, \tag{3.22}$$

$$b = -[(W_A - N_A \cos \beta) \sin \beta \tan \phi + (N_A \tan \delta + C_a)$$
$$\sin \beta \cos \beta + \sin \beta (C + W_p \tan \phi)], \text{ and} \tag{3.23}$$

$$c = (N_A \tan \delta + C_a) \sin^2 \beta \tan \phi \tag{3.24}$$

The resulting FS value is then obtained from the following equation:

$$FS = \frac{-b + \sqrt{b^2 - 4\,ac}}{2\,a}$$ (3.25)

where (in Figure 3.22a and in the above analysis)

W_A = total weight of the active wedge,
W_P = total weight of the passive wedge,
N_A = effective force normal to the failure plane of the active wedge,
N_P = effective force normal to the failure plane of the passive wedge,
γ = unit weight of the cover soil,
h = thickness of the cover soil,
L = length of slope measured along the geomembrane,
β = soil slope angle beneath the geomembrane,
ϕ = friction angle of the cover soil,
δ = interface friction angle between cover soil and geomembrane,
C_a = adhesive force between cover soil of the active wedge and the geomembrane,
c_a = adhesion between cover soil of the active wedge and the geomembrane,
C = cohesive force along the failure plane of the passive wedge,
c = cohesion of the cover soil,
E_A = interwedge force acting on the active wedge from the passive wedge,
E_P = interwedge force acting on the passive wedge from the active wedge, and
FS = factor of safety against cover soil sliding on the geomembrane

When the calculated FS value falls below 1.0, a stability failure of the cover soil sliding on the geomembrane is to be anticipated. Thus a value greater than 1.0 must be targeted as being the minimum factor of safety. How much greater than 1.0 the FS value should be is a design and/or regulatory issue. Example 3.12 illustrates the procedure.

Example 3.12

Given a cover soil slope of $\beta = 18.4°$ (i.e. 3H-to-1V), $L = 30$ m, $h = 900$ mm, $\gamma = 18$ kN/m³, $c = 0$, $\phi = 30°$, $c_a = 0$, $\delta = 18°$, determine the resulting factor of safety.

Solution:

$$W_A = \gamma h^2 \left(\frac{L}{h} - \frac{1}{\sin \beta} - \frac{\tan \beta}{2} \right)$$

$$= (18.0)(0.90)^2 \left(\frac{30}{0.90} - \frac{1}{\sin 18.4} - \frac{\tan 18.4}{2} \right)$$

$$= 14.58(33.3 - 3.17 - 0.17)$$

$$= 437 \text{ kN/m}$$

$$N_A = W_A \cos \beta$$
$$= 437 \cos 18.4$$
$$= 415 \text{ kN/m}$$

$$W_P = \frac{\gamma h^2}{\sin 2\beta}$$
$$= \frac{(18.0)(0.90)^2}{\sin 36.8}$$
$$= 24.3 \text{ kN/m}$$

$$a = (W_A - N_A \cos \beta) \cos \beta$$
$$= (437 - 415 \cos 18.4) \cos 18.4$$
$$= 41.0 \text{ kN/m}$$
$$b = -[(W_A - N_A \cos \beta) \sin \beta \tan \phi + (N_A \tan \delta + C_a) \sin \beta \cos \beta$$
$$+ \sin \beta (C + W_P \tan \phi)]$$
$$= -[(437 - 415 \cos 18.4) \sin 18.4 \tan 30 + (415 \tan 18 + 0) \sin 18.4 \cos 18.4$$
$$+ \sin 18.4(0 + 24.3 \tan 30)]$$
$$= -[7.84 + 40.4 + 4.43]$$
$$= -52.7 \text{ kN/m}$$
$$c = (N_A \tan \delta + C_a) \sin^2 \beta \tan \phi$$
$$= (415 \tan 18 + 0) \sin^2 18.4 \tan 30$$
$$= 7.8 \text{ kN/m}$$

$$\text{FS} = \frac{-b + \sqrt{b^2 - 4ac}}{2a}$$
$$= \frac{52.7 + \sqrt{(52.7)^2 - 4(41.0)(7.8)}}{2(41.0)}$$

FS = 1.11   which is too low for a final cover and an appropriate design option
              is to consider the use of geogrid veneer reinforcement

Figure 3.22b illustrates a growing application of geogrid reinforcement under the generic classification of *veneer reinforcement*. The geogrid embedded in its own anchor trench at the top of the slope is placed directly on the geomembrane. Soil backfilling (with lightweight construction equipment) proceeds from the toe to the crest of the slope. As backfill is placed, the geogrid reinforcement is tensioned, and, depending on the strength of the reinforcement, some or all of the gravitational stress of the soil is resisted. In the analysis that follows, the soil is assumed to be in contact with the geomembrane (acting through the apertures of the geogrid), the reinforcement is functioning at its allowable value (hence, reduction factors must be applied to the ultimate value), and the active wedge has included in it an additional vector—namely, the allowable geogrid tension, T. For the active wedge, we balance the forces in the vertical direction and the following formulation results.

$$E_A \sin \beta = W_A - N_A \cos \beta - \left(\frac{N_A \tan \delta + C_a}{\text{FS}} + T \right) \sin \beta$$

Hence the interwedge force acting on the active wedge is

$$E_A = \frac{(\text{FS})(W_A - N_A \cos \beta - T \sin \beta) - (N_A \tan \delta + C_a) \sin \beta}{\sin \beta (\text{FS})}$$

Again, by setting $E_A = E_P$ (recall E_P from the previous analysis), the resulting formulation can be arranged in the form of equation (3.21) where

$a = (W_A - N_A \cos \beta - T \sin \beta) \cos \beta$ (3.26)

$b = -[(W_A - N_A \cos \beta - T \sin \beta) \sin \beta \tan \phi + (N_A \tan \delta + C_a) \sin \beta \cos \beta$

$\qquad + \sin \beta (C + W_P \tan \phi)]$, and   (3.27)

$c = (N_A \tan \delta + C_a) \sin^2 \beta \tan \phi.$ (3.28)

Again, the resulting FS value can be obtained using equation (3.25). Example 3.13 illustrates the use of the above analysis.

Example 3.13

Let us continue Example 3.12, now using a geogrid with $T_{ult} = 150$ kN/m and cumulative reduction factors amounting to 4.5. What is the resulting factor of safety for this case of veneer reinforcement?

Solution: The W_A, N_A, and W_P values stay the same as in Example 3.12. The allowable tensile strength of the geogrid reinforcement is

$$T = T_{ult}/\Pi RF$$
$$= 150/4.5$$
$$= 33.3 \text{ kN/m}$$

Using equations (3.26), (3.27) and (3.28), together with equation (3.25) give the resulting factor of safety.

$a = (W_A - N_A \cos \beta - T \sin \beta) \cos \beta$
$\quad = (437 - 415 \cos 18.4 - 33.3 \sin 18.4) \cos 18.4$
$\quad = 31.4 \text{ kN/m}$

$b = -[(W_A - N_A \cos \beta - T \sin \beta) \sin \beta \tan \phi + (N_A \tan \delta + C_a) \sin \beta \cos \beta$
$\quad + \sin \beta (C + W_P \tan \phi)]$
$\quad = -[(437 - 415 \cos 18.4 - 33.3 \sin 18.4) \sin 18.4 \tan 30$
$\quad + (415 \tan 18 + 0) \sin 18.4 \cos 18.4 + \sin 18.4(0 + 24.3 \tan 30)]$
$\quad = -50.8 \text{ kN/m}$

$c = (N_A \tan \delta + C_a) \sin^2 \beta \tan \phi$
$\quad = (415 \tan 18 + 0) \sin^2 18.4 \tan 30$
$\quad = 7.8 \text{ kN/m}$

$$\begin{aligned}
\text{FS} &= \frac{-b + \sqrt{b^2 - 4ac}}{2a} \\
&= \frac{50.8 + \sqrt{(-50.8)^2 - 4(31.4)(7.8)}}{2(31.4)}
\end{aligned}$$

$$\text{FS} = 1.45 \qquad \text{which is acceptable}$$

This solution for veneer reinforcement agrees well with other methods in the literature and with a finite element solution (Wilson-Fahmy and Koerner [61]).

A significant issue, however, is the input variables for the analysis. This is particularly the case for the interface friction value and for the reduction factors on the geosynthetic reinforcement. Also, if a high strength geotextile is being used, the δ value will be for the geotextile to the geomembrane, since geotextiles do not allow for strike-through of the backfill soil. Concerning an acceptable value of the resulting factor of safety, the site-specific situation must be considered. For leachate collection soils in landfills, relatively low values of FS may be acceptable since the solid waste will provide a buttressing effect as it is placed in the landfill. Conversely, for final cover soils in the closure of landfills, quite high values of FS should be considered since the time frames for service life can be extremely long.

Lastly, in areas of anticipated earthquake activity, the slope stability analysis of a final cover soil over an engineered landfill, abandoned dump, or remediated site must consider seismic forces. In the United States, the Environmental Protection Agency (EPA) regulations require such an analysis for sites that have a probability of $\geq 10\%$ of experiencing a 0.10 g peak horizontal acceleration within 250 years.

The seismic analysis of cover soils of the type under consideration is a two-part process: (1) the calculation of a FS value using a pseudo-static analysis via the addition of a horizontal seismic force acting at the centroid of the cover cross section, and (2) a mandatory permanent deformation analysis if the FS value in the above calculation is less than 1.0. The calculated deformation is then assessed in light of the potential damage to the cover soil section and is accepted, or it is not and the slope will require an appropriate redesign. The redesign is then analyzed until the situation becomes acceptable.

The first part of the analysis is called a *pseudo-static approach*, which follows the previous examples except for the addition of a horizontal force at the centroid of the cover soil in proportion to the anticipated seismic activity. It is first necessary to obtain an average seismic coefficient (C_s) from a seismic zone map (e.g., Algermissen [62]). Such maps are available on a worldwide basis. The value of C_s is nondimensional and is a ratio of the bedrock acceleration to gravitational acceleration.

The additional seismic force is $C_s W_a$ on the active wedge and $C_s W_p$ on the passive wedge. By approaching the problem exactly as before and including the C_s-values, we obtain the following, based on equation (3.21) (see Koerner and Soong [57] for details):

$$a(FS)^2 + b(FS) + c = 0$$

where

$$a = (C_S W_A + N_A \sin \beta) \cos \beta + C_S W_P \cos \beta \qquad (3.29)$$

$$b = -[(C_S W_A + N_A \sin \beta) \sin \beta \tan \phi$$
$$+ (N_A \tan \delta + C_a) \cos^2 \beta$$
$$+ (C + W_P \tan \phi) \cos \beta] \tag{3.30}$$
$$c = (N_A \tan \delta + C_a) \cos \beta \sin \beta \tan \phi \tag{3.31}$$

The resulting FS value is then obtained from equation (3.25):

$$\text{FS} = \frac{-b + \sqrt{b^2 - 4ac}}{2a}$$

If the FS value from such a calculation is greater than 1.0, the analysis is complete. The assumption being that cover soil stability can withstand the short-term excitation of an earthquake and still not slide. However, if the value is less than 1.0, a second part of the analysis is required.

The second part of the analysis is directed toward calculating the estimated deformation of the lowest shear strength interface in the cross section under consideration. The deformation is then assessed in light of the potential damage that may be imposed on the system.

To begin the permanent deformation analysis, a yield acceleration, C_{sy}, is obtained from a pseudo-static analysis under an assumed FS = 1.0. We compare this value with the time history response assumed for the actual site location and cross section. If the earthquake time history response never exceeds the value of C_{sy}, there is no anticipated permanent deformation. However, whenever any part of the time history exceeds the value of C_{sy}, permanent deformation is expected. By double integration of the acceleration time history curve, to velocity and then to displacement, the cumulative value of deformation can be obtained. (See Matasovic et al. [63].) This value is considered to be permanent deformation and is then assessed based on the site-specific implications of damage to the final system.

3.3 DESIGN CRITIQUE

The design sections just presented use geogrids in their primary function, which is as soil reinforcement. This primary function comes about because of a number of features regarding geogrids.

- *Economy*, as in the reduction of base course thickness in unpaved roads
- *Practicality*, as in geogrid reinforced embankments and walls
- *Necessity*, as in veneer reinforcement of cover soils on geomembranes where traditional methods of construction are not adequate

The design methods in each of the above instances are direct adaptations of traditional geotechnical engineering methods—only now the designs include a reinforcement

material, namely geogrids. The liberties taken by making this change seem reasonable and justifiable on the basis of field performance and monitoring. In fact, the feedback seems to indicate that the design methods just presented are conservative. However, before we conclude that more liberal designs are in order, the nature of the actual situation must be considered. For example, embankment slopes, reinforced walls, and landfill reinforcement applications are generally permanent structures requiring long service lifetimes, which simply demand a conservative approach.

More uncertain than the design methods are the allowable properties of the geogrid and the proliferation of a wide variety of different geogrid types. Considerations of allowable strength lead directly to the subsequent factor of safety (Section 3.1.5). Bonaparte and Berg [64] subdivide applications into *permanent* versus *temporary*, and *critical* versus *noncritical*. It is a very perceptive approach, wherein the permanent and critical systems require the greatest amount of concern and caution. This, of course, is up to the designer on a site-specific basis. Regarding the variety of geogrid types, concern is warranted when a design is made and then an "or equal" specification is written. The introduction to this chapter has shown that geogrids vary considerably insofar as their physical, mechanical, and endurance properties. Hence a geogrid specification must be written around a set of performance characteristics. This, too, is a problem, since most of our experience has been in writing specifications for geotextiles, not for geogrids. Although the current situation could be easily dismissed as merely growing pains, this does little good for a designer who is unsure of a product or for manufacturers who are *very* sure of their product. Clearly, there is a need for generic specifications of all types of bidirectional and unidirectional geogrids.

3.4 CONSTRUCTION METHODS

As with geotextiles, geogrids come to the job site in rolls. However, they are often narrower than geotextiles. Typically geogrid roll widths are from 1 to 3 m wide for unitized geogrids and 3 to 4.5 m wide for coated yarn geogrids. Rod (strap) geogrid dimensions vary according to the manufacturer. Their deployment is straightforward unless some sort of tensioning or prestressing is desired. Because of their large aperture size, sewing is not possible to join the sides or ends together and some type of mechanical system is generally employed. Unitized unidirectional geogrids can be bent and the bent end inserted into the opening of an adjacent sheet. By placing a HDPE rod or bar down the slot that is formed, excellent load transfer is obtained. The rod is either 12 mm in diameter or a tapered bodkin. A number of joining techniques are under development with the flexible textilelike geogrids. Of course, adequate overlap can also be used to mobilize the tensile strength of the opposing materials via shear stresses. Wire cutters will suffice to cut or trim geogrids, but a circular saw is quicker and more efficient. The flexible coated yarn geogrids can generally be cut with a sharp knife.

Unitized geogrids have been used to anchor wall facing panels made from concrete in a manner similar to the metal strips of reinforced earth. The attachment of geogrids to facing panels involves the casting of small geogrid sections or metal hooks

into the concrete panels during their fabrication. The reinforcement geogrids are mechanically connected, directly or by means of a steel dowel running lengthwise behind the hooks and attached to the ends of the geogrids. Alternatively, geogrids can be used between layers of wall sections, gabions, concrete cells, or concrete blocks to anchor the walls and to reduce the earth pressure on the wall itself. Connection is by polymer or fiberglass dowels for unitized geogrids or by friction (sometimes between lock-and-key sections) for coated yarn and rod (strap) geogrids.

During the installation of geogrids for reinforcement purposes, the initial slack in the product must be removed before backfilling. This is sometimes a difficult task. Usually, laborers will use a crowbar, pick, or steel rod to pull the geogrid taut while it is being backfilled. The amount of tension is an estimate. It should be realized that too much tension might not be advisable, especially when the geogrid is attached to wall facing elements that are only temporarily supported. Clearly, tensioning is done on a trial-and-error basis. Its mobilization must be discussed by the parties involved before construction begins.

The above details are almost always geogrid product-specific. Thus the manufacturer's Web site or technical representative must be consulted to be assured that the construction details are adequate for the proposed material system—that is, with the particular geogrid and wall facing type. All geogrid manufacturers, to the author's knowledge, have well-trained geotechnical engineers on their staff to advise consultants and owners on the details and nuances of their products.

REFERENCES

1. Kinney, T. C., "Determining the Secant Aperture Stability Modulus of a Geogrid," Internal Report, Shannon and Wilson Inc., January 7, 2000.
2. Wilson-Fahmy, R., Koerner, R. M., and Fleck, J. A., "Unconfined and Confined Wide-Width Testing of Geosynthetics." In *Geosynthetic Soil Reinforcement Testing Procedures*, ASTM STP 1190, edited by S. J. Cheng. ASTM, 1993, pp. 49–63.
3. Sarsby, R. W., "The Influence of Aperture Size/Particle Size on the Efficiency of Grid Reinforcement," *Proceedings of the 2nd Canadian Symposium on Geotextiles and Geomembranes*, Edmonton, Canada, Geotechnical Society of Edmonton, 1985, pp. 7–12.
4. Ingold, T. S., "Laboratory Pull-Out Testing of Grid Reinforcement in Sand," *Geotechnical Testing Journal*, vol. 6, no. 3, 1983, pp. 212–217.
5. Koerner, R. M., Wayne, M. H., and Carroll, R. G., Jr., "Analytic Behavior of Geogrid Anchorage," *Proceedings of the Geosynthetics '89 Conference*. IFAI, 1989, pp. 525–536.
6. Wilson-Fahmy, R., and Koerner, R. M., "Finite Element Modeling of Soil-Geogrid Interaction in a Pull-out Loading Condition," *Geotextiles and Geomembranes*, vol. 12, no. 5, 1993, pp. 479–501.
7. Bathurst, R. J., and Simac, M. R., "Geosynthetic Reinforced Segmental Retaining Wall Structures in North America," *Proceedings of the 5th IGS Conference*, Special Volume. IGS, 1994, pp. 29–54.
8. Koerner, G. R., Koerner, R. M., and Elias, V., "Geosynthetic Installation Damage Under Two Different Backfill Conditions," *Geosynthetic Soil Reinforcement Testing Procedures*, ASTM STP 1190, edited by S. J. Cheng. ASTM, 1993, pp. 163–183.
9. Hsieh, C. W., and Wu, J. H., *Installation Survivability of Flexible Geogrids in Various Subgrade Materials*," Transportation Research Record No. 1772, Washington, DC: Transportation Research Board, 2001, pp. 190–196.
10. Sprague, C. J., and Allen, S. R., "Testing Installation Damage of Geosynthetics," *GFR*, vol. 21, no. 6, pp. 24–27.

11. McGown, A., Andrawes, K. Z., and Kabir, M. H., "Load-Extension Testing of Geotextiles Confined in Soil," *Proceedings of the 2nd International Conference on Geotextiles*. IFAI, 1982, pp. 93–96.

12. Ingold, T. S., Montanelli, F., and Rimoldi, P., "Extrapolation Techniques for Long-Term Strengths of Polymeric Geogrids," *Proceedings of the 5th International Conference on Geosynthetics*, IGS, 1994, pp. 1117–1120.

13. Miyata, K., "Walls Reinforced with Fiber Reinforced Plastic Geogrids in Japan," *Geosynthetics International*, vol. 3, no. 1, 1996, pp. 1–11.

14. Hsuan, Y. G., Koerner, R. M., and Koerner, G. R., "Field Measurements of Oxygen Temperature and Moisture Behind Segmental Retaining Walls," *Proceedings of the 7th International Conference on Geosynthetics*, September 22–27, 2002, A. A. Balkema, pp. 1431–1434.

15. Farrag, K. and Shirazi, H., "Development of an Accelerated Creep Testing Procedure for Geosynthetics—Part 1: Testing," *Geotechnical Testing Journal*, vol. 20, no. 4, December 1997, pp. 414–422.

16. Farrag, K., "Development of an Accelerated Creep Testing Procedure for Geosynthetics—Part 2: Analysis," *Geotechnical Testing Journal*, vol. 21, no. 1, March 1998, pp. 39–44.

17. Thornton, J. S., Allen, S. R., Thomas, R. W., and Sandri, D., "The Stepped Isothermal Method for Time-Temperature Superposition and Its Application to Creep Data on Polyester Yarn," *Sixth International Conference on Geosynthetics*, vol. 2, 1998, IFAI, pp. 699–706.

18. Greenwood, J. H., and Voskamp, W., "Predicting the Long-Term Strength of a Geogrid Using the Stepped Isothermal Method," *Proceedings of the 2nd European Geosynthetics Conference*, 2002, pp. 329–332.

19. Wrigley, N. E., "Durability and Long-Term Performance of Tensar Polymer Grids for Soil Reinforcement," *Materials Science and Technology*, vol. 3, no. 4, 1987, pp. 161–170.

20. Koerner, R. M., Lord, A. E. Jr., and Halse, Y., "Allowable Geosynthetic Strength and Flow Considerations," *Proceedings of the ASCE/Penn DOT Conference*, Central Pennsylvania Section, ASCE, 1988, pp. 1–19.

21. Haas, R., "Structural Behavior of Tensar Reinforced Pavements and Some Field Applications," *Proceedings of the Symposium on Polymer Grid Reinforcement in Civil Engineering*, Institution of Civil Engineers, 1984, pp. 166–170.

22. Abd El Halim, A. O. "Geogrid Reinforcement of Asphalt Pavements," PhD diss., University of Waterloo, Ontario, Canada, 1983.

23. Abd El Halim, A. O., Haas, R., and Chang, W. A., "Geogrid Reinforcement of Asphalt Pavements and Verification of Elastic Layer Theory," Research Board Record No. 949, TRB, 1983, pp. 55–65.

24. Carroll, R. G., Jr., Walls, J. G. and Haas, R., "Granular Base Reinforcement of Flexible Pavements Using Geogrids," *Proceedings of the Geosynthetics '87 Conference*. IFAI, 1987, pp. 46–57.

25. "Guide for Design of Pavement Structures," Washington, DC: AASHTO 1986.

26. Brown, S. F., Brodrick, B. V., and Hughes, D. A. B., "Tensar Reinforcement of Asphalt: Laboratory Studies," *Proceedings of the Symposium on Polymer Grid Reinforcement in Civil Engineering*. Institution of Civil Engineers, 1984, pp. 158–165.

27. Kennepohl, G.J.A. and Kamel, N. I., "Construction of Tensar Reinforced Asphalt Pavements," *Proceedings of the Symposium on Polymer Grid Reinforcement in Civil Engineering*. Institution of Civil Engineers, 1984, pp. 171–175.

28. Molenaar, A.A.A. and Nods, M., "Design Method for Plain and Geogrid Reinforced Overlays on Cracked Pavements," *Proceedings of the 3rd International RILEM Conference*, edited by L. Francken, E. Beuving, and A.A.A. Molenaar. E & FN Spon., 1996, pp. 311–320.

29. Giroud, J.-P., Ah-Line, C., and Bonaparte, R., "Design of Unpaved Roads and Trafficked Areas with Geogrids," *Proceedings of the Symposium on Polymer Grid Reinforcement in Civil Engineering*. Institution of Civil Engineers, 1984, pp. 116–127.
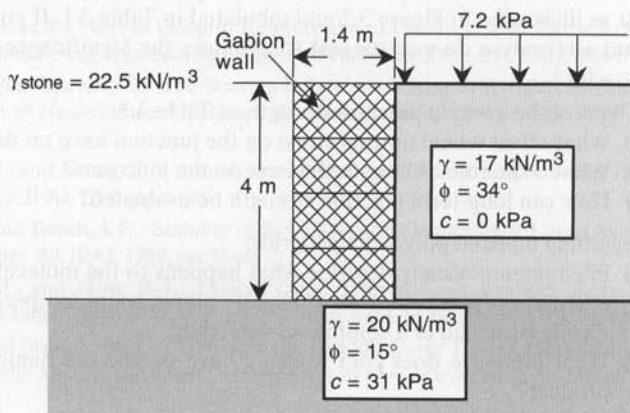
30. Forsyth, R. A., and Bieber, D. A., "La Honda Repair with Geogrid Reinforcement," *Proceedings of the Symposium on Polymer Grid Reinforcement in Civil Engineering*. Institution of Civil Engineers, pp. 54–57.

31. Berg, R. R., Anderson, R. P., Rose, R. J., and Chouery-Curtis, V. E., "Reinforced Soil Highway Slopes, *Proceedings of the TRB 69th Annual Meeting*. TRB, 1990.

32. Schmertmann, G. R., Chouery-Curtis, V. E., Johnson, R. D., and Bonaparte, R., "Design Charts for Ge-ogrid-Reinforced Soil Slopes," *Proceedings of the Geosynthetics '87 Conference*. IFAI, 1987, pp. 108–120.

33. Ingold, T. S., "An Analytical Study of Geotextile Reinforced Embankments," *Proceedings of the of 2nd International Conference on Geotextiles*, IFAI, 1982, pp. 683–689.

34. Murray, R. T., "Reinforcement Techniques in Repairing Slope Failures," *Proceedings of the Conference on Polymer Grid Reinforcement*. Institution of Civil Engineers, 1984, pp 47–53.

35. Jewell, R. A., "Application of Revised Design Charts for Steep Reinforced Slopes," *Journal Geotextiles and Geomembranes*, vol. 10, no. 3, 1991, pp. 203–233.

36. Leshchinsky, D., and Reinschmidt, A. J., "Stability of Membrane Reinforced Slopes," *Journal Geotechnical Engineering*, ASCE, vol. 111, no. 11, 1985, pp. 1285–1297.

37. Schneider, H. R., and Holtz, R. D., "Design of Slopes Reinforced with Geotextiles and Geogrids," *Journal Geotextiles and Geomembranes*, vol. 3, no. 1, 1986, pp. 29–52.

38. Reugger, R., "Geotextile Reinforced Soil Structures on Which Vegetation Can Be Established," *Proceedings of the 3rd International Conference on Geotextiles*. Austrian Society of Engineers, 1986, pp. 453–458.

39. Abu-Hejleh, N., Wang, T., and Zornberg, J. G., "Performance of Geosynthetic-Reinforced Walls Supporting Bridge and Approaching Roadway Structures." In *Advances in Transportation and Geoenvironmental Systems Using Geosynthetics*, edited by J. G. Zornberg and B. R. Christopher, ASCE, 2000, pp. 218–243.

40. Soong, T.-Y., and Koerner, R. M., "On the Required Connection Strength of Geosynthetically Reinforced Walls," *Journal Geotextiles and Geomembranes*, vol. 15, no. 4–6, 1997, pp. 377–394.

41. Tatsuoka, F., Murata, O. and Tateyama, M., "Permanent Geosynthetic Reinforced Soil Retaining Walls Used for Railway Embankments in Japan," *Proceedings of the Geosynthetic Reinforced Soil Retaining Walls*, edited by J. T. H. Wu. A. A. Balkema, 1992, pp. 101–130.

42. Bathurst, R. J., and Simac, M. R., "Geosynthetic Reinforced Segmental Retaining Wall Structures in North America," *Proceedings of the 5th IGS Conference*, IGS, 1994, pp. 29–54.

43. Koerner, J., Soong, T.-Y., and Koerner, R. M., "Earth Retaining Wall Costs in the USA," GRI Report No. 20, GII Publications, 1998.

44. Leshchinsky, D., "Issues and Nonissues in Block Walls as Implied Through Computer-Aided Design," *Proceedings of the GRI-12 Conference*, 1998: GII Publications, pp. 66–74.

45. Koerner, R. M., and Soong, T.-Y., "Geosynthetic Reinforced Segmental Retaining Walls," *Journal of Geotextiles and Geomembranes*, vol. 19, no. 6, August 2001, pp. 359–386.

46. Koerner, R. M., and Soong, T.-Y., "Drainage System Design Behind Segmental Walls," *EuroGeo III*, Munich, Germany, February, 2004, pp. 355–360.

47. Jarrett, P. M., "Evaluation of Geogrids for Construction of Roadways over Muskeg," *Proceedings of the Symposium on Polymer Grid Reinforcement in Civil Engineering*. Institute of Civil Engineers, 1984, pp. 149–153.

48. Milligan, G. W. E., and Love, J. P., "Model Testing of Geogrids Under an Aggregate Layer in Soft Ground," *Proceedings of the Symposium on Polymer Grid Reinforcement in Civil Engineering*. Institute of Civil Engineers, 1984, pp. 128–138.

49. Giroud, J.-P., Bonaparte, R., Beech, J. F., and Gross, B. A., "Design of Soil Layer-Geosynthetic Systems Overlying Voids," *Geotextiles and Geomembranes*, vol. 9, no. 1, 1990, pp. 11–50.

50. Edgar, S., "The Use of High-Tensile Polymer Grid Mattress on the Mussleburgh and Portobello Bypass," *Proceedings of the Symposium on Polymer Grid Reinforcement in Civil Engineering*. Institute of Civil Engineers, 1984, pp. 103–111.

51. Rueff, H., Stoffers, U. and Leicher, F., "Landfills on Soft Foundation Soils," Berlin, Germany: Ernst & Sohn, Bautechnik 69, vol. 5, 1992, pp 65–81.

52. Robertson, J. and Gilchrist, A. J. T., "Design and Construction of a Reinforced Embankment Across Soft Lakebed Deposits." *Proceedings of the Symposium on Polymer Grid Reinforcement in Civil Engineering*. Institute of Civil Engineers, 1984.

53. Jenner, C. G., Bush, D. I., and Bassett, R. H. "The Use of Slip Line Fields to Assess the Improvement in Bearing Capacity of Soft Ground Given by a Cellular Foundation Mattress Installed at the Base of an Embankment," *Proceedings of the Theory and Practice of Earth Reinforcement*. A.A. Balkema, 1988, pp. 209–214.

54. Han, J., and Gabr, M. A., "Numerical Analysis of Geosynthetic Reinforced and Pile-Supported Earth Platforms over Soft Soils," *Journal of Geotechnical and Geoenvironmental Engineering*, vol. 128, no. 1, pp. 44–53.

55. Han, J., and Akins, K., "Use of Geogrid Reinforced and Pile Supported Earth Structures," *Proceedings of the International Deep Foundations Congress*, Feb. 14–16, 2002, ASCE, pp. 668–679.

56. Paul, A., and Ponomarjow, A., "The Bearing Behavior of Geogrid Reinforced Crushed Stone Columns in Comparison to Nonreinforced Concrete Pile Foundations," *Proceedings of the EuroGeo3*, 2004, pp. 285–288.

57. Koerner, R. M., and Soong, T.-Y., "Analysis and Design of Veneer Cover Soils," *Proceedings of the 6th IGS Conference*, IFAI, 1998, pp. 1–26.

58. Giroud, J.-P., and Beech, J. F., "Stability of Soil Layers on Geosynthetic Lining System," *Proceedings of the Geosynthetics '89*. IFAI, 1989, pp. 35–46.

59. Koerner, R. M., and Hwu, B.-L., "Stability and Tension Considerations Regarding Cover Soils in Geomembrane Lined Slopes," *Journal of Geotextiles and Geomembranes*, vol. 10, no. 4, 1991, pp. 335–355.

60. Thiel, R. S., and Stewart, M. G., "Geosynthetic Landfill Cover Design Methodology and Construction Experience in the Pacific Northwest," *Proceedings of the Geosynthetics '93 Conference*, IFAI, 1993, pp. 1131–1144.

61. Wilson-Fahmy, R. F., and Koerner, R. M., "Finite Element Analysis of Cover Soil on Geomembrane Lined Slopes," *Proceedings of the Geosynthetics '93 Conference*. IFAI, pp. 1425–1437.

62. Algermissen, S. T., "Seismic Risk Studies in the United States," *Proceedings of the 4th World Conference on Earthquake Engineering*, vol. 1, 1969, pp. A1-14 to A1-27.

63. Matasovic, N., Kavazanjian, E., Jr., and Yan, L., "Newmark Deformation Analysis with Degrading Yield Acceleration," *Proceedings of the Geosynthetics '97 Conference*. IFAI, 1997, pp. 989–1000.

64. Bonaparte, R., and Berg, R., "Long-Term Allowable Tension for Geosynthetic Reinforcement," *Proceedings of the Geosynthetic '87 Conference*. IFAI, 1987, pp. 181–192.

PROBLEMS

3.1. List and describe the basic similarities and differences between geogrids and geotextiles.

3.2. List and describe the basic similarities and differences between geogrids and geonets.

3.3. Flexible geogrids are coated with latex, bitumen, or polyvinyl chloride. What is the reason for such coatings?

3.4. Derive an anchorage resistance formula on the basis of Figure 3.4 to include all three components of pullout resistance. (*Hint*: See [5].)

3.5. See again the anchorage analysis in Section 3.1.2.
   (a) Using the formula derived in Problem 3.4 for a geogrid in granular soil of $\phi = 35°$ at 19.5 kN/m^3 and 2.0 m depth, what is the ultimate pullout resistance for a length of 600 mm? The physical properties of the geogrid are 6.0 mm wide ribs at 50 mm centers in both directions, a rib thickness of 3.0 mm, and the friction angle mobilized by the rib's surface to the soil is 30°.
   (b) What is the relative proportion of the three components of anchorage strength calculated in part (a)?
   (c) If the wide-strip tensile strength of the above geogrid was 45 kN/m, could the anchorage force calculated in part (a) be mobilized? If not, what portion of it could be?

3.6. Repeat the calculations of Problem 3.5a using a rib width of 8.0 mm, then 10.0 mm, and then 12.0 mm. Plot the anchorage strength versus rib width.

3.7. What junction strength is required for the results of Problems 3.5a and 3.6, if all of the available anchorage strength is mobilized? (*Hint:* The transverse rib shear and transverse rib bearing must both be transmitted through the junction.)

3.8. Discuss the usefulness (or uselessness) of performing an in-isolation junction strength test as illustrated in Figure 3.2 and tabulated in Table 3.1. If you feel it has no relevancy, what alternative do you suggest to evaluate the significance of the transverse ribs of geogrids?

3.9. In light of the geogrid junction strength of Table 3.1:
 (a) What effect would normal stress on the junction have on the test results?
 (b) What is the role of long-term stress on the junctions?
 (c) How can long-term junction strength be evaluated?

3.10. Regarding unitized polyolefin geogrids:
 (a) Phenomenologically describe what happens to the molecular structure of polyethylene and polypropylene at or slightly above room temperature, when they are uniformly stretched in a continuous direction.
 (b) What influence does cold working have on the mechanical properties of the final product?

3.11. What is the effect of high temperature on the following mechanical properties of geogrids?
 (a) Modulus
 (b) Tensile strength
 (c) Elongation at failure
 (d) Creep behavior

3.12. If the ultimate tensile strength of a geogrid evaluated in wide-strip tensile strength test is 60 kN/m, what allowable strength should be used in design for the following situations?
 (a) Temporary unpaved access road for construction vehicle use for approximately one year
 (b) Stone base reinforcement in a permanent paved road for a 30-year lifetime
 (c) Differential settlement beneath a wall footing (i.e., improved bearing capacity) for a 50- to a 100-year lifetime

3.13. In using geogrids for reinforcement of paved roads, a possible mechanism involving increased bearing capacity is often mentioned. On a conceptual basis, how does this work?

3.14. How does the geogrid effectiveness factor (GEF) of Section 3.2.1 relate to the fabric effectiveness factor (FEF) of Section 2.10.2?

3.15. For the power law of equation (3.9), used to calculate the crack propagation through pavement overlays, what type of laboratory experiment would you devise to arrive at the $K, A,$ and n values required in the analysis?

3.16. Regarding geogrid reinforced unpaved roads:
 (a) What is the required aggregate thickness for an unpaved road carrying 10,000 vehicle passes of 80 kN with rut depths of 0.15 m on a soil subgrade whose undrained shear strength is 20 kN/m^2? (Use Figure 3.10.)
 (b) Using BX 1200 geogrid reinforcement, channelized traffic, and a high likelihood of aggregate contamination, how much aggregate can be saved?
 (c) What increase in load-spreading angle does this represent (assuming that the nonreinforced case is $\alpha_0 = 26.6°$)?

3.17. Repeat Problem 3.16 assuming that the soil subgrade has CBR = 2.0.

3.18. Repeat Problem 3.16 using UX 1200 geogrids.

3.19. Determine the factor of safety against sliding and overturning (i.e., the external stability) for the wall shown in the diagram below, carrying a surcharge load of 7.2 kPa.

γ stone = 22.5 kN/m^3

Gabion wall

1.4 m

7.2 kPa

4 m

$\gamma = 17$ kN/m^3
$\phi = 34°$
$c = 0$ kPa

$\gamma = 20$ kN/m^3
$\phi = 15°$
$c = 31$ kPa

3.20. Using the approach indicated by Figures 3.12 and 3.13, determine the number, spacing, and length of the geogrids needed to stabilize the embankment shown in the diagram below using a factor of safety of 1.3. Use combined reduction factors of 4.3 on the ultimate geogrid strength of the candidate geogrid of 180 kN/m to arrive at an allowable strength.

7 m

65°

$\gamma = 19$ kN/m^3
$\phi = 35°$
$c = 0$
$\mu = 0$
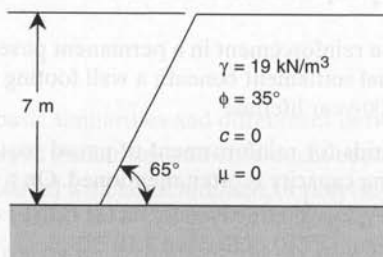
3.21. Figure 3.19 shows that at high deformations the load-carrying capacity of shallow footings can be increased considerably using geogrids. How can this feature be used without having the footing undergo large settlement? (Draw some sketches showing how this could be accomplished.)

3.22. Using the design guide of Figure 3.20, solve for T_{reqd} as in Example 3.11 (Section 3.2.6) for the following parametric variations (i.e., hold all values constant except the target parameter).
  (a) Vary H from 1 to 30 m
  (b) Vary R from 1 to 10 m
  (c) Vary q from 7 to 100 kPa at $H/B = 0.1$

3.23. For Example 3.12, concerning the nonreinforced cover soil (Section 3.2.7), recalculate the FS for δ values of 13, 15, 21 and 24° and plot the response along with that for 18° given in the example.

3.24. Recalculate Problem 3.23 varying the cover soil thickness, using 300, 600 and 1200 mm to compare with that given in Example 3.12 for 900 mm (use $\delta = 18°$).

3.25. For Example 3.13, for geogrid-reinforced cover soil (Section 3.2.7), recalculate the factor of safety for T_{ult} values results using 100, 200 and 250 kN/m and plot the results along with that for 150 kN/m given in the example.

3.26. A 30 m long slope has uniform thickness cover soil of 300 mm at a unit weight of 18 kN/m^3. The soil has a friction angle of 30° and zero cohesion (i.e., it is sand). The cover soil is on a geomembrane, as shown in Figure 3.22a. Direct shear testing has resulted in an interface friction angle of 22° with zero adhesion. The slope angle is 3(H)-to-1(V) (i.e., 18.4°). A design earthquake appropriately transferred to the site's cover soil results in an average seismic coefficient of 0.10. Using equations (3.21), (3.25), and (3.29–3.31), calculate the FS value and comment accordingly.

3.27. What are the various ways of transferring load from one sheet of geogrid to the next for the following:
(a) Homogeneous unidirectional geogrids
(b) Coated yarn geogrids
(c) Polymer rod (strap) geogrids

3.28. When using geogrids for reinforcement of masonry block facing retaining walls, what are the various ways of attaching the geogrids to such block facings?

4

Designing with Geonets

4.0 INTRODUCTION

A geonet can be defined as follows:

> *Geonet:* A geosynthetic material consisting of integrally connected parallel sets of ribs overlying similar sets at various angles for in-plane drainage of liquids or gases. Geonets are often laminated with geotextiles on one or both surfaces and are then referred to as geocomposite drainage materials.

As originally described in Section 1.5, geonets are formed by a continuous extrusion process into a netlike configuration of parallel sets of homogeneously interconnected ribs. Figure 1.18 shows how the extruded core is opened up into the final netlike configuration. Figures 4.1, 4.2, and 4.3 give a closer view of the details of various types of geonets. Each figure shows an overview, a closeup of the rib intersections, and a scanning electron micrograph of the rib intersection. The following types are illustrated:

- *Biplanar geonets consisting of solid extruded ribs*: These are the most common type of geonet (Figure 4.1).
- *Biplanar geonets consisting of foamed extruded ribs*: These result in greater overall thickness, and hence greater flow rate (Figure 4.2).
- *Triplanar geonets consisting of solid extruded ribs*: These allow for high preferential flow in the direction of the central ribs and also have the capability of sustaining high normal stresses (Figure 4.3)

Note, however, that there is considerable new product variation in this category of geosynthetics and it is still evolving (see Austin [1]).

All of the geonets currently available are made from polyethylene resin. The density varies from 0.94 to 0.96 mg/l, with the higher values forming the more rigid products. The resin is formulated with 2.0 to 2.5% carbon black (usually in a concentrated form mixed with a polyethylene carrier resin), and 0.25 to 0.75% additives that serve as processing aids and antioxidants. With these additives, even the lowest density resins fall into a HDPE category, which is how we will refer to all geonet products in this book.

4.1 GEONET PROPERTIES AND TEST METHODS

Since the primary function of a geonet is to convey liquid within the plane of its structure, the in-plane hydraulic flow rate, or transmissivity, is of paramount importance (see Williams et al. [2]). However, other features, which may influence this value over the service lifetime of the geonet, are also of importance. Thus a number of physical, mechanical, endurance, and environmental properties will also be presented in this section.

4.1.1 Physical Properties

The density or specific gravity of the polymer is an important property and it can be evaluated either by ASTM D1505 or D792. The former is preferred if an accuracy of at least 0.005 mg/l is required. Another physical property needed to characterize a geonet is its thickness, which can be determined using ASTM D5199 or ISO 9863. While there is no listing for geonets as such, it is recommended that geonet thickness be measured under a normal pressure of 20 kPa. (This is the same pressure that is recommended for measuring geomembrane thickness.) Note that geonets are not nearly as sensitive to
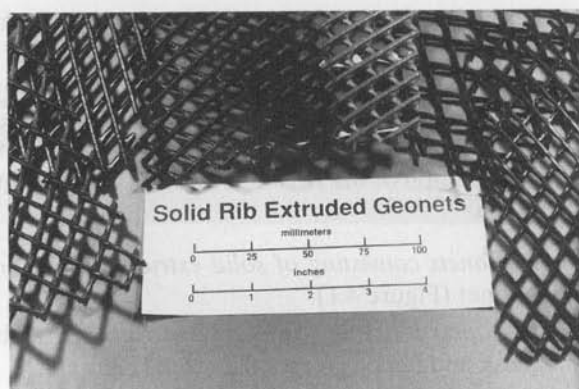
(a) Overview
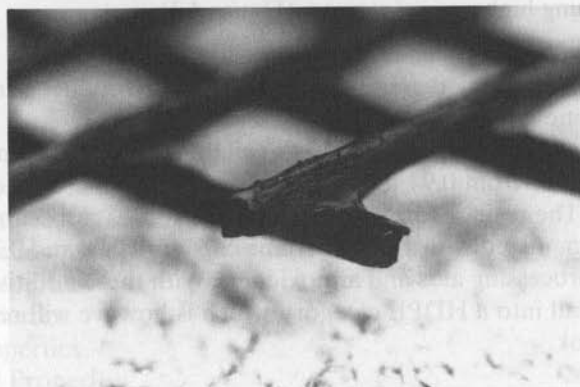
(b) Closeup of rib intersections
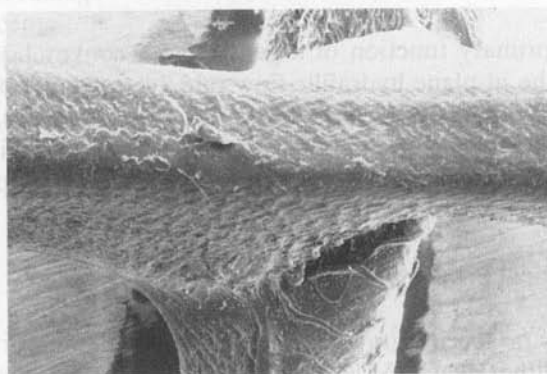
(c) Scanning electron micrograph of a rib intersection
(magnification × 20)

Figure 4.1 Biplanar geonets consisting of solid extruded ribs.
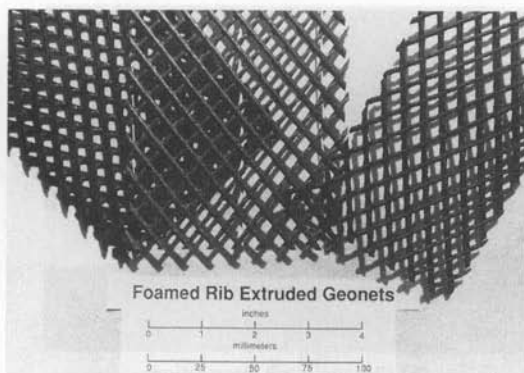
(a) Overview
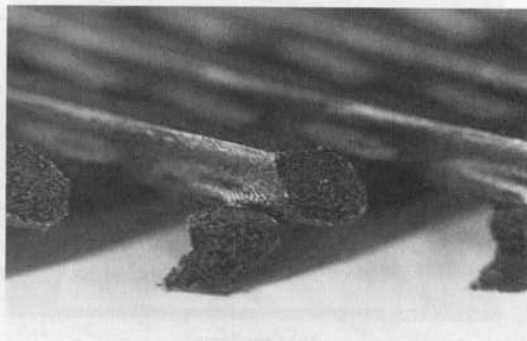
(b) Closeup of rib intersections
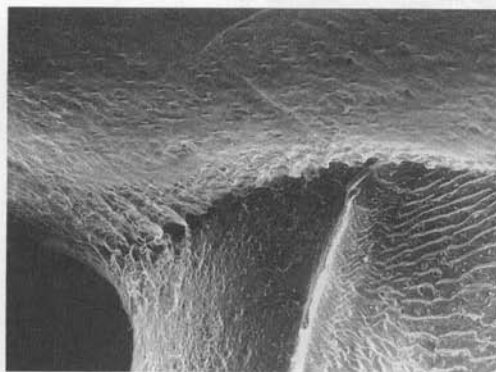
(c) Scanning electron micrograph of a rib
intersection (magnification × 20)
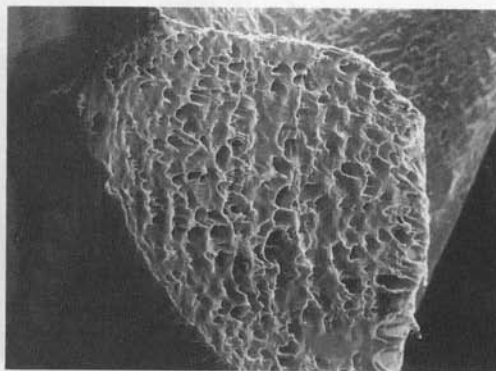
(d) Scanning electron micrograph of a rib
cross-section (magnification × 20)

Figure 4.2   Biplanar geonets consisting of foamed extruded ribs.

thickness variation under normal pressure as are geotextiles; they are similar to geomembranes in this regard.

Mass per unit area can be determined using ASTM D5261 or ISO 9864. For a 5.0 mm thick, solid-rib extruded biplanar geonet, the mass per unit area is usually in the range of 800 to 1600 g/m². It is not a design property per se, but it is informative from a manufacturer's point of view.

Other physical properties such as rib dimensions, planar angles made by the intersecting ribs, cross-planar angles made at the juncture locations, aperture size and shape, and so on, can be measured directly and are straightforward to obtain.
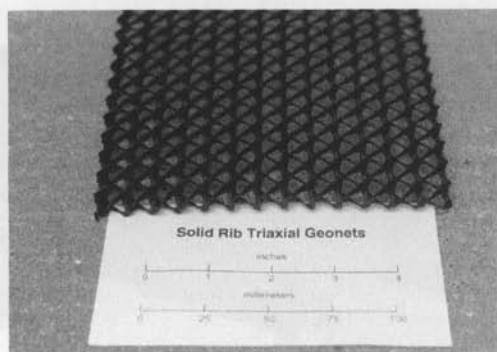
(a) Overview
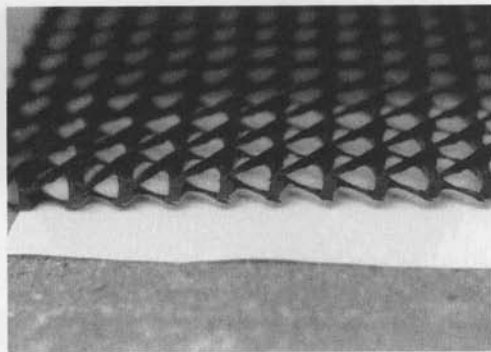
(b) Closeup of rib intersections
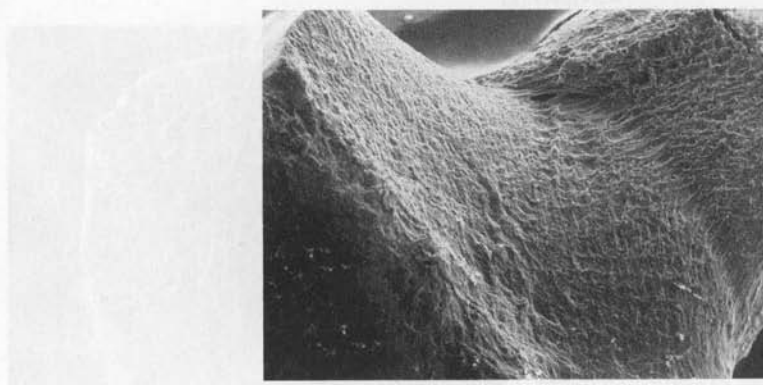
(c) Scanning electron micrograph of a rib intersection
(magnification × 20)

Figure 4.3   Triplanar geonets consisting of solid extruded ribs.

4.1.2 Mechanical Properties

A number of mechanical properties of geonets are important to consider.

Tensile Strength and Elongation.   The wide-width tensile strength curves of Figure 4.4 result from the testing of a 5.0 mm thick solid-rib biplanar extruded geonet in the machine and cross-machine directions. A 200 mm wide × 100 mm long test specimen was used in these tests. The strain rate was 10 mm/mm. Note the differences in behavior, suggesting that there is a preferential direction in strength between the machine and cross-machine directions. If site-specific conditions warrant a higher-strength direction, the geonet should be oriented with its machine direction positioned accordingly. Also note that geonets possess a low, but measurable, tensile strength. For

(a) Machine direction

(b) Cross-machine direction
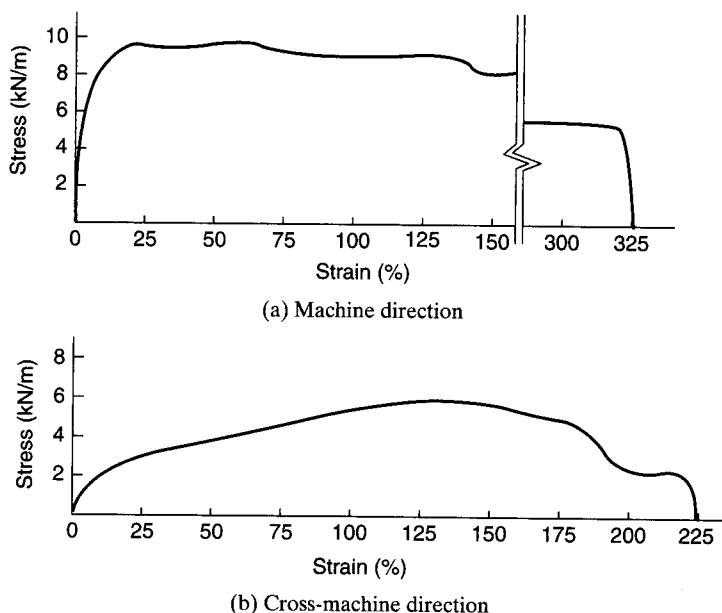
Figure 4.4   Tensile strength behavior of 5.0 mm thick solid-rib biplanar extruded geonet.

the solid-rib geonet illustrated in Figure 4.1 and shown in Figure 4.4, the average of a series of unconfined wide-width tensile tests gave the following information:

- Machine direction: peak strength = 9.9 kN/m, strain at peak = 23%, strain at failure = 290%
- Cross-machine direction: peak strength = 5.6 kN/m, strain at peak = 170%, strain at failure = 240%

If greater machine-direction tensile strength of a geonet is desired, consideration should be give to triplanar geonets oriented in the proper direction.

Compressive Strength and Deformation.   Of greater importance than the above-described in-plane tensile strength tests on geonets is the cross-plane compressive strength. This is because of the influence that compressive deformation or collapse has on the ability of the geonet to conduct liquid within its planar structure. There are a number of approaches to measuring a geonet's compressive strength. Using 150 mm square test specimens normally loaded under a constant strain rate load of 0.05 mm/min, the curves of Figure 4.5 are produced. Here it is shown that both the solid-rib extruded biplanar and the foamed-rib extruded biplanar geonets are initially quite stiff but
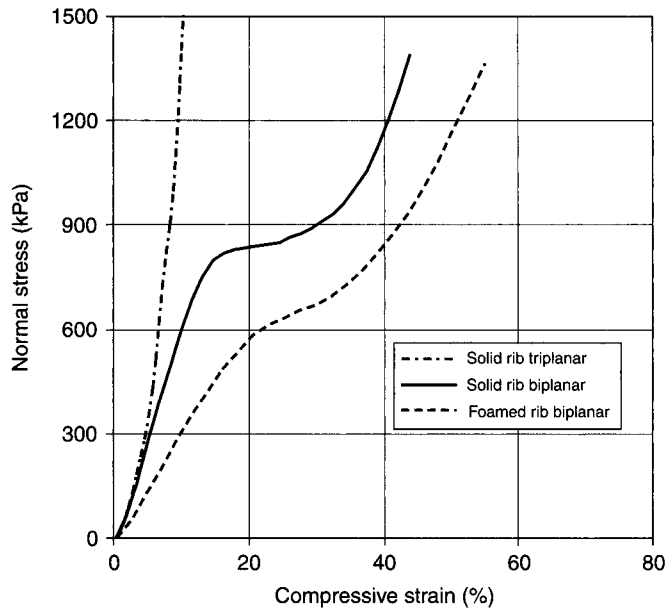
Figure 4.5   Compressive test data of various types of geonets.

begin to deform at normal stress between 600 and 850 kPa. This occurs because the parallel sets of ribs making up the respective geonets are not exactly perpendicular to one another at the junctions. Thus at high compressive stress, there is a *lay-down* or *roll-over* tendency, which gives rise to the characteristic behavior shown. Note that the geonet can still convey liquid beyond this point, but to a somewhat diminished degree. The reason for lay-down stress of the foamed rib geonet being lower than that of the solid-rib geonet is due to the relatively thicker ribs and hence higher flow rate capacity. Development is underway for biplanar geonets which do not have this tendency. The solid-rib extruded triplanar geones (with a still higher flow rate capacity) shows no inflection point since the central and thicker set of ribs is perpendicular to the normal stress. Thus its response to normal stress increases with compressive strain in direct proportion to the density of the resin.

Note that the long-term creep strength is not indicated by these short-term tests. High normal stress, indentation, and creep are discussed in Corcoran et al. [3]. Since creep testing is very time consuming, temperature-accelerated methods should be considered, among which is the stepped isothermal method (SIM) which has been applied to geonet compression testing (see Thornton et al. [4]).

Shear Strength.   A geonet's capacity for sustaining shear stress along a plane within its own thickness without collapsing may be of concern in certain situations. This arises when there are high opposing shear stresses acting on the top and bottom of the geonet, tending to put the material into a state of pure shear. This is not felt to be much

of a problem for the currently available unitized geonets. Considerably more concern should be focused on the interface friction behavior with respect to the materials above and beneath the geonet. This is particularly the case for geonet composites with a covering geotextile(s). Due to the generally low shear strength of a geotextile to a geonet, it is common practice to bond the geotextile(s) to the geonet at the manufacturer's facility. Bonding has been done in the past using adhesives, but most manufacturers currently use thermal methods (i.e., hot wedge, infrared, etc.). The test method commonly used as a quality control test to determine the tensile peel strength of the geotextile to the geonet is ASTM D413. The appropriate interface shear test method is ASTM D5321 or ISO 12957.1, and it is obviously a product-specific and site-specific test that must be performed for each set of conditions that arise (see Lydick and Zagorski [5]). There is no universal relationship between the tension peel and interface shear tests. It is an interesting research area. That said, minimum uniformly-bonded peel strengths often seen in specifications to avoid delamination and a subsequent interface shear failure are between 90 and 180 N/m. Higher values require greater melting of the geonet with proportionate loss of planar flow (or transmissivity), which is not desirable.

4.1.3 Hydraulic Properties

The in-plane hydraulic test to determine planar flow rate, or transmissivity, of geonets should be performed using ASTM D4716 or ISO 12958. Both test methods use a planar transmissivity device and not the radial transmissivity device that was described and illustrated in Section 2.3.4 on geotextiles. This is necessary because the flow regime in a geonet is surely turbulent (consisting of irregular flow paths and eddies) whereas in a geotextile it is probably laminar (thus allowing for radial flow and integration over the flow path length). Some relevant points regarding the test method are as follows.

- The specimen size must be 150 by 150 mm, or larger. Kolbasuk et al. [6] have shown that sample size and aspect ratio (i.e., length-to-width ratio) can have significant effect on the resulting measured flow rates.
- As an index test, the geonet test specimen is sandwiched between rigid plates. However, the cross-section can be varied as desired to approach becoming a site-specific performance test.
- Normal stresses are applied for a 15 min duration, and flow rates are measured at different hydraulic gradients during a subsequent 15 min duration.
- Stress is then increased to the next level and the cycle is repeated.
- De-aired water at 5 ppm, or lower, of dissolved oxygen is not explicitly specified, although for critical situations it might be necessary.
- A standard laboratory temperature of 20°C is required.

Following this procedure and using a 200 mm square test specimen with a 6.3 mm thick solid-rib extruded biplanar geonet in the test device shown in Figure 4.6, the flow rate
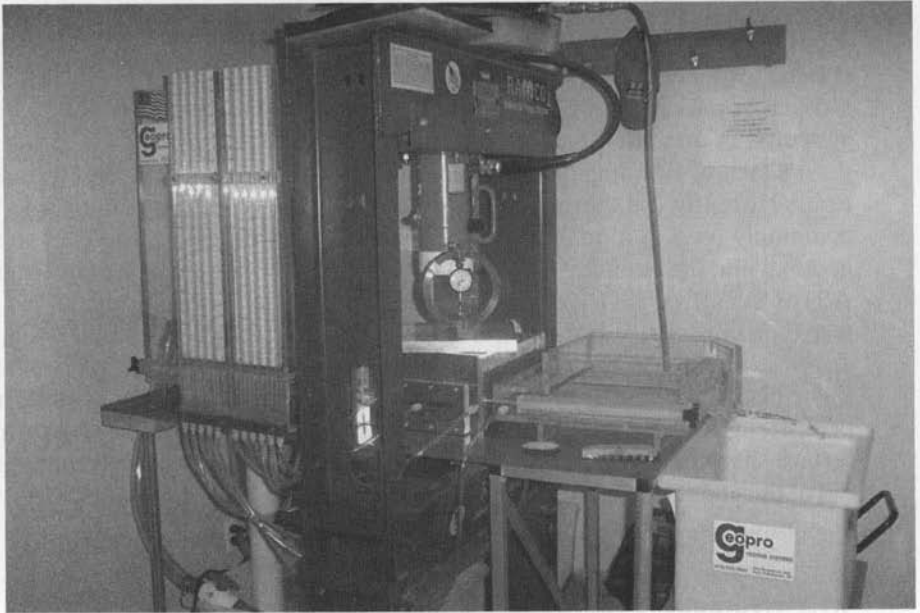
(a) A flow rate testing device
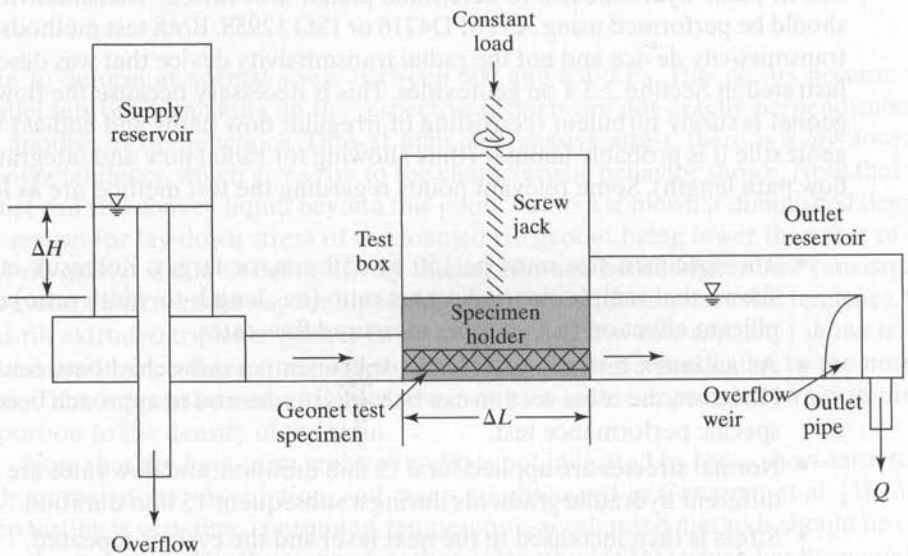
(b) Schematic diagram of flow rate testing device

Figure 4.6   Permeability device for measuring transmissivity (parallel in-plane flow) of a geonet.
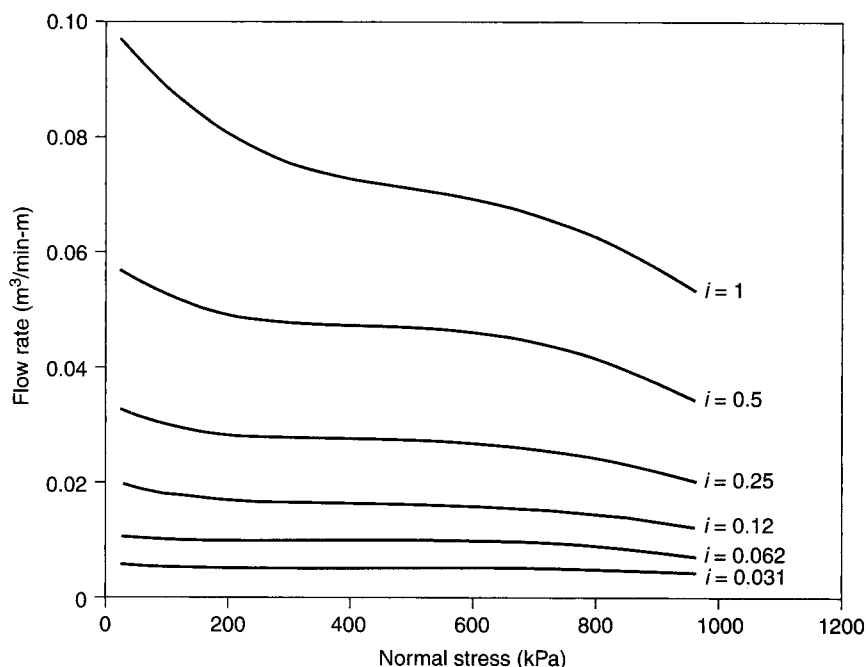
Figure 4.7   Flow rate behavior of a 6.3 mm thick biplanar geonet sandwiched between two 1.5 mm HDPE geomembranes.

curves of Figure 4.7 resulted. Here an increasing flow rate can be observed at each higher hydraulic gradient evaluated. From these data we can calculate a transmissivity value, the assumption being that the system is saturated at all times and flow is laminar. When we consider that these flow rates are extremely high in comparison to the flow rates in soil, it is clear that caution should be used when relying on transmissivity. For example, 300 mm of sand, having a permeability coefficient of 0.1 cm/s at a hydraulic gradient of 1.0, can carry only 0.018 m^3/min-m. Thus geonets can handle large flow rates compared with soil due to the higher velocity of flow within the significantly larger voids. Furthermore, the machine direction flow rate in triplanar geonets is even higher than in biplanar geonets. However, the flow regime in geonets is turbulent in its behavior. Thus the discussion in this chapter will generally be using flow rate values rather than transmissivity values.

The data shown in Figure 4.7 are of the *index* test type. Site-specific situations, however, can be included in the test procedure so as to make the test results more *performance* oriented. To do so we must have the representative conditions above and below the test specimen, and use liquids of the type (and sometimes at the temperature) to be conveyed in the actual system. Figure 4.8 illustrates the influence of one such variation. Here a cross-sectional profile consisting of a layer of clay (kaolinite clay at 15% water content), a 540 gm/m^2 nonwoven needle-punched polyester geotextile, a geonet, and a 1.5 mm HDPE geomembrane is used. Since the geonet is the same type
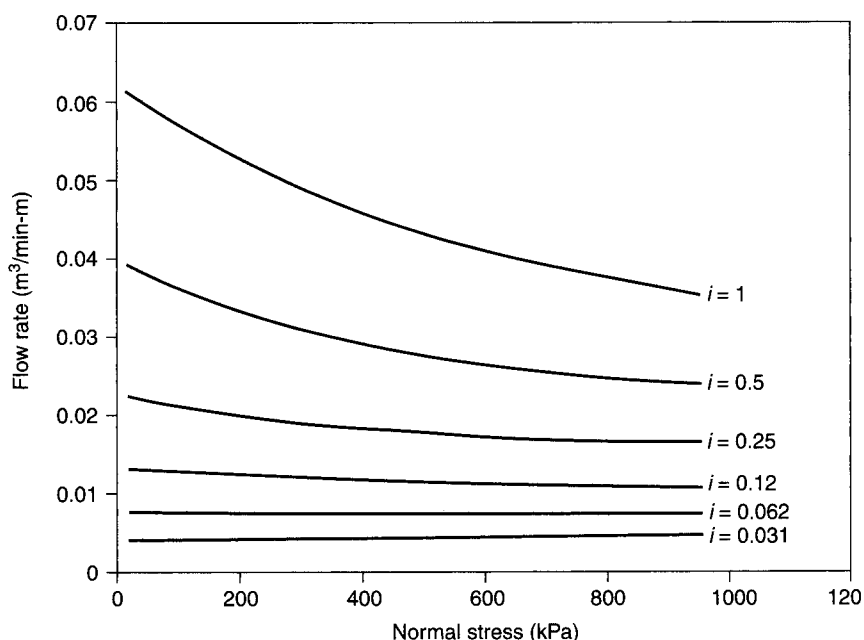
Figure 4.8 Flow rate behavior of a 6.3 mm thick biplanar geonet sandwiched between a 540 g/m² nonwoven needle-punched geotextile with clay above and a 1.5-mm HDPE geomembrane below.

as that producing the data in Figure 4.7, the results can be compared directly, the only difference being the clay soil/geotextile separator placed over the geonet. The marked decrease in the flow rates of Figure 4.8 as compared with Figure 4.7 comes from intrusion of the geotextile into the core space of the geonet via the pressure applied to the clay. Numerically the comparison results in Table 4.1, in which the reduction in flow rates is seen to be as high as 40% from the index test values. Additionally, the geotextile must be capable of sustaining the applied stress, suggesting that long-term tests are required to adequately assess such situations. Sustained load deformation, or creep, will be discussed later.

It should be emphasized that *flow rates per unit width* values are not *transmissivity* values. To convert flow rate per unit width to transmissivity, we use Darcy's formula, which tacitly assumes saturated conditions and laminar flow, neither of which are rigorously met with the typical flow regime in a geonet. Yet, current U.S. EPA leak detection regulations [7] state the following:

- For landfills and waste piles, the geonet's *transmissivity* (θ) must be

$$\theta \geq 3 \times 10^{-5} \text{ m}^2/\text{s}$$

TABLE 4.1   FLOW RATES (m³/min-m) AND REDUCTIONS (%) BETWEEN CURVES OF FIGURES 4.7 AND 4.8

Normal Stress (kPa)	Cross Section	Hydraulic Gradient (i)					
		0.03	0.06	0.12	0.25	0.50	1.00
50	HDPE (both sides)	0.005	0.011	0.019	0.032	0.055	0.095
	GT/clay (one side)	0.004	0.008	0.013	0.022	0.038	0.059
	Difference	0.001	0.003	0.006	0.010	0.017	0.036
	Reduction	20%	27%	31%	31%	31%	38%
250	HDPE (both sides)	0.005	0.011	0.017	0.028	0.048	0.077
	GT/clay (one side)	0.004	0.008	0.012	0.019	0.032	0.052
	Difference	0.001	0.003	0.005	0.009	0.016	0.025
	Reduction	20%	27%	29%	32%	33%	32%
500	HDPE (both sides)	0.005	0.010	0.017	0.027	0.047	0.072
	GT/clay (one side)	0.004	0.007	0.012	0.018	0.028	0.043
	Difference	0.001	0.003	0.005	0.009	0.019	0.029
	Reduction	20%	30%	29%	30%	40%	40%
950*	HDPE (both sides)	0.005	0.008	0.013	0.021	0.035	0.054
	GT/clay (one side)	0.004	0.007	0.011	0.017	0.024	0.035
	Difference	0.001	0.001	0.002	0.004	0.011	0.019
	Reduction	20%	12%	15%	19%	31%	35%

*Note that roll-over of the geonet structure has occurred at this normal stress (recall Figure 4.5). Thus the reduction percentages are not as large as they are with the other normal stress values.

- For surface impoundments, the geonet's *transmissivity* (θ) must be

$$\theta \geq 3 \times 10^{-4}\, m^2/s$$

We convert from flow rate per unit width to transmissivity as follows:

$$q \quad = kiA$$
$$q \quad = ki(W \times t) \tag{4.1}$$
$$q/W = i(k \times t)$$
$$q/W = i\theta \tag{4.2}$$

Thus it is seen in equation (4.2) that the units of q/W and θ are identical, but only at $i = 1.0$ are the numeric values the same. A hydraulic gradient of 1.0 occurs when the geonet is placed vertically, as in the lining of a tank wall, not on the sloping surfaces of a typical landfill or surface impoundment. Example 4.1 illustrates the numeric conversion.

Example 4.1

A geonet tested in the laboratory under site-specific conditions results in a flow rate per unit width of $0.65 \times 10^{-4}\, m^2/s$ at a hydraulic gradient 0.040. **(a)** What is the equivalent transmissivity in units of m^2/s, and **(b)** does this value meet the EPA criteria for landfills and surface impoundments?

Solution: Using equation (4.2) and converting units we have the following:

(a) The equivalent transmissivity is

$$\theta = \left(\frac{q}{W}\right)\left(\frac{1}{i}\right)$$

$$= 0.65 \times 10^{-4}(1/0.040)$$

$$\theta = 16.2 \times 10^{-4} \text{ m}^2/\text{s}$$

(b) Comparing the above to the EPA criteria,

$$162 \times 10^{-5} > 3.0 \times 10^{-5} \text{ m}^2/\text{s}$$

which is easily acceptable for landfills, with a resulting FS = 54.

$$16.2 \times 10^{-4} > 3.0 \times 10^{-4} \text{ m}^2/\text{s}$$

which is also acceptable for surface impoundments, with a resulting FS = 5.4.

4.1.4 Endurance Properties

The major endurance properties of concern when using geonets have to do with the long-term sustained deformation of the material and its ability to continue to transmit the required in-plane flow rate. Four issues are relevant: (1) type of polyethylene resin, (2) creep behavior of the geonet structure, (3) intrusion of adjacent materials into the geonet's apertures, and (4) the possible extrusion of clay through a covering geotextile. Each will be discussed.

Type of Polyethylene Resin.   Depending upon the type of polyethylene resin, primarily characterized by its density, the geonet will have different mechanical and endurance properties. The high density resins (e.g., greater than 0.950 mg/l), will result in relatively high modulus, high strength, and high creep resistance. Conversely, lower density resins (e.g., less than 0.945 mg/l) will be more flexible and can deform under high compressive stresses more easily. The lower density resins, however, often have the advantage of having better stress-crack resistance properties. (Stress-crack resistance is particularly critical for HDPE geomembranes, as will be discussed in Chapter 5.) The importance of stress-crack resistance for a geonet is a design issue and related to the site-specific situation.

Creep Behavior.   Sustained load (or creep) is the reduction in thickness of a geonet under an applied compressive stress. Here the density of the resin (as described above), type of structure, and composition of the rib junctions are all significant. Figure 4.9 presents geonet creep data at 480 kPa for 1000 hours. Note that even this is too short a time for conventional practice because the extrapolation of trends beyond one order of magnitude is questionable. Thus data for 10,000 hr, extrapolated to 100,000 hr ($\cong 11$ years), just begins to get into the frame of the life expectancy of many engineered systems using geonets. To shorten the testing time, other techniques
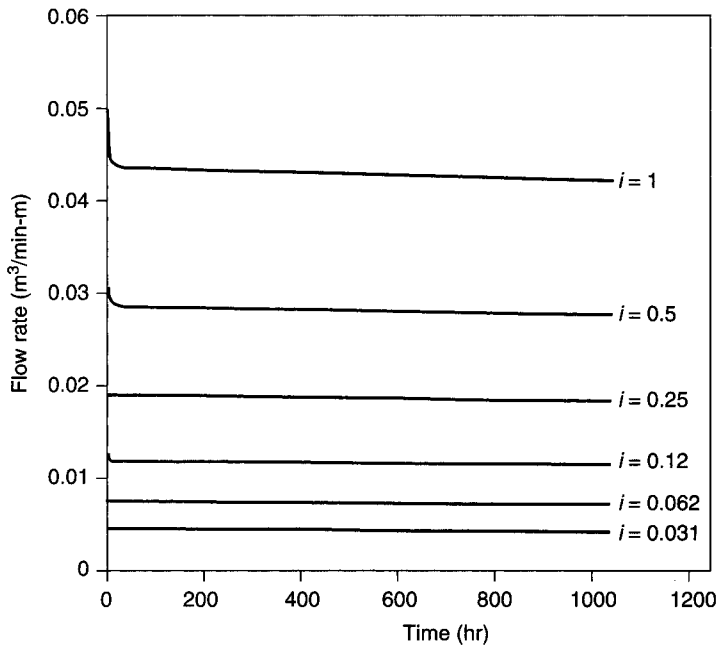
Figure 4.9   Long-term creep test results of the same cross section in Figure 4.8, except under a sustained load of 480 kPa.

such as time-temperature superposition (including the stepped isothermal method [4]) may be appropriate. Research is ongoing in this regard.

Intrusion of Adjacent Materials.   All geonets will necessarily be covered on the upper and lower surfaces with geotextile, geomembrane, concrete wall surface, or some other material. If the geonet's surfaces are not covered, soil will invade its apertures, rendering flow impossible. *Intrusion* refers to the deformation of the flexible covering materials, primarily geotextiles, occupying some of the geonet's void space, as illustrated by the flow rate reductions in Table 4.1. As seen by the data, intrusion into the core space is a very real phenomenon causing flow rate decrease. Figure 4.10 illustrates the phenomenon. Figure 4.10a, b, and c were made by using a compressible foam (representing soil) above the geomembrane or geotextile covering the geonet. Under load, the stiffer geomembranes (in this case, 1.5 mm HDPE geomembranes) have no observable intrusion. The stiff heat-bonded nonwoven geotextile on the upper surface of the geonet produces some intrusion. The flexible needle-punched nonwoven geotextile, however, has considerable intrusion. (See Hwu et al. [8] and Eith and Koerner [9] for data in this regard.) It should be mentioned that thermal bonding of the geotextile to the geonet has a tendency to decrease some of the intrusion.

Now superimpose on these short-term reductions, sustained compressive stresses for extended times. Figure 4.9 presents the results of such a test series, where each test has load maintained for 1000 hours. Note that the response curves are essentially

(a) No intrusion

(b) Low intrusion

(c) High intrusion
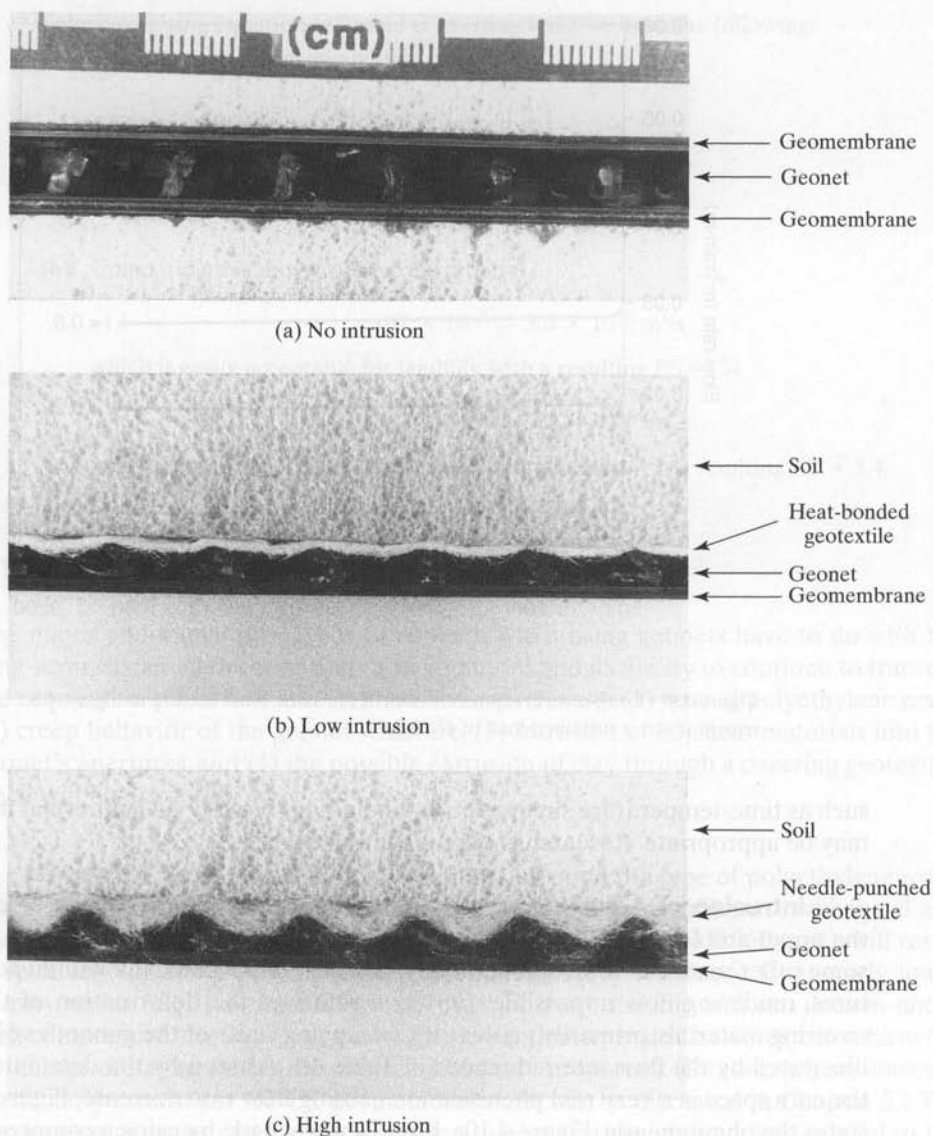
Figure 4.10   Intrusion of geotextiles and geomembranes into geonet's apertures.

horizontal. Thus creep intrusion (as contrasted to elastic, or initial, intrusion) is not an issue. The geotextile in this case is a nonwoven needle-punched polyester of 550 gm/m^2 mass per unit area with clay above. Clearly the selection of the geotextile is important in sustaining the applied compressive stresses. The initial amount of intrusion, not necessarily the long-term behavior, is primarily a function of the geotextile's initial modulus. All other things being equal, those nonwoven geotextiles with high modulus will have the minimum amount of initial intrusion and hence higher flow

rates. The long-term creep behavior depends upon the polymer type, stress level, distance between geonet ribs, and so on, and is best quantified by simulated laboratory testing.

Extrusion of Clay Materials.   If a compacted clay liner or a geosynthetic clay liner with bentonite is placed adjacent to a geonet composite, there is a possibility of the clay particles *extruding* through the geotextile's voids into the geonet. This is a disaster for the flow rate capability of the geonet; it must be avoided under all circumstances. Such a situation has happened in laboratory tests with woven monofilament geotextiles on the geonet and could happen with woven slit-film geotextiles as well. Conversely, nonwoven geotextiles have generally been effective in preventing soil extrusion. The minimum mass per unit area of the covering geotextile is a site-specific issue. Further studies are warranted in this regard.

4.1.5 Environmental Properties

A series of environmentally related issues can have an impact upon the flow rate performance of geonets. The first that comes to mind is temperature. Under high temperatures, flow rates increase over standardized laboratory test conditions. The converse is true for cold temperatures. These are usually minor effects that can be calculated on the basis of viscosity corrections (recall Section 2.3.4). Perhaps more important is that creep of the polymers (geonet and adjacent geotextile or geomembranes) increases under increasing temperature. Simulated testing under these conditions is possible but costly. In lieu of such testing, a conservative design approach regarding creep is warranted.

The second environmental consideration focuses on the nature of the liquid being transmitted. If chemicals or leachate are being transmitted, a number of questions arise. One of these is the chemical resistance of the polymers being used for the geonet and the covering geotextiles and/or geomembranes to the site-specific liquid. Here the choice of polyethylene for geonets is fortunate, since it is very resistant to most aggressive leachates. Again, laboratory testing can be performed using the actual or simulated leachate, but this can create concerns in a laboratory that is not equipped to handle contaminated liquids. ASTM is nicely set up with standards in this regard— i.e., laboratory immersion per D5322, geonet testing per D6388, and geotextile testing per D6389. The turbidity and viscosity effects of leachate (versus water) used in testing are another consideration, but these are often of second-order importance compared to some of the other issues being raised. Furthermore, they can be corrected by density and viscosity relationships (recall Section 2.3.4).

The third environmental consideration has to do with biological growth within the geonet and/or on the geotextiles that allow liquid to enter the geonet. In most transportation-related systems, such as roads and walls, the problem does not appear to be too serious. In systems related to waste containment (e.g., landfill leachate collection systems), the issue should be addressed. At the bottom of a landfill, temperatures can be high, ample organic material (as a biological food source) is available, and bacteria and fungi could indeed thrive. Whether oxygen is available or not only dictates

whether aerobic or anaerobic conditions prevail. Procedurally, we must use a high flow rate factor of safety or have systems designed so that flushing is possible. This area simply begs for future inquiry. Research should also focus on the filtration and drainage of agricultural runoff and wastewater sludges as well. Biological growth on geotextiles has been addressed and a design procedure is available (see Koerner et al. [10]).

The fourth environmental consideration, resistance to light and weather, is not felt to be a serious concern for most situations in which geonets are used. Polyethylene is quite resistant to weather-related degradation, and carbon black is included in all of the known products. Nevertheless geonets should be covered as soon as possible after placement. For geotextile covered geonets, the situation is controlled by the (more severe) ultraviolet degradation of the geotextile (recall Section 2.3.6).

4.1.6 Allowable Flow Rate

As described previously, the very essence of the design-by-function concept is the establishment of an adequate factor of safety. For geonets, where flow rate is the primary function, this takes the following form:

$$FS = \frac{q_{allow}}{q_{reqd}} \tag{4.3}$$

where

FS = factor of safety (to handle unknown loading conditions or uncertainties in the design and testing methods),

q_{allow} = allowable flow rate as obtained from laboratory testing, and

q_{reqd} = required flow rate as obtained from design of the actual system.

Alternatively, we could work from transmissivity to obtain the equivalent relationship;

$$FS = \frac{\theta_{allow}}{\theta_{reqd}} \tag{4.4}$$

where θ is the transmissivity, under definitions as above. As described previously, however, it is preferable to design with flow rate rather than transmissivity because of non-laminar flow conditions in geonets and the intuitive nature of the term.

Concerning the allowable flow rate or transmissivity value, which comes from hydraulic testing of the type described in Section 4.1.3, we must assess the realism of the test setup in contrast to the actual field system. If the test setup does not model site-specific conditions adequately, then adjustments to the laboratory value must be made. This is usually the case. Thus the laboratory-generated value is an ultimate value that must be reduced before use in design; that is,

$$q_{allow} < q_{ult}$$

One way of doing this is to ascribe reduction factors on each of the items not adequately assessed in the laboratory test. For example,

$$q_{\text{allow}} = q_{\text{ult}}\left[\frac{1}{RF_{IN} \times RF_{CR} \times RF_{CC} \times RF_{BC}}\right] \tag{4.5}$$

or if all of the reduction factors are considered together:

$$q_{\text{allow}} = q_{\text{ult}}\left[\frac{1}{\Pi RF}\right] \tag{4.6}$$

where

q_{ult} = flow rate determined using ASTM D4716 or ISO 12958 for short-term tests between solid platens using water as the transported liquid under laboratory test temperatures,

q_{allow} = allowable flow rate to be used in equation (4.3) for final design purposes,

RF_{IN} = reduction factor for elastic deformation, or intrusion, of the adjacent geosynthetics into the geonet's core space,

RF_{CR} = reduction factor for creep deformation of the geonet and/or adjacent geosynthetics into the geonet's core space,

RF_{CC} = reduction factor for chemical clogging and/or precipitation of chemicals within the geonet's core space,

RF_{BC} = reduction factor for biological clogging within the geonet's core space, and

ΠRF = product of all reduction factors for the site-specific conditions.

Some guidelines as to the various reduction factors to be used in different situations are given in Table 4.2. Please note that some of these values are based on relatively sparse information. Other reduction factors, such as overlapping connections, temperature effects, and liquid turbidity, could also be included. If needed, they can be included on a site-specific basis. On the other hand, if the actual laboratory test procedure has included the particular item, it would appear in the above formulation as a value of unity. Examples 4.2 and 4.3 illustrate two of the uses of geonets and serve to point out that high reduction factors are warranted in critical situations.

Example 4.2

What is the allowable geonet flow rate to be used in the design of a secondary leachate collection (or leak detection) system? Assume that laboratory testing at proper design load and proper hydraulic gradient gave a short-term between-rigid-plates value of $2.5 \times 10^{-4} \, \text{m}^2/\text{s}$.

TABLE 4.2 RECOMMENDED REDUCTION FACTOR VALUES FOR EQUATION (4.5) DETERMINING ALLOWABLE FLOW RATE OR TRANSMISSIVITY OF GEONETS

Application Area	Reduction Factor Values in Equation (4.5)			
	RF_{IN}*	RF_{CR}*	RF_{CC}	RF_{BC}
Sport fields	1.0–1.2	1.0–1.5	1.0–1.2	1.1–1.3
Capillary breaks	1.1–1.3	1.0–1.2	1.1–1.5	1.1–1.3
Roof and plaza decks	1.2–1.4	1.0–1.2	1.0–1.2	1.1–1.3
Retaining walls, seeping rock, and soil slopes	1.3–1.5	1.2–1.4	1.1–1.5	1.0–1.5
Drainage blankets	1.3–1.5	1.2–1.4	1.0–1.2	1.0–1.2
Infiltrating water drainage for landfill covers	1.3–1.5	1.1–1.4	1.0–1.2	1.5–2.0
Secondary leachate collection (landfill)	1.5–2.0	1.4–2.0	1.5–2.0	1.5–2.0
Primary leachate collection (landfills)	1.5–2.0	1.4–2.0	1.5–2.0	1.5–2.0

*These values are sensitive to the type of geonet, rib separation distance, and density of the resin used in the geonet's manufacture. The magnitude of the applied load is also of major importance.

Solution: Average values from Table 4.2 are used in equation (4.5) (however, note the large reduction).

$$q_{allow} = q_{ult}\left[\frac{1}{RF_{IN} \times RF_{CR} \times RF_{CC} \times RF_{BC}}\right]$$

$$= 2.5 \times 10^{-4}\left[\frac{1}{1.75 \times 1.7 \times 1.75 \times 1.75}\right]$$

$$= 2.5 \times 10^{-4}\left[\frac{1}{9.11}\right]$$

$$q_{allow} = 0.27 \times 10^{-4} \text{ m}^2/\text{s}$$

Example 4.3

What is the allowable geonet flow rate to be used in the design of a capillary break beneath a roadway to prevent frost heave? Assume that laboratory testing was done at the proper design load and hydraulic gradient and that this testing yielded a short-term between-rigid-plates value of 2.5×10^{-4} m^2/s.

Solution: Since better information is not known, average values from Table 4.2 are used in equation (4.5).

$$q_{allow} = q_{ult}\left[\frac{1}{RF_{IN} \times RF_{CR} \times RF_{CC} \times RF_{BC}}\right]$$

$$= 2.5 \times 10^{-4}\left[\frac{1}{1.2 \times 1.1 \times 1.3 \times 1.2}\right]$$

$$= 2.5 \times 10^{-4}\left[\frac{1}{2.06}\right]$$

$$q_{allow} = 1.21 \times 10^{-4} \text{ m}^2/\text{s}$$

4.2   DESIGNING FOR GEONET DRAINAGE

This section will be subdivided into a discussion of required theory (which somewhat repeats previously described issues, due to its importance), drainage examples in the waste containment–related field and drainage examples in the transportation-related field.

4.2.1 Theoretical Concepts

Design-by-function requires the formulation of a factor of safety as follows:

$$FS = \frac{\text{allowable (test) value}}{\text{required (design) value}}$$

For geonets serving as a drainage medium, the targeted value is flow rate and the above concept becomes equation (4.3):

$$FS = \frac{q_{\text{allow}}}{q_{\text{reqd}}}$$

where

q_{allow} = allowable flow rate (as discussed in Section 4.1), and

q_{reqd} = required flow rate (to be discussed here).

As stated previously, if we desire an alternative to the flow rate, calculations can be based on Darcy's formula (assuming saturated conditions and laminar flow) obtaining the transmissivity, θ. This important concept is repeated from equations (4.1) and (4.2):

$$q = kiA$$
$$q = ki(W \times t)$$
$$W = i(k \times t)$$
$$kt \equiv \theta = \frac{q}{iW}$$

where

q = volumetric flow rate (m³/s),

k = coefficient of permeability (m/s),

i = hydraulic gradient (dimensionless),

A = flow cross-sectional area (m²),

θ = transmissivity (m²/s),

W = width (m), and

t = thickness (m).

As in equation (4.2), it is seen that q/W and θ carry the same units and are directly related to one another by means of the hydraulic gradient i. At a hydraulic gradient of 1.0, they are numerically identical. At other values of hydraulic gradient they are not equal. Also note that the system should be saturated and flow must be laminar in order to use transmissivity. When in doubt, it is usually best to use flow rate per unit width.

4.2.2 Environmental-Related Applications

Geonets are widely used in landfill-liner systems as the primary leachate collection systems on side slopes and sometimes bottom slopes, and as leak detection systems between the primary and secondary liners (see Bonaparte et al. [11] and Lundell and Menoff [12]). They are also commonly placed above the barrier layer in final cover systems for drainage of surface water infiltrating the cover soil (Koerner and Soong [13]). All three of these applications will be illustrated by means of numeric examples. As such, geonets are placed with either a geomembrane on both sides, or a geomembrane beneath and a geotextile above. In this latter case, the geotextile has either granular soil or clay above it. Note that the inverse cross section is also possible—that is, there is a geomembrane above and a geotextile with soil below. The flow-rate results illustrated in Figures 4.7 and 4.8 indicate some of these alternatives. Lastly, the geonet can have geotextiles on both sides generally for the purpose of enhanced friction against the opposing surface(s) of textured geomembranes.

Example 4.4

Determine the flow rate factor of safety of a geonet that is used in a primary leachate collection system above a geomembrane and beneath a sand covering layer in a landfill cell whose plan view is as shown in the following diagram. The geonet delivers its flow to the central perforated header pipe leading to the downgradient removal sump. The landfill is 35 m high with a waste unit weight of 13 kN/m^3. The geonet being considered has been tested with the results shown in Figure 4.7. Site-specific reduction values will be necessary in order to obtain the allowable flow rate. The design inflow rate is 30,000 l/ha-day, which was the average leachate collected in all the New York state landfills in 2000. Note that this value is very much site-specific with hydrology, type of waste, and liquids management at the site all being major considerations.

Solution:

(a) The maximum length of geonet perpendicular to the central drainage pipe is calculated:

$$L_H = 14 + (150) \tan 5°$$
$$= 14 + 13.1$$
$$L_H = 27.1 \text{ m}$$

(b) The inflow rate is converted to units compatible with the test values:

$$r = 30,000 \text{ l/ha-day}$$
$$= 30,000 \frac{1000}{(10,000)(100)(100)(100)}$$
$$r = 0.003 \text{ m}^3/\text{day-m}^2$$
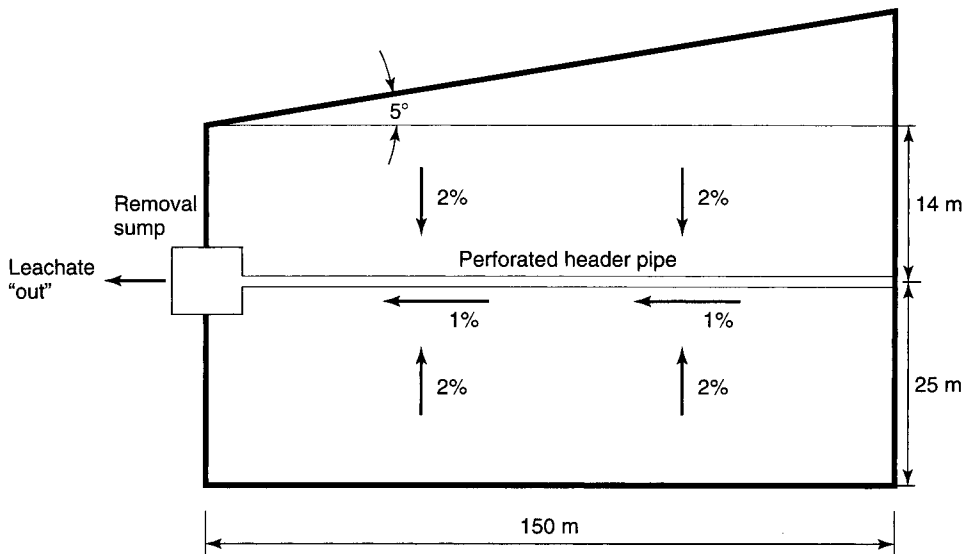
(c) The required (and maximum) flow rate per unit width is calculated (see Qian, et al [14]):

$$q_{reqd} = rL_H$$
$$= [0.003(27.1)]/[(24)(60)]$$
$$q_{reqd} = 0.0000565 \text{ m}^3/\text{min-m}$$

(d) The laboratory-obtained maximum flow rate is estimated from Figure 4.7 at $\sigma_n = 35 \times 13 = 455$ kPa, and $i = 0.02$:

$$q_{max} = 0.003 \text{ m}^3/\text{min-m}$$

(e) This is now reduced to an allowable value using average values from Table 4.2 except for intrusion, which is assumed to be at a maximum value:

$$q_{allow} = q_{ult}\left[\frac{1}{2.0 \times 1.7 \times 1.75 \times 1.75}\right]$$
$$= 0.003\left[\frac{1}{10.4}\right]$$
$$q_{all} = 0.000288 \text{ m}^3/\text{min-m}$$

(f) Finally, the FS-value is obtained:

$$FS = \frac{q_{allow}}{q_{reqd}}$$
$$= \frac{0.000288}{0.0000565}$$
$$FS = 5.1 \qquad \text{which is acceptable}$$

Example 4.5

Assuming that there are no regulations governing the situation, is the geonet whose response is shown in Figure 4.7 adequate for the following landfill leak detection and collection system? The geonet lies between two HDPE geomembranes (there is no pipe drainage system), and the design flow is 100 times *de minimis** leakage. (*De minimis* leakage is approximately 10 l/ha-day). The minimum slope of the bottom of the 300 m long landfill is 6%, and the landfill when completed will be 50 m high with a unit weight of waste being 11 kN/m^3.

Solution:

(a) The required flow rate converted to comparable units is

$$q_{reqd} = \frac{(100)(10)(0.001)}{(10,000)(24 \times 60)} \times 300$$

$$= 2.08 \times 10^{-5} \, \text{m}^3/\text{min-m}$$

(b) The ultimate flow rate is taken from Figure 4.7 (at $\sigma_n = 50 \times 11 = 550$ kPa and $i = 0.06$)

$$q_{ult} = 0.01 \, \text{m}^3/\text{min-m}$$

and from Table 4.2 it is reduced to obtain an allowable value using average values throughout:

$$q_{allow} = q_{ult}\left[\frac{1}{1.75 \times 1.7 \times 1.75 \times 1.75}\right]$$

$$= 0.01\left[\frac{1}{9.11}\right]$$

$$q_{allow} = 0.00110 \, \text{m}^3/\text{min-m}$$

(c) Therefore, the factor of safety is

$$FS = \frac{q_{allow}}{q_{reqd}}$$

$$= \frac{110 \times 10^{-5}}{2.08 \times 10^{-5}}$$

$$FS = 53 \qquad \text{which is more than adequate}$$

---

*U.S. EPA Regulatory Note: The primary (or upper) geomembrane of a hazardous waste facility should allow no more than *de minimis* leakage of all polluting species through the liner itself. The concept of *de minimis* comes from the legal principle *de minimis non curat lex* (the law does not concern itself with trifles). *De minimis* leakage is considered to be the amount that is of no threat to human health or the environment. It is recognized that geomembranes, since they are not impermeable, will allow some transmission of waste constituents, by such means as vapor permeation or via very small imperfections. The actual level of *de minimis* leakage of a constituent is specific to the site, the constituent's toxicity, and the mobility and biodegradability of the constituent. Specific levels for individual constituents have not been set, although the U.S. EPA believes that total *de minimis* leakage should be no more than 1 gallon per acre per day (gpad). This is approximately 10 l/ha-day. Current legislation [15], however, avoids setting a general action leakage rate (ALR) and instead requires each permit application to set its own site-specific ALR value.

(d) Note that for the data in Figure 4.8, for the geotextile and clay over the geonet, the flow rate is approximately half of the above and the factor of safety is reduced accordingly.

Example 4.6

What is the factor of safety of a geonet placed above a geomembrane and beneath a geotextile in the final cover of a completed solid waste facility (landfill or waste pile). As shown in the diagram below, the slope is 10% and the cover soil fill height is 1.25 m. Assume that the slope length is 120 m long. Short-term in-plane flow tests show that the flow rate is 2.5×10^{-4} m^2/s at a hydraulic gradient of 0.10 and at a normal pressure of 50 kN/m^2 (which includes soil weight plus equipment loads).
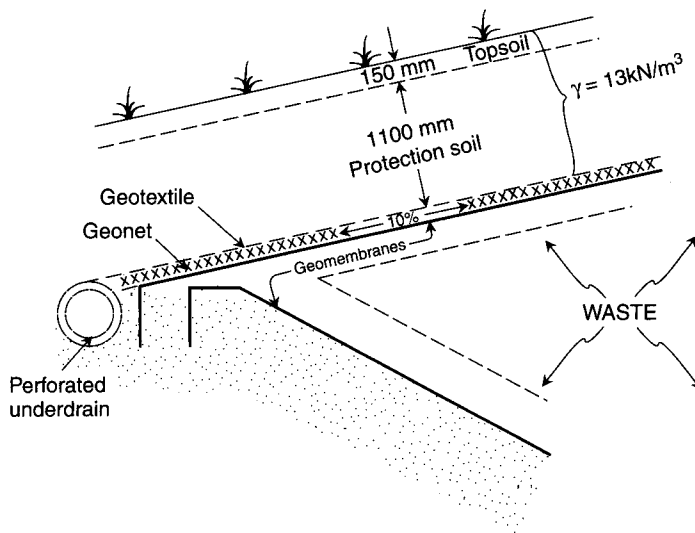
Solution:

(a) The allowable flow rate is again taken from equation (4.5) and Table 4.2, using average values

$$q_{\text{allow}} = 2.5 \times 10^{-4} \left[\frac{1}{1.4 \times 1.25 \times 1.1 \times 1.75} \right]$$

$$= 2.5 \times 10^{-4} \left[\frac{1}{3.37} \right]$$

$$q_{\text{allow}} = 0.74 \times 10^{-4} \text{ m}^2/\text{s}$$

(b) The required flow rate either must be approximated or must be determined by using a liquid-mass balance, including local hydrological data, soil storage, leakage, and so on. This was done in this case, following an hourly rainfall modeling procedure (see Koerner and Daniel [16]), giving a required flow rate 0.17×10^{-4} m^2/s at

the end of a 120 m long section of closure. Note that the computer model entitled Hydrologic Evaluation of Landfill Performance (HELP) is widely used by regulatory personnel and consultants working in the solid-waste field (Schroeder et al. [17]), but it can only track seepage on a daily basis and is not felt to adequately model intense storms. That said, the HELP model is recommended for determination of leachate arriving at the base of a landfill for subsequent drainage as depicted in Example 4.4.

(c) The final factor of safety becomes

$$FS = q_{allow}/q_{reqd}$$
$$= \frac{0.74 \times 10^{-4}}{0.17 \times 10^{-4}}$$
$$FS = 4.3$$

This value of factor of safety, being well above 1.0, is acceptable. However, seepage failures in landfill final covers have been so troublesome that very high FS values are required [13]. The final decision on acceptability is site-specific.

4.2.3 Transportation-Related Applications

Geonets have been well established as an alternative drainage material to granular soils in the environmental field, and there is no reason why they should not be used in transportation-related applications as well. This section addresses two such applications, both of which are very relevant.

Example 4.7

Given an area that is to be retrofitted with a new pavement because of past problems with frost heave, the new scheme is intended to have a geonet with thermally bonded geotextiles on both sides and will be placed immediately beneath the depth of maximum frost penetration, as shown in the diagram below. Based upon the rising capillary water, the required flow rate to be conveyed is estimated to be 0.17×10^{-4} m²/s. A candidate geonet has been selected, and tests performed at a gradient of 0.05 have resulted in a flow rate of 0.83×10^{-4} m²/s. What is the factor of safety?
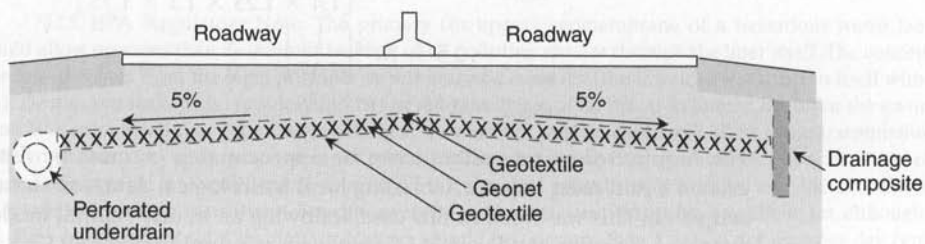
Solution:

(a) Assuming that the laboratory tests were short-term and between rigid plates, the value of 0.83×10^{-4} m²/s must be reduced according to Table 4.2, as per the earlier example problems. Using average values for the various reduction factors, we have

$$q_{allow} = 0.83 \times 10^{-4} \left[\frac{1}{1.2 \times 1.1 \times 1.3 \times 1.2} \right]$$

$$q_{allow} = 0.83 \times 10^{-4} \left[\frac{1}{2.06} \right]$$

$$= 0.403 \times 10^{-4} \text{ m}^2/\text{s}$$

(b) Now the actual flow rate factor of safety can be determined.

$$FS = q_{allow}/q_{reqd}$$

$$= \frac{0.403 \times 10^{-4}}{0.17 \times 10^{-4}}$$

$$FS = 2.4 \qquad \text{which is adequate}$$

Example 4.8

Determine the drainage factor of safety for the geonet behind an 8 m high cantilever retaining wall as shown in the diagram below. The geonet being used has a response as shown in Figure 4.7. In the field it will be placed against the concrete on one surface, and it will have a geotextile on the surface against the backfill soil. The soil backfill is a silty sand (ML-SW) with $k = 5.0 \times 10^{-5}$ m/s. Note this is the same problem that was attempted using a geotextile in Section 2.9.3 (Example 2.27), where the factor of safety was found to be 0.0062.
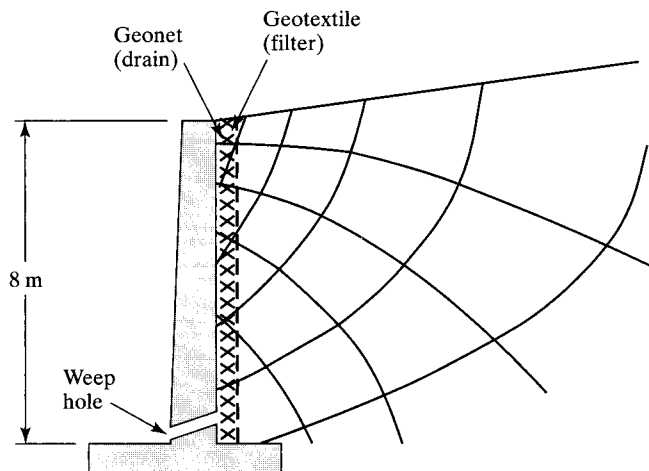
Solution:

(a) Calculate the maximum flow rate coming to the geonet. From the flow net sketched in the figure above, we have

$$q = kh\left(\frac{F}{N}\right)$$

$$= (5.0 \times 10^{-5})(8)\left(\frac{5}{5}\right)$$

$$= 4.0 \times 10^{-4} \text{ m}^2/\text{s}$$

(b) Determine the flow gradient within the geotextile:

$$i = \sin 90°$$

$$= 1.0$$

(c) Calculate the required transmissivity. Note that transmissivity is used so that the results can be directly compared to Example 2.27 using geotextiles:

$$q = kiA$$

$$= ki(t \times W)$$

$$= (kt)(i \times W)$$

$$(kt) = \theta = \frac{q}{i \times W}$$

$$= \frac{4.0 \times 10^{-4}}{1.0 \times 1.0}$$

$$\theta_{\text{reqd}} = 4.0 \times 10^{-4} \text{ m}^2/\text{s}$$

(d) From the laboratory data of Figure 4.7, obtain the ultimate flow rate, convert it to a transmissivity value, and then reduce it to an allowable transmissivity. The normal pressure is obtained first: $\sigma_n \cong 0.5(8)(18) = 72$ kPa and at $i = 1.0$ gives:

$$q = 0.094 \text{ m}^2/\text{min} = 15.6 \times 10^{-4} \text{ m}^2/\text{s}$$

For a vertical wall, where $i = 1.0$, the flow rate per unit width (q/W) is identical to the transmissivity θ (recall equation 4.2), so

$$\theta_{\text{ult}} = 15.6 \times 10^{-4} \text{ m}^2/\text{s}$$

Reducing the ultimate value according to Table 4.2 (with arbitrary selected values),

$$\theta_{\text{allow}} = 15.6 \times 10^{-4}\left[\frac{1}{1.4 \times 1.3 \times 1.2 \times 1.2}\right]$$

$$= 15.6 \times 10^{-4}\left[\frac{1}{2.62}\right]$$

$$\theta_{\text{allow}} = 5.95 \times 10^{-4} \text{ m}^2/\text{s}$$

(e) Knowing both allowable and required values of transmissivity, the factor of safety can now be calculated:

$$FS = \frac{\theta_{allow}}{\theta_{reqd}}$$

$$= \frac{5.95 \times 10^{-4}}{4.0 \times 10^{-4}}$$

$$FS = 1.48 \quad \text{which is marginally acceptable}$$

Thus, the geonet characterized by the Figure 4.7 data is only marginally adequate to drain the wall, whereas multiple layers of geotextiles were not adequate. However, even this factor of safety is somewhat questionable and a higher flow capacity drainage composite should be investigated—for example, a triplanar geonet or other type of drainage geocomposite. The problem will be repeated a third time in Chapter 9.

4.3 DESIGN CRITIQUE

The design examples just presented focused entirely on FS values based on either flow rate or transmissivity. This was done to reinforce the concept that in-plane drainage is the primary and unique function of geonets. In this regard, the geonet must be properly specified. At least three items are necessary to make a proper flow rate assessment: (1) flow rate (which is preferred to transmissivity), (2) the normal stress, and (3) the hydraulic gradient.

A few words about the normal stress are in order. To avoid rib lay-down and/or creep deformation, the compressive strength capability of the geonet must be higher than the design value. This value should be approximately 1.5 times (for short-service lifetimes) to 2 or more times (for long-service lifetimes in critical situations). Thus the structural stability of the geonet must be ensured against creep deformation and/or collapse (Narejo and Allen [18]). The actual flow rate value used for design purposes, however, can be taken from the curves at the design load at which the system will be operating.

When soil is adjacent to the geonet, the type of geotextile covering it is of great significance. While for most situations the geotextile is usually designed as a filter, it must also span the apertures of the geonet without excessively intruding or collapsing into the core space. There will always be some intrusion, and just how much is allowable depends on the site-specific situation. This can be evaluated experimentally, and values given in Table 4.2 reflect a series of such experiments. A possible method of minimizing intrusion could be the use of a high-modulus woven monofilament geotextile. For environmental-related facilities, however, this might not be appropriate. If hydrated clay or bentonite is above the geotextile and is under high pressure from the weight of the landfill above it, the clay will be extruded through the open spaces in the woven geotextile directly into the geonet openings. This is completely unacceptable. Thus, a nonwoven needle-punched geotextile with its labyrinth of overlapping fibers is necessary. However, some amount of intrusion must be anticipated and adequately

accounted for. A nonwoven heat-bonded geotextile might be a compromise geotextile with both high modulus (to prevent excessive intrusion) and high fiber overlapping (to prevent extrusion). Depending upon the actual stress level, a 200 g/m^2 geotextile should be the minimum mass per unit area. The major problem in using this type of geotextile appears to be thermal bonding the geotextile to the geonet. In general, geotextiles should be thermally bonded to geonets so as to avoid a potential shear plane. The bonding, however, should not be excessive since flow in the geonet can be compromised from excessive geonet melting during fabrication.

These same considerations must be expressed when a geosynthetic clay liner (GCL) is placed over a geonet. The lower geotextile of the GCL must be viewed in the same light as other geotextiles in this discussion. Depending upon the type of geotextile on the GCL facing the geonet, it is quite likely that an additional geotextile may be required between the GCL and the geonet.

4.4 CONSTRUCTION METHODS

Geonets are supplied in rolls from 2.0 to 6.7 m wide. They should be placed and covered in a timely manner. While UV and heat effects are not as severe in geonets as they are in geotextiles (because of thicker ribs in contrast to thin yarns and fibers), it is good practice not to leave the material exposed and subjected to accidental damage or contamination of any variety. Contamination can occur from soil, miscellaneous sediment, construction debris, ingrowing vegetation, and so on.

The rolls are usually placed with their roll directions oriented up-and-down slopes, rather than along (or parallel to) them. There are two reasons for this: First, the machine direction has the greatest strength (recall Figure 4.4) and flow rate; second, such orientation eliminates seams along the flow direction. If triplanar geonets are being used for their high flow in the machine direction, the proper orientation is critical during placement. For very long slopes or along the base of a facility, flow must continue unimpeded from one geonet to the next. When geotextiles are laminated to the geonet, the geotextiles must be stripped back from the overlapped area such that the upgradient geonet is directly on the downgradient geonet in shingled manner. There can be no geotextile sandwiched within this overlap area (see Daniel and Koerner [19]).

The seaming or joining of geonets is difficult. Assuming stress does not have to be transferred from one roll to the next, plastic electrical ties, threaded loops, and wires have all been used with a relatively small overlaps of 50 to 100 mm. Overall, there is room for improvement in this regard (see Zagorski and Wayne [20]). Metal hog rings should never be used when geonets are used adjacent to geomembranes. There are questions as to what influence overlapping has on the geonet's flow rate. The connection of geonets to perforated drainage pipes is difficult and extremely important. The geonet's outlet must be free draining at all times even in winter under freezing conditions. Details are available in manufacturers' literature (also see [19]).

Notwithstanding the above concerns, geonets are very impressive with respect to their flow rate capability, ease of construction, savings in airspace, and overall economy in many facilities where drainage must be accommodated. Some aspects of geonets will be revisited in Chapter 9 when we discuss additional geocomposite drainage materials.

REFERENCES

1. Austin, R. A., "The Manufacture of Geonets and Composite Products," *Proceedings of the GRI-8 on Geosynthetic Resins, Formulations and Manufacturing*. IFAI, 1995, pp. 127–138.

2. Williams N., Giroud, J.-P., and Bonaparte, R., "Properties of Plastic Nets for Liquid and Gas Drainage Associated with Geomembranes," *Proceedings of the International Conference on Geomembranes*. IFAI, 1984, pp. 399–404.

3. Corcoran, G. T., Cheng, S.-C.J. and Spear, A. D., "High Normal Stress Compression of Geosynthetic Lining Systems," *Proceedings of the 5th IGS Conference*. A. A. Balkema Publ., 1994, pp. 837–840.

4. Thornton, J. S., Allen, S. R., and Siebken, J. R., "Long-Term, Compressive Creep Behavior of High Density Polyethylene Geonets," *Proceedings of the 2nd European Geosynthetics Conference and Exhibition*, October 15–18, 2000, Bologna, Italy, pp. 869–874.

5. Lydick, L. D., and Zagorski, G. A., "Interface Friction of Geonets: A Literature Survey," *Journal of Geotextiles and Geomembranes*, vol. 10, nos. 5–6, 1991, pp. 167–176.

6. Kolbasuk, G. M., Lydick, L. D., and Reed, L. S., "Effects of Test Procedures on Geonet Transmissivity Results," *Journal of Geotextiles and Geomembranes*, vol. 11, nos. 4–6, 1992, pp. 153–166.

7. U.S. Environmental Protection Agency, EPA 40 CFR 260, 264, 265, 270 AND 271, *Federal Register*, vol. 57, no. 19, January 29, 1992, p. 3463.

8. Hwu, B.-L., Sprague, C. J., and Koerner, R. M., "Geotextile Intrusion into Geonets," *Proceedings of the 4th International Conference on Geotextiles and Geomembranes, and Related Products*. Rotterdam: A. A. Balkema, 1990, pp. 351–356.

9. Eith, A. W., and Koerner, R. M., "Field Evaluation of Geonet Flow Rate (Transmissivity) Under Increasing Load," *Journal of Geotextiles and Geomembranes*, vol. 11, nos. 5–6, 1992, pp. 153–166.

10. Koerner, G. R., Koerner, R. M., and Martin, J. P., "Geotextile Filters Used for Leachate Collection Systems: Testing, Design of Field Behavior," *Journal of Geotechnical Engineering Division*, vol. 120, no. 10, 1994, pp. 1792–1803.

11. Bonaparte, R., Williams, N., and Giroud, J-P, "Innovative Leachate Collection Systems for Hazardous Waste Containment Systems," *Proceedings of the Geotechnical Fabrics Conference '85*. IFAI, 1985, pp. 10–34.

12. Lundell, C. M., and Menoff, S. D., "The Use of Geosynthetics as Drainage Media at Solid Waste Landfills," *Proceedings of Geosynthetics '89*. IFAI. 1989, pp. 10–17.

13. Koerner, R. M., and Soong, T.-Y., "Analysis and Design of Veneer Cover Soils," *Proceedings of the 6th International Geosynthetic Society Conference*, IFAI., March 25–29, 1998, 1–26.

14. Qian X, Koerner R.M. and Gray V.H., *Geotechnical Aspects of Landfill Design and Construction*, Prentice Hall, Upper Saddle River, NJ, 2002, 717 pgs.

15. Matrecon, Inc., *Lining of Waste Containment and Other Impoundment Facilities*, 600/2-88/052, U. S: EPA, Cincinnati, OH: Risk Reduction Engineering Laboratory, September 1988.

16. Koerner, R. M., and Daniel, D. E., *Final Covers for Solid Waste Landfills and Abandoned Dumps*. ASCE Press, 1997.

17. Schroeder, P. R., Dizier, T. S., Zappi, P. A., McEnroe, B. M., Sjostrom, J. W., and Peyton, R. L., *The Hydrologic Evaluation of Landfill Performance (HELP) Model: Engineering Documentation for Version 3*, EPA/600/R-94/168b, U. S. E.P.A., Cincinnati, OH: Risk Reduction Engineering Laboratory, 1994.

18. Narejo, D., and Allen, S., "Using the Stepped Isothermal Method for Geonet Creep Evaluation," *Proceedings of EuroGeo3*, Munich, Germany, 2004, pp. 539–544.

19. Daniel, D.E. and Koerner R.M., *Waste Containment Facilities; Guidance for CQA and CQC of Liner and Cover Systems*, ASCE Press, 2nd Ed, 2005, 275 pgs.

20. Zagorski, G. A., and Wayne, M. H., "Geonet Seams," *Journal of Geotextiles and Geomembranes*, vol. 9, nos. 4–6, 1990, pp. 207–220.

PROBLEMS

4.1. Geonets are used specifically for their in-plane drainage capability. Give the reasons they are not used for the following:
(a) Separation
(b) Reinforcement
(c) Filtration
(d) Containment (moisture barrier)

4.2. When using geonets for drainage functions, what keeps the adjacent soil from getting in their apertures and blocking flow?

4.3. If a geotextile is placed adjacent to a geonet, what function(s) does the geotextile provide? How does the combination of geotextile and geonet accommodate flow?

4.4. All of the geonets described in this chapter are made of polyethylene. Could they be made from other polymers? Why do you suppose they are made from polyethylene?

4.5. It is noted in this chapter that the aperture size varies from product to product. What effect does aperture size have on flow and intrusion?

4.6. In the typical extruded biplanar geonets, the vertical axes of the intersecting ribs are not quite perpendicular to one another. What implications does this have for the compressive load-carrying capacity of the geonet?

4.7. For the foamed extruded geonets shown in Figure 4.2, answer the following questions:
(a) What are the foamed pores within the ribs filled with?
(b) What are the long-term implications of this?
(c) How would Fick's law (of diffusion) enter into this discussion?

4.8. For triplanar geonets, the flow rate is significantly higher than for biplanar geonets.
(a) Where in a typical landfill configuration can these geonets best be used?
(b) Why is knowledge of the slope direction critical to know?
(c) Why is the flow in the cross-machine direction not particularly important?

4.9. The shear strength between a geotextile and a geonet can be quite low and troublesome when used in side-slope design. Describe two methods by which the geotextile can be attached to the geonet to avoid the potential problem. Include the advantages and disadvantages of each method.

4.10. The flow-rate reductions between Figures 4.7 and 4.8 as tabulated in Table 4.1 are up to 40% for 500 kPa normal stress. Beyond this stress level the reductions are lower. Why are they lower at the higher stress levels?

4.11. Regarding the placement and use of a compacted clay liner over a geotextile bonded onto a geonet:
(a) What are the implications of using a lighter-weight geotextile for the results shown in Figure 4.8?
(b) What would happen if a woven monofilament geotextile of $\geq 6\%$ open area were used?
(c) What would happen if a nonwoven heat bonded geotextile were used?

4.12. Discuss the difference between extrusion and intrusion for a geotextile covering a geonet that has a clay liner placed above it.

4.13. The ultimate flow rate of a geonet being considered for the primary leachate collection system on a landfill side slope is 7.3×10^{-4} m²/s. Using the maximum values in Table 4.2, what is the allowable flow rate?

4.14. Using a geonet beneath an artificial surface in a tennis court requires an allowable flow rate of 1.6×10^{-4} m^2/s. What would be the necessary ultimate flow rate using the average values from Table 4.2?

4.15. Recalculate Example 4.5 (Section 4.2.2) concerning secondary leachate collection systems for design flows from 1 to 4000 times *de minimis*. Plot the resulting factors of safety against required flow rate.

4.16. A geonet is being considered for primary leachate collection on the 40 m long side slopes of a landfill. Using the data of Figure 4.8, interpolating at a normal stress of 700 kPa and a hydraulic gradient of 0.184, what is the factor of safety for a flow rate of 25,000 1/ha-day? The cumulative reduction factors should be 8.0. (Note that this leachate flow rate is typical of primary leachate flow rates in the state of New York.)

4.17. Recalculate Example 4.6 (Section 4.2.2) concerning a geonet in a landfill cover, where the required flow rate varies from 1×10^{-3} to 1×10^{-5} m^2/s. Plot the resulting factors of safety against slope angle.

4.18. What are the long-term normal stress implications for a geonet's flow-rate capability?

4.19. What are the long-term implications for a geonet's flow-rate capability in landfill liner design if the FS < 1.0?

5

Designing with Geomembranes

5.0 INTRODUCTION

According to ASTM D4439, a geomembrane is defined as follows:

> *Geomembrane*: A very low permeability synthetic membrane liner or barrier used with any geotechnical engineering related material so as to control fluid (or gas) migration in a human-made project, structure, or system.

Geomembranes are made from relatively thin continuous polymeric sheets, but they can also be made from the impregnation of geotextiles with asphalt or elastomer sprays or as multilayered bitumen geocomposites. In this chapter, we will focus on continuous polymeric sheet geomembranes. Impregnated geotextiles are covered in various parts of Chapter 2, and bituminous geomembranes are covered in Chapter 9.

Polymeric geomembranes are not absolutely impermeable (actually nothing is), but they are relatively impermeable when compared to geotextiles or soils, even to clay soils. Typical values of geomembrane permeability as measured by water-vapor transmission tests are in the range 1×10^{-12} to 1×10^{-15} m/s, which is three to six orders of magnitude lower than the typical clay liner. Thus the primary function is always as containment of, or barrier to, liquids or vapors. As noted in Section 1.6.3, the current market for geomembranes is extremely strong. New applications are regularly being developed, and this is directly reflected in sales volume; geomembranes are currently the largest segment of geosynthetics as far as product sales are concerned.

Since the primary function of geomembranes is always containment, as a barrier to a liquid and/or gas, this chapter is organized on the basis of different application areas. Liquid containment is treated first, and then solid waste containment, followed by numerous geotechnical applications.

As a counterpoint for the design calculations to follow, however, the next section describes geomembrane properties and the test methods used to obtain these properties. This information allows the design of the major geomembrane-related systems that are currently in use. The specific designs then form the subsequent parts of the chapter.

5.1   GEOMEMBRANE PROPERTIES AND TEST METHODS

To design-by-function (the theme of this book) is to make a conscious decision about the adequacy of the ratio of the allowable property of a geomembrane to the required property—that is, the factor of safety value. This section on properties is devoted to providing the test methods for the numerator of this ratio. The required, or design, value will come later.

5.1.1 Overview

The vast majority of geomembranes are relatively thin sheets of flexible thermoplastic polymeric materials (recall Figure 1.1). These sheets are manufactured in a factory and shipped to the job site, where placement and field seaming are performed to complete the job. Table 5.1 lists the materials in this category, the principal ones currently in use; these are the geomembranes that will be focused upon here. Section 1.2 gives an overview of the various polymers listed and describes a number of chemical identification or fingerprinting tests used to quantify their composition and formulation. Hybrid systems, many of which are made on-site by in situ methods, are quite different in their properties. For example, bitumen-impregnated geotextiles possess the fundamental properties of the base geotextile with the obvious exception of their modified hydraulic properties. In fact, impregnating a geotextile with bitumen essentially renders it impermeable, as does impregnating it with by bitumen/rubber or elastomeric materials (recall Sections 2.6.2 and 2.10.2). These modifications are each unique to the individual process, and consequently the performance properties of the resulting product must be individually assessed. Some of the tests to be described here do carry over (e.g., water-vapor transmission) to hybrid systems, but our concentration will be on continuous sheets of polymeric geomembranes.

TABLE 5.1   GEOMEMBRANES IN CURRENT USE

Most Widely Used

- High density polyethylene (HDPE)
- Linear low density polyethylene (LLDPE)
- Polyvinyl chloride (PVC)

Somewhat Less Widely Used

- Flexible polypropylene: nonreinforced (fPP) and reinforced (fPP-R)
- Chlorosulfonated polyethylene: reinforced (CSPE-R)
- Ethylene propylene diene terpolymer: nonreinforced (EPDM) and reinforced (EPDM-R)
- Ethylene interpolymer alloy: reinforced (EIA-R)

Many geomembrane test methods and standards are available or are being developed by standards-setting organizations around the world. Where appropriate, the ASTM and ISO standards will be referenced. The individual test methods will be grouped into three categories: (1) physical properties, (2) mechanical properties, and (3) endurance properties.

5.1.2 Physical Properties

Physical properties have to do with the geomembrane in an as-manufactured and/or as-received state. They are important for quality control, quality assurance, and proper identification.

Thickness.   Depending on the type of geomembrane, there are three types of thickness to be considered: (1) the thickness of smooth sheet, (2) the core thickness of textured sheet, and (3) the thickness (or height) of the asperities of textured sheet.

Smooth Sheet.   The determination of the thickness of a smooth geomembrane is performed by a straightforward measurement. The test uses an enlarged-area micrometer under a specified pressure, resulting in the desired value. ASTM D5199 and ISO 09863 are the test methods generally used for measuring geomembrane thickness. The pressure exerted by the micrometer is specified at 20 kPa. A number of measurements are taken across the roll width and an average value is obtained. When measuring the thickness of a smooth geomembrane, there is little ambiguity in the procedure. Nonreinforced geomembranes are made in thicknesses from 0.5 to 3 mm. When measuring materials with scrim reinforcement or aged membranes that have swelled, extreme care must be exercised, particularly in the preparation of the test specimen and in the application of pressure. Test conditions and applied pressures should always be given together with the actual values. Scrim-reinforced geomembranes are manufactured from multiple plies of materials which when laminated together result in geomembranes of thickness from 0.91 to 1.5 mm (recall Figure 1.25).

Textured Sheet.   The roughened surface of a textured geomembrane results in a significant increase in interface friction with adjacent materials versus the same geomembrane with a smooth surface. The thickness of such textured sheets is measured as the minimum core thickness between the roughened peaks or *asperities*. To measure the core thickness, a tapered-point micrometer for measuring machine screw threads is recommended. The tapered point-dimensions per ASTM D5994 are a 60° angle with the extreme tip at 0.08 mm diameter. The normal load on the tapered point is 0.56 N. For single-sided textured sheet, only one tapered point is needed, while double-sided textured sheet requires a micrometer with two opposing tapered tips. Within a limited area, the local minimum core thickness is obtained. Typically, 10 measurements across the roll width are taken and an average core thickness value is calculated and compared with the specification value.

Asperity Height.   For textured geomembranes, the roughness pattern is of interest insofar as it relates to mobilizing the maximum amount of interface shear strength with the opposing surface. Optimized texturing is a daunting task and a topic of interest

to both the manufacturing and user communities. Profilometry has been attempted (Dove and Frost [1]), as has an effort extended toward the use of fractals (Vallejo and Zhou [2]). Less involved, but still useful as a quality control and quality assurance method, is to merely measure the height of the asperities. To do so, a depth gauge micrometer with a 1.3 mm diameter pointed stylus is recommended. The gage is zeroed on a flat surface and then is placed on the peaks of the textured sheet with the stylus falling into the valley created by the texturing. The localized maximum depth is the asperity height. A number of measurements are taken across the roll width and an average asperity height is obtained and compared with the specification value.

Density.   The density or specific gravity of a geomembrane is dependent on the base material from which it is made. There are distinct differences, however, even in the same generic polymer. For example, polyethylene comes in several varieties: very low-density, low-density, linear low-density, medium-density, and high-density. The range for all geomembrane polymers falls within the general limits of 0.85 to 1.5 mg/l. The relevant test methods are ASTM D792 and ISO R1183. This test method is based on Archimedes' fundamental principle of specific gravity as the weight of the object in air divided by its weight in water.

A more accurate method is found in ASTM D1505, "Density Determination by the Density Column." Here a long glass column containing liquid varying from relatively high density at the bottom to low density at the top is used. For example, isopropanol with water is often used for measuring densities less than 1.0, while sodium bromide with water is used for densities greater than 1.0. Upon setup, spheres of known density are immersed in the column to generate a calibration curve. Small pieces of the polymer test specimen are then dropped into the column. Their equilibrium level within the column is used with the calibration curve to find the specimen's density. Accuracy is very good, within 0.002 mg/l when proper care is taken.

A comment on the density of HDPE geomembranes should be made. The ASTM classification for HDPE resin requires a density ≥ 0.941 mg/l. However, commercially available HDPE geomembranes use polyethylene resin from 0.934 to 0.938 mg/l; the resin itself is actually in the medium density range (MDPE). Only by adding carbon black and additives to the mixture is its formulated density raised to 0.941 mg/l or slightly higher. Thus what is called HDPE by the geomembrane industry is actually MDPE resin to the resin producer.

Melt (Flow) Index.   The melt-flow index or melt index (MI) test is used routinely by geomembrane manufacturers as a method of controlling polymer uniformity and processability. It relates to the flowability of the polymer in its molten state. It is used for both the incoming resin and the final formulated geomembrane sheet. The test method often used for geomembrane polymers is ASTM D1238. Here a given amount of the polymer is heated in a furnace until it melts. A constant weight forces the fluid mass through an orifice and out of the bottom of the test device. The MI value is the weight of extruded material in grams for a 10 min flow duration. The higher the value of melt-flow index, the lower the density of the polymer, all other things being equal. High MI values suggest a lower molecular weight, and vice versa, albeit by a relatively crude method in comparison with some of the techniques discussed in Section 1.2.2.

The test is also performed using two different weights forcing the molten polymer out of the orifice; for example, the standard test is performed at 2.16 kg, and then repeated at 5.0 kg. The resulting MI values are then made into the following ratio:

$$FRR = MI_{5.0}/MI_{2.16} \tag{5.1}$$

where

FRR   = flow rate ratio,

$MI_{5.0}$ = melt flow index under 5.0 kg weight, and

$MI_{2.16}$ = melt flow index under 2.16 kg weight.

High values of FRR indicate broad molecular weight distributions and various empirical relationships have been proposed.

Both MI and FRR tests are very important in the quality control and quality assurance of polyethylene resins and geomembranes.

Mass per Unit Area (Weight).   The weight of a geomembrane (actually its *mass per unit area* but invariably called simply *weight)* can be determined using a carefully measured area of a representative specimen and accurately measuring its mass. It is measured in units of g/m^2. The test is straightforward to perform and usually follows ASTM D1910 procedures.

Water-Vapor Transmission.   Since nothing is absolutely impermeable, the assessment of the relative impermeability of geomembranes is an often discussed issue. The discussion is placed along with physical properties for want of a better location. The test itself could use an adapted form of a geotechnical engineering test using water as the permeant; however, this would be impractical. In such a case, the hydraulic heads required are so great that leaks or failed specimens invariably result. At lower heads, long test times leading to evaporation problems become a major obstacle. Instead, a completely different approach is taken whereby water *vapor* is used as the permeant and diffusion is the fundamental mechanism of permeation. In the water-vapor transmission (WVT) test, a test specimen is sealed over an aluminum cup with either water or a desiccant in it and a controlled relative humidity difference across the geomembrane boundary is maintained. The ASTM test method is covered under E96. With water in the cup (i.e., 100% relative humidity) and a lower relative humidity outside of it, a weight loss over time can be monitored (see Figure 5.1). With a desiccant in the cup (i.e., 0% relative humidity) and a higher relative humidity outside of it, a weight gain over time can be seen and appropriately monitored. The required test time varies, but it is usually from 3 to 40 days. Water vapor transmission, permeance, and (diffusion) permeability are then calculated, as shown in Example 5.1.

Example 5.1

Calculate the WVT, permeance, and (diffusion) permeability of a 0.75 mm thick PVC geomembrane of area 0.003 m^2, which produced the test data in Figure 5.1 at an 80% relative-humidity difference while being maintained at a temperature of 30°C.
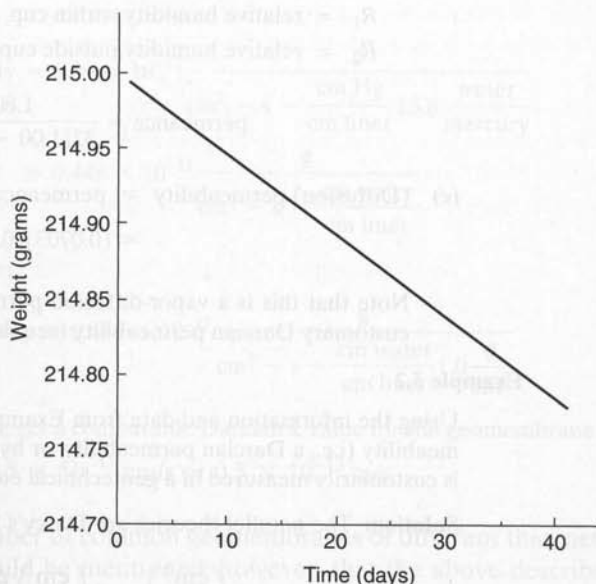
Figure 5.1   A water-vapor transmission test setup and resulting data for a 0.75 mm thick PVC geomembrane.

Solution: Calculations proceed in stages using the slope of the curve in Figure 5.1.

(a) Find the water-vapor transmission;

$$\text{WVT} = \frac{g \times 24}{t \times a} \tag{5.2}$$

where

> g = weight change (g),
> t = time interval (h), and
> a = area of specimen (m^2).

$$\text{WVT} = \frac{(0.216)(24)}{(40)(24)(0.003)} = 1.80 \text{ g/m}^2 - \text{day}$$

(b) The permeance is given as

$$\text{permeance} = \frac{\text{WVT}}{\Delta P} = \frac{\text{WVT}}{S(R_1 - R_2)}$$

where

> ΔP = vapor pressure difference across membrane (mmHg),
> S = saturation vapor pressure at test temperature (mmHg),

R_1 = relative humidity within cup, and

R_2 = relative humidity outside cup (in environmental chamber).

$$\text{permeance} = \frac{1.80}{32(1.00 - 0.20)} = 0.0703 \text{ metric perm}$$

(c) (Diffusion) permeability = permeance $\times$ thickness

$$= (0.0703)(0.75) = 0.0527 \text{ metric perm-mm}$$

Note that this is a vapor-diffusion permeability following Fickian diffusion, *not* the customary Darcian permeability (see the following example).

Example 5.2

Using the information and data from Example 5.1, calculate an equivalent hydraulic permeability (i.e., a Darcian permeability, or hydraulic conductivity) of the geomembrane as is customarily measured in a geotechnical engineering test on clay soils.

Solution: The parallel theories are Darcy's formula for hydraulic permeability, $q = kiA$,

$$q\left(\frac{\text{cm}^3}{\text{s}}\right) = k\left(\frac{\text{cm}}{\text{s}}\right)\frac{\Delta h}{\Delta l}\left(\frac{\text{cm H}_2\text{O}}{\text{cm soil}}\right)A(\text{cm}^2)$$

and the WVT test for Fickian diffusion permeability,

$$\text{flow}\left(\frac{\text{cm}^3}{\text{s}}\right) = k\left(\frac{\text{cm}^3}{\text{cm}^2 - \text{s} - \text{cm H}_2\text{O/cm liner}}\right)\text{pressure}\left(\frac{\text{cm H}_2\text{O}}{\text{cm liner}}\right)A(\text{cm}^2)$$

Thus we must now modify the data used in Example 5.1 into the proper units:

$$\text{WVT} = 1.80\frac{\text{g}}{\text{m}^2 - \text{day}}\frac{1}{(10^4)(24)(60)(60)}$$

$$= 2.08 \times 10^{-9}\frac{\text{g}}{\text{cm}^2 - \text{s}}$$

$$\text{permeance} = \frac{\text{WVT}}{\Delta P} = \frac{\text{WVT}}{S(R_1 - R_2)}$$

$$= \frac{2.08 \times 10^{-9}}{(32)(1.00 - 0.20)}$$

$$= 0.812 \times 10^{-10}\frac{\text{g}}{\text{cm}^2 - \text{s} - \text{mm Hg}}$$

$$\text{permeability} = \text{permeance} \times \text{liner thickness}$$

$$= 0.812 \times 10^{-10}(0.075)$$

$$= 0.609 \times 10^{-11}\frac{\text{g}}{\text{cm}^2 - \text{s} - \text{mm Hg/cm liner}}$$

$$= 6.09 \times 10^{-11}\frac{\text{g}}{\text{cm}^2 - \text{s} - \text{cm Hg/cm liner}}$$

In terms of water pressure,

$$\text{hydraulic conductivity} = 6.09 \times 10^{-11} \frac{\text{g}}{\text{cm}^2 - \text{s} - \frac{\text{cm Hg}}{\text{cm liner}} 13.6 \frac{\text{water}}{\text{mercury}}}$$

$$= 0.448 \times 10^{-11} \frac{\text{g}}{\text{cm}^2 - \text{s} - \frac{\text{cm water}}{\text{cm liner}}}$$

Now using the density of water,

$$\text{hydraulic conductivity} = 0.448 \times 10^{-11} \frac{\text{g}}{\text{cm}^2 - \text{s} - \frac{\text{cm water}}{\text{cm liner}} 1.0 \frac{\text{g}}{\text{cm}^3}}$$

and canceling the units out, we get a comparable Darcian k value for the geomembrane of

$$k \cong 0.5 \times 10^{-11} \text{ cm/s or } 0.5 \times 10^{-13} \text{ m/s}$$

The WVT values for a number of common geomembranes of different thicknesses are given in Table 5.2. It should be mentioned, however, that the above-described test method is extremely difficult to conduct for thick geomembranes and particularly for HDPE since its WVT values are so low. The least amount of leakage around the test specimen-to-container seal will greatly distort the resulting test results. As such the test is not recommended for general use and an entirely different configuration may be necessary, although the concept and theory will be the same.

Of particular interest is the conversion of 1.0 g/m²-day, approximately equal to 10 1/ha-day, which is the leakage sometimes associated with a flawlessly placed geomembrane. It has been referred to in various regulations as *de minimis* leakage (see footnote in Section 4.2.2). Note that if such a low value is used, it automatically eliminates some geomembrane materials, even without a single leak! It also suggests that

TABLE 5.2   WATER-VAPOR TRANSMISSION (WVT) VALUES

Geomembrane Polymer	Thickness (mm)	WVT	
		(g/m²-day)*	(perm-cm)
PVC	0.28	4.4	1.2×10^{-2}
	0.52	2.9	1.4×10^{-2}
	0.75	1.8	1.3×10^{-2}
CSPE-R	0.89	0.44	0.84×10^{-2}
EPDM-R	0.51	0.27	0.13×10^{-2}
	1.23	0.31	0.37×10^{-2}
HDPE	0.80	0.017	0.013×10^{-2}
	2.44	0.006	0.014×10^{-2}

*1.0 g/m²-day = 10.0 1/ha-day
Source: After Haxo et al. [3].

materials with extremely low WVT values are the best for all liquid containments. But, as we will see in the next section, this is not necessarily the case.

Solvent-Vapor Transmission.   When containing liquids other than water, the concept of *permselectivity* must be considered. Here the molecular size and attraction of the liquid vis-a-vis the polymeric liner material might result in vapor diffusion values that are very different than those found when using water. Organic solvents are in this category.

The test itself is a parallel to E96, the water vapor transmission test, except now the solvent of interest is placed within the cup. Obviously, care and proper laboratory procedures must be exercised when using hazardous or sometimes radioactive materials. As with the WVT test, proper sealing to prevent leakage is extremely difficult to achieve. However, some solvent-vapor transmission data are available and are reproduced in Table 5.3. Notice the tremendous range compared with the values given in Table 5.2 for water-vapor transmission. Clearly, if solvents are to be contained by a geomembrane, the site-specific solvent-vapor transmission test should be used to assess the geomembrane's containment capability in this regard.

The area of solvent vapor transmission has been extended by Rowe et al. [5] who used synthesized leachates to measure diffusion through different thicknesses of HDPE geomembranes. A number of organic compounds are evaluated to obtain their diffusion coefficients. It is shown that the geomembrane provides an excellent barrier to acetic acid and chloride. Conversely, organic compounds (such as dichloromethane, 1,1-dichloroethane, 1,2-dichloroethane, and 2-butanone [MEK]) can diffuse much

TABLE 5.3   SOLVENT-VAPOR TRANSMISSION (SVT) VALUES

		Geomembrane Polymer Type (Thickness)			
Property	Solvent	HDPE (0.80 mm)	HDPE (2.6 mm)	LDPE (0.75 mm)	CSPE-R (1.10 mm)
Solvent-vapor	Acetone	0.56	—	2.83	221
transmission	Methyl alcohol	0.16	—	0.74	—
(g/m²-day)	Cyclohexane	11.7	—	161	—
	Xylene	21.6	6.86	116	—
	Chloroform	54.8	15.8	570	—
Solvent-vapor	Acetone	0.26	—	1.33	104
permeance, (10^{-2}	Methyl alcohol	0.14	—	0.66	—
metric perms)	Cyclohexane	13.1	—	181	—
(SVT/mm Hg)	Xylene	308	97.9	1650	—
	Chloroform	30.8	8.88	320	—
Solvent-vapor	Methyl alcohol	0.01	—	0.05	—
permeability, (10^{-2}	Acetone	0.02	—	0.10	11.4
metric perms-cm)	Cyclohexane	1.05	—	13.6	—
	Xylene	24.6	25.6	124	—
	Chloroform	2.46	2.32	24.0	—

Source: Matrecon, Inc [4].

more rapidly. Several preventative options in this regard are available: using relatively thick geomembranes; treating the geomembrane's surface, by fluorination [6] or other strategies; including a back up of the geomembrane with a clay liner (CCL or GCL) for attenuation, thereby creating a composite liner; or using double-liner systems with an intermediate drainage layer. Note that diffusion tests of this type have the liquids stationary on the geomembrane, while in a typical landfill the sloped surface creates movement of the liquids to a sump area where they are removed.

5.1.3 Mechanical Properties

There are a number of mechanical tests that have been developed to determine the strength of polymeric sheet materials. Many have been adopted for use in evaluating geomembranes. This section attempts to sort out those having applicability to quality control or to design, i.e., index versus performance tests.

Tensile Behavior (Index).   Many tensile tests performed on geomembrane specimens are quite small in size and are used routinely for quality control and quality assurance (conformance) of the manufactured geomembranes. The test procedures generally used are covered in ASTM D6693 or ISO 527-3 as well as ASTM D6392, D882, D751, and D413. Table 5.4 gives the currently recommended tests for commonly used geomembranes.

The results for several of these geomembranes are given in Figure 5.2. The scrim-reinforced geomembrane CSPE-R resulted in the highest strength but failed abruptly when the fabric scrim broke. The response, however, did not drop to zero because the geomembrane plies on both sides of the scrim remained intact until ultimate failure occurred. This is typical of all fabric-reinforced geomembranes. The HDPE geomembrane responded in a characteristic fashion by showing a pronounced yield point, at 10 to 15% strain, dropping slightly, and then extending in strain to approximately 1000% when failure actually occurred. The PVC geomembrane gave a relatively smooth response, gradually increasing in strength until its failure at about 480% strain. The LLDPE geomembrane also gave a relatively smooth, but lower, response until it failed at approximately 700% strain.

The curves were generated using the specimen's original width and thickness to calculate stress and the original gage length to calculate strain. Thus the axes are engineering stress and strain, rather than true stress and strain. Quantitative data gained from these curves are focused around the following:

- Maximum stress (at ultimate for PVC and LLDPE, at scrim break for CSPE-R, and at yield for HDPE)
- Maximum strain (usually called *elongation* in the geomembrane literature)
- Modulus (the slope of the initial portion of the stress-strain curve)
- Ultimate stress at failure (or *strength*)
- Ultimate strain (or elongation) at complete failure

TABLE 5.4 RECOMMENDED TEST METHOD DETAILS FOR GEOMEMBRANES AND GEOMEMBRANE SEAMS IN SHEAR AND IN PEEL

Test and Selected Details	HDPE	LLDPE; fPP	PVC	fPP-R; EPDM-R; CSPE-R; EIA-R
Tensile Test on Sheet				
ASTM test method	D6693	D6693	D882	D751
Specimen shape	Dumbbell	Dumbbell	Strip	Grab
Specimen width (mm)	6.3	6.3	25	100 (25 grab)
Specimen length (mm)	115	115	150	150
Gauge length (mm)	33	33	50	75
Strain rate (mm/min)	50	500	500	300
Strength	Force/$(w \times t)$	Force/$(w \times t)$	Force/$(w \times t)$	Force
Strain (mm/mm)	Elong/33	Elong/33	Elong/50	Elong/75
Modulus	From graph	From graph	From graph	n/a
Shear Test on Seams				
ASTM test method	D6392	D6392	D882	D751
Specimen shape	Strip	Strip	Strip	Grab
Specimen width (mm)	25	25	25	100 (25 grab)
Specimen length (mm)	150 + seam	150 + seam	150 + seam	225 + seam
Gauge length (mm)	100 + seam	100 + seam	100 + seam	150 + seam
Strain rate (mm/min)	50	500	500	300
Strength	Force/$(w \times t)$	Force/$(w \times t)$	Force/$(w \times t)$	Force
Peel Test on Seams				
ASTM test method	D6392	D6392	D882	D413
Specimen shape	Strip	Strip	Strip	Strip
Specimen width (mm)	25	25	25	25
Specimen length (mm)	100	100	100	100
Gauge length (mm)	n/a	n/a	n/a	n/a
Strain rate (mm/min)	50	500	50	50
Strength	Force/$(w \times t)$	Force/$(w \times t)$	Force/w	Force/w

Abbreviations: n/a = not applicable
                 w = specimen width (mm)
                 t = specimen thickness (mm)
                 Force = maximum force attained at specimen failure (ultimate or break)

Table 5.5(a) gives these values for the four materials shown in Figure 5.2. While all of the listed values of strength are significant, attention is often focused on the maximum stress. It must be recognized, however, that polymers are viscoelastic materials and strain invariably plays an important role.

Tensile Behavior (Wide-Width). A major criticism of the previously described index test specimens is their contraction within the central region, giving a one-dimensional behavior not experienced with wide sheets in field situations. Thus uniform width and wider test specimens are desirable. Just how wide is a matter of debate. A width of 200 mm has been used for testing geotextiles and has been adopted for testing geomembranes; see ASTM D4885. The strain rate for testing geomembranes is,
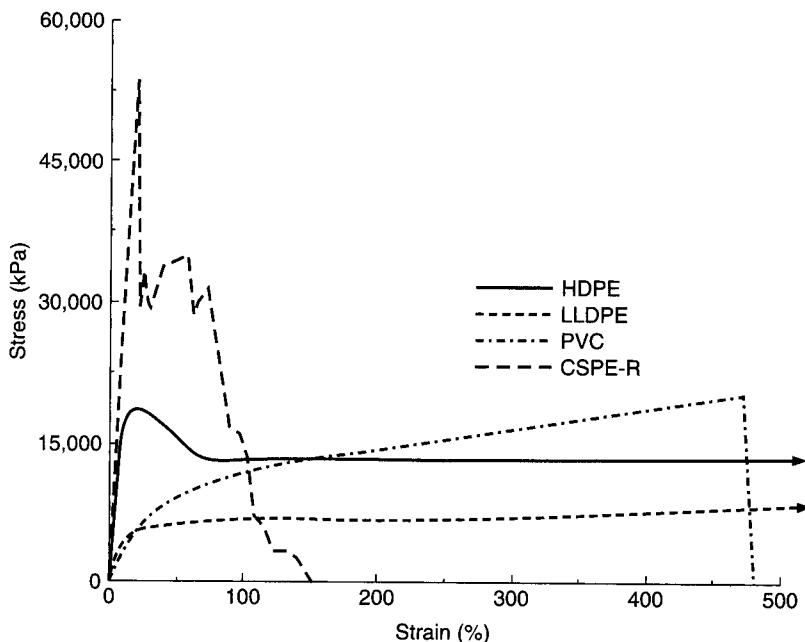
Figure 5.2   Index tensile test results of common geomembranes using criteria given in Table 5.4.

however, different from geotextiles. D4885 recommends using 1.0 mm/min. For a 100 mm long specimen with 200% strain at failure, the test would require 3.3 hours to complete. For a geomembrane with 1000% strain at failure, the test would require 16.7 hours. Clearly such tests are not of the index or quality-control variety and should be considered to be performance-oriented.

Figure 5.3 presents tensile stress-versus-strain curves on the same four geomembranes that are shown in Figure 5.2, but now for a uniform 200 mm width. While the general shape of each material is the same, the results of the various properties of interest are quite different. These results are tabulated in Table 5.5(b). It is felt that the use of a 200 mm width test specimen results in a much more design-oriented value than do test results from dumbbell or narrow-width specimens. This is particularly the case when plane-strain conditions are assumed in the design process (e.g., in side-slope stability calculations).

Tensile Behavior (Axi-Symmetric).   There are situations that call for a geomembrane's tensile behavior when it is mobilized by out-of-plane stresses. Localized deformation beneath a geomembrane is such a case. This type of behavior could well be anticipated for a geomembrane used in a landfill cover placed over differentially subsiding solid-waste material. The situation can be modeled by placing the geomembrane in a large empty container, as shown in Figure 5.4. An appropriate seal is made with the cover section and water or air is introduced above the geomembrane. Pressure is mobilized until the failure of the test specimen occurs. Beginning with

TABLE 5.5   TENSILE BEHAVIOR PROPERTIES OF VARIOUS GEOMEMBRANES

(a) Index Test Results (Figure 5.2)

Test Property	Units	HDPE	LLDPE	PVC	CSPE-R
Maximum stress	kPa	18,600	8,300	21,000	54,500
and corresponding strain	%	17	500[+]	480	19
Modulus	MPa	330	76	31	330
Ultimate stress	kPa	13,800	8,300	20,700	5,700
and corresponding strain	%	500[+]	500[+]	480	110

Nominal thicknesses are HDPE 1.5 mm, LLDPE 1.0 mm, PVC 0.75 mm, CSPE-R 0.91 mm.
Abbreviations: [+] = did not fail

(b) Wide Width Test Results (Figure 5.3)

Test Property	Units	HDPE	LLDPE	PVC	CSPE-R
Maximum stress	kPa	15,900	7,600	13,800	31,000
and corresponding strain	%	15	400[+]	210	23
Modulus	MPa	450	69	20	300
Ultimate stress	kPa	11,000	7,600	13,800	2,800
and corresponding strain	%	400[+]	400[+]	210	79

Nominal thicknesses are HDPE 1.5 mm, LLDPE 1.0 mm, PVC 0.75 mm, CSPE-R 0.91 mm.
Abbreviations: [+] = did not fail

(c) Axi-Symmetric Test Results (Figure 5.5)

Test Property	Units	HDPE	LLDPE	PVC	CSPE-R
Maximum stress	kPa	23,500	10,300	14,500	31,000
and corresponding strain	%	12	75	100	13
Modulus	MPa	720[−]	170[−]	100[−]	350[−]
Ultimate stress	kPa	23,500	10,300	14,500	31,000
and corresponding strain	%	25	75	100	13

Nominal thicknesses are HDPE 1.5 mm, LLDPE 1.0 mm, PVC 0.75 mm, CSPE-R 0.91 mm.
Abbreviations: [−] = values felt to be high

Steffen [7], a number of variations of this test have been made. It is currently formalized as ASTM D5716.

    The data generated by the test are pressure versus centerpoint deflection that can be plotted and used directly. To obtain stress-versus-strain (which is more desirable), certain assumptions must be made. The original analysis by Koerner et al. [8] has been modified by Merry and Bray [9]. Both are based on the assumption that the deflected shape is being deformed as a portion of a sphere with gradually moving center point along the centerline axis. The latter approach is preferred, however, since it is based on a constant geomembrane volume hypothesis. The resulting equations for stress and strain are as follows [9]:

$$\sigma = \frac{(L^2 + 4\delta^2)^2 p}{16(\delta)(L)^2(t)} \qquad \text{for all } \delta - \text{values} \qquad (5.3)$$
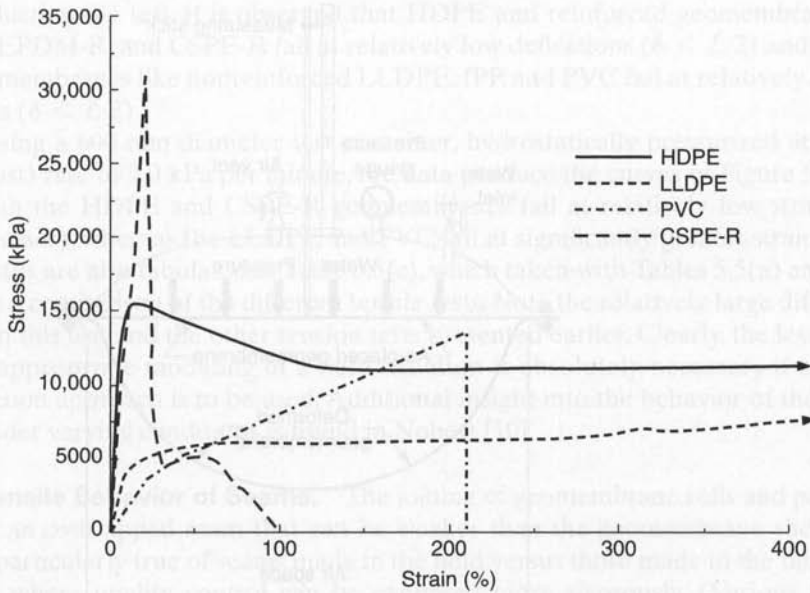
Figure 5.3 Tensile test results on 200 mm wide-width specimens of common geomembranes using ASTM D4885 test method.

and (for $\tan^{-1}$ in radians)

$$\epsilon(\%) = \left\{ \frac{\tan^{-1}\left[\left(\dfrac{4L\delta}{L^2 - 4\delta^2}\right)\right]\left(\dfrac{L^2 + 4\delta^2}{4\delta}\right) - L}{L} \right\} \times 100 \quad \text{for } \delta < L/2 \qquad (5.4)$$

$$\epsilon(\%) = \left\{ \frac{\left[\dfrac{L^2 + 4\delta^2}{4\delta}\right]\left[\pi - \sin^{-1}\left(\dfrac{4L\delta}{L^2 + 4\delta^2}\right)\right] - L}{L} \right\} \times 100 \quad \text{for } \delta \geq L/2 \qquad (5.5)$$

where

L = diameter of test specimen—that is, the container (mm)

δ = centerpoint deflection (mm)

p = pressure on test specimen (kPa)

t = original thickness of geomembrane (mm)

σ = geomembrane tensile strength (kPa)

ϵ = geomembrane tensile strain (%)
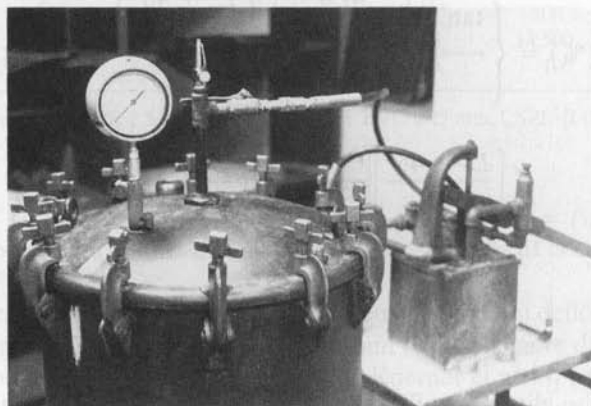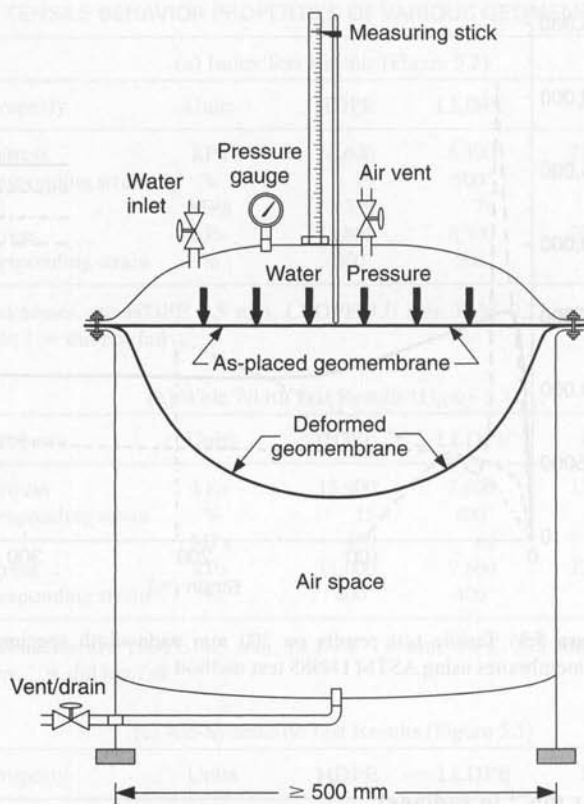
Figure 5.4 Schematic diagram and photograph of three-dimensional axi-symmetric geomembrane tension test apparatus.

In conducting the test, it is observed that HDPE and reinforced geomembranes like fPP-R, EPDM-R, and CSPE-R fail at relatively low deflections ($\delta < L/2$) and extensible geomembranes like nonreinforced LLDPE, fPP, and PVC fail at relatively high deflections ($\delta < L/2$).

Using a 600 mm diameter test container, hydrostatically pressurized at a (relatively fast) rate of 7.0 kPa per minute, the data produce the curves of Figure 5.5. Note that both the HDPE and CSPE-R geomembranes fail at relatively low strains (but high stresses), whereas the LLDPE and PVC fail at significantly greater strains. These test results are also tabulated in Table 5.5(c), which taken with Tables 5.5(a) and 5.5(b) provide a comparison of the different tensile tests. Note the relatively large differences between this test and the other tension tests presented earlier. Clearly, the lesson here is that appropriate modeling of a field situation is absolutely necessary if a design-by-function approach is to be used. Additional insight into the behavior of the test results under varying conditions is found in Nobert [10].

Tensile Behavior of Seams. The joining of geomembrane rolls and panels results in an overlapped seam that can be weaker than the geomembrane sheet itself. This is particularly true of seams made in the field versus those made in the fabrication factory, where quality control can be exercised more rigorously. (Various types of seaming methods will be discussed in Section 5.11.) To determine the strength of a geomembrane seam, a number of tests are available: typical shear tests are ASTM
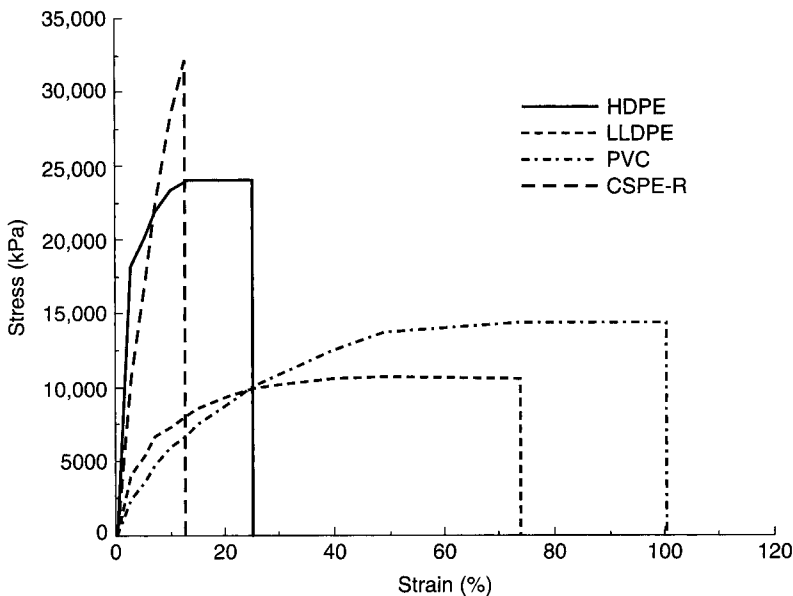
Figure 5.5 Stress-versus-strain response curves of various types of geomembranes under axi-symmetric hydrostatic pressure.

D6392, D882, and D751; typical peel tests are ASTM D6392, D882, and D413. Table 5.4 identifies them with respect to the type of geomembranes. In both shear and peel tests a representative specimen (usually 25 mm wide) is taken across the seam and the unseamed ends are placed in the grips of a tensile testing machine. For the shear test, the two separate ends of the seam are pulled apart, placing the joined or seamed portion between the geomembrane sheets in shear. For the peel test, one end of the geomembrane and the closest end of the adjacent piece are gripped, placing the seamed portion between them in a tensile mode. Figure 5.6 shows diagrams of the two configurations and also the results of tests on chemical (solvent) bonded PVC geomembrane seams compared with the sheet material itself with no seams, and extrusion fillet-welded HDPE geomembrane compared with the sheet itself. It is clearly seen that for these situations the peel test is a great deal more challenging than the shear test and that in all cases the seams have lower strength than the parent material. It is sometimes said that the shear test simulates a performance mode, whereas the peel test is more of an index test. It is important to perform both in order to fully evaluate the quality of the seam. It should be cautioned, however, that these results vary greatly with the type of geomembrane and the type of seam being evaluated. Of particular concern are the following questions.

- Which type of seam test (shear, peel, or both) should be used for construction quality control and quality assurance?
- Has the failure occurred in the seamed region or in the parent material adjacent to the seam?
- What percentage of parent material strength should the seam itself support?
- How much elongation in the shear test is necessary?
- How little separation (or incursion) in the peel test should be allowed?
- Is separation-in-plane (SIP) an allowable mode of failure if the seam meets all other separation criteria?
- Should seams be evaluated in wide-width or axi-symmetric modes that better simulate performance tests?

Haxo [11] has written extensively on the subject, as have Rollin and Fayoux [12] and Peggs [13], but the final decision rests with the specification writer and/or owner-permitting agency.

Tear Resistance. The measurement of tear resistance of a geomembrane can be done in a number of ways. ASTM D1004, D2263, D5884, D751, D1424, D1938, and ISO 34 all cover the general topic. ASTM D1004 uses a template to form a test specimen shaped such as to have a 90° angle where tear can begin to propagate. The two ends on each side of the specimen are gripped in a tensile testing machine, and tearing proceeds across the specimen perpendicular to the application of load. ASTM D2263, called *trapezoidal tear*, is sometimes recommended. In this test a geomembrane specimen is cut in the shape of a trapezoid of dimensions 100 mm on one side, 25 mm on the other, and 75 mm long. An initiating cut of 12.5 mm is made in the center of the 25 mm
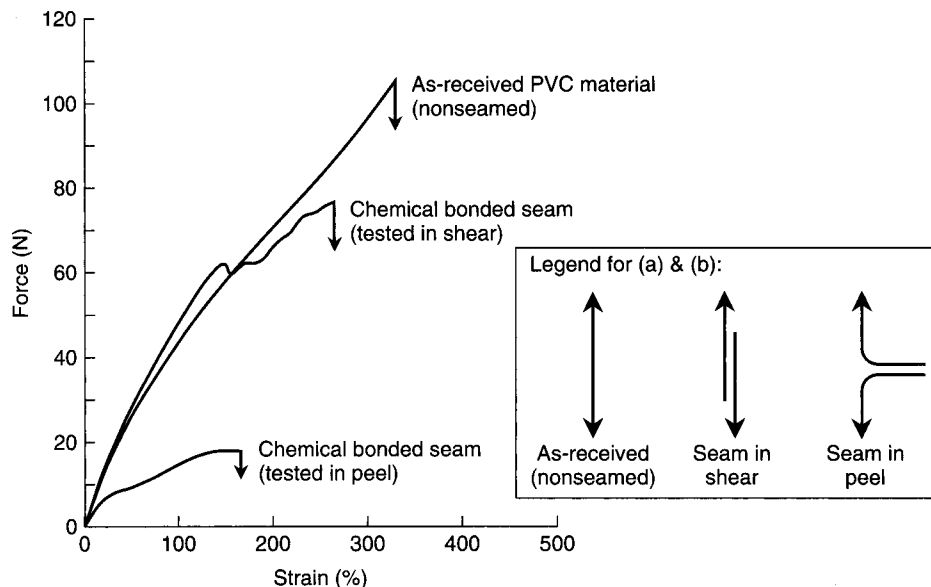
(a) Behavior of PVC sheet and seams
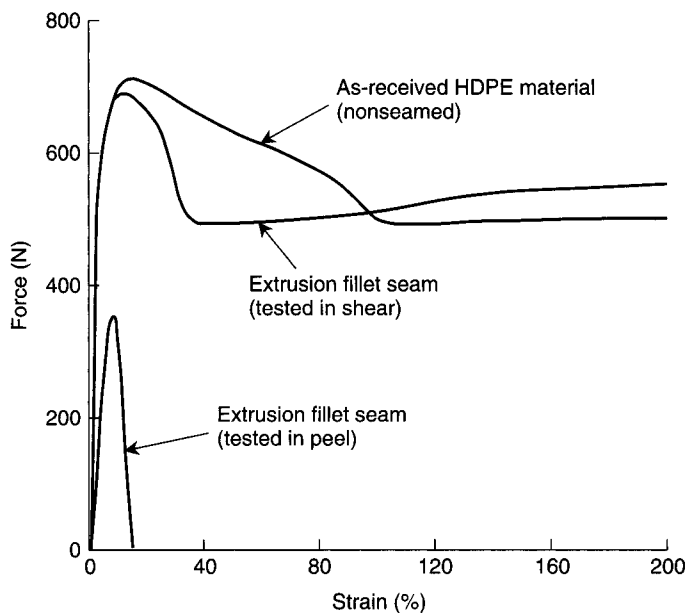
(b) Behavior of HDPE sheet and seams

Figure 5.6   Tensile test results on 25 mm wide and 0.5 mm thick PVC geomembrane compared with chemical-bonded seams on the same material tested in shear and in peel; and 25 mm wide and 1.5 mm thick HDPE geomembrane compared with extrusion fillet welded seams on the same material tested in shear and in peel.

side. This specimen is then mounted in the grips of a tensile testing machine in such a way that the 25 mm side (with the cut) is taut and the 100 mm side has 75 mm of slack in it. As the test machine elongates, the specimen tears from the 25 mm side to the 100 mm side, beginning at the initiating cut. In both of these above tests the maximum load is reported as the tear resistance.

The major difference in these two tests (D1004 and D2263) is the length of test specimen for the tear to propagate across. Here the D2263 is greater, 75 mm versus 12.5 mm, and a more accurate trend of behavior can be assessed. However, the required sample size is larger, which may be a limitation especially for incubated materials.

The tear resistance of many thin nonreinforced geomembranes is quite low, from 18 to 130 N. The implication of this is important for geomembrane handling and installation. Extreme care must be exercised during construction when moving rolls or panels into place and during periods of high wind. The placement of a scrim within the geomembrane greatly helps this situation. The tear test often recommended for scrim reinforced geomembranes is the tongue tear test, D5884. Here a 75 mm wide specimen with a 25 mm initiating cut is put in the grips of a tension testing machine and pulled against itself. The test specimen is 200 mm long and the maximum value of resistance is reported as the tear strength. Values of tear resistance for scrim reinforced geomembranes increase significantly, to the range 90 to 450 N.

As the geomembrane becomes thicker, tear during installation becomes less of an issue, and the design-related tear stresses become the critical values. These are site-specific situations that must be individually assessed.

Impact Resistance.   Falling objects, including cover soils, can penetrate geomembranes, either causing leaks themselves or acting as initiating points for tear propagation. Thus an assessment of geomembrane impact resistance is relevant. There are a number of ASTM options available; among them are ASTM D1709 or ISO 13433 (free-falling dart), ASTM D3029 (falling weight), and ASTM D1822, D746 and D3998 (pendulum types).

Rather than use a separate test device, it is sometimes convenient to use the Spencer impact adaptation of the Elmendorf tear test, ASTM D1424. The Elmendorf tear apparatus is a pendulum-type device that results in an energy-to-failure value in Joules. The Spencer impact attachment is merely a specimen-holding device for the penetration of a point at the end of the pendulum swing.

The results shown in Table 5.6 were obtained using such a device. It is clearly seen that the thicker geomembranes have greater impact resistance than do the thinner ones. The effect of scrim-reinforcement is also significant. The maximum value listed in the table is 21 J, which is the maximum capacity of the test apparatus just described. For geomembranes with greater impact resistance, or for geotextiles underlying and/or overlying the geomembrane, significantly higher impact resistances will result. Alternatively, a notched dumbbell-shaped test specimen can be used in which the pendulum imparts a tensile impact stress on the specimen. This is used with polyethylene geomembranes and can be done in cold temperatures; see ASTM D746 in this regard. For the testing of geocomposite systems, a larger floor-mounted pendulum device can

TABLE 5.6 IMPACT RESISTANCE (J) OF VARIOUS GEOMEMBRANES VIA ASTM D1424 SPENCER IMPACT METHOD

Geomembrane	Point Geometry Angle*				
	15°	30°	45°	60°	90°
PVC (0.50 mm)	6.5	8.9	14.9	>21	>21
PVC (0.75 mm)	9.2	13.6	18.3	>21	>21
HDPE (1.0 mm)	7.6	9.4	11.3	11.3	8.7
EPDM-R (0.91 mm)					
10 × 10 scrim	11.7	11.9	14.6	19.5	>21
CSPE-R (0.91 mm)					
10 × 10 scrim	12.2	12.7	14.0	19.3	>21

*These are conical points where the angle is measured from the central axis of the cone to its surface. In each case the total surface area of the points is kept constant.

be used. ASTM D3998 describes such a device. Data from such a test result in the curves shown in Figure 5.7. Here varying thicknesses of HDPE are evaluated with an approximate linear response as the result. When using a 400 g/m^2 nonwoven needle punched geotextile on the front or back of the geomembrane, an improvement in impact resistance is noted. Furthermore, a geotextile on both sides of the geomembrane improves the impact resistance even further. The response curves can be used to determine the economic efficiency of using a thicker geomembrane or geotextile with a thinner geomembrane.
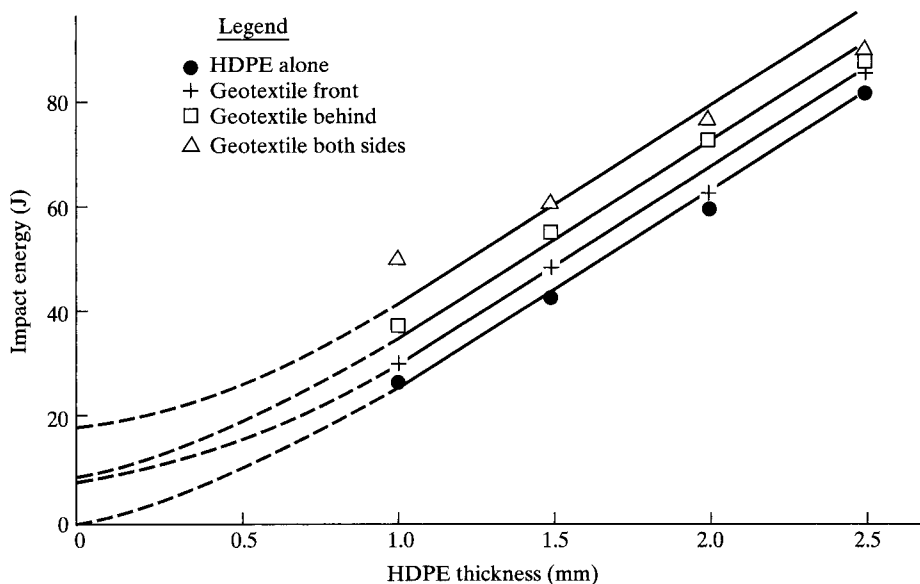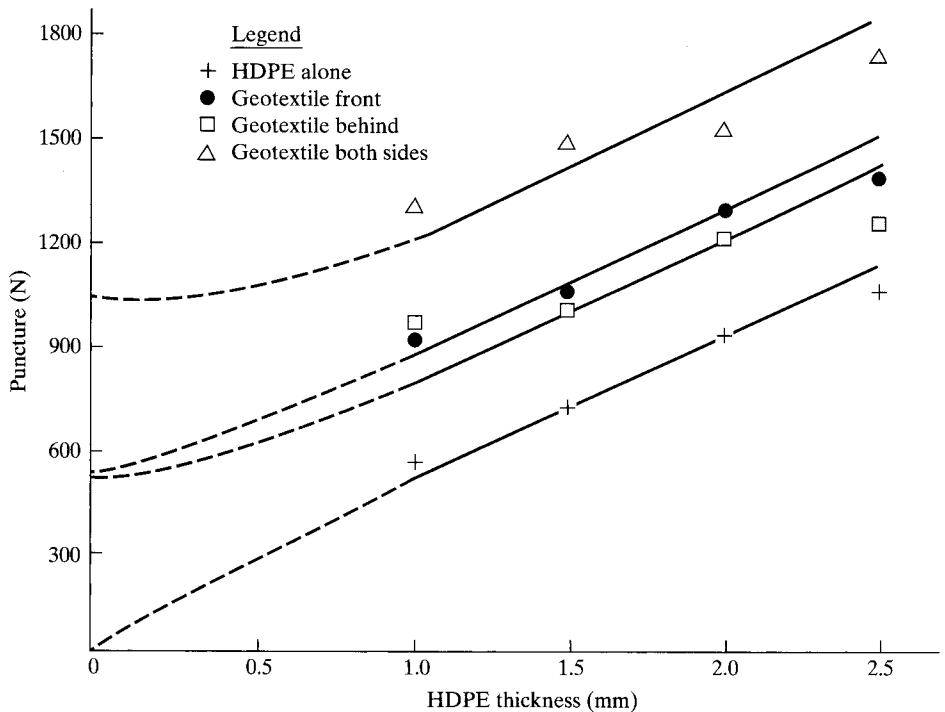

Figure 5.7 Falling pendulum impact test results on varying thicknesses of HDPE geomembranes and different combinations of geomembranes with 400 g/m^2 nonwoven needle-punched geotextiles. (After Koerner et al. [14])
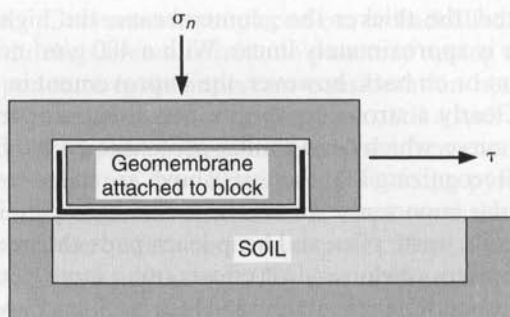
Puncture Resistance. Geomembranes placed on, or backfilled with, soil containing stones, sticks, or hard debris are vulnerable to puncture during and after loads are placed on them. Such puncture is an important consideration because it occurs after the geomembrane is covered and cannot be detected until a leak from the completed system becomes obvious. Repair costs at that time are often enormous.

The closest ASTM test modeling this situation is D5494, the pyramid puncture test, but it is used infrequently. Alternatively, D4833 is often used since it is the test method used by manufacturers for quality control purposes. Here a geomembrane is clamped over an empty mold 45 mm in diameter. The assembly is placed in a compression testing machine fitted with an 8 mm diameter rod with a flat but edge beveled bottom. The rod is pressed into the geomembrane until it punches through. The recommended load rate is 300 mm/min. The value reported as puncture resistance is the maximum load registered on the test machine. Typical values of geomembrane puncture resistance are 50 to 500 N for thin nonreinforced geomembranes and 200 to 2000 N for reinforced geomembranes. Here again the influence of the scrim reinforcement is seen. Note that the placement of a geotextile below and/or above a nonreinforced geomembrane greatly increases the puncture resistance of the geomembrane and essentially takes all the load before the geomembrane absorbs any of it. The results of the test for varying thicknesses of HDPE geomembrane are shown in Figure 5.8. As

Figure 5.8 Beveled flat-tip puncture test results on varying thicknesses of HDPE geomembranes and different combinations of geomembranes with 400 g/m^2 nonwoven needle-punched geotextiles. (After Koerner et al. [14])

expected, the thicker the geomembrane, the higher the puncture resistance. The response is approximately linear. With a 400 g/m^2 nonwoven needle-punched geotextile on front or on back, however, the improvement in puncture resistance is quite impressive. Clearly a strong composite action is occurring. This is further evidenced by the upper curve, which has a similar geotextile on the front and back of the geomembrane.

Recognizing that the tests above are index tests and that puncture resistance is of particular importance when large stone aggregate is used for leachate collection layers in landfills, waste piles, and heap leach pads, the need for a field-simulated performance test becomes obvious. Most efforts use a large-diameter pressure vessel with the subgrade beneath the geomembrane test specimen. Several variations can be evaluated: the actual subgrade (sand, gravel, stone, etc.) at the targeted density; the actual subgrade set in an epoxy cast (so-called "rock pizza"), so as to have the particles in the same configuration for each test; and truncated cones in a triangular array to simulate a worst-case subgrade condition. A test method is currently available, ASTM D5514, and a paper on the truncated cone test has evaluated a number of common geomembranes (HDPE, CSPE-R, PVC, and LLDPE), both with and without geotextile protection layers (Hullings and Koerner [15]). It has also been extended into creep testing to assess the viscoelastic properties of the geomembranes and protection layers (Narejo et al. [16]).

Interface Shear.   Critically important for the proper design of geomembrane-lined side slopes of landfills, reservoirs, and canals is the soil-to-geomembrane shear strength. As pointed out and analyzed by Koerner and Soong [17], numerous side slope failures have occurred. Often cover soils slide over geomembranes, but sometimes the geomembrane fails (or pulls out of the anchor trench) moving on a lower friction surface beneath. The test method used to access the situation is an adapted form of a geotechnical engineering direct shear test for determining soil-to-soil friction.

The experimental setup to evaluate soil-to-geomembrane friction uses the project-specific type of geomembrane in one-half of a direct shear box with the opposing soil surface in the other half; see Figure 5.9a. Generally the soil is compacted to its intended density and moisture content in the lower half and the geomembrane is firmly bonded to a wooden platen in the upper half. A number of site-specific conditions must be addressed in order to have performance-related results. Some examples would include the type and gradation of soil to be used, the density and moisture content of soil to be placed, the moisture condition during the test (i.e., dry, moist, or saturated), the normal stress(es) to apply, the time for saturation and/or consolidation, the strain rate to use during shear, and the deformation required to attain residual strength. In short, every geotechnical engineering question we might have in designing a soil system must be addressed when designing a geomembrane system.
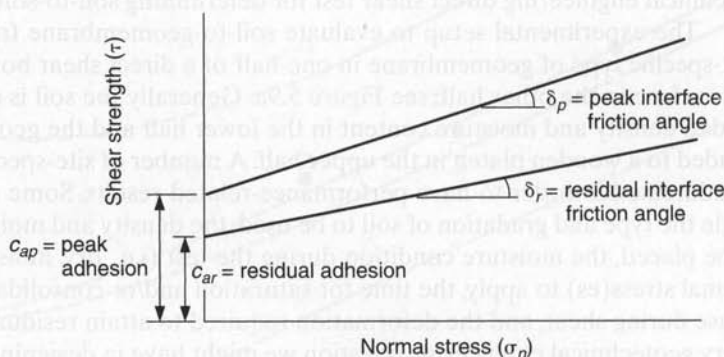
Additionally, the size of the shear box must be considered. For geomembranes against sands, silts, or clays, a 100 × 100 mm square shear box is recommended. Many commercial soil testing devices are available of this type. Only if we are evaluating gravel or other large open-sized material (like geonets or geogrids) against a geomembrane must the shear box be larger. This decision on shear box size should really be left to the design engineer. Unfortunately, ASTM D5321 on direct shear evaluation of geosynthetic-to-soil, or geosynthetic-to-geosynthetic, recommends a 300 × 300 mm square shear box for all situations (unless it can be proved that a smaller size is justified).

(a) Direct shear test device

Shear stress (τ)

σ_n(high)

σ_n(middle)

σ_n(low)

τ_p

τ_r

Shear displacement

(b) Direct shear test data

Shear strength (τ)

δ_p = peak interface friction angle

δ_r = residual interface friction angle

c_{ap} = peak adhesion

c_{ar} = residual adhesion

Normal stress (σ_n)
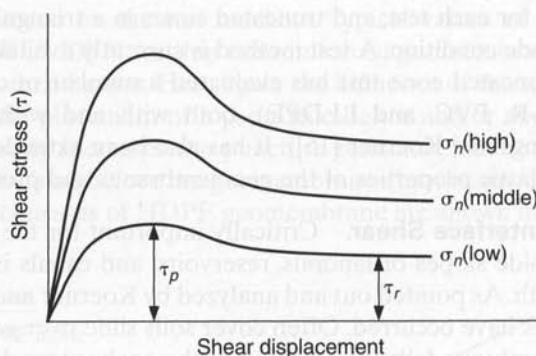
(c) Mohr-Coulomb failure envelopes

Figure 5.9 Direct shear testing concept and resulting shear strength parameters.

Although such a large shear box is appropriate for geogrid or geonet shear testing, it may be considered excessive, the paramount reasons being very long times for saturation, the nonuniform normal stresses (particularly during the test), and the insufficient travel to attain true residual strength.

Irrespective of box size, conducting a direct shear test is straightforward. Upon deciding the above-mentioned site-specific issues, a series of at least three separate tests (each time with new test specimens) is performed at different normal stresses (σ_n) centered around the site-specific normal stress. The data should be similar to that in Figure 5.9b. The peak and residual strengths are sometimes similar and sometimes very different.

Using the peak and residual shear stress values (i.e., the shear strengths) from these three graphs allows for a new graph to be developed, as shown in Figure 5.9c. This is the Mohr-Coulomb failure envelope, consisting of three failure points at the corresponding normal stresses for peak and (if different) residual strengths. The straight-line response results in the following equation:

$$\tau = c_a + \sigma_n \tan \delta \tag{5.6}$$

where

τ = shear strength of geomembrane to the opposing surface,

σ_n = normal stress on the shear plane,

c_a = adhesion of geomembrane to opposing surface, and

δ = friction angle of geomembrane to opposing surface.

If soil is the opposing surface, the tests can be repeated with soil in both halves of the shear box. Treating the data in an identical manner results in another Mohr-Coulomb failure envelope, which results in the following equation.

$$\tau = c + \sigma_n \tan \phi \tag{5.7}$$

where

τ = shear strength of soil,

c = cohesion of soil, and

ϕ = friction angle of soil.

As for other geosynthetics, efficiencies can be calculated in the standard manner.

$$E_c = (c_a/c)\ 100 \tag{5.8}$$

$$E_\phi = (\tan \delta/\tan \phi)\ 100 \tag{5.9}$$

There are hundreds of papers available on the interface friction between geomembranes and numerous other surfaces (soils and geosynthetics). Results from an early effort focusing on peak friction values (Martin et al. [18]) are given in Table 5.7. As shown, the peak friction angles of soil-to-geomembrane are always equal or less than soil-to-soil, with rough or textured surfaces being the highest, and the smoother,

TABLE 5.7   PEAK FRICTION VALUES AND EFFICIENCIES OF VARIOUS GEOSYNTHETIC INTERFACES*

(a) Soil-to-Geomembrane Friction Angles

Geomembrane	Soil type					
	Concrete Sand ($\phi = 30°$)		Ottawa Sand ($\phi = 28°$)		Mica Schist Sand ($\phi = 26°$)	
HDPE						
Textured	30°	(100%)	26°	(92%)	22°	(83%)
Smooth	18°	(56%)	18°	(61%)	17°	(63%)
PVC						
Rough	27°	(88%)	—	—	25°	(96%)
Smooth	25°	(81%)	—	—	21°	(79%)
CSPE-R	25°	(81%)	21°	(72%)	23°	(87%)

(b) Geomembrane-to-Geotextile Friction Angles

Geotextile	Geomembrane				
	HDPE		PVC		CSPE-R
	Textured	Smooth	Rough	Smooth	Undulating
Nonwoven needle-punched	32°	8°	23°	21°	15°
Nonwoven heat-bonded	28°	11°	20°	18°	21°
Woven monofilament	19°	6°	11°	10°	9°
Woven slit-film	32°	10°	28°	24°	13°

(c) Soil-to-Geotextile Friction Angles

Geotextile	Soil type					
	Concrete Sand ($\phi = 30°$)		Ottawa Sand ($\phi = 28°$)		Mica Schist Sand ($\phi = 26°$)	
Nonwoven needle-punched	30°	(100%)	26°	(92%)	25°	(96%)
Nonwoven heat-bonded	26°	(84%)	—	—	—	—
Woven monofilament	26°	(84%)	—	—	—	—
Woven slit-film	24°	(77%)	24°	(84%)	23°	(87%)

*Efficiency percentages (in parentheses) are based on Equations (5.8) at (5.9).
Source: Extended from Martin et al. [18].

harder geomembranes being the lowest. A much more extensive and recent paper is by Narejo and Koerner [19].

The frictional behavior of geomembranes placed on clay soils is of considerable importance for composite liners containing solid or liquid wastes. The current requirements are for the clay to have a hydraulic conductivity equal to or less than 1×10^{-7} cm/s and for the geomembrane to be placed directly upon the clay. While an indication of the shear strength parameters has been investigated (e.g., Narejo and Koerner [19] and Koerner et al. [20]), the data are so sensitive to the variables discussed

previously that site-specific and material-specific tests should always be performed. *In such cases, literature values should never be used for final design purposes.*

Much of the direct shear literature data is for peak shear strengths (e.g., the data of Table 5.7). Stark and Poeppel [21] have challenged this situation by testing various geosynthetic interfaces in a ring-shear device. In using such a device, significantly larger deformations can be mobilized than in conventional direct shear testing. In so doing, they found that residual strengths are often considerably lower than peak strengths. Among other findings, they identified a geomembrane *polishing action* that could occur at large deformations, decreasing peak friction angles by considerable amounts. Clearly, shear deformation tests must be continued further than has been done in past practice to see if, and how much, shear strength decreases beyond the peak values. The designer's dilemma of using peak or residual shear strength (or something between) is an actively disputed topic (Koerner [22]).

Anchorage.   In certain problem situations, a geomembrane might be sandwiched between two materials and then tensioned by an external force. The termination of a geomembrane liner within an anchor trench is such a situation. To simulate this behavior in a laboratory environment, we can use a 200 mm wide geomembrane embedded between back-to-back channels. Here the channels are placed under pressure using a hydraulic jack, and the exposed end is held fixed in the grips of a tension testing machine. The channel surfaces are fitted or faced with the actual or simulated (e.g., sandpaper) adjacent materials. Tension is mobilized from the fixed end of the geomembrane to the opposite end within the anchored zone. For design purposes we are searching for the anchorage depth necessary to mobilize the geomembrane's strength. The target value could be the tensile strength at yield, at scrim break, or at an allowable strain. Figure 5.10 shows the embedment depth required to mobilize full anchorage strength for HDPE, CSPE-R, and PVC geomembranes. Depending upon the applied normal stress, the anchorage distance varies from approximately 50 to 300 mm; that is, it is very small. Other curves for different geomembranes and confinement conditions can be similarly generated.

Stress-Cracking (Bent Strip).   Called *environmental stress-cracking* in ASTM D1693, this test is only applicable to semicrystalline materials like HDPE. Furthermore, the higher the density (hence, the crystallinity), the more significant the test. Small test specimens of 38 by 13 mm are prepared with a controlled imperfection on one surface—a notch about one-half of the thickness running centrally along the long dimension. The specimens are bent into a U-shape and placed within the flanges of a channel holder. This assembly is then immersed in a surface wetting agent at an elevated temperature, usually 50°C. Since stress-cracking is defined by ASTM as "an external or internal rupture in a plastic caused by tensile stress less than its short-time mechanical strength," the test records the proportion of the total number of specimens that crack in a given time. Geomembrane specifications in the past that call for this test require that there be no stress-cracked specimens within a given number of hours. However, the test is not a good challenge for currently used HDPE geomembranes and is not recommended for further use; *this test should be discontinued.*
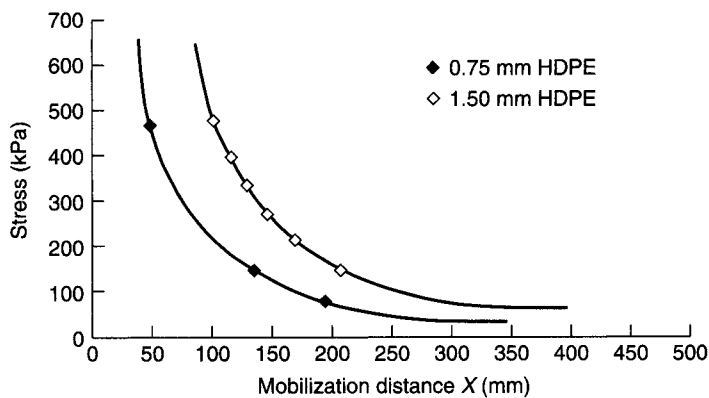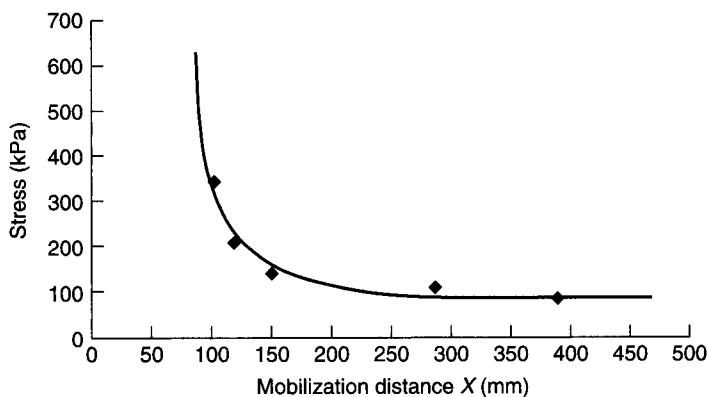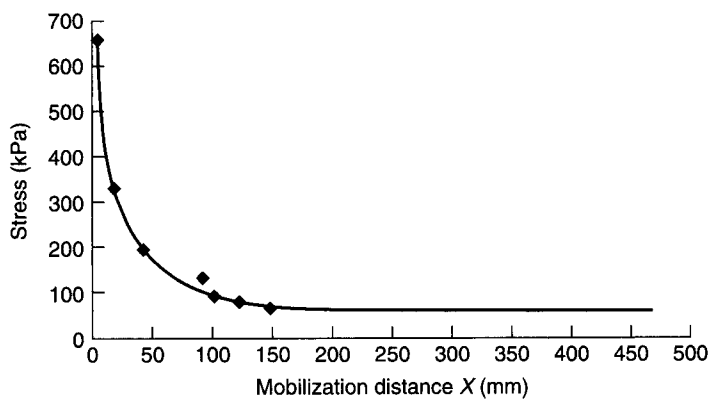
**Figure 5.10** Embedment depth curves versus applied normal stress for various geomembranes.

Stress-Cracking (Constant Load).   A more appropriate and stringent type of stress-cracking test for polyethylene geomembranes has been developed and adopted for HDPE geomembrane specifications. It is called the notched constant tension load (NCTL) test, designated ASTM D5397. The comparable ISO test method is 16700. It places centrally notched dumbbell-shaped test specimens under a constant load (at a known percentage of their yield stress) in a surface wetting agent at an elevated temperature. Igepal 630 is the usual wetting agent and 50°C is the recommended temperature. When a series of test specimens are evaluated at different percentages of their yield stress, a ductile-to-brittle behavior is indicated, as shown in Figure 5.11a. Evaluating 21
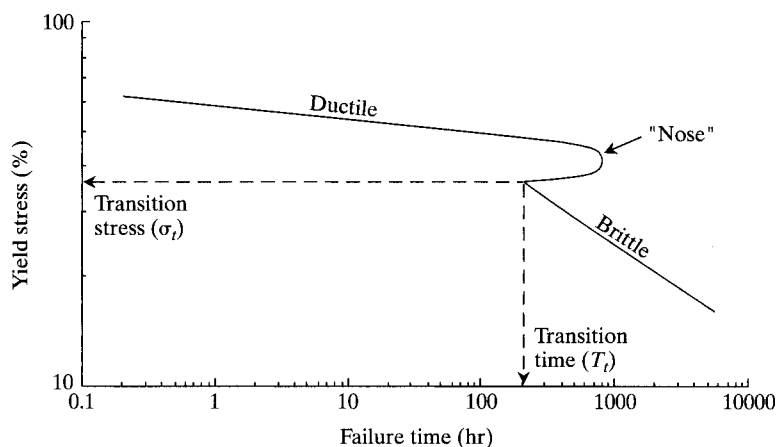
(a) A typical overshoot (or nose) response curve for a complete NCTL test
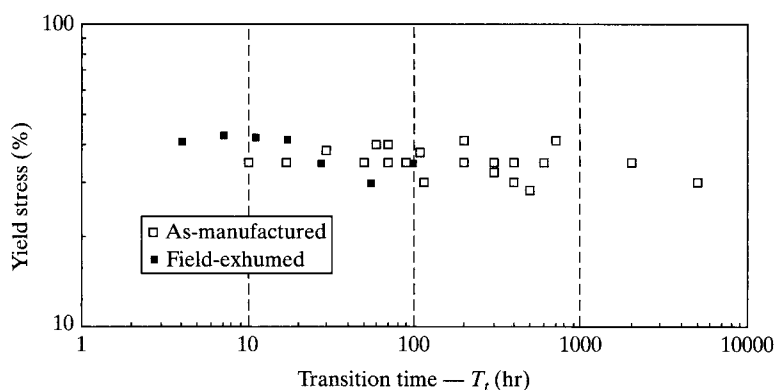
(b) Transition points for 21 virgin geomembranes and
7 field-retrieved geomembranes

Figure 5.11   Typical response of NCTL test to evaluate stress-crack resistance of HDPE geomembranes and resins and summary of transition point variations. (After Hsuan et al. [23])

commercially available virgin HDPE geomembranes, it is seen that the transition time (T_t) varies from 10 to 5000 hours. Additionally, seven field-retrieved HDPE geomembranes that had evidenced stress-cracking problems are evaluated. Their transition times range from 4 to 97 hr. These 28 data points are shown on Figure 5.11b. The current recommendation for an acceptable stress-crack resistant HDPE geomembrane is a transition time equal to or greater than 150 hr. Since stress-crack resistance is largely a resin-dependent mechanism, the NCTL test can be performed on samples made as plaques from the base resin, as well as on the finished geomembrane sheet. See ASTM D1928 for the preparation of plaques.

Stress-Cracking (Single Point).   Although the NCTL test just described is the premier test for evaluating the stress-cracking behavior of HDPE geomembranes, it has the disadvantage of requiring many tests and being quite lengthy in developing the full curve shown in Figure 5.11a. To make the procedure into more of a quality control test, a single-point version is available; called the SP-NCTL test, it is outlined in the appendix to ASTM D5397.

Procedurally we use the same type of test specimens and load device, but select a specific value of stress, in this case 30% of yield stress. If the specimen does not fail within 300 hr, it signifies that the transition time for the full curve is at least 150 hr and would thus fulfill the specified value mentioned in the previous section. The SP-NCTL test is further described by Hsuan and Koerner [24] and is recommended for use in HDPE geomembrane specifications.

5.1.4 Endurance Properties

Any phenomenon that causes polymeric chain scission, bond breaking, additive depletion, or extraction within the geomembrane must be considered as being detrimental to its long-term performance. There are a number of potential concerns in this regard. While each is material-specific, the general behavioral trend is to cause the geomembrane to become brittle in its stress-strain behavior over time. There are several mechanical properties to track in monitoring most types of long-term degradation: the decrease in elongation at failure, the increase in modulus of elasticity, the increase (then decrease) in stress at failure (i.e., strength), and the general loss of ductility. Obviously many of the physical and mechanical properties discussed in this section could be used to monitor the polymeric degradation process.

Ultraviolet.   As described in Section 2.3.6 for geotextiles, ultraviolet degradation of geomembranes occurs. Short-wave length energy for sunlight can penetrate the polymer structure causing chain scission, bond breaking, and surface degradation. Figure 2.27 presents the wavelength spectrum of natural sunlight and indicates that the UV-B range is the most sensitive region. By virtue of the specific surface area differences between geotextiles and geomembranes, however, the relative degree of ultraviolet degradation of geomembranes is much less than with geotextiles. Thus temporary coverings of geomembranes before placement is not generally necessary from an ultraviolet degradation perspective. Note in Table 1.6 that all polymers used for geosynthetics have carbon black or pigments (2 to 25%) included to act as screening or blocking

agents to minimize ultraviolet degradation. Furthermore, all have ultraviolet chemical stabilizers as part of their additive package. Thus the timely cover of geomembranes, written into many specifications, is often included to eliminate accidental or intentional damage of the geomembrane rather than because of ultraviolet degradation.

If we wish to estimate the UV-exposed lifetime of a particular geomembrane, a number of accelerated laboratory exposure tests are available—for example, the ultraviolet fluorescent tube method, ASTM G26, or the xenon arc method, ASTM D4355 and ISO 4892. Lifetime estimates are possible knowing site-specific exposure [25]. We can also perform outdoor weathering tests such as ASTM D1435, D3334, or D5970. These tests will generally require long exposure times and are sometimes accelerated by means of rotating mirrors that intensify the sunlight's energy. The general area of estimating lifetime from any of these tests (laboratory or field-exposed) is an important research topic.

The current trend for permanently exposed geomembranes (e.g., floating covers in reservoirs or exposed side slope liners of landfills and surface impoundments) is to use manufacturer's warranties. Warranties of up to 20 years can be obtained in some situations for CSPE-R and HDPE geomembranes. Other commonly used geomembranes have lower exposed lifetimes and must be covered with soil or with a sacrificial material such as a replaceable geotextile. For geomembranes that are backfilled or covered in a timely manner, ultraviolet degradation is a nonissue, and material warranties are generally irrelevant and unnecessary.

Radioactive Degradation.   It is quite possible that radioactivity higher than 10^6 to 10^7 rads will cause polymer degradation via chain scission. Thus the containment of high-level radioactive waste might not use geomembranes. Low-level radioactive waste, however, is much lower in its activity and can quite possibly be disposed of using geomembrane containment systems. Kane and Widmayer [26] describe a number of HDPE lined radioactive waste containment scenarios including landfill-liner systems, landfill-cover systems, below-ground vaults, uranium mill tailings disposal cells, and high-integrity containers. The last have been in use at low-level waste disposal facilities since 1979.

Other than internal government reports, however, there are very few references in the open literature on radioactive degradation of geomembranes. Since many countries are being required to site low-level radioactive waste landfills, additional research should be undertaken.

Biological.   There are a tremendous number of living organisms in the soil. Our discussion will focus only on areas where there is perceived concern.

Animals.   A major concern for soil-buried geomembranes is animals burrowing through them. Tests (Steiniger [27]) have focused on mice and rats. Technically, only those geomembraness harder than the burrower's tooth enamel or claws can avoid an attack if the animal is persistent enough. Thus geomembranes are indeed vulnerable to burrowing animals, but to what degree is largely unknown. Unfortunately, there are no established test procedures available; only intuitively can it be assumed that the stronger, harder, and thicker the geomembrane, the better its resistance to animal attack [27].

Fungi. Fungi include yeasts, molds, and mushrooms. They depend on organic matter for carbon, nitrogen, and other elements. Their numbers can be very large, as much as 10 to 20 million per gram of dry soil, and their population is constantly changing. Placing geomembranes in decomposing organic residue often causes concern about degradation. However, the high-molecular-weight polymers generally used for geomembranes seem very insensitive to such degradation. ASTM G21 deals with the resistance of plastics to fungi.

Bacteria. Bacteria are single-cell organisms, among the simplest and smallest known forms of life. They rarely exceed 5 μm in length and are usually round, rodlike, or spiral in shape. Their numbers are enormous: more than 1 billion per gram of soil. They participate in all organic transformations, and thus the discussion on fungi could essentially be repeated here. The test method for evaluation of resistance of plastics to bacteria is ASTM G22.

As with fungi, the greatest concern about bacteria regarding geomembranes is not polymeric degradation, but fouling and clogging of the drainage systems often constructed in conjunction with the liner.

Chemical. The chemical resistance of a geomembrane vis-a-vis the substance(s) it is meant to contain is always important, and often it is the foremost aspect of the design process. For example, in domestic-waste or hazardous waste containment, the pollutant will interface directly with the geomembrane. Thus the geomembrane's resistance must be assured for the life of the facility. This situation has long been recognized, and resin producers and manufacturers have evaluated many situations. This has resulted in various chemical resistance charts, such as Table 5.8, which lists generic

TABLE 5.8 GENERAL CHEMICAL RESISTANCE GUIDELINES OF SOME COMMONLY USED GEOMEMBRANES

	Geomembrane Type							
	HDPE		PVC		CSPE-R		EPDM-R	
Chemical	38°C	70°C	38°C	70°C	38°C	70°C	38°C	70°C
General								
Aliphatic hydrocarbons	✓	✓						
Aromatic hydrocarbons	✓	✓						
Chlorinated solvents	✓	✓					✓	
Oxygenated solvents	✓	✓					✓	✓
Crude petroleum solvents	✓	✓						
Alcohols	✓	✓	✓	✓			✓	✓
Acids								
Organic	✓	✓	✓	✓	✓		✓	✓
Inorganic	✓	✓	✓	✓	✓		✓	✓
Heavy Metals	✓	✓	✓	✓	✓		✓	✓
Salts	✓	✓	✓	✓	✓		✓	✓

Abbreviation: ✓ = generally good resistance.
Source: After Vandervoort [28].

chemicals against many common geomembranes on a relative basis. These charts and their tests are sometimes incorrectly called *chemical compatibility* charts or tests. To a chemist, compatibility is when two substances properly mix with one another; this is exactly the opposite of the trend we are considering in this section. *Chemical resistance* is the preferred term. Although such tables are generally reliable, there are many circumstances where geomembrane-specific testing is required:

- When the chemical is not a single-component material and possible synergistic effects are unknown.
- When the composition of the resulting chemical is simply not known, as in landfill leachates before the facility is constructed.
- When the geomembrane is not a single-component material but is made from a blend of materials.
- When the geomembrane is modified at the seams or is seamed with material that is different from that of the geomembrane sheets.
- When the containment must function over a very long period and the leachate may change over time during the course of the service lifetime.
- When untested circumstances, such as extreme heat or cold conditions, exist at the particular site.
- When the chart or table does not list new types and/or formulations of geomembranes; for example, Table 5.8 does not list LLDPE, fPP, and fPP-R.

Thus there exists a need for a specific test procedure. Chemical resistance tests on geomembranes for the specific conditions mentioned above require four important decisions to be made: the selection of the particular liquid to be used, the precise details of coupon incubation (temperature, atmosphere, orientation, and removal), the manner and type of specimen testing, and the assessment of the results of the testing.

The selection of the liquid is surely site-specific. A large database is given in [4], but the range of ingredients is enormous. Clearly, there is no typical leachate. What liquid is selected is a matter of agreement among the various parties involved. Often it is a difficult decision, and when the situation is critical it is decided on a worst-case basis. Thus the most aggressive liquid chemicals envisioned (e.g., various organic solvents) in the highest possible concentrations are often used for the incubating liquid.

The coupon incubation can sometimes be done in open containers or tubs, but generally it is being done in closed containers of the type shown in Figure 5.12. Here the container is sealed with the liquid circulating and being constantly monitored as to its consistency and temperature. There is no available headspace in the container, which means that organic solvents cannot escape from the completely filled chamber. Individual coupons are removed at 30, 60, 90, and 120 days, according to ASTM D5322 and D5496, and then cut into test specimens for evaluation.

There are many types of test(s) used to quantify the geomembrane's performance after chemical incubation. The following are most common:

- *Physical property tests:* These are for thickness, mass, length, width, and hardness and are the easiest and most straightforward to perform.
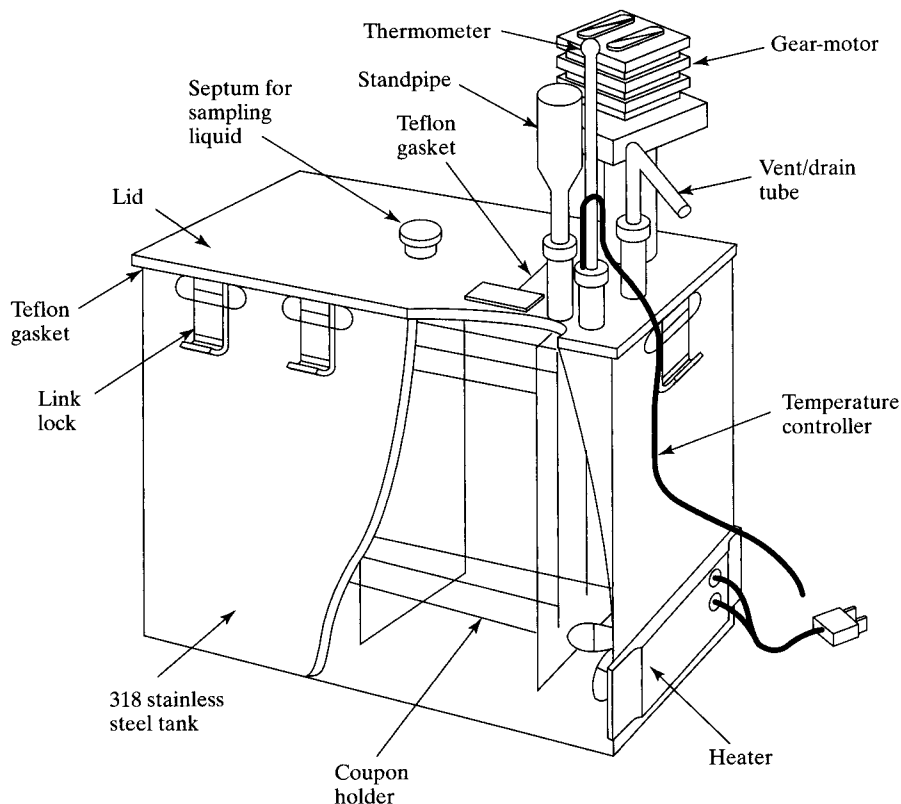
Figure 5.12   Schematic of incubation container for evaluating chemical resistance behavior of geomembranes. (After Metrecon [4])

- *Mechanical property tests:* The tensile test properties of strength at yield and/or break, elongation at yield and/or break, and modulus along with tear, puncture, and impact are the usual values measured. These are done as previously described.
- *Transport property tests:* Perhaps the most sensitive tests to perform (and undoubtedly the most difficult) are tests for water- or solvent-vapor transmission through the incubated geomembranes.

If a specific procedure, such as ASTM D5747, is followed, the test methods to be used will be prescribed and referenced accordingly. ISO 175 also covers the topic of chemical resistance to liquids.

For the assessment of the test results, the response curves for the above-mentioned tests should be plotted as the percent change in the measured property from the original versus the duration of incubation. Figure 5.13 shows such response curves for HDPE in a municipal solid-waste leachate at 50°C. The curves presented are the type often seen, in that the changes in the physical properties are significantly less than the
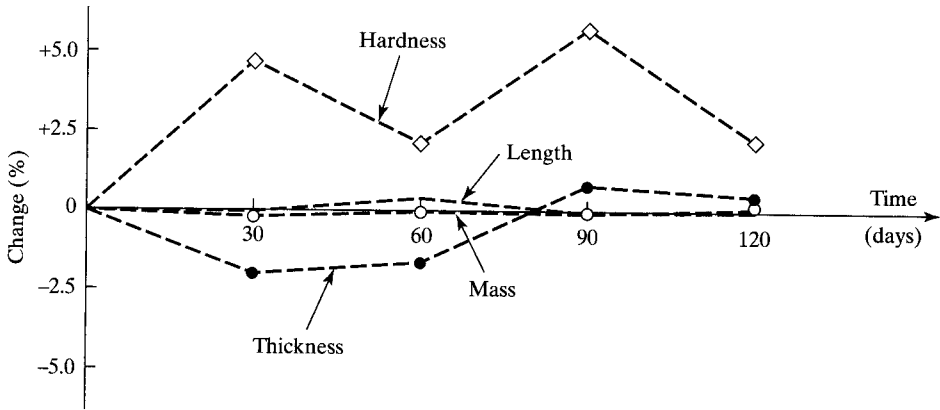
(a) Change in physical properties
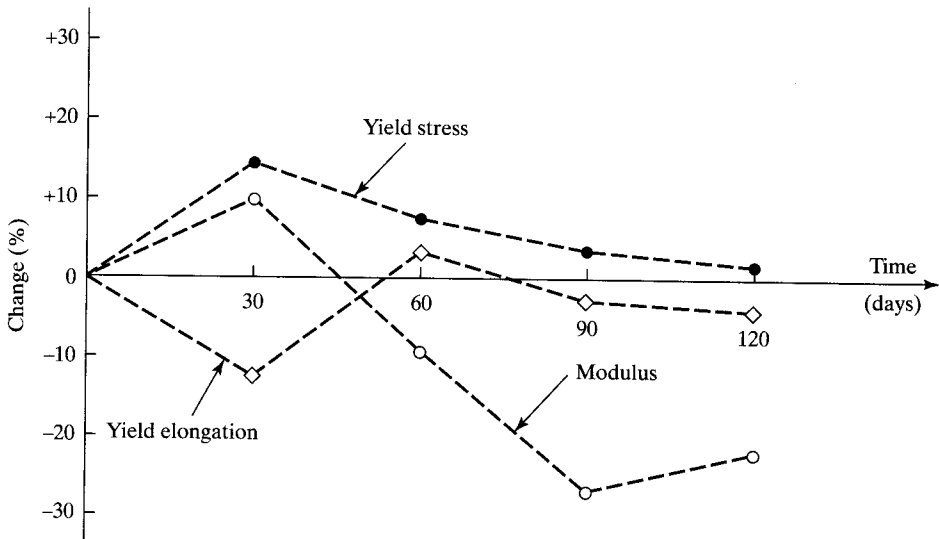
(b) Change in mechanical properties

Figure 5.13   Immersion behavior of HDPE samples to landfill leachate at 50°C up to 120 days. (After Tisinger [29])

changes in mechanical properties and no consistent trend is established, either a uniform increase or decrease. In this particular set of tests, the 23°C incubation data behaved similarly (see Tisinger [29]). If the geomembrane is reactive to the leachate, we expect uniform behavioral changes and the changes at the higher temperature to be greater than those at the lower temperature. With no discernible trend to indicate a reaction, and hence degradation, of the geomembrane, it may be concluded that the scatter results from inherent variation in the materials and the test methods themselves.

Furthermore, the property that changed the greatest amount, the modulus values in Figure 5.13(b) is subject to the greatest amount of judgmental error of all the values presented. While there are no established rules on allowable variation from the original test properties (see Table 5.9 for suggested values), it is clear that polyethylene will be more resistant to most organic solvents and aggressive chemicals than will other common geomembrane polymers. Furthermore, the higher the density, the better the chemical resistance. Thus high density polyethylene (HDPE) geomembranes are the material-of-choice for most landfill liners.

Thermal. Various properties of geomembranes, as they are made from polymers, are sensitive to changes in temperature. Both warm and cold temperatures have their own unique effects.

Warm Temperatures. Geomembrane materials exposed to heat can be subjected to changes in physical, mechanical, or chemical properties. The magnitude and duration of exposure determine the extent of this change. ASTM D794 covers the recommended procedure for determining permanent effects of heat on plastics—a tubular oven method (ASTM D1870), which consists of an oven with a coupon rack to

TABLE 5.9 SUGGESTED LIMIT OF CHANGES OF DIFFERENT TEST VALUES FOR INCUBATED GEOMEMBRANES

(a) Thermoset and Thermoplastic Polymers except HDPE (after Little [30])

Property	Resistant	Not Resistant
Permeation rate (g/m^2/hr)	<0.9	>0.9
Change in weight (%)	<10	>10
Change in volume (%)	<10	>10
Change in tensile strength (%)	<20	>20
Change in elongation at break (%)	<30	>30
Change in 100% or 200% modulus (%)	<30	>30
Change in hardness (points)	<10	>10

(b) Semicrystalline Polymers (such as HDPE)

Property	O'Toole [31]		Little [30]		Koerner	
	Resistant	Not Resistant	Resistant	Not Resistant	Resistant	Not Resistant
Permeation rate (g/m^2-hr.)	—	—	<0.9	≥0.9	<0.9	≥0.9
Change in weight (%)	<0.5	>1.0	<3	≥3	<2	≥2
Change in volume (%)	<0.2	>0.5	<1	≥1	<1	≥1
Change in yield strength (%)	<10	>20	<20	≥20	<20	≥20
Change in yield elongation (%)	—	—	<20	≥20	<30	≥30
Change in modulus (%)	—	—	—	—	<30	≥30
Change in tear strength (%)	—	—	—	—	<20	≥20
Change in puncture strength (%)	—	—	—	—	<30	≥30

allow for air circulation. Failure due to heat is defined as "a change in appearance, weight, dimensions, or other properties that alter the material to a degree that it is no longer acceptable for the service in question." This statement is of a qualitative nature and seems to suggest that comparison testing of candidate geomembranes for critical situations be done or that new samples be used for each incubation time and tensile tests be performed for comparison purposes.

Cold Temperatures.   Testing to evaluate the effect of cold on geomembranes follows along the same general lines as testing the effects of heat, but the behavior of the material is, of course, completely opposite. Cold will generally not degrade the geomembrane in any appreciable way, at least under temperatures normally encountered. Furthermore, tests on a variety of geomembranes and different seam types have shown no adverse effects to cyclic cold temperatures for 500 cycles (see Hsuan et al. [32]). The only meaningful effect that cold has on the constructability of the system is that flexibility is decreased and seams are more difficult to make. The latter point is perhaps the most significant aspect of extremely cold conditions. The proposed seaming method should be attempted at site-installation temperatures on test specimens on simulated subgrades and evaluated to see that a satisfactory seam strength will indeed result.

Thermal Expansion and Contraction.   There are a number of procedures that can be used to determine the coefficient of thermal contraction or expansion of a material—for example, ASTM D2102 and D2259 for contraction, and D1042 and D1204 for expansion and dimensional changes. All of them subject the test specimen to a constant source of cold (or heat) and carefully measure the separation distance between two given initial locations. Some typical data are presented in Table 5.10. Example 5.3 uses these data to illustrate the effect during the installation of a geomembrane.

TABLE 5.10   COEFFICIENTS OF THERMAL EXPANSION/CONTRACTION

Polymer Type	Thermal Expansion/Contraction ($\times 10^{-5}/°C$)
Polyethylene	
High density	11–13
Medium density	14–16
Low density	10–12
Linear low density	15–25
Polypropylene	5–9
Polyvinyl chloride	
Unplasticized (e.g., pipe)	5–10
Plasticized (e.g., geomembrane)	7–25
Polyamide	
Nylon 6	7–9
Nylon 66	7–9
Polystyrene	3–7
Polyester	5–9

Example 5.3

Calculate the amount of expansion that is generated during the installation of a HDPE liner for a surface impoundment anticipating a 40°C temperature increase. Base the calculations on a 30 m distance and the range of thermal expansion values of Table 5.10.

Solution:

$$\text{Minimum expansion: } 11 \times 10^{-5} \, (40)(30)(1000) = 132 \text{ mm}$$
$$\text{Maximum expansion: } 13 \times 10^{-5} \, (40)(30)(1000) = 156 \text{ mm}$$

It is easily seen that the calculated amounts in Example 5.3 are quite significant and that considerations for temperature expansion or contraction are important field-placement issues.

Oxidation.   Whenever a free radical is created (e.g., on a carbon atom in the polyethylene chain), oxygen can create progressive long-term degradation. Oxygen combines with the free radical to form a hydroperoxy radical, which is passed around within the molecular structure. It eventually reacts with another polymer chain, creating a new free radical and causing chain scission. The reaction generally accelerates once it is triggered, as shown in the following equations:

$$R^{\cdot} + O_2 \longrightarrow ROO^{\cdot}$$
$$ROO^{\cdot} + RH \longrightarrow ROOH + R^{\cdot}$$
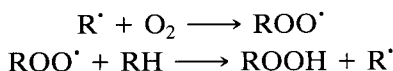
where

$R^{\cdot}$	=	free radical
$ROO^{\cdot}$	=	hydroperoxy free radical
RH	=	polymer chain
$ROOH$	=	oxidized polymer chain

Antioxidation additives (called antioxidants, or AOs) are added to the compound to scavenge these free radicals in order to halt, or at least to interfere with, the process. These additives, or stabilizers, are specific to each type of resin (recall Table 1.6). This area is very sophisticated and quite advanced, with all resin and additive producers being involved in a meaningful and positive way. The specific antioxidants that are used are usually proprietary (see Hsuan et al. [33] for a review of the topic). The removal of oxygen from the geomembrane's surface, of course, eliminates the concern. Thus, once placed and covered with waste or liquid, degradation by oxidation will be greatly retarded due to the starved oxygen conditions. Conversely, exposed geomembranes or those covered by nonsaturated soil will be proportionately more susceptible to the phenomenon. It should be recognized that oxidation of polymers will eventually, perhaps after hundreds of years, cause degradation even in the absence of other types of degradation phenomena.

There are two related test methods that are used to track the amount and/or depletion of antioxidants. They are called *oxidative induction time* (OIT) tests and are performed with a DSC device, as described in Section 1.2.2.

- *Standard OIT* (ASTM D3895 or ISO 11357): The oxidation is conducted at 35 kPa and 200°C. This test appears to misrepresent antioxidant packages containing thiosynergists and/or hindered amines due to the relatively high test temperature.
- *High Pressure OIT* (ASTM D5885): The oxidation is conducted at 3500 kPa and 150°C. This test can be used for all types of antioxidant packages and is the preferred test.

By conducting a series of simulated incubations at elevated temperatures, OIT testing can be conducted on retrieved specimens to monitor the antioxidant depletion rate. As will be seen in Section 5.1.5, this leads to lifetime prediction via Arrhenius modeling.

Synergistic Effects.   Each of the previous degradation phenomena has been described individually and separately. In practice, however, it is likely that two or more mechanisms are acting simultaneously. For example, a waste containment geomembrane may have anaerobic leachate above it and a partially saturated leak detection network containing oxygen below it. Thus chemical degradation from above and oxidation degradation from below will be acting on the liner. Additionally, elevated temperature from decomposing solid waste and the local stress situation may complicate the situation further. Evaluation of these various phenomena is the essence of lifetime prediction.

5.1.5 Lifetime Prediction

Clearly, the long-time frames involved in evaluating individual degradation mechanisms at field-related temperatures and stresses, compounded by synergistic effects, are not providing answers regarding geomembrane lifetime behavior fast enough for the decision-making practices of today. Thus accelerated testing, either by high stress, elevated temperatures and/or aggressive liquids, is very compelling. Lifetime prediction methods use the following ways of interpreting the data:

- *Stress limit testing:* A method used by the HDPE pipe industry in the United States for determining the value of hydrostatic design basis stress [34].
- *Rate process method:* Used for pipes and geomembranes, the method is comparable to the above and is common in Europe [35].
- *Hoechst multiparameter approach:* A method that utilizes biaxial stresses and stress relaxation for lifetime prediction [36] and can include seams as well [37, 38].
- *Arrhenius modeling:* The author's preferred method for geomembranes (and other geosynthetics) and will be described in detail.

Elevated Temperature Incubation and Arrhenius Modeling.   While the research community has regularly used elevated temperature incubation and Arrhenius modeling for lifetime prediction of plastics products [39], it was Mitchell and Spanner [40] who first attempted simulating in situ conditions of a geomembrane beneath a

solid waste landfill. They superimposed compressive stress, chemical exposure above and oxidation below, elevated temperature, and long testing time into a single experimental device. At the Geosynthetic Research Institute, 20 such columns have been constructed with five each maintained at 85, 75, 65 and 55°C constant temperatures (see Figure 5.14). Each is under a normal stress of 260 kPa and is under 300 mm of liquid head on its upper surface. The subgrade sand is dry and vented to the atmosphere. The test coupons are from a commercially available 1.5 mm thick HDPE geomembrane and are 150 mm in diameter. Coupons are removed periodically and evaluated for changes in numerous physical, mechanical, and chemical test properties. The typical behavior is shown in Figure 5.15a.

Stage A is the time required for depletion of the antioxidants. The assessment method is the oxidative induction time (OIT) test as described in Section 1.2.2. For this particular product the standard OIT response is shown in Figure 5.16a. By replotting on a semilog axis, as in Figure 5.16b, the slopes can be taken and plotted as in Figure 5.16c. The two curves are for standard OIT and high pressure OIT and are seen to be parallel. Thus for this antioxidant package either test can be used. (See Hsuan and Koerner [41] for relevant details.) Based on Figure 5.16b, the generalized equation for each straight line is

$$\ln(\text{OIT}) = \ln(P) - (S)(t) \tag{5.12}$$

where

OIT = oxidative induction time (min),
P = constant; the original value of OIT (min),
S = OIT depletion rate (min/mo), and
t = incubation time (mo).

The next step is to extrapolate the OIT depletion rate down to the site-specific temperature. The Arrhenius equation for Figure 5.16c is used:

$$S = A \exp[-E/(RT)] \tag{5.13}$$
$$\ln(S) = \ln(A) + [-E/(RT)] \tag{5.14}$$

where

E = activation energy under these conditions (kJ/mol),
R = gas constant (8.31 J/mol),
T = test temperature (K), and
A = constant.

Using the above from Figure 5.16c for standard OIT, $S = 56$ kJ/mol and for HP-OIT, $S = 58$ kJ/mol. That is, they are very close to one another, which indicates that either OIT
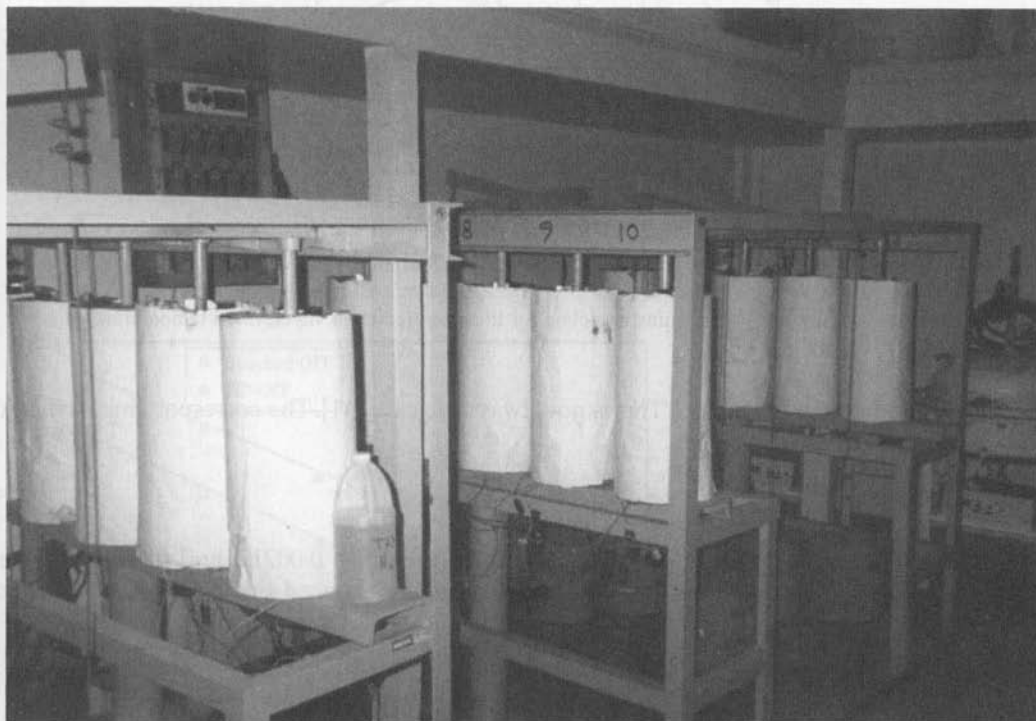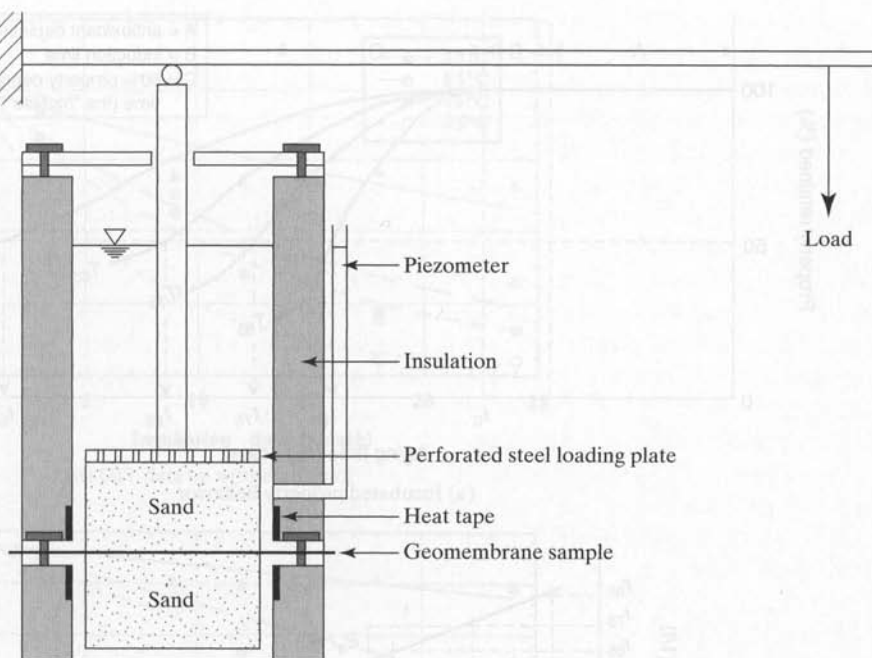
Figure 5.14   Diagram of the incubation setup for accelerated aging; photograph of a number of similar units used at the Geosynthetic Research Institute.
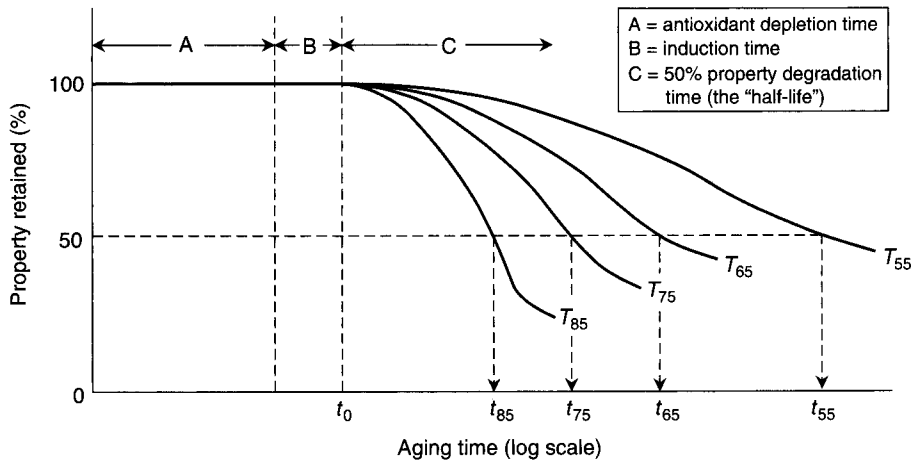
(a) Incubated property behavior
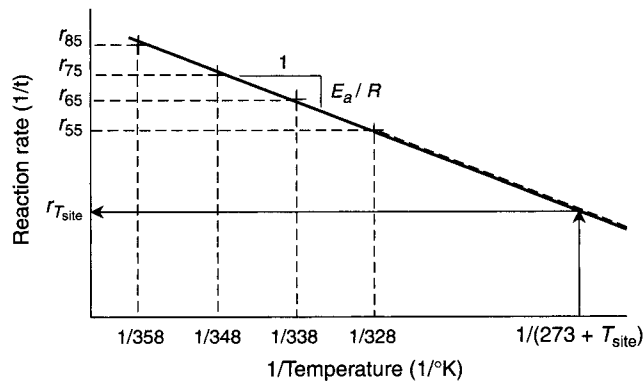
(b) Arrhenius plot for half-life property

Figure 5.15   Arrhenius modeling for lifetime prediction via elevated temperature aging.

test method could be used. This is not always the case [41]. The corresponding Arrhenius equation is the following:

$$\ln(S) = 17.045 - 6798/T \tag{5.15}$$

If a site-specific temperature of 20°C is used, then $S = 0.00212$, and the extrapolated lifetime for AO depletion (the value of 0.5 minutes is used since a log-scale does not allow for zero minutes) is as follows:

$$\ln(0.5) = \ln(80.5) - 0.000212t$$
$$t = 2,397 \text{ mo}$$
$$t = 200 \text{ yr}$$
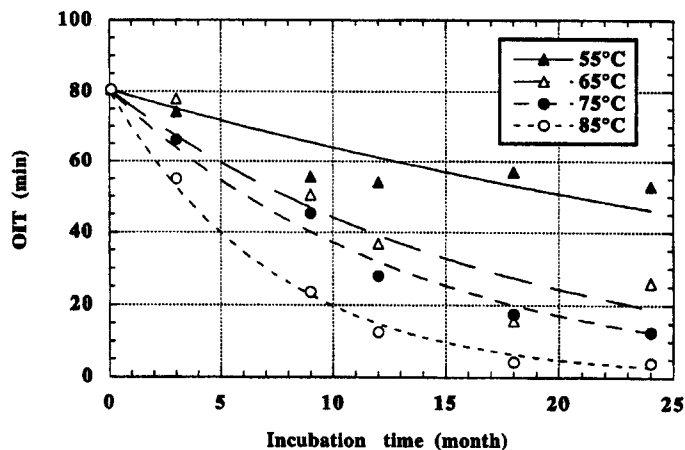
(a) OIT data on arithmetic plot
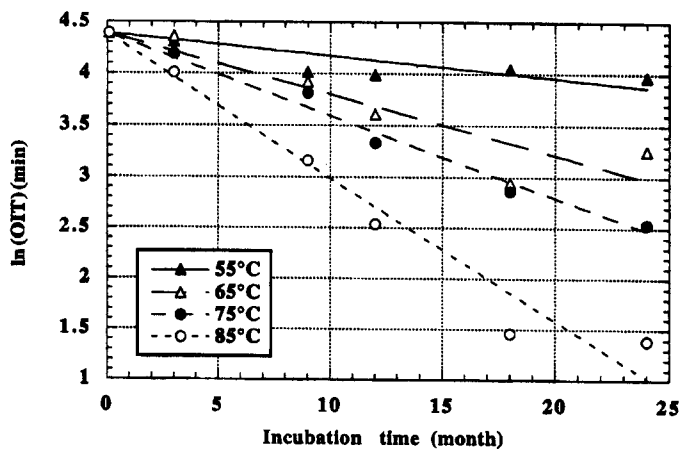
(b) OIT data replotted on semilog axis
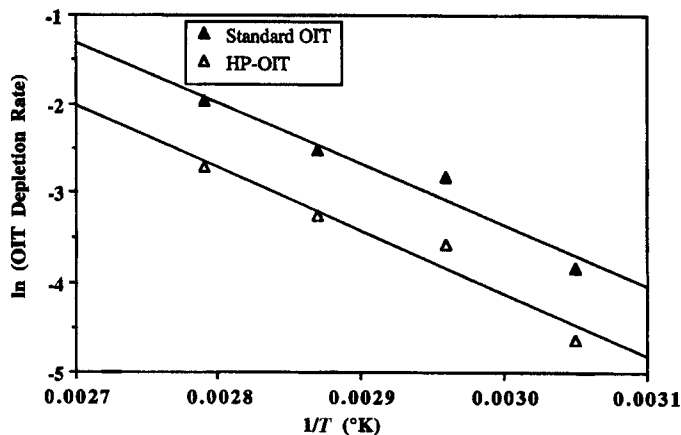
(c) Arrhenius plot of temperature response of OIT reduction

Figure 5.16 Procedure for determining antioxidant depletion time, which is Stage *A* in Figure 5.15a.

Had the calculation been done for HP-OIT from an original value of 210 mins down to 20 mins, the time would have been 215 yr.

Stage B in Figure 5.15a is the induction time. This can be described chemically but also intuitively. It is the time between depletion of the antioxidants and the onset of measurable degradation of engineering properties. These would include change of strength, loss of elongation, change in molecular weight, etc. In order to estimate this stage, the author located 30-year old HDPE milk and water containers at the bottom of a failed landfill and compared them with similar new containers. As is customary practice, short lifetime milk and water containers do not contain long-term antioxidants such that there is no stage A as there is for geomembranes. Table 5.11 shows that yield and modulus values remain the same, but break stress and strain were beginning to decrease beyond the statistical accuracy of the tests. The opinion reached is that the induction time is approximately 30 years at a temperature of 20°C, which was the situation for these containers.

Stage C must identify a target value of property change that is meaningful yet still acceptable. The 50% change in an engineering property (such as elongation at failure), the so-called half-life, is often selected. This is shown on Figure 5.15a for the four different temperature response curves. Taking the 50% property retained times and inverting these values to a reaction rate allows for plotting the Arrhenius plot, as in Figure 5.15b. Note that the abscissa is inverse temperature.

We can now extrapolate graphically to a lower site-specific temperature, as shown in Figure 5.15b, or we can extend the curve analytically. Examples 5.4 and 5.5 illustrate how this is accomplished analytically using literature values for the activation energy (see [39] for additional details). The essential equation for the extrapolation is

$$\frac{r_{T\text{-test}}}{r_{T\text{-site}}} = e^{-\frac{E_{act}}{R}\left[\frac{1}{T\text{-test}} - \frac{1}{T\text{-site}}\right]} \tag{5.16}$$

where

E_{act}/R = slope of Arrhenius plot,

T-test = incubated (high) temperature, and

T-site = site-specific (lower) temperature

TABLE 5.11   RESULTS OF TENSILE TESTING OF NEW VERSUS OLD HDPE CONTAINERS

Property	Milk Containers (average of 3 samples)			Water Container (1 sample)		
	New (average)	Old (average)	Change (%)	New	Old	Change (%)
Yield stress (MPa)	24	22	n/c	25	24	n/c
Yield strain (%)	11	11	n/c	11	11	n/c
Modulus (MPa)	550	507	n/c	650	580	n/c
Break stress (MPa)	22	14	−36	35	22	−37
Break strain (%)	990	730	−26	1700	970	−43

Abbreviations: n/c = no change

Example 5.4

Using experimental data from Martin and Gardner [42] for the half-life of the tensile strength of a PBT plastic, the E_{act}/R value is $-12,800$ K. Determine the estimated life, extrapolating from the 93°C actual incubation temperature (which took 300 hr to complete) to a site-specific temperature of 20°C.

Solution: After converting from centigrade to Kelvin

$$\frac{r_{93°C}}{r_{20°C}} = e^{-\frac{E_{act}}{R}\left[\frac{1}{93+273} - \frac{1}{20+273}\right]}$$

$$= e^{-12,800\left[\frac{1}{366} - \frac{1}{293}\right]}$$

$$= 6083$$

If the 93°C reaction takes 300 hr to complete, the comparable 20°C reaction would take

$$r_{20°C} = 6083(300)$$
$$= 1,825,000 \text{ hr}$$
$$= 208 \text{ yr}$$

Thus the predicted time for this particular polymer to reach 50% of its original strength at 20°C is approximately 200 yr, its predicted lifetime for Stage C.

Example 5.5

Using Underwriters Laboratory Standards [43] data for HDPE cable shielding, the E_{act}/R value is $-14,000$ K. This comes from the half-life of impact strength tests. One of the high temperature tests was at 196°C and it took 1000 hr to obtain these data. What is the life expectancy of this material at 90°C?

Solution: After converting from centigrade to Kelvin

$$\frac{r_{196°C}}{r_{90°C}} = e^{-\frac{E_{act}}{R}\left[\frac{1}{196+273} - \frac{1}{90+273}\right]}$$

$$= e^{-14,000\left[\frac{1}{469} - \frac{1}{363}\right]}$$

$$= 6104$$

If the 196°C reaction takes 1000 hr to complete, the comparable 90°C reaction will take

$$r_{90°C} = 6104(1000)$$
$$= 6,104,000 \text{ hr}$$
$$= 697 \text{ yr}$$

Thus the predicted time for this particular polymer to reach 50% of its original impact strength at 90°C is approximately 700 yr, its predicted lifetime for Stage C.

Summarizing the predicted lifetime of the HDPE geomembrane evaluated in this section leads to an estimated half-life of approximately 550 years (see Table 5.12). It is important to recognize, however, that temperatures higher than 20°C will cause lifetime to exponentially decrease. At 40°C, the predicted lifetime of the same geomembrane is approximately 90 years. In situ temperatures of landfill liners and covers (for both dry and wet landfills) is an ongoing research project at the Geosynthetic Research Institute.

TABLE 5.12 LIFETIME PREDICTION OF A BACKFILLED HDPE GEOMEMBRANE AS A FUNCTION OF IN SITU SERVICE TEMPERATURE[1]

In-Service Temperature (°C)	Stage A (yr)		Stage B (yr)	Stage C (yr)			Total Prediction[2] (yr)
	Std-OIT	HP-OIT		Ref. [44]	Ref. [42]	GSI Data	
20	200	215	30	740	208	8	555
25	135	144	25	441	100	7	348
30	95	98	20	259	49	6	221
35	65	67	15	154	25	5	142
40	45	47	10	93	13	4	93

[1]Exposed geomembrane lifetimes are considerably less than the values in this table.
[2]Total = Stage A (average) + Stage B + Stage C (average)

5.1.6 Summary

This relatively long section on properties and test methods has, hopefully, served to illustrate the wealth of test methods available for characterization and design considerations of geomembranes. Many of the tests and related test methods have come by way of the plastics and rubber industries for nongeotechnical-related uses. This is fortunate, for it gives a base or reference plane to work from. However, for many some variation is required before they can be used in below-ground construction. Still other demands require completely new tests and test methods. In standards-setting institutes throughout the world, there is an awareness of the problems and vibrant activity to develop such test methods and procedures. Until they are available, however, we must act on intuition and develop methods that model the required design information as closely as possible. Many of the tests conducted and the information presented in this section are done in that light. It should also be obvious that the complexity of the tests have progressed from the quite simple thickness test on smooth geomembranes to the very complex degradation tests. Indeed, a very wide range of test methods are available.

Finally, a rather lengthy discussion of durability and aging gives insight into the potential service lifetime of geomembranes. In a buried environment, the lifetimes promise to be very long. For example, the HDPE geomembrane evaluated promises to far outlast other engineering materials in comparable situations. In my experience with geosynthetics over the past 25 years, my original thought was that geosynthetics were easy to place but would not last very long. This has shifted dramatically to where I sense extremely long service lifetimes, but I have very real concerns as to the proper installation of geosynthetics. Clearly, the geosynthetic material must survive its initial placement if these long predicted lifetimes are to be achieved.

5.2 SURVIVABILITY REQUIREMENTS

In order for any of the design methods presented in this chapter to function properly, it is necessary that the geomembrane survive the packaging, transportation, handling,

and installation demands that are placed on it. This aspect of design cannot be taken lightly or assumed simply to take care of itself. Yet there is a decided challenge in presenting a generalized survivability design for every application, since each situation is unique. Some of the major variables affecting a given situation are the following:

- Storage at the manufacturing facility
- Handling at the manufacturing facility
- Transportation from the factory to the construction site
- Offloading at the site
- Storage conditions at the site
- Temperature extremes at the site
- Subgrade conditions at the site
- Deployment at the approximate location
- Movement into the final seaming location
- Treatment at the site during seaming
- Exposure at the site after seaming
- Placement of the cover material or soil backfill on the completed geomembrane

Note that each of these factors is largely out of the hands of the designer. Only by rigid specifications, a complimentary construction quality assurance (CQA) document, competent *full-time* inspection by CQA personnel, and cooperation of the installation contractor can the geomembrane survive to the point of beginning to function as designed. The U.S. Environmental Protection Agency has a technical guidance document focused on many of these issues [45]. Remembering that each situation is surely different, empirical guidelines are necessary and some properties and their minimum values are offered in Table 5.13.

TABLE 5.13   RECOMMENDED MINIMUM PROPERTIES FOR GENERAL GEOMEMBRANE INSTALLATION SURVIVABILITY

Property and Test Method	Required Degree of Installation Survivability			
	Low[1]	Medium[2]	High[3]	Very High[4]
Thickness (D1593) (mm)	0.63	0.75	0.88	1.00
Tensile D882 (25 mm strip) (kN/m)	7.0	9.0	11	13
Tear (D1004 Die C) (N)	33	45	67	90
Puncture (D4833) (N)	110	140	170	200
Impact (D3998 mod.) (J)	10	12	15	20

[1]Careful hand placement on a very uniform well-graded subgrade with light loads of a static nature, typical of vapor barriers beneath building floor slabs.

[2]Hand or machine placement on smooth machine-graded subgrade with medium load, typical of canal liners.

[3]Hand or machine placement on machine-graded subgrade of poor texture with high loads; typical of landfill liners and covers.

[4]Hand or machine placement on machine-graded subgrade of very poor texture with high loads, typical of liners for heap leach pads and construction/demolition wastes.

Geomembranes are most often vulnerable to tear, puncture, and impact while being stored, transported, handled, installed, and backfilled. Such events often come about accidentally, due to vandalism or to poor workmanship. Typical situations are the dropping of tools on the geomembrane, the driving of vehicles on the unprotected liner, the force of high winds getting beneath the geomembrane during placement, the awkwardness of moving large sheets of the geomembrane into position, and the quality of backfilling material and operations. The geomembrane property most involved with resistance or susceptibility to tear, puncture, and impact damage is thickness. At least a linear, and sometimes an exponential, increase in resistance to the above actions is seen as thickness increases. For this reason many agencies require a minimum thickness under any circumstance. For example, the U.S. Bureau of Reclamation requires a minimum thickness of 0.50 mm for canal liners, while the U.S. Environmental Protection Agency requires a minimum thickness for geomembranes for solid-waste liners of 0.75 mm. For similar applications in Germany, the use of a 2.0 mm thick geomembrane is required. Rather than use a single regulated value for all conditions, however, the minimum thickness and its subsequent properties should be related to site-specific conditions. Using a concept similar to the placement of geotextiles, Table 5.13 shows four required survivability levels. Note that these values are to be used as a check on design, not in place of design, to see that installation can be properly ensured.

5.3 LIQUID CONTAINMENT (POND) LINERS

The U.S. Environmental Protection Agency estimates that there are over 200,000 surface impoundments storing hazardous and nonhazardous liquids in the United States, the vast majority of which are unlined. This total does not include potable water and nonregulated reservoirs and impoundments. Worldwide, the number is unknown, but it is obviously enormous. Certainly there is a major need for and use of geomembranes to provide liquid containment of surface impoundments. In fact, the name *geomembrane* is actually one that supersedes the name *pond liner*, reflecting the original use of the polymeric materials to which this section is devoted. In addition to containment of the above types of liquids, the agriculture industry has a pressing need to store liquid waste and water, and hence both the U.S. Department of Agriculture and the U.S. Bureau of Reclamation were involved in early research into synthetic pond liners. While thermoset (rubber) liners may have been used prior to the 1930s, the use of polyvinyl chloride sheeting for liners began in the 1940s. When covered with a minimum of 300 mm of soil, these PVC liners apparently performed well. Uncovered, however, there was a tendency for progressive brittleness and cracking. Other thermoplastic liner materials, less susceptible to this problem, followed in rapid succession (e.g., CSPE-R). Today, all of the geomembrane materials listed in Table 5.1 are used for the containment of liquids with the various types of polyethylene being most common.

5.3.1 Geometric Considerations

Before selecting the geomembrane type, the desired liquid volume to be contained versus the available land area must be considered. Such calculations are geometric by

nature and result in a required depth on the basis of assumed sideslope angles. For a square or rectangular section with uniform side slopes, the general equation for volume is

$$V = HLW - SH^2L - SH^2W + 2S^2H^3 \tag{5.17}$$

where

V = volume of reservoir,

H = average height (i.e., depth) of the reservoir,

W = width at ground surface,

L = length at the ground surface, and

S = slope ratio (horizontal to vertical).

Equation (5.17) can be solved in a variety of ways, and various design curves can be generated. Such design curves are given in Figure 5.17 for a side-slope angle of 18.4°, which is 3 to 1 (horizontal to vertical), written as $3(H)$ to 1 (V), and a square configuration. Example 5.6 illustrates the use this concept.

Example 5.6

A square area 125 by 125 m is available for constructing a reservoir for storage of 60,000,000 liters of industrial process water. At estimated side slopes of $3(H)$ to $1(V)$, what is the required average height (i.e., depth of the pond)?

Solution:

$$\text{Volume} = 60,000,000 \text{ liters}$$
$$= 60,000 \text{ m}^3$$
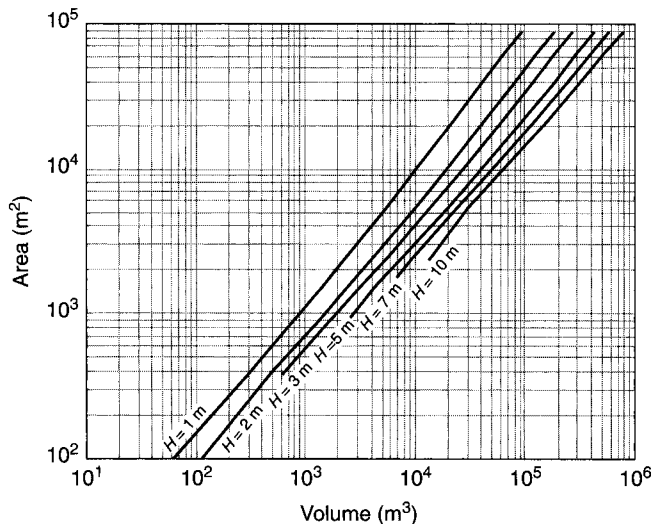
Figure 5.17 Volume-versus-area design chart for liquid containment ponds with side slopes of $3(H)$ to $1(V)$.

Using equation (5.17),

$$60,000 = H(125)(125) - (3)H^2(125)$$
$$- (3)H^2(125) + 2(9)H^3$$
$$60,000 = 15,625H - 750H^2 + 18H^3$$
$$H = 4.83 \text{ m}$$

Note that the above result agrees with the curves given in Figure 5.17; however, the lined impoundment must be somewhat deeper to allow for freeboard against overfilling, wave action, and so on.

From Example 5.6, it can be seen that to contain large volumes of liquids we will require massive land areas and/or deep containment pits. If such a land area is not available, the required depths often lead to additional problems, such as interception of the water table, difficulty in stabilizing the bottom and sides of the excavation, interception of unsuitable soil conditions, interception of bedrock, high excavation costs, and excavated soil disposal problems.

These problems are compounded in areas with soft cohesive soils or granular cohesionless soils in which very flat side slopes or geosynthetically reinforced slopes are required, as described in Section 3.2.7.

5.3.2 Typical Cross Sections

Upon first consideration, digging a hole, putting a liner in it, and then filling it with the liquid to be contained is simplicity itself. Indeed, for an ideal site, with proper liner material, proper construction techniques, and maintenance during its service lifetime, it is a straightforward task. Figure 5.18a shows such a liner on a prepared soil subgrade anchored in trenches around the perimeter of the site. Unfortunately, such ideal conditions and situations are seldom encountered.

The first complication has to do with atmospheric exposure and possible damage to the geomembrane. To shield the liner from ozone, ultraviolet light, temperature extremes, ice damage, wind stresses, accidental damage, and vandalism, a soil cover of at least 300 mm thickness is usually required. Vandalism is particularly troublesome in areas of noncontrolled site access. Figure 5.18b shows that the soil cover extends up out of the pit and over the liner anchorage areas. This soil cover is particularly troublesome on the side slopes, where gravitational sloughing of the cover soil compounded by liquid drawdown is often a problem. Friction between the liner and cover soil must be evaluated, and the appropriate design procedures must follow. This aspect is discussed later in this section.

The use of a geotextile beneath the geomembrane (Figures 5.18c, d), placed directly on the prepared soil subgrade before liner placement, is considered proper design for a number of reasons [46].

- It provides a clean working area for making field seams.
- It provides added puncture resistance when loads (either during construction or from the cover soil) are applied.
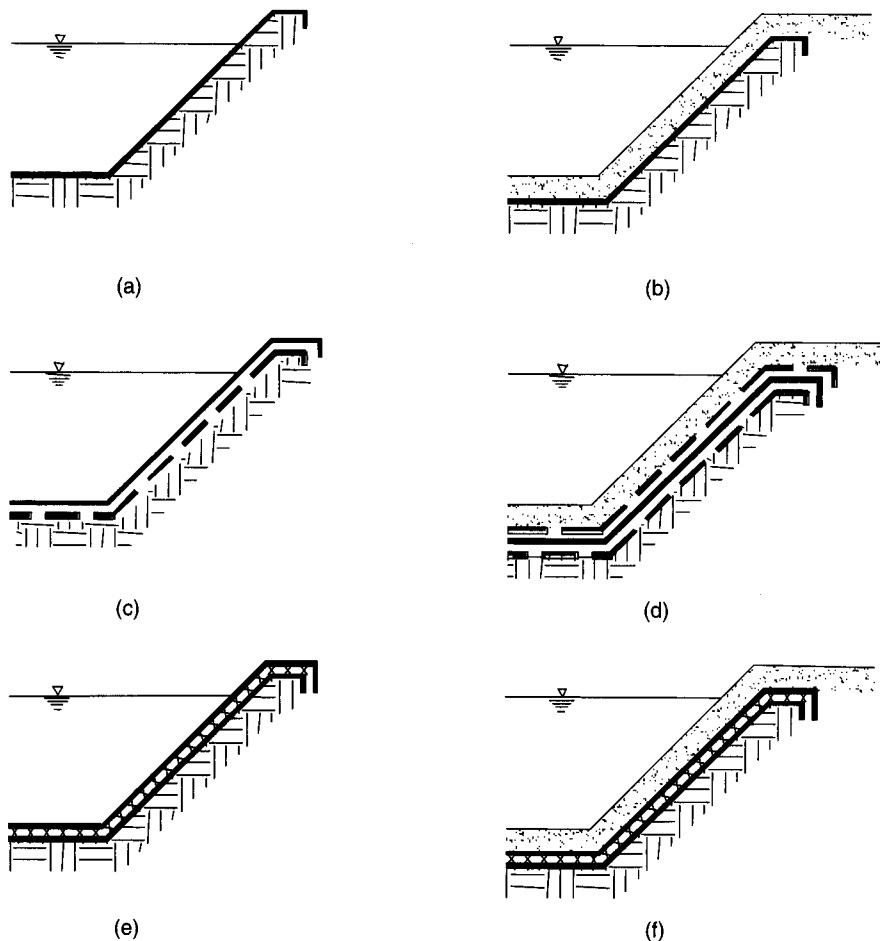
Figure 5.18 Various types of geomembrane liner systems for liquid-containment: (a) single unprotected liner system; (b) liner with soil covering; (c) liner with geotextile underliner; (d) liner with geotextile underliner and overliner with soil covering; (e) double-liner with geonet leak detection between liners; (f) double-liner with geonet leak detection between liners and soil covering, which may or may not contain a geotextile or geogrid as veneer reinforcement.

- It can add frictional resistance to the geomembrane-to-soil interface, thereby preventing excessive stresses on the geomembrane as it enters the anchor trench or allowing for steepened side slopes.
- If properly selected, the geotextile will allow for lateral and upward escape of subsurface water and gases that rise up beneath the geomembrane during its service life (see Figure 5.19). Upward-moving water is caused by high groundwater
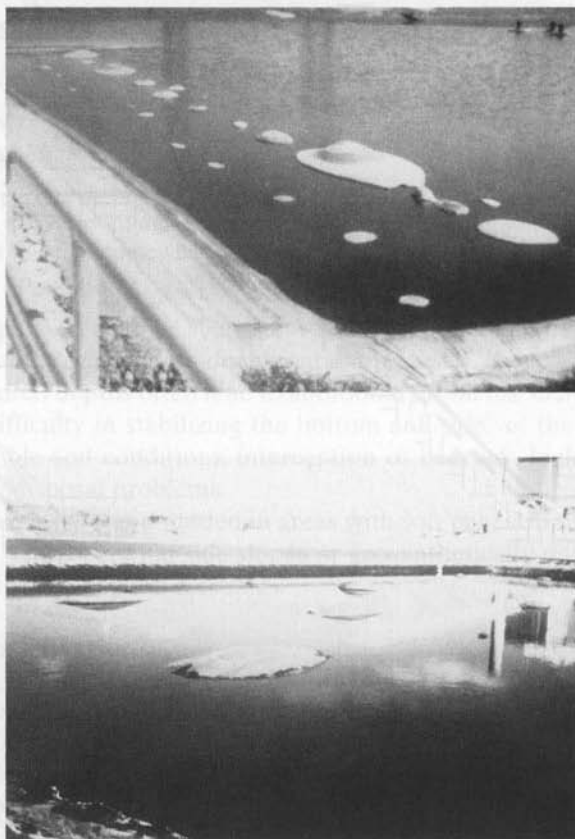
Figure 5.19 Subsurface generated gases pushing up a geomembrane reservoir liner, creating very high stresses on liner and seams.

levels and flooding conditions in nearby water courses. Upward-moving gases are caused by biodegradation of organic material in the subsurface soils and from rising water-table levels that expel the air from the soil voids. In such cases, nonwoven needle punched geotextiles, geonets, or drainage geocomposites with sufficient transmissivity to handle the estimated flows are required. Example 5.7 illustrates the procedure.

Example 5.7

Consider a 7 m deep geomembrane-lined pond that will create a barrier to rising gases from the biodegradation of the organic silt soil, as shown in the following diagram. The width of the impoundment is 200 m, with the grade rising up from the center as shown. An estimate of gas generation is 0.10 m^3/day-m^2 at a pressure of 7.0 kPa. Assume that the density of moist air is 0.0118 kN/m^3. The proposed underliner to be used is a 550 g/m^2 nonwoven needle-punched geotextile. What is the factor of safety of this geotextile's transmissivity for this set of conditions?
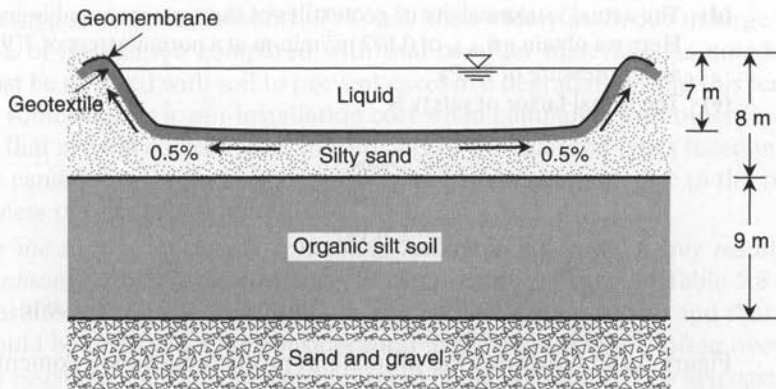
Solution:

(a) The flow rate is

$$q = 0.10 \left(\frac{200}{2} \times 1 \right)$$

$q = 10$ m³/day, at the higher elevation

$$= \frac{10}{(24)(60)}$$

$$= 6.94 \times 10^{-3} \text{ m}^3/\text{min}$$

(b) The air gradient, assuming a uniform distribution of 7.0 kPa at the center to zero at the edge, is

$$i = \frac{\Delta P / \gamma_{\text{air}}}{L/2}$$

$$= \frac{7.0/0.0118}{200/2}$$

$$i = 5.9$$

(c) Although this problem is probably not one of laminar-flow conditions, we use Darcy's formula since it is a conservative approach and air-flow transmissivity data are available in the literature.

$$q = kiA$$

$$= ki(t \times W)$$

$$kt = \theta_{\text{reqd}} = \frac{q}{i \times W}$$

$$\theta_{\text{reqd}} = \frac{6.94 \times 10^{-3}}{(5.9)(1.0)}$$

$$= 1.18 \times 10^{-3} \text{ m}^3/\text{min} - \text{m}$$

(d) The actual transmissivity of geotextiles of the type proposed is given in Figure 2.19a. Here we obtain a θ_{allow} of 0.192 m^3/min-m at a normal stress of 7(9.81) $\cong$ 70 kPa and an air pressure of 7 kPa.

(e) The actual factor of safety is

$$\begin{aligned} FS &= \frac{\theta_{allow}}{\theta_{reqd}} \\ &= \frac{0.192}{0.00118} \\ FS &= 162 \quad \text{which is more than adequate} \end{aligned}$$

Figure 5.18d illustrates the ultimate in protection of the geomembrane where it is sandwiched between two geotextiles. The underlying geotextile serves the same purposes just discussed. The overlying one is useful to maintain stability of the side slope cover soil and to prevent stones in the cover soil from puncturing the geomembrane. The latter point is a consideration only if properly graded cover soil is not available and poor-quality soil must be used. This type of composite design is also becoming customary in the secondary containment of underground storage tanks for groundwater protection.

Figure 5.18e illustrates a double-lined surface impoundment with a geonet leak detection system between liners. The first use of a geonet in 1984 was of this type, which is still in use for storing hazardous liquid at a private site in Virginia. The variation shown in Figure 5.18f has soil covering of the upper (primary) geomembrane for its protection and to shield it from ultraviolet degradation. Oftentimes, such coverings need reinforcement by means of a geotextile or geogrid inclusion. This topic is covered in Section 3.2.7 under veneer reinforcement.

Figure 5.18 does not show the various alternatives using geosynthetic clay liners and/or compacted clay liners. The variations are enormous and are clearly site-specific vis-a-vis the liquid to be contained.

It should also be mentioned that federal and state regulations could very well prescribe a cross section that is considered to be minimum technology guidance (MTG). Generally, a double liner cross section with leak detection is necessary if the stored liquid is hazardous and a single composite liner (geomembrane and compacted clay or a geosynthetic clay liner) if the liquid is nonhazardous. The variations in regulations are significant among the different regulatory agencies.

5.3.3 Geomembrane Material Selection

Concerning the selection of the type of resin to be used in the manufacture of the liner itself, chemical resistance to the contained liquid is of utmost importance. The entire design process becomes ludicrous in the absence of such chemical resistance. Furthermore, this resistance must be considered for the entire service life of the particular installation. Considerations for various liquids follow:

- *For potable water storage*, service lifetimes of approximately 20 years must be considered. This is similar to general water storage for agricultural use. Of the

liner types noted in Table 5.1, PVC has been widely used, due in large part to its ease of installation compared with that of other materials. As noted earlier, it must be covered with soil to prevent excessive degradation, and this tends to offset somewhat its lower installation cost when compared with other liner materials that are not soil covered. Indeed, any of the material types listed in Table 5.1 are candidates for potable or storage water containment, due to the relative inertness of this type of liquid.

- *For the storage of liquids containing known acids, bases, heavy metals, salts, or commonly stored chemicals*, the chemical resistance chart in Table 5.8 should be consulted. Note that most manufacturers have similar charts and that these too should be reviewed. One consideration in this regard that is often overlooked is the resistance of the seams to the liquid being contained. This is particularly important for adhesive-bonded seams and less so for thermal, extrusion, and solvent seams. (Seams are described in Section 5.11.)

- *For the storage of liquids that are combinations of industrial process effluents*, the most aggressive of the individual liquids to polymeric materials should be used for the selection process. This assumes that there are no synergistic effects occurring within the different liquids that may be placed in the reservoir. For the majority of these situations, chemical resistance charts are available (as in Table 5.8) for proper material selection.

- *For the storage of liquids that are an unidentifiable* or of an unknown variety (e.g., from industrial processes that are in the design stage and not yet on-stream) or for leachates of a very heterogeneous nature, extreme conservatism must be used. Because of its relative inertness with chemicals, HDPE will often be the material of choice. Seaming is done by thermal fusion or extrusion welding, with no foreign material additives used. It is prudent, however, and oftentimes required to incubate coupons in the laboratory using the synthesized liquid to see if reactions are occurring. This procedure is described in Section 5.1.4.

5.3.4 Thickness Considerations

There are several empirical relationships between geomembrane thickness and the depth of the contained liquid. While geomembrane thickness is indeed related to the pressures exerted upon it, such empirical guides are completely unfounded and certainly not in keeping with the technical-based design that will follow. This design is related to the subsurface deformation that the liner might experience during its service lifetime. Such deformations can come about in a number of ways: by random differential settlement of subgrade soils, by settlement of backfilled zones beneath the geomembrane (e.g., in pipe trenches), by localized settlements around soft areas beneath the geomembrane, by seismic disturbances that may modify the subgrade conditions, and by any kind of anomalous conditions that deforms the geomembrane and places it in tension.

The basic model we will work from (see Figure 5.20) requires a deformation mobilized tensile force to occur. Here deformation is induced by one of the settlement mechanisms mentioned above, thereby defining the value of β that must be assumed in
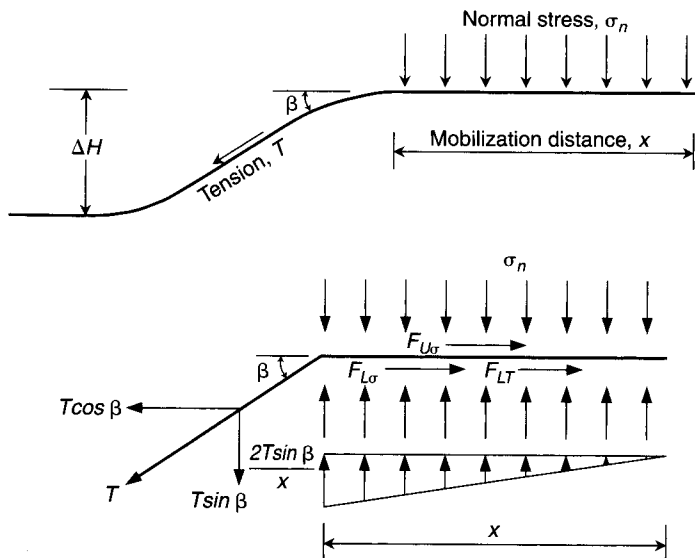
Figure 5.20 Design model and related forces used to calculate geomembrane thickness.

the design process. This induces tension in the geomembrane that is equal to the allowable stress times the unknown thickness.

$$T = \sigma_{\text{allow}} \, t$$

where

T = tension mobilized in the geomembrane,

σ_{allow} = allowable geomembrane stress, and

t = thickness of the geomembrane.

The tension is now resolved into its horizontal component, which must be resisted by the shear forces shown in Figure 5.20. Note that the vertical component (which is assumed to be dissipated along the mobilization distance x) must be added to the normal stress imposed by the overlying liquid (and soil if applicable). Thus,

$$\Sigma F_x = 0$$

$$T \cos \beta = F_{U\sigma} + F_{L\sigma} + F_{LT}$$

$$T \cos \beta = \sigma_n \tan \delta_U(x) + \sigma_n \tan \delta_L(x)$$

$$+ \, 0.5\left(\frac{2T \sin \beta}{x}\right)(x) \tan \delta_L$$

$$T = \frac{\sigma_n x (\tan \delta_U + \tan \delta_L)}{\cos \beta - \sin \beta \tan \delta_L}$$

But $T = \sigma_{allow}\, t$, so

$$t = \frac{\sigma_n x (\tan \delta_U + \tan \delta_L)}{\sigma_{allow}(\cos \beta - \sin \beta \tan \delta_L)} \tag{5.18}$$

where

β = settlement angle mobilizing the geomembrane tension,

$F_{U\sigma}$ = shear force above geomembrane due to liquid pressure (note that if liquid is being contained, the shear stress is zero; this is essentially the same even if a thin soil cover is above the geomembrane since cracking will likely occur),

$F_{L\sigma}$ = shear force below geomembrane due to the overlying liquid pressure (and soil if applicable),

F_{LT} = shear force below geomembrane due to the vertical component of T,

σ_n = applied stress from reservoir contents,

δ = angle of shearing resistance between geomembrane and the adjacent material (i.e., soil or geotextile), and

x = distance of mobilized geomembrane deformation.

The general ranges of the variables above are as follows:

σ_n = 20 to 100 kPa ($\cong 2$ to 10 m of liquid)

β = 0 to 60°,

x = 15 to 100 mm (determined from the laboratory test described in Section 5.1.3; see Figure 5.10),

σ_{allow} = 6000 to 30,000 kPa (determined from laboratory tests described in Section 5.1.3; see Figure 5.3),

δ_U = 0° for liquid containment and 10 to 40° for landfill containment (determined from laboratory tests described in Section 5.1.3), and

δ_L = 10 to 40° (determined from laboratory tests described in Section 5.1.3).

Example 5.8 shows the procedure to be used for a specific case.

Example 5.8

Determine the thickness of a geomembrane to be used in the containment of a 7 m deep water reservoir where the settlement over a backfilled collector pipe could result in a 45° settlement angle. The geomembrane is a textured LLDPE of 8000 kPa allowable stress. There is only a thin soil cover over the geomembrane (i.e., $\delta_U \cong 0$) and a nonwoven needle-punched geotextile is to be placed beneath it ($\delta_L = 25°$). The estimated mobilized distance for liner deformation is 50 mm.

Solution: Using equation (5.18), we obtain the required thickness:

$$t = \frac{\sigma_n x (\tan \delta_U + \tan \delta_L)}{\sigma_{allow}(\cos \beta - \sin \beta \tan \delta_L)}$$

$$= \frac{(68.7)(0.050)[\tan 0 + \tan 25]}{(8000)[\cos 45 - (\sin 45)(\tan 25)]}$$

$$= \frac{1.60}{3018}$$

$$= 0.00053 \text{ m}$$

$$t = 0.53 \text{ mm}$$

Figure 5.21 carries the procedure further into a set of design curves for the conditions cited therein. Note that the result is in terms of a thickness coefficient, which when multiplied by the height of liquid in meters (water is assumed) gives the required geomembrane thickness in millimeters. Other types of design charts can also be generated, but all are based on the premise that a subsidence occurs beneath the geomembrane, giving rise to the analysis. If no subsidence occurs, this type of analysis is not appropriate and thickness is based on installation and/or regulatory minimum values.

Note that adequate geomembrane thickness cannot be addressed solely on the basis of the analysis above. Other factors, such as construction equipment driving on the geomembrane during liner installation or reservoir cleaning operations during its service lifetime can impose severe stresses on the liner. Since all mechanical properties of the liner increase with thicker geomembranes, there is usually a minimum thickness that is recommended irrespective of design calculations. As shown in Table 5.13, this value is 0.63 mm. Some regulatory agencies, however, have their own minimum
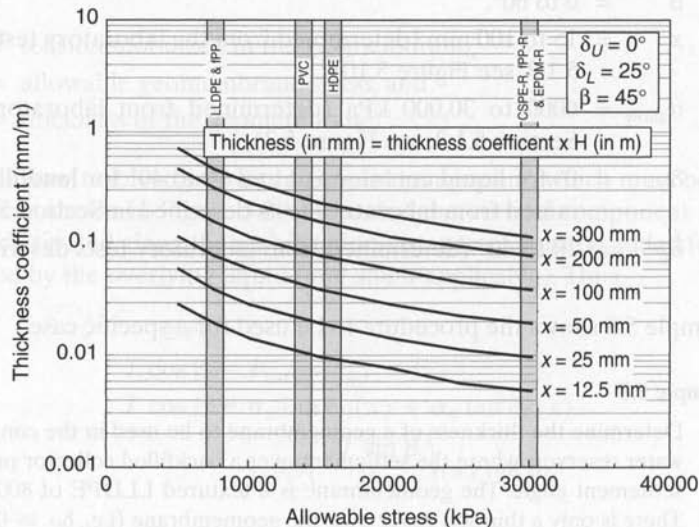
Figure 5.21 Design curves for geomembrane thickness based on unit height of water.

thickness standards that, if greater than the above value, would take precedence in those specific instances.

5.3.5 Side-Slope Considerations

The design of soil side slopes for liquid retention ponds falls within the scope of geotechnical engineering with some minor modifications. The analyses involved can be as simple or as detailed as the particular situation warrants. For the purposes of this particular section, separate aspects of the problem considering both side slope subgrade soil stability (with and without a geomembrane) and the stability of cover soils placed over the geomembrane will be treated.

Side Slope Subgrade Soil Stability. In considering the general slope stability of the soil mass beneath a geomembrane, a circular failure arc is generally assumed to be the mode of likely failure. In keeping with this assumption, several classes of failures can occur. As presented in Figure 5.22, these failures are base failure, toe failures (either beyond or within the anchor trench), and a slope failure.
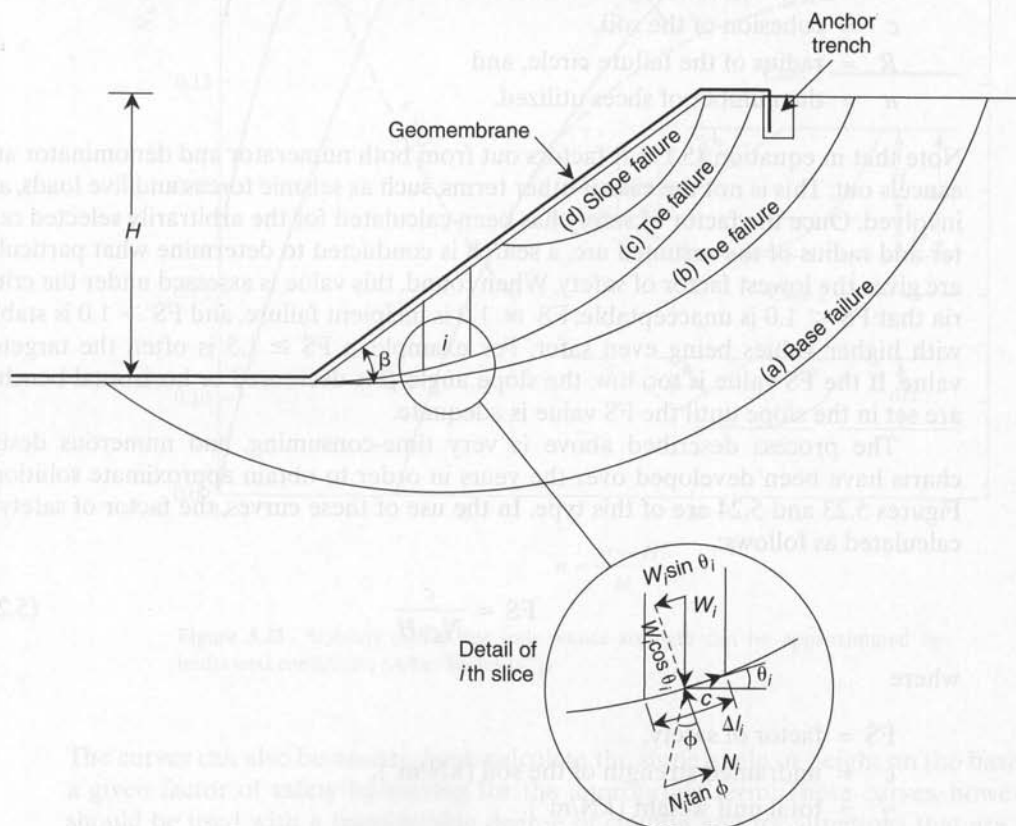
Figure 5.22   Various types of geomembrane-covered soil slope stability failures.

The usual design procedure involves the slope height, the soil properties, and the soil shear strength parameters, and has as its unknown the slope angle β. Furthermore, a total stress analysis is customary, since the entire site is generally above the water table and in an equilibrium state. Proceeding on the basis of an assumed center of rotation and radius, the procedure for the circles labeled (a) and (b) in Figure 5.22 is to subdivide the mass involved into vertical slices and to take moment equilibrium about the center of rotation. This yields the following factor of safety equation:

$$\text{FS} = \sum_{i=1}^{n} \frac{[(W_i \cos \theta_i) \tan \phi + \Delta l_i c] R}{(W_i \sin \theta_i) R} \tag{5.19}$$

where

W_i = weight of the ith slice,
θ_i = angle the ith slice makes with the horizontal,
Δl_i = arc length of the ith slice,
ϕ = angle of shearing resistance of the soil,
c = cohesion of the soil,
R = radius of the failure circle, and
n = the number of slices utilized.

Note that in equation (5.19) R factors out from both numerator and denominator and cancels out. This is not the case if other terms, such as seismic forces and live loads, are involved. Once the factor of safety has been calculated for the arbitrarily selected center and radius of the assumed arc, a search is conducted to determine what particular arc gives the lowest factor of safety. When found, this value is assessed under the criteria that FS < 1.0 is unacceptable, FS $\cong$ 1.0 is incipient failure, and FS > 1.0 is stable, with higher values being even safer. For example, a FS $\geq$ 1.5 is often the targeted value. If the FS value is too low, the slope angle β is decreased or horizontal benches are set in the slope until the FS value is adequate.

The process described above is very time-consuming, and numerous design charts have been developed over the years in order to obtain approximate solutions. Figures 5.23 and 5.24 are of this type. In the use of these curves, the factor of safety is calculated as follows:

$$\text{FS} = \frac{c}{N_S \gamma H} \tag{5.20}$$

where

FS = factor of safety,
c = undrained strength of the soil (kN/m^2),
γ = total unit weight (kN/m^3),
H = vertical height of slope (m), and
N_S = stability number taken from Figure 5.23 or 5.24.
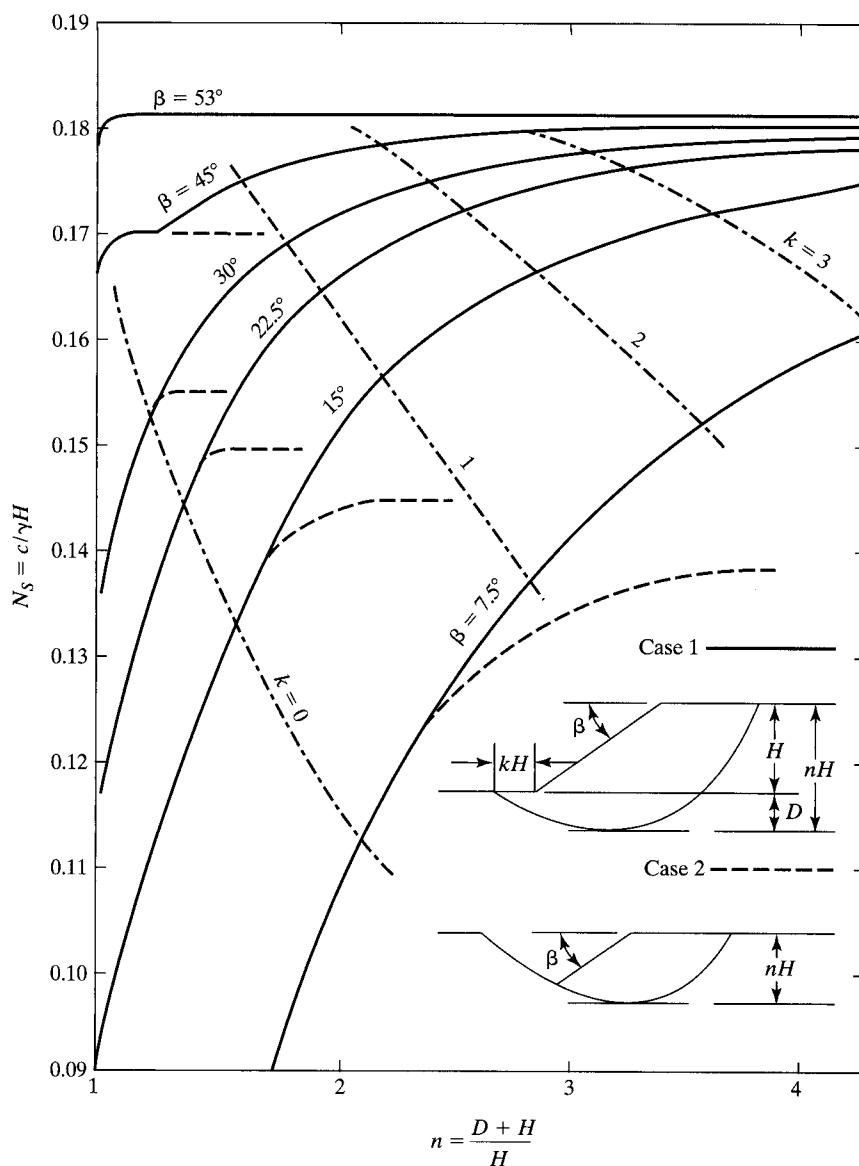
Figure 5.23 Stability curves for soils whose strength can be approximated by undrained conditions. (After Taylor [47])

The curves can also be used to back-calculate the slope angle or height on the basis of a given factor of safety by solving for the appropriate term. These curves, however, should be used with a considerable degree of caution and for situations that are not considered to be critical (e.g., where a failure would not cause loss of life or serious property damage). Example 5.9 demonstrates the use of one of the charts.
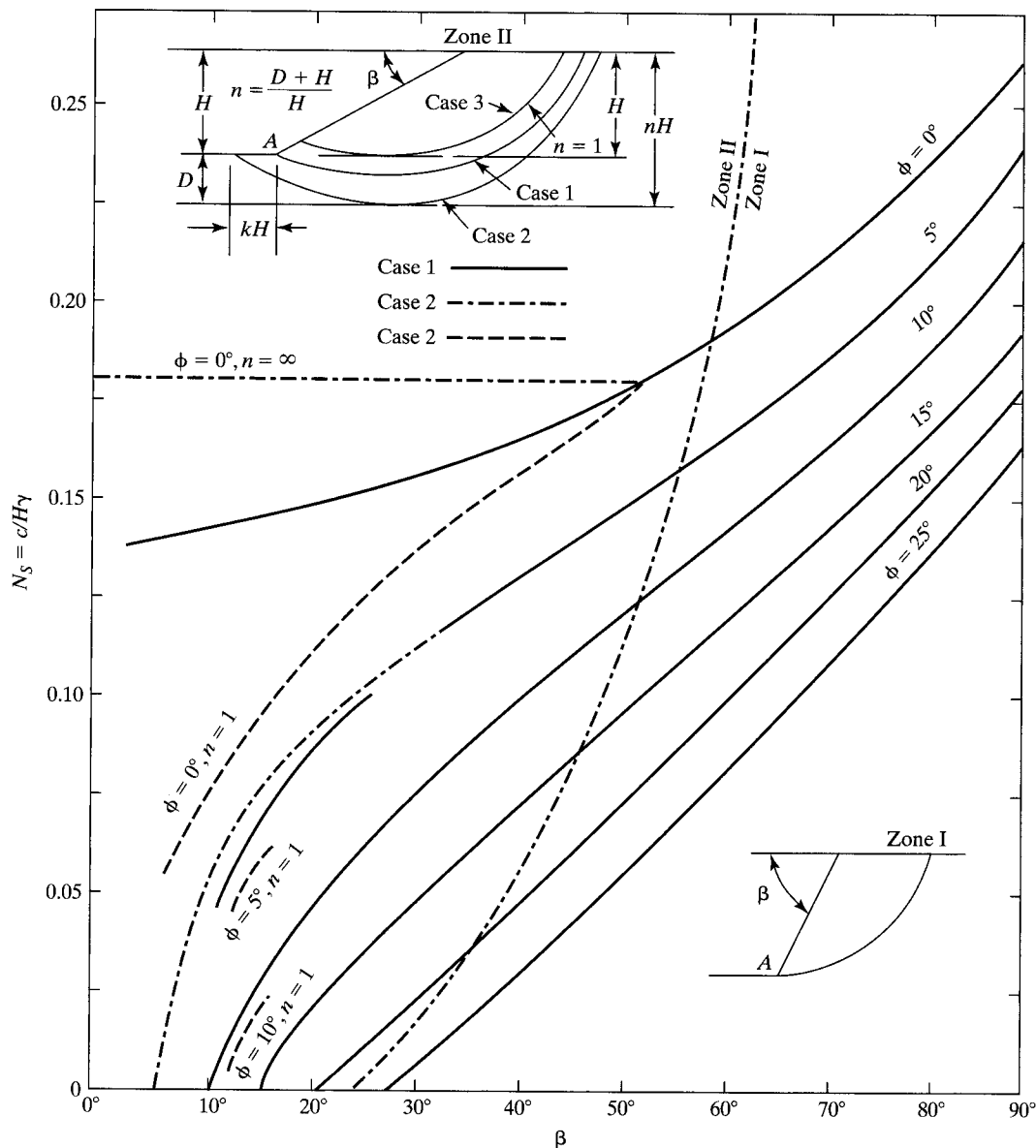
Figure 5.24 Stability curves for soils whose strength comes about from cohesion and friction. (After Taylor [47])

Example 5.9

A 4 m deep geomembrane-lined reservoir is to be placed in an area where the soil has an undrained shear strength of 14 kN/m² and a total unit weight of 15 kN/m³. There is a hard layer of sand and gravel 3 m beneath the bottom of the proposed reservoir; thus a base

failure to this depth is envisioned. What slope angle will be required on the basis of FS = 1.5?

Solution: Working from equation (5.20) for FS = 1.5 and Figure 5.23

$$FS = \frac{c}{N_S \gamma H}$$

$$1.5 = \frac{14}{N_S(15)(14)}$$

$$N_S = 0.155$$

and for

$$n = \frac{D + H}{H}$$

$$= \frac{3 + 4}{4}$$

$$= 1.75$$

using Figure 5.23, the required slope angle is 20°, which is approximately 2.7(H) to 1.0(V).

Regarding the failure circles labeled (c) and (d) in Figure 5.22, a slight variation can be considered. If the liner is covered with a soil layer and if the liner is in tension as it comes up the slope and enters into the anchor trench (as it usually is), a tensile force can be included in the analysis. The factor-of-safety equation then becomes

$$FS = \sum_{i=1}^{n} \frac{[(W_i \cos \theta_1) \tan \phi + (\Delta l_i)c]R + Ta}{(W_i \sin \theta_i)R} \tag{5.21}$$

where (in addition to the terms previously defined)

$T \quad = \sigma_{allow} \, t$, in which

$\sigma_{allow} =$ allowable strength of the geomembrane,

$t \quad =$ thickness of the geomembrane, and

$a \quad =$ the moment arm equal to R as its maximum.

If a geotextile underliner and/or overliner is used in conjunction with the geomembrane, it is to be included in a similar manner. Whatever the case, the net effect is to increase the factor of safety for a given circle location and radius. If we omit the term entirely, the error is on the conservative side. Regarding such a tensile force at the bottom of the failure arc, it is felt to be rarely of benefit. Certainly, if the liner is not covered with soil, there is no normal stress to mobilize resistance and, even if covered, the net effect is minimal.

Due to their tedious and repetitive nature, slope-stability calculations are well suited for computer adaptation. Many such programs exist and can readily be adapted for inclusion of the tensile forces just described.

Side Slope Cover Soil Stability—Infinite Slope.   In general, geomembranes should be covered. There are numerous reasons for this, including the following: protection against oxidation, protection against ultraviolet degradation, minimization of elevated temperature that increases degradation, protection against ice puncture in cold climates, protection against puncturing or tearing by sharp objects, elimination of wind uplift, protection against accidental damage, and protection against intentional

damage. The usual covering is a relatively thin layer of soil, which has the unfortunate tendency when placed on side slopes to slide gravitationally downward. The accumulated soil gathers at the toe of the slope and part of the denuded geomembrane is thereby exposed. The design method to prevent this unraveling of cover soils from occurring is straightforward and based on limit equilibrium conditions. Figure 5.25a shows a segment of subsoil, geomembrane, and cover soil having a uniform thickness. For this set of conditions a force summation equation along the slope angle β can be written, resulting in a factor of safety against failure.

$$FS = \frac{\text{resisting forces}}{\text{driving forces}}$$

$$= \frac{F}{W \sin \beta}$$

$$= \frac{N \tan \delta}{W \sin \beta}$$

$$= \frac{W \cos \beta \tan \delta}{W \sin \beta}$$

$$FS = \frac{\tan \delta}{\tan \beta} \tag{5.22}$$

where

β = slope angle, and

δ = friction angle between the geomembrane and its cover soil.

(Note that failure will occur at the cover soil interface because the geomembrane is held in place at the upper ground surface by the horizontal runout and anchor trench.) The design process for this situation is usually one where the slope angle β is known and a factor of safety is selected, leaving the friction angle between the geomembrane and the cover soil unknown. Since the type of geomembrane is probably already selected, it is seen that the quality of the cover soil or the possibility of geomembrane texturing are the ultimate variables.

Example 5.10

What type of soil is required for covering an CSPE-R liner on a 3(H) to 1(V) slope using a (relatively low) factor of safety of 1.3?

Solution: A 3-to-1 slope is a slope angle of 18.4°. Using equation (5.22) gives the required friction angle between the geomembrane and the cover soil.

$$FS = \frac{\tan \delta}{\tan \beta}$$

$$1.3 = \frac{\tan \delta}{\tan 18.4}$$

$$\tan \delta = 0.433$$

$$\delta = 23.4°$$

Going to the data in Table 5.7a for CSPE-R, we see that concrete sand has a δ-value that is acceptable. Also notice that neither the Ottawa sand nor Mica shist sand would be suitable.

(a) Infinite slope

To anchor trench

Geomembrane

W

$W \cos \beta$

$W \sin \beta$

$N \tan \delta$

N

δ

Cover soil

β

(b) Finite slope with uniform cover soil thickness

Active wedge

L

W_A

h

Geomembrane

W_P

E_P

$N_A \tan \delta$

C_a

Passive wedge

E_A

N_A

C

$N_P \tan \phi$

β

N_P

(c) Finite slope with tapered cover soil thickness

Active wedge

W_A

h_c

C_A

W_p

$E_P(\omega + \beta)/2$

Geomembrane

Passive wedge

y

E_A

$N_A \tan \delta$

C

$N_p \tan \phi$

N_A

D

L

ω

N_P

β
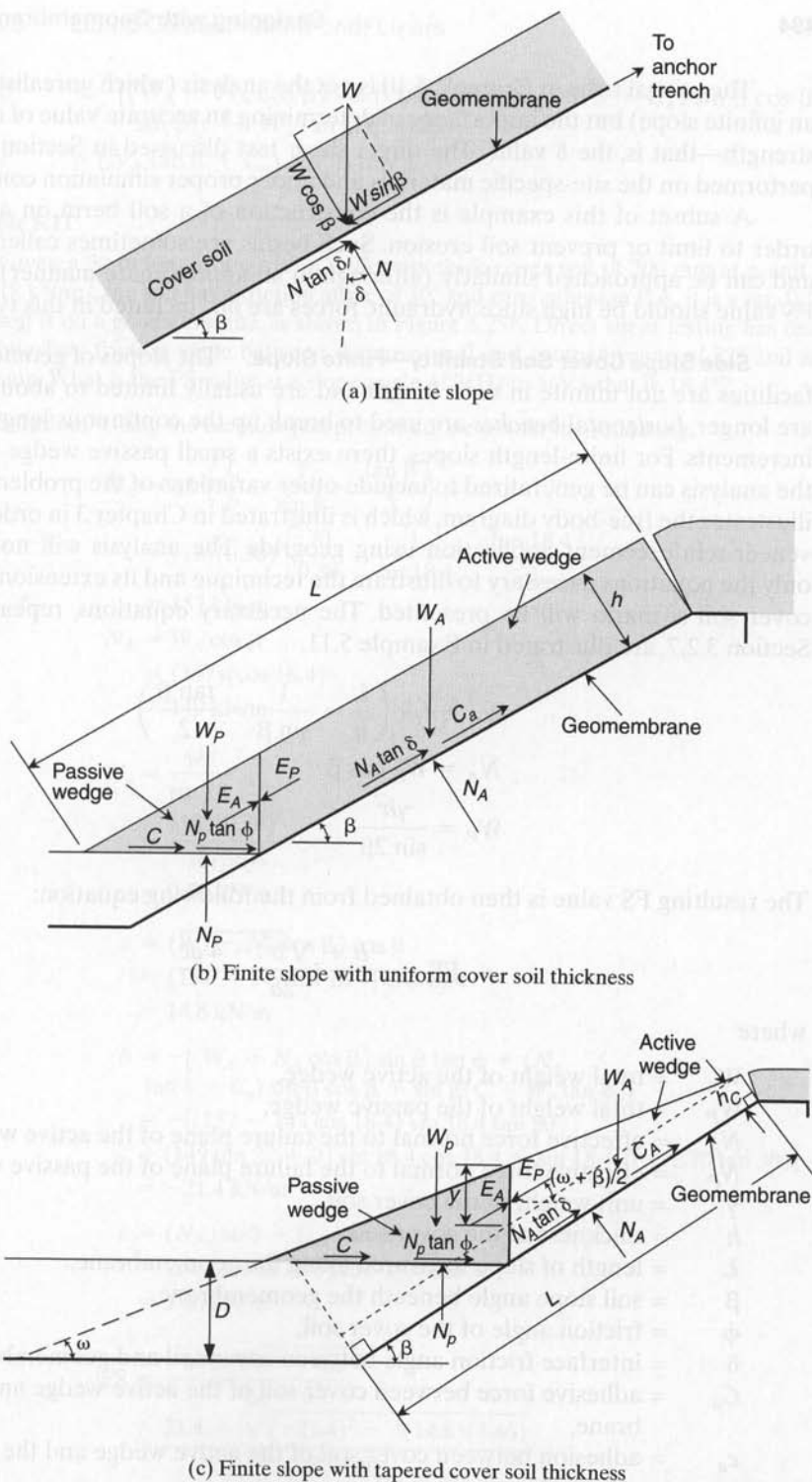
Figure 5.25 Schematic diagrams for forces involved with cover soils on geomembrane-lined slopes.

493

The critical issue in Example 5.10 is not the analysis (which unrealistically assumes an infinite slope) but the importance of determining an accurate value of interface shear strength—that is, the δ value. The direct shear test discussed in Section 5.1.3 must be performed on the site-specific materials and under proper simulation conditions.

A subset of this example is the construction of a soil berm on a long slope in order to limit or prevent soil erosion. Such berms are sometimes called *tack-on berms* and can be approached similarly (although in an approximate manner). The required FS value should be high since hydraulic forces are not included in this type of analysis.

Side Slope Cover Soil Stability—Finite Slope.   The slopes of geomembrane-lined facilities are not infinite in their length and are usually limited to about 30 m. If they are longer, *horizontal benches* are used to break up the continuous length into smaller increments. For finite-length slopes, there exists a small passive wedge at the toe and the analysis can be generalized to include other variations of the problem. Figure 5.25b illustrates the free-body diagram, which is illustrated in Chapter 3 in order to set up the veneer-reinforcement application using geogrids. The analysis will not be repeated; only the equations necessary to illustrate the technique and its extension into a tapered cover soil scenario will be presented. The necessary equations, repeated here from Section 3.2.7, are illustrated in Example 5.11.

$$W_A = \gamma h^2\left(\frac{L}{h} - \frac{1}{\sin \beta} - \frac{\tan \beta}{2}\right)$$

$$N_A = W_A \cos \beta$$

$$W_P = \frac{\gamma h^2}{\sin 2\beta}$$

The resulting FS value is then obtained from the following equation:

$$FS = \frac{-b + \sqrt{b^2 - 4ac}}{2a}$$

where

W_A = total weight of the active wedge,
W_P = total weight of the passive wedge,
N_A = effective force normal to the failure plane of the active wedge,
N_P = effective force normal to the failure plane of the passive wedge,
γ = unit weight of the cover soil,
h = thickness of the cover soil,
L = length of slope measured along the geomembrane,
β = soil slope angle beneath the geomembrane,
ϕ = friction angle of the cover soil,
δ = interface friction angle between cover soil and geomembrane,
C_a = adhesive force between cover soil of the active wedge and the geomembrane,
c_a = adhesion between cover soil of the active wedge and the geomembrane,
a = $(W_A - N_A \cos \beta) \cos \beta$,

$$b = -[(W_A - N_A \cos \beta) \sin \beta \tan \phi + (N_A \tan \delta + C_a) \sin \beta \cos \beta + \sin \beta (C + W_p \tan \phi)], \text{ and}$$

$$c = (N_A \tan \delta + C_a) \sin^2 \beta \tan \phi.$$

Example 5.11

Given a 30 m long slope with a uniformly thick cover soil of 300 mm at a unit weight of 18 kN/m³, the soil has a friction angle of 30° and zero cohesion (i.e., it is a sand). The cover soil is on a geomembrane, as shown in Figure 5.25b. Direct shear testing has resulted in a interface friction angle between the cover soil and geomembrane of 22° and zero adhesion. What is the FS value at a slope angle of 3(H) to 1(V), that is, 18.4°?

Solution: Using the formula just presented, we obtain the following:

$$W_A = \gamma h^2 \left(\frac{L}{h} - \frac{1}{\sin \beta} - \frac{\tan \beta}{2} \right)$$

$$= (18)(0.30)^2 \left[\frac{30}{0.30} - \frac{1}{\sin 18.4} - \frac{\tan 18.4}{2} \right]$$

$$= 157 \text{ kN/m}$$

$$N_A = W_A \cos \beta$$
$$= (157)(\cos 18.4)$$
$$= 149 \text{ kN/m}$$

$$W_p = \frac{\gamma h^2}{\sin 2\beta}$$

$$= \frac{(18)(0.30)^2}{\sin 36.8}$$

$$= 2.70 \text{ kN/m}$$

$$a = (W_A - N_A \cos \beta) \cos \beta$$
$$= (157 - 149 \cos 18.4) \cos 18.4$$
$$= 14.8 \text{ kN/m}$$

$$b = -[(W_A - N_A \cos \beta) \sin \beta \tan \phi + (N_A \tan \delta + C_a) \sin \beta \cos \beta + \sin \beta (C + W_p \tan \phi)]$$
$$= -[(157 - 149 \cos 18.4) \sin 18.4 \tan 30 + (149 \tan 22 + 0) \sin 18.4 \cos 18.4 + \sin 18.4(0 + 2.70 \tan 30)]$$
$$= -21.4 \text{ kN/m}$$

$$c = (N_A \tan \delta + C_a) \sin^2 \beta \tan \phi$$
$$= (149 \tan 22 + 0) \sin^2 18.4 \tan 30$$
$$= 3.46 \text{ kN/m}$$

$$FS = \frac{-b + \sqrt{b^2 - 4ac}}{2a}$$

$$= \frac{21.4 + \sqrt{(-21.4)^2 - 4(14.8)(3.46)}}{2(14.8)}$$

$$FS = 1.25 \text{ (vs. 1.21 for infinite slope)}$$

Slope ratio (Hor.: Vert.)
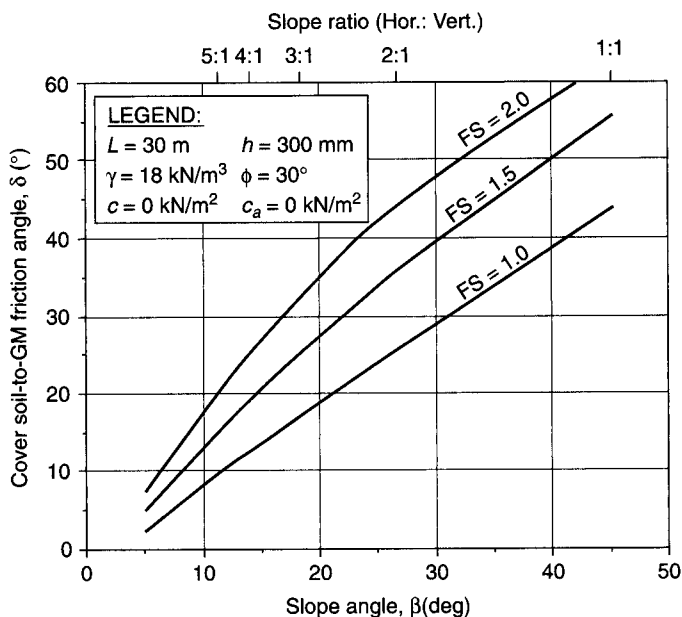
(a) FS values of uniform thickness cover soils

Slope ratio (Hor.: Vert.)
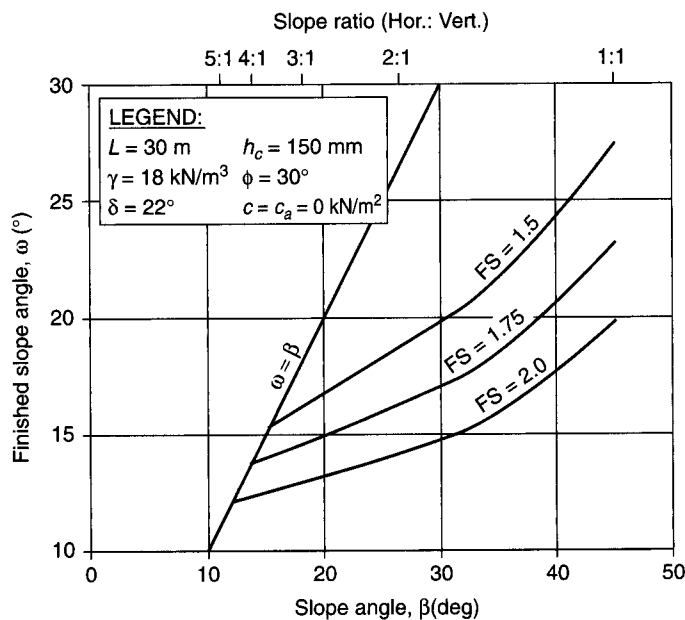
(b) FS values of tapered thickness cover soils

Figure 5.26   Design curves for cover soils on geomembrane-lined slopes.

Example 5.11 has been extended into a set of design curves in Figure 5.26a. As expected the FS value decreases for increasing slope angles and increases for increasing soil-to-geomembrane friction angles. Since the curves have been generated for the same conditions as the example problem, the resulting FS value is easily verified.

It should be noted that there can be a number of destabilizing forces that can reduce the FS value. These are equipment forces when moving *down* the slope, seepage forces within the cover soil, and seismic forces. They are addressed in the manner paralleling this section in Koerner and Soong [17].

Note that there are two commonly used methods to increase the FS value. One is the inclusion of a geogrid or geotextile as veneer reinforcement. This is covered in Section 3.2.7. Less common due to the additional toe space required, but certainly possible, is to use a tapered cover soil thickness.

Side Slope Cover Soil Stability—Tapered Thickness.   From Example 5.11 it is easily seen that cover soils over geomembranes can become unstable quite easily, even under static conditions. To alleviate this situation, it is possible to taper the cover soil, placing it so that it is thicker at the bottom and gradually thinner going toward the top (see Figure 5.25c). Note that the slope of the top of the cover soil is at an angle ω, where $\omega < \beta$. The formulation follows that of the previous section.

Considering the active wedge,

$$W_A = \gamma\left[\left(L - \frac{D}{\sin\beta} - h_c\tan\beta\right)\left(\frac{y\cos\beta}{2} + h_c\right) + \frac{h_c{}^2\tan\beta}{2}\right]$$

$$N_A = W_A\cos\beta$$

$$C_a = c_a\left(L - \frac{D}{\sin\beta}\right)$$

Balancing the forces in the vertical direction, the following formulation results;

$$E_A\sin\left(\frac{\omega + \beta}{2}\right) = W_A - N_A\cos\beta - \frac{N_A\tan\delta + C_a}{FS}(\sin\beta)$$

Hence the interwedge force acting on the active wedge is

$$E_A = \frac{(FS)(W_A - N_A\cos\beta) - (N_A\tan\delta + C_a)\sin\beta}{\sin\left(\dfrac{\omega + \beta}{2}\right)(FS)}$$

The passive wedge is considered in a similar manner:

$$W_P = \frac{\gamma}{2\tan\omega}\left[\left(L - \frac{D}{\sin\beta} - h_c\tan\beta\right)(\sin\beta - \cos\beta\tan\omega) + \frac{h_c}{\cos\beta}\right]^2$$

$$N_p = W_P + E_P\sin\left(\frac{\omega + \beta}{2}\right)$$

$$C = \frac{\gamma}{\tan\omega}\left[\left(L - \frac{D}{\sin\beta} - h_c\tan\beta\right)(\sin\beta - \cos\beta\tan\omega) + \frac{h_c}{\cos\beta}\right]$$

Balancing the forces in the horizontal direction, the following formulation results:

$$E_P \cos\left(\frac{\omega + \beta}{2}\right) = \frac{C + N_P \tan\phi}{FS}$$

Hence, the interwedge force acting on the passive wedge is

$$E_P = \frac{C + W_P \tan\phi}{\cos\left(\dfrac{\omega + \beta}{2}\right)(FS) - \sin\left(\dfrac{\omega + \beta}{2}\right)\tan\phi}$$

Again, by setting $E_A = E_P$, the following equation can be arranged in the quadratic equation form, which in our case is

$$a(FS)^2 + b(FS) + c = 0 \tag{5.23}$$

where

$$a = (W_A - N_A \cos\beta)\cos\left(\frac{\omega + \beta}{2}\right),$$

$$b = -\left[(W_A - N_A \cos\beta)\sin\left(\frac{\omega + \beta}{2}\right)\tan\phi + (N_A \tan\delta + C_a)\sin\beta\cos\left(\frac{\omega + \beta}{2}\right)\right.$$

$$\left. + \sin\left(\frac{\omega + \beta}{2}\right)(C + W_P \tan\phi)\right], \text{ and}$$

$$c = (N_A \tan\delta + C_a)\sin\beta\sin\left(\frac{\omega + \beta}{2}\right)\tan\phi.$$

Again, the resulting FS value can then be obtained as before:

$$FS = \frac{-b + \sqrt{b^2 - 4ac}}{2a} \tag{5.24}$$

where (see also Figure 2.25c and the preceding section)

D = thickness of cover soil at bottom of the slope, measured vertically,

h_c = thickness of cover soil at crest of the slope, measured perpendicular to the slope,

y = $\left(L - \dfrac{D}{\sin\beta} - h_c \tan\beta\right)(\sin\beta - \cos\beta \tan\omega)$, see Figure 5.25c, and

ω = final cover soil slope angle (note that $\omega < \beta$).

Example 5.12

A 30 m long slope has a tapered thickness cover soil of 150 mm at the crest extending at an angle ω of 16° to the intersection of the cover soil at the toe. The soil thickness at the bottom, D, is 300 mm. The unit weight of the cover soil is 18 kN/m³. The soil has a friction

angle of 30° and zero cohesion (i.e., it is a sand). The interface friction angle with the underlying geomembrane is 22° and zero adhesion. What is the FS value at an underlying soil slope angle β of 3(H) to 1(V) which is equal to 18.4°?

Solution:

$$y = \left(L - \frac{D}{\sin \beta} - h_c \tan \beta\right)(\sin \beta - \cos \beta \tan \omega)$$

$$= \left(30 - \frac{0.30}{\sin 18.4} - (0.15) \tan 18.4\right)(\sin 18.4 - (\cos 18.4)(\tan 16))$$

$$= 1.28 \text{ m}$$

$$W_A = \gamma\left[\left(L - \frac{D}{\sin \beta} - h_c \tan \beta\right)\left(\frac{y \cos \beta}{2} + h_c\right) + \frac{h_c^2 \tan \beta}{2}\right]$$

$$= 18\left[\left(30 - \frac{0.30}{\sin 18.4} - (1.28) \tan 18.4\right)\left(\frac{1.28 \cos 18.4}{2} + 0.15\right) + \frac{(0.15)^2 \tan 18.4}{2}\right]$$

$$= 390 \text{ kN/m}$$

$$N_A = W_A \cos \beta$$

$$= 390 \cos 18.4$$

$$= 370 \text{ kN/m}$$

$$W_p = \frac{\gamma}{2 \tan \omega}\left[\left(L - \frac{D}{\sin \beta} - h_c \tan \beta\right)(\sin \beta - \cos \beta \tan \omega) + \frac{h_c}{\cos \beta}\right]^2$$

$$= \frac{18}{2 \tan 16}\left[\left(30 - \frac{0.30}{\sin 18.4} - 1.28 \tan 18.4\right)(\sin 18.4 - \cos 18.4 \tan 16) + \frac{0.15}{\cos 18.4}\right]^2$$

$$= 65.1 \text{ kN/m}$$

$$a = (W_A - N_A \cos \beta) \cos\left(\frac{\omega + \beta}{2}\right)$$

$$= (390 - 370 \cos 18.4) \cos\left(\frac{16 + 18.4}{2}\right)$$

$$= 37.2 \text{ kN/m}$$

$$b = -\left[(W_A - N_A \cos \beta) \sin\left(\frac{\omega + \beta}{2}\right) \tan \phi + (N_A \tan \delta + C_a) \sin \beta \cos\left(\frac{\omega + \beta}{2}\right)\right.$$

$$\left. + \sin\left(\frac{\omega + \beta}{2}\right)(C + W_p \tan \phi)\right]$$

$$= -\left[(390 - 370 \cos 18.4) \sin\left(\frac{16 + 18.4}{2}\right) \tan 30 + (370 \tan 22 + 0)\right.$$

$$\sin 18.4 \cos\left(\frac{16 + 18.4}{2}\right) + \sin\left(\frac{16 + 18.4}{2}\right)(0 + 65.1 \tan 30)\right]$$

$$= -62.8 \text{ kN/m}$$

$$c = (N_A \tan \delta + C_a) \sin \beta \sin\left(\frac{\omega + \beta}{2}\right) \tan \phi$$

$$= (370 \tan 22 + 0) \sin 18.4 \sin\left(\frac{16 + 18.4}{2}\right) \tan 30$$

$$= 8.07 \text{ kN/m}$$

$$\text{FS} = \frac{-b + \sqrt{b^2 - 4ac}}{2a}$$

$$= \frac{62.8 + \sqrt{(-62.8)^2 - 4(37.2)(8.07)}}{2(37.2)}$$

$$\text{FS} = 1.55 \text{ (vs. 1.25 for the constant thickness cross section)}$$

Example 5.12 has also been extended to a set of design curves, as seen in Figure 5.26b. The anticipated trends are again noted, as is the agreement with the worked out example. Clearly, this type of stabilizing solution can be used if space at the toe of the slope is available. Often it is not or it occupies valuable air space and then geosynthetic reinforcement as discussed in Chapter 3 is the alternative solution.

5.3.6 Runout and Anchor Trench Design

As shown in Figure 5.18 and the profile sections of geomembrane-lined reservoirs, the liner coming up from the bottom of the excavation, covers the side slopes, and then runs over the top a short distance. It often terminates vertically down into an anchor trench. This anchor trench is typically dug by a small backhoe or trenching machine; the liner is draped over the edge, and then the trench is backfilled with the same soil that was there originally. The backfilled soil should be compacted in layers as the backfilling proceeds. Although concrete has been used as an anchorage block, it is rarely justified, at least on the basis of calculations, as will be seen in this section.

Regarding design, two separate cases will be analyzed: one with geomembrane runout only and no anchor trench at all (as is often used with canal liners), and the other as described above, with both runout and anchor trench considerations (as with reservoirs and landfills). Figure 5.27 defines the first situation, together with the forces and stresses involved. Note that the cover soil applies normal stress due to its weight but does not contribute frictional resistance above the geomembrane. This is due to the fact that the soil moves along with the geomembrane as it deforms and undoubtedly cracks, thereby losing its integrity.

From Figure 5.27, the following horizontal force summation results, which leads to the appropriate design equation:

$$\Sigma F_x = 0$$

$$T_{\text{allow}} \cos \beta = F_{U\sigma} + F_{L\sigma} + F_{LT}$$

$$= \sigma_n \tan \delta_U (L_{RO}) + \sigma_n \tan \delta_L (L_{RO}) + 0.5\left(\frac{2T_{\text{allow}} \sin \beta}{L_{RO}}\right)(L_{RO}) \tan \delta_L$$

$$L_{RO} = \frac{T_{\text{allow}}(\cos \beta - \sin \beta \tan \delta_L)}{\sigma_n(\tan \delta_U + \tan \delta_L)}$$

$$(5.25)$$
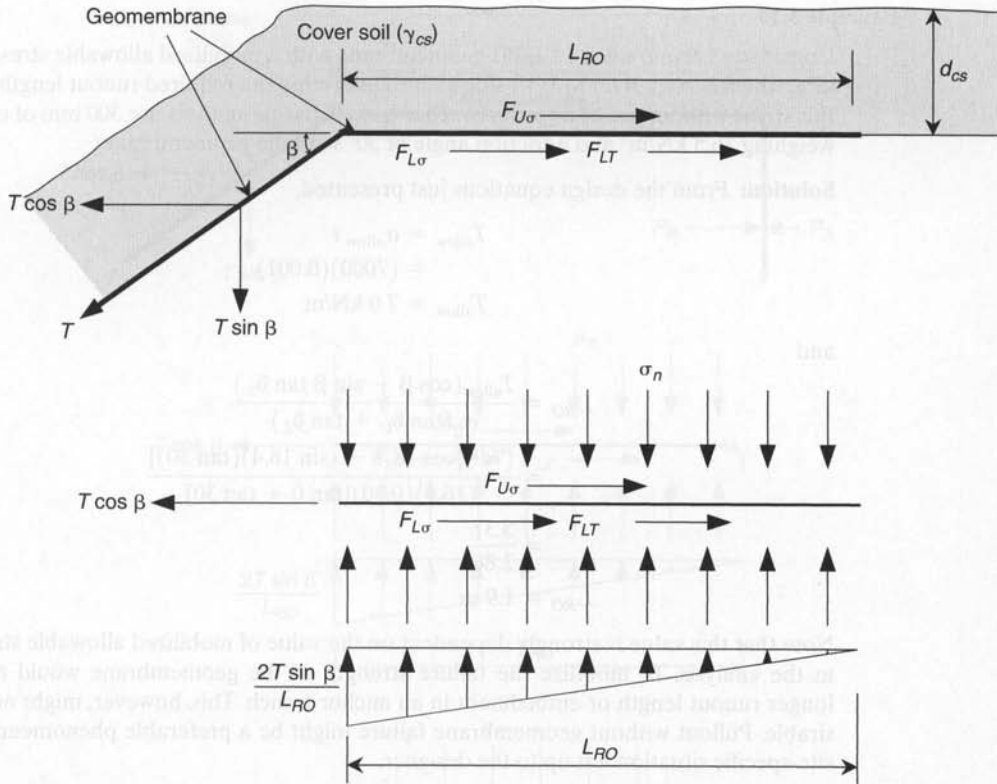
Figure 5.27 Cross section of geomembrane runout section and related stresses and forces involved.

where

T_{allow} = allowable force in geomembrane = $\sigma_{allow}\, t$, where

σ_{allow} = allowable stress in geomembrane, and

t = thickness of geomembrane;

β = side slope angle;

$F_{U\sigma}$ = shear force above geomembrane due to cover soil (note that for thin cover soils tensile cracking will occur and this value will be negligible);

$F_{L\sigma}$ = shear force below geomembrane due to cover soil;

F_{LT} = shear force below geomembrane due to vertical component of T_{allow};

σ_n = applied normal stress from cover soil;

δ = angle of shearing resistance between geomembrane and adjacent material (i.e., soil or geotextile); and

L_{RO} = length of geomembrane runout.

Example 5.13 illustrates the use of the concept and equations just developed.

Example 5.13

Consider a 1.0 mm thick LLDPE geomembrane with a mobilized allowable stress of 7000 kPa, which is on a 3(*H*) to 1(*V*) side slope. Determine the required runout length to resist this stress without use of a vertical anchor trench. In this analysis use 300 mm of cover soil weighing 16.5 kN/m^3 and a friction angle of 30° with the geomembrane.

Solution: From the design equations just presented,

$$T_{allow} = \sigma_{allow}\, t$$
$$= (7000)(0.001)$$
$$T_{allow} = 7.0 \text{ kN/m}$$

and

$$L_{RO} = \frac{T_{allow}(\cos\beta - \sin\beta \tan\delta_L)}{\sigma_n(\tan\delta_U + \tan\delta_L)}$$
$$= \frac{(7.0)[\cos 18.4 - (\sin 18.4)(\tan 30)]}{(16.5)(0.30)[\tan 0 + \tan 30]}$$
$$= \frac{5.37}{2.86}$$
$$L_{RO} = 1.9 \text{ m}$$

Note that this value is strongly dependent on the value of mobilized allowable stress used in the analysis. To mobilize the failure strength of the geomembrane would require a longer runout length or embedment in an anchor trench. This, however, might not be desirable. Pullout without geomembrane failure might be a preferable phenomenon. It is a site-specific situation left up to the designer.

The situation with an anchor trench at the end of the runout section is illustrated in Figure 5.28. The configuration requires some important assumptions regarding the state of stress within the anchor trench and its resistance mechanism. In order to provide lateral resistance, the vertical portion within the anchor trench has lateral forces acting upon it. More specifically, an active earth pressure (P_A) is tending to destabilize the situation, whereas a passive earth pressure (P_P) is tending to resist pullout. As will be shown, this passive earth pressure is very effective in providing a resisting force (see Holtz and Kovacs [48]). Using the free-body diagram of Figure 5.28,

$$\Sigma F_x = 0$$
$$T_{allow} \cos\beta = F_{U\sigma} + F_{L\sigma} + F_{LT} - P_A + P_P \tag{5.26}$$

where

T_{allow} = allowable force in geomembrane = $\sigma_{allow}\, t$, where

σ_{allow} = allowable stress in geomembrane, and

t = thickness of geomembrane;

β = side slope angle;

$F_{U\sigma}$ = shear force above geomembrane due to cover soil (note that for thin cover soils, tensile cracking will occur, and this value will be negligible);

Figure 5.28   Cross section of geomembrane runout section with anchor trench and related stresses and forces involved.

$F_{L\sigma}$ = shear force below geomembrane due to cover soil

F_{LT} = shear force below geomembrane due to vertical component of T_{allow};

P_A = active earth pressure against the backfill side of the anchor trench; and
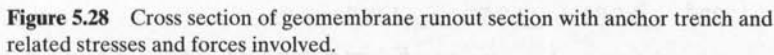
P_P = passive earth pressure against the in-situ side of the anchor trench.

The values of $F_{U\sigma}$, $F_{L\sigma}$, and F_{LT} have been defined previously. The values of P_A and P_P require the use of lateral earth pressure theory.

$$P_A = \frac{1}{2}(\gamma_{AT}d_{AT})K_A d_{AT} + (\sigma_n)K_A d_{AT}$$

$$P_A = (0.5\gamma_{AT}d_{AT} + \sigma_n)K_A d_{AT} \tag{5.27}$$

$$P_P = (0.5\gamma_{AT}d_{AT} + \sigma_n)K_P d_{AT} \tag{5.28}$$

where

γ_{AT} = unit weight of soil in anchor trench,
d_{AT} = depth of the anchor trench,
σ_n = applied normal stress from cover soil,
K_A = coefficient of active earth pressure = $\tan^2(45 - \phi/2)$,
K_P = coefficient of passive earth pressure = $\tan^2(45 + \phi/2)$, and
ϕ = angle of shearing resistance of respective soil.

This situation results in one equation with two unknowns; thus a choice of either L_{RO} or d_{AT} is necessary to calculate the other. As with the previous situation, the factor of safety is placed on the geomembrane force T, which is used as an allowable value, T_{allow}. Example 5.14 illustrates the procedure.

Example 5.14

Consider a 1.5 mm thick HDPE geomembrane extending out of a facility as shown in Figure 5.28. What depth anchor trench is needed if the runout distance is limited to 1.0 m? In the solution, use a geomembrane allowable stress of 16,000 kPa on a 3(H) to 1(V) side slope. Cover soil at 16.5 kN/m^3 and 300 mm thick is placed over the geomembrane runout and anchor trench (this is also the unit weight of the anchor trench soil). The friction angle of the geomembrane to the soil is 30° (although assume 0° for the top of the geomembrane under a soil-cracking assumption) and the soil itself is 35°. Also, develop a design chart for this example assuming that the runout length is not limited to 1.0 m.

Solution: Using the previously developed design equations based on Figure 5.28,

$$\begin{aligned}
T_{\text{allow}} &= \sigma_{\text{allow}}t \\
&= 16000(0.0015) \\
&= 24.0 \text{ kN/m}
\end{aligned}$$

and

$$\begin{aligned}
F_{U\sigma} &= \sigma_n \tan \delta_U (L_{RO}) \\
&= (0.3)(16.5) \tan 0(L_{RO}) \\
&= 0
\end{aligned}$$

$$\begin{aligned}
F_{L\sigma} &= \sigma_n \tan \delta_L (L_{RO}) \\
&= (0.3)(16.5) \tan 30(L_{RO}) \\
&= 2.86 L_{RO}
\end{aligned}$$

$$\begin{aligned}
F_{LT} &= T_{\text{allow}} \sin \beta \tan \delta_L \\
&= (24.0) \sin 18.4 \tan 30 \\
&= 4.37 \text{ kN/m}
\end{aligned}$$
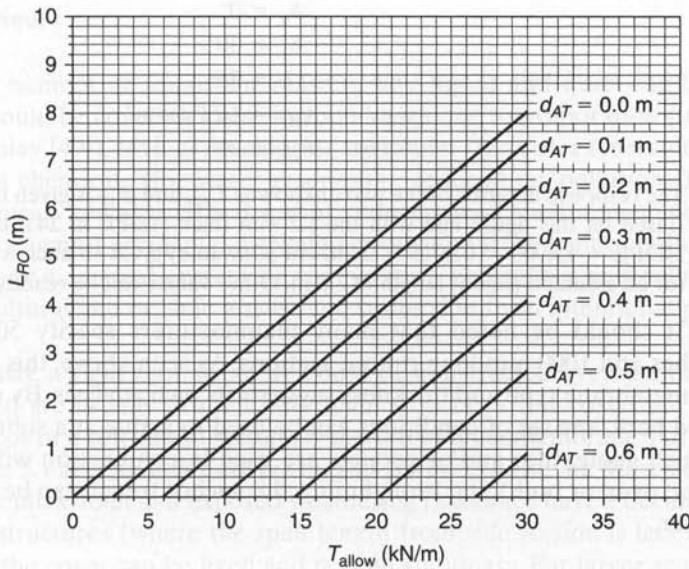
$$P_A = (0.5\gamma_{AT}d_{AT} + \sigma_n)K_Ad_{AT}$$
$$= [(0.5)(16.5)d_{AT} + (0.3)(16.5)]\tan^2(45 - 35/2)d_{AT}$$
$$= [8.25d_{AT} + 4.95](0.271)d_{AT}$$
$$= 2.24d_{AT}^2 + 1.34d_{AT}$$
$$P_P = (0.5\gamma_{AT}d_{AT} + \sigma_n)K_Pd_{AT}$$
$$= [(0.5)(16.5)d_{AT} + (0.3)(16.5)]\tan^2(45 + 35/2)d_{AT}$$
$$= [8.25d_{AT} + 4.95](3.69)d_{AT}$$
$$= 30.4d_{AT}^2 + 18.3d_{AT}$$

This is substituted into the general force equation (5.26) to arrive at the solution in terms of the two variables L_{RO} and d_{AT}:

$$T_{\text{allow}} \cos \beta = F_{U\sigma} + F_{L\sigma} + F_{LT} - P_A + P_P$$
$$(24.0) \cos 18.4 = 0 + 2.86 L_{RO} + 4.37 - 2.24d_{AT}^2$$
$$- 1.34d_{AT} + 30.4d_{AT}^2 + 18.3d_{AT}$$
$$18.4 = 2.86L_{RO} + 17.0d_{AT} + 28.2d_{AT}^2$$

Since $L_{RO} = 1.0$ m, the equation can be solved for the unknown d_{AT}.

$$d_{AT} = 0.50 \text{ m}$$

Using this formulation, we can develop a *design chart* for a wide range of geomembranes and thicknesses as characterized by different values of T_{allow}. For the specific conditions of Example 5.14, we obtain

$$\beta = 18.4°, \text{ which is } 3(H) \text{ to } 1(V)$$
$$\sigma_n = d_{cs}\gamma_{cs}$$
$$= (0.30)(16.5)$$
$$= 4.95 \text{ kN/m}^2$$

$$\delta_U = 0°$$
$$\delta_L = 30°$$
$$\phi = 35°$$
$$\gamma_{AT} = 16.5 \text{ kN/m}^3$$
$$\delta_{AT} = 30°;$$

The response in terms of the two unknowns L_{RO} and d_{AT} is given in the previous diagram. Based on this figure and with the 1.5 mm thick HDPE at 24.0 kN/m (from Table 5.5b, HDPE = 15,900 × 0.0015 = 24 kN/m allowable) gives an anchor trench depth of 0.50 m for an assumed runout length of 1.0 m. Other values can be readily selected.

It should be noted that many manufacturers specify 500 mm deep anchor trenches and 1000 mm long runout sections. As seen above, this is very simplistic, for each membrane type and thickness suggests its own analysis. By using a model as presented here, any set of conditions can be used to arrive at a solution. Even situations in which geotextiles and/or geonets are used in conjunction with the geomembrane (under, over, or both) and brought into the anchor trench can be analyzed in a similar manner.

5.3.7 Summary

Projects involving liquid containment using geomembranes are often extremely large. With large size come some inherent advantages over smaller projects. Foremost of these advantages is that most parties involved take the project seriously and approve of and enter into a planned and sequential design procedure. This section was laid out with this in mind, so that the design process proceeded step by step. Each element of design that is made leads to a new issue, which is followed by a new design element. Eventually, the quantitative process is concluded, and we must attend to extremely important details, often qualitative by nature, such as seam type, seam layout, piping layout, and appurtenance details. They are, however, common to all geomembrane projects and therefore will be handled in Sections 5.11 and 5.12.

Although such large projects obviously warrant a careful design procedure, it does not follow that smaller projects do not deserve the same attention. Indeed, failures of small liner systems can be significant. Many warrant a design effort comparable to that of large projects, as illustrated in this section.

With this section behind us, we can now focus on other applications involving geomembranes. Where a similar analysis is called for, reference will be made back to this section. Thus only new and/or unique features of geomembrane projects will form the basis of the sections to follow.

5.4   COVERS FOR RESERVOIRS AND QUASI-SOLIDS

Geomembrane covers are often used above the surface of storage reservoirs for liquids and quasi-solids such as industrial and agricultural sludges. They are of fixed, floating, or suspended types.

5.4.1 Overview

There are a number of important reasons why liquid and quasi-solid containment structures should be covered. These include losses due to evaporation (up to 84% per year; see Cooley [49]), savings on chlorine treatment (for water reservoirs), savings on algae control chemicals (for water reservoirs), reduced air pollution (for reservoirs holding chemicals and agricultural waste), reduced need for draining and cleaning, increased safety against accidental drowning, protection from natural pollution entering the reservoir (e.g., animal excretion), temperature control for anaerobic decomposition of agricultural and organic wastes, and protection from intentional pollution (i.e., terrorism).

Obviously, a rigid roof structure could be constructed over the facility, but the costs involved are usually prohibitively high. At a far lower cost, both during initial construction or in a retrofitted system, is the use of a geomembrane. All the materials listed in Table 5.1 are candidate covers for this purpose; however, those geomembranes with superior ultraviolet and exposed weathering resistance have a decided advantage. For smaller structures (where the span length from side to side is less than approximately 5 m) the cover can be fixed and remain stationary. For larger span lengths, the use of a floating cover that resides directly on the liquid's surface as it varies in elevation will be considered. Finally, the use of a totally encapsulated enclosure around the liquid or quasi-solid will be presented.

5.4.2 Fixed Covers

Fixed covers are usually used in conjunction with small-diameter tanks whose sides are made of wood, concrete, or steel. The geomembrane is fixed at the upper edge of the tank and takes a catenary shape toward the center. Positive fixity is required at the edges, since stress concentrations are very high when the tank's liquid level is beneath the elevation of the lower point of the cover. Small holes are put in the cover for rainwater drainage, but snow and wind loads can create a problem. The following example illustrates this situation.

Example 5.15

(a) Calculate the maximum edge stresses in a 0.91 mm thick geomembrane cover over a 6 m diameter wooden water storage tank, as shown in the following diagram. The combined loading to be used is 1.0 kPa, which will deflect the cover into a 15 m radius deformed shape. (b) If a CSPE cover is used with an ultimate strength of 4.5 kN/m when nonreinforced or 10.5 kN/m when reinforced (CSPE-R) with a 10 × 10 polyester scrim, what are the resulting factors of safety?

Solution:

(a) For a uniform loading on a horizontal projected area with tangential top edge support with $\theta \leq 90°$, the maximum edge stress is

$$\sigma_t = \frac{wR}{2t} \tag{5.29}$$
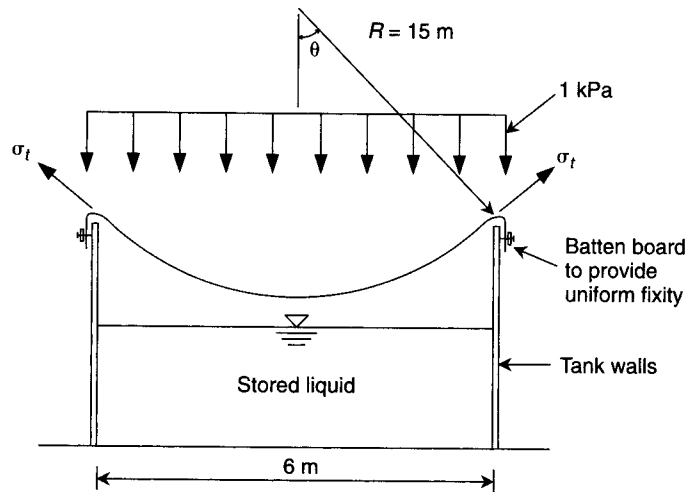
where

σ_t = maximum edge stress (kPa),
w = uniformly distributed load (kPa),
R = deformed radius (m), and
t = thickness of membrane (m).

Substituting into equation (5.29) gives:

$$\sigma_t = \frac{(1.0)(15)}{2(0.91/1000)}$$

$$= 8240 \text{ kPa}$$

(b) The strength and resulting FS of the nonreinforced CSPE cover are

$$\sigma_{\text{ult}} = \frac{4.5}{(0.91/1000)}$$

$$= 4950 \text{ kPa}$$

$$FS = \frac{\sigma_{\text{ult}}}{\sigma_{\text{reqd}}}$$

$$= \frac{4950}{8240}$$

$$= 0.60 \qquad \text{not acceptable}$$

(c) For the reinforced cover (CSPE-R), the strength and resulting FS are

$$\sigma_{\text{ult}} = \frac{10.5}{(0.91/1000)}$$

$$= 11{,}500 \text{ kPa}$$

$$FS = \frac{\sigma_{ult}}{\sigma_{reqd}}$$

$$= \frac{11,500}{8240}$$

$$= 1.40; \text{ acceptable}$$

It is easily seen in Example 5.15 that very high edge stresses occur, which gives a distinct advantage to scrim (fabric)-reinforced membranes. It should also be obvious that a very carefully planned and executed method of fixing the lining to the tank must be made. Such details will be addressed in Section 5.12. Since the edge stresses become extremely high for large-diameter tanks when the cover is fixed in position, the concept of floating covers has great appeal and current use.

5.4.3 Floating Covers

Floating covers of polymeric materials have made a strong impact on reservoir and liquid-holding facilities. All the materials listed in Table 5.1 are candidate cover materials, but superior ultraviolet and weathering resistance are an obvious advantage. Due to the desirability of decreasing the dead load, however, some additional materials have also been developed for this application. Foamed polymers (e.g., foamed EPDM rubber) in the form of a closed-cell structure of density as low as 0.16 mg/l have been successfully used. These lightweight foam liners have been on tanks up to 15 m diameter, and the design and construction procedure is somewhat unusual [50]. Small holes are cut into the liner to allow the cover to drain rainwater and snowmelt accumulating on top of it. The holes also help during installation, allowing any air trapped under the cover to escape. The edge is not attached to the tank but is stiffened by the addition of bonded foam-rubber strips, which prevent wind from getting beneath the cover. Wires are sometimes stretched across the top of the tank to prevent the loss of cover material when it is accidentally overfilled. A freeboard of 300 mm should be maintained.

However, for large water storage reservoirs of the type discussed in Section 5.3, the liner materials listed in Table 5.1 are generally used, particularly CSPE-R, HDPE, EPDM-R, and fPP-R. As can be intuitively appreciated, tensile strength as well as tear, puncture, and impact resistance are critical mechanical properties in this application. The covers are fixed to the sidewall of the tank or soil side-slope anchor trench in these cases. The dimensions of the cover must be greatest when the reservoir is empty. This creates a problem during filling, when the slack accumulates on the leeward sides. This results in the stressing of the cover on the windward sides and does not allow for rainwater or snowmelt collection and disposal in other areas. Thus accommodation of the slack is a major design consideration.

Gerber [51] presents a number of slack-accommodating designs using combinations of floats and sump weights. The floats are made of EPS or XPS materials (see Section 1.9 and Chapter 8) and are usually arranged beneath the cover and attached to its underside. Weights are similarly constructed, but the pockets are filled with sand and constructed on the top side of the cover. The designs are intricate and some are shown in Figures 5.29 and 5.30. In Figure 5.29 the central float grid is sufficiently stiff to
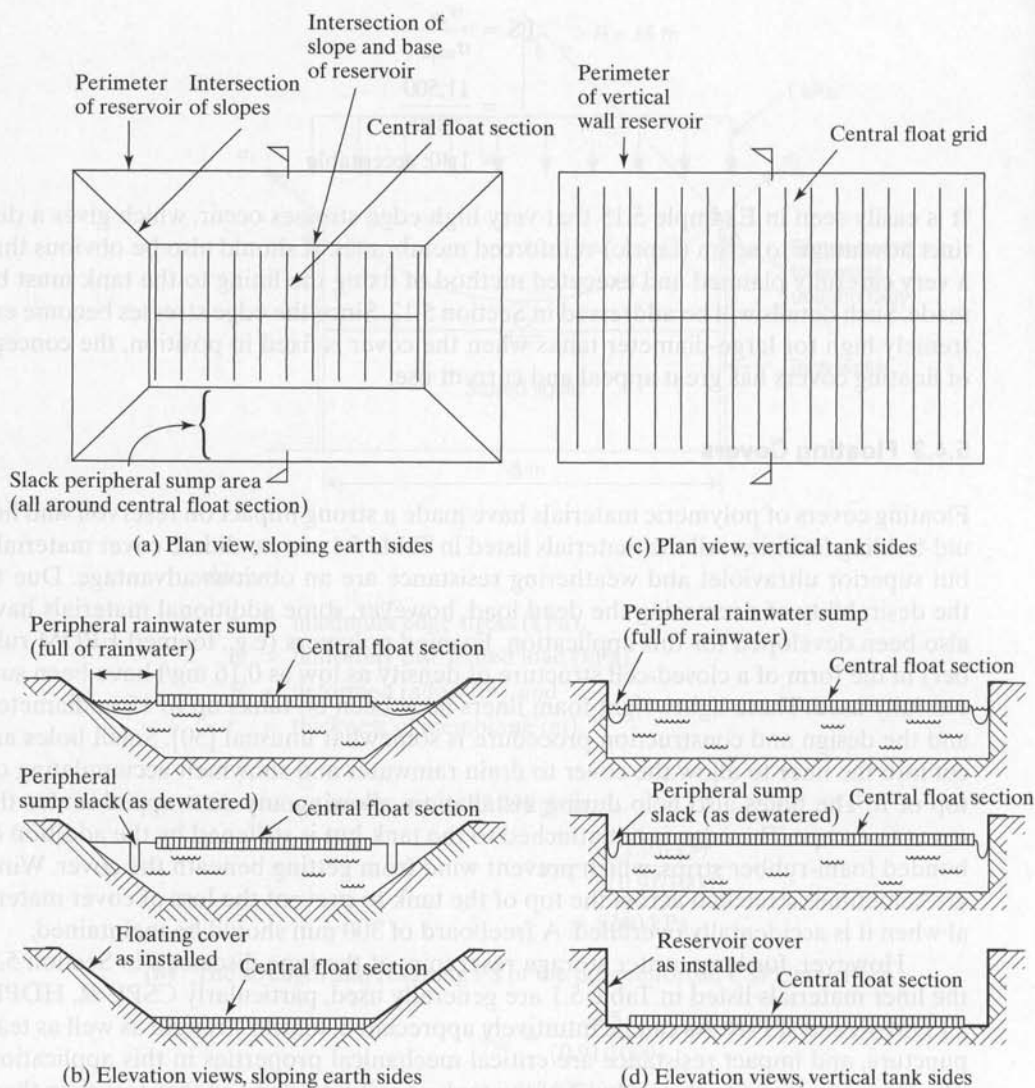
Figure 5.29 Designs for untensioned, centrally floated, peripheral sump reservoir covers. (After Gerber [51]).

maintain its integrity as the reservoir fills. All slack is forced to the sides, where rainwater and snowmelt collects and is pumped away when it becomes excessive. There are several drawbacks to these designs: (1) walking on the cover in the peripheral area is very unsafe; (2) wind pushes the central float section to the leeward side of the reservoir, leaving little or no slack on the windward side; and (3) rain puddles, ice, and debris tend to collect in certain areas of the central float section. Thus the concept of a *defined sump reservoir cover* is preferred. Figure 5.30 shows additional designs that essentially eliminate the previous problems.

(a) Plan and elevation views of sloping earth side cover reservoir, empty and full

(b) Plan and elevation view of vertical tank side reservoir, empty and full
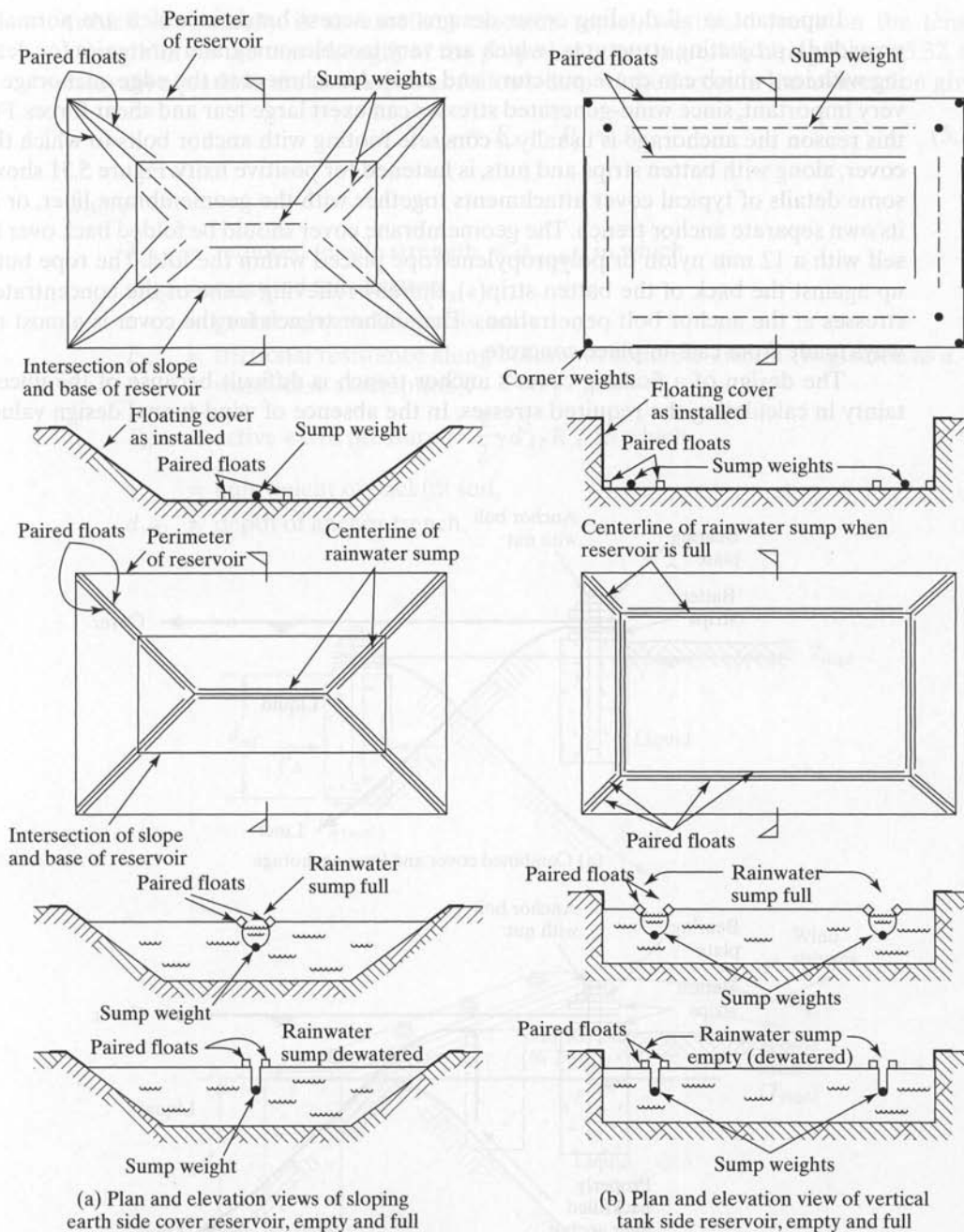
Figure 5.30 Designs for defined sump reservoir covers. (After Gerber [51]).

Important in all floating cover designs are access hatches (which are normally provided), projecting structures (which are very troublesome), and strategies for dealing with ice (which can cause puncture and tear). Attachment to the edge anchorage is very important, since wind-generated stresses can exert large tear and shear forces. For this reason the anchorage is usually a concrete footing with anchor bolts to which the cover, along with batten strips and nuts, is fastened for positive fixity. Figure 5.31 shows some details of typical cover attachments together with the geomembrane liner, or in its own separate anchor trench. The geomembrane cover should be folded back over itself with a 12 mm nylon or polypropylene rope placed within the fold. The rope butts up against the back of the batten strip(s), thereby relieving some of the concentrated stresses at the anchor bolt penetrations. The anchor trench for the cover is almost always made from cast-in-place concrete.

The design of a floating cover's anchor trench is difficult because of the uncertainty in calculating the required stresses. In the absence of wind-tunnel design values

(a) Combined cover and liner anchorage

(b) Separate cover and liner anchorage
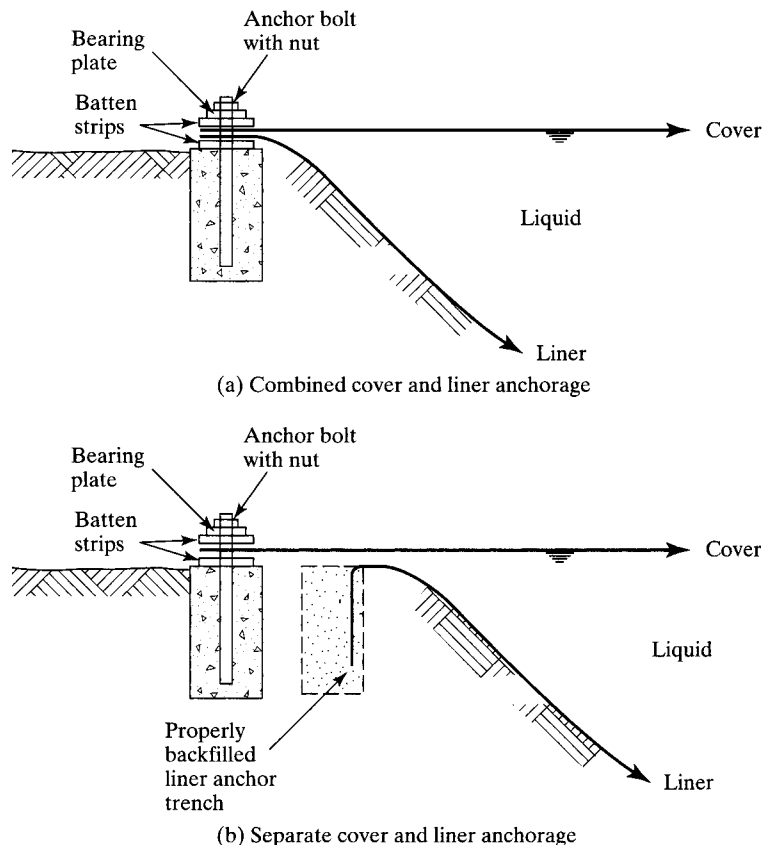
Figure 5.31 Typical configurations for anchoring geomembrane floating covers at their boundaries.

(which, incidentally, is an excellent research topic), we could focus on the tensile strength or on the tear strength of the proposed cover material. Using Figure 5.32, the relevant equations are developed as follows. Sum of the forces in the x-direction gives:

$$T_{\text{reqd}} = F_A + P_p - P_A \qquad (5.30)$$

where

T_{reqd} = required tensile strength = $\sigma_{\text{reqd}}\, t$, in which

σ_{reqd} = required tensile stress,

t = geomembrane thickness, and

F_A = frictional resistance along bottom of concrete anchor (neglected as a worst-case assumption);

P_A = active earth pressure = $\dfrac{1}{2}\gamma d_{AT}^2 K_A$, in which

γ = unit weight of backfill soil,

d_{AT} = depth of anchor trench,
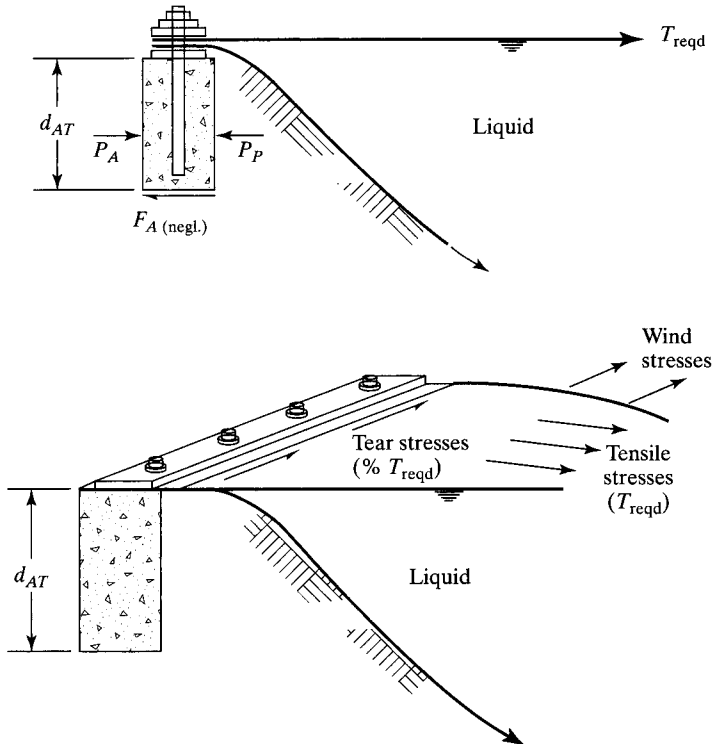
Figure 5.32   Design schemes for geomembrane floating covers.

K_A = $\tan^2(45 - \phi/2)$, where,

ϕ = angle of shearing resistance of soil; and

P_P = passive earth pressure = $\dfrac{1}{2}\gamma d_{AT}^2 K_P$, in which

K_P = $\tan^2(45 + \phi/2)$.

Example 5.16 illustrates the importance of this aspect of floating geomembrane covers.

Example 5.16

Calculate the factor of safety of a 1.15 mm thick reinforced CSPE-R geomembrane float-ing reservoir cover of allowable stress of 3500 kN/m^2 when it is connected to a 500 mm deep concrete anchor trench, as shown in Figure 5.32. The friction angle of the backfill soil is 35° and its unit weight is 19 kN/m^3.

Solution: Using the previously developed design equations with $F_A = 0$,

$$K_A = \tan^2(45 - \phi/2)$$
$$= \tan^2(45 - 35/2)$$
$$= 0.27$$

$$K_P = \tan^2(45 + \phi/2)$$
$$= \tan^2(45 + 35/2)$$
$$= 3.69$$

$$T_{\text{reqd}} = F_A + P_P - P_A$$
$$= 0 + (0.5)(19)(0.5)^2(3.69) - (0.5)(19)(0.5)^2(0.27)$$
$$= 0 + 8.76 - 0.64$$
$$= 8.12 \text{ kN/m}$$

Additionally,

$$T_{\text{reqd}} = \sigma_{\text{reqd}}\, t$$
$$\sigma_{\text{reqd}} = \frac{8.12}{(1.15/1000)}$$
$$= 7060 \text{ kN/m}^2$$

$$\text{FS} = \frac{\sigma_{\text{allow}}}{\sigma_{\text{reqd}}}$$
$$= \frac{3500}{7060}$$
$$\text{FS} = 0.50$$

thus the geomembrane cover will fail before the anchor trench is pulled out of its position. It also suggests that a geomembrane of twice the strength could be used to provide a bal-anced design between geomembrane failure and anchor trench failure.

The problem of estimating the actual tear stresses mobilized by wind acting over (and on) the central section is a very difficult one. To be sure, the stresses are high, and the survivability data of Table 5.13 in the very high category represents the absolute minimum values that should be used.

5.4.4 Quasi-Solids Covers

We have concentrated in this section on reservoirs containing liquids. Many times it is necessary to cover quasi-solid (or semiliquid) substances. An emerging application area is the covering of odorous substances, such as manure and other biodegradable farm wastes. As confined animal feedlot operations (CFOs)—mainly beef, pork, and poultry—grow larger and more numerous, growth in this application is obvious. For example, manure output in the United States is over 300 million metric tons, reflecting an increase of 72% between 1997 and 2002. Frobel [52] presents references on the chemistry of anaerobic digestors and the thermal energy that is produced. Frobel also focuses on the following geomembrane cover requirements: the polymer composition must resist animal waste and aqueous methane; the geomembrane must be low in gas vapor transmission; the geomembrane must be designed for fabrication into custom panels; the geomembrane must have high tensile, tear, and puncture resistance properties; the geomembrane must be repairable over the life of the project by conventional methods; and the geomembrane must be resistant to UV and ozone exposure with a relatively long-term weathering warranty provided by the manufacturer.

Other areas in which quasi-solids need to be covered is in the treatment of sewage sludge to increase the efficiency of anaerobic digestion. In addition to the geomembrane cover's low gas permeability, the black color increases the temperature beneath the cover, which further increases the bacterial activity. As with CFO's, the generated methane and hydrogen sulfide gases are collected at the high point of the site and used to generate electricity which is used on-site or sold to the local power grid. The situation is similar when treating papermill sludges.

The key to all of these application areas is just how solidlike or liquidlike the material is. If it is more solid, the cover will be designed as with solid-waste landfill closures, which will be described later in Section 5.7. If it is more liquid, the material must be placed in an excavation or large tank and the cover designed per the details of this section.

5.4.5 Complete Encapsulation

By lining the bottom and sides of reservoirs (as in Section 5.3) and now covering the contents with similar geomembrane materials (as in Section 5.4), it seems only natural that a completely fabricated enclosure should be considered. Indeed, such *superbags* are available, and in standard sizes up to 5 million liters! Even larger sizes can be fabricated by special order. The concept is straightforward in that the entire fabrication occurs at the factory, where the complete bag is transported to a prepared site (a 5 Ml nitrile rubber bag weighs only 55 kN) and placed accordingly. Filling with the liquid to be contained can begin immediately. Figure 5.33 shows such a bag inflated with air (to give visual impact) and installed in a prepared earth substructure after filling. Such huge bags have also been used to transport drinking water to the island of Cyprus from Turkey by being pulled by tugboats and anchored offshore, allowing the water to be used as required. Each bag contains drinking water supply for approximately 1 month. More water-borne transportation of various liquids is sure to engender active interest and activity in the near future.

(a) Air-inflated bag
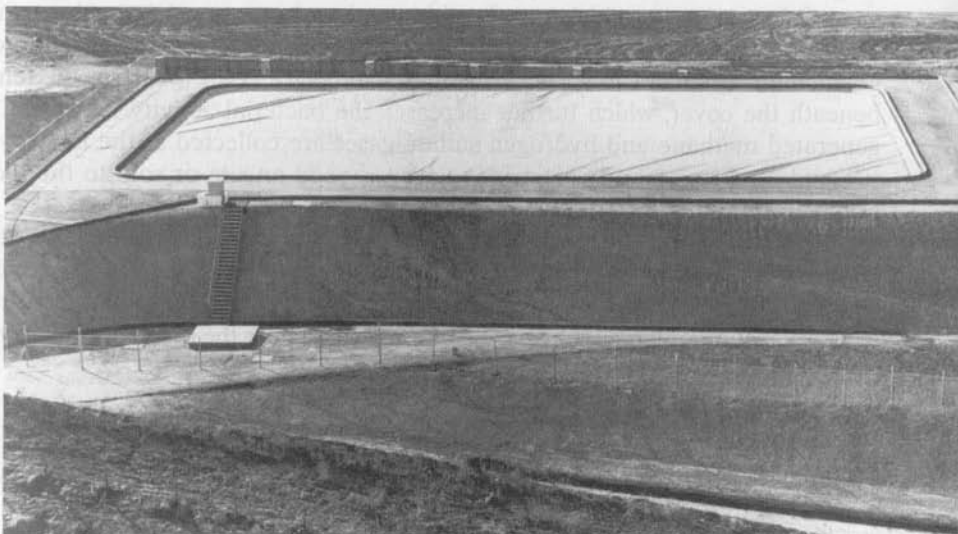
(b) Water-filled bag supported by soil berm
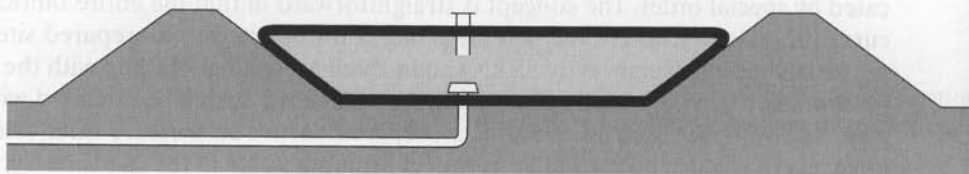
(c) Design sketch for soil berm stability

Figure 5.33   Inflatable reservoirs. (Compliments of Firestone Coated Fabrics Co. and Fabritank Co.)

5.5 WATER CONVEYANCE (CANAL) LINERS

This section covers the use of geomembranes to line canals in which the liquid is moving. The usual liquid is water, but many other liquids, including industrial chemicals and wastes, also need to be conveyed.

5.5.1 Overview

Often the source of water is located at a considerable distance from the intended user. As a result, many and varied attempts have been made to convey this valuable resource, sometimes requiring herculean feats. Consider, for example, the Romans, whose aqueducts are among the premier engineering achievements of recorded history. An important element in the economic functioning of such water conveyance canals is that they hold the water placed in them during the journey from source to user. Excessive leakage is obviously unacceptable, making the liner of the canal a key element in a successful system. With this in mind, engineers have tried almost everything to line their water conveyance canals at one time or another. These include soil liners (mainly clay soil), nonflexible liners (bricks, paving blocks, concrete, shotcrete, gunite, etc.), and flexible liners (bituminous panels, spray-on chemicals, geomembranes, and geosynthetic clay liners). The emphasis in this chapter, will be on polymeric geomembranes; GCLs will be covered in Chapter 6. When properly designed, constructed, and maintained, geomembrane materials have had a significant impact on the canal lining industry. As will be seen later in this section, this impact easily extends to the rehabilitation of old canals and their linings as well. The scope of the problem is enormous—indeed, it is worldwide.

Most countries have national committees and specific agencies studying canal linings. These organizations are specifying geomembranes regularly. In the United States, the American Society of Agricultural Engineers, the U.S. Bureau of Reclamation, and the U.S. Army Corps of Engineers have been active in this area. The activity is international: For instance a joint U.S.-Russian commission has made a series of tests and has reported on the subject. Many standards are available for geomembranes used specifically as canal linings. When searching the canal-related literature, however, the topic will usually come under a heading other than geomembranes, such as canal liners, synthetic canal liners, plastic canal liners, rubber canal liners, or polymeric canal liners.

5.5.2 Basic Considerations

With potable water shortages looming in many parts of the world—for example, Asia (particularly the Near East and China), the arid regions of Africa, and even in some areas in North and South America—the efficient transportation of water is absolutely necessary. Geomembranes liners represent an economical and realistic seepage control material in almost every instance.

Geometry.   The design of canal geometry for uniform flow is a well established branch of hydraulics within the general category of *open channel flow*. Many textbooks

are available on the subject and it is a required course in most undergraduate civil engineering curricula. It is well known that the preferred hydraulic cross sections are trapezoid (half of a hexagon), rectangle (half of a square), triangle (half of a square), semicircle, parabola, and catenary (hydrostatic).

Due to various layout, excavation, and compaction problems that are encountered, curved surfaces are not as widely used as those consisting of linear segments. Furthermore, rectangular sections must be supported by a separate structure of wood, concrete, or steel. The most common cross sections are therefore trapezoid (for large flows) and triangle (for small flows). Regarding the side-slope angles of these sections, the slope stability considerations of Section 5.3.5 are applicable.

Once the shape and side slopes are selected, the depth of the section is calculated from a *section factor* as follows:

$$AR^{2/3} = \frac{nq}{\sqrt{S}} \qquad (5.31)$$

where

$$AR^{2/3} = \text{section factor,}$$
$$A \quad = \text{area (m}^2\text{),}$$
$$R \quad = \text{hydraulic radius (m),}$$
$$n \quad = \text{Manning coefficient (the typical range of which is 0.020 to 0.035 depending on the flow; } n = 0.028 d_{50}^{0.1667} \text{ is sometimes used where } d_{50} \text{ is the average size of the cover soil in meters),}$$
$$q \quad = \text{flow rate (m}^3\text{/s), and}$$
$$S \quad = \text{slope of water surface (dimensionless).}$$

The A and R values are functions of the depth (in meters) and can be solved for explicitly or taken from design charts that are available [53].

Cross Sections.   When a geomembrane is used as the liner material, it is placed either directly on the prepared soil subgrade or on a previously installed geotextile. A uniform thickness soil cover is commonly placed over the geomembrane. Thus the completed cross section is typically like that shown in Figure 5.18b and d. The difference in this case, however, is that the liquid is flowing, and thus the possibility of scour of the cover soil must be addressed. Many studies (mostly empirical) have been directed at predicting a maximum permissible velocity of the liquid as a function of the type of cover soil. The values seem to range from 30 to 100 m/min, depending on cover soil type and the turbidity of the flowing water (see Table 5.14). This table also includes the tractive force mobilized by the flowing water. For a trapezoidal section, these forces are distributed as shown in Figure 5.34. If these forces are such that the soil cover is eroded (or if the geomembrane has no soil cover to begin with), they will act directly on the geomembrane. Particularly vulnerable are the seams, which have been shown to be low in strength in a peel or tension mode (recall Figure 5.6). Because of such problems, it is not uncommon to cover the liner with a nonerodable cover of asphalt, shotcrete, or

TABLE 5.14 MAXIMUM PERMISSIBLE VELOCITIES AND THE CORRESPONDING UNIT-TRACTIVE-FORCE VALUES

Material	Manning Coefficient	Clear water		Turbid Water	
		V (m/s)	T_0 (Pa)	V (m/s)	T_0 (Pa)
Fine sand, colloidal	0.020	0.45	1.29	0.76	3.59
Sandy loam, noncolloidal	0.020	0.54	1.77	0.76	3.59
Silt loam, noncolloidal	0.020	0.61	2.30	0.91	5.26
Alluvial silts, noncolloidal	0.020	0.61	2.30	1.07	7.18
Ordinary firm loam	0.020	0.76	3.59	1.07	7.18
Volcanic ash	0.020	0.76	3.59	1.07	7.18
Stiff clay, very colloidal	0.025	1.14	12.4	1.52	22.0
Alluvial silts, colloidal	0.025	1.14	12.4	1.52	22.0
Shales and hardpans	0.025	1.83	32.0	1.83	32.0
Fine gravel	0.020	0.76	3.59	1.52	15.3
Graded loam to cobbles when noncolloidal	0.030	1.14	18.2	1.52	31.0
Graded silts to cobbles when colloidal	0.030	1.22	20.6	1.68	38.0
Coarse gravel, colloidal	0.025	1.22	14.3	1.83	32.0
Cobbles and larger	0.035	1.52	44.0	1.68	53.0

Source: *V* values from Fortier and Scobey [54]. T_0 values converted by the U.S. Bureau of Reclamation.

concrete, although problems occur here too, including the oxidation of asphalts and the thermal shrinkage and cracking of cementatious materials. Steel reinforcement is often used to control thermal stresses. Alternatively, a precast articulating concrete mattress can be used (recall Figure 2.64b).

Since the quantity of liquid moving in the canal does not remain constant, a freeboard consideration must be addressed. Two definitions are needed: one of the height of the top of bank above the water surface (F_B), the other of the height of the geomembrane liner above the water surface (F_L). Figure 5.35 gives the Bureau of Reclamation's experience in this regard. Note that at high flow capacity generous amounts of freeboard are required in all cases, since overtopping would cause scour beneath the geomembrane and rapid undermining of the system. Also given is the height of a clay lining (F_E) above the water surface, which is less than that of a geomembrane liner. This probably reflects a caution in that scour is more serious in undermining geomembrane liners than it is with clay linings.

Material Selection.   For the conveyance of potable or agricultural water, all of the geomembranes listed in Table 5.1 are candidate materials. Due to its historical use and ease of construction, however, PVC is the most widely used liner material for water conveyance canals. Unless specifically formulated with high molecular weight plasticizers, PVC must be covered with soil or hard armoring of some type. Of course, certain situations may favor the choice of another material, but this choice would be on an individual basis. One situation of particular concern is in arid, desert areas, where consistently high temperatures are encountered. Here heat aging and weathering tests are critical in proper geomembrane selection.
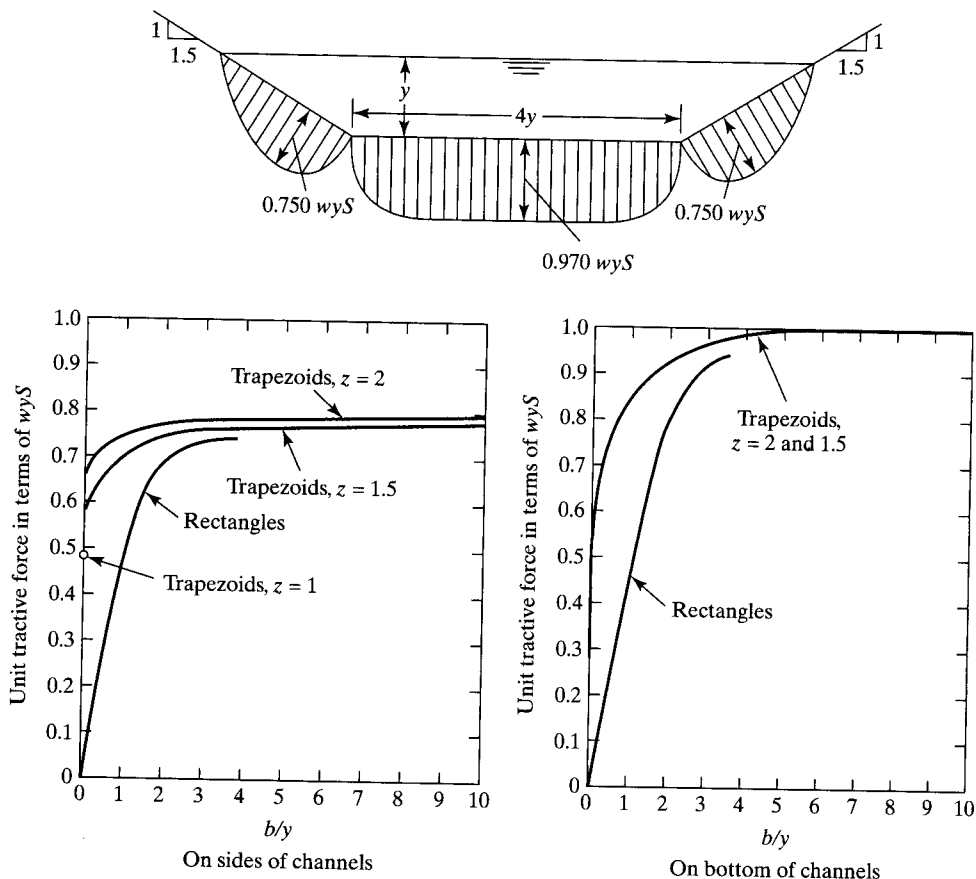
Figure 5.34 Distribution of tractive force in trapezoidal canal section. Values are in terms of wyS, where w = unit weight of fluid, y = depth, S = slope, and b = base width. (After Chow [53])

For the conveyance of liquids such as chemicals, the chemical resistance chart in Table 5.8 (or its equivalent) should be used. When a mixed waste stream or complex effluent is being transported, it may be necessary to run chemical resistance tests as described in Section 5.1.4. Where leak detection is important, a double liner with a drainage layer (sand, geonet, or drainage geocomposite) between the primary and secondary liners can be used, recall Figures 5.18e and f.

Thickness. A thickness design like that presented in Section 5.3.4 is certainly appropriate. However, the usual care in subgrade preparation, low normal stress, low hydraulic heads, moving water, and so on, make the design such that calculated thicknesses are quite low. For this application, it is best to use a minimum allowable thickness based on experience or the survivability chart in Table 5.13. The U.S. Bureau of
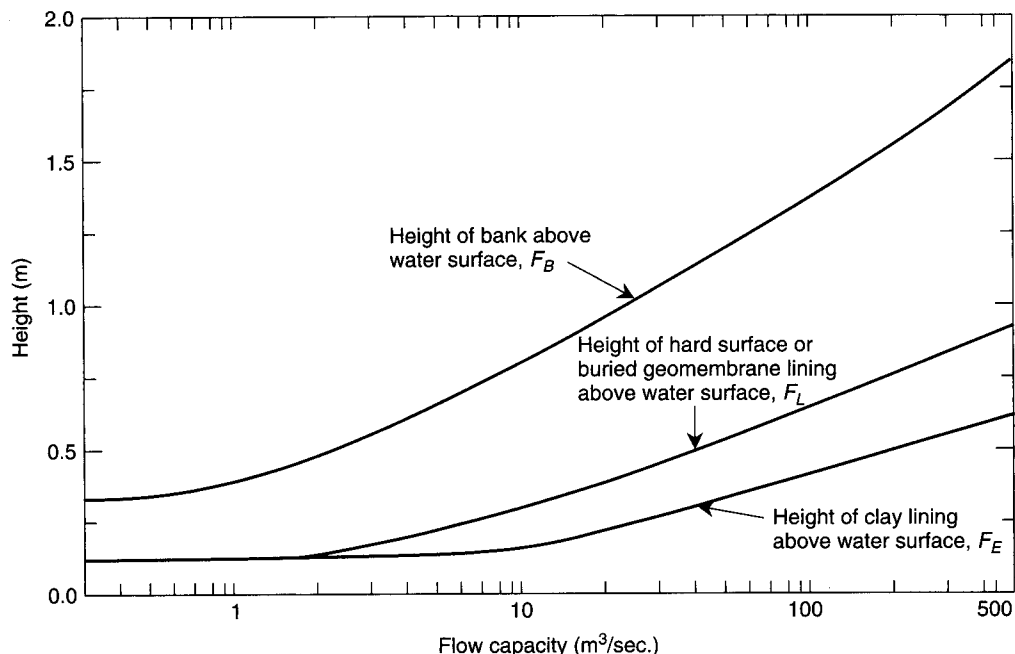
Figure 5.35 Bank heights for canals and freeboard for hard surfaces, buried geomembranes, and clay linings. (After Morrison and Starbuck [55])

Reclamation recommends a minimum 0.50 mm thickness for water-conveyance canals and sometimes uses 1.0 mm thick geomembranes.

Side Slopes.   The design of canal side slopes follows exactly the procedures described in Section 5.3.5.

Runout Length.   The design of geomembrane runout coming over the side slopes follows exactly the procedures described in Section 5.3.6. Quite often there is no anchor trench per se involved. Usual runout lengths are 1.0 to 1.5 m. The design follows exactly the procedure described in Section 5.3.6. When the canal is of a rectangular section, however, the liner must be anchored to a rigid structural member. Typical details for joining at connections are given in Section 5.12.1.

5.5.3 Unique Features

Due to the empirical nature of the use of geomembranes as canal liners, there are many specialty features that play a role in the success of a particular project.

Cover Soil.   Cover soils from 300 to 600 mm in thickness are needed on most geomembrane-lined canals for a number of reasons: to resist erosion, particularly at

the air-water interface; to hold the liner in place and to dissipate the tractive forces; to protect the liner from exposure from UV light, ozone, wind, and so on; and to protect the liner from damage from water action, plant growth, animals, vandalism, and canal maintenance equipment. However, due to the moving liquid in canal sections, the likelihood of cover soil scour is very high. Therefore, carefully selected cover soil particle sizes and shapes must be considered. The U.S. Bureau of Reclamation recommendations are given in Figure 5.36, where it is seen that the required cover soil is a well-graded sandy gravel. The material's particle shape should be angular or subangular so as to provide for a high in situ density with correspondingly high shear strength. Compaction to at least 95% standard Proctor compaction is necessary. Because of the angular nature of the cover soil, it is sometimes prudent to place at least a thin (say, 200 g/m^2) geotextile over the geomembrane, to use a composite geotextile/geomembrane, or to use a two-layer cover soil approach with finer-sized soil particles on the bottom layer next to the geomembrane. The thickness of each layer is usually 150 to 300 mm.
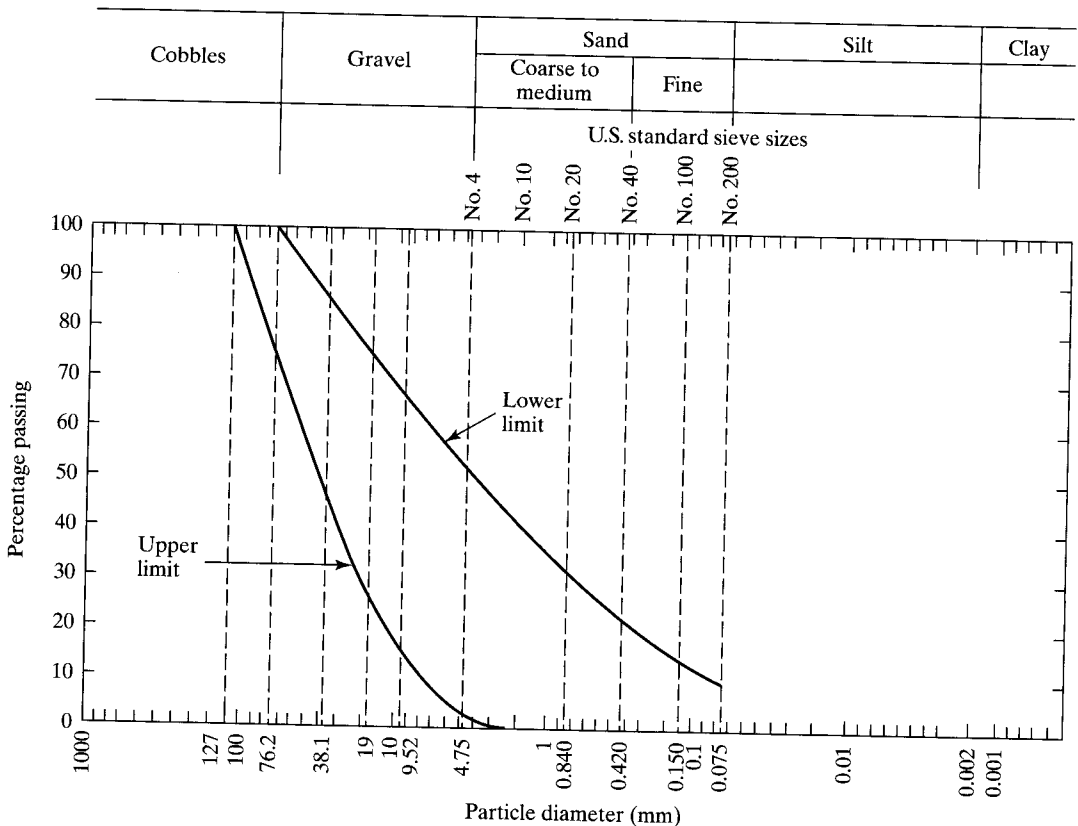
Figure 5.36 Limiting gradation curves for cover soil in canals. (After Morrison and Starbuck [55])

Seam-Joint Overlap.   Although geomembrane seams (joints) have not been specifically addressed (see Section 5.11), it should be intuitive that overlap should be placed downstream and should be relatively long. Thus 250 to 300 mm overlaps are recommended, not the usual 75 to 100 mm overlaps in other applications. If water is the transported liquid, seams are not as important as in other geomembrane applications since some water leakage can usually be tolerated. Often a long unseamed overlap is adequate. It obviously is a site-specific situation.

Remediation Work.   Since many canals in the past have been unlined or lined with nonflexible linings (asphalt, concrete, etc.) and have subsequently deteriorated, remediation projects are plentiful. They occur from a number of situations, such as settlement-induced cracking; thermal cyclic fatigue cracking; deteriorated expansion joints, opened construction joints; and deterioration due to chemical attack, oxidation and natural aging. When a crack occurs in a concrete lining, the amount of leakage is alarming. While crack filling with bitumen is a normal maintenance item, it is a temporary measure and becomes unwieldy as the situation grows progressively worse.

Geomembranes have served nicely as remediation liners, as shown in Figure 5.37a. The canal surface must be cleaned, and loose sections removed and repaired. No loose
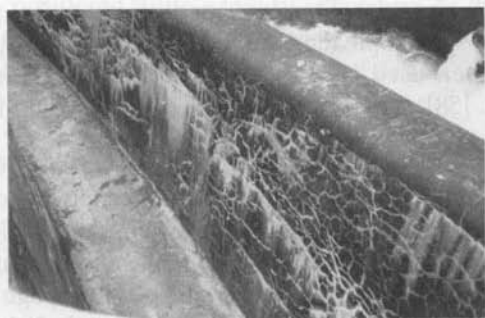
(a) Concrete canal in Italy: before and after

(b) Rock canal in United States: before and after

Figure 5.37   Examples of retrofitted leaking canals using exposed geomembranes.

sections of concrete can remain in place. Depending on the surface conditions, a thick nonwoven needle-punched geotextile protection layer is sometimes placed first, then the geomembrane. Bonding to the concrete is generally not necessary. Edge details, however, are very important, and positive fixity is required (see Section 5.12).

In the absence of a geotextile protection layer, the use of a thick geomembrane is required. Hammer et al. [56] report on the use of a 5.0 mm polypropylene liner placed in a live conveyance canal carrying paper mill effluent. The 3.2 km long project used a mechanical seal, since conventional seaming was not possible while working in live flowing water conditions.

Concrete Cover.   Rather than put the liner over the concrete (analogous to putting the cart before the donkey), new construction often justifies putting the geomembrane on the prepared soil subgrade and then concrete on top of it. What little water that comes through the concrete joints or cracks should be removed; this can be done by placing the concrete over a nonwoven needle-punched geotextile that is directly above the geomembrane. Since the flow rates of the geotextiles are drastically reduced because of intrusion of the wet concrete [57], geotextiles heavier than 350 g/m^2 will be required. The use of composite fabrics with a tight pore structure beneath the concrete, and then a high transmissivity portion, would also be possible.

The concrete used to pave over liners for canals is usually reinforced with welded wire mesh and is generally 150 to 300 mm thick. Standard road-paving techniques are used in most cases. In larger projects, special paving equipment can be developed and slip-form paving techniques have been used successfully even under conditions of retrofitting live canals (Comer et al. [58]). Alternatively, the concrete would be reinforced with polymer or steel fibers.

Low Cost Seepage Control.   In many locations irrigation canals run over exposed rock surfaces that are highly fractured. The seepage losses are significant, at times up to 75%. Alternatively, similar losses can occur with canals on sand or gravel subgrades. The U.S. Bureau of Reclamation has evaluated 34 different seepage control techniques/materials in central Oregon, each section being approximately 300 m long. The subgrade is a highly fractured volcanic basalt (see Figure 5.37b) which has been retrofitted with a number of alternatives:

* Shotcrete placed directly on the rock subgrade
* Shotcrete over a 0.75 mm PVC geomembrane
* Shotcrete with steel fibers over a 0.75 mm PVC geomembrane
* Shotcrete with polypropylene fibers over a 0.75 mm PVC geomembrane
* Shotcrete with polyethylene microgrids over a 0.75 mm PVC geomembrane
* Grout-filled mattress placed directly on the rock subgrade
* Grout-filled mattress over a 0.75 mm PVC geomembrane
* Geotextile/0.75 mm PVC geomembrane/geotextile composite
* Geotextile/0.91 mm CSPE-R geomembrane composite
* Geotextile/1.15 mm CSPE-R geomembrane composite

- Geotextile/1.0 mm textured HDPE geomembrane
- Textured 2.0 mm HDPE geomembrane
- Textured 2.5 mm HDPE geomembrane
- Various other combinations

The efficiency of the various sections has been evaluated by means of ponding tests conducted at 2, 5 and 10 year intervals. These values are contrasted to the initial construction cost of the installation plus maintenance costs, which are being kept by the local Water District, to arrive at a benefit/cost ratio (see Table 5.15). The preferred technique appears to be a geomembrane directly on the rock surface with a concrete or shotcrete cover placed above it. Considerable data are available in [59] on the 10-year behavior of the various materials that are involved, both geomembranes and hard surface coverings.

5.5.4 Summary

Geomembrane use in canal linings is a rapidly growing field for both new and remediation work. While most liners are covered with soil or concrete, uncovered geomembranes can also be used. As with any meaningful installation, design must be carefully considered using a logical procedure. In this section the design followed directly from the earlier section on reservoir liners, with some notable exceptions. As shown, the tools are available for a rational design.

5.6   SOLID-MATERIAL (LANDFILL) LINERS

The amount of municipal solid waste (MSW) and hazardous solid waste (HSW) generated is enormous by any standard of measure. Figure 5.38 shows the growth of MSW in the United States, of which approximately 55% is landfill. According to the United Nations Organization for Economic Cooperation and Development, greater percentages of MSW are landfilled by Mexico (99%), Greece (93%), United Kingdom (84%),

TABLE 5.15   BENEFIT/COST COMPARISONS OF VARIOUS SEEPAGE CONTROL LINING SYSTEMS

Type of Lining	Construction Cost ($/m^2)	Durability (years)	Maintenance Cost ($/m^2-yr)	Effectiveness at Seepage Reduction (%)	Benefit/Cost (B/C) Ratio
Fluid-applied membrane	$15.07–$46.60	10–15	$0.108	90	0.2–1.5
Concrete alone	$20.67–$25.08	40–60	$0.054	70	3.0–3.5
Exposed geomembrane	$8.40–$16.49	10–25	$0.108	90	1.9–3.2
Geomembrane with concrete cover	$26.16–$27.34	40–60	$0.054	95	3.5–3.7

Source: After Swihart and Haynes [59].
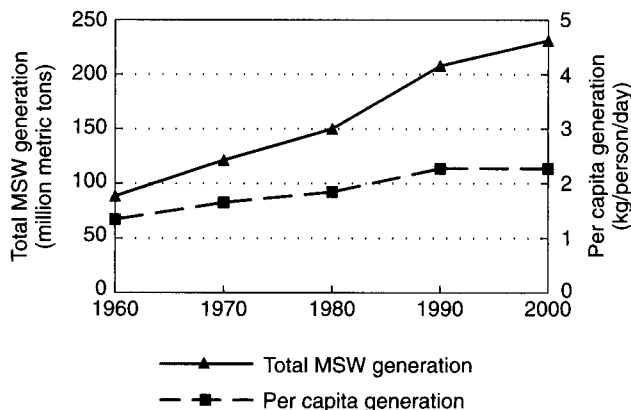
Figure 5.38 Municipal solid waste generation in the United States from 1960 to 2000. (After U.S. EPA [60])

Canada (75%), Korea (72%) and France (59%). Conversely, Sweden (39%), Japan (27%), Demark (22%), and Switzerland (14%) landfill less, but their incineration of MSW is relatively large. Thus, landfilling continues to be the primary disposal method in spite of great efforts for waste minimization and recycling. The amount of solid waste, including HSW, disposed in landfills worldwide is approximately 500 M metric tons per year.

Unfortunately, there are still additional quantities of solid waste *not* included in the above estimate. These materials include the following:

- Bottom and fly ash from incinerators, such as municipal incinerators, hazardous waste incinerators, and trash-to-steam facilities, where the concern is over concentrated heavy metals in the residual ash.
- Bottom and fly ash from coal-burning power plants, which represents a tremendous quantity of material.
- Dredged river and harbor sediments which may be contaminated to various levels with a wide range of possible pollutants.
- Biosolids residue from sewage treatment facilities, where the same concern of heavy metals is often expressed.
- Residue from precious metal extraction of previously mined rock through heap leach operations.
- Various types of construction and demolition (C & D) wastes.

Adequate and safe storage of all of the above material must be ensured. The situation is similar for all the industrialized nations and even looms as a problem for developing nations (see Mackey [61]). Since 1982, geomembranes have been used as a primary strategy for such containment. Their proper design and construction is at the heart of this important section.

5.6.1 Overview

As a groundwater pollution-control mechanism, the use of some type of liner on the bottom and sides of a landfill has been considered necessary since the 1970s when several notable incidents occurred, including Love Canal in the United States and Lekakurk in Holland. This necessity is created by the moisture in the incoming materials augmented by rainfall and snowmelt interacting with the already placed waste and forming a liquid called *leachate*. This leachate flows gravitationally downward and, if not for a liner, would continue to flow until it encountered groundwater or surface water, posing the threat of pollution. Although both the quantity and quality of leachate are of concern, it is the quality that can have horrendous characteristics while at the same time being extremely variable in its composition. Table 5.16 gives the range of leachate values at 18 MSW sites and the average of three HSW sites. Of particular note in this table is the variable nature of MSW leachates and the high levels of several types of organic solvents in HSW leachates.

The types of liners that have been used for leachate containment are indeed numerous (see Kays [64] for a historic review), but the predominant liner material until the early 1980s was compacted clay. When of the proper type, compacted clay liners (CCLs) can achieve hydraulic conductivity (or permeability) values in the range 1×10^{-6} to 5×10^{-8} cm/s and perform very satisfactorily. There are two drawbacks to CCLs, however, both of which have given impetus to the use of geomembranes for landfill liners:

- Clay liners must be 600 to 1500 mm thick, which takes up *airspace*, significant landfill volume that could be used to contain the waste itself.
- Clay liners have been shown to be subject to chemical reactions and subsequent shrinkage when evaluated in fixed-wall permeameters and exposed to full concentrations of organic solvent leachates (e.g., xylene, methanol, aniline, and acetic acid) (see Anderson et al. [65]).

This second feature of clay liners caused the U.S. Environmental Protection Agency (EPA) to promulgate the following regulations on July 6, 1982:

> Prevention (using geomembranes), rather than minimization (using compacted clay liners), of leachate migration produces better environmental results in the case of landfills used to dispose of hazardous wastes. A liner that prevents rather than minimizes leachate migration provides added assurance that environmental contamination will not occur.

The above events have ushered in increased awareness of, interest in, and demand for geomembranes made from polymeric materials. This section and the following one focus on geomembrane designs for landfill liners beneath the waste and closure systems above the waste, respectively.

Note, however, that all landfills are not hazardous, toxic, or radioactive. A suggested ranking of environmental and health concern from lowest to highest is as follows:

- Power plant bottom and fly ash
- Construction and demolition waste

TABLE 5.16 LEACHATE CHARACTERISTICS FROM MUNICIAL AND HAZARDOUS SOLID
WASTE LANDFILLS

Parameter	Unit	MSW (range)	HSW (average)
Chemical oxygen demand (COD)	mg/l	40–89520	37200
Biological oxygen demand (BOD)	mg/l	81–33360	19500
Total organic content (TOC)	mg/l	256–28000	—
pH-value	standard	3.7–8.5	9.1
Total solids (TS)	mg/l	0–59200	—
Total dissolved solids (TDS)	mg/l	584–44900	50100
Total suspended solids (TSS)	mg/l	10–700	212
Specific conductance	μS/cm	2810–16800	—
Alkalinity ($CaCO_3$)	mg/l	0–20800	11600
Hardness ($CaCO_3$)	mg/l	0–22800	—
Total phosphorous (P)	mg/l	0–130	21
Ortho-phosphorous (P)	mg/l	<None>6.5–85	—
NH_4-N	mg/l	0–1106	—
$NO_3 + NO_2$-N	mg/l	0.2–10.29	—
Calcium (Ca^{2+})	mg/l	60–7200	30
Chlorine (Cl^-)	mg/l	4.7–2467	12100
Sodium (Na^+)	mg/l	0–7700	13250
Sulfate $(-SO_3)^{2+}$	mg/l	1–1558	3850
Manganese (Mn)	mg/l	0.09–125	—
Magnesium (Mg)	mg/l	17–15600	16
Conductivity	μ Mhos	—	38575
Oil and grease	mg/l	—	210
Silica (SiO_2)	mg/l	—	141
Iron	mg/l	—	19
Nickel	mg/l	—	28
Potassium	mg/l	—	2715
Nitrate (N)	mg/l	—	51
Benzene	μg/l	—	6500
Chloroform	μg/l	—	1330
1,1 dichlorethane	μg/l	—	2900
Ethyl benzene	μg/l	—	35
Phenol	μg/l	—	14100
Styrene	μg/l	—	95
Toluene	μg/l	—	21100
m-xylene	μg/l	—	284
o-xylene	μg/l	—	93

Sources: MSW data from Chian and deWalle [62]; HSW data from Dudzik and Tisinger [63].

- Dredged river and harbor sediments
- Sewage-treatment sludge
- Treated or incinerated waste ash
- Nontreated nontoxic waste
- Untreated municipal waste

- Untreated biological (hospital) waste
- Heap leach residual waste
- Near hazardous waste
- Hazardous waste
- Radioactive waste: low level, transuranic, high level

To make regulatory distinctions in this listing of solid waste materials is extremely difficult. While MSW is extremely large in quantity, HSW is significantly more dangerous in quality. For this reason, the U.S. Environmental Protection Agency has expended considerable effort in making a distinction between hazardous and nonhazardous waste. For *hazardous waste* (as classified as having any one of 800^+ priority pollutants above legislated acceptable limits), federal regulations fall under 40 CFR 264.221 (1986). Such Subtitle C hazardous-waste landfills, surface impoundments, and waste piles must have

> ... two or more liners and a leak detection system between such liners. The liners and leak detection system must protect human health and the environment ... The requirement for the installation of two or more liners ... may be satisfied by the installation of a primary liner designed, operated, and constructed of materials to prevent the migration of any constituent into such liner during the period such facility remains in operation (including any post-closure monitoring period), and a secondary liner designed, operated, and constructed to prevent the migration of any constituent through such liner during such period.

Furthermore, the leachate collection and removal system regulations for double-lined waste piles and landfills specifically require that the system be designed and operated to ensure that the leachate depth over the primary liner does not exceed 300 mm. The system must also be chemically resistant to wastes and leachate, sufficiently strong to withstand landfill loadings, and protected from excessive clogging. Minimum technology guidance for double liners provides specific design criteria for the leachate-collection and leak detection systems. These criteria are as follows:

- The leachate collection system should be capable of maintaining a leachate head of less than 300 mm above the primary liner.
- Both leachate collection and leak detection systems should have at least 300 mm granular drainage layers that are chemically resistant to the waste and leachate, with a permeability not less than 0.01 cm/sec or an equivalent geosynthetic drainage material (e.g., a geonet or geocomposite).
- The minimum bottom slope of the facility should be 2%.
- The leachate-collection system should have a granular soil filter or geotextile above the drainage layer to prevent excessive clogging.
- Both systems when made of natural soils should have a drainage system of interconnected pipes to efficiently collect leachate; the pipes should have sufficient strength and chemical resistance to perform under anticipated landfill loadings.
- By virtue of the leak-detection rules 40 CFR 260, 264, 265, 270, 271 (1992), a site-specific action leakage rate (ALR) must be set for each facility.

- A construction quality assurance (CQA) program must be developed to see that the constructed facility meets or exceeds all design criteria, plans, and specifications.

Note that most federal and many state regulations refer to the leachate-collection systems above the primary liner as the primary leachate collection and removal systems (PLCRS), and to the leak-detection systems between the two liner systems as the secondary leachate collection and removal systems (SLCRS). For simplicity, we will refer to these two drainage systems as *leachate collection* (above the primary liner) and *leak detection* (between the primary and secondary liners).

For *nonhazardous waste*—those wastes that do not contain priority pollutants, or at least not higher than prescribed levels—federal regulations fall under 40 CFR Parts 257 and 258 Subtitle D for solid-waste disposal. These regulations clearly identify MSW as being the focus material of the regulations. However, it is presumed that non-hazardous industrial waste could fall under these Subtitle D regulations rather than under those of Subtitle C. Some salient points regarding Subtitle D liner systems are as follows:

- A leachate collection system should be located above the liner system.
- The leachate collection system should be capable of maintaining a leachate head of less than 300 mm on the liner system.
- The liner system could be a single composite liner (i.e., it is not required to have a double-liner system with leak detection capability).
- The single composite liner must be a geomembrane placed over a compacted clay liner.
- The geomembrane must be at least 0.75 mm thick, unless it is HDPE. A HDPE geomembrane must be at least 1.50 mm thick.
- The geomembrane must have "direct and uniform contact with the underlying compacted soil component." Furthermore, the phrase "intimate contact" is used in many state regulations.
- The compacted clay liner must be at least 600 mm thick and of a permeability of 1×10^{-7} cm/s or less.

Thus it is seen that by regulatory mandate there is an extremely large use of geomembranes and associated drainage systems for liner systems in the United States. In both hazardous and nonhazardous waste legislation, geosynthetic materials can be substituted for natural soil materials if technical equivalency can be shown. Thus geonets can often be used to replace drainage soils, geotextiles can often be used to replace filter soils, and geosynthetic clay liners can sometimes be used to replace compacted clay liners. It is quite clear that liner and drainage systems of this type are a major use of geosynthetics in North America.

The regulations just mentioned are minimum technology guidance (MTG) and individual states can, and often do, exceed these requirements. For example, in New York state all solid waste (both hazardous and nonhazardous) goes into landfills that consist of primary and secondary double-composite (geomembrane and compacted

clay) liner systems. Approximately 15 other states also have double liner regulations that are distinctly more restrictive than the federal standards. Indeed, a consulting engineering firm under contract to an owner/operator developing a landfill liner system must be fully cognizant of the state regulations where the facility will be located. It is typically this state that must issue the permit to proceed with construction.

While the preceding discussion on landfill liner regulations was focused on the United States, it must be noted the German regulations are also fully developed. Regulatory personnel from the two countries have long interacted with each other, resulting in largely parallel systems. The German regulations differ in the following ways:

- The only geomembrane resin type that is permitted is HDPE.
- The minimum thickness of the geomembrane must be 2.0 mm.
- The compacted clay liner beneath the geomembrane is highly engineered, thicker, and of lower hydraulic conductivity than in the United States.
- The drainage stone above the geomembrane is prescribed and must be 16/32 mm diameter rounded stone.
- The protection layer beneath the drainage stone must be such that no more than 0.25% strain is imposed to the underlying geomembrane.
- Intimate contact, translated directly as "press fit," must exist between the geomembrane and the underlying compacted clay.
- The seaming of the geomembranes is done under highly regulated circumstances.

These differences, and many similarities, between the two countries have been the subject of a 1996 workshop (Corbet and Peters [66]). It is an important report because many countries look to either the United States or Germany for guidance in formulating emerging landfill regulations. (See Koerner et al. [67] for a worldwide survey of landfill liner and cover regulations.)

5.6.2 Siting Considerations and Geometry

Due largely to nontechnical considerations (i.e., social, political, and legal), the siting of solid waste landfills of any type is very difficult. This difficulty is increased even further when the waste contains hazardous or radioactive materials. Nowhere is the NIMBY (*Not In My Backyard*) syndrome more obvious. An even higher (more politically oriented) level of difficulty is expressed by the acronym NIMTO (*Not In My Term of Office*). Yet when properly sited, designed, constructed, and maintained, landfills can be made secure for as long as they generate leachate—even in the case of landfills containing low-level radioactive waste. (High-level radioactive wastes have completely different containment strategies than those to be discussed in this book.) When siting a landfill, it is important to consider the following items: the stratigraphy and geology of the site, the depth to the watertable, the quality and significance of subsurface water, the use of down-gradient water, the population type and density, the weather conditions (particularly precipitation), the seismicity of the region, and any other concerns unique to the particular site.

Regarding the geometry for such landfills, the general recommendations and specific designs discussed in Section 5.3.1 have applicability here as well. A major difference, however, is the manner of placement of the contained materials, which are now solid rather than liquid. Solid waste landfills are of the following configurations: (1) in an excavation below grade, (2) as a fill above grade, (3) as a combination of below and above grade, and (4) within a canyon between two hillsides. The waste depths and/or elevations have no technical limits and the current tendency is toward large regionalized *megafills*, versus small localized sites.

The planning of the landfill must be done in the design stage with particular emphasis on the leachate collection (and leak detection, if doubly lined) system, and the leachate removal and subsequent treatment. Separate cells within a landfill are often made, each being an internal containment zone partitioned off by a *berm*, a small soil embankment. The external embankment dikes surrounding the site are usually quite steep and sometimes reinforced with geogrids or geotextiles. When below grade, a haul road is made at the top and used for access during construction and filling. Accepted solid-waste practices must be used (e.g., see Tchobanoglous et al. [68]). As an aside, it is suggested that future cells may be enclosed within a massive geomembrane (a super trash bag, if you will) or be placed beneath a temporary enclosure or canopy made as a tension structure or air-supported structure. Such actions would drastically reduce leachate generation, but are very expensive from an initial cost perspective.

5.6.3 Typical Cross Sections

A critical element in the proper functioning of a landfill is the containment system. This is often referred to as a *liner system* and thus includes geomembranes, compacted clay liners (CCLs), and geosynthetic clay liners (GCLs). Note that a geomembrane placed directly over a CCL or GCL is a single liner, albeit one of a composite nature. For solid-waste landfills, a leachate collection and removal system must be integrated into the system, and in cases of a double liner, a leak detection system is needed as well. The leachate collection and removal system is located above the uppermost, or primary, liner. For single-liner systems, the only way to monitor for a leak through the liner is when the leachate becomes fugitive. This has traditionally necessitated downstream monitoring wells and, for comparative purposes, upstream wells. If the wells are numerous enough and properly sited, the difference in water quality between downstream and upstream wells is indicative of the functioning of the landfill liner. If the quality is the same, the lined landfill is functioning as intended. If not, a leak is suggested and the local area is possibly contaminated. Considerably better than such a hit-or-miss leak detection approach is to construct a double-lined landfill liner with a leachate collection and removal system above and a leak detection system between them. When graded to a low spot beneath the landfill, any leachate getting through the primary (upper) liner is detected in the leak detection system and indicates an improperly functioning primary liner system.

Figure 5.39 presents average leakage rates from 287 double-lined landfill cells in the United States at different life cycle stages. Stage 1 occurs during construction and initial waste placement; Stage 2 occurs after considerable waste is placed; and Stage 3

(a) Sand leak detection system

(b) Geonet leak detection system
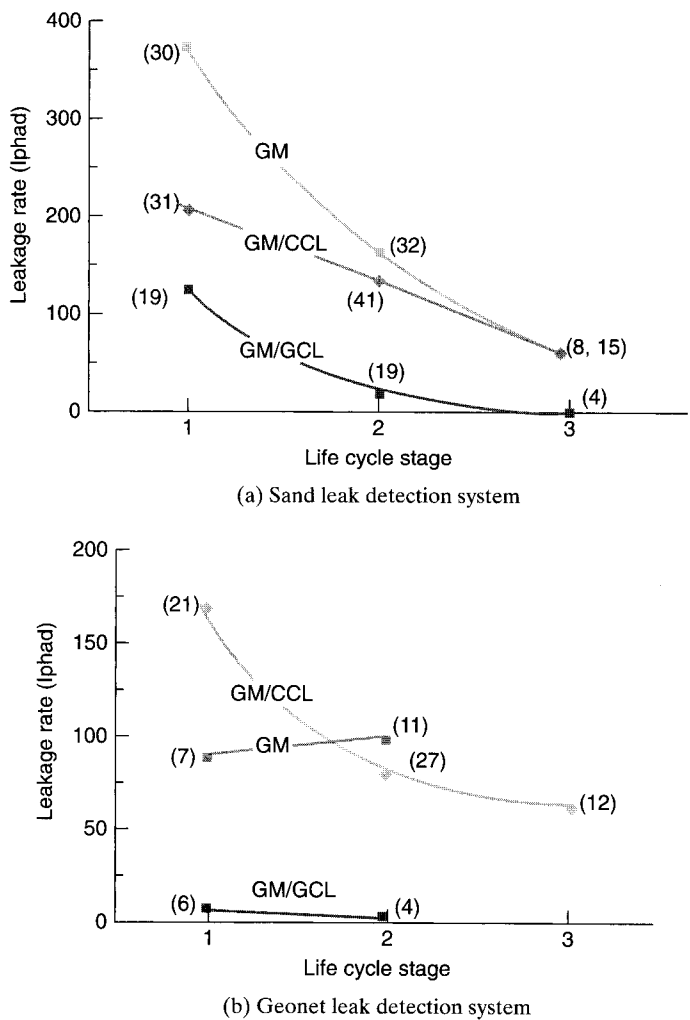
Figure 5.39   Leakage rates from 287 double-lined landfill cells in the United States with different types of primary liners. Each point represents the average of the number of cells in parentheses. (After Othman et al. [69] and Bonaparte et al. [70])

occurs after final cover is placed [69, 70]. The data clearly indicate that a geomembrane (by itself) as a primary liner allows for the highest leakage. A geomembrane over compacted clay liner (GM/CCL) composite results in almost as much leakage, the true amount of leakage being masked by expelled consolidation water from the CCL. A geomembrane over geosynthetic clay liner (GM/GCL) composite is clearly the preferred system for a primary liner resulting in extremely low leakage rates approaching negligible after Stage 2 is reached. Field data such as those shown in Figure 5.39 are very powerful in understanding the behavior of liner systems and in setting values for

action leakage rates (ALRs). Obviously, the situation can become quite contentious if an ALR has been set for the site and it is exceeded because of consolidation water from the overlying CCL, thus the preference for GM/GCL composite liners.

If, indeed, leachate leakage through the primary liner is noted above the ALR, corrective measures must be instituted. The prescribed corrective measures will be delineated in the response action plan (RAP), which necessarily accompanies the regulatory permit and sets the site-specific ALR value. Such actions might be continuous monitoring and tracking of the leakage rate; chemical analysis of both the liquid in the leak detection system and the leachate in the primary collection system for comparative purposes; placement of downstream monitoring wells (or additional ones); secession of waste placement in the facility; and removal of waste from the facility to find and repair the leak(s).

Using these concepts, Figure 5.40 shows the genesis of liner systems that have been used in the United States since the enactment of the 1982 legislation mentioned earlier. Table 5.17 contains details for each of the eight parts of the figure. Figure 5.40a shows the best that we could hope for in a solid waste liner system prior to 1982. There were no regulations on the clay thickness or on its permeability. (Recall that throughout this book, permeability is used rather than hydraulic conductivity.) The enactment of the 1982 regulations gave rise to the cross section of Figure 5.40b. Shortly thereafter, it was recognized in 1983 that redundancy of geomembrane liners was desirable, which allowed for a leak detection layer to be placed between the two geomembranes (see Figure 5.40c). However, CCLs were not to be denied. The study in Anderson et al. [65] was flawed to the extent that neat chemicals were used and evaluated in rigid wall permeameters. With additional research, CCLs reentered the cross section as part of a composite liner, as shown in Figure 5.40d [71]. Work by Giroud and Bonaparte [72] confirmed the low leakage rates that could be accomplished through composite liners having intimate contact with one another.

It was soon recognized that these layered geosynthetic and natural soil systems were difficult to construct, particularly due to the problem of the drainage soil's stability when placed on geomembranes on side slopes. Geonets entered as the leak detection network (no perforated pipes were required), as shown in Figure 5.40e. Thus stability was ensured, as well as considerable savings in volume (i.e., airspace).

The effectiveness of a composite liner is not to be denied. Furthermore, if it is the best strategy for the secondary liner, why not the primary liner as well? Hence we have the cross section in Figure 5.40f. The CCL above the geonet leak-detection system is however extremely difficult to properly place and compact. Furthermore, the consolidation water expelled during waste placement is so troublesome that an alternate scheme is very attractive. GCLs as the lower component of the primary liner nicely solve this situation, with the added attraction of saving additional volume; see Figure 5.40g.

Finally, the use of either geonets (biplanar or triplanar) or high compressive strength geocomposites for leachate collection above the primary liner is being used in some facilities, particularly on side slopes; see Figure 5.40h. Thus it is seen that geosynthetics have replaced natural soils in the entire cross section, with the exception of the lower component of the secondary liner. In this location, directly on top of
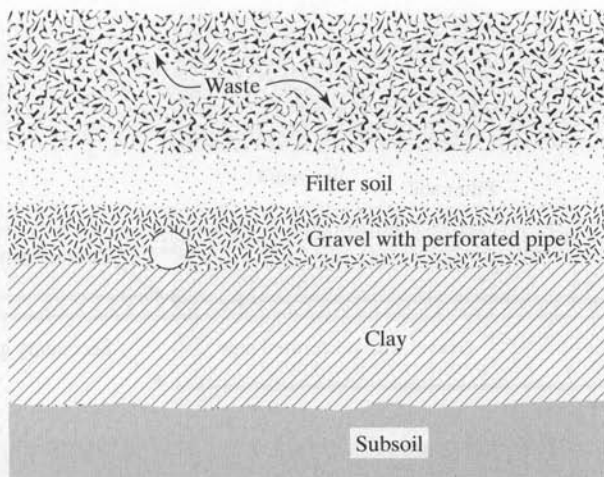
(a) Single-clay liner
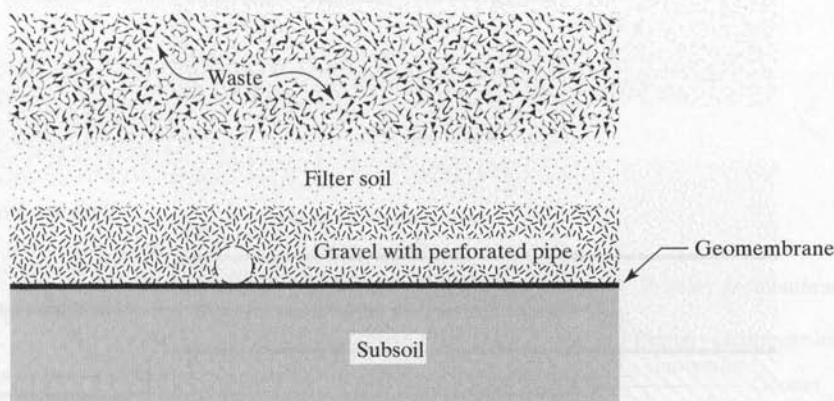
(b) Single-geomembrane liner

Figure 5.40a   Genesis of liner cross sections used to contain solid waste in the United States since 1982.

the soil subgrade, a CCL can be placed and compacted with no danger of damaging any underlying geosynthetic materials. More recently, however, in areas of low availability of clay soils a composite of GM/GCL/CCL (when the CCL $>1 \times 10^{-7}$ cm/s) has been used as the secondary liner system.

It is readily seen in the cross section of Figure 5.40h that great demands are being placed on geosynthetics in solid waste liner systems. The designs to follow, as well as others that have been already presented in this book, focus on many of these details. In this discussion on liner systems we mentioned savings in volume, or air space, several times. Example 5.17 illustrates the financial impact of air space on a facility's owner/operator.
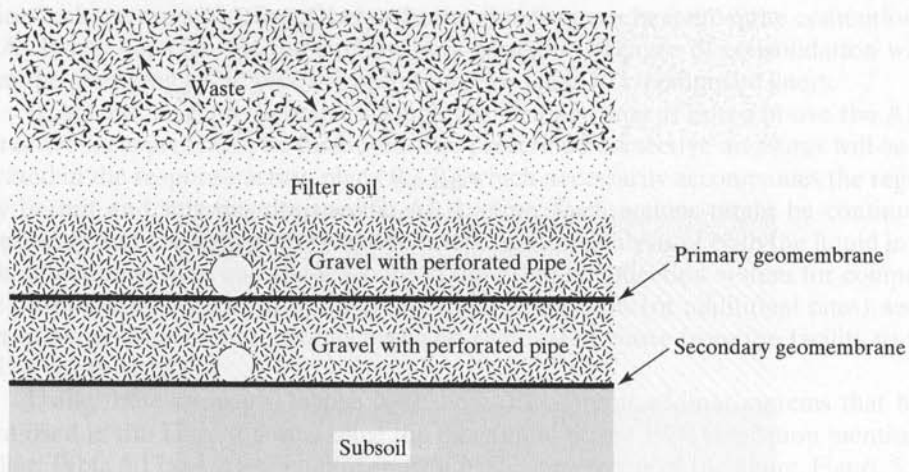
(c) Double-geomembrane liner
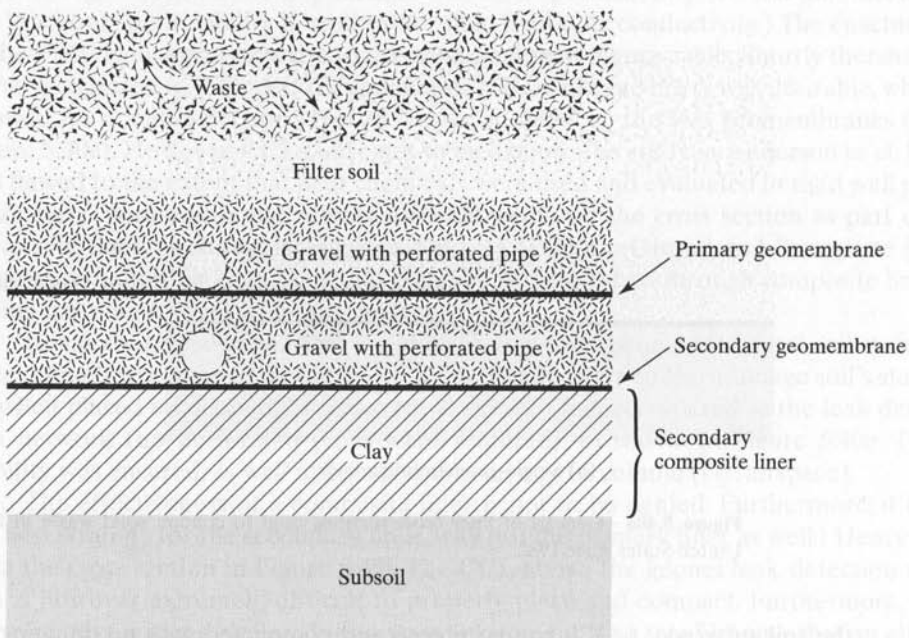
(d) Single-geomembrane, single-composite liner
(After Buranek and Pacey [71])

Figure 5.40b
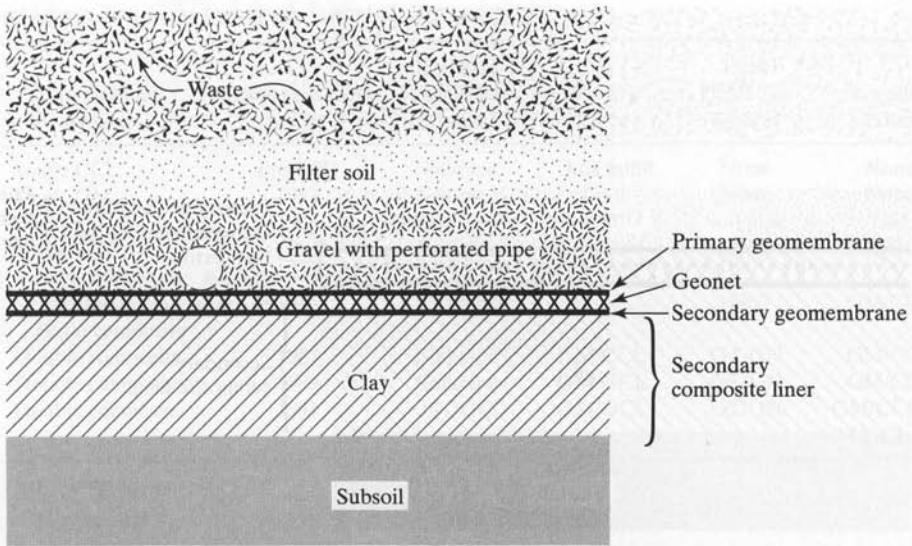
(e) Single-geomembrane, single-composite liner with geonet
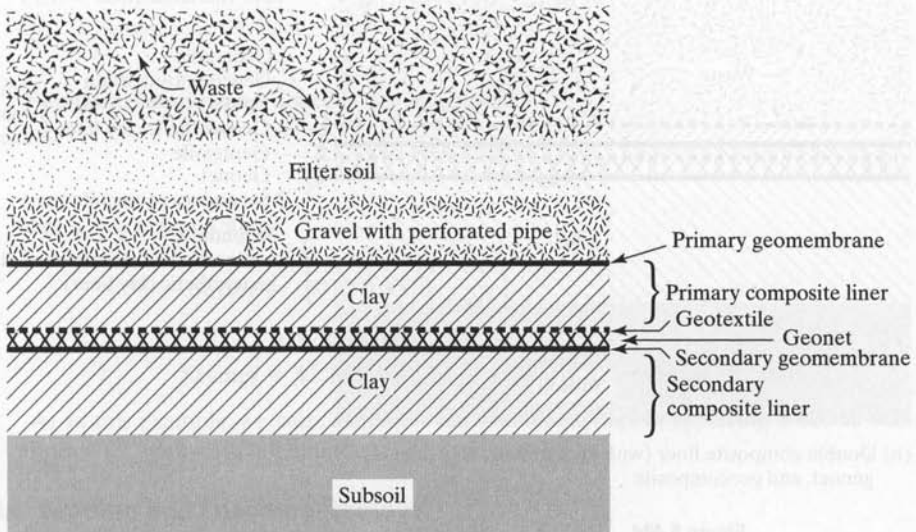
(f) Double-composite liner with geonet

Figure 5.40c

The profile (see cross section) of a landfill must be such that a minimum-
al flow (or leachate) (in a sump) always exists. This means to us for both the leachate
collection and, when present, for the leak detection system as well. Thus a certain grad-
ing of the bottom of the landfill (as well within a landfill) is very important. Conse-
quently, the very bottom (very deep) is continuous using a sump thick channel geonet to
avoid hanging. It can also send land into a leak detection layer. Volume is significant but to
discontinue the extensted gradient 4.0 and the lead to be transferred in the sand [1]. How much
of seal from outside a certain application is not a time optimal local lateral leak detection only
before it is carried through to make of where is the first drainage action.

(g) Double-composite liner (with geosynthetic clay liner) and geonet
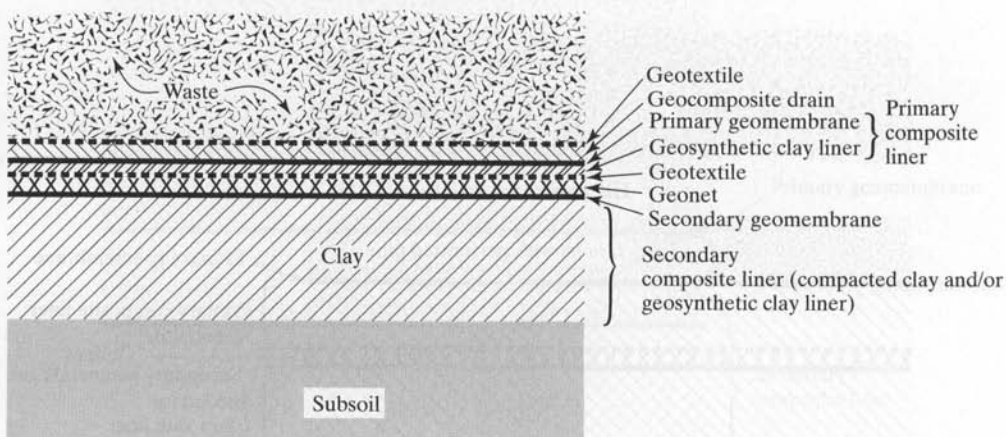
(h) Double-composite liner (with geosynthetic clay liner),
    geonet, and geocomposite

Figure 5.40d

Example 5.17

In a 5 ha landfill cell, a designer is considering using a 5 mm thick drainage geonet to re-
place a 300 mm thick sand layer as a leak detection layer. Technical equivalency has been
shown numerically in Section 4.2.2 and has been corroborated in the field [73]. How much
will the geosynthetic replacement save if the tipping fee of the solid waste is $80 per cubic
meter, as it is currently for municipal solid waste in the Philadelphia area.

TABLE 5.17   GENESIS OF LINER SYSTEMS USED IN THE UNITED STATES

Figure 5.40 (part)	Type of Liner System	Approximate Date in Use	Leachate Collection System	Primary Liner	Leak Detection System	Secondary Liner
(a)	Single CCL	Pre-1982	Soil/pipe	CCL	None	None
(b)	Single GM	1982	Soil/pipe	GM	None	None
(c)	Double GM	1983	Soil/pipe	GM	Soil/pipe	GM
(d)	Single GM, single composite	1984	Soil/pipe	GM	Soil/pipe	GM/CCL
(e)	Single GM, single composite	1985	Soil/pipe	GM	GN	GM/CCL
(f)	Double composite	1987	Soil/pipe	GM/CCL	GT/GN	GM/CCL
(g)	Double composite	1989	Soil/pipe	GM/GCL	GT/GN	GM/CCL
(h)	Double composite	1991	GT/GC	GM/GCL	GT/GN	GM/CCL, or GM/GCL/CCL

Abbreviations: GM = geomembrane
GN = geonet
GT = geotextile
GC = geocomposite
CCL = compacted clay liner
GCL = geosynthetic clay liner

Solution: The air space saved is first calculated.

$$\Delta H = 300 - 5$$
$$= 295 \text{ mm}$$

For a 5 ha cell at $80/m^3,

$$\text{Saving} = (80)(10{,}000)\left(\frac{295}{1000}\right)$$
$$= \$236{,}000/\text{ha}$$
$$\text{Savings} = \$1{,}180{,}000/5 \text{ ha} \qquad \text{Clearly a significant amount!}$$

As in this example, we can calculate even greater savings in replacing a 600 to 900 mm thick CCL with a 7 to 10 mm thick GCL.

5.6.4 Grading and Leachate Removal

The profile and configuration of the bottom of a landfill must be such that gravitational flow to a low point (a sump) always exists. This must be true for both the leachate collection and, when present, for the leak detection system as well. Thus accurate grading of the bottom of the landfill (or cell within a landfill) is very important. The consequence of improper design (localized low points, subsidence of subsoil, poor construction quality control and assurance, etc.) is that leachate will pond above the geomembrane and eventually diffuse through it, rather than being continuously removed and treated. Grading of the site for gravity flow leachate collection and leak detection is not only critically important but particularly difficult as well.

For large sites with no watertable restrictions, grades of 2% or higher can be de-signed and constructed with relative ease. However, such grades in a large landfill take considerable air space from the facility and alternate designs (e.g., accordion-shaped profiles) become advantageous. For smaller sites and/or high watertables, however, the design is usually on the basis of 0.5 to 1% slopes, which is very difficult and costly. Figure 5.41 gives some possible contours for gravity flow drainage. The low point of the leachate collection system must terminate at a sump with an outlet stemming from this location to beyond the landfill or cell.

For sites where removal pipe systems within the leachate collection soil must be periodically inspected, cleaned, and flushed, both access and egress must be available.

(a) V-shaped bottom

Outlet
well (sump)

Outlet
well (sump)

(b) Accordion-shaped bottom
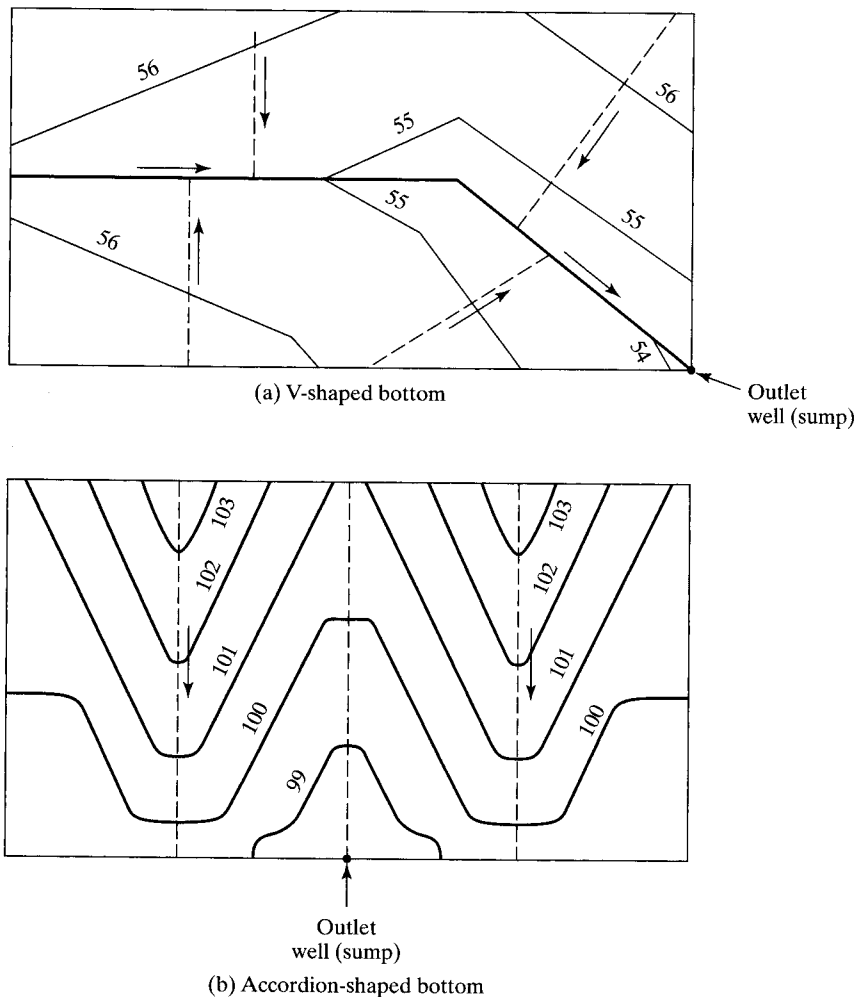
Figure 5.41 Two shapes of landfill bottoms for proper leachate collection and/or leak detection.

This will require careful planning and can completely dictate the nature of the grading plan. Some permits require only the header pipe to be cleaned; thus feeder liners can be laid out in a herringbone fashion, and V-shaped contours over the entire cell are acceptable. Figure 5.41a shows such a scheme, but sharp bends, both horizontal and vertical (i.e., up side slopes), must be made with wide-angle fittings. If all the pipes must be inspected, cleaned, and flushed, the accordion profile shown in Figure 5.41b must be considered. Within each trough will be a perforated pipe having access at the top of the slope and egress at the bottom of the slope. This latter case is very difficult to handle when constructing individual cells within a larger permitted facility.

There are three approaches toward the removal of leachate when it reaches the downgradient sump: (1) gravity flow, (2) vertical manholes, and (3) sidewall risers. These are shown in Figure 5.42. The gravity flow approach shown in Figure 5.42a has the advantage of not requiring pumps, but the disadvantage of requiring a difficult liner penetration at the lowest elevation in the cell. The vertical manhole approach shown in Figure 5.42b has the advantage of a large diameter pipe for pump insertion and inspection but the major disadvantage of downward pressure being exerted on the outside of the risers by the subsiding waste mass. Called *downdrag* or *negative skin friction* by geotechnical engineers in dealing with end bearing piles, piers, and caissons, it has resulted in very large downward pressures and crushing of the pipe and/or sump at the base. Numeric examples from Richardson and Koerner [74] illustrate this feature. To relieve the pressures somewhat, the outside of the concrete riser sections extending through the waste is sometimes wrapped in a low-friction material, such as HDPE. Other downdrag-reducing methods such as bitumen slip layers are also possible [75]. Vertical manhole risers of this type through the waste, however, are generally not recommended for leachate removal. The downdrag issue is essentially eliminated by using a sidewall riser scheme for leachate removal, as shown in Figure 5.42c. In doing so, the vertical risers through the waste mass itself, which result in many operational problems, are avoided. For sidewall risers, a large diameter HDPE pipe, typically 300 mm, terminates with a T-section in the sump that has numerous perforations in it. An HDPE rub sheet is placed under the T-section. The riser is brought up the side slope and into a shed. Here a submersible pump is lowered into the pipe for removal of leachate on demand. The pump can be withdrawn for maintenance or if problems arise. Figure 5.43a illustrates the type of sump area along with the riser pipes. Figure 5.43b illustrates the two large pipes for primary leachate removal, the smaller central pipe for header cleanout, and the smaller pipe on the right for leak detection monitoring. An additional favorable aspect of sidewall risers of the type shown in Figure 5.42c is that the sump can be quite large in area—for example, 5 to 10 m in length and width. By so doing, the depth of leachate in the sump can be limited to the usually prescribed value of 300 mm. Thus regulatory constraints are met and the penetrations and seaming of the geomembrane are much simpler than with the gravity flow system of Figure 5.42a.

Irrespective of the method of leachate removal, it must now be collected and properly treated before release into the local waterway or sewer system. Collection is in tank trucks for small landfills, or lined surface impoundments or steel storage tanks for large landfills. In some cases, the leachate is piped directly into the local sewage
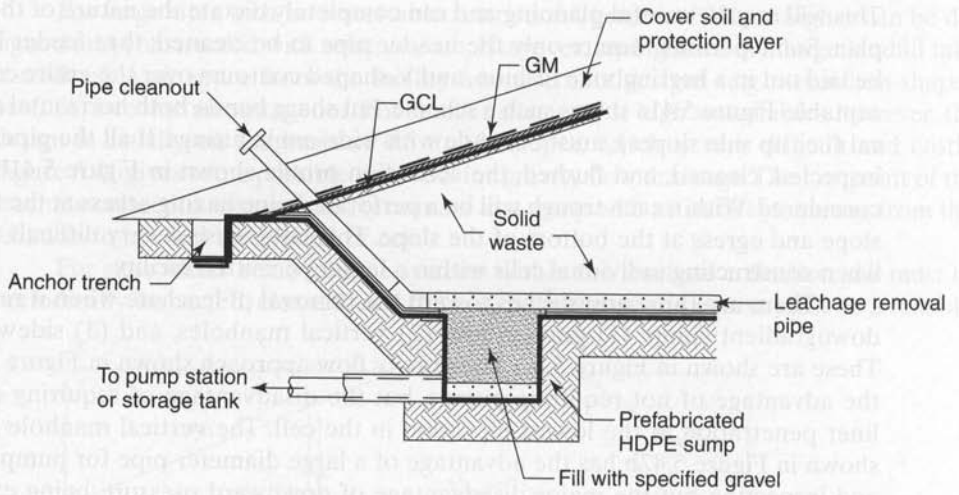
(a) Leachate removal by gravity flow from bottom of sump.
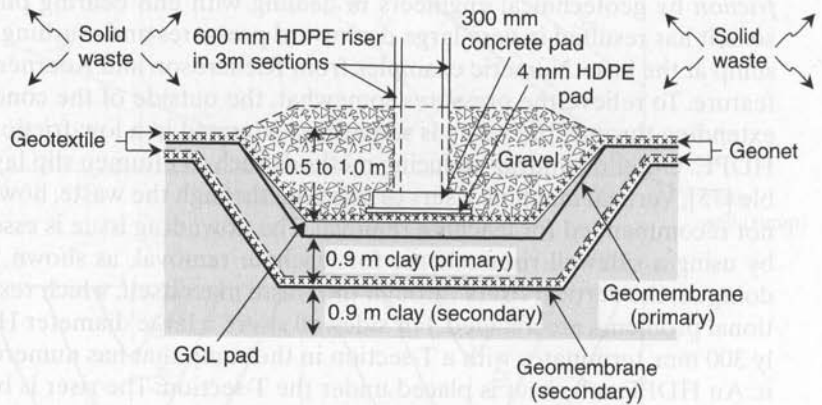
(b) Leachate removal from vertical manhole
extending up from sump
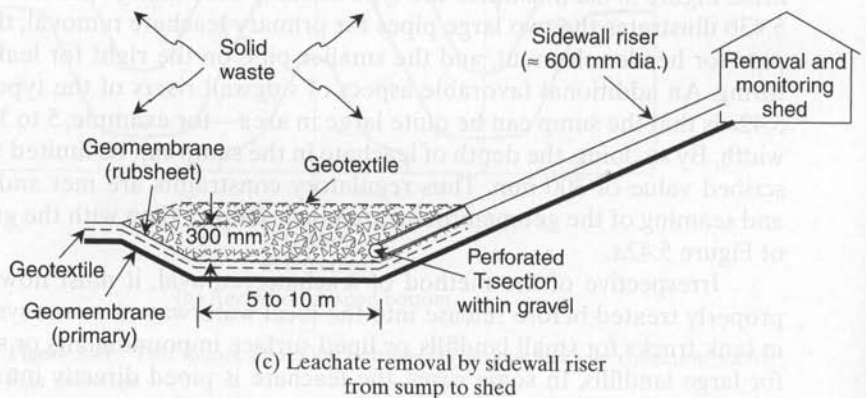
(c) Leachate removal by sidewall riser
from sump to shed

Figure 5.42 Various leachate removal designs for primary leachate collection systems.

(a) Two sidewall risers extending from large area sump
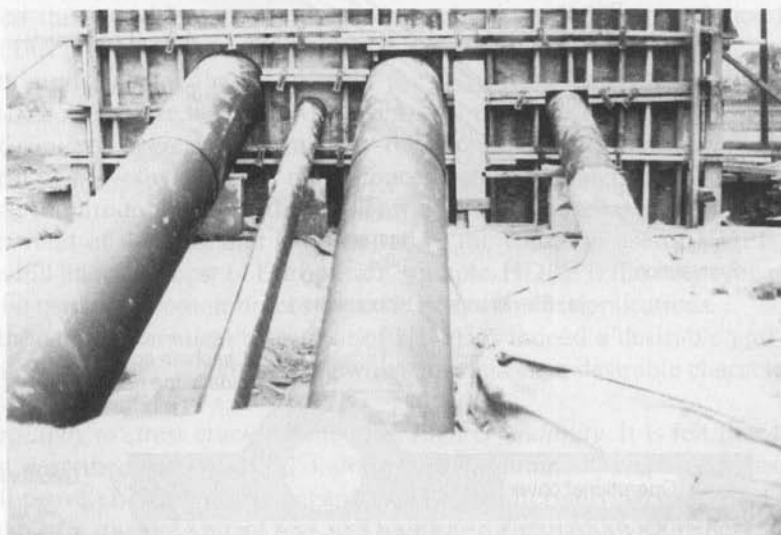
(b) Sidewall risers plus leak detection and cleanout pipes all leading
to shed at top of slope

Figure 5.43 Leachate removal pipe systems using sidewall risers.

treatment facility. Such treatment is clearly leachate-specific and site-specific and ad-
dressed in many textbooks, such as [68].

The monitoring and removal of liquid from the *leak detection system* between the
primary and secondary liners in a double-lined system is also necessary. To do so, a

HDPE pipe of 100 to 150 mm diameter is placed between the primary and secondary liners from a small sump in the secondary liner up the side slope, as shown in Figure 5.44. It is necessary to penetrate the primary liner at the upper slope, but pipe boots can be carefully fitted and seamed for this detail. A small diameter bailer or pump is generally used to extract and monitor the liquid within this leak detection piping system (see the right side pipe in Figure 5.43b).

Liquid in leak detection sumps can be quantitatively measured by a number of techniques. Some of the following have been noted at sites and mentioned in the literature: monitoring the change in liquid depth in the sump or riser pipe, using a flow meter with a mechanical or automatic accumulator coming from the sump, using a tipping bucket for gravity systems with a mechanical or automatic counter, and adapting a weir to the tipping bucket for gravity systems.

(a) Elevation view along slope

(b) Cross-section along slope
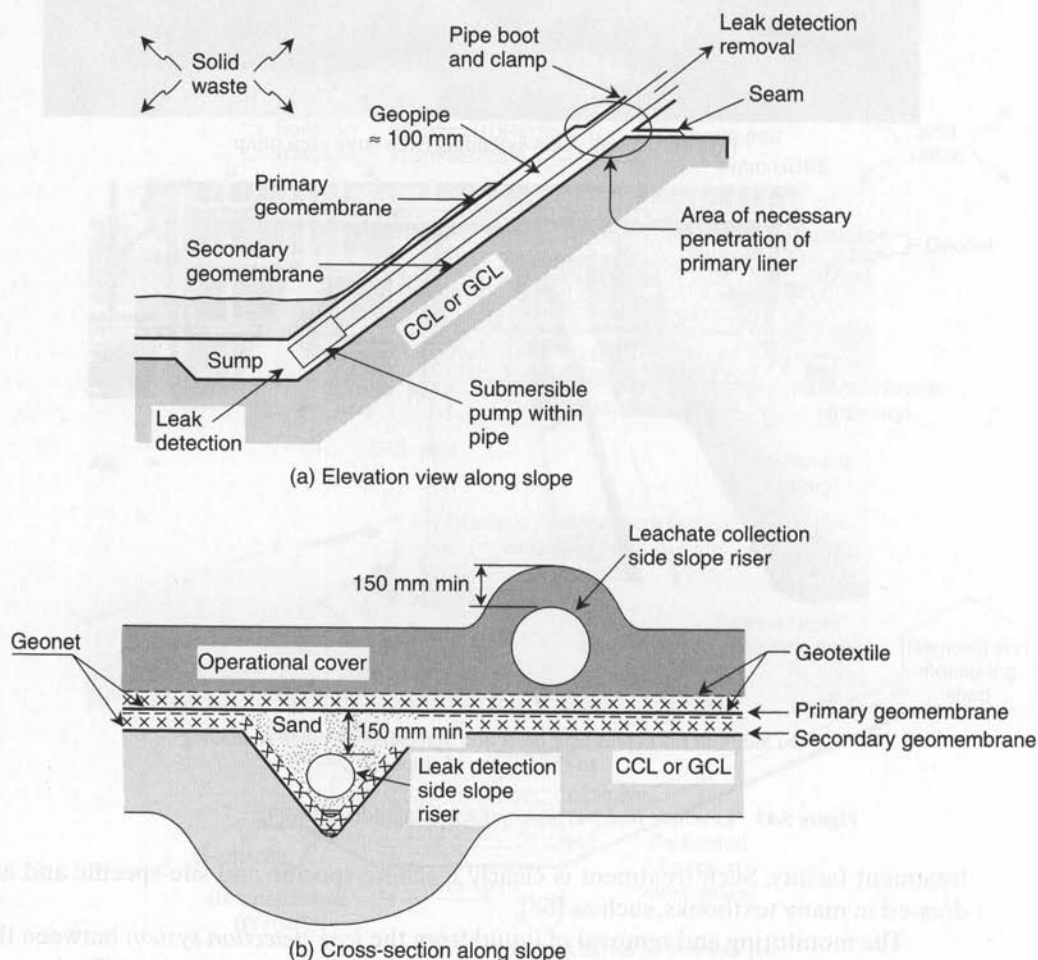
Figure 5.44 Leak detection removal pipe system using sidewall riser.

The quantity of the liquid gathered in the leak detection sump must, of course, be compared to the ALR, as prescribed in the site-specific response action plan (RAP). Recall the discussion in Section 5.6.3. The quantities of liquids found in the leak detection sumps of different facilities vary widely. The actual quantity appears to depend upon various factors: the attitude of the installation contractor, the workmanship of the contractors' personnel, appropriate CQA versus inappropriate (or no) CQA, the site operations (e.g., type of waste and daily cover), the site location (e.g., hydrology and precipitation), and the type of primary liner system, as seen in Figure 5.39.

5.6.5 Material Selection

The serious consequences of leachate leaks caused by chemical reactions with the geomembrane or its premature degradation makes solid waste landfill liner selection more critical than for any other application. Making the selection process more difficult is the extreme variety of solid waste leachates (recall Table 5.16). Thus candidate liner testing (generally via ASTM D5322) with the actual or synthesized leachate is often necessary to select the proper liner material. This incubation process is then followed by a series of physical and mechanical tests (generally via ASTM D5747) over varying time periods to determine if the original geomembrane properties have changed during the incubation period. If several geomembrane materials are being considered, the one with no change or the least change is the obvious choice. Recall the details of this procedure from Section 5.1.4.

The importance of the selection of the incubating leachate cannot be overemphasized. If a worst-case leachate is selected—for example, one containing organic solvents and similarly aggressive chemicals—the choice of geomembrane will probably be some form of polyethylene. The more concentrated and aggressive the leachate, the higher the required density of the PE. This worst-case leachate selection has indeed been the trend of the past and has resulted in the common use of HDPE for solid-waste landfill liners. In most of Europe, for example, HDPE is the only type of polymer that can be used for geomembranes in waste containment applications.

Although the chemical resistance of HDPE is indeed a desirable and necessary feature of the polymer, it comes along with some less than desirable characteristics:

- *Sensitivity to stress cracking due to its high crystallinity.* It is felt that the NCTL test described in Section 5.1.3 along with its minimum required transition time will prove effective in this regard (see [23]). Alternatively, the SP-NCTL test is more of a quality control test and requires a comparably shorter test time (see Section 5.1.3 and reference [24]).
- *Poor conformance to subgrade materials due to its stiffness and relatively high coefficient of thermal expansion* (recall Table 5.10). This leads to relatively large waves that challenge the requirements that a composite liner have intimate contact between the geomembrane and underlying CCL or GCL.
- *A low friction coefficient of smooth sheet leading to stability concerns.* These concerns are eliminated, however, when using textured HDPE. Although the processes by which texturing is accomplished differ between manufacturers, all result in a major improvement in interface friction.

- *Poor axi-symmetric tensile elongation* (recall Section 5.1.3). This is a concern only for those sites with poor subgrade stability, like piggybacked landfills and landfill covers above degrading waste. In general, it should not be a problem beneath the base of a properly sited and designed landfill. If questionable subgrades are anticipated, out-of-plane deformation can be offset by using coextruded HDPE/ LLDPE/HDPE geomembrane. As shown in Figure 5.5, the core of LLDPE is excellent in this particular stress mode.

In spite of the limitations noted previously, it is felt that, with proper selection of the resin, an awareness of proper design methods, and careful construction quality control and assurance, HDPE should be used for landfill liners that contain aggressive leachates. This is not to say that other existing geomembranes cannot to used, or that other new formulations will not appear in the future. It is only meant to explain the current widespread use of HDPE as landfill liners.

5.6.6 Thickness

According to U.S. EPA regulations, the required minimum thickness of a geomembrane liner for solid-waste containment is 0.75 mm and 1.5 mm if it is made from HDPE. Recall that German regulations require a minimum thickness for HDPE of 2.0 mm and, furthermore, that HDPE is the only polymer that can be used. Whatever the regulatory situation, the technical design should proceed along the same lines as that of any liner, as described in Section 5.3.4. As with thickness design dealing with reservoir liners, solid-waste geomembrane thickness can be calculated and then compared to the above minimum values if regulations apply, or to the minimum survivability values of Table 5.13 if there are no regulations. When the secondary liner is also a geomembrane, it should be the same thickness and type as the primary liner.

The design uses the same formulation as that developed in equation (5.18):

$$t = \frac{\sigma_n x(\tan \delta_U + \tan \delta_L)}{\sigma_{\text{allow}}(\cos \beta - \sin \beta \tan \delta_L)}$$

where

t = thickness of the geomembrane,

σ_n = applied stress from the landfill contents,

x = distance of mobilized geomembrane deformation,

δ_U = angle of shearing resistance between geomembrane and the upper material,

δ_L = angle of shearing resistance between geomembrane and the lower material,

σ_{allow} = allowable geomembrane stress, and

β = settlement angle mobilizing the geomembrane tension.

Example 5.18 illustrates the procedure.

Example 5.18

Obtain the required thickness of a smooth HDPE primary geomembrane beneath a 50 m high landfill containing solid waste of unit weight 12.5 kN/m^3. The localized subsoil settlement is estimated to result in a liner deformation angle of 20°. Drainage sand is above the geomembrane and a geonet is below it.

Solution: The necessary information for solving the design equation is

(a) For out-of-plane tension testing, the yield-stress of HDPE (from Table 5.5c) is conservatively estimated as 20,000 kPa.

(b) The mobilization distance for HDPE at 50 × 12.5 = 625 kPa (from Figure 5.10a) is approximately 80 mm.

(c) The friction angle (from Table 5.7) for smooth HDPE against Ottawa sand (δ_U) is 18°.

(d) The friction angle for HDPE against a geonet (separate test results) (δ_L) is 10°.

(e) These values give the required geomembrane thickness:

$$t = \frac{(625)(0.080)[\tan 18 + \tan 10]}{(20{,}000)[\cos 20 - (\sin 20)(\tan 10)]}$$

$$= \frac{25.1}{17600}$$

$$= 0.00143 \text{ m}$$

$$t = 1.43 \text{ mm}$$

Thus the regulated values of 1.5 mm in the United States or 2.0 mm in compliance with German regulations would control in this situation. Furthermore, the regulated values would be used since they also exceed the *very high* survivability value in Table 5.13 of 1.00 mm thickness.

5.6.7 Puncture Protection

There are many circumstances where geomembranes are placed on or beneath soils containing relatively large-sized stones — for example, poorly prepared clay soil subgrades with stones protruding from the surface or resting on the surface, soil subgrades over which geomembranes (particularly textured) have been dragged dislodging near-surface stones, and all cases where gravel drainage layers are placed above the geomembrane. All of these situations, particularly the last (which is unavoidable since it is a design situation), should use a protective geotextile to avoid puncturing of the geomembrane. Note that if the soil subgrade is a CCL, a geotextile cannot be used and the isolated stones must be physically removed. For the drainage layer case, which is common to all landfills, a nonwoven needle-punched geotextile can provide excellent puncture protection (recall Figure 5.8). However, the issue of required mass per unit area of the geotextile becomes critical.

In a series of papers, Wilson-Fahmy, Narejo and Koerner [76, 77, 78] have presented a design method that focuses on the protection of 1.5 mm thick HDPE geomembranes. The method uses the conventional factor of safety equation:

$$\text{FS} = \frac{p_{\text{allow}}}{p_{\text{reqd}}} \tag{5.32}$$

where

FS = factor of safety (against geomembrane puncture),

p_{reqd} = required pressure due to the landfill contents (or surface impoundment), and

p_{allow} = allowable pressure using different types of geotextiles and site-specific conditions

Based on a large number of ASTM 5514 experiments, an empirical relationship for p_{allow} has been obtained, as shown in equation (5.33). It requires the use of modification factors and reduction factors as given in Table 5.18. Note that in Table 5.18 all MF values ≤ 1.0 and all RF values ≥ 1.0.

$$p_{allow} = \left(50 + 0.00045\frac{M}{H^2}\right)\left[\frac{1}{MF_S \times MF_{PD} \times MF_A}\right]\left[\frac{1}{RF_{CR} \times RF_{CBD}}\right]$$
(5.33)

where

p_{allow} = allowable pressure (kPa),

M = geotextile mass per unit area (g/m^2),

H = protrusion height (m),

TABLE 5.18 MODIFICATION FACTORS AND REDUCTION FACTORS FOR GEOMEMBRANE PROTECTION DESIGN USING NONWOVEN NEEDLE-PUNCHED GEOTEXTILES

Modification Factors (all $\leq$ 1.0)

MF_s		MF_{PD}		MF_A	
Angular	1.0	Isolated	1.0	Hydrostatic	1.0
Subrounded	0.5	Dense, 38 mm	0.83	Geostatic, shallow	0.75
Rounded	0.25	Dense, 25 mm	0.67	Geostatic, mod.	0.50
		Dense, 12 mm	0.50	Geostatic, deep	0.25

Reduction Factors (all $\geq$ 1.0)

			RF_{CR}		
RF_{CBD}		Mass per Unit Area (gm/m^2)	Protrusion Height (mm)		
			38	25	12
Mild leachate	1.1	Geomembrane alone	N/R	N/R	N/R
Moderate leachate	1.3	270	N/R	N/R	>1.5
Harsh leachate	1.5	550	N/R	1.5	1.3
		1100	1.3	1.2	1.1
		>1100	$\cong$1.2	$\cong$1.1	$\cong$1.0

Abbreviations: N/R = not recommended

MF_S = modification factor for protrusion shape,

MF_{PD} = modification factor for packing density,

MF_A = modification factor for arching in solids,

RF_{CR} = reduction factor for long-term creep, and

RF_{CBD} = reduction factor for long-term chemical/biological degradation.

The situation can be approached from a given mass per unit area geotextile to determine the unknown FS value, or from an unknown mass per unit area geotextile and a given FS value. Example 5.19 uses the latter approach.

Example 5.19

Given a coarse-gravel (subrounded with d_{50} = 38 mm) leachate collection layer to be placed on a 1.5 mm HDPE geomembrane under a 50 m high landfill, what geotextile mass per unit area is necessary for a FS value of 3.0? Assume that the solid waste weighs 12 kN/m^3.

Solution: Use H = 25 mm = 0.025 m, which is an estimate since the gravel particles are not isolated but are adjacent to one another, MF_S = 0.5 for shape, MF_{PD} = 0.83 for packing density, MF_A = 0.25 for arching RF_{CR} = 1.5 for creep and RF_{CBD} = 1.3 for long-term degradation Now calculate the value of P_{allow} using equation (5.32):

$$FS = p_{allow}p_{reqd}$$
$$3.0 = p_{allow}(50)(12)$$
$$p_{allow} = 1800 \text{ kN/m}^2$$

Calculate the required mass per unit area of the geotextile using equation (5.33):

$$p_{allow} = \left(50 + 0.00045\frac{M}{H^2}\right)\left[\frac{1}{MF_S \times MF_{PD} \times MF_A}\right]\left[\frac{1}{FS_{CR} \times FS_{CBD}}\right]$$
$$1800 = \left[50 + 0.00045\frac{M}{(0.025)^2}\right]\left[\frac{1}{0.5 \times 0.83 \times 0.25}\right]\left[\frac{1}{1.5 \times 1.3}\right]$$
$$M = 436 \text{ g/m}^2; \text{ use } 500 \text{ g/m}^2$$

The isolated value of 50 kPa in the above equation represents the puncture resistance of the 1.5 mm HDPE geomembranes by itself. Other thicknesses of HDPE or other types of geomembranes will give proportionately different values.

5.6.8 Runout and Anchor Trenches

The terminus of geomembranes is a short horizontal runout at the top of the slope (recall Figure 5.27), and then (usually) a short drop into an anchor trench (recall Figure 5.28). The anchor trench is backfilled with soil and suitably compacted. Concrete anchor trenches with full fixity to the liner should generally not be used since geomembrane pullout is probably more desirable than geomembrane failure, although both should obviously be avoided.

The design method is explained and illustrated in Section 5.3.6 and will not be repeated here. Both analyses (runout alone and runout plus anchor trench) are applicable, with the latter being the most common. Alternatively, a V-trench configuration is also possible.

For termination of double liner systems, the designer is faced with a number of possible choices. Major considerations are to protect the integrity of both geomembranes and to keep surface water out of the leak detection system. In this regard, the two geomembranes can enter separate anchor trenches or come together in a common anchor trench. The primary geomembrane can also be cut short of the anchor trench and welded to the secondary geomembrane along the horizontal runout distance. In seismically active areas, consideration should be given to this latter approach with no vertical anchor trench at all; the logic being that geomembrane pullout is more desirable than geomembrane tensile failure somewhere along the side slope.

The terminus of the liner of a completed internal cell within a zoned landfill, with its eventual extension into an adjacent cell, is usually done by overlapping and seaming along the horizontal runout length of an intermediate berm. When waste fills the second cell, the berm is entombed and the process is then continued from cell to cell. Shear stresses on the geomembranes in both cells over this berm have been evaluated by large-scale laboratory models and found to be generally small and geomembrane-dependent (see Koerner and Wayne [79]). In high berms where higher stresses are generated, an auxiliary (or sacrificial) geomembrane rub-sheet over the crest of the berm should effectively dissipate the stresses before they propagate down to the underlying primary geomembrane.

5.6.9 Side Slope Subgrade Soil Stability

The design of the stability of the soil mass beneath the liner system of a solid-waste landfill is carried out in exactly the same manner as was discussed for liquid containment (reservoir) slopes and berms (recall Section 5.3.5). The process can include the strength of the covering liner materials, but if they are not included in the analysis, the error is on the conservative side. Interior berms, with or without geosynthetic inclusions, are also handled in the same manner as previously described.

5.6.10 Multilined Side Slope Cover Soil Stability

The situation of a liner and its leachate collection cover soil stability, or slumping, becomes quite complicated for multilined geomembrane and geonet collection systems of the type shown in Figure 5.40. Consider such a system, as shown in Figure 5.40e The leachate collection system soil gravitationally induces shear stress through the system, thereby challenging each of the interface layers that are in the cross section. If all of the interface shear strengths are greater than the slope angle, stability is achieved and the only deformation involved is a small amount to achieve elastic equilibrium (Wilson-Fahmy and Koerner [80]). However, if any interface shear strengths are lower than the slope angle, wide-width tensile stresses are induced into the overlying geosynthetics. This can cause the failure of the geosynthetics or pullout from the anchor trench, or it can result in quasistability via tensile reinforcement. If the last is the case, we can refer to the overlying geosynthetics as acting as *nonintentional* veneer reinforcement.

If the situation consists of the double liner system shown in Figure 5.45, all of the interface surfaces can be made quite stable by proper selection of the geosynthetics.
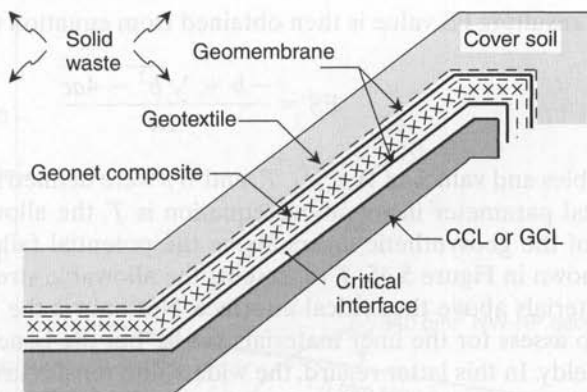
Figure 5.45   Geotextile/geomembrane/geonet composite/geomembrane above a CCL or GCL.

For example, textured geomembranes could be selected, and these together with non-woven needle-punched geotextiles will usually result in peak friction angles in excess of 25°. Furthermore, by thermally bonding the geotextiles in the leak detection system to the geonet, these surfaces are also stable at relatively high slope angles. Thus, the critical interfaces are at the upper (leachate collection sand or gravel) and the lower (CCL or GCL) surfaces. The upper surface is analyzed exactly as described in Section 3.2.7 for the case without geogrid reinforcement. The proper selection of cover soil against a nonwoven needle-punched geotextile (acting as a protection material, recall Section 5.6.7) should also result in a peak friction angle in excess of 25°. This leaves the lower surface of the secondary geomembrane against the clay liner as being the potentially low-interface surface. If the clay liner is a CCL, the concern is with the expelled consolidation water lubricating the interface. This surface has been involved in a major failure of a hazardous waste liner system, as reported by Byrne et al. [81] with an interface friction angle of 10°. If the liner is a GCL, the concern is the hydrated bentonite being extruded out of the upper geotextile and lubricating the interface with an interface friction angle of 5 to 10°. This surface was involved in two slides of full-scale field tests both involving woven geotextiles on the GCL, by Daniel et al. [82].

The analysis of multilined slopes of the type being discussed is a direct extension of the veneer reinforcement model presented in Section 3.2.7 on geogrids. Recalling Figure 3.22b, the analysis results in equation (3.21):

$$a(\text{FS})^2 + b(\text{FS}) + c = 0$$

where

$a = (W_A - N_A \cos \beta - T \sin \beta) \cos \beta,$

$b = -[(W_A - N_A \cos \beta - T \sin \beta) \sin \beta \tan \phi + (N_A \tan \delta + C_a) \sin \beta \cos \beta$
$\quad + \sin \beta(C + W_P \tan \phi)],$ and

$c = (N_A \tan \delta + C_a) \sin^2 \beta \tan \phi.$

The resulting FS value is then obtained from equation (3.22):

$$\mathrm{FS} = \frac{-b + \sqrt{b^2 - 4ac}}{2a}$$

The variables and values of W_A, N_A, T, and W_P were defined in Sections 3.2.7 and 5.3.5. The critical parameter in the above equation is T, the allowable wide-width tension strength of the geosynthetic layers above the potential failure surface. For the cross section shown in Figure 5.45, T represents the allowable strength of all of the geosynthetic materials above the critical interface. Not only is the issue of reduction factors difficult to assess for the liner materials per se, but the issue of strain compatibility is also unwieldy. In this latter regard, the wide-width tensile strength of each geosynthetic material must be determined, plotted on the same axes, and assessed at a specific value of strain. That is, the liner system components cannot act individually and must act as an equally strained unit. Example 5.20 illustrates the situation.

Example 5.20

For a 30 m long slope at 3(H) to 1(V)—i.e., $\beta = 18.4°$ — lined with a double liner system consisting of GT/GM/GC/GM/CCL or GCL (as in Figure 5.45), the lowest friction angle is assumed to be the secondary geomembrane to the underlying clay interface, which is 10°. All other interface friction angles are in excess of 18.4°. The wide-width tensile behavior of the various candidate geosynthetics is given in the following graph. The leachate collection cover soil is 450 mm thick with a unit weight of 18.0 kN/m³ and a friction angle of 30°. What is the factor of safety of the slope based on a cumulative reduction factor of 2.0?

Solution:

$$W_A = \gamma h^2 \left[\frac{L}{h} - \frac{1}{\sin \beta} - \frac{\tan \beta}{2} \right]$$

$$= (18.0)(0.45)^2 \left[\frac{30}{0.45} - \frac{1}{\sin 18.4} - \frac{\tan 18.4}{2} \right]$$

$$= 3.65[63.3]$$

$$= 231 \text{ kN/m}$$

$$N_A = W_A \cos \beta$$

$$= 231 \cos 18.4$$

$$= 219 \text{ kN/m}$$

$$W_P = \frac{\gamma h^2}{\sin 2\beta}$$

$$= \frac{(18.0)(0.45)^2}{\sin 36.8}$$

$$= 6.08 \text{ kN/m}$$

T_{ult} taken at the first geosynthetic failure, which is the nonwoven needle-punched geotextile at 25 kN/m, is

$$T_{\text{ult}} = 25 + 2(22) + 36$$

$$= 105 \text{ kN/m}$$
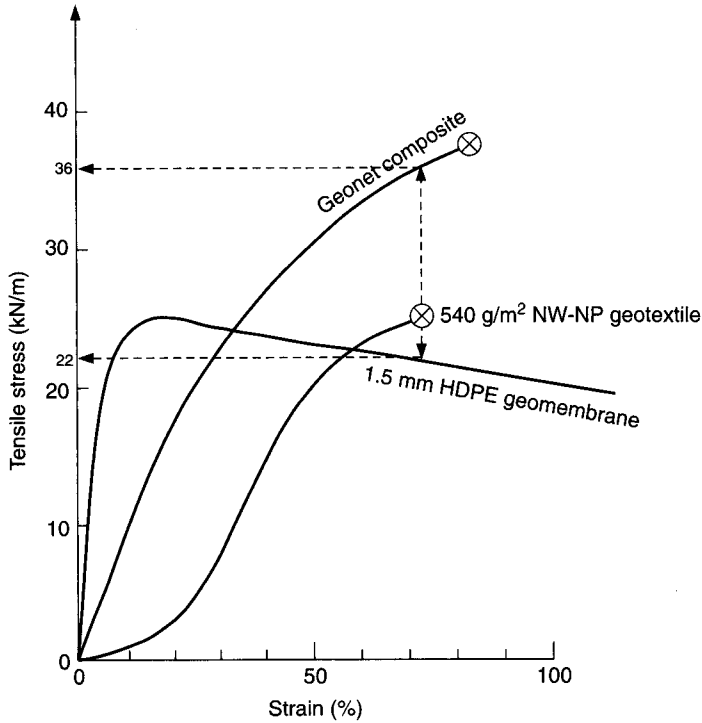
For a reduction factor of 2.0 to obtain T_{allow} gives

$$T_{allow} = 105/2.0$$
$$= 52.5 \text{ kN/m}$$

After calculating the individual values of a, b and c, the FS value will be

$a = (W_A - N_A \cos \beta - T \sin \beta) \cos \beta$
   $= (231 - 219 \cos 18.4 - 52.5 \sin 18.4) \cos 18.4$
   $= 6.1 \text{ kN/m}$

$b = -[(W_A - N_A \cos \beta - T \sin \beta) \sin \beta \tan \phi$
   $+ (N_A \tan \delta + C_a) \sin \beta \cos \beta + \sin \beta(C + W_p \tan \phi)]$
   $= -[(231 - 219 \cos 18.4 - 52.5 \sin 18.4) \sin 18.4 \tan 30$
   $+ (21.9 \tan 10 + 0) \sin 18.4 \cos 18.4 + \sin 18.4(0 + 6.08 \tan 30)]$
   $= -[1.17 + 11.57 + 1.11]$
   $= -13.8 \text{ kN/m}$

$c = (N_A \tan \delta + C_a) \sin^2 \beta \tan \phi$
   $= (219 \tan 10 + 0) \sin^2 18.4 \tan 30$
   $= 2.22 \text{ kN/m}$

$$FS = \frac{-b + \sqrt{b^2 - 4ac}}{2a}$$

$$= \frac{13.8 + \sqrt{(-13.8)^2 - 4(6.1)(2.22)}}{2(6.1)}$$

$$FS = 2.10$$

While the value appears to be acceptable, it is nevertheless disconcerting that the liner system per se is being used as the veneer reinforcement mechanism. Had higher reduction factors been used, the resulting FS value would be proportionately decreased. That said, when the solid waste is placed against the leachate collection soil, a resisting berm is created, bringing stability to the situation at that time.

5.6.11 Access Ramps

For below-grade landfills it is necessary to grade the subgrade to accommodate the necessary access ramp(s), line the entire facility, and then construct a road above the liner cross section. A typical geometry is shown in Figure 5.46a. A particularly troublesome aspect of this design is that the road must be built above the completed liner system. A variety of problems have occurred in the past:

- Inadequate drainage where the ramp meets the upper slope, with subsequent erosion and scour of the roadway itself.
- Inadequate roadway material above the liner system, with ramp soil sliding off the upper geomembrane due to truck traffic.
- Inadequate roadway thickness above the liner system, with the upper geomembrane failing in tension along the slope due to truck traffic.
- Inadequate roadway thickness above the liner system, with an underlying hydrated GCL creating slippage of the overlying geomembrane and entire roadway.

Clearly, a conservative design is required; Figure 5.46b presents some recommendations. While a 600 to 900 mm thickness might seen excessive, the dynamic stresses caused by braking trucks are high, and furthermore, the ramp soil can be removed in whole or in part as the waste elevation rises during filling operations.

5.6.12 Stability of Solid-Waste Masses

Upon first consideration, the stability of solid waste failing within itself should present no particular concern since its shear strength characteristics should be quite high. Singh and Murphy [83] present shear strength parameters of solid waste transitioning from high in friction (24 to 36°) to being high in cohesion (80 to 120 kPa). Obviously, the aging of the waste is an issue, but at all times the shear strength is quite high. A widely used MSW shear strength evelope assembled by Kavazanjian [84] indicates a bilinear response of 33° friction transitioning at less than 30 kPa normal stress to a cohesion of 24 kPa.

Paradoxically, there have been some massive failures of solid waste. Koerner and Soong [85] report on ten such failures of which half were unlined or soil-lined sites, and

(a) Geometry of typical ramp-grades from gentle to 25% (14.0°)

typ. 5–7 m

typ.
600–900 mm

Crushed stone
(SW-GW)

Leachate collection

Leachate collection

(W-MF) GT

(NW-NP) GT

(NW-NP) GT

Large stone and pipe

GM

(b) Suggested cross section
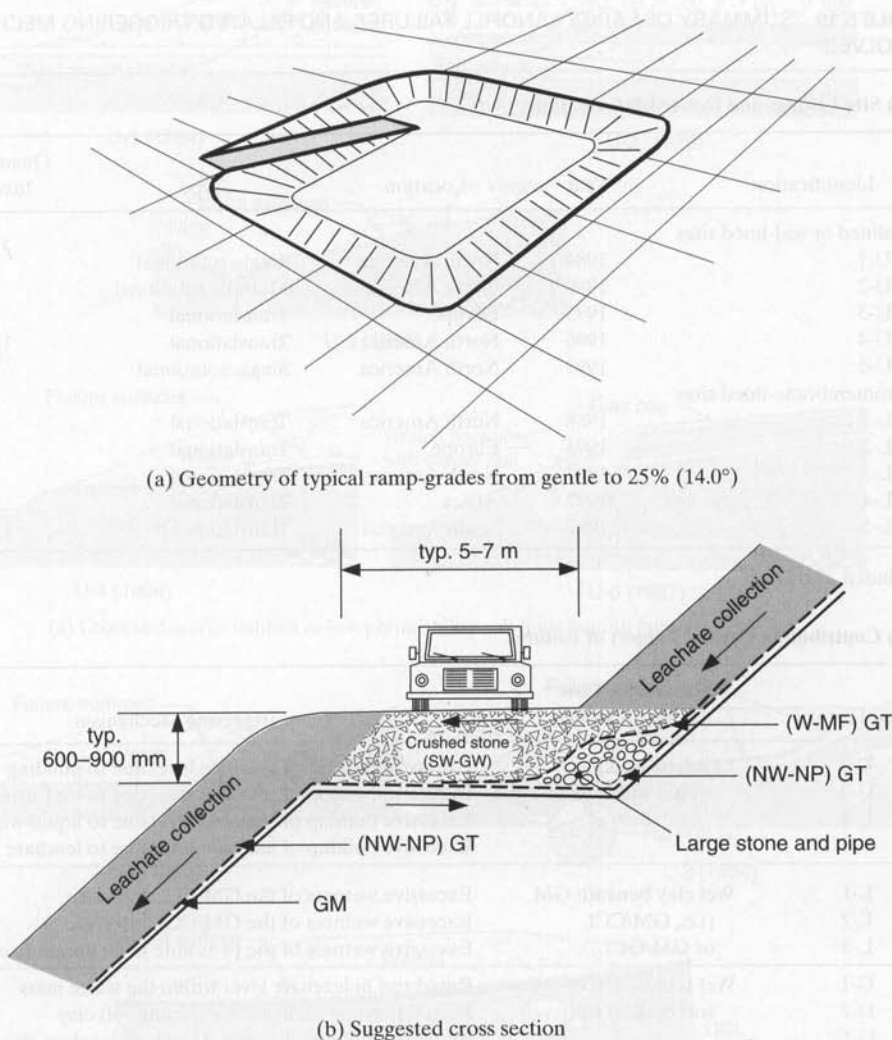
Figure 5.46   Typical geometry and cross section of a below-grade landfill access ramp.

half were at sites that contained geomembranes. Table 5.19a presents some details which were evaluated on the basis of both two-dimensional and three-dimensional analyses. On average the 3-D analyses were 16% higher than the comparable 2-D analyses. The 2-D representations of the individual failures are shown in Figure 5.47. Figure 5.48 shows the enormity of the problem at one of these sites. All of the failures were most dramatic and many involved litigation and fines, to say nothing of the deaths at one site and the environmental damage that ensued at all of the sites. The failure surfaces were either rotational or translational, the latter always occurring at the geomembrane-lined sites. Commercially available slope stability computer codes are

TABLE 5.19 SUMMARY OF LARGE LANDFILL FAILURES AND RELATED TRIGGERING MECHANISMS INVOLVED

(a) Site Listings and Related Information

Identification	Year	Location	Type	Quantity of Waste Involved (m³)
Unlined or soil-lined sites				
U-1	1984	North America	Single rotational	110,000
U-2	1989	North America	Multiple rotational	500,000
U-3	1993	Europe	Translational	470,000[1]
U-4	1996	North America	Translational	1,100,000
U-5	1997	North America	Single rotational	100,000
Geomembrane-lined sites				
L-1	1988	North America	Translational	490,000
L-2	1994	Europe	Translational	60,000
L-3	1997	North America	Translational	100,000
L-4	1997	Africa	Translational	300,000
L-5	1997	South America	Translational	1,200,000

[1]Included 27 deaths!

(b) Contributing Cause (Trigger) of Failures

Case History	Reason for Low Initial FS Value	Triggering Mechanism
U-3	Leachate buildup	Excessive buildup of leachate level due to ponding
U-4	within waste mass	Excessive buildup of leachate level due to ice formation
L-4		Excessive buildup of leachate level due to liquid waste injection
L-5		Excessive buildup of leachate level due to leachate injection
L-1	Wet clay beneath GM	Excessive wetness of the GM/CCL interface
L-2	(i.e., GM/CCL	Excessive wetness of the GM/CCL interface
L-3	or GM/GCL)	Excessive wetness of the bentonite in an unreinforced GCL
U-1	Wet foundation or	Rapid rise in leachate level within the waste mass
U-2	soft backfill soil	Foundation soil excavation exposing soft clay
U-5		Excessive buildup of perched leachate level on clay liner

Source: After Koerner and Soong [85].

readily configured to handle these failures provided that accurate values of shear strength of the material and surfaces involved are known. The importance of direct shear testing (as described in Section 5.1.3) cannot be overstated.

While the stability factors of safety of all of the sites were relatively low prior to failure, each had a unique aspect that Koerner and Soong [85] call a *triggering mechanism*. It was found that all ten failures had triggering mechanisms that involved liquids. Table 5.19b groups the failures according to triggering mechanisms where the excessive liquids are either (1) in the waste mass itself above the liner system, (2) within

(a) Cross sections of unlined or low permeability soil-lined landfill failures

(b) Cross sections of geomembrane-lined landfill failures
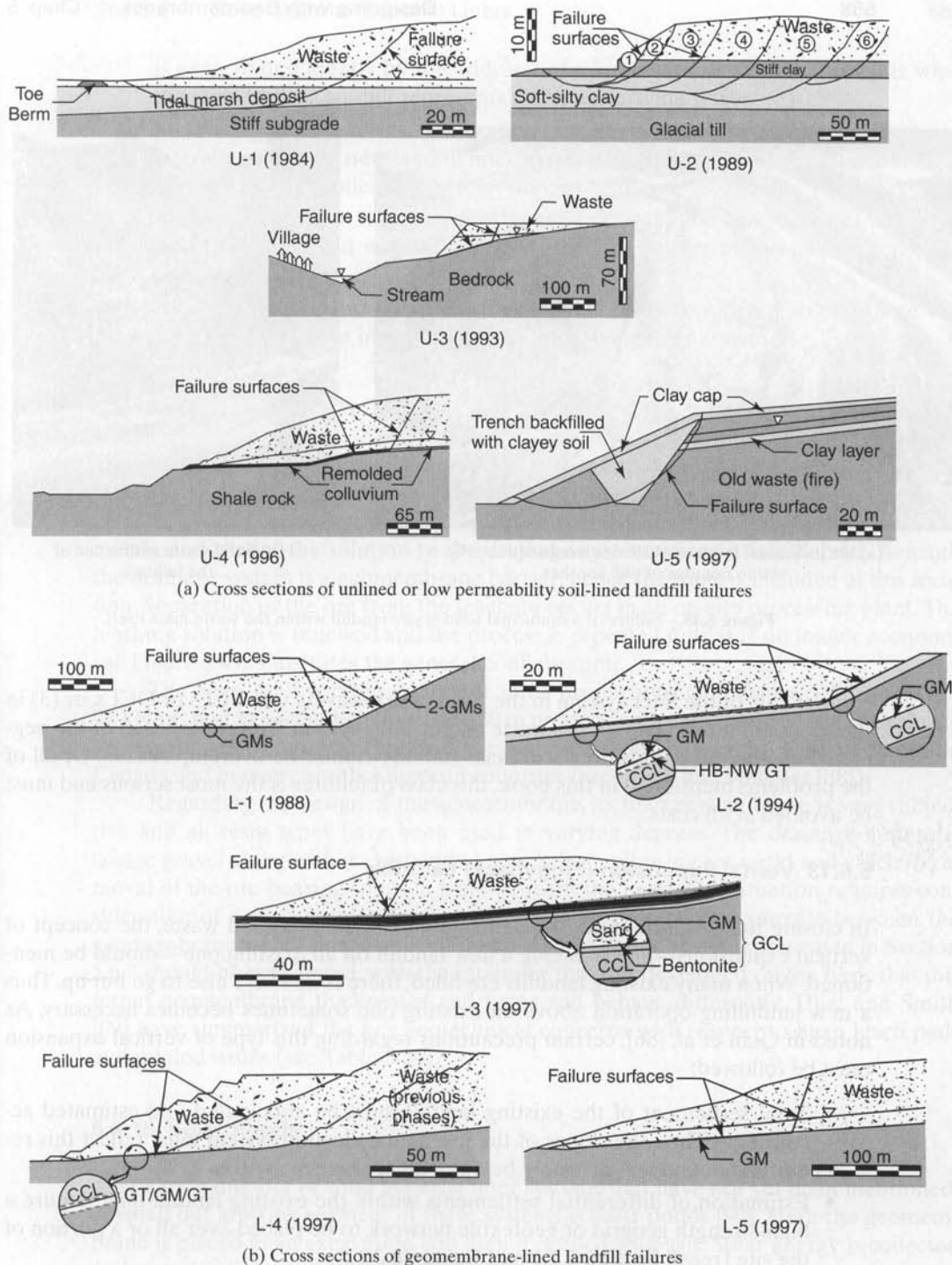
Figure 5.47 Two-dimensional cross sections of ten landfill failures. (After Koerner and Soong [85])

(a) Six individual failures which occurred sequentially
within minutes of one another

(b) Solid waste within one of
the failures

Figure 5.48   Failure of a municipal solid-waste landfill within the waste mass itself.

components of the liner system in the form of excessively wet CCLs or GCLs, or (3) in the foundation soil beneath the waste and/or liner system. This recognition of the negative influence of liquids on waste mass stability cannot be overemphasized. Of all of the problems mentioned in this book, this class of failures is the most serious and must be avoided at all costs.

5.6.13 Verital Expansion (Piggyback) Landfills

In closing this section on geosynthetic systems related to solid waste, the concept of vertical expansions—*piggybacking* a new landfill on an existing one—should be mentioned. When many existing landfills are filled, there is nowhere else to go but up. Thus a new landfilling operation above an existing one sometimes becomes necessary. As noted in Qian et al. [86], certain precautions regarding this type of vertical expansion must be followed:

- Total settlement of the existing landfill must be anticipated and estimated accordingly. Thus, the slopes of the leachate collection system must reflect this requirement and will probably be quite high, as much as 10 to 15%.

- Estimation of differential settlements within the existing landfill may require a high-strength geogrid or geotextile network to be placed over all or a portion of the site (recall Section 3.2.6 and Example 3.11).

- Waste placement in the new landfill must be carefully sequenced to balance stress on the existing landfill [86]. The stability of the waste situation just discussed

is exacerbated greatly by the addition of a large surcharge stress, which is what the piggybacked landfill represents to the underlying waste.

- Methane gas (if generated) migrating from the existing landfill must be carried laterally under the new landfill liner to side-slope venting and/or collection locations. Active gas collection systems may be required.
- Leachate collection from the existing landfill should be considered. If required, directionally drilled withdrawal wells at the perimeter of the facility may be a consideration.
- Access to the site via haul roads must be carefully considered so that there will be no damage to, or instability of, the underlying liner system.

5.6.14 Heap Leach Pads

Heap leach pads consist of a geomembrane with an overlying drainage system, and then a precious metal (gold, silver, or copper) bearing ore heaped above. A cyanide or sulfuric acid solution is sprayed on top of the ore, leaches through it reacting with the metals, and carries the solution to the drainage system where it is collected. Beneath the drainage system is a geomembrane barrier, hence the topic is included at this location. Separation of the ore from the leachate occurs in an on-site processing plant. The leaching solution is renewed and the process is repeated until it is no longer economical. Figure 5.49a illustrates the general configuration.

The heap itself is often enormous in its proportions (see Figure 5.49b). Ores of 22 kN/m^3 unit weight at heights up to 150 m produce enormous stresses on the drainage system and geomembrane. The concept is used widely in the western United States and Canada and in many South American countries (see Smith and Welkner [88]).

Regarding the design of the geomembrane, its thickness and type is very subjective and all resin types have been used to varying degrees. The drainage system is coarse gravel along with an embedded pipe system allowing for rapid and efficient removal of the ore-bearing solution from beneath the heap. This situation requires consideration of a sand cushion layer or a very thick protection geotextile between the geomembrane and drainage/collection gravel. The design method presented in Section 5.6.7 should be considered, with the reminder that it is developed on the basis that different geomembrane thicknesses and types will behave differently. Thiel and Smith [89] have summarized the key geotechnical concerns with respect to heap leach pads and related issues (see Table 5.20).

5.6.15 Solar Ponds

There are a number of solid material liner systems that have not yet been mentioned. A small but growing segment of these systems is solar ponds [90]. Here the geomembrane is placed in an excavation and then it is filled with salt. Solar energy is collected and stored as heat. A salt gradient effect is created, whereby zones are set up constantly replenishing new heat as it is gradually withdrawn from the lower storage zone for useful purposes. The main consideration insofar as the geomembrane is concerned is
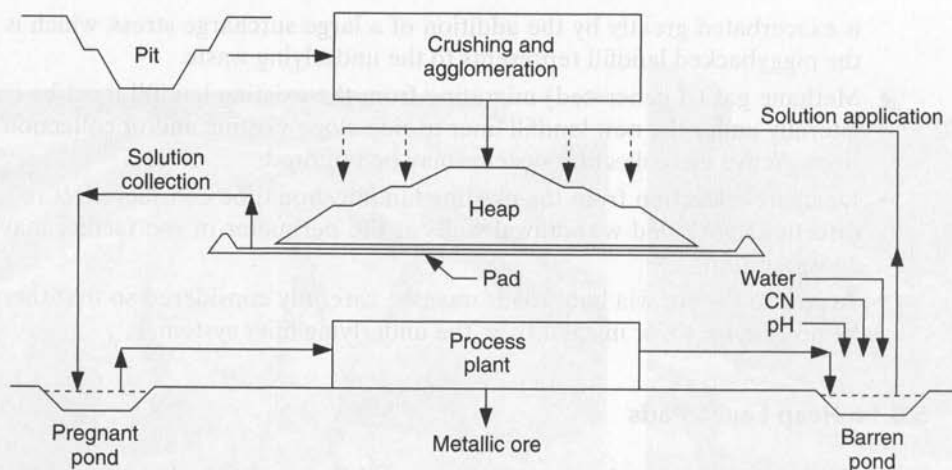
(a) General configuration of extraction process (After Leach et al. [87])

(b) A 65 ha South American heap facility (after Thiel and Smith [89])

Figure 5.49 Heap leach operation for extraction of metallic ores.

that temperatures up to 93°C must be withstood without excessive loss of the strength that is required for containment. The design, as with other situations not mentioned, should be possible using the guidelines set up in this section.

5.6.16 Summary

This section on the design of solid waste and related material containment liners followed closely the concepts developed in Section 5.3 on liquid containment (pond) liners.

TABLE 5.20   KEY GEOTECHNICAL CONCERNS REGARDING HEAP LEACH PADS AND RELATED APPURTENANCES

Performance Issue	Key Concerns
Slope stability	• Global and deep-seated failures due to extreme heights and slope angles • Sliding block stability along geomembrane interfaces • Effects of active leaching using elevated degrees of saturation • Effects of ponded liquid due to excessive clogging of collection and drainage system • Long-term chemical and biological degradation of geomembrane • First-lift stability affected by lift thickness (5 m to 50 m) and stacking direction
Liquefaction	• Earthquake-induced failures • Possible static liquefaction flowslides
Water management	• Tropical installations having large surplus water balances • Designs that include interim catch benches and temporary caps • Phreatic levels ranging from 1 to 60 m over the base liner
Liner survivability and leakage	• Coarse rock "overliner" systems • Extreme pressures caused by weight of heap and equipment • Durability against chemical attack, especially for high concentrations of sulfuric acid • Valley fill systems that create very high solution levels

Source: Modified from Thiel and Smith [89].

The notable exceptions are (1) that leachate collection systems above the primary geomembrane are always necessary; (2) cover soils (e.g., the leachate collection system) develop gravitational stresses that can fail or induce shear stresses in the liner system; (3) the shear stresses can result in tensile stresses in individual geosynthetic components that can be very high; (4) leak detection systems, and hence double liners, are often necessary or required by regulations and the cross sections can become very complex; (5) these extra design considerations require the determination of many physical and mechanical properties of the various geosynthetic and natural soil components and of the solid material itself; and (6) the criticality of proper laboratory testing of physical and mechanical properties for a rational design approach becomes obvious.

Table 5.21 summarizes the specific design problems for geomembranes and drainage geosynthetics. The large number of required properties of the geosynthetics and of the contained solid material are also indicated in the table. Keep in mind, however, that all of these values are obtainable, and a design-by-function approach is indeed possible for the solid-waste containment facilities described in this section.

With all of the geosynthetic components discussed in this section, and in the landfill covers to be discussed in the next section, it should come as no surprise that the solid-waste (landfill) area is pushing geosynthetics to new levels. Design models, testing methods, installation practices, inspection techniques, and geosynthetic product sales are all evident when considering the landfill liner and closure sketch of Figure 5.50. Here we see in a single cross section the impressive use of geosynthetics in the solid-waste containment application area. Yet, every component must be analyzed via a technically sound equivalency argument and justified via a reasonable benefit/cost

TABLE 5.21 VARIOUS DESIGN MODELS TO BE CONSIDERED IN LINER SYSTEMS FOR SOLID-WASTE DISPOSAL

(a) Geomembrane Design Elements

Design Element	Liner Stress	Required Properties Geomembrane	Required Properties Landfill	Typical Factor of Safety
Liner self-weight	Tensile	$G, t, \sigma_{allow}, \delta_L$	β, H	≥ 10
Weight of cover soil	Tensile	$t, \sigma_{allow}, \delta_U, \delta_L$	β, h, γ, H	0.5–2
Impact during construction	Impact	I	d, w	0.1–5
Weight of landfill	Compression	σ_{allow}	γ, H	≥ 10
Puncture	Puncture	σ_p	γ, H, P, A_p	0.5–3
Anchorage	Tensile	$t, \sigma_{allow}, \delta_U, \delta_L$	β, γ, ϕ	0.7–5
Settlement of landfill	Shear	τ, δ_U	β, γ, H	≥ 10
Subsidence under landfill	Tensile	$t, \sigma_{allow}, \delta_U, \delta_L, \chi$	α, γ, H	0.3–10

Geomembrane Properties:

G	=	specific gravity
t	=	thickness
σ_{allow}	=	allowable stress (yield, break, or allow.)
τ	=	shear stress
I	=	impact resistance
σ_p	=	puncture stress
δ_U	=	friction with material above
δ_L	=	friction with material below
χ	=	mobilization distance

Landfill Properties:

β	=	slope angle
H	=	height
γ	=	unit weight
h	=	lift height
α	=	subsidence angle
ϕ	=	friction angle
d	=	drop height
W	=	weight
p	=	puncture force
A_p	=	puncture area

(b) Drainage Composite Design Elements

Design Element	Issue	Approach	Required Properties Geosynthetic	Required Properties Landfill	Status of Problem
Stability of core	Avoid crushing of core	$FS = \sigma_{ult}/\sigma_{max}$	σ_{ult}	γ, H	Designable
Flow in core	First approximation	$FS = q_{allow}/q_{reqd}$	q_{allow}	γ, H, i, q_{reqd}	Designable
Creep of core	First reduction	$FS = q'_{allow}/q_{reqd}$	q'_{allow}	γ, H, q_{reqd}	Designable
Elastic intrusion of geomembrane	Second reduction	Elastic plate theory	E, μ, x, y	γ, H, q_{reqd}	Designable
Elastic intrusion of geotextile	Second reduction	Elastic plate theory	E, μ, x, y	γ, H, q_{reqd}	Designable
Creep intrusion of geomembrane	Third reduction	Creep theory	$\epsilon(\sigma, t), x, y$	γ, H, t	Unknown
Creep intrusion of geotextile	Third reduction	Creep theory	$\epsilon(\sigma, t), x, y$	γ, H, t	Unknown

Geocomposite Properties:

σ_{ult}	=	ultimate compression strength
q_{allow}	=	allowable flow rate
q'_{allow}	=	reduced allowable flow rate
t	=	time
E	=	modulus of elasticity
μ	=	Poisson's ratio
x, y	=	core dimensions
$\epsilon(\sigma, t)$	=	strain rate

Landfill Properties:

γ	=	unit weight
H	=	height
i	=	hydraulic gradient
q_{reqd}	=	actual (design) flow rate
t	=	time
σ_{max}	=	maximum stress
σ	=	applied stress

Source: Modified from Koerner and Richardson [91].
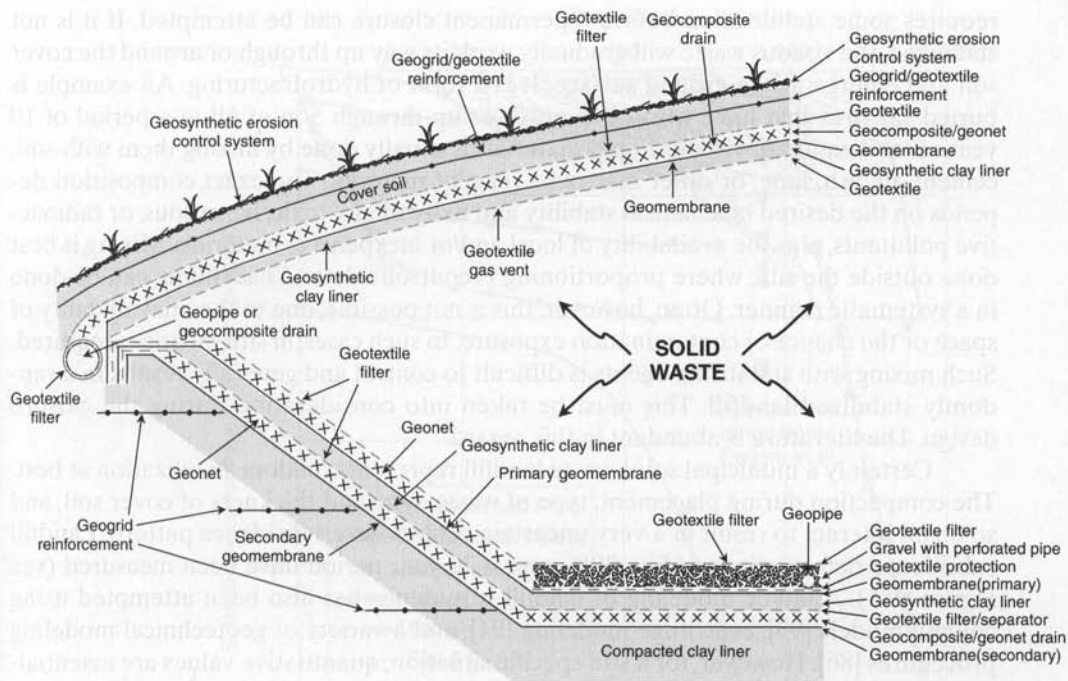
Figure 5.50   Solid-waste containment system with high geosynthetic utilization.

basis. In the liner system beneath the waste, each component should make sense and be justified accordingly. Now let's fill the site with solid waste and consider the cover system to be placed above the waste, which must be justified and designed in a similar manner.

5.7   LANDFILL COVERS AND CLOSURES

In order to minimize or entirely eliminate leachate generation after solid-waste filling is complete, a *cover* is required over a landfill, waste pile, or other mass of solid material. Covers are also referred to in the solid-waste literature as *final covers, landfill caps* and *landfill closures*.

5.7.1   Overview

There comes a time in the life of any landfill when it cannot accept additional material. When this occurs, it is necessary to construct a cover above the waste. Depending on its inherent stability, stabilization work on disposed waste materials may be necessary before closure begins. Take, for example, sludge lagoons of viscous fluids, or spent hydrocarbon wastes or suspensions of materials exhibiting Brownian motion, each of which

requires some stabilization before a permanent closure can be attempted. If it is not stabilized, the viscous waste will gradually work its way up through or around the cover soil and emerge at the ground surface. It is a form of hydrofracturing. An example is buried car tires that have worked themselves up through 5 m of fill in a period of 10 years. Stabilization of viscous liquid materials is usually done by mixing them with soil, cement, fly ash, lime, or other matrix or reagent material. The exact composition depends on the desired mechanical stability and fixity of any toxic, hazardous, or radioactive pollutants, plus the availability of local and/or inexpensive materials. Mixing is best done outside the site, where proportioning is controllable and backfilling can be done in a systematic manner. Often, however, this is not possible, due to the unavailability of space or the chance of contamination exposure. In such cases, in situ mixing is required. Such mixing with stabilizing agents is difficult to control and generally results in a randomly stabilized landfill. This must be taken into consideration during the closure design. The literature is abundant in this regard.

Certainly a municipal solid-waste landfill represents random stabilization at best. The compaction during placement, type of waste, type and thickness of cover soil, and so on all interact to result in a very uncertain post-closure subsidence pattern. Landfill subsidence deformations of 5 to 30% over a 20-year period have been measured (see Figure 5.51). Analytic modeling of landfill subsidence has also been attempted using column models [93], centrifuge modeling [94], and a variety of geotechnical modeling procedures [86]. However, for a site-specific situation, quantitative values are essentially unavailable (which, incidentally, makes it an area that clamors for research).

Whatever the situation, the landfill must eventually be covered and the following five components (from the waste up to the ground surface) must be considered: (1) gas collection layer, (2) liquid/gas barrier layer, (3) drainage layer, (4) protection layer, and (5) surface layer. Each of these components can be seen in the cover portion of the cross section in Figure 5.50. They are shown in the context of geosynthetic materials, but it should be noted that many regulations call for the use of natural soil materials. These same regulations also state that geosynthetics can be used as alternatives, if technical equivalency can be shown. In this, book, of course, geosynthetics will be emphasized.

5.7.2 Various Cross Sections

There are a large number of variations, using both geosynthetics and natural soils, that can be selected in designing the final cover for a landfill or (equally important) an abandoned dump site. Koerner and Daniel [95] use classifications for the existing waste mass as hazardous, nonhazardous, and abandoned, the last being essentially unknown in its classification. Equally (if not more) important is a knowledge of the regulations that apply for the site under consideration.

For final covers above *hazardous solid waste*, the EPA [96] requires the following technical details:

- The low-permeability soil layer, or CCL, should have a minimum thickness of 600 mm and a maximum in-place saturated hydraulic conductivity of 1×10^{-7} cm/s.
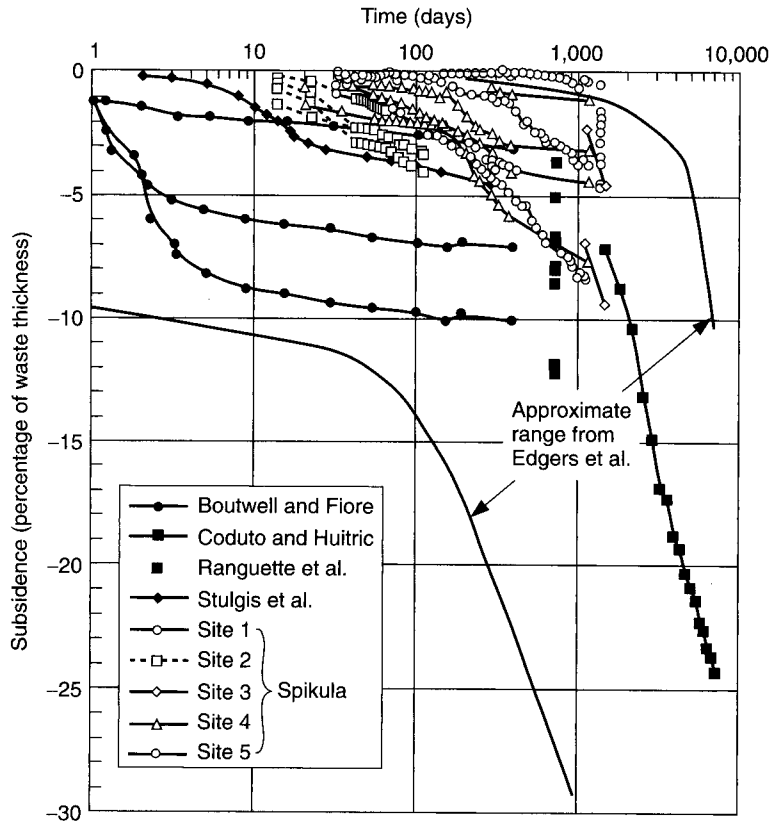
Figure 5.51   Municipal solid-waste landfill subsidence. (After Spikula [92])

- The geomembrane barrier above the compacted clay should have a minimum thickness of 0.75 mm.
- There should be adequate bedding above and below the geomembrane.
- The drainage layer above the geomembrane should have a minimum hydraulic conductivity of 0.01 cm/s and a final slope of 2% or greater after settlement and subsidence (thus necessitating subsidence predictions).
- The topsoil and protection soil above the drainage layer must have a minimum thickness of 600 mm.

As seen in Figure 5.50, there are many geosynthetic alternatives to the above-mentioned natural soils, for example:

- The CCL should be replaced by a GCL. (CCLs simply do not belong above a subsiding waste mass resulting in total and differential settlement.)
- The drainage layer could be replaced by a geocomposite or geonet drain.

- The filter layer above the drain could be replaced by a geotextile filter.
- The methane gas-collection layer could be replaced by a thick geotextile or geo-composite.
- For steep slopes, the cover soil may need geogrid or geotextile reinforcement acting as veneer reinforcement.
- The topsoil may need some type of geosynthetic erosion control system.

For final covers above municipal solid waste landfills, the EPA appears to be in a state of flux. The federal regulations [97] are quite loosely written and state that the cover must have a permeability as low as or lower than the liner system. Lending credibility to the importance of the cover system vis-a-vis the liner system beneath the waste, they also state that a "bathtub" effect is to be avoided. A "clarification" was issued in 1992 that has created considerable confusion in that it relaxes the regulations about the barrier layer of a landfill's composite liner to one requiring only a thin geomembrane of 0.5 mm thickness (1.5 mm if HDPE) placed over a soil of 1×10^{-5} cm/s permeability. In my opinion, such a regulation can never be interpreted as being comparable in its impermeability to a thicker geomembrane and a clay soil 100 times lower in permeability!

Lastly, as far as regulations are concerned, the U.S. Army Corps of Engineers guidance on abandoned dump final covers should be mentioned. In their documents they give equal credibility to 1.0 mm thick PVC and LLDPE geomembranes for covers. This is based on the usual conditions of having only surface water interface with the geomembrane and the possibility for geomembrane conformance to out-of-plane deformations beneath the cover. Recall Figure 5.5, which shows that these particular geomembranes perform very well in this type of stress state. The situation is further heightened by the fact that the EPA requires a landfill gas emission control system for any landfill of more than 2.5 million metric ton capacity or one that emits more than 50 metric tons of nonmethane organic compounds annually—that is, what would apply to most large landfills.

Instead of focusing so much on regulations, however, it is preferable to proceed from basics, particularly because the previous regulations are only for the United States. The five essential layers of a final cover for an engineered landfill or abandoned dump will be described in the sections that follow (for additional details see [95]).

5.7.3 Gas Collection Layer

Municipal solid waste (MSW) can generate tremendous quantities of gas during its decomposition. The two primary constituents are methane (CH_4) and carbon dioxide (CO_2). To provide an idea about the mechanisms and quantities, Baron et al. [98] cite the following series of events:

1. After closure, the aerobic phase of microorganism growth is relatively short, since oxygen supplies are rapidly (but not completely) depleted.
2. The anaerobic acid-forming microorganisms begin to appear.

3. The bacteriological organisms (aerobic and anaerobic) break down the long-chain organic compounds in the waste (mainly carbohydrates) to form organic acids, mainly CO_2.
4. This phase produces as much as 90% of the CO_2 and peaks 11 to 40 days after closure. It depletes the remainder of the available oxygen.
5. The methane-forming microorganisms become dominant.
6. The methane-forming anaerobic bacteria use the acids to form CH_4, some additional CO_2, and water.
7. Over time, the CH_4 increases and the CO_2 decreases. This takes about 180 to 500 days after closure. Thus one to two years is required to initiate a continuous flow of CH_4.
8. Within the next two-year period, approximately 30% of the CH_4 will be generated, and within five years approximately 50% will be generated. Thereafter, CH_4 generation continues but at a diminished rate. For example, 90% will have been generated after 80 years and 99% after 160 years. Note, however, that these values are very site-specific and are only meant to illustrate the trends and implications of methane gas generation in MSW landfills.
9. The range of quantities of CH_4 that are generated in a MSW landfill is 0.13 to 0.64 m^3 of CH_4 per kN of municipal solid waste per year. For a large landfill of 3 million metric tons per year, this results in 8,500 to 43,500 m^3 of CH_4 produced each day!

It is obviously necessary to provide a gas-collection layer and then a suitable venting and capturing system in order to avoid air pollution. Most large landfills use the gas for energy production at the landfill site or sell the energy over the local energy utility system. In the absence of such a gas-collection system, *blow-outs* of the geomembrane barrier, shown in Figure 5.52, are becoming more frequent. Note that the gas pressure generated from the decomposing waste has completely displaced the 1.2 m of cover soil at this particular site. Methane gas vents, typically on 15 to 50 m centers, must unfortunately penetrate and pass through the cover system. Figure 5.53 illustrates some of these details. Such vents, however, serve no function if the gas cannot enter at the lower level. To accomplish this, a nonwoven needle-punched geotextile or geocomposite drainage material is placed beneath the barrier system shown in Figure 5.50. The design is based on air transmissivity and is similar to Example 5.7 in Section 5.3.2 for the relief of air pressure beneath a liner system. The comments in that section apply here as well.

While the above discussion focuses on gases generated for municipal solid waste typical of the United States, waste in other countries may be more degradable and produce even greater gas quantities. Conversely, if the organic components of the waste are removed (as projected by European Union norms for 2006 and beyond), the waste (e.g., hazardous waste, ash, or building demolition waste) will be less degradable and produce lower quantities of landfill gases. Also note that wastes other than MSW may generally produce significantly lower quantities of gas. The gas generation rates are clearly waste-specific. Be cautioned, however, that if a geomembrane is located in the barrier layer, even small quantities of gases cannot be released and the situation shown in Figure 5.52 can easily result.

Figure 5.52   Geomembrane expanded by methane gas from a closed landfill pushing aside approximately 1.2 m of cover soil and topsoil.

5.7.4 Barrier Layer

In designing the barrier layer for a landfill closure, we might consider several options: a single compacted clay liner (CCL), a single geomembrane (GM), a single geosynthetic clay liner (GCL), two-component composites (GM/CCL or GM/GCL), and three-component composite liners (GM/CCL/GM or GM/GCL/GM). The last two options are sometimes attractive when the moisture content in the clay or bentonite components are particularly sensitive to environmental conditions (i.e., desiccation when dry or low shear strength when saturated).

Several critical factors affect the selection of a specific barrier layer: climate, the amount of differential settlement, the vulnerability of the cover soil to erosion or puncture, the amount of water percolation that can be tolerated through the cover system, the need for collecting waste-generated gas, and the slope steepness.

In assessing the seven barrier layer alternatives to the critical factors listed above, Daniel and Koerner [99] have scored each of those factors as 1 (not recommended) to 5 (recommended). For example, in cases involving large differential settlement, they scored a CCL as 1 and a geomembrane as 5. The authors suggest that designers consider these assessments for general guidance only. Unique conditions at a particular site will call for special design precautions. The assessed scores are then extended using a cost estimate and a general benefit/cost ratio can be computed for each of the alternate barrier layers.
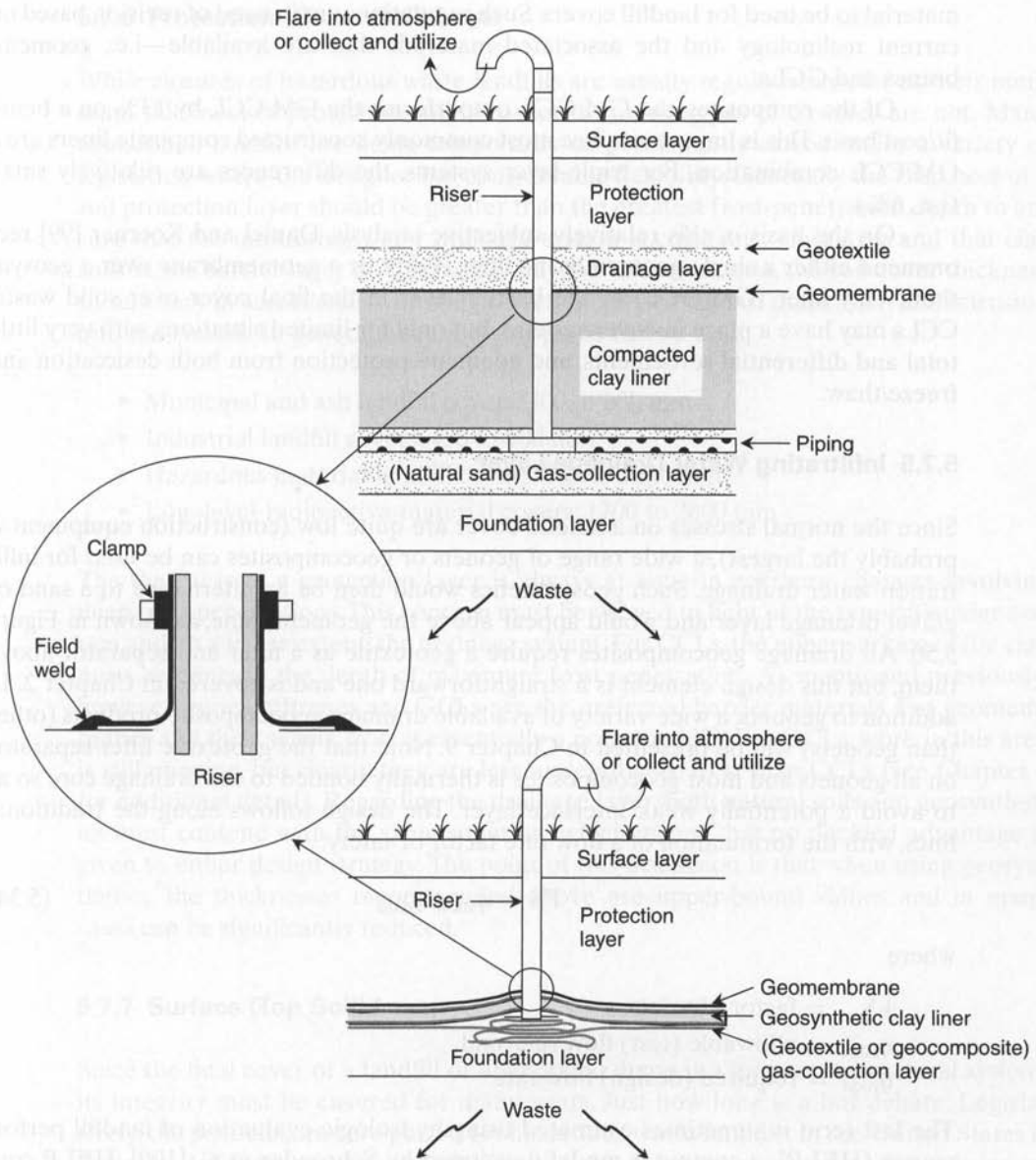
Figure 5.53 Selected venting systems to transmit landfill gases from the gas-collection layer (natural soil and geosynthetics) to the ground surface.

Among the single-layer systems, the single geomembrane (GM) outperforms the CCL by 77% in benefit/cost terms. Also, the GCL outperforms the CCL by 27% in benefit/cost terms. Thus the CCL is by far the poorest overall technical choice of any single-layer system. Paradoxically, a CCL is widely mentioned in regulations for a single-layer

material to be used for landfill covers. Such regulations are in need of revision based on current technology and the associated materials that are available—i.e., geomembranes and GCLs.

Of the composites, the GM/GCL outperforms the GM/CCL by 13% on a benefit/cost basis. This is important since most commonly constructed composite liners are a GM/CCL combination. For triple-layer systems, the differences are relatively small (i.e., 6%).

On the basis of this relatively subjective analysis, Daniel and Koerner [99] recommend either a single geomembrane liner (GM), or a geomembrane over a geosynthetic clay liner (GM/GCL) as the barrier layer in the final cover over solid waste. CCLs may have a place in cover systems, but only for limited situations with very little total and differential settlements, and adequate protection from both desiccation and freeze/thaw.

5.7.5 Infiltrating Water Drainage Layer

Since the normal stresses on a landfill cover are quite low (construction equipment is probably the largest), a wide range of geonets or geocomposites can be used for infiltration water drainage. Such geosynthetics would then be an alternative to a sand or gravel drainage layer and would appear above the geomembrane, as shown in Figure 5.50. All drainage geocomposites require a geotextile as a filter and separator above them, but this design element is a straightforward one and is covered in Chapter 2. In addition to geonets, a wide variety of available drainage geocomposite products (other than geonets) will be presented in Chapter 9. Note that the geotextile filter/separator on all geonets and most geocomposites is thermally bonded to the drainage core so as to avoid a potentially weak interface layer. The design follows along the traditional lines, with the formulation of a flow rate factor of safety:

$$FS = q_{allow}/q_{reqd} \tag{5.34}$$

where

$$
\begin{aligned}
FS &= \text{factor of safety,} \\
q_{allow} &= \text{allowable (test) flow rate, and} \\
q_{reqd} &= \text{required (design) flow rate.}
\end{aligned}
$$

The last term is sometimes estimated using hydrologic evaluation of landfill performance (HELP), a computer model developed by Schroeder et al. [100]. HELP contains hydrologic data from 200+ cities and has a great deal of design flexibility. Its limitation for this problem is that it calculates flow rate on a daily basis, which greatly understimates intense rainstorms. Thus, a hand calculation of the infiltration quantity on an hourly basis is recommended and is detailed in [99]. The allowable flow rate is obtained directly from laboratory testing via the ASTM D4716 test method, which is described in Chapter 4 and further described in Chapter 9. The simulated cross section at design pressures (or greater, if equipment or other live loads are of concern) should be used.

5.7.6 Protection (Cover Soil) Layer

While closures of hazardous waste landfills are usually regulated insofar as their minimum thickness of protection soil is concerned, other types of closures are not. Many abandoned landfills are being temporarily or permanently closed under a variety of legislation where the designer has considerable flexibility. Generally the thickness of a soil protection layer should be greater than the greatest frost-penetration depth to ensure that the infiltrating water drainage system is constantly operative and that clay soils in the barrier layer do not freeze. Beyond this restriction, the soil cover thickness should vary in accordance with the protection needed against infiltration and intrusion into the landfill. In general, the following guide can be used:

- Municipal and ash landfill covers: 300 to 600 mm
- Industrial landfill covers: 450 to 900 mm
- Hazardous material landfill covers: 750 to 1200 mm
- Low-level-radioactive-material covers: 1200 to 2000 mm

The thickness of a protection layer is always at issue in northern climates involving deep frost penetrations. This concern must be viewed in light of the type of barrier system and, to a lesser extent, the drainage system. For CCLs, the upper surface of the clay must be beneath the depth of maximum frost penetration. As mentioned previously, however, geomembranes and GCLs are the preferred barrier materials. For geomembranes and their seams, frost is essentially a nonissue [32]. For GCLs, work in this area is still ongoing, but clearly they are less susceptible to frost than CCLs (see Chapter 6 for additional detail). Regarding the drainage layer, both natural soils and geosynthetics must contend with the same situation, which means that no decided advantage is given to either design strategy. The point of this discussion is that when using geosynthetics, the thicknesses recommended above are upper-bound values and in many cases can be significantly reduced.

5.7.7 Surface (Top Soil) Layer

Since the final cover of a landfill or abandoned dump is a long-term structural system, its integrity must be ensured for many years. Just how long is a hot debate. Legislatively, the post-closure care period for hazardous waste landfills in the United States is 30 years. But to many, your author included, this is far too short a time. What happens after 30 years? Can rainwater and snowmelt enter the waste, generating new leachate for an unknown someone to remove and properly treat? Consider also radioactive waste with hundreds or thousands of years of active lifetime. Indeed, many questions arise, with too few answers.

With the above discussion in mind, it is necessary to anticipate the various mechanisms that might intrude or disturb the buried waste, thereby negating the cover system. Of major concern are the following mechanisms, which are offered with some selected comments. (See [99] for additional insight into this important area.)

- *Erosion by water:* With proper cover soil and vegetation, it is possible to design against water erosion. The local agricultural station, Soil Conservation Service, or local highway department can be consulted for the proper type of indigenous plants and shrubs. Gradients are very important. For above-grade landfills, they can be quite steep. In such cases, the use of erosion control geocomposites becomes important. Both temporary and permanent types are available, and they are discussed in Chapter 9.

- *Erosion by wind:* Wind erosion is quite difficult to design against because of the wind's widely varying velocity and direction. It is not a problem if vegetation is present over the entire cover area—hence proving again the importance of proper plants and shrubs. In arid regions it might be necessary to use some type of erosion control geocomposite or even hard armor treatment. Chapter 9 presents these materials and their alternatives.

- *Root penetration:* With some types of vegetation, deep root penetration into the cover soil can occur. The barrier layer should be chosen to prevent penetration, but even so, the drainage system above the geomembrane might become clogged. Proper plant and shrub selection is again important, as it was with both types of above-described erosion.

- *Burrowing animals:* When animals are burrowing, it is possible that the barrier layer could be encountered and penetrated. If this action poses a problem, the use of a rock layer or biobarrier above the drainage system might be necessary.

- *Accidental intrusion:* Of particular concern is accidental intrusion by drillers, pipeline excavators, site developers, and others who have interest or reason to investigate a closed landfill site. The proper posting of signs and maintained fencing should be adequate for preventing accidental intrusion by construction workers into capped landfill sites.

- *Intentional intrusion:* Why anyone would want to intrude through the final cover of an old landfill is beyond comprehension of the author. I suppose it is always possible and for some sites essentially impossible to prevent. Periodic inspections, with appropriate maintenance, are required for this and most of the other intrusion mechanisms as well.

5.7.8 Post-Closure Beneficial Uses and Aesthetics

To date, the final covers over completed landfills and abandoned dumps have been ominous zones, usually buffered from the public by fencing. The effect to the region is much like that obtained by quarantined areas: vast open spaces that appear to be permanently lost for public use. Recently some landfill owners have begun to explore alternatives for such culturally dead zones. Mackey [101], Phaneuf [102], Martin and Tedder [103], and Koerner et al. [104] report on closed landfill use for golf courses, sport fields, walking and jogging paths, parks, and many other uses. It is important to note that with a geomembrane in the barrier layer, the offensive odor of methane is eliminated. A different approach is the recent commissioning of a graphic artist by the Hackensack Meadowland Development Commission [105] to transform a New Jersey

municipal waste landfill final cover into an environmental art form. The 23 ha cover will be transformed into a Sky Mound that includes picturesque earth mounds which will frame sunrises and sunsets when viewed from the center of the cover. The astronomy theme is carried onto an interior lunar zone that is surrounded by a circular moat that serves as part of the surface water collection system and the looping arches of the methane recovery system. Pipe tunnels through selected mounds are aligned with stellar helical settings of the stars Sirius and Vega. These extraordinary features are shown in Figure 5.54. Land surrounding the landfill cover will be converted to a wild bird refuge.

It is clear that the negative impact of a landfill closure can be minimized. However, it should be cautioned that features such as earth mounds or surface impoundments within the cover must be carefully engineered to prevent damage to the underlying drainage and barrier system. The long-term performance of the cover must not be compromised by surface structures, regardless of their function or intent.

5.8 WET (OR BIOREACTOR) LANDFILLS

The liquids management practice of the previous two sections on solid waste landfill liners and covers can be described as *dry landfilling*. As such, liquids are limited to the maximum extent possible and are quickly and efficiently removed when they arrive at the leachate removal sump. This section is the counterpoint, wherein liquids are purposely added to the waste mass, hence the term *wet landfilling*. There are several wet landfill strategies possible including those known as *bioreactor landfills*.
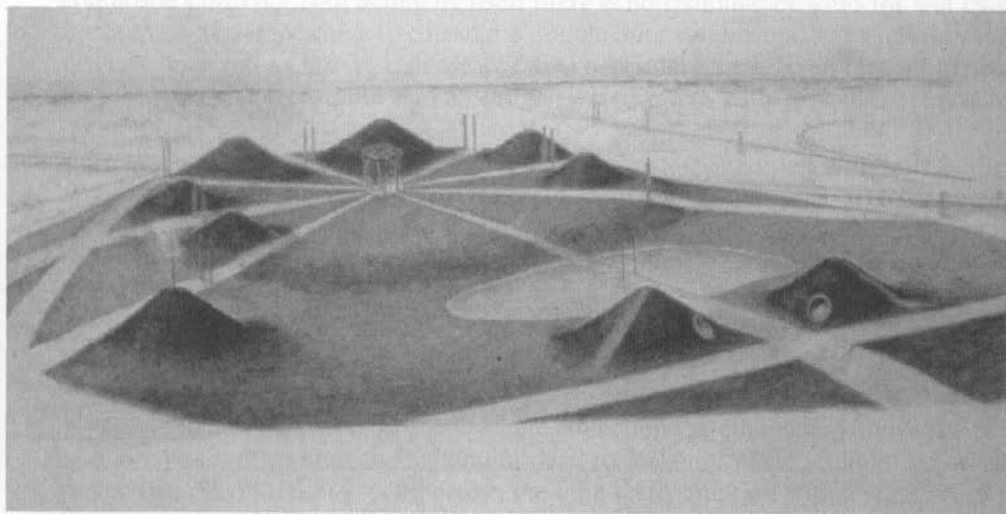
Figure 5.54   Artist's rendering of the topography of a final cover. (After Meadowlands Redevelopment Authority, Pinyon [105])

5.8.1 Background

To purposely add leachate back into or onto a municipal solid waste landfill is certainly not a new idea. Owners and operators have long used this liquids strategy, not only to temporarily avoid leachate treatment but also to enhance organic waste degradation, thereby gaining airspace and generating landfill gas (Pohland [106]). What is new is to consider various wet landfilling strategies and utilize the practice in full-scale situations. In this regard, there are at least three variations of wet landfilling. In Figure 5.55 conventional dry landfilling is compared with the wet landfilling strategies of (1) leachate recirculation, (2) anaerobic bioreactors, and (3) aerobic bioreactors. As the term implies, *leachate recirculation* is the redistribution of exiting landfill leachate back into the waste mass. To achieve an *anaerobic bioreactor*, the site's leachate must be augmented (examples are sewage sludge, industrial waste water, ground or surface water) to get the waste to an optimum moisture content called "field capacity." This varies with the type of waste but is a moisture content (based on dry unit weight) of 40 to 100% (Reinhart and Townsend [107]). Conceptually, it is the moisture content at which all of the organics have sufficient liquid to achieve complete degradation. At field capacity, the waste is indeed wet, but it is not fully saturated. Lastly, an *aerobic bioreactor* is a landfill that is at field capacity moisture and then purposely has air injected into it using perforated wells within the waste mass.

As seen in Figure 5.55 the stabilization time [108] rapidly decreases as we go from dry landfilling through the various types of wet landfilling. This is further related to the site's waste placement operations in that good waste contact by the liquids provides for much more rapid stabilization as well.
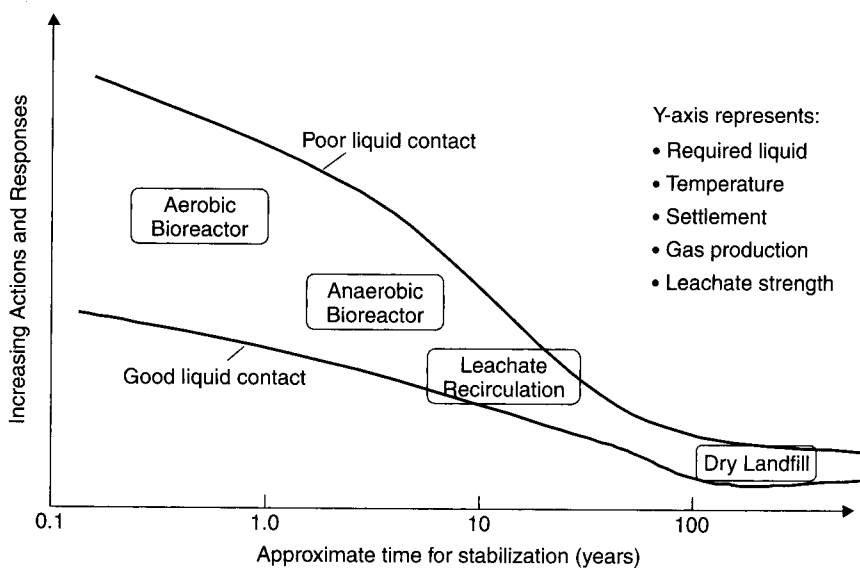
Figure 5.55 Various strategies of wet landfilling contrasted to dry or conventional landfilling insofar as liquids management practices are concerned.

In going from dry landfilling to the various wet landfill strategies, the required amount of liquid must increase, thus creating greater degradation, which causes the temperature to increase. This in turn results in increased landfill settlement and gas generation. Also, the leachate strength (turbidity and microorganisms) increases but by how much is a current research topic. As such, the liquid-generated elevated temperatures are a critical factor [109]. Figure 5.56 reinforces this statement in that field temperature data from a dry cell has been contrasted to a wet cell (anaerobic bioreactor) at the same landfill site. Thermocouples on the geomembrane beneath and above the two waste masses are used to obtain the data. Figure 5.56a shows that the dry cell liner temperature stayed at 20°C for about 5.5 years before degradation reactions occurred, raising the temperatures some 10°C where it seems to have stabilized. Conversely, the wet cell liner temperatures of Figure 5.56b began at 25°C and are over 40°C after 2.3 years. Cover temperatures are also interesting in that the annual summer/winter fluctuation can be easily seen in Figure 5.56c. It appears that the wet cell cover temperatures are higher, as shown in Figure 5.56d, but the data are sparse at this time; monitoring is ongoing.

As far as the geosynthetics in wet landfills are concerned there are a number of implications. They relate to the liner system, leachate collection system, leachate removal system, filter and/or operations layer, daily cover materials, final cover issues, and waste stability concerns. Each will be briefly commented upon in the sections that follow. (See reference [109] for additional details.)

5.8.2 Base Liner System

The addition of liquids in any of the wet landfill strategies illustrated here heightens the concern over liner leakage. As shown in Figure 5.39, the premier liner system is a composite GM/GCL, but acting by itself there is no redundancy. Thus for wet landfilling of MSW it is imperative to consider a double liner system consisting of GM/GCL as primary liner and a GM/GCL or GM/CCL as secondary liner. Even further, the action leakage rate (ALR) should be carefully selected along with remedial actions to be taken if it is exceeded.

It should also be noted that the lifetime of the liner materials will be decreased in direct relation to the increased temperature. (Recall Table 5.12, which shows this trend.) However, once the waste is stabilized, it should no longer pose a serious environmental threat and the two issues thus counterbalance one another. It is nonetheless a worthwhile consideration.

5.8.3 Leachate Collection System

As mentioned in Section 5.6.1 the leachate collection system located above the primary liner system must limit the maximum head to 300 mm. While straightforward in its design from an initial flow perspective, the long-term situation with a leachate of high turbidity and microorganism content presents a concern over excessive clogging. After evaluating a number of drainage materials, Koerner et al. [111] have concluded that gravel with a permeability of at least 1.0 cm/s should be chosen. This requires a rather
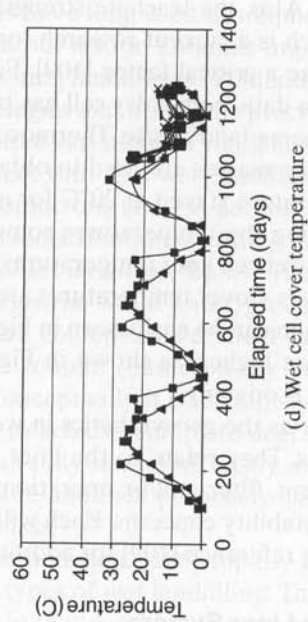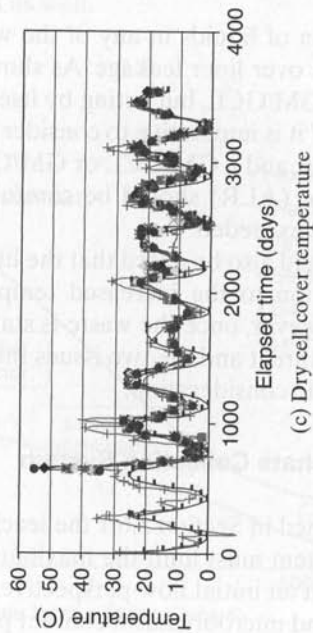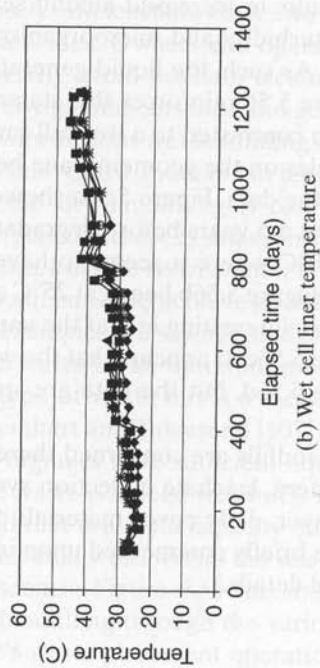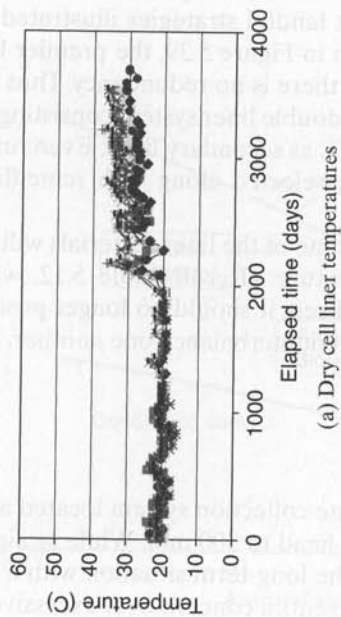
Figure 5.56 Long-term thermocouple obtained geomembrane temperatures beneath and above MSW at a landfill in Pennsylvania. (After Koerner and Koerner [109])

thick nonwoven geotextile cushion to be used to protect the geomembrane, a design that was presented in Section 5.6.7. Alternatively, a geonet composite with a low permeability sand above is possible and in many cases more economical.

5.8.4 Leachate Removal System

A perforated pipe removal system is embedded with the leachate collection system when it is a granular soil, such as sand or gravel. As will be seen in the discussion of plastic pipe in Chapter 7, the design is based on a limiting pipe deflection from the overlying solid-waste mass. In turn, this pipe deflection is also a function of the service temperature that was seen to be high for wet landfills. Thus, both high normal stresses and elevated temperature are major design considerations.

5.8.5 Filter and/or Operations Layer

Based on geotechnical engineering practice it is always recommended that a filter soil (or geotextile) be placed between dissimilar particle-sized materials. Clearly, solid waste and sand or gravel is in this category. Yet the filter is the material with the smallest porometry and thus the highest likelihood of becoming excessively clogged [110]. For this reason, and based on limited data, there are numerous landfills that place *select waste* directly on the leachate collection system (see Figure 5.57). This approach appears to be properly functioning and should be considered. Contrary to past landfill practice, there should be no *operations layer* placed on the leachate collection layer, which has typically been a 600 to 900 mm layer of local soil.

The concept for wet landfilling is to have the liquids permeate from the waste mass directly into the leachate collection and removal system. There should be no intermediate layers that retard or compromise the flow from reaching the sump area for removal and subsequent reuse on top of the landfill. *Perched leachate* within the waste mass above the liner system is not desirable in any type of solid-waste landfill.

5.8.6 Daily Cover Materials

In most cover materials, it is usually required that each lift of waste be covered by 150 mm of soil so as to eliminate odors, vectors, flying litter, and fires. Yet, in wet landfilling practice this soil layer can impede the flow of leachate through the waste mass. Alternative daily cover materials that are porous or can be removed are desirable. Pohland and Graven [112] report on four such categories: (1) polymer foams, (2) slurry sprays, (3) sludges and indigenous materials, and (4) reusable geosynthetics. They investigate the benefit/cost of the categories in which the reusable geosynthetics are the least expensive depending on the number of reuses.

5.8.7 Final Cover Issues

As shown in Figure 5.50, the engineered final cover should not be placed until the waste has stabilized. The majority of the settlement should be allowed to occur before a final compaction of the waste mass and construction of the final cover.

Figure 5.57 Select waste being placed directly on the leachate collection and removal system at a wet (bioreactor) landfill.

In this 2- to 20-year time period for wet landfilling, a temporary geomembrane cover is often necessary due to landfill gas emissions. A growing segment of geosynthetics, known as *exposed geomembrane covers*, can nicely satisfy this need. Gleason et al. [113] report on a number of case histories along with the important design aspects of anchoring the geomembranes during times of high wind exposure. The challenging research need of a cover that prevents gas from escaping the landfill while at the same time allowing precipitation to enter the landfill should be investigated (Hullings and Swyka [114]).

5.8.8 Waste Stability Concerns

With the introduction of relatively large amounts of liquids into the waste mass, there is a possibility of waste instability. Failure sites L-4 and L-5 in Table 5.19 were both wet landfills practicing leachate injection. Obviously, neither site was properly designed and, even further, the landfill operations were completely uncontrolled. Nevertheless, these two massive failures indeed occurred. Critical stability design parameters are the unit weight of the wet waste and the interface shear strengths along the projected failure surfaces. Dixon and Jones [115] present a review of these parameters and how they can effect various aspects of waste stability.

Stability calculations for wet landfills are a serious issue that must be thoroughly investigated. When relatively low factors of safety result, field monitoring is recommended.

Standard geotechnical monitoring is well suited for landfill monitoring as well as for soil materials.

5.8.9 Summary

Wet landfilling of municipal solid waste is being undertaken or being considered at hundreds of landfills. This practice should be encouraged since waste stabilization at the sites will occur rapidly and final closure will not leave the site as a future threat to the environment. Even further, many sites can be discreetly used for post-closure beneficial community uses (recall Section 5.7.8).

That said, the design of a wet, or bioreactor, landfill must be done with utmost care. The recent literature is abundant with references, and designers must be cognizant of the latest technology. In many cases, deformation surveys and monitoring (perhaps with slope indicators and even piezometers) would be a prudent auxiliary strategy to ensure safety and avoid an unforeseen event.

5.9 UNDERGROUND STORAGE TANKS

Leakage from underground storage tanks (many of which contain hydrocarbon products) represents a very serious threat to downgradient water supplies. Such leakage has necessitated various containment strategies, in the form of secondary containment, which are described in this section.

5.9.1 Overview

Depending on the study selected, there are as many as 6 million underground storage tanks in the United States containing hydrocarbon products. Of these, anywhere from 10 to 30% are thought to be leaking. To realize the seriousness of this number, consider that a 6 mm diameter hole in a standard 75,000 liter gasoline storage tank will pollute the drinking water supply of a 100,000-person community beyond acceptable background levels. As a result, many states have enacted legislation requiring secondary containment of underground storage tanks. Two different systems using geomembranes will be described.

5.9.2 Low-Volume Systems

As the secondary containment around a steel or fiberglass storage tank, we can wrap a geonet directly around the tank with a geomembrane around the geonet, as shown in Figure 5.58a. The geonet (also called a *stand-off mesh*) becomes the leak-detection network, while the geomembrane acts as the secondary liner. Both the geonet and geomembrane must be chemically resistant against the liquid in the tank, and HDPE is generally used in this particular approach. A leak monitoring and removal pipe is placed at the low point of the geonet to monitor for leaks in the primary liner (i.e., in the tank itself).
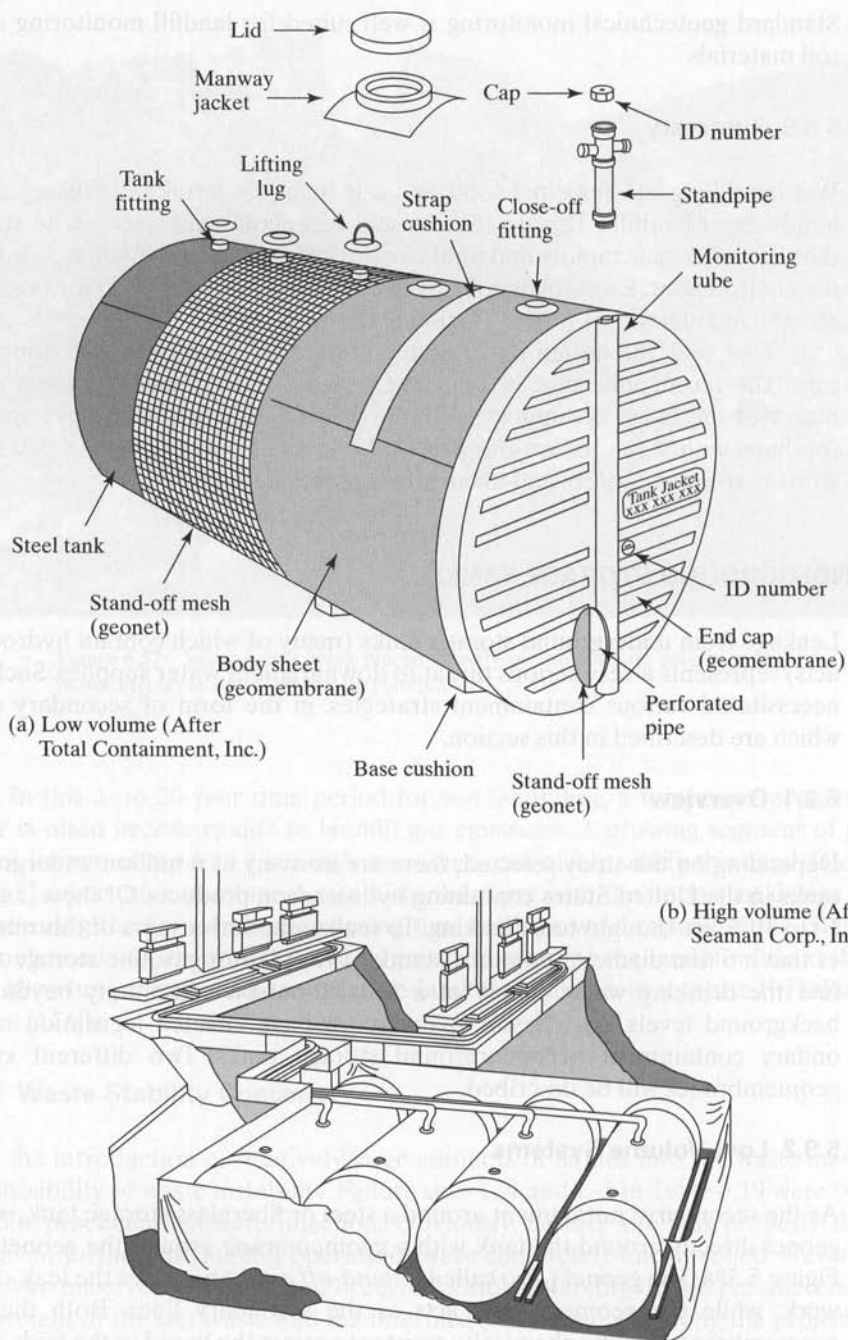
Figure 5.58 Schematic diagram of secondary leak detection and liner systems for underground storage tanks.

5.9.3 High-Volume Systems

For high-volume systems, an excavation for a number of underground tanks can be made, rather than fitting each tank individually, and the entire excavation lined with a geotextile-geomembrane-geotextile composite. Figure 5.58b illustrates such a procedure. The leak detection media is drainage stone, which also acts as bedding for the tanks. A pipe monitor is placed in this drainage system to check for tank leaks.

An interesting feature of this system is that the piping system leading to the gasoline station pumps can be handled in the same manner. Leaks often occur in or near the connections and fittings. The geomembrane composite actually encases the entire pipe network and travels with it wherever it goes. Hydrocarbon resistance of all the geosynthetic components is obviously necessary and EIA-R is often used in this particular approach, due to its greater flexibility over HDPE.

Underground storage tank owners who have sites that are underlain by granular soils with high seasonal watertables should be cognizant of these available geomembrane systems.

5.9.4 Tank Farms

Large holding tanks, some containing 40 Ml of liquid, require earth embankment containment, called *fire walls*, in case of leaks or rupture. These same embankments place the tanks in an underground category, even though they are located at the ground surface. Nevertheless, the need for secondary containment is required in many states. The resulting configuration appears exactly like any one of the sketches shown in Figure 5.18, with the exception that steel or concrete tanks are sitting in the center of the surrounding embankments. Thus any one of the geomembrane schemes illustrated can be used. For a long service lifetime, the geomembrane should be soil buried and it obviously must be chemically resistant to the liquid being contained in the tank. For hydrocarbon storage tanks, HDPE and EIA-R geomembranes are generally used. In this same type of application, GCLs have also been used, but they first must be exposed to water in order to hydrate the bentonite clay and mobilize its low permeability.

5.10 HYDRAULIC AND GEOTECHNICAL APPLICATIONS

Geomembranes have been used in many innovative ways in connection with traditional hydraulic and geotechnical engineering structures such as dams, tunnels and seepage control. An International Committee on Large Dams (ICOLD) report [116] presents over 300 case histories of the use of geomembrane waterproofing in various types of dams.

5.10.1 Earth and Earth/Rock Dams

In most situations where low-permeability materials are desired to inhibit high pore water pressure and/or excessive seepage, geomembranes offer a logical and competitive alternative to the use of clays. Zoned earth and earth/rock dams require an impervious

core, which has traditionally been of low-permeability silts, clays, or their mixtures. It seems natural to use a geomembrane as an alternative for cases where such fine-grained soils are difficult to obtain or to place.

Eigenbrod et al. [117] report on the use of an impervious upstream geomembrane blanket for controlling seepage in a tailings dam. Figure 5.59a presents a cross section of the completed structure, in which a geomembrane is positioned on the upstream face of the compacted tailings immediately beneath a crushed rock layer. A high-strength 300 g/m^2 woven polypropylene geotextile is placed between the geomembrane and the crushed rock to protect the geomembrane from puncture. The geomembrane is a 0.75-mm nonreinforced CSPE liner. It was selected on the basis of the following criteria: elongation sufficient to withstand 900 mm of settlement in a 3 m

Note: All measurements are in mm.

(a) On a tailings dam in Canada (After Eigenbrod et al. [117])

(b) On a roller-compacted concrete dam
in Italy (Compliments of CARPI, Inc.)

Figure 5.59   Geomembrane upstream blanket for seepage control.

diameter void, hence it was nonreinforced; resistance to the chemicals in the tailings materials being contained; satisfactory performance at $-40°C$; seams joinable at $+30°C$; and cost-competitiveness with other geomembranes.

Figure 5.59b shows such a geomembrane being placed on the upstream face of a roller-compacted concrete dam. When completed, a thick, nonwoven needle-punched protection geotextile will be placed over the geomembrane and then crushed rock, similar to Figure 5.59a. Sembenelli and Rodriguez [118] illustrate many additional uses of geosynthetics in earth and masonry dams.

5.10.2 Concrete and Masonry Dams

Many existing concrete dams and spillways are showing signs of deterioration due to old age. Leakage from cracks in such structures can be very large, hence remediation is often necessary. Monari [119] illustrates how a geomembrane was used to cover the upstream side of a 37 m high concrete dam. The liner was 2.0 mm PVC with 300% elongation. Fixity was achieved by a clever series of steel ribs that were fastened to the concrete prior to the geomembrane installation. In this way future repairs and/or replacement of the geomembrane could be made easily. This case history represents one of many ways in which geomembranes can be used to control seepage. Cazzuffi [120] reports on the use of exposed geomembrane waterproofing of concrete dams in the Alps region of northern Italy. Table 5.22 indicates that the geomembrane was directly against the concrete at the first three sites. Performance was less than expected during times of sudden drawdown when the geomembrane tended to become displaced due to seepage-generated hydraulic pressures behind the geomembrane. This issue was solved beginning with Lago Nero in 1980 when a thick needle-punched nonwoven geotextile was first placed against the concrete and then the geomembrane placed against it. The geotextile acted both as drainage material and for puncture protection against rough concrete. Subsequently, a geotextile bonded to the geomembrane has been used with the advantage of field placement of a single composite material. Scuero and Vaschetti [121] show how the same methods are adaptable to masonry dams of all types. Major design considerations include puncture resistance, particularly in areas where ice will form, and the lifetime of the exposed geomembranes. Several clever air bubbling systems have been devised to reduce the danger of puncture and Koerner and Hsuan [122] report on lifetime prediction of exposed geomembranes.

5.10.3 Roller-Compacted Concrete Dams

Existing roller-compacted concrete (RCC) dams that are leaking can be remediated in the same way that has just been described for concrete and masonry dams. However, for new RCC dams an alternative developed by CARPI [123] has been introduced. By fabricating large concrete panels of 150 mm thickness with a geomembrane/geotextile composite bonded to them (the fresh concrete bonds to the nonwoven geotextile very readily) and using these panels as the upstream forming system for the RCC, an excellent waterproofing barrier is created. The edges of the panels must be field seamed

TABLE 5.22 DAM AND GEOMEMBRANE CHARACTERISTICS FOR WATERPROOFING SEVERAL ITALIAN DAMS

	Contrada Sabetta	Lago Baitone	Lago Miller	Lago Nero	Locone	Castreccioni	Cignana	Piano Barbellino
Owner	ENEL	ENEL	ENEL	ENEL	CBAL	CBM	ENEL	ENEL
Type	R	M	M	C	Coff	C	C	C
Height (m)	32	37	11	40	13	67	58	69
Construction dates	1957–59	1927–30	1925–26	1924–29	1982	1981–86	1925–28	1926–31
Geomembrane (GM)								
Location	UF	UF	UF	UF	UF	RA	UF	UF
Slope	1/1	V	V	V	1/2.5	1/2.5–1/3.0	V	V
Surface (m²)	2600	3500	1500	4000	28,000	46,000	10,000	5500
Support behind GM	DC	DC	DC	GT	GT	GT	GT	GT
Protection to GM	CS	Exposed	Exposed	Exposed	Exposed	GT + RR	Exposed	Exposed
Installation of GM	1959	1969–71	1976	1980–81	1982	1984–85	1986–87	1986–87
Type of GM	EG	PIB	PVC	PVC	IIR	PVC	PVC	PVC
Thickness (mm)	2.0	2.0	1.8	1.9	1.5	1.2	2.5	2.5

Abbreviations:

R	= Rockfill dam	V	= Vertical
M	= Masonry dam	DC	= Direct contact
C	= Concrete dam	CS	= Concrete slabs
Coff	= Cofferdam	GT	= Geotextile
ENEL	= Ente Nazionale Energia Elettrica	RR	= Riprap
CBAL	= Consorzio Bonifica Apulo-Lucano	EG	= Elastomeric geomembrane
CBM	= Consorzio Bonifica Musone	PIB	= Polyisobutylene
UF	= Upstream face	PVC	= Polyvinyl chloride (high M_w plasticizer)
RA	= Reservoir area	IIR	= Isoprene-isobutylene rubber

Source: After Cazzuffi [120].

using thin cap strips from one panel to the next. Even further, the geomembrane is not exposed to either ultraviolet light or puncture since it is protected by the thickness of the concrete panel. The technique has been used on several RCC dams [122].

5.10.4 Geomembrane Dams

The use of water-inflated tubes to block off streams and create reservoirs or to control downstream water levels is possible. The tubes, made from geomembrane materials, have been used to contain water levels up to about 2.5 m in height. Various systems have been used, consisting of different materials. All have been of a reinforced variety (e.g., three- and five-ply CSPE-R, fPP-R, and EPDM-R). The seams are obviously critical, as are connections to the bottom and sides of the stream banks.

The most ambitious of all schemes of this type was the proposed damming of the three shipping channels in the Po River valley leading to Venice, Italy. Koerner and Welsh [124] show schematic drawings of the dams in their deflated and inflated positions. The intention was for them to remain deflated for most of the time, but when high waters in the Adriatic Sea occurred, the dams would be inflated, cutting off shipping but also foiling the destructive *aqua alta*, which has been doing damage to Venice itself. Unfortunately, an alternative scheme using large rotating concrete panels was used. Time will tell of the success of the selected scheme.

5.10.5 Tunnels

The waterproofing of tunnels has successfully deployed geomembranes, particularly in connection with the New Austrian Tunneling Method [125]. Here the tunnel is excavated and immediately shotcreted to prevent inward movement. The following series of steps are taken, leading to the completed section shown schematically in Figure 5.60.

1. Rock (usually) or soil (occasionally) is excavated.
2. The exposed surface is shotcreted immediately after excavation.
3. A thick nonwoven needle-punched geotextile of 400 g/m^2 minimum mass per unit area is attached by means of pins containing large polymer washers.
4. The geotextile is fitted to underdrains on each side of the tunnel base.
5. A geomembrane is placed over the geotextile, which is heat bonded to the previously placed washers.
6. The concrete liner segments or slip-formed concrete are placed against the geomembrane, completing the system.

Most mass transit systems, particularly passenger stations, are using this type of waterproofing system.

5.10.6 Vertical Cutoff Walls

The use of geomembranes to control seepage can be extended to their use in vertical cutoff trenches for remediation work. This type of cutoff can be placed in a number of

Rock tunnel
or excavation
with seepage

Shotcrete

Thick geotextile

Geomembrane

Permanent liner
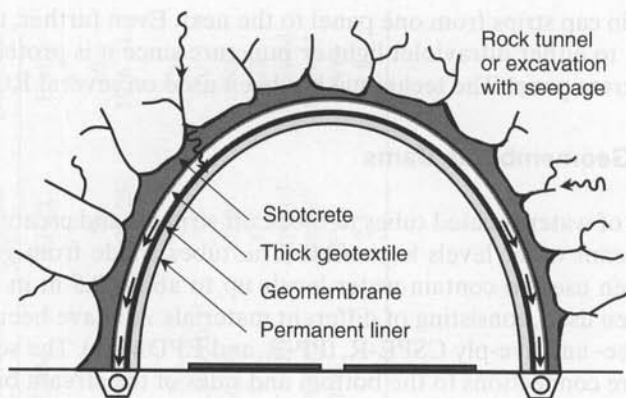
Figure 5.60 Procedure involved in tunnel waterproofing using geomembranes.

positions depending on actual circumstances: at or near the upstream toe (as shown in Figure 5.59a in place of the steel sheet piling); at or near the downstream toe (which is less desirable because of boiling considerations, but is sometimes necessary where dewatering cannot occur); vertically through the entire dam itself from its crest down to the top of the foundation or even into the foundation itself; as single or double seepage cutoff rings around the site (e.g., to contain seepage coming from landfills or hazardous waste sites (see Koerner and Gugliemetti [126]).

The construction process calls for excavating a trench and placing the joined geomembrane in it. It is then backfilled, thereby pushing the liner to the upward gradient side of the trench. For deep trenches this is usually not possible due to soil collapse, so the use of a slurry-supported trench is necessary. Here a mixture of water and bentonite (in approximate proportions of 20 to 1) is used to balance the pressures exerted by the in situ soil and groundwater so as to retain stability. Trenches 1 m wide and 20 m deep have been constructed in this manner. Once the trench is dug to its intended depth, the fabricated geomembrane is placed in the slurry. Since most geomembrane materials have a specific gravity near unity and the slurry is approximately 1.2, it is necessary to weight the bottom of the liner so that it sinks properly. Weights consisting of steel rods or metal pipes attached to the bottom edge of the geomembrane can be used. When the geomembrane is properly in place, the backfill is introduced, which displaces the slurry, forcing the geomembrane to the side of the trench. One representation of this concept in the form of a double wall is shown in Figure 5.61.

Since installation of the above scheme is very difficult, other competing systems on this same theme have become available. These usually center around thick HDPE or nonplasticized PVC, in the form of tongue-and-groove sheeting. It is exactly the same as with interlocking steel sheeting, except now with stiff (noncorroding) polymer materials. For seepage control within the interlocks, a water-expandable gasket or a polymer filled tube is used. Initial trials began with narrow sheets, but now wide sheets attached to an insertion plate are placed within a slurry supported trench (see Figure 5.62). The sheets are folded around the bottom of the insertion plate and held
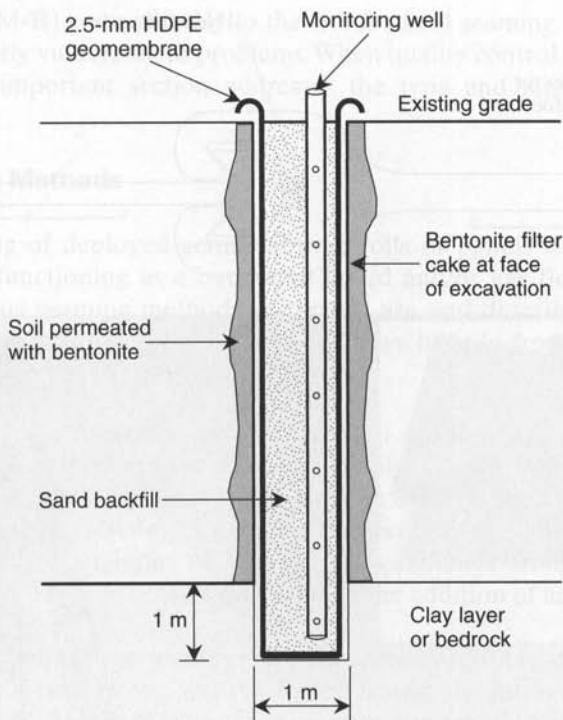
Figure 5.61 Concept of placing a geomembrane in a slurry-constructed trench to form a double seepage cut-off wall. (After ICOS of America, Inc.)

by pins until the proper depth is reached. The insertion plate is then removed, leaving the geomembrane cut-off wall in place and ready for the slurry displacing backfilling. The same system has been deployed in soft soil with no pre-excavated trench, using a vibratory pile hammer attached to the insertion plate. Several variations of the connections of one sheet to the next are shown in Koerner and Guglielmetti [126].

5.11 GEOMEMBRANE SEAMS

If a class were asked to make a list of the most important aspects of the installation of geomembranes, *seams* should be at the top of everyone's paper. Indeed, without proper seaming the whole concept of using a geomembrane as a liner or vapor barrier is foolish. The topic can be further viewed from the aspect of factory versus field seams. The individual geomembrane sheets are sometimes made into larger sheets by factory seaming them together (e.g., PVC and CSPE-R). These seams are generally very good, having been made in a controlled and clean environment with good quality control. The resulting panels are then brought to the project site and field seamed to their final configuration. Geomembranes supplied in wide-roll form (e.g., HDPE, LLDPE, fPP,

Connector profile

Hydrotite seal
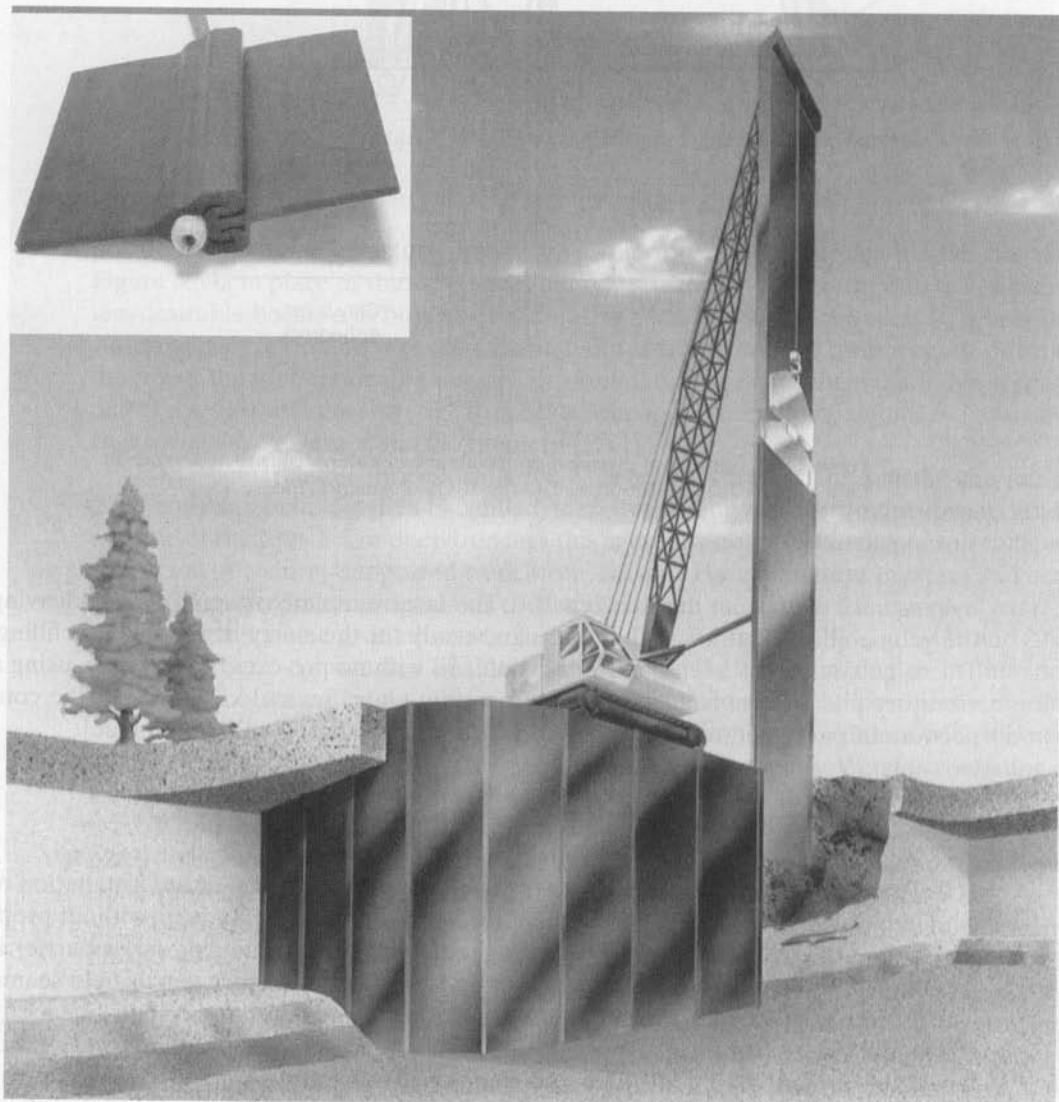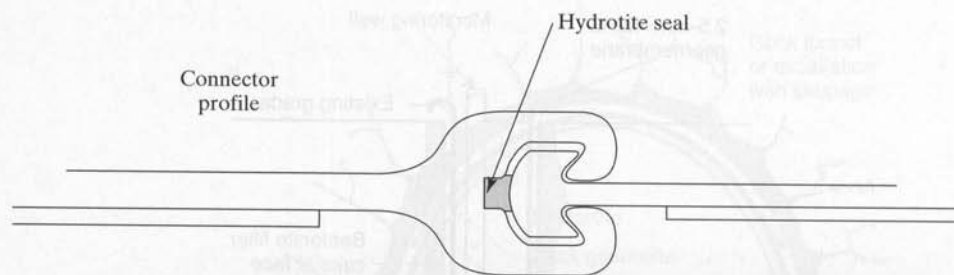
Figure 5.62   Vertical cut-off walls using HDPE interlocking sheet piles. (After GSE Lining Technology, Inc.)

fPP-R, and EPDM-R) come directly to the site for field seaming. It is the field seams that are particularly vulnerable to problems. When quality control is poor, leaks invariably arise. This important section addresses the type and manner of seaming of geomembranes.

5.11.1 Seaming Methods

The field seaming of deployed geomembrane rolls or panels is a critical aspect of their successful functioning as a barrier to liquid and/or gas flow. This section describes the various seaming methods in current use and describes the concept and importance of test strips (or trial seams). It draws heavily from an EPA Technical Guidance Document [45].

Overview.   The fundamental mechanism of seaming polymeric geomembrane sheets together is to temporarily reorganize the polymer structure (by melting or softening) of the two opposing surfaces to be joined in a controlled manner that, after the application of pressure, results in the two sheets being bonded together. This reorganization results from an input of energy that originates from either *thermal* or *chemical* processes. These processes may involve the addition of additional polymer in the bonded area.

Ideally, seaming two geomembrane sheets should result in no net loss of tensile strength across the two sheets, and the joined sheets should perform as one single geomembrane sheet. However, due to stress concentrations resulting from the seam geometry, current seaming techniques may result in minor tensile strength and/or elongation loss relative to the parent geomembrane sheet. The characteristics of the seamed area are a function of the type of geomembrane and the seaming technique used. Various factors, such as residual strength, geomembrane type, and seaming type, should be recognized by the designer when applying appropriate design factors of safety for the overall geomembrane function and facility performance.

The methods of seaming the geomembranes listed in Table 5.1 are given in Table 5.23 and shown schematically in Figure 5.63.

Seam Details.   Within the entire group of geomembranes that will be discussed there are four general categories of seaming methods (1) extrusion welding, (2) thermal

TABLE 5.23   VARIOUS METHODS FOR JOINING POLYMERIC GEOMEMBRANES

Thermal Processes	Chemical Processes
Extrusion	Chemical
Fillet	Chemical fusion
Flat (depreciated)	Bodied chemical fusion
Fusion	Adhesive
Hot wedge	Chemical adhesive
Hot air	Contact adhesive

Fillet type   Flat type (depreciated)

(a) Extrusion seams

Dual track hot wedge   Single track hot air
(single track is also possible)   (double track is also possible)

(b) Thermal fusion seams

Chemical fusion   Bodied chemical fusion

(c) Chemical seams

Chemical adhesive   Contact adhesive
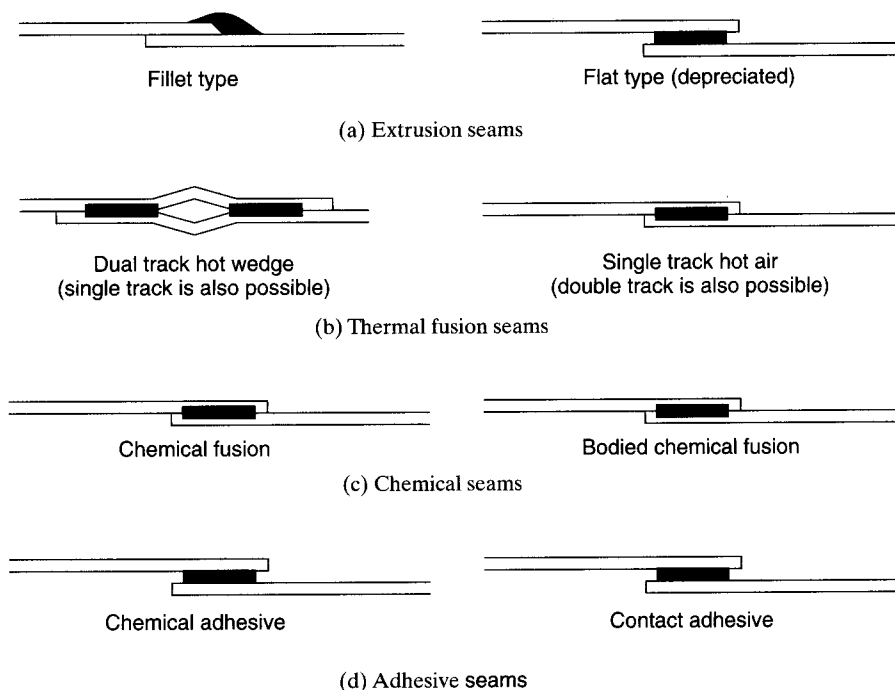
(d) Adhesive seams

Figure 5.63   Various methods available to fabricate geomembrane seams.

fusion or melt bonding, (4) chemical, and (5) adhesive seaming. Each will be explained along with its specific variations, so as to give an overview of field seaming technology.

Extrusion welding is used on polyolefin geomembranes—HDPE, LLDPE, fPP, and fPP-R. A ribbon of molten polymer is extruded over the edge of, or in between, the two slightly roughened surfaces to be joined. The molten extrudate causes the surfaces of the sheets to become hot and melt, after which the entire mass cools and bonds together. The technique is called *extrusion fillet seaming* when the extrudate is placed over the leading edge of the seam, and *extrusion flat seaming* when the extrudate is placed between the two sheets to be joined. The latter technique is no longer used in North America. It should be noted that extrusion fillet seaming is essentially the only method for seaming polyethylene geomembrane patches, for use in poorly accessible areas such as sump bottoms and around pipes, and for extremely short seam lengths. Temperature and seaming rate both play important roles in obtaining an acceptable bond; too much melting weakens the geomembrane and too little melting results in inadequate extrudate flow across the seam interface and in poor seam strength.

There are two *thermal fusion* or *melt bonding* methods that can be used on all of the thermoplastic geomembranes listed in Table 5.1. In both of them, the surface portions of the opposing surfaces are truly melted. This being the case, temperature, pressure, and seaming rate all play important roles in that excessive melting weakens the geomembrane and inadequate melting results in poor seam strength. The *hot wedge*

method consists of an electrically heated resistance element in the shape of a wedge that travels between the two sheets to be seamed. As it melts the surface of the two opposing sheets being seamed, a shear flow occurs across the upper and lower surfaces of the wedge. Roller pressure is applied as the two sheets converge at the tip of the wedge to form the final seam. Hot wedge units are automated as far as temperature, amount of pressure applied, and travel rate. A standard hot wedge creates a single uniform-width seam, while a dual (or *split*) hot wedge forms two parallel seams with a uniform unbonded space between them. This space is used to evaluate seam quality and the continuity of the seam by pressurizing the unbonded space with air and monitoring any drop in pressure that may signify a leak in the seam. *The dual hot wedge seam is considered by many, the author included, to be the premier seaming method for all thermoplastic geomembranes.* The technique can also be adapted to data acquisition welders (as is routinely done in Germany) and even for computer-controlled systems (see [127]). The *hot air* method makes use of a device consisting of a resistance heater, a blower, and temperature controls to force hot air between two sheets to melt the opposing surfaces. Immediately following the melting of the surfaces, pressure is applied to the seamed area to bond the two sheets. As with the hot wedge method, both single and dual seams can be produced, but the method is not nearly as controllable. In selected situations, this technique will be used to temporarily tack weld two sheets together until the final seam or weld is made and accepted.

There are two methods of chemically joining PVC and CSPE-R geomembranes. *Chemical fusion seams* make use of a liquid solvent applied between the two geomembrane sheets to be joined. After a few seconds to soften the surfaces, roller pressure is applied to make complete contact and bond the sheets together. As with any of the chemical seaming processes to be described, a portion of the two adjacent materials to be bonded is truly transformed into a viscous phase. The technique is used only for those geomembranes that can be dissolved by the applied solvent. Methyl ethyl keytone (MEK) is the solvent usually used. Excessive solvent will weaken the adjoining sheets, and inadequate solvent will result in a weak seam. *Bodied chemical fusion seams* are similar to chemical fusion seams except that 1 to 20% of the parent lining resin or compound is dissolved in the MEK solvent and then is used to make the seam. The purpose of adding the resin or compound is to increase the viscosity of the liquid for slope work and/or to adjust the evaporation rate of the solvent. This viscous liquid is applied by brush between the two opposing surfaces to be bonded. After a few seconds, roller pressure is applied to make complete contact.

For thermoset geomembranes, like EPDM and EPDM-R, adhesives are necessary. *Chemical adhesive seaming* makes use of a dissolved bonding agent (an adherent) in the chemical or bodied chemical, which is left after the seam has been completed and cured. The adherent thus becomes an additional element in the system. *Contact adhesives* are bonding agents applied to both mating surfaces. After reaching the proper degree of tackiness, the two sheets are placed on top of one another, followed by roller pressure. The adhesive forms the bond and is an additional element in the system.

Table 5.24 provides an overview of the seaming methods that are customarily used for each of the geomembranes in Table 5.1. It is generalized, and meant to suggest the primary seaming methods.

TABLE 5.24   AN OVERVIEW OF SEAMING METHODS FOR VARIOUS GEOMEMBRANE TYPES

Seaming Method	Type of Geomembrane								
	HDPE	LLDPE	fPP	fPP-R	PVC	CSPE-R	EIA-R	EPDM	EPDM-R
Extrusion (fillet and flat)	A	A	A	A	n/a	n/a	n/a	n/a	n/a
Thermal fusion (hot wedge and hot air)	A	A	A	A	A	A	A	n/a	n/a
Chemical fusion (solvent and bodied solvent)	n/a	n/a	n/a	n/a	A	A	A	n/a	n/a
Adhesive (chemical and contact)	n/a	n/a	n/a	n/a	A	A	A	A	A

Abbreviations:

A = method is applicable

n/a = method is not applicable

Test Strips (or Trial Seams).

Test strips (also called trial seams or qualifying seams) are an important aspect of field seaming procedures. They are meant to serve as a prequalifying experience for personnel, equipment, and procedures for making seams on the identical geomembrane material under the same climatic conditions as will be the actual field production seams. The test strips are usually made on two narrow pieces of excess geomembrane, varying in length from 1.0 to 3.0 m (see Figure 5.64). The test strips should be made in sufficient lengths, preferably as a single continuous seam, for all required testing purposes.

The goal of these test strips is to imitate all aspects of the actual production field seaming activities intended to be performed in the immediately upcoming work session, so as to determine equipment and operator proficiency. Ideally, test strips can estimate the quality of the production seams while minimizing the field sampling of the

Figure 5.64   Fabrication of a geomembrane test strip with wedge welder.

installed geomembrane through destructive mechanical testing. Test strips are typically made every four hours—for example, at the beginning of the workday and after the lunch break. They are also made whenever personnel or equipment are changed and when climatic conditions reflect wide changes in geomembrane temperature or other conditions that could affect seam quality.

The destructive testing of the test strips should be done as soon as the installation contractor feels that the strength requirements can be met. Thus it behooves the contractor to have all aspects of the test strip seam fabrication in complete working order, just as would be done in making production field seams. For extrusion and thermal fusion seams, destructive testing can be done as soon as the seam cools, which takes only a few minutes. For chemical fusion and adhesive seams, testing must wait for curing, possibly several days, and the use of a field oven to accelerate the curing of the seam is possible.

From two to six test specimens are cut from the test strip using a 25 mm wide die. The specimens are then tested in both peel and shear, using a field tensiometer (see Figure 5.65). If any of the test specimens fail, a new test strip is fabricated. If additional specimens fail, the seaming apparatus and seamer should not be accepted and should not be used for seaming until the deficiencies are corrected and successful trial welds are achieved. If the specimens pass, seaming operations can move directly to production seams in the field. Daniel and Koerner [45] discuss the situation in greater detail.

5.11.2 Destructive Seam Tests

After a field seaming crew has made a series of production seams, it is important to evaluate their performance. The procedure is to cut out a sample, send it to the laboratory, cut specimens and pull them until failure in either shear or peel modes (recall
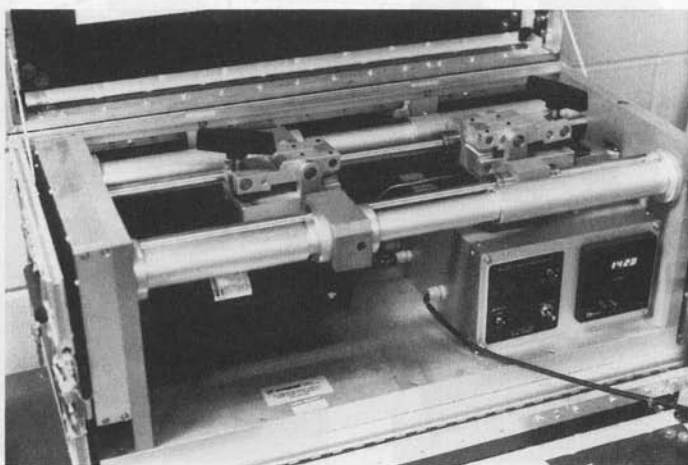
Figure 5.65   A field tensiometer for performing a geomembrane seam test. (Compliments of Wegener Co.)

Section 5.1.3). But considering a geomembrane sheet layout as shown in Figure 5.66, the questions becomes where and how many? Remember that each seam sample becomes a hole, which must be appropriately patched and then retested. For this reason it is common to reduce the number of field seam samples to a bare minimum, and then to assess only the method of seaming, not its continuity. By *method* we mean seaming type, temperature, dwell time, pressure, and other operational details affecting seam quality. Continuity of the entire seam is handled by nondestructive testing, which will be described later.
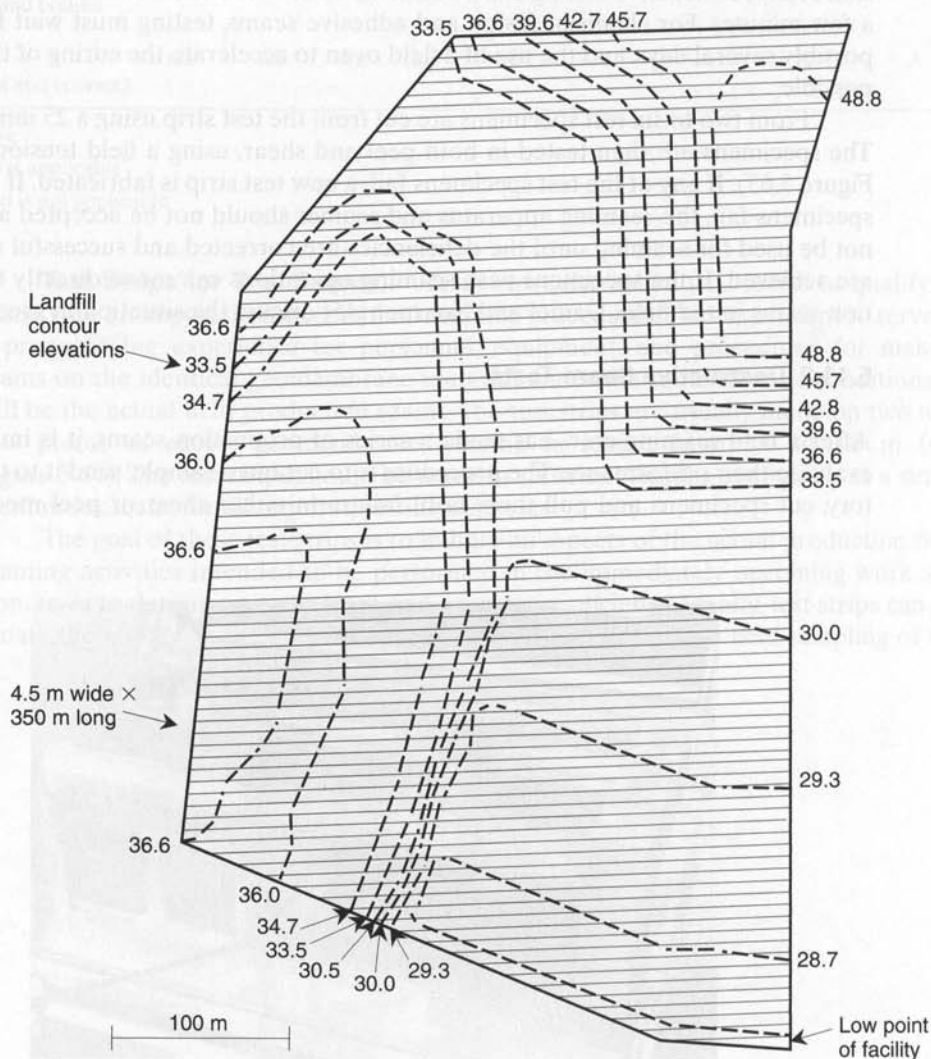
Figure 5.66 Geomembrane sheet layout for a solid-waste landfill; lined area equals approximately 76,800 m².

Sampling Protocol.   Destructive test sampling can be done on a random basis or on a periodic basis. Metrecon [4] recommends a frequency of six samples per kilometer of seam on a random basis, or one sample per 150 m of seam on a uniform basis. With current welding devices and certified personnel, this interval should be opened to one in 200 to 300 m of seam at least to begin a project. Recognize that even within a uniform interval the samples can be selected randomly (see [45]). Furthermore, there are sampling strategies that reward good seaming by requiring fewer samples and penalize poor seaming by requiring additional samples. See Richardson [128] for two such strategies, the method of attributes and the use of control charts; both of which have been standardized.

Sample Size.   The size of the destructive test sample depends on the specification and quality assurance plan at the site. It can be as small as 300 mm along the seam length or up to 1500 mm. After taking a sample, it is further subdivided among one or all of the following organizations: the owner/operator (for archiving), the construction quality control firm (for testing), the construction quality assurance firm (for testing), the general contractor (for archiving), and the regulatory agency (for inspection or archiving). Additional detail is given by Daniel and Koerner [45].

Shear and Peel Testing.   Figure 5.67 shows examples of shear and peel testing of geomembrane seam test specimens. Although such tests appear straightforward, there are many nuances depending on the type of geomembrane being evaluated.

(a) Typical shear test   (b) Typical peel test
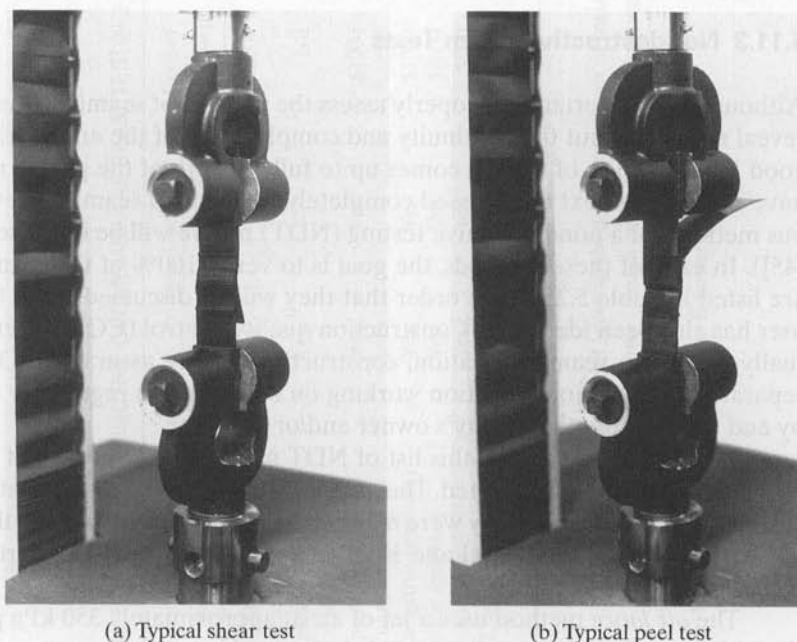
Figure 5.67   Basic types of geomembrane seam tests illustrated for HDPE.

Table 5.4 presents the current status of evaluating the various geomembranes mentioned in Table 5.1. Given is the type of shear test, peel test, and comparison test on the nonseamed sheet, unless the strength of the seam test is targeted to a limiting value. Insofar as a passing test is concerned, we are focusing on three issues.

- The sheet on either side of the seam must fail—that is, the seam cannot delaminate within itself. This is called a *film tear bond* failure as per Metrecon [4].
- The magnitude of the force required for failure should meet or exceed a specified value. For seams tested in a shear mode, failure forces of 85 to 95% of the unseamed sheet failure are usually specified. For seams tested in a peel mode, failure forces of 50 to 80% of the unseamed sheet are often specified for thermally bonded seams. Other strategies are used for chemical and adhesive bonded seams. These percentages underscore the severity of peel tests as compared with shear tests. As seen in the data in Figure 5.6, this is indeed the case. For assessing seam quality, the peel test is indeed the target test that should be focused on.
- The shear test must result in a minimum elongation of failure (e.g., 50% or larger), and the peel test must not delaminate, or separate, more than a given amount at failure (e.g., 25% or less).

Specifics of the above three issues must be embodied in the project specification, or reference made to a generic specification that is available through the Geosynthetic Research Institute.

5.11.3 Nondestructive Seam Tests

Although it is important to properly assess the method of seaming, shear and peel tests reveal nothing about the continuity and completeness of the entire seam. It does little good if one section of a seam comes up to full strength of the parent material, only to have the section next to it missed completely by the field seaming crew. Thus continuous methods of a nondestructive testing (NDT) nature will be discussed here (see also [45]). In each of these methods, the goal is to verify 100% of the seams. The methods are listed in Table 5.25 in the order that they will be discussed. Note that the primary user has also been identified. Construction quality control (CQC) refers to the firm actually doing the seam fabrication; construction quality assurance (CQA) refers to a separate inspection organization working on behalf of the regulatory agency, but paid by and reporting to the facility's owner and/or operator.

   In proceeding through this list of NDT methods the absence of three ultrasonic based methods should be noted. They are essentially laboratory oriented and have not yet been field perfected. They were mentioned in previous editions of this book and are written up in detail in Daniel and Koerner [45]. All of them are worthwhile research projects.

   The *air lance* method uses a jet of air at approximately 350 kPa pressure coming through an orifice of 5 mm diameter. It is directed beneath the upper edge of the overlapped seam to detect unbonded areas. When such an area is located, the air passes

TABLE 5.25 NONDESTRUCTIVE GEOMEMBRANE SEAM TESTING METHODS

Nondestructive Test Method	Primary User CQC	Primary User CQA	Cost of Equipment	Speed of Tests	Cost of Tests	Type of Result	Recording Method	Operator Dependency
Air lance	Yes	—	$200	Fast	Nil	Yes-no	Manual	Very high
Mechanical point (pick) stress	Yes	—	Nil	Fast	Nil	Yes-no	Manual	Very high
Dual seam (positive pressure)	Yes	Yes	$1000	Fast	Moderate	Yes-no	Manual	Low
Vacuum chamber (negative pressure)	Yes	Yes	$1000	Slow	Very high	Yes-no	Manual	High
Electric sparking	Yes	Yes	$3000	Fast	Low	Yes-no	Manual	Moderate
Electric wire	Yes	Yes	$500	Moderate	Nil	Yes-no	Manual	High
ELL survey	Yes	Yes	$20,000	Slow	High	Yes-no	Manual and automatic	Low

Abbreviations:

CQC = construction quality control (geomembrane manufacturer or installer)

CQA = construction quality assurance (design engineer or inspection organization)

ELL = electrical leak location

Source: Modified from Richardson and Koerner [74].

through, causing inflation and fluttering in the localized area. The audible sound also changes when unbonded areas are encountered. The method works best on relatively thin, less than 1.0 mm, flexible geomembranes, but it works only if the defect is open at the front edge of the seam, where the air jet is directed. It is essentially a contractor's or installer's tool to be used in a CQC manner.

The *mechanical point stress* or *"pick" test* uses a dull tool (such as a blunt screwdriver) under the top edge of a seam. With care, an installer can detect an unbonded area, which is easier to separate than a properly bonded area. It is a rapid test that obviously depends completely on the care and sensitivity of the person doing it. Detectability is similar to that using the air lance, and both are very operator-dependent. Again, this test is to be performed only by the installation contractor and/or geomembrane manufacturer. Design or inspection engineers have to business poking objects into seamed regions and should use one or more of the other available techniques.

The *pressurized dual seam* method was mentioned earlier in connection with the double-wedge thermal seaming method. The air channel that results between the two parallel seams is inflated using a hypodermic needle and is pressurized to approximately 200 kPa. If no drop on a pressure gauge occurs over a given time period, the entire seam is acceptable. The test method is standardized as ASTM D5820 for HDPE and by the Geosynthetic Research Institute for other geomembranes. If an excessive drop in pressure occurs, a number of actions can be taken: the distance can be systematically halved until the leak is located, the section can be tested by some other leak detection method, or a cap strip can be seamed over the entire exposed edge. The test is excellent and is considered by many, the author included, as the premier seam-testing method. Because there is no limitation in seam length, a single test can extend from one side of a facility to the other. The test is generally performed by the installation contractor, but with the CQA personnel viewing the procedure and assessing the results.

Vacuum chambers (boxes) are another technique that has been used. A 0.5 m long box with a transparent top is placed over the seam and a vacuum of approximately 15 kPa applied. When a leak is encountered, the soapy solution previously placed over the seam shows bubbles, thereby reducing the vacuum. This is due to air entering from beneath the liner and passing through the unbonded zone. The test is slow to perform, and it is often difficult to make a vacuum-tight joint at the bottom of the box where it passes over the seam edges. Due to upward deformations of the geomembrane into the vacuum box, only geomembrane thicknesses greater than 1.0 mm should be tested in this manner. For thin flexible geomembranes, the bottom of the box can be fitted with a steel mesh to avoid excessive deformations. It should be noted that vacuum boxes are a common form of nondestructive test used for patched areas, anchor trenches and sumps where a pressurized dual seam is not possible. The method is very labor-intensive and is essentially impossible to use on side slopes, since the adequate downward pressure required to make a good seal cannot be mobilized (as this is usually done by standing on top of the box).

Electric sparking originated as a factory technique used to detect pinholes in thin thermoplastic liners. The method uses a high-voltage (15 to 30 kV) current, and any leakage to ground (through a pinhole or flaw) will result in sparking to the metal support plate. The technique has been revived in a somewhat analogous form by manufacturing

a high carbon black coextruded polyethylene geomembrane on the lower surface of the sheet. By applying a suitable surface voltage, the entire geomembrane system (sheets and seams) can be monitored for leaks by electric spark testing.

The *electric wire* method places a copper or stainless steel wire between the overlapped geomembrane sheets, which actually embeds it into the completed seam. After seaming, a charged probe of about 20,000 volts is connected to one end of the wire and slowly moved over the length of the seam. A seam defect between the probe and the embedded wire results in an audible alarm from the unit. The method is advocated by some installation firms, giving rise to extremely low seam failure instances.

The *electric field test*, currently called the *electrical leak location (ELL) method*, was developed by Schultz et al. [129]. It utilizes a liquid-covered geomembrane to contain an electric field. The bottom of the lined facility should be covered with water, however the depth can be nominal and even a water film is adequate. An electrical source is used to impose current across the boundary of the liner. When a current is applied between the source and the remote current return electrodes, current flows either around the entire site (if no leak is present) or bypasses the longer travel path through the leak itself (when one is present). Potentials measured on the surface are affected by the distributions and can be used to locate the source of the leak. These potentials are measured by *walking* a probe across the surface. The operator walks on a predetermined grid layout and marks where anomalies exist. These can be rechecked after the survey is completed by other methods, such as a vacuum box.

Since its original development in the early 1980's, the method has been greatly expanded. Of significant importance is that ELL surveys have shown the majority (50 to 83%) of leaks in the geomembrane-lined facility are in the installed sheet itself rather than exclusively in the seams. In large part, this comes about from soil backfilling by the earthwork contractor. Surveying stakes penetrating through the underlying geomembranes are notorious in this regard, as are stone punctures and various-sized gouges from bulldozer blades. This issue is absolutely critical insofar as a total leak-free facility is concerned. The technique has emerged as being preferred in such a total system monitoring. Figure 5.68 illustrates the technique as it can be used on both single- and double-lined facilities. More importantly, it can be performed after the cover soil has been placed over the uppermost geomembrane. As indicated, the electrodes are connected to a high energy power supply with data taken within the facility and sometimes recorded on a digital data logger. Numerous references are available [130, 131] and the method is standardized as ASTM D6747, which provides additional details.

5.11.4 Summary

It is generally recognized that the geomembrane industry's ability to manufacture near-flawless sheets far surpasses its ability to seam separate sheets together. Furthermore, it is also recognized that the ability to make factory seams is generally considered to be better than the ability to make field seams. This difficulty regarding field seams is due to a number of factors: nonhorizontal (sloped) preparation surfaces; nonuniform and/or yielding preparation surfaces; nonconforming sheets to the subsurface; textured liners without smooth edges; wind-blown dirt in the areas to be seamed;

POWER
SUPPLY

DIGITAL
DATA
RECORDER

Soil backfill

Electrode

Current flow

Leak

Electrode

Primary geomembrane

Secondary geomembrane
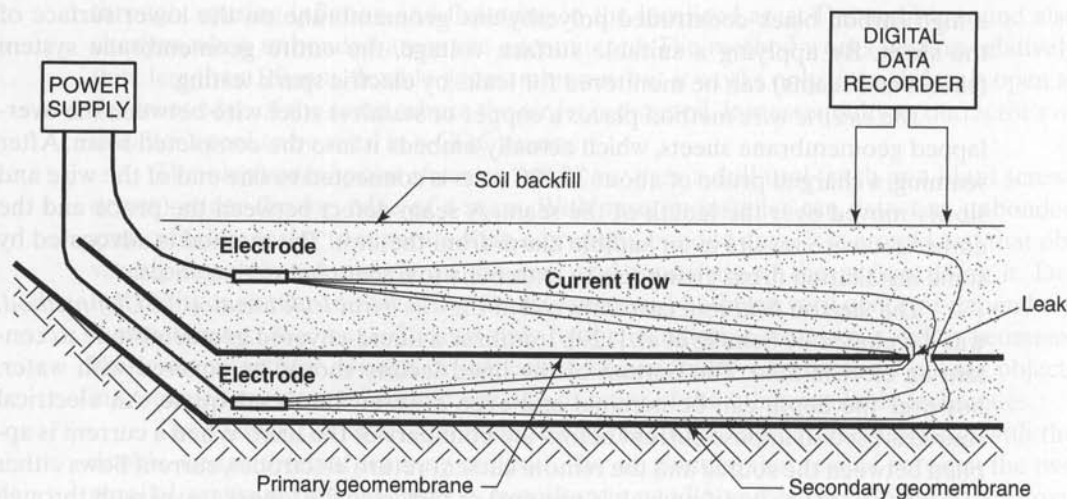
Figure 5.68 Principle of the electrical leak location (ELL) method for soil-covered geomembranes and for double-lined facilities. (After Laine and Darilek [130] and Darilek and Miller [131])

moisture and dampness in the subgrade beneath the seam; frost in the subgrade beneath the seam; moisture on the upper surface of the geomembrane; penetrations, connections, and appurtenances; wind fluttering the sheets out of position; ambient temperature variations during seaming; uncomfortably high temperatures for careful working; uncomfortably low temperatures for careful working; and expansion and/or contraction of sheets during seaming.*

With so many potential problems, it is natural that emphasis on high-quality field seams and on subsequent seam inspection is commonly referred to in the literature. This need grows progressively more important depending upon the implications of the contained material (usually liquid) escaping. Thus hazardous and radioactive waste facilities have the highest priority, while recreational reservoirs and aesthetic ponds have a much lower priority.

In this regard the dual track hot wedge fusion system deserves further commentary. At the outset it is helpful to recognize that *all* thermoplastic geomembranes can be seamed by this method. This includes every type of geomembrane listed in Table 5.1 except EPDM. The method has three controllable features: (1) wedge temperature, (2) nip roller pressure, and (3) travel rate (speed). Currently these controls are set manually, based in part on the outcome of trial seams, as previously discussed. Since trial seams are typically made at four-hour intervals, weather conditions can change, and the

---

*Note that in Germany geomembranes are required to have thin plastic tear strips (150 mm wide) on the top and bottom edges of the rolls, which are removed immediately before seaming, leaving the areas to be bonded both clean and dry.

operator must adjust the device accordingly. To avoid subjective modifications, current efforts are being made at data acquisition, on-line sensing, and computer-controlled feedback and adjustment [127]. Typically, the speed will be increased if the geomembrane temperature warms and decreased if it cools. A number of new and exciting systems are currently operational and are available in Europe.

Of equal importance to the type of seam are seam testing methods. Although destructive tests are invariably required, they are self-defeating at the outset. The worst-looking locations of a lined facility is at every location where a sample has been cut out for testing, patched, retested, and sometimes patched again. When samples must be taken by or distributed to the regulatory agency, the owner, the contractor, the designer, and the CQA organization, the situation can become ludicrous. It begs for a methodology that assesses both quality and continuity in the final product, even after backfilling.

Figure 5.69 presents such a methodology, which begins with the geomembrane being seamed by the dual track hot wedge method and a destructive test frequency of 1 sample per 150 m spacing. However, if an added level of quality is agreed upon by the installer (certified welders, taped edges, automatic welding devices, or infrared/ultrasonic testing), the spacing can be increased to 1 sample per 300 m. As production seaming begins, and the results of destructive tests becomes available, statistical methods, such as attributes or control charts, either open up the spacing (for good destructive test results) or close it (for poor destructive test results). Thus, good seaming is rewarded and poor seaming is penalized. Furthermore, the bold option is not to have routine
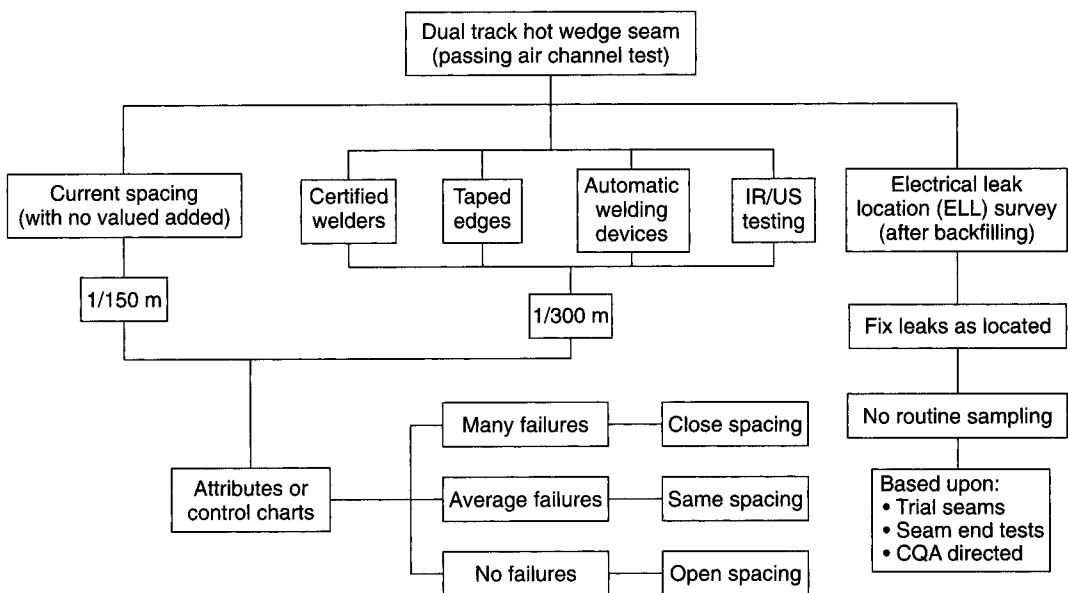
Figure 5.69   Recommended strategy for destructive test sample spacing assuming that the seam is made by dual track wedge welding and passes the specified air channel test.

sampling but instead to use the ELL method to test the entire facility, seams and sheet, after backfilling. Discovered leaks are fixed and retested by vacuum box as they are detected. Of course, trial seams, destructive tests at the anchor trench ends of long seams, and as directed by the CQA inspector must always be considered.

5.12 DETAILS AND MISCELLANEOUS ITEMS

As mentioned in the discussion on seams in Section 5.11, difficulties often arise when details are required. If the space is limited and automated equipment cannot be used, hand labor and experience are all important.

5.12.1 Connections

The primary guidelines that a designer should follow regarding geomembrane connections are to maintain as smooth a transition as possible and to use materials with the least possible change in stiffness. In this context, stiffness can be assessed by modulus, where the following ranking of materials (from highest to lowest modulus) is well known: steel (and other metals), concrete, wood, stiff polymers, soft polymers. Thus geomembranes connected to metal and concrete structures must be very carefully designed.

Design in this case is really a matter of detailing and visualizing how settlements, deformations, and other stress-and-strain-mobilizing phenomena might influence the connection. Experience is certainly important in this regard. Most manufacturers and installers of liners have details showing proper procedures. Some of these details are presented in Figure 5.70, where thick polyethylene strips (sometimes embedded in the concrete as it is poured) or woodstrips are used to make the transition from liner to concrete structure. Metal structures can be treated in a similar manner. Note that there is the possibility of making a pressure seal to concrete, as shown on the one detail. Such designs have been used to force subsurface groundwater to drainage sumps where gravitational flow was not possible.

Although these details are straightforward to visualize and easy to show, their proper construction is not so simple. Care and true craftsmanlike work are required for trouble-free and leak-free performance.

5.12.2 Appurtenances

Appurtenances are any adjunct item necessary for proper functioning of the total system. When dealing with geomembrane-related systems, this refers to inlet and outlet piping together with pipe racks, vents, sumps, structural support frames, and the like.

As for pipes penetrating the geomembrane, prefabricated *boots* are commonly used, which fit snugly over the pipe and are then sealed to the liner (see Figure 5.71). Mastic and O-rings around the pipe, and fillet extrusion welds on the skirt are used to complete the seal. The boot assembly should be made of the same material as the liner, and the mastic compound should be carefully selected. Direct connections to flanges

Corrosion resistant attachment

Screws or bolts
with sockets

Hardwood
timber batten

Geomembrane
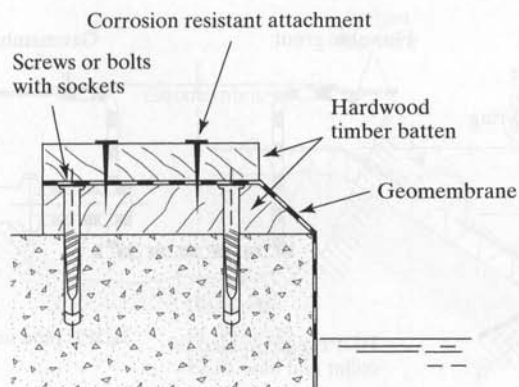
(a) Connection to existing structure

PE strip

Batten strip
Bolt and socket
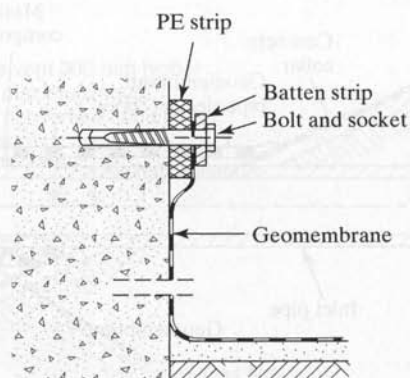
Geomembrane

(b) Connection to vertical face structure

Geomembrane

Batten strip

Percussion-
driven nail

PE strip
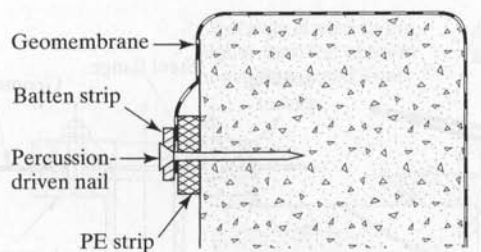
(c) Connection over concrete weir

PE strip

Batten strip
Geomembrane

Bolt and socket
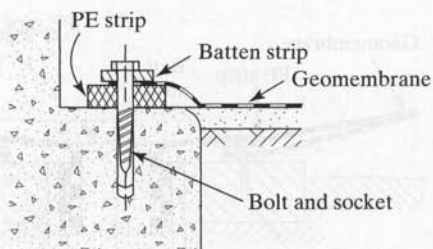
(d) Connection to horizontal structure

Joint insert
Mastic material
Site-poured
concrete member
Mastic material
Geomembrane

PE O-ring seal
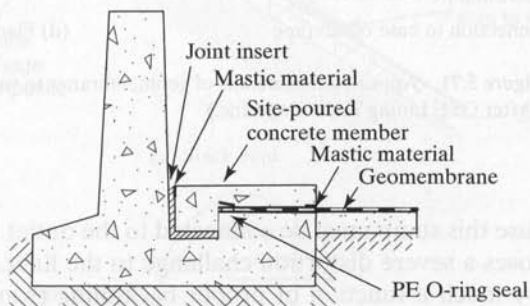
(e) Connection to structure forming
a concrete pressure seal

Figure 5.70   Connection details of geomembranes to different structures. (After
GSE Lining Technology, Inc.)

and base outlet pipes are even more difficult to construct, as the details in Figure 5.71
illustrate. Problems can arise here, not so much from the initial installation but because
such outlets represent a separate structure. These structures often have settlement pro-
files very different from the rest of the impoundment; hence, differential settlements
should be anticipated. An important example is the leachate collection sump of a landfill

Concrete collar

Geomembrane pipe sleeve ("boot")

Mastic compound

Flowable grout

Geomembrane

O-ring

Inlet pipe

Geomembrane

(a) Connection of concrete or steel inlet pipe

HDPE pipe welded to collar and base sheet

HDPE pipe section

(b) Connection of HDPE to prefabricated sump

Geomembrane

PE pipe section

PE strip   Batten strip

Sealing gasket

Steel flange

Geomembrane

Mechanical securing

Steel outlet pipe   O-ring

Mastic compound

Lower flange

(c) Connection to base outlet pipe

(d) Flange connection to pipe section

Figure 5.71 Appurtenance details of geomembranes to various pipe systems. (After GSE Lining Technology, Inc.)

liner. Because this sump must be connected to the outlet by pipe sections for liquid removal, it poses a severe distortion challenge to the liner. The degree of severity, however, is very much a function of proper backfilling (sometimes with flowable grout) which must be done with great care under close supervision. Great care in detailing, construction, and inspection should be exercised in these appurtenance items.

For gas-generating subsurface conditions, a geotextile underliner is recommended for collection and transmission, but eventually this gas must be released to a collection system or vented to the atmosphere. Vents are often made at the top of the side slope berm or along the runout length. They are either open cutout areas with flap vents (generally not recommended) or stack vents (preferred) at approximately 10 to 30 m centers (see Figure 5.72). An alternative is a rotating wind cowl assembly that always points downwind, thereby venting the system and at the same time pulling a slight vacuum that holds the liner snugly to the ground surface.

Air/gas
flap vent

Geomembrane

Place vent 300 mm higher
than maximum liquid
level at overflow conditions

50 mm minimum

Geotextile
or drainage
geocomposite

Gas flow

(a) Flap vent

Openings in vent to be
higher than top of berm
of overflow liquid level

Air/gas stack vent
assembly

Geomembrane

Approx. 150 mm

Bond skirt of
vent to liner

Geotextile
or drainage
geocomposite

Gas flow

(b) Stack vent

Wind cowl
detail

Geomembrane

Gas flow

Concrete

(c) Wind cowl vent

Figure 5.72 Typical gas vent details. (After Richardson and Koerner [74])

5.12.3 Leak Location (After Waste Placement) Techniques

Once a leak occurs in a lined impoundment or landfill it is often too late to initiate corrective action. However, such a passive approach cannot be taken when the leak is from a hazardous or radioactive waste site, and downstream water contamination can result. Thus numerous attempts have been made at solving the problem of leak location (versus leak detection from ELL surveys during installation, as described in Section 5.11.3). At the outset it should be mentioned that all the techniques to be reviewed are in various stages of research and development. None have been used with unconditional success and some are experimental. They are mentioned only to emphasize the importance of leak location and to illustrate that some of the efforts are currently ongoing.

Downstream well monitoring is generally held out as a possible approach to the problem. In this method, pollutants carried by the groundwater can possibly be detected in a well by proper sampling and testing methods. If this same pollutant is detected in other downstream wells and enough wells are available, pollution concentration gradients can be drawn. When back-extrapolated to beneath the landfill, some idea of the leak location might be possible. It is a long shot, however, and the number of wells required for accurate contouring is quite large, and hence very costly. In this regard, the author feels that double-lined facilities with leak detection capability are far superior to single-lined facilities with well monitoring [132].

Rather than using discrete data, we could possibly obtain continuous data from a nondestructive testing (NDT) technique. The geophysical method of *electrical resistivity* is a candidate method in this regard. Electrical resistivity (as with all electromagnetic methods) is very sensitive to high ion content concentrations. If a contaminated seepage plume (usually high in ionic content) forms downstream from a landfill, electrical resistivity traces can be made, detecting both the location of the plume and the concentration within the plume. By using back-extrapolated contours an approximate leak location can be determined. Problems do arise, however, because many other subsurface features such as stratigraphy, density, and buried objects also influence electrical resistivity. Even under ideal conditions, leak location under the landfill is approximate at best. Furthermore, the classical techniques are quite labor intensive. An alternative, based on the same principle of electrical resistivity, is a portable electromagnetic induction system. Using it makes the survey much more efficient and as accurate as older resistivity methods, at least for shallow-depth tracing.

The use of *tracers*, vegetable or chemical dyes, injected into various locations of the leachate collection system has been attempted. An estimate based on the time it takes for the tracer to reach a leak detection monitor (for double-lined facilities) or a downstream monitoring well (for single-lined facilities) serves to approximate where the leak is located. It is not known how successful this technique is or how tracer dilution or multiple leaks might complicate the process. It appears, however, that only very large leaks can be identified using such tracers.

Other leak location methods used within the boundaries of the facility itself must be designed before construction and installed accordingly. For example, when wires are

placed beneath the facility (e.g., in a geotextile underliner) during its construction, three different NDT methods can possibly be used to locate leaks. *Acoustic emission monitoring* senses the sounds that the leaks make as they pass over or near to the wires. By having a grid of wires, the emissions can be monitored at the edges of the impoundment. These pulses collected over a timespan of few minutes can be plotted in the x and y directions, and contours of equal emission count rate can be obtained. The convergence of these contours signifies the leak location. Feasibility and laboratory demonstrations have been attempted [133]. This technique could also be used for floating covers of surface impoundments if an accidental or intentional (terrorist) cut is made in the geomembrane. In a similar manner, *time-domain reflectometry* uses transmission-line wires placed beneath the geomembrane itself during construction. These are placed in sets, and depending on their response to questioning, signify leaks and, by implication, the location of these leaks. The technique has been attempted on a prototype landfill with success [134], but it suffers from the same drawback as acoustic emission, in that the conducting leads (wires) must be placed during liner construction. Long-term corrosion of the wires is a concern for both techniques. Thus, there must be a conscious effort by the designer before construction to include such a provision for potential leak location. Such a technique is available and has been used in final cover installations in Germany. Rödel [135] describes a set of electrodes placed under the geomembrane and another set placed perpendicularly above the geomembrane. When voltage is induced across the two sets of electrodes, the geomembrane acts as an insulator unless it has defects (holes). The resistance then drops on these electrodes near the defect, and it can be located by the electrode grid arrangement. Computer software is used for on-line monitoring and a graphic display.

5.12.4 Wind Uplift

When geomembranes are exposed during installation or permanently, they can be greatly affected by wind. Wind traveling over the geomembrane is influenced by friction and turbulence within the flowing air mass. Uplift forces develop as a result of wind flow separation that occurs when the air mass decelerates or when irregular boundary shapes are encountered. Downwind from the air-flow separation, a wake of turbulent eddies is formed and the air flow reverses. This results in uplift forces being exerted on the surface of the geomembrane. If forces are excessive with respect to the weight of the geomembrane and its anchorage (if any), it will be uplifted and unceremoniously pulled out of position in a very random manner. As seen in Figure 5.73, the geomembrane can easily be torn and severely damaged.

The obvious solution to this situation is to use sandbags to hold the deployed geomembrane in position until final cover is placed or suitable anchorage is provided. As indicated by Wayne and Koerner [136], however, the number of sandbags becomes unreasonably high as wind speeds become severe. While no easy solution is offered, the possibility of wind displaced geomembranes must be discussed by all parties *before* installation of the geomembrane begins. The proper time is at the preconstruction meeting when all parties are involved. Possible remedies are to merely reposition the disturbed geomembrane, reseam or cap strip the torn locations, test the damaged

Figure 5.73 Examples of wind-damaged geomembranes on two projects.

geomembrane at creases and severe distortions, or (in a worst-case situation) reject the roll(s) or panel(s) involved. It must be mentioned, however, that if rejection is decided upon, the installer may not have replacement material readily available and the project will probably be delayed. Furthermore, the important issue of payment for the replaced geomembrane must be openly and carefully discussed at the preconstruction meeting.

5.12.5 Quality Control and Quality Assurance

Of all the geosynthetic materials described in this book, none are as unforgiving as geomembranes. The smallest leak when placed under hydrostatic pressure can produce alarmingly high flow rates; see Giroud et al. [137]. Thus inspection is clearly warranted in almost all applications. Such inspection comes under the dual headings of quality control (QC) and quality assurance (QA). For geosynthetics that are both manufactured and constructed (often by different organizations), a further subdivision is necessary. Thus, it is important to keep four definitions in mind and to understand how the different activities contrast and/or complement one another [45].

- *Manufacturing quality control (MQC):* A planned system of inspections that is used to directly monitor and control the manufacture of a material that is factory originated. MQC is normally performed by the manufacturer (or fabricator) of geosynthetic materials and is necessary to ensure minimum, or maximum, specified values in the manufactured product. MQC refers to measures taken by the manufacturer to determine compliance with the requirements for materials and workmanship as stated in certification documents and contract plans and specifications.

- *Manufacturing quality assurance (MQA)*: A planned system of activities that provide assurance that the materials were manufactured as specified in the certification documents and contract plans and specifications. MQA includes manufacturing and fabrication facility inspections, verifications, audits, and evaluation of the raw materials and geosynthetic products to assess the quality of the manufactured materials. MQA refers to measures taken by the MQA organization to determine if the manufacturer or fabricator is in compliance with the product certification and contract plans and specifications for the project.

- *Construction quality control (CQC):* A planned system of inspections that are used to directly monitor and control the quality of a construction project. Construction quality control is normally performed by the geosynthetics installer to achieve the highest quality in the constructed or installed system. CQC refers to measures taken by the installer or contractor to determine compliance with the requirements for materials and workmanship as stated in the plans and specifications for the project.

- *Construction quality assurance (CQA):* A planned system of activities that provide assurance that the facility was constructed as specified in the design. Construction quality assurance includes inspections, verifications, audits, and evaluations of materials and workmanship necessary to determine and document the quality of the constructed facility. CQA refers to measures taken by the CQA organization to assess if the installer or contractor is in compliance with the plans and specifications for the project.

MQA and CQA are performed independently from MQC and CQC. Although MQA/CQA and MQC/CQC are separate activities, they have similar objectives and, in a smoothly running construction project, the processes will complement one another. An effective MQA/CQA program can lead to identification of deficiencies in the MQC/CQC process, but a MQA/CQA program by itself (in complete absence of a MQC/CQC program) is unlikely to lead to acceptable quality management. Quality is best ensured with effective MQC/CQC *and* MQA/CQA programs. Figure 5.74 illustrates the recommended interaction of the various organizations in a total quality program. Note that the flow chart includes both geosynthetic and natural soil materials, since both require similar concern and care. Of particular importance is the qualifications of the various parties involved. The current recommendations are given in Daniel and Koerner [45].

The proper and intended functioning of a geomembrane or other geosynthetic system in an engineered facility is strongly dependent on the MQC/MQA of its
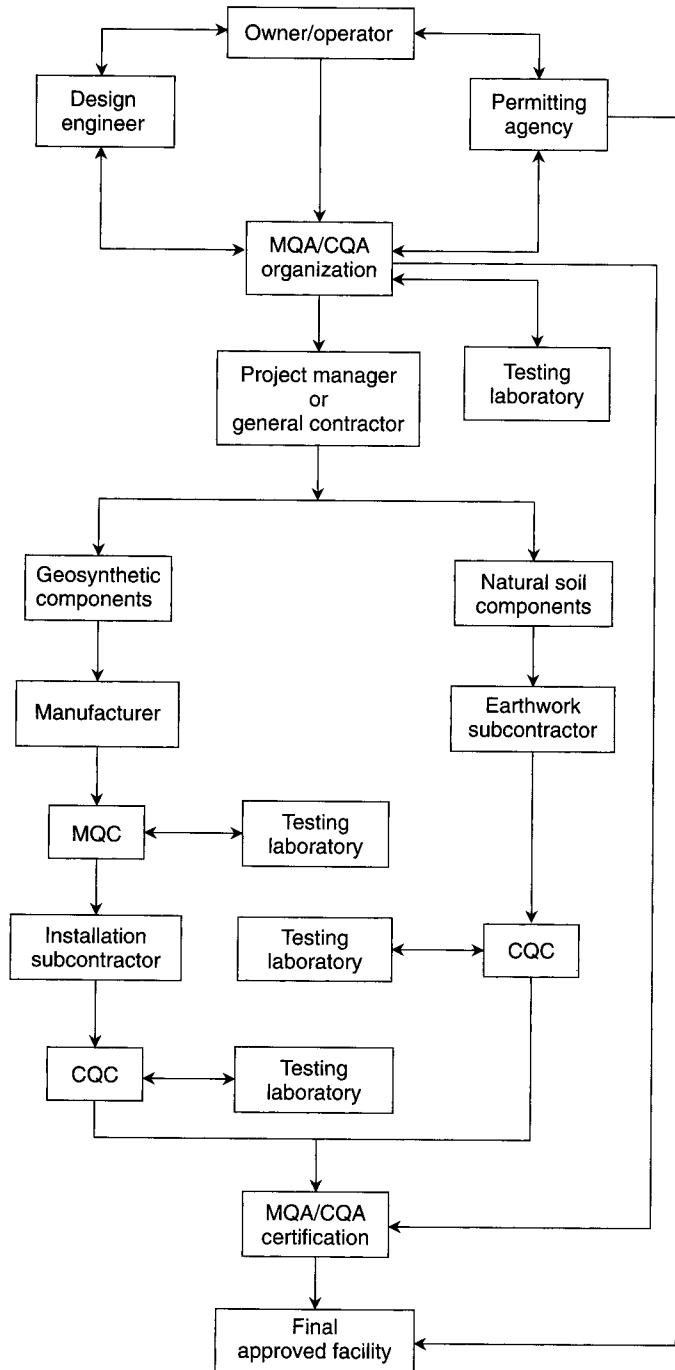
Figure 5.74 Organizational structure of MQC/MQA and CQC/CQA inspection activities. (After Daniel and Koerner [45])

manufacture and the CQC/CQA of its installation. This section has defined the scope and definition of those activities with emphasis on their interrelationship with one another. Although the level of effort will differ from project to project, the concepts outlined should be present for all situations. Geosynthetics are relatively new engineered materials in comparison to steel, concrete, timber, and so on, and every detail must be considered in order to avert failures—failures that are generally unacceptable if they occur any time up to the intended design lifetime of the facility. Proper consideration of MQC/MQA and CQC/CQA will serve well to establish geomembranes (and all types of geosynthetics) as bona fide engineering materials for the future.

5.13 CONCLUDING REMARKS

Throughout this chapter on geomembranes functioning as liquid or vapor barriers, the emphasis has been on a step-by-step design procedure. These steps generally are taken in the following order:

1. Site selection
2. Geometric layout (length, width and depth)
3. Geotechnical considerations (groundwater and subsurface foundation conditions)
4. Cross-section determination
5. Geomembrane material selection
6. Thickness determination
7. Side slope and cover soil details
8. Anchor trench details
9. Solid-waste stability (if applicable)
10. Final cover design and details (if applicable)
11. Seam type decision
12. Seam testing strategy (destructive and nondestructive)
13. Design of connections and appurtenances
14. Leak scenarios and corrective measures
15. Appropriate MQC and CQC
16. Appropriate MQA and CQA

Within the context of unifying a variety of geomembrane types, certain generalities have been made, but most of the elements above must be handled on a site-specific basis insofar as design and construction are considered.

As mentioned in Sections 5.11 and 5.12, the details and installation concerns cannot be denied. A complete conference [138] has been devoted to these concerns and the complementary nature of the included papers to the design of geomembranes should be apparent.

REFERENCES

1. Dove, J. E., and Frost, J. J., "A Method for Measuring Geomembrane Surface Roughness," *Geosynthetics Int.*, IFAI, vol. 3, no. 3, 1996, pp. 369–392.

2. Vallejo, L. E., and Zhou, Y., "Fractal Approach to Measuring Roughness on Geomembranes," *Journal of Geotechnical and Geoenvironmental Engineering*, ASCE, vol. 121, no. 5, pp. 442–447.

3. Haxo, H. E., Jr., Miedema, J. A., and Nelson, N. A., "Permeability of Polymeric Membrane Lining Materials," *Proceedings of the International Conference on Geomembranes*, IFAI, 1984, pp. 151–156.

4. Matrecon, Inc., *Lining of Waste Containment and Other Impoundment Facilities*, U.S. EPA/600/2-88/052, Cincinnati, OH, 1988.

5. Rowe, R. K., Hrapovic, L. and Armstrong, M. D., "Diffusion of Organic Pollutants through HDPE Geomembranes and Composite Liners and Its Influence on Groundwater Quality," *Proceedings Geosynthetics: Applications, Design and Construction*. Rotterdam: A. A. Balkema, 1996, pp. 737–742.

6. Sangam, H. P., Rowe, R. K., Cadwallader, M. W., and Kastelic, J. R., "Effects of HDPE Geomembrane Fluorination on the Diffusive Migration of MSW Organic Contaminants," *Proceedings Geosynthetics Conference*, IFAI, 2001, pp. 163–176.

7. Steffen, H., "Report on Two Dimensional Strain-Stress Behavior of Geomembranes With and Without Friction," *Proceedings of the International Conference on Geomembranes*: IFAI, 1982, pp. 181–185.

8. Koerner, R. M., Koerner, G. R., and Hwu, B.-L., "Three Dimensional, Axi-Symmetric Geomembrane Tension Test," *Proceedings Geosynthetic Testing for Waste Containment Applications*, STP 1081, edited by R. M. Koerner. ASTM, 1990, pp. 170–184.

9. Merry, S. M., and Bray, J. D., "Time-Dependent Mechanical Reponse of HDPE Geomembranes," *Journal of Geotechnical and Geoenvironmental Engineering*, ASCE, vol. 123, no. 1, 1957, pp. 57–68.

10. Nobert, J., "The Use of Multi-Axial Burst Test to Assess Field Performance of Geomembranes," *Proceedings Geosynthetics '93*. IFAI, 1993, pp. 685–702.

11. Haxo, H. E., Jr., "Quality Assurance of Geomembranes Used as Linings for Hazardous Waste Containment," *Journal of Geotextiles and Geomembranes*. vol. 4, no. 5, Elsevier, 1986, pp. 225–247.

12. Rollin, A. L., and Fayoux, D., "Geomembrane Seaming Techniques," In *Geomembranes: Identification and Performance Testing*, RILEM Report 4, edited by A. Rollin and J.-M. Rigo. London: Chapman and Hall, 1991, pp. 59–79.

13. Peggs, I. D., "Assessment of HDPE Geomembrane Seam Specifications," *Proceedings Geosynthetics: Applications, Design and Construction*. Rotterdam: A. A. Balkema, 1996, pp. 693–695.

14. Koerner, R. M., Monteleone, M. J., Schmidt, J. R., and Roethe, A. T., "Puncture and Impact Resistance of Geosynthetics," *Proceedings of the 3rd International Conference on Geotextiles*, 1986, Austrian Society of Engineers, Vienna, pp. 677–682.

15. Hullings, D. E., and Koerner, R. M., "Puncture Resistance of Geomembranes Using a Truncated Cone Test," *Proceedings Geosynthetics '91*. St. Paul, MN: IFAI, 1991, pp. 273–286.

16. Narejo, D. B., Wilson-Fahmy, R., and Koerner, R. M., "Geomembrane Puncture Evaluation and Use of Geotextile Protection Layers," *Proceedings PennDOT/ASCE Conference Geotechnical Engineering*, Harrisburg, PA: Central Pennsylvania Section, ASCE, 1993, pp. 1–16.

17. Koerner, R. M., and Soong, T.-Y., "Analysis and Design of Veneer Cover Soils," *Proceedings of the 6th IGS Conference*, 1998, IFAI., pp. 1–26.

18. Martin, J. P., Koerner, R. M., and Whitty, J. E., "Experimental Friction Evaluation of Slippage Between Geomembranes, Geotextiles, and Soils," *Proceedings of the International Conference on Geomembranes*, IFAI, 1984, pp. 191–196.

19. Narejo, D. and Koerner G. R., "Generic Recommendations for Interface Shear Strength of Geosynthetics." GRI Report Number 30, Geosynthetic Research Institute, 2005.

20. Koerner, R. M., Martin, J. P., and Koerner, G. R., "Shear Strength Parameters Between Geomembranes and Cohesive Soils," *Journal of Geotextiles and Geomembranes*, vol. 4, no. 1, 1986, pp. 21–30.

21. Stark, T. D., and Poeppel, A. R., "Landfill Liner Interface Strengths from Torsional-Ring-Stress Tests," *Journal of Geotechnical Engineering*, ASCE, vol. 120, no. 3, pp. 597–617.

22. Koerner, R. M., "Selected Papers on the Design Decision of Using Peak Versus Residual Shear Strengths," Geosynthetic Research Institute Report Number 29, September 30, 2003.

23. Hsuan, Y. G., Koerner, R. M., and Lord, A. E., Jr., "Stress Crack Resistance of High Density Polyethylene Geomembranes," *Journal of Geotechnical and Geoenvironmental Engineering*, ASCE, vol. 119, no. 11, 1993, pp. 1840–1855.

24. Hsuan, Y. G., and Koerner, R. M., "The Single Point–Notched Constant Tension Load Test: A Quality Control Test for Asseessing Stress Crack Resistance," *Geosynthetics International*, vol. 2, no. 5, 1995, pp. 831–843.

25. Hsuan, Y. G., and Koerner, R. M., "Can Outdoor Degradation be Predicted by Laboratory Acceleration Weathering?" *GFR* Magazine, November 1993, pp. 12–16.

26. Kane, J. D., and Widmayer, D. A., "Considerations for the Long-Term Performance of Geosynthetics at Radioactive Waste Disposal Facilities." In *Durability and Aging of Geosynthetics*, edited by R. M. Koerner. London: Elsevier, 1989, pp. 13–27.

27. Steiniger, F., "The Effect of Burrower Attack on Dike Liners," *Wasser und Boden*. Berlin: Ernst and Son, 1968, pp. 16–24.

28. Vandervoort, J., *The Use of Extruded Polymers in the Containment of Hazardous Wastes*, The Woodlands, TX: Schlegel Lining Technology, Inc., 1972.

29. Tisinger, L. G., "Chemical Compatibility Testing: A Typical Program," *GFR* Magazine, vol. 7, no. 3, 1989, pp. 22–25.

30. A. D. Little, Inc., "Resistance of Flexible Membrane Liners to Chemicals and Wastes," U. S. EPA Report PB86-119955, Cincinnati, OH, 1985.

31. O'Toole, J. L., *Design Guide, Modern Plastics Encyclopedia*. New York: McGraw-Hill, 1985–1986, pp. 398–446.

32. Hsuan, Y. G., Sculli, M. L., Guan, Z. C., and Comer, A. I., "Effects of Freeze-Thaw Cycling on Geomembrane Sheets and Their Seams," *Proceedings Geosynthetics '97*. IFAI, 1997, pp. 201–216.

33. Hsuan, Y. G., Koerner, R. M., and Lord, A. E., Jr., "A Review of the Degradation of Geosynthetic Reinforcing Materials and Various Polymer Stabilization Methods." In *Geosynthetic Soil Reinforcement Testing Procedure, STP 1190*, edited by S. C. Jonathan Cheng. ASTM, 1993, pp. 228–244.

34. Wolters, M., "Prediction of Long-Term Strength of Plastic Pipe Systems," *Proceedings of the 10th Plastic Fuel Gas Pipe Symposium*, American Gas Association, 1987, pp. 164–174.

35. Koerner, R. M., Halse, Y-H., and Lord, A. E., Jr., "Long-Term Durability and Aging of Geomembranes," *Proceedings Waste Containment Systems*, GSP No. 26 edited by R. Bonaparte. ASCE, 1990, pp. 106–134.

36. Koch, R., et al., "Long Term Creep Resistance of Sheets of Polyethylene Geomembrane," Report TR-88-0054. Frankfurt, Germany: Hoechst A. G., 1987.

37. Hessel, J., and John, P., "Long-Term Strength of Welded Joints in Polyethylene Sealing Sheets," *Werkstofftechnik*, vol. 18, 1987, pp. 228–231.

38. Gaube, E., Diedrick, G., and Muller, W., "Pipes of Thermoplastics; Experience of 20 Years of Pipe Testing, *Kunstoffe*, vol. 66, 1976, pp. 2–8.

39. Koerner, R. M., Lord, A. E., Jr., and Hsuan, Y. H., "Arrhenius Modeling to Predict Geosynthetic Degradation," *Journal of Geotextiles and Geomembranes*, vol. 11, no. 2, 1992, pp. 151–183.

40. Mitchell, D. H., and Spanner, G. E., "*Field Performance Assessment of Synthetic Liners for Uranium Tailings Ponds*," Status Report, Battelle PNL, U.S. NRC, NUREG/CR-4023, PNL-5005, 1985.

41. Hsuan, Y. G., and Koerner, R. M., "Antioxidant Depletion Lifetime for HDPE Geomembranes," *Journal of Geotechnical and Geoenvironmental Engineering*, vol. 124, no. 6, June 1998, pp. 532–541.

42. Martin, J. R., and Gardner, R. J., "Use of Plastics in Corrosion Resistance Instrumentation," paper presented at 1983 Plastic Seminar, NACE, October 24–27, 1983.

43. Underwriters Laboratory Standards, UL746B, "Polymeric Materials — Long-Term Property Evaluation," UL Laboratories, Inc., 1987.

44. Viebke, J., Ifwarson, M., and Gedde, U. W., "Degradation of Unstabilized Medium-Density Polyethylene Pipes in Hot-Water Applications," *Polymer Engineering and Science*, vol. 34, no. 17, 1994, pp. 1354–1361.

45. Daniel, D. E., and Koerner, R. M., "MQC/MQA and CQC/CQA of Waste Containment Liner and Cover Systems," U.S. EPA/600/R-93/182, Technical Resource Document, 2nd ed. ASCE: 2005.

46. Koerner, R. M., Bove, J. A., and Martin, J. P., "Water and Air Transmissivity of Geotextiles," *Journal of Geotextiles and Geomembranes*, vol. 1, no. 1, 1984, pp. 57–73.

47. Taylor, D. W., *Fundamentals of Soil Mechanics*. New York: Wiley, 1948.

48. Holtz, R. D., and Kovacs, W. D., *An Introduction to Geotechnical Engineering*. Englewood Cliffs NJ: Prentice Hall, 1981.

49. Cooley, K. R., "Evaporation Reduction: Summary of Long-Term Tank Studies," *Journal of Irrigation Drainage Division,* ASCE, vol. 109, no. 1, 1983, pp. 89–98.

50. Dedrick, A. R., "Foam-Rubber Covers for Evaporation Control," *Proceedings of the International Conference on Geomembranes*, IFAI, 1984, pp. 89–91.

51. Gerber, D. H., "Floating Reservoir Cover Designs," *Proceedings of the International Conference on Geomembranes*, IFAI, 1984, pp. 79–84.

52. Frobel, R. K. "Animal Waste Containment and Anaerobic Digestors," *Proceedings of the 17th GRI Conference*. GII Publication, pp. 94–111.

53. Chow, V. T., *Open Channel Hydraulics*. New York: McGraw-Hill, 1959.

54. Fortier, S., and Scobey, F. C., "Permissible Canal Velocities," *Transaction ASCE*, vol. 89, 1926, pp. 940–956.

55. Morrison, W. R., and Starbuck, J. G., *Performance of Plastic Canal Linings*, Bureau of Reclamation, REC-ERC-84-1, 1984.

56. Hammer, H., Ainsworth, J. B., and Beckham, R., "Case Study of an In-Situ, Uninterrupted Flow Repair of a Concrete Sluce Channel," *Proceedings of the International Conference on Geomembranes*. IFAI, 1984, pp. 343–345.

57. Koerner, R. M., and Lawrence, C. A., *Transmissivity of Geotextiles After Placement of Fresh Concrete*, Internal Report to U. S. Bureau of Reclamation: 1988.

58. Comer, A. I., Kube, M., and Sayer, M., "Remediation of Existing Canal Linings," *Journal of Geotextiles and Geomembranes*, vol. 14, nos. 5–6, 1996, pp. 313–326.

59. Swihart, J. J., and Haynes, J., "Canal Lining Demonstration Project: Ten Year Final Report," U. S. Bureau of Reclamation R-02-03, November 2002.

60. U. S. Environmental Protection Agency as reported in *MSW Magazine*, April 2002.

61. Mackey, R. E., "Is Thailand Ready for Lined Landfills?" *GFR Magazine*, vol. 14, no. 7, 1996, pp. 20–25.

62. Chian, E. S. K., and deWalle, F. B., "Sanitary Landfill Leachates and Their Treatment," *Journal of Environmental Engineering Division, ASCE*, vol. 102, no. EE2, 1976, pp. 411–431.

63. Dudzik, B. E., and Tisinger, L. G., "An Evaluation of Chemical Compatibiilty Test Results of HDPE Geomembrane Exposed to Industrial Waste Leachate." *Proceedings of Geosynthetic Testing for Waste Containment Applications, ASTM STP 1081*, edited by R. M. Koerner. Philadelphia, PA: ASTM, 1990, pp. 37–56.

64. Kays, W. B., *Construction of Linings for Reservoirs, Tanks, and Pollution Control Facilities*, 2nd ed. New York: Wiley, 1986.

65. Anderson, D. C., Brown, K. W., and Green, J., "Organic Leachate Effects on the Permeabilities of Clay Liners," *Proceedings of the Management of Uncontrolled Hazardous Waste Substances*. HMCRI, 1981, pp. 223–229.

66. Corbet, S., and Peters, M., "Workshop Report on 'USA-Germany Landfill Liner Practices,' " *Journal of Geotextiles and Geomembranes*, vol. 14, no. 12, 1996, pp. 647–726.

67. Koerner, J. R., and Koerner, R. M., *A Survey of Solid Waste Landfill Liner and Cover Regulations: Part II — Worldwide Status*, Geosynthetic Research Institute Report Number 23, 1999.

68. Tchobanoglous, G., Theisen, H. and Eliassen, R., *Solid Wastes*. New York: McGraw-Hill, 1997.

69. Othman, M. A., Bonaparte, R., and Gross, B. A., "Preliminary Results of Study of Composite Liner Field Performance," *Proceedings of the GRI-10 Conference*, GII Publications, 1997, pp. 115–142.

70. Bonaparte, R., Daniel, D. E., and Koerner, R. M., *Assessment and Recommendations for Improving the Performance of Waste Containment Systems*, U. S. Environmental Protection Agency, EPA/600/R-02/099, December 2002.

71. Buranek, D., and J. Pacey, "Geomembrane-Soil Composite Lining Systems Design, Construction, Problems and Solutions," *Proceedings of Geosynthetics '87*, vol. 2. IFAI, 1987, pp. 375–384.

72. Giroud, J. P., and Bonaparte, R., "Leakage Through Liners Constructed with Geomembranes. Part II Composite Liners," *Journal of Geotextiles and Geomembranes*, vol. 8, no. 2, 1989, pp. 71–112.

73. Eith, A. E., and Koerner, R. M., "Field Evaluation of Geonet Flow Rate (Transmissivity) Under Increasing Load," *Journal of Geotextiles and Geomembranes*, vol. 11, nos. 4–6, 1992, pp. 489–502.

74. Richardson, G. N., and Koerner, R. M., *Geosynthetic Design Guidance for Hazardous Waste Landfill Cells and Surface Impoundments*, Final Report U. S. EPA Contract No. 68-03-3338. Geosynthetic Research Institute, 1987.

75. Koerner, R. M., and Mukhopadhyay, C., *The Behavior of Negative Skin Friction on Model Piles in Medium Plasticity Silt*, Highway Research Record No. 405, 1972, pp. 34–44.

76. Wilson-Fahmy, R. F., Narejo, D., and Koerner, R. M., "Puncture Protection of Geomembranes. Part I: Theory," *Geosynthetics International*, vol. 3, no. 5, 1996, pp. 605–628.

77. Narejo, D., Koerner, R. M., and Wilson-Fahmy, R. F., "Puncture Protection of Geomembranes. Part II: Experimental," *Geosynthetics International*, vol. 3, no. 5, 1996, pp. 629–653.

78. Koerner, R. M., Wilson-Fahmy, R. F., and Narejo, D., "Puncture Protection of Geomembranes. Part III: Examples," *Geosynthetics International*, vol. 3, no. 5, 1996, pp. 655–676.

79. Koerner, R. M., and Wayne, M. H., "Geomembrane Anchorage Behavior Using a Large Scale Pullout Device," In *Geomembranes, Identification and Performance Testing*, edited by A. Rollin and J.-M Rigo, RILEM. Chapman and Hall, 1991, pp. 204–218.

80. Wilson-Fahmy, R. F., and Koerner, R. M., "Finite Element Analysis of Stability of Cover Soil on Geomembrane Lined Slopes," *Proceedings Geosynthetics '93*. IFAI, 1993, pp. 1425–1438.

81. Byrne, R. J., Kendall, J., and Brown, S., "Cause and Mechanism of Failure of Kettleman Hills Landfill," *ASCE Conference on Stability and Performance of Slopes and Embankments II*, ASCE, 1992, pp. 1–23.

82. Daniel, D. E., Koerner, R. M., Bonaparte, R., Landreth, R. E., Carson, D. A. and Scranton, H. B., "Slope Stability of Geosynthetic Clay Liner Test Plots," *Journal of Geotechnical and Geoenvironmental Engineering*, vol. 124, no. 7, 1998, pp. 628–637.

83. Singh, S., and Murphy, B., "Evaluation of the Stability of Sanitary Landfills," *Geotechnics of Waste Fills—Theory and Practice, ASTM STP 1070*, edited by Arvid Landva and G. David Knowles. ASTM, 1990, pp. 240–258.

84. Kavazanjian, E., "Evaluation of MSW Properties Using Field Measurements," *Proceedings of GRI-17 Conference on Hot Topics in Geosynthetics—IV*. GII Publications, 2003, pp. 52–93.

85. Koerner, R. M., and Soong, T.-Y., "Stability Assessment of Ten Large Landfill Failures," *Proceedings of GeoDenver 2000*, GSP No. 103, ASCE, 2000, pp. 1–38.

86. Qian, X., Koerner, R. M., and Gray, D. H., *Geotechnical Aspects of Landfill Design and Construction*, Upper Saddle River, NJ: Prentice Hall 2002.

87. Leach, J. A., Harper, T. G., and Tape, R. T., "Current Practice in the Use of Geosynthetics in the Heap Leach Industry," *Proceedings of Geosynthetics '87*. IFAI, 1987, pp. 365–374.

88. Smith, M. E., and Welkner, P. M., "Liner Systems in Chilean Cooper and Gold Heap Leaching," *Proceedings of the 5th IGS Conference*. Southeast Asia Chapter, 1994, pp. 1063–1068.

89. Thiel, R., and Smith, M. E., "State-of-the-Practice Review of Heap Leach Pad Design Issues," *Proceedings of GRI-17 Conference on Hot Topics in Geosynthetics—IV*, GII Publications, 2003, pp. 119–135.

90. Attaway, D. C., "New Applications for Geomembranes: Lining Solar Ponds," *Proceedings of the International Conference on Geomembranes*. IFAI, 1984, pp. 55–59.

91. Koerner, R. M., and Richardson, G. N., "Design of Geosynthetic Systems for Waste Disposal," *Proceedings of the Conference on Geotechnical Practice for Waste Disposal '87*. ASCE, 1987, pp. 65–86.

92. Spikula, D. R., "Subsidence Performance of Landfills," *Proceedings of the GRI-10 Conference*, GII Publications: 1997, pp. 237–244.

93. Murphy, W. L and Gilbert, P. A., "Estimation of Maximum Cover Subsidence Expected in Hazardous Waste Landfills," *EPA Proceedings on Land Disposal of Hazardous Waste*, EPA 600/9-84-007, 1984, pp. 222–229.

94. Sterling, H. J., and Ronayne, M. C., "Simulating Landfill Cover Subsidence," *Proceedings of the 11th Symposium on Land Disposal of Hazardous Waste*, U.S. EPA 600/9-85/013, 1985, pp. 236–244.

95. Koerner, R. M., and Daniel, D. E., *Final Covers for Engineered Landfills and Abandoned Dumps*, ASCE: 1997.

96. U.S. Environmental Protection Agency, *Covers for Uncontrolled Hazardous Waste Sites*, EPA-540/2-85-002, Cincinnati, OH, 1986.

97. U.S. Environmental Protection Agency, *Design and Construction of Covers for Solid Waste Landfills*, EPA-600/2-79-165. Cincinnati, OH: U.S. EPA, 1979.

98. Baron, J. L., et al., *Landfill Methane Utilization Technology Workbook*, U. S. DOE, CPE-810, Contract 31-109-38-5686, Argonne National Laboratory, 1981.

99. Daniel, D. E., and Koerner, R. M., *Final Cover Systems*, in *Geotechnical Aspects of Waste Disposal*, edited by D. E. Daniel. London: Chapman and Hall, 1992, pp. 455–496.

100. Schroeder, P. R., Dizier, T. S., Zappi, P. A., McEnroe, B. M., Sjostrom, J. W., and Peyton, R. L., "The Hydrologic Evaluation of Landfill Performance (HELP) Model: Engineering Documentation for Version 3," EPA/600/R-94/168b. Cincinnati, OH: U.S. EPA, Risk Reduction Engineering Laboratory, 1996.

101. Mackey, R. E., "Three End Uses for Closed Landfills and Their Impacts to the Geosynthetic Design," *Journal of Geotextiles and Geomembranes*, vol. 14, nos. 7–8, 1996, pp. 409–424.

102. Phaneuf, R. J., "Landfill End Uses in New York State," *Proceedings of the GRI-16 Conference on Hot Topics in Geosynthetics—III*. GII Publications: 2002, pp. 112–135.

103. Martin, W. L., and Tedder, R. B., "Use of Old Landfills in Florida, *Proceedings of the GRI-16 Conference on Hot Topics in Geosynthetics—III*, GII Publications, 2002, pp. 136–148.

104. Koerner, R. M., Gray, D. H., and Qian, X., "Post-Closure Beneficial Uses of Landfills," *Proceedings of the GRI-16 Conference on Hot Topics in Geosynthetics—III*, GII Publications, 2002, pp. 94–111.

105. Pinyan, C., "Sky Mound to Rise from Dump," *ENR*, June 11, 1987, pp. 28–29.

106. Pohland, F. G., "Landfill Bioreactors: Historical Perspective, Fundamental Principles, and New Horizons in Design and Operations," *Proceedings on Landfill Bioreactor Design and Operations*, EPA/600/R-95/146, September 1995, pp. 9–24.

107. Reinhart, D. R., and Townsend, T. G., *Landfill Bioreactor Design and Operation*. Boca Raton, FL: Lewis Publishers, 1998.

108. Carson, D. A., "The Municipal Solid Waste Landfill Operated as a Bioreactor," *Proceedings on Landfill Bioreactor Design and Operation*, EPA/600/R-95/146, September 1995, pp. 1–8.

109. Koerner, G. R., and Koerner, R. M., "Long-Term Temperature Monitoring of Geomembranes at Dry and Wet Landfills," *Journal of Geotextiles and Geomembranes*, vol. 23, no. 2, 2005.

110. Koerner, R. M., "Leachate Recycling Leading to Bioreactor Landfills for the Rapid Degradation of Municipal Solid Waste," *Proceedings of Great Lakes Region Solid Waste Conference*, Engineering Society of Detroit, March 15, 2000.

111. Koerner, G. R., Koerner, R. M., and Martin, J. P., "Geotextile Filters Used for Leachate Collection Systems: Testing, Design, and Field Behavior," *Journal of Geotechnical Engineering Division*, ASCE, vol. 120, no. 10, 1994, pp. 1792–1803.

112. Pohland, F., and Graven, J. P., "The Use of Alternative Materials for Daily Cover at Municipal Solid Waste Landfills," EPA/600/R-93/172, Washington, DC: U.S. Environmental Protection Agency, 1993.

113. Gleason, M. H., Houlihan, M. F., and Palutis, J. R., "Exposed Geomembrane Cover Systems: Technology Summary," *Proceedings of the Geosynthetics Conference*. IFAI, 2001, pp. 905–918.

114. Hullings, D. E., and Swyka, M. A., "Geosynthetics in Bioreactor Designs," *Proceedings of the GRI-13 Conference on Geosynthetics in the Future.* GII Publications, 1999, pp. 254–262.

115. Dixon, N., and Jones, R., "Engineering Properties of Municipal Solid Waste," *Proceedings of the GRI-17 Conference on Hot Topics in Geosynthetics—IV.* GII Publications, 2003, pp. 21–51.

116. ———, *Geomembrane Sealing Systems for Dams: Design Principles and Return of Experience,* International Committee on Large Dams, Paris, France, 2005.

117. Eigenbrod, K. D., Irwin, W. W., and Roggensack, W. D., "Upstream Geomembrane Liner for a Dam on a Compressible Foundation," *Proceedings of the International Conference in Geomembranes.* IFAI, 1984, pp. 99–103.

118. Sembenelli, P., and Rodriguez, E. A., "Geomembranes for Earth and Earth-Rock Dams: State-of-the-Art Report," *Proceedings on Geosynthetics: Applications, Design, and Construction,* edited by M. B. de Groot, G. den Hoedt, and R. J. Termaat. A. A. Balkema, 1996, pp. 877–888.

119. Monari, F., "Waterproofing Covering for the Upstream of the Lago Nera Dam," *Proceedings of the International Conference on Geomembranes.* IFAI, 1984, pp. 105–110.

120. Cazzuffi, D., "The Use of Geomembranes in Italian Dams," *International Journal of Water Power and Dam Construction,* vol. 26, no. 2, 1987, pp. 44–52.

121. Scuero, A. M., and Vaschetti, G. L., "Geomembranes for Masonry and Concrete Dams: State-of-the-Art Report," *Proceedings on Geosynthetics: Applications, Design, and Construction,* edited by M. B. de Groot, G. den Hoedt, and R. J. Termaat. A. A. Balkema, 1996, pp. 889–898.

122. Koerner, R. M., and Hsuan, Y. G., "Lifetime Prediction of Polymeric Geomembranes Used in New Dam Construction and Dam Rehabilitation," *Proceedings of the Association of State Dam Safety Officials,* June 4–6, 2003.

123. Scuero, A., and Vaschetti, G. L., "Exposed Waterstops for Joints and Cracks in RCC Dams," *Proceedings of the International Workshop on Roller Compacted Concrete Dam Construction in the Middle East,* Jordan, April 7–10, 2002.

124. Koerner, R. M., and Welsh, J. P., *Construction and Geotechnical Engineering Using Synthetic Fabrics,* New York: Wiley, 1980.

125. Frobel, R. K., "Geosynthetics in the NATM Tunnel Design," *Proceedings on Geosynthetics for Soil Improvement,* GSP Number 18, ASCE, 1988, pp. 51–67.

126. Koerner, R. M., and Guglielmetti, J., "Vertical Bariers: Geomembranes." In *Assessment of Barrier Technologies,* edited by R. R. Rumer and J. K. Mitchell. Washington DC, NTIS, PB96-180583, 1995, pp. 95–118.

127. U. S. Environmental Protection Agency, *Proceedings Workshop on Geomembrane Seaming, Data Acquisition, and Control,* EPA/600/R-93/112, 1993.

128. Richardson, G. N., *Construction Quality Management for Remedial Action and Remedial Design of Waste Containment Systems,* Technical Guidance Document, EPA/540/R-92/073, EPA, Cincinnati, OH: U. S. EPA, 1992.

129. Schultz, D. W., Duff, B. M., and Peters, W. R., "Performance of an Electrical Resistivity Technique for Detecting and Locating Geomembrane Failures," *Proceedings of the International Conference on Geomembranes.* IFAI, 1984, pp. 445–449.

130. Laine, D. L., and Darilek, G. T., "Locating Leaks in Geomembrane Liners Covered with a Protection Soil," *Proceedings of the Geosynthetics '93 Conference.* IFAI, 1993, pp. 1403–1412.

131. Darilek, G. T., and Miller, L. V., "Comparison of Dye Testing and Electrical Leak Location Testing of a Solid Waste Liner System," *Proceedings of the 6th International Conference on Geosynthetics.* IFAI, 1998, pp. 273–276.

132. Koerner, R. M., "Do We Need Monitoring Wells at Double-Lined Landfills?" *Civil Engineering,* February 2001, p. 96.

133. Koerner, R. M., Lord, A. E., Jr., and Luciani, V. A., "A Detection and Monitoring Technique for Location of Geomembrane Leaks," *Proceedings of the International Conference on Geomembranes.* IFAI, 1984, pp. 379–384.

134. Waller, M. J., and Singh, R., "Leak Detection Techniques and Repairability for Lined Waste Impoundment Sites," *Proceedings on Management of Unconfined Hazardous Waste Sites,* Hazardous Materials Central Research Institute, pp. 147–153.

135. Rödel, A., "Geologger—A New Type of Monitoring System for the Total Area of Geomembranes on Landfill Sites," *Proceedings on Geosynthetics: Applications, Design, and Construction*, edited by M. B. de Groot, G. den Hoedt, and R. J. Termaat. A. A. Balkema, 1996, pp. 625–626.

136. Wayne, M. H., and Koerner, R. M., "Effect of Wind Uplift on Liner Systems," *GFR Magazine* vol. 6, no. 4, 1988, pp. 26–29.

137. Giroud, J. P., Badu-Tweneboah, K., and Bonaparte, R., "Rate of Leakage Through a Composite Liner due to Geomembrane Defects," *Journal of Geotextiles and Geomembranes*, vol. 11, no. 1, 1992, pp. 1–28.

138. Koerner, R. M., ed., *Proceedings of the 6th GRI Seminar MQC/MQA and CQC/CQA of Geosynthetics*. IFAI, 1993.

PROBLEMS

5.1. What is the difference between thermoplastic and thermoset geomembranes? Why are thermoset geomembranes less used (and only have one product listed in Table 5.1)?

5.2. Describe the differences between noncrystalline and semicrystalline thermoplastic geomembranes with regard to their anticipated behavior. Draw a sketch of each type, showing proper mixtures within noncrystalline formulations like PVC and CSPE and the tie molecules bonding together crystalline regions in semicrystalline geomembranes like HDPE.

5.3. Describe the differences between geomembranes made from thermoplastic materials and polymer-impregnated geotextiles, as discussed in Section 2.6.2.

5.4. Regarding ASTM geomembrane test methods and standards:
   (a) In what committees would you expect to find relevant test methods for the materials from which geomembranes are made?
   (b) Why are there fewer existing standards under a geomembrane category?
   (c) What is the status of ISO-geomembrane standards?

5.5. Regarding common scrims used in reinforced geomembranes, such as CSPE-R, fPP-R, EPDM-R and EIA-R listed in Table 5.1:
   (a) Briefly describe how scrim-reinforced geomembranes are manufactured.
   (b) What do 20×20, 10×10, and 6×6 designations for the scrim mean?
   (c) Why are scrims less than 6×6 not available?
   (d) Why are scrims greater than 20×20 not available?
   (e) What kind of polymers are the scrim yarns generally made from?
   (f) Why is it a woven fabric rather than a nonwoven one?
   (g) What advantages and disadvantages do reinforced geomembranes have over those that are nonreinforced?

5.6. Describe the difference in behavior between a scrim-reinforced geomembrane and a spread-coated geomembrane if the scrim is a 10×10 polyester yarn and the spread-coated substrate is a 300 g/m^2 nonwoven needle-punched continuous-filament polyester fabric.

5.7. If an HDPE formulation is 97% resin at a density of 0.936 g/cc, 2.5% carbon black at a density of 1.85 g/cc, and 0.5% antioxidant at a density of 2.05 g/cc, what is its overall density?

5.8. Calculate the WVT, permeance, and permeability of a 1.5 mm HDPE geomembrane that showed a weight loss of 0.0045 g in 14 days at a relative humidity difference of 70% at a constant temperature of 20°C. The area of the test specimen is 0.0032 m^2.

5.9. For the 25 mm wide tensile test results shown in the graphs below, complete the table below.

fPP and fPP-R	0.75 mm	0.90 mm (6 × 6)	0.90 mm (10 × 10)
Strength at break (kN/m^2)			
Strain at break (%)			
Strength at failure (kN/m^2)			
Strain at failure (%)			
Modulus (kN/m^2)			

CSPE and CSPE-R	0.50 mm	0.75 mm	0.90 mm (10 × 10)
Strength at break (kN/m^2)			
Strain at break (%)			
Strength at failure (kN/m^2)			
Strain at failure (%)			
Modulus (kN/m^2)			
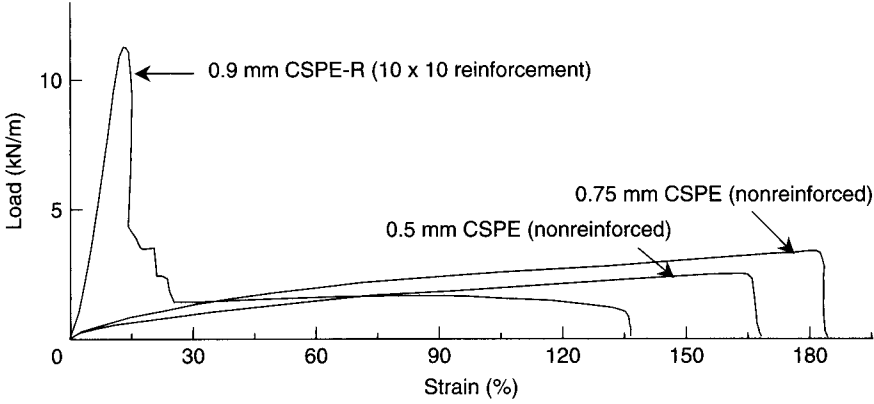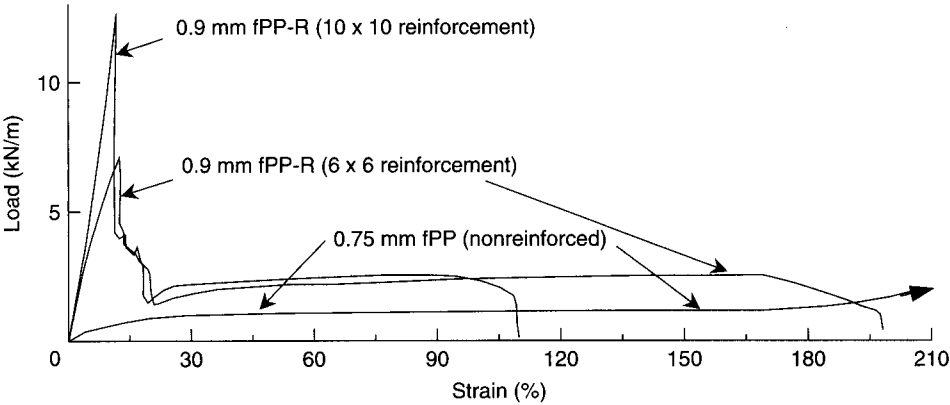
5.10. When could tensile test results from dumbbell-shaped specimens be used for design-simulation purposes? What is the basic purpose of such tests?

5.11. What type of tensile test would you use for the following design situations? Explain your answers.

    (a) A geomembrane coming up out of an excavation and over a berm into an anchor trench

    (b) Localized subsidence of a geomembrane beneath a reservoir due to gradual decay of organic subgrade material

    (c) Differential settlement of a geomembrane in the final cover (closure) of a municipal solid waste landfill

5.12. What proportion of full sheet strength is the shear and peel seam test data of Figure 5.6? Give answers for both PVC and HDPE, and comment on the adequacy of these seam strengths.

5.13. Plot the impact resistance of the five geomembranes listed in Table 5.6 against the point geometry angle listed. Comment on the various types of response curves that result.

5.14. Regarding interface friction tests:

    (a) Given the data shown below from direct shear tests of a CSPE-R geomembrane on Ottawa sand, calculate the resulting peak friction angle and its efficiency based on the friction angle of the sand as shown in Table 5.7.

Normal stress (kN/m^2)	35	70	105	140
Shear strength (kN/m^2)	12.5	25.0	40.7	53.0

    (b) For a LLDPE geomembrane on mica schist soil, the data shown below result. Calculate its peak friction angle and its efficiency based on the soil's friction angle of $26°$.

Normal stress (kN/m^2)	35	70	105	140
Shear strength (kN/m^2)	15.1	31.7	47.5	63.2

5.15. The stress and displacement direct shear curves in Figure 5.9b indicate that the residual strength is less than the peak strength. List the types of geomembranes where this is likely to occur.

5.16. Regarding stress cracking of geomembranes:

    (a) Stress cracking of geomembranes is usually considered to be possible in semicrystalline geomembranes such as HDPE. What are the conditions that can bring about this phenomenon?

    (b) Where are the most likely locations for stress cracking in field-deployed HDPE geomembranes?

    (c) Can stress cracking occur in other geomembranes? If so, describe the phenomenon for LLDPE, PVC, fPP, and CSPE-R.

5.17. The currently recommended acceptance level for HDPE geomembranes with respect to stress cracking via the NCTL test is a minimum transition time of 150 hours (recall

Figure 5.11b). How was this determined? How could this value change in the future? In which direction would it change?

5.18. The current recommendation of the SP-NCTL test presented in Section 5.1.3 is 300 hours. As a quality control test, this is too long. List ways and procedures by which the time might be shortened to a more practical value of 24 hours.

5.19. Think about what happens when there is ultraviolet degradation of geomembranes. (*Hint*: Recall Figure 2.27):
   (a) How does UV degrade the various polymers used to manufacture geomembranes?
   (b) How do manufacturers limit the phenomenon?
   (c) Rank the geomembranes listed in Table 5.1 according to their resistance to ultraviolet light degradation.

5.20. List a series of situations in which site-specific chemical immersion and subsequent testing as described in Section 5.1.4 are not necessary.

5.21. As a consultant or regulator, describe how you would select a leachate for chemical immersion tests like those described in Section 5.1.4 for a facility that is not built (i.e., it is in the proposal stage) for the following situations:
   (a) Hazardous waste landfill
   (b) Municipal solid waste (MSW) landfill
   (c) Surface impoundment of a chemical plant
   (d) Surface impoundment for sewage sludge

5.22. Given the chemical resistance immersion data of Figure 5.13, does this particular HDPE geomembrane qualify as being "resistant" in terms of O'Toole [31], Little [30], and Koerner, in Table 5.9?

5.23. What properties of a geomembrane would you require to be high when working in cold regions with liquid containment systems?

5.24. Immersing a geomembrane in water generally increases its weight (i.e., it swells via water absorption). In some cases, however, there is a weight loss. How can this occur?

5.25. Using average data from Table 5.10, calculate the change in length for 10, 20, 30, and 40°C variations of a 100 m long geomembrane roll if it were made from the following:
   (a) HDPE
   (b) LLDPE
   (c) Plasticized PVC

5.26. In the lifetime prediction technique discussed in Section 5.1.5, elevated temperatures are always involved. Explain why this is the case (that is, describe the concept of time-temperature superposition).

5.27. Consider the aging response curves in Figure 5.15a.
   (a) Describe how antioxidants function in generating Stage A of the curve.
   (b) Describe the mechanism involved in Stage B.
   (c) Describe the mechanism(s) involved in Stage C.

5.28. The discussion in Section 5.1.5 centered around HDPE geomembranes and pipe. What type of aging response would you expect from PVC geomembranes? Illustrate your answer with a set of curves similar to those in Figure 5.15a.

5.29. Using the data given in Table 5.12, plot the temperature versus lifetime behavior for the three stages of HDPE geomembrane lifetime, as well as the total predicted lifetime.

5.30. Regarding the minimum thickness of a geomembrane, three considerations are necessary: survivability, regulations, and estimated stresses.
  (a) From a survivability perspective, what is the minimum geomembrane thickness for the closure of a landfill? (See Table 5.13.)
  (b) A 1992 EPA clarification document on this topic calls for a minimum thickness of 0.50 mm. Please comment in light of your answer from a survivability perspective in part (a).

5.31. What liquid volume in liters will a liquid containment site hold that is 35 by 35 m at the ground surface, has $3(H)$-to-$1(V)$ side slopes, and is 3.5 m deep at its center?

5.32. A 60 million liter water reservoir is to be constructed on a site measuring 160 by 115 m. The reservoir is to have uniform side slopes but requires a minimum 10 m buffer zone around each side. Determine the required depth of the basin for the following:
  (a) 1-to-4 side slopes
  (b) 1-to-3 side slopes
  (c) 1-to-2 side slopes

5.33. Regarding a geotextile placed under a geomembrane as per Section 5.3.2:
  (a) What is the required air transmissivity of a geotextile underliner beneath a geomembrane in the case of a rising watertable of 1.2 m in a three-day period? The soil porosity is 0.32 and the covered site measures 15 by 45 m. The slope of the geotextile is 1.0%.
  (b) If the pond is filled with 7.5 m of water, what pressure is generated on the bottom of the liner?
  (c) If this pressure is a potential problem, what are some possible design alternatives?

5.34. Regarding composite geomembranes:
  (a) What would be the benefits and limitations of having a geotextile bonded directly to the geomembrane on its lower side?
  (b) Answer the question in part (a) for two geotextiles that are bonded to both the lower and upper surfaces of the geomembrane.

5.35. How thick should an unreinforced fPP geomembrane be if it subsides locally to a 45° angle under 5.0 m of water and is mobilized over a 50 mm length? The liner is not soil-covered and has a friction angle of 25° with the soil beneath it. The allowable strength is 7000 kN/m². Check your answer with the design chart in Figure 5.21.

5.36. Regarding the thickness design model presented in Section 5.3.4:
  (a) Which of the variables are experimentally obtained?
  (b) Which are design assumptions?
  (c) Which are dictated by the problem under consideration?

5.37. What is the factor of safety of a slope behind a geomembrane-lined pond when it is empty if the soil fails under undrained conditions? The slope is $2(H)$ to $1(V)$, 7.5 m deep, and will be of the toe failure type (i.e., $n = 1.0$). The soil's unconfined compression strength is $q_u = 35$ kN/m² (note $q_u = 2c$) and its unit weight is 18 kN/m³.

5.38. Repeat Problem 5.37 for side slopes of $3(H)$ on $1(V)$.

5.39. Using a factor of safety of 1.75, what is the maximum slope angle (and H on V values) for a 9.0 m high slope of 16.5 kN/m³ unit weight with cohesion of 10 kN/m² and a friction angle of 15°?

5.40. Recalculate the stability of the 300 mm uniform thickness cover soil in Example 5.11 (Section 5.3.5) for 600, 900, and 1200 mm thickness and plot the FS response curve.

5.41. Recalculate the stability of the 22° friction angle soil in Example 5.11 (Section 5.3.5) for soil-to-geomembrane friction angles of 10°, 14°, and 18°; compare to 22° (the example), and plot the FS response curve.

5.42. Recalculate the stability of the tapered thickness cover soil in Example 5.12 (Section 5.3.5) for ω values of 14, 15, 16 (the example), 17, and 18.4° and plot the FS response curve. (Does the 18.4° result check with the analysis given in Section 5.3.5 for uniformly thick cover soils?)

5.43. Regarding geomembranes in anchor trenches with runout only:
   (a) Recalculate Example 5.13 (Section 5.3.6) on runout length for various thicknesses of LLDPE geomembrane. Use 1.0 mm (example problem), 1.5, 2.0, and 2.5 mm values and plot the results.
   (b) Recalculate Example 5.13, assuming the geomembrane is fPP-R with an allowable stress of 30,000 kPa. Plot runout length versus thickness, where thickness varies between 1.0, 1.5, 2.0, and 2.5 mm.

5.44. Regarding geomembranes in anchor trenches with runout and vertical depth:
   (a) Recalculate Example 5.14 (Section 5.3.6) on runout length plus anchor trench depth for various thicknesses of HDPE geomembranes. Use 1.0, 1.5 (the example), 2.0, and 2.5 mm values and plot the results.
   (b) Recalculate Example 5.14, assuming the geomembrane is PVC with an allowable stress of 13,000 kPa. Plot runout length, and hold the anchor trench depth constant at 0.50 m; then reverse by holding runout length constant at 1.0 m and vary the anchor trench depth.

5.45. What would be the maximum stresses mobilized in a geomembrane covering a 10 m diameter wooden tank if the deformed radius conforms to a 25 m arc? The loading is 0.75 kN/m^2 and the thickness varies between 0.5, 1.0, 1.5, and 2.0 mm. Since some recent covers are made from foamed polyurethane up to 7.0 mm thick, include this value in your calculations and comment on such an approach.

5.46. When designing liquid containment systems, the term *freeboard* is used. What does this term mean?

5.47. In the design of floating covers for reservoirs, the location of floats and weights are critical.
   (a) How are floats made on a geomembrane?
   (b) How are weights made on a geomembrane?

5.48. Geomembranes that are used for floating covers must be exposed to the atmosphere indefinitely.
   (a) Which of the types of geomembranes listed in Table 5.1 are most suitable for long-term exposure?
   (b) How would you go about estimating the lifetime of such *exposed* geomembranes?
   (c) What mechanical and endurance properties should be emphasized in writing a specification for a floating cover?

5.49. For the large superbags shown in Figure 5.33, what type of lateral containment is necessary to prevent rupture of the enclosure?

5.50. Superbags are being used to transport liquids by being towed by barges in oceans and large lakes.
   (a) What liquids are likely to be transported?
   (b) What mechanical and endurance properties should be emphasized?

5.51. Covers over animal manure associated with large animal feedlot operations (AFO) are a growing segment of geomembrane use.
   (a) Describe the process involved.
   (b) What geomembrane property is very necessary?
   (c) What becomes of the residual degraded waste material?

5.52. Calculate the maximum tractive force on the bottom of a trapezoidal geomembrane-lined water canal of 1.5 m depth and 5.0 m width at a slope of 2%, and compare it with the allowable values given in Table 5.14.

5.53. Rank the low-cost canal liners mentioned in Section 5.5.3 when placed over highly fractured volcanic basalt rock foundation according to the following:
   (a) Their perceived seepage control (i.e., a benefit ranking)
   (b) A cost ranking on the basis of perceived cost for the various systems
   (c) The ranking of the subsequent benefit/cost ratio

5.54. Regarding the siting of a lined landfill (a *greenfield* site):
   (a) What are some of the major technical features to be considered?
   (b) What are some of the major nontechnical issues to be considered?

5.55. Describe the chemical interaction process by which organic solvents decrease the hydraulic conductivity (or coefficient of permeability) of clay soils.

5.56. When speaking of natural soil clay liners, the choices are either compacted clay liners or amended clay liners. Describe each of these types of soil liners.

5.57. The cost of an in-place natural soil liner can vary tremendously, while geomembranes (and geosynthetic clay liners) vary relatively little. Why is this the case and what are some of the major variables involved in natural clay soil liners?

5.58. Comment on the advantages and disadvantages of the composite geomembrane/natural clay secondary liner shown in Figure 5.40d and e.

5.59. Comment on the advantages and disadvantages of the composite geomembrane/natural clay primary liner shown in Figures 5.40f.

5.60. Comment on the advantages and disadvantages of the composite geomembrane/GCL primary liner shown in Figure 5.40g and h.

5.61. Regarding GM/CCL and GM/GCL composite liners:
   (a) For composite action to occur, do the geomembrane and clay have to be directly in contact?
   (b) Can a geotextile, for puncture resistance, be placed between them?
   (c) What is the effect of waves or wrinkles left in the geomembrane after backfilling?

5.62. For the outlet of a leachate collection and removal system beneath a landfill, a sump and collection well at its lowest elevation is necessary. Explain how the leachate is removed from each of these sumps (recall Figure 5.42) for the following:
   (a) The primary removal system
   (b) The leak-detection removal system

5.63. Prepare a specification for the gravel soil to be used around leachate collection and leak detection pipe systems, as shown in Figure 5.40a–g.

5.64. What are some technical equivalency issues that must be addressed to replace a gravel soil drain in either leachate collection or leak detection with the following:
   (a) Geonet, as in Figures 5.40e–h
   (b) Geocomposite, as in Figure 5.40h

5.65. Why is density control of subgrade soils beneath the lowest layer of a geosynthetic important when constructing a lined landfill facility? What density requirement should be specified?

5.66. Regarding geomembrane thickness:
   (a) What is the minimum thickness allowed by the U.S. EPA for a hazardous material geomembrane landfill liner?

(b) Why are geomembrane thicknesses for hazardous material landfill liners greater than the thicknesses required for other situations?

(c) Is geomembrane thickness the key issue in leak prevention in lined landfills?

5.67. What is the thickness required for a LLDPE liner containing a landfill of 13 kN/m^3 material 22 m deep under the following conditions: σ_{allow} = 8000 kN/m^2, β = 30°, x = 38 mm, δ_U = 20°, and δ_L = 35°?

5.68. Repeat Problem 5.67, using HDPE at σ_y = 16,000 kN/m^2.

5.69. Repeat Problem 5.67, using CSPE-R at σ_b = 30,000 kN/m^2.

5.70. The geomembrane puncture-protection design in Section 5.6.7 is based on 1.5 mm thick HDPE.

(a) How would the design vary for different thicknesses of HDPE?

(b) How would the design vary for the different types of geomembranes given in Table 5.1?

(c) How would the design vary for different types of geotextiles (i.e., other than nonwoven needle-punched geotextiles)?

5.71. Repeat Example 5.19 (Section 5.6.7) on geomembrane puncture protection for the following. Plot the response curve for each variation.

(a) Different FS values—that is FS = 1.0 to 10.0

(b) Different landfill heights—that is, 20 to 100 m

(c) Different protrusion heights—that is, 0.005 to 0.050 m

5.72. Repeat Example 5.20 (Section 5.6.10) for the multilined side slope stability using cumulative reduction factors 3.0 and 4.0, and plot the result against 2.0 (the example).

5.73. Calculate the required thickness of an access ramp, as shown in Figure 5.46b, based on trucks of 80 kN wheel loads at tire inflation pressures of 480 kPa. Assume that the liner beneath the ramp is a double-lined system with a biplanar leak detection geonet with a grade of 14° where the critical issues are the tensile strength of the 1.5 mm thick HDPE geomembranes and the roll-over compressive strength of the biplanar geonet. The critical shear interface is beneath the secondary geomembrane to the underlying CCL and its interface friction angle is 22°. [Hints: from Chapter 4 evaluate the crush strength of the geonet and from the unpaved road design of Chapter 2 calculate the stone thickness.]

5.74. Repeat Problem 5.73 assuming a dynamic impact factor of 3.0 times the static weight.

5.75. Describe and illustrate the concept of heap leach mining and the removal, treatment, and recirculation of the chemicals used in the process.

5.76. Describe and illustrate the concept of a solar pond together with the *salt gradient effect.*

5.77. List each of the geosynthetic materials shown in Figure 5.50 against its primary function in table below (either a *yes* or *no* is adequate).

Location	Type of Geosynthetic	Separation	Reinforcement	Filtration	Drainage	Barrier
Liner system						
Cover system						

5.78. Stabilization of liquid waste and quasi-solid waste materials is required before final capping and closure. What are the two basic functions of the stabilization process?

5.79. Incomplete in situ stabilization sometimes leaves unmixed zones in the area to be capped, which eventually results in *hydrofracturing*. What is meant by this term?

5.80. What are *bathtubs* with reference to stabilized landfill closures? What problems do they create?

5.81. Regarding the geotextile gas-transmission layer in a landfill closure:
  (a) Determine the required transmissivity of a nonwoven needle-punched geotextile beneath the barrier layer of a closure system as shown in Figure 5.50. The infiltration rate based on decomposition modeling is 0.1 m³/day and the grading of the system is 5%.
  (b) If the candidate geotextile has a measured transmissivity of 0.002 m³/min-m under a normal stress of 50 kPa, what is its resulting factor of safety?

5.82. Subsidence prediction of randomly placed municipal solid waste landfills represents a difficult challenge insofar as cap design is concerned.
  (a) For a deep municipal landfill consisting of domestic refuse, what steps would you take to quantify subsidence versus time?
  (b) What are the basic mechanisms?
  (c) How long do you suspect they will take to mobilize?

5.83. The thickness of a cover soil protection layer of a landfill closure discussed in Section 5.7.6 is generally required to be greater than the maximum depth of frost penetration. Is this same requirement justified for all barrier materials? Compare and contrast the situation for the following:
  (a) Compacted clay liners (CCLs)
  (b) Geosynthetic clay liners (GCLs)
  (c) Geomembranes (GMs)

5.84. List some possible uses for closed and properly capped landfill sites.

5.85. Section 5.8 introduced the concept of wet landfilling, also referred to as *bioreactor landfills*.
  (a) Why is the term *wet landfilling* preferred over bioreactor landfills?
  (b) What are the different methods of introducing liquids introduced into the landfill?
  (c) What is meant by the term *field capacity*?

5.86. What are the five primary stages of degradation of organics in a MSW landfill? (*Hint*: See references [106] and [107].)

5.87. When the organics in an MSW landfill have degraded, it is said to be *sustainable*. What are the characteristics of the landfill at that time?

5.88. Of the four liquids management strategies shown in Figure 5.55, what are the approximate times for the MSW to reach *sustainability*?

5.89. Corewalls in earth dams (whether of clay or a geomembrane) can be centrally located, located near the upstream side, or located near the downstream side. When using a geomembrane, where is the favored location and why?

5.90. List the durability issues of exposed geomembranes when placed on the upstream face of concrete and masonry dams, as described in Section 5.10.2.

5.91. How are durability issues of the geomembranes essentially avoided in roller-compacted concrete dams, as described in Section 5.10.3?

5.92. Geomembranes can be used as vertical cut-off walls in many situations, as described in Section 5.10.6. When placed in a slurry-filled trench, how are the seams made?

5.93. Thinner, more flexible geomembranes like PVC and CSPE-R are generally seamed into large panels in a fabrication facility; such seams are called *factory seams*. The subsequent joining of panels together at the job site is called *field seaming*. List some advantages of using factory seams rather than field seams for the same type of geomembrane.

5.94. Regarding factory seams and field seams:
   (a) What percentage of factory seams should be inspected via destructive tests? Via non-destructive tests?
   (b) What percentage of field seams should be inspected via destructive tests? Via nondestructive tests?

5.95. Why can't either thermal or solvent seam methods be used on thermoset elastomeric geomembranes like EPDM and EPDM-R?

5.96. The two fundamentally different seaming methods used to join thermoplastic geomembranes are either thermal or chemical methods (recall Table 5.23). List the advantages and disadvantages of each of these two seaming methods.

5.97. If thermal extrusion seaming methods are being used, the sheets to be joined require surface grinding.
   (a) Why is this required?
   (b) How deep should the grinding be?
   (c) What is the preferred grinding direction, or orientation, with respect to the direction of the seam?
   (d) What is the extent of the grinding with respect to the width of the extrudate?
   (e) How long before seaming should the surfaces be ground?

5.98. Describe the impacts of the following environmental situations on geomembrane seam quality:
   (a) Moisture
   (b) Soil particles
   (c) Extreme heat
   (d) Extreme cold

5.99. In thermal wedge welding of geomembrane seams, we often consider a two-dimensional window or even a three-dimensional bubble. Plot the seaming variables to describe both of these situations.

5.100. Regarding automated hot wedge welding devices:
   (a) What is meant by a *data acquisition welder*? What type of data would be acquired?
   (b) What is meant by a *process control welder*? How would an on-board computer help in this regard?

5.101. What is the fundamental problem with test strips made via solvent or adhesive seaming methods when it comes to taking and testing of destructive seam samples?

5.102. Using 4.5 m wide geomembranes from the site illustrated in Figure 5.66:
   (a) How many linear meters of field seams are required?
   (b) At one destructive test per 150 m, how many destructive tests are required?
   (c) For the CQC or CQA organization (which typically performs 5 shear and 5 peel tests for each sample), how many tests are required assuming that all samples pass and that no resampling is required?

5.103. The flowchart in Figure 5.69 presents the initial strategy of opening up the spacing of destructive tests from 1 in 150 m to 1 in 300 m if certified welder, taped edges, automatic welding devices or IR/US testing is performed. Describe these four possible actions.

5.104. The flowchart in Figure 5.69 notes that the statistical methods of attributes and control charts should be used to close, maintain, or open the destructive seam spacing as the project develops. What are these two methods?

5.105. Electrical leak location surveys (recall Figure 5.68) show great promise for controlling field acceptance of both seams and sheet.
   (a) What is the smallest size leak that can be typically located?
   (b) What type of leaks would we expect after the seamed geomembrane is backfilled?
   (c) After leaks are discovered, repaired and re-backfilled, what substantiation should the field inspector require?

5.106. What are the most commonly used nondestructive test for the following?
   (a) PVC geomembranes
   (b) Scrim-reinforced geomembranes
   (c) Extrusion-welded PE geomembranes
   (d) Hot wedge–welded PE geomembranes

5.107. If a second nondestructive test is required beyond your answer to Problem 5.106, what would be your choice for each geomembrane type?

5.108. Regarding leak location methods after waste is placed, which of those mentioned in Section 5.12.3 are field tested and functioning systems? Rate them as to advantages and disadvantages.

5.109. What are some test methods you would use to evaluate severely folded and/or creased geomembranes that are subjected to wind uplift and displacement? (Recall Section 5.12.4.)

5.110. Regarding quality control and quality assurance:
   (a) What technical skills are required to perform MQA?
   (b) What technical skills are required to perform CQA?
   (c) Can (or should) the MQA organization be the same as the CQA organization?

5.111. How early in the process of manufacturing geomembranes should the MQA organization become involved?

5.112. Regarding MQA/CQA:
   (a) Who contracts for (i.e., pays for) these services?
   (b) What is the QA plan or QA document all about?
   (c) When should a QA plan be developed?
   (d) What is the relationship between the QA organization and the site designer?
   (e) What is the relationship between the QA organization and the QC organization?
   (f) What is the relationship between QA organization and the regulatory permitting agency?
   (g) What do you estimate are costs of MQA/CQA as a percentage of the cost of the entire liner system?

5.113. Why is there no MQC/MQA involved with natural soil components in the flow chart in Figure 5.74?

5.114. List some advantages and disadvantages of requiring 1,000,000 m^2 of experience for a geosynthetic installer for minimum qualifications.

5.115. What is the necessity and/or value of having certified inspectors doing QC/QA work on geosynthetic systems?

5.116. In your opinion, is it necessary to accredit laboratories that do geosynthetic testing? Why?

5.117. List your ideas on the most common causes of failure in geomembrane systems.

5.118. What research and development areas do you feel are most important for the future development of geomembranes in civil engineering applications? Frame your comments into groupings related to the following:

(a) Transportation

(b) Environment

(c) Geotechnology

(d) Hydraulics

6

Geosynthetic Clay Liners

6.0   INTRODUCTION

Factory-fabricated clay products for use as a barrier to migrating liquids have been available to the building construction industry for many years. Such *waterproofing barriers* in the form of semirigid panels sandwiched between cardboard sheets have been used for over 30 years. What is new, and the focus of this chapter, are large *flexible* rolls of factory-fabricated clay barrier materials that can be used to great advantage in pollution control facilities as landfill liners, reservoirs liners, landfill covers, and containment

of underground storage tanks, not to mention the more traditional uses in geotechnical and transportation applications. A geosynthetic clay liner is defined as follows:

> *Geosynthetic clay liner (GCL):* A factory-manufactured hydraulic barrier consisting of a layer of bentonite or other very low permeability material supported by geotextiles and/or geomembranes, mechanically held together by needling, stitching, or chemical adhesives.

Section 1.7 describes the manufacturing of the currently available GCLs as well as the general application areas in which GCLs are currently used.

Note that GCLs were not known at the time that the first edition of this book was written (1986); they were only mentioned briefly in the second edition (1990), had a small chapter of their own in the third edition (1994), and had an expanded chapter devoted to their properties, equivalency (to other soil hydraulic barriers), design, and construction details in the fourth edition (1998). In the current edition, they have expanded into a plethora of new variations and styles. Figure 6.1 shows products available in North America. There are many additional products available elsewhere in the world.

The development and usage of geosynthetic clay liners is certainly a welcome addition to the field of geosynthetics. GCLs offer a bentonitic clay liner material in a factory-manufactured form and as such form a hydraulic barrier material somewhere between thick field-placed compacted clay liners (CCLs) and the polymeric geomembranes described in Chapter 5. There are currently two structurally different GCL types distinguished by the method of manufacturing the composite material: nonreinforced and internally reinforced. The two forms are based on the fact that hydrated bentonite is very low in its shear strength. Thus, nonreinforced GCLs are used on very flat surfaces and reinforced GCLs (by needle punching or stitch bonding) are used on relatively steep slopes. Each type has a number of subvariations.

Nonreinforced GCLs are either geotextile-related, geotextile/polymer-related, or geomembrane-related. The geotextile-related types have geotextiles on both surfaces and usually an adhesive mixed with the bentonite for bonding purposes, as shown in Figure 6.2a. The geotextile/polymer-related types are similar but have a polymer impregnated in the upper geotextile to decrease the permeability even lower than the bentonite itself. The geomembrane-related types have the bentonite adhesively bonded to a geomembrane (see Figure 6.2b). The geomembrane can be of any type, thickness, or texture.

More common than the above are *reinforced GCLs*. The usual method of reinforcement is by needle punching from a nonwoven geotextile through the bentonite and opposing geotextile, which thus creates a labyrinth of fibers throughout (see Figure 6.2c) Alternatively, we can stitch bond between two woven geotextiles through the sandwiched bentonite layer (see Figure 6.2d) Further variations of reinforced GCLs are geotextile-related, geotextile/polymer-related, and geotextile/film-related. The geotextile-related types have various geotextiles on both surfaces. The geotextile/polymer-related types have a polymer impregnated in the upper geotextile to lower the permeability beyond the bentonite itself. The geotextile/film-related types have a thin plastic film (≈ 0.10 mm thick) either above or beneath the upper geotextile. After needle punching, this film becomes part of the composite material and decreases the permeability lower than the bentonite itself.
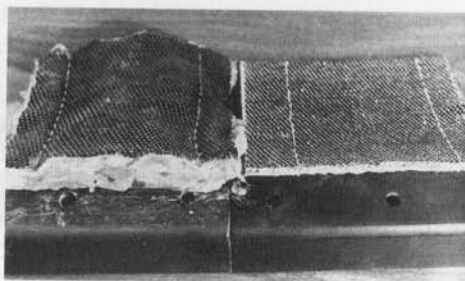
(a) Claymax from CETCO
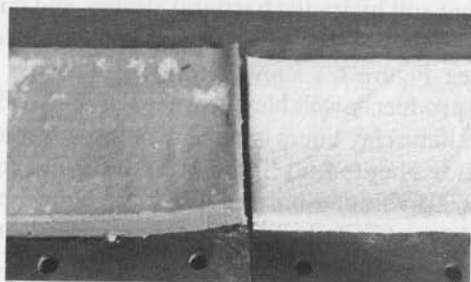
(b) Bentofix from BTI, Naue Fasertechnik, and Terrafix
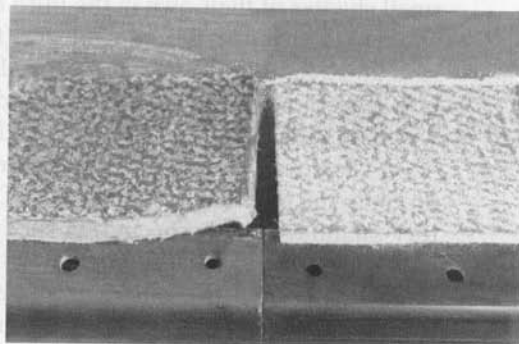
(c) Bentomat from CETCO
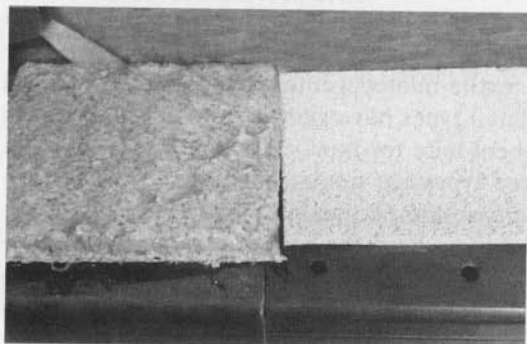
(d) Gundseal from GSE Lining Technology
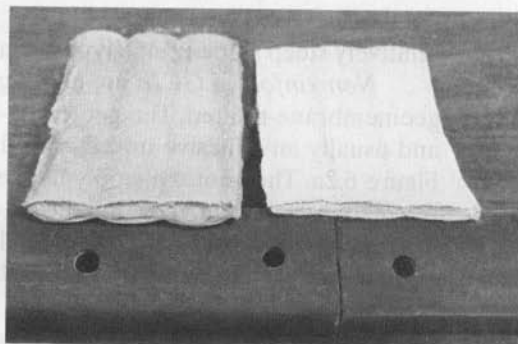
(e) NaBento from Huesker

Figure 6.1   A selection of commercially available GCLs with as-received product shown on right side and hydrated product on left side.

The newest type of GCL contains a *polymer-modified bentonite* that has lower permeability than the bentonite itself. The polymer can be adhered external to the bentonite particles, or internally bound within the microstructure of the bentonite lamella. This latter technique is truly nanotechnology within the GCL product industry. The usual carrier for the polymer-modified bentonite is within a needle-punched nonwoven geotextile where it can be subsequently needled to additional geotextiles. The lightweight
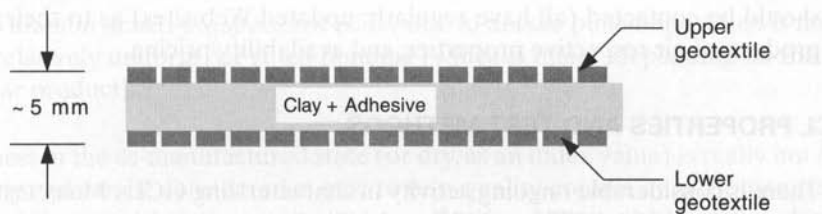
(a) Adhesive-bound clay between upper and lower geotextiles
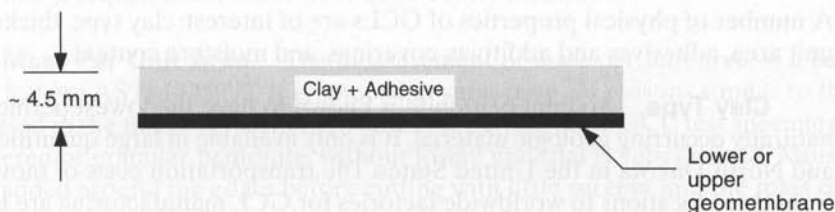
(b) Adhesive-bound clay above or below a geomembrane
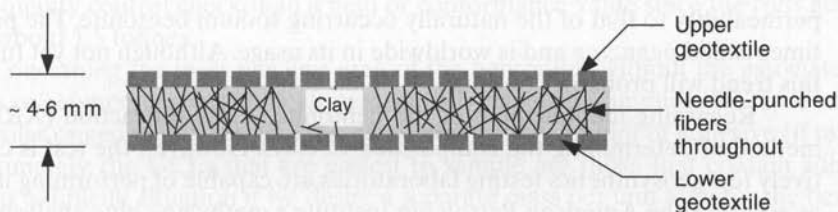
(c) Needle-punched clay through upper and lower geotextiles
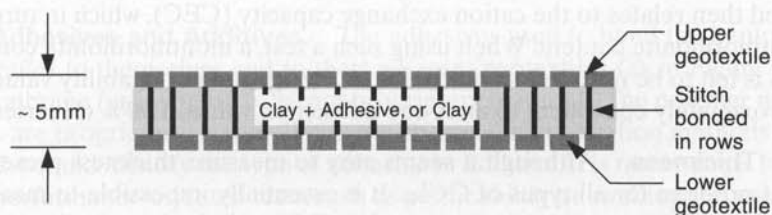
(d) Stitch-bonded clay between upper and lower geotextiles

Figure 6.2   Cross sections of currently available GCLs.

products are manufactured dry and have extremely low permeability. Perhaps the future will see an all-polymer product, but that remains for future research and development.

Additional details are available in Koerner [1] and in manufacturers' brochures and commercial literature for their respective products. The various manufacturers

should be contacted (all have regularly updated Web sites) as to their current line of products, their respective properties, and availability/pricing.

6.1 GCL PROPERTIES AND TEST METHODS

There is considerable ongoing activity in characterizing GCLs. Many test methods have been approved by ASTM and ISO and still others are in various stages of development.

6.1.1 Physical Properties

A number of physical properties of GCLs are of interest: clay type, thickness, mass per unit area, adhesives and additives, coverings, and moisture content.

Clay Type.   Sodium bentonite is known to have the lowest permeability of any naturally occurring geologic material. It is only available in large quantities in Wyoming and North Dakota in the United States. The transportation costs of moving bentonite from these locations to worldwide factories for GCL manufacturing are high. An alternative can be found in the large natural deposits of higher permeability calcium bentonite, which is much more available on a worldwide basis. By using sodium hydroxide to treat the calcium bentonite, a replacement of the calcium ions occurs, decreasing the permeability to that of the naturally occurring sodium bentonite. The process is sometimes called *peptizing* and is worldwide in its usage. Although not yet fully established, this trend will probably continue.

Regarding identification of the bentonite, X-ray diffraction (XRD) is a precise method of determining the composition of clays. However, the test is costly, and relatively few geosynthetics testing laboratories are capable of performing it. Although not as accurate, the American Petroleum Institute's methylene blue analysis is easy to perform and is thought to give conservative results. Methylene blue dye is added to a bentonite pyrophosphate solution in 1 ml increments. Dye is added to the solution until a spot of the solution forms a *blue halo* when placed on a filter paper. The volume of dye added then relates to the cation exchange capacity (CEC), which in turn relates to the montmorillonite content. When using such a test, a montmorillonite content of at least 70% is felt to be required to yield adequate swell and permeability values. This value is approximately equivalent to an X-ray diffraction value of 90% (Heerten et al. [2]).

Thickness.   Although it seems easy to measure, thickness presents a measurement problem for all types of GCLs. It is essentially impossible to measure the thickness of the bentonite component of a GCL within its associated geotextiles or geomembrane. Even if it were possible to measure, the moisture content of the bentonite would have to be measured and accounted for. As a result, the thickness of a GCL usually refers to the composite material. Three items influence variations in thickness measurements:

- *Moisture content of the bentonite*, which can be controlled by stipulating oven dry test specimens.
- *Geotextile thickness variation under pressure*, which can be controlled by stipulating a precise pressure.

- *Variation across the specimen width* due to needle punching (which is minor and relatively uniform) or stitch bonding (which is major, depending on the particular product).

Thickness in the as-manufactured state (or dry, as an index value) is really not a critical property and can be considered at best to be a quality-control item for manufacturing. It is usually not included in a product specification. Where thickness is relevant in a performance role is in permeability testing to convert a flow rate (or flux) value to a hydraulic conductivity or permeability value. Here the thickness of the hydrated test specimen is required and the issue is quite controversial.

Mass Per Unit Area.   The measurement of mass per unit area of a composite GCL follows ASTM D5993. It is somewhat subjective for reasons similar to those just discussed in the thickness section. In addition, cutting out a GCL test specimen, having powdered or granular bentonite, without losing material is very difficult. Moisture has been added around the edges before cutting with little success, and the mass of the adsorbed water must be deducted, which is difficult if a water spray is used.

A measurement that can be made with assurance is the roll average mass per unit area of the complete GCL roll. This is a relevant property but it is more of a manufacturing quality control check than a field or conformance value since the rolls generally weigh about 1.5 tonnes.

Concerning the mass per unit area of the bentonite (without the associated geotextiles or geomembranes), difficulties arise with respect to sampling, the removal of the geotextiles or geomembrane, and the deduction for the amount of adhesive (if present). Unfortunately, the GCLs that are easiest to sample are those that contain adhesives, which is a difficult situation if we desire a separate mass per unit area for the bentonite component. Note that most GCLs are targeted to have 3.7 kg/m^2 of bentonite.

Clearly work needs to be done in evaluating mass per unit area of GCLs, particularly from a field-conformance perspective.

Adhesives and Additives.   The adhesives used to bond the bentonite powder or granules to themselves and to their adjacent geotextiles (as in Figure 6.2a) or to a geomembrane (as in Figure 6.2b) are proprietary materials. The polymer modified bentonites are proprietary as well. While the chemical identification methods described in Table 1.4 could identify the type of adhesive or additive, it is rarely done. Instead, other more performance-oriented tests, such as permeability or swelling, are used to see that the adhesive or additive is not detrimental to the performance of the final product.

Coverings.   As shown in Figure 6.2 a, c, and d, geotextiles cover the upper and lower surfaces of these types of GCLs, whereas a geomembrane covers the surface of one of them (see Figure 6.2b). Specific details on all of the geotextiles and geomembranes used for GCLs are described in Chapters 2 and 5, respectively. However, this should not be taken as meaning that the geotextiles or geomembranes are not an important element of GCLs. The following properties are directly related to the covering materials: the uniformity of bentonite distribution, the containment of the hydrated bentonite during installation and service lifetime, the shear strength of the geocomposite at

its two external surfaces and internally, the puncture resistance of the geocomposite, the cross-plane permeability, and the overlap seam permeability. It should be cautioned, however, that the original properties of the geotextiles (or geomembrane) will be significantly altered by virtue of the GCL-manufacturing process. For example, the grab tensile strength of the original geotextile will be decreased considerably after needle or stitch bonding during the production process. Thus if the geotextile is removed from the GCL, its physical, mechanical, and hydraulic properties will be significantly changed from the original geotextile properties as received by the GCL manufacturer before fabrication. If the properties of the geotextile(s) or geomembrane are to be measured, a separate sample must be obtained from the manufacturer before GCL fabrication into the final product and tested accordingly.

Moisture Content.   Bentonite is a very hydrophilic mineral. As such it will generally have a measurable moisture content at all times. The value can be as high as 10% (the shrinkage limit) yet this is still considered to be the as-received, or dry, condition. The situation is further complicated by those GCLs that contain adhesives in the bentonite. Generally, some adhesive in liquid form remains after oven heating. This, along with the humidity adsorption of the bentonite, can lead to a total moisture content of up to 15% as the product leaves the manufacturing facility. For GCLs that have water added to the bentonite during manufacturing, the moisture content will be even higher.

The measurement of moisture content is straightforward via ASTM D5993 and is defined as the moisture content divided by the oven-dry weight of the specimen expressed as a percentage. Some manufacturers base the moisture content on the wet weight of the test specimen, which results in somewhat lower values.

If a high moisture content GCL loses its moisture in the field it will shrink, losing some or all of its overlap. With other contributing factors, panel separation might even occur. Under such circumstances greater overlap should be considered.

6.1.2 Hydraulic Properties

Since GCLs are used in their primary function as hydraulic barriers, this section is critically important. The hydraulic properties considered here are hydration liquid, swell index, moisture absorption, fluid loss, and permeability (or flux).

Hydration Liquid.   Bentonite, the essential low permeability component of GCLs, is known to hydrate differently depending upon the nature of the hydrating liquid. It is also known to hydrate differently as a function of the applied normal stress. Figure 6.3 illustrates the hydration response of four GCLs to the following five liquids: (1) distilled water, (2) Philadelphia tap water, (3) mild landfill leachate, (4) harsh landfill leachate, and (5) automotive diesel fuel. In all cases, the distilled water hydrated the GCLs to the greatest degree. In contrast, the diesel fuel resulted in no hydration. Obviously, with diesel fuel the adsorbed water layer on the bentonite particles never developed and no swelling occurred. This is an important and well-known finding, in that GCLs must be pre-hydrated with water if they are to be used to contain hydrocarbons and nonpolar fluids. The two types of landfill leachates and tap water fall at
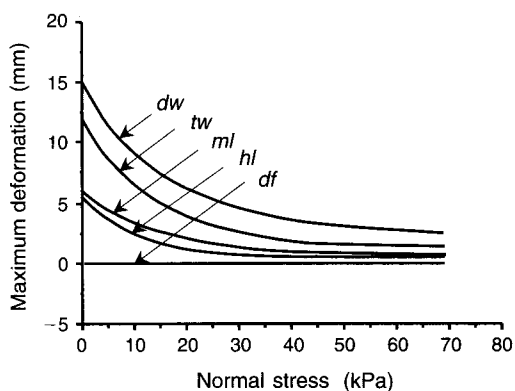
(a) Results for GCL-1
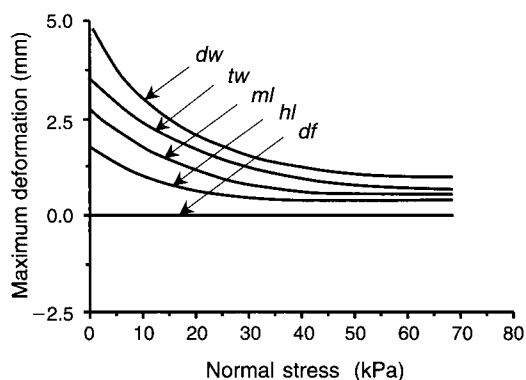
(b) Results for GCL-2

LEGEND
dw = distilled water
tw = tap water
ml = mild leachate
hl = harsh leachate
df = diesel fuel
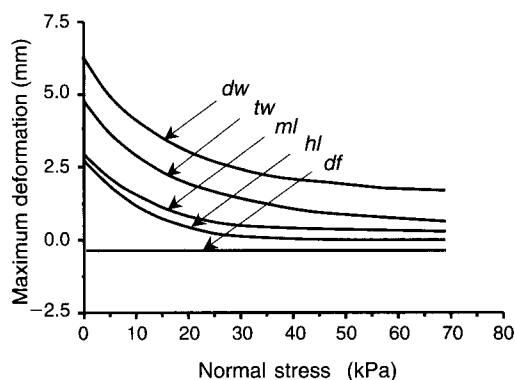
(c) Results for GCL-3
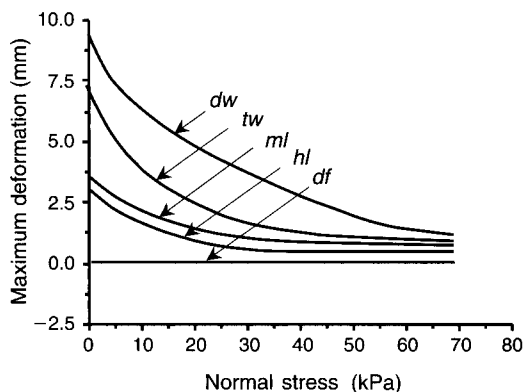
(d) Results for GCL-4

Figure 6.3   Hydration of GCLs using different liquids. (After Leisher [3])

an intermediate point between these two extremes. All three fluids have anions and cations within them, which diminish the hydration potential of the bentonite from the ideal case of distilled water. It is somewhat disconcerting to see that local Philadelphia tap water was found to be quite close in its response to leachate, but at least it was the mild leachate!

Swell Index.   The amount of swelling of bentonite under zero normal stress has been formalized in a test known as the *swell index*, and designated as ASTM D5890. In this test, a graduated cylinder is filled with 100 ml of water, to which 2.0 g of bentonite is added. The bentonite is milled to a powder and added to the water slowly so as to allow the clay to flocculate and settle to the bottom of the cylinder. After leaving the cylinder undisturbed for 24 hours, the volume occupied by the clay is measured and a recommendation is given. Heerten et al. [2] recommend a minimum swell index value of 24 ml per 2.0 g of bentonite.

A similar test, albeit under a very low seating load but one that can be readily performed in the field as a conformance test, is GRI test method GCL-1. In this procedure a CBR swelling test device is used, wherein 100 g of the GCL clay component (along with its adhesive, if present) is removed from the product and placed in the mold. A light seating load of 0.68 kPa is placed on the test specimen with a dial gage attached. The test specimen is saturated and readings are taken for 24 hours. The hydration behavior is recorded (see Figure 6.4) and if the swelling meets or exceeds the manufacturer's value, the clay component is acceptable.

Moisture Absorption.   The fact that the bentonite in GCLs can readily absorb water from the adjacent soil has been shown by Daniel et al. [4]. They placed samples of GCLs on sand soils of varying water contents from 1 to 17% and measured the uptake of water in the GCL. Figure 6.5 shows the resulting curves. Two important messages stem from this data: soils as dry as 1% can result in GCL hydration to 50% and the time for hydration is quite rapid (e.g., within 5 to 15 days).

For a laboratory determination of absorption, some GCL manufacturers report a plate water absorption test, performed in accordance with ASTM E946, to determine the volumetric increase of a clay sample as it draws water from an underlying saturated porous stone. Alternatively, Heerten et al. [2] recommend the Enslin-Neff test, which uses 0.4 g of bentonite on a glass filter within a cylinder. The cylinder funnels into a graduated capillary tube filled with water. The bentonite draws the water through the filter, causing a reduction in the water level of the tube. After 24 hours, the change in volume and the corresponding weight of water is recorded as a percentage of the original weight of bentonite.

Fluid Loss.   Another index text now focused on the fluid loss of the bentonite tested under pressure is ASTM D5891. It is an indirect measure of the adhesive characteristics of the pore water to the clay particles. In this test a carefully prepared bentonite slurry is poured into an assembled cell that has a filter paper suspended on a support screen in its base. The cell is then placed in a filter press that is pressurized to 700 kPa. The clear water collected from the base outlet of the cell between 7.5 and 30 min is the fluid loss. A maximum value of 18 ml is often specified for this test.

Permeability (Hydraulic Conductivity) and Flux.   Although the proper term is *hydraulic conductivity*, we will continue to use the word *permeability* since it is embedded in the GCL literature at this time. As with CCLs, the permeability of a GCL should be evaluated under field-simulated pressure conditions in a flexible wall permeameter.
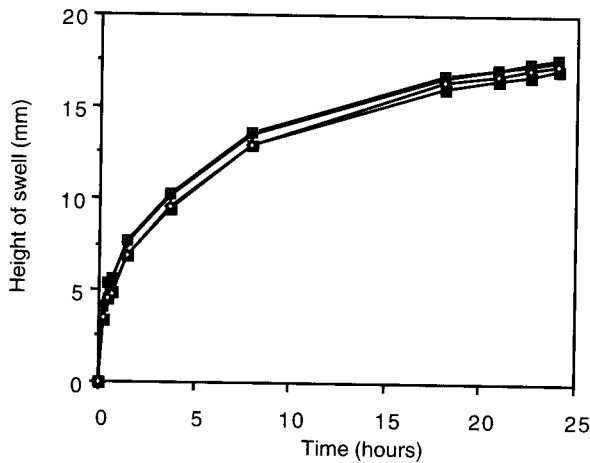
(a) Type of swell behavior from Product A
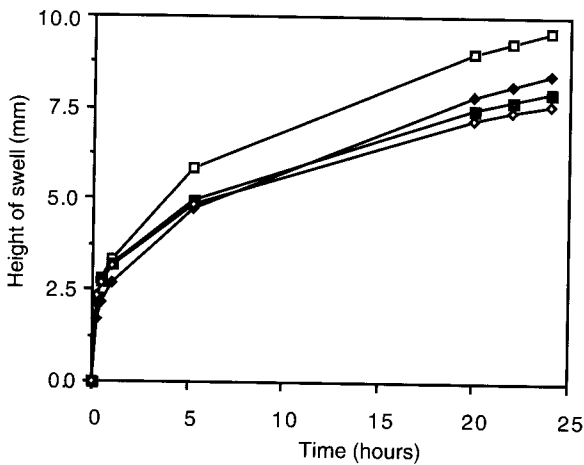
(b) Type of swell behavior from Product B

Figure 6.4   Typical hydration response curves for 100 g of clay component removed from two commercially available GCLs (each graph shows the reproducibility of four replicate tests).

Rigid wall permeameters cannot be used (see Koerner [5]). The general performance test for GCLs is ASTM D5887, which results in a "flux" value in units of m^3/sec-m^2.

A 100 mm diameter GCL test specimen is placed within a rubber membrane that is then placed in a triaxial permeameter. It is subjected to a total stress of 550 kPa and then back pressure saturated at 515 kPa with deionized water for 48 hr. Permeation through the specimen is initiated by raising the pressure on the influent side of the test specimen to 530 kPa. Permeation is continued until inflow and outflow are equal to
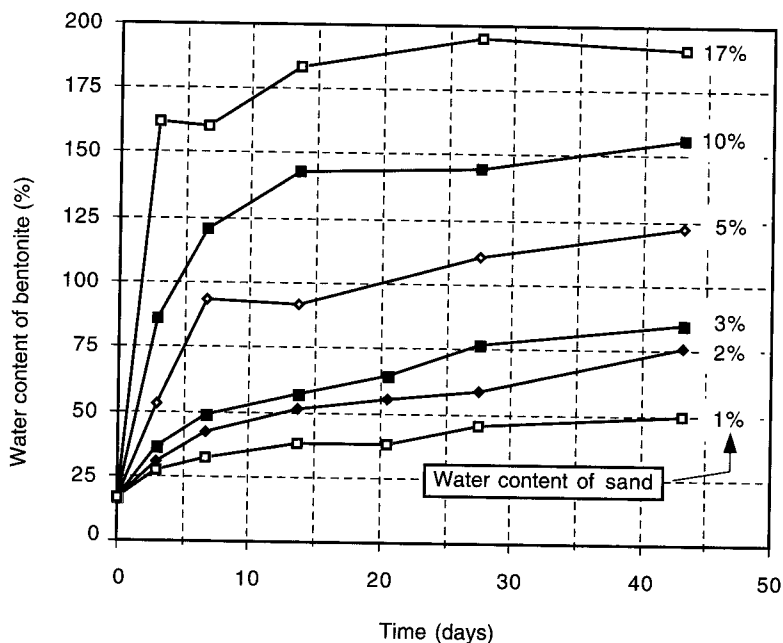
Figure 6.5　Water content versus time for GCL samples placed in contact with sand at various water contents. (After Daniel et al. [4])

±25%, or until the flow rate is sufficiently low to ensure conformance with a required value. The final value of flux or permeability is then obtained and reported. The test can also be conducted using site-specific conditions set forth by the parties involved. Permeants that are potentially incompatible with the bentonite can also be evaluated. ASTM D6766 provides such a test protocol in which two variations are mentioned. One is with initial GCL saturation using water, the second saturates the GCL with a specific test liquid. Both are followed by permeation with the specific test liquid. The second option is the most aggressive.

In the experimental procedures described above, a flow rate per unit area through the test specimen is actually measured. This value is also called the *flux*. It is plotted, along with the hydraulic gradient, for different values of total head to produce the permeability. Darcy's formula in terms of flow rate and flux illustrates the numeric procedure:

$$q = kiA \tag{6.1}$$

$$\frac{q}{A} = k\left(\frac{\Delta h}{t}\right) \tag{6.2}$$

where

$\quad q$ = flow rate (m³/s),
$\quad A$ = area (m²),

tank. The tank bottom was fitted with a centrally located rubber bladder filled with water, and the GCL test specimen was placed above it. Both full sections of GCLs and overlapped GCLs were evaluated. After 300 mm of gravel was placed above the GCL and the system was saturated, the bladder was sequentially emptied, producing an out-of-plane deformation in the GCL. The deformation was characterized by a Δ/L ratio, where Δ is the settlement and L is the radius of the deformation. Although the results were clearly product-specific, several conclusions could be drawn:

- The integrity of the different overlapped seams is compromised at Δ/L values of 0.12 to 0.81. (Note, however, that the tests were conducted at very low normal stresses.)
- Vertical separation of the overlapping sheets can occur at very low normal stresses.
- There is a potential for resealing after an initial movement in the overlapped region has occurred.
- In cases of anticipated differential settlement and low normal stresses, LaGatta recommends a larger overlap distance—for example, 225 mm instead of the customary 150 mm.

6.1.3 Mechanical Properties

GCLs placed on side slopes, under high shear stresses, adjacent to rough or yielding subgrades, under thermal stresses, and so on can readily challenge the individual product's mechanical properties thereby affecting its functionality as a hydraulic barrier. Invariably, some aspect of tensile stress will be involved. In addition, the critically important aspect of shear strength will be addressed in this section.

   Wide-Width Tension.   Using ASTM D6768, a GCL can be evaluated for its wide-width tensile behavior. Since the clay component has little tensile strength, either dry or saturated (in comparison to the geosynthetics), the recommended manner of testing is the dry state. The resulting strength will be essentially that of the geotextiles or geomembrane involved. The GCL should be tested as a composite, however, not as individual geosynthetics or according to the published values of the individual original geosynthetic materials. Thus, finding bentonite all over the testing machine should be anticipated. It is possible to seal the test specimen edges with hot glue, but if this is done carelessly it could affect the tensile strength response.
   Two GCLs were tested in their as-received dry state, with results given in Figure 6.6. The first, referred to as GCL-A, consisted of bentonite clay sandwiched between a needle-punched geotextile on one side and a composite geotextile on the other. The composite was a woven slit-film geotextile incorporated into a needle-punched geotextile. The second, GCL-B, consisted of bentonite clay sandwiched between a woven slit-film geotextile and a nonwoven needle-punched geotextile. All the geotextiles used in the manufacture of GCL-A and GCL-B were made from polypropylene yarns. Note that the tests were first conducted at zero normal stress (the
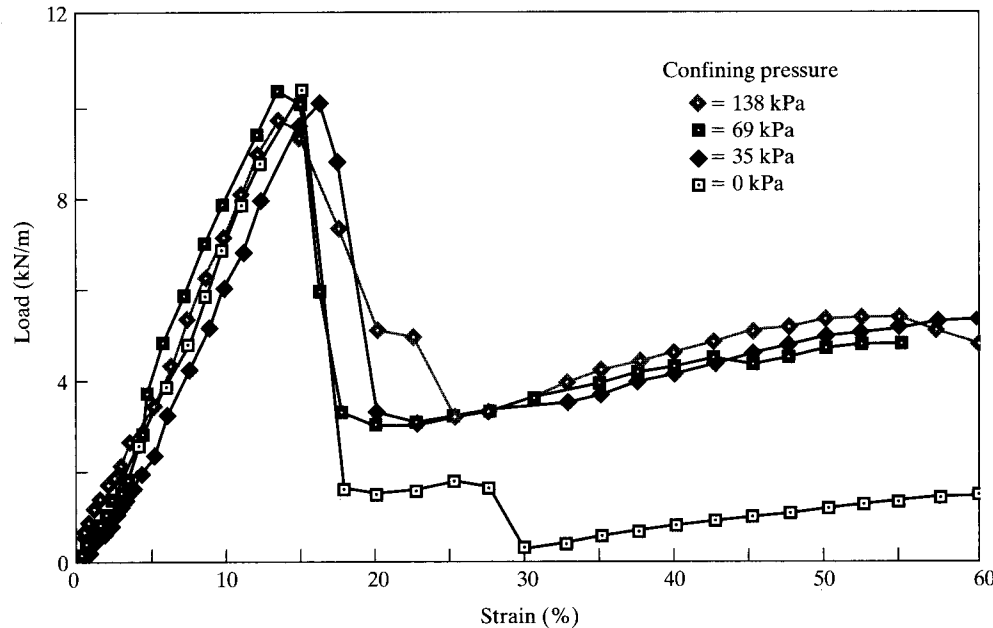
(a) Load-extension behavior of GCL-A
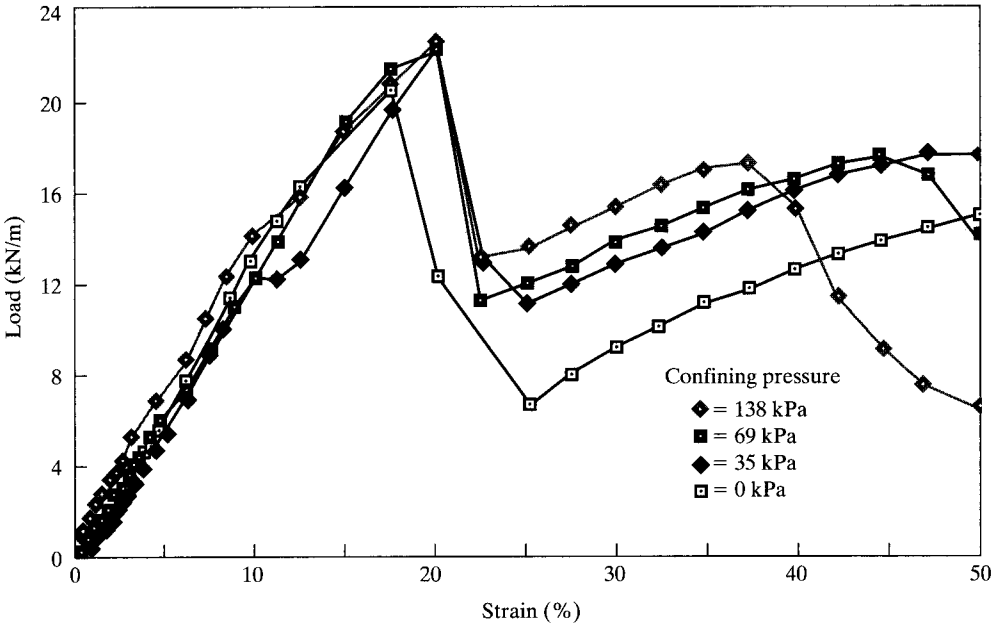
(b) Load-extension behavior of GCL-B

Figure 6.6 Wide-width tensile behavior of two GCLs per ASTM test method D6768. (Wilson-Fahmy et al. [9])

q/A = flux (m/s) as measured in the above test,
k = permeability (m/s) as often desired,
Δh = total head (m), and
t = thickness (m).

All of the values, with the notable exception of the thickness, are readily measured. The thickness of the hydrated specimen at the conclusion of the test is very troublesome to measure. The edges of the test specimen are often thinner or thicker than the center. For stitch-bonded GCLs a waved surface is observed. Deciding what measurement to use is elusive, and consequently ASTM D5887 calls for only the flux to be measured and reported. While this is completely appropriate and can be done accurately, it leaves both the designer and regulator at a loss as to how to compare a GCL's permeability to another clay barrier such as a CCL.

To assess the accuracy of the above procedure, Daniel et al. [6] conducted an interlaboratory testing program among 18 commercial laboratories and found that the permeability of a specific GCL ranged from 2×10^{-11} to 2×10^{-12} m/s. This is the general range for geotextile-related GCLs made from sodium bentonite. If calcium bentonite is used, the value of the permeability will be considerbly higher. As mentioned previously, if the calcium bentonite is treated with sodium, the permeability is reduced to approximately the value for naturally occurring sodium bentonite. A considerable body of literature is available on bentonite modification and its subsequent engineering properties.

Permeability of Overlap Seam.   Because GCL roll edges and ends are placed in the field by an overlap configuration, it is important that flow does not occur between the upper and lower GCL panels.

Using a large laboratory test tank measuring 2.4 m long × 1.2 m wide × 0.9 m high with an overlap seal along the long direction of the tank, Estornell and Daniel [7] measured the permeability in the overlap region. The amount of overlap was 150 mm. Above the GCLs, 300 mm of gravel supplied the applied normal stress. Within experimental error, the overlap permeability was as low as with the control sample having no overlap seam. This study, in general, confirms the manufacturers' recommendations of a minimum overlap requirement of 150 mm. A smaller version of this test is currently under investigation.

It is important to mention that those GCLs with nonwoven needle-punched geotextiles on both upper and lower surfaces *must* have bentonite powder or paste placed within the overlap area. The amount is typically recommended to be 0.4 kg/m, but it does depend on the type of geotextiles that are involved. Alternatively, one manufacturer's product has an exposed bentonite clay strip ($\simeq$10 mm wide) with no geotextile covering. As a result, the bentonite is self-sealing when hydrated. In all cases, the manufacturers' recommendations should be followed.

Permeability Under Deformation.   Recognizing that GCLs are being used in landfill caps and closures and that differential subsidence is likely in such applications, the issue of GCL permeability in an out-of-plane deformation mode must be addressed. LaGatta [8] has evaluated a number of conditions in a large-scale laboratory

customary manner) and then at varying amounts of confined normal stress. The following comments focus only on the unconfined behavior.

The initial response of both GCLs was strongly influenced by the woven slit-film geotextiles, which took the load uniformly until this component failed. The loss of strength between 10 and 20% is seen to be quite pronounced. Thereafter, the nonwoven component took the load until its ultimate failure beyond 50 to 60% strain. The modulus, strain at initial failure, and peak strength are the targeted values from such tests, but clearly, they are product-specific and dominated by the type of geotextile(s).

For the geomembrane-associated GCL of Figure 6.2b, the tensile behavior is anticipated to be quite close to that of the geomembrane by itself; see [9] for selected data from geomembranes in this same mode of testing.

Confined Wide-Width Tension.   Using a confined wide-width tension device (recall Section 2.3.3), the same two GCLs as in the previous section were evaluated, but now at 35, 69, and 138 kPa normal pressures [9].

Figure 6.6a shows the load-extension response of GCL-A at these pressures and compares the responses with the zero confining pressure. It can be seen that up to peak load, there is practically no effect of confinement. This is not surprising since most of the load is carried by the woven slit-film geotextile, which has a much higher modulus compared with the needle-punched geotextiles making up the remainder of the product. In fact, the peak load is always associated with the rupture of the woven geotextile. The same behavior is noticed in Figure 6.6b for GCL-B where the load up to peak is again carried by the woven slit-film geotextile. After peak is reached in both types of GCLs, the stress drops off significantly and very erratic behavior is observed. This behavior is quite complex in that the nonwoven needle-punched geotextiles, the needling process, and the interaction of the clay particles are all involved in some way. For the purposes of reinforcement, however, this behavior is academic since the modulus, peak strength, and associated peak strain are the focal points for any design process.

The conclusion of confined wide-width testing appears to be that *if* a woven slit-film geotextile (also a woven monofilament or even a woven/nonwoven composite) is in the upper or lower geotextile, the effect of lateral confinement is negligible and the unconfined tension test is adequate. Use of ASTM D6768 in isolation is recommended. It is also much easier to set up and is considerably faster to perform. This probably holds true for GCLs with geomembranes as well. However, if, the GCL has only nonwoven needle-punched geotextiles associated with it, the effect of confinement is measurable and tests with lateral confinement as illustrated in this section are warranted.

Axi-symmetric Tension.   The question frequently arises as to the axi-symmetric tensile behavior of GCLs, particularly when used in landfill closure applications. Koerner et al. [10] have used an axi-symmetric tension test setup for geomembranes and modified it for GCLs. The test setup shown in Figure 5.4 was used with a LLDPE geomembrane over the GCL test specimen. Hydrostatic pressure is applied until failure occurs, which is always in the GCL before the LLDPE geomembrane. The load taken by the geomembrane is deducted (via a separate test on the geomembrane by itself), and

the stress-versus-strain behavior of the GCL is obtained. In general, the failure strain for the geotextile-related GCLs is from 10 to 19%, and for HDPE geomembrane related GCLs from 15 to 22%. Such values are orders of magnitudes higher than CCLs, and in keeping with stiffer geomembranes like HDPE and fabric-reinforced geomembranes (e.g., fPP-R, CSPE-R, and EPDM-R). Geomembranes with the highest flexibility, like LLDPE, fPP, and PVC, strain considerably further (50 to 100%) in this type of test (recall Figure 5.5).

Direct Shear.   A series of *direct shear tests* have been performed using a 100 mm × 100 mm shear box with the center of the GCL test specimens located at the split in the upper and lower shear boxes. The strain rate in all cases was 1.0 mm/min. Note that this is a relatively rapid strain rate and creep shear tests are available for comparison purposes [11]. Normal stresses varied from 0.7 to 140 kPa. The same four GCLs hydrated in the same five liquids described in Section 6.1.2 were used for these internal shear tests. The tests were performed in three different states: as-received condition (dry), hydration while under zero normal stress (free swell), and hydration under the same normal stress as the respective shear tests (constrained swell). Table 6.1 presents the resulting shear strength parameters. (See Sections 2.3.3 and 5.1.3 for details on the direct shear test.) These internal shear test results included the following observations:

- The GCLs were strongest in the dry condition and weakest in the free swell condition. The results from constrained swell conditions were intermediate between the two extremes.
- The type of hydrating liquid affected shear strength, but to a lesser extent than other factors. Hydration with distilled water was the worst-case condition in this regard.
- GCLs fabricated by needle punching between two geotextiles required much larger displacements than unreinforced GCLs to reach their limiting shear strength stress.
- Needle punching significantly increased the shear strength under all conditions. (Note that stitch-bonded GCLs were not evaluated in this series of tests, but similar and even greater improvements have been measured in separate tests.)

Depending upon the nature of the upper and lower surfaces of the GCL and on the adjacent soil or other geosynthetic materials, separate *interface shear tests* will be needed. These interfaces must be evaluated with respect to the adjacent site-specific materials: geotextiles (Section 2.3.3), geogrids (Section 3.1.2), geonets (Section 4.1.2), or geomembranes (Section 5.1.3). Also note that the interface surface may be considerably changed from the as-received geosynthetic materials, due to hydrated bentonite intruding into nonwoven needle-punched geotextiles or extruding out of the woven geotextiles into the interface of concern. Slit-film, spun-laced, and monofilament geotextiles with even the slightest open area between fibers or yarns are all of great concern in this regard. Product-specific simulated testing is called for in most circumstances.

TABLE 6.1   SUMMARY OF REINFORCED GCL (INTERNAL) DIRECT SHEAR TEST RESULTS[1]

	Hydration with Distilled Water			Hydration with Tap Water		
	Dry	Constrained Swell	Free Swell	Dry	Constrained Swell	Free Swell
GCL-1 ϕ (degrees)	37	16	0	37	18	0
c (kPa)	6.9	2.8	4.1	6.9	2.8	3.4
GCL-2 ϕ (degrees)	36	31	10	36	34	15
c (kPa)	68	6.9	9.0	68	6.9	6.9
GCL-3 ϕ (degrees)	42	37	23	42	43	26
c (kPa)	14	8.5	4.8	14	5.5	10
GCL-4 ϕ (degrees)	26	19	0	26	18	0
c (kPa)	50	4.8	2.8	50	4.8	3.4

	Hydration with Mild Leachate			Hydration with Harsh Leachate		
	Dry	Constrained Swell	Free Swell	Dry	Constrained Swell	Free Swell
GCL-1 ϕ (degrees)	37	24	4	37	19	0
c (kPa)	6.9	6.2	3.4	6.9	5.5	2.8
GCL-2 ϕ (degrees)	36	43	20	36	39	30
c (kPa)	68	4.8	12	68	4.1	8.3
GCL-3 ϕ (degrees)	42	39	25	42	45	32
c (kPa)	14	8.3	14	14	4.8	12
GCL-4 ϕ (degrees)	26	18	13	26	13	0
c (kPa)	50	4.8	3.4	50	7.6	3.4

	Hydration with Diesel Fuel						
	Dry	Constrained Swell	Free Swell			Dry	Constrained Swell	Free Swell
GCL-1 ϕ (degrees)	37	44	38	GCL-3 ϕ (degrees)	42	42	40
c (kPa)	6.9	4.1	6.2	c (kPa)	14	6.2	4.8
GCL-2 ϕ (degrees)	36	51	46	GCL-4 ϕ (degrees)	26	24	29
c (kPa)	68	4.1	4.8	c (kPa)	50	4.1	6.2

[1]*Dry* refers to the GCL as received, placed under desired normal stress, then sheared at midplane. *Constrained swell* refers to GCL hydrated under the desired normal stress, then sheared at the midplane. *Free swell* refers to GCL hydrated under zero normal stress, then placed under the desired normal stress, and immediately sheared at midplane.

Source: After Leisher [3].

Peel Strength.   ASTM D6496 addresses the peel strength between upper and lower geotextiles of reinforced GCLs. In this test, a 100 mm wide specimen has its cap and carrier geotextiles gripped individually in opposing tensile grips and pulled at a constant rate of extension by a tensile testing machine until the layers of the specimen separate. The reinforcing fibers or stitches are successfully placed in tension and have the effect of bundling against one another. The average peel strength is calculated and reported in units of kN/m. The test is an index test used to evaluate the quality of the

reinforcement process. Numerous attempts have been made at rating peel strength with internal direct shear strength but without complete success (von Maubeuge and Lucas [12]). Considering the relative ease of the peel test, obtaining such a relationship is a good research topic.

Puncture and/or Squeezing Resistance.   Due to the relative thinness of GCLs compared with CCLs, puncture and/or squeezing resistance concerns are understandably often voiced. There are a number of tests that can be used with GCLs, including ASTM D4883, which uses a 8.0 mm probe; ASTM D6241, which uses a CBR probe of 50 mm diameter; and ISO 12236, which also uses a 50 mm diameter probe. Although all of these tests are straightforward to perform, it is important to recognize the self-healing puncture characteristics of GCLs which contain bentonite. Figure 6.7 illustrates this feature for a hole made by a bolt that penetrated the GCL, which upon hydration appears to have sealed itself quite nicely. No puncture test by itself can reproduce this self-sealing mechanism, since the GCL is being used as a hydraulic barrier and puncture per se may not be a defeating, or even limiting, phenomenon. Lateral squeezing, however, can occur if a nonpuncturing load is stationed on a GCL with insufficient cover soil. The degree of squeezing is dependant on the bentonite's initial moisture content and the type of GCL [13].

6.1.4 Endurance Properties

Since the solid component of the barrier material in a GCL is clay, its long-term integrity is generally assured. However, the liquid that activates and permeates the bentonite, resulting in its low permeability, is certainly an issue insofar as moisture barrier endurance is concerned. Recall the ASTM D6766 test that was discussed in Section 6.1.2.

Figure 6.7 Bolt puncture of a GCL, illustrating self-healing quality of bentonite clay. (Photograph courtesy of CETCO)

Freeze-Thaw.   The central property of a hydrated GCL insofar as freeze-thaw behavior is concerned is its permeability. Daniel et al. [14] used a rectangular laboratory flow box and subjected the entire assembly to 10 freeze-thaw cycles. The permeability showed a slight increase from 1.5×10^{-9} to 5.5×10^{-9} cm/sec. Kraus et al. [15] report no change in flexible wall permeability tests of the specimens evaluated after 20 freeze-thaw cycles.

While the moisture in the bentonite of the GCL can freeze, causing disruption of the soil structure, upon thawing the bentonite is very self-healing and apparently returns to its original state. In this regard, it is fortunate that most GCLs have geotextile or geomembrane coverings so that fugitive soil particles cannot invade the bentonite structure during the expansion cycle.

Shrink-Swell.   The behavior of alternate wet and dry cycles insofar as a GCL's permeability is important in many circumstances, particularly so when the duration and intensity of the dry cycle is sufficient to cause desiccation of the clay component of the GCL. Boardman and Daniel [16] evaluated a single, albeit severe, wet-dry cycle on a number of GCLs and found essentially no change in the permeability. The results are encouraging and mimic the freeze-thaw results, but the results of numerous wet-versus-dry cycles await further investigation.

Perhaps more significant than change in permeability is that shrinkage can cause loss of overlap and even separation at the roll edges or ends. If this occurs in the field, friction with the underlying surface will prevent expansion back to the original overlapped condition. Thus cover soil, placed in a timely manner and sufficiently thick to resist shrinkage, is necessary.

Adsorption.   The adsorptive capacity of GCLs is important when they are used for landfill liners and interface with the various leachates that they are meant to contain. Both organic and inorganic solutes are of concern. The situation is described in [17], particularly in comparison to CCLs and addressing the issue of making an equivalency assessment. The cation exchange capacity of the bentonite clay must be determined and, along with its thickness, such a comparison can be made. It is in this particular instance that GCLs usually are not considered to be equivalent to the much thicker CCLs. For this reason there is a tendency to use a three-component composite liner (i.e., GM/GCL/CCL—recall Section 5.6.3). The CCL component, however, can be significantly higher in its permeability than the usual regulated value. The hydraulic conductivity of the GCL/CCL system has been analytically investigated by Giroud et al. [18].

Water Breakout Time.   Water breakout time is of particular interest for GCLs used in landfill closures. It is at this point that steady-state seepage will occur through the GCL and into the underlying solid waste. The data can be obtained from a permeability test, as described in Section 6.1.2, but now starting with the as-received dry GCL instead of starting with a fully saturated test specimen.

Solute Breakout Time.   For a GCL placed beneath a landfill or surface impoundment, it is the solute breakout time (rather than water) that is of concern. The

test method is again the permeability test (see Section 6.1.2), but now with the liquid of concern (e.g, with the leachate), as the permeant. This is an area where research seems to be warranted, particularly in light of showing the equivalency of GCLs to CCLs.

Geotextile Durability.   The durability of geotextile coverings of GCLs, as well as the needle-punched fibers or sewing yarns providing internal reinforcement, is similar to that discussed in Section 2.3.6 on geotextiles. The exceptions are that the adjacent or surrounding medium is hydrated bentonite and required lifetimes are always long when GCLs are used as solid-waste barriers. Thus, recent efforts have focused on geotextile fiber and fabric lifetime [19–21]. The approach is similar to that described in Section 5.1.5 for geomembrane lifetime prediction, with the exception that the simulated laboratory incubation setup is very challenging. The topic is of considerable research value.

6.2   EQUIVALENCY ISSUES

Since CCLs (both natural soil and amended soil types) have been used historically as liquid barriers, it is only fitting that GCLs should have to compare favorably with, *or be better than*, CCLs in order to be used as replacement barrier materials. They may have to be better than CCLs since GCLs are the replacement material, and concerns are often voiced when the use of new materials is contemplated. The obvious issues are due to the fundamental differences listed in Table 6.2.

As first glance, we would assume that a technical equivalency argument could be based on the flow rate or flux through the competitive materials. Such a calculation is straightforward (it is illustrated in Section 6.3.1) and is routinely used for such purposes. However, this particular calculation is only the beginning of a complete equivalency comparison since numerous hydraulic, physical/mechanical, and construction issues need evaluation. Within each issue there are specific questions that can be raised in

TABLE 6.2   DIFFERENCES BETWEEN GEOSYNTHETIC CLAY LINERS AND COMPACTED CLAY LINERS

Characteristic	GCLs	CCLs
Material	Bentonite clay, adhesives, geotextiles, and/or geomembranes	Native soils or blends of soil and bentonite clay
Construction	Factory-manufactured and then installed in the field	Constructed and/or amended in the field
Thickness	$\cong 6$ mm	300 to 900 mm
Permeability of clay	10^{-10} to 10^{-12} m/s	10^{-9} to 10^{-10} m/s
Speed and ease of construction	Rapid, simple installation	Slow, complicated construction
Installed cost	$0.05 to $0.10 per m^2	Highly variable (estimated range $0.07 to $0.30 per m^2)
Experience	CQC and CQA are critical	Has been used for decades

order to arrive at a complete equivalency assessment. Furthermore, for waste containment systems, we can identify functional differences between a barrier material beneath a waste facility (e.g., landfills, surface impoundments, heap leach pads, and waste piles) and a barrier material placed above a waste facility (e.g., landfill and agricultural covers and closure situations). In addition, the comparison may differ depending on whether the GCL is compared to a CCL when each is used by itself (as with a single barrier) or when they are used in a composite barrier, as with a GM/GCL compared with a GM/CCL.

The aforementioned contrasts can be arranged via a comparison that includes the various issues for liners versus covers. See Tables 6.3 and 6.4 respectively, for a relatively complete set of equivalency issues that often require an analysis. The tables can serve best as a guide or checklist for a site-specific comparison to be made by the user.

In both Table 6.3 (for liners) and Table 6.4 (for covers) it is seen that regarding the *hydraulic issues*, the chemical adsorptive capacity of a GCL compared with the typical CCL is generally not equivalent. It is site-specific just how dominant an issue this is. If it is significant, the use of a combined GCL/CCL composite is an alternative (see

TABLE 6.3 GENERALIZED TECHNICAL EQUIVALENCY ASSESSMENT FOR GCL LINERS BENEATH LANDFILLS AND SURFACE IMPOUNDMENTS

Category	Criterion for Evaluation	Probably Superior	Probably Equivalent	Probably Not Equivalent	Equivalency Dependent on Site or Product
Hydraulic issues	Steady flux of water		✓		
	Steady solute flux		✓		
	Chemical adsorption capacity			✓	
	Breakout time				
	Water				✓
	Solute				✓
	Horizontal flow in seams or lifts		✓		
	Horizontal flow beneath geomembrane		✓		
	Generation of consolidation water	✓			
Physical/ mechanical issues	Freeze-thaw behavior	✓			
	Total settlement		✓		
	Differential settlement	✓			
	Stability on slopes				✓
	Squeezing or bearing stability			✓	
Construction issues	Puncture resistance			✓	
	Subgrade conditions			✓	
	Ease of placement	✓			
	Speed of construction	✓			
	Availability of materials	✓			
	Requirements for water	✓			
	Air pollution concerns	✓			
	Weather constraints				✓
	Quality assurance considerations		✓		

Source: After Koerner and Daniel [17].

TABLE 6.4 GENERALIZED TECHNICAL EQUIVALENCY ASSESSMENT FOR GCL COVERS ABOVE LANDFILLS AND ABANDONED DUMPS

Category	Criterion for Evaluation	Probably Superior	Probably Equivalent	Probably Not Equivalent	Equivalency Dependent on Site or Product
Hydraulic issues	Steady flux of water		✓		
	Breakout time of water				✓
	Horizontal flow in seams or lifts		✓		
	Horizontal flow beneath geomembrane		✓		
	Generation of consolidation water	✓			
	Permeability to gases		✓		
Physical/ mechanical issues	Freeze-thaw behavior	✓			
	Shrink-swell behavior	✓			
	Total settlement		✓		
	Differential settlement	✓			
	Stability on slopes				✓
	Vulnerability to erosion				✓
	Squeezing or bearing stability			✓	
Construction issues	Puncture resistance			✓	
	Subgrade conditions			✓	
	Ease of placement	✓			
	Speed of construction	✓			
	Availability of materials	✓			
	Requirements for water	✓			
	Air pollution concerns	✓			
	Weather constraints				✓
	Quality assurance considerations		✓		

Source: Koerner and Daniel [17].

Giroud et al. [18]). Similarly the water and solute breakout times for the geotextile-covered GCLs are probably not equivalent to CCLs, but the geomembrane backed GCL probably is. Again the relevancy of breakout time must be assessed in light of site-specific considerations. Intimate contact of geomembranes with both GCLs and CCLs is an area in need of appropriate CQC and CQA.

Regarding *physical/mechanical issues*, GCLs are generally equivalent to or better than CCLs, with the exception of squeezing or bearing capacity when the GCLs are of high moisture content and trafficked without sufficient soil cover. This issue must be avoided by proper specification values and follow-through in the CQC and CQA activities. The all-important issue of shear strength (internal and interface) is a site-specific and/or product-specific issue.

Regarding *construction issues* it appears that only the puncture resistance and need for very careful subgrade preparation of GCLs are limiting issues. The self-healing characteristics of bentonite clay, however, must be considered in regard to puncture (recall the bolt puncture shown in Figure 6.7). Regarding subgrade conditions Scheu et al. [22] describe GCLs placed over very rough subgrades. Even further, GCLs are sometimes used as protection mats in Germany placed *over* geomembranes

and beneath coarse drainage stone in leachate collection layers. Lastly, a key issue, as with all geosynthetics and natural soil materials, is proper CQC and CQA insofar as their installation is concerned.

Thus it is felt that in most cases a GCL can replace a CCL on the basis of technical equivalency. One important issue not addressed in Tables 6.3 or 6.4 is cost. In areas where proper natural clay soils are plentiful and air space is not important, CCLs will be competitive with GCLs. In areas where they are not, and blending of native soils with admixed bentonite clay is necessary for a proper CCL, the GCLs will usually be very cost effective. This is obviously a site-specific consideration.

6.3   DESIGNING WITH GCLS

The single, and obviously primary, function of a GCL is as a liquid barrier. Thus the examples given in this section will illustrate the function of containment for different applications.

6.3.1 GCLs as Single Liners

GCLs have been used as single liners—i.e., by themselves with no composite or back-up geomembranes—in a number of notable cases. In this section, two will be described: canal liners and underground storage tank liners.

Heerten and List [23] report on GCLs being used to rehabilitate old clay liners in German canals. The study cites a canal that was dewatered and properly regraded and then had the GCL placed directly on the soil subgrade. The particular GCL was of the needle-punched type shown in Figure 6.2c with an 800 g/m^2 nonwoven carrier geotextile and a 300 g/m nonwoven cap geotextile. The permeability of the calcium bentonite was 1×10^{-10} m/s. A 300 mm thick gravel soil layer was placed over the GCL (see Figure 6.8a). The side slopes varied segmentally from 4.8 to 18.4 to 26.6 to 29.7° as the cross section rose to the top of the slope. Internal shear tests on this particular product resulted in friction angles of approximately 34°, according to the data in Table 6.1. Thus the needling process for internal shear strength and upper and lower nonwoven geotextiles for external shear strength provide the assurity of adequate slope stability for all sections along the side slopes.

There are a huge number of steel storage tanks that require secondary containment liners for environmental safety in case of a failure. The usual situation is shown in Figure 6.8b. The purpose of the GCL is to contain the liquid in the storage tank in the event of a pipe burst or tank leak. It is the same application as described in Section 5.9, where the solution was to use a geomembrane. Since side slope distances are usually quite small, most GCLs are candidates for this application. However, one caution must be raised. If the soil cover, typically a gravel, placed over the GCL is limestone, the leaching of calcium and magnesium from the stone into the sodium bentonite may cause a base exchange to occur, thereby increasing the permeability of the bentonite in the GCL. Thus it is important to prehydrate GCLs with water whenever they will not
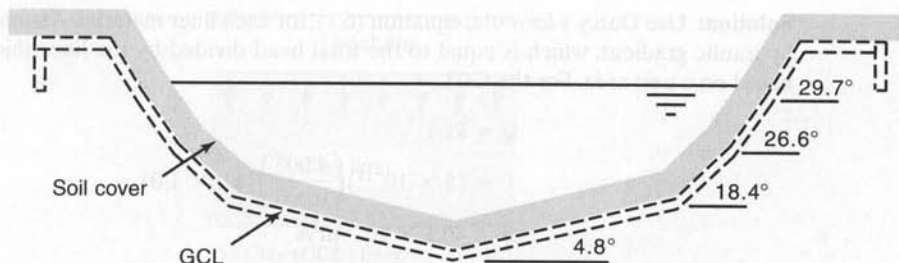
(a) GCL as a canal liner (After Heerten and List [23])
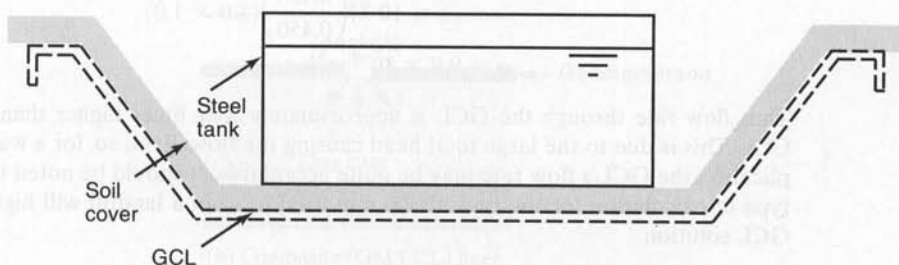
(b) GCL as a storage tank liner

Figure 6.8   Cross section of GCLs used as single liners.

be water-saturated during their initial liquid containment (recall the diesel fuel hydration tests in Figure 6.3).

The general issues in the design of a GCL used as a single liner are as follows:

1. Calculate the flow rate in the context of alternative materials (see Example 6.1), adsorption, and breakout time for both water and the solute in the containment application.
2. Calculate shear strength for side slopes under internal and both external interface conditions (recall Section 3.2.7)
3. Assess the possible implications of puncture, tear, and loss of bentonite, considering both the materials above and below the GCL.
4. Carefully consider installation survivability of the GCL, considering both the subgrade and the backfill materials.

Example 6.1

Calculate the water flow rate coming from a GCL in a 4.0 m deep canal if the permeability of the GCL is 5×10^{-11} m/s and it is 5 mm thick. Compare this value with a CCL that is 450 mm thick with a permeability of 1×10^{-9} m/s, and comment accordingly.

Solution: Use Darcy's formula, equation (6.1), for each liner material. Assume that i is the hydraulic gradient, which is equal to the total head divided by the liner thickness and is based on a unit area. For the GCL,

$$q = kiA$$
$$= (5 \times 10^{-11})\left(\frac{4.005}{0.005}\right)(1.0 \times 1.0)$$
$$q = 40.1 \times 10^{-9} \, \text{m}^3/\text{s}$$

For the CCL we have

$$q = kiA$$
$$= (1 \times 10^{-9})\left(\frac{4.450}{0.450}\right)(1.0 \times 1.0)$$
$$q = 9.9 \times 10^{-9} \, \text{m}^3/\text{s}$$

Thus flow rate through the GCL is approximately four times higher than through the CCL. This is due to the large total head causing the flow. Even so, for a water canal application the GCL's flow rate may be quite acceptable. It should be noted that the same type of calculation for the typical 300 mm total head in a landfill will highly favor the GCL solution.

6.3.2 GCLs as Composite Liners

GCLs have seen their greatest use to date as the lower component of a composite liner for landfills and surface impoundments. Thus a geomembrane will be the upper component and the GCL the lower component. Such a composite liner has been used to great advantage as the primary liner of a double-lined landfill facility, as was shown in Figures 5.40g and h. The reduction in leakage rates for facilities constructed with a GM/GCL composite, versus GM alone *or* a GM/CCL composite, is remarkable (recall Figure 5.39). In the case of the GM by itself, the occurrence of a hole brings leachate directly into the leak detection system, while consolidation water from a GM/CCL is very large and difficult to distinguish from actual leakage. The GCL, being placed dry, attenuates any leakage through holes or flaws in the geomembrane, giving in many cases near-zero leakage rates.

Such a composite GM/GCL can also be used as a secondary liner system, but regulations sometime require a GM/CCL secondary liner. Thus we would have to show complete equivalency of the GCL to the CCL. Although this can be done (recall Section 6.2), some regulators are reluctant to give changes for traditionally thick elements of the cross section, such as a CCL. An alternative composite liner that has been used is a three-component GM/GCL/CCL; although the CCL component can be somewhat higher in permeability than the regulated value, the GCL/CCL together will give the regulated value or lower (Giroud et al. [18]).

In a GM/GCL composite liner application, the upper geotextile covering of the GCLs is controversial. This raises the issue of intimate contact. The original concept of composite liner behavior is shown by comparing parts (a) and (b) in Figure 6.9. Here a potential hole in the geomembrane directly meets the underlying clay, where it is

Leachate

↓ ↓ ↓ ↓ ↓ ↓ ↓ ↓

Clay liner

(a) Clay (CCL) liner
(CCL by itself)

Leachate

← Geomembrane

Clay liner

(b) Composite (GM/CCL) liner
(geomembrane and CCL
with intimate contact)

Leachate

← Geomembrane
← Geotextile*
GCL
← Geotextile

* Does this geotextile's transmissivity
compromise the composite liner concept?

(c) Composite (GM/GCL) liner
(geomembrane and GCL with
questionable intimate contact)

Figure 6.9   Composite liner concept, illustrating the issue of intimate contact.

forced to radially propagate through the clay soil. No drainage layer (sand or geotextile) is generally allowed between the two materials. Thus it is reasonable to express a concern when a GCL is used instead of a CCL and the GCL has a geotextile as its upper surface. Figure 6.9c illustrates the essence of this concern. Here the lateral transmission of the leachate in the plane of the geotextile, allowing for the attack of the clay component over an area larger than the hole itself, can be envisioned. While this is a reasonable concern, we must realistically question the transmissivity of the geotextile in light of the *quantity* of liquid being transmitted. Table 2.7 presented the transmissivity of various geotextiles. Generally, woven slit-film and woven monofilament geotextiles are not of concern and furthermore, the extrusion of bentonite through the open

voids of such woven geotextiles will probably lower the transmissivity value to that of the bentonite itself. Thus the concern in this situation is the lowering of the shear strength of the interface between the bottom of the geomembrane and the top surface of the GCL. This situation has resulted in two slides of full scale test plots at 2(H)-to-1(V) slopes (Koerner et al. [25]). As a result, when GCLs are on relatively steep side slopes, the upper geotextile (beneath the covering geomembrane) should be a nonwoven needle-punched type. The minimum mass per unit area becomes a trade-off between being sufficiently thick to avoid the extrusion of the hydrated bentonite and sufficiently thin so that composite action is not an issue [26]. To assess the situation, the radial transmissivity test described by Wilson-Fahmy and Koerner [27] can be considered. Polymer impregnation of the upper geotextile is of interest in this regard.

The general issues involved in a composite GM/GCL liner are as follows:

1. Calculate composite liner flow rate for water containment applications, and the flow rate adsorption and breakout time for leachate (solute) containment applications. (See Examples 6.2 and 6.3.)
2. Assess the internal and interface shear strengths for the side slopes and intermediate berms under short- and long-term loading conditions, (recall Section 3.2.7).
3. Consider the GCL wide-width strength design and anchor trench reaction. If the interface friction angle below the GCL is lower than those above it and also lower than the side slope angle, the difference must be carried by the GCL in tension. Thus, the importance of the anchor trench design becomes apparent (see Section 5.6.8).
4. Avoid puncture, tear, and loss of bentonite by using carefully worded specifications followed by strict CQC and CQA. Both static and dynamic conditions must be addressed (the latter being of concern for access ramps).
5. Avoid lateral migration, or squeezing, and loss of thickness of the hydrated bentonite under heavy long-term static loads, as listed in Table 6.3. A suitably thick soil cover layer is necessary before trafficking.
6. Avoid the contamination of overlying geomembrane seam areas from loss of bentonite. This has been a problem particularly with textured geomembranes.
7. Consider both the GCL's subgrade and backfill materials insofar as survivability during installation.

Example 6.2

What is the upper-bound leakage through a 2.0 mm wide slit in a geomembrane overlying a 10 mm thick GCL having a permeability of 7.0×10^{-12} m/s? The slit is long with respect to its width. The composite liner is under a constant total head of 300 mm. Use the formulation presented by Giroud and Bonaparte [28].

Solution: Assuming radial flow through the underlying GCL, the following formula gives the flow rate per unit length of slit in the geomembrane.

$$q = \pi k_s(h_w + t)/\ln(2t/b) \tag{6.3}$$

where

q = flow rate,
k_s = GCL permeability,
h_w = total head loss,
t = GCL thickness, and
b = width of slit in geomembrane.

$$q = \pi(7.0 \times 10^{-12})(0.300 + 0.010)/\ln(0.020/0.002)$$

$$q = 3.0 \times 10^{-12}\,\text{m}^3/\text{s} - \text{m of slit length}$$

Example 6.3

What is the upper-bound leakage through a 2.0 mm circular hole in a geomembrane over-lying a 10 mm thick GCL having a permeability of 7.0×10^{-12} m/s? The composite liner is under a constant total head of 300 mm. Again use the formulation presented by Giroud and Bonaparte [28].

Solution: Assuming radial flow through the underlying GCL, the following formula gives the estimated leakage rate.

$$q = \pi k_s (h_w + t)d/(1 - 0.5d/t) \tag{6.4}$$

where

d = hole diameter

$$q = \pi(7.0 \times 10^{-12})(0.300 + 0.010)(0.002)/(1 - 0.001/0.010)$$

$$q = 0.015 \times 10^{-12}\,\text{m}^3/\text{s}$$

6.3.3 GCLs as Composite Covers

In exactly the same way as they are used for liners beneath solid waste, a composite GM/GCL can be used in a cover above the solid waste (see Koerner and Daniel [29]). In describing such barrier strategy for landfill covers (also called closures or caps), the typical benefit/cost ratios decidedly favor a GM/GCL over a GM/CCL (see Koerner and Daniel [30]).

The fundamental difference between the two applications of a composite liner above the waste and below the waste is that differential settlement will likely occur in cover situations. The GM/GCL application has been developed and used in a number of covers for abandoned dumps, many with no liner of any type beneath the waste.

The general issues involved in the design for a composite GM/GCL final cover placed above a solid waste landfill are as follows:

1. Calculate the composite cover flow rate for water, as illustrated in Examples 6.2 and 6.3.
2. Assess the internal and interface shear strengths for cover slopes under short- and long-term loading conditions, including live loadings, (recall Section 3.2.7)

3. Assess the GCL strength design and factor of safety. If the interface friction angle below the GCL is lower than those above it and also lower than the slope angle, the difference must be carried by the GCL in tension.

4. Carry the tensile stresses via anchor trenches per Section 5.6.8 or, if symmetry of the cover exists, via equal and opposite reactions on each side of the crest.

5. Evaluate the retention of the GCL's low permeability in the event of out-of-plane deformation due to subsidence of the underlying solid waste material (i.e., due to differential settlement); see Example 6.4.

6. Avoid puncture, tear, and loss of bentonite, considering both the materials above and below the GCL.

7. Avoid the contamination of geomembrane seam areas from loss of bentonite. This has been a problem, particularly with textured geomembranes.

8. Consider both the subgrade and the backfill materials in the GCLs survivability during installation. This may require test pads simulating field conditions, followed by exhuming the GCL and observing or testing for possible damage.

Example 6.4

For the out-of-plane deformation configuration shown in the diagram below, calculate the approximate tensile strain in the GCL and in the geomembrane. What is the factor of safety of each material if the GCL loses its hydraulic barrier integrity at 14% tensile strain and the geomembrane is LLDPE and loses its hydraulic barrier integrity at 100 percent tensile strain (recall Figure 5.4 and equation 5.4, which is in radians).

Out-of-plane deformation
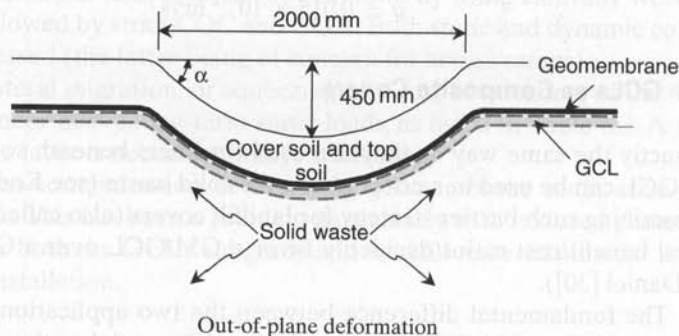
Solution: The deflected shape is used for calculations as follows:

$$\epsilon(\%) = \left\{ \frac{\tan^{-1}\left[\left(\dfrac{4L\delta}{L^2 - 4\delta^2}\right)\right]\left(\dfrac{L^2 + 4\delta^2}{4\delta}\right) - L}{L} \right\} \times 100 \quad \text{for } \delta < \frac{L}{2}$$

$$\epsilon(\%) = \left\{ \frac{\tan^{-1}\left[\left(\dfrac{4(2.0)(0.45)}{(2.0)^2 - 4(0.45)^2}\right)\right]\left(\dfrac{(2.0)^2 + 4(0.45)^2}{4(0.45)}\right) - 2.0}{2.0} \right\}(100)$$

$$\epsilon(\%) = 13.0\%$$

Thus the GCL is barely satisfactory, having FS = 14.0/13.0 = 1.1; while the GM is quite satisfactory, having FS = 100/13.0 = 7.7.

6.3.4 GCLs on Slopes

The 14 test plots—9 on 2(H)-to-1(V) slopes and 5 on 3(H)-to-1(V) slopes—described in [25] are focused on assessing the long-term internal shear strength of various types of GCLs. It is a worthwhile and on-going effort since the shear strength of hydrated bentonite is low. How low is a matter of the site-specific conditions as assessed by simulated direct shear tests (recall Table 6.1).

This issue, insofar as GCLs on slopes is concerned, is that the bentonite must either remain dry (e.g., protected between two geomembranes) or be internally reinforced. The most common methods of internal reinforcement are by needle punching or stitch bonding. Examples 6.5 and 6.6 illustrate the magnitude of the required internal strength—first with no support from above, then with overlying geosynthetics providing additional reinforcement.

Example 6.5

What is the required long-term strength of the internal reinforcement of a hydrated GCL (i.e., the needle-punched fibers or stitch-bonded yarns) to achieve a FS = 1.5 when it is placed on a 3(H)-to-1(V) slope that is 30 m long and is covered with 450 mm of well-graded sand (ϕ = 35°) weighing 17 kN/m³? Assume that no tensile strength is afforded by the upper geotextile (i.e., worst-case assumption). Also assume that the upper and lower surfaces of the GCL have sufficient interface shear strength so as to force the potential failure plane within the internal structure of the GCL. Use δ = 6° for the shear strength of the hydrated bentonite.

Solution: The formulation given in Section 3.2.7 on geogrid veneer reinforcement can be used to find the required reinforcement strength from back-calculation, based on a given value for the factor of safety. (Actually a computer program was written for the solution.) Look again at equations (3.14), (3.15), (3.17), and (3.22):

$$W_A = \gamma h^2 \left(\frac{L}{h} - \frac{1}{\sin \beta} - \frac{\tan \beta}{2} \right)$$

$$= (17.0)(0.45)^2 \left[\frac{30}{0.45} - \frac{1}{\sin 18.4} - \frac{\tan 18.4}{2} \right]$$

$$= 218 \text{ kN/m}$$

$$N_A = W_A \cos \beta$$
$$= (218) \cos 18.4$$
$$= 207 \text{ kN/m}$$

$$W_P = \frac{\gamma h^2}{\sin 2\beta}$$
$$= \frac{(17.0)(0.45)^2}{\sin 36.8}$$
$$= 5.75 \text{ kN/m}$$

$$FS = \frac{-b + \sqrt{b^2 + 4ac}}{2a}$$

where

$$a = (W_A - N_A \cos \beta - T \sin \beta) \cos \beta$$
$$= (218 - 207 \cos 18.4 - T \sin 18.4) \cos 18.4$$
$$= 21 - 0.299\, T$$

$$b = -[(W_A - N_A \cos \beta - T \sin \beta) \sin \beta \tan \phi$$
$$+ (N_A \tan \delta + C_a) \sin \beta \cos \beta$$
$$+ \sin \beta (C + W_P \tan \phi)]$$
$$= -[(218 - 207 \cos 18.4 - T \sin 18.4) \sin 18.4 \tan 35$$
$$+ (207 \tan 6 + 0) \sin 18.4 \cos 18.4$$
$$+ \sin 18.4(0 + 5.75 \tan 35)]$$
$$= -[(39.5 - 35.6 - 0.057\, T) + 8.4]$$

$$c = (N_A \tan \delta + C_a) \sin^2 \beta \tan \phi$$
$$= (207 \tan 6 + 0) \sin^2 18.4 \tan 35$$
$$= 1.52$$

When equation (3.22) is set equal to FS = 1.5 this results in the required strength of the internal reinforcement.

$$T = 51.0 \text{ kN/m}$$

Example 6.5 could certainly be modified to account for the tensile strength of the covering geotextile and perhaps other overlying geosynthetics as well. Example 6.6 illustrates this more realistic situation.

Example 6.6

Continue with the calculations in Example 6.5, taking into account that the upper geotextile of the GCL is a nonwoven needle-punched fabric with wide-width strength of 16 kN/m. Furthermore, it is overlain by a 1.5 mm thick HDPE geomembrane with a wide-width strength of 13 kN/m. Assume that strain compatibility exists and that both the upper geotextile and geomembrane are held firmly in the anchor trench at the crest of the slope.

Solution: The required strength of the internal GCL reinforcement is reduced in direct proportion to the overlying geosynthetics since they are acting as nonintentional veneer reinforcement. Thus,

$$T = 51.0 - 16 - 13$$
$$= 22 \text{ kN/m}$$

Alternatively, an FS = 1.5 (it might be considered as a reduction factor on the overlying geosynthetics) could be put on both the geotextile and geomembrane, resulting in a balanced factor of safety for each component of the system. Thus,

$$T = 51.0 - (16/1.5) - (13/1.5)$$
$$= 31.7 \text{ kN/m}$$

What remains at this point is to calculate the actual internal resisting strengths of the various needle-punched and stitch-bonded GCLs. This is a very interesting and difficult textile engineering problem, which is being investigated. Until such time as quantified answers are available, long-term laboratory shear tests [11] and field test plots [25] are providing the confidence needed to use GCLs on relatively steep slopes.

6.4 DESIGN CRITIQUE

When designing with GCLs, several factors must be kept in mind. First, we must recognize that a liquid barrier is the focal point of attention. Thus the flow rate for water containment problems and flow rate, adsorption and breakout time for solute problems are involved. For water, the situation is more straightforward due to bentonite's long history as a waterproofing material. The solute aspects are more difficult due to the complex nature of leachate and its many possible constituents.

Second, shear strength considerations (generally the bentonite is considered to be hydrated) are very important when GCLs are placed on side slopes. Direct shear testing (of both interfaces and internally) is necessary and site-specific conditions should be simulated in every way possible. Bentonite is a known material to geotechnical engineers and the superposition of geosynthetic considerations (e.g., needle-punching or stitch-bonding) should not be overwhelming. Limit equilibrium is illustrated in Section 5.6.10 for multilined slopes, and the inclusion of GCLs into the cross section is straightforward. Perhaps the greatest uncertainty in a strength design with respect to side slopes are the long-term considerations. Long-term direct shear and wide-width creep tension tests are both required if the situation warrants this feature. This is clearly the case for landfill final closures, but generally *not* the case for landfill liners. This is because solid waste will be placed against the liner system during filling of the landfill, thus providing a passive and stabilizing force.

Third, we must consider the possibility of puncture. In the geotextile chapter, a puncture analysis was provided (recall Section 2.5.4). Using this model and the puncture resistance of the GCL, a factor of safety could be formulated. However, the calculation may not be relevant. If an object punctures the GCL and the bentonite provides a seal against it, the liquid barrier function might still be adequate (recall Figure 6.7). On the other hand, if we have a GM/GCL composite liner, such a puncturing situation could be very significant. This leads directly to the importance of construction methods—that is, CQC and CQA—when using GCLs.

Finally, we must consider that the GCL will hydrate quickly and its bearing capacity against lateral squeezing is quite low [13, 31]. To avoid this situation, an adequately thick soil fill must be placed over the GCL (and covering geosynthetics if they are involved) before trafficking the site with construction equipment. This also leads directly to the importance of CQC and CQA when using GCLs.

The design process just described usually concludes with a recommended specification for the site specific conditions. While ASTM D5889 addresses the situation and provides test method guidance, it is only a template without specific property values. Table 6.5 provides more quantified information. It is a *draft* specification but one that

TABLE 6.5 DRAFT SPECIFICATION FOR GENERAL GCL APPLICATIONS

Property	ASTM Test Method	Reinforced GCL			Non-Reinforced GCL			Testing Frequency
		GT-Related	GT Polymer-Related	GM-GF-Related	GT-Related	GT Polymer-Related	GM-GF-Related	
Clay (as received)								
Swell index (ml)	D5890	24	24	24	24	24	24	50 tonnes
Fluid loss (ml/2g)[1]	D5891	18	18	18	18	18	18	50 tonnes
Geotextiles (as received)								
Cap fabric—mass per unit area (g/m²)	D5261	200	200	200	70	100	n/a/70	20,000 m²
Carrier fabric—mass per unit area (g/m²)	D5261	(4)	(4)	(4)	90	100	n/a/90	20,000 m²
Coating mass per unit area (g/m²)[2]	D5261	n/a	100	n/a	n/a	100	n/a	4,000 m²
Geomembrane/Geofilm (as received)								
Thickness[3] (mm)	D5199/D5994	n/a	n/a	0.40/0.50/0.10	n/a	n/a	0.40/0.75/0.10	20,000 m²
Density (gm/cc)	D1505/D792	n/a	n/a	0.92	n/a	n/a	0.92	20,000 m²
Break tensile strength, MD&XMD (kN/m)	D6693	n/a	n/a	n/a	n/a	n/a	6.0	20,000 m²
Break tensile strength, MD (kN/m)	D882	n/a	n/a	2.5	n/a	n/a	2.5	20,000 m²
GCL (as manufactured)								
Mass of GCL (g/m²)	D5993	4000	4050	4100	4000	4050	4100	4,000 m²
Mass of bentonite (g/m²)	D5993	3700	3700	3700	3700	3700	3700	4,000 m²
Moisture content[1] (%)	D5993	(4)	(4)	(4)	(4)	(4)	(4)	4,000 m²
Tensile str., MD (kN/m)	D6768	4.0	4.0	4.0	4.0	4.0	4.0	4,000 m²
Peel strength (N/m)	D6496	400	400	400	n/a	n/a	n/a	20,000 m²
Permeability[1] (m/sec), "or"	D5887	5×10^{-12}	5×10^{-12}	5×10^{-12}	5×10^{-11}	5×10^{-12}	5×10^{-12}	Weekly
flux[1] (m³/sec-m²),	D5887	1×10^{-8}	1×10^{-9}	1×10^{-9}	1×10^{-8}	1×10^{-9}	1×10^{-9}	Weekly
Bentonite permeability[1-5] (m/sec) (at 35 kPa)	D6766	1×10^{-9}	1×10^{-10}	1×10^{-10}	1×10^{-9}	1×10^{-10}	1×10^{-10}	Yearly
Bentonite permeability[1-5] (m/sec) (at 500 kPa)	D6766 mod.	1×10^{-10}	1×10^{-11}	1×10^{-11}	1×10^{-10}	1×10^{-11}	1×10^{-11}	Yearly
Component Durability								
Geotextile[6] (% strength retained)	D4632	65	65	n/a	65	65	n/a	Yearly
Geomembrane	D6693	n/a	n/a	GM Spec[7]	n/a	n/a	GM Spec[7]	Yearly
Geofilm/polymer treated[6] (% strength retained)	D6693	n/a	85	80	n/a	80	80	Yearly

Abbreviations: n/a = not applicable with respect to this property

(1) These values are maximum (all others are minimum).
(2) Calculated value is obtained from difference of coated fabric to as-received fabric.
(3) First value is for smooth geomembrane, second for textured geomembrane, third for geofilm.
(4) Value is both site specific and product specific and is currently being evaluated
(5) Value represents as-used bentonite permeability after permeation with a 0.1 M calcium chloride solution.
(6) Value represents the minimum percentage strength retained from the as-manufactured value after oven aging.
(7) Durability criteria should follow the appropriate specification for the geomembrane type used—i.e., GRI GM-13 for HDPE, GRI GM-17 for LLDPE or GRI GM-18 for fPP.

addresses the currently available GCLs, with the exception of polymer modified bentonites that are still emerging. The property values provided are subject to change, and substantiation work is ongoing.

6.5 CONSTRUCTION METHODS

The site-specific contract plans and specifications involving GCLs should be very detailed as to their installation. Panel layouts, as with geomembranes, should be addressed. The orientation of the overlap-seam shingling and the length of overlap must be clearly stated. It is considered good practice in GCL manufacturing to have an overlap line marked on the products for guidance in this regard. If additional bentonite (dry or paste) is to be placed in the overlapped region, it must be stated accordingly and constructed in the recommended manner. Generally, those GCLs with nonwoven needle-punched geotextiles on both sides should be treated in this manner.

The manner of placement should also be mentioned. Vehicles and equipment should never ride directly on geosynthetics of any type, including GCLs. Even though puncture might not occur, the thinning of the material will play havoc with the flow-rate calculations. This is the squeezing or bearing capacity issue mentioned previously. Once the first geosynthetic of any type, including GCLs, is placed, only lightweight units, such as all-terrain vehicles (ATVs), can be permitted. Trauger and Tewes [32] provide information on four different installation methods that are acceptable. Table 6.6 gives the description, along with advantages and disadvantages of each method. Additionally, Figure 6.10 is keyed into each of these four methods.

Storage and handling of GCLs is covered in ASTM D5888. The premature wetting of GCLs before they are covered or backfilled is often a problem. The contract documents must be clear—such as, a maximum moisture content—as to the disposition

TABLE 6.6 FIELD INSTALLATION TECHNIQUES

Installation Method	Description	Advantages	Disadvantages
Manual unroll	GCL placed on ground and moved manually.	Minimum equipment required. Applicable for confined spaces.	Low production rates; labor-intensive.
Controlled downslope release	GCL lowered downslope by slowly releasing from a harness assembly.	Applicable for slopes that are too steep for traditional equipment.	May be difficult to guide GCL as it unrolls; may be unsafe.
Stationary roll pull	Roll suspended at site perimeter; one end pulled out into areas to be lined.	Equipment can be kept out of lined area.	Modest production rates; coarser subgrades may damage underside of GCL.
Moving roll pull	One end of roll placed on ground or suspended from equipment that moves backward along area to be lined.	High production rates possible.	Equipment may damage underlying geosynthetic materials or cause rutting of subgrade surfaces.

Source: After Trauger and Tewes [32].

(a) Manual method

(b) Controlled downslope release

(c) Stationary roll pull

(d) Moving roll pull

Figure 6.10   Various acceptable methods of field deployment of GCLs.

of hydrated GCLs before covering. In a completely opposite manner to the above, the drying of GCLs has been a problem. If the GCL at its as-received moisture content dries, it will shrink and a loss of some of the overlap distance will occur. The situation may not be noticed if a geomembrane is placed over the GCL and then left exposed to summer sunlight, particularly on side slopes. In addition to the above shrinkage possibility, tensile stresses on a GCL underlying an exposed geomembrane might even give rise to further loss of overlap and even panel seperation. The issue is currently being investigated.

There are two aspects to be considered in quality control and assurance: the manufacturing and the field construction. These are referred to as MQC/MQA and CQC/CQA, respectively (see the definitions in Section 5.12.5). For MQC/MQA purposes, the specification of Table 6.5, perhaps modified to site specific conditions, should be considered.

For field CQC/CQA, many of the tests in Table 6.5 cannot be readily performed. Sampling is most difficult for GCLs and the seriousness of edge disturbance and redistribution of bentonite is yet to be resolved for the various products. Thus the search is currently for field-oriented test methods (i.e., for conformance tests), that can be done

to assure that the intended product is delivered and properly installed. Some detail in this regard is found in Daniel and Koerner [33]. A possible field permeability test has been proposed by Didier and Cazaux [34]. A guide for installation is available as ASTM D6102.

In summary, GCLs are indeed viable and true geosynthetic materials. They deserve to be included in a book such as this and to have a separate chapter devoted to them. Many applications are being developed and implemented on a regular basis, not only in the environmental containment area but also in transportation areas (highways, airfields, etc.) and obviously in the hydraulics area. As with all geosynthetic materials, the GCL market is quite mobile with new styles and products being developed on a regular basis. This vitality is considered to be a welcome asset and will hopefully be sustained into the future.

REFERENCES

1. Koerner, R. M., "Perspectives on Geosynthetic Clay Liners." In *Testing and Acceptance Criteria for Geosynthetic Clay Liners*, ASTM STP 1308, edited by Larry W. Well. ASTM, 1997, pp. 3–20.
2. Heerten, G., von Maubeuge, K., Simpson, M., and Mills, C., "Manufacturing Quality Control of Geosynthetic Clay Liners—A Manufacturers Perspective," *Proceedings of the 6th GRI Seminar, MQC/MQA and CQC/CQA of Geosynthetics*, IFAI, 1993, pp. 86–95.
3. Leisher, P. J., "Hydration and Shear Strength Behavior of Geosynthetic Clay Liners," MSCE Thesis, Drexel University, Philadelphia, PA, 1992.
4. Daniel, D. E., Shan, H.-Y., and Anderson, J. D., "Effects of Partial Wetting on the Performance of the Bentonite Component of a Geosynthetic Clay Liner," *Proceedings of Geosynthetics '93*, IFAI, 1993, pp. 1483–1496.
5. Koerner, G. R., "Comparing GCL Performance Using Rigid vs. Flexible Wall Permeameters," *Second Symposium on Geosynthetic Clay Liners*, STP1456, ASTM 2004. pp. 110–120.
6. Daniel, D. E., Bowders, J. J., and Gilbert, R. B., "Laboratory Hydraulic Conductivity Testing of GCLs in Flexible-Wall Permeameters." In *Testing and Acceptance Criteria for Geosynthetic Clay Liners*, ASTM STP 1308, edited by Larry W. Well. ASTM, 1997, pp. 208–228.
7. Estornell, P., and Daniel, D. E., "Hydraulic Conductivity of Three Geosynthetic Clay Liners," *Journal of Geotechnical Engineering*, ASCE, vol. 118, no. 10, 1992, pp. 1592–1606.
8. LaGatta, M. D., "Hydraulic Conductivity Tests on Geosynthetic Clay Liners Subjected to Differential Settlement," MSCE Thesis, University of Texas, Austin, TX, 1992.
9. Wilson-Fahmy, R. G., Koerner, R. M., and Fleck, J. A., "Unconfined and Confined Wide-Width Testing of Geosynthetics," *ASTM STP 1190*, edited by S. J. Cheng. ASTM, 1993, pp. 44–63.
10. Koerner, R. M., Koerner, G. R., and Eberlé, M. A., "Out-of-Plane Tensile Behavior of Geosynthetic Clay Liners," *Geosynthetics International*, vol. 3, no. 2, 1996, pp. 277–296.
11. Koerner, R. M., Soong, T.-Y., Koerner, G. R., and Gontar, A., "Creep Testing and Data Extrapolation of Reinforced GCLs," *Proceedings of the GRI-14 Conference*. GII Publications, December 2000, pp. 189–210.
12. von Maubeuge, K. P., and Lucas, S. N., "Peel and Sheer Test Comparison and Geosynthetic Clay Liner Shear Strength Correlation." *Proceedings on Clay Geosynthetic Barriers*, edited by H. Zanzinger, R. M. Koerner, and E. Gartung. A. A. Balkema, 2002, pp. 104–110.
13. Koerner R. M., and Najero D., "On the Bearing Capacity of Hydrated GCL's," *Journal of Geotechnical and Geoenvironmental Engineering*, vol. 121, No. 1, 1995, pp. 82–87.
14. Daniel, D. E., Trautwein, S. J., and Goswami, P. K., "Measurement of Hydraulic Properties of Geosynthetic Clay Liners Using a Flow Box." In *Testing and Acceptance Criteria for Geosynthetic Clay Liners*, ASTM STP 1308, edited by Larry W. Well. ASTM, 1997, pp. 196–207.

15. Kraus, J. B., Benson, C. H., Erickson, A. E., and Chamberlain, E. J., "Freeze-Thaw Cycling and Hydraulic Conductivity of Bentonite Barriers," *Journal of Geotechnical and Geoenvironmental Engineering* ASCE, vol. 123, no. 3, 1997, pp. 229–238.

16. Boardman, B. T., and Daniel, D. E., "Hydraulic Conductivity of Desiccated Geosynthetic Clay Liners," *Journal of Geotechnical and Geoenvironmental Engineering*, vol. 122, no. 3, 1996, pp. 204–208.

17. Koerner, R. M., and Daniel, D. E., "A Suggested Methodology for Assessing the Technical Equivalency of GCLs to CCLs." In *Geosynthetic Clay Liners*, edited by R. M. Koerner, E. Gartung, and H. Zanzinger. A. A. Balkema, 1995, p. 73–100.

18. Giroud, J.-P., Badu-Tweneboah, K., and Soderman, K. L., "Comparison of Leachate Flow Through Compacted Clay Liners and Geosynthetic Clay Liners in Landfill Liner Systems," *Geosynthetics International*, vol. 4, nos. 3–4, 1997, pp. 391–431.

19. Mueller, W., and Jakob, I., "Comparison of Oxidation Stability of Various Geosynthetics," *Proceedings of EuroGeo II Conference*, Bologna, Italy, 2000, pp. 449–454.

20. Hsuan, Y. G., and Koerner, R. M., "Durability and Lifetime of Polymer Fibers with Respect to Reinforced Geosynthetic Clay Barriers," *Proceedings Clay Geosynthetic Barriers*, edited by H. Zanzinger, R. M. Koerner, and, E. Gartung. A. A. Balkema, 2002, 73–86.

21. Thomas, R. W., "Thermal Oxidation of Polypropylene Geotextiles Used in a Geosynthetic Clay Liner," *Proceedings on Clay Geosynthetic Barriers*, edited by H. Zanzinger, R. M. Koerner, and, E. Gartung. A. A. Balkema, 2002, 105–110.

22. Scheu, C., Johannssen, K., and Soatloff, F., "Nonwoven Bentonite Fabrics—A New Fiber Reinforced Mineral Liner System," *4th International Conference on Geotextiles, Geomembranes, and Related Products*, edited by Den Hoedt. A. A. Balkema, 1990, pp. 467–472.

23. Heerten, G., and List, F., "Rehabilitation of Old Liner Systems in Canals," *4th International Conference on Geotextiles, Geomembranes, and Related Products*, edited by Den Hoedt. A. A. Balkema, 1990, pp. 453–456.

24. Othman, M. A., Bonaparte, R., and Gross, B. A., "Preliminary Results of Study of Composite Liner Field Performance," *Journal of Geotextiles and Geomembranes*, vol. 15, nos. 4–6, 1997, pp. 289–312.

25. Koerner, R. M., Carson, D. A., Daniel, D. E., and Bonaparte, R., "Current Status of the Cincinnati GCL Test Plots," *Journal of Geotextiles and Geomembranes*, vol. 15, nos. 4–6, 1997, pp. 313–340.

26. Rowe, K., and Orsini, C., "Internal Erosion of GCLs Placed Directly Over Fine Gravel," *Proceedings on Clay Geosynthetic Barriers*, edited by H. Zanzinger, R. M. Koerner, and E. Gartung, A. A. Balkema, 2002, 199–208.

27. Wilson-Fahmy, R. F., and Koerner, R. M., "Leakage Rates Through Holes in Geomembranes Overlying Geosynthetic Clay Liners," *Proceedings on Geosynthetics 95*, IFAI, 1995, pp. 655–668.

28. Giroud, J.-P., and Bonaparte, R., "Leakage Through Liners Constructed with Geomembranes. Part II. Composite Liners," *Journal of Geotextiles and Geomembranes*, vol. 8, no. 2, 1989, pp. 71–112.

29. Koerner, R. M., and Daniel, D. E., *Final Covers for Solid Waste Landfills and Abandoned Dumps*, New York: ASCE Press, 1997.

30. Koerner, R. M., and Daniel, D. E., "Better Cover-Ups," *Civil Engineering*, ASCE, 1992, pp. 55–57.

31. Fox, P. J., DeBattista, D. J., and Chen, S.-H., "A Study of the CBR Bearing Capacity Test for Hydrated Geosynthetic Clay Liners." In *Testing and Acceptance Criteria for Geosynthetic Clay Liners, ASTM STP 1308*, edited by L. W. Well. ASTM, 1997, pp. 251–264.

32. Trauger, R., and Tewes, K., "Design and Installation of a State-of-the-Art Landfill Liner System," *Proceedings of GCL Conference*, 1995, Nuremberg, Germany, pp. 175–182.

33. Daniel, D. E., and Koerner, R. M., "MQC/MQA and CQC/CQA of Waste Containment Liner and Cover Systems," *U.S. EPA Technical Resource Document*, EPA/600/R-93/182 (2nd Edition available through ASCE Press, 2005).

34. Didier, G., and Cazaux, D., "Field Permeability Measurement of Geosynthetic Clay Liners," *Proceedings on Geosynthetics: Applications, Design and Construction*, edited by M. B. deGroot, G. den Hoedt, and R. J. Tremaat. A. A. Balkema, 1996, pp. 837–843.

PROBLEMS

6.1. Regarding clay mineral soils (from a mineralogical perspective):
   (a) Sketch the chemical structure of montmorillonite clay.
   (b) Compare this structure to kaolinite and illite clays.
   (c) How does bentonite clay relate to the clay soils in parts (a) and (b)? What is its background and past usage?

6.2. Most bentonite clay deposits in Wyoming and North Dakota are sodium bentonites. Elsewhere in the world, there are large deposits of calcium bentonite clay.
   (a) What is the difference between sodium and calcium bentonite clays?
   (b) How does one sodium activate a calcium clay?
   (c) What is the permeance of such an activation process?

6.3. Some GCLs are made from bentonite powder and others from bentonite granules. What are the pros and cons of each?

6.4. If the moisture content of an as-received GCL is 18.5% based on the measured values of $W_w = 28.1$ g and $W_s = 152$ g, using dry weight (as in standard geotechnical engineering practice), what is its moisture content based on wet weight?

6.5. Describe how anions and cations in the hydrating liquid of a GCL might affect hydration behavior. How do you think this would affect its internal shear behavior?

6.6. The wide-width tension behavior of both GCLs shown in Figure 6.6 give little increase due to the effect of lateral confinement. What is the main contributing component in these GCLs that resulted in this lack of response?

6.7. For the two wide-width tensile response curves shown in Figure 6.6, there is a post-peak response that continues, albeit at lower strength, out to a 50 to 60% strain. What is the main contributing component in these GCLs that resulted in this response?

6.8. Regarding the internal direct shear tests shown in Table 6.1:
   (a) The distilled water free swell tests in GCLs 1 and 4 gave a zero friction angle. Why is this the case?
   (b) In the same tests, GCLs 2 and 3, which are both needle-punched products, give higher but different values (10 and 23° respectively). Why is this the case and what are the possible reasons for the differences in the needle-punched products?
   (c) Constrained swell tests in this same series give increases of 16, 21, 14, and 19°, respectively (over the free swell friction angle results). Why is this the case?
   (d) In comparison to parts (a)–(c), the diesel fuel tests give tremendously high friction angles in both free and constrained swell conditions, 24 to 51°. Why is this the case?

6.9. With respect to the GCL to CCL equivalency summary in Tables 6.3 and 6.4, discuss the following issues.
   (a) Intimate contact is product-specific. Why? Which are the preferred GCLs in this situation?
   (b) Water breakout time is product-specific. Which is the preferred GCL in this situation?
   (c) Slope stability is product-specific. Why?
   (d) Erosion potential is product-specific and site-specific. Why?
   (e) Lateral squeezing is product-specific. Why is it important?
   (f) Subgrade condition is site-specific. Why?
   (g) Why are CQC/CQA procedures significant in such an equivalency comparison?

6.10. The puncture resistance of a GCL in Tables 6.3 and 6.4 is noted as being probably not equivalent to a CCL. Why is this the case and why may it not be significant?

6.11. Calculate the water flux ratios of a GCL to CCL, as per Example 6.1 (Section 6.3.1) for total hydraulic heads of 8, 4 (the example), 2, 1, 0.5, 0.30 (the common regulatory limit), and 0.15 m, and graph the result of each calculation.

6.12. Calculate the tensile strain in a GCL as it deforms in an out-of-plane mode as per Example 6.4 (Section 6.3.3) for deformations of 100, 300, 450 (the example), and 1000 mm and graph the resulting values. The radius of the depression remains constant at 1.0 m.

6.13. Recalculate the required long-term shear strength of the internal reinforement of a GCL presented in Example 6.5 (Section 6.3.4) for the following cover soil thickness: 300, 600, and 900 mm, and graph the results along with that for 450 mm (the example).

6.14. What long-term internal reinforcement concerns of GCLs might be expressed for the following:
   (a) Needle-punched types
   (b) Stitch-bonded types
   (c) Nonreinforced types when placed between two geomembranes

6.15. Why should construction equipment be prohibited from traveling directly on a deployed GCL? Is the situation more critical with certain GCLs? What is the effect on an equivalency calculation for those GCLs that may have thinned?

6.16. What is the flow rate (water flux) through an intact GCL having a permeability of 5×10^{-12} m/s under 300 mm of total head difference if it is originally 10 mm thick? What is it if it has been thinned during construction and placement to 8 mm and then to 5 mm and to 2 mm? Plot the resulting response curve.

6.17. Regarding the GCL specification of Table 6.5, describe the following:
   (a) A GT polymer-related product.
   (b) A geofilm-related product
   (c) A geomembrane-related product

6.18. Why is the increase in permeability of the D6766 testing in Table 6.5 higher at 35 kPa than at 500 kPa?

6.19. What are the implications for a GCL that is deployed and then hydrates before it can be covered?

6.20. The loss of seam overlap in the field after deployment (e.g., by shrinkage) may be a concern in certain unique situations. How can GCL seams be given structural integrity? In other words, list and describe some possible GCL seam-joining methods or some newer GCLs that have internal structural stability.

7

Designing with Geopipes

7.0   INTRODUCTION

The traditional materials used for the underground pipeline transmission of water, gas, oil, and various other liquids have been steel, cast iron, concrete, and clay. These pipe materials are classified as *rigid* and are strength-related as far as their material behavior is concerned. Significant inroads into these markets are, however, being made by polymers in the form of plastic pipe, and they certainly deserve a separate chapter in a book devoted to geosynthetic materials. Recall Table 1.10 in this regard. Pipes made from polymeric materials are classified as *flexible* and are deflection-related as far as their material behavior is concerned. This chapter deals with geopipes — that is, plastic pipe placed beneath the ground surface and subsequently backfilled.

There are a number of polymer resins used in the fabrication of plastic pipe. Currently they are high density polyethylene (HDPE), polyvinyl chloride (PVC), polypropylene (PP), polybutylene (PB), acrylonitrile butadiene styrene (ABS), and cellulose acetate butyrate (CAB). They all entered the market as solid wall constant-thickness pipes of relatively small diameter. For example, every hardware store handles small diameter PVC pipe and fittings for household water and drainage systems for do-it-yourselfers. Today's plastic pipes, however, can be very large in diameter and very thick in their wall dimension (see Figure 7.1). Advanced extrusion and seaming processes have also led to differing types of wall sections consisting of ribs, cores, and corrugated profiles of a wide variety of cross-sectional shapes and sizes. These pipes are collectively referred to as profiled, ribbed, or corrugated wall pipes. Additionally, many applications such as agriculture drains and leachate collection systems require holes, slots, or other types of perforations through the wall section to allow for the inflow of fluid. Geopipe of the types just mentioned are being used at a tremendously increasing rate. They offer the user many significant advantages. They are low in initial cost, lightweight, and easy to install and to join together. They also have numerous prefabricated appurtenances and an excellent flow regime and durability.

As with all pipe materials, there are a number of potential failure modes of geopipe that must be assessed by the design engineer. They include the following, each of which has had attention drawn to it due to past problems and current concerns:

- Excessive pipe deflection due to improper backfilling, leading to excessive deflection or localized material overstressing
- Seam separation of joined pipe ends due to ring compression stress
- Wall crushing due to high overburden stress
- Wall buckling due to external pressure and/or internal vacuum
- Impact cracking of pipe in extremely cold environments
- Stress cracking, both slow crack growth and rapid crack propogation
- Melting or burning due to accidental or intentionally set fires.

Within this list of concerns, there are three areas in need of a focused discussion: (1) properties, (2) design, and (3) construction. These are the topics in this chapter.
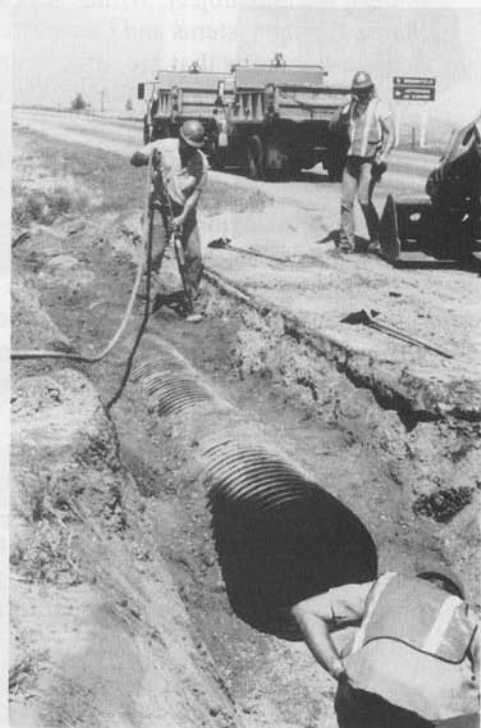
Figure 7.1 Plastic pipes used in below-ground construction. (Compliments of Phillips Driscopipe, Carlon, and ADS)

It should be clearly recognized that plastic pipe is an extremely large and well-developed area with respect to the other types of geosynthetic materials. There are large numbers of books, reports, test methods, manufacturers' guides, and so on that are available. In particular, note that the Plastic Pipe Institute (PPI) is very active in providing a wealth of information through its own literature and that of its member companies. A joint conference with other plastic pipe groups provides considerable information [1]. To make the chapter manageable in size, it will focus only on gravity flow situations involving either profiled or solid wall pipe. This arbitrary selection eliminates water and gas pipelines, which function under positive pressure and are the focus of many other publications.

7.1 GEOPIPE PROPERTIES AND TEST METHODS

Various test methods for evaluating the properties of plastic pipe are available from standardization organizations throughout the world. Among the most active is the American Society for Testing and Materials (ASTM), which has several specific committees on the subject. Within ASTM, the main committees are Committee F-17 on Plastic Piping Systems and Committee D20 on Plastics. Other organizations have plastic pipe standards that are often oriented toward specific application areas. For example, the American Water Works Association (AWWA) has standards oriented toward drinking water pipe conveyance, the Underwriters Laboratory (UL) has standards for cable shielding, the National Sanitation Foundation (NSF) has standards for waste water pipe conveyance, and AASHTO has standards and specifications for highway drainage applications. Also note that the PPI has general plastic pipe standards for various applications.

For the sake of uniformity with other chapters in this book, we will subdivide this section on properties and test methods not by application (since geopipes always act in a drainage function), but by the category that best fits the various tests into a design mode: physical, mechanical, chemical, biological, and thermal properties, followed by the relevant specifications.

7.1.1 Physical Properties

Physical properties have to do with the pipe in the as-received and nonstressed state. These properties are important for proper identification, for comparing one style or product with another, and for conformance and quality assurance purposes.

Wall Thickness.   The thickness of smooth wall constant-thickness pipe can be measured according to ASTM D2122. It is a straightforward measurement that uses a caliper accurate to 0.02 mm. The value reported is the minimum wall thickness of the pipe at any cross section. Wall thicknesses and tolerances for HDPE pipe are given in ASTM D2447.

When dealing with profiled pipe (either corrugated or spiral wound) the situation is more difficult. The number of variations in this regard are enormous; Figure 7.2
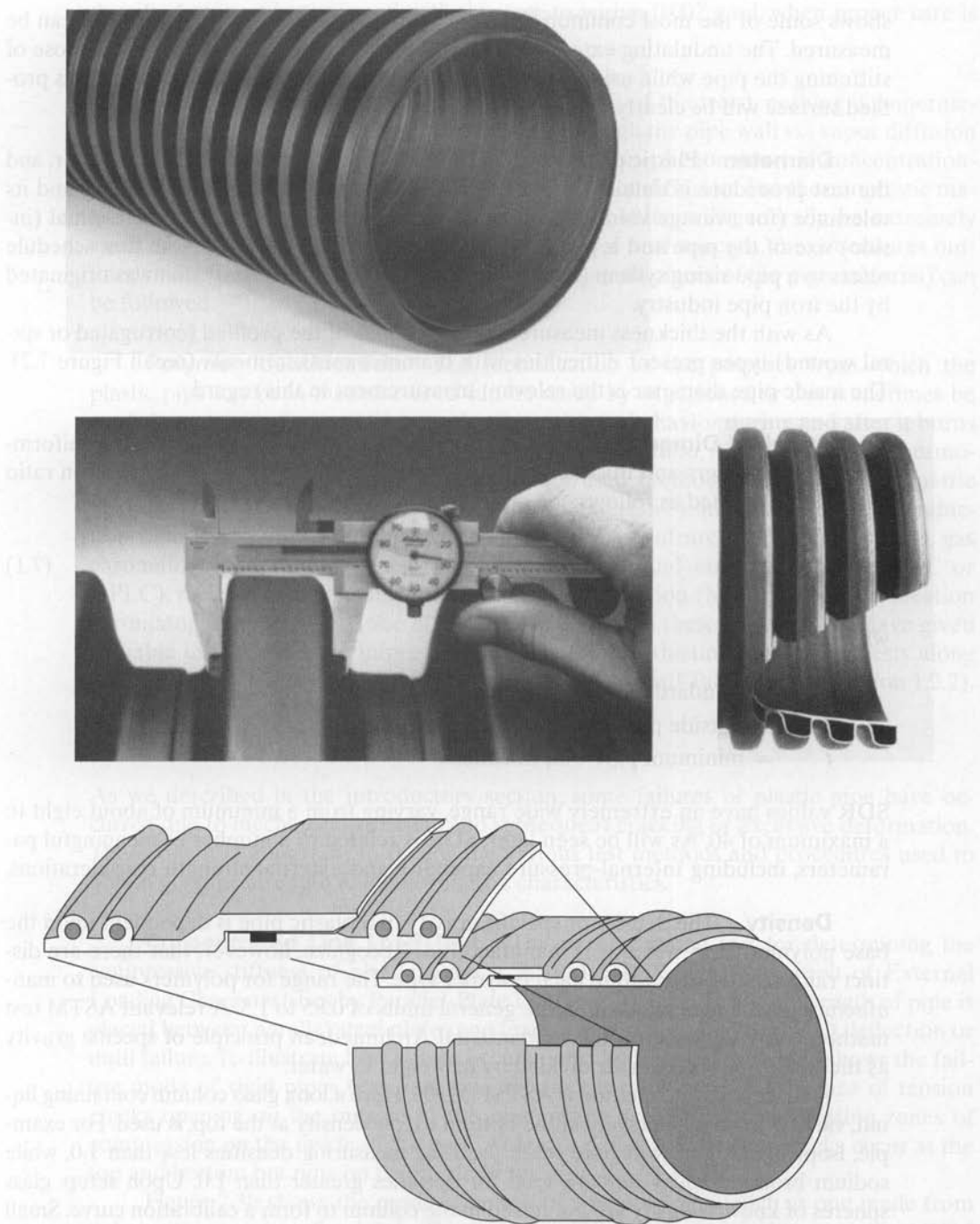
Figure 7.2 Various cross sections of profiled geopipe used for a variety of drainage applications. (Compliments of ADS, Spirolite, and Hancor)

shows some of the most common types. At minimum, the inner liner thickness can be measured. The undulating external surface of the pipe is fabricated for the purpose of stiffening the pipe while using a minimum amount of polymer. The effects of this profiled surface will be clearly evidenced in Section 7.1.2, on mechanical testing.

Diameter.   Plastic pipes are generally measured by their outside diameter, and the test procedure is detailed in ASTM D2122. The average outside diameter and its tolerance (for average values and for out-of-roundness) is based on the nominal (inside) size of the pipe and is given by "schedule" in ASTM D2447. Note that schedule refers to a pipe sizing system (outside diameter and wall thickness) that was originated by the iron pipe industry.

As with the thickness measurements, geopipes of the profiled (corrugated or spiral wound) types present difficulties with diameter measurements (recall Figure 7.2). The inside pipe diameter is the relevant measurement in this regard.

Standard Dimension Ratio.   Of importance in comparing different uniform-wall pipe diameters and thicknesses with one another is the standard dimension ratio (SDR). It is defined as follows:

$$SDR = \frac{D}{t} \tag{7.1}$$

where

SDR = standard dimension ratio,
D = outside pipe diameter, and
t = minimum pipe wall thickness.

SDR values have an extremely wide range, varying from a minimum of about eight to a maximum of 40. As will be seen later, SDR is related to a number of meaningful parameters, including internal-pressure capability and external strength considerations.

Density.   The density or specific gravity of a plastic pipe is dependent upon the base polymer from which it is manufactured. Recognize, however, that there are distinct ranges of density within each polymer type. The range for polymers used to manufacture plastic pipe falls within the general limits of 0.85 to 1.5. A relevant ASTM test method is D792, based on the fundamental Archimedean principle of specific gravity as the weight of object in air divided by its weight in water.

A more accurate method is ASTM D1505. Here a long glass column containing liquid, varying from high density at the bottom to low density at the top, is used. For example, isopropanol and water are often used for measuring densities less than 1.0, while sodium bromide and water are used for densities greater than 1.0. Upon setup, glass spheres of known density are immersed in the column to form a calibration curve. Small pieces of the test specimen weighing about 20 to 30 mg are then dropped into the column after they have been properly cleaned of surface impurities. Their equilibrium position within the column is located and used with the calibration curve to find the unknown

density. Accuracy is very good with this test, to within 0.002 g/ml, when proper care is taken; see Section 5.1.2.

Vapor Transmission.   In the absolute sense of the word, nothing is impermeable. As such, liquids within a pipe can diffuse through the pipe wall via vapor diffusion and recondense on the other side. This permeation phenomenon is concentration-driven and is generally assumed to obey Fick's law of diffusion. For thermoplastic materials of the type and thickness of geopipes, the value will generally be extremely small. Nevertheless, if water vapor or solvent vapor is of concern, the procedures outlined in Section 5.1.2 (using a plaque made from small pieces of the pipe material) can be followed.

Polymer Identification.   The identification of the polymer from which the plastic pipe has been manufactured can be made by experience or can sometimes be made by putting a flame to the sample and noting its behavior during and after it burns (recall Table 1.4). For a much more definitive identification, however, various thermochemical tests are required. The most widely used methods are thermogravimetric analysis (TGA), differential scanning calorimetry (DSC), including oxidative induction time (OIT), thermomechanical analysis (TMA), infrared spectroscopy (IR), gas chromatography (GC), regular or high pressure liquid chromatography (RLC or HPLC), melt index (MI), molecular weight determination (MW), and gel permeation chromatography (GPC). Halse et al. [2] have described these methods and have given valuable insight as to the information obtained in conducting the various tests along with the tests' major advantages and disadvantages (recall Table 1.5 and Section 1.2.2).

7.1.2 Mechanical Properties

As we described in the introductory section, some failures of plastic pipe have occurred due to mechanical stressing and subsequent cracking or excessive deformation. Therefore, it is important to review the various test methods and procedures used to obtain geopipe strength and deformation characteristics.

Concentrated Line Load Test.   The most common test for determining the compressive stiffness of plastic pipes is ASTM D2412 "Determination of External Loading Characteristics by Parallel-Plate Loading." A short (150 mm) length of pipe is placed between parallel steel plates and loaded in compression to a given deflection or until failure. To illustrate how failure occurs, consider Figure 7.3a, which shows the failure mode of rigid pipes (e.g., concrete or clay pipes). Note the existence of tension cracks opening on the outside of the pipe, which accompanies contrasting zones of compression on the inside of the pipe. At larger deflection, tension cracks occur at the top and bottom but now on the inside of the pipe.

Figure 7.3b shows the mode of failure of a flexible pipe (such as one made from polymers) in an *unconfined* state. This is the condition of the pipes when tested in ASTM D2412. Note that the plastic pipe does not crack, but instead deforms and eventually buckles when the deflection becomes excessive. While the entire load-versus-deflection

(a) Rigid pipe brittle failure mode

(b) Unconfined flexible pipe buckling failure mode

(c) Confined flexible pipe behavior
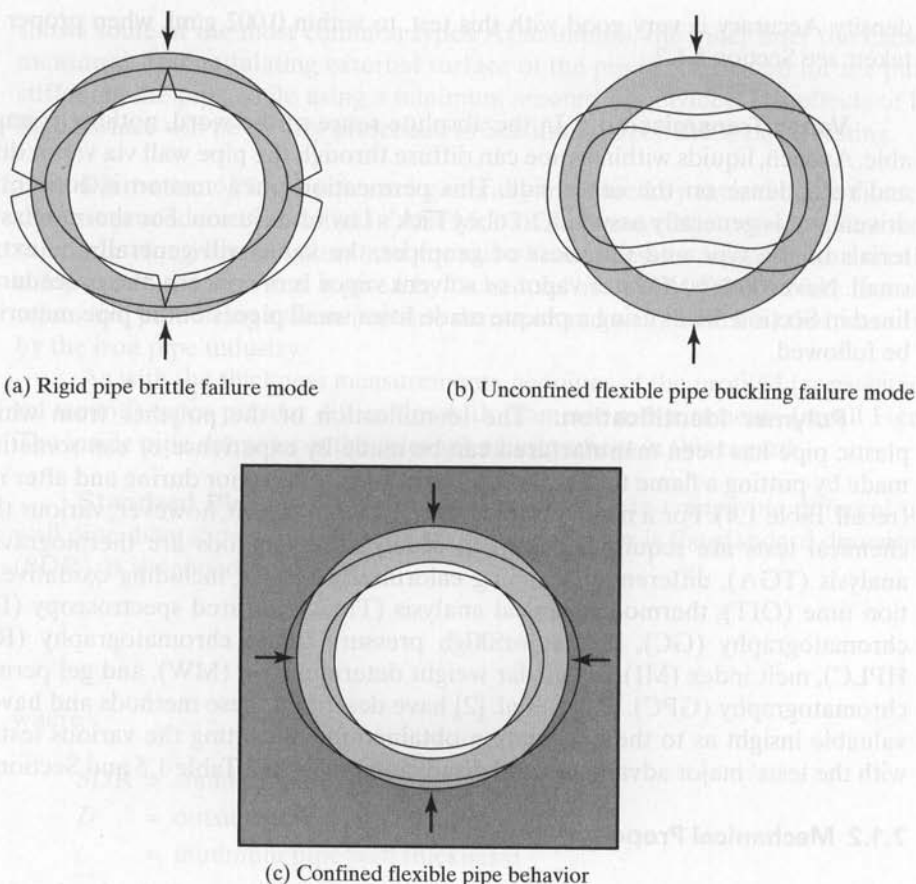
Figure 7.3 Behavior of rigid-versus-flexible geopipe due to external loads.

curve is interesting to observe, pipe stiffness is usually calculated at either 5 or 10% deflection. The relevant equations for pipe deflection, pipe stiffness, and stiffness factor calculations according to D2412 are as follows:

$$P = \frac{y}{d}(100) \tag{7.2}$$

where

P = pipe deflection (%),

y = measured change of inside diameter (deflection) (m), and

d = initial inside pipe diameter (m).

$$PS = \frac{F}{y} \tag{7.3}$$

where

PS = pipe stiffness (kPa),
F = force per unit length of pipe (kN/m), and
y = deflection (m).

Also,

$$SF = 0.149\, r^3\, (PS) \tag{7.4}$$

where

SF = stiffness factor (kPa-m^3), and
r = midwall radius (m).

Note that this plate load test is clearly of the index variety because when in service the pipe will be confined by the backfill soil, as shown in Figure 7.3c. The passive pressure exerted by the soil will be seen to be extremely effective and very necessary in the proper functioning of flexible plastic pipes to help support the imposed vertical loads.

The complementary theoretical equivalents to the pipe stiffness terms just mentioned are as follows:

$$\text{Stiffness factor SF} = EI \tag{7.5}$$
$$\text{Pipe stiffness PS} = 6.71\, EI/r^3 \tag{7.6}$$
$$\text{Ring stiffness RS} = EI/r^3 \text{ (sometimes } EI/D^3) \tag{7.7}$$

where

E = modulus of elasticity (kPa),
I = moment of inertia of pipe cross section per unit length (m^3),
r = mean radius of pipe (m), and
D = mean diameter of pipe (m).

The values of E, I, r, and D for commonly used pipe materials and sizes are found in various pipe manufacturers' literature, technical brochures, and Web sites.

   Distributed Load Tests.   In order to better simulate the effects of soil bearing beneath the pipe and load spreading above the pipe, several variations of ASTM D2412 have been developed. Figure 7.4a–d, illustrates some of these variations. Note, however, that their past use has generally been with rigid pipes and such testing is not common with flexible polymeric pipes. For flexible plastic pipes of the type described in this chapter, the complete lateral confinement of the soil should be considered. Watkins and Reeve [3] have performed tests, as shown in Figure 7.4e. Here the pipe is completely confined in its simulated environment and loaded accordingly.

The pressure-versus-deflection response is very different than that with nonconfined boundary conditions. Furthermore, there is even a meaningful difference in response between backfill soils at 75 and 85% relative density (see Figure 7.4f). This type of simulated performance test illustrates the importance of uniform backfill around the entire circumference of the pipe. Unfortunately, this type of test is not regularly used nor standardized at this time.

   Hydrostatic Pressure Test.   This test method, ASTM D1598, consists of subjecting samples of thermoplastic pipe or reinforced thermosetting-resin pipe to a constant internal pressure until loss of pressure, rupture, or ballooning of the pipe occurs. The data obtained from the test are subsequently used to establish stress-versus-failure time relationships, from which the hydrostatic design stress can be obtained.

(a) Two-edge bearing   (b) Three-edge bearing

(c) Minnesota bearing   (d) Sand bearing
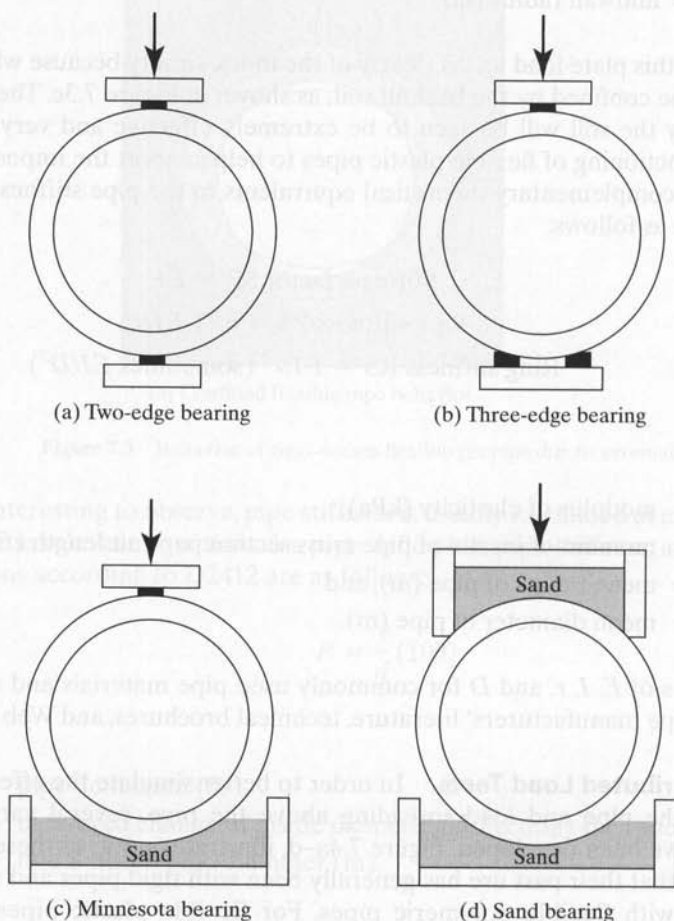
Figure 7.4 Various types of pipe load test configurations and selected results. (Parts [e] and [f] after Watkins and Reeve [3])
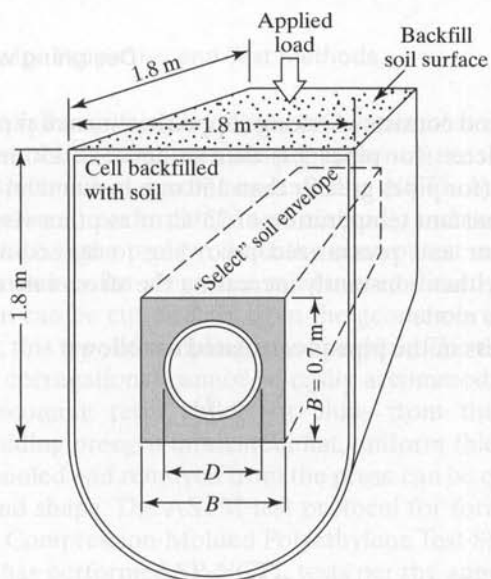
(e) Confined soil bearing
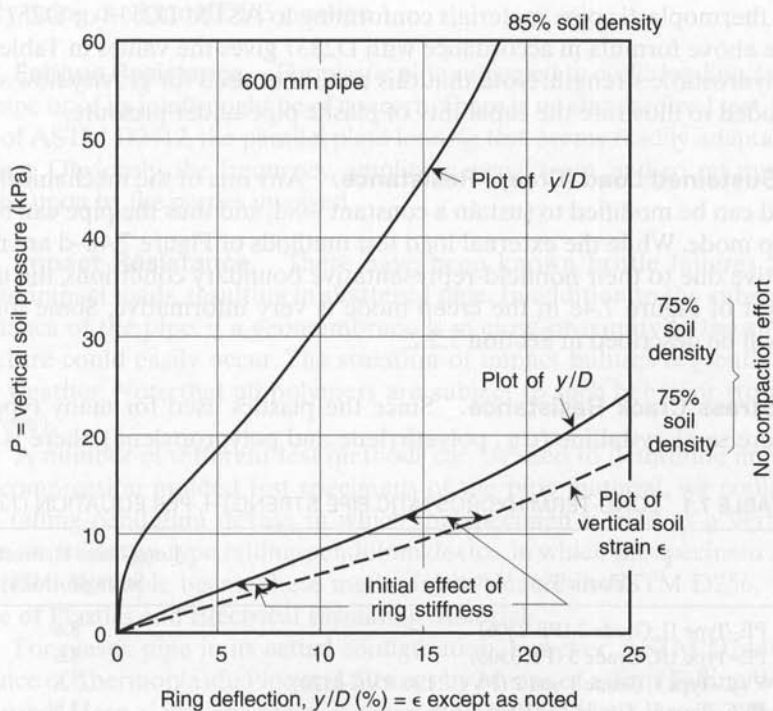
(f) Confined soil bearing results

Figure 7.4 (Continued)

679

The test method consists of taking capped sections of pipe having lengths that are five times the diameter (for pipes less than or equal to 150 mm in diameter) or three times the diameter (for pipes greater than 150 mm in diameter), and immersing them in a water bath at a constant temperature of 23°C, or as otherwise agreed upon. The pipes are filled with water and pressurized according to agreed-upon sequences; the two major options are either constantly increasing the stress rate or maintaining the stress over time in a creep mode.

The hoop stress in the pipe is calculated as follows:

$$\frac{2S}{P} = \frac{D}{t} - 1 \tag{7.8}$$

where

S = hydrostatic design stress (MPa),
P = internal pressure rating that includes a factor of safety (MPa),
D = average outside diameter (mm), and
t = minimum wall thickness (mm).

Using thermoplastic pipe materials conforming to ASTM D2513 or D2517 and analyzing the above formula in accordance with D2837 gives the values in Table 7.1 for long-term hydrostatic strength. Note that this test is not used for gravity flow situations but is included to illustrate the capability of plastic pipe under pressure.

Sustained Load (Creep) Resistance.   Any one of the mechanical tests just described can be modified to sustain a constant load, and thus the pipe can be forced into a creep mode. While the external load test methods of Figure 7.4a–d are not overly informative due to their nonfield-representative boundary conditions, the uniform pressure test of Figure 7.4e in the creep mode is very informative. Some long-term field tests will be described in Section 7.2.2.

Stress Crack Resistance.   Since the plastics used for many types of flexible pipes are semicrystalline (e.g., polyethylene and polypropylene), there is a propensity

TABLE 7.1   LONG-TERM HYDROSTATIC PIPE STRENGTH, PER EQUATION (7.8)

Plastic Pipe Material	Long-Term Hydrostatic Strength (MPa)
PE–Type II, Grade 3 (PE 2306)	8.6
PE–Type III, Grade 3 (PE 3306)	8.6
PVC–Type I, Grade 1 and 2 (PVC-1120, PVC-1120)	27.6
PVC–Type II, Grade 1 (PVC-2110)	13.8
ABS – Type I, Grade 2 (ABS-1210)	13.8
CAB–MH (CAB-MH08)	11.0
CAB–S (CAB-S004)	5.5

for a brittle type failure, which is called *environmental stress cracking* or simply *stress cracking*. The tests used to evaluate this phenomenon are the bent strip test covered in Section 5.1.3 (which is not recommended), the NCTL test covered in Section 5.1.3 (which is the preferred performance test method), and the SP-NCTL test covered in Section 5.1.3 (which is the preferred quality control test method). In all of these tests, the material comes in a flat sheet that can be used directly. For example, a dumbbell-shaped specimen can be cut directly from the geomembrane sheet for its subsequent testing. For pipe, this type of sampling is not possible. The thickness, curvature, and surface detail (like corrugations) cannot be easily accommodated. As a result it is necessary to melt incoming resin pellets or chips from the manufactured pipe in a compression molding press to fabricate a flat, uniform thickness sheet or *plaque* that, when properly cooled and removed from the press, can be die-cut into the required test specimen size and shape. The ASTM test protocol for forming these sheets is D1928, "Preparation of Compression-Molded Polyethylene Test Sheets and Test Samples."

Hsuan [4] has performed SP-NCTL tests per the appendix to ASTM D5397 on a number of HDPE pipe resins and chips. The results are presented in Table 7.2 for loadings at 10 and 20% of yield stress. The data show that the time for failure to occur in a brittle mode is significantly different for the various materials evaluated. Although the significance of this data with respect to stress crack performance in the field is still being developed, the results clearly show that a wide variety of different resins are currently being used for HDPE geopipe.

Fatigue Resistance.   For plastic pipe subjected to cyclic loading, fatigue failure of the pipe or of its joints might be of concern. There is no standardized test, but a modification of ASTM D2412, the parallel plate loading test, seems readily adaptable to dynamic loading. Obviously, the frequency, amplitude, wave form, and so on must be mutually agreed upon by the parties involved.

Impact Resistance.   There have been known brittle failures of plastic pipe due to impact loads, resulting in shattered pipe. In addition to the subsequent nonperformance of the pipe, if a geomembrane is in close proximity to the shattered pipe, a puncture could easily occur. The situation of impact failures is greatly aggravated in cold weather. Note that all polymers are subject to such behavior (to widely varying degrees).

A number of different test methods can be used to determine impact resistance. For compression molded test specimens of the pipe material, we could use an Izod-type falling-pendulum device, in which the specimen is held as a vertical cantilever beam, or a Charpy-type falling-pendulum device, in which the specimen is supported as a horizontal simple beam. These methods are treated in ASTM D256, "Impact Resistance of Plastics and Electrical Insulating Materials."

For plastic pipe in its actual configuration, however, ASTM D2444, "Impact Resistance of Thermoplastic Pipe and Fittings by Means of a Tup (Falling Weight)," is usually used. Here a test specimen is supported on a V-block or on a flat plate with a seating groove in it. The pipe specimen is usually of a length equal to its diameter but not less than 150 mm. Temperature control is important, and the procedure usually calls for the pipe to be maintained at a subfreezing temperature and then rapidly

TABLE 7.2   SINGLE POINT-NOTCHED CONSTANT TENSION LOAD (SP-NCTL) TEST
DATA ON RESINS USED FOR GEOPIPE PER ASTM D5397

Resin Code	Resin Description	Failure Time at 20% Yield Stress	Failure Time at 10% Yield Stress
Virgin Resins			
1	HDPE-A	1.8	16
2	HDPE-B	7.3	80
3	MDPE-A	3000	–
5	HDPE-C	553	4000[1]
6	HDPE-D	1.4	14
7	HDPE-E		35
8	HDPE-F		25
9	HDPE-G		38
10	HDPE-H		72
11	HDPE-I		21
12	100% rework HDPE-J		850[1]
Blended Resins with Post-Consumer Recycle (PCR)			
1	HDPE-K with PCR (I)	0.8	3.4
2	HDPE-L with PCR (II)	0.9	6
3	HDPE-M with 25% PCR (III)	3.3	41
4	HDPE-N with PCR (IV)		260[1]
5	HDPE-O with PCR (V)		1400[1]
6	HDPE-J with 50% PCR (VI)		960[1]
7	HDPE-C with 25% PCR (VII)		930[1]
8	HDPE-C with 50% PCR (VII)		263
9	HDPE-C with 75% PCR (VII)		75
12	HDPE-H with 25% PCR (VII)		55
13	HDPE-H with 50% PCR (VII)		34
14	HDPE-H with 75% PCR (VII)		24
16	100 PCR (VII)		21
17	HDPE-P with 25% PCR (VIII)		27
18	HDPE-P with 50% PCR (VIII)		24
19	HDPE-P with 75% PCR (VIII)		16

1. Data obtained by extrapolation.
Source: After Hsuan [4].

removed from the chamber and tested. A *tup* (that is, a falling weight) of 2.5, 5, 10, or 15 kg is then dropped within a tube of sufficient length to cause impact failure. The tube is approximately 4 m tall and must be aligned so that chattering of the falling tup does not occur, or, at least, is minimized. The tup nose detail is important and the test method allows for three different types. One type is tapered to a 13 mm radius, another is hemispherical with a 50 mm radius, and the third has a protruding tip of 6 mm at its end.

Twenty test specimens are initially required to determine the proper combination of the above variables to cause the pipe to fail and then up to 150 test specimens are required to generate the required statistical data set. With a set of failures and nonfailures, the two percentages are plotted on probability graph paper for the desired value of impact resistance of the pipe.

Abrasion Resistance.   The *external* abrasion of geopipes is not considered to be of concern for most situations of static loads on or within stable backfill soils. For exposed pipes or water-submerged pipes, problems could certainly exist but are beyond the scope of this chapter.

The *internal* abrasion of geopipes, however, does occurr. Slurry pipelines, used to convey solid particulates like dredged soil materials are applications where moving particles will cause abrasion. Haas and Smith [6] have performed erosion studies that compare the abrasion performance of several types of plastic pipe with steel and aluminum pipe. The test setup consisted of a closed loop of test pipe with a sand slurry continuously circulated by a pump. Four sets of data were generated; two silica sand gradations (coarse [d_{50} = 0.58 mm] and fine [with d_{50} = 0.31 mm] at 40% by weight in a water slurry), each at two velocities, 2.1 and 4.6 m/s. The annual wear rates were measured in terms of loss of thickness and are given in Table 7.3. Overall, the results indicate the following:

- The wear rates vary considerably, from about 0.1 to 7 mm per year under continuous flow of abrasive slurry.
- Polyethylene pipe has good abrasion resistance compared with the other materials tested, including other types of polymers.

The above study indicates that the plastics used for the pipe tested are comparable with or better than metals in resistance to abrasion by sand slurries. PVC, while not covered in the reported tests, has modulus, yield strength, and ultimate strength (the significant parameters in abrasion resistance) in the range of ABS and acrylic.

Regarding a laboratory index test for abrasion, we could consider using ASTM D1175. This test method covers six abrasion methods directed at geotextiles placed in a flat configuration (recall Section 2.3.5). Pipe materials could be evaluated by any one of these techniques but only after they were recast into plaques by the compressive molding techniques discussed above.

Connection Tests.   As with most geosynthetic materials, the connections between separate geopipe sections can be the weak link of the completed pipe system.

TABLE 7.3   WEAR RATE OF PLASTICS AND METALS UNDER ABRASIVE SLURRIES

| | Wear Rate (mm/year) | | | |
| | Coarse Sand | | Fine Sand | |
Pipe Material	@ 2.1 m/s	@ 4.6 m/s	@ 2.1 m/s	@ 4.6 m/s
Steel	0.65	1.81	0.04	0.02
Aluminum	1.81	7.48	0.14	0.86
Polyethylene (PE)	0.06	0.46	nil	0.06
Acrylonitrile butadiene styrene (ABS)	0.36	2.07	0.07	0.51
Acrylic	0.99	4.10	0.17	1.42

Source: After Haas and Smith [6].

The various joining techniques are described in Section 7.5.2. There are no specific connection strength tests of a formalized nature; however, many of the tests described in this section on mechanical testing can be modified to include a joined section. If the pipe is solid wall, the adaptation is straightforward, since plastic pipes are often butt joined in a thermal fusion procedure. If the pipe is profiled, however, joining is usually accomplished by a prefabricated fitting or coupling. In this case longitudinal tension and/or large scale three-point bending tests might be considered. Future research efforts on pipe connections appear to be warranted. It should be noted that there is an ASTM test for joint watertightness, D3212, when using push-on or mechanical-type joints. In this test either internal pressure or a vacuum on the capped sections of pipe is used with the connections in the center of the test section.

7.1.3 Chemical Properties

Geopipes are often called upon to convey aggressive chemicals or are immersed in chemicals. Both within and without, the chemical resistance of the pipe must be assured. A number of different mechanisms might be considered.

Swelling Resistance.   The test for liquid absorption and the monitoring of the amount of swelling of a plastic material is a standard test (ASTM D570) and is covered in Section 5.1.4. The test must be modified for a pipe configuration or be conducted on compression molded samples of the polymer from which the pipe is manufactured.

Chemical Resistance.   Most manufacturers have a good database on the chemical resistance of their pipe materials to commonly conveyed liquids. Heterogeneous liquids, like landfill leachates and heap leach chemicals, however, can be somewhat problematic. As with the geomembrane chemical resistance tests described in Section 5.1.4, pipe specimens must be incubated, periodically removed, and then tested to evaluate whether changes have occurred when compared with the as-received material. There is no established test procedure for geopipe. Even the incubation of full cross sections of pipe is problematic because large containers must be used to accommodate the required number of pipe sections. For example, if a 150 mm diameter pipe is being evaluated in D2412 concentrated line load tests, the pipe lengths must be 450 mm long and five replicates at 30, 60, 90, and 120 day incubation times would require a container of approximately 600 1. When handling this much leachate, health and safety issues must be considered and testing costs will certainly rise accordingly.

To greatly alleviate the problem of testing laboratory containers with large amounts of leachate, we might consider cutting 90 or 120° sections of the candidate pipe and immersing these in a stacked configuration. The stacking and incubation container would appear as shown in Figure 7.5a In such a case, as little as 75 1 of leachate would be required. The load-versus-deflection test would be conducted in a steel channel section, as shown in Figure 7.5b. Note that careful machining of the supporting ends of the pipe is important to alleviate stress concentrations as much as possible. Preliminary data from this type of laterally confined test match remarkably well with those from geopipe tests under full soil confinement. Work is ongoing in this regard.

(a) Suggested immersion stacking

(b) Suggested test setup and specimen configuration
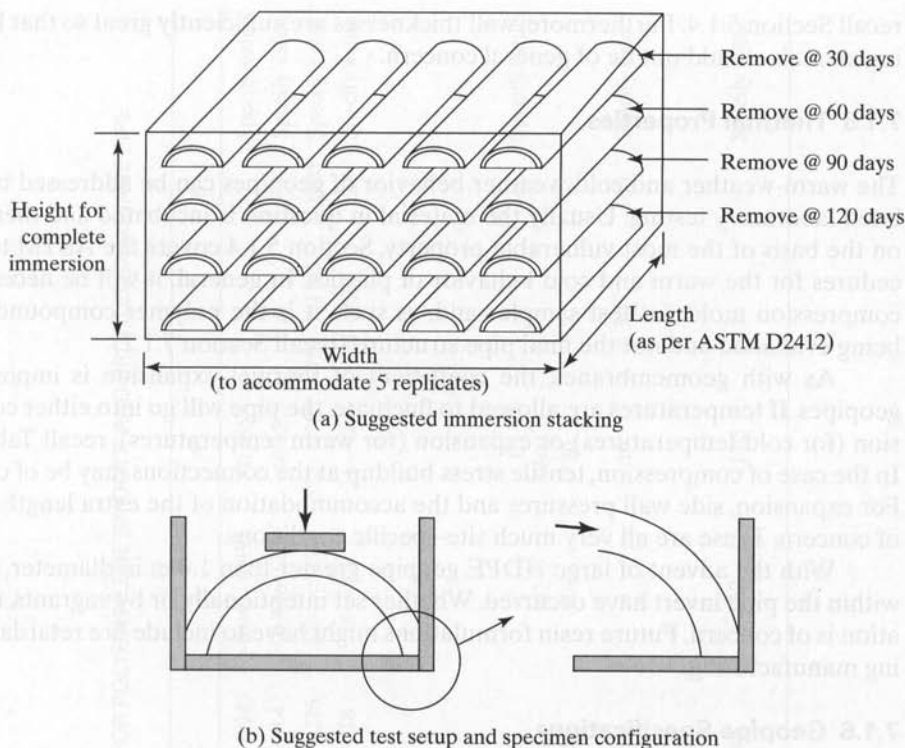
Figure 7.5 Suggested incubation setup and testing configuration for chemical resistance evaluation of geopipes.

Ultraviolet Light Resistance. All plastics will suffer from ultraviolet degradation if left exposed to sunlight for long enough. There are a number of outdoor tests that are available, as well as accelerated laboratory tests. Most notable in this latter group are two ASTM tests: D4355, "Deterioration of Geotextiles from Exposure to Ultraviolet Light and Water (Xenon-Arc Type Apparatus)" and G53, "Operating Light-and Water-Exposure Apparatus (Fluorescent UV-Condensation Type) for Exposure of Nonmetallic Materials." That said, the susceptibility of geopipe to ultraviolet light with respect to other geosynthetics is relatively low. This is based upon the low surface area of geopipes and the usually high wall thickness in comparison with geotextiles, geogrids, and geomembranes. Thus, with timely cover, geopipes (with properly formulated compounding materials including antioxidants and carbon black) should not be of concern as far as ultraviolet degradation is concerned.

7.1.4 Biological Properties

The resistance of plastic pipe to animals and to smaller forms of life (like fungi and bacteria) might be considered. Under usual conditions, high molecular weight polymers are not felt to be a source of great concern as to their biological degradation;

recall Section 5.1.4. Furthermore, wall thicknesses are sufficiently great so that burrowing animals should not be of general concern.

7.1.5 Thermal Properties

The warm-weather and cold-weather behavior of geopipes can be addressed by simulated laboratory testing. Usually the material in question is incubated and then tested on the basis of the most vulnerable property. Section 5.1.4 covers the ASTM test procedures for the warm and cold behavior of plastics. In general, it will be necessary to compression mold flat test samples and, as such, it is the polymer compound that is being evaluated and not the final pipe structure (recall Section 7.1.2).

As with geomembranes, the coefficient of thermal expansion is important in geopipes. If temperatures are allowed to fluctuate, the pipe will go into either compression (for cold temperatures) or expansion (for warm temperatures); recall Table 5.10. In the case of compression, tensile stress buildup at the connections may be of concern. For expansion, side wall pressures and the accommodation of the extra length may be of concern. These are all very much site-specific conditions.

With the advent of large HDPE geopipe greater than 1.0 m in diameter, fires set within the pipe invert have occurred. Whether set intentionally or by vagrants, the situation is of concern. Future resin formulations might have to include fire retardants during manufacturing.

7.1.6 Geopipe Specifications

With the variety of material properties that are available to geopipe manufacturers, even within a specific resin type, it is only natural that some standardization be attempted. This is the case with HDPE pipe, which has been put in *cell* classifications in accordance with the resin's density (see Table 7.4a). As expected, the properties are interrelated in that higher density produces a lower melt index, a higher flexural modulus, a higher yield strength, and a higher hydrostatic design basis strength.

Also note the seemingly uncertain position regarding stress crack resistance. The issue is controversial. It is generally accepted that ASTM D1693, the bent strip test, is not challenging (and hence unacceptable) in its assessment of stress crack resistance. Furthermore, quantification insofar as the relative ranking of resins is not possible using this method. As a result, the current tendency is to use a notched molded plaque under a constant tensile stress. It is formalized as ASTM F1473. Alternatively, ASTM D5397, the NCTL test described in Section 5.1.3, will be the stress crack test used for HDPE profiled drainage pipe (recall the data of Table 7.2). The complementary specification for HDPE profiled wall drainage pipe is available as AASHTO M294, and the required mechanical properties are given as Table 7.4b.

The requirements for PVC pipe resin and its related properties are also available in specification form via ASTM D1784. Table 7.5a presents the minimum values that determine the relevant cell number for use in different applications. The complementary specification for PVC profiled wall drainage pipe is available as AASHTO M304 and the required mechanical properties are given in Table 7.5b.

TABLE 7.4A PRIMARY PROPERTIES: CELL CLASSIFICATION LIMITS FOR POLYETHYLENE SMOOTH AND PROFILED DRAINAGE PIPE MATERIALS, PER ASTM D3350

Property	Test Method	0	1	2	3	4	5	6	7
1 Density, g/cm³	D1505	Unspecified	≤0.925	0.926–0.940	>0.940–0.955	>0.955	—	—	Specify value
2 Melt index	D1238	Unspecified	>1.0	1.0 to 0.4	<0.4 to 0.15	<0.15	A	—	Specify value
3 Flexural modulus, MPa	D790	Unspecified	<138	138–<276	276–<552	552–<758	758–<1103	>1103	Specify value
4 Tensile strength at yield, MPa	D638	Unspecified	<15	15–<18	18–<21	21–<24	24–<28	>28	Specify value
5 Slow crack growth Resistance									
I. ESCR	D1693	Unspecified							
a. Test duration, (100% Igepal)			A	B	C	C		—		Specify value
b. Test duration, h			48	24	192	600				
c. Failure, max (%)			50	50	20	20				
II. PENT (hours)	F1473	Unspecified								
Molded plaque, 80°C, 2.4 MPa Notch depth, F1473, Table 1		Unspecified	0.1	1	3	10	30	100		Specify value
6 Hydrostatic design basis, Mpa, (23°C)	D2837	Not rated	5.52	6.89	8.62	11.03	—	—	—	Specify value

TABLE 7.4B   MECHANICAL PROPERTIES OF HDPE PROFILED WALL DRAINAGE PIPE PER AASHTO M294

Diameter (mm)	Wall Thickness (mm)	Pipe Stiffness (kPa)	Rows of Perforations[1]	H, Max,[2] (mm)	L, Min[2] (mm)
300	0.9	345	6	138	192
375	1.0	290	6	184	256
450	1.3	275	6	207	288
525	1.5	260	6	230	320
600	1.5	235	8	230	320
675	1.5	205	8	230	320
750	1.5	195	8	230	320
900	1.7	150	8	230	320
1050	1.8	140	8	230	320
1200	1.8	125	8	230	320
1350	2.0	110	8	230	320
1500	2.0	95	8	230	320

1. Minimum number of rows. A greater number of rows for increased inlet area shall be subject to agreement between purchaser and manufacturer.

2. $H(\max) = 0.46 D$; $L(\min) = 0.64$, where D = nominal diameter of pipe, mm.

Note: AASHTO M294 requires a classification of 345400 for profiled HDPE pipe. In Table 7.4A, this means that density is cell 3; melt index is cell 4; modulus is cell 5; strength is cell 4; SCGR is unspecified; and HDB is not rated.

TABLE 7.5A   CLASS REQUIREMENTS FOR RIGID PVC DRAINAGE PIPE COMPOUNDS PER ASTM D1784

Property and Unit	Cell Limits								
	0	1	2	3	4	5	6	7	8
Base resin	Unspecified	PVC homo-polymer	Chlorinated PVC	Vinyl copolymer					
Impact strength (Izod), min: (J/m of notch)	Unspecified	<35	35	80	270	535	800		
Tensile strength, min (MPa)	Unspecified	<35	35	40	50	55			
Modulus of elasticity in tension, min (MPa)	Unspecified	<1900	1900	2200	2500	2750	3000		
Deflection temperature under load, min 1.82 MPa (°C)	Unspecified	<55	55	60	70	80	90	100	110
Flammability	A	A	A	A	A	A	A	A	A

A = All compounds covered by this specification when tested in accordance with Method D635 shall yield the following results: average extent of burning <25 mm and average time of burning of <10 s.

TABLE 7.5B   MECHANICAL PROPERTIES OF PVC PROFILED WALL DRAINAGE PIPE PER AASHTO M304

Nominal Pipe Size (mm)	Minimum Average Inside Diameter[1] (mm)	Minimum Waterway Wall (mm)	Minimum Pipe Impact Strength (J)	Minimum Pipe Stiffness (kPa)
100	100.0	0.56	108	318
150	149.7	0.64	108	318
200	199.7	0.89	136	318
250	249.6	1.14	136	318
300	296.8	1.52	136	318
375	363.3	1.90	136	262
450	444.8	2.16	136	221
525	524.7	2.54	136	193
600	594.7	2.92	136	165
675	669.8	3.18	136	152
450	746.4	3.43	163	131
900	898.4	3.94	163	110
1050	1050.9	4.32	163	97
1200	1202.9	4.83	163	83

[1]Tolerance on inside diameter shall be +2% of nominal pipe size, but not to exceed 13 mm.

7.2   THEORETICAL CONCEPTS

Before considering design examples, some consideration must be given to selected theoretical concepts. These concepts have to do with the hydraulic considerations of pipes flowing full and pipes that are only partially full. Also in this section are selected concepts and formulas associated with the stresses imposed by soil backfill on the pipe during its service lifetime. For a more in-depth treatment of these topics, there are numerous textbooks available (for example, see [7]–[10]).

7.2.1 Hydraulic Issues

For pipelines that are flowing full, the *Hazen-Williams formula* is often used to describe flow behavior. It is empirical and is only used for pipes greater than 50 mm in diameter and velocities less than 3 m/s.

$$V = 0.85 \, C \, R_H^{0.63} S^{0.54} \tag{7.9}$$

where

V = velocity of flow (m/s),
R_H = hydraulic radius (m) = flow area/wetted perimeter
     = $(\pi D^2/4)/\pi D = D/4$,
D = internal diameter of pipe (m),
S = slope or gradient of pipeline (m/m), and

C = a constant that depends on the pipe material and the condition of the inner surface (dimensionless). Hwang [7] gives $C = 140–150$, but does not distinguish between different types of plastic pipe, smooth versus profiled inner surfaces or pipes with perforations.

The previous formula can be readily converted to flow rate, Q, by multiplying the velocity by the cross-sectional area A of the pipe.

For pipelines that are either flowing full or flowing partially full, the *Manning equation* is generally used:

$$V = \frac{1}{n}R_H^{0.66}S^{0.5} \tag{7.10}$$

where

V = velocity of flow (m/s),
R_H = hydraulic radius (m),
S = slope or gradient of pipeline (m/m), and
n = coefficient of roughness (see Table 7.6) (dimensionless).

Plastic pipe of the type discussed in this chapter, with a *smooth interior*, has a Manning coefficient from 0.009 to 0.010. Plastic pipe with a *profiled or corrugated interior* has a Manning coefficient ranging from 0.018 to 0.025.

Equations (7.9) and (7.10) are generally used in the form of charts or nomographs to determine pipe sizes, flow velocity, or discharge flow rates (see Figures 7.6 and 7.7). For each chart we include an example from Hwang [7], which is illustrated on the respective nomographs by heavy lines. Note that both nomographs are for pipes flowing full.

TABLE 7.6   VALUES OF MANNING ROUGHNESS COEFFICIENT, n, FOR REPRESENTATIVE SURFACES

Type of Pipe Surface	Representative n Value
Lucite, glass, or *plastic*[1]	0.010
Wood or finished concrete	0.013
Unfinished concrete, well-laid brickwork, concrete, or cast iron pipe	0.015
Riveted or spiral steel pipe	0.017
Smooth, uniform earth channel	0.022
Corrugated flumes, typical canals, river free from large stones and heavy weeds	0.025
Canals and rivers with many stones and weeds	0.035

[1]The table does not distinguish between different types of plastic pipes, smooth versus profiled inner surfaces or pipes with perforations.

Source: After Fox and McDonald [9].
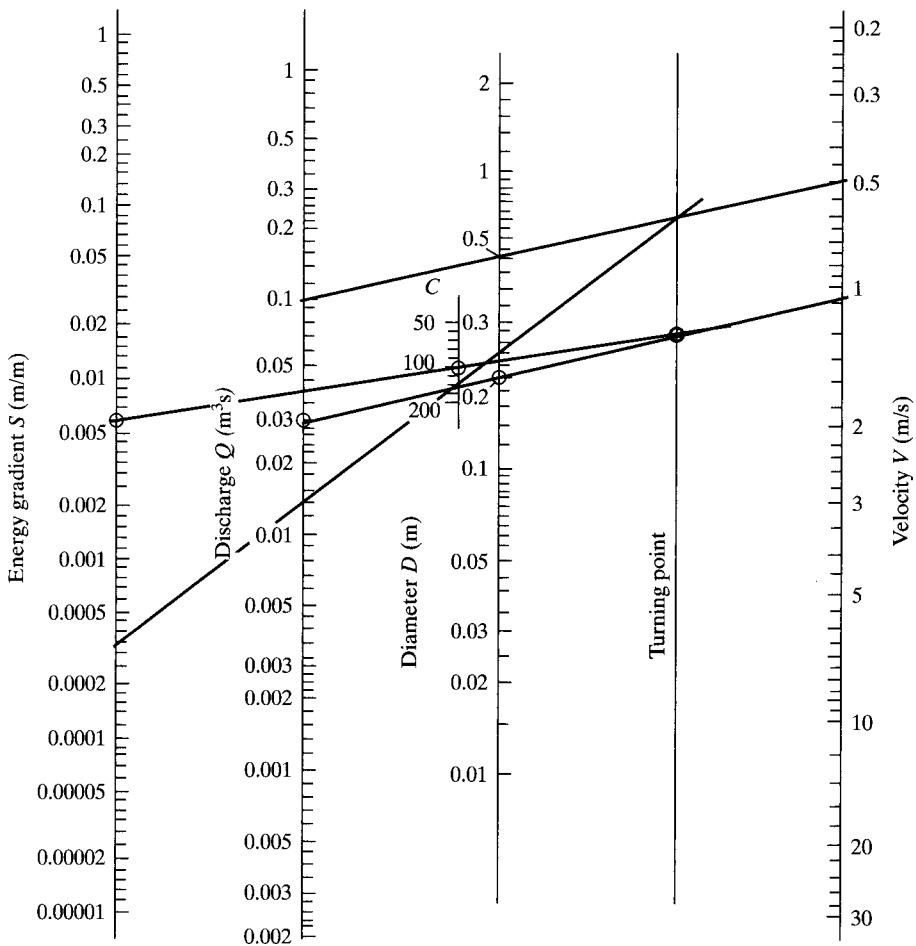
Figure 7.6   Solution nomograph for Hazen-Williams formula.

Example 7.1

A 100 m long pipe with $D = 200$ mm and $C = 120$ carries a discharge of 30 l/s. Determine the head loss in the pipe. (See the Hazen-Williams nomograph in Figure 7.6.)

Solution: Applying the conditions given to the solution nomograph in Figure 7.6, the energy gradient is obtained.

$$S = 0.0058 \text{ m/m}$$

The energy gradient is defined as the energy loss per unit pipe length or

$$S = \frac{h_f}{L} = 0.0058 \text{ m/m}$$
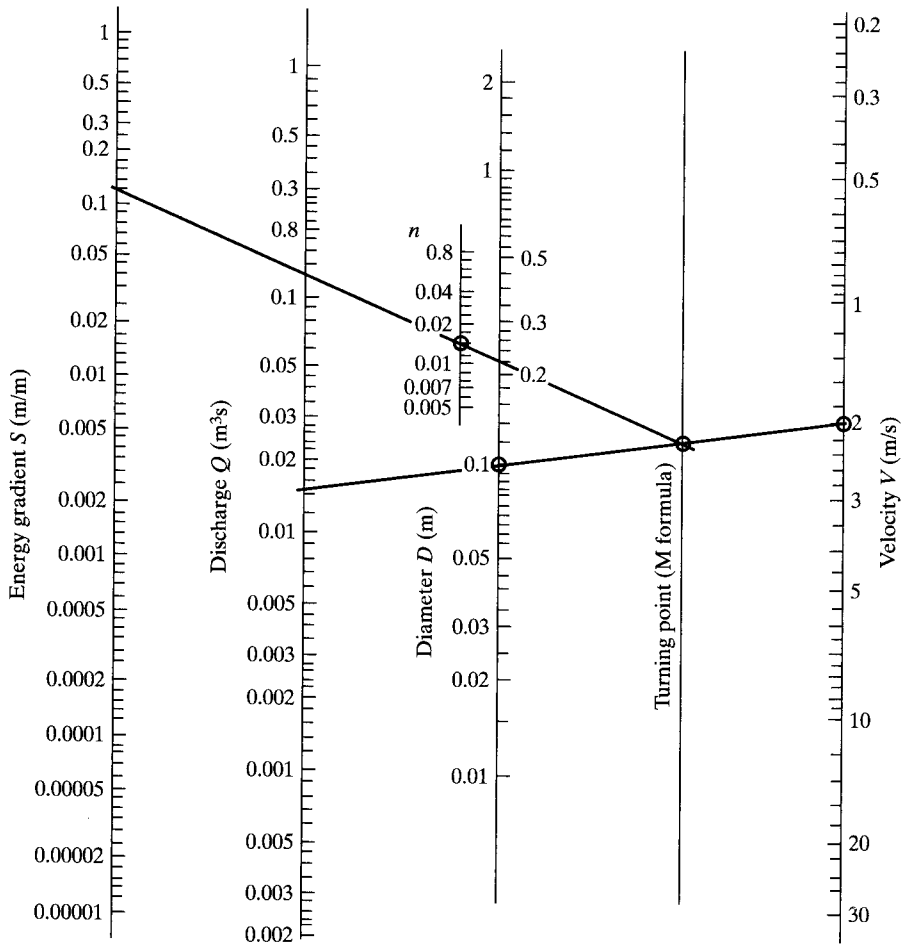
Figure 7.7 Solution nomograph for Manning formula.

Hence,

$$h_f = (0.0058 \text{ m/m})(100 \text{ m}) = 0.58 \text{ m}$$

Example 7.2

A horizontal pipe with 100 mm uniform diameter is 200 m long. The Manning roughness coefficient is $n = 0.015$ and the measured drop is 24.6 m in a water column. Determine the discharge. (See the Manning nomograph in Figure 7.7.)

Solution: The energy gradient in the pipe is

$$S = \frac{h_f}{L} = \frac{24.6}{200} = 0.123$$

Applying this value and the conditions given to the solution chart in Figure 7.7, we obtain the following discharge:

$$Q = 0.015 \text{ m}^3/\text{sec.}$$

For many of the examples of gravity drainage using perforated plastic pipe that are discussed in Section 7.3, the partially full condition is the typical case. The modified Manning equations are as follows [11]:

$$Q = 1.137 A R_H^{0.66} S^{0.5} \tag{7.11}$$

$$V = \frac{Q}{A} \tag{7.12}$$

where

Q = flow rate (m^3/s),
V = velocity of flow (m/s),
A = flow area cross section (m^2),
R_H = hydraulic radius (mm) = (flow area cross section divided by the wetted perimeter), and
S = slope or gradient (m/m)

Another relationship used in the analysis of pipeline flow is the Darcy-Weisbach equation for head loss, which is as follows:

$$h_L = (f)\left(\frac{LV^2}{2gD}\right) \tag{7.13}$$

where

h_L = head loss (m),
f = friction factor (dimensionless),
L = pipe length (m),
D = pipe diameter (m), and
V = flow velocity (m/s).

For laminar flow, equation (7.13) becomes

$$h_L = \left(\frac{64}{N_R}\right)\left(\frac{LV^2}{2gD}\right) \tag{7.14}$$

where

f = $64/N_R$, and
N_R = Reynold's number (dimensionless).

In general, the dimensionless friction factor f in equation (7.14) is related to both the pipe roughness and the Reynold's number and is usually the major pipe loss factor. The Colebrook-White expression that follows is sometimes used for its evaluation:

$$\frac{1}{\sqrt{f}} = -2\log\left(\frac{2.51}{N_R\sqrt{f}} + \frac{\epsilon/D}{3.7}\right) \tag{7.15}$$

where

f = friction factor or resistance coefficient,
D = pipe diameter,
N_R = Reynold's number, and
ϵ = smoothness factor.

The Reynold's number defines the flow boundary between laminar and turbulent conditions. It is defined as follows:

$$N_R = \frac{VD\rho}{\mu} = \frac{VD}{\nu} \tag{7.16}$$

where

N_R = Reynold's number (dimensionless),
V = flow velocity (m/s),
D = pipe diameter (m),
ρ = fluid density (kN-s^2/m^4) = specific weight divided by g = 9.81 m/s^2,
μ = coefficient of viscosity (kN-s/m^2), and
ν = kinematic viscosity (m^2/sec) = μ/ρ.

The above rather nonintuitive set of relationships is greatly sorted out by use of a Moody's diagram, as shown in Figure 7.8. In this important graph it is seen that laminar flow conditions exist for $N_R < 2000$. Above 2000, flow becomes more and more unstable, until at higher N_R values it eventually becomes turbulent. These turbulent values are seen to be highly dependent on the pipe's roughness.

7.2.2 Deflection Issues

An engineering approach to the quantification of deflection of buried pipelines has been developed by a sequential group of research faculty and students at Iowa State University. Beginning with Marston in the 1920s evaluating rigid conduits (the term used for shallow buried pipes), followed by Spangler between 1950 and 1970 evaluating flexible conduits, and into the present time by Watkins, the group and their colleagues have "written the book" for this type of research [12]. Key issues in the development are the use of arching theory for gravitational force dissipation, the
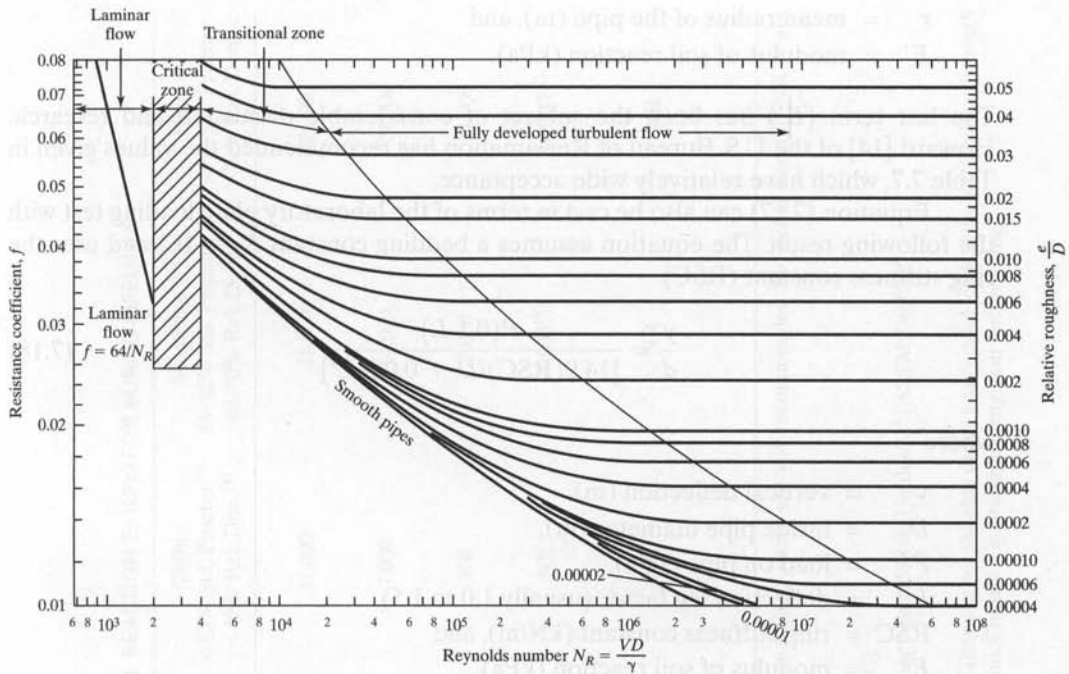
Figure 7.8 Moody chart of resistance to uniform flow in circular pipes. (After Hwang [7])

importance of subgrade stability, backfill type, and compaction conditions, and finally the flexibility of the pipe structure itself. Moser [13] presents the following equation summarizing the Iowa State group's effort for the deflection behavior of flexible (in our case plastic) pipe:

$$\Delta x = \frac{D_L K_b W_c}{(EI/r^3) + (0.061E')} \cong y \tag{7.17}$$

where

Δx = horizontal increase in diameter (m),

y = vertical deflection (m),

D_L = deflection lag factor, which varies from 1.0 to 1.5 (dimensionless),

K_b = bedding constant, which varies from 0.83 to 0.110 (dimensionless),

W_c = Marston's prism load per unit length of pipe (kN/m) (note that arching is not taken into account in this formula),

E = modulus of elasticity of the pipe material (kPa),

I = moment of inertia of the pipe wall per unit length (m³),

EI = bedding stiffness of the pipe ring per unit length (kN-m),

r = mean radius of the pipe (m), and
E' = modulus of soil reaction (kPa).

The last term (E') has been the subject of considerable discussion and research. Howard [14] of the U.S. Bureau of Reclamation has recommended the values given in Table 7.7, which have relatively wide acceptance.

Equation (7.17) can also be cast in terms of the laboratory plate loading test with the following result. The equation assumes a bedding constant $K_b = 0.2$ and uses the ring stiffness constant (RSC).

$$\frac{y}{d} = \frac{P(0.1\,L)}{[14.9(\text{RSC})/D + 0.061E']} \tag{7.18}$$

where

y = vertical deflection (m),
D = inside pipe diameter (m),
P = load on pipe (kPa),
L = deflection lag factor (usually 1.0 to 1.5),
RSC = ring stiffness constant (kN/m), and
E' = modulus of soil reaction (kPa).

The ring stiffness constant (RSC) reflects the sensitivity of the pipe to installation stresses. It is defined in terms of the pipe's deflection resulting from the load applied between parallel plates as per ASTM D2412 (recall Section 7.1.2). As described in ASTM F894, RSC is the value obtained by dividing the parallel plate load by the resulting deformation (as a percentage) at 3% deflection. Note that most plastic pipe manufacturers have an empirical formula, along with the necessary tables of their pipe products, for the evaluation of RSC values (e.g., see [15]). Equation (7.18) also reflects strongly on the type, condition, and placement of backfill both on the sides of the pipe and above it (recall Table 7.7), for values of the modulus of soil reaction E'.

Due to the importance of the above formulation, several full-scale field and large-scale laboratory trials have been published, which give valuable information. Watkins and Reeve [3] have evaluated 375, 450, and 600 mm corrugated plastic pipe under standard H-20 truck loadings to determine the minimum cover necessary to prevent pipe damage, and they have also performed high pressure large-scale laboratory tests. Regarding the minimum cover tests, their results show the response given in Figure 7.9. Here it can be seen that for a limiting ring deflection of 5% (for this particular pipe) 300 to 375 mm of soil cover is necessary. For the large-scale laboratory tests, the setup and typical data are shown in Figure 7.4e.

Using the finite element computer program "Culvert Analysis and Design" (CANDE), Katona [16] has developed a series of design charts for allowable maximum fill heights. The program has the pipe and surrounding soil in an incremental plane strain formulation. The pipe is modeled with connected beam-column elements and the soil with continuous elements. The assumptions used are all reasonable, with the possible exceptions of a bonded pipe-to-soil interface and linear elastic polyethylene

TABLE 7.7 U.S. BUREAU OF RECLAMATION VALUES OF MODULUS OF SOIL REACTION E' (kPa) FOR BURIED PIPELINES

Class ASTM D2321	Soil Type for Pipe Bedding Material (Unified Classification System[1])	Dumped	Slight <85% Std. Proctor[3] <40% Rel. Den.[4]	Moderate 85–95% Std. Proctor 40–70% Rel. Den.	High >95% Std. Proctor >70% Rel. Den.
I	Crushed rock: Manufactured angular, granular material with little or no fines (6 to 38 mm)	7,000	21,000	21,000	21,000
II	Coarse-grained soils with little or no fines: GW, GP, SW, SP[2] containing less than 12% fines (max. particle size 38 mm)	NR	7,000	14,000	21,000
III	Coarse-grained soils with fines: GM, GC, SM, SC[2] containing more than 12% fines (maximum particle size 38 mm)	NR	NR	7,000	14,000
IV(a)	Fine-grained soil (LL < 50): soils with medium to no plasticity CL, ML, ML-CL, with more than 25% coarse-grained particles	NR	NR	7,000[5]	14,000[5]
IV(b)	Fine-grained soils (LL > 50): soils with high plasticity CH, MH, CH-MH Fine-grained soils (LL < 50): soils with medium to no plasticity CL, ML, ML-CL with less than 25% coarse-grained particles	NR	NR	NR	NR

Organic soils OL, OM, and PT as well as soils containing frozen earth, debris, and large rocks are not recommended for initial backfill; NR = not recommended for use per ASTM D2321; LL = liquid limit.

[1] ASTM Designation D2487

[2] Or any borderline soil beginning with some of these symbols (i.e., GM, GC, GC-SC).

[3] Percent Proctor based on laboratory maximum dry density from test standards using about 598,000 joules/m^3 (ASTM D698).

[4] Relative density per ASTM D2049.

[5] Under some circumstances Class IV(a) soils are suitable as primary initial backfill. They are not suitable under heavy dead loads, dynamic loads, or beneath the water table. Compact with moisture content at optimum or slightly dry of optimum. Consult a geotechnical engineer before using.

Source: After Howard [14].
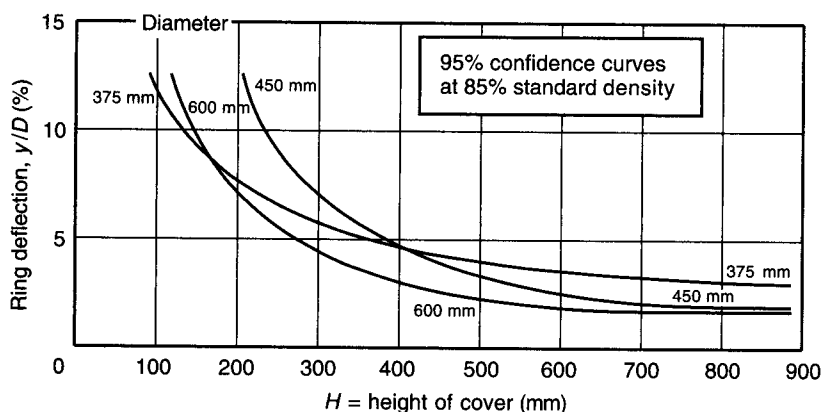
Figure 7.9   Minimum cover values for H-20 loading on HDPE pipe. (After Watkins and Reeve [3])

properties. Allowable fill heights for 108 cases were analyzed. The variations are as follows: pipe diameters ranging from 100 to 750 mm; three pipe corrugation areas in each pipe size; good and fair soil backfills and short-term and long-term pipe properties ($E = 750$ MPa and $\sigma_y = 20$ MPa for a short-term life of 0.05 years, and $E = 150$ MPa and $\sigma_y = 6.2$ MPa for a long-term life of 50 years). Table 7.8 gives Katona's results for these variations.

The values listed in Table 7.8, however, may be somewhat conservative, as indicated by the full-scale field study of Selig and Hashash [17]. A 600 mm corrugated HDPE pipe was placed in a carefully constructed trench and backfilled with a well-graded sand and gravel. It was then backfilled with 30 m of highly compacted soil of 23 kN/m^3 density. Pipe wall strain, circumferential shortening, trench strain, free field soil strain, temperature, soil stress, and shape changes were monitored over a two-year period. (The evaluation is still ongoing.) Some indication of the information gained is given in Figure 7.10a for the change in pipe diameter and Figure 7.10b for the circumferential shortening. All the values are within reason and the performance seems to indicate the proper functioning of the pipe under this very heavy static overburden stress that is approximately twice the value predicted in Table 7.8. This information seems to suggest that predicted values of overburden stress on polymer pipes (when properly placed and backfilled) may be quite conservative.

Regarding the *internal* stress mobilization from pressurized fluids or gases, there is a tremendous body of knowledge that is available. Pressurized water and natural gas transmission lines form the bulk of this information. However, the focus of this chapter is on gravity flow situations.

7.3   DESIGN APPLICATIONS

This section will illustrate the design of various situations that use either profile wall or solid wall plastic pipes. In general, underdrains will require perforated, profile wall

TABLE 7.8   DESIGN TABLE FOR ALLOWABLE FILL HEIGHT

Pipe Properties		Allowable Fill Heights			
		Good Quality Soil		Fair Quality Soil	
Inside Pipe Diameter (mm)	Corrugated Area (mm²/m)	S (m)	L (m)	S (m)	L (m)
100	1.0	13.7	7.8	9.6	3.7
	2.3	26.6	12.6	19.3	7.2
	3.6	38.2	17.3	23.4	10.7
150	1.3	11.9	7.0	8.1	3.1
	2.5	20.9	10.5	15.6	5.5
	3.8	29.1	13.7	20.0	7.9
200	1.5	10.9	6.7	7.2	2.9
	2.8	17.7	9.3	12.9	4.6
	4.1	24.1	11.8	17.9	6.5
250	2.0	11.4	6.9	7.6	3.1
	3.3	16.9	9.1	12.2	4.5
	4.6	22.1	11.0	16.7	5.9
300	2.5	11.7	7.1	7.9	3.2
	3.8	16.3	8.9	11.7	4.4
	5.1	20.7	10.5	15.6	5.6
375	3.8	13.4	7.9	9.4	3.7
	5.1	17.0	9.2	12.4	4.6
	6.3	20.6	10.5	15.4	5.5
450	5.1	14.7	8.4	10.4	3.9
	6.3	17.6	9.6	12.9	4.8
	7.6	20.6	10.6	15.4	5.6
600	6.3	14.6	8.7	10.2	4.0
	7.6	17.0	9.6	12.2	4.6
	8.9	19.4	10.5	14.2	5.2
750	7.6	13.3	8.1	9.2	3.7
	8.9	15.1	8.8	10.7	4.2
	10.2	16.9	9.6	12.3	4.7

Abbreviations: S = Short-term design life (0.05 years)
L = Long-term design life (50 years)
Source: After Katona [16].

pipes and will be under gravity-flow conditions. Conversely, landfill pipe risers and manholes will generally be solid wall pipes, also with gravity-flow conditions.

7.3.1 Pavement Underdrains — Perforated Profiled Collection Pipes

An underdrain system should be installed parallel to the downward sloping side of all highways, airfields, railroads, parking lots, staging areas, and so on, to collect the water that is transmitted beneath and above the pavement's surface. That this is necessary has been ably documented by Cedergren [18], who shows that pavement life is seriously
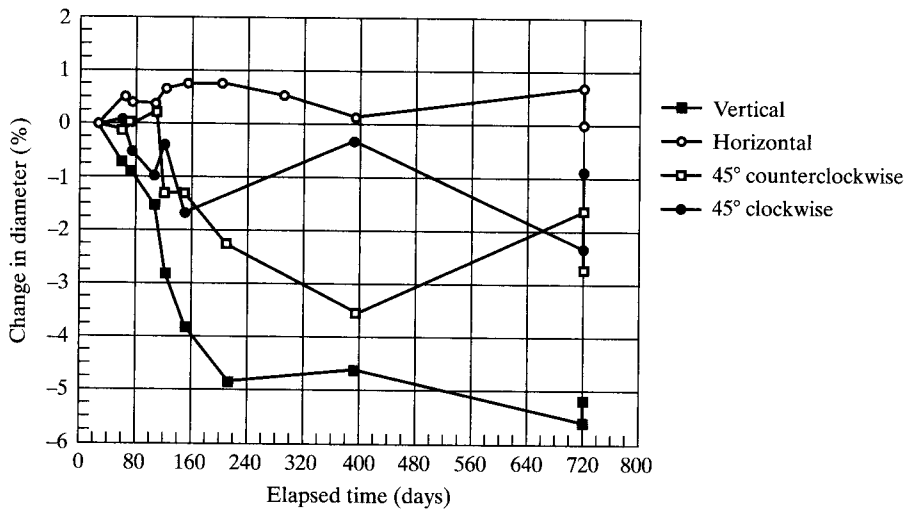
(a) Diameter changes along various axes
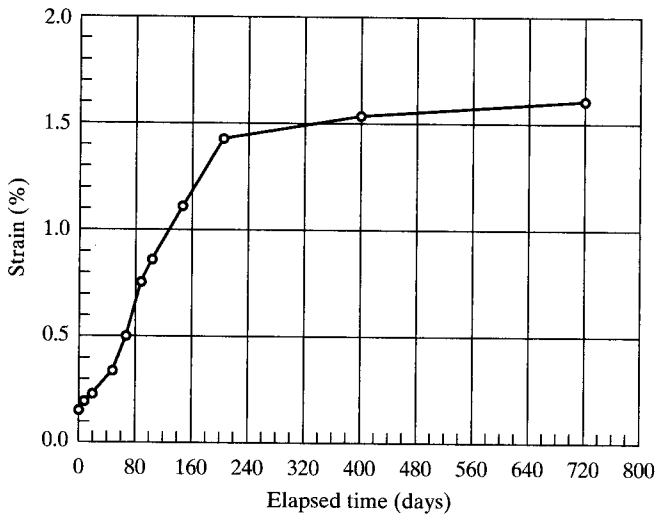
(b) Shortening of circumference with time

Figure 7.10   Results of 700 kPa highway loading on a 600 mm diameter profiled pipe. (After Selig and Hashash [17])

reduced when water remains within the pavement cross section, (see Figure 7.11). This figure also shows that the situation of reduced pavement life is greatly aggravated by cold weather conditions.

The water that penetrates through cracks in the pavement's surface flows within the stone base (on a gravitational basis) to the edge of the highway where it must be collected and transported away from the pavement area (e.g., into a drainage swale, ditch,
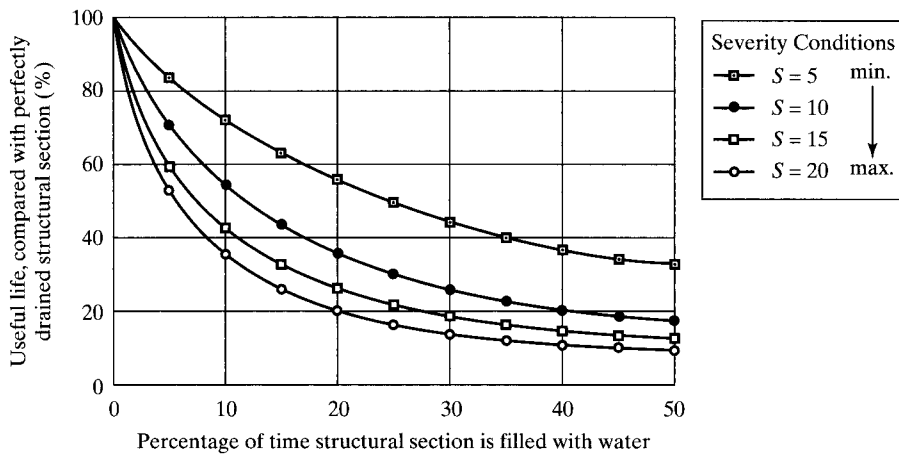
Figure 7.11   Curves showing the effect of water in pavement base course on service life. (After Cedergren [18])

or stream). This quantity is added to the surface runoff occurring above the pavement and shoulder if the latter is present. A variety of configurations of underdrain systems exist (recall Figure 2.63), but many use a perforated pipe as the central conveyance element. This type of drain is often surrounded by gravel with a sand filter and/or a geotextile filter, as shown in Example 7.3.

Example 7.3

Consider a 7.5 m wide pavement in an area with an extremely high rainfall intensity of 150 mm/hr as the 10-year design storm. The runoff coefficient is 0.50. The infiltration coefficient from the pavement is 0.30; thus 80% of the rainfall will reach the underdrain in a relatively short time. (Consider the release factor from an open graded stone base to be 1.0.) What quantity of flow will the underdrain have to convey at the end of a 50 m section between inlets at an average slope of 0.03, and what size profiled pipe is necessary? (Use a roughness coefficient of 0.010 for smooth interior pipe — i.e., CPP-SP pipe.)

Solution: Using a straightforward approach (see Gupta [10] and Koerner and Hwu [19]), the following formulation is obtained:

$$q = i_R (c_i f_R + c_s)W \tag{7.19}$$

where

q = flow rate per meter of length,
i_R = rainfall intensity,
c_i = pavement infiltration coefficient,
f_R = release factor for the stone base,
c_s = pavement surface runoff coefficient, and
W = pavement width,
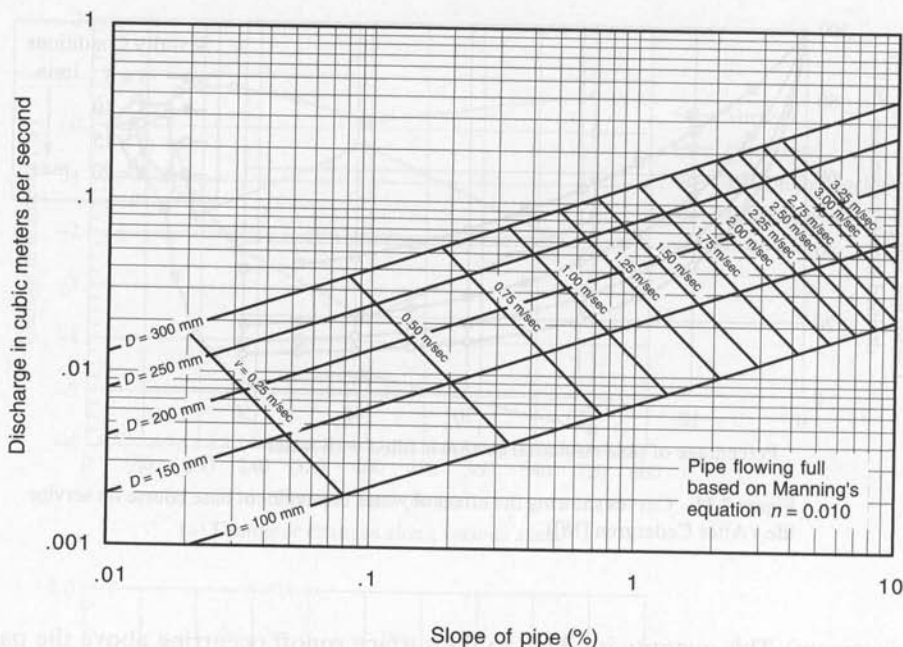
Figure 7.12 Sizing of leachate collection pipe. (After EPA [20])

$$q = \frac{0.150 \left[0.30(1.0) + 0.50 \right] 7.5}{(60)(60)}$$

$$= 0.00025 \text{ m}^2/\text{s}$$

$$= 0.00025(50)$$

$$q = 0.0125 \text{ m}^3/\text{s}$$

From this point either the Hazen-Williams or the Manning chart is used for the proper pipe size. Figure 7.12, based on the Manning formula, has been prepared for $n = 0.010$. Using a slope of 3% and a flow rate of 0.0125 m³/s gives the required pipe size of 100 mm diameter.

7.3.2 Primary Leachate Collection Systems — Perforated Profiled Collection Pipes

Contained within the drainage sand or gravel of a leachate collection system (e.g., located above a primary liner system of a landfill) is a pipe-manifold system consisting of interconnected perforated pipes. These pipe systems have made a complete change in recent years from concrete to plastic pipes. Although a number of polymers are possible, high density polyethylene is widely used due to its excellent chemical resistance to a wide range of leachates. Furthermore, the pipes usually have a profiled configuration, and they have to be designed on the basis of both spacing and diameter considerations. The example that follows shows how an estimate of the allowable head on the liner is critical.

Example 7.4

Consider a 3 ha landfill cell ($L = 300$ m and $W = 100$ m) with a tentative primary leachate removal system and perforated pipe as shown in Figure 7.13. The cell is uniformly sloped to the sump at 2% for both header and feeder pipes. The maximum head on the liner (via EPA regulations) is 300 mm. The landfill is located near Philadelphia, Pennsylvania. Determine the feeder pipe spacing for an inflow of 3176 mm/year and a sand collection layer with a permeability of 0.01 cm/s. Note that 3176 mm/year is equivalent to 93,000 1/ha-day which is over three times the leachate collected in a climate such as Philadelphia. Consequently, we have included an FS $\cong$ 3.0.
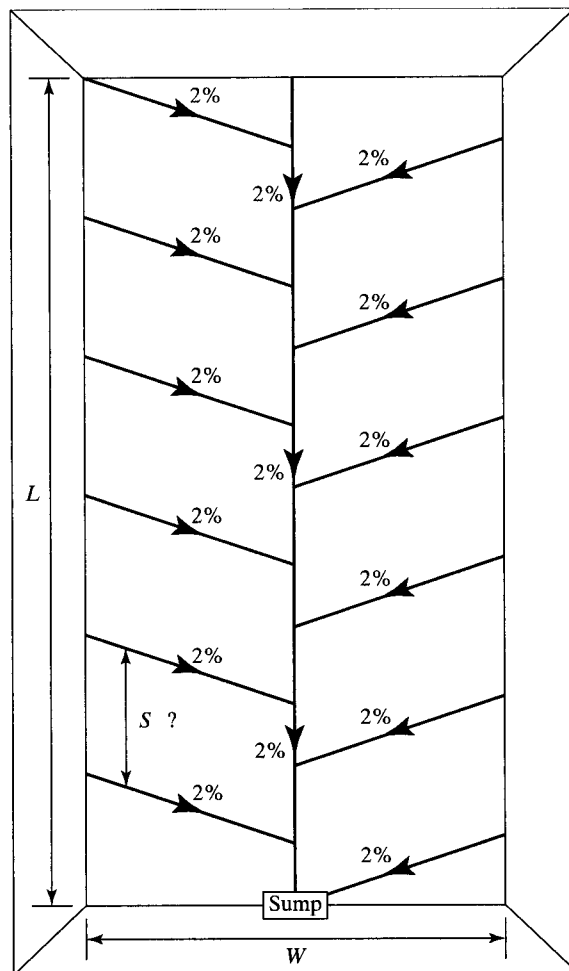
Figure 7.13   Typical plan view of the perforated pipe network of the leachate collection system for a landfill.

Solution: We use a form of the so-called "mound equation" of which the McEnroe method will be used [21]. For the above 2% slope, the resulting angle $\alpha = 1.15°$. Therefore,

$$R = \frac{r}{k \sin^2 \alpha}$$

$$= \frac{3176}{(0.01)(100)(60)(60)(24)(365) \sin^2(1.15)}$$

$$R = 0.25 \tag{7.20}$$

In the McEnroe formulation, $R = 0.25$ has the mound reaching from one feeder pipe to the next with the resulting formula for spacing. Note that there are other formulas for different conditions of the mound [21]:

$$\frac{y_{max}}{L} = \frac{SR(1 - 2RS)}{1 - 2R} \exp \frac{2R(S - 1)}{(1 - 2RS)(1 - 2R)} \tag{7.21}$$

where

y_{max} = maximum head (normal height) on the liner (m)
L = feeder pipe spacing (m)
S = slope between the feeder pipes = $\tan \alpha = 0.02$
R = 0.25 (dimensionless)

$$\frac{0.30}{L} = \frac{(0.02)(0.25)[1 - 2(0.02)(0.25)]}{1 - 2(0.25)} \exp \frac{2(0.25)(0.02 - 1)}{[1 - 2(0.25)(0.02)][1 - 2(0.25)]}$$

$$= \frac{(0.02)(0.25)(0.99)}{(0.5)} \exp \frac{(-0.49)}{(0.99)(0.50)}$$

$$= (0.0099) \exp (-0.99)$$

$$= (0.0099) \frac{1}{2.69}$$

$$\frac{0.30}{L} = 0.00368$$

$$L = 81.5 \text{ m (or less, since this is an upper-bound value)}$$

7.3.3 Liquid Transmission — Solid-Wall Nonperforated Pipe with Deflection Calculations

The design of a full-flow buried transmission pipeline requires both pipe sizing and the verification of a limiting deformation. The first part uses the Hazen-Williams formula developed in Section 7.2.1; the second part uses the modified Iowa State equation developed in Section 7.2.2.

Example 7.5

Consider a long gravity transmission PVC pipeline ($C = 150$) with a 0.035% slope and a required discharge of 0.1 m³/s. What is the required diameter? Consider that this pipe is buried under 6 m of soil weighing 19 kN/m³ and that the pipe bedding material is Class II with high compaction. What is the total deflection from the soil backfill when added to an assumed installation load deflection?

Solution: Using the Hazen-Williams nomograph in Figure 7.6, the heavy lines indicate that the necessary pipe diameter is 0.5 m.

To enter into the deflection calculation, assume that the pipe is the next largest nominal size, which has the following characteristics for T1-PVC pipe from ASTM F 679:

Diameter (inside) = 525 mm
Diameter (outside) = 560 mm
Wall thickness = 16.0 mm
Pipe stiffness = 317 kN/m^2

In the modified Iowa State formula given as equation (7.17), assume that D_L = 1.2, K_b = 0.2, and E' = 21,000 kPa.

$$W_c = H(\gamma)D_0$$
$$= (6.0)(19)(0.560)$$
$$W_c = 63.8 \text{ kN/m} \tag{7.22}$$

Note that this is the full weight of the soil prism above the diameter of the pipe. There is no reduction due to soil arching via pipe deflection.

$$\Delta x = \frac{D_L K_b W_c}{(EI/r^3) + (0.061E')}$$
$$= \frac{(1.2)(0.2)(63.8)}{(317/6.71) + (0.061)(21,000)}$$
$$= 0.0115m$$
$$\Delta x = 11.5 \text{ mm } (\cong y, \text{ per ASTM D2412})$$

Therefore,

$$\delta = \frac{y}{D} = \frac{11.5}{525}$$
$$= 0.0219 \times 100$$
$$= 2.2\%$$

The installation deflection is now estimated from the empirical values in Table 7.9. For a pipe stiffness of 317 kN/m^2 and a high compaction density, the installation deflection is 2.0%. Thus the total deflection is 2.2 to 2.0% which is 4.2%. This is seen to be acceptable since maximum allowable values are in the 5 to 10% range.

7.4   DESIGN CRITIQUE

The designs just presented are a selection of geopipe topics that are felt to be of interest to those involved in geosynthetics. They are far from being representative of the general use of plastic pipe. Clearly the major use for HDPE pipe is natural gas transmission pipelines. Equally, the use of PVC pipe in water transmission and plumbing pipelines is widespread. The use of pipe in these types of public utility applications

TABLE 7.9   DESIGN INSTALLATION DEFLECTIONS FOR HAUNCHED PIPE

Pipe Stiffness (kPa)	Installation Deflection (%)[1]		
	Less than 85% of Max. Dry Density[2] or Dumped[3]	85 to 95% of Max. Dry Density[2]	Greater Than 95% of Max. Dry Density[2]
<275	6+	4	3
275 – 700	4+	3	2
>700	2+	2	1

1. Deflections of unhaunched pipe are significantly larger.
2. Maximum dry density determined in accordance with AASHTO T 99.
3. Dumped materials and materials with less than 85% of maximum dry density are not recommended for embedment. Deflection values are provided for information only.

Source: After Chambers et al. [22].

dwarfs the use of plastic pipe in geosynthetics-related applications. It is nevertheless a growing area within geosynthetics (recall Table 1.10) and it is hoped that these applications have given some insight into the technology.

Perhaps of most current research interest is the load-carrying capacity behavior of geopipe in collection systems beneath large landfills, and heap leach piles. The theories presented in this chapter were originally developed with significantly lower normal stresses in mind. For large megafills, it appears as though design models incorporating soil arching are appropriate; this comes about from the deflections of the pipe itself as the overlying lifts of waste are imposed. Research and full-scale field testing are ongoing. Of significance is work at Ohio University evaluating a number of leachate collection cross sections (see Sargand et al. [23]). Both short-term and long-term tests are being evaluated using HDPE (smooth and profiled) and PVC pipes. Deflection calculations are further complicated when dealing with high temperatures that occur in wet landfills of the bioreactor types (recall Section 5.8).

One additional detail that is extremely difficult to design is the connection of plastic pipe to plastic manholes, such as those shown in Figure 7.14. In this case there are many applications with an extremely wide variety of possibilities. One driving force for the use of these plastic manholes is the necessity of providing chemical resistance against various leachates in solid-waste landfilling operations. The growing tendency in this regard is to use high density polyethylene for both the pipe and manhole system. In so doing, factory prefabrication can be utilized to great advantage. Standardized systems are becoming available. The manufacturers of HDPE pipe and fittings should be consulted for information and details

7.5   CONSTRUCTION METHODS

Subgrade preparation, joining, placement, and backfilling of plastic pipe is relatively simple in comparison to pipes made from other materials. This comes about by virtue

Figure 7.14 Illustrations of the use of plastic pipe with plastic manholes. (Compliments of Driscopipe and ADS)

of their light weight, relatively long lengths, and ease of joining. As with all geosynthetics, however, there are proper procedures that must be followed. CQC and CQA are as important with geopipe as they are with any other type of geosynthetic material.

7.5.1 Subgrade Preparation

Plastic pipe is usually placed in a prepared trench or within other prepared subgrade materials. If soil is the subgrade, as it usually is, the compaction should be to 95% of Standard Proctor compaction so as to minimize the deformation of the pipe while it is in service. Note that pipe trenches are often overexcavated so that bedding soil of a cohesionless nature can bring the grade up to the plan elevation (see Figure 7.15a). Granular soil can easily be graded, gives uniform support to the pipe, and is readily compacted beneath and above after the pipe is placed. Sufficient trench length should be available such that pipe laying can continue in a uniform manner. Conversely, too much open trench may allow for local instability or sloughing failures and negatively influence pipe placement and/or backfilling. Decisions related to such factors will depend greatly on the soil type and depth of trench. In some cases, trench support systems may be required. Local conditions and safety considerations will govern each situation.

If the pipe is to be placed directly on a geomembrane (as in the leachate collection system shown in Figure 7.15b), the full-depth drainage stone should be placed before pipe installation. Small excavations of at least the diameter of the pipe are then made, and the pipe is placed in these shallow excavations. Thus we end up with a trench, albeit a shallow one, even in cases of pipe placement in leachate collection systems.

Native soil backfill

$\approx D$

D

Secondary
backfill

$\approx 0.75D$

Primary
backfill

100–150 mm

Bedding
soil

$\leftarrow$ $D + 300$ mm $\rightarrow$
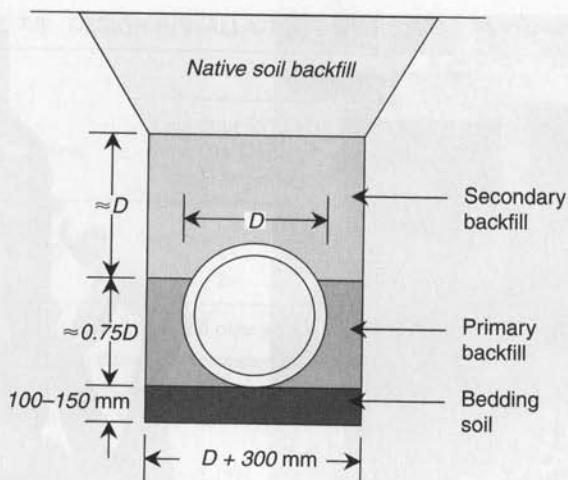
(a) Excavated trench method

Select gravel

Leachate
collection
gravel/sand

300 to 750 mm
typical

Bedding soil

Geomembrane
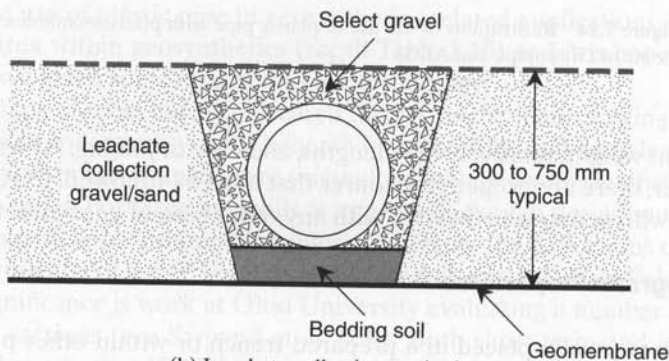
(b) Leachate collection method

Figure 7.15   Pipe placement and backfilling procedures.

Note that various organizations have guides or practices such as the following relating to underground installation methods for plastic pipe: ASTM D2774, "Underground Installation of Thermoplastic Pressure Piping;" ASTM F481, "Standard Practice for Installation of Thermoplastic Pipe and Fittings;" AWWA M23; "PVC Pipe Design and Installation;" PPI TR8; "Installation Procedures for Polyethylene Plastic Pipe;" and PPI TR31; "Underground Installation of Polyolefin Piping."

An approach completely different from the excavation, placement, and backfilling just described can be taken under certain circumstances. Figure 7.16 presents an example of a trenchless pipe placement. It uses a saw-type digging chain followed immediately by a pipe boot into which the pipe is transferred to the bottom of the trench. The soil collapses around the pipe after it leaves the boot and a vibratory sled compactor completes the procedure. This same concept, using a rotary wheel excavator,
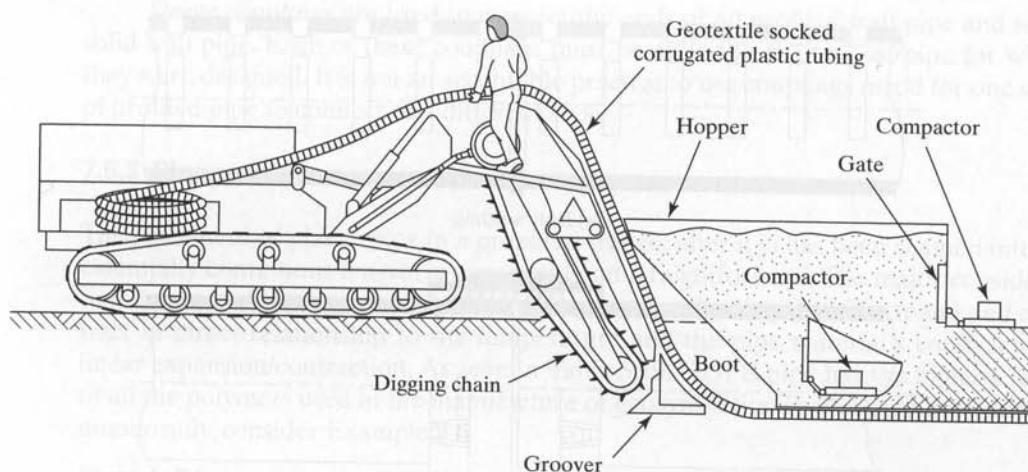
Figure 7.16 Trenchless installation of perforated profiled drainage pipe. (After Chambers et al. [22])

is being used for geocomposite edge drain installation, as will be described in Chapter 9.

7.5.2 Connections

There are a number of methods used to connect the ends of geopipe together, as shown in Figure 7.17:

The *butt welding* method is used for thick-walled HDPE pipe (either solid or perforated) and is exactly the same as that used in the natural gas pipe industry, (see ASTM D2657). The ends of the pipe are properly aligned with a heated plate placed between them. A longitudinal force brings the ends of each pipe against opposite sides of the heat plate. When adequate thermal energy is generated and the pipe ends become viscous, the heat plate is removed and the pipe ends are quickly brought together. Adequate force is applied to the opposing pipes to extrude a slight amount of the molten plastic out from the seam area. After cooling, the force is released and the seam is completed. This technique is routinely used in natural gas pipeline installation and has been shown to make seams of quality equal to that of the pipe itself. *Electric-socket welding* is similar. In contrast, PVC pipe is usually chemically seamed using a solvent on the pipe ends before pressure joining them together, (see ASTM D2672).

The *screw connection* can only be made if the plastic pipe thickness is adequate to form or machine the pipe ends to accept one another. Various configurations can be made and several patents are available on specialty products. To make a tight connection, gaskets are sometimes used, which reside in slotted seats of the thicker section of the connection. To make a leak-free connection it is possible to *extrusion seam* the outside separation for small diameter pipe or to extrusion seam the inside for very large diameter pipe. This latter situation could easily arise in connecting HDPE plastic pipe to HDPE plastic manholes (recall Figure 7.14).
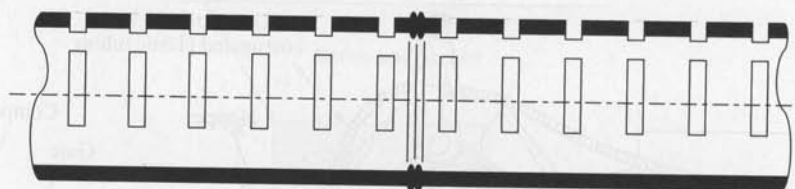
(a) Butt welding
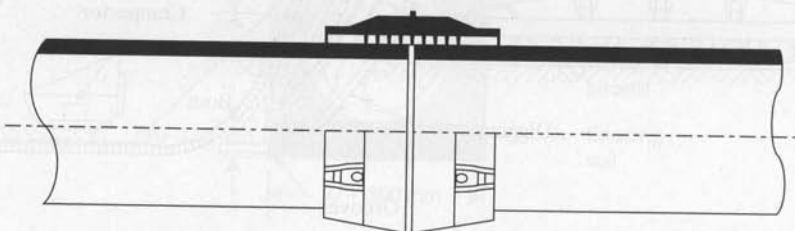
(b) Electric-socket welding
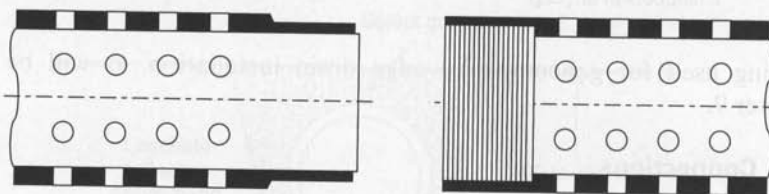
(c) Screw connection
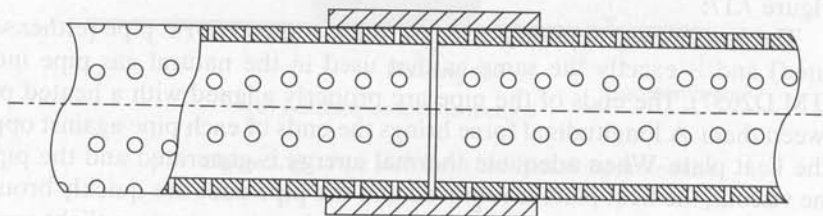
(d) HDPE sleeves
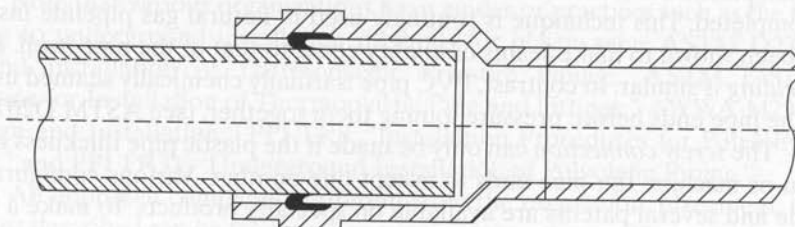
(e) Pressure sleeves with lip seal

Figure 7.17   Methods of joining geopipe.

Sleeve couplings are used to connect the ends of all profiled wall pipe and some solid wall pipe. Each of these couplings must be mated to the type of pipe for which they were designed. It is not an acceptable practice to use couplings made for one style of profiled pipe to connect to a different style.

7.5.3 Placement

The placement of plastic pipe in a prepared trench, after it is has been seamed into an essentially continuous length, is very rapid and straightforward. The major consideration that *must* be addressed is ambient temperature. Plastic pipe will expand and contract in direct relationship to the temperature and the pipe material's coefficient of linear expansion/contraction. As seen in Table 5.10, HDPE pipe has the highest value of all the polymers used in the manufacture of geosynthetics. To illustrate these effects numerically, consider Example 7.6.

Example 7.6

Calculate the elongation of 30 m of HDPE pipe in a trench undergoing a 25°C temperature increase, if it is allowed to deflect in an unrestricted manner. Also calculate the compressive stress mobilized if the same pipe is constrained in a fixed position.

Solution: Using a coefficient of expansion of $12 \times 10^{-5}/°C$ for HDPE, the elongation of the pipe if unconstrained is

$$\delta = \alpha(\Delta T)\, L \qquad\qquad (7.23)$$
$$= (12 \times 10^{-5})(25)(30)(1000)$$
$$\delta = 90\ \text{mm}$$

It the pipe is restricted (fixed) in position, the compressive stress that is induced is as follows (assuming a modulus of elasticity of HDPE of 760 MPa):

$$\sigma_c = \alpha(\Delta T)\, E \qquad\qquad (7.24)$$
$$= (12 \times 10^{-5})(25)(760)$$
$$\sigma_c = 2.3\ \text{MPa} \ (\simeq 12\% \text{ of the yield strength of typical HDPE})$$

Obviously, if the temperature decreases after the pipe is laid, the movement will tend to be a contraction and, if constrained, the stress will be tensile. To avoid problems due to thermal effects after backfilling is complete and the pipe is in service, the installation temperature should be within 10°C, and preferably 5°C, of the backfilled service temperature. This certainly could limit the time of day when pipe installation and/or backfilling is performed. The number of variations on this theme is essentially limitless.

7.5.4 Backfilling Operations

The backfilling of plastic pipe is performed in stages, as shown in Figure 7.15a. The primary backfill, which is usually a granular soil with adequate fines to provide good placement stability, is most important and requires special care in its placement in the haunch areas beneath the pipe. If soil is not placed beneath the pipe, voids will result

and when loaded the pipe will deform into these voids. Such deformations will always be excessive, thereby jeopardizing the pipe material in a manner not intended in the pipe's design. Conversely, too much compaction (called *slicing* since it is usually done by shovels in a sideways jabbing motion) will lift the pipe off of the subgrade and destroy the elevation control. Also the backfilling should be done in a reasonably symmetric manner so the pipe is not pushed laterally out of alignment. With the proper backfill soil, such as Class I or II material in Table 7.7, the lift thickness can be up to 450 mm. For Class III material, the lift thickness should be a minimum of 200 to 300 mm. Cavalier dumping of backfill soil adjacent to and above the pipe is simply courting disaster. The backfill soil cannot contain oversized material. A relatively large stone impinging against the pipe results in a stress concentration of the highest order. Such practices must be not permitted under any circumstances.

The secondary backfill provides support and load transfer to the top of the pipe and support for the subsequent backing operation. The soil type is often one grade class lower than the primary backfill soil; for example, if Class II soil is used as primary backfill, then Class III is used for secondary backfill. The thickness of this layer should be at least one-half of the diameter of the pipe itself and preferably equal to the diameter. Backfilling can be mechanized but never on a lift thickness less than 300 mm (recall Figure 7.9).

Following placement of the secondary backfill, natural soil or the soil or solid waste being used to construct the facility is brought up to final grade in lifts, as per the plans and specifications. This aspect follows standard earthwork construction procedures.

REFERENCES

1. *Proceedings of Plastics Pipes XII*, Milan, Italy, April 19–22, 2004. Washington, DC: Plastics Pipe Conference Association.

2. Halse, Y., Wiertz, J., Rigo, J. M., and Cazzuffi, D., "Chemical Identification Methods Used to Characterize Polymeric Geomembranes." In *Geomembranes: Identification and Performance Testing*, edited by A. L. Rollin and J. M. Rigo. Chapman and Hall, 1990, pp. 316–336.

3. Watkins, R. K., and Reeve, R. C., "Structural Performance of Buried Corrugated Polyethylene Testing," *30th Annual Geology Symposium*, Federal Highway Administration, Washington, DC, 1979.

4. Hsuan, Y. G., "Evaluation of Stress Crack Resistance of Polyethylene Non-Pressure Pipe Resins," Final Report, Plastic Pipe Institute, Washington, DC, 1997.

5. Hsuan, Y. G., and McGrath, T. J., "HPDE Pipe: Recommended Material Specifications and Design Requirements," NCHRP Report 429, Transportation Research Board, Washington, DC, 1999.

6. Haas, D. B., and Smith, L. G., "Erosion Studies," A Report of Canada Ltd., Saskatchewan Research Council, E 57–7, 1975.

7. Hwang, H. C., *Fundamentals of Hydraulic Engineering Systems*. Englewood Cliffs, NJ: Prentice Hall, 1981.

8. Viessam, W., Jr., and Hammer, M. J., *Water Supply and Pollution Control*, 4th ed. New York: Harper and Row, 1985.

9. Fox, R. W., and McDonald, A. T., *Introduction to Fluid Mechanics*, 3rd ed. New York: Wiley, 1985.

10. Gupta, R. S., *Hydrology and Hydraulic Systems*. Englewood Cliffs, NJ: Prentice-Hall, 1989.

11. *Driscopipe Systems Design*. Bartlesville, OK: Phillips Driscopipe, Inc.

12. Spangler, M. G., *Soil Engineering*, 2nd ed. Scranton, PA: International Textbook Co., 1971.

13. Moser, A. P., *Buried Pipe Design*. New York: McGraw-Hill, 1990.

14. Howard, A. K., "Soil Reaction for Buried Flexible Pipe," *Journal Geotechnical Engineering Division*, ASCE, vol. 103, no. GT1, 1977, pp. 33–43.

15. Spirolite HDPE Pipe Product Data CHM-916, Chevron Chemical Co., Reno, NV, 1989.

16. Katona, M. G., "Allowable Fill Height for Corrugated Polyethylene Pipe," TRB #1191, Transportation Research Board, National Research Council, Washington, DC, 1988.

17. Selig, E. T., and Hashash, N., "Analysis of the Performance of a Buried High Density Polyethylene Pipe." In *Structural Performance of Flexible Pipes*, edited by S. M. Sargand, G. G. Mitchell, and J. O. Hurd. Rotterdan: A. A. Balkema, 1990, pp. 95–103.

18. Cedergren, H. R., *Drainage of Highway and Airfield Pavements*. New York: Wiley, 1974.

19. Koerner, R. M., and Hwu, B-L., "Prefabricated Highway Edge Drains," ASCE/PennDOT Geotechnical Seminar, Hershey, PA, April 1990.

20. U.S. EPA, "Lining of Waste Containment and Other Impoundment Facilities," Report No. 600/2-88/052, 1988.

21. McEnroe, B. M., "Maximum Saturated Leachate Depth over Landfill Liner," *Journal of Environmental Engineering*, ASCE, vol. 119, no. 2, 1993, pp. 262–270.

22. Chambers, R. E., McGrath, T. J., and Heger, F. J., "Plastic Pipe for Subsurface Drainage of Transportation Facilities," NCHRP Report 225, Transportation Research Board, National Research Council, Washington, DC, 1980.

23. Sargand, S. M., Mitchell, G. G., and Hurd, J. O., eds., *Structural Performance of Flexible Pipes*. Rotterdam: A. A. Balkema, 1993.

PROBLEMS

7.1. Why are profiled pipes not directly measurable in terms of SDR or schedule?

7.2. How do you find an equivalent SDR of a profiled pipe?

7.3. What are some possible differences between the formulations of an HDPE geomembrane and an HDPE pipe?

7.4. What are some possible differences between the formulations of a PVC geomembrane and a PVC pipe?

7.5. On a normalized graph of stress-versus-deformation, sketch the relative behavior of a plastic pipe, concrete pipe, and steel pipe in an unconfined compression mode, such as ASTM D2412.

7.6. Why is the ultimate deflection of a plastic pipe usually taken as 10%?

7.7. The seaming of solid wall HDPE and PVC pipe is fundamentally different than the seaming of geomembranes.

    (a) What are the general seaming methods for solid wall plastic pipe?

    (b) What property does pipe have, versus geomembranes, that allows this to be accomplished?

    (c) What do you suspect is the general strength requirement for geopipe seams?

7.8. How are profiled HDPE pipes joined?

7.9. The use of geopipe as leachate collection removal pipes in landfills are of concern because of high vertical stresses. Describe how these considerations are handled when using equation (7.17) for the calculation of pipe deflection.

7.10. Describe how the modulus of soil reaction (E') in equation (7.17) is obtained and discuss its sensitivity.

7.11. Calculate and graph the deflection response for Example 7.5 (Section 7.3.3) for varying values of modulus of soil reaction (E').

7.12. Repeat Problem 7.11, varying the depth at which the pipe is buried.

7.13. Recalculate Example 7.4 (Section 7.3.2) using the same parameters except vary the maximum head (the mound) on the liner from 0.1, 0.2, 0.5, 0.75, and 1.0 m.

7.14. In the installation of geopipes, the backfilling beneath the pipe and under the haunches is critical. How do you inspect these two areas of backfilling?

7.15. Why is it necessary to have a minimum amount of soil cover over a geopipe before it can be trafficked by construction equipment? (*Hint*: Recall Figure 7.9).

8

Designing with Geofoam

8.0   INTRODUCTION

As described in Section 1.9, geofoam is expanded polystyrene (EPS) or extruded polystyrene (XPS) manufactured into large blocks, as shown in Figure 1.29. According to ASTM D4439, geofoam is defined as follows:

> *Geofoam:* Block or planar rigid cellular foamed polymeric material used in geotechnical engineering applications.

Yet, this definition is extremely broad and does not capture the issues of possible non-polystyrene materials and the necessary expansion process as well as the fact that the cells are gas-filled with solid material cell walls, or that discrete units can be used to form an intermediate structure.

The primary function for geofoam that we listed in Table 1.1 is that of separation and this is indeed the case, but it is quite limiting because geofoam is used in much broader applications—the major ones being as lightweight fill, compressible inclusions, thermal insulation, and (when appropriately formed) drainage. Figure 8.1 shows these applications, each of which will be addressed in the design section that follows geofoam properties and test methods.

It should be noted that the area of geofoam can nicely segue into what Horvath [1] calls *geocombs*, previously called ultralight cellular structures which he defines as "any manufactured material created by an extrusion process that results in a final product that consists of numerous open-ended tubes that are glued, bonded, fused or otherwise bundled together." The cross-sectional geometry of an individual tube typically has a simple geometric shape (circle, ellipse, hexagon, octagon, etc.) and is of the order of 25 mm across. The overall cross-section of the assemblage of bundled tubes resembles a honeycomb that gives rise to the name geocomb. Only rigid polymers (polypropylene and PVC) have been used to date as geocomb material.

The focus in this chapter will be on geofoam that is generally in the form of large blocks or plates, as shown in Figure 8.1.

8.1 GEOFOAM PROPERTIES AND TEST METHODS

Although somewhat arbitrary, geofoam properties and test methods will be grouped into physical, mechanical, thermal, and endurance categories. Of the various tests to be described, the specification for various grades of EPS and XPS shown in Table 8.1 should be kept in mind. Note that the these designations correspond to the respective geofoam densities. That said, the ASTM specification is instructive but quite liberal in its numeric values. For more demanding criteria, particularly with respect to load-bearing applications, the emerging specifications by AASHTO should be investigated.

8.1.1 Physical Properties

Dimensions.   Among the physical properties of geofoam are length, width, and height, but these are straightforward measurements with little ambiguity. Table 8.2 gives dimensions of the commonly available products in North America.

Density.   Density is measured according to ASTM C578, which results in extremely low values ranging from 11 to 48 kg/m^3. This is from 0.6 to 2.5% of the weight of a typical sand at a density of 1940 kg/m^3. Thus, lightweight fill applications are ideally

(a) Lightweight highway fill in Salt Lake City, Utah
    (Compliments of John Volk, URS Corp.)

(b) Compressible inclusion behind retaining wall
    (Compliments of John Henry, ACF Corp.)

(c) Thermal insulation beneath building
    (Compliments of Archie Filshill, InterGeo Corp.)

(d) Drainage channels beneath building slab
    (Compliments of John Horvath, Manhattan College)

Figure 8.1   Major applications of geofoam in engineering construction works.

suited for geofoam. Also, one person can easily handle and maneuver extremely large blocks of geofoam.

Moisture Absorption.   As described in Section 1.9, the manufacturing of geofoam precludes a permeability per se, but absorption can be important in certain applications—for example, in thermal insulation applications. The maximum absorption is about 0.3% by volume, per ASTM C578, and its effect is to somewhat reduce the R-value which will be discussed later.

TABLE 8.1 PHYSICAL PROPERTY REQUIREMENTS OF GEOFOAM ACCORDING TO ASTM D6817

Property and Units	EPS12	EPS15	EPS19	EPS22	EPS29	XPS20	XPS21	XPS26	XPS29	XPS36	XPS48
Density, min., kg/m^3	11.2	14.4	18.4	21.6	28.8	19.2	20.8	25.6	28.8	35.2	48.0
Compressive strength, min., kPa at 1%	15	25	40	50	75	20	35	75	105	160	280
Compressive strength, min., kPa at 5%	35	55	90	115	170	85	110	185	235	335	535
Compressive strength, min., kPa at 10%	40	70	110	135	200	104	104	173	276	414	690
Flexural strength, min., kPa	69	172	207	276	345	276	276	345	414	517	689
Oxygen index, min., volume %	24.0	24.0	24.0	24.0	24.0	24.0	24.0	24.0	24.0	24.0	24.0

TABLE 8.2   COMMONLY MANUFACTURED
DIMENSIONS OF GEOFOAM ACCORDING
TO ASTM D6817

Dimension (mm)	All EPS Types	All XPS Types
Width	305–1219	406–1219
Length	1219–4877	1219–1743
Thickness	25–1219	25–102

Oxygen Index. Since geofoam is readily combustible, an oxygen index (OI) test method is necessary for its evaluation. Note that this property is listed in the specification in Table 8.1. The OI method is defined in ASTM D2873 as the minimum percentage of oxygen in the site-specific gaseous environment required to support combustion. A material with an OI $\leq 21\%$ would burn freely in air that contains approximately 21% oxygen. Polystyrene has an OI of about 18%, however, a flame-retardant EPS is available that has a minimum OI of 24%. As noted by Horvath [2], geofoam should not be exposed to conditions in which temperatures are in excess of 95°C.

8.1.2 Mechanical Properties

The mechanical properties of geofoam, of which there are many, are of major importance. The most significant follow.

Compression Behavior. The compressive strength of a geofoam specimen is measured according to ASTM C165 or D1621 and uses a cube of 50 mm dimensions. Crosshead movement is 5.0 ± 0.5 mm/min equivalent to 10% strain per minute. As indicated in Table 8.1, measurements are to be taken at 1, 5, and 10% strain. Typical behavior of EPA and XPS at various densities is shown in Figure 8.2 (after Negussey [3]). The effects of density are clearly evident as well as the transition points of the curves. Larger test specimens or lateral confinement would give a stiffer response and be more of a performance test method [4].

Compression Creep Behavior. The sustained compressive load applied to a geofoam specimen results in behavior as shown in Figure 8.3 (after Negussey [3]). It is clearly seen in the EPS behavior that tertiary creep can be entered if too high a load is applied. In this regard the higher density products are an advantage. The current trend in geosynthetic long-term testing, however, is to use time-temperature-superposition (TTS) as an accelerated creep method. More specifically, the stepped isothermal method (SIM) has been attempted with limited success (Hsuan, et al [5]). Additional research appears to be warranted.

Tension and Flexure Resistances. ASTM C1623 evaluates the tensile strength of geofoam using a dumbbell-shaped specimen of 645 mm^2 cross section at its narrowest location. A strain rate of 5% per minute is used until failure. Figure 8.4 gives
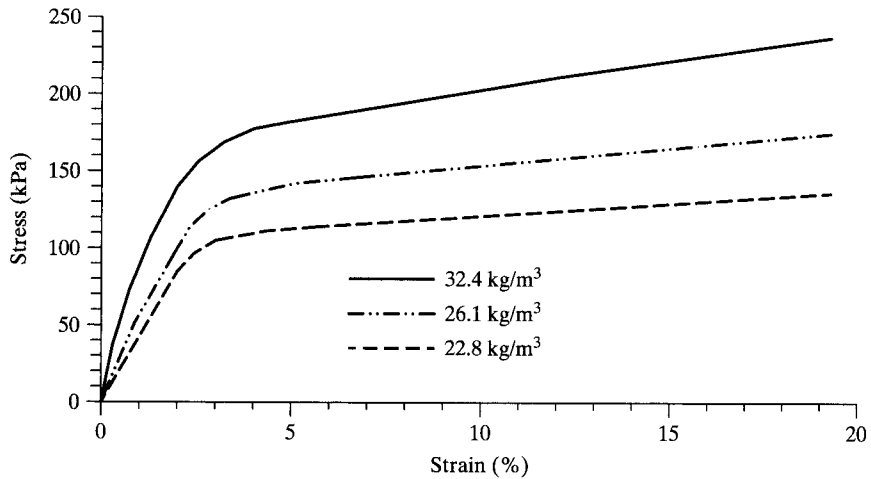
(a) Behavior of EPS geofoam
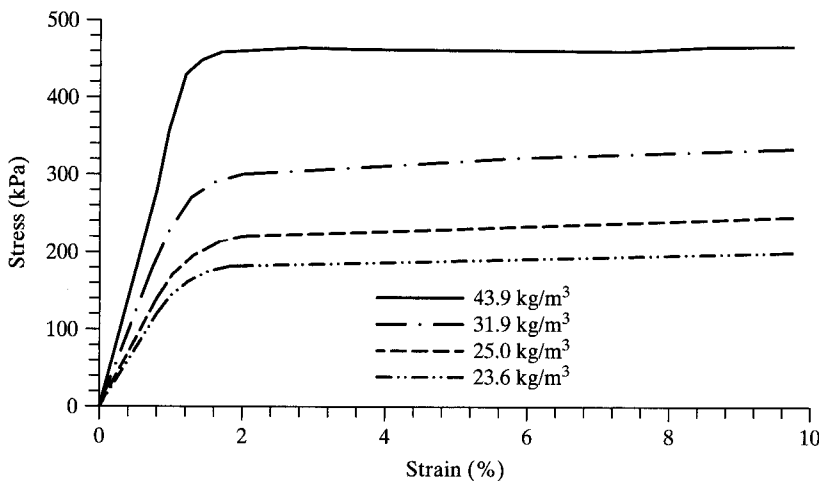
(b) Behavior of XPS geofoam

Figure 8.2   Unconfined compression behavior of geofoam as a function of density. (After Negussey [3])

EPS tensile strength as a function of density [6]. The tension-related value of flexure is covered in ASTM C203 and uses a geofoam beam in 3-point loading. The beam measures 250 mm long by 150 mm wide and is of varying thickness. The maximum stress is calculated in the conventional manner, and when plotted as in Figure 8.4 it shows similar behavior to tension, as it should.

Shear Strength.   There are numerous aspects of shear strength that are of interest: internal, external between geofoam blocks, and external to other surfaces such
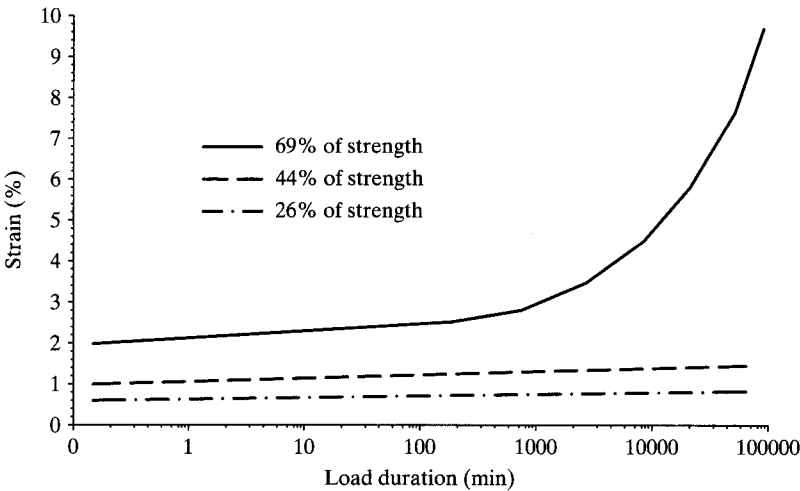
(a) EPS geofoam (density = 23.5 kg/m^3) creep behavior
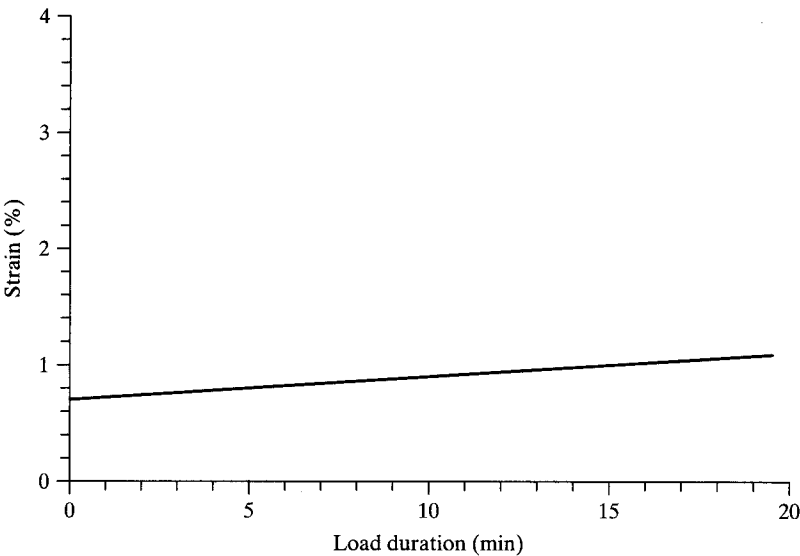
(b) XPS geofoam (density = 30.9 kg/m^3) creep behavior

Figure 8.3   Creep behavior of geofoam. (After Negussey [3])

as soil backfill or a geomembrane. ASTM C273 covers geofoam internal shear strength, and other standards such as ASTM D5321 cover shear strength between blocks and to other geosynthetics or soil surfaces. Perhaps most revealing is the shear strength between geofoam blocks, and its response to varying density is shown in Figure 8.4. The parallel behavior to the 10% compression response is of interest.
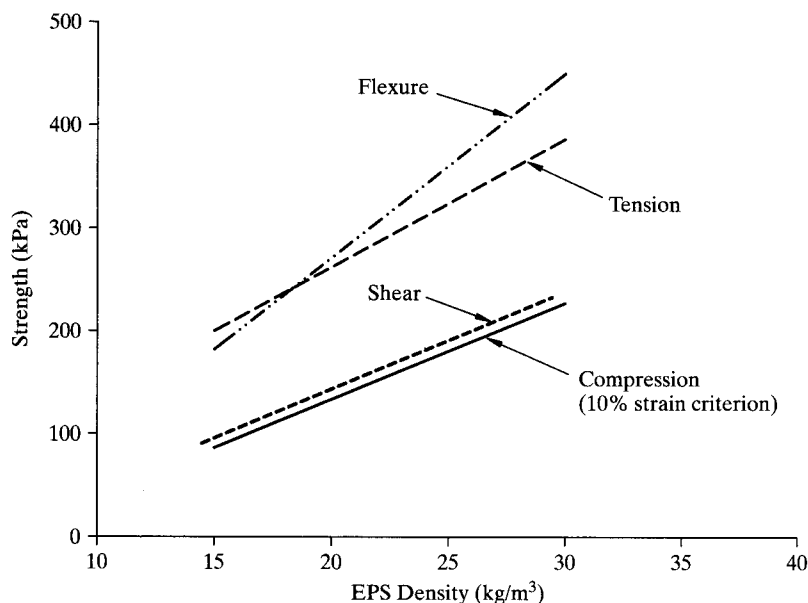
Figure 8.4   Various strength values of EPS as a function of density [6].

Other Mechanical Tests.   As with other geosynthetics, there are a variety of tests and test configurations that we might evaluate, such as cyclic load or fatigue behavior (see Horvath [2]). In this regard, the effects of temperature, confinement and concentrated load behavior come to mind. All are to be considered to be viable research topics for additional investigation.

8.1.3 Thermal Properties

Since geofoam is regularly used for its insulating value, the resistance to thermal gradients is an important property.

Thermal Resistance.   ASTM C578 measures thermal resistance in terms of an R-value, which is the resistance to heat flow in a unit width of geofoam. Its units are "m° C/W." The related R-value numbers are designated in the test standard. Figure 8.5 presents data for XPS and two densities of EPS as a function of temperature. As noted previously, moisture has the effect of reducing R-values. For comparison purposes, R-values of soil and concrete are less than one. R-value losses of 33 to 44% for EPS and 10 to 22% for XPS have been found for geofoam with full moisture absorption [2].

Thermal Cycling.   In some applications the temperature cycles and hence the resulting R-values fluctuate. In this regard it is prudent to use a conservative value in design. The topic is a good research area.
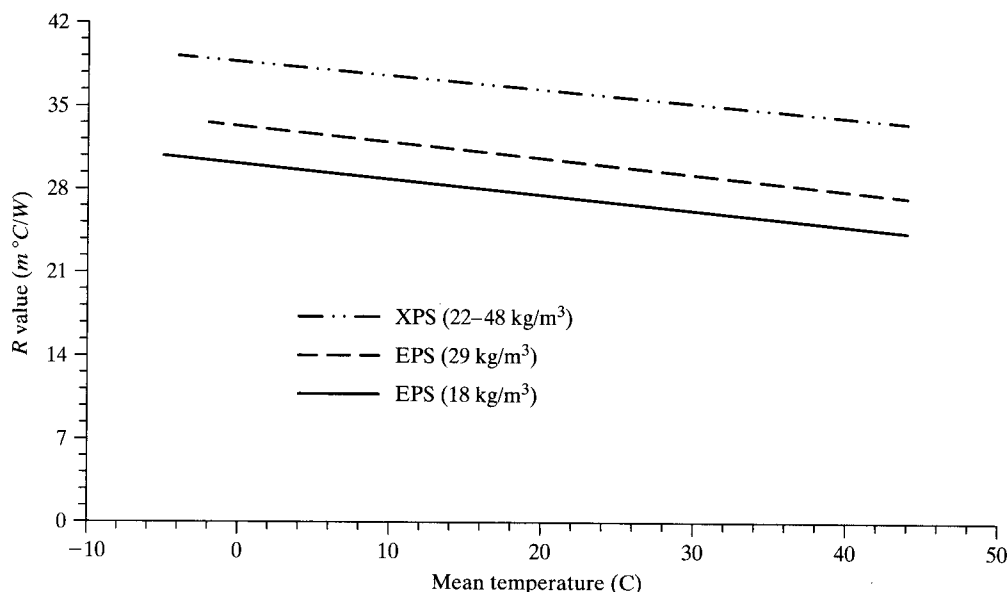
Figure 8.5   Geofoam R values (in SI units) as a function of temperature per ASTM D578. (After Negussey [3])

8.1.4 Endurance Properties

Most of the previously described tests were short-term, the exception being creep testing. There are numerous other actions of a long-term nature that will be described here under the topic of endurance properties.

Chemical Resistance.   Since many geofoam applications are related to highway, airfields, and railroads, gasoline and diesel spills are possible. Geofoam is readily attacked by hydrocarbons of all types. Other organic fluids, and perhaps even vapors, are potential degradation environments. Geomembrane encapsulation of the geofoam is common in this regard, and the design must adequately address this specific situation. The geomembrane chemical resistance chart of Table 5.8 is the first step in selecting the geomembrane type. Of course, seams and other aspects of constructability must be addressed accordingly.

Ultraviolet Degradation.   Initial discoloration followed by degradation (powdering) will result for geofoam subjected to long-term UV exposure. Since geofoam is invariably soil backfilled, *timely cover* is important. Maximum exposure times up to one month should be stipulated in the specifications depending on site-specific ambient conditions.

Flammability.   Geofoam is combustible and for this reason (in addition to UV degradation) it should be backfilled as soon as possible. This same precaution holds for stockpiled geofoam as well.

Biological Degradation.   Since polystyrene contains no food source, algae and fungi will not consume it, but infestation by insects and the like has occurred. Additives can be included during manufacturing to deter the situation, if warranted.

Lifetime Prediction.   As with all geosynthetics, an estimate of buried lifetime is of interest and geofoam is no exception. In the design applications to be presented next, required lifetimes of 75 to 100 years are not uncommon. The methodology for a lifetime assessment is incubation at several elevated temperatures—i.e., time-temperature superposition, followed by Arrhenius modelling. The procedure was described in Section 5.1.5. The vexing issue for geofoam, however, is what parameter to track to determine the *half-life*. Since compression is invariably involved, we could target a modulus value at 5 or 10%. It is felt to be the preferred method. Alternatively, tension or flexural resistance could be selected but specimen preparation and/or size could be a disadvantage.

8.2   DESIGN APPLICATIONS

This section presents geofoam used in four different types of applications. Figure 8.1 illustrates each of them. By way of historical development, Horvath [2] and Negussey [4] devote complete sections to the topic.

8.2.1 Lightweight Fill

The Norwegian Road Research Laboratory (NRRL) has focused on the use of geofoam as lightweight fill since 1970 [7]. There are many other early references as well [8]. The NRRL, however, has constructed hundreds of such projects [9] as have other Scandinavian countries. With the publication of the proceedings of an entire conference on the subject [8], this application is the one most widely used and accepted. A recent example (and one of the largest) as reported by Volk [10] is in Salt Lake City, Utah. Example 8.1 illustrates this type of application.

Example 8.1

A very wide 4.0 m high embankment is to be placed over a saturated organic silt (OL) foundation that is 13.4 m thick, as shown in the following diagram. What is the anticipated settlement based on the embankment being built with soil (γ_{soil} = 18.5 kN/m^3)? What if it is built with geofoam of unit weight γ_{GF} = 0.18 kN/m^3 as shown (thus a density of 18.4 kg/m^3) and the combined soil/pavement covering above it is at γ_{SP} = 19.0 kN/m^3)? Note that between the foundation soil and the geofoam is a geosynthetic drainage composite (geotextile/drainage core/geotextile) that functions as a drainage blanket for laterally transmitting consolidation water coming from the foundation soil.
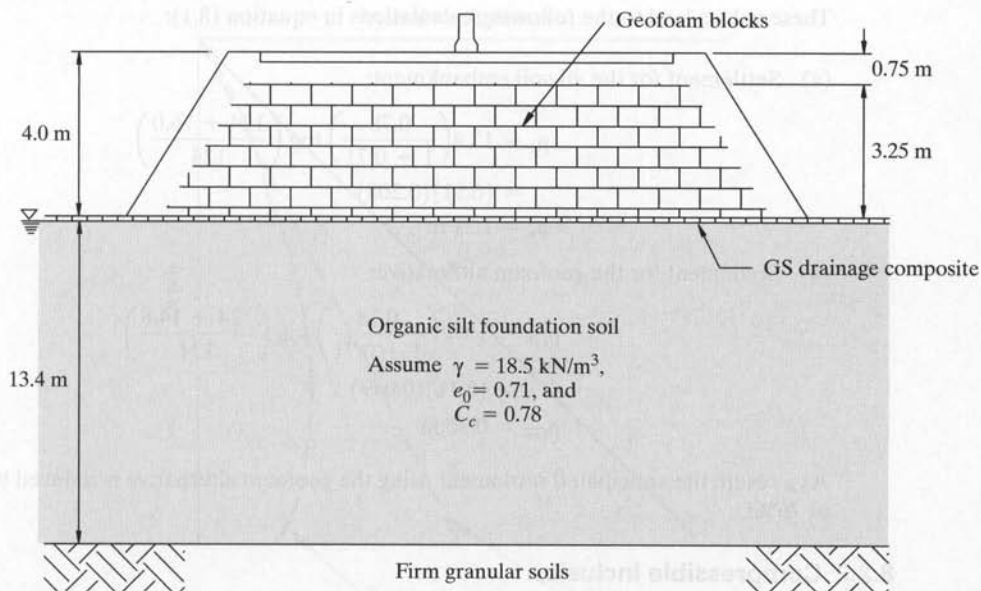
Solution: Using standard consolidation theory as described in all geotechnical engineering textbooks, (see Holtz and Kovacs [11]), it is well established that

$$\rho = H \frac{C_c}{1 + e_0} \log \frac{p_1 + \Delta p}{p_1} \qquad (8.1)$$

where

ρ = anticipated settlement,
H = thickness of compressible layer,
e_0 = original void ratio of compressible layer,
p_1 = existing pressure at mid-height of compressible layer, and
Δp = embankment load causing settlement.

Thus

$$p_1 = \frac{13.4}{2}(18.5)$$

$$= 124 \text{ kN/m}^2$$

and

$$\Delta p_s = (4.0)(19.0)$$

$$= 76.0 \text{ kN/m}^2 \quad \text{for the all-soil embankment}$$

whereas

$$\Delta p_{gf} = (0.75)(19.0) + (3.25)(0.18)$$

$$= 14.2 + 0.59$$

$$= 14.8 \text{ kN/m}^2 \quad \text{for the geofoam alternative}$$

These values lead to the following calculations in equation (8.1):

(a) Settlement for the all-soil embankment:

$$\rho_s = 13.4\left(\frac{0.78}{1 + 0.71}\right)\log\left(\frac{124 + 76.0}{124}\right)$$
$$= (6.11)(0.208)$$
$$\rho_s = 1.27 \text{ m}$$

(b) Settlement for the geofoam alternative:

$$\rho_{GF} = 13.4\left(\frac{0.78}{1 + 0.71}\right)\log\left(\frac{124 + 14.8}{124}\right)$$
$$= (6.11)(0.049)$$
$$\rho_{GF} = 0.30 \text{ m}$$

As a result, the anticipated settlement using the geofoam alternative is reduced by 0.97 m, or 76%!

8.2.2 Compressible Inclusion

The initial paper regarding geofoam as a compressible inclusion appears to be by Partos and Kazaniwsky [12]. This involved a below-grade parking garage wherein the opposing walls were braced against one another in a manner so as to generate *at-rest earth pressures*. Use of geofoam behind the walls ensured that only *active earth pressures* would be realized—approximately a 35% reduction. Subsequently, Horvath [13,14] has shown that geofoam can actually reduce lateral earth pressures to even less than active conditions. Figure 8.6 shows the typical situations from geotechnical engineering where the following equations for lateral earth pressures are common knowledge.

$$K = \frac{\sigma_h}{\sigma_v} \tag{8.2}$$

where

K = coefficient of earth pressure,
σ_h = horizontal stress acting on wall, and
σ_v = vertical stress at a given depth.

Furthermore,

K_p = passive earth pressure [K_p = $\tan^2(45 + \phi/2)$],   (8.3)
K_o = at-rest earth pressure [$K_o \simeq (1 - \sin \phi)$],   (8.4)
K_a = active earth pressure [$K_a = \tan^2(45 - \phi/2)$], and   (8.5)
ϕ = friction angle of the backfill soil.

Note that the at-rest pressure is uniformly higher than the active earth pressure and that both are linearly increasing with depth. The passive earth pressure (not shown) is the highest of all, but it is not particularly relevant in the walls to be discussed. Horvath

Lateral earth pressure
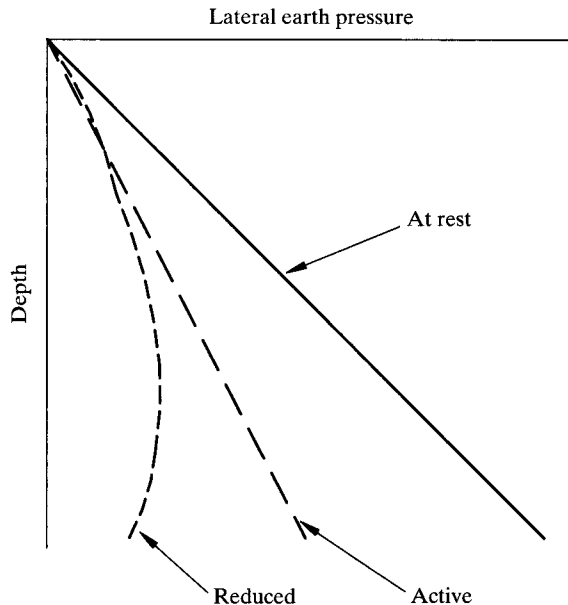
Figure 8.6 Conceptual lateral earth pressure distributions under different in situ stress conditions.

indicates that a compressible inclusion allows for arching in the backfill soil and that the subsequent earth pressure is curved, with a peak value near mid-height of the structure. Depending on the geofoam's thickness, the values are generally less than active earth pressure, and as depth increases the difference becomes substantial. In Figure 8.7, the behavior is quantified based on a FEM procedure that was developed by Horvath [13]. The trend is clearly evident and furthermore, the thicker geofoam reduces the wall pressures to almost a negligible amount. Example 8.2 illustrates the different magnitudes of lateral earth pressure against retaining walls under different scenarios.

Example 8.2

A 7.0 m high cantilever retaining wall is backfilled with soil at 18.5 kN/m^3 and $\phi = 33°$. Determine the following lateral earth pressures: **(a)** at-rest conditions, **(b)** active conditions, **(c)** conditions using Figure 8.7 with 50 mm geofoam, **(d)** conditions using Figure 8.7 with 150 mm geofoam, and **(e)** conditions using Figure 8.7 with 600 mm geofoam.

Solution: Use conventional geotechnical engineering for parts (a) and (b), and scaled values from Figure 8.7 for parts (c), (d), and (e):

(a)   At-rest conditions: $K_o = 1 - \sin \phi = 0.455$

$$P_o = \frac{1}{2}\gamma H^2 K_o$$

$$= \frac{1}{2}(18.5)(7.0)^2(0.455)$$

$$= 206 \text{ kN/m}$$
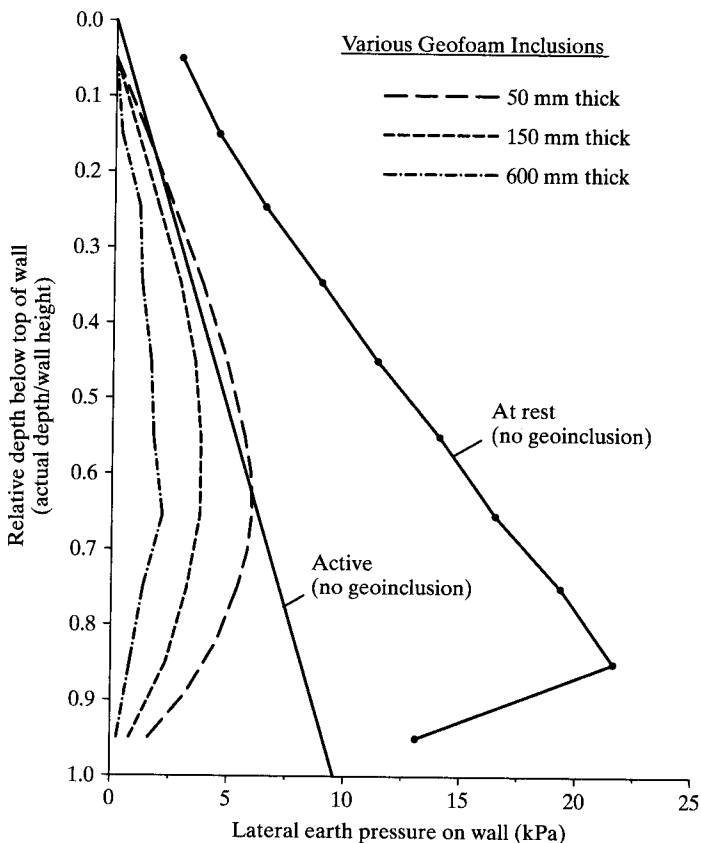
Figure 8.7 Lateral earth pressures for reduced earth pressure (REP) wall case. (After Horvath [13])

(b) Active conditions: $K_A = \tan^2(45 - \phi/2) = 0.295$

$$P_A = \frac{1}{2}\gamma H^2 K_A$$

$$= \frac{1}{2}(18.5)(7.0)^2(0.295)$$

$$= 134 \text{ kN/m}$$

(c) 50 mm of geofoam (scaled from Figure 8.7 using arbitrary units)

$$P_{50} = \frac{\text{Area under 50 mm curve}}{\text{Area under active curve}}(134)$$

$$= (138/184)(134)$$

$$= 101 \text{ kN/m } (75\% \text{ of active})$$

(d) 150 mm of geofoam (scaled from Figure 8.7 using arbitrary units)

$$P_{150} = \frac{\text{Area under 150 mm curve}}{\text{Area under active curve}} (134)$$

$$= (88/184)(134)$$

$$= 64 \text{ kN/m (48\% of active)}$$

(e) 600 mm of geofoam (scaled from Figure 8.7 using arbitrary units)

$$P_{600} = \frac{\text{Area under 600 mm curve}}{\text{Area under active curve}} (134)$$

$$= (40/184)(134)$$

$$= 29.1 \text{ kN/m (22\% of active)}$$

It is easily seen that the total earth pressures against the wall are significantly reduced in going with successively thicker layers of geofoam.

A completely different application than the above is the use of geofoam (as a compressible inclusion) beneath building and pavement slabs in areas where *expansive soils* are present in the subgrade soils. Expansive soils are widespread in many locations of the world, and upheaval of all types or roads and structures is a serious and costly situation. Geofoam represents a cost-effective solution to the expansive soil problem.

8.2.3 Thermal Insulation

This application of geofoam should be obvious to everyone since EPS is used to manufacture coffee containers and a wide range of commonly used articles in need of thermal insulation. All earth sheltered dwellings (houses, industrial buildings, garages, etc.) can have external temperatures muted by installing geofoam on the outside of the concrete or masonry walls or beneath floor slabs. In so doing the adverse effects of cold and hot temperatures are diminished. The key to the amount of change is the geofoam's resistance to thermal flow (hot or cold), as shown below. From standard physics texts, such as, Tipler [15], we have the following:

$$I = \frac{\Delta Q}{\Delta t} = kA\frac{\Delta T}{\Delta x} \tag{8.6}$$

where

I = heat current or heat flow,
ΔQ = heat energy,
Δt = time interval,
k = coefficient of thermal conductivity,
A = cross sectional area of heat flow,
ΔT = temperature difference across the material, and
Δx = thickness of the material.

Solving equation 8.6 for ΔT:

$$\Delta T = \left[\frac{\Delta x}{kA}\right]I = (I)(R_t) \qquad (8.7)$$

where

$$R_t = \text{thermal resistance}$$
$$= \frac{\Delta x}{kA} \qquad (8.8)$$

The thermal resistance per unit area is the R factor and is merely the thickness of the insulator divided by the thermal conductivity.

$$R = \frac{\Delta x}{k} \qquad (8.9)$$

Values of k and R are given in Table 8.3 in both SI units and English units. In contrast, Figure 8.5 presents the R values of geofoam, which are seen to be among the highest of the materials listed in Table 8.3—e.g., air, glass, wool, and rock wool. The numeric values of geofoam have been added to Table 8.3 accordingly.

The use of R values showing heat (or cooling) savings is shown in Example 8.3.

Example 8.3

A refrigerated building (with an inside temperature to be maintained at $-10°C$) for the storage of perishable foods is sited on a high water content soil adjacent to a river. The building's footprint is 25 m by 10 m. The concerns are twofold: (1) to prevent the groundwater beneath the building from freezing, which would lift the floorslab (a form of *icejacking*) and (2) to save refrigerant over time. The floor slab is 225 mm of reinforced concrete ($R = 0.9 \text{ m°C/W}$) on gravel ($R = 0.1 \text{ m°C/W}$) for conventional design, or on 150 mm thick geofoam ($R = 35 \text{ m°C/W}$). Do the example first without geofoam, then with geofoam and compare the results. Rewrite equation 8.6, which using equation 9.9 can be done in terms of an R factor as follows:

$$\frac{\Delta Q}{\Delta t} = kA \frac{\Delta T}{\Delta x}$$

$$\frac{\Delta Q}{\Delta t} = \frac{A \cdot \Delta T}{R} \qquad (8.10)$$

Solution:

(a) With gravel and no geofoam; (i.e., with a conventional design):

$$\frac{Q}{t} = \frac{(25)(10)(20)}{(0.9 + 0.1)}$$
$$= 5000 \ W$$

TABLE 8.3 THERMAL CONDUCTIVITIES *(k)* AND *R* VALUES FOR VARIOUS MATERIALS COMPARED TO GEOFOAM

Material	$k^{(1)}$	$R^{(2,5)}$	$k^{(3)}$	$R^{(4,5)}$
Air (27°C)	0.026	38.5	0.18	5.56
Ice	2.21	0.452	15.3	0.065
Water (27°C)	0.609	1.64	4.22	0.237
Aluminum	237	0.004	1644	6.08×10^{-4}
Copper	401	0.002	2780	3.60×10^{-4}
Gold	318	0.003	2200	4.55×10^{-4}
Iron	80.4	0.012	558	0.002
Lead	353	0.003	2450	4.08×10^{-4}
Silver	429	0.002	2980	3.36×10^{-4}
Steel	46	0.022	319	0.003
Oak	0.15	6.67	1.02	0.980
Maple	0.16	6.25	1.1	0.909
White pine	0.11	9.09	0.78	1.28
Brick	0.4–0.9	2.5–1.1	3–6	0.33–0.17
Concrete	0.9–1.3	1.1–0.77	6–9	0.17–0.11
Corkboard	0.04	25	0.3	3.33
Glass	0.7–0.9	1.4–1.1	5–6	0.2–0.17
Glass wool	0.042	23.8	0.29	3.45
Masonite	0.048	20.8	0.33	3.03
Plaster	0.3–0.7	3.3–1.4	2–5	0.5–0.2
Rock wool	0.039	25.6	0.27	3.71
Geofoam (EPS)	0.029–0.042	24–35	0.20–0.29	3.46–5.05
Geofoam (XPS)	0.025–0.031	32–40	0.17–0.22	4.61–5.77

$^{(1)}$ k in SI units of W/m · °C.

$^{(2)}$ R in SI units of m · °C/W.

$^{(3)}$ k in English units of Btu · in./h · ft^2 · °F.

$^{(4)}$ R in English units of h · ft^2 · °F/Btu · in.

$^{(5)}$ Conversion is as follows: $R_{SI} = 6.93\ R_{English}$

Source: Modified from Tipler [15].

(b) With geofoam:

$$\frac{Q}{t} = \frac{(25)(10)(20)}{(0.9 + 35)}$$

$$= 139\ W$$

(c) Thus the savings in refrigeration inside of the building per unit of time using geofoam is 4861 *W*, which is 36 times less expensive using geofoam as an insulator.

8.2.4 Drainage Applications

The relative ease with which geofoam can be machined allows for grooves or slots to be fabricated into the product as it is manufactured. When placed in a continuous alignment in the field, this creates a channel that serves as a pipe or conduit for the

transmission of liquids or gases. This is, of course, the drainage function that now can be juxtaposed onto one of the other geofoam's applications discussed in this section. We can visualize conducting groundwater or infiltration water from behind retaining walls or beneath building slabs in this manner. As the channels become sufficiently large, we have created geopipes, albeit in a square or rectangular cross section. Alternatively, the geofoam can be manufactured with pedestals that allow for drainage in all directions and that are not to be constrained to a linear orientation. The variations are essentially limitless. These drainage concepts are ideally positioned for alternative geofoam products like geocombs, as mentioned in the introduction to this chapter.

In most instances, a geotextile serving as a separator and filter must be placed against the soil. The design of the geotextile follows its respective sections in Chapter 2. The geotextile can be bonded to the geofoam in the factory if it is desirable to do so.

The design methods for geofoam or geocombs in various drainage applications were discussed in Chapter 4 and will be discussed further in Chapter 9.

8.3 DESIGN CRITIQUE

Designing with geofoam is a logical extension of basic principles. Clearly, technology transfer can be employed to a considerable extent.

Lightweight fill is probably the greatest single application of geofoam and clearly uses the greatest quantities of the material. Settlement prediction using standard geotechnical engineering principles is readily adaptable, even considerations of long-term creep deformations. Slope stability and/or direct sliding can also be handled, and there are several publications that address this topic [4, 16]. In this regard the block layout is important and three-dimensional staggering is recommended. Dynamic, seismic, and wind loadings are more difficult to deal with, but they are problematic in all geotechnical design as well, particularly the magnitude of the applied loadings.

Geofoam as a compressible inclusion is very capable of ensuring active earth pressures behind retaining walls. To have pressures lower than active, however, is not an intuitive approach. Championed by Horvath [13, 14], this concept is very provocative and could be advanced by field monitoring and, perhaps, centrifuge modeling as well (although scaling of various components promises to be difficult).

The thermal insulation applications of geofoam are well founded in fundamental heat flow (physics) theory and its practical extension to all types of home and industrial insulation materials and practices is commonplace. The necessary R values are available under the important assumption that proper installation has been achieved. Construction aspects of geofoam will follow in the next section.

The last area presented is utilization of geofoam drainage, which depends on the block manufacturing process. A flow rate factor of safety can be calculated in the standard manner and has been illustrated with geotextiles, geonets, and (in the next chapter) drainage geocomposites.

Vibration damping (steady state and random) is provocative but little information is available. It is, however, mentioned in Horvath [2] with respect to motor vehicle damping. The seismic behavior is essentially unknown but is of obvious interest.

Design, of course, must address service life, which means that durability is an issue for many of the applications presented. Embankments, walls, structures, and the like have targeted lifetimes of 75 to 100 years, and geosynthetics are regularly challenged in this regard. The focus to date on lifetime prediction has been on geomembranes (from an environmental protection aspect), and this same type of predictive methodology should be used to assess geofoam. Section 8.1.4 briefly discusses the recommended approach. Although neither quick nor inexpensive, it seems obvious that work must be initiated to answer this very meaningful question.

For the academician, the *research needs* section in Horvath [2] is a invaluable guide for future geofoam activity. Clearly, much has been done and much more remains to be done with this type of geosynthetic material

8.4   CONSTRUCTION METHODS

The planar surfaces of geofoam blocks allow for direct "butt" contact between one another. This assumes that the soil subgrade for the first layer of geofoam blocks is compacted, leveled, and true-to-grade. A block structure, albeit with huge blocks is then built. If the subgrade is not true with respect to the lowest course of blocks, the situation will only be aggravated as it becomes higher. Geofoam blocks can be cut using a chain saw or a hot-wire device.

The attachment of the blocks to one another is made using thin steel plates (some galvanized) with pointed barbs facing up and/or down (see Figure 8.8). They readily penetrate the geofoam blocks and hold them together.

Since geofoam should never be used in an exposed condition, covering (usually by soil) must be carefully considered. This is an application-specific issue, but the placement of soil must be done with care. As with all geosynthetics, construction equipment should never travel directly on geofoam. There can be no exceptions since concentrated wheel loads can locally deform and even crush the blocks. If this occurs, the
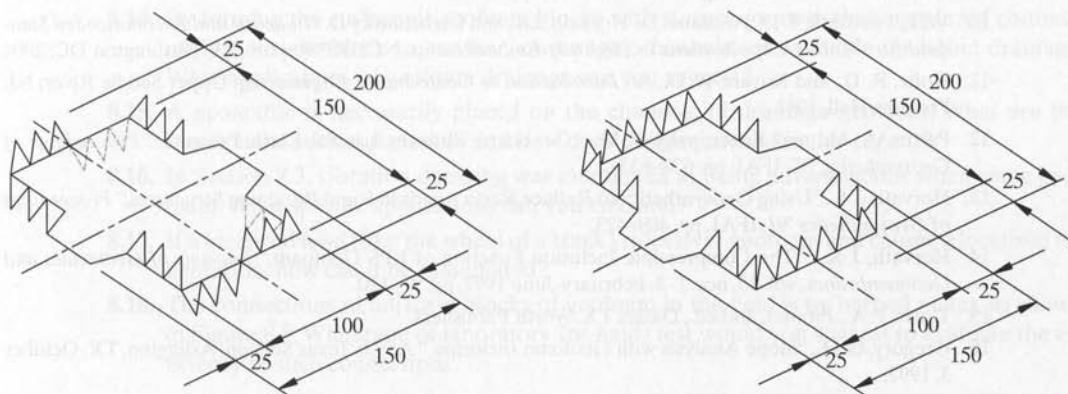
Figure 8.8 Various types of barbed connection plates for geofoam; all dimensions are in millimeters [3].

affected blocks must be discarded. The issue of minimum soil cover before construction equipment trafficking is subjective, but 450 mm of soil is a typical construction specification value.

Adverse weather conditions (rain or snow) are not harmful to the geofoam blocks, although wind is troublesome from the perspective of manual handling. If stored at the construction site for longer than approximately one month, the blocks should be covered with a plastic membrane or a tarpaulin.

A number of standards organizations, most notably ASTM and ISO, are active in the area of geofoam. Not only are test methods being developed but also specifications like Table 8.1 and possible construction guides as well. Clearly, geofoam as a geosynthetic material belongs in a book such as this, and previous editions now seem incomplete without having the topic as a stand-alone chapter.

REFERENCES

1. Horvath, J. S., "Geofoam and Geocomb," *Proceedings of the GRI-13 Conference*, December 14–15, 1999, GII Publication, pp. 72–104.
2. Horvath, J. S., *Geofoam Geosynthetic*. Scarsdale, NY: Horvath Engineering P. C. Publisher, 1995, 217 pgs.
3. Negussey, D., "Properties and Applications of Geofoam," Society of Plastics Engineers, 1997.
4. Negussey, D., *Slope Stabilization with Geofoam*, Syracuse, NY: Geofoam Research Center, Syracuse University, 2001.
5. Hsuan, Y. G., Yeo S.-S., and Koerner R.M., "Compression Creep Behavior of Geofoam Using the Stepped Isothermal Method," Proceedings of GSI-18 at GeoFrontiers, 2005, ASCE.
6. Styropor, "Construction, Highway Construction and Ground Insulation," Tech. Info. Bulletin No. 1-800e, BASF AG, Ludwigshafe, Germany, June 1991 (rev. September 1993).
7. National Road Research Laboratory (NRRL), "Expanded Polystyrene Used in Road Embankments; Design, Construction and Quality Assurance," Form 582E, Oslo, Norway, September 1992.
8. *Proceedings of the International Geotechnical Symposium on Polystyrene Foam in Below-Grade Applications*," edited by J. S. Horvath, May 1994, Manhattan College, NY.
9. Dahlberg, R. G., and Refsdal, G., "Polystyrene Foam for Lightweight Road Embankments," *Proceedings of the 16 World Road Congress*, Vienna, 1979, pp. 27–33.
10. Volk, J. in Stark, T. D., Arellano, D., Horvath, J.S., and Leshchinsky D. *Guideline and Recommended Standard for Geofoam Applications in Highway Embankments*, NCHRP Report 529, Washington DC; 2004
11. Holtz, R. D., and Kovacs, W. D., *An Introduction to Geotechnical Engineering*. Upper Saddle River; NJ: Prentice Hall, 1981.
12. Partos, A. M., and Kazaniwsky, P. M., "Geoboard Reduces Lateral Earth Pressure," *Proceedings of Geosynthetics '87*, IFAI, pp. 628–633.
13. Horvath, J. S., "Using Geosynthetics to Reduce Earth Loads in Rigid Retaining Structures," *Proceedings of Geosynthetics '91*, IFAI, pp. 409–423.
14. Horvath, J. S., ""The Compressible Inclusion Function of EPS Geofoam," *Journals of Geotextiles and Geomembranes*, vol. 15, nos. 1–3, February-June 1997, pp. 77–120.
15. Tipler, P. A., *Physics*, 2nd ed., Dallas, TX, Worth Publishers.
16. Gregory, G. H., "Slope Analysis with Geofoam Inclusion," ASCE Texas Section, Arlington, TX, October 3, 1997.

PROBLEMS

8.1. The most widely used geofoam application is for lightweight fills. Why is this the case?

8.2. List the types of subgrade conditions where geofoam should be considered insofar as lightweight fill is concerned.

8.3. What is the significance of the oxygen index measurement for geofoam?

8.4. The compression behavior curves shown in Figure 8.2 indicate a piecewise liner trend. In the initial portion of the curves what is occurring at less than 2%? What is occurring in the latter portion greater than 3%?

8.5. Depending upon the stress level applied to geofoam, compressive creep many be a concern (recall Figure 8.3). Unfortunately, conventional creep testing is very long and tedious. What techniques could be used to greatly decrease the time involved?

8.6. What is the difference between standard time-temperature-superposition (TTS) testing and the stepped isothermal method (SIM)?

8.7. Figure 8.4 indicates very similar trends in (a) flexure and tension, and (b) shear and compression. Describe why these respective sets of curves are so close to one another?

8.8. Why are R values decreased when geofoam absorbs moisture?

8.9. Recalculate Example 8.1 using different values of the compression index of the foundation soil, varying from 0.25 to 1.50. What general types of soils do these various C_c values represent?

8.10. Recalculate Example 8.1 using different values of surcharge fill height, varying the geofoam thickness from 1.5 to 7.5 m.

8.11. In considering lateral earth pressures behind retaining walls, three coefficients (K_A, K_o, and K_p) are discussed in Section 8.2.2. Describe the backfill soil's condition in these three states.

8.12. Figures 8.6 and 8.7 indicate that lateral earth pressures can be reduced to less than active conditions. Describe how this is possible.

8.13. Geofoam placed behind a retaining wall obviously acts as an inclusion to reduce lateral earth pressure (recall Example 8.2). In northern climates, however, it also acts as an insulating material. Describe how this function works to advantage in the performance of the wall.

8.14. By forming the surface of geofoam blocks with slots or grooves that are placed continuously from one block to another, continuous channels are available for liquid drainage. What applications of geofoam drainage can you suggest?

8.15. A geotextile is necessarily placed on the channels of drainage geofoam. What are the functions of such a geotextile and how does design proceed in this regard?

8.16. In Section 8.3, vibration damping was mentioned as being advantageous when using geofoam. What specific applications can you envision?

8.17. If a localized load (like the wheel of a truck) rides over geofoam and causes a localized indentation, how can it be remediated?

8.18. The connections of adjacent blocks of geofoam in the field is by barbed plates, as shown in Figure 8.8. What type of laboratory (or field) test would you suggest to evaluate the efficiency of such connections?

9

Designing with Geocomposites

9.0 INTRODUCTION

As originally described in Section 1.10, geocomposites consist of various combinations of geotextiles, geogrids, geonets, geomembranes, and other materials. In keeping with the general theme of this book, the geocomposites to be discussed will be made from synthetic, or human-made, materials rather than naturally occurring ones. Sometimes, however, it is necessary to include gravel, sand, silt, and/or clay within the composite system. For background information, the reader should review Section 1.10. The general reason for the existence of geocomposites is the higher performance that can often be attained by combining the attributes of two or more materials. Such high performance can be used for any of the basic functions that have already been introduced to the reader: separation, reinforcement, filtration, drainage, and containment. This chapter focuses on these five functions insofar as they are addressed by geocomposites. Some of the individual sections will be subdivided according to application area due to the large amount of material to be discussed (e.g., drainage geocomposites).

Although the general situation might change with time, the growth rate of geocomposites is currently proceeding faster than most areas discussed thus far. Of course, some of these hybrid materials have been introduced only recently, but selected application areas have completely swung in their direction. Drainage composites having high flow capability are such a situation. Examples are discussed in connection with wick drains, sheet drains, and edge drains. Note that high-performance reinforcement systems can be obtained by different approaches; the role of geocomposites in reinforcement will be emphasized. The area is so dynamic that GCLs were only mentioned in the second edition of the book as liquid containment geocomposites. In subsequent editions they were treated as a geosynthetic in their own right.

Before beginning the chapter, however, the reader is cautioned that many of these geocomposites serve multiple functions. While the primary function will always be the focus, the proper performance of secondary (and perhaps tertiary) functions is also required. If the design of these additional functions has been covered previously in this book, it will not be repeated here; the appropriate sections will, however, be cross-referenced.

9.1 GEOCOMPOSITES IN SEPARATION (EROSION CONTROL SYSTEMS)

When geotextiles are designed as separators between dissimilar materials (Section 2.5), the mechanical demands on the material are quite low. Many geotextiles between 200 and 300 g/m^2 are adequate to handle general situations (e.g., where a stone base is being separated from soil subgrade or different zones are separated within an earth dam). Values such as tensile strength, modulus, burst strength, puncture strength, and tear strength are rarely used fully for the geotextiles discussed. In fact, the recommended installation survivability properties often take precedence over the calculated values. However, in the above situations, the geotextile was usually not used as a ground surface cover by itself; it was not separating the ground surface from the prevailing atmospheric conditions (wind, rain, snow, etc.). Although an extremely porous

geotextile could be used for this purpose, specialty geocomposites have been developed for the specific purpose of *erosion control*.

The general goal of erosion-control geocomposites is to protect the soil from sheet, rill, or gully erosion either indefinitely or until vegetation can establish itself. While water is the predominant medium for erosion (or detachment) and the subsequent transportation of soil particles, wind is also a potential medium, as shown in Figure 9.1. Here the interaction of the water or air velocity and the size of soil particles gives rise to the sequence of soil erosion—namely, detachment, transportation, and deposition. The figure also shows that water is somewhat more severe than air in causing erosion.

The International Erosion Control Association (IECA) is an organization that focuses on erosion control practices, materials, conferences, publications, and standards. Most of the products dealt with by erosion control specialists use geosynthetic materials in whole or in part; they are shown collectively in Figure 9.2. The relatively large number of erosion control products can be broadly separated into temporary and permanent materials, as will be further described later.

The installation of many of the flexible erosion-control products is straightforward. Figure 9.3 illustrates the use of geocomposites as erosion protection in a water channel and on a steep side slope. The products are usually placed on a prepared soil subgrade by pinning them to the soil with U-shaped staples or small ground anchors. *Intimate contact* of the blanket or mat to the soil subgrade is very important, since
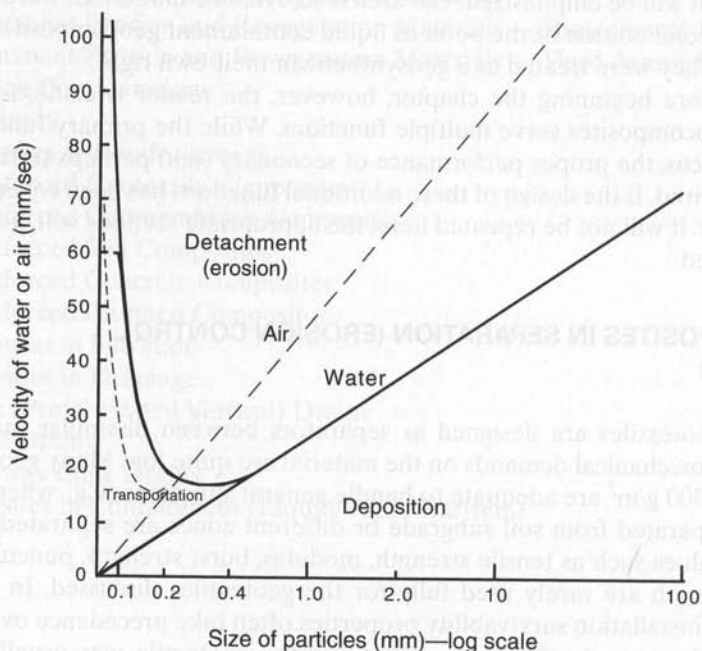
Figure 9.1 Comparison of detachment (or erosion), transportation, and deposition responses due to air and water. (Modified from Garrels [1])
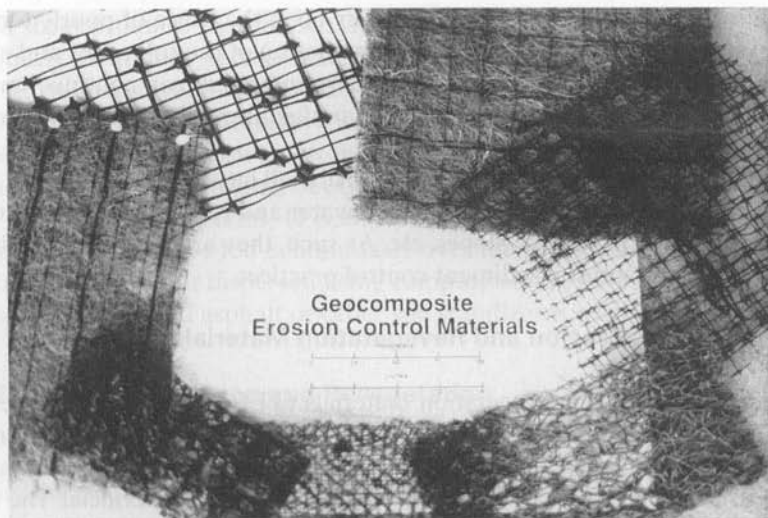
Figure 9.2   Geocomposites used in erosion control.

(a) As installed erosion control material in water runoff channel
(Compliments of TC Nicolon, Inc.)

(b) After growth erosion control material in water runoff channel
(Compliments of TC Nicolon, Inc.)

(c) Erosion control material on steep side slope
(Compliments of Colbond, Inc.)

Figure 9.3   Use of geocomposite separators in the two major erosion control applications.

water flow beneath the material has usually been the cause of poorly functioning and failed systems. In a similar vein, proper installation of the roll edges and ends is important, so that flow does not cause local undermining that can continue under the adjacent rolls in a progressive manner. The manufacturers' installation recommendations must be closely followed.

All of the products to be described easily fall into categories of best management practices (BMPs) for the control of storm water and runoff into local waterways, from construction sites, roadways, slopes, etc. As such, they are appropriate when considering clean streams and soil sediment control practices.

9.1.1 Temporary Erosion and Revegetation Materials

Temporary erosion and revegetation materials (TERMs) consist of materials that are wholly or partly degradable. They provide temporary erosion control and are either degradable after a given period, or only function long enough to facilitate vegetative growth; after the growth is established, the TERM becomes sacrificial. The natural products are completely biodegradable, while the polymer products are only partially so.

Theisen [2] groups the following materials (listed in Table 9.1) in the TERM category. The first two products are self-explanatory, consisting of traditional methods of soil erosion control using straw, hay, or mulch loosely bonded by asphalt or adhesive. Their stability in remaining as-placed is often quite poor. Geofibers in the form of short pieces of fibers or microgrids can be mixed into soil with machines or rototillers to aid in lay-down and continuity. The fiber or grid inclusions provide for greater stability over straw, hay, or mulch simply broadcast over the ground surface.

Erosion-control meshes and nets (ECMNs) are biaxially oriented nets manufactured from polypropylene or polyethylene. They do not absorb moisture, nor do they dimensionally change over time. They are lightweight and are stapled to the previously seeded ground using hooked nails or U-shaped pins. This is the practice for many of the

TABLE 9.1   GEOSYNTHETIC EROSION CONTROL MATERIALS

TERMs	PERMs	
	Biotechnical-Related	Hard Armor-Related
Straw, hay, and hydraulic mulches	UV stabilized fiber roving systems (FRSs)	Geocellular containment systems (GCSs)—concrete filled
Tackifiers and soil stabilizers	Erosion-control revegetation mats (ECRMs)	Fabric-formed revetments (FFRs)
Hydraulic mulch geofibers	Turf reinforcement mats (TRMs)	Vegetated concrete block systems
Erosion-control meshes and nets (ECMNs)	Discrete-length geofibers	Concrete block systems
Erosion-control blankets (ECBs)	Geocellular containment systems (GCSs)—vegetated	Stone riprap
Fiber roving systems (FRSs)		Gabions

Source: After Theisen [2].

rolled sheet products that follow. The stability is obviously greatly improved over the previously mentioned natural materials.

Erosion-control blankets (ECBs) are also biaxially oriented nets manufactured from polypropylene or polyethylene, but these are now placed on one or both sides of a blanket of straw, excelsior, cotton, coconut, or polymer fibers. The fibers are held to the net by glue, lock stitching, or other threading methods.

Fiber roving systems (FRSs) are continuous strands, or yarns, usually of polypropylene, that are fed continuously over the surface that is to be protected. They can be hand placed or dispersed using compressed air. After placement on the ground surface, an emulsified asphalt or other soil stabilizer is used for controlled positioning.

9.1.2 Permanent Erosion and Revegetation Materials — Biotechnical-Related

Within the permanent erosion and revegetation materials (PERMs) are a biotechnical-related group, as shown in Table 9.1. These polymer products furnish erosion control, aid in vegetative growth, and eventually become entangled with the vegetation to provide reinforcement to the root system. As long as the material is shielded from sunlight, via shading and soil cover, it will not degrade (at least within the limits of other polymeric materials). The seed is usually applied after the PERM is placed and is often carried directly in the backfilling soil.

The polymers in FRSs can be stabilized with carbon black and/or chemical stabilizers, so they can be sometimes considered in the PERM category (see Table 9.1). They are described earlier.

Erosion-control revegetation mats (ECRMs) and turf reinforcement mats (TRMs) are closely related to one another. The basic difference is that ECRMs are placed on the ground surface with a soil infill, while TRMs are placed on the ground surface with soil filling in and above the material. Thus TRMs can be expected to provide better vegetative entanglement and longer performance. Other subtle differences are that ECRMs are usually of greater density and lower mat thickness. Seeding is generally done prior to installation with ECRMs, but it is usually done while backfilling within the structure of TRMs.

Discrete-length geofibers are short pieces of polymer yarns mixed with soil for the purpose of providing a tensile strength component against sudden forces for facilities such as athletic fields, trafficked slopes, and so on. Geocellular containment systems (GCSs) consist of three-dimensional cells of geomembranes or geotextiles that are filled with soil and, when used for erosion control, are vegetated. They are described in Section 9.2.3 from the perspective of their reinforcement capabilities.

9.1.3 Permanent Erosion and Revegetation Materials—Hard Armor-Related

In a separate category of inert materials, we can include a number of PERMs that are essentially hard armor systems (see Table 9.1).

Whenever the infill material is permanent, as with concrete or grout, GCSs can be considered in this category. Clearly, fabric-formed revetments (FFRs) which are covered in Section 2.10.4, are hard armor materials. They were included in Chapter 2, because the geotextiles in the upper and lower surface hold the key to the installation, but it should be clearly recognized that erosion control is the major feature that is being provided.

Numerous concrete block systems are available for erosion control. Hand-placed interlocking masonry blocks are very popular for low-traffic pavement areas such as carports, driveways, off-street parking, and so on. The voids in the blocks and between them are usually vegetated. Alternatively, the system can be factory-fabricated as a unit, brought to the job site, and placed on prepared soil (recall Figure 2.64b). The prefabricated blocks are either laid on or bonded to a geotextile substrate. The finished mat can bend and torque by virtue of the blocks being articulated with mechanical joints, weaving patterns, or cables. Such systems are generally not vegetated.

Stone riprap can be a very effective erosion-control method whereby large rock is placed on a geotextile substrate. A geotextile placed on the proposed soil surface before rock placement serves as a filter and separator and is described in Section 2.8.5. The stone can vary from small hand-placed pieces to machine-placed pieces of enormous size. Canals and waterfront property are often protected from erosion using stone riprap.

Closely related are gabions, which consist of discrete cells of wire netting filled with hand-placed stone. The wire is usually galvanized steel hexagonal wire mesh, but in some cases it can be a plastic geogrid. Gabions require that a geotextile be placed behind them, acting as a filter and separator for the backfilled soil. The topic is covered in Section 2.8.3.

9.1.4 Design Considerations

While Figure 9.1 shows the general behavior of the soil erosion process, it does little to quantify the variety of complex processes that are involved. In this regard, Weggel and Rustom [3] have nicely explained the process. Beginning with the impact of a raindrop on the soil, a splash mechanism is set up whereby the shear strength of the soil can be exceeded. Once detachment occurs, surface flow transports the individual particles in a gravitational manner until the hydraulics and topography result in final deposition of the soil particles. There are an incredible number of variables involved in the three basic mechanisms of detachment, transportation, and deposition. Somewhat as a compromise position, design is distinguished between either slope erosion or channel/ditch erosion, channels simply being large ditches (recall Figure 9.3). Each will be described accordingly.

Slope Erosion.   The most often-used model for soil loss by erosion is the Universal Soil Loss Equation (USLE) developed by Wischmeier and Smith [4]. The equation is as follows:

$$E = RK\,(LS)\,CP \tag{9.1}$$

where

E = soil loss (tons per square kilometer per year depending upon constants used),

R = rainfall factor (dimensionless),

K = soil erodibility factor (dimensionless),

LS = length of slope or gradient factor (dimensionless),

C = vegetative cover factor (dimensionless), and

P = conservation practice factor (dimensionless).

Charts and tables in [4] describe the various factors involved. This material, however, focuses on various types of bare or vegetated soil. With geosynthetic erosion-control materials being involved, the C factor in the above equation is markedly reduced. Table 9.2 presents C factors for many of the products described previously. In all cases, the values are much lower than those of unprotected soil. Thus, the design procedure is to first calculate the soil loss of the bare soil and then to compare this value to a calculated soil loss with the candidate geosynthetic erosion-control material. The difference is always substantial.

There are many limitations to equation (9.1). Among them are that it is not applicable for predicting erosion from the following: gully-type runoff, small localized sites, steep slopes, seasonal variations, and short-term water surges. The equation is, however, useful in a global sense, and it is often embedded in regulations that make it very important for

TABLE 9.2   RECOMMENDED C FACTORS FOR USE IN EQUATION 9.1 AND ALLOWABLE SHEAR STRESSES (FOR USE WITH EQUATION 9.3 TO CALCULATE SOIL LOSS FROM SLOPE AND CHANNEL/DITCH EROSION, RESPECTIVELY)

Category (all RECMs)	Composition	Time (mos.)	H-to-V (max.)	C Factor (for USLE)	τ_{allow} (Pa)
TERM	MCN	≤3	5:1	0.10	12
	ECS	≤3	4:1	0.10	24
	ECB/OWT	≤3	3:1	0.15	72
	ECB double	≤3	2:1	0.20	84
TERM	MCN	≤12	5:1	0.10	12
	ELC	≤12	4:1	0.10	24
	ECB/OWT	≤12	3:1	0.15	72
	ECB double	≤12	2:1	0.20	84
PERM	MCN	≤24	5:1	0.10	12
	ECB/OWT	≤24	1.5:1	0.25	96
PERM	ECB double	≤36	1:1	0.25	108
PERM	TRM-A	n/a	1:1	n/a	288
	TRM-B	n/a	0.5:1	n/a	480

Abbreviations: RECM = rolled erosion control materials; other acronyms explained in Table 9.1.

n/a = not available

Source: After Erosion Control Technology Council [5].

such applications as landfill final covers, construction sites, and land development sites. Note that a modified USLE for point-source erosion in also available.

Channel and Ditch Erosion.   A very different approach to erosion design than illustrated above focuses on channel and ditch erosion. Here we consider either the velocity of the flowing water or the shear strength of the soil subgrade versus the protection afforded by the geosynthetic erosion-control material. Both situations will be described and illustrated by examples.

The *velocity approach* for channels and ditches calculates a required (or design) velocity and compares it with an allowable velocity for determining a factor of safety.

$$V_{\text{reqd}} = \frac{1.0}{n} R^{2/3} S_f^{1/2} \tag{9.2}$$

where

V_{reqd} = flow velocity (m/sec),
n = Manning's coefficient (see Table 9.3) (dimensionless),
R = hydraulic radius = A/P,
A = cross-sectional area (m^2),
P = wetted perimeter (m), and
S_f = slope of channel (dimensionless)

TABLE 9.3   MANNING'S ROUGHNESS COEFFICIENTS, I.E., *n*-VALUES

Lining Category	Lining Type	Depth Ranges		
		0–15 cm	15–60 cm	>60 cm
Rigid	Concrete	0.015	0.013	0.013
	Grouted riprap	0.040	0.030	0.028
	Stone masonry	0.042	0.032	0.030
	Soil cement	0.025	0.022	0.020
	Asphalt	0.018	0.016	0.016
Unlined	Bare soil	0.023	0.020	0.020
	Rock cut	0.045	0.035	0.025
Temporary	Woven paper net	0.016	0.015	0.015
	Jute net	0.028	0.022	0.019
	Fiberglass roving	0.028	0.021	0.019
	Straw with net	0.065	0.033	0.025
	Curled wood mat	0.066	0.035	0.028
	Synthetic mat (RECM)	0.036	0.025	0.021
Gravel riprap	2.5 cm average size	0.044	0.033	0.030
	5 cm average size	0.066	0.041	0.034
Rock riprap	15 cm average size	0.104	0.069	0.035
	130 cm average size	—	0.078	0.040

Source: *Hydranlic Reference Manual* [6].

Example 9.1

Given a channel of 2.75 m² area, wetted perimeter of 7.16 m, depth $\cong$ 0.50 m, slope of 0.030 and bare soil, what is the factor of safety using different RECMs with allowable velocities per Figure 9.4?

Solution:

(a) Calculate the required (or design) velocity for $n = 0.025$, which is obtained from Table 9.3 for bare soil using equation (9.2):

$$R = \frac{2.75}{7.16} = 0.384$$

$$R^{2/3} = (0.384)^{2/3} = 0.528 \quad \text{and} \quad S^{1/2} = (0.03)^{1/2} = 0.173$$

$$V_{\text{reqd}} = \frac{1.0}{0.025}(0.528)(0.173)$$

$$V_{\text{reqd}} = 3.65 \text{ m/sec}$$

(b) Obtain V_{allow} of RECMs from Figure 9.4.
   - Nonvegetated TRM or ECRM

   Short to long flow duration = 4.2 to 2.5 m/sec
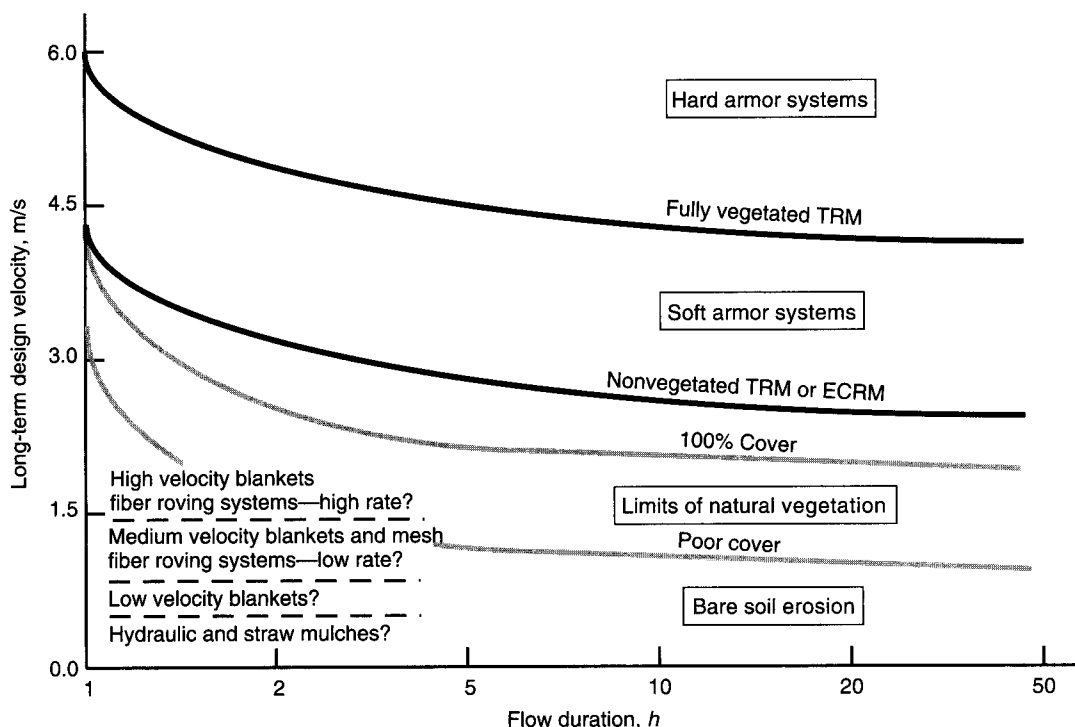
Figure 9.4   Recommended maximum design velocities for various classes of rolled erosion control materials. (After Theisen [2])

- Fully Vegetated TRM

$$\text{Short to long flow duration} = 6.0 \text{ to } 4.3 \text{ m/sec}$$

(c) Calculate the range of FS values.
- Nonvegetated TRM or ECRM

$$\text{FS}_{max} = \frac{4.2}{3.65} = 1.15; \text{ FS}_{min} = \frac{2.5}{3.65} = 0.68$$

- Fully vegetated TRM

$$\text{FS}_{max} = \frac{6.0}{3.65} = 1.64; \text{ FS}_{min} = \frac{4.3}{3.65} = 1.18$$

(d) Thus, a fully vegetated TRM is the preferred strategy.

The *shear stress approach* for channels and ditches calculates a required (or design) shear stress and compares it with an allowable shear stress for determining a factor of safety:

$$\tau_{reqd} = \gamma_w d S_f \tag{9.3}$$

where

τ_{reqd} = required shear stress (strength) (kN/m^2)
γ_w = unit weight of water (kN/m^3)
d = depth of flow (m)
S_f = slope of channel (dimensionless)

When the depth of flow is not known, we can proceed by knowing the flow rate or the hydraulic radius. Numerous nomographs are available on this topic [6].

Example 9.2

A ditch has a depth of 17 cm and a slope of 0.040. Determine the factor of safety for different RECMs with allowable shear strengths per Table 9.2 using erosion-control blankets (ECBs).

Solution

(a) Calculate the required (design) shear stress using equation (9.3):

$$\begin{aligned} \tau_{reqd} &= \gamma_w d S_f \\ &= (9.81)(0.17)(0.040) \\ \tau_{reqd} &= 0.067 \text{ kN/m}^2 \end{aligned}$$

(b) Obtain the allowable shear stress from Table 9.2:

$$\text{TERM: ECB double} = 84 \text{ Pa} = 0.084 \text{ kPa} = 0.084 \text{ kN/m}^2$$
$$\text{PERM: ECB double} = 108 \text{ Pa} = 0.108 \text{ kPa} = 0.108 \text{ kN/m}^2$$

(c) Calculate the FS-values:

$$\text{TERM ECB double: FS} = 0.084/0.067 = 1.25$$
$$\text{PERM ECB double: FS} = 0.108/0.067 = 1.61$$

Hence, both types are satisfactory solutions.

9.1.5 Summary

A study and understanding of soil erosion is a major area of concern and is worldwide in its occurrence. Certainly erosion control using geosynthetics is a worthwhile target and is the focus of this section. The rolled erosion-control materials (RECMs) described are positioned nicely between traditional mulching and hard armor strategies (recall Table 9.1). Hundreds of different RECMs fall within these two extremes.

Design of RECMs is emerging and is being distinguished between large area soil slopes and narrowly confined channels and ditches. The former is being designed using the Universal Soil Loss Equation (USLE), and the latter using either velocity or shear stress. Such calculations result in a required, or design, value. This value must be compared with an allowable value that is laboratory-generated to arrive at a factor of safety. Activity in this regard goes from bench scale tests [7] to large water flumes in hydraulics laboratories or dedicated field sites for product calibration and approval. Many standards-setting organizations are involved in this process with the ultimate goal of a generic specification, but it is too early for consensus in this regard. Eventually, field monitoring will justify and/or modify the appropriate performance tests and design models that were presented.

9.2 GEOCOMPOSITES IN REINFORCEMENT

Although conventional geotextiles can be made very strong—woven multifilament fabrics have been made with tensile strengths up to 350 kN/m—the use of polymeric fibers with other materials can make the result synergistically stronger, and sometimes for less cost too. Furthermore, configurations completely different from the fabriclike systems we've discussed can sometimes be created. The focus in this section is the use and potential synergism between two (or more) materials in reinforced geocomposites: reinforced geotextiles, reinforced geomembranes, reinforced soil, or other reinforced construction materials, such as concrete or bitumen. As will be seen, many innovative systems have been developed and are currently available.

9.2.1 Reinforced Geotextile Composites

Geotextiles have been reinforced by various polymers, by fiberglass, and by steel. Each will be described in this section.

Polymers.   Many possibilities exist for making fibers from two polymers or fabrics from two fibers. One of the early bicomponent fiber types, made into a nonwoven

heat-bonded geotextile, was of the former type. It had a polyester core surrounded by a polypropylene sheath. The outer polypropylene sheath was bonded to crossover fibers at the intersections. This was nicely designed, since the melting temperature of polypropylene is somewhat lower than polyester. More common, however, is the use of bundled high-strength fibers protected by an outer covering. Some of these systems consist of parallel high-tenacity polyester or polyaramid (nylon) fibers encased in a polyolefine sheath. The polyolefine is either polypropylene or polyethylene. The core, however, is what gives the material its high strength. These materials are available in a number of different forms, some having wide-width tensile strengths up to 250 kN/m.

Fiberglass.   As a synthetic material, fiberglass represents a great potential for geotechnical engineering reinforcement applications. Fiberglass has excellent mechanical properties, including high tensile strength, high modulus, and high creep resistance. Conversely, when buried in soil, fiberglass can experience corrosion or pitting with a related strength loss (unless specifically formulated), and its resistance to abrasion is low. Nevertheless, many uses of fiberglass have been successful. Fiberglass geogrids are being manufactured and installed on a regular basis in pavements to prevent reflective cracking (recall Chapter 3). For reinforcement, fiberglass certainly can be used in conjunction with polymeric fibers or as a product by itself. Some possible manufacturing processes for accomplishing a fiberglass fiber inclusion in a geotextile are weft- or warp-insertion knit fabrics, and triaxial, diagonal, or bias woven fabrics. Most systems of this type are still in the development stage.

Steel.   In a manner similar to that just described, steel strand can be used with different polymeric fabrics as the host material. DeGroot [8] describes a woven network of steelcord and geotextile fibers with tensile strengths up to 3000 kN/m developed in Belgium. Such high-strength materials are used as direct road support, sometimes being placed directly beneath the asphalt surfacing where strains tend to be at a maximum. Field results show that the number of load repetitions can be raised from 3 to 10 times over nonreinforced sections.

Kenter et al. [9] report on a steel reinforced polypropylene woven geotextile with strength up to 2000 kN/m. This material, developed in the Netherlands, acts as a direct unpaved road support without aggregate. This type of "instant road," however, when placed on soft subgrade soils, must act as its own anchoring system. For the prevention of continuing rutting, the product has prestressing rods or springwire bars in the cross machine direction. Two types are available, depending on the stability of the subsoil.

The joining of these products is a potential problem, since load transfer across transverse joints is difficult with extremely high strength geocomposites. The longitudinal joint would be even a larger potential problem if the width of the mat were smaller than the width of the roadway. Sewing is simply not possible; for example, Figure 2.12 shows that strength efficiencies become unacceptably low long before the strengths of these types of geocomposites are realized. This leaves resin bonding, perhaps in conjunction with mechanical joining, as the only possibility. A major research effort seems to be warranted in this regard. The other option might be to design the system to avoid connections altogether. A spectacular case in the Netherlands illustrates how this could be accomplished.

In this application, steel-reinforced woven geotextiles have been used to great advantage as the support system for the sea-bottom mattresses used to support large concrete piers in the Netherlands. These mattresses consist of three layers of filter soils, each 120 mm thick. Each mattress measures 42 m × 200 m and weighs 5500 tonnes. The high strength fabric supports the mattress as it is being constructed, rolled onto a handling drum, and transported onto a seagoing vessel. The mattresses are deployed from the roll directly onto the ocean floor in water up to 35 m deep. This particular steel-reinforced fabric has steel cable running in the length direction and is capable of developing a 790 kN/m tensile strength. The manufacturer worked with the consortium of companies that constructed the Eastern Scheldt Storm Surge Barrier. For this project a special on-site factory was constructed for the fabrication of the mattress. Its details will be described later in Section 9.3 on geocomposite filtration. A major point regarding the high strength fabric support material is that seams were not necessary. The mats were constructed in one huge continuous roll!

9.2.2 Reinforced Geomembrane Composites

While the primary function of a geomembrane is indeed as liquid or vapor containment, it still can be subjected to tensile stresses and, as such, must be capable of adequate performance in this regard. The scrim-reinforced multiple materials described in Chapter 5 are of this type. Also described in Chapter 5 are spread-coated geomembranes, in which the polymer is applied directly to a geotextile substrate. Here the geotextile vastly changes the tensile performance of the composite and is certainly a reinforcement component. Not described in Chapter 5 are geomembrane/geonet composites and geomembrane/geogrid composites. These variations will be described in Section 9.5 on geocomposites in containment for moisture barriers.

9.2.3 Reinforced Soil Composites

By suitably mixing soil and polymer element(s), a reinforced soil composite results. These interesting systems are described in this section.

Fibers and Meshes. Fiber reinforcement has long been used to enhance the brittle nature of cementatious materials, so it should come as no surprise that similar attempts should be made with polymer fibers in soil. Most work has been done with cohesionless sands and gravels, but cohesive silts and clays might benefit as well. Usually, the fibers [10] are 25 to 100 mm in length; meshes, or microgrids [11], are of a similar size. The composite material must be uniformly mixed as a first step and then placed and compacted in layers or sections where desired. Based on laboratory tests, McGown et al. [12] have found that mesh elements in 0.18% weight proportion resulted in an apparent cohesion of 50 kPa for a granular soil. What the optimal behavior is for different soils, different fibers or meshes, different sizes and percentages of fibers or meshes, and so on, all awaits additional research. The technique is particularly appropriate for slope stabilization, either in new construction or in rehabilitation [13].

Continuous Fibers   Leflaive [14] has pioneered the application of mixing continuous polyester threads with granular soil to steepen and/or stabilize embankments and slopes. The technique uses a specially designed machine capable of dispensing 23 m^3/hr of soil mixed with fibers coming from 40 bobbins, resulting in a weight percentage of 0.1 to 0.2%. The finished fiber-reinforced soil has fascinating properties. The system has been used in France where highway slopes of 60° have been constructed and have remained stable. Large field trials with enormous surcharges have failed to destroy the thread-reinforced soil mass. Laboratory studies on continuous fiber-reinforced granular soils have resulted in apparent cohesion values in excess of 100 kPa [15]. The use of the technique in the widening of highways or railroads that are in cut areas is quite attractive.

Three-Dimensional Geocells   Rather than rely on friction, arching, and entanglements of fiber or mesh for improved soil performance, geosynthetics can be manufactured so that they physically confine the soil. Such confinement is known to vastly improve granular soil shear strength, as any triaxial shear test will substantiate. Furthermore, the increased shear strength due to confinement results in excellent bearing capacity.

The U.S. Army Corps of Engineers [16] in Vicksburg, Mississippi, has experimented with a number of confining systems, from short pieces of sand-filled plastic pipes standing on end to cubic confinement cells made from slotted aluminum sheets to prefabricated polymeric systems called sand grids or *geocells*. Geocells are typically made from HDPE strips 100 mm wide and approximately 1.2 mm thick. They are ultrasonically welded along their 100 mm width at approximately 300 mm intervals and are shipped to the job site in a collapsed configuration (see Figure 9.5). At the job site they are placed directly on the subsoil's surface and propped open in an accordian-like fashion with an external stretcher assembly. This section expands to a 5 by 10 m area of hundreds of individual cells, each approximately 250 mm in size. They are then filled with sand and compacted using a vibratory hand-operated plate compactor. The final step involves spraying the surface with an emulsified asphalt (approximately 60% asphalt in a 40% water suspension) at the rate of approximately 5 l/m^2. The water drains through the sand, leaving the asphalt globules in the upper portion of the sand, thereby forming a temporary wearing surface. In its expanded form, the system appears as shown in Figure 9.5. Tests have been conducted that have supported tandemaxle truck loads of 230 kN for 10,000 passes with only slight rutting. Without the system, the same trucks become bogged down in deep ruts after only 10 passes. There are a number of manufacturers that make different products within the geocell category. Most use high density polyethylene for the cell material, while a few use geotextiles for the cell materials. The various manufacturers should be consulted for their different material and geometric properties and for the latest styles that are available.

In terms of design, such systems are quite complex to assess. If we adapt the conventional plastic limit equilibrium mechanism as used in statically loaded shallow foundation bearing capacity (see Figure 9.6a), the failure mode is interrupted by the geocell system. For such a failure to occur, the sand in a particular cell must overcome the side friction, punch out of it, thereby loading the sand beneath the level of the mattress (see Figure 9.6b). This in turn fails in bearing capacity, but now with the positive
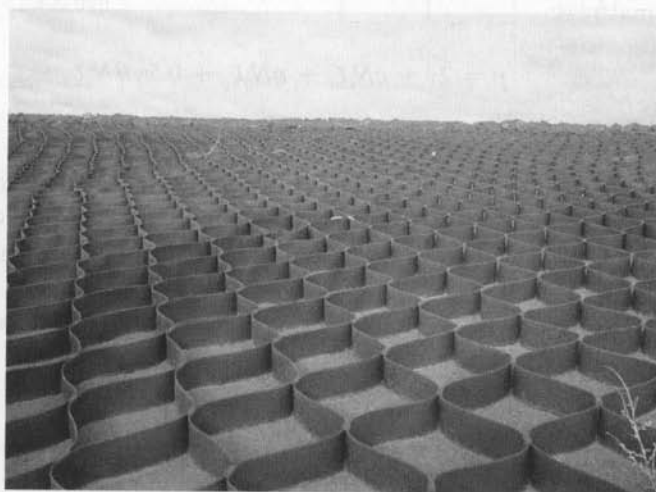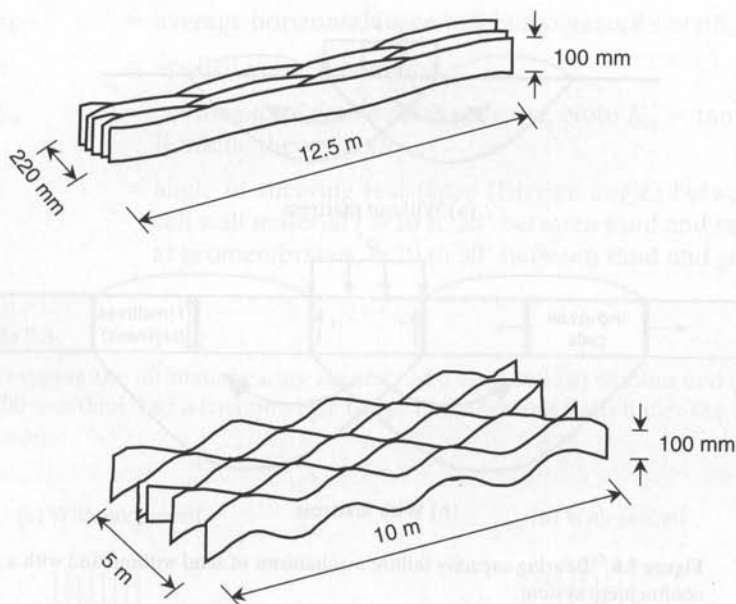
Figure 9.5 Diagrams and a photograph of a three-dimensional geocell for soil stabilization. (Compliments of Tenax Corp.)

effects of a small surcharge loading and typically higher-density conditions. The relevant equations are as follows, illustrated by Example 9.3:

Without mattress:

$$p = cN_c\zeta_c + qN_q\zeta_q + 0.5\gamma BN_\gamma\zeta_\gamma \tag{9.4}$$

(a) Without mattress
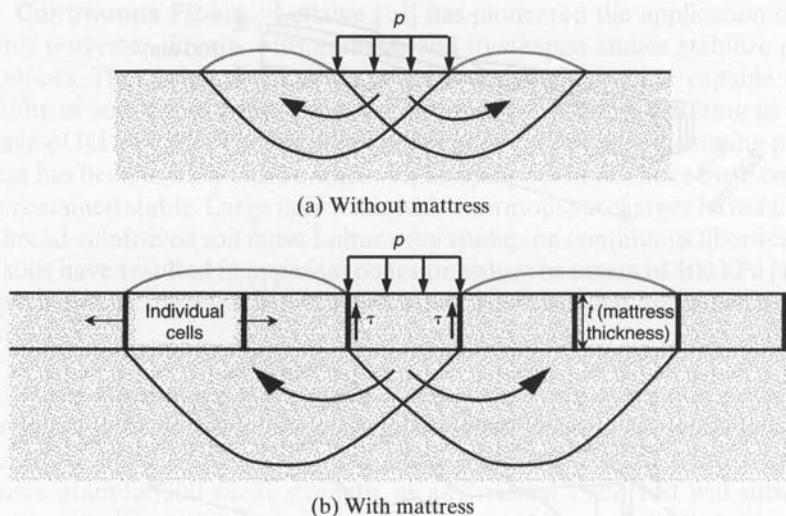
(b) With mattress

Figure 9.6 Bearing capacity failure mechanisms of sand without and with a geocell confinement system.

With mattress:

$$p = 2\tau + cN_c\zeta_c + qN_q\zeta_q + 0.5\gamma BN_\gamma\zeta_\gamma \qquad (9.5)$$

where

p	= maximum bearing capacity stress ($\cong$ tire inflation pressure of vehicles driving on the system if this is the application);
c	= cohesion (equal to zero when considering granular soil such as sand);
q	= surcharge load ($= \gamma_q D_q$), in which
γ_q	= unit weight of soil within geocell, and
D_q	= depth of geocell (recall Figure 9.6b);
B	= width of applied pressure system;
γ	= unit weight of soil in failure zone;
N_c, N_q, N_γ	= bearing capacity factors, which are all functions of ϕ (where ϕ = the angle of shearing resistance [friction angle] of soil; see any geotechnical engineering text);
$\zeta_c, \zeta_q, \zeta_\gamma$	= shape factors used to account for differences from the plane strain assumption of the original theory (see geotechnical engineering texts) and
τ	= shear strength between geocell wall and soil contained within it; note that $\tau = \sigma_h \tan \delta$ (for granular soils), in which

σ_h = average horizontal force within the geocell ($\cong pK_a$),

p = applied vertical pressure,

K_a = coefficient of active earth pressure. Note $K_a = \tan^2(45 - \phi/2)$, for Rankine theory, and

δ = angle of shearing resistance (friction angle) between soil and the cell wall material ($\cong 10$ to $30°$ between sand and smooth or textural geomembranes, $\cong 20$ to $30°$ between sand and geotextiles).

Example 9.3

Compare the ultimate bearing capacity of a sand soil (**a**) without and (**b**) with a geocell 200 mm thick and a friction angle of 18° to the geocell walls under the conditions shown below.

(a) Without geocell   (b) With geocell
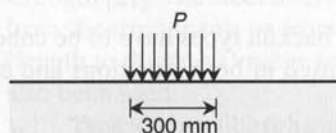
$\gamma = 15$ kN/m³
$\phi = 20°$
$c = 0$
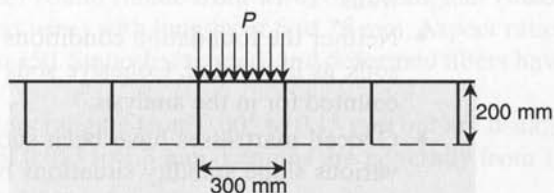
$\gamma = 16$ kN/m³
$\phi = 27°$
$c = 0$
$\sigma_h = 20$kPa (est.)
$\delta = 18°$

Solution:

(a) Without a geocell

$$p = cN_c\zeta_c + qN_q\zeta_q + 0.5\gamma BN_\gamma\zeta_\gamma$$

Since $c = 0$ and $q = 0$;

$$p = 0 + 0 + (0.5)(15)(0.30)(5.39)(0.60)$$
$$= 7.3 \text{ kPa}$$

(b) With a geocell, only $c = 0$.

$$p = 2\tau + cN_c\zeta_c + qN_q\zeta_q + 0.5\gamma BN_\gamma\zeta_\gamma$$
$$= 2(20) \tan 18° + 0 + (0.2)(16)(13.2)(1.51)$$
$$+ 0.5(16)(0.30)(14.47)(0.60)$$
$$= 13.0 + 0 + 63.8 + 20.8$$
$$= 97.6 \text{ kPa; which is 13 times greater than without the geocells}$$

We can add the following to the description of geocells, the design method, and the various types of geocell products that are available:

- The bearing capacity improvement shown using geocells is very large.
- The use of thicker (i.e., greater depth) geocells will give proportionately greater improvement (see next topic).
- The use of a geotextile cell wall material with higher friction values than that used in the above analysis will give a proportionate improvement.
- With an increased densification of the soil infill, the improvement can be exponential.
- The dynamic effects of sand working under the mattress and gradually lifting it up out of position due to moving vehicles has not been considered. It is relevant, however, since it is a possible mode of failure.
- The solution given is for static bearing capacity; thus it is also suited for such problems as building foundations, embankment loads, earth dams, and retaining walls.
- Neither the foundation conditions nor the backfill types have to be cohesionless soils, as illustrated. Cohesive soils can be used in both situations and easily accounted for in the analysis.
- Geocell mattresses have been successfully used to construct *live* walls and for various slope stability situations by placing one section on top of the previous (with or without geosynthetic reinforcement). The analysis follows that presented in Chapters 2 and 3. Designs are also described by Richardson [17].

Three-Dimensional Mattresses.   A deeper, more substantial mattress can be developed using a three-dimensional geosynthetic structure consisting, for example, of gravel-filled geogrid cells (recall Figure 3.21). These cells are typically 1.0 m deep and can be either square or triangular in plan view. They are joined together by a *bodkin* joint, an interlocking knuckle joint with a steel or plastic rod threaded through the intersection forming the coupling. Unitized polyolefin geogrids can be joined in this manner. Other geogrids must be joined by hog rings or other mechanical fasteners. The filling sequence is important, and John [18] suggests the following:

1. Fill the first two rows of cells to half height.
2. Fill the first row to full height.
3. Fill the third row to half height.
4. Fill the second row to full height.
5. Advance by repeating the sequence of half-height and full-height filling in Steps 1–4.

Edgar [19] reports on a three-dimensional geogrid mattress that somewhat parallels the geocells described above. The soil-filled geogrid mattress was constructed over soft fine-grained soils. A 32 m high embankment was successfully placed on top of it. It

was felt that the nonreinforced slip plane was forced to pass vertically through the mattress and therefore deeper into the stiffer layers of the underlying subsoils. This improved the stability to the point where the mode of failure was probably changed from a circular arc to a less critical plastic failure of the soft clay. The application was considered to be a successful (and economical) one and parallels similar mattress support systems being used as foundations over soft soils for the support of landfills—for example, in Germany [20]. Many other applications, along with the related design methods are available, Richardson [17]

9.2.4 Reinforced Concrete Composites

Historically, fibers have been used to reinforce many different types of building materials. Some classic uses are straw in bricks, animal hair in plaster, and asbestos in cement. More recently, however, fiber-reinforced concrete has concentrated on steel, glass, and plastic fibers being placed in mortar, concrete, gunite, and shotcrete to improve their mechanical characteristics, particularly those of tensile, flexural, and impact strength [21]. The steel fibers are either round (made from wire) or rectangular (made from shearing sheets or from flattened wire) with lengths of 6 to 75 mm. Aspect ratios (length to thickness) range from 30 to 150. Smooth, crimped, and deformed fibers have also been used.

Typical glass fibers have diameters ranging from 0.005 to 0.15 mm but are usually bonded together to form diameters of 0.013 to 1.3 mm. Lengths are generally from 13 to 50 mm.

Typical plastic fibers that have been used are nylon, polypropylene, polyethylene, polyester, and rayon. Fiber diameters of 0.020 to 0.38 mm have been used; lengths of 13 to 50 mm are customary.

In general, the addition of fibers to cementatious materials results in the following improvements: greater resistance to cracking; holding cracked sections together; greater resistance to thermal changes, particularly shrinkage; thinner design sections; less maintenance, and longer life.

There is little standardization available regarding the amount of fibers to add to cementatious materials. The criterion is often dictated by how much fiber can be added before the mix becomes unworkable. This depends not only on volume, aspect ratio, type, and kind of fiber but also on the aggregate size, amount of sand, and amount of cement.

9.2.5 Reinforced Bitumen Composites

Including polymeric geogrids within bituminous pavement base courses with the idea of increasing the lateral modulus has been attempted. A number of the geogrids mentioned in Chapter 3 have been used. The attempts have only been of marginal success for two reasons: the softening (and sometimes the partial loss of prestress) of the polymers under the rather high temperature of the bituminous material as it is placed, and placement difficulties where the paving machine tends to pick up the geogrid and distort or tear it.

Rather than using geogrids, an alternative is to use discrete fibers generally made from polypropylene, although polyester is also a possibility. The fibers are usually No. 4 denier, approximately 10 to 12 mm in length with tensile strength of 15 g or higher. The melting point must be at least 160°C. The fibers (approximately 3 kg/ton) have been used in many applications where measurable benefits have arisen, most importantly, that crack formation is delayed for an additional one to four years over nonreinforced mixes, and that the tendency of creep is also delayed, leading to less rutting of the pavement's surface. Jenq [22], among others, suggests that rigorous field testing be pursued for further quantification.

9.3   GEOCOMPOSITES IN FILTRATION

When a geosynthetic material is asked to perform multiple functions, a geocomposite can be formed wherein each function is addressed using a single material. When an ample market is available, or envisioned, such products are quick to appear. An example is in the railroad industry, where two material properties of geotextile separators are critically important: high abrasion resistance on the upper side against ballast stone and filtration of very fine particles on the lower side against the subsoil (recall Figure 2.71). To accomplish this with a single geotextile, for example, is quite difficult. The high abrasion resistance can be achieved nicely with a resin dipped, force-air-dried geotextile, but this process leaves quite large voids in the fabric, where loss of soil would likely be a problem. The problem is overcome by attaching (such as by needling) the abrasion-resistant geotextile on top with a tight nonwoven geotextile on the underside, to allow for the desired result.

Another example is that of a geotextile required above a drainage geonet and below the clay layer of a composite primary liner in a landfill (recall Figure 5.40f). In order for the clay not to extrude into the geonet, we require the use of a nonwoven geotextile. Yet such geotextiles, particularly if needle-punched, have relatively low modulus values and intrude into the geonet's core space, markedly reducing flow capacity. One possible solution to this situation is the use of a scrim-reinforced nonwoven needle-punched geotextile. The resulting geocomposite filter serves both the filtration and the reinforcement functions. Potentially any number of such combinations is possible.

By far, the most elaborate filtration application using geosynthetics in connection with natural soils has been by the Dutch in connection with the Eastern Scheldt Storm Surge Barrier. (A series of papers from the Second International Conference on Geotextiles provides many details on this fascinating project [23, 24, 25]). To form a gate-type dam across the delta of the Scheldt River, 66 prefabricated piers with sliding gates fitting between the piers have been constructed. The gates are open during normal flow and closed only when high seas are in the North Sea. To ensure the stability of the sandy soil beneath the piers (which are 35 to 45 m high and weigh 18,000 kg each), a very elaborate filter mattress consisting of geotextiles, wire-mesh containment baskets, and natural soils was developed. Each bottom mattress, measuring 200 m × 42 m and 0.36 m thick, consists of three layers: a lower layer of 110 mm of sand (0.3 to 2.0 mm), a middle layer of 110 mm of sand-gravel (2.0 to 8.0 mm), and an

upper layer of 140 mm of gravel (8.0 to 40 mm). The lower support geotextile is a woven multifilament geotextile reinforced with steel cables described previously in Section 9.2.1. Its function is reinforcement, since it supports the entire 5,000,000 kg mattress during its deployment. Above this, and separating the three soil layers, is a lightweight nonwoven heat-bonded polypropylene geotextile used as a separator between the different-sized soils. Within each layer of filter soil, partitions are created by using steel wire baskets lined with geotextiles to prevent the soils from laterally shifting during fabrication and installation. The uppermost fabric is a 400 g/m^2 knit polypropylene geotextile. To tie the mat together vertically, steel pins 6 mm in diameter are inserted and secured with the snap-lock grommets on the top and bottom of the mattress.

    This entire mattress is placed on a vibratory compacted seafloor in water up to 35 m deep at 90° to the axis of the dam itself. Each mattress is centered under each concrete pier, the piers being placed at 45 m spacings; thus a 3 m space is between each mattress. It was felt that the stiffness of the mat was too great for a continuous system, which therefore necessitated the gap. This gap was filled in later with larger stones, forming in effect another filter.

    A second and smaller mattress measuring 60 m × 31 m and 0.36 m thick was placed above the lower one. This upper mat is assembled in exactly the same way as the lower mat except that it is composed of three layers of uniform-size 8.0 to 40 mm gravel. The purpose of this upper mat is to distribute the weight of the concrete pier sitting directly on top of it and to protect the lower mat. The remainder of the concrete pier is protected with large armor stone.

    Indeed, this project is among the greatest achievements of any type of heavy construction and is one that uses geocomposites as filter mattresses as a key element in its successful construction and anticipated durability, which is estimated to be 200 years [26].

9.4 GEOCOMPOSITES IN DRAINAGE

Geocomposites used as drainage media have completely taken over certain geotechnical application areas in an amazingly short time. *Wick drains*, used instead of sand drains, and *sheet drains* behind retaining walls are such areas. Prefabricated *highway edge drains* are also being used to a great extent. These three topics will be discussed individually after some general comments.

    All of the drainage products to be discussed consist of a geotextile encapsulated polymeric core for transmitting the anticipated in-plane flow. This is necessary since the typical geotextiles described in Chapter 2 are generally not thick enough to handle the required flow rates by themselves. For example, the different types of geotextiles have been evaluated by Gerry and Raymond [27], who give typical values of transmissivity. However, as shown in the examples of Section 2.9, some drainage situations result in flow rates that are too great to be handled by any conventional geotextile. Thus there exists a need for specialty products capable of handing significantly higher flow rates.

    As a benchmark for many of the problems to follow, it is customary to see drainage designs using 300 mm of clean sand soil. For a typical permeability of 0.001

m/s at a hydraulic gradient of 1.0, this is equivalent to the following Darcian flow rate, which can be modified into a flow rate per unit width or q/W value:

$$q = kiA$$
$$q = ki(W \times t) \tag{9.6}$$
$$q/W = (k)(i)(t) \tag{9.7}$$

where

q = in-plane flow rate (m^3/s),
k = hydraulic conductivity (permeability) (m/s),
i = hydraulic gradient (dimensionless),
A = total cross-sectional area of flow (m^2),
W = width of flow (m), and
t = thickness (m).

$$q/W = 0.001(1.0)(0.3)$$
$$q/W = 3 \times 10^{-4} \, m^2/s$$

In comparison with even the very thick nonwoven geotextiles, this value is two orders of magnitude higher; hence the need for specialized geocomposite drainage materials.

9.4.1 Wick (Prefabricated Vertical) Drains

Generally, geosynthetic materials made from polymers (polypropylene, polyester, polyethylene, etc.) *do not wick*. These polymers by themselves are quite hydrophobic; they actually repel water. If the fabric pore structure is filled with water, however, it will exist in the voids and wait for some external source like gravity or pressure to initiate its movement. So why do most people refer to the subject of this section as *wick drains*? The answer is probably that when these geocomposites are vertically inserted in the ground with their ends protruding at the ground surface and with water being forced out of them under pressure, they resemble a set of giant wicks. The mechanism of flow, however, is *not* by wicking, as with a candle wick, so it must be clearly explained. A far better term for these materials is *prefabricated vertical drains* (PVDs), which is a commonly used term in Europe and Asia. It is also a somewhat limiting term since the drains are often used at an angle other than vertical, and sometimes they are even used horizontally.

The method of rapid consolidation of saturated fine-grained soils (silts, clays, and their mixtures) has been actively pursued using *sand drains* since the 1930s. The practice involves the placement of vertical columns of sand (usually 200 to 600 mm in diameter) at spacings of 1.5 to 6.0 m centers throughout the soil profile to be dewatered. Their lengths are site-specific but usually extend to the bottom of the soft layer(s) involved. Once installed, a surcharge load is placed on the ground surface so as to mobilize excess

pore pressure in the water within the soil voids. This surcharge load is placed in incremental lifts, and with each increment (and the simultaneous increase in excess pore water pressure in the underlying saturated soil) drainage occurs via the installed sand drains. The water takes the shortest drainage path—which is horizontally—to the sand drain, at which point flow becomes vertical and very rapid since the sand is many orders of magnitude greater in permeability than the fine-grained soil being consolidated. Critical in this method of consolidating soils rapidly (it does little insofar as the amount or magnitude of settlement is concerned) is the rate at which surcharge fill is added. Surcharge fill placement is controlled by the effective stress equation

$$\overline{\sigma} = \sigma - u_w \qquad (9.8)$$

where

$\overline{\sigma}$ = effective (or intergranular) stress,

σ = total stress, and

u_w = excess pore water pressure (*excess*, since it is higher than normal hydrostatic conditions).

The increase in excess pore water pressure increment (via the surcharge) should never be higher than the increase in the total stress increment. Thus the effective stress (directly related to the soil's shear strength) is never decreased, and as surcharge loading proceeds it should actually increase. Surcharge loads are usually earth fills but have also been accomplished using a geomembrane-contained water loading and by pulling a vacuum under a geomembrane ground cover.

    With this brief background of the concept (there is a wealth of information available on the technique), and recognizing that millions of sand drains have been installed, there are nonetheless the following shortcomings:

- There is a distinct possibility that the sand drain may not be continuous if the installation mandrel is withdrawn too fast or if insufficient sand is in the mandrel during the withdrawal.
- There is a a vulnerability to shear failure of the weak soil mass as surcharge load is being placed. Since the small diameter sand drains offer essentially no shear resistance, the technique is limited to very slow placement of the surcharge. Often this is as little as 2.0 kPa per day, which is only 100 mm per day, and even then pore water monitoring of the site is mandatory.
- A relatively large crane is needed to install the sand drains. This in turn requires a substantial soil layer, typically 1 to 2 m thick, to be placed over the site to begin the project, for the purpose of adequate bearing capacity.
- The sand for this soil layer and for the sand drains themselves may be difficult and costly to obtain.
- The material for the surcharge (which should be somewhat greater in its final ground surface pressure than the bearing pressure of the proposed structure) might be difficult to obtain. Surcharge fill heights of up to 10 m are not uncommon.

- Most of this surcharge fill must be removed once the site is consolidated, which is sometimes difficult to do and often expensive.

By contrasting sand drains to the alternative of geocomposite wick drains (see Figure 9.7), a number of interesting features are revealed. The wick drains, usually consisting of plastic fluted or nubbed cores that are surrounded by a geotextile filter, have considerable tensile strength. Typically, the breaking strength of a wick drain 100 mm wide is 5 to 15 kN. When threaded throughout a site on centers of 1 to 2 m, such drains offer a sizable reinforcing effect. Although the effect has not been quantified in a three-dimensional analysis, the equivalent plane strain force is sizable. Furthermore, wick drains do not require any sand to transmit flow. Figure 9.8 illustrates the installation process.

The wick drains arrive at the site in rolls and are placed on the installation rig in dispensers like a huge roll of toilet paper. The end is threaded down inside a hollow steel lance, which must be as long as the depth to which the wick drains are to be installed. As it emerges from the bottom of the lance, the wick drain is folded around a steel bar or base plate. The base plate is preferred so as to keep the wick drain down at the bottom of the lance and at the same time to keep the soft soil through which it will be placed out of the lower portion of the lance so that the drain properly releases when the lance is withdrawn. The entire assembly (lance, base plate, and wick drain) is now pressed into the ground to the desired depth. If a hard crust of soil or a high strength geotextile or geogrid is at the original ground surface, it must be pre-augered or suitably pierced beforehand. When it reaches the desired depth, the lance is withdrawn, leaving the base plate and wick drain behind. The rig moves and the process is repeated at the next location. It is a very rapid construction cycle (approximately 1 min), requiring no
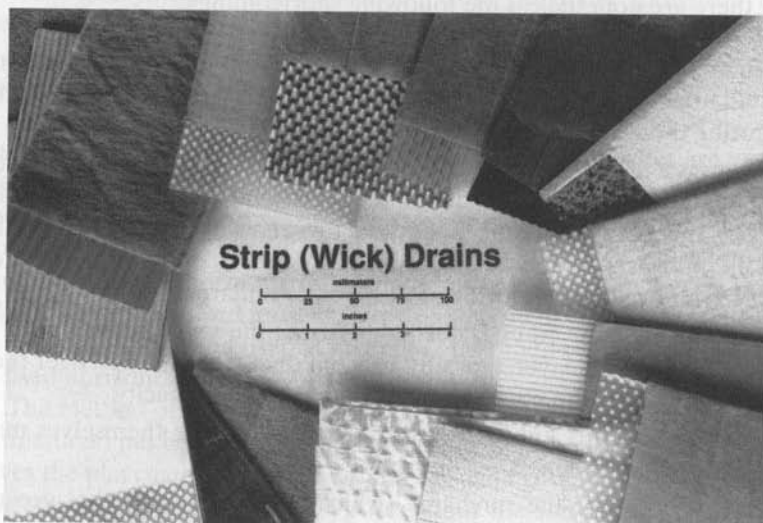
Figure 9.7 Various commercially available geocomposite wick drains, also called *strip drains* and *prefabricated vertical drains* (PVDs).
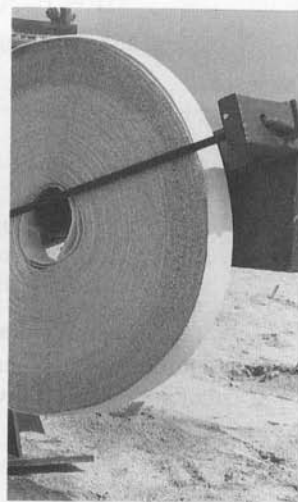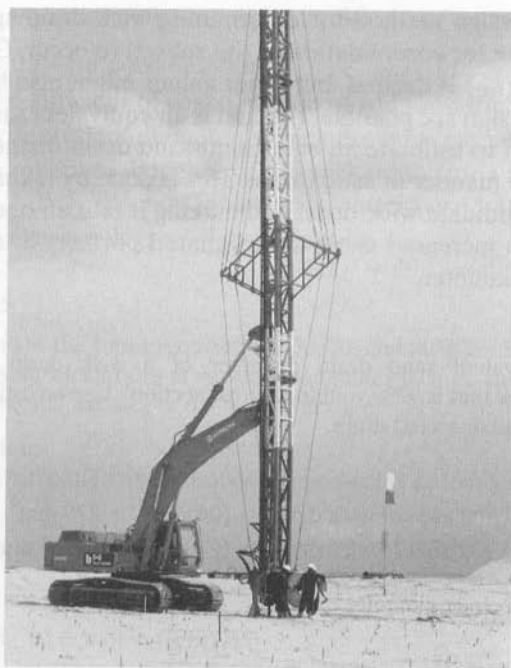
Figure 9.8 Installation rig and associated details for the installation of wick (prefabricated vertical) drains. (Compliments of Colbond, Inc.)

other materials than the wick drains and base plates. At the ground surface the ends of the wick drains (typically at 1 to 2 m spacing) are interconnected by a granular soil drainage layer or a geocomposite sheet drain layer. There are a number of commercially available wick drain manufacturers and installation contractors who readily provide information on the current products, styles, properties, and estimated costs.

Concerning the design method for determining wick drain spacings, the initial focal point is on the time for consolidation of the subsoil to occur. Generally, the time for 90% consolidation (t_{90}) is desired, but other values might also be of interest. Two approaches to such a design are possible. The first is an equivalent sand drain approach that uses the wick drain to estimate an equivalent sand drain diameter and then proceeds with design in the manner of sand drains. This is done by taking the actual cross-sectional area of the candidate wick drain and making it into an open void circle. This open void circle is then increased using the estimated porosity of sand to obtain the equivalent sand drain diameter.

Example 9.4

What is the equivalent sand drain diameter of a wick drain measuring 96 mm wide $\times$ 2.9 mm thick that is 92% void in its cross section? Use an estimated sand porosity of 0.3 for typical sand in a sand drain.

Solution:

$$\text{Total area of wick drain} = (96)(2.9) = 279 \text{ mm}^2$$
$$\text{Void area of wick drain} = (279)(0.92) = 257 \text{ mm}^2$$

The equivalent void circle diameter is

$$d_v = \sqrt{\frac{(4)(257)}{\pi}}$$
$$= 18.1 \text{ mm}$$

The equivalent sand drain diameter is

$$d_{sd} = \sqrt{\frac{d_v^2}{0.3}} = \sqrt{\frac{(18.1)^2}{0.3}}$$
$$= 33 \text{ mm}$$

Note that equivalent sand drain diameters for the various commercially available wick drains vary from 30 to 50 mm. Design for spacing versus time for consolidation now proceeds as per standard radial consolidation theory.

The second approach to wick drain design is more straightforward than the preceding approach and is the preferable one. As developed by Hansbo [28], the time for consolidation is given by the following equations, which are illustrated in Example 9.5:

$$t = \frac{D^2}{8c_h}\left[\frac{\ln(D/d)}{1 - (d/D)^2} - \frac{3 - (d/D)^2}{4}\right]\ln\frac{1}{1 - \overline{U}} \tag{9.9}$$

This can be simplified, since the d/D term is small, to the following:

$$t = \frac{D^2}{8c_h}\left(\ln\frac{D}{d} - 0.75\right)\ln\frac{1}{1 - \overline{U}} \tag{9.10}$$

where

t = time for consolidation,

c_h = coefficient of consolidation of soil for horizontal flow,

d = equivalent diameter of wick drain ($\cong$ circumference/π),

D = sphere of influence of the wick drain (for a triangular pattern use 1.05 × spacing; for a square pattern use 1.13 × spacing), and

$\overline{U}$ = average degree of consolidation.

Example 9.5

Calculate the times required for 50, 70, and 90% consolidation of a saturated clayey silt soil using wick drains at various triangular spacings. The wick drains measure 100 × 4 mm and the soil has a $c_h = 6.5 \times 10^{-6}$ m²/min.

Solution:
In the simplified formula above for a d-value as follows:

$$d = \frac{100 + 100 + 4 + 4}{\pi}$$

$$= 66.2 \text{ mm}$$

Now using equation (9.10),

$$t = \frac{D^2}{8(6.5 \times 10^{-6})}\left(\ln\frac{D}{0.0662} - 0.75\right)\ln\frac{1}{1 - \overline{U}}$$

which results in the following table for consolidation times at various $\overline{U}$ values:

Assumed Wick Drain Spacing,	Percent Consolidation Value ($\overline{U}$)		
D (m)	50%	70%	90%
2.1	159,000 (110)	276,000 (192)	529,000 (367)
1.8	110,000 (77)	192,000 (133)	366,000 (254)
1.5	71,000 (49)	123,000 (86)	236,000 (164)
1.2	41,000 (29)	72,000 (50)	137,000 (95)
0.9	20,000 (14)	35,000 (24)	67,000 (46)
0.6	7,000 (4.8)	12,000 (8.4)	23,000 (16)
0.3	910 (0.6)	1,590 (1.1)	3,030 (2.1)

Note: Consolidations times are in minutes; the equivalent number of days are in parentheses.

These values are now plotted to obtain the design curves shown in the following diagram. Note that the D spacings must be decreased by 1.05 using a triangular strip drain pattern. When compared with the results using the equivalent sand drain method, these values are seen to agree very closely. Note the agreement in the 90% consolidation curves.
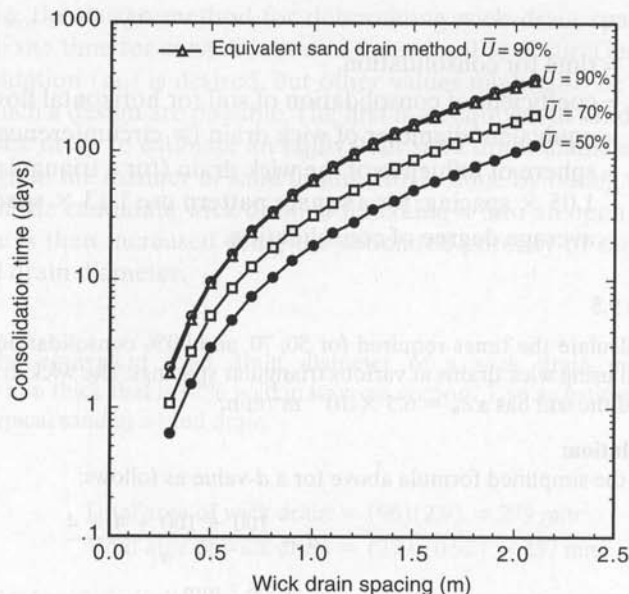
In summary, it is clear to me that wick drains offer so many advantages over sand drains that wick drains should be used exclusively in the future. The following points are strongly in their favor:

- The analytic procedure is available and straightforward in its use.
- Tensile strength is definitely afforded to the soft soil by the presence of the numerous wick drains. It is, however, a difficult three-dimensional problem to quantitatively assess making it a good research topic.
- There is only nominal resistance to the flow of water once it enters the wick drain.
- Construction equipment is relatively small, imparting low ground contact pressures on the soft soils.
- Installation is simple, straightforward, fast, and economic.

Additional research into wick drains is needed in the areas of the effects of soil smear on the geotextile filter and the effects of the kinking of the wick drain core [29]. Soil smear stems from the distortion of the soil due to installation, withdrawal, and subsequent collapse of the in situ soil on the wick drain. Its effect is mainly on the horizontal coefficient of consolidation (c_h) and is currently being evaluated (Welker, et al. [30]).

Kinking refers to the necessary shortening of the wick drains during the consolidation process. In some wick drains the tendency might be to fold into a tight S-shape—that is, to kink, thereby restricting or even cutting off flow. The subject of kinking on actual flow rates has been evaluated by Suits et al. [31], and Lawrence and Koerner [32]. The experimental device is shown in Figure 9.9. The flow rate in a wick drain in a standard (unkinked) condition can be evaluated and then compared to a kinked, or crimped, condition
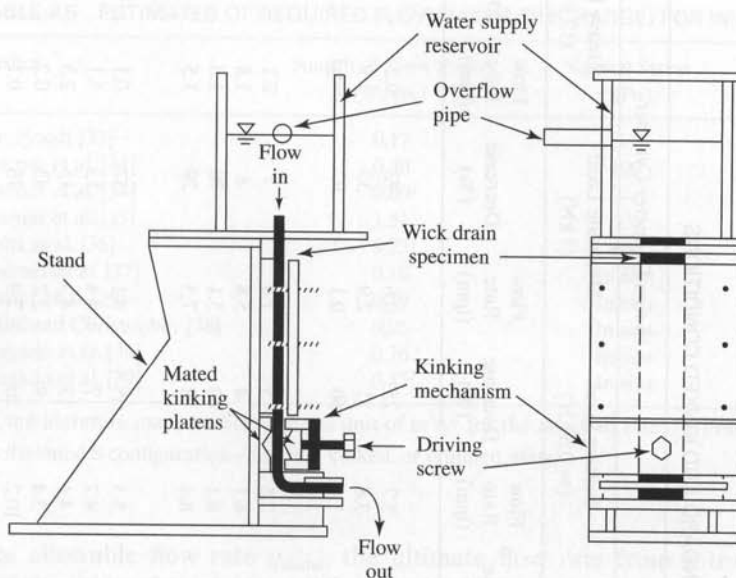
Figure 9.9 Side and front views of a laboratory kinking (or crimping) test device.

to determine what reduction is occurring. The results from two different kinking devices (one rounded and one pointed) at different applied pressures are shown in Table 9.4. Here the types of wick drains evaluated are classified according to their perceived stiffness as rigid, semiflexible, or flexible. The data indicate, however, that such apparent stiffness is not a particularly good indicator of flow rate behavior in a kinked state. Indeed, if kinking is a concern, the candidate wick drain(s) should be experimentally assessed.

The importance of knowing the flow rate in a kinked state is in allowing the required flow to pass through the wick drain at all times during its operational lifetime. This is the second part of design using wick drains (the first is to determine the spacing for a required time for consolidation). Here the required flow rate (q_{reqd}) has been investigated by a number of researchers (see Table 9.5). A value from this table must now be compared with an allowable flow rate (q_{allow}) for the conventional design factor of safety used throughout this book.

$$FS = \frac{q_{allow}}{q_{reqd}} \qquad (9.11)$$

where

    FS   = factor of safety,
    q_{allow} = allowable flow rate for the candidate wick drain, and
    q_{reqd} = required flow rate from Table 9.5.

TABLE 9.4 FLOW RATE (DISCHARGE) TEST RESULTS FOR WICK DRAINS UNDER STANDARD AND KINKED CONDITIONS

	Standard (Initial) Flow Rate (lpm)	90° Wedge						13-mm Diameter Cylinder					
		Seating Load (≅0.6 kN)		Moderate Load (3 kN)		Heavy Load (12 kn)		Seating Load (≅0.6 kN)		Moderate Load (3 kN)		Heavy Load (12 kN)	
	Flow Rate (lpm)	Flow Rate (lpm)	Decrease (%)	Flow Rate (lpm)	Decrease (%)	Flow Rate (lmp)	Decrease (%)	Flow Rate (lpm)	Decrease (%)	Flow Rate (lpm)	Decrease (%)	Flow Rate (lpm)	Decrease (%)
Rigid types													
Bando	7.6	6.4	16	5.4	29	0.3	97	5.7	25	0.6	92	0.2	98
Castle Board	4.3	1.6	62	1.4	67	0.9	78	3.8	11	2.9	33	1.1	75
Desol	3.3	0.9	72	0.6	81	0.2	95	1.6	50	0.1	97	Negl	100
Semiflexible types													
Aliwick	7.9	6.9	13	6.7	15	3.6	54	7.5	5	7.4	7	2.1	73
Ameridrain	6.3	5.1	20	4.5	28	0.3	95	6.1	4	5.8	8	1.8	71
Mebra	10.2	8.2	20	6.7	34	1.3	87	6.1	40	3.1	70	1.8	82
Vinylex	10.2	6.4	37	6.1	41	5.1	50	8.4	18	7.3	29	1.5	86
Flexible types													
Alidrain	8.5	7.7	9	4.4	48	1.8	79	5.5	35	4.1	52	0.1	99
Alidrain "S"-F	5.1	4.0	21	3.9	23	3.4	32	4.7	7	4.4	13	3.1	38
Alidrain "S"-B	5.1	3.1	40	2.6	48	2.3	54	4.4	13	4.3	15	2.3	54
Colbond	3.8	2.8	25	2.4	36	0.6	85	3.4	9	2.2	43	0.2	96
Hitek Flodrain	12.8	6.5	49	2.2	83	0.1	99	10.2	20	2.9	78	0.1	99

Source: After Lawrence and Koerner [32].

TABLE 9.5 ESTIMATES OF REQUIRED FLOW RATES (DISCHARGE) FOR WICK DRAINS

Author	Required Flow Rate[1] (1/min.)	Normal Stress (kPa)	Hydraulic Gradient
den Hoedt [33]	0.17	—	—
Kremer et al. [34]	0.30	100	0.62
Kremer et al. [34]	0.09[2]	—	—
Kremer et al. [35]	1.51	15	1.00
Holtz et al. [36]	0.23	400	—
Koerner et al. [37]	0.10	In situ	1.00
Rixner et al. [29]	0.19	In situ	1.00
Holtz and Christopher [38]	0.95	In situ	1.00
Bergado et al. [39]	0.76	In situ	1.00
Bergado et al. [39]	0.47[2]	In situ	1.00

[1]In the literature many authors use the unit of m^3/yr for the required rate; 1.0 l/min = 526 m^3/yr.
[2]In flattened S configuration—i.e., in a kinked, or crimped, state.

For the allowable flow rate q_{allow}, the ultimate flow rate from a transmissivity test method should be obtained (recall Section 4.1.3). Typical values of ultimate flow rate at a hydraulic gradient of 1.0 under 200 kPa normal stress vary from 2.5 to 5.0 1/min for a 100 mm wide wick drain. This value must then be reduced on the basis of site-specific reduction factors,

$$q_{allow} = q_{ult}\left[\frac{1}{RF_{IN} \times RF_{CR} \times RF_{CC} \times RF_{BC}}\right] \qquad (9.12)$$

where

q_{allow} = allowable flow rate to be used in design,

q_{ult} = ultimate flow rate (as determined from ASTM D4716 or ISO-12958) for short-term tests,

RF_{IN} = reduction factor for elastic deformation of the adjacent geotextile intruding into the drainage core space,

RF_{CR} = reduction factor for creep deformation of the drainage core itself and/or creep intrusion of the adjacent geotextile into the drainage core space,

RF_{CC} = reduction factor for chemical clogging and/or precipitation of chemicals onto the geotextile or within the drainage core space, and

RF_{BC} = reduction factor for biological clogging of the geotextile or within the drainage core space.

A guide for typical values of reduction factors is presented as Table 9.6 (compare that with Table 4.2 for geonets). Note, however, that wick drains are temporary construction expedients, thus the chemical and biological clogging potential is comparatively low. Creep is dependent on the time the wick drains are required and the normal stress arising from the depth within the soil to be consolidated. For intrusion RF_{IN},

TABLE 9.6 RECOMMENDED REDUCTION FACTORS FOR EQUATION (9.12) TO DETERMINE ALLOWABLE FLOW RATE OF DRAINAGE GEOCOMPOSITES (SHEET DRAINS [MOST APPLICATIONS], WICK DRAINS AND EDGE DRAINS)

Application Area	RF_{IN}	RF_{CR}[1]	RF_{CC}	RF_{BC}
Sport fields	1.0–1.2	1.0–1.5	1.0–1.2	1.1–1.3
Capillary breaks	1.1–1.3	1.0–1.2	1.1–1.5	1.1–1.3
Roof and plaza decks	1.2–1.4	1.0–1.2	1.0–1.2	1.1–1.3
Retaining walls, seeping rock and soil slopes	1.3–1.5	1.2–1.4	1.1–1.5	1.0–1.5
Drainage blankets	1.3–1.5	1.2–1.4	1.0–1.2	1.0–1.2
Surface water drains for landfill caps	1.3–1.5	1.2–1.4	1.0–1.2	1.5–2.0
Secondary leachate collection (landfill)	1.5–2.0	1.4–2.0	1.5–2.0	1.5–2.0
Primary leachate collection (landfill)	1.5–2.0	1.4–2.0	1.5–2.0	1.5–2.0
Wick drains (or PVDs)[2]	1.5–2.5	1.0–2.5	1.0–1.2	1.0–1.2
Highway edge drains	1.2–1.8	1.5–3.0	1.1–5.0	1.0–1.2

[1]These values assume that the ultimate value was obtained using an applied normal pressure of approximately 1.5 times the field-anticipated maximum value. If it was not, the values must be increased.

[2]An addition-term for kinking, or crimping, should be included, where $RF_{KG} = 1.0$ to 4.0.

the laboratory test can be evaluated with soil above and below the wick drains. In this case, the intrusion reduction factor would be included in Equation (9.12) as a value of unity. Now, having an in situ modified value of q_{allow}, a traditional design-by-function can be performed, as shown in Example 9.6.

Example 9.6

What is the flow rate factor of safety for a wick drain in a stratified soil profile requiring a flow rate of 0.10 1/min? (Note from Table 9.5, however, that there is quite a difference of opinion as to the proper value of required flow rate.) The laboratory measured value of the candidate wick drain using solid plates was 2.8 1/min.

Solution

Using Equation (9.12) but now adding an additional term for kinking (RF_{KG}), and estimated values from Table 9.6, we have

$$q_{\text{allow}} = q_{\text{ult}} \left[\frac{1}{RF_{IN} \times RF_{CR} \times RF_{CC} \times RF_{BC} \times RF_{KG}} \right]$$

$$= 2.8 \left[\frac{1}{2.0 \times 1.5 \times 1.0 \times 1.0 \times 1.5} \right]$$

$$= 2.8 \left(\frac{1}{4.5} \right)$$

$$q_{\text{allow}} = 0.62$$

Using equation (9.11), we have

$$FS = \frac{q_{allow}}{q_{reqd}}$$

$$= \frac{0.62}{0.10}$$

$$FS = 6.2$$

which is acceptable and would be so even if a significantly higher required flow rate had been used.

Additional details on wick drains (prefabricated vertical drains) are found in Holtz et al. [36].

9.4.2 Sheet Drains

In a number of drainage application areas involving large planar areas, the requirements are higher than those indicated in Table 2.7 for geotextiles. Such applications include a variety of uses: behind retaining walls, against fractured rock slopes that are seeping, against soil slopes that are seeping, beneath athletic fields, beneath geomembrane liners, beneath floor slabs, beneath plaza decks, beneath surcharge fills, as capillary breaks, as vertical drainage inceptors, and as horizontal drainage inceptors. To meet these needs, there are a number of geocomposite sheet drainage systems available. Some of these products are illustrated in Figure 9.10. We will refer to them collectively as *sheet drains*, although other names such as *geomats* and *geospacers* are also used. All have high flow capacities in their as-manufactured state, but they vary greatly in their
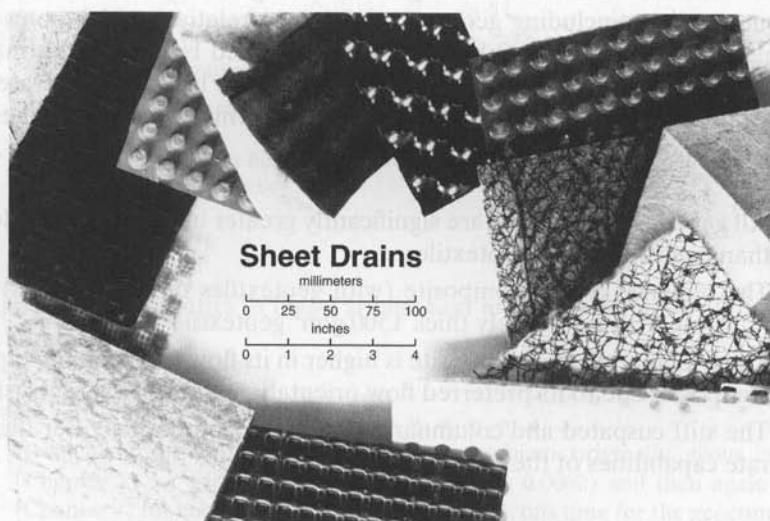
Figure 9.10 Various commercially available geocomposite sheet drains.
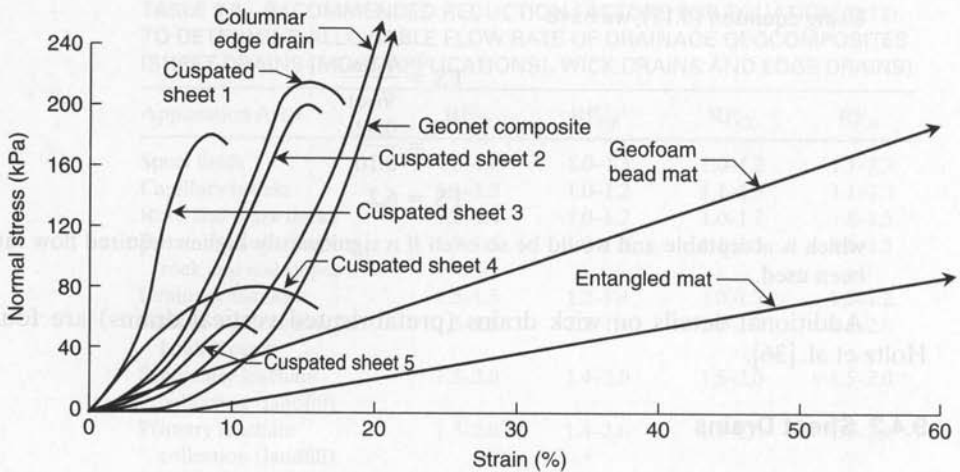
Figure 9.11 Compressibility behavior of selected geocomposite sheet drain materials.

normal compression behavior (see Figure 9.11). It is, of course, the behavior in the compressed state that will dictate the amount of flow available for a given situation.

Most manufacturers have quantified their products for the actual flow rates under load and at various flow gradients. Figure 9.12 presents the typical type of information: illustrating a stiff core behavior in Figure 9.12a, a flexible core behavior in Figure 9.12b, two types of geonets in Figure 9.12c and d. Note, however, that these are index tests conducted between rigid platens and do not account for intrusion or creep. Figure 9.13 illustrates a better perspective of how these various geocomposite drains compare with one another. Here eight different geocomposite drains are compared with one another (including geonets), and to two relatively thick nonwoven needle-punched geotextiles. Figure 9.13a has been generated by holding normal stress constant and varying the hydraulic gradient. Figure 9.13b has been generated by holding the hydraulic gradient constant and varying the normal stress. From these curves the following trends are indicated:

- All geocomposite drains are significantly greater in their in-plane flow capability than even very thick geotextiles.
- The biplanar geonet composite (with geotextiles on the surfaces) is greater in flow rate than a relatively thick 1500 g/m² geotextile.
- The triplanar geonet composite is higher in its flow rate than the biplanar geonet composite due to its preferred flow orientation and its lower intrusion.
- The stiff cuspated and columnar drainage geocomposites offer the highest flow rate capabilities of the products evaluated.

Note that the design procedure for geocomposite drains is exactly like that described in Chapter 4 for geonets. Geonets and geocomposite sheet drains are indeed
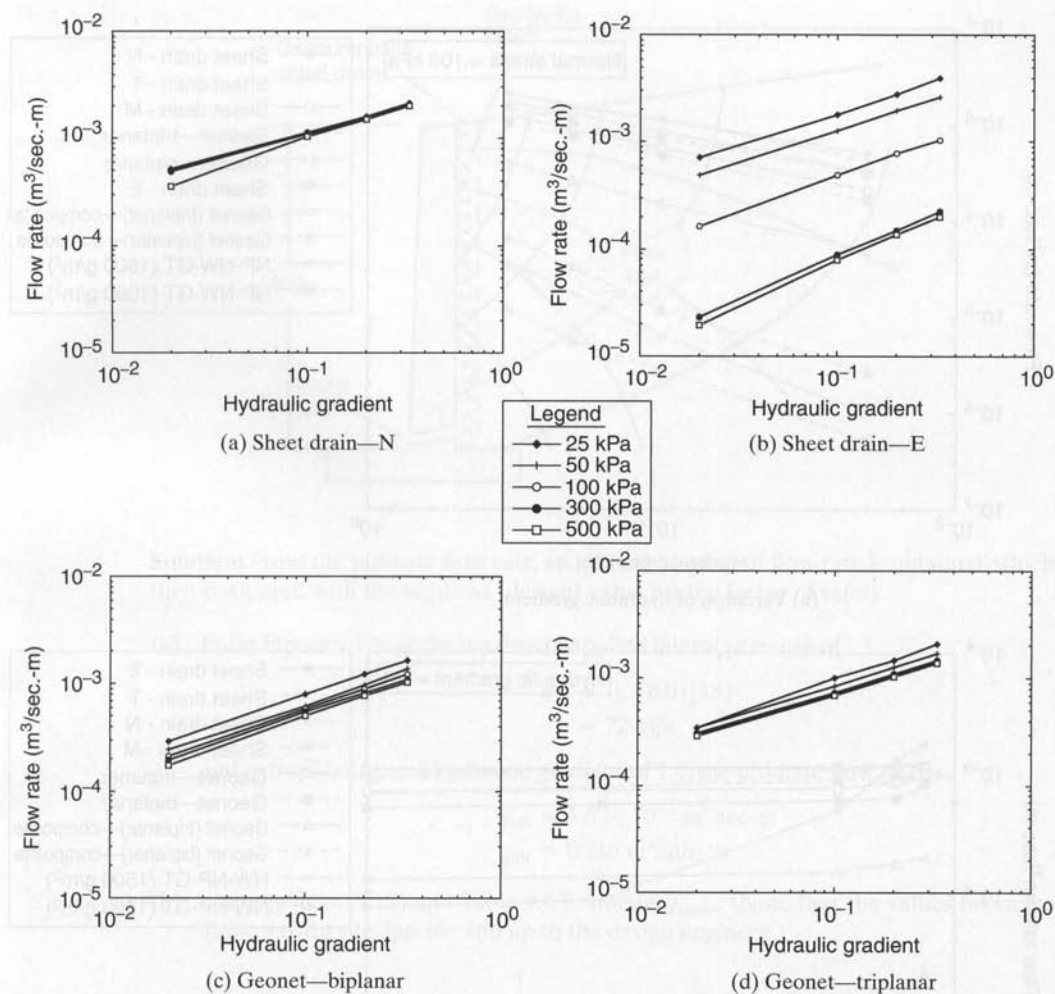
Figure 9.12   Index flow rate behavior of selected sheet drains compared with different types of geonets.

competing geosynthetics in many application areas. Example 9.7 illustrates the use of sheet drains.

Example 9.7

Recalculate the retaining wall drainage problem originally given in Example 2.27 (Chapter 2) for geotextiles (where the FS was 0.0062) and then again in Example 4.8 (Chapter 4) for geonets (where the FS was 1.48), this time for the geocomposite whose response is given in Figure 9.12a. Recall that the required flow rate (which is equal to the transmissivity since the hydraulic gradient is 1.0) is 0.024 m^3/min-m.
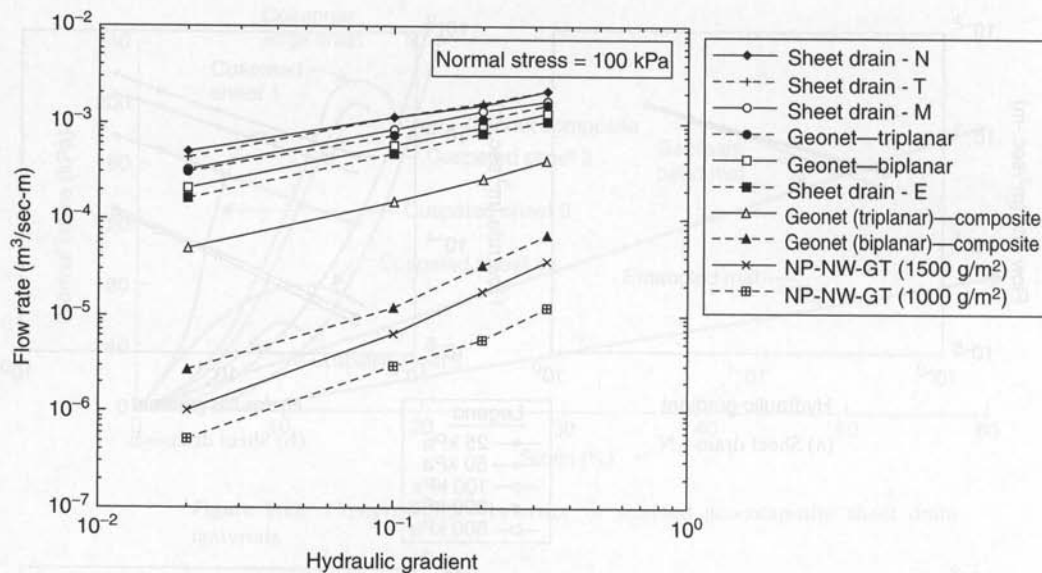
(a) Variation of hydraulic gradient
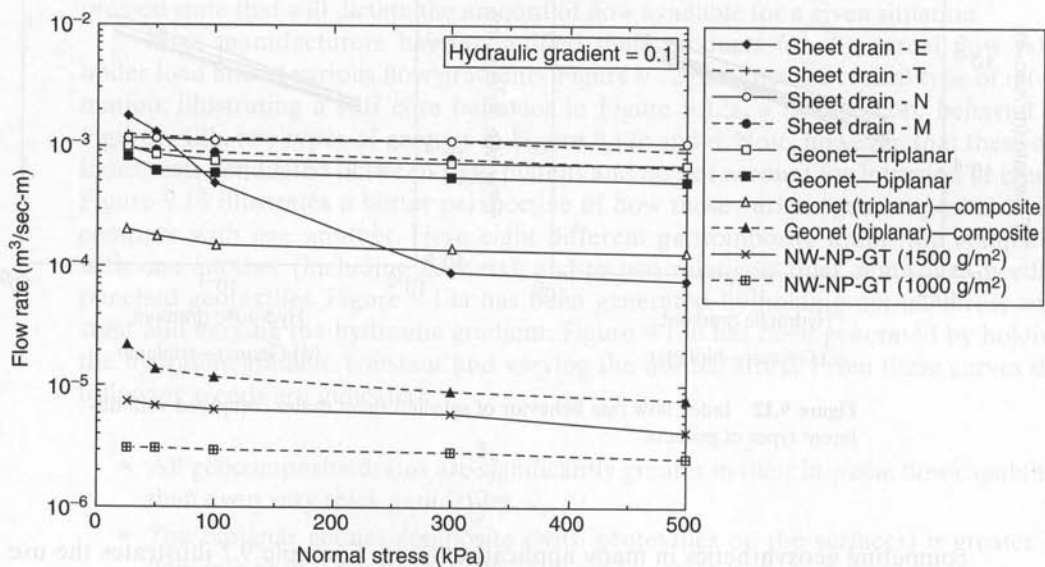
(b) Variation of normal stress

Figure 9.13 Index flow rate behavior of various sheet drains compared with thick geotextiles and geonets.

Geotextile
(filter)

Geocomposite
sheet drain

Flow
Net

8 m

Weep
hole
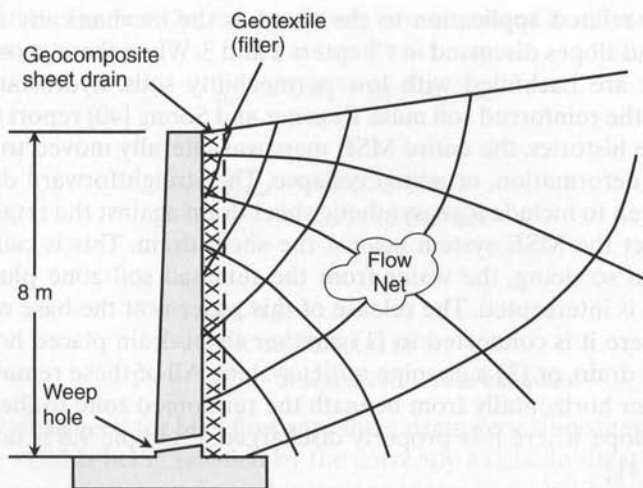
Solution: From the ultimate flow rate, an allowable value of flow rate is obtained, which is then compared with the required (design) value for the factor of safety.

(a) From Figure 9.12a at the maximum applied lateral pressure of

$$\sigma_n \cong 0.5(8.0)(18)$$
$$= 72 \text{ kPa}$$

and extrapolating to a hydraulic gradient of 1.0, the ultimate flow rate is

$$q_{ult} = 3.6 \times 10^{-3} \text{ m}^3/\text{sec-m}$$
$$q_{ult} = 0.216 \text{ m}^3/\text{min-m}$$

(b) Use equation (9.12) and Table 9.6 to obtain q_{allow}. (Note that the values taken from Table 9.6 are site-specific and up to the design engineer.)

$$q_{allow} = q_{ult}\left[\frac{1}{RF_{IN} \times RF_{CR} \times RF_{CC} \times RF_{BC}}\right]$$

$$= 0.216\left[\frac{1}{1.4 \times 1.3 \times 1.3 \times 1.25}\right]$$

$$= 0.216\left(\frac{1}{2.96}\right)$$

$$q_{allow} = 0.073 \text{ m}^3/\text{min-m}$$

(c) The final comparison can now be made using equation (9.11).

$$FS = q_{allow}/q_{reqd}$$
$$= 0.073/0.024$$
$$FS = 3.0 \qquad \text{which is acceptable}$$

Note that this is twice as great as the geonet solution (FS = 1.48) of Example 4.8 and almost 500 times greater than the geotextile solution (FS = 0.0062) of Example 2.27.

A related application to the above is the mechanically stabilized earth (MSE) walls and slopes discussed in Chapters 2 and 3. When these geosynthetically reinforced systems are backfilled with low permeability soils, hydrostatic pressures can arise against the reinforced soil mass. Koerner and Soong [40] report that in 20 out of 26 failure case histories, the entire MSE mass was laterally moved to the point of either excessive deformation, or actual collapse. The straightforward design approach should have been to include a geosynthetic sheet drain against the retained soil zone and then construct the MSE system against the sheet drain. This is called a *back* or *chimney drain*. In so doing, the water from the retained soil zone plus drainage from other sources is intercepted. The release of this water is at the base of the wall or slope system where it is connected to (1) another sheet drain placed horizontally, (2) a gravel blanket drain, or (3) a geopipe outlet system. All of these removal alternatives convey the water horizontally from beneath the reinforced zone to the face of the wall or toe of the slope where it is properly discharged. Example 9.8 is taken from Koerner and Soong [41].

Example 9.8

A 7.0 m high geogrid-reinforced segmental retaining wall has a 2(H) to 1(V) (i.e., 26.6°) backslope as shown in the diagram below, which has been backfilled with a relatively impermeable clayey silt soil. Based on a required flow rate of 2.70×10^{-6} m²/sec and a geosynthetic sheet drain characterized as shown in Figure 9.13(a) as sheet drain E, what is the flow rate factor of safety? Use a cumulative reduction factor (Π RF) of 5.0.

$\beta = 26.6°$

Retained soil
($k_{ret} = 5 \times 10^{-5}$ cm/sec)

Reinforced soil
($k = 1 \times 10^{-6}$ cm/sec)

7.0 m

Geosynthetic
drainage product

Flow discharge
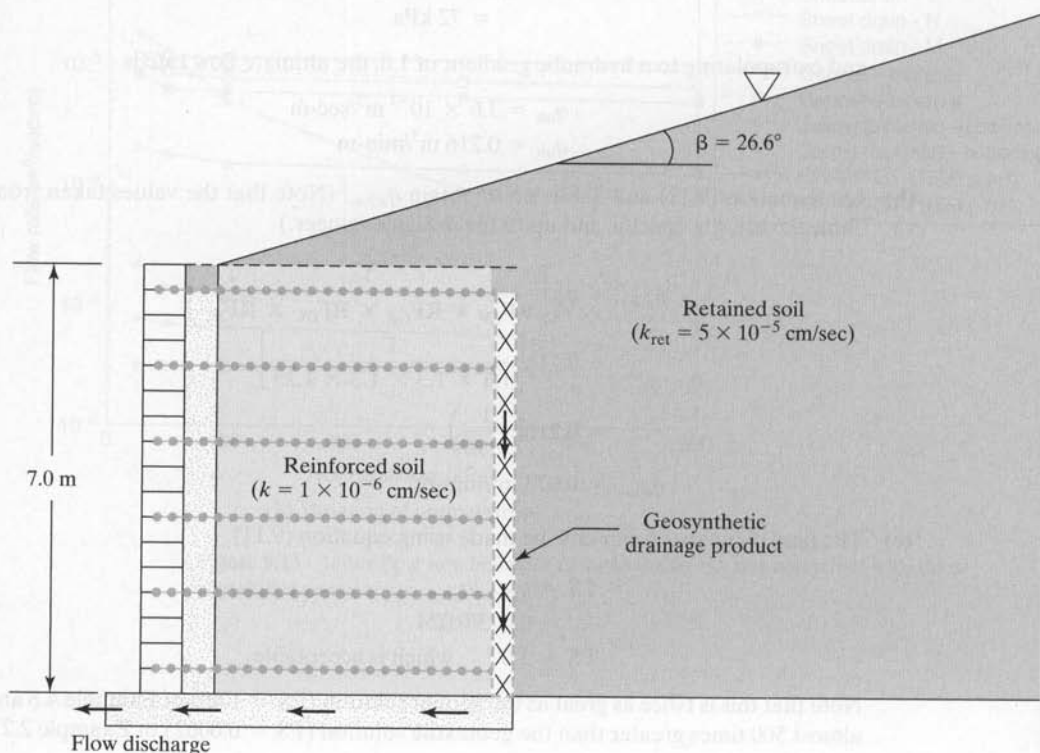
Solution: Using Figure 9.13a, for sheet drain E, extrapolated to a hydraulic gradient of 1.0, we have

$$q_{ult} = 2.0 \times 10^{-3} \, m^2/sec$$

and then,

$$q_{allow} = 0.002/5.0$$
$$= 4.0 \times 10^{-4} \, m^2/sec$$

Thus

$$FS = q_{allow}/q_{ult}$$
$$= 4.0 \times 10^{-4}/2.70 \times 10^{-6}$$
$$FS = 148 \qquad \text{which is more than adequate}$$

There is a clear need for high flow rate sheet drain geocomposites in myrid applications, and the need is being satisfied by the currently available sheet drain products. There are, however, some unanswered questions that will probably lead to variations of the existing products and to the development of new ones as well.

- As seen in Figures 9.11 and 9.13, the core material strength and drainage response varies significantly from product to product.
- The creep of the system is of concern, particularly with respect to the breakdown stress of the cuspated cores for permanent installations and at high normal stress levels.
- The strength and creep of the geotextile filter are important in that the filter must span between protrusions of the core material. Flow rates will rapidly diminish if it excessively intrudes or plastically deforms into the flow channels of the core material, and will shut off completely if it fails.
- The geotextile covering must be designed with respect to the flow passing through it and the soil to be retained since it is indeed a filter in every sense of the word. The designs offered in Section 2.8 must be considered in this regard.
- The connection of the sheet drain to the base (bottom) drain must be such that flow is uniform and continuous. It involves both the drainage core and the geotextile filter.
- In some extreme cases, high or low temperatures may adversely affect the systems. High temperatures may lead to creep, while low temperatures can cause icing problems that block upstream flow.
- Claims about the insulation value of some of the systems have been noted, particularly when they are used adjacent to earth-sheltered structures. Although possible, the effect of moisture in the system versus its insulation value needs to be properly quantified. In this regard, consider using geofoam (Chapter 8) against the wall and then the geocomposite drain between the geofoam and the backfill soil.
- If a vapor barrier is required when placing the system next to an earth-sheltered structure, this can possibly be achieved by using a thin geomembrane on the side of the core facing the structure.

- Traditional bitumen vapor barriers on walls must be protected against some of the geocomposite sheet drain products that have hollow recesses on the side facing the structure. These recesses can indent the waterproofing, rendering it thinner than desired. A geomembrane on the back side of the sheet drain avoids the potential problem.

- The allowable flow rate to be used in a functional factor of safety design must come from a laboratory test replicating the actual in situ conditions. If not possible or practical, a modification of the laboratory determined value using reduction factors must be made. Equation (9.12) and Table 9.6 are recommended.

9.4.3 Highway Edge Drains

Highway performance and lifetime are both directly related to the drainage capability of the stone base course beneath the pavement. This was clearly illustrated in Chapter 2, dealing with geotextiles as separators for the purpose of preserving stone base drainage, as well as for geotextile filters protecting the perforated pipe underdrain system at the edge of the pavement. But why do we need a perforated pipe, embedded in drainage stone, and further enclosed with a geotextile? Why not use a prefabricated drainage geocomposite serving as a complete edge drain system by itself? Indeed such systems are now available under the category of geocomposite *highway edge drains* (see Figure 9.14).

    The concept of prefabricated highway edge drains was brought into a rational design context by Dempsey [42]. Of particular note is that the flow mechanism within highway edge drains is very different than the wick drains and sheet drains described
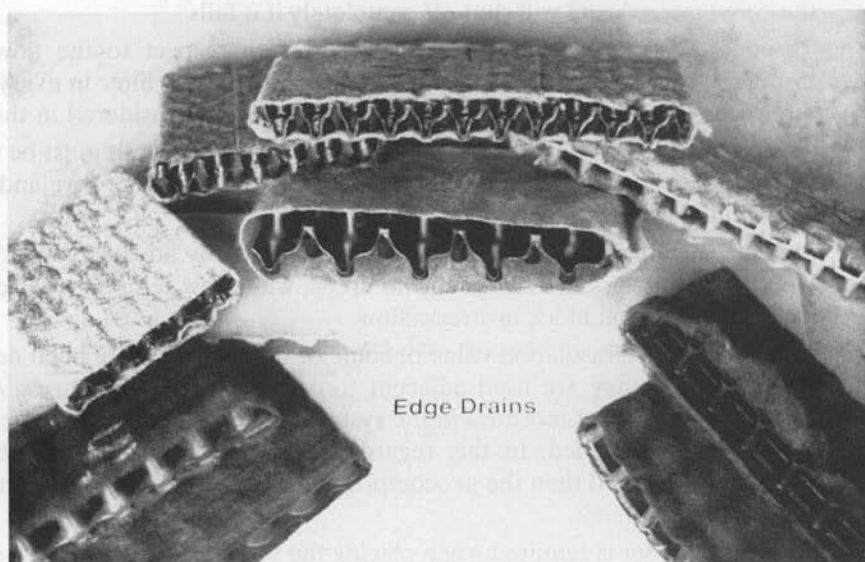
Edge Drains

Figure 9.14   Various commercially available geocomposite highway edge drains.

in Sections 9.4.1 and 9.4.2. Figure 9.15 indicates that flow comes mainly from the stone base, through the geotextile filter, and then drops into the bottom portion of the vertically deployed core. Additional flow comes from the surface, where the shoulder often pulls away from the more stationary highway pavement. Generally no flow (or certainly very little) will come from the subsoil beneath the stone base or from the soil beneath the shoulder. Note that conceptually only the region of the geocomposite edge drain beneath the bottom of the stone base is carrying flow. The rest of the edge drain above this flow zone is just acting as an accumulator for the incoming water. The flow region then conveys the gathered water parallel to the highway to an appropriate outlet. Outlets are required at intervals of 50 to 150 m, depending upon the highway grade and hydrologic conditions. There are numerous types of product-specific prefabricated fittings that fit directly into the end of the drain and exit the accumulated water at 45, 60 or 90° away from the pavement section.

Regarding design, the basic flow rate equation will again apply equation (9.11):

$$FS = \frac{q_{allow}}{q_{reqd}}$$

where

   FS   = factor of safety,
   q_{allow} = allowable flow rate from a laboratory test (to be described), and
   q_{reqd} = required (or design) flow rate.

The laboratory-obtained flow rate should be determined by a flow box contained within a laboratory hydraulic flume. The simulation can model the actual flow regime quite nicely [42]. In the laboratory, however, it is limited by length considerations.
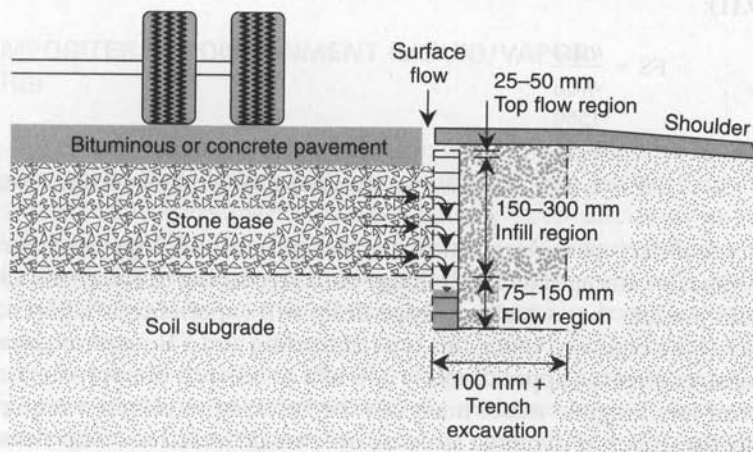
Figure 9.15 Flow path and configuration using prefabricated highway edge drains.

Other nonrepresentative conditions such as solid side walls, short-term conditions, and the effects of liquids other than tap water can be handled according to equation (9.12) and Table 9.6. Thus a q_{ult} value obtained from this type of test can be modified to a q_{allow} value for design.

The required flow rate q_{reqd}, has also been measured by Dempsey [42] at a number of sites within precipitation rates from 20 to 35 mm/hr, giving required values ranging from 760 to 1900 l/hr. Note, however, that this is a very site-specific value depending upon the following: type of pavement surface, condition and age of pavement, type of stone base, thickness of stone base, fouling (contamination) of stone base, edge joint condition, rainfall and snow melt, temperature, shoulder type, system gradient, outlet spacing, outlet type, normal stress, and response initiation time. Example 9.9 illustrates the design methodology.

Example 9.9

The maximum anticipated flow rate to a highway edge drain is 1150 l/hr. What is the factor of safety using a geocomposite edge drain whose laboratory ultimate flow rate is 4000 l/hr?

Solution: First calculate an allowable flow rate using equation (9.12) along with the values of Table 9.6 tuned to the site-specific conditions.

$$q_{allow} = q_{ult}\left[\frac{1}{RF_{IN} \times RF_{CR} \times RF_{CC} \times RF_{BC}}\right]$$

$$q_{allow} = 4000\left[\frac{1}{1.3 \times 1.5 \times 1.2 \times 1.1}\right]$$

$$= 4000\left(\frac{1}{2.57}\right)$$

$$= 1560 \text{ l/hr}$$

Then calculate the flow-rate factor of safety in the conventional manner per equation (9.11):

$$FS = \frac{q_{allow}}{q_{reqd}}$$

$$= \frac{1560}{1150}$$

$$FS = 1.4 \quad \text{which is low, but acceptable for this noncritical situation}$$

A secondary consideration in the design methodology considers the issue of the compressive strength of the drainage core. According to Koerner and Hwu [43], the maximum loading that a highway edge drain will experience is a parked truck on the shoulder of the highway. Using this type of loading and a Boussinesq analysis, the maximum normal stress is approximately 140 kPa at a depth of approximately 165 mm. A number of less tangible issues must now be resolved to obtain a required value—for example, the effect of dynamic stresses, overweight vehicles, creep stresses (such as, a broken or abandoned truck), and inclined loads due to friction. Thus the calculated

value should be increased by a load factor. Koerner and Hwu [43] use a factor of 3.0, while some highway engineers use 2.0. Thus the required strength should probably be between 280 and 420 kPa.

Concerning the field performance of all types of highway edge drains, Koerner et al. [44] have exhumed 91 sites across the United States, including 41 geocomposite edge drains of the type described in this section. The cores were seen to perform quite well. The only failures per se were due to the use of a compressible product that was never intended for this application and a geotextile that was punctured by the core protrusion, due to its inadequate strength.

Problems were encountered, however, with the geotextile filter enclosing the drainage cores. In the above total of 41 exhumed geocomposite edge drains, there were eight sites that allowed excessive amounts of soil to pass the geotextile and fully clog the core. It was found that the soil that passed through the geotextile was always less than the #100 sieve in its particle size characteristics. Since the geotextiles used on these products were #40 to #70 AOS sieve size, it was felt that the failures were construction-related, in that intimate contact of the upstream soil to the geotextile did not occur. Figure 9.16a illustrates that the situation usually occurs with machine excavated trenches, which sometime create overexcavation beneath the pavement slab, particularly when coarse gravel or boulders are present. The suggested remedy (Koerner, et al. [44]) shown in Figure 9.16b is to move the edge drain to the shoulder side of the small 100 mm wide trench and then backfill with sand that is slurried into the open space. The water should carry the sand beneath the slab to fill any voids that may be present. In this situation the geotextile is designed as a filter for the sand, which is readily accomplished using the principles described in Section 2.8.

Clearly, geocomposite highway edge drains are the future in both retrofitted highway pavements and also in new construction. Their installed costs are extremely low due to the automated method of installation [44]. With adequate design of the geotextile filters [45], either through use of upstream sand or proper design to handle local situations, it is felt that these products can be used with confidence.

9.5 GEOCOMPOSITES IN CONTAINMENT (LIQUID/VAPOR BARRIERS)

There are a wide variety of geosynthetic combinations that can be used as moisture barriers either to keep liquids and gases within an area or out of an area. Membrane encapsulated soil layers (MESLs) have already been discussed in connection with paved or unpaved road construction (see Section 2.6.2) and asphalt saturated geotextiles for use in the prevention of bituminous pavement crack reflection problems (see Section 2.10.2). Both of these situations utilize composite behavior, but the discussions pertaining to them fell more appropriately in Chapter 2 than in this section. This does not imply that this section has a lower priority. Indeed, there is so much innovation occurring in the development of geocomposite moisture barriers that we scarcely know where to begin (for example, see Figure 9.17). Thus without any particular order, a description will be made of various products fitting into this category.
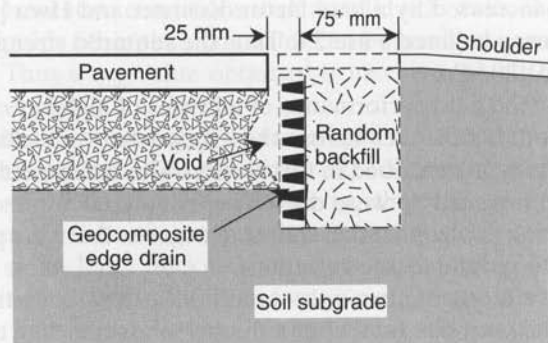
(a) Occurence of large void(s) beneath pavement slab preventing intimate
contact of geotextile with upstream stone base and subgrade soil.
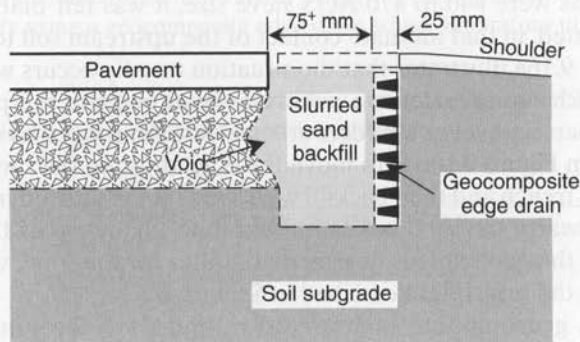
(b) Suggested remedy for backfilling large voids via slurried sand with
geocomposite edge drain moved to shoulder side of trench.

Figure 9.16   Intimate contact issue and the avoidance of upstream voids using geo-
composite highway edge drains.

GEOCOMPOSITES - MOISTURE BARRIER
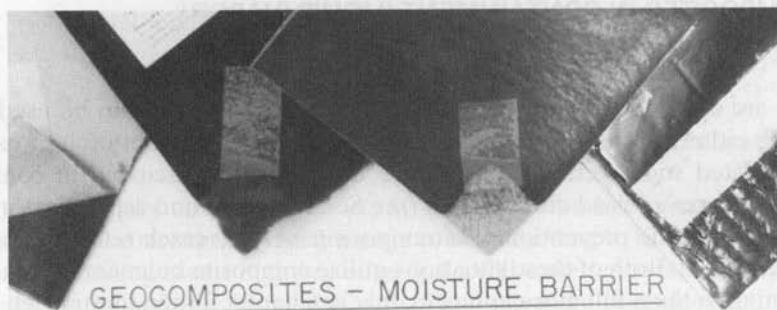
Figure 9.17   Various types of geocomposite moisture barriers.

Prefabricated *geotextile/bitumen* products are available wherein the two-ply systems are discrete, yet act together in composite form. The geotextile gives tensile strength, while the bitumen provides the moisture barrier. One particular variant of this class is the use of woven fiberglass fabric as the geotextile. This high strength, high modulus, low creep material is best used in the prevention of reflective cracking in distressed pavements. Rather than covering the entire roadway surface, as described in Section 2.10.2, however, these materials are meant for application directly spanning the cracks. The materials are laid down in 450 mm wide strips and undoubtedly provide a reinforcement function as well as a moisture barrier function.

Another product in this category but now serving as a containment material consists of the following nine layers: (1) strip-film on top; (2) slate, sand, or geotextile; (3) bitumen; (4) polyester film; (5) bitumen; (6) reinforcement geotextile; (7) bitumen; (8) sand or nonwoven geotextile; (9) strip-film on bottom. The product is supplied in large rolls (hence the need for the strip films) placed directly on a prepared subgrade for landfill or reservoir containment liners. The seams are made using a hot bitumen mix poured directly on the overlapped joint. In this sense the product is actually a geomembrane and could have been included in Chapter 5; it is not because usual practice uses polymer-base (noncomposite) liners almost exclusively. However, in some countries (such as, France and the Netherlands) bituminous liners and bituminous composite liners are seeing some use for lining of reservoirs, surface impoundments, and landfills.

Recognizing that geotextile underliners beneath geomembranes serve a number of valuable purposes, several one-piece *geotextile-geomembrane* geocomposites are available. These two-ply laminates are generally meant to serve as conventional geomembranes but can be placed much more efficiently than in two separate steps. Conceivably, any combination of geomembrane and/or geotextile could be developed in this manner. An area that promises to see growing use is a *geotextile-geomembrane-geotextile* composite used as a secondary containment system into which are placed underground gasoline storage tanks. Leaks from such tanks pose a serious threat to aquifers unless suitably contained.

The idea of encapsulating a thin metallic sheet between geomembranes has as its goal the complete barrier to the permeation of HC, CHC, and CFC organic liquids and vapors. Composite HDPE/aluminum/HDPE products that are 2.0 to 3.0 mm thick and supplied in rolls in a standard format are available. Complete impermeability of certain organics, such as trichlorethylene, chloroform, tetrachlorethylene, toluene, tetrachlormethane, xylene, chlorobenzene, octave, and so on, is possible with such liner systems. The bonding of the layers is very strong and seaming is afforded by the HDPE covering layers using conventional thermal fusing methods.

Using this same concept, radioactive wastes can be contained by encapsulating lead sheet between two HDPE outer layers. Lead is, of course, known to be resistant to the permeation of radioactive vapors and liquids.

Still further, a geomembrane with uniformly spaced protrusions, or nubs, rising out from its surface is available. Such protrusions can be any height up to 25 mm and placed at any spacing or pattern. With a geotextile as a filter lying on top of the nubs, we have a combined liquid barrier and drainage system in the form of an integral *geonet-geomembrane* composite. With a geomembrane covering the top of the nubs, we have a double liner system with leak detection capability.

A parallel development, now with a high strength (in the *supertuff* class of polymers) geogrid manufactured with the geomembrane, is also in the prototype stage. Indeed, the era in which completely prefabricated, reinforced, filter-drainage-barrier systems are mass-produced in the factory, with superb quality control, is about to begin. Truly a thrilling development is occurring.

9.6   CONCLUSION

The word *innovation* best summarizes the heart of this chapter. By knowing the strongest and weakest points of two materials, we can sometimes combine them to emphasize the strongest points of both of them. When done cleverly, even a synergistic effect can be the result, where the combined effect is better than the sum of the performances of the separate materials. These performance thoughts, however, must be weighed in light of the economics of the production of the geocomposites.

It is of little surprise that manufacturers are taking the lead in the area of geocomposites. New products appear regularly, leaving the designer to play catch-up in assessing these new applications. The phrase *or equal*, which is commonly used in specification writing, is completely inappropriate in this area. Certainly new products will appear and old ones will disappear in the future. It is up to the designer to understand the application, evaluate the function or functions, and compare these requirements with that of the candidate geocomposite's properties. The resulting factor of safety is then assessed in light of the particular application. The process is not different in any way from other engineering materials utilizing *design-by-function* — the byword of this entire book.

REFERENCES

1. Garrels, R. M., *A Textbook of Geology*. New York: Harper, 1951.
2. Theisen, M. S., "The Role of Geosynthetics in Erosion and Sediment Control: An Overview," *Journal of Geotextiles and Geomembranes*, vol. 11, nos. 4–6, 1992, pp. 199–214.
3. Weggel, J. R., and Rustom, R., "Soil Erosion by Rainfall and Runoff — State of the Art," *Journal of Geotextiles and Geomembranes*, vol. 11, nos. 4–6, 1992, pp. 215–236.
4. Wishmeier, W. H., and Smith, D. D., "A Universal Soil-Loss Equation to Guide Conservation Farm Planning," *Proceedings of the 7th International Conference on Soil Science*, Soil Science Society of America, 1960.
5. Erosion Control Technology Council (ECTC), 2002, St. Paul, MN.
6. *Hydraulic Reference Manual*, HEC-RAS River Analysis, U.S.A. COE, Hydrologic Engineering Center, Version 3.1, 2002.
7. Sprague, C. J., Carver, C. A., and Allen, S., "Development of RECM Performance Tests," *Geotechnical Testing Journal*, ASTM, vol. 25, no. 3, December 2002, pp. 1–20.
8. DeGroot, M. T., "Woven Steelcord Networks as Reinforcement of Asphalt Roads," *Proceedings of the 3rd International Conference on Geotextiles*, Austrian Society of Engineers and Architects, Vienna, 1986, pp. 113–118.
9. Kenter, C. J., DeGroot, M. T., and Dunnewind, H. J., "An Instant Road of Steel Reinforced Geotextile," *Proceedings of the 3rd International Conference on Geotextiles*, Austrian Society of Engineers and Architects, Vienna, 1986, pp. 67–70.

10. Hoare, D. J., "Laboratory Study of Granular Soils Reinforced with Randomly Oriented Discrete Fibers," *Proceedings of the International Conference on Soil Reinforcement*, International Society of Soil Mechanics and Foundation Engineering, French Chapter, Paris, 1979, pp. 47–52.

11. Mercer, F. B., Andrawes, K.Z., McGown, A., and Hytiris, N., "A New Method of Soil Stabilization." In *Polymer Grid Reinforcement*. London: Thomas Telford, 1985, pp. 244–249.

12. McGown, A., Andrawes, K. Z., Hytiris, N. and Mercer, F. B., "Soil Strengthening Using Random Distributed Mesh Elements," *Proceedings of the 11th ISSMFE Conference.*, BiTech Publications Ltd., 1985, pp. 1735–1738.

13. Gregory, G. H., and Chill, D. S., "Stabilization of Earth Slopes with Fiber Reinforcement," *Proceedings of the 6th International Conference on Geosynthetics*, IFAI, 1998, pp. 1073–1078.

14. Leflaive, E., "The Reinforcement of Granular Materials with Continuous Fibers," *Proceedings of the 2nd International Conference on Geotextiles*, IFAI, 1982, pp. 721–726.

15. Leflaive, E., and Liausu, Ph., "The Reinforcement of Soils by Continuous Threads," *Proceedings of the 3rd International Conference on Geotextiles*, Austrian Society of Engineers and Architects, Vienna, 1986, pp. 1159–1162.

16. "WES Developing Sand-Grid Confinement System," *Army Research Development Acquisition Magazine*, July-August, 1981, p. 7.

17. Richardson, G. N., "Geocells; A 25-Year Perspective," GFR, vol. 22, nos, 6 & 8, 2004, pp. 14–19 & 22–27.

18. John, N. W. M., *Geotextiles*. Glasgow: Blackie, 1987.

19. Edgar, S., "The Use of High Tensile Polymer Grid Mattress on the Musselburgh and Portobello Bypass." In *Polymer Grid Reinforcement*. London: Thomas Telford, 1985, pp. 103–111.

20. Rueff, H., Stoffers, U., and Leicher, F., " Landfills Placed on Soft Foundation Soils" Bautechnik vol. 69, no. 5, 1992, pp. 69–77.

21. Batson, G. B., "Introduction to Fibrous Concrete," *Proceedings on the CERL Fibrous Concrete Conference* University of Illinois Press, 1972, pp. 1–25.

22. Jenq, Y.-S., "Peformance Evalution of Fiber Reinforced Asphalt Concrete," FHWA/OH/94/018, Washington, DC, 1994.

23. Visser, T., and Mouw, K. A. G., "The Development and Application of Geotextiles on the Oosterschelde Project," *Proceedings of the 2nd International Conference on Geotextiles*, IFAI, 1982, pp. 265–270.

24. Door, H. C., and DeHaan, D. W., "The Oosterschelde Filter Mattress and Gravel Bag," *Proceedings of the 2nd International Conference on Geotextiles*, IFAI, 1982, pp. 271–276.

25. Van Harten, K., "Analysis and Experimental Testing of Load Distribution in the Foundation Mattress," *Proceedings of the 2nd International Conference on Geotextiles*, IFAI, 1982, pp. 277–282.

26. Wisse, J. D. M., and Birkenfeld, S., "The Long-Term Thermo-Oxidative Stability of Polypropylene Geotextiles in the Oosterschelde Project," *Proceedings of the 2nd International Conference on Geotextiles*, IFAI, 1982, pp. 283–286.

27. Gerry, B. S., and Raymond, G. P., "The In-Plane Permeability of Geotextiles," *Geotechnical Testing Journal*, ASTM, vol. 6, no. 4, 1983, pp. 181–189.

28. Hansbo, S., "Consolidation of Clay by Band-Shaped Perforated Drains," *Ground Engineering* 1979, pp. 16–25.

29. Rixner, J. J., Kraemer, S. R., and Smith, A. D., *Prefabricated Vertical Drains*, Report No. FHwA/RD-86/168, Washington, DC, 1986.

30. Welker, A.L., Devine, B.J., and Goughnour, R.R., "Development of a PVD Permeater," Proceedings of GRI-18 in Geofrontiers, ASCE, 2005, Paper 1.29.

31. Suits, L. D., Gemme, R. L., and Masi, J.J., "The Effectiveness of Prefabricated Drains in the Laboratory Consolidation of Remolded Soils," *ASTM Symposium Consolidation of Soils: Laboratory Testing*, ASTM, 1985, pp. 114–126.

32. Lawrence, C. A., and Koerner, R. M., "Flow Behavior of Kinked Strip Drains," *Proceedings Geosynthetics for Soil Improvement*," ASCE, 1988, pp. 22–39.

33. den Hoedt, G., "Laboratory Testing of Vertical Drains," *Proceedings of the 10th ICSMFE*, Swedish Society of Civil Engineers, Stockholm, 1981, pp. 627–630.

34. Kremer, R., et al., "Quality Standards for Vertical Drains," *Proceedings of the 2nd International Conference on Geotextiles*, IFAI, 1982, pp. 319–324.

35. Kremer, R., et al., "The Quality of Vertical Drainage," *Proceedings of the 8th European Conference SSMFE*, Finnish Society of Civil Engineers, Helsinki, 1983, pp. 721–726.

36. Holtz, R. D., Jamiolkowski, M., Lancelotta, R., and Pedroni, S., *Prefabricated Vertical Drains*, Newton, MA: Butterworth/Heinemann, 1990.

37. Koerner, R. M., Fowler, J., and Lawrence, C. A., "Soft Soil Stabilization Study for Wilmington Harbor South Dredge Materials Disposal Area," U.S. Army Corps of Engineers, WES, Misc. Paper GL-86-38 1986.

38. Holtz, R. D., and Christopher, B. R., "Characteristics of Prefabricated Vertical Drains for Accelerating Consolidation," *Proceedings of the 9th European Conference SSMFE*, Irish Society of Civil Engineers, Dublin, 1987, pp. 453–466.

39. Bergado, D. T., Manivannan, R., and Balasubramanian, A. S., "Proposed Criteria for Discharge Capacity of Prefabricated Vertical Drains," *Journal of Geotextiles and Geomembranes*, vol. 14, no. 9, 1996, pp. 481–506.

40. Koerner, R. M., and Soong, T.-Y., "Geosynthetic Reinforced Segmental Retaining Walls," *Journal of Geotextiles and Geomembranes*, vol. 19, no. 6, August 2001, pp. 359–386.

41. Koerner, R. M., and Soong, T.-Y., "Drainage System Design Behind Segmental Walls," *18th PennDOT/ASCE Conference on Geotechnical Engineering*, Hershey, PA, 2000; also *Proceedings of the GRI-14 Conference*, GII Publications, December 2000, pp. 323–351.

42. Dempsey, B. J., "Core Flow Capacity Requirements of Geocomposite Fin-Drain Materials Utilized in Pavement Subdrainage," 67th Annual Transportation Research Board Meeting, Washington, DC, 1988.

43. Koerner, R. M., and Hwu, B.-L., "Prefabricated Highway Edge Drains," *Transportation Research Record No. 1329*, Transportation Research Board, Washington, DC, 1991, pp. 14–20.

44. Koerner, G. R., Koerner, R. M., and Wilson-Fahmy, R. F., "Field Performance of Geosynthetic Highway Drainage Systems." In *Recent Developments in Geotextile Filters and Prefabricated Drainage Geocomposites, ASTM STP 1281*, 1996, pp. 165–181.

45. Wilson-Fahmy, R. F., Koerner, G. R., and Koerner, R. M., "Geotextile Filter Design Critique," In *Recent Developments in Geotextile Filters and Prefabricated Drainage Geocomposites, ASTM STP 1281*, 1996, pp. 132–161.

PROBLEMS

9.1. List some of the various joining methods that you could suggest to make a laminated geocomposite from different geosynthetic materials.

9.2. Describe or illustrate the differences between sheet, rill, and gully erosion mechanisms.

9.3. Using the Unified Soil Classification System or typical soil particle sizes, show by means of Figure 9.1, what velocities are required for the erosion and deposition of gravels, sands, silts, and clays. Answer the problem for both water and air.

9.4. What test methods and properties should be included in a generic specification for an erosion control geocomposite such as a turf reinforcement mat?

9.5. When used on exposed slopes, synthetic materials eventually degrade. Why does this occur? How is it usually minimized by geosynthetic manufacturers? How is it prevented when using a PERM?

9.6. Erosion control is very much related to intimate contact of the system with the soil that it is to protect.
   (a) Why is this the case, that is, what happens if intimate contact is not achieved?
   (b) Do natural fibers or polymeric fibers have the advantage?
   (c) How would intimate contact of polymeric erosion control materials be assured?

9.7. Section 9.1.4 made the design distinction using erosion control materials between **(a)** slope erosion, and **(b)** channel and ditch erosion. Why is this situation logical and what design methodologies apply to each.

9.8. Recalculate Example 9.1 by holding all values constant except the wetted perimeter of flow in the channel. Using perimeters of 5.0, 7.0, and 9.0 m, calculate the FS values based on an allowable velocity of a particular RECM of 4.5 m/sec.

9.9. For the shear stress design of an RECM per Equation 9.3, we need an allowable value for comparison and the resulting factor of safety. Such values were given in Table 9.2. How are such values obtained or verified?

9.10. In Section 9.2.1 it is mentioned that a steel reinforced woven geotextile could be used for direct support of vehicles without any soil or paved surface covering. In such instances, what test methods and properties should be included in a generic specification?

9.11. What shear strength properties of a sand are modified by the inclusion of fibers per Section 9.2.3? What differences do you envision between short fibers and continuous fibers?

9.12. Determine the ultimate bearing capacity of a cohesionless sand using a geocell reinforcement with $\delta = 18°$ as described in Example 9.3 as a function of the depth of the mattress. Vary the depth using 50, 100, 200 (the example), and 300 mm, and plot the response curve. Use the following soil properties: $\gamma = 16$ kN/m^3, $\phi = 27°$, and $\sigma_h = 20$ kPa (avg.).

9.13. Three-dimensional geogrid mattress filled with gravel are mentioned in Section 9.2.3. When placed on soft foundation soil, how do these mattresses provide stability—that is, what are the design elements that are improved? (*Hint:* Revisit Chapter 3 for information on this topic.)

9.14. What are the advantages and disadvantages of mixing polymeric fibers into the following materials:
   (a) Portland cement concrete, per Section 9.2.4
   (b) Bituminous materials, per Section 9.2.5

9.15. As with graded soil filters, geotextiles can be used in a similar composite form, as discussed per Section 9.3. If a cohesionless silt (ML Classification) were to be placed adjacent to a poorly graded gravel (GP Classification), how could a single geotextile versus two geotextiles (a composite geotextile) be fabricated to accommodate these very dissimilar soils? (Use assumed values for your opening size design.)

9.16. Concerning the wick drains described in Section 9.4.1, answer the following questions:
   (a) Do these geocomposites actually *wick* the water out of the soil as a wick in a candle brings wax up to the flame?
   (b) Does the installation of wick drains affect the amount of settlement or the rate of settlement?
   (c) What function does the geotextile covering the plastic core play?
   (d) What is the role of the core?
   (e) How does the expelled water exit the wick drain (top and/or bottom) so that excess pore water pressures do not build up under the surcharge?

9.17. Describe and illustrate what is meant by wick drain *smear*, as probably occurs during installation.

9.18. What is meant by *well resistance*, as might occur in the performance of sand drains versus wick drains?

9.19. What is the time for 95% consolidation of a proposed building site using wick drains measuring 92 mm by 10 mm in a cross-sectional area to be placed on a square pattern of 1.25 m centers in a saturated silt having a horizontal coefficient of consolidation of 12 mm^2/min?

9.20. Regarding the Hansbo analysis for wick drain spacing:
   (a) What spacing is required for wick drains of 100 mm by 6 mm placed on a triangular pattern if the required time for 50% consolidation is 90 days in a saturated silty clay with a horizontal coefficient of consolidation of 0.65 mm^2/min?
   (b) Check the spacing from part (a) if the time for 90% consolidation is 300 days.

9.21. Regarding traditional consolidation soil testing:
   (a) Describe how you measure the vertical coefficient of consolidation (c_v) of an undisturbed soil sample in the laboratory.
   (b) On a conceptual basis, how could this value in part (a) be related to the horizontal coefficient of consolidation (c_h)?
   (c) How could a soil sample be oriented to obtain c_h directly?

9.22. Calculate the time for 90% consolidation settlement for a silty clay soil with $c_h = 4.5$ mm^2/min using wick drains measuring 100 mm by 3.8 mm on triangular spacings of 4.0, 3.0, 2.0, and 1.0 m and plot the results on a semilog graph, as shown in Example 9.5 (Section 9.4.1).

9.23. Repeat Problem 9.22 for 70% and 50% consolidation, and compare the three response curves.

9.24. Given a measured flow rate between solid end platens of a wick drain in the laboratory ASTM D4716 test of 45 1/min-m at site-specific pressure and a hydraulic gradient of 1.0:
   (a) Reduce this value according to Table 9.6 to an allowable value (use average values).
   (b) Calculate the flow rate factors of safety using the required flow rates from Table 9.5 following the Koerner value of 0.10 1/min and then Holtz/Christopher value of 0.95 l/min.
   (c) The calculation in part (b) is based on a typical length of wick drain. What are the implications of extremely long wick drains?

9.25. Given the measured flow rate of a sheet drain geocomposite of 95 1/min-m when tested between solid platens in a planar flow test, what would be the allowable flow rate using average values in Table 9.6 if used in (a) sport field drainage?, (b) a roof or plaza deck?, and (c) a landfill cap?

9.26. Using sheet drain-E, shown in Figure 9.12b, check to see if it could handle the flow in Example 9.7 (Section 9.4.2) for drainage of the concrete cantilever retaining wall.

9.27. Determine the flow rate that can be handled by sheet drain N, shown in Figure 9.12a, for the drainage of a roof garden shown in the following diagram. Repeat the problem, but now use sheet drain E from Figure 9.12b.
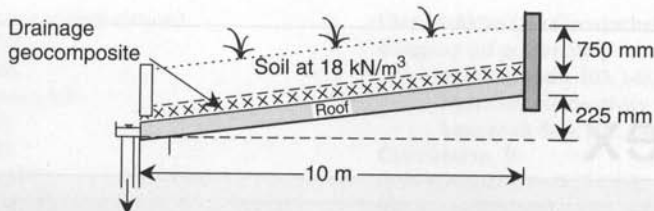
9.28. Of all the geosynthetic drainage materials that currently exist, the highway edge drains presented in Section 9.4.3 have the highest flow rates. Their thicknesses range from 12 to 38 mm. Estimate where their response curve falls in Figure 9.13. What is the range of flow rates for these products?

9.29. For geocomposite highway edge drains, why is the test method described in Section 9.4.3 using a laboratory water flume preferred over the ASTM D4716 test method? If the only laboratory test data available is from an ASTM D4716 test, how do you modify the value to be representative (i.e., what additional reduction factor should be used)?

9.30. For the geocomposite containment barriers in Section 9.5:

   (a) What are some reasons for attaching a geotextile to the upper side of a geomembrane used in a landfill cover?

   (b) What are some reasons for attaching a geotextile to the underside of a geomembrane that is used as a single moisture barrier for a building foundation?

   (c) In such cases, why are the seams difficult to make?

9.31. For geocomposite barriers per Section 9.5, an aluminum sheet (acting as a hydrocarbon barrier) and a lead sheet (acting as a radioactive barrier) were mentioned.

   (a) How is the HDPE bonded to the metallic sheet?

   (b) How are seams made?

   (c) What installation difficulties do you envision?

9.32. In Section 9.6 it was mentioned that the phrase *or equal* in specifications is inappropriate. Why is this the case?

Index

StudentAid.ed.gov
FUNDING YOUR FUTURE